THE

LONDON, EDINBURGH, AND DUBLIN

PHILOSOPHICAL MAGAZINE

AND

JOURNAL OF SCIENCE.

CONDUCTED BY

SIR OLIVER JOSEPH LODGE, D.Sc., LL.D., F.R.S.
SIR JOSEPH JOHN THOMSON, O.M., M.A., Sc.D., LL.D., F.R.S.
ALFRED W. PORTER, D.Sc., F.R.S.

AND

ALLAN FERGUSON, M.A., D.Sc.

"Nec aranearum sane textus ideo melior quia ex se fila gignunt, nec noster vilior quia ex allenis libamus ut apes."
JUST. LIPS. *Polit.* lib. i. cap. 1. Not.

VOL. XXV.—SEVENTH SERIES.

JANUARY—JUNE 1938.

LONDON:

TAYLOR AND FRANCIS, LTD., RED LION COURT, FLEET ST.

Agents: WM. DAWSON AND SONS, LTD., CANNON HOUSE, PILGRIM ST., E.C. 4.

"Meditationis est perscrutari occulta; contemplationis est admirari perspicua .... Admiratio generat quæstionem, quæstio investigationem, investigatio inventionem."—*Hugo de S. Victore.*

—— "Cur spirent venti, cur terra dehiscat,
Cur mare turgescat, pelago cur tantus amaror,
Cur caput obscura Phœbus ferrugine condat,
Quid toties diros cogat flagrare cometas,
Quid pariat nubes, veniant cur fulmina cœlo,
Quo micet igne Iris, superos quis conciat orbes
Tam vario motu."

J. B. Pinelli ad Mazonium.

CONTENTS OF VOL. XXV.

(SEVENTH SERIES).

NUMBER CLXVI.—JANUARY.

Page

Dr. W. S. Kimball on the Differentiation of Line Integrals by Parallel Displacement. 1

Messrs. E. A. Guggenheim and L. A. Wiseman on the Activity Coefficients of Potassium Chloride and of Calcium Chloride.... 45

Mr. R. Thornton Coe on the Bending of Beams on Elastic Foundations 49

Mr. E. A. Meyerovitz on the Method of Images for calculating Electric and Magnetic Fields 66

Messrs. I. Ramakrishna Rao and P. Koteswaram on Additional Raman Frequencies for Water 90

Messrs. C. R. Bailey and J. B. Hale on the Infra-red Absorption Spectrum of Phosgene 98

Mr. Weng Wen-Po on the Atomic Forces of Solid State 111

Prof. H. Spencer-Gregory and Mr. E. H. Dock on the Effect of Temperature on the Thermal Conductivity and the Accommodation Coefficient of Hydrogen below 0° C. 129

Dr. L. G. H. Huxley on the Propagation of Electromagnetic Waves in an Ionized Atmosphere 148

Mr. M. N. S. Immelman on the Point-discharge Currents during Thunderstorms 159

Messrs. A. Žáček and V. Petržílka on the Radial and Torsional Vibrations of Annular Quartz Plates 164

Prof. Preston B. Carwile on the Reciprocals to Ampere's Law ... 175

Prof. John J. Dowling on the Zero-Shunt Valve A.C. Potentiometer. 184

Notices respecting New Books :—

Mr. Francis Bitter's Introduction to Ferromagnetism..... 189

Dr. R. W. Gurney's Ions in Solution 190

Mr. Alfred Landé's Principles of Quantum Mechanics 191

Mr. A. S. Ramsey's Electricity and Magnetism 192

Mr. A. S. Ramsey's Dynamics.—Part II. 192

NUMBER CLXVII.—FEBRUARY.

Messrs. H. Warburton Hall and W. Hunter on the Form assumed by a Steadily Rotating Thread 193

Dr. S. S. Bhatnagar and Messrs. Mohan Lal Khanna and M. B. Nevgi on the Paramagnetism of the Iron Group 234

Mr. J. M. Thomson on the Magnetic Fields in Transformers at Low Frequencies (25 to 75 cycles per second) 242

Mr. P. Görlich on Measurements on Photocathodes in Contact ... 256

Dr. N. W. McLachlan on Operational Systems 259

Mr. Horst Teichmann on the Blocking Layer Photoelectric Effect of Cæsium Oxide 269

Dr. John R. Airey on the Radiation Integrals $\int_x^\infty \frac{dx}{x^2(e^x-1)}$ 273

Page

Mr. C. Hurst on the Potential Problem of a Sphere lying between Infinite Conducting Planes 282
Mr. N. F. Astbury on the Primary Standard of Mutual Inductance of the National Physical Laboratory 290
Dr. W. Fabian on Lebesgue Complex Integration 318
Dr. W. Fabian on the Zeta-function of Riemann 321
Dr. J. Alan Chalmers on the Reflexion of β-Rays..... 322
Dr. William Hume-Rothery and Mr. Geoffrey Vincent Raynor on the Nature of Intermetallic Compounds of the Type Mg_2Sn.... 335
Dr. Ronold King on the Capacitance at Ultra-High Frequencies . 339
Dr. R. M. Davies on the Frequency of Longitudinal and Torsional Vibration of Unloaded and Loaded Bars 364
Mr. C. E. Wright: Note on the Paper "A Note on the Vibrations of a Rotating Rope"..... 387
Dr. L. G. H. Huxley's Supplementary Note to the Paper "The Propagation of Electromagnetic Waves in an Ionized Atmosphere" 388
Notices respecting New Books :—
Messrs J. H. Michell and M. H. Belz's Mathematical Analysis. 389
Mr. F. B. Pidduck's Lectures on the Mathematical Theory of Electricity 389
Prof. Edward S. Allen's Plane Trigonometry 390
Mr. A. S. Ramsey's Hydrostatics 390
Mr. K. Henney's Electron Tubes in Industry 391
Mr. A. V. Eastman's The Fundamentals of Vacuum Tubes . 392

NUMBER CLXVIII.—MARCH.

Dr. Samuel C. Curran on the Complete Detection of Beta-particles. 393
Prof. S. C. Dhar on the Operational Representation of M-functions of the Confluent Hypergeometric Type 416
Dr. J. J. Hermans on Charged Colloid Particles in an Ultrasonic Field 426
Mr. Harold Ward Gardner on the Gradient Diagram 438
Mr. W. J. G. Beynon on the Ultra-Violet Absorption Bands of Ethyl Alcohol, *n*-Propyl Alcohol, and *n*-Butyl Alcohol in relation to Magneto-optical Dispersion 443
Mr. W. T. Howell on Integral Representations for Products of Weber's Parabolic Cylinder Functions 456
Prof. J. S. Townsend on the Diffusion of Electrons in a Magnetic Field 459
Dr. D. B. McNeill on some Aspects of Active Nitrogen 471
Mr. W. J. G. Beynon and Prof. E. J. Evans on the Ultra-Violet Absorption Bands of Methyl Alcohol and Allyl Alcohol and their Relation to Magneto-Optical Dispersion..... 476
Mr. R. P. Bell on the Wave Functions and Permeabilities for a new type of Potential Barrier..... 488
Mr. J. L. Sharma on Whittaker's Confluent Hypergeometric Function 491
Mr. G. F. Partridge on a Method of Harmonic Analysis.—A Study of the Rotational Frequencies of Screw Propellers ... 505
Mr. Andrew Gemant on Fractional Differentials 540
Dr. W. S. Kimball on the Application of Derivatives of Line Integrals 549
Prof. Atsushi Miyadzu: Note on the Equilibrium of a Vortex maintained in a sudden Expanding Stream..... 567

Page

Mr. A. H. A. Hogg on the Equilibrium of a thin Plate, symmetrically loaded, resting on an Elastic Foundation of Infinite Depth 576

Notices respecting New Books :—

Mr. Harald Cramér's Random Variables and Probability Distributions 583

Dr. J. W. Mellor's A Comprehensive Treatise on Inorganic and Theoretical Chemistry.—Vol. XVI. Pt. and General Index 584

NUMBER CLXIX.—APRIL.

Dr. Louis A. Pipes on Operational and Matrix Methods in Linear Variable Networks 585

Mr. W. T. Howell : a Note on Hermite Polynomials 600

Prof. B. Dasannacharya on the Development of the Minor Axis in a Foucault's Pendulum 601

Mr. W. T. Howell on a Class of Functions which are Self-reciprocal in the Hankel Transform 622

Prof. W. J. Duncan : Note on Galerkin's Method for the Treatment of Problems concerning Elastic Bodies 628

Prof. W. J. Duncan : Applications of the Galerkin Method to the Torsion and Flexure of Cylinders and Prisms 634

Prof. E. L. E. Wheatcroft, Dr. R. B. Smith, and Mr. J. Metcalfe on Pre-striking Currents in a Thyratron 649

Mr. Hikosaburo Ataka on an Extension of Thévénin's Theorem.. 663

Messrs. H. Lessheim and R. Samuel : Note on Numerical Valency in Polyatomic Molecules 667

Mr. Th. Pöschl : Remarks on the more Accurate Calculation of the Deflexion of Beams and Struts 678

Prof. E. Taylor Jones on Magnetism and the Vibratory Electron . 682

Mr. D. V. Gogate on a Relativistic Study of Joule-Thomson Effect and Adiabatic Processes in a Gas.—Part I. 694

Notices respecting New Books :—

Measurement of Radiant Energy (edited by Mr. L. E. Forsythe) 703

Mr. Gerhard Herzberg's Atomic Spectra and Atomic Structure 703

Mr. J. M. Thomas's Differential Systems 704

NUMBER CLXX.—MAY.

Dr. D. M. Wrinch on the Hydration and Denaturation of Proteins. 705

Dr. R. A. Frazer, Mr. W. P. Jones, and Miss Sylvia W. Skan : Note on Approximations to Functions and to Solutions of Differential Equations 740

Dr. W. G. Bickley on the Secondary Flow due to a Sphere rotating in a Viscous Fluid 746

Prof. Alfred W. Porter on the Calculation of Surface Tension from Measurement of Sessile Drops 752

Mr. J. Allen : Experiments on Water Waves of Translation in Small Channels 754

Dr. L. L. Bircumshaw and Mr. G. D. Preston : Studies on the Oxidation of Metals.—Part V. The Oxidation of Molten Lead . 769

Mr. G. R. Stibitz on the Potentials in Curved Surfaces 783

Dr. Malcolm Fraser on the Thermo-Electric Effects in Homogeneous Conductors 785

Page

Mr. Manindra Kumar Chakravarty and Dr. S. R. Khastgir on the Direct Determination of the Electrical Constants of Soil at Ultra-high Radio-frequency 793
Mr. Frederick Record on Thick Lenses and Combinations of Thin Lenses 801
Dr. W. Fabian on Lebesgue Complex Integration and Generalized Differentiation 807
Notices respecting New Books :—
Mr. H. Kestelman's Modern Theories of Integration 811
Mr. Enrico Fermi's Thermodynamics 812
Messrs. S. Barnard and J. M. Child's Higher Algebra 813
Mr. Herbert Dingle's Through Science to Philosophy 814
Messrs. Max Morris and O. E. Brown's Analytic Geometry and Calculus 816

NUMBER CLXXI.—JUNE (SUPPLEMENT).

Messrs. Balth. van der Pol and H. Bremmer on the Propagation of Radio Waves over a Finitely Conducting Spherical Earth... 817
Dr. A. L. Reimann on the Evaporation of Atoms, Ions and Electrons from Tungsten..... 834
Prof. T. M. MacRobert : a Proof by Induction of the Analytical Continuations of certain Generalized Hypergeometric Functions. 848
Mr. F. J. Turton on new Forms of the Theorem of Three Moments. 852
Mr. Weng Wen-Po on Molecular Force and Viscosity of Gases. .. 865
Mr. Sukhamaya Gangopadhyaya and Dr. S. R. Khastgir on the Dielectric Constant of Ionized Gases.—II..... 883
Mr. S. M. Mitra on the Raman Effect in Solid Cyclohexane..... 895
Dr. Edmund C. Stoner on Collective Electron Energy and Specific Heat 899
Dr. Preston B. Carwile : Suggested Explanation of the Contradiction between the Rayleigh-Jeans Formula and Experiment.... 926
Mr. N. A. Shastri on Lommel Functions 930
Dr. Louis A. Pipes on the Operational Theory of Solid Friction . 950
Mr. P. J. Rigden on the Viscosity of Air, Oxygen, and Nitrogen . 961
Dr. T. Walmsley on the Impedance Characteristics of Short-Wave Dipoles 981
Profs. K. Prosad and D. N. Sen on the Trajectory of Ash Particles in Air and the Determination of their Size 993
Dr. Ludwik Silberstein on the Summation of the Series $1+x^3/3\,!+x^6/6\,!+\ldots$ 1003
Notices respecting New Books :—
Dr. George Kaván's Factor Tables giving the Complete Decomposition into Prime Factors of all Numbers up to 256,000 1004
Messrs. C. V. Durell and A. Robson's Advanced Algebra.—Vols. II. and III. 1005
Prof. A. Cornelius Benjamin's An Introduction to the Philosophy of Science 1006
Prof. L. Susan Stebbing's Philosophy and the Physicists ... 1007

NUMBER CLXXII.—JUNE.

Messrs. N. F. Astbury and L. H. Ford on a Screened Sub-Standard Inductometer 1009
Dr. S. S. Banerjee and Mr. R. D. Joshi on Dielectric Constant and Conductivity of Soil at High Radio Frequencies..... 1025

Page

Mr. U. C. Bardhan on the Nuclear Structure of Radioactive Substances 1033

Messrs. S. R. Craxford, O. Gatty, and T. Teorell on the Theory of Electrocapillarity.—VII. The Theory of Surface Films 1041

Messrs. S. R. Craxford, O. Gatty, and T. Teorell : A Note on Surface pH 1061

Dr. J. P. Andrews on the Thermal Diffusivity of the Soil at Colombo Observatory 1066

Dr. H. C. Hepburn on Electrolytic Water-Transport and Ionic Hydration Numbers 1074

Dr. T. H. Goodwin and Mr. R. Hardy on the Computation of Three-dimensional Fourier Syntheses in Crystal Structure Analysis 1096

Drs. G. C. Seager and F. C. Thompson : a Note on a suggested Intermetallic Reaction in a Liquid Antimony-Copper-Tin-Lead Alloy 1104

Dr. Bruce Chalmers and Mr. R. H. Humphry on the Specific Resistance and the Temperature Variation of Resistance of Tin Crystals 1108

Mr. W. T. Howell on a Definite Integral for Legendre Functions. 1113

Notices respecting New Books :—

Mr. J. V. Uspensky's Introduction to Mathematical Probability 1115

Synthetic Resins and Allied Plastics. Edited by Mr. R. S. Morrell, in collaboration with Messrs. T. H. Barry, R. P. L. Britton, and H. M. Langton 1117

Messrs. M. and B. Ruhemann's Low Temperature Physics... 1119

Mr. W. F. Osgood's Mechanics 1120

Dr. N. Feather's An Introduction to Nuclear Physics 1120

Bessel Functions.—Part I. Functions of Orders Zero and Unity 1121

Index 1122

PLATES.

I. Illustrative of Messrs. I. R. Rao and P. Koleswaram's Paper on Additional Raman Frequencies for Water.

II.–IV. Illustrative of Messrs. A. Žáček and V. Petržílka's Paper on Radial and Torsional Vibrations of Annular Quartz Plates.

V. Illustrative of Mr. N. F. Astbury's Paper on the Primary Standard of Mutual Inductance of the National Physical Laboratory.

VI.–VIII. Illustrative of Mr. G. F. Partridge's Paper on a Method of Harmonic Analysis.—A Study of the Rotational Frequencies of Screw Propellers.

IX. Illustrative of Dr. D. M. Wrinch's Paper on the Hydration and Denaturation of Proteins.

X. Illustrative of Mr. S. M. Mitra's Paper on the Raman Effect in Solid Cyclohexane.

XI. Illustrative of Profs. K. Prosad and D. N. Sen's Paper on the Trajectory of Ash Particles in Air and the Determination of their Size.

ERRATA.

December 1937.

Page 1079, bottom line :

For $(x)=\alpha_m(\ldots$, read $\xi_m(x)=\alpha_m(\ldots$.

Page 1085 :

"Arbitrary," in line following equation (2.1) to be read $R(\lambda)$ and $R(\mu)>0$.

Page 1086 :

The right-hand side of equation (2.5) to be multiplied by p.

Page 1090 :

The right-hand side of equation (5.2) to be multiplied by $\sqrt{\pi}$.

THE

LONDON, EDINBURGH, AND DUBLIN

PHILOSOPHICAL MAGAZINE

AND

JOURNAL OF SCIENCE.

[SEVENTH SERIES.]

JANUARY 1938.

I. *Differentiation of Line Integrals by Parallel Displacement.* *By* W. S. KIMBALL, *Ph.D., Michigan State College, East Lansing, Michigan* *.

Introduction.

FORMULÆ for the derivatives of line integrals are derived by the same method of differentials previously † used to get the new critical equations in the calculus of variations, but attention is no longer restricted to cases where the integrals are maxima and minima. Line integrals with fixed integration limits are treated, those with fixed lower and variable upper limit, and those with fixed upper and variable lower limit.

The variations $\delta x=h$, and $\delta y=k$ of the independent variables measure *parallel* displacements of the original path for its entire extent between whatever limits are chosen for the line integral which is the dependent variable J_i^k. Hence, outside of dependence on the original path and limits, the dependent variable is a unique *two*-point function, two being enough to determine its straight line variations. This two-point function J_i^k has ordinarily unique rates of changes with respect to x or y referring

* Communicated by the Author.

† W. S. Kimball, Phil. Mag. xxiii. p. 114 (1937).

to any point on the path of integration, being independent of which point:

$$\frac{\partial J_i^k}{\partial x}=\frac{\partial J_i^k}{\partial\, dx}=M(x_iy_i)+\int_{x_iy_i}^{x_ky_k} M_x\,dx+N_x\,dy-M(x_ky_k)$$

$$=(f-y'f_{y'})_i+\int_{x_i}^{x_k} f_x\,dx-(f-y'f_{y'})_k;$$

$$\frac{\partial J_i^k}{\partial y}=\frac{\partial J_i^k}{\partial\, dy}=N(x_iy_i)+\int_{x_iy_i}^{x_ky_k} M_y\,dx+N_y\,dy-N(x_ky_k)$$

$$=f_{y'}(x_iy_i)+\int_{x_i}^{x_k} f_y\,dx-f_{y'}(x_ky_k).$$

Here the right members when set equal to zero include the new critical equations * (48) in the calculus of variations.

Besides first and second partial derivatives, an area derivative is obtained that is a special case of Volterra's derivative, and the differentials are line integrals around a closed differential circuit, and hence are expressible in terms of the curl of the vector integrand.

The area derivative is taken with respect to the area $d\sigma=\delta x\,dy-\delta y\,dx$ adjoining the path, and when set equal to zero gives Euler's equations

$$\frac{dJ}{d\sigma}=\frac{d}{dy}\left(\frac{\partial J}{\partial x}\right)=-\frac{d}{dx}\frac{\partial J}{\partial y}=N_x-M_y=\frac{d}{dx}f_{y'}-f_y.$$

In the right members above, the vector integrand is $F=i(f-y'f_{y'})+jf_{y'}$, which for an extremal arc must be perpendicular to the line on which a variable end-point is to lie according to the transversality condition.

In Part I. we differentiate the sum that approximates the integral and obtain in the limit unique derivatives. In Part II. we reverse the procedure and start with an integral and differentiate, using parallel path displacements. Differentiation with respect to these parallel path displacements h and k turns out to be the same as differentiation with respect to x and y treated as *independent* variables, *i. e.*, using the differentials δx and δy instead of $dy=\phi'dx$, which latter are related to each other by the path-equation $y=\phi(x)$. We obtain the same derivatives as in Part I., thereby showing that the limit

* W. S. Kimball, Phil. Mag. xxiii. p. 114 (1937).

processes of differentiation and integration as applied here are commutative. In Part III. we apply the new rules for differentiation with respect to differentials and obtain the same derivatives as in the first two parts. First partials and an area derivative are also obtained where the slope y' is included in the vector integrand as in the calculus of variations proper, whereby Euler's and Du Bois Raymond's and the new critical conditions (48) of the previous paper are interpreted geometrically with reference to parallel displacements of the path of integration. Second partial derivatives of this type of integral having y' in the vector integrand are not considered.

Three special advantages are to be emphasized: (*a*) the parallel displacement requirement for path-variations simplifies the analysis, since most integrals are continuous functions of such displacements or of the two points which determine them; (*b*) the arbitrary nature of the choice of limit points on the integration path permits a ready extension of the method to the calculus of variations; (*c*) the derivatives are unique in that differentiation by delta process before passing to the limit as in Part I. introduces automatically the parallel path displacements and prescribes how these are to be used with an integral as in Part II. to give results commutative with those of Part I., whose method thus forms the basis of the theory.

Applications to various types of line integrals are given in a sequel article.

Part I.

Differentiation before passing to the Limit as in Integration.

§1. *The Derivatives of a Line Integral* * *with fixed Limits of Integration.*

We consider a line integral with fixed limits of integration:

$$J=\int_{x_0y_0}^{a,\,b} M(x,\,y)\,dx+N(x,\,y)\,dy \quad . \quad . \quad . \quad (1)$$

* All the formulæ and analysis of Part I. may be extended without change of form to include the calculus of variations proper, where the vector integrand is a function of y', and is given by $R=i(f-y'f_{y'})+jf_{y'}$. Compare with Part III.

and the sum that approximates it

$$\mathrm{F}=\sum_{i=1}^{n}(\mathrm{M}(x_iy_i)\,\Delta x_i+\mathrm{N}(x_iy_i)\Delta y_i), \quad . \quad . \quad . \quad (2)$$

where M and N have continuous first and second derivatives, and the vector integrand, $\mathrm{R}=i\mathrm{M}+j\mathrm{N}$ is a function * of x and y only, and

$$\left.\begin{aligned} x_i&=x_0+\sum_{j=1}^{i}\Delta x_j,\\ y_i&=y_0+\sum_{j=1}^{i}\Delta y_j,\end{aligned}\right\}. \quad . \quad . \quad . \quad . \quad . \quad . \quad (3)$$

and

$$\left.\begin{aligned} a&=x_0+\sum_{j=1}^{n}\Delta x_j,\\ b&=y_0+\sum_{j=1}^{n}\Delta y_j,\end{aligned}\right\}. \quad . \quad . \quad . \quad . \quad . \quad . \quad (4)$$

where a, b, x_0, y_0 are constants.

Certain consequences of (3) and (4) are to be used below:

$$\left.\begin{aligned} \frac{\partial x_j}{\partial\,\Delta x_i}&=0,\text{ or }1,\\ \frac{\partial y_j}{\partial\,\Delta y_i}&=0,\text{ or }1,\end{aligned}\right\}. \quad . \quad . \quad . \quad . \quad . \quad . \quad (5)$$

according as j is less than i or otherwise.

Eqs. (4) put a single restriction on the $n\,\Delta x$'s, and another on the $n\,\Delta y$'s. Hence there are only $n-1$ independent variables in each set. We take Δx_k and Δy_k as the dependent variables, and from (4) we have

$$\left.\begin{aligned} \frac{\partial\,\Delta x_k}{\partial\,\Delta x_i}&=-1,\\ \frac{\partial\Delta y_k}{\partial\,\Delta y_i}&=-1.\end{aligned}\right\}. \quad . \quad . \quad . \quad . \quad . \quad . \quad (6)$$

Since Δx_i and Δy_i are the last of the variables that sum up according to (3) to x_i and y_i, their increments $d\Delta x_i$ and $d\,\Delta y_i$ measure (provided the Δx's and Δy's of lower index are constant, *i. e.*, if $k>i$) the *sole* increase in x_i and y_i, and being added at the outer ends they are identi-

* See preceding footnote.

cally equal to the increments of x_i and y_i given by the familiar dx_i and dy_i. Hence * (see figs. 1 and 2)

$$\left.\begin{aligned} \frac{d\,\Delta x_i}{dx_i} &= 1 = \frac{\delta x}{dx_i}, \\ \frac{d\,\Delta y_i}{dy_i} &= 1 = \frac{\delta y}{dy_i}, \end{aligned}\right\} \quad \ldots\ldots \quad (7)$$

provided no path displacement occurs between $(x_0 y_0)$ and (x_i, y_i), *i. e.*, the Δx's and Δy's of lower index are constant $(k > i)$.

On the other hand, if $k < i$ all Δx's and Δy's of higher index than i are constant for partial derivatives with respect to Δx_i and Δy_i, and likewise each (x, y) of index equal to or greater than i will be constant since the upper limits (a, b) are fixed. An increase in Δx_i will then *decrease* x_{i-1} by its identical amount $d\,\Delta x_i$, as shown in figs. 1 and 2. Hence instead of (7) we have

$$\left.\begin{aligned} \frac{d\,\Delta x_i}{dx_{i-1}} &= -1 = -\frac{\delta x}{dx_{i-1}}, \\ \frac{d\,\Delta y_i}{dy_{i-1}} &= -1 = -\frac{\delta y}{dy_{i-1}}, \end{aligned}\right\} \quad \ldots\ldots \quad (8)$$

provided no path displacement occurs between (x_i, y_i) and (a, b) (see figs. 1 and 2, *i. e.*, the Δx's and Δy's of higher index are constant $(k < i)$

As the norms of the Δx and Δy partitions defined by (4) approach zero, the sum (2) is assumed to approach the limit (1), the line integral defined as usual.

Now take the partial derivatives of (2) with respect to Δx_i and Δy_i, treating Δx_k and Δy_k as the dependent variables :

$$\left.\begin{aligned} \frac{\partial F}{\partial\,\Delta x_i} &= M(x_i y_i) + \sum_{j=i}^{n} (M_{x_j}\Delta x_j + N_{x_j}\Delta y_j) \\ &\quad + \left[M(x_k, y_k) + \sum_{j=k}^{n} M_{x_j}\Delta x_j + N_{x_j}\Delta y_j\right]\frac{\partial\,\Delta x_k}{\partial\,\Delta x_i}, \\ \frac{\partial F}{\partial\,\Delta y_i} &= N(x_i y_i) + \sum_{j=i}^{n} (M_{y_j}\Delta x_j + N_{y_j}\Delta y_j) \\ &\quad + \left[N(x_k, y_k) + \sum_{j=k}^{n} M_{y_j}\Delta x_j + N_{y_j}\Delta y_j\right]\frac{\partial\,\Delta y_k}{\partial\,\Delta y_i}. \end{aligned}\right\} \quad \ldots \quad (9)$$

* The right members are added because $d\,\Delta x_i$ and $d\,\Delta y_i$ turn out to be the " variations " of Euler and Lagrange as indicated by the customary notation ; see figs. 1 and 2.

The summation terms range only from $j=i$ to n and $j=k$ to n because of (5), and the last three terms come from differentiating with respect to the dependent variables, Δx_k and Δy_k, and the subscripts indicate partial derivatives.

Introduce (6) into (9), then

$$\left.\begin{aligned}\frac{\partial F}{\partial \Delta x_i} &= M(x_i y_i) + \sum_{j=i}^{n} (M_{x_j}\Delta x_j + N_{x_j}\Delta y_j) \\ &\quad - M(x_k y_k) - \sum_{j=k}^{n} (M_{x_j}\Delta x_j + N_{x_j}\Delta y_j), \\ \frac{\partial F}{\partial \Delta y} &= N(x_i y_i) + \sum_{j=i}^{n} (M_{y_j}\Delta x_j + N_{y_j}\Delta y_j) \\ &\quad - N(x_k y_k) - \sum_{j=k}^{n} (M_{y_j}\Delta x_j + N_{y_j}\Delta y_j).\end{aligned}\right\} \quad . \; . \; . \quad (10)$$

Simplify the right members and multiply the left members by (7) and (8) for $k>i$ and $k<i$ respectively, then (10) becomes

$$\left.\begin{aligned}\frac{\partial F}{\partial x_i} &= M(x_i y_i) + \sum_{j=i}^{k} (M_{x_j}\Delta x_j + N_{x_j}\Delta y_j) - M(x_k, y_k), \\ \frac{\partial F}{\partial y_i} &= N(x_i y_i) + \sum_{j=i}^{k} (M_{y_j}\Delta x_j + N_{y_j}\Delta y_j) - N(x_k, y_k).\end{aligned}\right\} (k>i). \quad . \; . \; . \quad (11)$$

$$\left.\begin{aligned}\frac{\partial F}{\partial x_{i-1}} &= M(x_k y_k) - \sum_{j=i}^{k} (M_{x_j}\Delta x_j + N_{x_j}\Delta y_j) - M(x_i y_i), \\ \frac{\partial F}{\partial y_{i-1}} &= N(x_k y_k) - \sum_{j=i}^{k} (M_{y_j}\Delta x_j + N_{y_j}\Delta y_j) - N(x_i y_i).\end{aligned}\right\} (k<i). \quad . \; . \; . \quad (12)$$

Now pass to the limit in the usual way as the norms of the Δx and Δy partitions approach zero. Then the sum (2) approaches the limit (1); and $x_{i-1}=x_i-\Delta x_i$ approaches x_i and eqs. (11) approach in general a limit (13) with an integral term

$$\left.\begin{aligned}\frac{\partial J_i^k}{\partial x_i} &= M(x_i y_i) + \int_{x_i y_i}^{x_k y_k} (M_x\,dx + N_x\,dy) - M(x_k y_k), \\ \frac{\partial J_i^k}{\partial y_i} &= N(x_i y_i) + \int_{x_i y_i}^{x_k y_k} (M_y\,dx + N_y\,dy) - N(x_k y_k),\end{aligned}\right\} . \quad (13)$$

and (12) approaches the limit (14)

$$\left.\begin{aligned}\frac{\partial \mathrm{J}^{i}_{k}}{\partial x_{i}} &= \mathrm{M}(x_k y_k) + \int_{x_k y_k}^{x_i y_i} (\mathrm{M}_x\,dx + \mathrm{N}_x\,dy) - \mathrm{M}(x_i y_i)\,,\\ \frac{\partial \mathrm{J}^{i}_{k}}{\partial y_{i}} &= \mathrm{N}(x_k y_k) + \int_{x_k y_k}^{x_i y_i} (\mathrm{M}_y\,dx + \mathrm{N}_y\,dy) - \mathrm{N}(x_i y_i).\end{aligned}\right\}. \quad (14)$$

Eqs. (13) and (14) are derivatives of a certain kind which we shall see are the actual rates of change with respect to x_i and y_i of that part of the line integral (1) included between the dependent variables (x_k, y_k) and the independent variables $(x_i y_i)$, as indicated by the subscripts and superscripts on the J's.

A special case of (13) occurs when (x_k, y_k), a fixed point during the above operations according to (6), is taken at the upper limit. For (x_k, y_k) equal to (a, b) at this upper limit of (1) we have

$$\left.\begin{aligned}\frac{\partial \mathrm{J}^{n}_{i}}{\partial x_{i}} &= \mathrm{M}(x_i y_i) + \int_{x_i y_i}^{a,\,b} \mathrm{M}_x\,dx + \mathrm{N}_x\,dy - \mathrm{M}(a, b)\,,\\ \frac{\partial \mathrm{J}^{n}_{i}}{\partial y_{i}} &= \mathrm{N}(x_i y_i) + \int_{x_i y_i}^{a,\,b} \mathrm{M}_y\,dx + \mathrm{N}_y\,dy - \mathrm{N}(a, b)\end{aligned}\right\}. \quad (15)$$

Another special case occurs when $(x_k y_k)$ of (14) is taken as the *lower* limit $(x_0 y_0)$. Then we have from (14)

$$\left.\begin{aligned}\frac{\partial \mathrm{J}^{i}_{0}}{\partial x_{i}} &= \mathrm{M}(x_0 y_0) + \int_{x_0 y_0}^{x_i y_i} \mathrm{M}_x\,dx + \mathrm{N}_x\,dy - \mathrm{M}(x_i y_i)\,,\\ \frac{\partial \mathrm{J}^{i}_{0}}{\partial y_{i}} &= \mathrm{N}(x_0 y_0) + \int_{x_0 y_0}^{x_i y_i} \mathrm{M}_y\,dx + \mathrm{N}_y\,dy - \mathrm{N}(x_i y_i).\end{aligned}\right\}. \quad (16)$$

To get the derivatives of the entire line integral (1), we have only to use the appropriate limits in these last four derivative formulæ and get

$$\left.\begin{aligned}\frac{\partial \mathrm{J}}{\partial x_{i}} &= \mathrm{M}(x_0 y_0) + \int_{x_0 y_0}^{a,\,b} \mathrm{M}_x\,dx + \mathrm{N}_x\,dy - \mathrm{M}(a, b)\,,\\ \frac{\partial \mathrm{J}}{\partial y_{i}} &= \mathrm{N}(x_0 y_0) + \int_{x_0 y_0}^{a,\,b} \mathrm{M}_y\,dx + \mathrm{N}_y\,dy - \mathrm{N}(a, b).\end{aligned}\right\}. \quad (17)$$

In (17) the range of J from $(x_0 y_0)$ to (a, b) is not indicated, because these equations give the derivatives as the indicated rates of change of the complete integral (1), in contrast to (13) to (16), which are derivatives of those parts of (1) between the indicated limits along the integration path. Also the subscripts i for the independent

variable are intended to indicate that (17) holds for the differentiation of (1) with respect to x_i and y_i, either at the upper limit $(x_iy_i)=(a, b)$ in (16) or at the lower limit $((x_iy_i)=(x_0y_0)$ in (15)), and also for any (x_iy_i) on the path of integration between these limits as shown by Theorem 1, § 5 below.

§ 2. *Geometrical Interpretation of the Derivatives of Line Integrals by Parallel Displacement of the Path of Integration.*

The geometrical significance of (11) and (12) becomes clear if we examine fig. 1, which shows how a positive increment given to Δx_i operates (*a*) to shove the broken

Fig. 1.

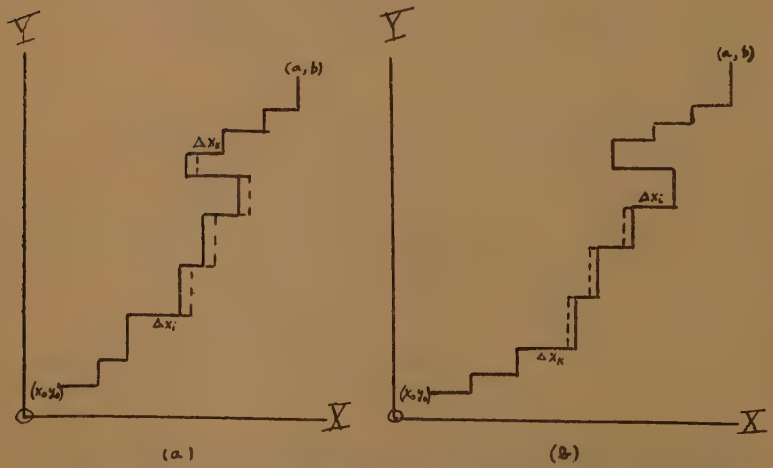

The parallel displacements of the path of the sum (2) indicating (*a*), the shift or variation in the positive x direction equal to $\delta x=d\,\Delta x_i$ when the dependent variable Δx_k has $k>i$ as in (11); and (*b*), the equal and opposite shift or variation $\delta x=-d\,\Delta x_i$ that occurs when the dependent variable Δx_k is of lower index, $k<i$, as in (12).

line to the right for all Δx's and Δy's of index between i and k (when $k>i$). This is because all these interval variables are kept constant except Δx_i and the dependent Δx_k according to (4). We hence must have $d\,\Delta x_i=-d\,\Delta x_k$ according to (6), whereby the shift is exactly compensated and an upper limit is indicated for the parallel path displacements shown in fig. 1 *a*. In fig. 1 *b*, where $k<i$, there is no chance for a shift between x_i and "a" since all the intervening Δx's are kept constant, but the x's that are smaller than x_i are shoved to the left due to this

increase in Δx_i until the position of Δx_k is reached where the shift ends due to the compensating $d\Delta x_k = -d\Delta x_i$ according to (6).

Note that, due to the fact that all Δx's are constant except these two, there is no shift anywhere along the path except between these two arbitrary positions; and, secondly, note that between these limiting positions the shifts are equal to the variation $\delta x = d\Delta x_i$ which measures the *parallel* displacement of the broken line or path.

As the norms of the Δx and Δy partitions shown in fig. 1 approach zero, the broken line approaches a curve and the parallel displacements of fig. 1 approach those of a curve such as shown by fig. 3 and in Part II. And for a given variation $\delta x = d\Delta x_i$ the area enclosed between the original and displaced paths $(y_k - y_i)\delta x$ is independent of how fine the partition is. During this limiting process the derivatives (11) and (12) of the sum (2) for various partitions will ordinarily approach unique limits, which are shown herein below to be the actual partial derivatives of (1) with respect to x_i and y_i in the sense of being the corresponding rates of change.

Along with the concept of (13) and (14) as derivatives of (1), we have the concept of J_i^k as a unique function of its parallel displacements, or a *two-point* function of (x', y') and (x, y) as explained in section 9 below, since these two points (x', y') on the original path, and $(x, y) = (x' + \delta x, y' + \delta y)$ on the displaced path are enough to determine uniquely the varied integral J_i^k that emerges under rectilinear parallel path displacements as herein.

Furthermore, just as (11) and (12) give only the rates of change of the sum (2) between the arbitrarily chosen limits (x_i, y_i) and (x_k, y_k) indicated by fig. 1, so the derivatives (13) and (14) of J give only the rates of change of that part of J included between the same indicated arbitrary limits whose position need not be affected by the limiting process whereby the partitions approach zero. Likewise with (15) and (16), but (17) gives the partial derivatives of the entire integral.

§ 3. *The Derivatives of a Line Integral having Variable Upper Limit.*

Instead of (1), we now have

$$J = \int_{x_0 y_0}^{\xi, n} M\,dx + N\,dy, \quad . \quad . \quad . \quad . \quad . \quad (18)$$

where ξ and η replace the constants (a, b) of (4):

$$\xi = x_0 + \sum_{i=1}^{n} \Delta x_i; \quad \eta = y_0 + \sum_{i=1}^{n} \Delta y_i. \quad . \quad . \quad (19)$$

With (ξ, η) a variable point, (19) impose no restriction on the Δx's and Δy's which hence constitute n pairs of independent variables and formulæ (6) arising from the dependent Δx_k will drop out. Using (2) again the Δ process is exactly the same as for section one, except for the absence of the last three terms of (9) and (10) due

Fig. 2.

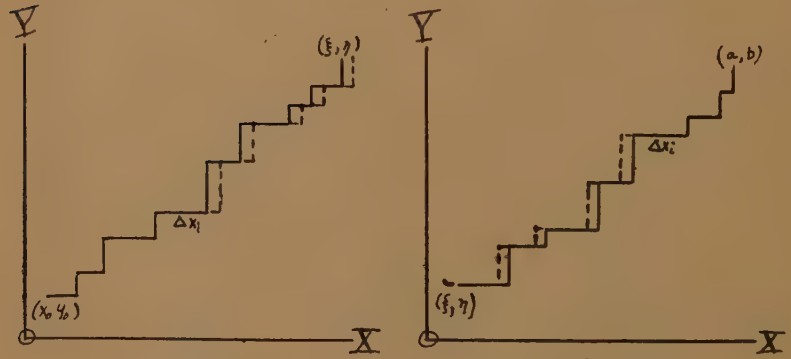

The path of the sum (2) showing the *shift* of path due to $d\,\Delta x_i$ and extending from x_i to the variable limit as a parallel displacement of the path.

to the now absent dependent variable Δx_k. Hence instead of (10) we have

$$\left.\begin{aligned} \frac{\partial F}{\partial x_i} = \frac{\partial F}{\partial \Delta x_i} &= M(x_i, y_i) + \sum_{j=i}^{n} M_{x_j} \Delta x_j + N_{x_j} \Delta y_j \,, \\ \frac{\partial F}{\partial y_i} = \frac{\partial F}{\partial \Delta y_i} &= N(x_i, y_i) + \sum_{j=i}^{n} M_{y_j} \Delta x_j + N_{y_j} \Delta y_j \,, \end{aligned}\right\} . \quad (22)$$

where the left members are introduced with the help of (7), which still applies here as shown by fig. 2 *a*.

The summation terms range between i and n as before, since (5) still applies when (18) is under consideration as the limit of (2).

As the norms of the Δx and Δy partitions indicated

by fig. 2 *a* approach zero, (2) approaches the limit (1) and (22) approaches the limit :

$$\left.\begin{aligned}\frac{\partial \mathrm{J}_i^n}{\partial x_i} &= \mathrm{M}(x_i y_i) + \int_{x_i y_i}^{\xi,\eta} \mathrm{M}_x\,dx + \mathrm{N}_x\,dy\,,\\ \frac{\partial \mathrm{J}_i^n}{dy_i^i} &= \mathrm{N}(x_i y_i) + \int_{x_i y_i}^{\xi,\eta} \mathrm{M}_y\,dx + \mathrm{N}_y\,dy.\end{aligned}\right\} \quad . \quad . \quad (23)$$

A special case of (23) occurs when we differentiate (18) with respect to the upper limit. Then $(x_i y_i) = (\xi, \eta) = (xy)$ is the only pair of variables involved, and so we drop the subscripts and the integral terms of (23) drop out,

$$\left.\begin{aligned}\frac{\partial \mathrm{J}}{\partial x} &= \mathrm{M}(x, y)\,,\\ \frac{\partial \mathrm{J}}{\partial y} &= \mathrm{N}(x, y),\end{aligned}\right\} \quad . \quad . \quad . \quad . \quad . \quad . \quad (24)$$

which are the familiar formulæ for the derivatives of an integral with respect to its variable upper limit. Note the contrast between (23) and (24). The former gives the rates of change of a definite integral taken over the indicated part of the path subjected to parallel displacement and marked by the dotted line variation of fig. 2 *a*, whereas (24) gives mere differentiation of an anti-derivative and the displacements concerned occur for this case all at the upper limit $(\xi, \eta) = (x, y)$.

§ 4. *The Derivatives of a Line Integral having Variable Lower Limits.*

Instead of (1) or (18), we now have

$$\mathrm{J} = \int_{\xi,\eta}^{a,b} \mathrm{M}\,dx + \mathrm{N}\,dy, \quad . \quad . \quad . \quad . \quad (25)$$

where the variable point (ξ, η) replaces (x_0, y_0) in (3) and (4).

$$x_i = \xi + \sum_{j=1}^{i} \Delta x_j\,; \quad y_i = \eta + \sum_{=1}^{i} \Delta y_j. \quad . \quad . \quad (26)$$

$$a = \xi + \sum_{j=1}^{n} \Delta x_j\,; \quad b = \eta + \sum_{j=1}^{n} \Delta y_j. \quad . \quad . \quad (27)$$

Note that the variable (ξ, η) replacing (x_0, y_0) will do so in *both* (3) and (4) to give (26) and (27) in contrast to (19), where (ξ, η) replaced the constants (a, b) in (4) and

left (3) unchanged. Eqs. (26) and (27), however, are equivalent to a single pair obtained by eliminating ξ and η between them :

$$a=x_i+\sum_{j=i+1}^{n}\Delta x_j\,;\quad b=y_i+\sum_{j=i+1}^{n}\Delta y_j,\quad .\quad .\quad (28)$$

and hence, instead of (5), we now have

$$\frac{\partial x_j}{\partial \Delta x_i}=-1 \text{ or } 0,\quad .\quad .\quad .\quad .\quad .\quad .\quad (29)$$

according as j is less than i or otherwise.

As with (19) eqs. (28) impose no restriction on the now independent variables Δx and Δy, so that when we apply the Δ process using (2), there are no last three terms like those of (9) and (10) due to the dependent variable Δx_k. Hence using (8), which evidently applies here (it is a special case of (29) ; also see fig. 2 *b*),

$$\left.\begin{aligned}-\frac{\partial F}{\partial x_{i-1}}=\frac{\partial F}{\partial \Delta x_i}&=M(x_iy_i)-\sum_{j=1}^{i}(M_{x_j}\Delta x_j+N_{x_j}\Delta y_j),\\ -\frac{\partial F}{\partial y_{i-1}}=\frac{\partial F}{\partial \Delta y_i}&=N(x_iy_i)-\sum_{j=1}^{i}(M_{y_j}\Delta x_j+N_{y_j}\Delta y_j).\end{aligned}\right\}\quad (30)$$

The summation terms are negative and range from 1 to i because of (29), which replaces (5) as applied to the case in hand (see fig. 2 *b*). As the norms of the Δx and Δy partitions approach zero $x_{i-1}=x_i-\Delta x_i$ approaches x_i, and likewise with the y's. Hence (30) become

$$\left.\begin{aligned}\frac{\partial J_0^i}{\partial x_i}&=\int_{\xi,\,\eta}^{x_iy_i}M_x\,dx+N_x\,dy-M(x_iy_i),\\ \frac{\partial J_0^i}{\partial y_i}&=\int_{\xi,\,\eta}^{x_iy_i}M_y\,dx+N_y\,dy-N(x_iy_i).\end{aligned}\right\}\quad .\quad .\quad (31)$$

A special case of (31) occurs when we differentiate with respect to the lower limit, *i. e.*, take $(x_iy_i)=(\xi,\,\eta)$. Then the integral term vanishes and we have the familiar formulæ, dropping the subscripts,

$$\left.\begin{aligned}\frac{\partial J}{\partial x}&=-M(x,\,y),\\ \frac{\partial J}{\partial y}&=-N(x,\,y).\end{aligned}\right\}\quad .\quad .\quad .\quad .\quad (32)$$

Like the contrast between (24) and (23), (32) is differentiation of an anti-derivative where the displacements concerned occur at the *lower* variable end *only* of the broken line path shown in fig. 2*b*. On the other hand, (31) is the rate of change of a line integral between the limits $(x_i y_i)$ and (ξ, η) shown in the figure.

It is illuminating to compare (23) with (31) in the light of fig. 2. Note that the rate of change of the one is minus the rate of change of the other (for the same integration interval) and that this is due to the fact that the *lower* limit of (18) is fixed, whereas it is the *upper* limit of (25) that is the fixed one.

§ 5. *Theorem I.—When the path of* (1) *has fixed limits* (x_0, y_0) *and* (a, b), *the derivatives* (13) *and* (14) *of that part of the line integral* (1) *between* (x_i, y_i) *and* (x_k, y_k) *on its path are the same whether the independent variables are taken at the upper end, the lower end, or anywhere on the path between these limits* (x_i, y_i) *and* (x_k, y_k).

Consider (14), the derivative of that part of (1) between (x_i, y_i) and (x_k, y_k), where the dependent variables (x_k, y_k) are smaller than $(x_i y_i)$ as shown in fig. 1 *b*. We may use different notation in (14), letting $(x_k y_k)$ stand for the independent variables and $(x_i y_i)$ for the dependent ones instead of *vice versa*. When we make these replacements (14) becomes

$$\left.\begin{aligned} \frac{\partial \mathrm{J}_i^k}{\partial x_k} &= \mathrm{M}(x_i y_i) + \int_{x_i y_i}^{x_k y_k} (\mathrm{M}_x\, dx + \mathrm{N}_x\, dy) - \mathrm{M}(x_k, y_k), \\ \frac{\partial \mathrm{J}_i^k}{\partial y_k} &= \mathrm{N}(x_i y_i) + \int_{x_i y_i}^{x_k y_k} (\mathrm{M}_y\, dx + \mathrm{N}_y\, dy) - \mathrm{N}(x_k, y_k). \end{aligned}\right\} \quad (33)$$

Eqs. (33), however, are identical in their right members with (13), even though they are derivatives with respect to the variables at the upper limit $(x_k y_k)$. Thus, comparison of (13) and (33) shows that the derivatives of J_i^k are the same, whether they be taken with respect to the variables at the upper limit $(x_k y_k)$ or the lower limit $(x_i y_i)$.

Suppose we differentiate with respect to x_j and y_j at some point on the path between these interval limits. For the part of the rate of change between $(x_j y_j)$ and the upper limit $(x_k y_k)$ we substitute $(x_j y_j)$ for $(x_i y_i)$ in (13)

because we are differentiating with respect to variables of lower index $j<k$. Thus

$$\left.\begin{aligned}\frac{\partial \mathrm{J}_j^k}{\partial x_j} &= \mathrm{M}(x_j y_j) + \int_{x_j y_j}^{x_k y_k} \mathrm{M}_x\, dx + \mathrm{N}_x\, dy - \mathrm{M}(x_k y_k),\\ \frac{\partial \mathrm{J}_k}{\partial y_j} &= \mathrm{N}(x_j y_j) + \int_{x_j y_j}^{x_k y_k} \mathrm{M}_y\, dx + \mathrm{N}_y\, dy - \mathrm{N}(x_k y_k).\end{aligned}\right\} \quad (34)$$

For the part between $(x_i y_i)$ and $(x_j y_j)$ we substitute $(x_j y_j)$ for $(x_k y_k)$ in (33), since we are differentiating with

Fig. 3.

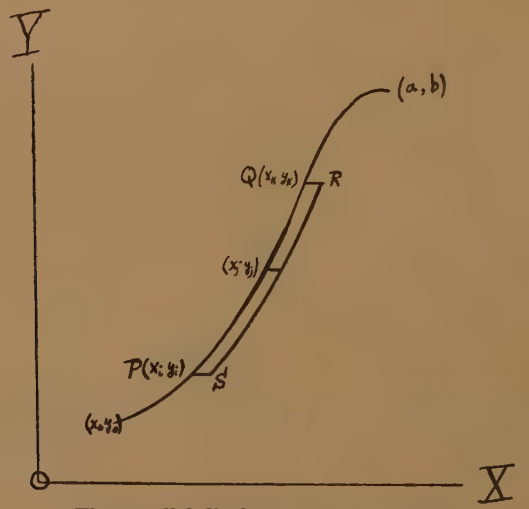

The parallel displacement of the path.

respect to the variables at the *upper* limit $(x_j y_j)$ of the lower part of the path interval shown in fig. 3.

$$\left.\begin{aligned}\frac{\partial \mathrm{J}_i^j}{\partial x_j} &= \mathrm{M}(x_i y_i) + \int_{x_i y_i}^{x_j y_j} \mathrm{M}_x\, dx + \mathrm{N}_x\, dy - \mathrm{M}(x_j y_j),\\ \frac{\partial \mathrm{J}_i^j}{\partial y_j} &= \mathrm{N}(x_i y_i) + \int_{x_i y_i}^{x_j y_j} \mathrm{M}_y\, dx + \mathrm{N}_y\, dy - \mathrm{N}(x_j y_j).\end{aligned}\right\} \quad (35)$$

If we add (34) and (35) we have

$$\left.\begin{aligned}\frac{\partial \mathrm{J}_i^k}{\partial x_j} &= \frac{\partial(\mathrm{J}_i^j + \mathrm{J}_j^k)}{\partial x_j} = \mathrm{M}(x_i y_i) + \int_{x_i y_i}^{x_k y_k} \mathrm{M}_x\, dx + \mathrm{N}_x\, dy - \mathrm{M}(x_k y_k),\\ \frac{\partial \mathrm{J}_i^k}{\partial y_j} &= \frac{\partial}{\partial y_j}(\mathrm{J}_i^j + \mathrm{J}_j^k) = \mathrm{N}(x_i y_i) + \int_{x_i y_i}^{x_k y_k} \mathrm{M}_y\, dx + \mathrm{N}\ dy - \mathrm{N}(x_k y_k)\end{aligned}\right\} \quad . \quad . \quad . \quad (36)$$

The right members of (36), (13), and (33) are identical. Hence, the derivatives of a part : J_i^k of (1) along that part of the path between the limits (x_iy_i) and (x_Ky_k) are the same if taken with respect to any (x_jy_j) en route *between* the limits as they are when taken with respect to the variables at the limits as given by (13) and (33).

Examination of figs. 1, 2, and 3 shows why these derivatives are the same, *i. e.*, every Δx and x along the interval has the same increment, and also each and all are associated with the same increment for the dependent variable J_i^k over the stretch between these limits.

Since (x_jy_j) is a general point on the integration path of (1) between (x_iy_i) and (x_ky_k) we may indicate its generality by dropping its subscripts :

$$\left.\begin{aligned}\frac{\partial}{\partial x}(J_i^k)&=M(x_iy_i)+\int_{x_iy_i}^{x_ky_k} M_x\,dx+N_y\,dy-M(x_ky_k),\\ \frac{\partial}{\partial y}(J_i^k)&=N(x_iy_i)+\int_{x_iy_i}^{x_ky_k} M_y\,dx+N_y\,dy-N(x_ky_k).\end{aligned}\right\}\quad(37)$$

Eqs. (13) to (16) are evidently special cases of (37), where the derivatives of the indicated part of (1) are taken with respect to variables at one of the ends of the part of the integration path under consideration. And (17) is the special case of (37) where differentiation is of the entire integral (1).

Likewise in case of the line integrals (18) and (25) having a variable limit, the derivatives (23) and (31) are the same as if taken with respect to any (x, y) between the limiting points of the indicated part of the integral :

$$\left.\begin{aligned}\frac{\partial}{\partial x}J_i^\eta&=M(x_iy_i)+\int_{x_iy_i}^{\xi,\eta} M_x\,dx+N_x\,dy,\\ \frac{\partial}{\partial y}J_i^\eta&=N(x_iy_i)+\int_{x_iy_i}^{\xi,\eta} M_y\,dx+N_y\,dy.\end{aligned}\right\}\quad(38)$$

$$\left.\begin{aligned}\frac{\partial}{\partial x}J_0^i&=\int_{\xi,\eta}^{x_iy_i} M_x\,dx+N_x\,dy-M(x_iy_i)\,;\\ \frac{\partial}{\partial y}J_0^i&=\int_{\xi,\eta}^{x_iy_i} M_y\,dx+N_y\,dy-N(x_iy_i).\end{aligned}\right\}\quad(39)$$

These formulæ may be derived like (37) by choosing as $(xy)=(x_jy_j)$ any point on the path between (x_iy_i)

and (ξ, η). Then for the part of (18) or (25) included between $(x_j y_j)$ and $(x_i y_i)$ formulæ (34) or (35) apply; and for the other part, we have formulæ like (23) and (31) which, when added to the derivatives of the first part of the integral, give (38) and (39).

§ 6. *The Degenerate Case.*

The definite integral for a single variable of integration is the degenerate case of (1) that occurs when the y's are absent:

$$J = \int_{x_0}^{a} M(x)\,dx. \quad . \quad . \quad . \quad . \quad . \quad (40)$$

When (37) is applied to (40) we have

$$\frac{\partial J}{\partial x} = M(x_i) + \int_{x_i}^{x_k} M_x\,dx - M(x_k) \equiv 0. \quad . \quad . \quad (41)$$

This result, identically zero for the rate of change of any part of a definite integral, is a check on the validity of (37) as applied to this degenerate case.

When one of the limits of integration is variable, we have

$$J = \int_{x_0}^{\xi} M(x)\,dx; \quad \text{or} \quad J = \int_{\xi}^{a} M(x)\,dx, \quad . \quad . \quad (42)$$

whose derivatives given by (38) and (39) respectively, are:

$$\frac{\partial J_i^n}{\partial x} = M(x_i) + \int_{x_i}^{\xi} M_x\,dx \equiv M(\xi). \quad . \quad . \quad . \quad (43)$$

$$\frac{\partial J_0^i}{\partial x} = \int_{\xi}^{x_i} M_x\,dx - M(x_i) \equiv -M(\xi). \quad . \quad . \quad (44)$$

Note that these derivatives are each equal to the integrand with suitable sign at the variable limit, even though differentiation is taken with respect to any x included between the integration limits. This contrasts with (38) and (39), but affords a check on their validity by confirming the elementary theory involved in the degenerate cases here considered.

Part II.

Differentiation by Parallel Displacement of the Path of a Line Integral after *passing to the Limit as in Integration.*

§ 7. *The increment ΔJ_i^k of a line integral may be taken as a closed circuit integral expressible as the surface integral of the curl of the vector integrand, and obtained by parallel path displacements.*

In Part II. we develop a geometrical method of differentiation by parallel path displacements. The guide and objective of the procedure have been to obtain results that check the formulæ of Part I. We shall see that this object has been attained by a most simple and elegant geometrical method, and with results immediately applicable to the Calculus of Variations.

We consider a line integral (1) and let the part of its path $y=\phi(x)$ between (x_iy_i) and (x_k, y_k) be displaced parallel to the x axis and y axis by amounts h and k respectively. Then the line integral around this resulting closed circuit PSRQ is given by

$$\int_{x_iy_i}^{x_i+h,\ y_i+k} \mathrm{M}\delta x+\mathrm{N}\,\delta y+\int_{x_iy_i}^{x_ky_k} \mathrm{M}(x'+h,\ y'+k)\,dx'$$

$$+\mathrm{N}(x'+h,\ y'+k)\,dy'-\int_{x_ky_k}^{x_k+h,\ y_k+k} \mathrm{M}\delta x+\mathrm{N}\delta y$$

$$-\int_{x_iy_i}^{x_ky_k} \mathrm{M}\,dx'+\mathrm{N}\,dy'$$

$$\equiv\int_{x_iy_i}^{x_ky_k}\int_{x',\,y'}^{x'+h,\ y'+k} (\mathrm{N}_x-\mathrm{M}_y)(\delta x\,dy'-\delta y\,dx')=\Delta \mathrm{J}_i^k. \quad . \ . \ . \quad (45)$$

Here the primes are used for the special values of x and y subject to the relation $y=\phi(x)$ and thus refer to points $(x'y')$ on this original undisplaced path from $\mathrm{P}(x_iy_i)$ to $\mathrm{Q}(x_ky_k)$, whereas x and y are unrelated independent variables since h and k are arbitrary.

Here the right member is the surface integral of the curl of the vector integrand $\mathrm{R}=i\mathrm{M}+j\mathrm{N}$, according to Stokes's Theorem. The differential area $d\sigma=\delta x\,dy-\delta y\,dx$ is shown as one of the infinitesimal parallelogram areas in the shaded strip shown in fig. 4. Note that $dx=dx'$

and $dy=dy'$ always refer to displacements along or parallel to the original integration path $y=\phi(x)$ satisfied by $(x'y')$ while the point (x, y) is free to take any new position, indicating x and y as *independent* variables related to $x'y'$ by the arbitrary addition of h and k. The four integrals of the left member are taken along the four parts of the closed circuit : PS, SR, RQ, and QP in the order named. The path of integration for the fourth and second integrals is $y=\phi(x)$ and $y=\phi(x-h)+k$ respectively, being the

Fig. 4.

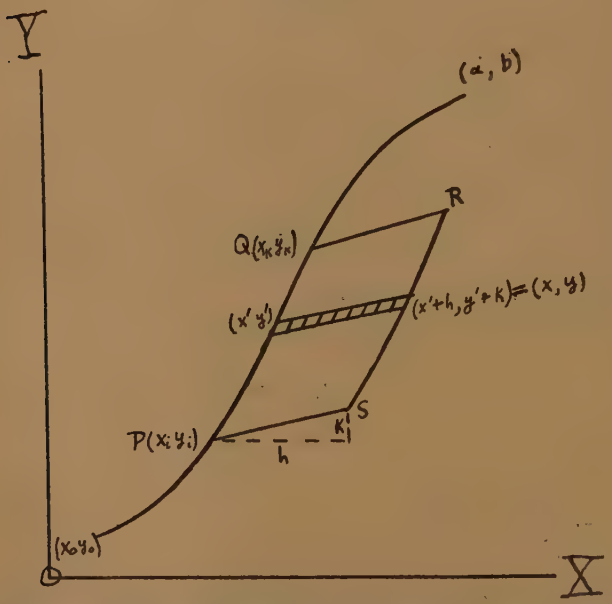

The closed circuit path PQRS of the increment (45) due to parallel path displacements h and k.

original and displaced paths, the former being satisfied by $(xy)=(x'y')$ and the latter by $(x, y)=(x'+h, y'+k)$. For the first and third integrals we have the rectilinear paths

$$\left.\begin{aligned} y-y_i&=\frac{k}{h}(x-x_i)=\frac{\delta y}{\delta x}(x-x_i),\\ y-y_k&=\frac{k}{h}(x-x_k)=\frac{\delta y}{\delta x}(x-x_k),\end{aligned}\right\} \quad . \quad . \quad . \quad (46)$$

in which we note the constant slope

$$\frac{\delta y}{\delta x} = \frac{k}{h}.$$

We take (45) as the increment of the line integral (1) between the points (x_i, y_i) and (x_k, y_k) on its path as indicated by the expression on the right. This identity (45) may, of course, be checked by taking the partial derivatives with respect to h or k and then removing the integral signs by total differentiation along the path $y=\phi(x)$ taking either the upper or lower limit as variable. This procedure reduces both members of (45) to the integrand of the right member :

$$\mathrm{N}_x(x'+h,\ y'+k)-\mathrm{M}_y(x'+h,\ y'+k)=\mathrm{N}_x(x,\ y)-\mathrm{M}_y(x,\ y).$$

Or we may first differentiate along the path $y=\phi(x)$, taking, say, $(x_k y_k)$ as the variable point, with $(x_i y_i)$ and h and k constant. Then the derivatives of the second and fourth integrals are exactly cancelled by the derivatives of the third integral with respect to its upper and lower limits respectively. The integrand, also of the third integral, however, depends on $(x_k y_k)$ being taken along the path given by the second of (46). Thus the derivative in question with respect to y_k is given by

$$\frac{d}{dy_k}\,\Delta \mathrm{J}_i^k = \Big[-\int_{x_k y_k}^{x_k+h,\ y_k+k} \frac{d}{dy_k}\Big(\mathrm{M}(x,\ y_k+\frac{k}{h}(x-x_k))\delta x + \frac{d}{dy_k}\,\mathrm{N}(x_k+\frac{h}{k}(y-y_k),\ y)\Big)\delta y \Big]_{(x_k y_k)=(x'y')}$$

$$\equiv \int_{x'y'}^{x'+h,\ y'+k} (\mathrm{N}_x-\mathrm{M}_y)\,\frac{\delta x\,dy-\delta y\,dx}{dy}. \quad . \quad . \quad . \quad (47)$$

The bracket reduces identically to the right member when the indicated operations are carried out using

$$\frac{k}{h}=\frac{\delta y}{\delta x} \quad \text{and} \quad \frac{dx_k}{dy_k}=\frac{dx}{dy}=\frac{dx'}{dy'}.$$

§8. *The line integral* $\mathrm{J}_i^k\ (h,\ k)=(\mathrm{J}+\Delta \mathrm{J})_i^k$ *may ordinarily be expanded in powers of its parallel displacements.*

If we assume differentiability of (45) with respect to h and k and convergence of its Maclaurin expansion, the integral (1) as given by (48) along the varied path in three

sections from P to S, from S to R, and R to Q as shown in fig. 4, may also be so expanded :

$$\mathrm{J}_i^k(h,\,k)=(\mathrm{J}+\Delta\mathrm{J})_i^k=\int_{x_iy_i}^{x_i+h,\,y_i+k}\mathrm{M}\delta x+\mathrm{N}\delta y$$

$$+\int_{x_iy_i}^{x_ky_k}\mathrm{M}(x'+h,\,y'+k)\,dx'+\mathrm{N}(x'+h,\,y'+k)\,dy'$$

$$-\int_{x_ky_k}^{x_k+h,\,y_k+k}\mathrm{M}\delta x+\mathrm{N}\delta y. \quad . \quad . \quad . \quad . \quad . \quad . \quad (48)$$

The derivatives of (48) at $h=k=0$ are readily found :

$$\left.\begin{aligned}
\frac{\partial \mathrm{J}_i^k}{\partial h}(0,\,0)&=\mathrm{M}(x_iy_i)+\int_{x_iy_i}^{x_ky_k}\mathrm{M}_x\,dx+\mathrm{N}_x\,dy-\mathrm{M}(x_ky_k)\\
&\equiv\int_{y_i}^{y_k}(\mathrm{N}_x-\mathrm{M}_y)\,dy=\frac{\partial \mathrm{J}_i^k}{\partial x},\\
\frac{\partial \mathrm{J}_i^k}{\partial k}(0,\,0)&=\mathrm{N}(x_iy_i)+\int_{x_iy_i}^{x_ky_k}\mathrm{M}_y\,dx+\mathrm{N}_y\,dy-\mathrm{N}(x_ky_k)\\
&\equiv\int_{x_i}^{x_k}(\mathrm{M}_y-\mathrm{N}_x)\,dx=\frac{\partial \mathrm{J}_i^k}{\partial y},\\
\frac{\partial^2 \mathrm{J}_i^k}{\partial h^2}(0,\,0)&=\mathrm{M}_x(x_iy_i)+\int_{x_iy_i}^{x_ky_k}\mathrm{M}_{xx}\,dx+\mathrm{N}_{xx}\,dy-\mathrm{M}_x(x_ky_k)\\
&\equiv\int_{y_i}^{y_k}(\mathrm{N}_{xx}-\mathrm{M}_{xy})\,dy=\frac{\partial^2 \mathrm{J}_i^k}{\partial x^2},\\
\frac{\partial}{\partial k}\frac{\partial \mathrm{J}_i^k}{\partial h}(0,\,0)&=\mathrm{M}_y(x_iy_i)+\int_{x_iy_i}^{x_ky_k}\mathrm{M}_{xy}\,dx+\mathrm{N}_{xy}\,dy-\mathrm{M}_y(x_ky_k)\\
&\equiv\int_{y_i}^{y_k}(\mathrm{N}_{xy}-\mathrm{M}_{yy})\,dy=\frac{\partial^2 \mathrm{J}_i^k}{\partial y\,\partial x},\\
\frac{\partial}{\partial h}\frac{\partial \mathrm{J}_i^k}{\partial k}(0,\,0)&=\mathrm{N}_x(x_iy_i)+\int_{x_iy_i}^{x_ky_k}\mathrm{M}_{xy}\,dx+\mathrm{N}_{xy}\,dy-\mathrm{N}_x(x_ky_k)\\
&\equiv\int_{x_i}^{x_k}(\mathrm{M}_{xy}-\mathrm{N}_{xx})\,dx=\frac{\partial^2 \mathrm{J}_i^k}{\partial x\,\partial y},\\
\frac{\partial^2 \mathrm{J}_i^k}{\partial k^2}(0,\,0)&=\mathrm{N}_y(x_iy_i)+\int_{x_iy_i}^{x_ky_k}\mathrm{M}_{yy}\,dx+\mathrm{N}_{yy}\,dy-\mathrm{N}_y(x_ky_k)\\
&\equiv\int_{x_i}^{x_k}(\mathrm{M}_{yy}-\mathrm{N}_{xy})\,dx=\frac{\partial^2 \mathrm{J}_i^k}{\partial y^2}.
\end{aligned}\right\}$$

. . . (49)

Here we have dropped the superfluous primes from dx' and dy', etc., which refer to the variables of integration of definite integrals.

Eqs. (49) are shown on the right also as surface * integrals of the curls of

$$R = iM + jN, \quad \text{or} \quad R_x = iM_x + jN_x, \quad \text{or} \quad R_y = iM_y + jN_y,$$

being identical with the left members, as is readily shown by taking the total derivative with respect to one of the limits along the path so as to remove the integral signs. These surface integrals are also obtainable by differentiating the right member of (45) and setting $h=k=0$. On the extreme right, (49) are shown as the partials with respect to the coordinates of any point (x, y) which here becomes $(x'y')$ (since $h=k=0$) and the point is hence located on the path of integration $y=\phi(x)$, as proved below in §§ 10 and 11.

With the help of (49) we may expand (48) in powers of h and k, the constant parallel displacements, which may be put under the integral signs :

$$J_i^k(h, k) = \int_{x_i y_i}^{x_k y_k} M\,dx + N\,dy + \int_{x_i y_i}^{x_k y_k} (N_x - M_y)(h\,dy - k\,dx)$$
$$+ \frac{h}{2}\int_{x_i y_i}^{x_k y_k} (N_{xx} - M_{xy})(h\,dy - k\,dx)$$
$$+ \frac{k}{2}\int_{x_i y_i}^{x_k y_k} (N_{xy} - M_{yy})(h\,dy - k\,dx) + \ldots . \qquad (50)$$

Likewise (48) may be expanded in powers of h and k using the *middle members* of (49).

Suppose for brevity we take $k=0$, so that the parallel displacement is entirely in the x-direction. Then the expansion of (48), using these middle members of (49) becomes

$$J_i^k(h, 0) = h\left[\, M(x_i y_i) + \frac{h}{2}(M_x(x_i y_i) + \ldots \,\right]$$
$$+ \int_{x_i y_i}^{x_k y_k} \left(M + hM_x + \frac{h^2}{2}M_{xx} + \ldots\right) dx$$

* For surfaces of unit width in the x or y directions taking $\delta x = 1$ or $\delta y = 1$. Since δx and δy are constants for the integration along $y=\phi(x)$, they may be removed from under the integral sign and set equal to unity, as explained in sections 13 and 14 below. See (59) and fig. 6.

$$+\left(\mathrm{N}+h\mathrm{N}_x+\frac{h^2}{2}\mathrm{N}_{xx}+\dots\right)dy$$

$$-h\left[\mathrm{M}(x_k y_k)+\frac{h}{2}\mathrm{M}_x(x_k y_k)+\dots\right], \quad . \quad . \quad . \quad (51)$$

which is identical according to (49) with (50) when $k=0$. The three integrals (48) are shown as the three expansions of (51) and in the same order.

§ 9. *Assuming an integration path* $y=\phi(x)$ *with limit points on it* $(x_i y_i)$ *and* $(x_k y_k)$, *the line integral* $\mathrm{J}_i^k\ (h,\ k)$, *given by* (48) *and obtained by parallel displacement is a function* (a) *of the parallel displacements* h *and* k ; *or* (b) *a two-point function determined by* $(x'\ y')$ *on* $y=\phi(x)$ *and a second related point* $(xy)=(x'+h,\ y'+k)$ *on the displaced path* $y-\phi(x-h)+k$.

The integral (48), being the integral (1) taken along the three section path from P to S, from S to R, and from R to Q, is evidently uniquely determined by the three paths $y=\phi(x-h)+k$ and the two lines (46). And these in turn are determined by h and k, once $y=\phi(x)$ with its limit points $(x_i y_i)$ and $(x_k y_k)$ are given. Hence we note that this line integral is a *function* of its parallel displacements h and k in the sense of being determined by them in the premises ($y=\phi(x)$ with its limits being given).

Again we note that two end points $(x'y')$ and $(x,\ y)$ are sufficient to determine a connecting straight vector such as the rectilinear displacements shown in fig. 4. We may choose any point $(x',\ y')$ on the path and its displaced position $(xy)=(x'+h,\ y'+k)$ on the displaced path as the two points whose choice determines h and k, and hence the line integral in question. Hence our line integral is a *two-point* function as well as a function of h and k, the two points being $(x',\ y')$ on $y=\phi(x)$ and $(xy)=(x'+h,\ y'+k)$ on the displaced path $y=\phi(x-h)+k$.

These two points, such as those in fig. 4, are sufficient to determine our line integral uniquely.

Hence (48) may be written $\mathrm{J}_i^k\ (h,\ k)=\mathrm{J}_i^k\ (x-x',\ y-y')$.

Although (48) is a line function, *i. e.*, a function of the path of integration $y=\phi(x)$, yet we thus see that, once this is chosen with its limits, (48) becomes a variable dependent on $(x',\ y')$, any point on this path and on (x,y), its displaced position under parallel path displacements $h=x-x'$, $k=y-y'$, as shown in fig. 4.

§ 10. *The two-point function* (48) $\mathrm{J}_i^k(x-x', y-y') = \mathrm{J}_i^k(h, k)$ *of any point* $(x'y')$ *on* $y=\phi(x)$ *and* (x, y) *on the displaced path, has ordinarily unique partial derivatives with respect to the independent variables* x *and* y.

Since $x=x'+h$ and $y=y'+k$, we have for a given fixed (x', y') on a fixed $y'=\phi(x')$, $\delta x=\delta h$ and $\delta_y=\delta_k$ where the usual Greek symbols indicate that the changes in x and y measure the path variations δh and δk as parallel displacements according to the method herein. Hence the partial derivatives of (48) with respect to x and y are the same as the partials with respect to h and k respectively :

$$\left.\begin{aligned}
\frac{\partial \mathrm{J}_i^k}{\partial h}(h, k) &= \frac{\partial \mathrm{J}_i^k}{\partial x}(x-x', y-y') \\
&= \mathrm{M}(x_i+h, y_i+k) + \int_{x_iy_i}^{x_ky_k} \mathrm{M}_x(x'+h, y'+k)\,dx' \\
&\quad + \mathrm{N}_x(x'+h, y'+k)\,dy' - \mathrm{M}(x_k+h, y_k+k), \\
\frac{\partial \mathrm{J}_i^k}{\partial k}(h, k) &= \frac{\partial \mathrm{J}_i^k}{\partial y}(x-x', y-y') \\
&= \mathrm{N}(x_i+h, y_i+k) + \int_{x_iy_i}^{x_ky_k} \mathrm{M}_y(x'+h, y'+k)\,dx' \\
&\quad + \mathrm{N}_y(x'+h, y'+k)\,dy' - \mathrm{N}(x_k+h, y_k+k).
\end{aligned}\right\} \quad (52)$$

These are the same as the first two of (49) except that we have not yet set h and k equal to zero. Apart from the path of integration $y=\phi(x)$ and the limit points (x_iy_i) and (x_ky_k) on it, (52) are uniquely determined by h and k, according to the indicated functional dependence. Also (52) are each two-point functions of (xy) independent variables and (x', y') variables of integration related by $y'=\phi(x')$ the equation of the original path of integration. Thus we see that the derivatives (52) of (48) are also *two-point* functions in precisely the same way that the line integral (48) itself is, *i. e.*, because it takes two end points $(x'y')$ and (xy) to determine the vectors which measure our parallel displacements h and k.

When we set $(x, y)=(x'y')$, h and k become zero and (52) reduces to the first two of (49), which are hence proved to be the partials of J_i^k with respect to x and y at the particular place $(x'y')$ on the original path of

integration $y=\phi(x)$. Just as the line integral (48) is independent of $(x'y')$, variables of integration of a definite integral, so its derivatives (52) are independent of $(x'y')$ and so we note that (52) has the same value, no matter where $(x'y')$ is chosen along the path of integration $y=\phi(x)$, provided only $h=x-x'$ and $k=y-y'$ remain the same.

Likewise with the first two of (49) (as well as the higher derivatives). But (49) is special, in that for it $(xy)=(x'y')$ whereby $h=k=0$, and hence h and k, being zero, have to remain the same for changes in $(x'y')$ along the path of integration, so that the formulæ (49) appear as derivatives of J_i^k with respect to x and y and independent of where they are chosen along the path of integration. It is thus to be emphasized that the independent variables x and y appearing in the denominators of the differential quotients of (49) and (52) play a different rôle from the $(x'y')$ variables of integration of the definite integrals which latter are subject to the relation $y'=\phi(x')$, as shown by (52). The mere fact that we choose to emphasize (49) as the important special case of (52) need not obscure the fact that the (x, y) of the differential quotients of (49) are the independent variables for the indicated partial rates of change, and hence are not subject to $y=\phi(x)$ which restricts the variations of the variables of integration. In (49) we merely fix attention on what the rates of change (52) become at the places $(x'y')=(xy)$ on the path of integration.

The striking fact about (49) as compared with (52), however, lies in that (49) give the partial rates of change of a part J_i^k of any line integral (1), with respect to x and y at any position (x', y') on the path of integration ; and these derivatives, moreover, are uniquely determined by *precisely* the *same* quantities as the original line integral J_h^k itself, *i. e.*, they depend only on the path of integration $y=\phi(x)$, the limit points on that path (x_iy_i) and (x_ky_k) and the vector integrand $\mathrm{R}=i\mathrm{M}+j\mathrm{N}$ and its derivatives.

Since the first two of (49) are identical with (37) of Part I., they serve to give a geometrical interpretation of (37), obtained by differentiation with respect to differentials. The equivalence of (37) and (49) also shows that the limit process of integration is commutative with the limit process of differentiation as performed herein, since the order of application of these two limit processes

is reversed in (49) from what it was in (37). Hence any difficulty that might arise from the complications of the double limit is surmounted by the choice of method herein of differentiation of line integrals by parallel displacements.

§ 11. *The general rule for finding the derivatives of a line integral by parallel displacements.*

We noted above that (52), the derivatives of (48) with respect to x and y or h and k as well as (48) itself are two-point functions of the arbitrary point (x, y) and the point $(x'y')$ restricted to lie on the path of integration $y=\phi(x)$. Hence we may differentiate (52) with respect to x and y just as we differentiated (48), remembering that $(x'y')$ remains fixed on the original path of integration $y=\phi(x)$ during this process: and hence $\delta x=\delta h$ and $\delta y=\delta k$ and $h=x-x'$; $k=y-y'$.

$$\begin{aligned}
\frac{\partial^2 \mathrm{J}_i}{\partial h^2} &= \frac{\partial^2 \mathrm{J}_i^k}{\partial x^2}(x-x', y-y') \\
&= \mathrm{M}_x(x_i+h, y_i+k)+\int_{x_iy_i}^{x_ky_k} \mathrm{M}_{xx}(x'+h, y'+k)\,dx' \\
&\quad +\mathrm{N}_{xx}(x'+h, y'+k)\,dy'-\mathrm{M}_x(x_k+h, y_k+k), \\
\frac{\partial}{\partial k}\frac{\partial \mathrm{J}_i^k}{\partial h} &= \frac{\partial}{\partial y}\frac{\partial \mathrm{J}_i^k}{\partial x}(x-x', y=y') \\
&= \mathrm{M}_y(x_i+h, y_i+k)+\int_{x_iy_i}^{x_ky_k} \mathrm{M}_{xy}(x'+h, y'+k)\,dx' \\
&\quad +\mathrm{N}_{xy}(x'+h, y'+k)\,dy'-\mathrm{M}_y(x_k+h, y_k+k), \\
\frac{\partial}{\partial h}\frac{\partial \mathrm{J}_i^k}{\partial k} &= \frac{\partial}{\partial x}\frac{\partial \mathrm{J}_i^k}{\partial y}(x-x', y-y') \\
&= \mathrm{N}_x(x_i+h, y_i+k)+\int_{x_iy_i}^{x_ky_k} \mathrm{M}_{xy}(x'+h, y'+k)\,dx' \\
&\quad +\mathrm{N}_{xy}(x'+h, y'+k)\,dy'-\mathrm{N}_x(x_k+h, y_k+k), \\
\frac{\partial^2 \mathrm{J}_i^k}{\partial k^2} &= \frac{\partial^2 \mathrm{J}_i}{\partial y^2}(x-x', y-y') \\
&= \mathrm{N}_y(x_i+h, y_i+k)+\int_{x_iy_i}^{x_ky_k} \mathrm{M}_{yy}(x'+h, y'+k)\,dx' \\
&\quad +\mathrm{N}_{yy}(x'+h, y'+k)\,dy'-\mathrm{N}_y(x_k+h, y_k+k).
\end{aligned} \quad \ldots \quad (53)$$

When we set $(x, y)=(x', y')$ we have $h=k=0$, and eqs. (53) reduce to the last four of eqs. (49) which are thus proved to be the second partials of J_i^k as given by (53) with respect to x and y at the particular place where $(x, y)=(x'y')$, *i. e.*, for positions on the path of integration $y=\phi(x)$. Thus all of eqs. (49) are shown to be special cases of (52) and (53) and their importance lies in that they represent *rates of change* of J_i^k, the part of the line integral (1) between the limits along the path in question, and, moreover, give these rates of change in terms of *precisely* the *same quantities* that determine the original integral, *i. e.*, the path $y=\phi(x)$, its limit points (x_iy_i), (x_ky_k) and the vector integrand $R=iM+jN$ with its derivatives.

As with the first two of (49), it is to be emphasized with the last four derivatives, that the variations δx and δy of the *independent* variables x and y of the differential quotients are *not* subject to $y=\phi(x)$ that restricts the variables of integration $(x'y')$ and $dy'=\phi' dx'$ of the definite integrals between the limits (x_iy_i) and (x_ky_k), but play a different rôle from these latter just as the x and y of (53) do not function in the same way as the x' and y' that are restricted by $dy'=\phi' dx'$, a distinction that is not to be obscured by our exercised right to dwell on the special case of (53) given by (49) where (xy) refers to the same localities as $(x'y')$.

Higher derivatives than the second partials of (1) are evidently obtainable by the same procedure as used in obtaining (49), *i, e.*, by successive differentiation of (48) with respect to h and k and then setting these parallel displacements equal to zero. Thus we have :—

The General Rule.—The partial derivatives (49) or of higher order, of a line integral (1) with respect to the *independent* variables x and y, taken on its path of integration, are given by the corresponding partials at $h=k=0$, with respect to h and k, respectively, of the integral (48) $J_i^k(h, k)$, being the part of (1) between the original limits (x_iy_i) and (x_ky_k), but along the three section path PSRQ obtained by parallel displacements h and k as shown in fig. 4, instead of along the original $y=\phi(x)$.

§ 12. *Derivatives of Line Integrals with Variable Limits.*

We consider the line integral (18) with variable upper limit point (ξ, η) and subject its path to parallel displace-

ments h and k as shown by fig. 5, and instead of (48) obtain:

$$J_i^n(h, k) = (J + \Delta J)_i^n = \int_{x_i y_i}^{x_i+h,\, y_i+k} M\delta x + N\delta y$$

$$+ \int_{x_i y_i}^{\xi,\, \eta} M(x'+h, y'+k)\, dx' + N(x'+h, y'+k)\, dy'. \quad (56)$$

Fig. 5.

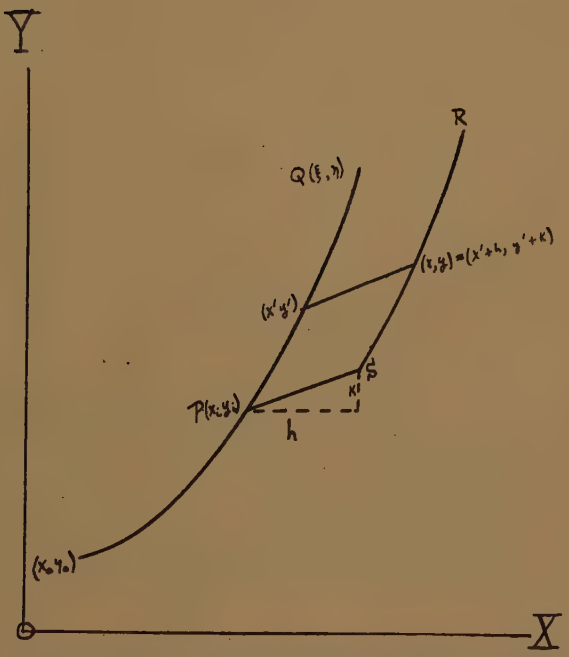

The path PSR of the displaced integral (56) with variable upper limit.

The third integral in (48) is absent from (56) because the variable limit Q is shifted to R along with the displaced path, and hence no back track integral from R to Q is present. We obtain the derivatives (38) as well as higher derivatives with respect to x and y, independent variables, having variations δx and δy not subject to $y = \phi(x)$, but nevertheless at the localities on this path where $(xy) = (x'y')$ determined by $h = k = 0$, precisely as done in

deriving (49) for the case of fixed limits in §§ 10 and 11 above. The general rule of § 11 will thus be seen to apply here also, so that we obtain the first derivatives (38) of (18) as well as higher ones, by differentiating (56) with respect to h and k and setting these displacements h and k equal to zero :

$$\left.\begin{aligned}
\frac{\partial \mathrm{J}_i^n}{\partial h}(0,\,0) &= \mathrm{M}(x_i y_i) + \int_{x_i y_i}^{\xi,\,\eta} \mathrm{M}_x\,dx + \mathrm{N}_x\,dy = \frac{\partial \mathrm{J}_i^n}{\partial x}, \\
\frac{\partial \mathrm{J}_i^n}{\partial k}(0,\,0) &= \mathrm{N}(x_i y_i) + \int_{x_i y_i}^{\xi,\,\eta} \mathrm{M}_y\,dx + \mathrm{N}_y\,dy = \frac{\partial \mathrm{J}_i^n}{\partial y}, \\
\frac{\partial^2 \mathrm{J}_i^n}{\partial h^2}(0,\,0) &= \mathrm{M}_x(x_i y_i) + \int_{x_i y_i}^{\xi,\,\eta} \mathrm{M}_{xx}\,dx + \mathrm{N}_{xx}\,dy = \frac{\partial^2 \mathrm{J}_i^x}{\partial x^2}, \\
\frac{\partial}{\partial k}\frac{\partial \mathrm{J}_i^n}{\partial h}(0,\,0) &= \mathrm{M}_y(x_i y_i) + \int_{x_i y_i}^{\xi,\,\eta} \mathrm{M}_{xy}\,dx + \mathrm{N}_{xy}\,dy = \frac{\partial^2 \mathrm{J}_i^n}{\partial y \partial x}, \\
\frac{\partial}{\partial h}\frac{\partial \mathrm{J}_i^n}{\partial k}(0,\,0) &= \mathrm{N}_x(x_i y_i) + \int_{x_i y_i}^{\xi,\,\eta} \mathrm{M}_{xy}\,dx + \mathrm{N}_{xy}\,dy = \frac{\partial^2 \mathrm{J}_i^n}{\partial x \partial y}, \\
\frac{\partial^2 \mathrm{J}_i^n}{\partial k^2}(0,\,0) &= \mathrm{N}_y(x_i y_i) + \int_{x_i y_i}^{\xi,\,\eta} \mathrm{M}_{yy}\,dx + \mathrm{N}_{yy}\,dy = \frac{\partial^2 \mathrm{J}_i^n}{\partial y^2}.
\end{aligned}\right\} \quad (57)$$

Since (56) is not part of a closed circuit integral such as (48), having a closed circuit (45) for its increment, Stokes's Theorem is not applicable so as to express its derivatives (57) as surface integrals of the curl of its vector integrand as done for (48) in formulæ (49). The line integral (56), however, is still to be thought of as a *two-point* function uniquely determined by $(x',\ y')$ on the original path and $(x,\ y)$ its new position on the displaced path as shown in fig. 5.

In case the *lower* limit is the variable one as with (25) instead of (18) ,the derivatives are the same as (57) except for reversal of sign. These also are obtained by applying the general rule of § 11 to the line integral :

$$\mathrm{J}_0^i(h,k) = (\mathrm{J} + \Delta\mathrm{J})_0^i = \int_{\xi,\,\eta}^{x_i y_i} \mathrm{M}(x'+h,\ y'+k)\,dx' + \mathrm{N}(x'+h,\ y'+k)\,dy' - \int_{x_i y_i}^{x_i+h,\ y_i+k} \mathrm{M}\,\delta x + \mathrm{N}\,\delta y. \quad (58)$$

where, this time it is the *lower* end piece of the closed circuit of fig. 4 which is absent, instead of the upper end piece absent from fig. 5.

§ 13. *The differentials of line integrals are line integrals around the closed differential circuit made by the original path and that due to its parallel displacement of a differential extent.*

When we consider only the terms in the expansions (50) and (51) that are of first degree in h and k, transposing $\int \mathrm{M}dx+\mathrm{N}dy$ to the left member, then we obtain the first approximation to (45); *i. e.*, the differential or first variation of J_i^k; and we now set $h=\delta x$ and $k=\delta y$:

$$d\mathrm{J}_i^k = \frac{\partial \mathrm{J}_i^k}{\partial x}\,\delta x + \frac{\partial \mathrm{J}_i^k}{\partial y}\,\delta y$$

$$= \left[\mathrm{M}(x_i y_i) + \int_{x_i y_i}^{x_k y_k} \mathrm{M}_x\,dx + \mathrm{N}_x\,dy - \mathrm{M}(x_k y_k)\right]\delta x$$

$$+ \left[\mathrm{N}(x_i y_i) + \int_{x_i y_i}^{x_l y_k} \mathrm{M}_y\,dx + \mathrm{N}_y\,dy - \mathrm{N}(x_l y_k)\right]\delta y$$

$$\equiv \int_{x_i y_i}^{x_l y_k} (\mathrm{N}_x - \mathrm{M}_y)\,(\delta x\,dy - \delta y\,dx) \equiv \int (\mathrm{N}_x - \mathrm{M}_y)\,d\sigma, \qquad (59)$$

where on the right we have set $d\sigma=\delta x\,dy-\delta y\,dx$, the parallelogram area determined by the points $(x,\ y)$, $(x+dx,\ y+dy)$ and $(x+\delta x,\ y+\delta y)$, the first two of which lie on the original path of integration and the last one on the displaced path.

Like (45), this is the line integral around the closed circuit (first approximation to it) indicated by fig. 6, but here the parallel displacements are of infinitesimal extent and given by the variations δx and δy. Note that the differential (59) also is expressed as the surface integral of the curl of the vector integrand $\mathrm{R}=i\mathrm{M}+j\mathrm{N}$ over the enclosed area.

§ 14. *The derivatives of line integrals having fixed limits of integration are*: (a) *the line integrals around the closed circuit made by the original and displaced paths per* unit *displacement*, i. e., *the changes that would occur if the rates of change at the path were maintained over* unit *path displacement*; (b) *the surface integrals of the curl of the vector integrand over the surface enclosed by this same circuit.*

If we set $\delta x=1$ and $\delta y=0$ in (59) we obtain the first of (49) and taking $\delta y=1$ and $\delta x=0$ gives the second of (49).

The derivatives (49) are thus seen to be line integrals around the closed circuit * such as shown in fig. 6, but for *unit* displacements. This, of course, is to be understood in the usual calculus sense of a rate of change, *i. e.*, the changes that would occur in unit path displacement, in case the rates at the path were maintained over the entire unit interval displacement $\delta x = 1$ or $\delta y = 1$. Thus

Fig. 6.

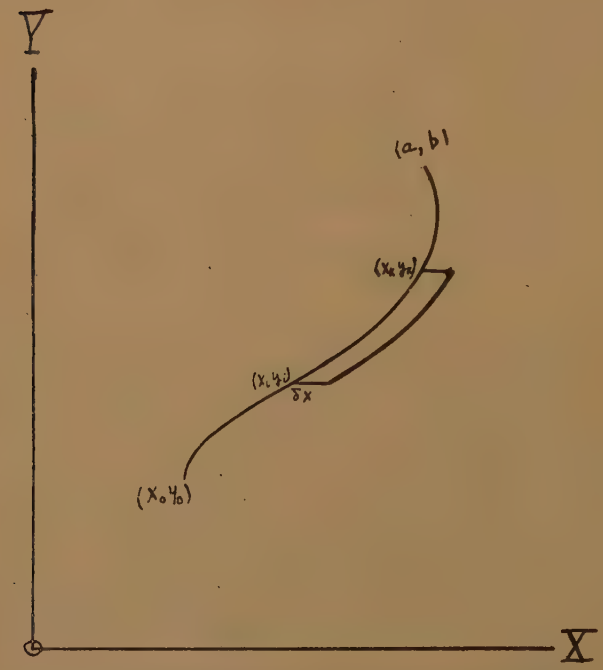

The closed differential circuit around which (1) is taken as given by (59) when $\delta y = 0$.

(49) are *rates* of change of J or the changes (59) per unit change in the independent variable x or y, and this means, according to the method herein, the change in J given by (59) per unit parallel displacements h or k of the path of integration.

* This holds also for second and higher derivatives, all of which are identically equal to the appropriate surface integrals over the enclosed circuit.

§ 15. *The area derivative of a line integral is the total derivative of the partial derivatives* :

$$\frac{d}{dy}\left(\frac{\partial \mathrm{J}}{\partial x}\right) = -\frac{d}{dx}\left(\frac{\partial \mathrm{J}}{\partial y}\right).$$

We may remove the integral signs from (49) and (59) by letting the upper or lower limit be variable and taking the total derivative along the path of integration. Then, noting the appropriate values of σ that apply, we have :

$$\left.\begin{aligned} &\frac{d\mathrm{J}}{d\sigma} = \frac{d}{dy}\left(\frac{\partial \mathrm{J}}{\partial x}\right) = -\frac{d}{dx}\left(\frac{\partial \mathrm{J}}{\partial y}\right) = \mathrm{N}_x - \mathrm{M}_y, \\ &\frac{d}{dx}\left(\frac{\partial \mathrm{J}}{\partial x}\right) = y'\frac{d\mathrm{J}}{d\sigma}\,; \quad \frac{d}{dy}\left(\frac{\partial \mathrm{J}}{\partial y}\right) = -\frac{1}{y'}\frac{d\mathrm{J}}{d\sigma}. \end{aligned}\right\} \quad (60)$$

This $\frac{d\mathrm{J}}{d\sigma}$ is a special case of Volterra's well-known derivative of a line integral or a function of a line or functional, being the rate of change of J with respect to the area enclosed between the original and the displaced path. The fact that the right member is the curl of the vector integrand of the line integral checks the definition of curl in vector analysis, for the curl of a vector has been described as the " circuitation " or line integral per unit area *, or rate of change of a closed line integral per unit area enclosed. Note that the area derivative is a function of (x, y), only as indicated by dropping the subscripts which is in contrast to the previous derivatives which have an integral term (usually non-vanishing) and depend on a path interval from $(x_i y_i)$ to $(x_k y_k)$.

Fig. 7 shows the geometrical interpretation of the area derivative (60) (which is a case of Volterra's derivative) as given by the *total* derivative of the partial $\frac{\partial \mathrm{J}}{\partial x}$. For this latter gives the change in J due to unit † change in x only and due to such path shifts to the right as indicated by fig. 7, where if δx is unity the enclosed area will be

$$y_k - y_i = (y_k - y_i)\,\delta x = \delta x \int_{y_i}^{y_k} dy.$$

* In the calculus sense, *i. e.*, what this unit closed circuit integral would be in case the indicated rates involved were the same throughout the circuit as at (x, y) the point in question.

† As a rate of change in the calculus sense.

Now, if we wish to find the rate of change per *unit* area adjoining the curve as indicated by the shaded part of fig. 7 and required by the above analysis, then the variations of $\frac{\partial J}{\partial x}$ due to y must be due to dy instead of δy, and must accordingly take place along the curved integration path $y=\phi(x)$ indicated by fig. 7 and precisely as is provided for by total differentiation, whose process, using the equa-

Fig. 7.

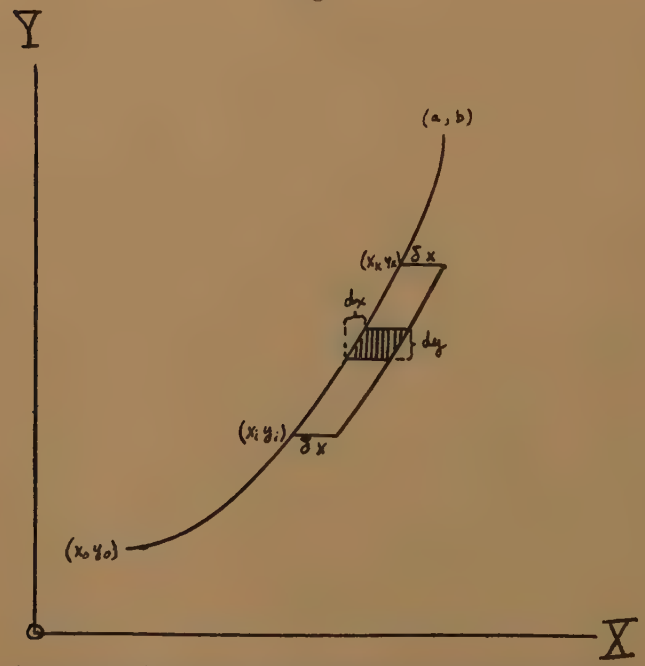

The area $d\sigma=\delta x\,dy$ used as the independent variable for the area derivative where $\delta y=0$ as in the first of (49) or (60).

tion of the path, tells x and y how they are to vary with respect to each other. Likewise when the order of differentiation is reversed.

§ 16. *The Second Order area Differential and Volterra's First Order Differential.*

The second order area differential is obtained by multiplying (60) by $d\sigma$ or dropping the integral sign from (59) :

$$dJ=(N_x-M_y)\,d\sigma=(N_x-M_y)(\delta x\,dy-\delta y\,dx). \quad (61)$$

When (61) is integrated along the path with δx and δy constant we obtain (59), which, if we take the limits as (x_0, y_0) and (a, b) instead of arbitrary, gives the special case of (59) that is the differential of J along its *entire* length :

$$\begin{aligned} d\mathrm{J} &= \int_{x_0}^{a} (\mathrm{N}_x - \mathrm{M}_y) \frac{d\sigma}{dx}(x)\, dx \\ &\equiv \delta x \int_{y_0}^{b} (\mathrm{N}_x - \mathrm{M}_y)\, dy + \delta y \int_{x_0}^{a} (\mathrm{M}_y - \mathrm{N}_x)\, dx \\ &\equiv \delta x \left[\mathrm{M}(x_0 y_0) + \int_{x_0 y_0}^{a, b} \mathrm{M}_x\, dx + \mathrm{N}_x\, dy - \mathrm{M}(a, b) \right] \\ &\quad + \delta y \left[\mathrm{N}(x_0 y_0) + \int_{x_0 y_0}^{a, b} \mathrm{M}_y\, dx + \mathrm{N}_y\, dy - \mathrm{N}(a, b) \right]. \end{aligned} \qquad . \ . \ . \quad (62)$$

Here $\dfrac{d\sigma}{dx}(x) = y'\delta x - \delta y$ is a function of x since the slope y varies with x along the path of integration, and in the right members * we remove δx and δy, taken to be constants for the present theory, from under the integral sign.

Eq. (62) may be compared † with Volterra's differential :

$$\delta \mathrm{F} = \int_{x_0}^{a} \mathrm{F}'(f(x)\xi)\, \delta f(\xi)\, d\xi = \oint \mathrm{M}\, d\xi + \mathrm{N}\, d\eta. \qquad (63)$$

Here the right member is added because whenever Volterra's derivative can be interpreted (as ordinarily) as taken with respect to the area adjoining the path of a line integral, in some coordinates or other, then it will be the curl of a corresponding vector integrand that can be read into his integral, This is because a curl is identically just such an area rate of change. Hence by Stokes's Theorem, Volterra's differential is the line integral about the area enclosed by the original and displaced paths, such as indicated herein by the right member of (63) and by figs. 6 and 7. However, (63) is more general than (62) in that the variations of its displaced path need not be constants along the path between

* A. G. Webster, ' Dynamics,' p. 85, gives the left members of this equation (62).

† V. Volterra, ' Functions of Lines,' Ch. 2, pp. 24, 25 (1913). ' Theory of Functionals,' Ch. 1, pp. 23, 24 ; eq. (2), p. 24 (1931).

(x_iy_i) and (x_ky_k) such as δx and δy used herein. Otherwise (63) is equivalent to (62) and includes it as a special case, as may be shown by replacing y by $f(x)$ and x by ξ in (62) and $\frac{d\sigma}{dx}(x)$ by $\delta f(\xi)$.

Two important advantages of (59) over Volterra's (63) may be noted. The first is due to greater *specialization* in that the δx and δy are constants along the path interval considered. This makes the part J_i^k of the integral (1) a uniquely determined two-point function of any $(x'y')$ on the path and (xy) its displaced position, or again, a function of its parallel displacements h and k; and a continuous function (in the usual sense) for variations $\delta x=h$ and $\delta y=k$ of x and y in many cases where the same does not hold for Volterra's integral under variations $\delta y=\eta(x)$. See § 9 above. Thus the length integral is not continuous in the Volterra sense (see Bliss, Proc. Nat. Acad. of Science, i. p. 174, 1915), whereas it will readily be seen from fig. 6 that J_i^k whose differential is given by (59) is continuous in that the usual inequalities which are the criteria for its continuity are satisfied.

The second great advantage of (59) over Volterra's (63) comes from the variable arbitrary limits. For where one of these limits is taken as the variable point $(x, y)=(x_iy_i)$ and the derivative (53) set equal to zero, we get the new conditions like (48) of the previous * paper for extrema in the calculus of variations.

Part III.

Differentiation by Application of the New Rules for Differentiation with Respect to Differentials.

§17. *Working Rules (I.) and (II.) for differentiation with respect to differentials of an integral in the calculus of variations yield identically formulas* (38) *for the derivatives of the corresponding line integral with variable upper limit.*

These working rules † may be stated for reference.

Working Rule (I.).—The partial derivative of an integral with respect to a differential that appears *explicitly* under

* Kimball, W. S., *loc. cit.* sec. 9, p. 143.
† Kimball, W. S., *loc. cit.* Sec. 10, p. 144.

the integral sign is given by (*a*) dropping the integral sign, and (*b*) differentiating with respect to this differential, treating it as an ordinary finite variable.

Working Rule (*II.*).—The partial derivative with respect to a differential (say dx), of an integral that depends *implicitly* on this differential by virtue of explicit dependence on the corresponding integral variable x, as by $x=x_0+\int_{x_0}^{x} dx$, is given by (*a*) differentiating under the integral sign with respect to this integral variable x, and (*b*) setting as *lower* limit, that same or other integral variable x or y, with respect to which the integration is to be carried out.

The application of these rules to (18) being an integral with a variable limit (ξ, η) involves the application of Working Rule (I.) to the dx and dy that appear explicitly, and the application of Working Rule (II.) to the functions M and N of x and y :

$$\left.\begin{aligned} \frac{\partial J}{\partial dx} &= M(x, y)+\int_{xy}^{\xi, \eta} M_x\,dx+N_x\,dy=\frac{\partial J_i^n}{\partial x}, \\ \frac{\partial J}{\partial dy} &= N(x, y)+\int_{xy}^{\xi, \eta} M_y\,dx+N_y\,dy=\frac{\partial J_i^n}{\partial y}, \end{aligned}\right\} \quad (64)$$

where the right members come from multiplying the left members by (7), or by comparison with (38). Note that these rules give the rate of change of that part of the integral (18) that is included between the points (xy) and (ξ, η) along the path of integration.

§ 18. *Differentiation with respect to differentials of the integral $J=F-G$ yields identically the derivatives* (37) *of that part of a line integral J included between (xy) and the fixed upper limit along the path of integration.*

The condition $G=0$, used previously * with Calculus of Variations problems was taken of the form :

$$\begin{aligned} G&=c_1[\textstyle\int dx-(a-x_0)]+c_2[\int dy-)(b-y_0)] \\ &\equiv M(a, b)[\textstyle\int dx-(a-x_0)]+N(a, b)[\int dy-(b-y_0)]=0, \end{aligned} \quad . \; . \; . \quad (65)$$

* Kimball, *loc. cit.* uses this $G=0$ as an isoperimetric condition on the differentials whereby fixed end points are provided for the integrating path of a definite integral.

where the undetermined constants c_1 and c_2 of the Lagrange method always turned out to be the corresponding components of the vector integrand at the upper limit, as indicated.

Now form the function $J=F-G$, using for F the line integral (1) and G of (65); and differentiate with respect to differentials as per Working Rules (I.) and (II.) above:

$$\left.\begin{aligned}\frac{\partial J}{\partial dx}&=M(x,y)+\int_{xy}^{a,b} M_x\,dx+N_x\,dy-M(a,b)=\frac{\partial J_i^n}{\partial x},\\ \frac{\partial J}{\partial dy}&=N(x,y)+\int_{xy}^{a,b} M_y\,dx+N_y\,dy-N(a,b)=\frac{\partial J_i^n}{\partial y},\end{aligned}\right\} \quad . \quad . \quad . \quad (66)$$

where, as before, the right members come from multiplying the left members by (7) or by comparison with (37). Eqs. (66) are identical with (37) for the indicated limits which include, like (64), the part of J between (x, y) and the upper limit. The reason why Working Rules (I.) and (II.) give these particular limits, *i. e.*, refer to the derivatives of that part of J between (x, y) and (a, b) is to be found in the particular way the Δ process was applied in the calculus of variations, in that it used

$$x=x_0+\int_{x_0}^{x} dx\,;\quad y=y_0+\int_{y_0}^{y} dy,$$

whereby the sums start from the lower limit (x_0y_0) and range up, instead of starting from (a, b) and ranging down, or from some intermediate point (x_ky_k). This particular method of making x and y dependent on dx and dy always leads in connexion with the Lagrange method (which treats Δx_i and Δy_i as all independent variables) to results equivalent to taking $\Delta x_n=dx_n$ and $\Delta y_n=dy_n$ for the *dependent* variables. Thus differentiation with respect to differentials of $J=F-G$ using (1) for F and (65) for G is identical with differentiation of (1) according to (37), taking the dependent differentials as Δx_n and Δy_n whereby $(x_k, y_k)=(x_n, y_n)=(a, b)$. This arbitrary specialization in the choice of upper limit is inherent in the particular method employed in working out by Δ process the second rule for differentiation with respect to differentials. It will be seen that this choice of the upper limits in (37) is the choice best adapted to applications to maxima and

minima problems such as treated in the calculus of variations. Hence the specialization in question is a happy one.

§ 19. *General Rules for Differentiation with respect to Differentials.*

Note that Working Rule (II.) (not Working Rule (I.)) for differentiation with respect to differentials would have to be revised if it is to express the results of §4 referring to variable lower limits, so as to take care of a dependence of x and y on dx and dy as per $x=a-\int_x^a dx$ and $y=b-\int_y^b dy$ which are the limits of (28) in order to obtain (39) by the application of Working Rule (II.) to (25).

We easily find the general inclusive form of Working Rule (II.) by referring back to formula (10) Part I. Simplify the summation terms of the right members, and then pass to the limit *before* using (7) or (8). Then (10) becomes :

$$\left.\begin{aligned}\frac{\partial \mathrm{J}_i^k}{\partial\, dx} &= \mathrm{M}(x_i y_i)+\int_{x_i y_i}^{x_k y_k} \mathrm{M}_x\, dx+\mathrm{N}_x\, dy-\mathrm{M}(x_k y_k)=\frac{\partial \mathrm{J}_i^k}{\partial x}\,,\\ \frac{\partial \mathrm{J}_i^k}{\partial\, dy} &= \mathrm{N}(x_i y_i)+\int_{x_i y_i}^{x_k y_k} \mathrm{M}_y\, dx+\mathrm{N}_y\, dy-\mathrm{N}(x_k y_k)=\frac{\partial \mathrm{J}_i^k}{\partial y}\,.\end{aligned}\right\} \quad . \quad . \quad . \quad (67)$$

Here again the right members come from comparison with (37).

We may generalize the two rules for differentiation with respect to differentials so as to include all the cases here treated as well as the special extremum problems of the calculus of variations formerly treated :—

Working Rule (*I.*).—The partial derivative of a part J_i^k of a line integral J with respect to a differential that appears *explicitly* under the integral sign is given by (*a*) dropping the integral sign, (*b*) differentiating with respect to this differential, treating it as an ordinary finite variable, (*c*) *subtracting* the resulting derivative at the upper fixed limit $(x_k y_k)$ from the value at the lower fixed limit $(x_i y_i)$.

Working Rule (*II.*).—The partial derivative with respect to a differential, say dx, of the part J_i^k of a line integral J that depends implicitly on this differential by virtue of explicit dependence on the corresponding integral variable

(x), is given by (a) differentiating this part J_i^k of this integral under the integral sign with respect to this integral variable x, and (b) keeping its upper and lower limits, unchanged.

Supplement to Rule (*I.*).—In case of a definite integral with variable upper or lower limit, the derivative referred to by (c) of Rule I. at the *variable* limit is absent.

These rules, it will be noted, include as special cases the rules as stated in § 17 above and applied in (64) and (66) to line integrals with variable and fixed limits, and may be considered as established by the argument of Part I. that leads to (10) and hence to (67) of this section, which is the resulting formula which they always yield when properly applied. Since (67) is the same as (37) and the first two of (49), we note again that differentiation with respect to differentials as herein, always gives the partial derivatives with respect to the corresponding integral variables x and y, for any point along the path of integration, it being understood that all x's (or y's) along that part of the path included by the dependent variable J_j^k take on the same increments according to the method of differentiation by parallel displacement developed in this article. (See Part II., §§ 10 and 11.)

§ 20. *The Geometrical Meaning of Working Rules I. and II. for Differentiating with respect to Differentials: Rule I. gives the differential circuit integral over the end pieces of the strip. Rule II. gives it along the parallel curved paths.*

We saw above in Part II., §§ 13 and 14, that the derivatives (49) or (67) represent line integrals around the closed differential circuit, such as indicated by fig. 8 taking $\delta x = 1$. The part of the line integral along P to S, *i. e.*, from $(x_i y_i)$ to $(x_i + \delta x, y_i)$ was given by $M(x_i y_i)\delta x$ which became $M(x_i, y_i)$ when δx was divided out or set equal to unity as in (49) and (67). Likewise $M(x_k y_k)$ is the part of the line integral along R to Q shown * in fig. 8. These two terms are the part of (67) given by application of Working Rule (I.) for differentiating with respect to differentials, being the part outside the integral

* These are first approximations to the expansions (51).

term. Likewise for partial derivatives with respect to y. Hence, for Working Rule (I.), we have the formulæ :

$$\left.\begin{aligned}\left(\frac{\partial \mathrm{J}_i^k}{\partial x}\right)_{\mathrm{I}} &= \mathrm{M}(x_i y_i) - \mathrm{M}(x_k y_k) \\ &= (f - y' f_{y'})_{x_i y_i} - (f - y' f_{y'})_{x_k y_k} = \left(\frac{\partial \mathrm{J}}{\partial \bar{dx}}\right)_{\mathrm{I}}, \\ \left(\frac{\partial \mathrm{J}_i^k}{\partial y}\right)_{\mathrm{I}} &= \mathrm{N}(x_i y_i) - \mathrm{N}(x_k y_k) \\ &= f_{y'}(x_i y_i) - f_{y'}(x_k y_k) = \left(\frac{\partial \mathrm{J}}{\partial dy}\right)_{\mathrm{I}},\end{aligned}\right\} \quad (68)$$

Fig. 8.

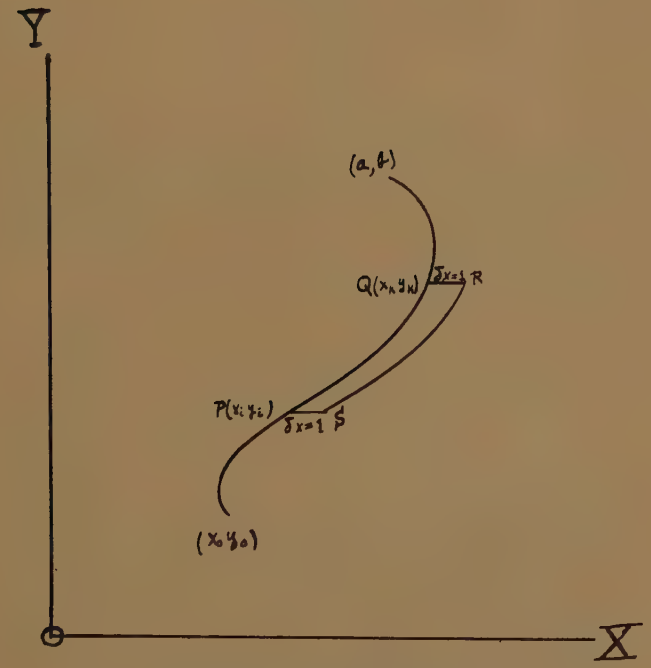

The closed circuit of unit displacement which is the integration path of derivatives.

which refer to a line integral (69) in terms of M and N or $f(xyy')$ where y' is necessarily the slope along the path of integration : $dy \equiv y' dx$.

$$\mathrm{J} = \int \mathrm{M}\, dx + \mathrm{N}\, dy = \int f(x, y, y')\, dx \equiv \int (f - y' f_{y'})\, dx + f_{y'}\, dy. \quad (69)$$

And these derivatives (68) give the part of the closed circuit line integral (67) per unit displacement shown in fig. 8 out along $\delta x=1$ or $\delta y=1$ at P and back again at Q in the usual sense of the calculus, *i. e.*, they are what those parts of the line integral would be in case M and N had the same value all along this unit displacement that they have at $P(x_i y_i)$ and $Q(x_k y_k)$.

Application of the Working Rule (II.) to (69) gives the integral terms of (67) :

$$\left.\begin{aligned}\left(\frac{\partial \mathrm{J}_i^k}{\partial x}\right)_{\mathrm{II}} &= \int_{x_i y_i}^{x_k y_k} \mathrm{M}_x\,dx+\mathrm{N}_x\,dy = \int_{x_i}^{x_k} f_x\,dx = \left(\frac{\partial \mathrm{J}}{\partial dx}\right)_{\mathrm{II}},\\ \left(\frac{\partial \mathrm{J}_i^k}{\partial y}\right)_{\mathrm{II}} &= \int_{x_i y_i}^{x_k y_k} \mathrm{M}_y\,dx+\mathrm{N}_y\,dy = \int_{x_i}^{x_k} f_y\,dx = \left(\frac{\partial \mathrm{J}}{\partial dy}\right)_{\mathrm{II}}.\end{aligned}\right\} \quad . \quad . \quad . \quad (70)$$

And these we have seen in §§ 13 and 14 above, represent the difference between the line integral (69) along the original and the displaced path per unit displacement in case the rate of change were maintained over the entire unit displacement, and shown in fig. 8 as the integral difference along the two curved paths from P to Q and S to R, respectively.

Summarizing the results of this section we have :—

Rule I. gives the difference between the values of J along the vector displacements PS and QR at the ends of the unit displacement circuit (see figs. 4 and 8), *i. e.*, along the straight lines (46) per unit displacement in the calculus sense.

Rule II. gives the difference between the values of the line integral J along the original path $y=\phi(x)$ from P to Q and along the parallel displaced path from S and R obtained from $y=\phi(x)$ by unit parallel displacement in the calculus sense of a rate of change.

Note that the choice of M and N in terms of f and $f_{y'}$ given by (69) is determined according to (68) by application of Rule I. to the various members of (69) which requires $\mathrm{M}=f-y'f_{y'}$ and $\mathrm{N}=f_{y'}$ in case $\int f(xyy')\,dx$ is to be a line integral with vector integrand $\mathrm{R}=i\mathrm{M}+j\mathrm{N}$ having components given by *application* of Working Rule I.

Note also, that in consequence of this choice of M and N, we have :

$$M_{y'}+y'N_{y'}=f_{y'}-f_{y'}-y'f_{y'y'}+y'f_{y'y'}\equiv 0, \quad . \quad (71)$$

and hence the derivatives (70) are independent of $y'=\frac{dy}{dx}$ being obtainable by differentiation under the integral sign partially with respect to x and y only, treating y' as constant.

§ 21. *The Vector Integrand for Integrals in the Calculus of Variations, and the Transversality Condition.*

The geometrical interpretation of Working Rules I. and II. shows the part that each contributes to the line integral around the closed differential circuit which makes up the complete derivatives $\frac{\partial J}{\partial x}$ and $\frac{\partial J}{\partial y}$ given by (67). And (68) shows the combinations of $f(xyy')$ and its derivative $f_{y'}$ (xyy') that are required by Working Rule I. when f replaces M and N in the derivative formulæ (67). The line integral (1), however, involves the scalar product of two vectors in its integrand, *i. e.*, $R=iM+jN$ and $ds=i\,dx+j\,dy$, and so may be written :

$$J=\int M\,dx+N\,dy$$

$$=\int |R|\,|ds|\left(\frac{M}{R}\frac{dx}{ds}+\frac{N}{R}\frac{dy}{ds}\right)=\int |R|\,|ds|\cos\theta. \quad (72)$$

Accordingly, if we refer to R as the vector integrand of (1), the corresponding vector integrand of (69) is given by replacing M and N by their values in terms of f and $f_{y'}$:

$$F=i(f-y'f_{y'})+jf_{y'}=iM+jN. \quad . \quad . \quad . \quad (73)$$

The problem of obtaining the extremal arc from a point to a line in the calculus of variations requires that the well-known * transversality condition shall be satisfied :

$$F\cdot ds=(f-pf_{y'}\ dx+f_{y'}\,dy=M\,dx+N\,dy=0, \quad (74)$$

where $ds=i\,dx+j\,dy$ is a differential arc along the line in question, and y' of (73) takes on the special value p for one of the extremal arcs of the family through the fixed limit of the integral to be made a minimum, *i. e.*, (73)

* Bliss, *loc. cit.* p. 167.

is here the vector integrand of J when the path of integration is an *extremal* arc.

The geometrical interpretation is that the transversality condition given by (74) requires the vector integrand of J along an extremal arc to be perpendicular (where intersecting it) to the line on which the variable end point is required to lie. Whenever $N=pM$ (as is the case where $f(x, y, y')=\phi(x, y)\sqrt{1+y'^2}$) this means that the extremal arc also will be perpendicular to this line, but if N is not equal to pM the extremal arc will not be perpendicular to this line.

§ 22. *The first partial derivatives and the area derivative for line integrals having the slope of the path y' in the vector integrand, and the geometrical meaning of the Euler and Du Bois Raymond equations in the calculus of variatoins.*

The partial derivatives (67) for the line integral (69) with y' (=slope) in the vector integrand (73) are given by using (68) and (70) in (67) :

$$\left.\begin{aligned} \frac{\partial J_i^k}{\partial x} = \frac{\partial J_i^k}{\partial\, dx} &= (f-y'f_{y'})_i+\int_{x_i}^{x_k} f_x\, dx-(f-y'f_{y'})_k \\ &\equiv \int_{y_i}^{y_k}\left(\frac{d}{dx}f_{y'}-f_y\right)dy, \\ \frac{\partial J_i^k}{\partial y} = \frac{\partial J_i^k}{\partial\, dy} &= f_{y'}(x_iy_i)+\int_{x_i}^{x_k} f_y\, dx-f_{y'}(x_ky_k) \\ &\equiv \int_{x_i}^{x_k}\left(f_y-\frac{d}{dx}f_{y'}\right)dx. \end{aligned}\right\} \quad (75)$$

The right members show the form which the curl of the vector integrand (73) takes for problems in the calculus of variations :

$$\text{Curl } F=N_x-M_y=\frac{d}{dx}f_{y'}-f_y. \quad . \quad . \quad . \quad (76)$$

To obtain the area derivative (60) as applied to (69) let the upper * limit point (x_ky_k) be variable and take the total derivatives of (75) along the integration path :

$$\frac{dJ}{d\sigma}=\frac{d}{dy}\left(\frac{\partial J}{\partial x}\right)=-\frac{d}{dx}\left(\frac{\partial J}{\partial y}\right)=\frac{d}{dx}f_{y'}-f_y. \quad . \quad (77)$$

* Differentiation with respect to a variable lower limit gives eqs. (50) of the previous paper, being the negative of the area derivative.

The vanishing of (77) is Euler's well-known condition in the calculus of variations. We thus see, according to (60) and (77), that it specifies that the rate of change of the integral J with respect to the area *adjoining* the integration path shall be zero everywhere on the path. It refers to the *adjoining* area because in taking the total derivatives of the partials as above, the denominator of the differential quotient becomes a case of $d\sigma=\delta x\,dy-\delta y\,dx$ (for δy or $\delta x=0$), and, as noted in Part II. above, this is the parallelogram area determined by (x, y), $(x+dx, y+dy)$ and $(x+\delta x, y+\delta y)$ where the first two points lie on the path of integration of the line integral (see fig. 7). If we set (75) equal * to zero, and let $(x_i, y_i)=(x, y)$ a variable point, we obtain the Du Bois Raymond equation

$$f_{y'}=\int_{x_k}^{x} f_y\,dx+c_2, \quad \text{where } c_2=f_{y'}(x_k, y_k), \quad . \quad (78)$$

which, according to (75), means that the partial rate of change of J_i^k is zero, where the independent variable y may be taken at any point on the path between the limits (x, y) and (x_k, y_k), *i. e.*, the change in J_i^k per unit parallel displacement of the path in the *y-direction*, is zero for every path interval (x, y) to (x_k, y_k). Likewise the equally significant equation (79) comes from vanishing of the first of (75) :

$$f-y'f_{y'}=\int_{x_k}^{x} f_x\,dx+c_1, \quad \text{where } c_1=(f-y'f_{y'})_{(x_k y_k)}, \quad (79)$$

which says that the change in J_i^k per unit parallel displacement of the path in the *x-direction* is zero for every such included interval of the path of integration.

Second partial derivatives of (69) where the slope y' is included in the vector integrand as in the calculus of variations are *not* considered here, because, unlike (49), they involve difficulties beyond the scope of the present article.

In conclusion, note that these geometrical interpretations of the Euler and Du Bois Raymond conditions and the equally significant (79) are forced into view by the method of differentiation with respect to differentials as applied in Part I. and Part III. as well as the previous

* These are the new critical conditions (48) for extremal arcs in the calculus of variations.

paper *. For we have identified $d(dx)$ and $d(dy)$ with δx and δy, the "variations" of Euler and Lagrange, which are required by this method and technique herein to measure *parallel* displacements of the path of integration along its entire extent between whatever limits are chosen for the dependent variable J_i^k. Thus the method of differentiation with respect to differentials and its automatic introduction of parallel path displacements is the keystone of the arch upon which rest the inevitable geometrical interpretations and developments that are here shown to be its consequences, and it is a striking coincidence as well as consequence that the method affords such a simple and elegant interpretation of the Euler and Du Bois Raymond equations.

§ 23. *Theorem II.—Every integral of the calculus of variations* $\int f(x, y, y')dx$ *along any path* $y=\phi(x)$ *is equal to, and has the same first partial and area derivatives as the ordinary line integral* $J=\int (f-\phi' f_{y'})dx+f_{y'}\,dy$ *along the same path whose slope* $\phi'(x, y)$ *replaces* y' *in the vector integrand.*

This theorem follows at once from the above equations whose unified results it expresses. Thus (69) shows that the two indicated integrals are identical as long as y' of $f(x, y, y')$ is taken as the slope ϕ' of the path of integration. Likewise (67), (68), (70), and (75) show that the first partial derivatives are the same for one integral as for the other, provided the slope ϕ' of the path equals the third argument of $f(x, y, y')$, whereas (60), (76), and (77) show that the area derivatives are the same. On the other hand, *second partial* derivatives of $\int f(x, y, y')dx$ are outside the scope of the present article, and hence are not considered.

It is to be noted that $\phi'(x, y)$, the slope of the path of integration $y=\phi(x)$ can usually in simple cases be expressed in terms of either x or y or both, so that the indicated notation is to be understood in this way. Furthermore, it will be understood that, since the relation $y=\phi(x)$ is used in evaluating the integrals as well as the derivatives, the resulting values will be independent of

* Kimball, *loc. cit.*

whether $\phi'(x, y)$ appears in the integral (80) previous to the evaluation process as a function of x or y or both.

The advantage of this theorem is that it supplies an ordinary line integral with no y' in its vector integrand :

$$J=\int (f-\phi' f_{y'})\,dx+f_{y'}\,dy,$$

$$\text{with} \quad \begin{cases} M(x, y)=f(x, y, \phi')-\phi' f_{y'}(x, y, \phi'), \\ N(x, y)=f_{y'}(x, y, \phi'), \end{cases} \qquad . \ . \ . \quad (80)$$

but associated with (69) in such a way as to have the same first partial and area derivatives and be equal to it along any arc $y=\phi(x)$ admitted * to consideration. Along paths of integration other than $y=\phi(x)$, however, (69) and (80) are seen to be different integrals, having different derivatives.

Corollary, every integral (69) *of the calculus of variations has an equal associated line integral* (80) *where the integration path is an extremal arc, and with likewise vanishing first partial and area derivatives.*

This corollary is evidently the special case of the above general theorem where $y=\phi(x)$ is the extremal arc characterized by the vanishing of the first partial and area derivatives of (69) and (80).

The writer is very specially indebted to Professor G. Y. Rainich, of Ann Arbor, for valuable criticism and discussions. Special thanks are also due to Dr. B. F. Kimball, of Delmar, N.Y., for valuable constructive criticism.

II. *The Activity Coefficients of Potassium Chloride and of Calcium Chloride.* *By* E. A. Guggenheim *and* L. A. Wiseman †.

IN previous papers ‡ formulæ have been obtained for the activity coefficient of each electrolyte and for the osmotic coefficient of the solvent in dilute solutions

* Admissible in the sense of providing integrals and derivatives that exist.

† Communicated by Prof. F. G. Donnan.

‡ E. A. Guggenheim, Rep. of Scandinavian Science Congress, Copenhagen, 1929, p. 298; Phil. Mag. ser. 7, xix. p. 588 (1935); Phil. Mag. ser. 7. xxii. p. 322 (1936).

of mixed electrolytes. These formulæ involve parameters λ called interaction coefficients; there is one such for each electrolyte, having the same value in all dilute solutions containing that particular electrolyte. In the

TABLE I.

Mean Activity Coefficient of KCl in Aqueous Solution at 25° C.

$$\log_{10} f_{KCl} = -0{\cdot}500 \frac{C^{\frac{1}{2}}}{1+C^{\frac{1}{2}}} + \lambda_{KCl}\, C\,; \quad \lambda_{KCl} = 0{\cdot}083.$$

C.	$C^{\frac{1}{2}}$.	f calc.	f' calc.	f' obs.	f' calc. (S. & MacI.).
0·005008	·07077	·9277	·9277	·9273	·9276
·010003	·10002	·9022	·9021	·9024	·9024
·010053	·10026	·9020	·9019	·9024	·9023
·020002	·14143	·8704	·8702	·8702	·8707*
·030000	·17320	·8486	·8484	·8494	·8490
·030285	·17403	·8480	·8478	·8482	·8485
·040000	·20000	·8318	·8315	·8320	·8321
·050106	·22384	·8181	·8177	·8187	·8183
·059995	·24494	·8065	·8061	·8071	·8067
·080004	·28285	·7878	·7872	·7872	·7874
·10000	·31623	·7730	·7723	·7718	·7719

simplest case of a solution of a single electrolyte the formula for the mean activity coefficient f reduces to

$$\log_{10} f = -0{\cdot}500 \frac{C^{\frac{1}{2}}}{1+C^{\frac{1}{2}}} + \lambda C \quad . \quad . \quad . \quad . \quad (1)$$

for a uni-univalent electrolyte and to

$$\log_{10} f = -0{\cdot}500 \frac{2I^{\frac{1}{2}}}{1+I^{\frac{1}{2}}} + \frac{4}{3}\lambda C \quad . \quad . \quad . \quad . \quad (2)$$

for a bi-univalent electrolyte. Here C denotes molar concentration and I denotes ionic strength. The numerical coefficient 0·500 is sufficiently accurate between 15° C. and 25° C., whereas at 0° C. the slightly lower value 0·486 should be used. Such experimental data as are available indicate that for ionic strengths below 0·1 the formulæ are accurate to within a few parts per thousand

* Schedlovsky and MacInnes give ·8701, but this appears to be a slight numerical inaccuracy.

in the activity coefficients, and in almost all cases as accurate as the best experimental data. We propose to consider the application of these formulæ to some recent data of Schedlovsky and MacInnes * for KCl and $CaCl_2$.

The results of the comparison are given in Tables I. and II. At the top of each table is given the formula used with the value assumed for λ. The column headed "f calc." gives the mean activity coefficient so calculated. These are the rational activity coefficients. Since Schedlovsky and MacInnes use activity coefficients related to

TABLE II.

Mean Activity Coefficient of $CaCl_2$ in Aqueous Solution at 25° C.

$$\log_{10} f_{CaCl_2} = -0{\cdot}500 \frac{2I^{\frac{1}{2}}}{1+I^{\frac{1}{2}}} + \frac{4}{3}\lambda_{CaCl_2} C\,; \quad \lambda_{CaCl_2} = 0{\cdot}75.$$

C.	$I^{\frac{1}{2}}$.	f calc.	f' calc.	f' obs.	f' calc. (S. & MacI.).
·0018153	·073796	·8572	·8571	·8588	·8586
·0060915	·13518	·7709	·7707	·7745	·7746
·0095837	·16956	·7320	·7327	·7361	·7364
·024167	·26926	·6488	·6483	·6514	·6510
·037526	·33553	·6114	·6106	·6097	·6085

the volume concentration scale, we have converted these f values to the slightly different values of this scale; these are denoted by "f' calc." The columns headed "f' obs." give the experimental values of Schedlovsky and MacInnes. The last column of each table gives the values calculated by Schedlovsky and MacInnes from a formula of the Debye-Hückel type with an arbitrary value assigned to the mean ionic diameter. For KCl our formula fits the experimental data to one part in a thousand. For $CaCl_2$ our formula fits the experimental data to within about five parts in a thousand, whereas Schedlovsky and MacInnes' formula fits to within about one part in a thousand. The experimental accuracy is certainly very high and appears to be more exact thau our formula.

* Schedlovsky and MacInnes, J. Am. Chem. Soc. lix. p. 503 (1937)

Nevertheless we believe our formula to be useful for three reasons :—

(1) An accuracy of $\frac{1}{2}$ per cent. in an activity coefficient is more than adequate for practically all applications.

(2) The values given by our formula can be calculated with great rapidity once one has a graph of $x/(1+x)$.

(3) The λ value in our formula can be used for computing activity coefficients in solutions containing several electrolytes, while the " mean ionic diameter " for one solution bears no simple relation to that in another solution.

There are no other accurate data for $CaCl_2$ with which to compare those of Schedlovsky and MacInnes. For KCl there are several sets, and a comparison is of interest *. Güntelberg's measurements of f_{HCl} in mixtures of HCl and KCl at 20° C. lead to a value $-0{\cdot}168$ of $\lambda_{KCl}-\lambda_{HCl}$, while there are numerous data for HCl which show that $\lambda_{HCl}=0{\cdot}240$ and within the experimental accuracy this value is independent of temperature between 0° C. and 25° C. Combining these data we obtain $\lambda_{KCl}=0{\cdot}072$ at 20° C. This value is in perfect agreement with the value at 0° C. given by the freezing-point data of Adams and those of Hovorka and Rodebush, but agrees less well with the freezing-point data of Scatchard and Prentiss, which give $\lambda_{KCl}=0{\cdot}056$ at 0° C. Since λ_{HCl} hardly varies between 0° C. and 25° C., it would be surprising if λ_{KCl} varied much over the same temperature range. It was therefore suggested that the experimental value of λ_{KCl} from the data of Scatchard and Prentiss might possibly be too low and less accurate than the value given by the earlier data of Adams. It is therefore rather striking that the new value $\lambda_{KCl}=0{\cdot}083$ is nearer to Adams's value and on the opposite side of it to that of Scatchard and Prentiss. To avoid misconception we would emphasize that this method of comparison is a very sensitive one, and the maximum discrepancy involved is one of only six parts per thousand in f_{KCl} at a molarity 0·1.

The Sir William Ramsay Laboratories of
Inorganic and Physical Chemistry,
University College, London, W.C. 1.

* For full references to all the data, here referred to, see Guggenheim, *loc. cit.*

III. *The Bending of Beams on Elastic Foundations.*

By R. Thornton Coe, *M.A., M.Sc.Tech., A.M.I.E.E.**

I. *Introduction.*

THE present paper is intended to facilitate the application of theory to a class of problem which arises in engineering, such as that associated with the stress distribution in cylindrical bodies arising from some form of centrifugal loading or from thermal expansion. A particular application is that of determining the stress distribution in the band of binding wires used to secure the end windings of a rotating armature of an electrical machine against the effects of centrifugal force. In most cases the binding wire cannot be extended to the edge of the end windings, and a knowledge of the greatest stress which occurs in the outermost wire is of some

Fig. 1.

Arrangement of force applied at one end of beam.

importance. The results may also be applied in the study of stresses in cylindrical retaining rings.

The paper deals first with the separate effects of a single force or couple acting at the end of a finite length of beam resting on an elastic foundation. The results are expressed in terms of suitable parameters, and values of these are tabulated to facilitate their application to particular problems.

The method of dealing with the more general case of several loads and discontinuities in the beam section is then indicated.

II. *Effect of External Force applied at one end of Beam.*

Referring to fig. 1, let a downward force P be applied to the left-hand end A of the beam.

* Communicated by the Author.

Further, let

k=foundation force, per unit length of beam, per unit compression ;

E=Young's modulus for beam ;

I=moment of inertia of beam section about its neutral axis,

Taking the origin at A, and measuring x and y in the conventional directions (thus giving positive deflexion upwards), the differential equation satisfied by the beam is obtained from the rate of increase of shearing force which is provided by the elastic foundation.

Thus $$\mathrm{EI}\frac{d^4y}{dx^4}=-ky$$

or $$\frac{d^4y}{dx^4}+\frac{k}{\mathrm{EI}}y=0. \quad \ldots\ldots \quad (1)$$

The above equation implies of course that where the beam deflexion is positive, that is upwards, the foundation will pull the beam downwards. This will not be at variance with practice, since usually there will be additional uniform loading sufficient to keep the whole foundation in compression.

The roots of the auxiliary equation are $\left(-\frac{k}{\mathrm{EI}}\right)^{\frac{1}{4}}$,

i. e.,

$$(1+i)\alpha, \quad (-1+i)\alpha, \quad (-1-i)\alpha, \quad \text{and} \quad (1-i)\alpha,$$

where $i=\sqrt{-1}$ and α=the positive value of $\left(\frac{k}{4\mathrm{EI}}\right)^{\frac{1}{4}}$.

The solution is

$$y=e^{\alpha x}(\mathrm{A}\cos\alpha x+\mathrm{B}\sin\alpha x)+e^{-\alpha x}(\mathrm{E}\cos\alpha x+\mathrm{F}\sin\alpha x),$$

or, in a form more convenient for the present purpose,

$$y=(p\cosh\alpha x+q\sinh\alpha x)\cos\alpha x$$
$$+(r\cosh\alpha x+s\sinh\alpha x)\sin\alpha x. \quad (2)$$

The boundary conditions to be satisfied are

when $x=0$, $\frac{d^2y}{dx^2}=0$ and $\mathrm{EI}\frac{d^3y}{dx^3}=-\mathrm{P}$,

and when $x=\mathrm{L}$, $\frac{d^2y}{dx^2}=0$ and $\mathrm{EI}\frac{d^3y}{dx^3}=0$.

Substituting the above,

$$2\alpha^2 s = 0, \quad (3)$$

$$EI\,2\alpha^3(r-q) = -P, \quad (4)$$

$$(s \cosh \alpha L + r \sinh \alpha L) \cos \alpha L - (q \cosh \alpha L + p \sinh \alpha L) \sin \alpha L = 0, \quad (5)$$

and

$$\{(r-q) \cosh \alpha L + (s-p) \sinh \alpha L\} \cos \alpha L - \{(s+p) \cosh \alpha L + (r+q) \sinh \alpha L\} \sin \alpha L = 0. \quad (6)$$

Solving equations (3) to (6) we get

$$p = -\frac{P}{kL}(2\alpha L)\frac{\cosh \alpha L \sinh \alpha L - \cos \alpha L \sin \alpha L}{\sinh^2 \alpha L - \sin^2 \alpha L}, \quad (7)$$

$$q = \frac{P}{kL}(2\alpha L)\frac{\sinh^2 \alpha L}{\sinh^2 \alpha L - \sin^2 \alpha L}, \quad (8)$$

$$r = \frac{P}{kL}(2\alpha L)\frac{\sin^2 \alpha L}{\sinh^2 \alpha L - \sin^2 \alpha L} = q - \frac{P}{kL}2\alpha L, \quad (9)$$

and $s = 0$. (10)

The deflexions at the two ends of the beam due to the load P at $x=0$ are :

when $x=0$,

$$y_a = p, \quad (11)$$

and when $x=L$

$$y_b = -\frac{P}{kL}(2\alpha L)\frac{\sinh \alpha L \cos \alpha L - \cosh \alpha L \sin \alpha L}{\sinh^2 \alpha L - \sin^2 \alpha L}. \quad (12)$$

Also the slopes at the two ends of the beam are :

when $x=0$,

$$\left(\frac{dy}{dx}\right)_a = \alpha(q+r) = \frac{P}{kL^2}2\alpha L\left(\frac{q}{\frac{P}{kL}} - \alpha L\right), \quad (13)$$

and when $x=L$,

$$\left(\frac{dy}{dx}\right)_b = \frac{P}{kL^2}4(\alpha L)^2\frac{\sinh \alpha L \sin \alpha L}{\sinh^2 \alpha L - \sin^2 \alpha L}. \quad (14)$$

For small values of αL the various coefficients and deflexions are best expressed as series of ascending powers

of αL for the purpose of numerical evaluation. The following series are rapidly convergent, and the few terms given will yield six-figure accuracy for values of αL up to about 1·2.

$$p = -\frac{4P}{kL}\left\{1+\frac{48}{7!}(\alpha L)^4-\frac{218112}{7.12!}(\alpha L)^8 + \frac{4681728}{7.15!}(\alpha L)^{12}+\dots\right\}$$

$$= -\frac{4P}{kL}\left\{1+\frac{1}{105}(\alpha L)^4-\frac{71}{1091475}(\alpha L)^8 + \frac{254}{496621125}(\alpha L)^{12}+\dots\right\}, \quad (15)$$

and

$$q = \frac{P}{kL}\left(\frac{3}{\alpha L}\right)\left\{1+\tfrac{1}{3}(\alpha L)^2+\frac{176}{7!}(\alpha L)^4-\frac{57088}{7.11!}(\alpha L)^8 + \frac{14528512}{7.15!}(\alpha L)^{12}+\dots\right\}$$

$$= \frac{P}{kL}\left(\frac{3}{\alpha L}\right)\left\{1+\tfrac{1}{3}(\alpha L)^2+\frac{11}{315}(\alpha L)^4-\frac{223}{1091475}(\alpha L)^8 + \frac{7094}{4469590125}(\alpha L)^{12}+\dots\right\}. \quad (16)$$

When $x=L$,

$$y_b = \frac{2P}{kL}\left\{1-\frac{72}{7!}(\alpha L)^4+\frac{35104}{7.11!}(\alpha L)^8 - \frac{9320832}{7.15!}(\alpha L)^{12}+\dots\right\}$$

$$= \frac{2P}{kL}\left\{1-\frac{1}{70}(\alpha L)^4+\frac{1097}{8731800}(\alpha L)^8 - \frac{899}{882882000}(\alpha L)^{12}+\dots\right\}, \quad (17)$$

and

$$\left(\frac{dy}{dx}\right)_b = \frac{6P}{kL^2}\left\{1-\frac{104}{7!}(\alpha L)^4+\frac{53792}{7.11!}(\alpha L)^8 - \frac{14416768}{7.15!}(\alpha L)^{12}+\dots\right\}$$

$$= \frac{6P}{kL^2}\left\{1 - \frac{13}{630}(\alpha L)^4 + \frac{1681}{8731800}(\alpha L)^8 - \frac{112631}{71513442000}(\alpha L)^{12} + \ldots\right\}. \quad (18)$$

For the limiting case where $\alpha L = 0$ the deflexion of the beam at the end $x=0$ is $-\frac{4P}{kL}$, and that at the end $x=L$ is $\frac{2P}{kL}$. For this case the deflexion curve becomes a straight line of slope $\frac{6P}{kL^2}$, and it can readily be verified that the above results lead to zero shearing force and zero bending moment at the end B of the beam, which is in accord with the assumed boundary conditions.

For large values of αL the various coefficients are best calculated from expansions in powers of $\frac{1}{\sinh \alpha L}$. Thus

$$p = -\frac{P}{kL} 2\alpha L\left\{1 + \frac{1}{\sinh^2 \alpha L}\left(\tfrac{1}{2} + \sin^2 \alpha L - \sin \alpha L \cos \alpha L\right) + \ldots\right\}, \quad (19)$$

$$q = \frac{P}{kL} 2\alpha L\left(1 + \frac{\sin^2 \alpha L}{\sinh^2 \alpha L} + \ldots\right), \quad (20)$$

$$y_b = -\frac{P}{kL}\frac{2\alpha L}{\sinh \alpha L}\left\{\cos \alpha L - \sin \alpha L - \frac{\sin \alpha L}{\sinh^2 \alpha L}\left(\tfrac{1}{2} + \sin^2 \alpha L - \sin \alpha L \cos \alpha L\right) + \ldots\right\}, \quad (21)$$

and $$\left(\frac{dy}{dx}\right)_b = \frac{P}{kL^2} 4(\alpha L)^2 \frac{\sin \alpha L}{\sinh \alpha L}\left(1 + \frac{\sin^2 \alpha L}{\sinh^2 \alpha L} + \ldots\right). \quad (22)$$

Numerical values of $y_a = p$, q, y_b, and $\left(\frac{dy}{dx}\right)_b$ have been calculated from the various expressions given above for a large number of values of αL in the range from 0 to 7·5, and are given in Table I.

The values of parameters given in Table I. enable the deflexion along the beam to be calculated from equation (2)

with an accuracy of about one part in 100,000 of the maximum deflexion which occurs at $x=0$, for values of αL up to about 5. For larger values of αL it is

TABLE I.—Constants for determining Beam Deflexion due to Concentrated Load P at end $x=0$.

αL.	$\frac{y_a}{\frac{P}{k}} = \frac{p}{\frac{P}{k}}$.	$\frac{q}{\frac{P}{k}}$.	$\frac{r}{\frac{P}{k}}$.	$\frac{y_b}{\frac{P}{k}}$.	$\frac{\left(\frac{dy}{dx}\right)_b}{\frac{P}{k^2}}$.
0	4·00000	∞	∞	2·00000	6·00000
0·1...	4·00000	30·10010	29·90010	2·00000	5·99999
0·2...	4·00006	15·20084	14·80084	1·99995	5·99980
0·3...	4·00031	10·30282	9·70282	1·99977	5·99900
0·4...	4·00097	7·90660	7·10660	1·99928	5·99683
0·5...	4·00238	6·51309	5·51309	1·99821	5·99227
0·6...	4·00493	5·62261	4·42261	1·99620	5·98397
0·7...	4·00913	5·02160	3·62160	1·99315	5·97034
0·8...	4·01556	4·60351	3·00351	1·98834	5·94948
0·9...	4·02488	4·30941	2·50941	1·98136	5·91926
1·0...	4·03784	4·10415	2·10415	1·97168	5·87734
1·2 ..	4·07789	3·87887	1·47887	1·94182	5·74816
1·4...	4·14262	3·82405	1·02405	1·89383	5·54090
1·6...	4·23903	3·88845	0·68845	1·82300	5·23568
1·8...	4·37361	4·04297	0·44297	1·72571	4·81771
2·0...	4·55034	4·26829	0·26829	1·59979	4·28045
2·5...	5·18405	5·04941	0·04941	1·17488	2·49738
3·0...	6·03937	6·00119	0·00119	0·67801	0·50723
3·5...	7·00753	7·00315	0·00315	0·24767	−1·03950
4·0...	8·00621	8·00616	0·00616	−0·03041	−1·77621
4·5...	9·00555	9·00425	0·00425	−0·15346	−1·76027
5·0...	10·00307	10·00167	0·00167	−0·16750	−1·29251
5·5...	11·00110	11·00037	0·00037	−0·12716	−0·69781
6·0...	12·00025	12·00002	0·00002	−0·07374	−0·19947
6·5...	13·00004	13·00001	0·00001	−0·02977	0·10932
7·0...	14·00002	14·00002	0·00002	−0·00247	0·23485
7·5...	15·00002	15·00002	0·00002	0·00981	0·23346

necessary to have rather more accurate values of p, q, and r than are given in Table I., in order to retain the same accuracy of the calculated deflexion along the beam. Recourse should be made to the expansions for p and q in powers of $\frac{1}{\sinh \alpha L}$, the first few terms which are given

in equations (19) and (20) being sufficient for the purpose. For values of αL greater than about 12 the same degree of accuracy in the calculated deflexion curve can be obtained by using as an approximation the expression for a semi-infinite beam as given below in equation (23).

Fig. 2.

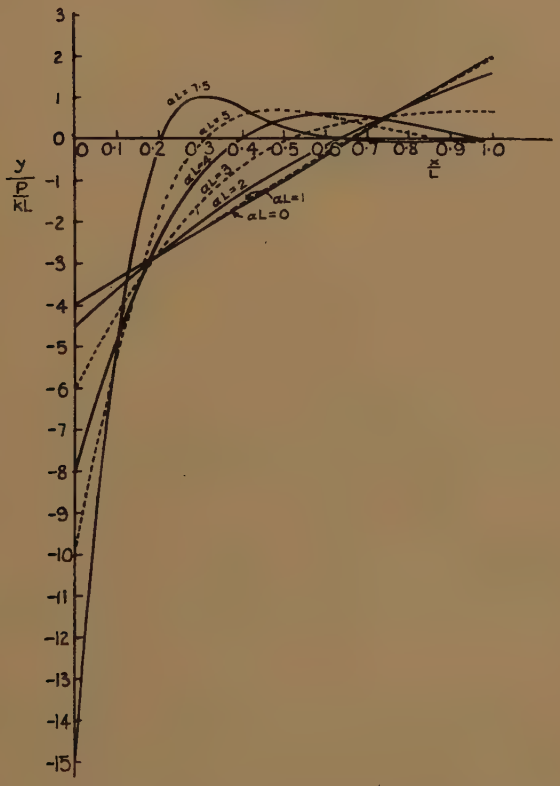

Deflexion of beam on elastic foundations due to load P at end $x=0$.

The deflexion along the beam at intervals of one-tenth of the whole span has been calculated for the following values of αL :—0, 1, 2, 3, 4, 5, and 7·5. These results are given in Table II. and are also shown graphically in fig. 2.

For the limiting condition where the beam and its elastic support extend from $x=0$ to $x=+\infty$ the parameter $\alpha L=\infty$, whence, substituting in equations (7) to (10),

$p=-\frac{P}{kL}(2\alpha L)$, $q=-p$, and $r=s=0$, and the equation of the deflexion curve reduces to

$$y=-\frac{P}{kL}2\alpha L(\cosh\alpha x-\sinh\alpha x)\cos\alpha x$$

$$=-\frac{P}{2\alpha^3 EI}e^{-\alpha x}\cos\alpha x, \quad . \quad . \quad . \quad . \quad . \quad . \quad (23)$$

which is a well-known result.

TABLE II.—Beam Deflexion y due to Force P applied at end $x=0$.

$\frac{x}{L}$	$\frac{y}{P}\cdot\frac{}{kL}$						
	$\alpha L=0.$	$\alpha L=1.$	$\alpha L=2.$	$\alpha L=3.$	$\alpha L=4.$	$\alpha L=5.$	$\alpha L=7{\cdot}5.$
0 ..	−4·000	−4·038	−4·550	−6·039	−8·006	−10·003	−15·000
0·1.	−3·400	−3·418	−3·652	−4·285	−4·940	−5·324	−5·184
0·2	−2·800	−2·801	−2·803	−2·755	−2·500	−1·987	−0·237
0·3.	−2·200	−2·188	−2·030	−1·549	−0·863	−0·154	0·993
0·4.	−1·600	−1·582	−1·342	−0·678	0·063	0·571	0·739
0·5.	−1·000	−0·981	−0·735	−0·098	0·472	0·671	0·289
0·6.	−0·400	−0·386	−0·198	0·256	0·559	0·509	0·034
0·7.	0·200	0·206	0·287	0·455	0·476	0·295	−0·042
0·8.	0·800	0·796	0·738	0·562	0·322	0·100	−0·037
0·9.	1·400	1·384	1·171	0·626	0·147	−0·037	−0·014
1·0.	2·000	1·972	1·600	0·678	−0·030	−0·167	0·010

For this case the deflexion and slope at the end $x=0$ of the beam become $-\frac{2P\alpha}{k}$ and $\frac{2P\alpha^2}{k}$ respectively.

III. *Effect of External Couple applied at one End of Beam.*

Consider a beam as an elastic foundation, as shown in fig. 3, where a couple of moment M acts in an anti-clockwise direction on the end $x=0$ of the beam.

The deflexion y in terms of x can be written in the same form as for the concentrated force, namely :

$$y=(p\cosh\alpha x+q\sinh\alpha x)\cos\alpha x+(r\cosh\alpha x+s\sinh\alpha x)\sin\alpha x. \quad . \quad . \quad . \quad (24)$$

In the present case the arbitrary constants p, q, r, and s are determined from the boundary conditions, that

when $x=0$, $\mathrm{EI}\dfrac{d^2y}{dx^2}=-\mathrm{M}$ and $\dfrac{d^3y}{dx^3}=0$,

and when $x=\mathrm{L}$, $\dfrac{d^2y}{dx^2}=0$ and $\dfrac{d^3y}{dx^3}=0$.

Substituting these conditions in equation (24), and solving, we get

$$p=-\frac{\mathrm{M}}{k\mathrm{L}^2}2(\alpha\mathrm{L})^2\frac{\sinh^2\alpha\mathrm{L}+\sin^2\alpha\mathrm{L}}{\sinh^2\alpha\mathrm{L}-\sin^2\alpha\mathrm{L}}, \quad . \quad . \quad . \quad . \quad (25)$$

$$q=\frac{\mathrm{M}}{k\mathrm{L}^2}2(\alpha\mathrm{L})^2\frac{\sinh\alpha\mathrm{L}\cosh\alpha\mathrm{L}+\sin\alpha\mathrm{L}\cos\alpha\mathrm{L}}{\sinh^2\alpha\mathrm{L}-\sin^2\alpha\mathrm{L}}, \quad (26)$$

$$r=q, \quad . \quad . \quad . \quad . \quad . \quad . \quad . \quad . \quad . \quad . \quad . \quad . \quad (27)$$

$$s=-\frac{\mathrm{M}}{k\mathrm{L}^2}2(\alpha\mathrm{L})^2. \quad . \quad . \quad . \quad . \quad . \quad . \quad . \quad . \quad . \quad (28)$$

Fig. 3.

Arrangement of couple applied at one end of beam.

The deflexions at the two ends of the beam due to the applied moment M at the end $x=0$ are :

when $x=0$, $y_a=p$, ... (29)

and when $x=\mathrm{L}$, $y_b=\dfrac{\mathrm{M}}{k\mathrm{L}^3}4(\alpha\mathrm{L})^2\dfrac{\sinh\alpha\mathrm{L}\sin\alpha\mathrm{L}}{\sinh^2\alpha\mathrm{L}-\sin^2\alpha\mathrm{L}}$. (30)

Also the end slopes are :

when $x=0$,

$$\left(\frac{dy}{dx}\right)_a=2\alpha q=\frac{\mathrm{M}}{k\mathrm{L}^3}2\alpha\mathrm{L}\frac{q}{\dfrac{\mathrm{M}}{k\mathrm{L}^2}}, \quad . \quad . \quad . \quad . \quad . \quad . \quad . \quad . \quad (31)$$

and when $x=\mathrm{L}$,

$$\left(\frac{dy}{dx}\right)_b=\frac{\mathrm{M}}{k\mathrm{L}^3}4(\alpha\mathrm{L})^3\frac{\sinh\alpha\mathrm{L}\cos\alpha\mathrm{L}+\cosh\alpha\mathrm{L}\sin\alpha\mathrm{L}}{\sinh^2\alpha\mathrm{L}-\sin^2\alpha\mathrm{L}}. \quad (32)$$

For small values of αL the various coefficients are again best evaluated from power series in αL.
Thus

$$p = -\frac{6M}{kL^2}\left\{1+\frac{176}{7!}(\alpha L)^4-\frac{57088}{7.11!}(\alpha L)^8 + \frac{14528512}{7.15!}(\alpha L)^{12}+\dots\right\}$$

$$= -\frac{6M}{kL^2}\left\{1+\frac{11}{315}(\alpha L)^4-\frac{223}{1091475}(\alpha L)^8 + \frac{7094}{4469590125}(\alpha L)^{12}+\dots\right\}, \quad (33)$$

$$q = \frac{M}{kL^2}\frac{6}{\alpha L}\left\{1+\frac{624}{7!}(\alpha L)^4-\frac{135936}{7.11!}(\alpha L)^8 + \frac{2256896}{7.14!}(\alpha L)^{12}+\dots\right\}$$

$$= \frac{M}{kL^2}\frac{6}{\alpha L}\left\{1+\frac{13}{105}(\alpha L)^4-\frac{59}{121275}(\alpha L)^8 + \frac{1102}{297972675}(\alpha L)^{12}+\dots\right\}, \quad (34)$$

and when $x = L$,

$$y_b = \frac{6M}{kL^2}\left\{1-\frac{104}{7!}(\alpha L)^4+\frac{53792}{7.11!}(\alpha L)^8 - \frac{14416768}{7.15!}(\alpha L)^{12}+\dots\right\}$$

$$= \frac{6M}{kL^2}\left\{1-\frac{13}{630}(\alpha L)^4+\frac{1681}{8731800}(\alpha L)^8 - \frac{112631}{71513442000}(\alpha L)^{12}+\dots\right\}, \quad (35)$$

and

$$\left(\frac{dy}{dx}\right)_b = \frac{12M}{kL^3}\left\{1-\frac{216}{7!}(\alpha L)^4+\frac{122784}{7.11!}(\alpha L)^8 - \frac{33413760}{7.15!}(\alpha L)^{12}+\dots\right\}$$

$$= \frac{12M}{kL^3}\left\{1-\frac{3}{70}(\alpha L)^4+\frac{1279}{2910600}(\alpha L)^8 - \frac{5801}{1589187600}(\alpha L)^{12}+\ldots\right\}. \quad (36)$$

As in the case of the results for the applied force the terms of the series given above yield six-figure accuracy for values of αL up to about 1·2.

For the limiting case where $\alpha L=0$ the above series show that

$$y_a = -\frac{6M}{kL^2} \quad \text{and} \quad y_b = \frac{6M}{kL^2}.$$

The deflexion curve becomes a straight line, and the equal and opposite deflexions at the two ends of the beam are in accord with the fact that there must be no resultant force on the flexible foundation.

For large values of αL

$$p = -\frac{M}{kL^2}4(\alpha L)^2\left(\tfrac{1}{2}+\frac{\sin^2\alpha L}{\sinh^2\alpha L}+\ldots\right), \quad (37)$$

$$q = \frac{M}{kL^2}2(\alpha L)^2\left\{1+\frac{1}{\sinh^2\alpha L}(\tfrac{1}{2}+\sin^2\alpha L + \sin\alpha L\cos\alpha L)+\ldots\right\}, \quad (38)$$

$$y_b = \frac{M}{kL^2}4(\alpha L)^2\frac{\sin\alpha L}{\sinh\alpha L}\left(1+\frac{\sin^2\alpha L}{\sinh^2\alpha L}+\ldots\right), \quad (39)$$

and

$$\left(\frac{dy}{dx}\right)_b = \frac{M}{kL^3}4(\alpha L)^3\frac{1}{\sinh\alpha L}\left\{\cos\alpha L+\sin\alpha L + \frac{\sin\alpha L}{\sinh^2\alpha L}(\tfrac{1}{2}+\sin^2\alpha L+\sin\alpha L\cos\alpha L)+\ldots\right\}. \quad (40)$$

Numerical values of $y_a=p$, q, y_b, and $\left(\frac{dy}{dx}\right)_b$ have been calculated from the above expressions, and are given in Table III.

Table IV. gives the deflexion along the beam at intervals of one-tenth of the span as calculated from the above expressions, while fig. 4 shows these same results graphically.

For the limiting case, where the beam extends from $x=0$ to infinity, $\alpha L=\infty$ and the coefficients reduce to $s=p=-\frac{M}{kL^2}2(\alpha L)^2$ and $q=r=-p$, giving for the deflexion curve the equation

TABLE III.—Constants for determining Beam Deflexion due to Couple M applied at end $x=0$.

αL.	$\frac{y_a}{-\frac{M}{kL^2}}=\frac{p}{-\frac{M}{kL^2}}$	$\frac{q}{\frac{M}{kL^2}}$	$\frac{s}{-\frac{M}{kL^2}}$	$\frac{y_b}{\frac{M}{kL^2}}$	$\frac{\left(\frac{dy}{dx}\right)_b}{\frac{M}{kL^2}}$
0	6·00000	∞	0	6·00000	12·00000
0·1....	6·00002	60·00074	0·02	5·99999	11·99995
0·2....	6·00034	30·00594	0·08	5·99980	11·99918
0·3....	6·00169	20·02006	0·18	5·99900	11·99583
0·4....	6·00528	15·04754	0·32	5·99683	11·98684
0·5....	6·01309	12·09283	0·5	5·99227	11·96788
0·6....	6·02713	10·16038	0·72	5·98397	11·93344
0·7....	6·05024	8·82599	0·98	5·97034	11·87682
0·8....	6·08562	7·87973	1·28	5·94948	11·79023
0·9....	6·13694	7·20682	1·62	5·91926	11·66483
1·0....	6·20831	6·73996	2·00	5·87734	11·49094
1·2....	6·42929	6·27337	2·88	5·74816	10·95587
1·4....	6·78734	6·29419	3·92	5·54089	10·09973
1·6....	7·32303	6·71810	5·12	5·23568	8·84434
1·8....	8·07470	7·50044	6·48	4·81771	7·13622
2·0....	9·07316	8·60955	8·0	4·28045	4·96240
2·5....	12·74703	12·62944	12·5	2·49738	−2·02962
3·0....	18·00715	18·06799	18·0	0·50723	−9·14572
3·5....	24·52204	24·58518	24·5	−1·03950	−13·35765
4·0....	32·04926	32·06739	32·0	−1·77621	−13·24600
4·5....	40·53824	40·53324	40·5	−1·76027	−9·63130
5·0....	50·01670	50·01042	50·0	−1·29251	−4·55144
5·5....	60·50402	60·50201	60·5	−0·69781	0·01689
6·0....	72·00028	72·00055	72·0	−0·19947	2·91587
6·5....	84·50007	84·50058	84·5	0·10932	3·93629
7·0....	98·00028	98·00047	98·0	0·23485	3·53034
7·5....	112·50024	112·50023	112·5	0·23346	2·39798

$$y=-\frac{M}{kL^2}2(\alpha L)^2(\cosh\alpha x-\sinh\alpha x)(\cos\alpha x-\sin\alpha x)$$

$$=-\frac{M}{2\alpha^2 EI}e^{-\alpha x}(\cos\alpha x-\sin\alpha x), \quad . \quad . \quad . \quad . \quad . \quad . \quad . \quad . \quad (41)$$

which is again a well-known result.

IV. *Application of Results to General Case.*

For the general case of any form of loading it is necessary to consider the beam in separate sections the divisions of which are determined by the positions of external forces and couples, and by any discontinuities in uniform loads, in the beam section and in the resilience of the foundation.

TABLE IV.—Beam Deflexion y, due to Couple M applied at end $x=0$.

$\frac{x}{L}$	$\frac{y}{\frac{M}{kL^2}}$						
	$\alpha L=0.$	$\alpha L=1.$	$\alpha L=2.$	$\alpha L=3.$	$\alpha L=4.$	$\alpha L=5.$	$\alpha L=7{\cdot}5.$
0.....	−6·000	−6·208	−9·073	−18·007	−32·049	−50·017	−112·500
0·1 ...	−4·800	−4·880	−5·947	−8·765	−11·399	−12·018	−2·660
0·2 ...	−3·600	−3·591	−3·432	−2·501	0·357	5·546	23·269
0·3 ...	−2·400	−2·337	−1·466	1·297	5·609	10·363	16·675
0·4 ...	−1·200	−1·114	0·036	3·236	6·819	9·015	6·336
0·5 ...	0·000	0·083	1·170	3·891	5·946	5·814	0·656
0·6 ...	1·200	1·260	2·030	3·739	4·285	2·894	−0·968
0·7 ...	2·400	2·423	2·706	3·136	2·534	0·921	−0·829
0·8 ...	3·600	3·578	3·271	2·318	0·958	−0·198	−0·360
0·9 ...	4·800	4·728	3·784	1·421	−0·445	−0·825	−0·016
1·0 ...	6·000	5·877	4·280	0·507	−1·776	−1·293	0·233

Let the external force P_1 and couple M_1 be considered as acting at the left-hand end of the first section of the beam, and similar forces and couples P_2, M_2, P_3, M_3 etc. at the left-hand ends of succeeding sections of the beam, as indicated in fig. 5.

In order to make the actual beam continuous between the first and second sections a mutual force Q_2 and couple C_2 must be introduced, acting in opposite directions on the two adjacent portions of beam. Mutually opposed forces and couples must similarly be introduced at other division points.

Fig. 4.

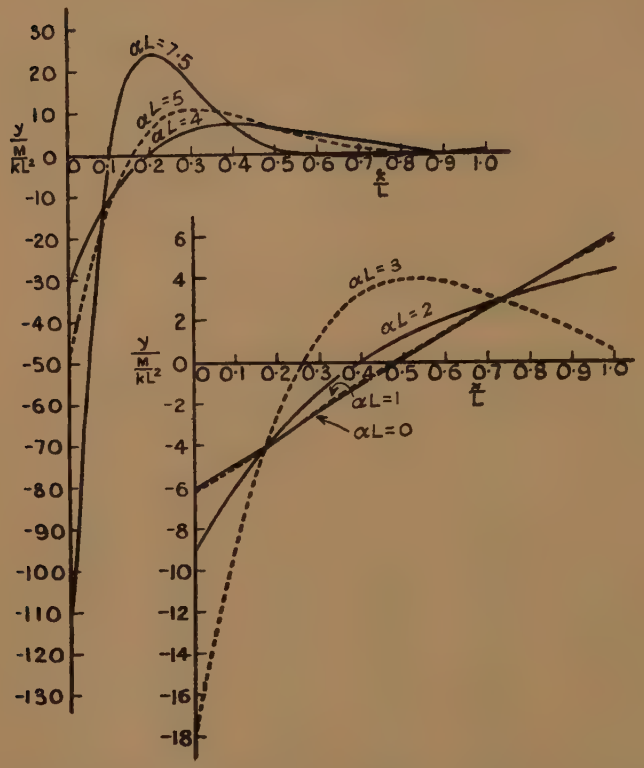

Deflexion of beam on elastic foundations due to couple M at end $x=0$.

Fig. 5.

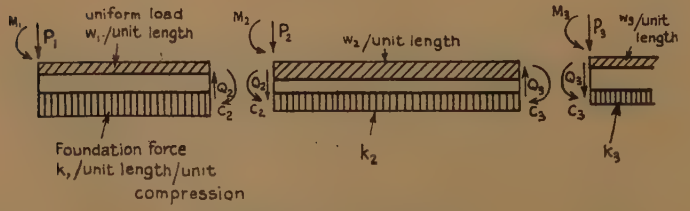

Arrangement of general case.

The requisite number of equations to give the unknowns Q_2, C_2 etc. can be obtained by writing down the condition that the deflexion is the same and the slope is the same

on the two sides of each division line. Thus for the first and second sections of the beam

$$y_2 = -\frac{w_1}{k_1} - Q_2 y_{1a} + P_1 y_{1b} + C_2 y'_{1a} + M_1 y'_{1b}$$

$$= -\frac{w_2}{k_2} + (P_2 + Q_2) y_{2a} - Q_2 y_{2b} + (M_2 + C_2) y'_{2a} + C_2 y'_{2b}, \quad \ldots \quad (42)$$

Fig. 6.

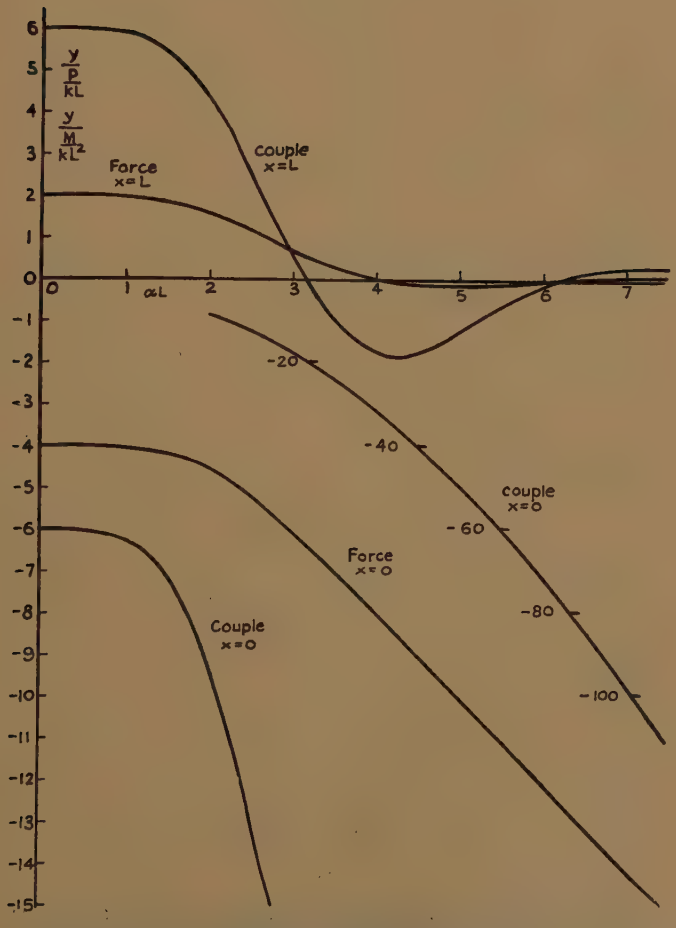

Variation with αL of deflexions at both ends of beam due to force P and couple M applied at end $x=0$.

and

$$\left(\frac{dy}{dx}\right)_2 = Q_2\left(\frac{dy}{dx}\right)_{1a} + P_1\left(\frac{dy}{dx}\right)_{1b} - C_2\left(\frac{dy}{dx}\right)'_{1a} + M_1\left(\frac{dy}{dx}\right)'_{1b}$$

$$= (P_2+Q_2)\left(\frac{dy}{dx}\right)_{2a} + Q_3\left(\frac{dy}{dx}\right)_{2b}$$

$$+ (M_2+C_2)\left(\frac{dy}{dx}\right)'_{2a} - C_3\left(\frac{dy}{dx}\right)'_{2b}, \quad (43)$$

Fig. 7.

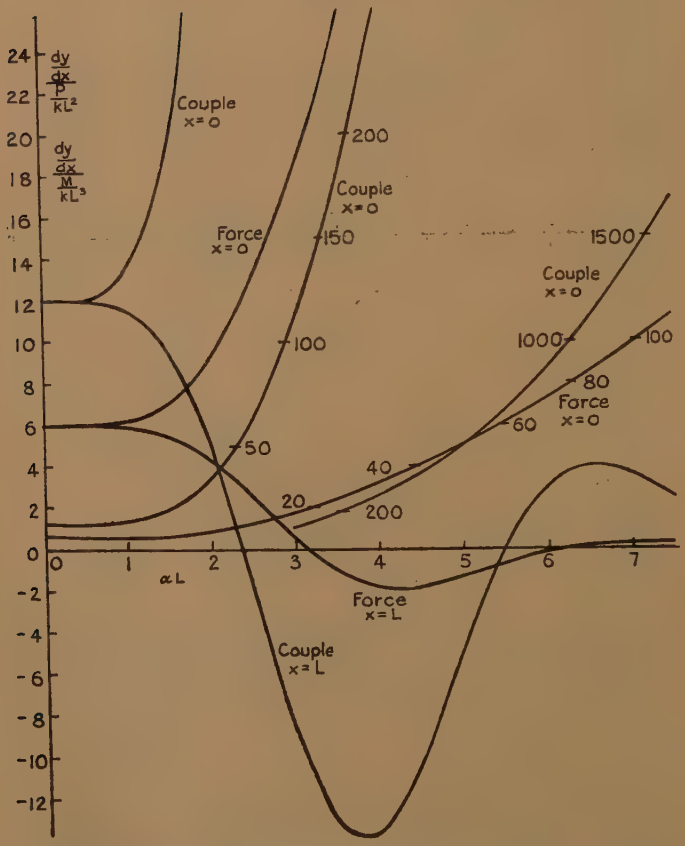

Variation with αL of slopes at both ends of beam due to force P and couple M applied at end $x=0$.

where y_{1a} and y'_{1a} are the deflexions at the left-hand end and y_{1b} and y'_{1b} those at the right end of section 1 of the beam, due to unit downward force and unit anti-clockwise couple respectively applied at the left-hand end, as in the cases dealt with in sections II. and III. of this paper.

Similarly $\left(\frac{dy}{dx}\right)_{1a}$ and $\left(\frac{dy}{dx}\right)'_{1a}$ are the slopes at the left-hand end, and $\left(\frac{dy}{dx}\right)_{1b}$ and $\left(\frac{dy}{dx}\right)'_{1b}$ are those at the right-hand end due to unit force and couple respectively applied at the left-hand end.

The end deflexions of a section of beam arising from a force or couple at the left-hand end are shown plotted against αL in fig. 6, while fig. 7 shows similar curves for the end slopes. Both these curves are derived from the results given in Tables I. and III.

Having determined the mutual reactions and couples Q_2, C_2, Q_3, C_3, etc., the deflexion curve of any section of the beam can be determined by superposing the separate deflexions arising from the force and couple at each end of this section of beam. The stress in the foundation is determined directly by the deflexion at any point.

The variation of bending stress along the beam is determined by the bending moment $EI\frac{d^2y}{dx^2}$ at any point which can be found graphically from the final deflexion curve, or by calculation from the expression

$$\frac{d^2y}{dx^2} = 2\alpha^2\{(s\cosh\alpha x + r\sinh\alpha x)\cos\alpha x - (q\cosh\alpha x + p\sinh\alpha x)\sin\alpha x\}, \quad (44)$$

for each of the end forces and couples on the given portion of the beam.

Consulting Engineers Department,
The British Thomson-Houston Co., Ltd., Rugby.
June 1937.

IV. *The Method of Images for calculating Electric and Magnetic Fields.* *By* E. A. Meyerovitz, *Moscow Krzizanovsky Power Institute of the Academy of Sciences of the U.S.S.R.*†

Summary.

In this paper a method for field calculation is described, giving a rather simple result which may be of great practical importance in many cases. The application of this method is closely associated with the formation of the Riemann surface in accordance with each given problem and the distribution on this surface of a system of images of the sources exciting the field. The method is used for calculating the field of charges in proximity to conducting surfaces and the field of currents in proximity to iron masses. Simultaneously the possibility is also examined of combining the generalized method of images with the method of conformal transformation. In conclusion it is shown that the examination method used is also suitable for some cases of the finite magnetic permeability of iron or the finite dielectric constant of the dielectric.

ONE of the highly efficient and exceedingly simple methods for solving a series of problems has been found in the method of images applied by W. Thomson in calculating the electrostatic field. This method is based on the substitution of the action of conducting masses by the action of a certain system of charges distributed in the region occupied by these masses. Here the problem of field calculation within some limited region develops into a problem of field calculation for the total unlimited space, making allowances for an additional system of charges, described as the electric image of the primary system relative to the interfaces of the conducting and dielectric medium. This method has also proved suitable for calculating a magnetic field, brought about by currents distributed in proximity to iron masses. Here the images of the given system of currents relative to iron surfaces are introduced in the calculation. An account kept of the action of these images fully substitutes the account kept of the action of iron masses.

† Communicated by the Author.

Although this method has proved very efficient, still it has only been applied for calculating electric and magnetic fields in a very small number of instances. A solution has been arrived at by the method of images in the case of spherical surfaces, in some cases of plane surfaces and some cylindric surfaces.

And yet, on closer examination, it appears that the image method can be satisfactorily used in solving problems of a far more general character, a great many of these problems being of great practical importance in designing electrical machinery. For this purpose it is necessary to determine the analytic foundations on which this method is based, but so far this work has been accomplished only to a small degree. Such investigations show, at least in respect of the plane-parallel field, a quite simple association with several generally known functionally theoretic notions which contribute to this method the necessary analytic rigidity. In the present paper the solution of some problems is given, based on the results of our examination, which permits us to pass judgement on the practical value of the suggested calculation method.

In the present paper we deal only with instances of a plane-parallel field. We assume that the currents or charges are distributed along linear conductors placed perpendicularly to the plane in which the calculation is made. This "linearness" does not, of course, limit the generality of the conclusions arrived at, inasmuch as by integration it is always possible to revert to the conductors of finite section. The magnetic permeability of iron is assumed in the first part of our paper as infinitely great. Henceforth the subject is being more generally examined.

§ 1. *Method of the Function of the Complex Potential as applied to Problems of the Type under Examination.*

The general type of the problems which we intend specifying henceforth corresponds to the image given in fig. 1.

As shown in fig. 1, we have a system of linear currents or charges a, a', a'' . . . distributed in region g bounded by surfaces—p, p', p'' . . ., of iron masses or conductors occupying regions—μ, μ', μ'' . . . . Let us assume that on the boundaries no currents or charges exist. Region g

may also include the infinitely remote point. Inasmuch as we examine a plane-parallel field, the calculation may be made in plane xy, and the solution of the field calculation problem in respect of region g may be arrived at by finding some function $\phi(z)=u+iv$ of the complex variable $z=x+iy$. In points a, a', a'' . . . the function must possess logarithmic singularities. On curves p, p', p'', which represent the boundaries of region g, the function $\phi(z)$ must comply with the given conditions. Let us assume these curves to consist of several segmentary-analytic curves of finite or infinite length.

If we exclude the many-valuedness obtained in evading the logarithmic singularities in points a, a', a'' . . . or regions μ, μ', μ'' . . . function $\phi(z)$ must be a single-valued

Fig. 1.

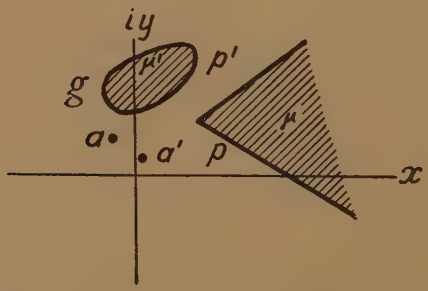

function in region g. If we do not exclude the said evasion paths, then the many-valued function is obtained at the expense of the imaginary part. A complete single-valued $\phi(z)$ function is attained in region g by accordingly drawing the cuts.

§ 2. *Some Peculiarities in the Calculation of an Electric or Magnetic Field.*

In solving electrostatic problems the real part of the function of the complex potential $\phi(z)=u+iv$ is equivalent to the electrostatic potential and is the solution of the equation $\nabla^2 u=0$ throughout the g region with the exception of points a, a', a'' . . ., and approaching these points it tends towards logarithmic infinitude. On curves p, p', p'' . . . potential u has a constant given value. In the infinitely remote point of the g region, provided no charges exist there, u assumes a value which equals zero. The

lines of force of the electric field are given by curves v=const.

In calculating the magnetic field the real part of function $\phi(z)$ is equivalent to the vector potential of the magnetic field : the lines of force of the field are given by curves u=const.

In our problems the vector-potential has only one component perpendicular plane in which the calculation is done and may be treated as a scalar value. Accordingly, the real part of $\phi(z)$ in the magnetic problem is within the g region in agreement with the same ratio as the real part of $\phi(z)$ in a similar electrostatic problem. The solutions of these two problems only differ from one another as regards the boundary conditions and the condition in the infinitely remote point.

In calculating the magnetic field of currents distributed in proximity to iron masses, in the case of region g containing an infinitely remote point it is assumed that the sum of the currents in the region equals zero. Should the sum of the currents distributed at the finite distances from part of the region examined not equal zero, then in the infinitely remote point a linear conductor is presumed with a current of such magnitude that the total sum of currents of this region should equal zero, the lines of force of the field being orthogonal to the boundary curves p, p', p'' .... On these curves the condition v=const. is, therefore, everywhere complied with, with the exception of the points lying on the section lines, where v makes a leap.

Whenever the g region is bounded and the sum of currents in the region does not equal zero, the conditions on the boundaries become implicated. The lines of force of the field do not enter into the iron in this case perpendicularly to its surface. The total field may be divided into two components which are determined separately. One component is determined under the condition that on the boundaries v= const. and the other component is determined under the condition of u=const., this being similar to the condition in calculating the electric field. The resulting field is found by superposition. Thus, in the majority of cases, the boundary conditions may either be reduced to the condition u=const. or to v=const. on the boundaries. This leads to full uniformity in solving the problems.

§ 3. *Association of the Image Method with the Principle of Symmetric Continuation.*

The image method applied to the case in fig. 1 means a substitution of the influence produced by masses μ, μ', μ'' ... by some system of charges or currents distributed beyond the g region. Supposing we succeeded in distributing within the regions μ, μ', μ'' ... the system of conductors b, b', b'' ... in such a manner that on joint examination of the action of conductors a, a', a'' ... and b, b', b'' ... the given conditions are fulfilled on the boundaries of the g region . We thereby determine for the whole of plane z some analytic function $\varphi(z)$ which is continuous when passing through p, p', p'' ... and is identical with the function sought for in the g region. It possesses logarithmic singularities b, b', b'' ... in the regions μ, μ', μ'' ...

Function $\varphi(z)$ effects, accordingly, the analytic continuation of function $\phi(z)$ in the regions μ, μ', μ'' ... through the arcs of curves p, p', p'' ... In the joining points of the analytic arcs of the boundaries of the g region function $\varphi(z)$ must either have branching points or crossing-points.

In our example the possibility of distributing the images in points b, b', b'' ... means that the joining points must be crossing-points, because otherwise the analytic continuations through two adjacent boundary arcs could not be identical with one another.

Seeing that analytic continuation can only be effected in one unique manner, it is apparent that the $\varphi(z)$ function is fully determined by this method.

Let us examine by what method the distribution of points b, b', b'' ... could be determined in the region μ, μ', μ'' ...

On curves p, p', p'' ... the condition is given : either v=const. or u=const. Therefore the analytic continuation through the arcs of these curves may be effected by the Riemann-Schwartz symmetry principle. According to this principle, symmetric values of the function must correspond to points symmetric to our analytic arcs. If on the arc the equality $u=0$ occurs, then the function values in the symmetric points must be

$$\varphi(z) = u+iv$$

and

$$\varphi(z_*) = -u+iv.$$

If in point z the function has a logarithmic singularity, then in point z_*, which is symmetric with it, the function has a logarithmic singularity of the opposite sign.

Under the condition of $v=0$ on the boundaries, the logarithmic singularities in symmetric points have the same sign.

In the example examined by us points b, b', b'' . . . represent points that are symmetric with a, a', a'' . . . relatively to the arcs of curves p, p', p'' . . . The signs of charges or currents in points b, b', b'' . . . are determined depending on the conditions prevalent on the boundaries.

We infer that the problem of electric or magnetic reflexion is solved by determining points symmetric to the arcs of curves p, p', p'' . . . The problem approaches the type examined, and its solution may be arrived at by distributing the images in regions μ, μ', μ'' . . ., if the process of determining the symmetric points yields equal results for all arcs and if uninterrupted analytic continuation is attained in the regions μ, μ', μ'' . . . This is exactly the type of problem whose solution has already been obtained.

§ 4. *Distribution of Images of Riemann Surfaces.*

In the general case analytic continuations through the arcs constituting the boundaries of the field region do not yield identical results, or the analytic continuation in the regions μ, μ', μ'' . . . cannot be made uninterrupted. The problem may then be reduced to the preceding one, if we examine all branches of the suitably built function $\varphi(z)$, provided by the uninterrupted continuation of $\phi(z)$ on the Riemann surface positioned above plane z. The images of currents or charges may be distributed in this case on other sheets of the surface with respect to the function element in the g region that is of interest to us. The aspect of the Riemann surface for $\varphi(z)$ is fully determined by the character of the curves bounding the g region and is to be found by examining the symmetric points for each arc of these curves. By determining on each sheet the points symmetric with a, a', a'' . . of the g region we ascertain the distribution of the images b, b', b''.

In this form the problem is reduced to finding the enclosed Riemann surface corresponding to the given boundary curve and to the construction of a single-valued function on it (if we exclude the many values

obtained in evading logarithmic points) possessing logarithmic singularities and branching points at the given places.

§ 5. *Solution of Problems in the Case of Surface consisting of Segments of Circular Cylinders or Segments of Planes.*

By using as examples some problems of practical bearing we intend showing how the above described method of solution is applied.

(a) *A current in proximity to an unbounded right angle of iron.*

Supposing, as is shown in fig. 2, a linear conductor, along which the current is flowing, is situated in proximity to a right angle of iron with $\mu = \infty$.

Fig. 2.

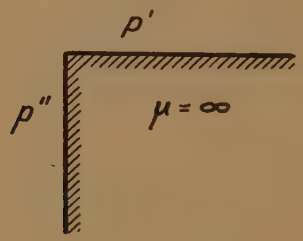

The g region—apparently the total region beyond the right angle $\phi(z)$—is given in this region by a logarithmic singularity at point "a" and by the condition $v = \text{const.}$ on the boundary. Analytic continuations through the two sides of the right angle are different within the hatched region. An uninterrupted and single-valued continuation may be produced if we distribute function $\varphi(z)$ over three sheets of the Riemann surface that are pasted together along the straight line p' and have branching points at the vertex of the right angle and at the infinitely remote point of the straight line p' (fig. 3).

As we see, all images of point "a" are distributed on sheets II and III of the Riemann surface. On the straight lines p_*' and p_*'' the function values are symmetric with the function values on the straight lines p' and p'' which are equivalent to the iron surface. Let us assume that at the point where the vertex of the right angle is situated, $z = 0$.

The function determined on the thus constructed Riemann surface and having logarithmic singularities at the point "a" and in its three magnetic images b, b', b'' complies with the condition of symmetry to both straight lines p' and p''.

Such a function, representing the solution of our problem, is easily found. With this object in view let us find the single-valued function on the three-sheet Riemann surface with an algebraic branching point of $z=0$ and $z=\infty$. Such a function, with an exactitude up to the rational transformations, of it and of z, is given as

$$R(z)=z^{\frac{1}{3}} \quad . \quad . \quad . \quad . \quad . \quad . \quad . \quad (1)$$

Therefore the complex potential, complying with all conditions of our problem, will be

$$\varphi(z)=0{\cdot}2\zeta \ln (z^{\frac{1}{3}}-z_0^{\frac{1}{3}})(z^{\frac{1}{3}}-\bar{z}_0^{\frac{1}{3}})(z^{\frac{1}{3}}+z_0^{\frac{1}{3}})(z^{\frac{1}{3}}+\bar{z}_0^{\frac{1}{3}})=$$
$$=0{\cdot}2\zeta \ln (z^{\frac{1}{3}}-z_0^{\frac{1}{3}})(z^{\frac{1}{3}}-\bar{z}_0^{\frac{1}{3}}), \quad . \quad . \quad . \quad . \quad . \quad . \quad . \quad (1\,a)$$

Fig. 3.

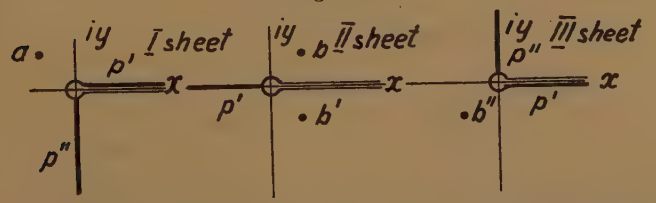

where ζ is the current in conductor a, z_0—the distribution point of the conductor and $\bar{z}_0$—the conjugated point with z_0.

It is obvious that the problem can be solved by a similar method not only in the case of a field situated outside of the straight angle, but also in the case of angles of different value. In the case of the electrostatic problem with the value $u=$const. on the straight lines p' and p'' the electric image b' has the same sign as "a," while the images b and b'' have the opposite sign.

(b) *A current in proximity to an iron sheet of finite width.*

The second example which we intend examining corresponds to fig. 4. As shown in fig. 4, here the conductor is situated in proximity to an iron plate BC with $\mu=\infty$.

Let us assume the plate to be infinitely thin. In the direction perpendicular to the drawing the dimensions

of the plate and current are, as formerly, unbounded. On both sides of the plate the condition v=const. must be complied with. This problem differs from the preceding one inasmuch as the g region, including the boundaries, occupies the total plane z. In the general case the analytic continuation of the field function on both sides of BC is different. The complex potential representing the solution of our problem may be found with the aid of the single-valued function, on the two-sheet Riemann surface, that has branching points in B and C with sheets pasted together along the straight line BC (fig. 5).

The image of point "a" is distributed symmetrically to the straight line BC at point b. Let us mark the

Fig. 4.

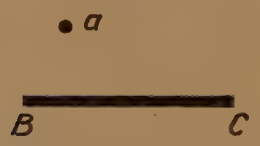

Fig. 5.

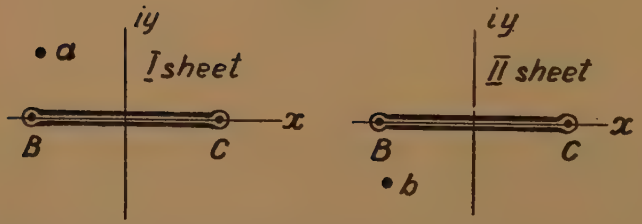

width of the plate as $2h$ and place point $z=0$ in the middle of it.

The single-valued function on our Riemann surface

$$\sqrt{\frac{z-h}{z+h}} \quad \ldots\ldots\ldots \quad (2)$$

has branching points at points $\pm h$.

The complex potential with logarithmic singularities at points a and b will be

$$\varphi(z)=0{\cdot}2\zeta ln\left\{\left[\sqrt{\frac{z-h}{z+h}}-\sqrt{\frac{z_0-h}{z_0+h}}\right]\left[\sqrt{\frac{z-h}{z+h}}+\sqrt{\frac{z_0-h}{z_0+h}}\right](z+h)\right\}, \quad \ldots \quad (2\,a)$$

where ζ is the current of the conductor, z_0 the affix of point a, $\bar{z}_0$ the affix of point b.

The function given by the expression (2a) has a logarithmic singularity in the infinity on both sheets, according to the purport of the problem. In a similar way, on a two-sheet Riemann surface, however, with a different number of branchings, the problem is solved in the case of the current being situated in proximity to several plates, distributed, as shown in fig. 6, along one straight line.

Fig. 6.

Fig. 7.

(c) *The field of a current situated within an iron circular cylinder with a slot* (fig. 7).

In calculating the field in this case the same two-sheet Riemann surface may be used as in the previous case, but with a different distribution of the cuts (fig. 8).

The first sheet is equivalent to the region of the actual field, and the complex potential in this region has a logarithmic singularity at the point where the conducting wire is situated and a logarithmic singularity of the opposite sign at the infinitely remote point. By cutting the sheets along the cylinder arc and pasting them together along this cut, we obtain a two-sheet surface with branching points B and C. When producing the symmetric continuation of the complex potential's function on the second sheet, we must distribute on this sheet the loga-

rithmic singularity of the same sign as in a at point b, which is inverse to a with respect to the circumference bend. At point b', in the centre of the circumference, we must place the logarithmic singularity of the inverse sign. This is the image of the singularity at the infinitely remote point of the first sheet. The function, which is single-valued on our surface, is exactly as in the previous example,

$$\sqrt{\frac{z-z_1}{z-z_2}},$$

Fig. 8.

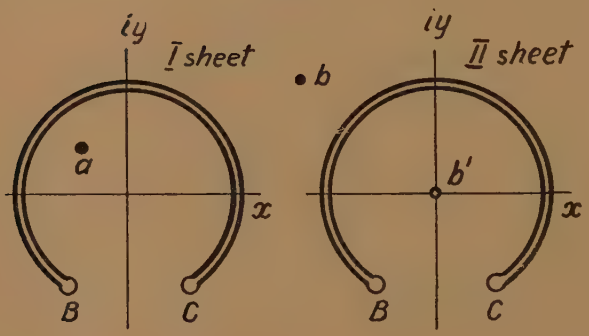

and the complex potential will then be

$$\varphi(z) = 0{\cdot}2\zeta \ln \frac{\left(\sqrt{\frac{z-z_1}{z-z_2}} - \sqrt{\frac{z_0-z_1}{z_0-z_2}}\right)\left(\sqrt{\frac{z-z_1}{z-z_2}} + \sqrt{\frac{z_{01}-z_1}{z_{01}-z_2}}\right)}{\left(\sqrt{\frac{z-z_1}{z-z_2}} + \sqrt{\frac{z_1}{z_2}}\right)\left(\sqrt{\frac{z-z_1}{z-z_2}} - 1\right)} \quad . \quad . \quad . \quad . \quad (3)$$

where z_1 and z_2 are affixes of points B and C and z_0 and z_{01} are affixes of points a and b, while $z=0$ is in the centre of the bend.

The previous examples have shown how the method is applied in the case when the process of determining the symmetric points is single-valued (the symmetry to the straight line and circumference). To simplify matters, we have chosen such examples where the number of sheets of the Riemann surface and of the images

thereon is finite. The number of problems that have such a simple solution can be essentially increased. In the case of an infinite number of sheets the solution method does not differ from the one described above. More complex, however, and calling for special discussion are such cases when the curves by which the g region is bounded are not composed of circumference bends or segments of straight lines.

§ 6. *The Symmetry Relative to Algebraic Curves.*

The case is sufficiently general for the ordinary calculation problems when the arcs of the curves, by which the field region is bounded, are given as an algebraic equation of the form

$$F(xy)=0. \quad . \quad . \quad . \quad . \quad . \quad . \quad (4\,a)$$

It was just for this case that C. Carathéodory † suggested the method of analytic continuation with the aid of finding symmetric points. According to C. Carathéodory, we obtain from simple considerations the algebraic dependence between the affixes of the points symmetric to the curves (4 *a*)

$$F\left(\frac{z+\bar{z}_*}{2}, \frac{z-z_*}{2i}\right)=0, \quad . \quad . \quad . \quad . \quad (4)‡$$

where $z=x+iy$ and $z_*=x_*+iy_*$ are affixes of two points that are mutually symmetric relatively to the curve.

In respect of all cases solved hitherto by the image method the formula (4) also gives a direct result.

In the case of a region bounded by a straight line

$$y=0, \quad . \quad . \quad . \quad . \quad . \quad . \quad . \quad (5)$$

we obtain from (4) the ratio

$$z=\bar{z}_*, \quad . \quad . \quad . \quad . \quad . \quad . \quad . \quad (5')$$

which corresponds to the case of mirror reflexion relatively to the plane.

In the case of a field of current or charge in proximity to a circular cylinder we deduce from the circular equation for curve p

$$x^2+y^2=r^2, \quad . \quad . \quad . \quad . \quad . \quad . \quad (6)$$

† C. Carathéodory, ' Conformal Representation,' Cambridge, 1932.

‡ Exactly the same ratio has been obtained considerably earlier by D. A. Grave (' On Fundamental Problems of the Mathematical Theory of compiling Geographic Maps,' Petersburg, 1896). The latter, however, did not associate it with analytic continuation.

on the basis (4), the following condition of symmetry

$$z\bar{z}_* = r^2. \quad . \quad . \quad . \quad . \quad . \quad . \quad (6')$$

Equivalent to expression (6′) is the transfiguration of the inversion when reflecting towards the circular cylinder.

In the general case, when equation (4) contains z_* of power n, we find for one point z a system of points n that are symmetric with it. By substituting for z in the original equation (4), each of the z_* values found, we find a system of points z_*' that are symmetric to z. By substituting in the like manner $z^{*\prime}$ we find a system of points $z^{*\prime\prime}$ which is symmetric with $z^{*\prime}$ etc. Should every subsequent substitution provide each time new points, then the total number of mutually symmetric points is liable to become infinitely great. In the case when we revert in our substitutions to points already previously found, the number of symmetric points may prove to be finite †.

§ 7. *Calculation of the Field for Regions bounded by Algebraic Curves.*

The method of determining points that are symmetric to the curves enables us to find for problems of a sufficiently general type (guided by the given distribution of currents or charges) a system of electromagnetic images. These images may be distributed on a Riemann surface, which consists of a finite or infinite number of sheets and is constructed for the given curve that bounds the field region by the method of analytic continuation, as has already been shown in the examples of § 5. These examples may be treated as particular cases of problems of a more general type mentioned above, Below we give several examples which show the solution method also for these more general cases.

§ 8. *Applying the Methods of Electromagnetic Images to some Problems.*

(a) *The field of a current situated in the hyperbolic space* (fig. 9).

Supposing the curve bounding the field region is given

† D. A. Grave, *loc. cit.*

as an equation of an equilateral hyperbola $xy=c$. The expression (4) is then

$$z^2-\bar{z}^2{}_*=4ic.$$

We get two points that are symmetric with z,

$$z_{*1,\,2}=\pm\sqrt{\bar{z}^2+4ic}. \quad . \quad . \quad . \quad . \quad . \quad (7)$$

The point symmetric with z_{*1} and z_{*2} is determined in the singular :

$$z'_*=-z. \quad . \quad . \quad . \quad . \quad . \quad . \quad . \quad (8)$$

Fig. 9.

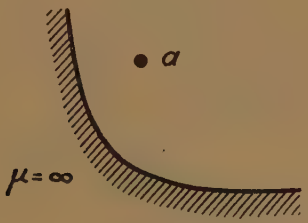

Fig. 10.

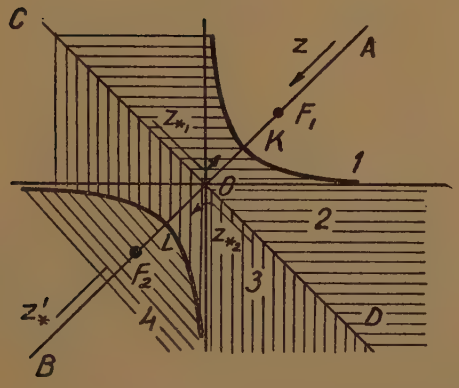

If we lend z an optional value within the hyperbolic space 1, then points z_{*1}, z_{*2}, and z'_* will be displaced within regions 2, 3, and 4 shown in fig. 10.

As point z proceeds along the axis AF_1, point z'_* proceeds along BF_2, point z_{*1} along CO, and point z_{*2} along DO. Both points z_{*1} and z_{*2} are convergent at point O. During further displacement of z from F_1 towards the vertex of the K hyperbola these points move

along OK and OH. The congruence in the displacement of the points is shown in the drawing by pointers.

By placing the current at point " a " with the affix z_0 and producing the analytic continuation of the field function determined by it through the hyperbola curve which is bounding region 1 and then across the CD boundary of regions 2 and 3 and, finally, through the hyperbola which is bounding region 4, we obtain the b, b', and b'' images of the " a " current at points

$$\sqrt{z_0^2+4ic},\ -\sqrt{z_0^2+4ic}$$

and $-z_0$ that are symmetric with z_0 (fig. 11).

The system of four currents found of the same sign and value gives rise within the hyperbolic space to a magnetic

Fig. 11.

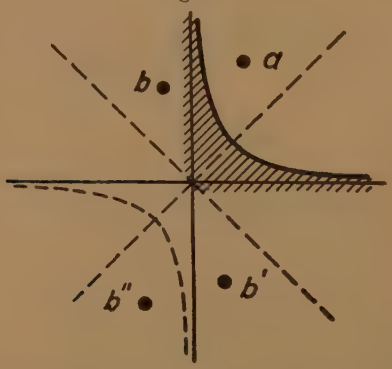

field, which is equivalent to the actual field caused by current a, allowance being made for the influence of the iron surface.

As we note from this example, it is possible to produce an analytic continuation of the field function over the entire plane z on one single sheet.

Let us examine another case.

(b) *The field of a current in a channel bounded by hyperbolic surfaces* (fig. 12).

Supposing that, similarly to the previous example, the equation of hyperbolic surfaces by which the field region is bounded is given in the form of $xy=c$ We will assume, however, the " a " current to be situated in the channel between the two branches of the hyperbolic surface by

which the space filled with iron is bounded. The symmetry transfiguration will have the same aspect as that examined in the previous case (7, 8).

In the event of analytic continuation into the space filled by iron we obtain in region 1′ (fig. 13 *a*) at the symmetric points such values of the field function that are symmetric with the values of the same function in region 1, while in region 2′ we obtain such values of the

Fig. 12.

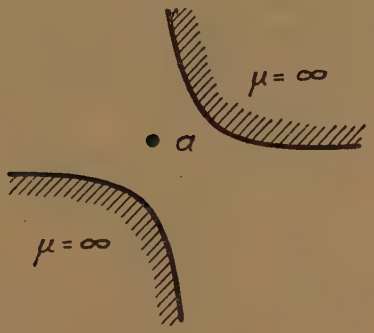

Fig. 13.

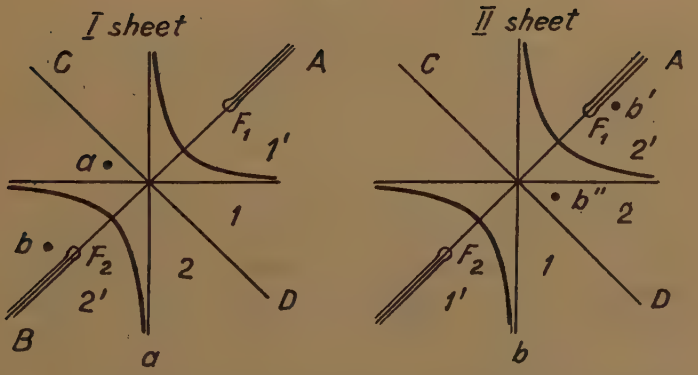

function that are symmetric with its values in region 2. Along the straight lines AF_1 and BF_2 the function sustains in the course of such a continuation a leap. By drawing a cut along these straight lines and continuing the field function on sheet II. (fig. 13 *b*), we obtain on this sheet the same values of the function as on sheet I. at the points turned symmetrically towards the straight line CD.

On these two sheets it appears to be possible to continue the field function uninterruptedly along all paths evading the particular points. One image of the linear conductor with the current "a" appears to be situated on sheet I. (point b), and the two others on sheet II. (points b' and b'').

If we mark the affixes of points F_1 and F_2 as z_1 and $-z_1$, then the function which is single-valued on our two-sheet surface may be obtained in the form of $\sqrt{\frac{z-z_1}{z+z_2}}$, and if we mark the affixes of points a, b, b', and b'' as z_a, z_b, z_b' and z_b'', then, considering that $z_a=-z_b''$ and $z_b'=-z_b$, we obtain the field function in the region lying between the hyperbolic surfaces in the form of

$$\varphi(z)=0{\cdot}2\zeta \ln \left[\left(\sqrt{\frac{z-z_1}{z+z_1}}-\sqrt{\frac{z_a-z_1}{z_a+z_1}}\right)\left(\sqrt{\frac{z-z_1}{z+z_1}}-\sqrt{\frac{z_b-z_1}{z_b+z_1}}\right)\left(\sqrt{\frac{z-z_1}{z+z_1}}+\sqrt{\frac{z_{b'}-z_1}{z_{b'}+z_1}}\right)\left(\sqrt{\frac{z-z_1}{z+z_1}}+\sqrt{\frac{z_{b''}-z_1}{z_{b''}+z_1}}\right)(z_1+z)\right]^2, \quad . \quad . \quad (9)$$

The $\varphi(z)$ function has logarithmic singularities at points a, b, b', and b'', and likewise at the infinitely remote point on both sheets. Consequently, this function complies with the symmetry relatively to the hyperbola curves and represents the solution of our problem.

§ 9. *Combining the Image Method with the Method of Conformal Transformation.*

We have shown on several examples that it is possible to arrive at a simple solution of the problem of field calculation by using the well-known method of images in cases when such a solution could not be previously arrived at by its method. With this object in view we have generalized this method by placing the images on Riemann surfaces whose aspect must be obtained in conformity with the character of the surfaces that are bounding the field region tested. In some cases, however, it is found to be more convenient to combine the image method with the method of conformal transformation, as by so doing it is often possible to solve problems that

are otherwise diffcult to solve. Below we give a practical example of the solution of a problem by this method.

§ 10. *The Field of a Winding placed round an Iron Core.*

The distribution scheme to be calculated is shown in fig. 14. Instead of an actual plane-meridial field we suppose the field to be plane-parallel. We also assume the conductor with current I to be a linear conductor.

A similar problem has already been solved by us in one of our previous works. There, however, we assumed the conductor to be lying directly on the iron surface Currents are then absent in the field region tested. The iron surface was assumed to be an equipotential surface with a leap of the magnetic potential at the point where the current is situated.

Fig. 14.

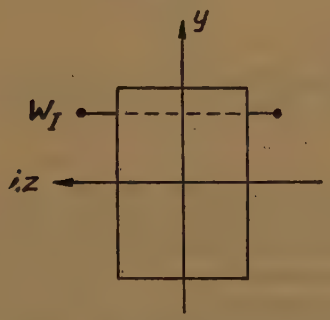

The problem thus put could be solved by the usual methods similar to methods used in solving electrostatic problems. However, in the case shown in fig. 14 some new solution should be found. Let us try to find this solution in form of the analytic function $\phi(w)$ whose real part is the vector potential of the field.

In solving this problem let us avail ourselves of the fact that the "y" axis is the symmetry axis of the field and, therefore, convergent with the direction of the line of vector B of magnetic induction.

We shall examine the field only on one side of the symmetry axis (fig. 15 *a*). The conformal representation of the region bounded by the broken line $-\infty$ ABCD $+\infty$ in the plane $w=y+iz$ on the upper semiplane $\xi=\gamma+i\eta$

(fig. 15 *b*) is given with the aid of the Christoffel-Schwartz formula. It is

$$W = C\left\{(K^2-1)\int_0^{\xi}\frac{dt}{\sqrt{(1-K^2t^2)(1-t^2)}} + \int_0^{\xi}\sqrt{\frac{1-K^2t^{2'}}{1-t^2}}dt, \quad . \quad . \quad . \quad . \quad . \quad . \quad . \quad (10)\right.$$

i. e., the dependence between W and ξ is represented by the sum of the elliptic integrals of the I. and II. kind. The constants C and K are readily found, depending upon the geometric dimensions of the core, and the result obtained may be presented in the form of curves. Equivalent to point W_I, where the conductor carrying the current is situated in region (w), is the point ξ_T in zone (ξ). The lines of vector B enter into the iron (while $\mu = \infty$) perpendicularly to the surface, *i. e.*, on the iron

Fig. 15.

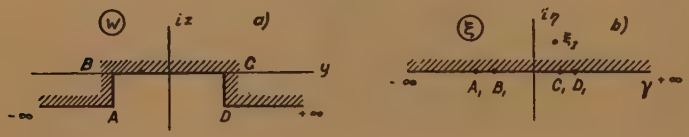

surface the imaginary part of the complex potential may be assumed as being constant. The condition of the constancy of the imaginary part of the complex potential is complied with in our problem along the ABCD line. Equivalent to the broken line ABCD of region (W) is the straight line $A_1B_1C_1D_1$ of region (ξ).

Along the line $D+\infty -\infty A$ in region (W) and the equivalent line $D_1+\infty -\infty A_1$ of region (ξ) the condition of the constancy of the real part of the complex potential is complied with. The function of the complex potential of our problem $\phi(W)$, which is an analytic function in region (W), corresponds to an analytic function $\phi'(\xi)$ in region (ξ). In the upper semiplane of the region (ξ) the function $\phi'(\xi)$ is given by a logarithmic singularity at point ξ_1 and by the condition along the real axis. Let us continue this function into the lower semiplane. The continuation through the segment of the real axis $A_1B_1C_1D_1$ and through the segment $D_1+\infty -\infty A_1$ is different in character owing to the difference in the conditions set in these segments.

At point ξ_{0I}, symmetric with ξ_I, in the first case will be distributed the logarithmic singularity of the same sign as in ξ_I, whereas in the second case the logarithmic singularity has an inverse sign. (This is equivalent to the reflexion of the current with a direct and inverse sign.)

It presents no difficulty to construct either of these two analytic continuations if we introduce in conformity with the double valuedness of function $\phi'(\xi)$ two sheets of plane (ξ) pasted together along the cut drawn between points A_1 and D_1 similarly to the case in figs. 4 and 5.

The problem in region (ξ) results, accordingly, in finding a double-valued analytic function that would have the branching points A_1 and D_1, as well as logarithmic singularities at point ξ_I and ξ_{0I} of both branches in conformity

Fig. 16.

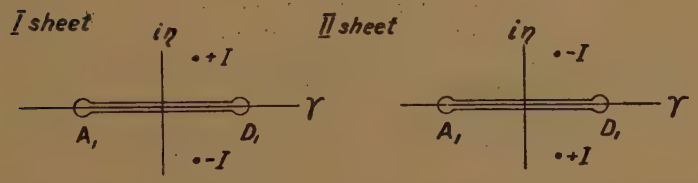

with fig. 16. According to what has been previously stated, such a function is readily found and is expressed as $\phi'(\xi) = 0{\cdot}2\mathrm{I}.\ln$

$$\frac{\left[\sqrt{\frac{\xi-1}{\xi+1}}-\sqrt{\frac{\xi_y-1}{\xi_y+1}}\right]\left[\sqrt{\frac{\xi-1}{\xi+1}}+\sqrt{\frac{\xi_y^0+1}{\xi_y^0-1}}\right]}{\left[\sqrt{\frac{\xi-1}{\xi+1}}-\sqrt{\frac{\xi_y^0-1}{\xi_y^0+1}}\right]\left[\sqrt{\frac{\xi-1}{\xi+1}}+\sqrt{\frac{\xi_y-1}{\xi_y+1}}\right]} \quad . \quad . \quad . \quad . \quad (11)$$

Here it is assumed that the affixes of points D_1 and A_1 ($+1$ and -1) are in agreement with the condition assumed in developing the formula (10) of the representation of region (W) on region (ξ). The formula (10) gives the dependence of W on ξ. By substituting in (11) it is rendered possible to determine $\phi(W)$—the function of the complex potential sought for in the region of the actual field.

§ 11. *The Case of Finite Permeability or the Finite Dielectric Constant.*

In the previous problems the lines of force of the field near the boundary surfaces were directed perpendicularly to the latter. The curves bounding the region occupied by iron could be supposed to be lines of constant value of the real or imaginary part of some function of the complex variable which represented the solution of our problem. If, however, in our problems of calculating the magnetic field we assume that the magnetic permeability of iron has some finite value, or if we examine in the problems of calculating the electric field the charges situated at the interface of two dielectrics with finite values of dielectric constants, then we shall have to impose other conditions upon the behaviour of the lines of force of the field near the interfaces. Such conditions are the continuity of the tangential component and the leap of the normal component of the vector of magnetic or electric intensity. It is well known that several problems, where such a condition exists on the boundary, are solved by the image method †. Below we intend showing that the examination method previously applied by us is also suitable for the solution of problems of this nature and that, consequently, this is a general calculation method covering all cases where a solution is sought for with the aid of reflexion.

§ 12. *Conditions on the Interface of Two Mediums.*

In the problems previously examined, owing to the simple character of the boundary conditions, we were justified in searching for the field in some region without being interested in the field that actually exists beyond its boundaries. In the problems that we have now examined it is necessary, so as to comply with the boundary conditions, to determine the field within the entire region where it exists. Let $\phi_1(z)=u_1+iv_1$, be the field function in some region g_1, occupied by a medium with index (1), and $\phi_2(z)=u_2+iv_2$ be the field function in the region adjoining g_1 which we will mark as g_2. The g_2 region is occupied by a medium with index 2.

† B. Hague, ' Electromagnetic Problems in Electrical Engineering.' Oxford University Press, London, 1929.

In the calculation of the electric field u_1 and u_2 represent the electric potential. In the calculation of the magnetic field these values determine the vector potential of the magnetic field. The condition of the continuity of the tangential component of the electric intensity of the electric field on the interface of mediums 1 and 2 is given as follows

$$\frac{\partial u_1}{\partial t} = \frac{\partial u_2}{\partial t}. \quad \ldots\ldots\ldots \quad (1)$$

This very ratio is equivalent, in the case of a magnetic problem, to the condition of the continuity of the normal component of the magnetic induction vector.

The condition of the leap of the normal component of the electric intensity may be introduced with the aid of the ratio

$$\frac{\partial u_1}{\partial n} = \alpha \frac{\partial u_2}{\partial n}. \quad \ldots\ldots\ldots \quad (2)$$

This ratio is equivalent to the condition of the leap of the tangential component of the vector of magnetic induction. In the electric problem $\alpha = \frac{\epsilon_2}{\epsilon_1}$. In the magnetic problem $\alpha = \frac{\mu_1}{\mu_2}$.

§ 13. *The Construction of Functions complying with Conditions* (1) *and* (2).

Let us present the functions $\phi_1(z)$ and $\phi_2(z)$ each in form of two items :

$$\phi_1(z) = \phi_1'(z) + \phi_2''(z) = (u_1' + iv_1') + (u_1'' + iv_1'')$$
$$\phi_2(z) = \phi_2'(z) + \phi_2''(z) = (u_2' + iv_2'') + (u_2'' + iv_2'')$$
$$\ldots \quad (3)$$

Let us introduce the following condition for the determination of the items of expression (3), making also allowance for the Cauchy-Riemann equations :

$$\frac{\partial u_1'}{\partial t} = \frac{\partial v_1'}{\partial n} = 0 \ldots\ldots\ldots \quad (4)$$

$$\frac{\partial u_2'}{\partial t} = \frac{\partial v_2'}{\partial n} = 0. \quad \ldots\ldots\ldots \quad (5)$$

$$\frac{\partial u_1''}{\partial n} = \frac{\partial v_1''}{\partial t} = 0 \quad . \quad . \quad . \quad . \quad . \quad . \quad . \quad . \quad (6)$$

$$\frac{\partial u_2''}{\partial n} = \frac{\partial v_2''}{\partial t} = 0 \quad . \quad . \quad . \quad . \quad . \quad . \quad . \quad . \quad (7)$$

$$\frac{\partial u_1'}{\partial n} = -\frac{\partial v_1'}{\partial t} = \alpha \frac{\partial u_2'}{\partial n} = -\alpha \frac{\partial v_2'}{\partial t} \quad . \quad (8)$$

$$\frac{\partial u_2''}{\partial t} = \frac{\partial v_1''}{\partial t} = \frac{\partial u_2''}{\partial t} = \frac{\partial v_2''}{\partial t} \quad . \quad . \quad . \quad (9)$$

Expressions (4) . . . . (9) determine the functions $\phi_1(z)$ and $\phi_2(z)$, whose real parts comply with conditions (1) and (2).

$$\frac{\partial u_1}{\partial t} = \frac{\partial u_1''}{\partial t} = \frac{\partial u_2}{\partial t} = \frac{\partial u_2''}{\partial t}$$

$$\frac{\partial u_1}{\partial n} = \frac{\partial u_1'}{\partial n} = \alpha \frac{\partial u_2'}{\partial n} = \alpha \frac{\partial u_2}{\partial n} . \quad . \quad . \quad (11)$$

The functions of field $\phi_1(z)$ and $\phi_2(z)$ are characteristic of the field in region (1) and (2) respectively. Each of them can be continued beyond the boundaries of the region. By using the introduced component functions $\phi_1'(z)$, $\phi_1''(z)$ and $\phi_2'(z)$,$\phi_2''(z)$ the continuation may be produced by the image method. Conditions (4), (5), (6), and (7) are similar to the conditions of the problems whose solutious have already been previously examined by us.

§ 14. *Field Determination in the Case of a Single Reflexion.*

If the interface of the regions g_1 and g_2 represents a circular cylinder or an infinite plane, then we have to deal with a case when the problem may be solved with the aid of a single reflexion. Supposing the source of the field is situated at point " a " of medium 1. Let us mark the intensity of the source as T and determine the function $\phi_1''(z)$ in such a manner that it should have logarithmic singularities equivalent to sources of an intensity of T_1'' of the same sign at point " a " and at point " a_0" symmetric with " a " relatively to the interface, while the real and imaginary parts of $\phi_1''(z)$ are in agreement with ratio 6. $\phi_1'(z)$ we determine in such a manner that it should have logarithmic singularities T_1', positive at

point "a" and negative at point "a_0". Thereby ratio 4 is complied with. We similarly determine functions $\phi_2(z)$ and $\phi_2''(z)$. We determine function ϕ_2'' as having logarithmic singularities T_2'' of the same sign and function, ϕ_2' as having singularities T_2' of different sign at the same points "a" and "a_0". Thereby ratios (5) and (7) will be complied with.

In order that the expressions (8) and (9) should be complied with let us choose

$$T_1''=T_2'' \text{ and } T_1'=\alpha T_2'. \quad . \quad . \quad . \quad (12)$$

$\phi_1(z)$ must have at point "a" a logarithmic singularity equivalent to the source T; $\phi_2(z)$ must have no singularity at point "a_0". These conditions will be complied with if the following ratio is introduced between the quantities examined:

$$\left.\begin{aligned} T_2''-T_2'=0, \\ T_1'+T_1''=T. \end{aligned}\right\} \quad . \quad . \quad . \quad . \quad . \quad (13)$$

On the basis of (12) and (13) we find

$$T_1'=T\frac{\alpha}{1+\alpha},\ T_1''=T_2''=T_2'=T\frac{1}{1+\alpha}.$$

Function $\phi_1(z)$ has at point "a" a singularity which is equivalent to the field source T and a singularity equivalent to the fictitious source $T_1''-T_1'=T\frac{1-\alpha}{1+\alpha}$ at point "a_0." The function $\phi_2(z)$ has a singularity which is equivalent to a source of the intensity of $T_2''+T_2'=T\frac{2}{1+\alpha}$ at a point "a."

The solution obtained fully agrees with the solutions arrived at by other methods of a more particular character. Allowance should also be made for the singularities that may occur at the infinitely remote point of the field.

§ 15. *The Case of Multiple Reflexion.*

In the case of multiple reflexion it is possible to find with the aid of the same formulæ (4) . . . . (9) the field function which complies with conditions 1, 2 on the boundary of two mediums. Additional difficulties, however, are encountered in the endeavour to comply with the

condition of bringing the logarithmic singularities of the function found into agreement with the actual source of the field both as regards the position and the intensity. The cases commonly met are those when the field sources are situated between two interfaces in form of circular cylinders or infinite planes, and they may be easily examined with the aid of our method.

V. *Additional Raman Frequencies for Water. By* I. Ramakrishna Rao *and* P. Koteswaram, *Andhra University, Waltair* *.

[Plate I.]

1. *Introduction.*

NO substance has been the subject of investigation by as many authors as water, and surprisingly, for no other substance is there greater divergence between the results obtained by them. The main cause of this divergence is the large diffuseness of the principal water band whose Raman frequency ranges from 3200–3600. During the course of the last five years, many workers reported having observed a number of high and low frequency bands other than the above for water. A systematic and thorough examination of these frequencies was recently made by Magat † and Hibben ‡.

As workers in this line ever since the discovery of the Raman effect, we were following with interest the results of different experimenters on this problem of water. The new frequencies reported by others were not unnoticed by us, but were rejected as either spurious mercury lines making their appearance during long exposures of the photographic plate, or genuine Raman bands of frequency 3200–3600, excited not by the mercury line assigned by these authors, but arising out of other comparatively feeble lines of the mercury arc. Finding that even systematic investigations of the type of those of Magat and Hibben reveal these new lines, a critical study of the Raman spectrum of water was made by us which confirmed our previous interpretation.

* Communicated by the Authors.
† M. Magat, *Ann. d. Phys.* vi. p. 108 (1936).
‡ J. H. Hibben, Journ. of Chem. Physics, v. p. 166 (1937).

Table I.

Raman frequencies of water as reported by other workers.

Author	Magat.				Bolla *.		Cabbannes & Riols †.	Hulubei ‡.	Others.	Hibben.	
Exciting line ..	4358		2537		2537		2537	2537	2537	2537	
	$\Delta\nu$.	Int.	$\Delta\nu$.	Int.	$\Delta\nu$.	Int.	$\Delta\nu$.	$\Delta\nu$.	$\Delta\nu$.	$\Delta\nu$.	Int.
Raman frequencies	..	..	..	..	60	f	..	..	..	..	..
	152–225	Ff	175	32	172	F	..	..	..	141	1
	600	ff	500	40	510	f	550	..	600 §	440	4
	..	..	740	29	780	f	700	..	..	—	..
	1659	f	1659	?	1645	f	1643	1654	..	1627	3
	..	..	2135	14	2150	ff	..	..	2190 ‖	2170	2
	3221	F	3150	70	3200	F	3224	3233	..	3219	8
	3435	FF	3480	86	3435	F	3436	3443	..	3445	10
	..	..	..	..	3630	Ff	3625	..	..	..	..
	..	..	4023	47	3990	Ff	..	..	..	..	..
	5090	Ff	5100	45	..	..	..	..	..	..	..

FF in the Table indicates a very strong line ; F=strong ; Ff=medium ; f=feeble ; and ff=very feeble.

* Bolla, *Nuovo Cimento*, ix. p. 290 (1930) ; x. p. 101 (1933).
† Cabbanes and Riols, *C. R.* cxcviii. p. 30 (1934).
‡ Hulubei, *C. R.* cxciv. p. 1475 (1930).
§ Segre, *Rendiconti Lincei*, xiii. p. 959 (1931).
‖ Brunetti and Ollano, *Rendiconti Lincei*, xii. p. 252 (1930).

Before giving our results on this subject, the results obtained by others are reproduced in the Table I. to indicate the large discrepancies both in their frequency and intensity values. The table is copied from Magat's * paper, the last column containing the most recent values of Hibben † being the only addition to it.

As regards the results given in the above table, much significance cannot be attached to differences in Raman frequencies between the values of various authors as they arise out of the uncertainty in the location of the maximum of the band, which is more so when they are faint. What is more important is the discrepancy in the relative intensities of the bands as observed by different workers.

The 3200–3600 band is so strong that there is no scope for any doubt as to its assignment. Hence this band will be left out of consideration in the rest of this paper.

2. *Discussion of the Raman Frequencies.*

Frequency 60.—Taking the other frequencies one by one, Bolla obtained a faint one equal to 60 by excitation by the 2537 line of the mercury arc. It was not observed by others. A perusal of the microphotometric curve of the spectrum of the direct mercury arc, given in fig. 1 (Pl. I.) clearly indicates a strong continuous band with a number of discontinuities accompanying the 2537 line marked in the figure. As the above Raman line falls within the region of the continuous band, any one of the discontinuities may be construed to be a Raman line. These discontinuities correspond to a number of faint mercury arc lines, which may appear with considerable intensity in the spectrum of the light scattered by water. Thus the presence of a line in this region in the Raman spectrum of water does not necessarily indicate that it is a Raman line. The genuineness of this line is therefore very doubtful.

Frequencies 162–225 and 600.—For these two Raman frequencies, even Magat's results with excitation by the 4358 and 2537 lines are inconsistent among themselves. While by excitation by the 4358 line the latter frequency is much fainter than the former, with the 2537 line they are of the same order of intensity. Actually the relative intensities of these must be the same irrespective of the

* M. Magat, *Ann. d. Phys.* vi. p. 108 (1936).

† J. H. Hibben, Journ. of Chem. Physics, v. p. 166 (1937).

exciting line. This is a clear indication that there is something wrong with the assignment made by Magat. On comparing Magat's result with that of Hibben, who also claims to have observed these frequencies, the latter finds that the frequency equal to 600 is about four times the intensity of the former. We have taken the spectrum of the direct mercury arc with a spectrograph of large dispersion in the region between 4358 and 4916 and found, on very long exposure, a number of very faint lines with frequency shifts up to 600 from the 4358 line. Magat might have observed them in the Raman spectrum of water and might have assumed them to be genuine Raman lines.

As regards the same frequencies obtained by the 2537 excitation, there is, in this region, a number of mercury lines of wave-lengths 2540, 2545, 2549, 2556, 2572, 2576, and 2578 with frequency shifts ranging from 59 to 638 rom the 2537 line. Superposed on these there are the following Raman bands of water: the 3200–3600 band excited by the 2345 line of the mercury arc, the 1650 band excited by the 2464 line, and the 3200–3600 one excited by the 2378 line. We believe that the maxima with frequency shifts from the 2537 line equal to 175, 500, and 700 are really the maxima indicated above, and not any genuine Raman lines of low frequency excited by the 2537 line. The high intensities of these Raman lines indicated by other observers seem to arise out of this superposition. In the microphotometric curve of the Raman spectrum of water in this region given in fig. 1 (Pl. I.), and also in the curves given by both Magat and Hibben, all these bands are so mixed up that a continuous band is obtained with intensity gradually diminishing from the 2537 line to the larger wave-length side.

An additional band, unresolved in the microphotometric curves (which have a smaller magnification than ours) given by the above two authors, is apparent in our diagram and is marked with an arrow. Its frequency shift from the 2537 line is 1145, and if resolved in their curves it would have been assigned by them as another new Raman line with the above frequency. It is, however, the 3200–3600 band excited by the strong 2399 line of the mercury arc.

Frequency 1650.—The only line for which the results

of all the observers are consistent is this. Unfortunately, it falls in inconvenient regions for excitation by all mercury lines. This is perhaps the reason why it escaped detection for a long time, though it was known to be a fundamental frequency for water. Corresponding to its excitation by the 4358 line, it falls in the same region as the strong 3200–3600 band excited by the 4047 line. This is much fainter than the other band, and hence even the use of filters to cut off the 4047 line was not effective in bringing it out with large intensity, as even the feeble transmission of the 4047 line by the filters may be sufficient to bring out its corresponding Raman band with sufficient intensity to mask the 1650 line.

Corresponding to excitation by the 4047 line, it falls in the region of the strong 4358 mercury triplet. Similarly, for every other exciting line of the mercury arc in the ultra-violet, it is either masked by the 3200–3600 band excited by the neighbouring mercury lines or by the fainter lines of the mercury arc itself.

In the case of excitation by the 2537 line, however, though the 1650 Raman band falls over the 2640 line of mercury, the difference in the diffuseness of this place in the Raman spectrum and that of the direct mercury arc, indicates the irrefutable presence of this band, and though the bands of frequency 3200–3600 excited by the 2447 and 2467 lines fall in this region, the latter are so faint that their superposition may be ignored. Thus, this is the only frequency among all those mentioned by others which is, in our opinion, genuine.

Frequency 2150.—In Magat's values, though the intensity of this band, as excited by the 2537 line, is as much as 14, he did not find it at all with the 4358 excitation. If it were really a 2150 band, for excitation by the 4358 line, it should fall at 4811 Å.U., which is a region free from any mercury lines, and should therefore be noticeable. The fact that it is not found either by us or by Magat is sufficient indication as to the incorrectness of the assignment.

This band, obtained by Magat and others with a frequency shift of about 2150 from the 2537 line, is actually the result of the supperposition of the two Raman bands of frequency 3200–3600 excited by the strong mercury lines 2482 and 2464. The larger width of this band in our microphotometric curve (fig. 1, Pl. I.) compared to the width

of other bands in this region, is a clear indication of its excitation by two mercury lines. The large intensity of this band indicates that it should be a strong Raman band excited by a strong mercury line, and not a feeble one excited by the 2537 line as explained by others.

Frequency 4023—This band of Magat has been mentioned by no other worker except Bolla. According to Magat, this is a very strong band of intensity 47 when excited by the 2537 line, but is not to be found at all with excitation by any other line, though corresponding to the 3650, 4047, and 4358 excitations, it should fall at 4283, 4835, and 5286 Å.U. regions which are perfectly free from any mercury lines. It may be argued that this band corresponding to 4358 is in a region which is insensitive to the photographic plate, but no argument can explain its absence in the case of excitation by the other two lines. The only possible explanation for this anomaly is that Magat's assignment is wrong, the band with a frequency shift of 4023 from the 2537 line being excited, not by this mercury line as reported by him, but only the 3200–3600 band excited by the strong 2576 line, the effect of which seems to be ignored by all other observers including Magat and Hibben. The correctness of our assignment will be evident from Table II.

Frequency 5100.—This is mentioned only by Magat as having been excited by the 2537 as well as the 4358 lines. The band corresponding to the latter falls between the green line and the yellow doublet of the mercury arc. The continuous spectrum itself in this region is sufficiently large to mask any Raman line or band, and the presence of some mercury lines in this region may be easily construed to be a genuine Raman band. Excited by 4047 line, this falls in nearly the same position as the 3200–3600 band for the 4358 line. Hence no definite conclusion can be reached from this result. But the absence of its excitation by the 3650 group of lines is again a clear indication of the wrong assignment of Magat. If this frequency was a genuine one, it should appear at 4485 Å.U. corresponding to the 3650 group. This being, according to Magat, a strong Raman frequency of intensity 45, it should be clearly observed in the region between the 4358 and 4916 line of the mercury arc. But not even the faintest trace of it is found by us and Magat does not mention it at all.

As regards the real origin of this band appearing in the Raman spectrum of water in the ultra-violet, it is the 3200–3600 excited by the strong mercury triplet at 2652 Å.U. This assignment will be evident from Table II.

The following table contains the comparative statement of the assignment of other workers given side by side with ours. The first column contains the frequency shift of the observed Raman band from the 2537 line of the mercury line. These shifts were considered to be genuine Raman frequencies by the other workers. In

TABLE II.

Assignment of other workers.			Our assignment.		
$\Delta\nu$.	ν_{Hg}.	ν_R.	λ_{Hg}.	Hg.	$\Delta\nu_R$.
175 (32)	39412	39237	2345 (4)	42622	3385
740 (24)	....	38672	2378 (5)	42032	3360
2150 (14)	....	37262	2464 (4)	40570	3308
....	....	....	2482 (6)	40276	....
3200 3400 (80) 3600	....	36012	2537 (10 R)	39412	3400
4023 (47)	....	35389	2576 (6)	38803	3414
5100 (45)	....	34312	2652 (8)	37695	3383
500 (40)	....	38912	2464 (4)	40571	1659
1659 (?)	....	37753	2537 (10 R)	39412	1659
1145*	....	38267	2399 (8)	41633	3396

the second column is given the frequency of the 2537 line which is supposed by them to excite these frequencies. The third column represents the actual frequencies of the Raman bands. The other columns in the table give respectively the correct mercury arc lines (exciting these bands), their frequencies, and the differences between the values in columns 5 and 3, which give the actual Raman frequencies according to our assignment. The values given within brackets are the intensities.

* This Raman band was not pointed by other workers. It is noted for the first time by us, but represents only the 3200–3600 band excited by the strong 2399 line of mercury.

3. *Discussion of the Results.*

The values in the last column of the table are nearly equal to one another and clearly represent the same frequency which corresponds to that of the central maximum of the principal Raman band of water. Taking into consideration the diffuseness of these bands and the possibility of the superposition of a number of mercury lines over them, which may give rise to a shift in the position of the maxima, the differences are within the order of accuracy of fixing this position. The table irrefutably supports our view-point that the Raman lines observed by the different authors correspond, not to different frequencies natural to the water molecule arising out of a single exciting line, but actually to the same Raman frequency arising out of different lines of the mercury arc.

The 2537 line is no doubt very strong for exciting Raman lines, but, accompanied as it is by a large number of both strong and weak mercury lines on its longer and shorter wave-length sides, is most unsuitable for analysis of the Raman spectrum of a substance like water which gives very broad and diffuse bands. It is really a surprise to us as to how all these observers ignored the possibility of excitation by the neighbouring lines. The fact that not even a trace of these new frequencies is to be found by excitation with other equally strong mercury lines like the 3126–32 doublet, the 3650 triplet, and the 4047 line is sufficient to prove the incorrectness of their assignments. As regards the bands observed with the 4358 excitation, arguments were already given taking the frequencies one by one. Thus in spite of the fact that the concensus of opinion of the other observers is in favour of these new frequencies, we are obliged to contradict them on account of the strong evidence in favour of our interpretation.

4. *Effect of Temperature and Addition of Electrolytes.*

Another argument put forward in support of these new frequencies is the changes observed with temperature and addition of electrolytes. We reproduce in fig. 1 (Pl. I.) the microphotometric curves of the Raman spectra of water at 37° and 90° C. The changes in the intensity of the bands reported by Magat are not noticed

in our curves at all, and as such, the question of explaining his results does not arise. In this connexion, it may be pointed out that the curves reproduced by Hibben are themselves inconsistent with those of Magat. There is closer agreement between the curves of Hibben and our own. The slight changes in intensity attributed by Hibben to suppression of these additional frequencies at the higher temperature may partly arise out of changes in the distribution of intensity of the 3200–3600 band, and partly out of changes in the intensities of the superposed Rayleigh lines from one temperature to another.

The above arguments hold good to explain the results of Hibben with solutions of electrolytes.

5. *Summary.*

A number of workers have reported the following Raman frequencies for water :—60, 175, 500, 700, 1650, 2150, 3200, 3400, 3600, 4023, and 5100. A critical study of the intensity and frequency values of the Raman bands of water in both the visible and ultra-violet regions of the spectrum, is found by us to reveal that all these are not bands of different Raman frequencies excited by the same mercury line, but correspond to the same principal Raman band of water of frequency 3200–3600 arising out of different strong lines of the mercury arc, the excitation by which was ignored by them. The only genuine frequency other than this being at 1650, which happens to be the other fundamental for water.

VI. *The Infra-red Absorption Spectrum of Phosgene.*

By C. R. Bailey *and* J. B. Hale, *University College, London* *.

THE spectroscopic data for carbonyl chloride are scanty. The Raman spectrum has been explored by Dadieu and Kohlrausch [1], and by Henri and Howell [2], who also examined the ultra-violet region [3], while a preliminary examination in the infra-red up to $4{\cdot}5\,\mu$ was made by Marton [4]. The present investigation covers the region from 1 to $20\,\mu$.

* Communicated by Prof. F. G. Donnan, F.R.S.

Experimental.

The apparatus, consisting of a spectrometer provided with quartz, fluorite, rock-salt, and sylvine prisms, giving direct energy readings by means of a thermopile and a photo-relay, has been adequately described before [5], [6], [7]. The phosgene was taken from a commercial cylinder and dried with P_2O_5; it was used in the vapour state.

The infra-red data are collected in Table I.; the intensities are given in arbitrary units and are only approxi-

TABLE I.

The Infra-red Spectrum of $COCl_2$ Vapour.

Band.	Band centre. λ (μ).	Band centre. ν (cm.$^{-1}$).	Intensity.	Slit width (cm.$^{-1}$).	Prism.
A_1	2·755	3630	12	24	Fluorite.
A_2	3·270	3058	1	21	,,
A_3	3·597	2780	1	18	,,
	3·685	2714	2	18	,,
B	4·281	2336	11	14	,,
C	4·849	2062	10	11	,,
D	5·474	1827	95	8	,,
E	6·004	1666	80	7	,,
F	7·131	1403	60	6	,,
G	7·78	1285	4	13	Rock-salt.
H	8·64	1157	21	10	,,
I	9·91	1009	90	7	,,
K	11·84	845	100	6	,,
L	13·40	746	10	3	,,
	13·60	735	10	3	,,
M_1	14·32	698	7	3	,,
M_2	15·15	660	17	5	Sylvine.
N	17·35	576	90	3	,,
	17·75	563	78	3	,,

mate. The general appearance of the spectrum is shown in fig. 1, and fig. 2 gives many of the bands under the higher resolution afforded by chosen pressures and appropriate prism materials. The individual bands do not call for description, since, with the possible exception of the band L at 741 cm.$^{-1}$, no structure has been revealed.

Note.—Throughout the following all frequencies are in wave numbers (cm.$^{-1}$), interatomic distances in Ångstroms (1×10^{-8} cm.), and force constants in dynes per cm. $\times 10^5$.

Assignments.

The molecule belongs to the symmetry group C_{2v}; there being no axis of symmetry of order greater than two, vibrational degeneracy is absent, and we must

Fig. 1.

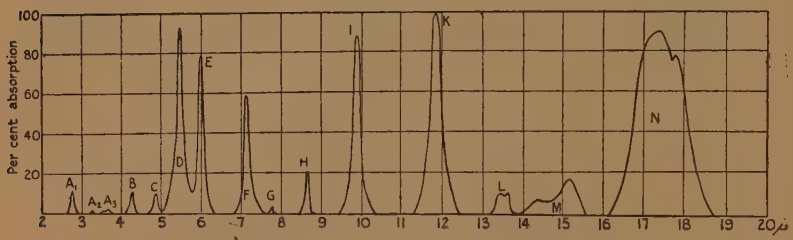

The infra-red absorption spectrum of phosgene.

Fig. 2.

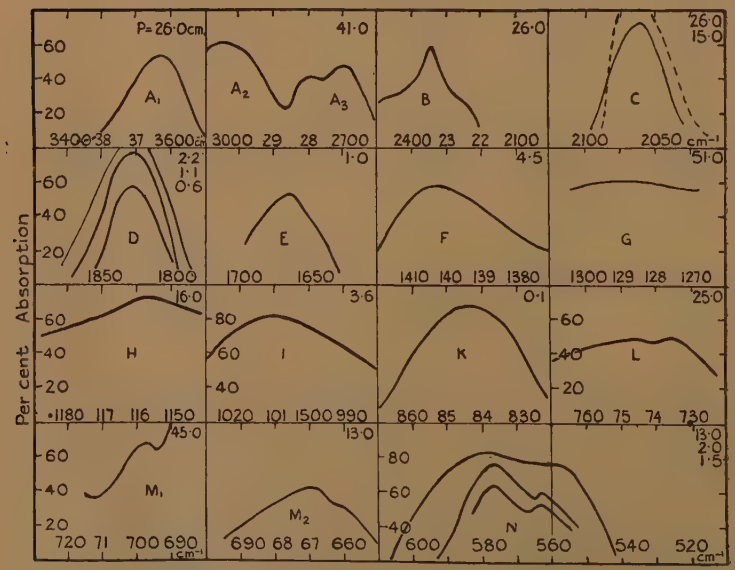

The individual infra-red bands of phosgene.

expect six modes, active in both Raman and infra-red. If the molecule is as represented in fig. 3 we have three modes, $\omega_{1,2,3}$, totally symmetrical with respect to the planes $\sigma(xy)$, $\sigma(yz)$: two, $\omega_{4,5}$, antisymmetrical with

respect to $\sigma(yz)$; and one, ω_6, perpendicular to the molecular plane $\sigma(xy)$. The modes are shown in fig. 4. We can at once place ω_1, the C=O frequency, as 1827 cm.$^{-1}$ in the infra-red, the liquid giving the Raman value of 1810 cm.$^{-1}$.

Help in assigning the other bands is obtained from the models constructed by Trenkler for four-mass systems [8]. It will be seen from these that motion in ω_1 is confined almost entirely to the carbon and oxygen atoms, while

Fig. 3.

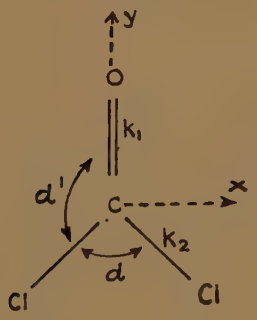

Fig. 4

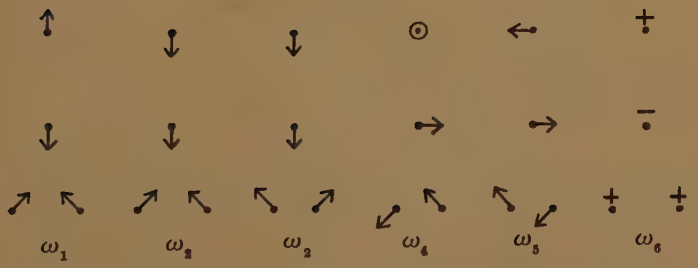

in ω_4 the oxygen atom is still. Hence ω_4 is in effect the asymmetric vibration of the triatomic grouping CCl_2, with ω_2 and ω_3 very close respectively to the corresponding high and low symmetric vibrations. The calculations below confirm the choice of 845 cm.$^{-1}$ for ω_4, 576 cm.$^{-1}$ for ω_2 and probably both ω_3 and ω_5 at 300 cm.$^{-1}$, in agreement with the infra-red and Raman intensities. This leaves 444 cm.$^{-1}$ as the bending frequency ω_6.

These assignments had been made and the work completed for publication when polarization measurements for the Raman spectrum were published by Anan-

thakrishnan [40]. They confirm the suggested assignment in preference to that of Kohlrausch [13] or Mecke [27], since the first three vibrations, $\omega_{1,2,3}$, are polarized ($\rho > 6/7$), the second three depolarized ($\rho = 6/7$).

The two spectra are summarized in Table II.

TABLE II.

I.R. (g) (cm.$^{-1}$).	Raman (l) (cm.$^{-1}$).	Mode.	Calc. (cm.$^{-1}$).
3630	....	$2\omega_1$	3654
3058	....	$2\omega_1 - \omega_2$	3078
		$\omega_1 + 2\omega_2$	2979
2780	....	?	
2714	....	$\omega_1 + 2\omega_6$	2715
2336	....	$\omega_1 + \omega_2$	2403
2062	....	$\omega_1 + \omega_{3,5}$	2127
		$\omega_6 + 2\omega_4$	2134
1827	1810 (P)	ω_1	—
1666	....	$2\omega_4$	1690
1403	....	$\omega_2 + \omega_4$	1421
		$\omega_2 + 2\omega_6$	1459
		$\omega_3 + 2\omega_2$	1452
1285	....	$\omega_2 + \omega_6$	1285
1157	....	$2\omega_2$	1152
		$\omega_2 + 2\omega_6$	1188
1009	....	$\omega_2 + \omega_6$	1020
845	834 (D)	ω_4	—
		$\omega_2 + \omega_{3,5}$	871
746, 735	....	$\omega_6 + \omega_{3,5}$	744
698, 660	....	$2\omega_{3,5}$	600 ?
576, 563	571 (PP)	ω_2	—
	444 (D)	ω_6	—
	300 (P)	$\omega_{3,5}$	—

PP = strongly polarized ; P = polarized ; D = depolarized.

The above assignments agree in the more important respects with those suggested by Corin [26].

The Force Constants.

Lechner [9] has considered the vibrations of the various possible configurations for a four-mass system. Using modified valence forces he obtains the following expressions for the frequencies of molecules of the phosgene type :—

$$\lambda_1 . \lambda_2 . \lambda_3 = k_1 . k_2 . (2d + d') \left(\frac{s}{s_{13}} \right)^2 . D.$$

$$\lambda_1\lambda_2+\lambda_1\lambda_3+\lambda_2\lambda_3=k_1.k_2.\mathrm{E}+k_1(2d+d')\left(\frac{s}{s_{13}}\right)^2.\mathrm{F}$$
$$+k_2(2d+d')\left(\frac{s}{s_{13}}\right)^2.\mathrm{G}.$$

$$\lambda_1+\lambda_2+\lambda_3=k_1.\mathrm{H}+k_2.\mathrm{I}+(2d+d')\left(\frac{s}{s_{13}}\right)^2.\mathrm{K}.$$

$$\lambda_4.\lambda_5=k_2.d'\left(\frac{s}{s_{13}}\right)^2\mathrm{A}.$$

$$\lambda_4+\lambda_5=k_2.\mathrm{B}+d'\left(\frac{s}{s_{13}}\right)^2\mathrm{C}.$$

Here A, B, C, etc. are functions of the masses, distances and angles of the molecule, and may be found in the original paper. $\lambda_i=4\pi^2c^2.\omega_i^2/\mathrm{N}=5{\cdot}863\times10^{-2}.\omega_i^2$; k_1, k_2, d and d' are as in fig. 3. s_{12} is the carbon-oxygen distance, s_{13} the carbon-chlorine distance, s is taken as the mean of the two, and N is the Avogadrian number. Electron diffraction measurements [10] give C–O = 1·28 ± ·03, C–Cl = 1·68 ± ·02 and the angle Cl–C–Cl = 117 ± 2°: the absolute values are not critical. Inserting the frequencies given in Table II., it is possible to obtain approximate values for the force constants; we find $k_1=12{\cdot}14$, $k_2=2{\cdot}27$, $d=1{\cdot}05$, $d'={\cdot}20$. Calculating back from these values we obtain $\omega_1=1834$ (obs. 1827), $\omega_2=543$ (obs. 576), $\omega_3=316$ (obs. ? 300), $\omega_4=836$ (obs. 845), and $\omega_5=299$; the force system chosen thus satisfactorily represents the molecule, with the exception that λ_6 vanishes.

The double nature of the band at 17·5 μ may, perhaps, be due to the isotope effect. The abundance ratio of the molecules $CO^{35}Cl_2$, $CO^{35}Cl^{37}Cl$, and $CO^{37}Cl_2$ is approximately 9 : 6 : 1; Salant and Rosenthal's expression [11] for the parallel frequencies ω_1 and ω_2 of the triatomic molecule may be applied with reasonable approximation to the phosgene frequencies ω_2 and ω_3. We have

$$\frac{\Delta\omega_2}{\omega_2}+\frac{\Delta\omega_3}{\omega_3}=\frac{-(\mu+1)\Delta m}{2(2m+\Delta m)},$$

μ being M/(2m+M); if the C and O masses are considered as moving together (=M) in these two vibrations we obtain $\Delta\omega_2+1{\cdot}9\,\Delta\omega_3=-10{\cdot}2$ cm.$^{-1}$ for the sum of the parallel isotopic shifts in the molecules $CO^{35}Cl_2$ and

$CO^{35}Cl^{37}Cl$. A rough trial with the values of k_2 and d obtained above shows $\Delta\omega_3$ to be of the order of 2, and $\Delta\omega_2$ will then be about 6. The observed difference between the peaks is 13 ; the lack of agreement is probably due to the overlapping of the bands. The relative intensities of 3 : 2, however, are approximately correct. The shift for the perpendicular frequency at 845 cm.$^{-1}$ is about 3 cm.$^{-1}$, which would not be seen in the conditions of experiment.

Comparison with other Molecules.

Phosgene, formaldehyde, urea, ethylene, and tetrachlorethylene have certain configurative resemblances, and the related molecular constants may be summarized in Table III.

The data provide a test for the general theory that the molecular forces characteristic of certain groupings remain constant in the passage from one molecule to another. Innumerable Raman spectra testify to this phenomenon as far as the simplest diatomic groups are involved. The extension to polyatomic groups has been treated by Sutherland and Dennison [23], and by Miss Rosenthal in a number of papers [22], [24]. It will be seen that on the whole there is a satisfactory persistence of force constants, distances, and frequencies throughout the table. The force constant, the type of linkage, and the interatomic distance are related, and many formulæ have been devised to express the relationship. Douglas Clark [29] has examined a number of these, and as a rule very close agreement is to be obtained between the calculated and observed interatomic distances when the force constants are known. In particular the modified Badger expression [30], $r_e=(C_{ij}/k_e)^{\frac{1}{3}}+d_{ij}$, is of wide application, and where the constants C_{ij} and d_{ij} are accurately known gives reasonably good results. It is interesting to note that the Badger relationship fails to the extent of about 8 per cent. in the carbon-carbon linkages, the estimated value of the interatomic distance, r_e, being in all cases too small. Table IV. exemplifies this.

It seems safe to apply the rule when carbon is linked to another element : amongst the diatomic molecules we have k_e for CO $=18{\cdot}8$, for CN $=16{\cdot}2$; the calculated and observed values for r_e agree in both cases at 1·14 and 1·17 respectively.

TABLE III.

Molecular Constants of Phosgene and Associated Molecules.

	$COCl_2$.	COH_2.	$CO(NH_2)_2$.	C_2Cl_4.	C_2H_4.	CCl_4.	CH_4.
ν_{CO}	1827	1744 [12]	1655 [13]	—	—	—	—
$\nu_{C=C}$	—	—	—	1570 [14]	1621 [15]	—	—
ν_{CX_2} (a).....	834	2974	1157	862 [28]	3019	—	—
ν_{CX_2} (s).....	576	2874	1001	446 ?	2988	—	—
δ_{CX_2} (s).....	300 ?	1503	586	235	1444	—	—
r_{CO}	1·12 [16] / 1·28 [10]	1·15 ? [17]	1·25 [18]	—	—	—	—
r_{CX}	1·80 [16] / 1·68 [10]	1·04 ?	1·37 [18]	1·74 [10], [25]	1·04 [19]	1·76 [21], [25]	1·06
$r_{C=C}$	—	—	—	1·38 [10]	1·37 [19]	—	—
k_{CO}	12·14	12·0	(10·2)	—	—	—	—
$k_{C=C}$	—	—	—	6·15 [20]	9·79 [23]	—	—
k_{CX}	2·27	4·4	(5·5)	4·48 [33]	4·37 [23]	3·61 [22]	4·92 [22]

If these relationships are to be used for the purpose of recognizing the existence and extent of resonance among possible structures the force constants must be known to a high degree of accuracy, and true weight must be given to the type of potential function assumed in evaluating the frequencies. Thus the Urey and Bradley force-field offers a convenient method of handling tetrahedral pentatomic molecules, such as CCl_4 [31], but since the molecule is represented as being in a state of strain the force constant for the C—Cl link does not correspond to the equilibrium atomic separation. It is necessary to apply a correction for the strain, which raises the value of the force constant from 1·74 to 3·85 according to Urey and Bradley's calculations. The real value is difficult to ascertain. Miss Rosenthal's estimates [22] show that

TABLE IV.

The Observed and Calculated Carbon-carbon Distances.

Link.	k.	r_e. (Badger)	r_e. Obs.	Ratio.
C—C	4·96	1·40	1·54	1·10
Benzene	7·6	1·30	1·39	1·07
C=C	9·8	1·25	1·37	1·10
C≡C	14·9	1·18	1·28	1·06

it must lie between 2·64 and 6·24, with the probable value of 3·61. Now the corresponding value for methane is 4·92 ; if we assume that the breathing frequency, $\omega_1 = 2915$, does not involve interaction between the hydrogen atoms, we can determine k from the relationship $k = 5{\cdot}863 \times 10^{-2} . m\,\omega_1^2$ as 5·01, in close agreement. For CCl_4, however, with $\omega_1 = 467$, $k = 4{\cdot}54$, while Badger's rule for an interatomic separation of 1·76 gives $k = 2{\cdot}78$.

Linnett and Thompson [32] have proposed using values of the force constants in tetrachlorethylene, C_2Cl_4, compared with those of carbon tetrachloride, to show the presence of a considerable contribution from structures of the type

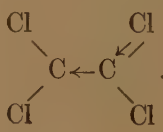

A shortening of the C—Cl bond and a lengthening of the C=C bond are thus to be expected, together with corresponding modifications in the force constants. Unfortunately even the comparatively refined methods of electron diffraction cannot distinguish between a supposed C=C separation in ethylene of 1·37 and in C_2Cl_4 of 1·38 (assumed by Brockway, Beach and Pauling [10]); the lengths of the C—Cl link in CCl_4 and C_2Cl_4 again are respectively 1·76 and 1·74, but the difference is hardly outside the experimental error. The potential functions designed by Sutherland and Dennison [23] and by Delfosse [35] have been applied to C_2H_4 and C_2Cl_4 by Duchesne [20], [33] with the result that the C=C force constants are 9·79 and 6·15 respectively; if we assume that the force constant 9·79 for ethylene gives a corrected C=C distance of 1·37 from the Badger relationship, then the C_2Cl_4 force constant would correspond to a distance of 1·45. Such an increase represents on Pauling's well-known curve [34] a 75 per cent. single bond effect!

The Raman spectra of a very large number of ethylenic compounds have been examined by Bourguel [36] and others, and, apart from a slight variation between the extreme limits of about 1650 to 1560—that is, of the order of 5·5 per cent.—the ethylenic frequency remains remarkably constant. This is the type of effect shown in Trenkler's models, particularly as in the case of ω_1 for phosgene cited above, and it seems that the expressions used to describe the potential energy do not take enough account of the lack of influence of the external masses on this frequency. Indeed, if we neglect the external atoms altogether we obtain from 1621 cm.$^{-1}$ for C_2H_4, $k_{C=C}=9{\cdot}25$, and from 1569 cm.$^{-1}$ for C_2Cl_4, $k=8{\cdot}66$, the corresponding interatomic separations being 1·37 and 1·38 as expected.

There is an additional effect neglect of which may possibly lead to wrong interpretation of results. The energy expression for any vibrational level in a polyatomic molecule is of the type

$$\begin{aligned} E_{000}=&X_1V_1+X_2V_2+\ldots\\ &+X_{11}V_1^2+X_{22}V_2^2+\ldots\\ &+X_{12}V_1V_2+X_{23}V_2V_3+\ldots, \end{aligned}$$

where $V_i=(n_i+\frac{1}{2})$, n_i being the quantum number for the ith vibration, and X_i=frequency of ith vibration. If

there is a high degree of anharmonicity, and if there is considerable interaction between modes, indicated by large values of X_{ii} and X_{ij} respectively, then the observed value for any fundamental may depart largely from the values for infinitesimal amplitude: and since it is the latter values which strictly should be used in the potential energy expressions, force constants derived by neglect of this consideration may appear considerably smaller than they really are.

We have carefully examined various force systems for the three molecules phosgene, formaldehyde, and urea, and for purposes of comparison have adopted one in which the motion in ω_1 is regarded as being, in accordance with experiment [8], confined largely to carbon and oxygen, the external atoms remaining fixed; it will be seen that the concordance is satisfactory. The calculations show that some reconciliation is necessary between the results of electron diffraction, X-ray analysis, and vibrational frequencies.

Thus Pauling [34] ascribes some 28 per cent. double bond character to the C–N link in urea, in accordance with Wyckoff and Corey's X-ray measurements [18] of C−N=1·37; but at the same time these two investigators give the C=O link as 1·25, which is less than Pauling's normal double bond value of C=O=1·28, whereas, if the first hypothesis is true, there should be a marked single bond contribution. Again, Pauling allots a 17 per cent. double bond character to the C−Cl link in phosgene, and then takes the C=O link in this compound as a normal double bond. Formaldehyde, according to Bru [17], has C=O=1·15, while for phosgene Dornte [16] gives C=O=1·12: these results may be a little too low, but qualitatively their indications are correct, since it seems certain from the position and intensity of the CO frequency in phosgene as compared with formaldehyde that if the latter, as it is reasonable to suppose, contains a normal double bond C=O, then in phosgene there must be a considerable triple bond effect.

We find that the modified potential energy expression which regards the motion in ω_1 as being confined largely to the C and O atoms gives k_{CO} for phosgene, formaldehyde and urea as 12·3, 11·5, and 10·2 respectively, with the corresponding interatomic distances by Badger's rule of

1·21, 1·23, and 1·25, the last being in agreement with Wyckoff and Corey's result. The force constants for the link between carbon and an external atom (Cl, H, or N) are for phosgene 2·27 (C_2Cl_4=4·48, CCl_4=3·61), for formaldehyde 4·4 (C_2H_4=4·37, CH_4=4·92), for urea 5·5 (*cf.* tetraethylammonium iodide [41], ω_1=1466, $k \triangleq 3{\cdot}6$). The closeness between the force constants in the case of formaldehyde and its related compounds enables one to make reasonable deductions concerning the links in the other groups of compounds. For the nitrogen compound, k=5·5 corresponds to r_e (C—N)=1·38 (found [18] 1·37), which agrees with Pauling's estimate of 17 per cent. double bond contribution; $k \triangleq 3{\cdot}6$ for $N(C_2H_5)_4I$ corresponds to r_e(C—N)=1·48, while Pauling's table [37] gives 1·47 and electron diffraction for trimethylamine [38] gives C—N=1·5.

In guanidonium chloride, $C(NH_2)_3$. Cl, the resonance is complete: the breathing frequency is 1006 [42], which gives a force constant $k+2k'$=9·5. In plane equilateral triangular molecules k' for the interaction of the C—NH_2 links is of the order of 1, so that k for this link is not far removed from 7, and the C—N distance will be near 1·3. Theilacker [39] by X-ray methods finds C—N=1·18, but this value is probably too small, since the double bond C=N from Pauling's table must lie near 1·32, and the 33⅓ per cent. double bond contribution in the guanidonium ion will result in an interatomic distance of about 1·35.

With the true C—Cl distance as 1·76, k=4·48 from C_2Cl_4 gives C—Cl as 1·68 (Pauling [10] finds 1·68), k=2·27 from phosgene gives C—Cl as 1·89. As an absolute value this may be too high, but relatively there seems no doubt that the C—Cl distance in phosgene is greater than the normal, while the C=O distance is less, in conflict with Pauling's electron diffraction measurements. Hence it seems likely that the structure

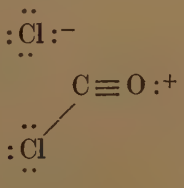

makes a more important contribution to the ground state than does

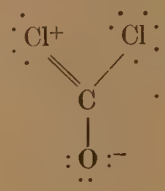

References.

(1) Dadieu, A., Kohlrausch, K. W. F., *Wien. Ber.* cxxxix. p. 717 (1930).
(2) Henri, V., Howell, O. R., Proc. Roy. Soc. A, cxxviii. p. 190 (1930).
(3) Henri, V., Howell, O. R., *ibid.* p. 192.
(4) Marton, L., *Zeits. f. physikal. Chem.* cxvii. p. 97 (1925).
(5) Bailey, C. R., Cassie, A. B. D., Angus, W. R., Proc. Roy. Soc. A, cxxx. p. 134 (1930).
(6) Cassie, A. B. D., Bailey, C. R., *ibid.* cxxxii. p. 252 (1931).
(7) Bailey, C. R., Thompson, J. W., Hale, J. B., J. Chem. Phys. iv. p. 625 (1936).
(8) Trenkler, F., *Physikal. Zeits.* xxxvi. p. 423 (1935).
(9) Lechner, F., *Wien. Ber.* cxli. p. 634 (1932).
(10) Brockway, L. O., Beach, J. Y., Pauling, L., J. Amer. Chem. Soc. lvii. p. 2693 (1935).
(11) Salant, E. O., Rosenthal, Jenny E., Phys. Rev. xlii. p. 812 (1932).
(12) Nielsen, H. H., Phys. Rev. xlvi. p. 117 (1934).
(13) Kohlrausch, K. W. F., Pongratz, A., *Zeits. Phys. Chem.* B, xxvii. p. 176 (1934).
(14) Heidenreich, F., *Zeits. Physik*, xcvii. p. 277 (1935).
(15) Bhagavantam, S., ' Nature,' cxxxviii. p. 1098 (1936).
(16) Dornte, R. W., J. Amer. Chem. Soc. lv. p. 4128 (1933).
(17) Bru, L., *Anal. Fis. Quim.* xxx. p. 483 (1932).
(18) Wyckoff, R. W. G., Corey, R. B., *Zeits. Krist.* lxxxix. p. 462 (1934).
(19) Badger, R. M., Phys. Rev. xlv. p. 648 (1934).
(20) Duchesne, J., ' Nature,' cxxxix. p. 288 (1937).
(21) Sutton, L. E., Brockway, L. O., J. Amer. Chem. Soc. lvii. p. 473 (1935).
(22) Rosenthal, Jenny E., Phys. Rev. xlix. p. 535 (1936).
(23) Sutherland, G. B. B. M., Dennison, D. M., Proc. Roy. Soc. A, cxlviii. p. 250 (1935).
(24) Voge, H. H., Rosenthal, Jenny E., J. Chem. Phys. iv. p. 137 (1936).
(25) De Laszlo, H., ' Nature,' cxxxv. p. 474 (1935).
(26) Corin, C., *J. Chim. phys*, xxxii. p. 241 (1935).
(27) Mecke, R., "Structure of Molecules," *Leipziger Vorträge*, p. 50 (1931).
(28) Wu, T-Y., Phys. Rev. xlvi. p. 465 (1934).
(29) Clark, C. H. Douglas, Stoves, J. L., Phil. Mag. xxii. p. 1137 (1935).
(30) Badger, R. M., J. Chem. Phys. iii. p. 710 (1935).
(31) Urey, H. C., Bradley, C. A., Phys. Rev. xxxviii. p. 1969 (1931).
(32) Linnett, J. W., Thompson, H. W., ' Nature,' cxxxix. p. 509 (1937).
(33) Duchesne, J., ' Nature,' cxxxix. p. 634 (1937).
(34) Pauling, L., Brockway, L. O., Beach, J. Y., J. Amer. Chem. Soc. lvii. p. 2705 (1935).
(35) Delfosse, J. M., *Ann. Soc. Sci. Brux.* lv. p. 114 (1935).

(36) Bourguel, P., *Comptes Rendus*, cxciv. p. 1736 (1932).
(37) Pauling, L., Proc. Nat. Acad. Sci. xviii. p. 293 (1932).
(38) Richter, H., *Physikal. Zeits.* xxxvi. p. 85 (1935).
(39) Theilacker, W., *Zeits. Krist.* xc. p. 256 (1935).
(40) Ananthakrishnan, R., Proc. Ind. Acad. Sci, v. p. 285 (1937).
(41) Syrkin, J. K., Wolkenstein, M. W., *Acta Phys.-Chem. U.S.S.R.* ii. p. 303 (1935).
(42) Ananthakrishnan, R., Proc. Ind. Acad. Sci. v. p. 200 (1937).

VII. *On the Atomic Forces of Solid State.*

By Weng Wen-Po *.

Part VII.

(20) *ATOMIC VOLUME.*—This part is a direct continuation of the previous parts published recently †. Some refinements of the former treatment are now presented, and followed by some new development of the investigation after section (23).

We have first assumed that an atom, which is displaced a distance x from its neutral position, will be acted upon by a force $f(r_0+x)$ exerted by all the atoms from which the displaced atom starts to move and another force $f(r_0-x)$ exerted by all the atoms which it approaches. The solid is assumed to be isotropic, and the atom treated is supposed to be the average case of all the atoms. The symbol r_0 represents the average distance of two adjacent atoms.

The value of r_0 has been defined by the equation

$$r_0=kn^{-\frac{1}{3}}=k\left(\frac{W}{\rho N_0}\right)^{\frac{1}{3}}, \quad . \quad . \quad (9) \text{ \& } (10)$$

where W is the atomic weight, ρ the density, and N_0 the Avogadro's number. k is a constant which will vary for different crystal systems, and was taken to be 1·38 as an average. According to the conception of atomic volume we can define r_0 in a more precise way as the average diameter of a unit cell of the imaginary atom which has its specific shape and volume. For our purpose, the unit cell may be visualized as being bounded by the surface in which an imaginary exploring atom

* Communicated by the Author.
† Parts I.–II., Phil. Mag. xxii. p. 49 (1936); Part III., xxii. p. 281 (1936); Parts IV.–V., xxiii. p. 33 (1937); Part VI., xxiv. p. 466 (1937).

experiences no radial force toward the atom which forms the centre of the cell. Therefore for one value of atomic volume there are still as many possible values r_0 as the shapes of the unit cell.

As it is practically impossible to know the shape of the atomic unit cell as defined we can only work out some simple cases which will show the approximate effect. Taking the simplest case of a spherical cell which has been used quite frequently in expressing the atomic volume, the value of the unit cell is

$$\frac{4}{3}\pi\left(\frac{r_0}{2}\right)^3 = \frac{W}{\rho N_0}.$$

Thus, $$k = \left(\frac{6}{\pi}\right)^{\frac{1}{3}} = 1{\cdot}24.$$

A more general case is an ellipsoid of revolution. In the polar coordinate of variables ρ_1, θ_1, and ϕ_1 an ellipsoid of revolution with its principal axis $\theta = 0$ can be represented by

$$\rho_1^2 = \frac{\gamma^2 a_1^2}{(\gamma^2-1)\sin^2\theta_1 + 1},$$

where $2a_1$ is the length of either of the equal axes and γ the ratio of the principal axis to the equal axis. By present definition $\frac{r_0}{2}$ will be the space average of ρ_1, *i. e.*,

$$\frac{r_0}{2} = \frac{1}{4\pi}\int_0^{\pi}\int_0^{2\pi} \rho_1 \sin\theta_1 \, d\theta_1 \, d\phi_1,$$

which gives the ratio $\frac{r_0}{a_1}$ after the quadrature. As the unit cell has an average volume $\frac{W}{\rho N_0}$, we can determine a_1 by $\frac{4}{3}\pi a_1^3 \gamma = \frac{W}{\rho N_0}$, and r_0 by $r_0^3 = \frac{3}{4\pi\gamma}\left(\frac{r_0}{a_1}\right)^3 \frac{W}{\rho N_0}$.

It follows $$k = \left(\frac{3}{4\pi\gamma}\right)^{\frac{1}{3}}\left(\frac{r_0}{a_1}\right).$$

The results of the evaluation of the integrals give

$$k = \left(\frac{6}{\pi\gamma}\right)^{\frac{1}{3}} \frac{\gamma}{\sqrt{\gamma^2-1}} \sin^{-1}\frac{\sqrt{\gamma^2-1}}{\gamma} \qquad \text{when } \gamma > 1,$$

$$k = \left(\frac{6}{\pi\gamma}\right)^{\frac{1}{3}} \frac{\gamma}{\sqrt{\gamma^2-1}} \log_e \frac{\sqrt{1-\gamma^2}+1}{\gamma} \qquad \text{when } \gamma < 1.$$

In Table XIX. the values of k corresponding to several values of γ are calculated.

For our purposes it will be good enough to use $k=1{\cdot}24$ except in those cases where the compressibility constant are involved. When compressibility is used to represent the atomic force a certain correction seems to be absorbed in the constant k, and a bigger apparent value of k results. One cause of the correction is due to an approximation in equation (4). This can be shown in a qualitative way as below. The force $f(r_0+x)$ is defined as the derivative of the potential energy of the atom due to certain numbers of surrounding atoms with respect to the displacement of the atom concerned—that is to say, the atom upon which the force $f(r_0+x)$ acts is alone displaced. Evidently it is different from the case of a compressed solid, where all neighbouring atoms draw nearer to each other. In this case the mutual distance between all atoms becomes

TABLE XIX.

γ	1/3	2/5	1/2	2/3	1	3/2	2	5/2	3
k	1·12	1·15	1·19	1·22	1·24	1·23	1·19	1·16	1·12

variable; but the difference is not large as long as the inverse index of the force is not too small. This can be proved in a limiting case of a number of positive and negative charges arranged alternatively at an equal distance r apart from each other along the x axis as an analogy to the atomic arrangement of alkaline halides. The derivative of the potential energy of a terminal charge with respect to r is

$$-\frac{e^2}{r^2}\left(1-\frac{1}{2}+\frac{1}{3}-\frac{1}{4}\cdots \text{ to } \infty\right).$$

The sum in the parenthesis is log 2, or 0·694. The derivative of the same quantity with respect to the displacement of the terminal charge alone for infinite small displacement is

$$-\frac{e^2}{r^2}\left(1-\frac{1}{4}+\frac{1}{9}-\frac{1}{16}\cdots \text{ to } \infty\right).$$

The sum in the parenthesis is $\frac{\pi^2}{12}$, or 0·822. The difference will be smaller in the three-dimensional case.

(21) *Anharmonic Motion.*—When the displacement of the atom is not very large it is convenient to express $f(r_0+x)$ in a power series of x as

$$f(r_0+x)=-ax+bx^2-cx^3+\ldots$$

The actual force experienced by an atom is the resultant of $f(r_0+x)$ and $-f(r_0-x)$, due to all the surrounding atoms. The resultant force $\mathrm{F}(x)$ is hence

$$\mathrm{F}(x)=-2ax-2cx^3-\ldots$$

The contribution of the anharmonic term to the kinetic energy has been discussed in section (8) of Part II.

Unfortunately the method used was not rigorous, though the final result was not affected. In this section we will treat the same problem again by means of Clausius's virial theory. Let the average value of kinetic energy and potential energy through a long period of time and of many atoms be denoted by $\overline{\mathrm{E}_{\text{kin.}}}$ and $\overline{\mathrm{E}_{\text{pot.}}}$ respectively. By virial theory we have

$$\overline{\mathrm{E}_{\text{kin.}}}=-\tfrac{1}{2}\overline{\mathrm{F}(x).x}=a\bar{x}^2+c\bar{x}^4,$$

where $\overline{\mathrm{F}(x).x}$, $\bar{x}^2$, and $\bar{x}^4$ are the average values of $\mathrm{F}(x).x$, x^2, and x^4 respectively. The average potential energy, on the other hand, is

$$\overline{\mathrm{E}_{\text{pot.}}}=-\overline{\int_0^x \mathrm{F}(x)\,dx}=a\bar{x}^2+\tfrac{1}{2}c\bar{x}^4,$$

where $\overline{\int_0^x \mathrm{F}(x)\,dx}$ means the average value of $\int_0^x \mathrm{F}(x)\,dx$. Therefore the fraction of the average kinetic energy in the total energy can be expressed as

$$\frac{\overline{\mathrm{E}_{\text{kin.}}}}{\overline{\mathrm{E}_{\text{kin.}}}+\overline{\mathrm{E}_{\text{pot.}}}}=\frac{1}{2}\left[1+\frac{1}{4}\cdot\frac{c}{a}\cdot\frac{\bar{x}^4}{\bar{x}^2}\right],$$

when $\left(\frac{cr_0^2}{a}\right)\left(\frac{x}{r_0}\right)^2$ is small enough to compare with unity.

To work out the correction the approximation $x=X_1 \cos 2\pi\nu t$ can be used. The result is

$$\frac{\overline{E_{kin.}}}{\overline{E_{kin.}}+\overline{E_{pot.}}}=\frac{1}{2}\left[1+\frac{3}{16}c'\left(\frac{X_1}{r_0}\right)^2\right],$$

where $c'=\frac{cr_0^2}{a}$. If we express the total energy by $\frac{1}{2}mv_0^2$, where v_0 is the velocity of the atom at the point of zero force, or equilibrium point, we can easily change the expression by the equation

$$aX_1^2=\tfrac{1}{2}mv_0^2\left(1-\frac{cm}{4a^2}v_0\right),$$

which is an approximate solution of the equation of motion at $\frac{dx}{dt}=0$. Thus we obtain

$$\overline{E_{kin.}}=\tfrac{1}{2}m\left[\frac{v_0^2}{2}-\frac{3cm}{64a^2}v_0^4\right]. \quad . \quad . \quad . \quad (30)$$

This is the same equation (30) which we obtained in Part II. by actually averaging the kinetic energy.

In section (8) we held the classical view of temperature, namely, that the average kinetic energy equals to $\frac{1}{2}k_0T$ for each degree of freedom. By this assumption we arrived at equation (34),

$$c'=\frac{cr_0^2}{a}=21\times10^{-9}\frac{WC}{\rho\beta_0},$$

where CT is defined as the increase of specific heat above 3R at the temperature T. We obtained thereby $C'\times10^{-1}$ for Ag, Au, Pt, Cu, and Pb to be 5·4, 6·0, 29, 9·3, and 11·4 respectively. (Some misprints were made in equation (33) and Table IX.) If we set q, the index of the inverse repulsive part of $f(r_0+x)$, to be 35 as an average, we get by equation (59) of Part VI. $c'\times10^{-1}=20$. So far we have neglected the free electrons altogether. $1{\cdot}6\times10^{-4}$ should be subtracted from C according to Sommerfield's assumption; but the data are not accurate enough to make the correction worth while. Moreover, a treatment of anharmonic motion by statistics is lacking. It is not quite certain whether the result will be reduced

to the classical conception of temperature in a degenerated case of high temperature.

(22) *The Value of* $\frac{br_0}{a}$.—In the expansion

$$f(r_0+x)=-ax+bx^2-cx^3\ldots$$

the fraction $\frac{br_0}{a}$ was found to be more or less the same for all substances. Extension of the assumption to non-metallic elements yielded fairly good agreement. This assumption also provides a good chance to test our former hypothesis of thermal conduction in non-metallic crystals described in Part IV. Equation (52), which expressed the coefficient of thermal conductivity K in terms of density ρ, atomic weight W, as

$$K=1{\cdot}5\times10^{-39}W^{\frac{1}{3}}\rho^{-\frac{1}{3}}\nu^3T^{-1}\ \text{watt/cm./sec.},\quad .\quad (52)$$

TABLE XX.

	$\nu^*\times10^{-12}$.	K at °C. (calc.).	K at °C. (obs.).
I	1·58	0·008	0·0044
Dia.	39	3·9	1·5
Si	10	1·2	0·93

gave the right order of magnitude of K for several alkaline halides. If $\frac{br_0}{a}$ is a constant, and the numbers of neighbouring atoms which contribute the conduction is the same, equation (52) will also give the order of magnitude of K for non-metallic elements. Unfortunately there are only three non-metallic elements whose thermal conductivity in the solid state has been accurately measured and whose characteristic frequency is unique and known. For these elements—namely, diamond, iodine, and silicon—the calculation was carried out, and the results are shown in Table XX. The calculated figures are in favour of our assumption.

* Taken from Table XVII.

Before we go into a further investigation we need a clearer and more exact idea of the true value of $\frac{br_0}{a}$ or b' for all elements. The method for the estimation of b' which we employed in equation (29) of Part II. was chosen for the sake of easy manipulation; but it contains the uncertainty of involving the compressibility β_0, which is difficult to measure accurately. Moreover, the representation of the atomic force by compressibility is a rough one. Here we will calculate b' again by the same principle but using the known values of characteristic frequency instead of the compressibility. Equations (8) and (44) of Part IV. give the equation required for the purpose,

$$b' = \frac{12\pi^2 k^2}{N_0^{\frac{2}{3}}} W^{\frac{2}{3}} \rho^{-\frac{2}{3}} \nu^2 \left[\frac{\alpha(T)}{S(T)}\right],$$

$$= 2{\cdot}54 \times 10^{-14} W^{\frac{2}{3}} \rho^{-\frac{2}{3}} \nu^2 \left[\frac{\alpha(T)}{S(T)}\right], \quad . \quad (62)$$

where $k = 1{\cdot}24$ has been used. As there is no direct precision method for the measurement of the characteristic frequency we have to choose one of the many indirect methods. To keep our argument in a logical order we should not use Lindemann's and similar formulæ, which in our opinion are merely consequences of b' being constant. The only reliable source of the value ν with comprehensive data and solid theoretical basis * is Debye's specific heat data. In Table XXI. the results of the calculation, using specific heat data, are shown.

It is shown in Table XXI. that the tendency of the deviation of b' from a constant value survives, although we may neglect the big discrepancy in the case of Bi and Sb, which is probably due to their particular crystal structure. Moreover, the deviation is a systematic one according to the order of groups in the periodic table. We should conclude that the index of the inverse repulsive term in $f(r_0+x)$ on which b' mainly depends is not exactly a constant.

(24) *The Latent Heat of Vaporization.*—An analysis of the force $f(r_0+x)$ in section (19) of Part VI. led us to the conclusion that $f(r_0+x)$ is the sum of two terms each

* Blackman, P. R. C. L. cxlviii. p. 365 (1935); cxlix. p. 117 (1935).

proportional to a certain power of r. The form of the function $f(r)$ we assume at present is then

$$f(r) = \frac{A}{r^p} + \frac{B}{r^q}, \quad \ldots\ldots \quad (60)$$

where the $\frac{B}{r^q}$ term is assigned as the repulsive term for definiteness. The value b', which is equal to $\frac{1}{2}(p+q+1)$, will be nearly constant if p and q are also nearly constant.

TABLE XXI.

Elements.	$\nu \times 10^{-12}$.	$\frac{\alpha(T)}{S(T)} \times 10^{12}$.	p.	b'.	q.
Ag	*4·50	8·09	10·5	19·5	36
Al	*8·34	2·56	2·70	21·0	39
As	†5·76	1·37	5·7	11·5	..
Au	*3·77	10·89	19·3	19·6	34
Bi	‡2·06	10·9	9·8	9·0	..
Ca	§4·44	3·85	1·55	16·8	..
Cd	*3·35	13·50	8·6	21·4	40
Cu	*6·59	4·31	8·92	17·6	32
Fe	*8·80	2·63	7·86	19·1	35
K	*2·08	11·2	0·86	14·2	25
Mg	§6·43	2·49	1·74	15·2	27
Na	*3·33	5·84	0·97	13·6	24
Ni	†7·90	2·92	8·90	16·3	30
Pb	*1·84	22·8	11·34	13·6	24
Pt	*4·71	6·55	21·45	16·1	29
Sb	‖2·95	5·55	6·68	8·5	..
Tl	†1·89	21·51	11·85	13·2	..
Zn	*4·90	8·53	7·14	22·7	42

When q is much larger than p, as we may assume to be sensibly the case, we are not very sure about the constancy of p. However, p is expected to be a constant for those elements which have the same type of attractive force.

It is difficult to study the attractive force alone, since here is no physical property which is a direct measure

* *Handb. d. Exper. Phys.* viii. p. 245.
† *Tables Annu. Intern. d. Numero const. et Donn.* x. p. 58 (1930).
‡ *P.K. Akad. Amsterdam*, xxxiii. p. 243 (1930).
§ J. A. C. S. xl. p. 489 (1918).
‖ *Ann. der Physik.* lxiii. p. 476 (1920).

of the attractive force only. Although the repulsive force of $f(r_0+x)$ dwindles very quickly as r increases, matter does not usually occur in a state where the repulsive term vanishes altogether but the attractive term survives. The usual state of matter is either aggregate or gaseous. In the latter state of matter the molecular attraction is again too feeble. The only property which depends largely upon the attractive force is the latent heat of vaporization. Fortunately the amount of heat energy required to take an atom from the lattice to infinity against the atomic force $f(r_0+x)$ is very easily calculated, provided the expression of $f(r_0+x)$ assumed is accurate enough within the range of the first few values of r_0. This can be done by considering the potential of the atom due to the force $f(r)$ to be $\int_{r_0}^{\infty} f(r)\,dr$. According to the definition $f(r)$ is the force exerted by half the surrounding atoms; so the potential energy due to all the atoms in the bulk is $2\int_{r_0}^{\infty} f(r)\,dr$. If we write $\mathscr{L}$ for the latent heat of vaporization in ergs per gram, we have then

$$m\mathscr{L}=2\int_{r_0}^{\infty} f(r)\,dr. \quad . \quad . \quad . \quad . \quad . \quad (63)$$

By equation (60), and considering $f(r_0)=0$, we obtain

$$m\mathscr{L}=\frac{2(q-p)}{(p-1)(q-1)}\times\frac{-A}{r_0^{p-1}}.$$

By equation (61), *i. e*, $-A(q-p)=ar_0^{p+1}$, we get

$$m\mathscr{L}=\frac{2}{(p-1)(q-1)}ar_0^2. \quad . \quad . \quad . \quad . \quad (64)$$

Before we make any use of equation (64) let us get some idea of the value p first. By means of equation (28) of Part II., which can be written after transposing as

$$b'=\frac{q+p+1}{2}=\frac{6ar_0^2}{m}\left[\frac{\alpha(T)}{S(T)}\right], \quad . \quad . \quad . \quad (65)$$

where $\left[\frac{\alpha(T)}{S(T)}\right]$ is the ratio of the coefficient of linear

thermal expansion over specific heat, we are able to find the value $\frac{1}{2}(p+q+1)$. Since q is in the order of 30 or 40, as we can estimate from alkaline halides, we may cancel $(p+q+1)$ by $(q-1)$ as a very rough approximation. Then the equations (64) and (65) yield

$$p=1+\frac{1}{6}\frac{1}{\mathscr{L}}\left[\frac{S(T)}{\alpha(T)}\right]. \quad . \quad . \quad . \quad . \quad (66)$$

TABLE XXII.

Element.	$\mathscr{L}W\times10^{-12}$.	$S(20°\text{ C.}).W\times10^{-7}$.	$\alpha(20°\text{ C.})\times10^{5}$.	p.
Ag	2·49	25·2	1·89	1·9
Al	2·25	24·2	2·30	1·8
Au	3·68	25·7	1·42	1·8
Cs	6·70	29·0	0·97	1·8
Co	3·80	24·8	1·23	1·9
Fe	3·80	24·9	1·17	1·9
Hg.....	5·93	28·0	0·90	1·9
K.....	0·84	29·0	8·3	1·7
Mn	2·40	24·6	2·3	1·8
Ni	3·80	25·8	1·28	1·9
Pb	1·93	26·5	2·91	1·8
Pt	5·20	26·5	2·91	1·8
Rb.....	0·74	28·7	9·0	1·7
Zn	0·99	25·3	3·3	2·2

Strictly speaking the value of $\mathscr{L}$ so defined should be the latent heat at absolute zero. Since the amount of energy $\mathscr{L}$ is generally very large compared with other corrections, we can use the latent heat of vaporization at the boiling-point instead. In Table XXII. values of p for some metals calculated by means of equation (66) are shown.

Owing to the crude processes of simplification and the complication of the lattice structure, which we neglected altogether, the result tabulated in Table XXII. is just good enough to suggest an inverse square rule of attraction

for metals. Therefore we shall use $p=2$ for metals for the sake of simplicity.

Now we can make use of equation (63) to calculate the characteristic vibrational frequency ν of the metallic elements. We have already proved

$$\nu=\frac{1}{2\pi}\sqrt{\frac{2a}{m}}$$

in equation (8). Eliminating a from this and equation (64), we get

$$\nu=\frac{\sqrt{(q-1)(p-1)}}{2\pi}\frac{\mathscr{L}^{\frac{1}{2}}}{r_0}, \quad . \quad . \quad . \quad (67)$$

which can be transformed by means of $r_0=k\left(\frac{W}{\rho N_0}\right)^{\frac{1}{3}}$ to

$$\nu=\frac{\sqrt{(q-1)(p-1)}}{2\pi k}\mathscr{L}^{\frac{1}{2}}\rho^{\frac{1}{2}}W^{-\frac{1}{6}}. \quad . \quad . \quad . \quad (68)$$

Let $k=1{\cdot}24$, $p=2$, and $b'=15$ as an average value taken from Table XX., or $q=2b'-p-1=27$; we have

$$\nu=5{\cdot}5\times10^7\times(\mathscr{L}W)^{\frac{1}{2}}\rho^{\frac{1}{2}}W^{-\frac{2}{3}} \quad . \quad . \quad . \quad (69)$$

for metallic elements. Using the physical constants given in the International Critical Tables, vol. i. pp. 102–105, values of ν for metals were calculated by equation (69) and tabulated in Table XXIII., where they are compared with those obtained from specific heat data by Debye's theory. Whenever specific heat data are lacking data from other sources are inserted. It is very interesting to see that the agreement is generally good.

For non-metallic elements the value of p is not exactly known; so we have to determine the constants of equation (68) by means of the known values of ν obtained by other methods. By doing this we get

$$\nu=11\times10^7(\mathscr{L}W)^{\frac{1}{2}}\rho^{\frac{1}{2}}W^{-\frac{2}{3}} \quad . \quad . \quad . \quad . \quad (69')$$

for non-metallic elements. The calculated values of ν by equation (69′) were listed in the lower part of Table XXIII.

Comparing equations (68) and (69) we obtain

$$(p-1)(q-1)=104$$

for most non-metallic elements. If the value of q is still

Table XXIII.

Elements.	$\nu \times 10^{-12}\,\mathscr{L}$.	$\nu \times 10^{-12}$ sp.ht.* etc.	$\frac{\mathscr{L}W}{T_m} \times 10^{-9}$.	Elements.	$\nu \times 10^{-12}\,\mathscr{L}$.	$\nu \times 10^{-12}$ sp.ht.* etc.	$\frac{\mathscr{L}W}{T_m} \times 10^{-9}$.
			Metals.				
Ag	3·8	4·5	2·0	Mn	5·9	7·5†	1·9
Al	7·4	8·4	2·4	Mo	7·1	7·9	2·5
As	5·6	5·8	..	Na	4·1	3·3	2·8
Au	3·5	3·8	2·8	Ni	7·5	7·9	2·2
Ba	2·6	2·4	3·2	Pb	2·0	1·8	3·2
Bi	1·9	2·1	3·5	Pt	4·3	4·7	2·6
Co	7·4	8·2 †	2·2	Rb	1·1	1·5 †	2·4
Cr	7·0	8·3 †	1·7	Sb	2·6	2·9	2·1
Cs	0·99	0·95 †	2·4	Si	8·7	10	3·1
Cu	7·7	6·6	3·4	Sn	3·4	3·4 ‡	..
Fe	8·3	8·8	2·1	Sr	3·6	3·0 †	3·5
Hg	1·2	1·8	2·5	Tl	1·4	1·8	..
K	2·3	2·1	2·5	W	5·8	6·7 §	2·5
Mg	7·5	6·4	2·8	Zn	3·8	4·9	1·9
			Non-Metals.				
A	1·5	1·8	0·75	I	1·6	1·6	0·57
Br	1·7	1·8	0·56	N	2·1	2·1	0·44
Cl	2·2	2·3	0·58	Ne	1·2	1·2	0·71
F	8·3	8·3	..	O	2·3	2·4	0·63
H	3·2	1·9	..	Se	2·7	2·7	0·63
He	0·64	0·7 (?)	..				

* Data, if not noted otherwise, has been previously referred to.
† Not from sp.ht. data. W. C. M. Lewis, Text-books of Phys. Chem. iii. p. 61 (1919).
‡ *Handb. d. exper. phys.* viii. p. 245.
§ *Zeits. f. Phys.* xi. p. 343 (1924).

the same as metals p will be equal to 5. It is quite likely that the attraction in the non-metallic elements is around an inverse fifth value. For the time being we cannot draw any further conclusion before sufficient physical constants for an accurate determination of b' are available.

To conclude this section let us examine the ratio $\frac{\mathscr{L}W}{T_m}$, which should be nearly constant, as we will show later. Here T_m is the melting-point on the absolute scale and is not too near to zero. The numerical values of the quotient are shown in Table XXIII. This appears very like Trouton's rule.

(24) *Fusion.*—With the aid of the knowledge of $f(r_0+x)$ at fairly big values of r we can test our theory of fusion once again, as we did in Section 11 of Part IV. Apart from the fact that the fuller form of $f(r_0+x)$ is used, some necessary refinements in the calculation of the average specific heat from the absolute zero to the melting-point are made. It makes very little difference to the metals if the specific heat at the room-temperature is used; but for the non-metallic elements the difference can be very large. The zero-point energy, whose amount is rather obscure for atoms, is neglected. As before, we assume that fusion begins to take place when the maximum linear amplitude of the atomic oscillation excited by all the absorbed heat energy from absolute zero to the melting-point reaches the range where $\frac{df(r)}{dr}=0$. The idea of concentrating the total energy in one direction is also consistent with the explanation of Trouton's rule of heat fusion which we suggested in section (12).

The average atomic heat can be calculated by Debye's theory as

$$\overline{W.S\left(\frac{\Theta}{T}\right)}=3R\left(\frac{T}{\Theta}\right)^3\int_0^{\frac{\Theta}{T}}\frac{y^3\,dy}{e^y-1}=3RD\left(\frac{\Theta}{T}\right),$$

where the notation $D\left(\frac{\Theta}{T}\right)$ is used to denote the Debye's energy integral. The integral has been well worked out

by J. A. Beattie * in 1925. From his results a table of $D\left(\frac{\Theta}{T}\right)$ was constructed to suit our purpose.

$\frac{T}{\Theta}$.	1.	2.	3.	4.	5.	6.	7.	8.	9.	10.
	..	..	..	·909	·928	·940	·946	·954	·958	·963

$\frac{T}{\Theta}$.	0.	0·1.	0·2.	0·3.	0·4.	0·5.	0·6.	0·7.	0·8.	0·9.
3.....	·880	·883	·886	·889	·893	·896	·899	·901	·904	·906
2.....	·825	·832	·840	·845	·852	·859	·864	·869	·872	·876
1.....	·674	·698	·742	·742	·758	·773	·785	·797	·808	·817
0.....	..	..	·118	·245	·354	·441	·510	·564	·610	·644

$\frac{T}{\Theta}$.	0·10.	0·11.	0·12.	0·13.	0·14.	0·15.	0·16.	0·17.	0·18.	0·19.
	..	·0193	·0327	·0408	·0498	·0598	·0702	·0811	·0929	·1053

By equating the total energy $m\overline{S\left(\frac{\Theta}{T}\right)}T_m$, where J is the mechanical equivalent of heat, to $2\pi^2\nu^2 m X_1^2$, where X_1 is the maximum linear amplitude, we have

$$2\pi^2\nu^2 X_1^2 = 3RT_m D\left(\frac{\Theta}{T}\right).$$

Substituting

$$r_0 = k\left(\frac{W}{N_0\rho}\right)^{\frac{1}{3}} \quad \text{and} \quad k = 1{\cdot}24,$$

we get

$$\frac{X_1}{r_0} = 2{\cdot}43\times10^{11}\times\sqrt{D\left(\frac{\Theta}{T}\right)}\,\frac{\rho^{\frac{1}{2}}T_m^{\frac{1}{2}}}{\nu W^{\frac{5}{6}}}, \quad . \quad . \quad (70)$$

where $2{\cdot}43\times10^{11}$ is the numerical approximation of

$$\frac{\sqrt{N_0^{\frac{1}{3}}}}{k\pi\sqrt{2}}\times\sqrt{3R}.$$

Comparing this with Lindemann's equation, whose constant is $2{\cdot}8\times10^{12}$, and assuming $\sqrt{D\left(\frac{\Theta}{T}\right)}$ to be 0·9 roughly, $\frac{X_1}{r_0}$ should be around 0·1.

* Jour. of Mathematics and Physics, vi. p. 1 (1926–7).

On the other hand, by equating the derivative

$$\frac{d}{dr}\left[\frac{A}{(r_0+x)^p}+\frac{B}{(r_0+x)^q}\right]$$

TABLE XXIV.

Element.	$\nu\times10^{12}$.	$\sqrt{D\left(\frac{\Theta}{T}\right)}$.	$\frac{X_1}{r_0}$.	q.
Ag	4·50	·967	·0815	38
Al.....	8·34	·922	·0731	44
Au	3·77	·971	·0748	43
Bi.....	2·06	·967	·0653	45
Ca	4·44	·963	·0924	32
Cd	3·35	·950	·0670	40
Cu	6·59	·954	·0842	36
Fe	8·80	·954	·0867	36
K	2·08	·942	·0950	30
Mg	6·43	·938	·0904	32
Mo	7·94	·975	·0773	41
Na	3·33	·921	·0937	31
Ni	7·90	·959	·0850	36
Pb	1·84	·971	·0826	37
Pt	4·71	·975	·0773	41
Sb	2·95	·971	·0828	37
Tl	1·89	·971	·0808	39
Zn	4·90	·937	·0720	45
A	1·78	·818	·0560	34
Br	1·80	·939	·0628	37
Cl	2·31	·879	·0763	28
H.....	1·19	·245	·0157	..
N.....	2·05	·687	·0724	30
O	2·35	·910	·0731	30

to zero, and bearing in mind $f(r_0)=0$, we get

$$\frac{X_1}{r_0}=\frac{\log\frac{q}{p}}{q-p} \quad . \quad . \quad . \quad . \quad . \quad . \quad (71)$$

at the melting-point. Equations (71) and (70) enable us to calculate q from ν and the melting-point if p is supposed to be known. In Table XXIV. values of $\frac{X_1}{r_0}$

at the melting-point are calculated from the known values of ν determined by specific heat alone. By setting $p=2$ for metallic elements and $p=5$ for non-metallic elements the values of q were computed as shown in the last column.

The most efficient way of testing our theory is to compare the values of q so obtained. We have so far three methods of determining q by known values of ν: they are from melting-point, from thermal expansion, and from latent heat of vaporization by equation (68). In the last-named method we have also to assume the value of p to be 2 and 5 respectively.

TABLE XXV.

Elements.	$q(\mathscr{L})$.	$q(T_m)$.	$q(\alpha_e)$.	Elements.	$q(\mathscr{L})$.	$q(Tm)$.	$q(\alpha_e)$.
Ag	37	38	36	Mo	33	41	..
Al.....	34	44	39	Na	18	31	24
Au	31	43	34	Ni	30	36	30
Ca	..	32	30	Pb	25	37	24
Cu.....	20	36	32	Pt	32	41	39
Fe.....	30	36	35	Sb	35	37	..
K	22	30	25	Tl.....	>45	39	..
Mg	20	32	27	Zn	44	45	42
A	38	44	..	N	27	30	..
Br	30	37	..	O	29	30	..
Cl	29	28	..				

In Table XXV. values of q calculated from these three methods are compared. Considering that all these equations are directly derived from our few assumptions, and that no arbitrary constant whatever has been introduced, we should say that the agreement was very good. It is shown in these figures that the variation of q from element to element has a constant tendency. For example, the values of q for Na, K, Mg, and Ca are always lower than the average.

The results also show that the general influence of the complication of the crystal structure on the physical quantities is not big enough to conceal the evident variation of the value q. It follows that both Lindemann's, Gruneisen's, and latent heat formulæ are by no means

the best way to determine ν. It takes a suitable average of the values obtained from these formulæ to get rid of the influence of q.

It is perhaps worth mentioning that the value q for hydrogen is 12 calculated from the latent heat, but 250 calculated from the melting-point. It is probably due to the zero-point energy, which is big enough to conceal the amount of energy $m\overline{\mathrm{JS}\left(\frac{\Theta}{\mathrm{T}}\right)}\mathrm{T}_m$ altogether. If this is the case, the zero-point energy will be in the order of 0·1 to 0·5 $h\nu$. There are probably other complications at those temperatures.

The values for q for the non-metals given in the table are probably not so near to their true value as those of metals. There are several reasons. In the first place, a modification of our treatment should be made for elements like O_2 and N_2 if their molecules are actually bound together in the way that the dissociation energy indicated by the spectroscopic data suggests; in the second place, the zero-point energy, whose existence might affect the result by a considerable amount in the case of elements of low melting-point, has been neglected; in the third place, the assumption $p=5$ is not beyond doubt.

Combining equations (68), (70), and (71), we have

$$\frac{\mathscr{L}\mathrm{W}}{\mathrm{T}_m} \propto \left[\frac{q-p}{\log\frac{q}{p}}\right]^2 \frac{\mathrm{D}\left(\frac{\Theta}{\mathrm{T}}\right)}{(q-1)(p-1)},$$

which has been shown to be nearly constant at high temperature. The approximate inverse square rule of attraction in metals is in favour of the electrostatic hypothesis. The recent works in electrostatic attraction for metals by K. F. Herzfeld *, P. Gombas †, and others are not without success.

(25) *Supplements.*—For the inert elements like Ne, A and He there is no marked change in the atomic structure during the transition from gaseous state to aggregate

* *Handb. d. exper. Phys.* xxiv. (2) p. 252.

† *Zeits. f. Physik.* xcv. p. 687 (1935); xciv. p. 473 (1935); xcl. p. 400 (1934).

state. Then we do not expect the attractive force, say $\frac{A}{r^p}$, will undergo any abrupt change during the transition. A numerical estimation will show that the correction term of pressure in van der Waals's equation is much too small to account for $\frac{A}{r^p}$'s existence if $p=4$, but it will be big enough to compare with the homopolar force if $p=6$.

Based on the results of infra-red absorption of sulphur Taylor and Rideal * suggested that the homopolar attraction is due to the alternate positive and negative polarities of the atom. If the alternate positive and negative polarities are due to the moving electrons and he nucleus the force reduces to a van der Waals force

TABLE XXVI.

Elements.	S_m†.	$\nu \times 10^{-12}$ (S_m).	$\nu \times 10^{-12}$ sp. ht.
Ag	800	3·5	4·5
Cu	1103	5·3	6·6
Na	222	3·9	3·3
Pt	1819	3·9	4·7
Sb	350	2·2	2·9

as treated by Heitler and London ‡, who estimated $p=7$ at long distances.

The formula of surface tension and the characteristic frequency for metals, namely, equation (55), have been tested for some more elements with less definite data, as shown in Table XXVI.

If the surface energy is proportional or equal to the energy required for the atom to travel from the interior of the liquid to the surface it will be $\int_{r_0}^{\infty} f(r)\,dr$, or half the latent heat of evaporation. By this assumption we can easily derive the formulæ of surface tension and the

* Proc. Roy. Soc. A, cxv. p. 589 (1927).
† International Critical Tables, iv. p. 439.
‡ *Zeit. f. Phys.* lx. p. 491 (1930); lxiii. p. 245 (1930).

characteristic frequency for both metallic and non-metallic elements from equation (69) and (69′), but not the numerical constant. That the surface energy is half the energy of infinite separation has been considered by H. Margenau * in a very simple but elegant manner. However, a precise verification of the hypothesis needs some definite knowledge of the surface structure.

Imperial College of Science and Technology,
London

VIII. *The Effect of Temperature on the Thermal Conductivity and the Accommodation Coefficient of Hydrogen below* 0° *C. By* Assistant Professor H. Spencer-Gregory *and* E. H. Dock, *Imperial College of Science and Technology, South Kensington* †.

EXPERIMENTAL investigations relevant to the effect of temperature on the heat conduction through gases are few in number, and comparatively little work has been done on the subject above and below the range of temperature −182° C. to 300° C.

Above 300° C., the troublesome effects associated with mass motions of the gas and the temperature discontinuity between the heated solid and the adjacent gas are of serious magnitude and difficult to disentangle from the effect due to pure conduction. The radiation also becomes increasingly important as the temperature increases, and is only of less importance in the hot-wire method by reason of the small diameters of the wires used.

From a theoretical aspect, it was shown by Maxwell [1] in terms of the kinetic theory, that for perfectly elastic spherical molecules between which forces of attraction and repulsion are non-existent, the thermal conductivity should, along with the coefficient of viscosity, be proportional to the square root of the absolute temperature.

From considerations of the hypothesis of decreasing intermolecular action with increasing temperature, due

* Phys. Rev. xxxviii. p. 365 (1931).
† Communicated by Prof. H. Spencer-Gregory.

to an apparent decrease in the molecular diameter, the collision paths, and therefore the thermal conduction and viscosity, would be expected to increase rather more rapidly than the square root of the temperature, a conclusion which was first supported by some early experiments due to Winkelmann [2].

In 1912, Chapman [3], applying Maxwell's Theory in a more generalized form, and making use of the hypothesis that forces of repulsion exist between molecules varying inversely as the nth power of the distance ($F \propto r^{-n}$) deduced for molecules possessing translational energy only, a relation in which K, the thermal conductivity, is expressed in terms of the coefficient of viscosity η, and the specific heat at constant volume C_v

$$K = f\eta C_v,$$

where f is a constant factor depending on the law of force and has a calculated value 2·5 exactly for $n=5$, and although this value of f can be regarded as being satisfactory for monatomic gases, the law of force on which its evaluation depends ($n=5$) theoretically predicts that η should vary directly as the absolute temperature, a prediction which has been found to be experimentally incorrect.

For gases in the monatomic state, since f and C_v are invariable with temperature, the variation of K will be parallel with that of η, and a law of force $\propto r^{-n}$ Chapman [4] has shown that the dependence on temperature of the viscosity is represented by the formula

$$\eta = AT^{1/2+2/(n-1)},$$

where A is a constant.

Weber [5], in an investigation on the heat conduction through pure neon for a range of temperature between −182° C. and 10° C., found that his experimental results could be very accurately represented by the formula

$$K/K_0 = (T/T_0)^{1/2+1/5}$$

where K_0 is the thermal conductivity at the temperature of melting ice T_0. The measurements give for the temperature coefficient between 0° C. and 100° C., ·00226 ; this agrees very closely with the temperature

coefficient of the viscosity for which Rankine [6] found 0·00225.

If Chapman's relation is assumed to be correct for polyatomic gases, then, apart from the possibility of a change in the factor f, it would be expected that K will vary more rapidly with the temperature than η on account of the effect of the rotational and vibrational energies of the molecules on the specific heat C_v.

This conclusion is fully supported by the recent [7] experiments of Mr. C. T. Archer on the heat conduction through CO_2 between 0° C. and 330° C., for which the dependence on temperature was found to be represented by the relation

$$K/K_0=(T/T_0)^{1\cdot216},$$

a result which exhibits a much greater rate of increase than is shown by the viscosity of CO_2 over a similar range of temperature.

The present investigation in relation to hydrogen between 0° C. and −182° C. has been undertaken to furnish information in respect of the thermal conductivity, and, in addition, to determine the effect of accommodation and its dependence on temperature. The possibility of calculating the coefficient of accommodation from the experimentally determined heat losses in conjunction with the theoretical aspect of the temperature drop effect was made the subject of a recent paper [8] by Dr. Gregory in which the temperature discontinuity between a uniformly heated wire and the adjacent gas was found to be expressible in the form of a general relation, applicable to permanent gases of all molecular weights.

As associated with the Fourier Law of heat conduction for a cylindrical distribution of temperature, the temperature drop effect is represented by the equation [8]

$$\delta\theta=F(Q/p)$$

$$=\frac{Q\sqrt{T_1}}{pr_1A}\left(\sqrt{1+\frac{Q^2T_1}{(2-\alpha)^2p^2r_1^2A^2T_1^2}}-\frac{Q\sqrt{T_1}}{(2-\alpha)pr_1AT_1}\right). \quad \ldots \quad (1)$$

in which r_1 and T_1 denote the radius and the absolute temperature of the wire, Q the rate of loss of heat, p the

pressure of the gas, while A is a quantity defined by the relation

$$A = \frac{\sqrt{R}2\pi l(\beta+1/2)2\alpha}{\sqrt{2\pi M}(2-\alpha)}, \quad . \quad . \quad . \quad . \quad (2)$$

where l is the length of the uniformly heated wire, M the molecular weight of the gas, α the coefficient of accommodation as defined by Knudsen, and βR the molecular heat of the gas.

If $\delta\theta_1$ and $\delta\theta_2$ represent the temperature discontinuities at the surfaces of the wire and wall respectively, then applying (1) to the modified Fourier equation, we obtain

$$\begin{aligned}\frac{Q \log_e (r_2-\lambda_2)}{2\pi kl\ (r_1+\lambda_1)} &= (T_1-T_2-\delta\theta_1-\delta\theta_2) \\ &= (T_1-T_2)-\frac{Q\sqrt{T_1}}{pr_1A_1}\left(\sqrt{1+\frac{Q^2T_1}{(2-\alpha)^2p^2r_1^2A_1^2T_1^2}}\right) \\ &\quad -\frac{Q\sqrt{T_2}}{pr_2A_2}\left(\sqrt{1+\frac{Q^2T_2}{(2-\alpha')p^2r_2^2A_2^2T_2^2}}\right) \\ &\quad +\frac{Q^2}{p^2}\left(\frac{1}{(2-\alpha)r_1^2A_1^2}+\frac{1}{(2-\alpha')r_2^2A_2^2}\right). \\ &\qquad . \quad . \quad . \quad (3)\end{aligned}$$

In (3) r_2 denotes the radius of the internal surface of the tube coaxially disposed with respect to the heated wire and A_1 and A_2 the values of A at the surfaces of the wire and tube respectively. A_1 and A_2 will differ slightly by reason of the dependence on temperature of α and β.

In respect of a range of pressures such that the average collision paths λ_1 and λ_2 of the gas molecules are of negligible magnitude in comparison with the curvatures r_1 and r_2, equation (3) reduces to the form

$$Q \log_e \frac{r_2}{r_1} = 2\pi kl(T_1-T_2)-2\pi kl(\sqrt{T_1}/r_1A_1+\sqrt{T_2}/r_2A_2)Q/p. \quad . \quad . \quad . \quad (4)$$

In applying (4) to the experimental data associated with the heat conduction above or below 0° C., allowance must be made for a possible variation in temperature of the external surface of the tube, due to the difficulty

of obtaining perfect control of the thermostatic arrangement associated with the experimental procedure.

If the variation of the bath temperature is of serious magnitude during the course of time occupied by the experiment, then, corresponding to a change of temperature δT of the internal surface of the tube wall, the change in the thermal conductivity K of the gas is given by

$$\pm\delta K = \pm K \cdot \gamma\delta T/2,$$

where K represents the thermal conductivity at a mean temperature $(T_1+T_2)/2$ and γ the temperature coefficient of K.

In relation to the present investigation, the maximum aberration recorded was about 0·5° C. in the case of the CO_2 bath, and this corresponds for a value of $\gamma = \cdot 0045$ to a change in K of amount not exceeding one-fifth of 1 per cent.

The variation of the quantity (T_1-T_2) arising from the same effect can be fully compensated by writing equation (4) in a form in which the variables considered are $(T_1-T_2)/C^2$ and $1/p$.

$$\frac{(T_1-T_2)}{C^2} = \frac{R_1 \log r_2/r_1}{2\pi K l} + \frac{R_1}{pA}(\sqrt{T_1}/r_1+\sqrt{T_2}/r_2), \quad (5)$$

where C denotes the current strength required to ensure constancy of the temperature T_1 of the wire at a pressure p of the gas and R_1 the corresponding resistance of the heated filament. Also since the variation of α and β as contained in A_1 and A_2 is small over the range of temperature from T_1 to T_2, a further simplification has been effected by writing $A_1 = A_2 = A$ in (4).

Radiation Correction.

The corrections to be applied in respect of the loss of heat by radiation have been found to be of negligible importance in relation to the present investigation, partly on account of the fine wires used in the tube system, and also from considerations of the low temperatures employed in the experiments.

The radiation, calculated from the Helfgott formula,

$$E = 2\pi r_1 l \sigma T^4(1-e^{-\alpha T}),$$

where r_1 and l are the radius and length of the compensated element of wire, T the temperature of the wire on the absolute scale, and σ and α constants given by

$$\sigma = 5{\cdot}72 \times 10^{-12} \text{ watts per cm.}^2,$$

$$\alpha = 1{\cdot}25 \times 10^{-4} \text{ for platinum}$$

was of the order of about 0·1 per cent. of the total heat loss at 0° C., a correction quite beyond the estimated accuracy of the thermal conductivity.

Thermostatic System.

In order to produce temperatures in the neighbourhood of −182° C. and −78° C., a vacuum vessel of approximately one gallon capacity was mounted in a wooden box, the space between the two being occupied by cotton wool. A motor-driven stirrer immersed in the thermostatic fluid ensured a constancy of temperature throughout the vessel while the experiment was in progress.

For the oxygen point pure liquid oxygen was used, but for the investigation on heat conduction of the gas, liquid air was found to be the more convenient and economical. The bath temperature, as measured by the external platinum wire fused on the wall of the tube, was found to vary only by a maximum amount of about 0·03° C. and in most cases was considerably less.

Temperatures in the neighbourhood of −78° C. were produced by adding powdered solid CO_2 to aviation spirit, the whole sludge being stirred by the motor-driven propeller. It was found that the temperature of the sludge depended on the degree to which the sludge was saturated by the CO_2. For an initially highly saturated solution the temperature was found to decrease at first rather rapidly, attain a minimum, and then rise again slowly.

By very carefully adjusting the amount of CO_2, a constancy of temperature throughout the experiment was ensured to within about 0·5° C., to which the modified equation (5) was found to be applicable. In the extreme cases such variation in the bath temperature corresponded to corrections in the thermal conductivity of the order of about two in one thousand.

A diagram of the thermostatic arrangement is shown in fig. 1 along with a plan of the tube and wire system.

Corrections to be applied to the platinum scale of temperature between 0° C. and −182° C.

From 0° C. and 660° C. the temperature t on the international scale of temperature is deducible from the

Fig. 1.

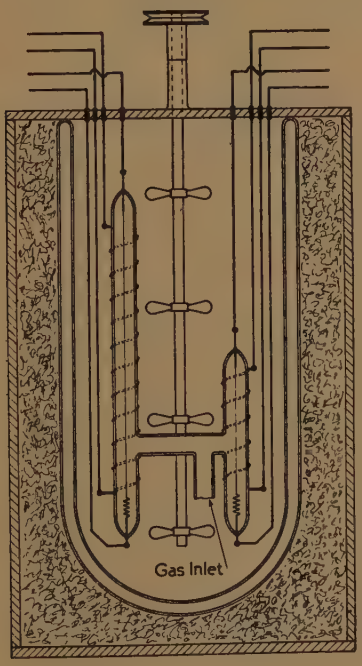

measured resistance R_t of the compensated element of platinum wire by means of the relation

$$R_t = R_0(1 + At + Bt^2), \quad . \quad . \quad . \quad . \quad (6)$$

in which the constants A and B are determined by calibration at the fixed temperature points of ice, steam, and sulphur. In this way the constants A and B have been found to be related to each other in the manner given by the equation

$$\delta = -\frac{10B}{A + 100B}, \quad . \quad . \quad . \quad . \quad . \quad . \quad (7)$$

where δ is a constant for a particular specimen of platinum and has been found to vary with the purity of the specimen.

The temperature pt on the platinum scale is defined by the relation

$$pt = \frac{R_t/R_0 - 1}{R_{100}/R_0 - 1} \times 100, \quad . \quad . \quad . \quad . \quad (8)$$

where R_{100} is the resistance at the normal boiling-point of water. In this way from (6), (7), and (8)

$$t = \frac{1 + 100\delta - \sqrt{(1+100\delta)^2 - 4\delta pt}}{2\delta}; \quad . \quad . \quad (9)$$

hence values of t between 0° C. and 660° C. can be calculated from the corresponding values of pt.

Below 0° C. (6) requires modification and internationally has been defined as

$$R_t/R_0 - 1 = At + Bt^2 + Ct^3(t - 100), \quad . \quad . \quad (10)$$

where C is an additional constant which can be determined from the boiling-point of liquid oxygen, and which in terms of the barometric pressure p mm. Hg is given by the relation

$$t_p = -182{\cdot}97 + 0{\cdot}0126\,(p - 760) + {\cdot}0000065\,(p - 760)^2.$$

Since the values of A, B, and C are known for the specimen of platinum employed, it is possible to construct a table of values of the quantity $R_t/R_0 - 1$ corresponding to intervals of 1° C. of t, and from (8) the corresponding values of pt can be calculated.

In the present instance the resistance of the compensated platinum wire was measured at temperatures corresponding to those of ice, steam and liquid oxygen, the determination of the resistance relative to the sulphur point being found impossible with the experimental system of tubes and wires ; it was necessary, therefore, in order to calculate A, B and C, to make use of the value of δ supplied by the makers of the wire (1·495). The experimental procedure of determining the fixed point resistances was similar in each case. A series of currents of small strengths was passed through the bridge system, and the corresponding balance points determined ; the problem is strictly one related to the thermal conductivity of the gas surrounding the wires, and it has been shown

by Gregory [9] that the appropriate working relation is given by

$$W = mx + c, \quad . \quad . \quad . \quad . \quad . \quad . \quad (11)$$

where W denotes the rate of heat development in the wire and x the corresponding distance of the balance point from the true mid-point of the bridge system; in this way a value of x corresponding to $W = 0$ can be

Fig. 2.

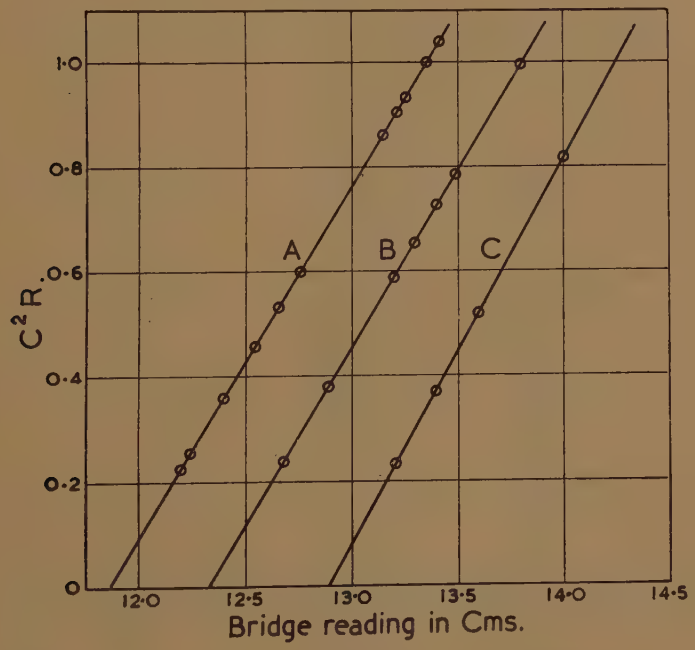

found by extrapolation, and hence the resistance of the wire at the external temperature of the bath is known.

Examples of this procedure in relation to the particular case of the oxygen bath are shown in fig. 2.

This method of determining the fixed point resistances was found to be necessary only in the case of the centrally disposed wires; in the case of the wires fused on the tube wall, the fixed point resistances were found to be invariable with the strength of the bridge current, providing that this did not exceed a definite small value.

The constants A, B and C as associated in equation (10)

for both the internal and external system of wires are given below.

Internal Wires.

$$R_t/R_0 - 1 = 3{\cdot}933 \times 10^{-3}t - 5{\cdot}812 \times 10^{-7}t^2 - 4{\cdot}594 \times 10^{-12}t^3(t-100).$$

External Wires.

$$R_t/R_0 - 1 = 3{\cdot}911 \times 10^{-3}t - 5{\cdot}779 \times 10^{-7}t^2 - 3{\cdot}792 \times 10^{-12}t^3\,(t-100).$$

TABLE I.

$t°$ C.	pt.	$(t-pt)$.
−190	−200·62	+10·62
−189	−199·51	+10·51
−188	−198·39	+10·39
−187	−197·28	+10·28
−186	−196·16	+10·16
−185	−195·05	+10·05
−184	−193·94	+9·94
−183	−192·83	+9·83
−182	−191·71	+9·71
−181	−190·60	+9·60
−180	−189·50	+9·50
−179	−188·39	+9·39
−178	−187·28	+9·28
−177	−186·16	+9·16
−176	−185·07	+9·07
−175	−183·97	+8·97
−174	−182·86	+8·86
−173	−181·76	+8·76
−172	−180·66	+8·66
−171	−179·56	+8·56
−170	−178·46	+8·46
−169	−177·36	+8·36
−168	−176·26	+8·26
−167	−175·16	+8·16
−166	−174·07	+8·07
−165	−172·97	+7·97
−164	−171·88	+7·88
−163	−170·78	+7·78

The corrections to be applied to the temperatures calculated in relation to the platinum scale have been tabulated in Tables I. and II., and refer only to the internal wires.

Since $(t-pt)$ is known for any value of pt, the corresponding value of t can be found from the Tables.

Experimental Details.

The experimental procedure is similar to that developed by Gregory [10] in his investigation of the effect of temperature on the heat conduction through H_2 between 0° C. and 330° C.

In the present instance the more accurate form of the modified Fourier relation (5) was applied to calculate the thermal conductivity and the coefficient of accommodation from the experimental data.

Briefly, the temperature of the compensated element of wire was maintained at a constant value by varying the strength of the current through the bridge system,

TABLE II.

t° C.	pt.	$(t-pt)$.
−80	−82·27	+2·27
−79	−81·23	+2·23
−78	−80·18	+2·18
−77	−79·14	+2·14
−76	−78·1	+2·10
−75	−77·06	+2·06
−74	−76·02	+2·02
−73	−74·97	+1·97
−72	−73·93	+1·93
−71	−72·89	+1·89

while the pressure of the gas was altered by definite amounts, and simultaneously the bath temperature T_3 was measured by the platinum wire fused on the external surface of the tube. As the quantity (T_1-T_2) refers strictly to the difference of temperature between the central wire and the internal surface of the tube, it is necessary, therefore, in order to determine the value of T_2, to calculate the drop of temperature δt across the wall of the tube, which is deducible from the known rate of heat development in the central wire (C^2R_1), the curvatures of the internal and external surfaces of the tube r_2 and r_3, and the thermal conductivity K_g of the material of the tube wall. The corresponding value of T_2 is then obtained from

$$T_2=\delta t+T_3, \quad . \quad . \quad . \quad . \quad . \quad . \quad (12)$$

where δt is known from the relation

$$\delta t = \frac{C^2 R_1 \log_e \frac{r_3}{r_2}}{2\pi K_g l} \quad . \quad . \quad . \quad . \quad . \quad . \quad (13)$$

The order of magnitude of δt as associated with the present investigation was found to be not greater than

TABLE III.—CO_2 Bath.

Temperature of Central Wire $T_1 = -63{\cdot}79°$ C.

p cm. Hg.	$1/p$ (cm. Hg.)$^{-1}$.	$(T_1-T_2)/C^2$.	(T_1-T_2) °C.
78·10	0·0128	107·66	14·24
58·83	0·0170	107·74	14·06
50·98	0·0196	107·85	14·00
45·58	0·0219	107·85	13·95
41·90	0·0239	107·93	13·93
36·72	0·0272	108·01	13·89
34·02	0·0294	108·21	13·86
31·22	0·0320	108·33	13·79
28·40	0·0352	108·29	13·70
26·34	0·0380	108·44	13·64
23·76	0·0421	108·72	13·58
21·18	0·0472	108·77	13·52
19·05	0·0525	109·05	13·48
16·92	0·0591	109·19	13·43
14·87	0·0672	109·48	13·39
13·16	0·0760	109·84	13·34
11·77	0·0850	110·15	13·30

$K = 3{\cdot}110 \times 10^{-4}$ cals./cm./sec./deg.
Mean gas temperature $= 202{\cdot}44°$ abs.

0·02° C., and for this reason it is not necessary to know the value of K to a high degree of accuracy.

From (5), a linear relation operates between the quantities $(T_1-T_2)/C^2$ and $1/p$, and typical examples of the many observations recorded are tabulated in Tables III. and IV., and as applied to equation (5) are represented graphically in fig. 3.

Values of the thermal conductivity, corresponding to the average temperature $(T_1+T_2)/2$, are calculable from the intercept

$$\frac{R_1 \log r_2/r_1}{2\pi kl}$$

of such lines, while the coefficient of accommodation α at a temperature T_1 can be calculated from the relation

$$m=(\sqrt{T_1}/r_1+\sqrt{T_2}/r_2) \cdot 1/A,$$

where m is the slope of (5) and A a quantity defined by (2).

TABLE IV.—Liquid-Air Bath.

Temperature of Central Wire $T_1=-164{\cdot}76°$ C.

p. cm. Hg.	$1/p$ (cm. Hg.).	$(T_1-T_2)/C^2$.	(T_1-T_2) °C.
69·51	0·0144	92·09	18·08
39·83	0·0251	92·22	18·07
24·94	0·0401	92·26	18·06
15·98	0·0527	92·38	18·07
15·57	0·0642	92·47	18·07
9·82	0·1018	92·81	18·09
7·87	0·1270	93·02	18·10
7·01	0·1427	93·16	18·10
6·01	0·1664	93·33	18·10
4·90	0·2041	93·68	18·11
3·76	0·2660	94·17	18·12
2·96	0·3378	94·77	18·12

$K=1{\cdot}603\times10^{-4}$ cals./cm./sec./deg.
Mean gas temperature $=99{\cdot}30°$ abs.

Values of the thermal conductivity k, and the coefficient of accommodation α, corresponding to the average gas temperatures, are tabulated in Table V. and represented graphically in regard to their dependence on temperature in figs. 4 and 5.

From the results contained in fig. 4 the dependence on temperature of the heat conduction has been found to be expressible with satisfactory accuracy by a relation of the form

$$K_T=AT^n,$$

in which K_T represents the thermal conductivity at a temperature T (abs.) and n and A constants given by

$$A = 2{\cdot}14 \times 10^{-6},$$

$$n = 0{\cdot}938.$$

Fig. 3.

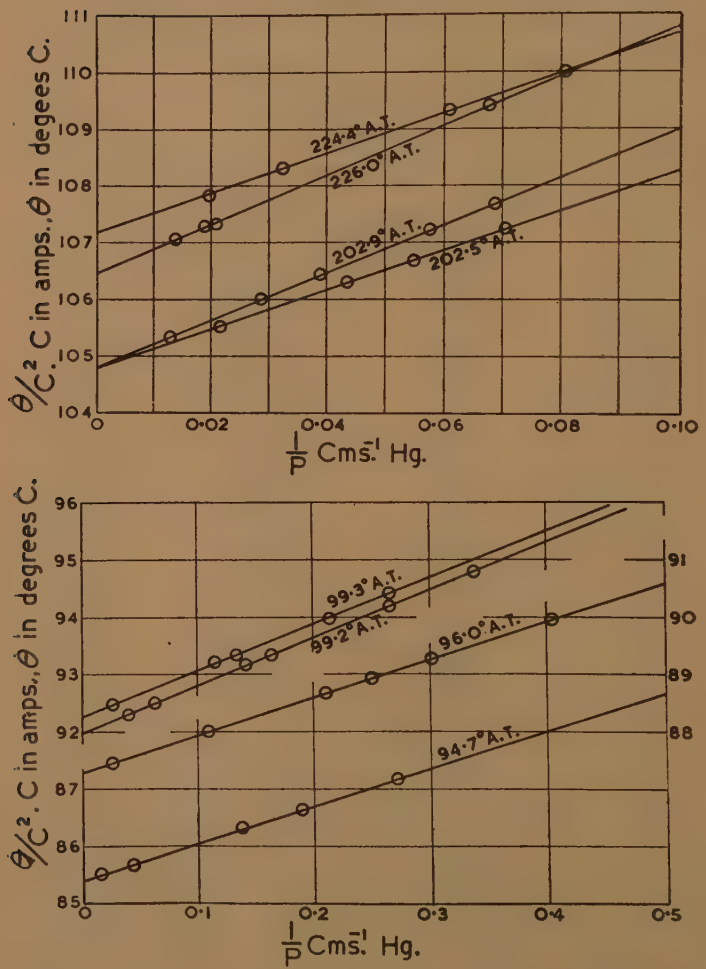

Values of the thermal conductivity resulting from an earlier investigation by Dr. Gregory [10] at various temperatures above 0° C. have been included in fig. 4 for purposes of comparison.

TABLE V.

$(T_1+T_2)/2$. deg. abs.	$k \times 10^4$ cals./cm./sec./deg.	α.
280·36	4·22	0·23
226·03	3·50	..
224·48	3·45	0·23 (5)
222·75	3·39	0·240
209·36	3·17	..
202·46	3·11	..
99·29	1·60	0·43
99·07	1·59	..
96·27	1·56	0·44 (5)
96·57	1·55	0·460
94·58	1·53	0·465

Fig. 4.

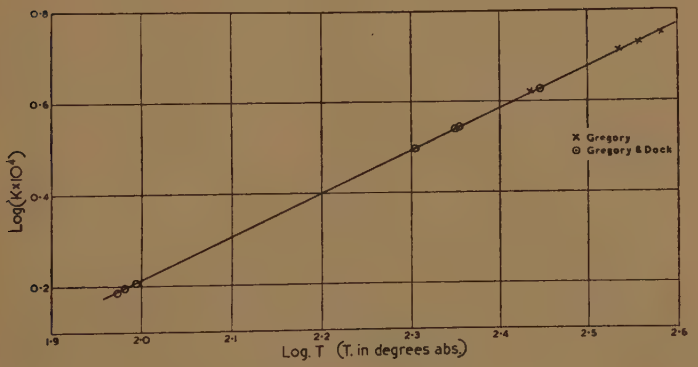

Fig. 5.

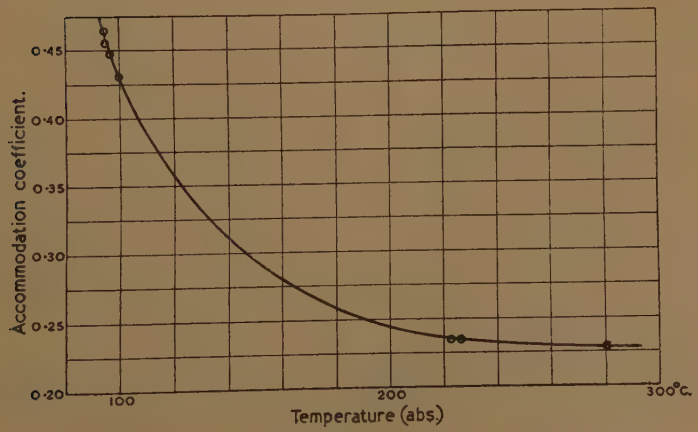

The temperature coefficient of thermal conductivity γ has been calculated from the definition

$$\gamma = \frac{1}{K_T}\left(\frac{dK}{dT}\right)_T,$$

in conjunction with the relation $K_T = 2{\cdot}14 \times 10^{-6} \times T^{0{\cdot}938}$ at the absolute temperatures 273·1, 203·8, 94·6, respectively, and the results are compared in Table VI. with those obtained from measurements carried out at various temperatures in the neighbourhood of each of the temperatures referred to above. The latter procedure is the more usual, and has been fully explained in previous papers on the subject.

TABLE VI.

Mean temp. abs.	From definition.	Usual procedure.
273·1	·0034	·0031
203·8	·0046	·0049
94·6	·0099	·0101

The Coefficient of Accommodation.

The results for the coefficient of accommodation α, calculated from the temperature drop theory, are found to vary in magnitude (fig. 5) from a value 0·48 at the temperature of liquid oxygen to a value 0·23 at 0° C., the rate of change at the former temperature being abnormally high. This aspect of the dependence on temperature has yet to receive confirmation from purely theoretical considerations. A mechanism for the effect of accommodation was proposed by Mott and Jackson [11] in relation to perfectly clean metallic surfaces and received support from the experimental investigations of Roberts [12]. More recently, Mann and Newell [13] determined the rates of increase of the coefficient of accommodation of H_2 relative to platinum after the surface had been cleaned by prolonged heating to a high temperature ; on lowering the temperature to a normal value (100° C.), the coefficient was found to increase very rapidly at first from a small value (·11) to the normal

value 0·30, representing a saturated condition of the surface, the attainment of the latter state requiring a comparatively long period for completion. It was found that, after saturation, evacuation and heating to a high temperature, the evolved volume of gas measured at atmospheric pressure and room-temperature was of the order of seventy times that of the wire. It would seem that the adsorption process is accompanied by a slow diffusion of gas into the platinum, and this very probably accounts for the very slow rate at which saturation is attained. For normal adsorption on smooth platinum the above volume would correspond to about 2000 hydrogen atoms for every exposed atom of platinum.

The existence of such adsorbed layers at every interface (solid-liquid), (liquid-gas) or (gas-solid), has been shown to be a necessary consequence of molecular attraction by Dr. S. C. Bradford ([14]), who has established its actual existence by applying it to calculate the vapour densities and boiling-points of liquids along with the viscosities of liquids and gases, which results are shown to be in excellent agreement with the experimentally observed values.

According to Dr. Bradford [14], the gas adsorbed at a solid surface exists in a quasi-liquid condition, in which the condensed molecules may be treated as a three-dimensional liquid in interaction with its vapour phase and possessing a definite surface energy.

Such a viewpoint would seem consistent with the large volume of gas which is emitted when a metal is strongly heated to a high temperature, and inconsistent with the hypothesis that surface saturation is effected when the surface is completely covered with a monomolecular layer.

The present calculations of the accommodation coefficient as defined by Knudsen, in terms of the temperature drop theory, have clearly indicated that the effect is independent of pressure over a wide range and depends only on temperature. It has also been shown by Gregory and Stephens [17] in a recent investigation that the coefficient of accommodation for the helium-platinum and the hydrogen-platinum phase are almost identical within experimental error of the results obtained by Mann [18] under conditions when the gas was strongly rarefied.

This aspect of the effect of accommodation suggests that the energy exchanges at constant temperature, together with the surface conditions, remain very sensibly the same from very low pressures up to pressures of the order of several cm. of Hg.

The process of adsorption would therefore seem to be one associated primarily with the diffusion of a relatively large volume of gas into the solid, which finally terminates with the formation of a stable film when the surface becomes saturated.

This implies that the average density of the film is independent of the external gas pressure and depends at a definite temperature almost entirely on the predominating attraction of the solid particles.

The factor f defined by the relation

$$f = \frac{K}{\eta C_v},$$

where K, η, and C represent the thermal conductivity, the coefficient of viscosity, and the specific heat at constant volume per gram of gas respectively, has been calculated at various temperatures between 0° C. and −182° C. from the experimental data for K associated with the present investigation, in conjunction with the most accurate available data for η and C_v.

Errors of the order of 2 per cent. are possible in the measured values of K and η at low temperatures, while even greater errors in the case of C_v are probable, for which a notable example is that of hydrogen.

The results (Table VII.) at the various temperatures are very approximately the same $f=2{\cdot}00$, with the exception of the value at the temperature of liquid oxygen, for which $f=2{\cdot}27$, a discrepancy accounted for probably by the experimentally observed decrease in C_v due to the loss in rotational energy at low temperatures.

Calculations of the factor f have also been made (Table VII.) from equations of semiempirical basis (14) and (15) deduced by Eucken [15] and Jeans [16], in conjunction with the experimental results of the molecular heats of H_2 between 0° C. and −182° C.

Eucken. $$f = 2{\cdot}5\frac{C_t}{C_v} + \frac{C}{C_v}. \quad . \quad . \quad . \quad . \quad . \quad . \quad (14)$$

Jeans. $$f = \frac{9\gamma - 5}{4}. \quad . \quad . \quad . \quad . \quad . \quad . \quad . \quad (15)$$

In (14) and (15), C_t and C_r represent the contributions of translational and rotational energies to the specific heat at constant volume C_v, and γ the ratio of the specific heats of the gas. For a rigid diatomic molecule with no vibration, $C_t+C_r=C$ also.

Both equations (14) and (15) give results which are equally good and support the high value obtained from the relation $K=f\eta C_v$ at the temperature of liquid oxygen.

TABLE VII.

Temp. abs.	$\eta\times10^7$.	$K\times10^4$.	Molecular heat βR cals.	$f=\frac{K}{\eta C_v}$.	Eucken (14).	Jeans (15).
89·6	392	1·45	3·29	2·27	2·36	2·37
192	666	2·97	4·48	2·01	2·01	2·00
195	670	3·01	4·51	2·01	1·99	1·99
213	710	3·27	4·62	2·01	1·97	1·97
233	760	3·56	4·73	2·00	1·95	1·95
273·1	860	4·14	4·86	2·01	1·93	1·93

References.

(1) Maxwell, J. C., Collected Works, vol. ii. p. 23.
(2) Winkelmann, *Pogg. Ann.* vol. clvi. p. 497 (1876).
(3) S. Chapman, Lond. Phil. Trans. A, vol. ccxi. p. 433 (1912).
(4) S. Chapman, Lond. Phil. Trans. A, vol. ccxvi. p. 279 (1916).
(5) S. Weber, Comm. Phys. Lab. Univ. of Leiden. Supplement no. 42 *b*, Deel 26, pp. 1338–1352 (1918).
(6) A. O. Rankine, *Physik Z. S.* vol. xi. pp. 497 and 745 (1910).
(7) C. T. Archer, Phil. Mag. ser. 7, vol. xix. p. 901 (1935).
(8) H. Spencer-Gregory, Phil. Mag. ser. 7, vol. xxii. p. 262 (1936).
(9) H. S. Gregory and S. Marshall, Proc. Roy. Soc. A, vol. cxviii, p. 597 (1928).
(10) H. S. Gregory, Proc. Roy. Soc. series A, no. 866, vol. cxlix. pp. 35–56 (March 1935).
(11) Proc. Roy. Soc. A, vol. cxxxvii. (1932).
(12) Proc. Roy. Soc. A, vol. clii. p. 464 (1935).
(13) Mann and Newell, Proc. Roy. Soc. A, no. 894, vol. clviii. (Jan. 1937).
(14) S. C. Bradford, Proc. Phys. Soc. vol. xlix. pt. vi. no. 275 (1937).
(15) Eucken, A., (A) *Phys. Z.* xiv. p. 329 (1913).
(16) Jeans, J. H., ' Dynamical Theory of Gases,' 3rd ed., p. 302.
(17) H. Spencer-Gregory and R. W. B. Stephens, ' Nature,' vol. cxxxix. p. 28 (January 1937).
(18) W. B. Mann, Proc. Roy. Soc. series A, no. 859, vol. cxlvi. pp. 776–791 (Oct. 1934).

IX. *The Propagation of Electromagnetic Waves in an Ionized Atmosphere.*

By L. G. H. Huxley, *M.A., D.Phil., F.Inst.P., F. W. Bennett Lecturer in Physics, University College, Leicester* *.

I. *Introduction.*

THE theory of the propagation of electromagnetic waves in the ionosphere, developed successively by various investigators within the last twenty-five years, assumes its most complete form in the magneto-ionic theory, in which the effect of the earth's magnetic field on the motions of the ions is fully considered.

This theory leads to two fundamental formulæ [1] and [2] independently derived by Appleton and Hartree. From these formulæ the refractive index of the medium and the absorption coefficient and state of polarization of the waves may be deduced for any direction of propagation relative to the earth's magnetic field.

The general features of the propagation are in conformity with the theory, and in special cases, such as when the waves are propagated along the earth's field, the simplified forms which the complicated general formulæ assume lead to predictions in close agreement with observation.

Nevertheless, the physical basis of this theory is in certain respects unsatisfactory in so far as the essential gaseous character of the ionic cloud is not specifically considered.

The electrical properties ascribed to the medium are rather those of a set of ions or electrons, free or loosely bound, imbedded in a quasi-viscous medium, their principal motions being the vibrations excited under the action of the applied electromagnetic field. The agitational motions of the ions, if accounted for at all, appear only indirectly in a damping factor.

It is known, however, from the theory of the interaction of electromagnetic waves in the ionosphere given by Bailey and Martyn [3], that the motions of electrons among the molecules of the ionosphere under the action of the electric field of the electromagnetic wave are essentially the same as the motions of electrons in gases.

* Communicated by the Author.

investigated by Townsend and his associates in the laboratory. The electrons acquire, under the action of either a steady or a high frequency electric force, a mean energy of agitation which exceeds the mean energy of thermal agitation of the molecules of the gas among which they move. The velocity of drift W of a group of such electrons in the direction of an applied electric force is usually much smaller than the mean velocity of agitation U of the molecules [4]. A theory which appears to presuppose the contrary must therefore be open to criticism.

In a previous paper [5], I have obtained expressions for the conductivity of an ionized gas under the influence of an alternating electric force of any frequency, and in what follows these results are used to develop a theory of the propagation of radio waves in the ionosphere, free from the objection mentioned above.

II. *Propagation of Electromagnetic Waves.*

General Formulæ.

The ordinary "cross and dot" notation of vector analysis is used for vector and scalar products respectively. In this notation Maxwell's equations for the electromagnetic field become

$$\nabla \times \mathrm{E} = -\frac{\mu \dot{\mathrm{H}}}{c}; \quad \nabla . \mathrm{E} = 4\pi\rho;$$

$$\nabla \times \mathrm{H} = \frac{\dot{\mathrm{E}} + 4\pi \mathrm{I}}{c}; \quad \nabla . \mathrm{H} = 0;$$

where the current density I is the sum of the conduction current density and the rate of change of the electrostatic polarization, and the density ρ is the sum of the true and "fictitious" charge densities. When I and ρ are so expressed it is unnecessary to consider independently the dielectric properties of the medium. H is expressed in gauss, and all other quantities in electrostatic units.

On eliminating H we obtain

$$\nabla^2 \mathrm{E} - \mathrm{Grad}\ (\mathrm{Div}\ \mathrm{E}) = \frac{\mu}{c^2} \frac{d^2 \mathrm{E}}{dt^2} + \frac{4\pi\mu}{c^2} \frac{d\mathrm{I}}{dt}. \quad . \quad (1)$$

We shall assume that the field vectors are those of a plane electromagnetic wave propagated at phase velocity v,

so that they may be represented as the product of complex amplitudes which involve the phase constants, and the common factor

$$e^{jp\left(t-\frac{\mathrm{R}\,.\,\mathrm{N}}{v}\right)} \equiv e^{jp\left(t-\frac{lx+my+nz}{v}\right)},$$

where p is the angular frequency and N the unit vector normal to the wave front whose direction cosines are l, m, and n.

The scalar product R . N is $(lx+my+nz)$, x, y, and z being the coordinates of any point on the plane wave front.

It is also convenient to introduce a vector P which may be termed the "generalized polarization," and is defined as follows:

$$\mathrm{I} = \frac{d\mathrm{P}}{dt} = jp\mathrm{P}$$

or

$$\frac{d\mathrm{I}}{dt} = -p^2\mathrm{P}.$$

Equation (1) may now be transformed to

$$\nabla^2\mathrm{E} - \frac{\mu}{c^2}\frac{d^2\mathrm{E}}{dt^2} = \mathrm{Grad\ (Div\ E)} - \frac{4\pi\mu p^2}{c^2}\mathrm{P}. \quad . \quad . \quad (2)$$

On eliminating E from Maxwell's equations we find

$$\nabla^2\mathrm{H} - \frac{\mu}{c^2}\frac{d^2\mathrm{H}}{dt^2} = -\frac{4\pi}{c}(\nabla \times \mathrm{I}). \quad . \quad . \quad . \quad (3)$$

The following results are easily obtained:

$$\nabla^2\mathrm{E} \equiv -\frac{p^2\mathrm{E}}{v^2}; \quad \nabla^2\mathrm{H} \equiv -\frac{p^2\mathrm{H}}{v^2};$$

$$\mathrm{Grad\ (Div\ E)} \equiv \nabla(\nabla\,.\,\mathrm{E}) \equiv -\left(\frac{p^2\mathrm{S}}{v^2}\right)\mathrm{N},$$

where S is the scalar product N . E;

$$\mathrm{Curl\ I} \equiv \nabla \times \mathrm{I} \equiv -\frac{jp}{v}(\mathrm{N} \times \mathrm{I}) = \frac{p^2}{v}(\mathrm{N} \times \mathrm{P}).$$

When these substitutions are made in equations (2) and (3) we find

$$\left(\frac{c^2}{v^2} - \mu\right)\mathrm{E} = \left(\frac{\mathrm{S}c^2}{v^2}\right)\mathrm{N} + 4\pi\mu\mathrm{P}, \quad . \quad . \quad . \quad (4)$$

$$\left(\frac{c^2}{v^2} - \mu\right)\mathrm{H} = \frac{4\pi c}{v}(\mathrm{N} \times \mathrm{P}). \quad . \quad . \quad . \quad . \quad . \quad (5)$$

Form the scalar product of each side of (4) and the unit vector N to obtain

$$\mathrm{H}=\frac{c}{\mu v}(\mathrm{N}\times\mathrm{E}). \quad . \quad . \quad . \quad . \quad . \quad . \quad . \quad (6)$$

The scalar product of N and each side of (4) leads to

$$\mu\mathrm{N}\,.\,(\mathrm{E}+4\pi\mathrm{P})=\mu\mathrm{N}\,.\,\mathrm{D}=0, \quad . \quad . \quad . \quad . \quad (7)$$

where $\mathrm{D}=\mathrm{E}+4\pi\mathrm{P}$ is the "generalized displacement." Equation (4) may also be written in the alternative form

$$\frac{c^2}{v^2}\mathrm{E}-\mu\mathrm{D}-\left(\frac{\mathrm{S}c^2}{v^2}\right)\mathrm{N}=0. \quad . \quad . \quad . \quad . \quad (4\,a)$$

Thus from (4 *a*) we deduce that E, D, and N are coplanar; from (6) that H is normal to these three vectors; and from (7) that D is perpendicular to N as well as to H.

Thus the electromagnetic wave is propagated as transverse vibrations of D and of H.

The relations between the vectors which appear above may be treated as relations between their complex amplitudes by dividing throughout by the common factor

$$e^{jp\left(t-\frac{\mathrm{R}.\mathrm{N}}{v}\right)}.$$

III. *Electrical Conductivity of an Ionized Gas.*

Let a permanent magnetic field H_0 gauss exist throughout the gas and choose a coordinate system whose Oz axis is in the direction of H_0.

Under the action of an alternating e.m.f. $\mathrm{X}=\mathrm{X}_0\cos pt$ directed along O*x*, the ions acquire velocities of drift W_x and W_y, which are related to X_0, p, and H_0 by formulæ obtained in a previous paper [5]. These formulæ are conveniently expressed in terms of the following symbols:

$\omega=\dfrac{\mathrm{H}_0 e}{mc}=\dfrac{\mathrm{H}_0\rho}{c}$ [H_0 in gauss].

$\rho=\dfrac{e}{m}$ = charge-mass ratio of the ion [e in e.s.u.].

$\mathrm{T}=\dfrac{l}{\mathrm{U}}=\dfrac{1}{\nu}$ = mean interval between collisions of an ion with molecules of the gas, ν being the collision frequency.

n=ionic concentration.

$\sigma=\frac{2}{3}\frac{ne^2}{m}\mathrm{T}$= direct current conductivity of the ionized gas, so that

$$\frac{\sigma}{2ne}=\frac{1}{3}\rho\mathrm{T}.$$

$$\mathrm{F}^{\pm}=\frac{1}{1+(p\pm\omega)^2\mathrm{T}^2}\left(1+\frac{(p\pm\omega)^2\mathrm{T}^2}{1+(p\pm\omega)^2\mathrm{T}^2}\right),$$

$$f^{\pm}=\frac{(p\pm\omega)\mathrm{T}}{1+(p\pm\omega)^2\mathrm{T}^2}\left(\frac{1}{2}+\frac{(p\pm\omega)^2\mathrm{T}^2}{1+(p\pm\omega)^2\mathrm{T}^2}\right),$$

F and f merely being abreviations for the above functions.

$$\mathrm{S}=\mathrm{F}^{+}+\mathrm{F}^{-};\quad s=f^{+}+f^{-}.$$
$$\mathrm{D}=\mathrm{F}^{+}-\mathrm{F}^{-};\quad d=f^{+}-f^{-}.$$

We define also the functions G and g as the forms assumed respectively by F and f when $\omega=0$.

When the distribution of the velocities U about the mean is neglected the velocity components

W_x and W_y due to the force $\mathrm{X}=\mathrm{X}_0\cos pt$ are [5]

$$\mathrm{W}_x=\frac{\mathrm{X}_0\sigma}{2ne}[\mathrm{S}\cos pt+s\sin pt],$$

$$\mathrm{W}_y=\frac{\mathrm{X}_0\sigma}{2ne}[\mathrm{D}\sin pt-d\cos pt].$$

The component W_z depends only on the force $\mathrm{Z}=\mathrm{Z}_0\cos pt$ along Oz and is

$$\mathrm{W}_z=\frac{\mathrm{Z}_0}{ne}[\mathrm{G}\cos pt+g\sin pt].$$

IV. *Propagation of Electromagnetic Waves in an Ionized Medium.*

Let the components of the electric and other vectors in the electromagnetic wave be of the form

$$\mathrm{X}=\mathrm{E}_x e^{ip\left(t-\frac{\mathrm{R}.\mathrm{N}}{v}\right)},\ \text{etc.}$$

The components of the current density are then given by

$$\mathrm{I}_x=ne\mathrm{W}_x=\frac{\sigma\mathrm{E}_x}{2}[\mathrm{S}+js]-\frac{\sigma}{2}\mathrm{E}_y[\mathrm{D}-jd],$$

$$I_y = neW_y = \frac{\sigma}{2} E_y[S+js] + \frac{\sigma}{2} E_x[D-jd],$$

$$I_z = neW_z = \sigma E_z[G+jg].$$

The components of the polarization are therefore

$$\begin{aligned} P_x &= \frac{I_x}{jp} = \frac{\sigma}{2p}[s-jS]E_x + \frac{\sigma}{2p}[d+jD]E_y \\ &= AE_x + BE_y, \\ P_y &= AE_y - BE_x, \\ P_z &= CE_z, \end{aligned}$$

where
$$A = \frac{\sigma}{2p}[s-jS]\,; \quad B = \frac{\sigma}{2p}(d+jD)\,; \quad C = \frac{\sigma}{p}[g-jG]. \qquad (8)$$

Equation (4) becomes ($\mu=1$)

$$\begin{aligned} (a)\quad & \left(\frac{c^2}{v^2}-1\right)E_x = \left(\frac{Sc^2}{v^2}\right) l + 4\pi(AE_x+BE_y), \\ (b)\quad & \left(\frac{c^2}{v^2}-1\right)E_y = \left(\frac{Sc^2}{v^2}\right) m + 4\pi(AE_y-BE_x), \\ (c)\quad & \left(\frac{c^2}{v^2}-1\right)E_z = \left(\frac{Sc^2}{v^2}\right) n + 4\pi CE_z. \end{aligned} \qquad (9)$$

For equation (5) we obtain

$$\begin{aligned} (a)\quad & \left(\frac{c^2}{v^2}-1\right)H_x = \frac{4\pi c}{v}[mCE_z - n(AE_y - BE_x)], \\ (b)\quad & \left(\frac{c^2}{v^2}-1\right)H_y = \frac{4\pi c}{v}[n(AE_x+BE_y) - lCE_z], \\ (c)\quad & \left(\frac{c^2}{v^2}-1\right)H_z = \frac{4\pi c}{v}[l(AE_y-BE_x) - m(AE_y+BE_x)]. \end{aligned} \qquad (10)$$

and for (6)

$$\begin{aligned} (a)\quad & H_x = \frac{c}{v}(mE_z - nE_y), \\ (b)\quad & H_y = \frac{c}{v}(nE_x - lE)_z, \\ (c)\quad & H_z = \frac{c}{v}(lE_y - mE_x). \end{aligned} \qquad (11)$$

These equations contain all the information necessary to determine the polarization and absorption of the waves and the refractive index of the medium.

Special Cases.

(a) *Propagation along the Field.*

$$l=m=0\,; \quad n=1\,; \quad \mathrm{S}=\mathrm{E}_z.$$

Equation (9) becomes

$$\frac{1}{4\pi}\left(\frac{c^2}{v^2}-1\right)=\mathrm{A}+\mathrm{B}\frac{\mathrm{E}_y}{\mathrm{E}_x}=\mathrm{A}-\mathrm{B}\frac{\mathrm{E}_x}{\mathrm{E}_y},$$

$$\frac{1}{4\pi}\left(\frac{c^2}{v^2}-1\right)\mathrm{E}_z=\frac{v^2}{4\pi c^2}\mathrm{E}_z+\mathrm{CE}_z,$$

whence $$\mathrm{E}_z=0,$$

$$\left(\frac{\mathrm{E}_y}{\mathrm{E}_x}\right)^2=-1, \quad \text{or} \quad \mathrm{E}_y=\pm j\mathrm{E}_x,$$

and from (11),

$$\mathrm{H}_z=0,$$

$$\frac{\mathrm{H}_y}{\mathrm{H}_x}=-\frac{\mathrm{E}_x}{\mathrm{E}_y}=\pm j.$$

Consequently, the permanent and independent wave forms propagated along Oz are two oppositely rotating circularly polarized waves both of E and of H. The refractive indices μ and absorption coefficients k are obtained from equations (9) in the special form given above.

We find

$$\frac{c^2}{v^2}=(\mu-jk)^2=1+4\pi(\mathrm{A}\pm j\mathrm{B})$$

$$=1+\frac{4\pi\sigma}{2p}(s\mp\mathrm{D})-j.\frac{4\pi\sigma}{2p}(\mathrm{S}\mp d),$$

whence $$\mu^2-k^2=1+\frac{2\pi\sigma}{p}(s\mp\mathrm{D}),$$

$$\mu k=\frac{\pi\sigma}{p}(\mathrm{S}\mp d)\,;$$

on eliminating μ and k in turn we obtain

$$2k^2 = -\left[1+\frac{2\pi\sigma}{p}(s\mp \mathrm{D})\right] + \left\{\left[1+\frac{2\pi\sigma}{p}(s\mp \mathrm{D})\right]^2 + \frac{4\pi^2\sigma^2}{p^2}(\mathrm{S}\mp d)^2\right\}^{1/2},$$

$$2\mu^2 = \left[1+\frac{2\pi\sigma}{p}(s\mp \mathrm{D})\right] + \left\{\left[1+\frac{2\pi\sigma}{p}(s\mp \mathrm{D})\right]^2 + \frac{4\pi^2\sigma^2}{p^2}(\mathrm{S}\mp d)^2\right\}^{1/2}.$$

The positive sign is taken before the radical since k and μ are real quantities.

When $\frac{2\pi\sigma}{p} >> 1$ and $(p\pm\omega)\mathrm{T} << 1$ the medium acquires metallic conductivity.

We have, in this instance,

$$\mathrm{S}=2\ ;\ s=d=\mathrm{D}=0,$$

$$k^2 \to \frac{2\pi\sigma}{p} \to \mu^2,$$

which is Drude's expression for the absorption coefficient and refractive index of electromagnetic waves in a highly conducting medium.

If, however, the waves traverse a region for which

$$\frac{2\pi\sigma}{p} << 1, \quad \text{and} \quad (p\pm\omega)\mathrm{T}$$

compared with unity is not too large or too small, then

$$k^2 \to \frac{\pi^2\sigma^2}{p^2}[\mathrm{S}+s\mp(d+\mathrm{D})].$$

Consequently, the circularly polarized waves are differentially absorbed and one alone may perhaps emerge.

(b) *Propagation Transverse to the Field.*

Without loss of generality the symmetry of the problem permits the assumption $m=0$.

Then $l=1\ ;\quad m=n=0\ ;\quad \mathrm{S}=\mathrm{E}_x.$

From equation (11) we have

$$\mathrm{H}_y = -\frac{c}{v}\mathrm{E}_z,$$

$$H_z = \frac{c}{v} E_y,$$

$$H_x = 0.$$

From (9 *c*) we conclude

$$E_z = 0, \quad \text{or} \quad \frac{c^2}{v^2} = 1 + 4\pi C.$$

If $E_z = 0$, then $H_y = 0$, and the wave consists of a plane polarized wave H_z.

(9 *a*) gives the ratio

$$\frac{E_x}{E_y} = -\frac{B}{(1+4\pi A)},$$

while the complex refractive index obtained from (9 *b*) is

$$(\mu - jk)^2 = \frac{c^2}{v^2} = 1 + 4\pi\left(A - B\frac{E_x}{E_y}\right) = 1 + 4\pi\left(A + \frac{B^2}{1+4\pi A}\right).$$

If $E_x \neq 0$, then in general, $E_x = E_y = H_z = 0$,

$$H_y = -\frac{c}{v} E_z,$$

$$(\mu - jk)^2 = 1 + 4\pi C.$$

Thus normal to the field the magnetic vector is propagated as two independent plane polarized waves H_y and H_z, which travel with different phase velocities and are differentially absorbed.

V. *Propagation in any Direction.*

Without loss of generality we may put $m = 0$, so that the wave normal lies in the xOz plane.

Let the direction cosines of the unit vector N be $(l, 0, n)$.

The component of the magnetic vector in the plane xOz is

$$H' = -nH_x + lH_z,$$

its component normal to this plane being H_y.

The simple forms assumed by the polarization in the special instances considered above for which l and n were respectively zero, suggest the following assumption for the general case of propagation in any direction.

Write

$$H' = \alpha H_y,$$

then, from (11), since $m=0$,

$$H' = -nH_x + lH_z = \frac{c}{v} E_y,$$

$$H_y = \frac{c}{v}(nE_x - lE_z),$$

$$\therefore \quad \alpha = \frac{E_y}{nE_x - lE_z},$$

or

$$-lE_z = \frac{E_y}{\alpha} - nE_x,$$

also from (10)

$$\left(\frac{c^2}{v^2} - 1\right) H' = \frac{4\pi c}{v}(AE_y - BE_x),$$

$$\alpha = \frac{AE_y - BE_x}{n(AE_x + BE_y) - lCE_z},$$

so that,

$$-lCE_z = -E_x\left(nA + \frac{B}{\alpha}\right) + E_y\left(\frac{A}{\alpha} - nB\right) = \frac{CE_y}{\alpha} - nCE_x,$$

$$\therefore \quad \frac{E_y}{E_x} = \frac{n(A-C)\alpha + B}{(A-C) - nB\alpha} \quad \ldots\ldots \quad (12)$$

We may obtain another expression for $\frac{E_y}{E_x}$ as follows:—

Multiply equations (9 *a*) and (9 *c*) respectively by l and n, and add; then, since

$$S = lE_x + nE_z,$$

$$l(1+4\pi A)E_x + 4\pi lBE_y = -n(1+4\pi C)E_z,$$

$$\therefore \quad -lE_z = l^2\left\{\frac{(1+4\pi A)E_x + 4\pi BE_y}{n(1+4\pi C)}\right\} = \frac{E_y}{\alpha} - nE_x,$$

whence, on taking (12) into account,

$$\frac{E_y}{E_x} = \left\{\frac{l^2(1+4\pi A) + n^2(1+4\pi C)}{n(1+4\pi C) - 4\pi l^2 B\alpha}\right\}\alpha = \frac{n(A-C)\alpha + B}{(A-C) - nB\alpha}. \quad (13)$$

We thus eliminate $\frac{E_y}{E_x}$, and after reduction the following reciprocal quadratic equation is found for α:

$$\alpha^2 - \frac{l^2[(A-C)(1+4\pi A) + 4\pi B^2]}{nB(1+4\pi C)}\alpha + 1 = 0.$$

Consequently, if $\alpha=\beta$ is one root of the above equation, $\beta'=\frac{1}{\beta}$ is the other root.

The permanent wave forms at an arbitrary direction to the field are therefore elliptically polarized waves of the magnetic vector, such that in the one the ratio of the amplitudes is $\frac{H'}{H_y}=\beta$, and in the other $\frac{H'}{H_y}=\frac{1}{\beta}$.

In the case of propagation along the field $l=0$ and $\alpha^2=-1$; $\beta=\pm j$ as before.

Normal to the field $n=0$, so that $\beta=0$; $\beta'=\infty$ in agreement with previous conclusions.

From equations (9 *b*) and (13)

$$(\mu-jk)^2=\frac{c^2}{v^2}=1+4\pi\left(A-B\frac{E_x}{E_y}\right)$$

$$=1+4\pi\left\{A-\frac{B[n(1+4\pi C)-4\pi l^2B\alpha]}{\alpha[l^2(1+4\pi A)+n^2(1+4\pi C)]}\right\}$$

$$=1+4\pi\left\{A-\frac{B[(A-C)-nB\alpha]}{n(A-C)\alpha+B}\right\}.$$

On substituting the appropriate root $\alpha=\beta$ or β', we obtain the complex refractive index for the corresponding wave.

Conclusion.

It is not the purpose of this paper to enter into detailed discussions of particular problems relating to the ionosphere, but rather to indicate the lines along which a more satisfactory theory might be developed.

The present theory leads to conclusions concerning the propagation of waves in an arbitrary direction to the field essentially different from those which are derived from the Appleton-Hartree formulæ. In the latter formulæ the components H_{0L} and H_{0T} of the permanent magnetic field along and transverse to the direction of propagation appear individually, whereas from the standpoint of the theory given above such a resolution of the magnetic force is inadmissible, since the total field strength H_0 alone appears in the expressions for the conductivity, and, moreover, not linearly.

In certain special cases the Appleton-Hartree formulæ reduce to forms which involve the total field H_0 only,

and they would then lead to conclusions not essentially different from those to be derived from the present theory.

It is improbable that the neglect in this paper of the distribution of the electronic velocities U about the mean would introduce serious error, since it is known that under the action of the field the velocity distribution is in many instances narrower than that given by Maxwell's law.

The Lorentz correction to the effective electric field on account of the polarization of the medium has been neglected as probably unimportant when the lateral dimensions of the wave front are great in comparison with the wave-length.

The ionic charge has throughout been considered positive. If the ions are electrons then the quantity ω must be considered negative. On substituting ω in the formulæ for S, s, D, and d, we find that S and s remain unaffected while D and d change sign. It is easily seen that in the case of propagation along the permanent magnetic field, the effect of reversing the sign of the ionic charge is to cause the right-handed and left-handed circularly polarized waves to exchange properties.

References.

(1) Appleton, E. V., "Radio Exploration of Upper Atmospheric Ionization," Physical Society Reports on Progress in Physics, vol. ii. p. 129.
(2) White, F. W. G., 'Electromagnetic Waves,' chaps. v. and vi. (Methuen).
(3) Bailey, V. A., and Martyn, D. F., "Influence of Electric Waves on the Ionosphere," Phil. Mag. vol. xviii. p. 369 (August 1934).
(4) Townsend, J. S., 'Motion of Electrons in Gases,' Oxford.
(5) Huxley, L. G. H., "Motions of Electrons in Magnetic Fields and Alternating Electric Fields," Phil. Mag. vol. xxiii. p. 442 (March 1937).

X. *Point-discharge Currents during Thunderstorms.* By M. N. S. Immelman, *Senior Lecturer in Physics, University of Pretoria* *.

DURING fine weather there is a positive potential gradient over the surface of the earth, the average value of this gradient for the whole earth being about 120 volts per metre. In this fine-weather field positive

* Communicated by the Author.

ions are driven towards the earth and negative ions way from it, giving rise to a downwardly directed electric current.

The mean value of the fine-weather current between the earth and the upper atmosphere is about 2×10^{-16} amperes per square centimetre, or about 1000 amperes for the whole earth.

To this must be added a precipitation current which has been estimated by Wigand * to be about 400 amperes for the whole world directed towards the earth.

In spite of these two effects the earth's electrical charge is maintained.

It was due to a suggestion by C. T. R. Wilson that regions of disturbed weather were examined for a possible cause of replenishment. It was found that under thunder-clouds and during rain the potential gradient is as a general rule in the reverse direction and has also an abnormally high value. Fields of 10,000 volts per metre and more are often observed under thunder-clouds.

Wormell † designed a microvoltameter which enabled him to keep a continuous record of the sign and magnitude of the vertical current due to the point-discharge of electricity from an elevated metal point during periods of disturbed weather. He erected an observation station at Cambridge, and his results, taken over a period of several years, show that there is a considerable net transfer of positive electricity upwards from the earth to the atmosphere during the intense electric fields associated with thunderstorms and showers.

Although Wormell's results are very complete it is desirable to have results of similar observations in other parts of the world where weather conditions are different.

The author, using a microvoltameter similar to that described by Wormell, kept a record of point-discharges during thunderstorms at Pretoria, South Africa.

The pole on which the discharge-point was mounted was about 7 metres high. It was in the centre of an empty field, which was, however, surrounded by trees on all sides. The nearest tree to the pole was about 30 metres away.

The voltameter was not housed in a separate hut at some

* *Ann. d. Physik*, lxvi. p. 81 (1921).

† Proc. Roy. Soc. A, cxv. p. 443 (1927); Proc. Roy. Soc. A, cxxvii. p. 567 (1930).

distance from the pole, but was kept in a box attached to the pole itself.

Difficulties were at first experienced due to leakage across the glass surface of the voltameter as a result of the acid in the voltameter "creeping" along the glass. The trouble was overcome by surrounding each of the open ends with an oil-bath, as shown at B, C, and D in the figure.

The cross-piece T connecting the two limbs was directly sealed on instead of being connected by rubber tubing. A was connected to the discharge-point at the top of the pole and B was connected to earth.

Now if V_A c.c. of mixed gas collects at the electrode in A and V_E c.c. collects in B for a definite period, then

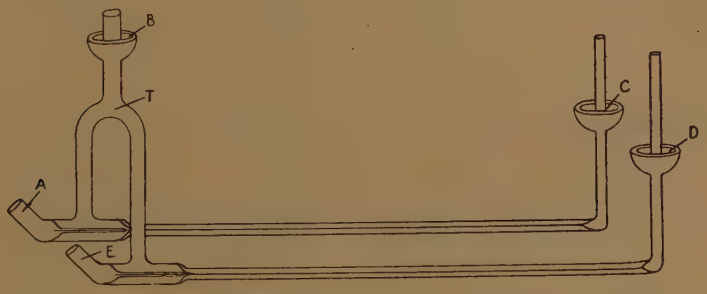

if q_A units of electricity enter the voltameter at A and q_E enter at E, we have that

$$cq_A+2cq_E=V_A,$$

also

$$2cq_A+cq_E=V_E,$$

where c c.c. and $2c$ c.c. are the quantities of oxygen and hydrogen respectively that are liberated in electrolysis by 1 unit of electricity. Hence by measuring V_A and V_E the quantities q_A and q_E can be determined. In the results that follow q_A and q_E are in millicoulombs.

Results.

Date.	q_A.	q_E.	
28. 8. 33	2·0	25	Very severe dust-storm all day, few clouds in distance.
27. 9. 33	Trace.	..	Wind and slight dust in afternoon, sky clear.

Date.	q_A.	q_E.	
28. 9. 33	..	28·5	Severe dust-storm in afternoon and evening, sky overcast, no rain.
10. 10. 33	10·5	1·5	Sky overcast during afternoon, sheet lightning in the distance during evening, no rain.
11. 10. 33	..	11·5	Sky overcast, dust-storm during evening, no lightning.
13. 10. 33	16·0	2·0	Wind and dust, few clouds overhead.
16. 10. 33	..	2·0	Wind, dust, and distant lightning, sky overcast, very slight rain.
17. 10. 33	..	8	Sky overcast, thundery conditions, distant lightning, *very* little rain.
26. 10. 33	3·0	24·5	Sky overcast, severe dust-storm, no rain, no lightning.
27. 10. 33	..	3	Sheet lightning in distance, no dust, very little rain, sky heavily overcast.
1. 11. 33	..	24·5	Instrument not read for few days of hot sultry weather, slight rain on morning of 1. 11. 33.
12. 11. 33	0	20·5	Bad thunderstorm and rain previous night, plenty of lightning in vicinity.
24. 11. 33	3·5	..	Heavy shower of rain previous night, few claps of thunder.
28. 11. 33	2·5	8·5	Bad thunderstorm accompanied by heavy rain.
1. 12. 33	5	0	Lightning and thunder, little rain, weather sultry with overcast sky.
8. 12. 33	5·5	23	Dust-storm followed by heavy thunderstorm, rain previous afternoon.
13. 12. 33	..	Trace.	Cloudy but little lightning, storm about 10 miles away.
17. 12. 33	Trace.	..	Small storm ± 6 miles away, little lightning, strong wind.
14. 1. 34	..	2·5	Distant storm at night, heavy rains.
30. 1. 34	..	Trace.	Small storms all round, thundery conditions.
14. 2. 34	..	Trace.	.....
29. 10. 34	1·5	1·0	Plenty of sheet lightning previous night.
14. 11. 34	..	30·5	Plenty of thunder, lightning, and rain.
28. 11. 34	5	3	.....
24. 3. 35	6	1·5	Plenty of lightning, heavy rain.
1. 9. 35	1	1	Plenty of lightning, heavy rain.
16. 9. 35	2	1·5	Thunder, very little rain.
6. 10. 35	..	8·5	Lightning and rain.
10. 10. 35	3	6	Thunderstorm and heavy rain.
13. 10. 36	0	3·5	Slight rain, wind N.E., thunder and lightning previous night.
14. 10. 36	2	3·5	Rain, hail, and thunder previous afternoon, 5.30 to 9 P.M.

Date.	q_A.	q_E.	
16. 10. 36	0	4	Thunderstorm with slight rain.
28. 10. 36	2	11	Strong wind, thunderstorm 3 miles west.
29. 10. 36	0	6·0	Fork and chain lightning, with slight rain.
6. 11. 36	1·5	4	Good thunderstorm in distance, slight rain.
9. 11. 36	4	1	Good rain, severe short thunderstorm.
12. 11. 36	5	26·5	Two days of rain with severe thunderstorms.
17. 11. 36	5	8·5	Thunderstorm accompanied by rain.
19. 11. 36	6·5	2·5	Short sharp storm, much rain.
24. 11. 36	7	24·5	Beautiful sheet lightning with some chain, little rain.
30. 11. 36	5	5·5	Slight storms for three nights (instrument not read).
17. 12. 26	7·5	3·5	Sheet lightning and some rain.
29. 12. 36	0·5	7	Steady soft rain, with few thunderclaps.
15. 1. 37	12	1	Sultry weather, ending with slight storm.
5. 2. 37	1·5	4	Small thunderstorm.

At Pretoria rain is almost invariably accompanied by thunderstorms; the season for rain and thunderstorms is limited to about five months during the year, usually from about October to February.

Very few results were obtained during the two seasons 1934–1935 and 1935–1936, as the author was away on leave and the instrument was not attended to.

Several severe dust-storms occurred during the latter part of 1933. Very big discharges were recorded, and in all cases except two the discharge was from the earth to the atmosphere.

For the two complete seasons there was a net transfer of positive electricity from the earth to the atmosphere amounting to 185 millicoulombs for the two. If the discharges during the dust-storms be left out of account then the results show a net loss of positive electricity of 65 millicoulombs for the 1933–1934 season and 57 millicoulombs for the 1936–1937 season.

In conclusion, I wish to thank the Institute of Electrical Engineers, Johannesburg, for a grant which made it possible for these observations to be taken. I also wish to thank Professor Schonland, Chairman of the Lightning Research Committee, for suggesting the experiments and for his interest in them.

XI. *Radial and Torsional Vibrations of Annular Quartz Plates.* *By* A. Žáček *and* V. Petržílka *.

[Plates II.–IV.]

VARIOUS kinds of vibrations of quartz rings [1], [2] and of hollow quartz cylinders [3], [1] have been recently studied. In all the cases the research has been concerned with vibrating systems in which the thickness was comparable with the other dimensions. In our work, however, we have studied the vibrations of very thin circular plates having in their middle a circular opening of varying radius. The thickness of the plate was so small that it was negligible as compared with the radius of the plate.

First we give the results of the theoretical and experimental study of free extensional vibrations of circular annular plates. We call extensional vibrations those in which the elastic displacements take place in the plane of the plate. Annular plates, as well as full plates [4], [5], can perform the following three kinds of extensional vibrations: 1, radial; 2, torsional; 3, vibrations that may be called a combination of radial and torsional vibrations. As lengthy numerical calculations would be necessitated by the third type of vibration this paper confines itself to radial and torsional vibrations only. The piezo-electric material employed consisted in quartz plates cut normal to the optical axis, which behave in their plane in the same way as plates of isotropic material.

The Theoretical Part.

In deriving the relations for the frequency and nodal lines of free extensional vibrations of circular annular plates we start from the equations derived by Love [4]; these relations can also be derived directly if we assume that elastic displacements take place only in the plane x, y, which we draw through the middle plane of the plate, whereas there do not exist any elastic displacements in the direction of the axis z, *i. e.*, in the direction of the thickness of the plate.

* Communicated by Prof. E. V. Appleton.

Between the elastic stress-components

$$X_x, Y_y, X_y = Y_x$$

and the elastic displacements

$$x_x = \frac{\partial u}{\partial x}, \quad y_y = \frac{\partial v}{\partial y}, \quad x_y = y_x = \frac{\partial u}{\partial y} + \frac{\partial v}{\partial x}$$

there exist the relations

$$\left.\begin{aligned} X_x &= F\left(\frac{\partial u}{\partial x} + \sigma \frac{\partial v}{\partial y}\right), \\ Y_y &= F\left(\frac{\partial v}{\partial y} + \sigma \frac{\partial u}{\partial x}\right), \\ X_y = Y_x &= G\left(\frac{\partial u}{\partial y} + \frac{\partial v}{\partial x}\right), \end{aligned}\right\} \quad \ldots \quad (1)$$

where F and G are given by the expressions

$$F = \frac{E}{1-\sigma^2}, \quad G = \frac{E}{2(1+\sigma)}, \quad \ldots \quad (2)$$

E denoting the modulus of elasticity, σ Poisson's ratio Substituting these expressions in the equations of motion (ρ is the density of the solid employed), we get

$$\left.\begin{aligned} \rho \frac{\partial^2 u}{\partial t^2} &= F \frac{\partial p}{\partial x} - G \frac{\partial \epsilon}{\partial y}, \\ \rho \frac{\partial^2 v}{\partial t^2} &= F \frac{\partial p}{\partial y} + G \frac{\partial \epsilon}{\partial x}, \end{aligned}\right\} \quad \ldots \quad (3)$$

on introducing the areal dilatation p, the rotation ϵ by means of relations

$$p = \frac{\partial u}{\partial x} + \frac{\partial v}{\partial y}, \quad \epsilon = \frac{\partial v}{\partial x} - \frac{\partial u}{\partial y}. \quad \ldots \quad (4)$$

From the equations (3) we get the final equations for extensional vibrations in the form of

$$\left.\begin{aligned} \rho \frac{\partial^2 p}{\partial t^2} &= F \Delta p, \\ \rho \frac{\partial^2 \epsilon}{\partial t^2} &= G \Delta \epsilon. \end{aligned}\right\} \quad \ldots \quad (5)$$

The plate in our case being a circular one it is appropriate to transpose p and ϵ into polar coordinates r and Θ.

Substituting for u and v the new variables U and V by means of relations

$$u=\mathrm{U}\cos\Theta-\mathrm{V}\sin\Theta,\quad v=\mathrm{U}\sin\Theta+\mathrm{V}\cos\Theta,$$

in which U denotes displacement in the direction of the radius and V normal to the direction of the radius of the plate, the relations holding for p and ϵ are

$$p=\frac{\mathrm{U}}{r}+\frac{\partial \mathrm{U}}{\partial r}+\frac{1}{r}\frac{\partial \mathrm{V}}{\partial\Theta},$$

$$\epsilon=\frac{\mathrm{V}}{r}+\frac{\partial \mathrm{V}}{\partial r}-\frac{1}{r}\frac{\partial \mathrm{U}}{\partial\Theta}$$

Subsequently we shall study two types of extensional vibrations of circular annular plates: (1) vibrations in which elastic displacements occur only in the direction of the radius of the plate, and which, therefore, we shall call radial; (2) vibrations in which elastic displacements take place normal to the radius of the plate, and which, therefore, we shall call torsional.

1. *Radial Vibrations.*

For radial vibrations in which $\mathrm{U}\neq 0$ is independent on Θ, whereas $\mathrm{V}=0$, the equations (5) are reduced to one differential equation,

$$\rho\frac{\partial^2 \mathrm{U}}{\partial t^2}=\mathrm{F}\frac{\partial}{\partial r}\left\{\frac{1}{r}\frac{\partial}{\partial r}(r\mathrm{U})\right\},\quad\ldots\quad(6)$$

with the boundary condition (see equations (1))

$$\mathrm{X}_x=\mathrm{Y}_y=\mathrm{F}\left\{\frac{\partial \mathrm{U}}{\partial r}+\sigma\frac{\mathrm{U}}{r}\right\}_{\substack{r=a\\ r=b}}=0\quad\ldots\quad(7)$$

for $r=a$ and $r=b$, where a denotes the external, b the internal radius of the plate. For the nth overtone the integral of this equation, which may be written in the form of $\mathrm{U}_n=\mathrm{R}_n(r)\mathrm{T}_n(t)$, is given by the expression

$$\mathrm{U}_n=\{\mathrm{C}_1^{(n)}\mathrm{I}_1(\kappa_n^{(r)}r)+\mathrm{C}_2^{(n)}\mathrm{N}_1(\kappa_n^{(r)}r)\}\{\mathrm{A}_n\sin\omega_n^{(r)}t+\mathrm{B}_n\cos\omega_n^{(r)}t\},$$

$$\ldots\quad(8)$$

in which

$$\omega_n^{(r)}=\kappa_n^{(r)}\sqrt{\frac{\mathrm{E}}{\rho(1-\sigma^2)}}\quad\ldots\quad(9)$$

denotes the frequency of this vibration, $I_1(\kappa_n^{(r)}r)$, $N_1(\kappa_n^{(r)}r)$ Bessel's and Neumann's functions. The constant $\kappa_n^{(r)}$ we shall calculate as the nth root of the equation (7), which, on substituting from equation (8), will pass into the form of

$$-\frac{C_1^{(n)}}{C_2^{(n)}}=\frac{x_n^{(r)}N_0(x_n^{(r)})-(1-\sigma)N_1(x_n^{(r)})}{x_n^{(r)}I_0(x_n^{(r)})-(1-\sigma)I_1(x_n^{(r)})}$$

$$=\frac{\xi_n^{(r)}N_0(\xi_n^{(r)})-(1-\sigma)N_1(\xi_n^{(r)})}{\xi_n^{(r)}I_0(\xi_n^{(r)})-(1-\sigma)I_1(\xi_n^{(r)})}, \quad . \quad (10)$$

where

$$\kappa_n^{(r)}=\frac{x_n^{(r)}}{a}=\frac{\xi_n^{(r)}}{b}. \quad . \quad . \quad . \quad . \quad . \quad (11)$$

The nodal lines are circles that arise for such values of radius r for which $U_n=0$, *i. e.*,

$$\frac{I_1(\kappa_n^{(r)}r)}{N_1(\kappa_n^{(r)}r)}=-\frac{C_2^{(n)}}{C_1^{(n)}}. \quad . \quad . \quad . \quad . \quad (12)$$

2. *Torsional Vibrations.*

For torsional vibrations in which $V\neq 0$ is independent on Θ, whereas $U=0$, we get from equations (5) quite analogically as in radial vibrations only one differential equation,

$$\rho\frac{\partial^2 V}{\partial t^2}=G\frac{\partial}{\partial r}\left\{\frac{1}{r}\frac{\partial}{\partial r}(rV)\right\}, \quad . \quad . \quad . \quad (13)$$

with the boundary condition (see equations (1))

$$X_y=Y_x=G\left\{\frac{\partial V}{\partial r}-\frac{V}{r}\right\}_{\substack{r=a\\ r=b}}=0 \quad . \quad . \quad (14)$$

for $r=a$ and $r=b$.

Introducing into equation (13) the torsional angle ϕ in the relation $V=r\phi$, we get the equation

$$\rho r^3\frac{\partial^2\phi}{\partial t^2}=G\left\{\frac{\partial}{\partial r}\left(r^3\frac{\partial\phi}{\partial r}\right)\right\}. \quad . \quad . \quad . \quad (15)$$

This equation, however, is identical with Grammel's [7], [8] equation

$$\rho r^3 z\frac{\partial^2\phi}{\partial t^2}=G\frac{\partial}{\partial r}\left(r^3 z\frac{\partial\phi}{\partial r}\right),$$

where $z=f(r)$ denotes the thickness of the plate, this thickness being constant in our case.

The equations (13) and (14) can be satisfied by the functions in the form of $V_n=R_n(r)T_n(t)$, the resulting expression for the nth overtone thus being

$$V_n=\{D_1^{(n)}I_1(\kappa_n^{(t)}r)+D_2N_1(\kappa_n^{(t)}r)\}\{A_n'\sin\omega_n^{(t)}t+B_n'\cos\omega_n^{(t)}t\}, \quad . \quad . \quad . \quad (16)$$

where

$$\omega_n^{(t)}=\kappa_n^{(t)}\sqrt{\frac{E}{2(1+\sigma)}} \quad . \quad . \quad . \quad . \quad (17)$$

denotes the frequency of this vibration. The constant $K_n^{(t)}$ will be calculated from the equation [6]

$$-\frac{D_2^{(n)}}{D_1^{(n)}}=\frac{I_2(\kappa_n^{(t)}a)}{N_2(\kappa_n^{(t)}a)}=\frac{I_2(\kappa_n^{(t)}b)}{N_2(\kappa_n^{(t)}b)}=\frac{I_2(x_n^{(t)})}{N_2(x_n^{(t)})}=\frac{I_2(\xi_n^{(t)})}{N_2(\xi_n^{(t)})}, \quad (18)$$

in which

$$\kappa_n^{(t)}=\frac{x_n^{(t)}}{a}=\frac{\xi_n^{(t)}}{b}.$$

The radii of the nodal lines will be calculated from the equation $V_n=0$, *i. e.*,

$$\frac{I_1(\kappa_n^{(t)}r)}{N_1(\kappa_n^{(t)}r)}=-\frac{D_2^{(n)}}{D_1^{(n)}}. \quad . \quad . \quad . \quad . \quad . \quad . \quad (19)$$

The Experimental Part.

The plates employed in our experiments were four circular annular plates the radii of which are given in Table I. All the plates were cut normal to the optical

Table I.

Quartz plate.	External radius a in cm.	Internal radius b in cm.	Thickness d in cm.	b/a.
A.....	1·491	0·0	$0·101_5$	—
B.....	1·477	0·339	0·097	$0·229_6$
C.....	1·499	0·602	0·102	$0·401_9$
D.....	1·500	0·900	0·103	0·600

axis, the electric axes thus lying in the plane of the plate. In the quartz the modulus of elasticity, E_{11} [9],

$$E_{11}=1/s_{11}=7{\cdot}862.10^{11} \text{ (cm.-g.-sec. system)},$$

and Poisson's ratio, σ [9], [10],

$$\sigma=-s_{12}/s_{11}=0{\cdot}130,$$

are constant in the plane perpendicular to the optical axis, the plates accordingly behaving in this plane just as a plate of isotropic solid. On calculating the frequencies the value $\rho=2{\cdot}65$ g./cm.^{3} was employed for the density of quartz.

The vibrations were excited piezo-electrically by putting the plate on an insulating foundation between six electrodes placed in a circle (fig. 1). Radial vibrations were excited while the plate was turned so that the electrodes were

Fig. 1.

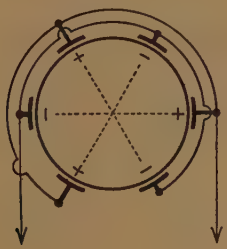

opposite to the ends of the electric axis, while when torsional vibrations were being excited the plate was placed in the holder in such a way that the ends of the electric axis found themselves between the electrodes. Thus it was possible to excite tangentia stress in the torsional vibrations. The electrodes were interconnected as shown in fig. 1, and attached to the oscillating circuit of a small transmitter. The frequency of the transmitter was slowly changed until the moment when, the frequency of the transmitter being equal to the actual frequency of the free radial or torsional vibrations, there was produced on the plate a picture of the nodal lines. To produce nodal lines lycopodium was employed; the frequency was measured by means of a wave-meter with 0·1 per cent. precision.

1. *Radial Vibrations.*

Radial vibrations were submitted to observation in all the plates, with frequencies given in Tables II., III., IV., and V. The resulting measurements of frequency

TABLE II.—Plate A (full).

n.	$x_n^{(r)}$.	Calculated frequency f_c in kc.	Measured frequency f_m in kc.	$\delta=\frac{f_c-f_m}{f_m}$ parts per 1000.	Figure.
0	1·935	$113{\cdot}4_7$	$114{\cdot}3_1$	−7·3	2
1	5·357	$314{\cdot}1_3$	$315{\cdot}3_4$	−3·8	3
2	8·552	$501{\cdot}4_8$	$502{\cdot}4_5$	−1·9	4
3	11·717	$687{\cdot}0_7$	$689{\cdot}5_7$	−3·6	—

TABLE III.—Plate B.

n.	$x_n^{(r)}$.	Calculated frequency f_c in kc.	Measured frequency f_m in kc.	$\delta=\frac{f_c-f_m}{f_m}$ parts per 1000.	Figure.
0	1·717	$101{\cdot}6_7$	$101{\cdot}9_5$	−2·8	5
1	4·895	$289{\cdot}8_5$	$290{\cdot}2_8$	−1·5	6
2	8·579	$507{\cdot}9_9$	$509{\cdot}3_6$	−2·7	7
3	12·510	$740{\cdot}7_7$	$742{\cdot}3_2$	−2·1	—

TABLE IV.—Plate C.

n.	$x_n^{(r)}$.	Calculated frequency f_c in kc.	Measured frequency f_m in kc.	$\delta=\frac{f_c-f_m}{f_m}$ parts per 1000.	Figure.
0	1·471	85·83	85·76	+0·8	8
1	5·622	$328{\cdot}0_2$	$331{\cdot}9_6$	−11·9	9
2	10·688	$623{\cdot}5_9$	$632{\cdot}6_1$	−14·3	10
3	15·891	$927{\cdot}1_8$	$935{\cdot}0_2$	−8·4	—

are in good agreement with the frequencies calculated from equation (9); the nodal lines can be seen in figs. 2 to 13 (Pl. II.). For the sake of comparison we also give the

results of observation in a full plate. The fundamental vibration does not show any nodal line in an annular plate; in case of overtones the nodal lines are circles. The radii of nodal lines obtained from measurement and calculation are given in Table VI. Radii of nodal lines are reduced to radius $a=1$.

TABLE V.—Plate D.

n.	$x_n^{(r)}$.	Calculated frequency f_c in kc.	Measured frequency f_m in kc.	$\delta=\frac{f_c-f_m}{f_m}$ parts per 1000.	Figure.
0	1·255	73·14	73·22	−1·1	11
1	8·015	$467{\cdot}1_7$	$471{\cdot}7_0$	−9·6	12
2	15·786	$920{\cdot}1_1$	$930{\cdot}2_3$	−10·9	13
3	23·616	$1376{\cdot}0_5$	$1401{\cdot}0_9$	−18·1	—

TABLE VI.—Radii of the Nodal Lines reduced to Radius $a=1$.

Plate.	r_k. e	$m=0$.	$m=1$.		$m=2$.		
		r_0.	r_0.	r_1.	r_0.	r_1.	r_2.
A	Calculated ..	0	0	0·712	0	0·447	0·819
	Measured ...	0	0	0·72	0	0·42	0·83
B	Calculated ..	—	—	0·688	—	0·450	0·821
	Measured ...	—	—	0·69	—	0·44	0·83
C	Calculated...	—	—	0·728	—	0·560	0·853
	Measured ...	—	—	—	—	—	—
D	Calculated...	—	—	0·809	—	0·703	0·903
	Measured ...	—	—	0·81	—	0·72	0·91

2. *Torsional Vibrations.*

Torsional vibrations could also be excited in all the plates, at frequencies given in Tables VII., VIII., IX., X. The nodal lines in these vibrations should also be

circles, but figures 14–25 (Pl. III.) show trigonal symmetry; the axes of symmetry of these pictures halve the angles of electric axes, thus it was possible to determine in a simple way the position of the electric axes. The radii calculated from the equation (19) are compiled in Table XI.; the radii of the nodal circles in a full plate are the same as in radial vibrations. As can be seen from the pictures of the nodal lines a great number

TABLE VII.—Plate A (full).

n.	$x_n^{(t)}$.	Calculated frequency f_c in kc.	Measured frequency f_m in kc.	$\delta = \frac{f_c - f_m}{f_m}$ parts per 1000.	Figure.
0	5·136	$198{\cdot}6_2$	$197{\cdot}5_4$	+5·4	14
1	8·412	$325{\cdot}3_1$	$325{\cdot}1_6$	+0·5	15
2	11·620	$449{\cdot}3_7$	$448{\cdot}5_2$	+1·9	16
3	14·796	$572{\cdot}1_9$	$571{\cdot}9_2$	+0·5	—

TABLE VIII.—Plate B.

n.	$x_n^{(t)}$.	Calculated frequency f_c in kc.	Measured frequency f_m in kc.	$\delta = \frac{f_c - f_m}{f_m}$. parts per 1000.	Figure.
0	5·273	$205{\cdot}9_2$	$205{\cdot}5_0$	+2·0	17
1	8·990	$351{\cdot}0_8$	$350{\cdot}4_3$	+1·9	18
2	12·842	$501{\cdot}5_1$	$500{\cdot}4_3$	+2·2	19
3	16·788	$655{\cdot}6_1$	$654{\cdot}4_3$	+1·8	—
4	20·778	$811{\cdot}4_2$	$799{\cdot}2_0$	+2·7	—
5	24·794	$968{\cdot}2_6$	$965{\cdot}8_9$	+2·5	—

of circles is produced in case of torsional vibrations, but no one of the radii observed could be safely identified with the radius, calculated from theoretic formulæ *.

* *Notice in proof.*—In a recently published paper [12] E. Lonn explains the mentioned deviations from the theory in the following way: The extensional vibrations are accompanied with transversal vibrations of the same frequency. so that lycopodium figures show, therefore, not only the nodal lines of extensional vibrations, but also the nodal lines of transversal vibrations. In the case of torsional vibrations the transversal vibrations of such a symmetry are much more easily excited, which agrees with the symmetry of the crystal plate. But this conception does not hold in general.

TABLE IX.—Plate C.

n.	$x_n^{(t)}$.	Calculated frequency f_c in kc.	Measured frequency f_m in kc.	$\delta=\frac{f_c-f_m}{f_c}$ parts per 1000.	Figure.
0	5·978	$230{\cdot}0_3$	$231{\cdot}3_4$	−5·7	20
1	10·925	$420{\cdot}3_9$	$423{\cdot}5_9$	−7·6	21
2	16·047	$617{\cdot}4_9$	$623{\cdot}5_4$	−9·8	22
3	21·230	$816{\cdot}9_3$	$824{\cdot}7_0$	−9·5	—
4	26·440	$1017{\cdot}4_1$	$1023{\cdot}4_1$	−5·9	—

TABLE X.—Plate D.

n.	$x_n^{(t)}$.	Calculated frequency f_c in kc.	Measured frequency f_m in kc.	$\delta=\frac{f_c-f_m}{f_c}$ parts per 1000.	Figure.
0	8·227	$316{\cdot}2_5$	$318{\cdot}0_2$	−5·6	23
1	15·887	$610{\cdot}7_0$	$611{\cdot}6_5$	−1·6	24
2	23·694	$910{\cdot}8_0$	$909{\cdot}0_8$	+1·9	25
3	31·515	$1211{\cdot}0_4$	$1205{\cdot}0_2$	+5·1	—

TABLE XI.—Radii of the Nodal Lines reduced to Radius $a=1$.

Plate.	$m=0$.	$m=1$.		$m=2$.		
	r_0.	r_0.	r_1.	r_0.	r_1.	r_2.
B	0·752	0·490	0·843	0·398	0·649	0·898
C	0·788	0·588	0·882	0·523	0·722	0·923
D	0·843	0·721	0·921	0·681	0·816	0·950

APPENDIX.

In studying radial vibrations we have observed another interesting secondary effect, namely, that the air-layer in the opening of the plate is also brought into vibration by the vibration of the plate. The frequency of the vibration being very high, and the wave-length consequently very

short, standing waves will be produced inside the plate. The lycopodium, poured into the opening of the vibrating plate, will assemble in the same places where the nodal lines are situated, as can be seen in fig. 26 (Pl. IV.) (plate C, $n=1$, $f_1=331{\cdot}9_6$ kc.) and fig. 27 (Pl. IV.) (plate D, $n=1$, $f_1=471{\cdot}7$ kc.). The appearance of a similar acoustic field has been observed in other types of vibrations, and will subsequently be studied also in liquids.

Annular plates can be applied as resonators in various devices, it being possible to use for this purpose not only radial vibrations but also torsional ones.

Summary.

This paper describes the radial and torsional vibrations of circular annular plates.

In the case of radial vibrations it has been established that, in accordance with the theory, the frequency of the fundamental mode of vibrations in a full plate is higher than the frequency of corresponding vibrations in annular plates, which frequency declines with the increasing internal radius of the plate. The nodal lines are circles, and their radii, observed in individual plates, accord, within the limits of precision attainable, with the radii figured out from theory.

In the case of torsional vibrations it is exactly the other way about. The frequency of the fundamental mode of vibrations in a full plate is, in accordance with the theory, lower than the frequency of corresponding vibrations in annular plates, which frequency increases with increasing internal radius of the plate. The nodal lines are also circles. In the case of all torsional vibrations the experiments have shown the nodal lines to be circles, but none of the radii of these circles is in accordance with the radii given by theory.

In the opening of the plates there arise in case of radial vibrations standing waves in the air, which can easily be shown by lycopodium figures.

Both the radial and the torsional vibrations in annular plates can be technically applied in their use as resonators.

List of References.

(1) E. Giebe and A. Scheibe, *E. N. T.* v. p. 65 (1928).
(2) S. Chaikin, *Ztschr. f. Hochfrequenztechnik*, xxxv. p. 6 (1930).
(3) Tsi-Zé Ny, Ling-Chao Tsien, and Sun-Hung Fang, Proc. I. R. E. xxiv. p. 1484 (1936).

(4) A. E. H. Love, 'A Treatise on the Mathematical Theory of Elasticity,' p. 497 (Cambridge, 1927).
(5) V. Petržílka, *Ann. d. Phys.* xv. p. 881 (1932); *Handb. d. Experimental-Physik*, Bd. xvii. Teil 1, p. 368 (1934); *Ann. d. Phys.* xxiii. p. 156 (1935).
(6) A. Kalähne, *Ann. d. Phys.* xviii. p. 92 (1905); xix. p. 80 (1906); *Ztschr. f. Mathematik u. Physik*, liv. p. 55 (1907).
(7) R. Grammel, *Ztschr. f. angewandte Mathematik u. Mechanik*, v. p. 193 (1925).
(8) V. Petržílka, *Čas. pro pěst. mat. a fys.* lxv. p. 110 (1936).
(9) E. Giebe and E. Blechschmidt, *Ann. d. Phys.* xviii. p. 417 (1933).
(10) R. B. Wright and D. M. Stuart, Bur. of Standard, Journal of Res. vii. p. 519 (1931).
(11) L. Essen, Proc. Roy. Soc. London, ser. A, clv. p. 498 (1936).
(12) E. Lonn, *Ann. d. Phys.* xxx. p. 420 (1937).

Physical Institute of the
Charles' University, Prague.

XII. *Reciprocals to Ampere's Law.* *By* Preston B. Carwile, *Ph.D., Lehigh University, U.S.A.**

Summary.

An application of the well-known principle of reciprocity between corresponding electric and magnetic entities leads to an explicit statement of the reciprocal to a common form of Ampere's law. The same principle leads to the law of equivalent electric shells. These laws are believed to reduce certain aspects of magneto-electric fields to a more elementary level than has been common. Applications are made to several simple theorems. The laws are briefly discussed as to formal and physical significance.

Notation.

$\mathbf{E}$=Electric field.
$\mathbf{H}$=Magnetic field.
V=Electromotive force (sometimes induced electric potential).
$\mathbf{i}$=Electric convection current.
$\mathbf{y}$=Magnetic convection current.
$\mathbf{j}$=Electric convection current density.
$\dot{\mathbf{N}}$=Time rate of change of total electric flux.

* Communicated by the Author.

$\dot{\Phi}$=Time rate of change of total magnetic flux.

$\dot{\mathbf{B}}$=Time rate of change of magnetic flux density.

$d\mathbf{s}$=Line element.

$\mathbf{r}$=Displacement of region of $d\mathbf{E}$ or $d\mathbf{H}$ from $d\mathbf{s}$.

ρ=Strength of equivalent magnetic shell.

σ=Strength of equivalent electric shell.

μ=Magnetic permeability of medium (assumed constant).

μ_0=Magnetic permeability of free space.

k=Dielectric constant of medium.

k_0=Dielectric constant of free space.

Ω=Solid angle.

c=Ratio of the electromagnetic to the electrostatic unit of electric charge.

$\oint$=Line integral once around any closed path.

Introduction.

EQ. (1), (3), (5), (7) below are variant forms of Ampere's law. Eq. (6), (8) are variant forms of Faraday's law of electromagnetic induction. Eq. (7), (8) are reciprocal in character; likewise (5), (6). The purpose of this paper is to present the missing eq. (2), (4), which should exist as reciprocals to (1), (3) respectively, or as variants to (6), (8), but which the writer has not found in print in the explicit forms [1] to be given here. Gibbs's vector notation is employed. Ordinary electromagnetic units are used except where subscripts are given.

$$d\mathbf{H}=\frac{id\mathbf{s}\times\mathbf{r}}{r^3}. \quad . \quad . \quad (1) \qquad\qquad (2)$$

$$\rho=\mu_0 i \quad . \quad . \quad . \quad (3) \qquad\qquad (4)$$

$$\nabla\times\mathbf{H}=4\pi\mathbf{j}. \quad . \quad . \quad . \quad (5) \qquad \nabla\times\mathbf{E}=-\dot{\mathbf{B}} \quad . \quad . \quad (6)$$

$$\oint \mathbf{H}.d\mathbf{s}=4\pi i \quad . \quad . \quad . \quad (7) \qquad \oint \mathbf{E}\,.\,d\mathbf{s}=-\dot{\Phi}. \quad . \quad . \quad (8)$$

When eq. (7), (8) [or (5), (6)] are expressed in Heaviside-Lorentz rational units, and are generalized to include electric displacement current and magnetic convection current, they disclose analogy, symmetry, and reciprocity. Of these characteristics analogy is superficial and

symmetry is formal. Reciprocity has a deeper significance. Reciprocity may be described as the reversible cross-relation between electric and magnetic entities. More specifically, it is the inductive action-and-reaction between corresponding electric and magnetic entities. In classical electromagnetic theory magnetism, and therefore the principle of reciprocity, were regarded as convenient fictions only. Dirac [2] has shown that quantum mechanics demands the physical existence of free magnetic poles. This, conceptually at least, gives magnetism the same aspect of physical reality that has long been ascribed to electricity. Reciprocity likewise assumes a new significance. Although free poles have not yet been detected experimentally, the term for magnetic convection current is used in certain equations below for clarity in applying the principle of reciprocity.

Derivations.

Let us write eq. (1) in Heaviside-Lorentz rational [3] units and generalize it to include electric displacement current. Using the subscript r to indicate rational units, we shall then have

$$d\mathbf{H}_r = \frac{(i_r + \dot{\mathrm{N}}_r)\, d\mathbf{s} \times \mathbf{r}}{4\pi c r^3}, \quad \ldots \quad (1_r)$$

where we assume for simplicity that $\mathbf{i}_r$ and $\dot{\mathbf{N}}_r$ have the same direction. Now let us replace $\mathbf{H}_r$, i_r, and $\dot{\mathrm{N}}_r$ by their analogous entities $\mathbf{E}_r$, y_r, and $\dot{\Phi}_r$ respectively, and reverse the analogous vector sense on the assumption that reaction is opposite to primary action. We then have

$$d\mathbf{E}_r = -\frac{(y_r + \dot{\Phi}_r) d\mathbf{s} \times \mathbf{r}}{4\pi c r^3} \quad \ldots \quad (2_r)$$

This equation is the exact reciprocal to eq. (1_r). Dropping the term for magnetic convection current y, and converting back into ordinary electromagnetic units, we have

$$d\mathbf{E} = -\frac{\dot{\Phi} d\mathbf{s} \times \mathbf{r}}{4\pi r^3} \quad \ldots \quad (2)$$

This is the effective reciprocal to eq. (1). It is just as real and adaptable. It may also be regarded as a variant

form of Faraday's law ; as such, *it is unique in giving the element of induced electric field* rather than the integral of the field around a closed path. The law expressed by eq. (2) is independent of any condition as to open or closed circuit. The presence of conductors in the neighbourhood will generally give rise to secondary fields (magneto-electric, electrostatic, or both), but any such effects will simply be superposed on the original field.

When the law is stated in non-vector form, such as eq. (11) below, the sense of the induced electric field is given by the reciprocal to Ampere's familiar right-hand rule—that is, the analogous left-hand rule, which may be stated as follows : *Grasp the element of changing magnetic flux by the left hand so that the thumb points in the sense of increasing flux, then the fingers indicate the sense of the encircling electric field.*

In order to obtain the reciprocal to eq. (3) we follow the same procedure. After converting to Heaviside-Lorentz rational units, and generalizing to include electric displacement current, we have

$$\rho_r = \frac{\mu_{0r}(i_r + \dot{\mathrm{N}}_r)}{c} \quad . \quad . \quad . \quad . \quad . \quad . \quad (3_r)$$

The reciprocal to this is

$$\sigma_r = \frac{k_{0r}(y_r + \dot{\Phi}_r)}{c} \quad . \quad . \quad . \quad . \quad . \quad . \quad (4_r)$$

We now drop the term y and convert back into electromagnetic units, obtaining

$$\sigma = \frac{k_0 \dot{\Phi}}{4\pi} \quad . \quad . \quad . \quad . \quad . \quad . \quad . \quad (4)$$

This equation is the effective reciprocal to eq. (3). We can now formulate the reciprocal to the law of equivalent magnetic shells. It is the law of equivalent electric shells, which may be stated as follows : *Every linear circuit in which magnetic flux is changing is equivalent (as regards the induced electric field) to any simple electric shell the bounding edge of which coincides with the flux circuit and the strength (moment per unit area) of which is given by eq.* (4). *The positive side of a plane equivalent electric shell is the forward side with respect to the advance of a left-hand screw as it rotates with the increasing magnetic flux.*

If we express σ and k_0 in electrostatic units and leave $\dot{\Phi}$ in electromagnetic units eq. (4) becomes

$$\sigma_s = \frac{k_{0s}\dot{\Phi}}{4\pi c} \quad . \quad . \quad . \quad . \quad . \quad . \quad . \quad (4')$$

Perhaps the use of μ_0 and k_0 in eq. (3) and (4) should be justified. If we define a simple magnetic shell as a permanently magnetized and impenetrable sheet, having a constant magnetic moment per unit area, then, according to Wilberforce [4] and Page [5], the field in the neighbourhood of such a shell is independent of the permeability of the surrounding medium. Thus eq. (3) is valid regardless of the medium.

If, on the other hand, we were to define a simple magnetic [electric] shell as a slightly separated double layer of opposite poles [charge] having constant magnetic [electric] moment per unit area and having the same medium *inside* and outside the shell, then the conclusions of Wilberforce and Page would not be applicable, and μ_0, k_0 would have to be replaced by μ, k in eq. (3), (4) respectively.

On casual observation these definitions seem equivalent, yet they lead to different results. The first definition is the one commonly used for a magnetic shell. For an electric shell the second definition would be the natural one to choose, since it corresponds with a parallel plate condenser charged to a fixed voltage rather than a permanently polarized dielectric. Evidently we require a more discriminating definition of a simple shell than has generally been considered necessary. Of the two definitions the former is preferable for both magnetic and electric shells, since it leads to simpler results. Eq. (3) and (4) are then valid regardless of the medium.

The law of equivalent electric shells reduces the general treatment of induced electric fields and potentials to solid angle methods similar to the methods used with magnetic shells. For instance, the induced electric potential V at any point in the neighbourhood of a thin magnetic circuit in which the flux is changing is

$$V = \sigma\,\Omega, \quad . \quad . \quad . \quad . \quad . \quad . \quad . \quad (9)$$

where Ω is the solid angle subtended at the point by the magnetic circuit and where this angle is taken as positive

for points on the positive side of the shell, and *vice versa*. The induced electric field at any point is

$$\mathbf{E} = -\nabla V = -\sigma \nabla \Omega. \quad . \quad . \quad . \quad . \quad . \quad (10)$$

Applications.

As a simple application of the law expressed by eq. (2) let us determine the induced electric field at a point P (fig. 1) situated a distance a from a long, thin, straight core, in which the magnetic flux is increasing toward the right at the rate $\dot{\Phi}$. According to eq. (2) the magnitude

Fig. 1.

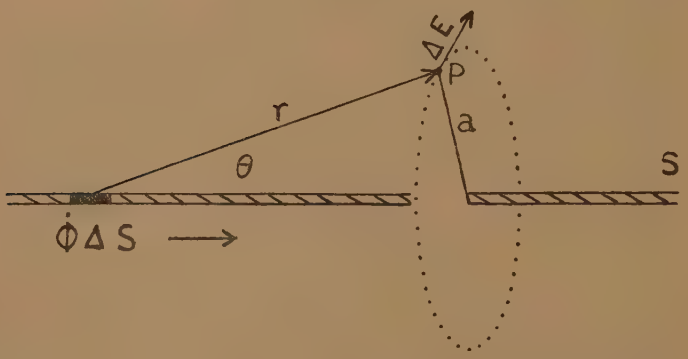

Element $\Delta\mathbf{E}$ of induced electric field (at any point P, in the vicinity of a long, thin, straight core) due to an element $\dot{\Phi}\,\Delta s$ of increasing magnetic flux (left to right) in the core.

of the electric field at P due to the element of changing flux $\dot{\Phi} ds$ is

$$dE = \frac{\dot{\Phi} ds \sin\theta}{4\pi r^2} \quad . \quad . \quad . \quad . \quad . \quad (11)$$

and

$$E = \int_{s=-\infty}^{s=+\infty} dE = \frac{\dot{\Phi}}{4\pi} \int_{-\infty}^{+\infty} \frac{\sin\theta}{r^2}\, ds$$

$$= \frac{\dot{\Phi}}{4\pi a} \int_0^{\pi} \sin\theta\, d\theta = \frac{\dot{\Phi}}{2\pi a}. \quad . \quad . \quad . \quad . \quad (12)$$

According to the left-hand rule the direction of $\mathbf{E}$ is into the paper, tangent to the circle drawn through P about the core as its axis.

Allowing for the factor 4π, which is due to the lack of symmetry of units in the electromagnetic system, we recognize in eq. (12) the reciprocal to the Biot-Savart law as given by

$$H=\frac{2i}{a}. \quad . \quad . \quad . \quad . \quad . \quad . \quad . \quad (13)$$

The total electromotive force induced in a circular path (or path of any shape) of one turn around the same core is

$$V_1=\int_0^{2\pi a} E dl = \frac{\dot{\Phi}}{2\pi a}\int_0^{2\pi a} dl=\dot{\Phi}. \quad . \quad . \quad . \quad (14)$$

As another application of the law expressed by eq. (2) let us determine the induced electric field at any point P (fig. 2) on the axis of a thin, circular ring, in which magnetic flux is increasing in the counter-clockwise sense as seen

Fig. 2.

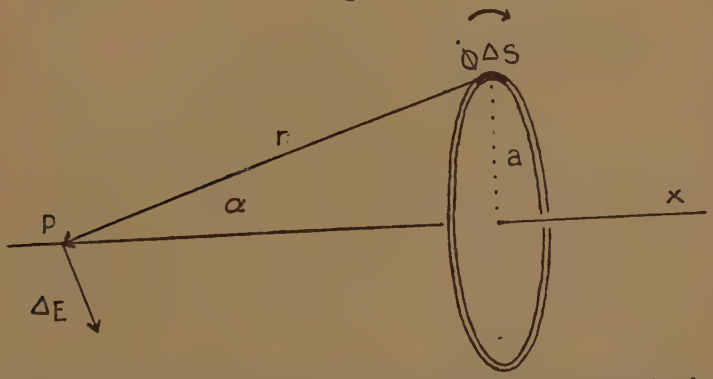

Element $\Delta\mathbf{E}$ of induced electric field (at any point P, on the axis of a thin, circular ring) due to an element $\dot{\Phi}\Delta\mathbf{s}$ of increasing magnetic flux (counter-clockwise, viewed from the left) in the ring.

from the left. The angle between $\mathbf{r}$ and $\dot{\Phi}d\mathbf{s}$ is $\pi/2$, the scalar r is constant, angle α is constant, and the transverse components of the electric field neutralize while the axial components combine additively, giving

$$E_x=\int_{s=0}^{s=2\pi a} dE_x=(\sin\alpha)\int_{s=0}^{s=2\pi a} dE$$

$$=(\sin\alpha)\int_0^{2\pi a}\frac{\dot{\Phi}ds}{4\pi r^2}=\frac{\dot{\Phi}\sin^3\alpha}{2a}. \quad . \quad . \quad . \quad (15)$$

This field has a maximum value of $\dot{\Phi}/(2a)$ at the centre of the ring, and diminishes rapidly as the distance of P increases from the centre of the ring in either sense. Eq. (15) is the reciprocal to the familiar equation for the magnetic field at a point on the axis of a circular electric current, viz.,

$$H=\frac{2\pi i \sin^3 \alpha}{a}. \quad . \quad . \quad . \quad . \quad . \quad . \quad (16)$$

Eq. (15) [unlike eq. (12), (14)] is not readily derived from eq. (8), nor is it derivable in so elementary a way as that shown above by any method in common use.

Let us continue and evaluate the total electromotive force induced along the whole axis.

$$V=\int_{-\infty}^{+\infty} E_x\, dx=\frac{\dot{\Phi}}{2a}\int_{-\infty}^{+\infty} \sin^3 \alpha\, dx$$

$$=\frac{\dot{\Phi}}{2a}\int_0^{\pi} (\sin^2 \alpha) r\, d\alpha=\frac{\dot{\Phi}}{2}\int_0^{\pi} \sin \alpha\, d\alpha=\dot{\Phi}. \quad . \quad . \quad . \quad . \quad (17)$$

Discussion.

The magnetic flux through a finite cross-section cannot increase indefinitely at a steady rate. Hence eq. (2), (4) have physical significance for transient or cyclic processes only. On the other hand, such transients or cycles must be slow (quasi-stationary) in order for the equations to apply, since no allowance is made for the time required for the propagation of a field from one region to another. The laws are precise, however, for every frequency whose wave-length is large compared with r.

The electric field which may be realized physically by the direct application of eq. (2), (4) is rather small in magnitude. This may be seen by inserting reasonable experimental values in eq. (15). Suppose, for instance, that we have an iron ring whose effective radius a is 5 cm. and in which the flux changes from zero to 100,000 lines in a time of 0·001 sec. The average electric field induced at the centre of the ring is $(100{,}000)/(0{\cdot}001 \times 2 \times 5)$ lines per sec. per cm., or 0·01 volt per cm.

Although these induced fields are small we have free charges to react with them; whereas, in dealing with

Ampere's law, we do not yet have free poles to react with the magnetic fields. Furthermore, the high voltages furnished by step-up transformers are produced by the integration of precisely these small electric fields.

In the present view of the writer another observation is of interest. The kinetic energy of an electric current is the volume integral through surrounding space of the associated magnetic energy density. Reciprocally, a circuit of changing magnetic flux has kinetic (?) energy equal to the volume integral through surrounding space of the associated electric energy density. This electric field exists only while the magnetic flux is changing. The electric energy is therefore associated directly with $\dot{\Phi}$ rather than with Φ itself. When Φ is changing the associated electric energy opposes any change in the rate of change. Thus when $\dot{\Phi}$ is maintained by an accelerating electric charge in a surrounding winding then the charge has inertia toward change in acceleration as well as inertia toward change in velocity. *This gives physical meaning to the third derivative of displacement of charge with respect to time.*

Eq. (7), (8) apply to closed paths only. Although eq. (5), (6) are stated in differential form, they likewise are based on the idea of closed paths whose dimensions are small. Eq. (5), (6) serve admirably as twin cornerstones for symbolic electromagnetic theory. In comparison, eq. (1), (2) exhibit relationships which are fine-grained, point-to-point, and immediately applicable to open circuits. This combination of characteristics is not apparent in eq. (5) to (8); the application of the latter equations to open circuits is an intricate process. For elementary presentations, for some aspects of physical interpretation, and for basic concept it appears that eq. (1), (2) hold places which are individually unique.

References.

(1) See, however, John J. Tate, National Research Council Bulletin, iv. pt. 6, p. 80 (1922).
(2) P. A. M. Dirac, Proc. Roy. Soc. A, cxxxiii. p. 60 (1931).
(3) For conversion factors see Leigh Page, 'Introduction to Theoretical Physics,' p. 425 (1929).
(4) L. R. Wilberforce, Proc. Phys. Soc. London, xlv. p. 82 (1933).
(5) Leigh Page, Phys. Rev. xliv. p. 112 (1933).

Bethlehem, Pennsylvania.
July 24, 1937.

XIII. *The Zero-Shunt Valve A.C. Potentiometer.*

By Prof. John J. Dowling, *M.A., F.Inst.P., M.R.I.A.**

Summary.

The use of the zero-shunt in the anode circuit of a detector valve enables the P.D. across an impedance carrying an alternating current to be balanced against the P.D. across an adjustable resistance in which the same a.c. flows. Measurements are possible of impedances, phase-angle, frequency, etc. at high or low frequency and with considerable precision.

THE application of the potentiometer principle to a.c. measurements is, of course, well established; but in practice it is complicated by the necessity for

Fig. 1.

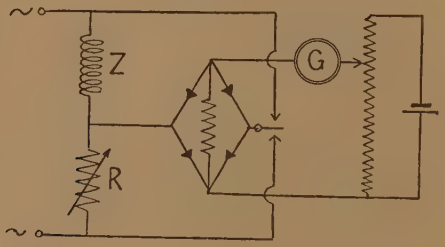

balancing both the *in-phase* and *in-quadrature* components. The employment of a rectifying device in conjunction with the galvanometer enables much of the original simplicity of the D.C. system to be regained, and the present paper describes some investigations made on these lines.

Although a Westinghouse detector may be employed (as indicated in fig. 1), the fact that the detector bridge is of relatively low impedance limits the range of its application. For this reason the valve arrangement described is altogether preferable, and to this I will confine my remarks.

The simplest example, and that first experimented with, deals with the measurement of a mutual inductance.

* Communicated by the Author.

The original lay-out is shown in fig. 2, the coils being two large coaxial single layer cylindrical coils, of which the mutual inductance could be calculated from the dimensions.

In the first determination 4 v. : 50 ~ supply was employed, the grid bias being 2 v. and the anode voltage 50 v. The valve used in this and most other cases was a 2 v. detector valve. The resistance R was made up of two non-inductive plug boxes, while S was a 2000 ohm rheostat. The galvanometer was a unipivot micro-ammeter. The procedure was as follows :—

With the grid key " up," S is adjusted to an approximate balance for M. The key is then depressed and R adjusted to near balance. These adjustments are

Fig. 2.

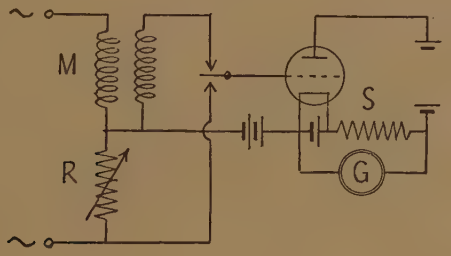

repeated until the galvanometer remains at balance for either position of the key. Since the same current flows in R and M, we have

$$2\pi f.\mathrm{M}=\mathrm{R}\ *.$$

The following were the results obtained at the first trial :—

Mutual inductance (calculated approximately from dimensions)	4·012 *m*H.
Mutual inductance measured by Maxwell's method	4·073 ,,
Mutual inductance measured by Pirani's method	4·080 ,,
Mutual inductance measured by new method.	4·076 ,,

* Actually $f=50$ ~ and $r=1{\cdot}28$ ohm $\therefore$ M = 4·076 mH.

These results being so satisfactory the possibilities of the method were gone into more fully.

The method is applicable to many measurements other than mutual inductance, but it must be emphasized at the outset that there are three sources of error, which are all the more serious because they are insidious and easily overlooked.

(*a*) The source of alternating current must be capable of yielding a *pure* sine wave, without appreciable harmonics, since it is essential that the potential wave shapes across inductances or capacities should be similar to those across resistances. This consideration restricts the method to inductances without iron cores.

(*b*) The frequency must be accurately known at the time that the balance is obtained *. For work at higher frequencies a heterodyne oscillator was tried, but it had to be abandoned owing to frequency drift. An exceedingly satisfactory supply was obtained from a magnetostriction oscillator with one stage of amplification. A long bar of " 2729 (Telcron) " alloy vibrates at its natural frequency of 2250 $\sim$ when energized by coils of 0·1 Henry (5000 turns). By tuning the output transformer a supply of excellent wave-form and very constant frequency is obtained.

(*c*) The third source of error may lead to altogether erroneous results, but it is easy to evade. The grid must be heavily biassed to ensure that it produces no shunting effect on the part of the circuit to which it is connected.

In fig. 3 is shown the lay-out finally adopted for the measurement of impedances. A mirror galvanometer together with an universal shunt replaces the microammeter, and *two* non-inductive resistance boxes (R_1 R_2) are employed so as to facilitate rapid balancing. The sum (R_1+R_2) is always kept the same, so that the rebalancing of Z with S, which was previously necessary, is no longer required. The celerity of adjustment afforded by this largely nullifies trouble due to drifting of the galvanometer caused by the valve circuit, and I have

* I find that the A.C. supply in the I. F. S. is admirable as regards wave shape, although its frequency is not exactly constant.

not found it necessary to adopt any form of balancing in the valve-circuit.

The method is not restricted to sonic frequencies, and, indeed, is quite satisfactory at radio frequencies. In such cases instead of a resistance a calibrated condenser can be employed. If a previously calibrated mutual inductance is available, together with a calibrated condenser, the method enables quite accurate frequency determinations to be effected—always provided that the wave-form is known to be sinoidal. An interesting application is to the study of the behaviour of coupled circuits and filters generally, since the measurement is made under working conditions.

Fig. 3.

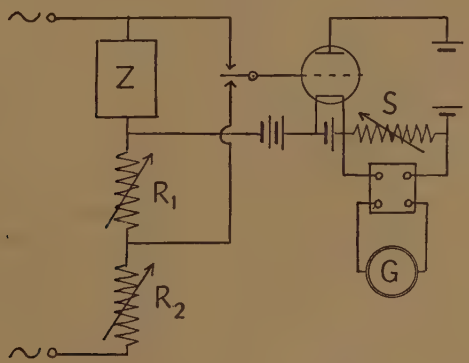

So far I have not referred to the phase-angle (θ) of the impedance. A simple modification of the procedure enables this to be determined. If a mutual inductance (M) is available this may be introduced, as shown in fig. 4, and a second reading of R_1 obtained. In lieu of M an air condenser of capacity K may be likewise employed, as indicated in fig. 5. Even if M (or K) have unknown values the measurement of θ can be carried out by obtaining the value of R_1 to which M (or K) corresponds when balanced *alone*.

The graphic method (figs. 6 and 7) is the simplest way to treat the results. In these figures OA is drawn equal to the value of R_1, which balances Z alone; OB equals that balancing Z with M (or K) in series; AB

equals R_1 for M (or K) alone *. OP is then drawn perpendicular to AB, and it makes the angle $AOP=\theta$.

Fig. 4.

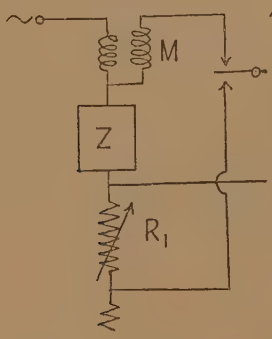

Fig. 5.

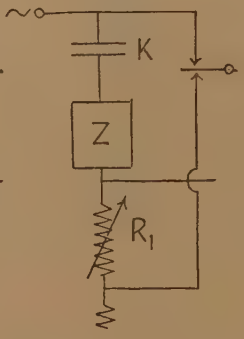

Fig. 6.

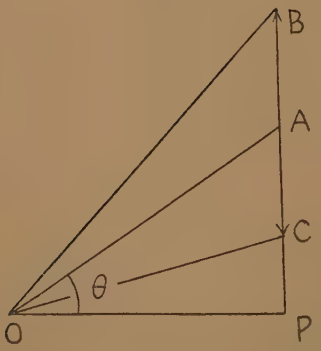

$AB=+MP.\quad AC=-M.\quad OA=Z.$

Fig. 7.

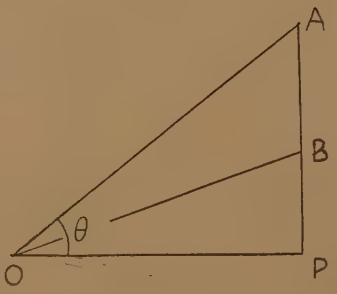

$AB=1/KP.\quad OA=Z.$

I desire to record my thanks to my students Sr. M. Anthony, Sr. M. Bernadette, and Mr. Fahie, who carried out the experimental work for me.

University College, Dublin.
August 8th, 1937.

* M may be positive or negative. The other solution is obtained by drawing AC to represent (−M), and, of course, OC to represent the corresponding series measurement.

XIV. *Notices respecting New Books.*

Introduction to Ferromagnetism. By FRANCIS BITTER. [Pp. xii+314.] (McGraw-Hill, London and New York, 1937. Price 24*s*.)

THE appearance of "Introduction" in the title of this book, and of others of a similar character, suggests that the word is acquiring a new meaning! Although there are a number of chapters of an introductory character, the greater part of the book is taken up by very full accounts of particular aspects of ferromagnetism, aspects which, the author considers, "give promise of being of outstanding interest during the next few years." With this criterion a much fuller discussion of alloys might have been expected, and also some account of developments on the theoretical side which have followed from the application of the Bloch method to the basic problem rather than the original method of Heisenberg, and which have resulted in bringing the theory of ferromagnetism into much closer relation with the general theory of metals. Some limitations are inevitable in so extensive a subject, and with this indication of the nature of the limitations in this book the way is opened for a proper appreciation of its many valuable features.

The book opens with a general introduction, in which the main concepts and phenomena are briefly discussed; an account of the historical development, chiefly concerned with the Weiss treatment; and an outline of the properties of metals and alloys. An interesting section on the use of magnetic powders and suspensions for revealing surface structures—a method due to Bitter—is contributed by Elmore. The next chapter, comprising sixty pages, on magnetic materials and their preparation, is by Yensen. As would be expected, this provides a masterly survey of the technologically important materials; it contains, moreover, a full account of the methods of preparing and analysing materials of high purity, and there are extensive references.

The major theme of the book is developed in three long chapters entitled "Internal Fields," "Magnetization," and "Mechanical Deformation." The first describes the Heisenberg theory, and developments of Ising's treatment of the linear chain. There is also a good account of the Seitz method for deriving the forms of energy expressions consistent with crystal symmetry, this being particularly useful as rendering more widely available—and intelligible—a powerful weapon of attack on an extensive range of problems. With the aid of

this weapon the author is able to give a very full and satisfying treatment of the magnetic and magneto-elastic properties of single crystals. The results are then utilized in the calculation and interpretation of the properties of polycrystalline material, much of this work being original.

There follows a brief account of the electrical properties of ferromagnetics, and a final chapter on the evolution of thermal energy in magnetic processes. Earlier in the book (p. 29) it is stated that "it is possible to relate by means of the first law such phenomena as, for instance, the change in length produced by a change in magnetization with the change in magnetization produced by a change in length." Whether or not this is an unintentional revelation of the author's opinion of the power of thermodynamics, the thermodynamic treatment given is certainly not applied to much greater effect. There is also a summary of the facts relating to the Barkhausen effect in the last chapter, rather curiously separated from the discussion of magnetization given earlier. An appendix by Zwicky on co-operative phenomena is useful in bringing together evidence bearing on the question of secondary structure in crystals, even though it by no means solves the problems at issue in connexion with ferromagnetics.

As an artistic whole the book to some extent lacks coherence, due in part to the varying level of treatment. The three chapters developing the main theme, and Yensen's chapter on magnetic materials—together occupying some two hundred pages—will, however, be indispensable to both physicists and technologists concerned with magnetism, and are more than sufficient to make this book an outstanding contribution to the literature on the subject.

Ions in Solution. By R. W. Gurney. (Cambridge University Press, 1936. Price 10*s.* 6*d.*)

The theoretical treatment of problems presented by solutions of electrolytes has received comparatively little attention from the physicist. It is probably for this reason that many well-known effects, such as the potential differences at contact surfaces between metals and solutions and between pairs of solutions, continue to be interpreted in terms of views which are linked up with that period of development of physical chemistry which recalls the names of van't Hoff, Ostwald, Nernst and Arrhenius. The most notable advances since that time were made about 1920, and are embodied in the Debye-Hückel theory, by which many well-known facts are correlated and interpreted satisfactorily on the basis of interionic forces, which were largely ignored in the classical period.

In the present volume Dr. Gurney has directed attention to the importance of energy changes in ionic systems, and by the application of considerations similar to those used by Bohr in the study of ions in gaseous systems he shows convincingly that the behaviour of ions in solution and the many phenomena with which they are associated can be systematically explained in a simple manner.

There can be no doubt that the author's general method of treatment represents a noteworthy contribution to the problem of dissolved electrolytes, and the book is bound to be found stimulating by all who are interested in this important field of chemical physics.

It is perhaps unfortunate that no attempt should have been made by the author to indicate, where possible, the relationship between his views on electrochemical problems and those which are familiar as a matter of history to large numbers of students who are primarily by training chemisst rather than physicists.

Principles of Quantum Mechanics. By ALFRED LANDÉ. [Pp. xii+120.] (Cambridge University Press, 1937. Price 7*s.* 6*d.*)

THE aim of this book, as stated in the preface, is " to develop the principles of quantum mechanics on the basis of a few standard observations." The quantum theory is treated as a general mathematical method of finding the relation between the corpuscular and wave quantities obtained as complementary sets of data. The procedure followed is that of generalization from the relations suggested by a consideration of typical simple observations. These are discussed in the first part of the book in some detail, particular stress being laid on the invalidity of attempts to fuse the two complementary pictures into one, in which either waves or corpuscles are treated as the more fundamental. Subsequent parts deal with the uncertainty relations; the principle of interference of probabilities, and Schrödinger's equation; the principle of correspondence; and general transformation theory.

The programme of the book is very similar to that of Heisenberg's ' Physical Principles of the Quantum Theory,' but the interrelation between the various general mathematical methods is developed more fully.

It is an amazing *tour de force* to have covered so much ground in such short compass. Inevitably the book makes heavy demands on the reader, for it is very largely a concentrated exposition of abstract theory unrelieved by illustrative applications. The earlier sections might be read

with advantage by those in the early stages of study of the theory for the clear account of its general character and aim. It is, however, for those who are familiar with particular aspects of the theory that the book will be most valuable for its illuminating survey and summary of the theory in its more general aspects.

Electricity and Magnetism. By A. S. Ramsey. [Pp. 267+x.] (Cambridge University Press. Price 10*s.* 6*d.*)

This introduction to the mathematical theory of electricity and magnetism is based upon lectures given by the author at intervals over a period of many years, and will be especially useful to university students attending first and second year courses. The first chapter provides the preliminary mathematics necessary to the understanding of the ensuing discussions of the fundamental ideas of electrostatics, Gauss's theorem, Poisson's equation, systems of conductors, dielectrics, electrical images, permanent and induced magnetism, and electromagnetism.

As is usual in Mr. Ramsey's books, the methods are illustrated by numerous worked examples, and many more graded problems are suggested for the reader's consideration.

Dynamics.—Part II. By A. S. Ramsey. [Pp. 344+xi.] (Cambridge University Press. Price 15*s.*)

The author offers a supplement to his 'Dynamics,' which appeared a few years ago and was intended for the use of scholarship candidates and first year students at the universities. The new volume, which deals with more advanced work in particle and rigid dynamics, and especially with problems in three dimensions, and includes the use of generalized coordinates, is suitable for candidates proceeding to an honours degree.

Vectorial methods are not employed in the text, but the fundamental equations of dynamics are obtained by such methods in an appendix. Many worked examples appear in the chapters, each of which is terminated by a collection of suitable problems for solution by the reader.

[*The Editors do not hold themselves responsible for the views expressed by their correspondents.*]

Fig. 1.

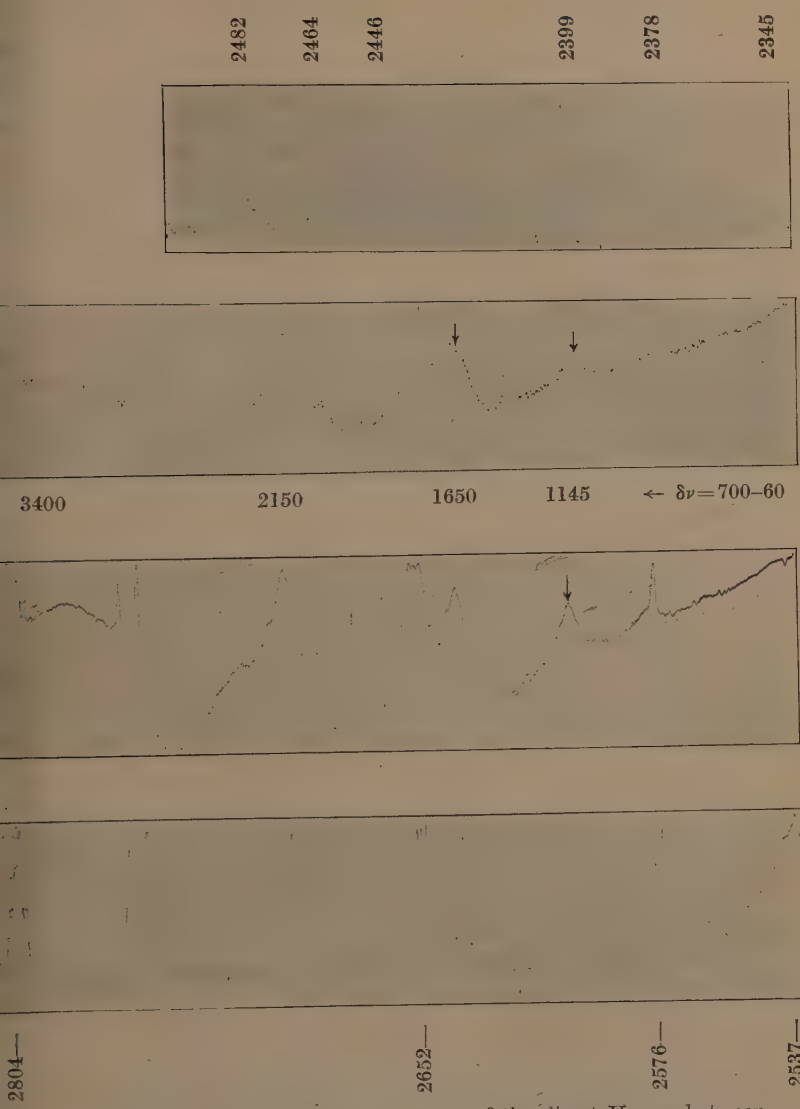

a represents the microphotometric curve of the direct Hg arc between 2345 and 2482. The wave-lengths of the exciting lines according to our assignment are noted. *b* is for water at 90°. The correspondence between the exciting and excited lines in *a* and *b* is clear. *c* is for water at 37°, and *d* for the Hg arc between 2537 and 2804, indicating the superposition of the large number of the Hg lines in *d* over the Raman bands in *c*. Values marked in *b* are frequency shifts from the 2537 line.

Figs. 2–13.

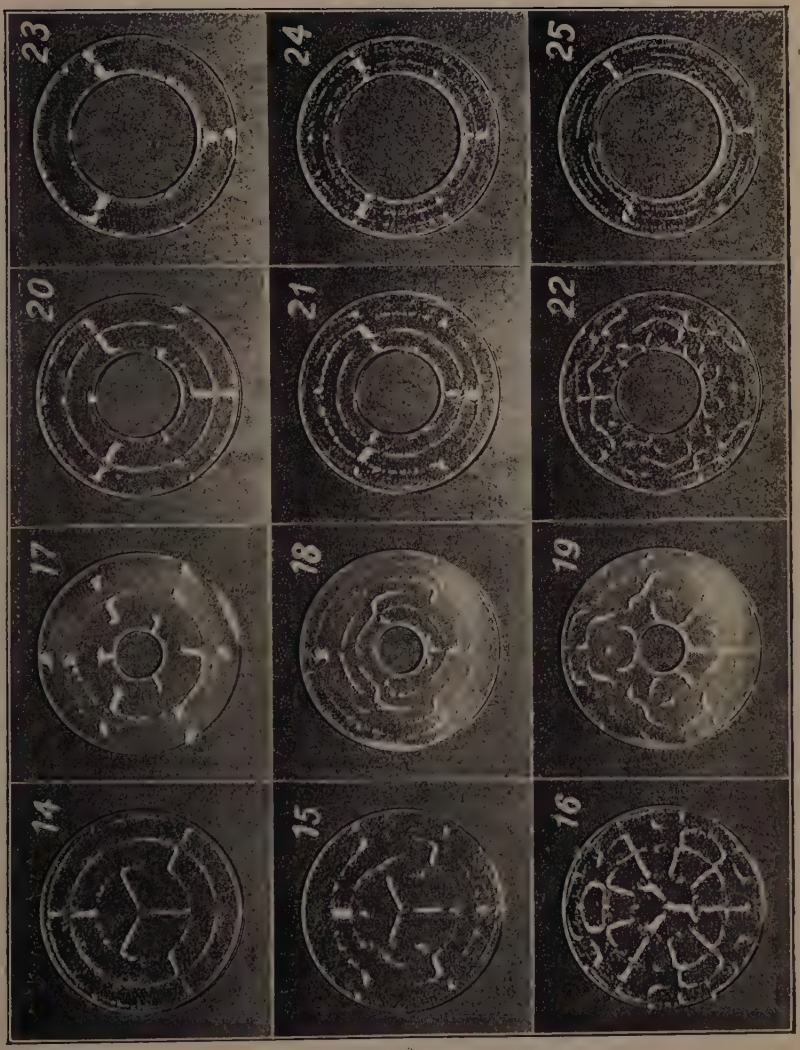

Figs. 14–25.

Fig. 26. Fig. 27.

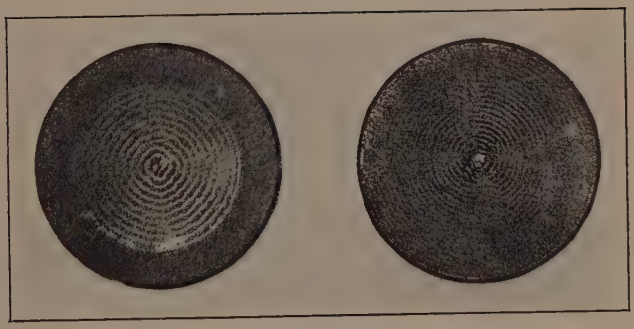

Enlarged size.

THE

LONDON, EDINBURGH, AND DUBLIN

PHILOSOPHICAL MAGAZINE

AND

JOURNAL OF SCIENCE.

[SEVENTH SERIES.]

FEBRUARY 1938.

XV. *On the Form assumed by a Steadily Rotating Thread.* *By* H. WARBURTON HALL, *M.Sc.*, *and* W. HUNTER, *M.A.**

1. THE results obtained in this paper arose from the investigations, undertaken by one of us †, into the anomalies in the behaviour of the tension in a thread wound from a fixed bobbin. If the thread from the bobbin is passed through an eyelet fixed on the axis of the bobbin and then carried off at a given rate, the motion round the bobbin of the point at which the thread leaves as it unwinds causes rotation of the portion of the thread between the bobbin and the eyelet. For certain distances of the eyelet from the point where the thread leaves the bobbin abrupt changes occur in the form of the rotating thread, with accompanying changes in the tension of the thread beyond the eyelet. It was

* Communicated by Prof. D. R. Hartree, M.A., Ph.D., F.R.S.

† H. W. Hall, of the Experimental Department, The Fine Cotton Spinners' and Doublers' Association, Ltd., Rock Bank, Bollington, Cheshire. A brief account of the experiments is given in a letter to 'Nature,' cxxxviii. p. 932 (Nov. 28, 1936). We should like to thank Mr. F. P. Slater, the Director of the above Department, for permission to make use of experimental results obtained there. We should also like to thank Prof. Hartree, who read the MS. of this paper, and made several helpful suggestions as to the presentation of the work.

the incidence of these changes which it was desired to investigate.

There are two questions involved: the conditions to be assumed at the place where the thread leaves the bobbin, and the stability of the form assumed by the rotating thread. In order to separate these two questions we have considered first a problem in which the former question does not arise. That is, we here consider the stability of form only, by taking the case of a thread one end of which is attached to a steadily rotating arm and the other end of which supports a mass either hanging freely (with the arm rotating in a horizontal plane), or after the thread has passed through an eyelet on the axis of rotation (with the arm rotating in a vertical plane, so that the axis of rotation is horizontal, and the part of the thread beyond the eyelet hangs vertically with the mass at its end). The similarity of the form of the thread in these conditions to that in the original problem appears sufficient to make it worth while investigating the possible forms of the thread. Further, the problem is not without interest in itself as an example of the motion of a thread or string of which an exact solution in finite terms is obtainable, the variability of the tension being taken into account, and no restriction as to the magnitude of the displacement being necessitated.

We obtain first a complete solution of the equations of motion of a steadily rotating thread in terms of elliptic functions. When we introduce the particular end conditions envisaged, we obtain a transcendental equation to determine the modulus of the elliptic functions involved. The equations thus obtained have, in the one case an infinity of solutions, in the other case a finite number of solutions, and the actual form assumed by the thread is determined by consideration of the energy. It is then possible to obtain the relations between the dimensions of the system for which change of form can occur. We exhibit these relations finally in graphical form.

In obtaining our solution we have had to neglect the effect of air resistance. Actually experiment shows that this effect is by no means negligible; to mention one point, theoretically the thread should rotate in the form of a plane curve, but observation shows that, apparently owing to air resistance, it is dragged into a spiral form; and it appears that, in the case of the thread

supporting a mass hanging freely, the air resistance has an important effect on the stability. We therefore introduce a general argument showing the effect to be expected; and as an illustration we consider the effect on the position and stability of the suspended mass of a resistance proportional to its velocity, in the special case when the inertia of the thread is neglected. (We have not so far found it possible to obtain a solution of the equations of motion in the general case when the inertia of the thread and the resistance experienced by the thread are *both* taken into account.) It appears that the general effect may be to cause the thread to take up a position in which the resistance is small, in preference to a position which, in the absence of resistance, would be the most stable. Since the resistance is thus reduced to a minimum, the solution obtained by neglecting the resistance may still give a good approximation to the form of the thread and, in particular, give an indication of the incidence of instability. This conclusion is confirmed by the good results obtained from a comparison of the calculated and observed lengths of thread for which instability sets in. This comparison is made at the end of the paper.

2. The general solution of the equations of motion of a thread in steady rotation with angular velocity ω can be expressed in terms of Weierstrassian elliptic functions. We take the axis of rotation as axis of z and reduce the system to rest, so that the equations of relative equilibrium (*i. e.*, the equations referred to axes rotating with angular velocity ω) are

$$\frac{d}{ds}\left(\mathrm{T}\frac{dx}{ds}\right) = -m\omega^2 x, \quad . \quad . \quad . \quad . \quad (2.1)$$

$$\frac{d}{ds}\left(\mathrm{T}\frac{dy}{ds}\right) = -m\omega^2 y, \quad . \quad . \quad . \quad . \quad (2.2)$$

$$\frac{d}{ds}\left(\mathrm{T}\frac{dz}{ds}\right) = 0, \quad . \quad . \quad . \quad . \quad . \quad . \quad (2.3)$$

where T is the tension, m the mass per unit length of the thread; and we have ignored the weight of the thread, taking it as negligible in comparison with the centrifugal force.

Multiplying these equations by $\frac{dx}{ds}, \frac{dy}{ds}, \frac{dz}{ds}$ respectively

and adding (which is equivalent to resolving along the tangent) we obtain

$$\frac{d\mathrm{T}}{ds} = -m\omega^2\left(x\frac{dx}{ds} + y\frac{dy}{ds}\right). \quad . \quad . \quad . \quad (2.4)$$

From (2.1) and (2.2), or by taking moments about the axis of rotation, we have also

$$\frac{d}{ds}\left[\mathrm{T}\left(x\frac{dy}{ds} - y\frac{dx}{ds}\right)\right] = 0. \quad . \quad . \quad . \quad (2.5)$$

Hence

$$\mathrm{T} = \tfrac{1}{2}m\omega^2(b - x^2 - y^2),$$

and then

$$\frac{dz}{ds} = \frac{c}{b - x^2 - y^2}, \quad . \quad . \quad . \quad . \quad (2.6)$$

$$x\frac{dy}{ds} - y\frac{dx}{ds} = \frac{a}{b - x^2 - y^2}, \quad . \quad . \quad . \quad . \quad (2.7)$$

where a, b c, are arbitrary constants of integration.

Then

$$\left(\frac{dx}{dz}\right)^2 + \left(\frac{dy}{dz}\right)^2 = \left(\frac{ds}{dz}\right)^2 - 1 = \left[\frac{b - x^2 - y^2}{c}\right]^2 - 1.$$

Hence, if we write v for $x^2 + y^2$, we have

$$\frac{1}{4}\left(\frac{dv}{dz}\right)^2 = v\left[\left(\frac{dx}{dz}\right)^2 + \left(\frac{dy}{dz}\right)^2\right] - \left(x\frac{dy}{dz} - y\frac{dx}{dz}\right)^2.$$

$$= v\left[\left(\frac{b - v}{c}\right)^2 - 1\right] - \frac{a^2}{c^2}.$$

Putting $v = w + \frac{2}{3}b$, $z = c(u + \alpha)$, where α is arbitrary, and taking $g_2 = \frac{4}{3}(b^2 + 3c^2)$, $g_3 = 4a^2 - \frac{8}{27}b(b^2 - 9c^2)$, we obtain

$$\left(\frac{dw}{du}\right)^2 = 4w^3 - g_2 w - g_3.$$

$$\therefore \qquad w = \wp(u\,;\ g_2,\ g_3).$$

Thus

$$x^2 + y^2 = \wp u + \tfrac{2}{3}b, \quad . \quad . \quad . \quad . \quad . \quad (2.8)$$

and, therefore,

$$x\frac{dx}{du} + y\frac{dy}{du} = \tfrac{1}{2}\wp' u.$$

Also, from (2.6) and (2.7),

$$x\frac{dy}{du} - y\frac{dx}{du} = a.$$

Solving for $\frac{dx}{du}$, $\frac{dy}{du}$, we obtain

$$(\wp u+\tfrac{2}{3}b)\frac{dx}{du}=\tfrac{1}{2}x\wp' u-ay,$$

$$(\wp u+\tfrac{2}{3}b)\frac{dy}{du}=\tfrac{1}{2}y\wp' u+ax,$$

and, therefore,

$$(\wp u+\tfrac{2}{3}b)\frac{d}{du}(x+iy)=\tfrac{1}{2}(\wp' u+2ia)(x+iy).$$

In view of the values of g_2, g_3 we can choose u_0 uniquely, so that

$$\wp u_0=-\tfrac{2}{3}b, \quad \wp' u_0=-2ia,$$

and then

$$\frac{1}{x+iy}\frac{d}{du}(x+iy)=\frac{1}{2}\frac{\wp' u-\wp' u_0}{\wp u-\wp u_0}$$

$$=\zeta(u+u_0)-\zeta u-\zeta u_0.$$

$$\therefore \quad x+iy=C\frac{\sigma(u+u_0)}{\sigma u}e^{-u\zeta u_0}$$

$$=\frac{\sigma(u+u_0)}{\sigma u\sigma u_0}e^{-(u+\beta)\zeta u_0}, \quad . \quad . \quad . \quad (2.9)$$

where β is a new arbitrary constant of integration.

Also from (2.8) we have

$$x^2+y^2=\wp u-\wp u_0=-\frac{\sigma(u+u_0)\sigma(u-u_0)}{\sigma^2 u\sigma^2 u_0}.$$

$$\therefore \quad x-iy=-\frac{\sigma(u-u_0)}{\sigma u\sigma u_0}e^{(u+\beta)\zeta u_0}. \quad . \quad . \quad . \quad (2.10)$$

Since $z=c(u+\alpha)$, equations (2.9), (2.10) give the curve formed by the thread as it rotates.

3. With the special end conditions we are going to consider, the constant of integration a vanishes, and the solution can readily be expressed in terms of Jacobian elliptic functions. Instead of transforming the general solution, however, it is simpler to obtain the necessary results directly from equations (2.3), (2.4), and (2.5).

Using polar coordinates r, θ in the plane perpendicular

to the axis of rotation, the integrals of these three equations may be written

$$T\frac{dz}{ds} = \text{constant}, \quad . \quad . \quad . \quad . \quad (3.1)$$

$$T + \tfrac{1}{2}m.\omega^2 r^2 = \text{constant}, \quad . \quad . \quad . \quad . \quad (3.2)$$

$$Tr^2\frac{d\theta}{ds} = \text{constant}. \quad . \quad . \quad . \quad (3.3)$$

Now if the thread passes through an eyelet on the axis of rotation, $r=0$ at this point. If the rotating arm is horizontal with the thread supporting a hanging mass, we must have equilibrium between the weight, the centrifugal force and the tension in the thread; by resolving in the horizontal plane perpendicular to the radius vector we obtain the condition $Tr\frac{d\theta}{ds}=0$ at this end *. In both cases the constant of integration in (3.3) vanishes; and hence $\frac{d\theta}{ds}$ must vanish, since we cannot have T or r vanishing at all points of the curve. Hence θ is constant ($\theta=0$, say), and the thread must rotate in the form of a plane curve.

If we combine equations (3.1), (3.2), using the fact that now

$$\left(\frac{dr}{ds}\right)^2 + \left(\frac{dz}{ds}\right)^2 = 1, \quad . \quad . \quad . \quad . \quad (3.4)$$

we obtain an equation between r and z, the solution of which is immediately expressible in terms of Jacobian functions. Since the form of the solution is slightly different in the two cases, we consider them separately from this point.

4. *Case I.—Thread passing through eyelet on axis of rotation and supporting a hanging mass M.*

In this case we take the origin at the eyelet, so that $r=0$ and $T=Mg$ when $z=0$. If the length of the rotating

* A solution for the case when the resistance experienced by the hanging mass, but not by the thread itself, is taken into account can be obtained by equating $Tr\frac{d\theta}{ds}$ to this resistance, assuming it to act in the opposite direction to that of the rotation of M. In that case we no longer obtain a plane curve. The solution is still expressible in terms of elliptic functions, since it is only the end conditions which are affected.

arm is a, and if it is at a distance h from the eyelet, we must also have $r=\pm a$ when $z=h$.

Then

$$T = Mg - \tfrac{1}{2}m\omega^2 r^2,$$

$$T\frac{dz}{ds} = \text{constant} = q.Mg \quad \text{(say)}.$$

Putting

$$\eta^2 = \frac{m\omega^2 a^2}{2Mg}, \quad \ldots\ldots \quad (4.1)$$

so that η is a constant depending on the dimensions of the system, we have

$$\frac{dz}{ds} = \frac{qa^2}{a^2 - \eta^2 r^2},$$

$$\left(\frac{dr}{ds}\right)^2 = 1 - \frac{q^2 a^4}{(a^2 - \eta^2 r^2)^2},$$

and, therefore,

$$\left(\frac{dr}{dz}\right)^2 = \frac{(a^2 - \eta^2 r^2)^2 - q^2 a^4}{q^2 a^4}. \quad \ldots \quad (4.2)$$

If we write for the moment $\eta r = a\sqrt{1-q}\,.\,t$, $\sqrt{1+q}\,.\,\eta z = aqv$, and $\dfrac{1-q}{1+q} = k^2$, this becomes

$$\left(\frac{dt}{dv}\right)^2 = (1-t^2)(1-k^2t^2),$$

and hence

$$t = \operatorname{sn}(v\,;\ k).$$

i. e.,

$$\eta\frac{r}{a} = \sqrt{\frac{2k^2}{1+k^2}}\operatorname{sn}\left[\frac{\sqrt{2(1+k^2)}}{1-k^2}\eta\frac{z}{a}\right]. \quad \ldots \quad (4.3)$$

This is the equation of the curve formed by the thread. The modulus k depends on the arbitrary constant q, and has to be chosen so as to satisfy the remaining condition $r=\pm a$ when $z=h$. If we introduce another dimensionless constant,

$$\zeta = \frac{\eta h}{a}, \quad \ldots\ldots\ldots \quad (4.4)$$

this condition is

$$\eta^2 = \frac{2k^2}{1+k^2}\operatorname{sn}^2\left[\frac{\sqrt{2(1+k^2)}}{1-k^2}\zeta\right] \ldots \quad (4.5)$$

We may remark that for a solution to be possible we must have $\eta^2 \leqslant 1$, *i. e.*, $\frac{1}{2}m\omega^2 a^2 \leqslant Mg$. If this condition is not satisfied, equilibrium is impossible except when the mass M is drawn right up to the eyelet.

5. For given values of η and ζ we shall find that equation (4.5) has an infinity of solutions. Now in a motion of the type here considered stability is assured if $U-T_0$ is a minimum in the configuration of relative equilibrium, where U is the potential energy and T_0 is the kinetic energy of the system when rotating as a whole *. Here $U-T_0$ can be taken as $Mgs-\frac{1}{2}\int m\omega^2 r^2\,ds$, where s is the length of thread between the eyelet and the rotating arm, and the sufficiency of the condition can be deduced directly. For the equations of motion relative to rotating axes,

$$m(\ddot{x}-2\omega\dot{y}-\omega^2 x) = \frac{\partial}{\partial s}\left(T\frac{\partial x}{\partial s}\right),$$

$$m(\ddot{y}+2\omega\dot{x}-\omega^2 y) = \frac{\partial}{\partial s}\left(T\frac{\partial y}{\partial s}\right),$$

$$m\ddot{z} = \frac{\partial}{\partial s}\left(T\frac{\partial z}{\partial s}\right),$$

give, when integrated along the thread,

$$\frac{d}{dt}\left\{\frac{1}{2}\int m(\dot{x}^2+\dot{y}^2+\dot{z}^2)\,ds - \frac{1}{2}\int m\omega^2 r^2\,ds\right\}$$

$$= \int\left[\Sigma\dot{x}\frac{\partial}{\partial s}\left(T\frac{\partial x}{\partial s}\right)\right]ds$$

$$= \left[T\Sigma\dot{x}\frac{\partial x}{\partial s}\right]_0^h - \int\left[T\Sigma\frac{\partial x}{\partial s}\frac{\partial^2 x}{\partial s\,\partial t}\right]ds.$$

But $\Sigma\left(\frac{\partial x}{\partial s}\right)^2 = 1$, and thus $\Sigma\frac{\partial x}{ds}\frac{\partial^2 x}{\partial s\,\partial t} = 0$; also at the end $z=h$ we have $\dot{x}=\dot{y}=\dot{z}=0$, and at the end $z=0$,

* See Lamb, Proc. Roy. Soc. A, lxxx. p. 168 (1908); or 'Hydrodynamics,' Ch. VIII. Actually, owing to the "gyroscopic" terms in the equations of disturbed motion, the condition is not essential, and there may even be stability with $U-T_0$ a maximum, but the point does not arise in this case.

$\Sigma\dot{x}\frac{\partial x}{\partial s}$ =resolved part of velocity along tangent $=\dot{s}$, and from the motion of M, $T=Mg+M\ddot{s}$. Thus we have

$$\frac{d}{dt}[\mathbb{T}+U-T_0]=0,$$

where $$\mathbb{T}=\frac{1}{2}\int m(\dot{x}^2+\dot{y}^2+\dot{z}^2)\,ds+\tfrac{1}{2}M\dot{s}^2$$

=K.E. of motion relative to rotating axes.

Hence if $U-T_0$ is a minimum, $\mathbb{T}$ must decrease as the thread moves away from the equilibrium configuration.

We write

$$U-T_0=\int(Mg-\tfrac{1}{2}m\omega^2r^2)\,ds=\frac{Mga}{\eta}V,$$

where $$V=\int\left(1-\frac{\eta^2r^2}{a^2}\right)\frac{\eta\,ds}{a}.$$

Of all the possible configurations, the thread will tend to take up that for which V has the least possible value. In order to compare the values of V in the different configurations, we shall regard η as given and discuss ζ and V as functions of the parameter q. It will be found that the possible equilibrium configurations group themselves in pairs, of which one is then presumably stable and the other unstable. Each such pair is possible only up to a certain value of ζ, so that for this value of ζ an abrupt change in form must occur.

6. Using equation (4.2) and putting $\frac{\eta r}{a}=u$, we have

$$\frac{\eta}{a}\frac{dz}{du}=\pm\frac{q}{\sqrt{(1-u^2)^2-q^2}}=\pm f(u), \quad \text{say},$$

the sign of $\frac{dz}{du}$ changing when $u=\pm\sqrt{1-q}$. Hence the value of ζ will be of the form

$$\zeta=2n\int_0^{\sqrt{1-q}}f(u)\,du\pm\int_0^{\eta}f(u)\,du. \quad . \quad . \quad (6.1)$$

Here n is an arbitrary integer, giving the number of arches of the sn-curve, *i. e.*, the number of complete (or

nearly complete *) " balloons " formed by the rotating thread.

Since

$$\left(1-\frac{\eta^2 r^2}{a^2}\right)\frac{\eta}{a}\,ds = \pm\frac{(1-u^2)^2\,du}{\sqrt{(1-u^2)^2-q^2}} = \pm\phi(u)\,du, \quad \text{say,}$$

the corresponding value of V will be given by

$$V = 2n\int_0^{\sqrt{1-q}}\phi(u)\,du \pm \int_0^{\eta}\phi(u)\,du. \quad . \quad . \quad (6.2)$$

We must have $\eta \leqslant \sqrt{1-q}$ for the solution to be real, and hence we consider only the range of values

$$0 \leqslant q \leqslant 1-\eta^2.$$

Now

$$\frac{\partial\phi}{\partial q} = \frac{q(1-u^2)^2}{[(1-u^2)^2-q^2]^{3/2}} = q\frac{\partial f}{\partial q},$$

$$\frac{d}{dq}\int_0^{\sqrt{1-q}} f(u)\,du = \frac{d}{dq}\int_0^{\pi/2}\frac{q\,dx}{\sqrt{(1+q)-(1-q)\sin^2 x}}$$

$$= \frac{1}{2}\int_0^{\pi/2}\frac{2+q-(2-q)\sin^2 x}{[1+q-(1-q)\sin^2 x]^{3/2}}\,dx,$$

$$\frac{d}{dq}\int_0^{\sqrt{1-q}}\phi(u)\,du$$

$$= \frac{d}{dq}\int_0^{\pi/2}\frac{[1-(1-q)\sin^2 x]^2}{\sqrt{1+q-(1-q)\sin^2 x}}\,dx$$

$$= \frac{1}{2}\int_0^{\pi/2}\frac{[1-(1-q)\sin^2 x][-1+(4+3q)\sin^2 x-3(1-q)\sin^4 x]}{[1+q-(1-q)\sin^2 x]^{3/2}}\,dx$$

$$= \frac{q}{2}\int_0^{\pi/2}\frac{2+q-(2-q)\sin^2 x}{[1+q-(1-q)\sin^2 x]^{3/2}}\,dx$$

$$- \frac{1}{2}\int_0^{\pi/2}\frac{1+q-4\sin^2 x+3(1-q)\sin^4 x}{\sqrt{1+q-(1-q)\sin^2 x}}\,dx$$

$$= q\frac{d}{dq}\int_0^{\sqrt{1-q}} f(u)\,du,$$

* If the portion of the curve between the rotating arm and the first node is greater than half an arch, the negative sign in (6.1) must be taken, and the number of complete " balloons " is then $n-1$.

since

$$\int_0^{\pi/2} \frac{1+q-4\sin^2 x+3(1-q)\sin^4 x}{\sqrt{1+q-(1-q)\sin^2 x}}\,dx$$
$$= \left[\sin x \cos x \sqrt{1+q-(1-q)\sin^2 x}\right]_0^{\pi/2} = 0.$$

Hence we obtain

$$\frac{d\zeta}{dq} = n\int_0^{\pi/2} \frac{2+q-(2-q)\sin^2 x}{[1+q-(1-q)\sin^2 x]^{3/2}}\,dx$$
$$\pm\int_0^{\eta} \frac{(1-u^2)^2}{[(1-u^2)^2-q^2]^{3/2}}\,du, \quad (6.3)$$

$$\frac{dV}{dq} = q\frac{d\zeta}{dq}. \quad (6.4)$$

7. We consider the two expressions

$$\zeta = 2n\int_0^{\sqrt{1-q}} \frac{q\,du}{\sqrt{(1-u^2)^2-q^2}} + \int_0^{\eta} \frac{q\,du}{\sqrt{(1-u^2)^2-q^2}}, \quad (7.1)$$

$$\zeta = (2n+2)\int_0^{\sqrt{1-q}} \frac{q\,du}{\sqrt{(1-u^2)^2-q^2}} - \int_0^{\eta} \frac{q\,du}{\sqrt{(1-u^2)^2-q^2}}, \quad (7.2)$$

which, with the corresponding expressions for V, have a common value when $q=1-\eta^2$, *i. e.*, when the rotating arm is situated at a maximum point of the corresponding sn-curve.

When $q=0$, $\zeta=0$ in both cases, for if we put $\frac{1-q}{1+q}=k^2$,

$$\int_0^{\sqrt{1-q}} \frac{q\,du}{\sqrt{(1-u^2)^2-q^2}} = \frac{k'^2\mathrm{K}}{\sqrt{2(1+k^2)}},$$

and when $q\to 0$, $k\to 1$, $k'\to 0$ and also $k'\mathrm{K}\to 0$.

If ζ is given by (7.1), both terms of $\frac{d\zeta}{dq}$ are essentially positive, and ζ increases steadily as q increases from 0 to $1-\eta^2$, the value of $\frac{d\zeta}{dq}$ tending to $+\infty$ when q approaches $1-\eta^2$. Since $\frac{dV}{d\zeta}=q$, the corresponding value of V also increases as ζ increases.

If ζ is given by (7.2), so that

$$\frac{d\zeta}{dq} = (n+1)\int_0^{\pi/2} \frac{2+q-(2-q)\sin^2 x}{[1+q-(1-q)\sin^2 x]^{3/2}}\,dx - \int_0^{\eta} \frac{(1-u^2)^2}{[(1-u^2)^2-q^2]^{3/2}}\,du,$$

then $\frac{d\zeta}{dq} \to -\infty$ when $q \to 1-\eta^2$. As q decreases, the first term in $\frac{d\zeta}{dq}$ increases and the second decreases, so that eventually $\frac{d\zeta}{dq} = 0$ for some value $q = q_n$. Hence, as q increases from 0 to $1-\eta^2$, this value of ζ increases from 0 to a maximum when $q = q_n$*, and then decreases again to unite with the other branch, thus giving a complete loop having a vertical tangent at $q = 1-\eta^2$.

When $q = q_n$, the value of $\frac{dV}{dq}$ is also zero, so that this part of the (V, ζ) graph has a cusp, the gradient of the tangent there being q_n. Hence, taking both branches together, the (V, ζ) graph starts from the point $\zeta = 0$, $V = \frac{4}{3}n + \frac{1}{3}\eta(3-\eta^2)$ when $q = 0$, and ζ, V increase together, the gradient increasing from 0 to $1-\eta^2$. Changing to the other branch, ζ and V continue to increase, while the gradient decreases from $1-\eta^2$ to q_n (the point corresponding to $q = 1-\eta^2$ is thus a point of inflexion). Finally, as the gradient decreases from q_n to 0, ζ and V decreases together, so that this portion of the graph lies above the other portion, and ends at the point $\zeta = 0$, $V = \frac{4}{3}(n+1) - \frac{1}{3}\eta(3-\eta^2)$. The general form of the graph is illustrated in fig. 1, which is calculated for the case $\eta = 0{\cdot}5$.

8. Since the form taken by the thread is that for which the value of V is least, it follows that the thread will tend to take up the form corresponding to the smallest

* The amplitude and the wave-length of the curve defined by (4.3) are so related that one increases as the other decreases. Since the length of the rotating arm gives a lower limit to the amplitude, there is an upper limit to the distance that can be spanned with a given number of semi-waves of the curve.

possible value of n, and there will be changes of form at the maximum values of ζ given by

$$\zeta=(2n+2)\int_0^{\sqrt{1-q}}\frac{q\,du}{\sqrt{(1-u^2)^2-q^2}}-\int_0^{\eta}\frac{q\,du}{\sqrt{(1-u^2)^2-q^2}}, \quad \ldots \quad (8.1)$$

Fig. 1.

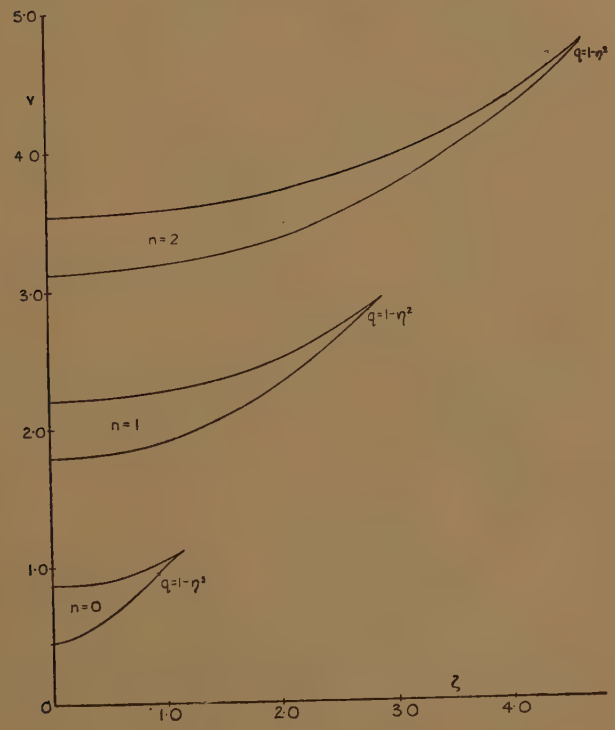

i. e., for the values $q=q_n$ which satisfy

$$(n+1)\int_0^{\pi/2}\frac{2+q-(2-q)\sin^2 x}{[1+q-(1-q)\sin^2 x]^{3/2}}\,dx = \int_0^{\eta}\frac{(1-u^2)^2\,du}{[(1-u^2)^2-q^2]^{3/2}}. \quad (8.2)$$

Since the integral on the right increases as q increases, q_n increases with n, and for large values of n approaches

the limiting value $1-\eta^2$. If we put $q=1-\eta^2-x^2$, and assume $x^2/(1-\eta^2)$ small, we have

$$\zeta=(2n+1)\int_0^{\sqrt{\eta^2+x^2}}\frac{(1-\eta^2-x^2)\,du}{\sqrt{(\eta^2+x^2-u^2)(2-\eta^2-x^2-u^2)}}$$
$$+\int_\eta^{\sqrt{\eta^2+x^2}}\frac{(1-\eta^2-x^2)\,du}{\sqrt{(\eta^2+x^2-u^2)(2-\eta^2-x^2-u^2)}}$$
$$=(2n+1)\mathrm{I}_1+\mathrm{I}_2, \quad \text{say.}$$

In I_1 put

$$u=\sqrt{\eta^2+x^2}\,\mathrm{sn}\,(z\,;\,k), \qquad \eta^2=\frac{2k^2}{1+k^2},$$

and then

$$\mathrm{I}_1=\frac{1-\eta^2-x^2}{\sqrt{2-\eta^2}}\int_0^{\mathrm{K}}\left[1-\frac{1+k^2}{2}\frac{1+\mathrm{sn}^2 z}{\mathrm{dn}^2 z}x^2\right]^{-\frac{1}{2}}dz$$
$$=\frac{1-\eta^2-x^2}{\sqrt{2-\eta^2}}\int_0^{\mathrm{K}}\left[1-\frac{x^2}{1-\eta^2}\left\{\frac{(1+k^2)\,\mathrm{dn}^2 z-(1-k^2)}{2k^2}\right\}\right]^{-\frac{1}{2}}dz,$$

on replacing z by $\mathrm{K}-z$. Since the term multiplying $x^2/(1-\eta^2)$ lies between 1 and $\frac{1}{2}k'^2$, we can expand the integrand, giving

$$\mathrm{I}_1=\frac{1-\eta^2}{\sqrt{2-\eta^2}}\left[\mathrm{K}-\frac{x^2}{1-\eta^2}\cdot\frac{(1+3k^2)\mathrm{K}-(1+k^2)\mathrm{E}}{4k^2}+\ldots\right].$$

Again, if we put $u^2=\eta^2+x^2(1-v^2)$, we obtain

$$\mathrm{I}_2=x(1-\eta^2-x^2)\int_0^1\frac{dv}{\sqrt{[\eta^2+x^2(1-v^2)][2(1-\eta^2)-x^2(2-v^2)]}}.$$

If x^2/η^2 is small as well as $x^2/(1-\eta^2)$ (which will certainly be the case if $\eta^2\geqslant 1-\eta^2$, i. e., $\eta^2\geqslant\frac{1}{2}$), we obtain on expansion

$$\mathrm{I}_2=x\sqrt{\frac{1-\eta^2}{2\eta^2}}\left[1-\frac{4+3\eta^2}{12}\cdot\frac{x^2}{\eta^2(1-\eta^2)}+\ldots\right].$$

Thus we have approximately

$$\zeta=(2n+1)\frac{1-\eta^2}{\sqrt{2-\eta^2}}\left[\mathrm{K}-\frac{x^2}{1-\eta^2}\cdot\frac{(1+\eta^2)\mathrm{K}-\mathrm{E}}{2\eta^2}\right]+\sqrt{\frac{1-\eta^2}{2\eta^2}}x.$$

The value of x for which $\dfrac{d\zeta}{dx}=0$ is then approximately

$$x=\frac{1}{2n+1}\cdot\frac{\eta}{(1+\eta^2)\mathrm{K}-\mathrm{E}}\sqrt{\tfrac{1}{2}(1-\eta^2)(2-\eta^2)}, \qquad (8.2)$$

giving as an approximation to the critical value of ζ,

$$\zeta=(2n+1)\frac{1-\eta^2}{\sqrt{2-\eta^2}}\left[\mathrm{K}+\frac{1}{4}\frac{2-\eta^2}{(1+\eta^2)\mathrm{K}-\mathrm{E}}\cdot\frac{1}{(2n+1)^2}\right]. \quad (8.3)$$

If x is given by (8.2) we have

$$\frac{x^2}{1-\eta^2}=\frac{1}{(2n+1)^2}\cdot\frac{\eta^2(2-\eta^2)}{2[(1+\eta^2)\mathrm{K}-\mathrm{E}]^2}. \quad (8.4)$$

Hence the assumption that $x^2/(1-\eta^2)$ is small will always be justified for sufficiently large n. In fact, when η is very close to unity the term $(1+\eta^2)\mathrm{K}-\mathrm{E}$ in the denominator becomes very large, and the right-hand side of (8.4) is small even for small values of n. Thus, although $1-\eta^2$ is small, the assumption is still valid and the approximation (8.3) can be used for quite small values of n.

9. For small values of η we can calculate ζ in another manner. Putting

$$\frac{1-q}{1+q}=k^2,$$

the value of ζ is given by

$$\zeta=\frac{1-k^2}{\sqrt{2(1+k^2)}}[(2n+2)\mathrm{K}-\mathrm{F}(k,\psi)], \quad (9.1)$$

where

$$\eta^2=\frac{2k^2}{1+k^2}\sin^2\psi, \quad (9.2)$$

and $\mathrm{F}(k,\psi)$ is Legendre's standard integral

$$\int_0^{\psi}\frac{dx}{\sqrt{1-k^2\sin^2 x}}.$$

The condition $\dfrac{d\zeta}{dq}=0$ becomes

$$2(n+1)k^2\int_0^{\pi/2}\frac{3+k^2-(1+3k^2)\sin^2 x}{(1-k^2\sin^2 x)^{3/2}}\,dx = \int_0^{\psi}\frac{1+k^2-2k^2\sin^2 x}{\cos^2 x(1-k^2\sin^2 x)^{3/2}}\,dx,$$

i. e.,

$$k^2\left[(2n+2)\int_0^{\pi/2}f(k,x)\,dx-\int_0^{\psi}f(k,x)\,dx\right]=\frac{(1-k^2)\tan\psi}{\sqrt{1-k^2\sin^2\psi}}, \quad (9.3)$$

where $$f(k, x) = \frac{3+k^2-(1+3k^2)\sin^2 x}{(1-k^2\sin^2 x)^{3/2}}.$$

Since, even if n is small, the critical values of ζ are given by values of q not very far from $1-\eta^2$ *, the corresponding values of k^2 lie in the neighbourhood of $\eta^2/(2-\eta^2)$ and will be small if η is small. We therefore expand both sides of (9.3) in powers of k^2. If we write

$$u = \frac{2\tan\psi}{[5(n+1)\pi - 5\psi + \tan\psi]} \quad . \quad . \quad . \quad (9.4)$$

this gives

$$k^2 = u - k^4\left[\frac{19}{40} + \frac{5\cos 2\psi - 13}{160}u\right] - k^6\left[\frac{15}{64} + \frac{11\cos 4\psi + 134\cos 2\psi + 95}{512}u\right] - \ldots$$

If u is small, this gives the value of k^2 in the form

$$k^2 = u - \frac{19}{40}u^2 + \frac{477 - 50\cos 2\psi}{1600}u^3 - \ldots \quad . \quad (9.5)$$

We can then regard equations (9.1), (9.2), (9.4), and (9.5) as giving the critical values of ζ and η in terms of a parameter ψ.

The graphs of the critical values of ζ, *i. e.*, $\omega h\sqrt{\frac{m}{2Mg}}$ against η, i. e., $\omega a\sqrt{\frac{m}{2Mg}}$ for values of n from 0 to 5 have been calculated and are shown in fig. 2.

10. *Case II.—Axis of rotation vertical and thread supporting a mass* M *hanging freely.*

Taking the positive sense of the axis OZ as downwards, but leaving the position of the origin undetermined for the moment, the conditions for the relative equilibrium of the mass M give, at the lower end of the thread,

$$T\frac{dz}{ds} = Mg, \quad . \quad . \quad . \quad . \quad . \quad . \quad (10.1)$$

* When $q = 1-\eta^2$, the amplitude of the sn-curve is equal to the length of the rotating arm and the wave-length is a maximum. By varying q, the value of ζ can be increased, owing to the greater distance between the rotating arm and the first node of the curve, but this effect is soon counteracted by the decrease in wave-length. The proximity of the cusp to the point for which $q = 1-\eta^2$ is indicated in fig. 1.

$$T\frac{dr}{ds} = M\omega^2 r. \quad . \quad . \quad . \quad . \quad . \quad (10.2)$$

Since $T\dfrac{dz}{ds}$ is constant, the relation (10.1) holds at all points of the thread. We have also

$$T + \tfrac{1}{2}m\omega^2 r^2 = \text{constant} = Mg\,p, \text{ say.}$$

Fig. 2.

Hence, writing as before, $\frac{1}{2}m\omega^2 a^2 = Mg\,\eta^2$,

$$T = Mg\left(p - \eta^2\frac{r^2}{a^2}\right), \quad . \quad . \quad . \quad . \quad (10.3)$$

$$\frac{dz}{ds} = \frac{1}{p - \eta^2 r^2/a^2}, \quad . \quad . \quad . \quad . \quad . \quad (10.4)$$

$$\left(\frac{dr}{ds}\right)^2 = 1 - \frac{1}{(p - \eta^2 r^2/a^2)^2}, \quad . \quad . \quad . \quad (10.5)$$

If ρ is the radius of the path described by M, we can then write (10.2) in the form

$$M\omega^2\rho = Mg\sqrt{(p-\eta^2\rho^2/a^2)^2-1},$$

or, putting $$\mu = \frac{M\omega^2}{mg},$$

$$2\mu\frac{\eta^2\rho^2}{a^2} = \left(p-\frac{\eta^2\rho^2}{a^2}\right)^2 - 1.$$

We can regard this as an equation for ρ, and remembering that, since $\frac{dz}{ds}<1$, we must have $\eta^2\rho^2/a^2<p-1$, we obtain

$$\frac{\eta^2\rho^2}{a^2} = p+\mu-\sqrt{\mu^2+2\mu p+1}. \quad . \quad . \quad (10.6)$$

Finally, from (10.4) and (10.5) we have

$$\left(\frac{dr}{dz}\right)^2 = \left(p-1-\frac{\eta^2r^2}{a^2}\right)\left(p+1-\frac{\eta^2r^2}{a^2}\right).$$

Putting $\frac{p-1}{p+1}=k^2$, so that $k'^2=1-k^2=\frac{2}{p+1}$, we find that the equation of the curve formed by the thread is

$$\frac{\eta r}{a} = \sqrt{2}\frac{k}{k'}\,\mathrm{sn}\left[\frac{\sqrt{2}}{k'}\frac{\eta}{a}(z+z_0)\right]. \quad . \quad . \quad (10.7)$$

The arbitrary constants k and z_0 have to be chosen so that at one end $r=\pm a$ (where a is the length of the rotating arm as before), and at the other end $r=\rho$.

11. As in the previous case, it is better to work in terms of elliptic integrals. We denote the total length of the thread by l, and write

$$\sigma = \frac{\eta l}{a} = \omega l\sqrt{\frac{m}{2Mg}}.$$

Putting $\frac{\eta r}{a}=u$, $\frac{\eta\rho}{a}=u_0$, we have from (10.5)

$$\frac{dr}{ds} = \pm\frac{\sqrt{(p-u^2)^2-1}}{p-u^2},$$

and hence σ is given by an expression of the form

$$\sigma = 2n\int_0^{\sqrt{p-1}} g(u)\,du + \int_0^{u_0} g(u)\,du \pm \int_0^{\eta} g(u)\,du, \quad (11.1)$$

where $g(u) = (p-u^2)/\sqrt{(p-u^2)^2-1}$

and $u_0^2 = p+\mu-\sqrt{\mu^2+2p\mu+1}$ . . (11.2)

The sign of the second term in σ is necessarily positive since from (10.2) the signs of r and $\frac{dr}{ds}$ must be the same at this end of the thread ; n is an arbitrary integer, having the same significance as before.

By taking different values of n we obtain the same value of σ for different values of p, and hence there are, in general, alternative forms of relative equilibrium. The appropriate form for the function $U-T_0$ (in the notation of § 5) in this case is

$$-Mgz-\tfrac{1}{2}M\omega^2\rho^2-\tfrac{1}{2}m\omega^2\int r^2\,ds \equiv \frac{Mga}{\eta}V, \quad \text{say.}$$

Since this is always negative, we consider the value of $-V$, which, using (10.4), is given by

$$-V = \int\left[u^2+\frac{1}{p-u^2}\right]\frac{\eta\,ds}{a}+\frac{1}{2}\frac{\omega^2\eta\rho^2}{ga}.$$

Hence the value of $-V$ corresponding to (11.1) is given by

$$-V = 2n\int_0^{\sqrt{p-1}}\psi(u)\,du+\int_0^{u_0}\psi(u)\,du + \sqrt{\frac{\mu}{2}}u_0^2 \pm \int_0^{\eta}\psi(u)\,du, \quad (11.3)$$

where $\psi(u)=(1+pu^2-u^4)/\sqrt{(p-u^2)^2-1}$.

Taking η and μ as known, we shall regard (11.1), (11.2), and (11.3) as giving $-V$, σ in terms of the parameter p. The solution is real if $\eta \leqslant \sqrt{p-1}$, and we need only consider, therefore, the range of values of p given by $1+\eta^2 \leqslant p$.

12. Writing

$$\sigma = 2n\int_0^{\pi/2}\frac{p-(p-1)\sin^2 x}{\sqrt{p+1-(p-1)\sin^2 x}} + \int_0^{u_0} g(u)\,du \pm \int_0^{\eta} g(u)\,du,$$

and using

$$2u_0\frac{du_0}{dp}=1-\frac{\mu}{\sqrt{\mu^2+2p\mu+1}}=\frac{p-{u_0}^2}{p+\mu-{u_0}^2},$$

$$\sqrt{(p-{u_0}^2)^2-1}=\sqrt{2\mu}\,u_0,$$

we find, after a little transformation, that

$$\frac{d\sigma}{dp}=\frac{n}{p+1}\int_0^{\pi/2}\frac{p+1-p\sin^2x}{\sqrt{p+1-(p-1)\sin^2x}}dx$$

$$+\frac{(p-{u_0}^2)^2}{2\sqrt{2\mu}\,{u_0}^2(p+\mu-{u_0}^2)}-\int_0^{u_0}\frac{du}{[(p-u^2)^2-1]^{3/2}}$$

$$\mp\int_0^{\eta}\frac{du}{[(p-u^2)^2-1]^{3/2}}; \quad (12.1)$$

and treating $-V$ in the same way, we also find

$$-\frac{dV}{dp}=p\frac{d\sigma}{dp}. \quad . \quad . \quad . \quad . \quad . \quad (12.2)$$

The first term in $\frac{d\sigma}{dp}$ is finite and essentially positive. In fact, putting

$$\frac{p-1}{p+1}=k^2,$$

$$\frac{1}{p+1}\int_0^{\pi/2}\frac{p+1-p\sin^2x}{\sqrt{p+1-(p-1)\sin^2x}}dx$$

$$=\frac{k'}{2\sqrt{2}\,k^2}[(1+k^2)\mathrm{E}-(1-k^2)\mathrm{K}],$$

and the term on the right decreases steadily from $\frac{3\pi}{8\sqrt{2}}$ to 0 as k increases from 0 to 1, *i. e.*, as p increases from 1 to ∞ *.

Again, we can write

$$\frac{(p-{u_0}^2)^2}{2\sqrt{2\mu}\,{u_0}^2(p+\mu-{u_0}^2)}-\int_0^{u_0}\frac{du}{[(p-u^2)^2-1]^{3/2}}$$

* The limiting values are determinate in view of the well-known results

$$\lim_{k\to0}\frac{\mathrm{K}-\mathrm{E}}{k^2}=\frac{\pi}{4} \quad \lim_{k\to1}k'\mathrm{K}=0, \quad \lim_{k\to1}\mathrm{E}=1.$$

$$= \frac{1}{2(p^2-1)} \left\{ \int_0^{u_0} \frac{p(p-u^2)-1}{\sqrt{(p-u^2)^2-1}}\, du \right.$$

$$\left. + \frac{\sqrt{\mu}\,(p^2-1)(2p\mu+1)}{\sqrt{2(\mu^2+2p\mu+1)}\,[\mu p+1+p\sqrt{\mu^2+2p\mu+1}]} \right\} \geqslant 0,$$

since $p \geqslant 1+u^2$;

and

$$\frac{(p-u_0^2)^2}{2\sqrt{2\mu}\,u_0^2(p+\mu-u_0^2)} - \int_0^{u_0} \frac{du}{[(p-u^2)^2-1]^{3/2}}$$

$$< \frac{(p-u_0^2)^2}{2\sqrt{2\mu}\,u_0^2(p+\mu-u_0^2)}$$

$$= \sqrt{\left\{ \frac{\mu}{2(\mu^2+2p\mu+1)} \right\}} + \frac{1}{2\sqrt{2\mu}\,(p^2-1)}$$

$$+ \frac{p+\mu}{2(p^2-1)\sqrt{2\mu(\mu^2+2\mu p+1)}},$$

showing that these two terms in combination give a contribution to $\frac{d\sigma}{dp}$ which is always positive and finite when $p \geqslant 1+\eta^2$, and which tends to zero when p tends to infinity.

Finally, the last term $\int_0^{\eta} \frac{du}{[(p-u^2)^2-1]^{3/2}}$ decreases from infinity to zero as p increases from $1+\eta^2$ to infinity.

13. We take the two expressions for σ,

$$\sigma = 2n \int_0^{\sqrt{p-1}} g(u)\, du + \int_0^{u_0} g(u)\, du + \int_0^{\eta} g(u)\, du, \quad (13.1)$$

$$\sigma = (2n+2) \int_0^{\sqrt{p-1}} g(u)\, du + \int_0^{u_0} g(u)\, du - \int_0^{\eta} g(u)\, du, \quad (13.2)$$

$$g(u) = (p-u^2)/\sqrt{(p-u^2)^2-1},$$

which have a common value when $p = 1+\eta^2$.

When σ is given by (13.2) and $n \geqslant -1$, $\frac{d\sigma}{dp}$ is the sum of positive terms and is thus positive and decreases from $+\infty$ to 0 as p increases from $1+\eta^2$ to ∞. Hence this

value of σ increases steadily from its value when $p=1+\eta^2$ to infinity.

When σ is given by (13.1) and $n \geqslant 0$, $\frac{d\sigma}{dp} \to -\infty$ when $p \to 1+\eta^2$, and the value of σ initially decreases as p increases. But when $p \to \infty$, $\sigma \to \infty$, so that eventually σ must increase. Hence there must be a value $p=p_n$ for which $\frac{d\sigma}{dp}=0$; and this value of σ decreases from its value when $p=1+\eta^2$ to a minimum when $p=p_n$, and then increases again, tending to infinity when $p \to \infty$ *.

Since $-\frac{dV}{d\sigma}=p$, we see that when $n \geqslant 0$, the $(-V, \sigma)$ graph has a cusp when $p=p_n$ and a point of inflexion when $p=1+\eta^2$. On the branch given by (13.2) σ and $-V$ increase together as p increases from $1+\eta^2$ to ∞. On the branch given by (13.1), σ and $-V$ continue to decrease as p increases from $1+\eta^2$ to p_n, and then start to increase again, increasing to infinity as $p \to \infty$. Since the gradient $-\frac{dV}{d\sigma}$ is increasing, the latter portion of the graph lies above the former.

When $n=-1$ we need only consider that part of the graph for which σ is positive; hence we take only the branch (13.2) with $u_0 \geqslant \eta$. Then $\sigma=0$ when $p=\sqrt{1+2\mu\eta^2+\eta^2}$, and as p increases, $-V$ and σ both increase to infinity.

The general form of the graph is illustrated in fig. 3. Here the values of σ and $-V$ have been calculated for the case $\eta=0{\cdot}5$, $\mu=30$, and are shown by the full-line curves in the figure.

14. The form of the $(-V, \sigma)$ graph shows that new positions of relative equilibrium appear at points corresponding to the minimum values of σ; but the values of V for these new positions are algebraically greater than those corresponding to the branch (a) in fig. 3, so that apparently this branch, which corresponds to the case when the mass M rotates in a fashion similar to that

* In this case amplitude and wave-length increase or decrease together. Hence there is a lower limit, but no upper limit, to the distance that can be spanned with a given number of arches of the curve given by (10.7).

of a conical pendulum, should always represent a stable position. (The configurations corresponding to the branches (*a*), (*b*), and (*c*) of fig. 3 are shown in fig. 4, which is drawn for the case $\sigma = 1{\cdot}65$. The rotating arm is represented by OA, and OZ is the axis of rotation.)

Experiment shows, however, that if the thread is sufficiently long it does take up a sinusoidal form. If the

Fig. 3.

thread is then progressively shortened (other things being unchanged), a stage is reached at which the motion tends to become unsteady ; beyond this point the motion of the thread becomes erratic until a further stage is reached, at which the thread again settles down in a sinusoidal form, but with the number of nodes reduced by unity. Thus we have ranges of instability alternating with ranges of stability, until finally a length is reached

at which the mass M commences to swing outwards in larger and larger circles.

It seems possible that these results are attributable to the effect of air resistance, though in the absence of a solution of the equations of resisted motion a complete discussion cannot be given. If we treat the equations of motion as in § 5, using the end conditions appropriate to this case, and introducing extra terms to represent the resistance, we obtain

$$\frac{d}{dt}[\mathrm{T}+\mathrm{U}-\mathrm{T}_0] = -\int(\mathrm{X}\dot{x}+\mathrm{Y}\dot{y}+\mathrm{Z}\dot{z})\,ds, \quad . \quad (14.1)$$

where X, Y, Z are the components of resistance per unit length of the thread, and $\mathrm{U}-\mathrm{T}_0$ has the value given in §11. If X, Y, Z depended only on the *relative* disturbance $\dot{x}$, $\dot{y}$, $\dot{z}$, the expression $\mathrm{T}+\mathrm{U}-\mathrm{T}_0$ would continually decrease, so that the system would tend to a configuration in which $\mathrm{U}-\mathrm{T}_0$ were a minimum. This is the basis of the statement that only such a configuration could be "permanently" stable *. But actually X, Y, Z will contain terms arising from the rotation *as a whole*, and therefore depending on x, y, z. If we could write the contribution of such terms to the right-hand side of (14.1) in the form $-\dfrac{d\mathrm{F}}{dt}$, then it is the sum $\mathrm{T}+\mathrm{F}+\mathrm{U}_0-\mathrm{T}$ which we should expect to decrease, so that the system would tend to a configuration in which $\mathrm{F}+\mathrm{U}_0-\mathrm{T}$ were as small as possible, F depending on the resistance to steady rotation; and even if the terms could not be put in this form, the effect would be roughly the same, to impart a tendency towards the position in which the resistance due to steady rotation would be a minimum.

In the present case, since the resistance may be expected to increase with the distance from the axis of rotation, it will be least when the amplitude of the sn-curve is least, and therefore in the configuration corresponding to the greatest possible value of n †. Hence when the minimum value of σ is reached for which a new configuration with a greater value of n is possible, we should expect a tendency towards this new configuration to show itself;

* See, for example, Lamb, *op. cit.*

† In case i. the configuration with the least amplitude also corresponds to the least possible value of $\mathrm{U}-\mathrm{T}_0$, so no difficulty arises.

and thus the lower limits of the ranges of instability should approximate to these minimum values of σ. Numerical values are compared with the experimental results in § 21 and show that this expectation is realized.

The determination of an upper limit for the range of instability is more difficult. The existence of a range of instability appears to arise from the fact that the new position of equilibrium corresponds to a *maximum* of $U-T_0$, and so would not necessarily be a position of stable equilibrium in the absence of air resistance. Since the change is from a configuration in which the resistance is large to one in which the resistance is small, it may be possible for the old position to become untenable without the resistance in the new position being sufficient to have a pronounced effect on the stability. This possibility is illustrated by the examination which follows of the special case when the inertia of the thread is neglected completely.

We should therefore expect the upper limit of the range of instability to approximate to the value of σ for which the new configuration would ordinarily become stable. Unfortunately, an exact determination of this value seems impossible *. Observation suggests that stability is not attained until the portion of the thread between the rotating arm and the first node of the curve is greater than half an arch ; this would imply a value of σ given by (13.2), and means that the portion of each branch in fig. 3 between the cusp and the point for which $p=1+\eta^2$ is always unstable. The comparison of the experimental limits of stability with the values of σ for $p=1+\eta^2$, made in § 21, shows that the limit actually lies beyond this point of inflexion. On the other hand, the fact that the difference between the values is roughly constant (for given values of η and μ) suggests that the two are connected ; and if it were a matter of practical importance it should be possible to obtain an approximate formula for this difference.

15. If the mass of the thread is ignored, the problem reduces to that of a conical pendulum whose point of suspension A (*cf.* fig. 4) is describing a circle of centre O

* The equations for small displacements from the steady state are simultaneous equations whose coefficients depend on the equation of the undisturbed curve, *i. e.*, involve elliptic functions of the independent variable.

and radius a with angular velocity ω. In order to have a problem which yields to exact treatment, we will assume a resistance which is proportional to the velocity, writing the factor of proportionality in the form $\kappa M\omega$. Since its inertia is neglected, the thread will now hang in a straight line, and we will denote by λ the inclination of the thread to the vertical and by χ the angle which the vertical plane through A containing the mass M makes with the rotating arm *. Then the equations of motion referred to rotating axes are

$$M(\ddot{x}-2\omega\dot{y}-\omega^2x) = T\sin\lambda\cos\chi-\kappa M\omega(\dot{x}-\omega y), \quad (15.1)$$

$$M(\ddot{y}+2\omega\dot{x}-\omega^2y) = T\sin\lambda\sin\chi-\kappa M\omega(\dot{y}+\omega x), \quad (15.2)$$

Fig. 4.

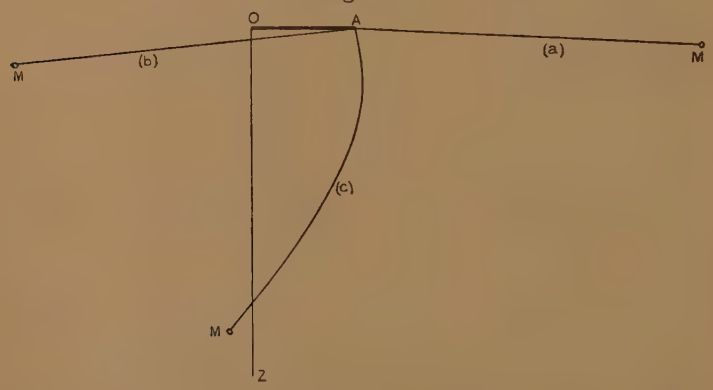

$$M\ddot{z} = Mg-T\cos\lambda-\kappa M\omega\dot{z}. \quad . \quad . \quad (15.3)$$

If we put

$$x=a-l\sin\lambda\cos\chi, \quad y=-l\sin\lambda\sin\chi, \quad z=l\cos\lambda,$$

where l is, as before, the length of the thread, elimination of T gives two equations, which we can put in the form

$$\ddot{l\lambda}-l\sin\lambda\cos\lambda\dot{\chi}^2-2\omega\dot{l}\sin\lambda\cos\lambda\dot{\chi}-\omega^2\cos\lambda(l\sin\lambda-a\cos\chi)$$
$$+\kappa\omega(\dot{l\lambda}-a\omega\cos\lambda\sin\chi) = -g\sin\lambda, \quad (15.4)$$

* The angle χ will be taken as 0 when the mass is in a position corresponding to (b) in fig. 4; when the mass is dragged behind the rotating arm (which is assumed to lie along the x-axis) χ will be taken as positive, increasing to π when the mass is in a position corresponding to (a) in fig. 4.

$$l\sin\lambda\ddot{\chi}+2l\cos\lambda\dot{\lambda}\dot{\chi}+2\omega l\cos\lambda\dot{\lambda}-\omega^2 a\sin\chi$$
$$+\kappa\omega[l\sin\lambda\dot{\chi}+\omega(l\sin\lambda-a\cos\chi)]=0. \quad (15.5)$$

We obtain the conditions for steady motion with the thread inclined at a constant angle α to the vertical, in a plane making a constant angle β with the rotating arm, by putting $\lambda=\alpha$, $\chi=\beta$ in (15.4) and (15.5), giving

$$l\sin\alpha-a\cos\beta+\kappa a\sin\beta=\frac{g}{\omega^2}\tan\alpha, \quad . \quad (15.6)$$

$$a\sin\beta=\kappa(l\sin\alpha-a\cos\beta). \quad . \quad . \quad . \quad (15.7)$$

To obtain the conditions for stability, we substitute $\lambda=\alpha+\delta$, $\chi=\beta+\xi$ in (15.4), (15.5), neglecting terms of order higher than the first in δ, ξ *. This gives, using (15.6) and (15.7),

$$l(\ddot{\delta}+\kappa\omega\dot{\delta})+\omega^2[l\sin^2\alpha-a\operatorname{cosec}\alpha(\cos\beta-\kappa\sin\beta)]\delta$$
$$-\omega l\sin\alpha\cos\alpha(2\dot{\xi}+\kappa\omega\xi)=0,$$
$$l\sin\alpha(\ddot{\xi}+\kappa\omega\dot{\xi})-\omega^2 a(\cos\beta-\kappa\sin\beta)\xi$$
$$+\omega l\cos\alpha(2\dot{\delta}+\kappa\omega\delta)=0.$$

These equations have solutions of the type

$$\delta=\delta_0 e^{-\frac{1}{2}\kappa\omega t\pm iq\omega t}, \quad \xi=\xi_0 e^{-\frac{1}{2}\kappa\omega t\pm iq\omega t},$$

provided

$$[lq^2+\tfrac{1}{4}\kappa^2 l+a\operatorname{cosec}\alpha(\cos\beta-\kappa\sin\beta)]$$
$$\times[lq^2+\tfrac{1}{4}\kappa^2 l+a\operatorname{cosec}\alpha(\cos\beta-\kappa\sin\beta)-l\sin^2\alpha]$$
$$=4l^2\cos^2\alpha q^2.$$

For stability the roots of this equation in q^2 must be such that the real part of $-\frac{1}{2}\kappa\pm iq$ is negative. This implies the three inequalities

$$a^2\operatorname{cosec}^2\alpha(\cos\beta-\kappa\sin\beta)^2+\kappa^2 l^2\cos^2\alpha$$
$$>al\sin\alpha(\cos\beta-\kappa\sin\beta), \quad (15.8)$$

$$l(\sin^2\alpha+4\cos^2\alpha)>2a\operatorname{cosec}\alpha(\cos\beta-\kappa\sin\beta), \quad . \quad . \quad (15.9)$$

$$l[(\sin^2\alpha+4\cos^2\alpha)^2+2\kappa^2(\sin^2\alpha+2\cos^2\alpha)]$$
$$>4(4\cos^2\alpha+\kappa^2)a\operatorname{cosec}\alpha(\cos\beta-\kappa\sin\beta). \quad (15.10)$$

* We make no assumption here as to the magnitude of the resistance, and the coefficient κ need not be small. We are only assuming that the initial disturbance from the steady state is small, and then determining whether the disturbance will increase with the time or be damped out.

16. If $\kappa=0$, then from (15.7) $\sin\beta=0$, and (15.6) gives

$$\beta=0, \quad \frac{l}{a}=\gamma\sec\alpha+\operatorname{cosec}\alpha, \quad . \quad . \quad (16.1)$$

$$\beta=\pi, \quad \frac{l}{a}=\gamma\sec\alpha-\operatorname{cosec}\alpha, \quad . \quad . \quad (16.2)$$

where $$\gamma=\frac{g}{a\omega^2}.$$

These equations are the limiting forms assumed by (13.1), with $n=0$, and (13.2), with $n=-1$, when $\frac{m}{M}\to 0$. For then $\eta\to 0$, $\mu\to\infty$, while $\eta\sqrt{2\mu}=\frac{a\omega^2}{g}\to\frac{1}{\gamma}$. Hence

$$\frac{l}{a}=\frac{\sigma}{\eta}=\lim_{\eta\to 0}\frac{1}{\eta}\left[\int_0^{u_0}\pm\int_0^{\eta}\frac{p-u^2}{\sqrt{(p-u^2)^2-1}}du\right]$$

$$=\frac{p}{\sqrt{p^2-1}}\left[\lim_{\eta\to 0}\frac{u_0}{\eta}\pm 1\right].$$

But $$u_0^2=(p^2-1)/[p+\mu+\sqrt{\mu^2+2p\mu+1}],$$

$$\therefore \quad \frac{u_0^2}{\eta^2}\to\frac{p^2-1}{2\mu\eta^2}=\gamma^2(p^2-1),$$

$$\frac{l}{a}=\gamma p\pm p/\sqrt{p^2-1},$$

which may be identified with the equations above by putting

$$p=\sec\alpha.$$

If $\frac{l}{a}$ is given by (16.2), then $\frac{l}{a}$ increases from 0 to ∞ as α increases from $\tan^{-1}\frac{1}{\gamma}$ to $\frac{\pi}{2}$, so that there is always one position of equilibrium, corresponding to the position (a) in fig. 4.

If $\frac{l}{a}$ is given by (16.1), then there is a minimum value

$$\frac{l}{a}=(1+\gamma^{2/3})^{3/2}, \quad . \quad . \quad . \quad . \quad . \quad (16.3)$$

given by $\alpha=\alpha_0$, where $\cot^3\alpha_0=\gamma$. If $\frac{l}{a}$ is greater than this

minimum, there are two further positions of equilibrium ; one for which $\alpha>\alpha_0$, i. e., $p>p_0$, corresponding to the position (*b*) in fig. 4 ; and one for which $\alpha<\alpha_0$, i. e., $p<p_0$. This last case corresponds only partially to the position (*c*) ; for if the inertia of the thread is ignored we no longer have the possibility of the thread ballooning out beyond the end of the rotating arm (as shown in fig. 4), it can only hang at a small inclination (less than α_0) to the vertical, as if the curve shown in fig. 4 were flattened down.

In this limiting case, $\frac{l}{a}$ increases to infinity while p decreases from p_0 to 1 ; in the general case p only decreases from p_0 to $1+\eta^2$, and then we pass to the form given by (13.2) with $n=0$, so that $\frac{l}{a}$ increases to infinity while p increases again from $1+\eta^2$ to ∞ . The resemblance between the two cases is thus incomplete, there being nothing in the limiting case corresponding to the branches with $n>0$. If we calculate the corresponding values of V *, then instead of a point of inflexion at $p=1+\eta^2$, as on branch (*c*) in fig. 3, the limiting case gives a curve on which $-\mathrm{V}$ and σ continue to increase to infinity, but with $-\frac{d\mathrm{V}}{d\sigma}$ decreasing to 1. The solution in the limiting case at this point separates from the general solution in which $m\neq0$. This departure is indicated in fig. 3, where the curves for the limiting case are represented by the dotted lines.

The minimum value of $\frac{l}{a}$ corresponds to a point before the solutions separate and can be used to give an approximation to the smallest critical value of σ, which is the minimum value from (13.1) with $n=0$. Thus, if $\eta=0{\cdot}5$, $\mu=30$, we have $\gamma=\frac{1}{\eta\sqrt{2\mu}}=\frac{1}{\sqrt{15}}$, and (16.3) gives

* We can disregard the presence of the factor η in the coordinates in fig. 3, since removing this factor is merely equivalent to a change of scale. Thus we take $\mathrm{M}ga\mathrm{V}=-\mathrm{M}gz-\frac{1}{2}\mathrm{M}\omega^2\rho^2$, *i. e.*, $-\mathrm{V}=l/a\cos\alpha+(1\mp l/a\sin\alpha)^2/2\gamma$; and to get a curve comparable with that in fig. 3 we must introduce a factor $\frac{1}{2}$ (since, in the case there shown, $\eta=\frac{1}{2}$).

$\frac{l}{a}=1{\cdot}666$, as compared with the value $\frac{l}{a}=1{\cdot}675$ obtained from fig. 3, which gives the exact curves for these values of η and μ. For larger values of μ the approximation is even better.

Putting $\kappa=0$ in the inequalities (15.8), (15.9), (15.10), we see that they are trivial in the case $\beta=\pi$, so that, in the absence of resistance, the position (a) is always a possible position of stable equilibrium; this confirms the result stated at the beginning of § 14 *. In the case $\beta=0$, using (16.1), the inequalities reduce to

$$\cot^3\alpha>\gamma, \quad . \quad . \quad . \quad . \quad . \quad . \quad . \quad . \quad . \quad (16.4)$$

$$\gamma>\frac{\tan^2\alpha-2}{\tan\alpha(\tan^2\alpha+4)}, \quad . \quad . \quad . \quad (16.5)$$

$$\gamma>\frac{\tan\alpha\,(8-\tan^2\alpha)}{(\tan^2\alpha+4)^2}. \quad . \quad . \quad . \quad (16.6)$$

The first of these shows that the position (b) is always unstable. In the position (c), where $\alpha<\alpha_0$, $\cot^3\alpha>\cot^3\alpha_0=\gamma$, and (16.4) is satisfied; but there may still be a restriction implied by (16.5), (16.6). In fact, if $\gamma<\frac{1}{8}$ †, α must not exceed the least (positive) root of the equation.

$$\gamma\,(\tan^2\alpha+4)^2=\tan\alpha\,(8-\tan^2\alpha). \quad . \quad . \quad (16.7)$$

and there is a lower limit to the value of $\frac{l}{a}$ for stability on this branch. Unfortunately, this value may belong to a region where the solutions separate, and so give no indication of the limit of stability when the inertia of the thread is taken into account.

Thus, taking the data from experiment (iii.) in § 21, we have $a=2{\cdot}5$ cm., $\omega=48{\cdot}67\,\pi$ rad./sec., and hence $\frac{1}{\gamma}=59{\cdot}57$. The limiting value of α is then given by

* The results as to stability in the case $\kappa=0$ are stated, without detailed analysis, by Lamb in the paper referred to in § 5, footnote.

† If $\frac{1}{8}<\gamma<\frac{1}{192}\sqrt{1654+146\sqrt{73}}$, there are two ranges of stability, since then the inequalities are also satisfied when α lies between the value given by the larger root of (16.7) and α_0; and if $\frac{1}{192}\sqrt{1654+146\sqrt{73}}<\gamma$ the inequalities are satisfied for all values of α less than α_0. These large values of γ, however, correspond to speeds of rotation much smaller than those used in the experiments, and we therefore confine our attention to the behaviour for values of γ less than $\frac{1}{8}$.

tan $\alpha = \cdot 0336$, and the limiting value of l for stability is 74·5 cm. The experiment gives the value $l = 25 \cdot 4$ cm., and the discrepancy is due to the fact that in the experiment $1+\eta^2 = 1 \cdot 0302$, while the limiting value $l = 74 \cdot 5$ cm. corresponds to a value of α for which $p = \sec \alpha = 1 \cdot 00056$, *i. e.*, to a value of p which is less than $1+\eta^2$.

Fig. 5.

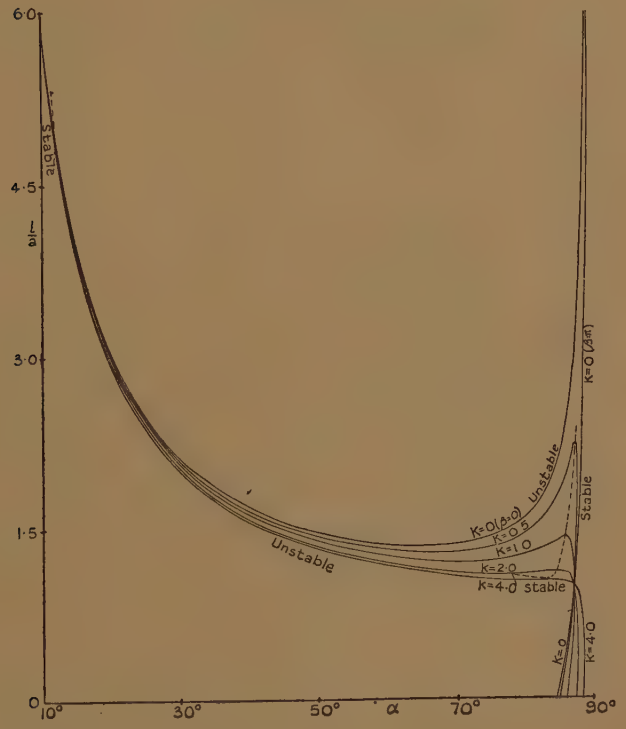

17. If $\kappa > 0$, we can write *

$$\frac{l}{a} = \operatorname{cosec} \alpha \left(\cos \beta + \frac{1}{\kappa} \sin \beta \right), \quad . \quad . \quad (17.1)$$

* To avoid irrationalities, we retain both equations; it may be noted that

$$\frac{l}{a} = \frac{\gamma}{1+\kappa^2} \sec \alpha \pm \operatorname{cosec} \alpha \sqrt{1 - c^2 \tan^2 \alpha},$$

an equation which, when k is small, gives values of $\frac{l}{a}$ differing only slightly from those in § 16 except when α is nearly equal to $\frac{\pi}{2}$.

where $$\sin\beta = c\tan\alpha \quad . \quad . \quad . \quad . \quad . \quad (17.2)$$

and $$c = \frac{\kappa\gamma}{1+\kappa^2}.$$

From (17.2) we see that α cannot exceed $\tan^{-1}\frac{1}{c}$, and that, provided this condition is satisfied, to each value of α corresponds two values of β and, therefore, two values of $\frac{l}{a}$, though one of these values may be negative, and is then disregarded. If we take $\beta > \frac{\pi}{2}$, so that $\cos\beta$ is negative, then $\frac{l}{a}$ increases from 0 to $\sqrt{1+c^2}/\kappa$ as α increases from $\tan^{-1}(\sqrt{1+\kappa^2}/\gamma)$ to $\tan^{-1}(1/c)$. This gives a position of equilibrium more or less corresponding to the position (a), the mass swinging outwards but being dragged behind the rotating arm, the greatest inclination α occurring when $\beta = \frac{\pi}{2}$, *i. e.*, when the vertical plane containing the thread is at right angles to the rotating arm.

If we take $\beta < \frac{\pi}{2}$, the variation of $\frac{l}{a}$ with α depends on the relative magnitudes of κ and γ. For we have, from (17.1) and (17.2),

$$\frac{d}{d\alpha}\left(\frac{l}{a}\right) = \frac{\tau^3 - \kappa[\tau^4 + c^2(1+\tau^2)^2]}{\kappa c\tau(1+\tau^2)}\operatorname{cosec}\alpha, \quad . \quad (17.3)$$

where $$\tau = \tan\beta.$$

If

$$\frac{1}{c^2} > \frac{16}{27}\kappa\,[(3+4\kappa^2)^{3/2} + \kappa(9+8\kappa^2)], \quad . \quad (17.4)$$

the equation,

$$\tau^3 = \kappa\,[\tau^4 + c^2(1+\tau^2)^2], \quad . \quad . \quad . \quad (17.5)$$

has two real positive roots and there are two distinct values of β, and therefore of α, for which $\frac{d}{d\alpha}\left(\frac{l}{a}\right) = 0$. Since, in any case, $\frac{d}{d\alpha}\left(\frac{l}{a}\right) \to -\infty$ when $\tau \to 0$ and when $\tau \to \infty$, it follows that if κ is small enough for (17.4) to hold, the

value of $\frac{l}{a}$ first decreases to a minimum as α increases, then increases to a maximum, finally decreasing again as α tends to $\tan^{-1}(1/c)$, for which value of α this branch unites with the other branch, the value of $\frac{l}{a}$ being $\sqrt{1+c^2}/\kappa$, and β again being equal to $\frac{\pi}{2}$. If κ is so large that (17.4) no longer holds, then equation (17.5) has no real roots and $\frac{d}{d\alpha}\left(\frac{l}{a}\right)$ never vanishes; as α increases from 0 to $\tan^{-1}\left(\frac{1}{c}\right)$, β increases from 0 to $\frac{\pi}{2}$, and $\frac{l}{a}$ decreases from ∞ to $\sqrt{1+c^2}/\kappa$.

In fig. 5 we show the graph of $\frac{l}{a}$ against α for different values of κ, taking $\gamma=0{\cdot}1$. In this case the value of κ for which (17.4) ceases to hold is approximately $\kappa=3{\cdot}37$, and the change in the form of the graph may be seen by comparing the curve for $\kappa=4$ with the curves for smaller values of κ.

It will be seen that for small values of κ the curves at first follow closely the corresponding curve for the case $\kappa=0$, given by (16.1), until the maximum point is nearly reached, and then turn over to follow the curve given by (16.2); and though for larger values of κ the departure from the curve $\kappa=0$ increases, this departure is mainly confined to the parts of the curve where α is large *. Thus the effect of the resistance is mainly to exclude those positions of equilibrium, corresponding to the positions (*a*) and (*b*) in fig. 4, in which the thread is inclined at a large angle to the axis of rotation, for all values of $\frac{l}{a}$ above a certain maximum. For small values

* To avoid complicating the figure the variation of β is not indicated, except in the case $\kappa=0$, where $\beta=0$ along one branch and $\beta=\pi$ along the other. On the remaining curves β increases from 0 when $\alpha=0$ to $\tan^{-1}(-\kappa)$ when $\frac{l}{a}=0$. Since c is small (i. e., $c\leqslant\gamma/2$), the variation in β is mainly confined to the parts of the curves for which α is nearly equal to $\frac{\pi}{2}$.

of κ (say $\kappa<1$ for the value of γ considered), the range of values of $\frac{l}{a}$ for which positions of equilibrium of the types (a) and (b) are possible may extend above the minimum point of the curve $\kappa=0$; as κ increases this range decreases, but even for comparatively large values of κ (say $\kappa=4$) still reaches to a point not very far below that minimum.

The inequalities expressing the conditions for stability are necessarily satisfied when $\cos\beta$ is negative, so that the parts of the curves where $\beta>\frac{\pi}{2}$ always represent stable positions of equilibrium. If $\beta<\frac{\pi}{2}$, then, using (17.1) and (17.2), and again putting $\tan\beta=\tau$, we have

$$\tau^3<\kappa[\tau^4+c^2(1+\tau^2)^2], \quad . \quad . \quad . \quad . \quad . \quad . \quad . \quad (17.6)$$

$$\kappa[\tau^2-2c^2(1+\tau^2)] < \tau[(1+2\kappa^2)\tau^2+2(2+\kappa^2)c^2(1+\tau^2)], \quad . \quad . \quad (17.7)$$

$$\kappa\tau[(2\kappa^2-1)\tau^2+2(4+\kappa^2)c^2(1+\tau^2)] < [\tau^2+4c^2(1+\tau^2)]^2+2\kappa^2[\tau^2+10c^2(1+\tau^2)] \times[\tau^2+c^2(1+\tau^2)]+4\kappa^4[\tau^2+c^2(1+\tau^2)]^2. \quad (17.8)$$

Comparison of (17.3) and (17.6) shows that the part of the curve between the minimum and maximum values of $\frac{l}{a}$ always represents unstable positions of equilibrium. This is the counterpart of the result found for the case $\kappa=0$, that the position (b) of fig. 4 is always unstable.

A detailed discussion of the other inequalities would involve some rather tedious algebra; we may content ourselves with remarking that they are necessarily satisfied when β is small and when β is nearly $\pi/2$, but may exclude a range of intermediate values of β (and therefore also of α) which may, or may not, overlap with the range of values excluded by (17.6) *. In fig. 5 the

* It is, perhaps, also worth mentioning that, owing to this possibility of non-overlapping, there may, as in the case $\kappa=0$ when $\gamma>\frac{1}{8}$, be two ranges of instability separated by a range of stability. Thus when $\kappa=3$ (the graph of l/a for this value of κ is not drawn, but lies between those for $\kappa=2$ and $\kappa=4$) the limits derived from (17.8) are $\alpha=11°{\cdot}78$, $\alpha=77°{\cdot}99$, and those derived from (17.6) are $\alpha=80°{\cdot}77$, $\alpha=83°{\cdot}85$, so that there is a small range of stability from $\alpha=77°{\cdot}99$ to $\alpha=80°{\cdot}77$.

boundaries of the region of instability are roughly indicated by the dotted lines. The upper boundary is always defined by (17.8), *i. e.*, is obtained by taking the value of $\frac{l}{a}$ corresponding to the smaller value of τ for which (17.8) becomes an equality. The lower boundary is partially defined by (17.6), *i. e.*, is partially formed by the locus of the maxima and minima of $\frac{l}{a}$ for different values of κ; and partially by (17.8), which still imposes a restriction even when κ is so large that (17.4) is not satisfied, *i. e.*, when (17.6) is satisfied for all values of τ. The inequality (17.7) does not impose any restriction outside those imposed by the other two.

18. From the analysis of the preceding sections we see that by introducing a resistance we can reproduce the phenomenon of a range of instability intervening between two ranges of stability, provided the resistance is not too small. If κ is small, the maximum point of the graph may rise above the level of the upper limit of the region of instability (in the particular example illustrated this would occur roughly when $\kappa < 0{\cdot}2$), and there would always be a possible position of stable equilibrium for a given value of $\frac{l}{a}$. For larger values of κ, on the other hand, there will be a range of values of $\frac{l}{a}$ for which there is no position of stable equilibrium. The position of the lower limit of the range of instability thus introduced may depend largely on the value of κ when κ is still small, but ultimately tends to lie close to, though rather below, the minimum value of $\frac{l}{a}$ as given by the case $\kappa = 0$. This is in accordance with the results given in § 21, where it will be seen that though the minimum values of $\frac{l}{a}$ do give good approximations to the lower limits of instability, the experimental values consistently lie slightly below the calculated values.

In the particular example illustrated, the value of $\frac{l}{a}$

at the upper boundary of the region of instability is very little affected by the value of κ; as κ ranges from 0 to 4 $\frac{l}{a}$ decreases only from 5·074 to 4·901. It would probably be affected more if the resistance experienced by the thread itself could be taken into account. On the other hand, if the resistance were taken as proportional to a higher power of the velocity than the first, it would increase with greater rapidity as the distance from the axis of rotation increased, and could still produce a large effect on the positions (*a*) and (*b*) without having so much effect on the position (*c*). In any case it would appear reasonable, in the absence of a complete solution of the equations of resisted motion, to take the upper limit of instability as coinciding approximately with that for the unresisted motion.

19. We have seen that an approximation to the minimum value of σ, as defined in equation (13.1), is given by (16.3) when $n=0$. In calculating the remaining values, *i. e.*, for $n \geqslant 1$, we shall disregard the term in u_0. For since we have neglected the weight of the thread in comparison with the centrifugal force, the solution is really only applicable when $\mu = \frac{\omega^2}{g} \cdot \frac{M}{m}$ is fairly large, and then the second term in σ is small in comparison with the first, at any rate in the region where the minima of σ lie.

In fact, putting $\frac{p-1}{p+1} = k^2$, $k' u_0 = \sqrt{2}\, k \sin \phi_0$, the contribution to $\frac{l}{a}$ of the term in question is

$$\frac{\sqrt{2}}{\eta k'} \int_0^{\phi_0} \left[\sqrt{1-k^2 \sin^2 \phi} - \frac{k'^2}{2} \cdot \frac{1}{\sqrt{1-k^2 \sin^2 \phi}} \right] d\phi,$$

and is, therefore, less than

$$\frac{\sqrt{2}}{\eta k'} (1 - \tfrac{1}{2} k'^2)\, \phi_0.$$

Also

$$k'^2 u_0^2 = 1 + k^2 + k'^2 \mu - k' \sqrt{k'^2 (1+\mu^2) + 2(1+k^2)\mu},$$

$$\sin \phi_0 = \frac{1}{2k} \left[\sqrt{(1+k)^2 + k'^2 \mu} - \sqrt{(1-k)^2 + k'^2 \mu} \right]$$

$$= \frac{2}{k'} \cdot \frac{1}{\sqrt{\mu + \tan^2 \frac{\psi}{2}} + \sqrt{\mu + \cot^2 \frac{\psi}{2}}},$$

where $\psi = \cos^{-1} k$,

$$< \frac{1}{k'\sqrt{\mu}}.$$

$$\therefore \qquad \phi_0 \leqslant \frac{\pi}{2} \sin \phi_0 < \frac{\pi}{2k'\sqrt{\mu}}.$$

Hence the term in question is less than

$$\frac{\sqrt{2}}{\eta k'} \cdot \frac{1+k^2}{2} \cdot \frac{\pi}{2k'\sqrt{\mu}} = \frac{\pi}{2} \cdot \frac{1+k^2}{1-k^2} \cdot \frac{g}{a\omega^2}$$

$$= p \cdot \frac{\pi}{2} \frac{g}{a\omega^2};$$

But the minimum values of σ are given by values of p which approach $1+\eta^2$ with increasing n, so that the term in question is negligible if $\frac{a\omega^2}{g}$ is large, save possibly when $1+\eta^2$ is also large.

In disregarding this term we are really assuming that, since the mass M will tend to settle down almost on the axis of rotation (except when $n=0$), we may neglect, in comparison with the whole length, the small portion of the thread between M and the axis. The proviso that η must not be large excludes the case when the speed of rotation is so high that $\frac{a\omega^2}{g}$ is large in comparison with $\frac{M}{ma}$ $\left(\text{for } 2\eta^2 = \frac{a\omega^2}{g} \Big/ \frac{M}{ma}\right)$, since the mass M is then too small to keep the end of the thread down.

20. When $n \geqslant 1$ we therefore determine the minimum values of σ from

$$\sigma = 2n \int_0^{\sqrt{p-1}} \frac{p-u^2}{\sqrt{(p-u^2)^2-1}}\, du + \int_0^{\eta} \frac{p-u^2}{\sqrt{(p-u^2)^2-1}}\, du;$$

so that p must satisfy the equation

$$\frac{n}{p+1} \int_0^{\pi/2} \frac{p+1-p\sin^2 x}{\sqrt{p+1-(p-1)\sin^2 x}}\, dx$$

$$= \int_0^\eta \frac{du}{[(p-u^2)^2-1]^{3/2}}$$

$$= \frac{1}{2(p^2-1)}\left[\frac{(p^2+1)\eta-p\eta^3}{\sqrt{(p-\eta^2)^2-1}} - \int_0^\eta \frac{p^2-1-pu^2}{\sqrt{(p-u^2)^2-1}}\,du\right]. \quad . \quad . \quad . \quad (20.1)$$

If we put $$\frac{p-1}{p+1} = k^2$$

and $$\frac{\eta}{\sqrt{2}} = \frac{k}{k'}\sin\phi \quad . \quad . \quad . \quad . \quad (20.2)$$

we can write the value of σ (putting $u=\sqrt{p-1}\sin x$) in the form

$$\frac{\sigma}{\sqrt{2}} = \frac{1}{k'}[2n(\mathrm{E}-\tfrac{1}{2}k'^2\mathrm{K})+\mathrm{E}(k,\phi)-\tfrac{1}{2}k'^2\mathrm{F}(k,\phi)], \quad (20.3)$$

where $\mathrm{E}(k,\phi)$ is the standard elliptic integral

$$\int_0^\phi \sqrt{1-k^2\sin^2 x}\,dx.$$

From (20.1) we derive the equation to be satisfied by k in the form

$$k^2\left[2n\int_0^{\pi/2} g(k,x)\,dx + \int_0^\phi g(k,x)\,dx\right]$$

$$= \frac{\tan\phi}{\sqrt{1-k^2\sin^2\phi}}[(1+k^4)-k^2(1+k^2)\sin^2\phi], \quad (20.4)$$

where $$g(k,x) = \frac{2-(1+k^2)\sin^2 x}{\sqrt{1-k^2\sin^2 x}}.$$

Expanding both sides in powers of k^2, we obtain an equation which may be written

$$k^2 = v+\tfrac{1}{8}k^4[1+\tfrac{3}{4}(3+5\cos 2\phi)v]$$

$$+\tfrac{1}{64}k^6[1+\tfrac{1}{8}(9+10\cos 2\phi-35\cos 4\phi)v]+\ldots,$$

where $$v = 2\tan\phi/[3(n\pi+\phi)+\tan\phi].$$

If v is small, this gives the value of k^2 in the form

$$k^2 = v+\tfrac{1}{8}v^2+\tfrac{3}{64}(7+10\cos 2\phi)v^3+\ldots \quad . \quad (20.5)$$

We can then regard equations (20.2), (20.3), and (20.5) as giving the critical values of σ and η in terms of a parameter ϕ. In fig. 6 we give the graph of $\frac{\sigma}{\sqrt{2}} \equiv \frac{1}{2}\omega l\sqrt{\frac{m}{\mathrm{M}g}}$

against $\frac{\eta}{\sqrt{2}} \equiv \frac{1}{2}\omega a\sqrt{\frac{m}{Mg}}$ for values of $\eta/\sqrt{2}$ from 0 to 0·5 and for values of n from 1 to 5.

21. In case II. experimental results have been obtained which can be compared with the theoretical results. We tabulate below the results of three experiments, in which the following values were used (the measurements

Fig. 6.

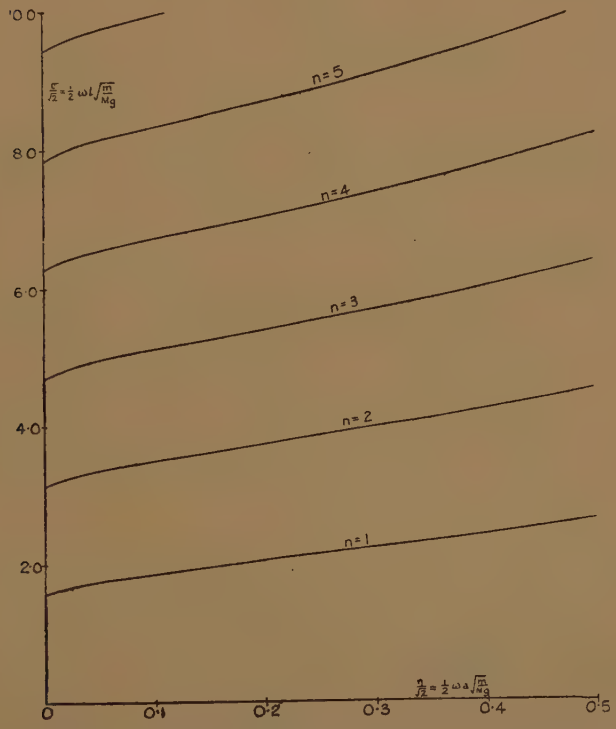

are all given in C.G.S. units, so that $g=981$; we give the appropriate values of the three constants $\eta \equiv \omega a\sqrt{\frac{m}{2Mg}}$ $\mu \equiv \frac{M\omega^2}{mg}$, $\gamma \equiv \frac{g}{a\omega^2}$, which have been used in the previous analysis) :—

(i.) $a=1·0$, $m=0·001456$, $M=3·538$ $\omega=39·54\pi$;

so that

$$\eta=0{\cdot}0569\ \left(\frac{\eta}{\sqrt{2}}=0{\cdot}0402\right),\quad \mu=3{\cdot}82\times10^4,\quad \gamma=0{\cdot}0636.$$

(ii.) $a=2{\cdot}5$, $m=0{\cdot}00157$, $M=3{\cdot}538$, $\omega=39{\cdot}54\ \pi$;

so that

$$\eta=0{\cdot}1477\ \left(\frac{\eta}{\sqrt{2}}=0{\cdot}1044\right),\quad \mu=3{\cdot}54\times10^4,\quad \gamma=0{\cdot}0254.$$

(iii.) $a=2{\cdot}5$, $m=0{\cdot}00081$, $M=2{\cdot}0$, $\omega=48{\cdot}67\ \pi$;

so that

$$\eta=0{\cdot}1737\ \left(\frac{\eta}{\sqrt{2}}=0{\cdot}1228\right),\quad \mu=5{\cdot}88\times10^4,\quad \gamma=0{\cdot}0168.$$

Length (in centimetres) of thread at lower limit of instability.

	(i.) $\eta=0{\cdot}0569$.		(ii.) $\eta=0{\cdot}1477$.		(iii.) $\eta=0{\cdot}1737$.	
n.	Calculated.	Observed.	Calculated.	Observed.	Calculated.	Observed.
1	42·8	41·8	44·8	43·1	38·9	34·1
2	82·8	82·0	84·2	82·0	72·6	67·3
3	122·6	121·3	123·0	119·2	105·4	99·7
4	..	..	..	..	138·7	129·4

For each value of η the critical values of σ can be obtained from the graph and the corresponding values of l calculated, giving a theoretical approximation to the lower limits of the ranges of instability *.

It will be seen that on the whole there is good agreement between the calculated and the experimental

* The values of n given in the tables are those to be used in the equations of § 20 for the calculation of σ. This means that the range of instability for given n is that which intervenes between the ranges in which the thread rotates steadily with n nodes (counting the position of M as one) and with $n+1$ nodes, *i. e.*, with the thread forming $n-1$ and n complete " balloons " respectively, there being an incomplete " balloon " between the upper node and the rotating arm. No measurements were made beyond the point where M began to leave the axis of rotation; and hence for $n=0$ only an upper limit is given, no results being available for comparison with the theoretical values calculated from equation (16.3).

results, particularly in the cases where the larger M was used *.

In the second table we compare the experimental values of l at the upper limit of instability with the values l_i for which the rotating arm is situated at the middle point of an arch of the rotating arm ; *i. e.*, with the values of l corresponding to the points of inflexion $p=1+\eta^2$. Again neglecting the small portion of the thread between M and the axis of rotation, these values are given by

$$\sigma_i=(2n+1)\frac{\sqrt{2}}{k'}[\mathrm{E}-\tfrac{1}{2}k'^2\mathrm{K}], \quad . \quad . \quad (21.1)$$

where $\sigma_i=\omega\sqrt{\frac{m}{2\mathrm{M}g}}l_i$, and $k=\eta/\sqrt{2+\eta^2}$.

Length (l) of thread (in centimetres) at upper limit of instability.

	(i.) $\gamma=0{\cdot}0636$.			(ii.) $\gamma=0{\cdot}0254$.			(iii.) $\gamma=0{\cdot}0168$.		
n.	l_i.	l.	$l-l_i$.	l_i.	l.	$l-l_i$.	l_i.	l.	$l-l_i$.
0 ..	19·5	35·5	16·0	19·0	34·8	15·8	16·2	25·4	9·2
1 ..	58·6	75·0	16·4	56·9	73·5	16·6	48·5	56·5	8·0
2 ..	97·7	116·5	18·8	94·8	114·1	19·3	80·8	93·9	13·1
3 ..	136·8	151·0	14·2	132·7	150·8	18·1	113·2	121·3	8·1
4 ..	..	..	..	..	..	..	145·5	146·8	1·3
	(Aver. diff.) $\div a=16{\cdot}4$			(Aver. diff.) $\div a=7{\cdot}0$.			(Aver. diff.) $\div a=3{\cdot}2$		

It will be seen that the difference $(l-l_i)$ remains fairly steady in each experiment (save possibility the third), suggesting that, if it were necessary, an approximate formula for the upper limit of stability could be obtained. The values given for $\frac{l-l_i}{a}$ suggest that this difference

* The values for the smaller M were obtained in an earlier experiment performed with rather crude apparatus which was afterwards improved ; the experimental results in this case may therefore be somewhat less reliable.

depends mainly on the value of γ, rather than on the values of η and μ separately.

It appears, therefore, that the theoretical form for the thread found by ignoring the effect of air resistance can still serve as a guide to the range where instability is to be expected, and in particular gives a good approximation to the lower limit of this range.

It should be noted that the limits measured experimentally are the limiting values of l for which it is possible to get a steady rotation of the thread with the mass M hanging at a constant depth. When this limit is passed the mass M at first oscillates only slightly in a vertical line, so that it is possibly merely oscillating about a position of stable equilibrium. This cannot be avoided, since the nearer the approach to the region of instability the more sensitive is the thread to extraneous disturbances, and it is not possible to avoid a certain amount of vibration being communicated to the rotating arm from the motor by which it is driven. It would, however, be difficult to draw a clear line of demarcation between such oscillations and the beginning of instability. The experimental results may therefore be taken as giving extreme limits for the range of instabilitv.

XVI. *Paramagnetism of the Iron Group. By* S. S. Bhatnagar, *O.B.E., D.Sc. (Lond.), F.Inst.P.*, Mohan Lal Khanna, *M.Sc., and* M. B. Nevgi, *M.Sc.**

A LARGE number of thorough investigations [1] of the variation of paramagnetic susceptibility with temperature have been made, and it has been shown by various workers that the Curie-Weiss law holds good in most of these cases. The observed p_B values of the ions of the iron group do not agree at all with those deduced theoretically from expressions advanced by different authors. It seems most probable that the anomalies observed in these cases may be explained in terms of the partial or complete independence of L– and S– moments and of the partial or complete ineffectiveness of the L– moment owing to interaction with neighbouring ions,

* Communicated by S. S. Bhatnagar, O.B.E., D.Sc. (Lond.).

in accordance with Van Vleck's [2] theory of the quenching of the orbital magnetic moment. The present work was undertaken to augment the experimental knowledge of the magnetic properties of the ions of the iron group by investigating the cobalt and nickel salts of the organic acids, which could be obtained in a high state of purity.

Experimental.

The apparatus employed during this investigation is Gouy's balance. For higher temperature measurements an electric furnace made of mica pieces and nichrome wire was used. In order to avoid any error due to the changes in the field at different temperatures the balance was standardized separately for each of the temperatures employed. It has already been shown in a previous paper [3] that the substances in the tube attained the temperature recorded by the thermometer placed in the electric furnace.

The values of the magnetic susceptibility of the substance under investigation have been calculated according to the equation

$$\chi = \frac{1}{m}\left\{(\chi_0 \cdot m_0 - \chi_a \cdot m_{a.0})\frac{\omega}{\omega_0} + \chi_a \cdot m_a\right\},$$

where

χ_0 = specific susceptibility of the standard substance;
χ = " " " specimen;
χ_a = " " " air;
m_0 = mass of the standard substance;
m = " " specimen;
$m_{a.0}$ = mass of the air displaced by the standard;
ma = " " " specimen;
ω_0 = pull due to the standard substance;
ω = " " specimen.

The substances used were B.D.H. extra-pure. The anhydrous salts were prepared from those substances, and special precautions were taken to ensure that all the water of crystallization had actually been removed. In order to be certain that the compounds did not decompose on heating the magnetic observations were repeated at room-temperature after heating to the highest one. From the mean values, $\overline{C}_m$ and θ, the values of χ

at different temperatures were calculated and added for comparison. As the temperatures recorded are within an error of $\pm 0{\cdot}1^\circ$ C., there is no point in giving the value of θ up to the second decimal. The calculated values for χ have been obtained with the help of that rounded-off value of θ; this is the reason why there is no *complete* agreement between them and the observed values even at those temperatures on which the determination of $\overline{C}_m$ and θ was based.

Experimental Results.

Table I.

T° (abs.).	$\chi \times 10^6$. Obs.	$\chi \times 10^6$. Calc.	$\chi_M \times 10^6$.	$\chi_{Co^{++}} \times 10^6$.	$1/\chi_{Co^{++}}$.	C_m.	$\overline{C}_m$.	p_B.	θ.
Cobalt acetate (anhydrous).									
303	58·32	58·32	10322	10380	96·3	3·549	3·496	5·31	−33·8
343	52·19	52·09	9236	9294	107·6	3·493			
383	47·13	47·06	8341	8399	119·1	3·445			
423	42·92	42·92	7595	7653	130·7				
Cobalt oxalate (anhydrous).									
303	57·53	57·50	8454	8482	117·9	3·055	3·060	4·97	−58·0
343	51·64	51·75	7588	7616	131·3	3·122			
383	47·04	47·04	6912	6940	144·1	3·082			
423	43·13	43·11	6338	6366	157·1				
Cobalt lactate (anhydrous).									
303	49·50	49·52	11732	11823	84·6	3·384	3·254	5·12	+27·9
343	43·38	43·18	10282	10373	96·4	3·182			
383	38·33	38·28	9085	9176	109·0	3·203			
423	34·35	34·36	8142	8233	121·5				
Cobalt thiocyanate (anhydrous).									
303	63·33	63·31	11088	11139	89·8	3·633	3·575	5·37	−18·0
343	56·38	56·26	9871	9923	100·8	3·591			
383	50·74	50·62	8884	8935	111·9	3·503			
423	46·01	46·00	8056	8108	123·3				
Cobalt cyanide (anhydrous).									
303	34·48	34·47	3825	3847	259·9	1·219	1·206	3·12	−10·5
343	30·59	30·64	3394	3416	292·8	1·223			
383	27·58	27·42	3061	3082	324·5	1·143			
423	24·88	24·88	2760	2782	359·5				

TABLE II.

T° (abs.).	$\chi \times 10^6$. Obs.	$\chi \times 10^6$. Calc.	$\chi_M \times 10^6$.	$\chi_{Ni^{++}} \times 10^6$.	$1/\chi_{Ni^{++}}$.	C_m.	C_m.	p_B.	θ.
				Nickel acetate (anhydrous).					
311	24·70	24·70	4366	4424	226·0	1·162	1·139	3·03	+53·5
348	21·61	21·55	3820	3878	257·9	1·169			
383	19·33	19·23	3417	3474	287·8	1·095			
423	17·12	17·12	3025	3083	324·4				
				Nickel oxalate (anhydrous).					
311	20·51	20·51	3009	3037	329·3	0·949	0·939	2·75	+1·8
348	18·32	18·30	2687	2716	368·3	0·947			
383	16·63	16·60	2440	2468	405·2	0·924			
423	15·01	15·01	2202	2230	448·5				
				Nickel lactate (anhydrous).					
311	17·58	17·58	4164	4255	235·0	1·101	1 121	3·01	+47·7
348	15·34	15·36	3671	3762	268·7	1·147			
383	13·74	13·72	3252	3343	299·1	1·114			
423	12·22	12·23	2894	2985	335·0				
				Nickel tartrate (anhydrous).					
311	20·56	20·56	4250	4311	232·0	1·085	1·085	2·96	+59·3
348	17·88	17·88	3697	3758	266·1	1·085			
383	15·92	15·92	3291	3352	298·4				
				Nickel citrate (anhydrous).					
311	21·06	21·05	11668	3942	253·7	1·128	1·122	3·01	+26·3
348	18·60	18·64	10310	3490	286·5	1·117			
383	16·74	16·74	9279	3146	317·9				
				Nickel benzoate (anhydrous).					
311	20·08	20·07	6038	6165	162·2	1·293	1·293	3·20	+101·2
348	17·00	17·00	5114	5241	190·8	1·294			
383	14·84	14·84	4463	4589	217·9				

DISCUSSION OF RESULTS.

A glance at the tables will reveal the fact that the p_B values of the Co^{++} ion fall between 5·37 and 4·97, while those of the Ni^{++} ion lie between 2·75 and 3·20, with the exception of cobalt cyanide, in which case the p_B value is 3·12. In the following tables the theoretical and experimental values for the Co^{++} and Ni^{++} ions, as obtained by different authors, are given for comparison.

Table III.—Co^{++} ion.

Theoretical Values [4].

			p_B.
Van Vleck	....	....	5·21
Bose	....	....	3·88
Sommerfeld ..	....	....	4·03
Hund	....	....	6·64

Experimental.

Authors.	Salt.	State.	
Chatillon [5] ..	$CoSO_4$.	Solution.	4·8-5·2
,,	$CoCl_2$.	In different solvents.	5·0–5·3
Weiss [6]	....	....	5
Foëx [7]	$CoSO_4$.	....	4·8–5·1
Serres [8].....	$CoSO_4$.	Anhydrous and hydrated salts.	5·0–5·3
Jackson [9] ...	$CoSO_4 . 7H_2O$.	Crystals along different axes.	$p_1=5·11$ $p_2=5·05$ $p_3=4·91$
Honda and Ishiwara [10].	$CoCl_2$.	....	5·01
	$CoSO_4$.	....	4·85
Théodorides [11].	$CoSO_4$.	....	5·07
,,	$CoCl_2$.	....	5·05
Cabrera [12] ...	$CoSO_4$.	In solution.	4·9–5·0
Trümpler [13] .	$CoSO_4$.	,,	4·95–4·97
Bhatnagar and Kapur [14].	$CoCl_2$.	In different solvents.	4·4–5·5
Datta [15]	Complex cobalt salts.	Solid.	4·69–4·81
Present authors.	$Co(CH_3 . COO)_2$.	,,	5·31
		,,	4·97
	$Co(CH_3 . CH(OH) . COO)_2$	,,	5·12
	$CO(SCN)_2$.	,,	5·36
	$Co(CN)_2$.	,,	3·12

Table IV.—Ni^{++} ion.

Theoretical [16].

			p_B.
Van Vleck	....	....	4·48
Sommerfeld ..	....	....	2·83
Bose	....	....	2·83
Hund	....	....	5·59

Experimental.

Authors.	Substance.	State.	
Cabrera [17] ...	$NiSO_4$. $NiCl_2$. $Ni(NO_3)_2$.	In solution.	3·2 3·2 3·2
Cabrera and Duperier [18].	$NiSO_4$.	Anhydrous.	3·035
Foëx [19]	$NiCl_2$.	In solution.	99
Honda and.. Ishiwara [10].	$NiCl_2$.	....	32·2

TABLE IV. (*cont.*).

Authors.	Substance.	State.	
Théodorides [11].	$NiCl_2$.	....	3·2–3·4
Datta [15]	Complex nickel salts.	Solid.	2·8–3·0
Woltjer [20] ...	$NiCl_2$.	....	3·17
Serres [21]	$NiSO_4$.	Anhydrous	3·2
	$NiCl_2$.	and hydrated	3·2
	$Ni(CN)_2$.	salts.	1·2–1·4
Present authors.	$Ni(CH_3 . COO)_2$.	Solid.	3·03
	$\begin{matrix} COO \\ \vert \\ COO \end{matrix}\!\!>\!Ni$.	,,	2·75
	$Ni(CH_3 . CH(OH) . COO)_2$.	,,	3·01
	$\begin{matrix} CH(OH) . COO \\ \vert \\ CH(OH) . COO \end{matrix}\!\!>\!Ni$.	,,	2·96
	$Ni_3\left[\begin{matrix} CH_2 . COO— \\ \vert \\ C(OH) . COO— \\ \vert \\ CH_2 . COO— \end{matrix}\right]_2$	,,	3·01
	$Ni(C_6H_5 . COO)_2$.	,,	3·20

Hund's formula [22],

$$p = 4{\cdot}97g\sqrt{J(J+1)},$$

and Van Vleck and Frank's formula [23],

$$\chi_M = \frac{Ng^2\beta^2J(J+1)}{3kT} + N\alpha,$$

which have been so successful in dealing with the rare earth salts and ions, fail completely to account for those of the iron group. The Co^{++} ion has 25 electrons and has a $^4F_{9/2}$ term as its ground state, whereas the Ni^{++} ion with 26 electrons is in $^3F_4$.

According to Van Vleck [2] we have in the iron group:—

(i.) For wide multiplet intervals, $h\triangle r \gg kT(\triangle r \to \infty)$:

$$p'_B = g\sqrt{J(J+1)};$$

for Co^{++}, $g=4/3$, $J=9/2$, and $p'_B = 6{\cdot}64$;

for Ni^{++}, $g=5/4$, $J=4$, and $p'_B = 5{\cdot}59$.

(ii.) For narrow multiplets, $h\triangle r \ll kT(\triangle r \to 0)$:

$$p'_B = \sqrt{L(L+1)+4S(S+1)};$$

for Co^{++}, $p'_B = 5{\cdot}20$;

for Ni^{++}, $p_B = 4{\cdot}47$.

(iii.) For comparable multiplet intervals, $h\triangle r \approx kT$, using the actual multiplet intervals calculated by Laporte [24] and corrected by Van Vleck and Frank [23] by the introduction of the term $\alpha(J)$, the value for Co^{++} is 6·56, while for Ni^{++} the value is 5·56.

(iv.) If the orbital moment is completely quenched by a crystalline field only the spin moment is effective, and

$$p'_B = \sqrt{4S(S+1)},$$

for Co^{++}, $p_B' = 3{\cdot}87$,

and for Ni^{++}, $p_B' = 2{\cdot}83$.

In the rare earth ions there is no possibility of an interaction between the electrons responsible for paramagnetism, which are below an inert gas configuration of eight electrons of higher total quantum number, and the neighbouring molecules or ions (both in solid and solutions) ; in the case of the iron group, however, the incomplete 3*d* sub-shell, lying just below the valence electrons, which are removed by ionization, will be open to the action of the molecules of the solvent. This is sufficient to disturb the orbital magnetic moment and render it completely or partially ineffective in responding to an external field, and to leave only the spin moment to account for their paramagnetic behaviour. This view of interaction effects was advanced by Stoner [25], Brunetti [26], and Van Vleck [2] independently. Under these conditions the p_B values for the ions of the iron group will not fall between the wide limits indicated by (i.) and (ii.), but should lie between the limits given by the following equations :—

$$p_B = \sqrt{4S(S+1)},$$

and

$$p_B = \sqrt{4S(S+1)+L(L+1)};$$

the values of p_B for Co^{++} and Ni^{++} found in the present investigation go in support of the above views.

Serres [21] has shown that the value of the magnetic moment of the Ni^{++} ion in anhydrous nickel cyanide lies between 1·4 and 1·2 instead of 3·02 as in the other nickel salts. In the present work anhydrous thiocyanate

and cyanide have been investigated. The p_B value for the Co^{++} ion in the former case is the same as that obtained experimentally from other salts, while in the latter case it is 3·12. This is possibly due to the fact that, although the linkage in the other salts may be of the electrovalent type, it is covalent in the cyanides.

Our thanks are due to Dr. H. Lessheim for his help in calculations and discussions.

References.

(1) *Cf.* references (5) to (21).
(2) J. H. Van Vleck, ' Theory of Electric and Magnetic Susceptibilities ' (Oxford, 1932), particularly xi. p. 73.
(3) S. S. Bhatnagar, M. B. Nevgi, and R. L. Sharma, Phil. Mag. xxii. p. 409 (1936).
(4) *L. c.*, reference (2), chapter xi. p. 72.
(5) A. Chatillon, *Ann. de Phys.* ix. p. 187 (1928) ; *C. R.* clxxvi. p. 1608 (1923).
(6) P. Weiss, J. Phys. Radium, v. p. 129 (1924).
(7) G. Foëx, *C. R.* clxxx. p. 919 (1925).
(8) A. Serres, *Ann. de Phys.* xvii. p. 5 (1932).
(9) L. C. Jackson, Proc. Roy. Soc. (A) cxl. p. 695 (1933).
(10) K. Honda and Y. Ishiwara, Sci. Rep. Tohoku Imp. Univ. (ii.) iv. p. 215 (1915).
(11) P. Théodorides, *J. de Phys.* iii. p. 1 (1922).
(12) J. and M. Cabrera, *Anal. Soc. Espan. Fis. Quim.* (B) xiv. p. 357 (1916).
(13) Trümpler, Thesis, Zurich, 1917.
(11)–(13) Quoted from ref. (5).
14) S. S. Bhatnagar and A. N. Kapur, J. Indian Chem. Soc. ix. p. 341 (1932).
(15) S. Datta, Phil. Mag. xvii. p. 585 (1934).
(16) *L. c.*, ref. (2).
(17) B. Cabrera, E. Moles, and J. Guzman, *Arch. Sci. Phys. Nat.* (v.) xxxvii. p. 32 (1914) ; *Anal. Soc. Espan. Fis. Quim.* xii. p. 131 (1914).
(18) B. Cabrera and A. Duperier, *Anal. Soc. Espan. Fis. Quim.* xxix. p. 5 (1931).
(19) G. Foëx, J. Phys. Radium (7) iii. p. 337 (1932).
(20) H. R. Woltjer, *Proc. K. Akad. Wetensch. Amsterdam*, xxviii. p. 536 (1925).
(21) A. Serres, *Ann. de Phys.* xx. p. 441 (1933).
(22) F. Hund, *Zs. f. Phys.* xxxiii. p. 855 (1925).
(23) *L. c.*, ref. (2), chapter ix. p. 55.
(24) C. Laporte, *Zs. f. Physik*, xlvii. p. 761 (1928).
(25) E. C. Stoner, Phil. Mag. viii. p. 250 (1929).
(26) R. Brunetti, *Rendic Acc. Lincei*, ix. p. 754 (1929).

University Chemical Laboratories,
Lahore (India).

XVII. *Magnetic Fields in Transformers at Low Frequencies (25 to 75 cycles per second).* *By* J .M. Thomson *.

ONE of the most important problems in the design of a transformer is the predetermination of the reactive drop of voltage at the secondary terminals when the transformer is loaded. The exact calculation is a matter of considerable difficulty, and designers usually employ approximate formulæ for the computation of the leakage reactance corrected by some factor which experience and the results of tests have shown to be necessary.

A further problem of extreme practical importance is the calculation of the magnetic field itself. In large current windings there is a non-uniform distribution of current which causes an increase in the copper resistance loss in the winding. This loss can be reduced by making the conductor of a number of strands and transposing the strands in such a way as to make the distribution of current more uniform. To do this properly, accurate plots of the magnetic field are necessary, and at present no work has been done on the type of windings analysed in this paper. As a result of this, the work described in this paper was done in an effort to obtain reasonably correct flux plots and a more accurate formula for the calculation of the leakage reactance in certain types of transformers.

In practice transformers are made in a great variety of forms. An analysis will be made of the type known as the core concentric type with a divided core. The core may have two or four yokes. The high and low tension windings will consist of concentric coaxial cylinders.

The permeability of all the iron parts is assumed to be so large that H is equal to zero in the iron, and the flux enters the iron at right angles to the surface. The permeability will usually lie between 1000 to 5000, and the difference from true normality will be within three minutes or less. The iron parts are assumed to be perfectly laminated, so that when the alternating currents flow in the windings no eddy currents can be induced in the iron by the varying flux. It is also assumed

* Communicated by E. F. Burton.

that the current density over the section of the conductors is constant. This means that in heavy current windings the conductors are laminated, and so transposed

Figs. 1*a*–1*d*.

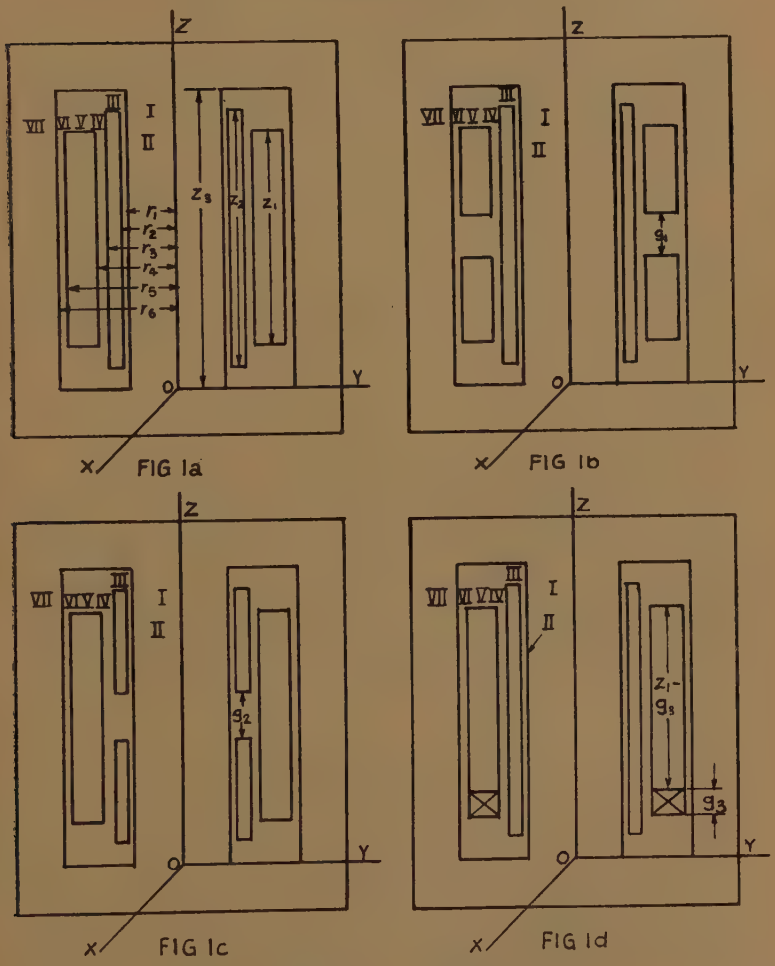

that the current density is constant. The insulation between the conductors is neglected.

It is also assumed that the only field present is that due to the windings. The frequency is so low that all capacity effects can be neglected.

Figs. 1 *a*, 1 *b*, 1 *c*, 1 *d* are cross-sections of the winding that will be analysed in this paper.

Fig. 1 *a* will be considered the standard arrangement.

Fig. 1 *b* has a large tap in the high-tension winding.

Fig. 1 *c* is similar to 1 *b*, but with the gap in the low tension winding.

Fig. 1 *d* has the high-tension winding displaced, as shown, by taps at one end of the winding.

The core-window, which contains the windings, is divided up into the seven regions—I, II, III, IV, V, VI, and VII—as marked on figs. 1 *a*, 1 *b*, 1 *c*, and 1 *d*.

Region I is the volume $-0 \leqq r \leqq r_1$ for $-\infty \leqq z \leqq +\infty$.

Region II is the volume $+r_1 \leqq r \leqq r_2$ for $-\infty \leqq z \leqq +\infty$.

Region III, etc.

Region VII is the volume $+r_6 \leqq r \leqq +\infty$, $-\infty \leqq z \leqq +\infty$.

Mathematical Solution.

List of Symbols.

δ_p=HT current density vector.

δ_s=LT current density vector.

In this problem the choice of cylindrical coordinates makes the components of δ_p and δ_s in the direction of the z- and r-axis zero, since δ_p and δ_s are vectors normal to the cross-section of the winding by planes through the z-axis. Since the components of the flux-density, B_r, B_ϕ, and B_z, are independent of ϕ, we finally obtain differential equations in which δ_p and δ_s are scalar quantities. We thus have

$$\delta_p = \frac{-N_1 I_1}{\text{effective cross-section of the HT winding}},$$

$$\delta_s = \frac{N_2 I_2}{\text{effective cross-section of the LT winding}}.$$

The LT current is assumed to be flowing in the positive direction, and, therefore, since the HT current is flowing in the opposite direction, the HT current density will be negative when compared with the LT current density.

B=magnetic flux density in gauss with components B_r, B_ϕ, B_z.

H=magnetic intensity with components H_r, H_ϕ, H_z.

$B=\mu H$, where μ is the permeability of the space under examination.

N_1I_1=ampere-turns in the high-tension winding.

N_2I_2=ampere-turns in the low-tension winding.

It is assumed that the magnetizing current of the core is neglected, and under these conditions we have $N_1I_1=N_2I_2$. Further, for simplicity in numerical calculations, we assume that the HT and LT windings have the same number of turns, and, therefore, $I_1=I_2=I$, numerically:

a_m, b_m, c_m, d_m, f_m, g_m, h_m, j_m, p_m, q_m, s_m, t_m, u_m, v_m, etc., are constants.

The transformer is divided into seven regions: I, II, III, IV, V, VI, VII, and the following system of identification has been carried out:

B_z^{II} is the flux-density in region II in the direction of the z-axis.

L_{II} is the inductance in region II, etc.

L=leakage inductance of a transformer in abhenries.

=inductance measured between the two HT terminals with the LT winding short-circuited.

=self-inductance of the HT winding plus the self-inductance of the LT winding minus twice the mutual inductance between the HT and the LT windings (1 : 1 turn ratio assumed)

$$=L_I+L_{II}+L_{III}+L_{IV}+L_V+L_{VI}+L_{VII},$$

where

$$L_I=\frac{2}{I^2\mu}\int_{vol}\frac{H.B}{8\pi}dv \quad \text{over region I,}$$

$$L_{II}=\frac{2}{I^2}\int_{vol}\frac{H.B}{8\pi}dv \quad \text{over region II,}$$

etc.

It is evident from the symmetry of the problem that cylindrical coordinates will give the simplest results, and that all quantities are independent of ϕ; also that

$$B_\phi=0.$$

On examining Maxwell's equations it is at once evident that there is a function ψ which can be considered to be

a generalized flux-function such that $\psi=a$ constant will give the flux-lines in the transformer.

A further transformation is made assuming ψ is equal to $r\mathrm{A}$.

The equations of Maxwell then reduce to

$$\frac{\partial^2 \mathrm{A}}{\partial r^2}+\frac{1}{r}\frac{\partial \mathrm{A}}{\partial r}+\frac{\partial^2 \mathrm{A}}{\partial z^2}-\frac{\mathrm{A}}{r^2}=-4\pi\mu\delta, \quad . \quad . \quad (1)$$

with equations

$$\mathrm{B}_r=-\frac{\partial \mathrm{A}}{\partial z}, \quad . \quad . \quad . \quad . \quad . \quad . \quad . \quad (2)$$

and

$$\mathrm{B}_z=\frac{1}{r}\frac{\partial}{\partial r}(r\mathrm{A}). \quad . \quad . \quad . \quad . \quad . \quad . \quad (3)$$

We thus have to solve

Regions I, II, IV, VI, VII :

$$\frac{\partial^2 \mathrm{A}}{\partial r^2}+\frac{1}{r}\frac{\partial \mathrm{A}}{\partial r}+\frac{\partial^2 \mathrm{A}}{\partial z^2}-\frac{\mathrm{A}}{r^2}=0. \quad . \quad . \quad . \quad . \quad (4)$$

Region III :

$$\frac{\partial^2 \mathrm{A}}{\partial r^2}+\frac{1}{r}\frac{\partial \mathrm{A}}{\partial r}+\frac{\partial^2 \mathrm{A}}{\partial z^2}-\frac{\mathrm{A}}{r^2}=-4\pi\delta_s. \quad . \quad . \quad (5)$$

Region V :

$$\frac{\partial^2 \mathrm{A}}{\partial r^2}+\frac{1}{r}\frac{\partial \mathrm{A}}{\partial r}+\frac{\partial^2 \mathrm{A}}{\partial z^2}-\frac{\mathrm{A}}{r^2}=4\pi\delta_p, \quad . \quad . \quad (6)$$

where

$$\mathrm{B}_r=-\frac{\partial \mathrm{A}}{\partial z} \quad \text{and} \quad \mathrm{B}_z=\frac{1}{r}\frac{\partial \mathrm{A}}{\partial r}(r\mathrm{A}),$$

and the boundary conditions are

$$\mathrm{B}_r^{\mathrm{I}}=\mathrm{B}_r^{\mathrm{II}};\ \mathrm{B}_r^{\mathrm{II}}=\mathrm{B}_r^{\mathrm{III}}, \text{ etc.}, \quad . \quad . \quad . \quad . \quad (7)$$

for $r=r_1$; $r=r_2$,

and

$$\mathrm{H}_z^{\mathrm{I}}=\mathrm{H}_z^{\mathrm{II}};\ \mathrm{H}_z^{\mathrm{II}}=\mathrm{H}_z^{\mathrm{III}}, \text{ etc.}, \quad . \quad . \quad . \quad . \quad (8)$$

for $r=r_1$; $r=r_2$.

Since the permeability of the end-yokes is very great, these yokes will act as magnetic mirrors ; and from the theory of images it is known that the yokes can be

eliminated if the image conductors are put in place of the yokes. Fig. 2 shows the position of the conductors and the first two image windings. It is obvious that δ is a periodic function of z with period z_3.

In the regions III and V the current density δ is a function of z, and since δ satisfies Dirichlet's conditions,

Fig. 2.

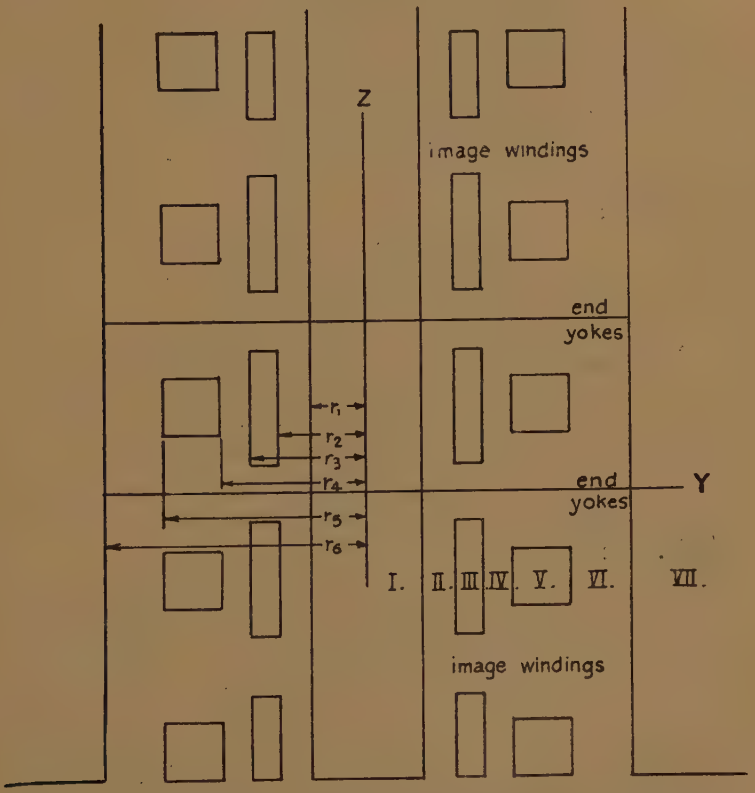

it can be expressed as a Fourier Series in z. We have, therefore,

Region III :

$$\delta_s = \delta_{20} + \sum_{m=1}^{\infty} \delta_{2m} \cos \frac{m\pi}{z_3} z. \quad . \quad . \quad . \quad . \quad (9)$$

Region V :

$$\delta_p = \delta_{10} + \sum_{m=1}^{\infty} \delta_{1m} \cos \frac{m\pi}{z_3} z, \quad . \quad . \quad . \quad (10)$$

where the values of δ_{10}, δ_{1m}, δ_{20}, and δ_{2m} for the types of windings considered in this analysis are as follows :

Fig. 1*a* :

$$\delta_{10} = \frac{z_1}{z_3}\delta_p, \quad \ldots\ldots \quad (11)$$

$$\delta_{1m} = \frac{4\delta_p}{m\pi}\cos\frac{m\pi}{2}\sin\frac{m\pi}{2}\frac{z_1}{z_3}, \quad \ldots \quad (12)$$

$$\delta_{20} = \frac{z_2}{z_3}\delta_s, \quad \ldots\ldots \quad (13)$$

$$\delta_{2m} = \frac{4\delta_s}{m\pi}\cos\frac{m\pi}{2}\sin\frac{m\pi}{2}\frac{z_2}{z_3}. \quad \ldots \quad (14)$$

Fig. 1*b* :

$$\delta_{10} = \left(\frac{z_1 - g_1}{z_3}\right)\delta_p, \quad \ldots\ldots \quad (15)$$

$$\delta_{1m} = \frac{4\delta_p}{m\pi}\cos\frac{m\pi}{2}\left[\sin\frac{m\pi}{2}\frac{z_1}{z_3} - \sin\frac{m\pi}{2}\frac{g_1}{z_3}\right], \quad \ldots \quad (16)$$

$$\delta_{20} = \frac{z_2}{z_3}\delta_s, \quad \ldots\ldots \quad (17)$$

$$\delta_{2m} = \frac{4\delta_s}{m\pi}\cos\frac{m\pi}{2}\sin\frac{m\pi}{2}\frac{z_2}{z_3}. \quad \ldots \quad (18)$$

Fig. 1*c* :

$$\delta_{10} = \frac{z_1}{z_3}\delta_p, \quad \ldots\ldots \quad (19)$$

$$\delta_{1m} = \frac{4\delta_p}{m\pi}\cos\frac{m\pi}{2}\sin\frac{m\pi}{2}\frac{z_1}{z_3}, \quad \ldots \quad (20)$$

$$\delta_{20} = \left(\frac{z_2 - g_2}{z_3}\right)\delta_s, \quad \ldots\ldots \quad (21)$$

$$\delta_{2m} = \frac{4\delta_s}{m\pi}\cos\frac{m\pi}{2}\left[\sin\frac{m\pi}{2}\frac{z_2}{z_3} - \sin\frac{m\pi}{2}\frac{g}{z_3}\right]. \quad \ldots \quad (22)$$

Fig. 1*d* :

$$\delta_{10} = \left(\frac{z_1 - g_3}{z_3}\right)\delta_p, \quad \ldots\ldots \quad (23)$$

$$\delta_{1m} = \frac{4\delta_p}{m\pi}\left[\cos\left(\frac{m\pi}{2}\frac{z_3 + g_3}{z_3}\right)\sin\left(\frac{m\pi}{2}\frac{z_1 - g_3}{z_3}\right)\right], \quad (24)$$

$$\delta_{20} = \frac{z_2}{z_3}\delta_s, \quad \ldots \ldots \quad (25)$$

$$\delta_{2m} = \frac{4\delta_s}{m\pi}\cos\frac{m\pi}{2}\sin\frac{m\pi}{2}\frac{z_2}{z_3}. \quad \ldots \quad (26)$$

It is evident from these equations that δ_{11}, δ_{13}, δ_{21}, δ_{23}, etc., are equal to zero when the windings are symmetrical with respect to the centre of the window.

B_r is a periodic function of z with period z_3, and by symmetry it is an odd function. Thus B_r may be expanded into a Fourier Series for the range $-z_3$ to z_3 in the form

$$-\frac{\partial A}{\partial z} = B_r = \sum_1^\infty \sin\frac{m\pi z}{z_3} F_m(r). \quad \ldots \quad (27)$$

Hence a solution of

$$\frac{\partial^2 A}{\partial r^2} + \frac{1}{r}\frac{\partial A}{\partial r} + \frac{\partial^2 A}{\partial z^2} - \frac{A}{r^2} = 0 \quad \ldots \quad (28)$$

will have the form

$$A = ar + \frac{b}{r} + \sum_1^\infty \left[\cos\frac{m\pi z}{z_3} \{a_m I_1(k_m r) + b_m K_1(k_m r)\} \right], \quad (29)$$

where

$$k_m = \frac{m\pi}{z_3}, \quad \ldots \ldots \quad (30)$$

$$m = 1, 2, 3, 4, \infty, \quad \ldots \ldots \quad (31)$$

and I_1, K_1 are modified Bessel functions of the first and second kind.

In region III we have to find the solution of the equation

$$\frac{\partial^2 A}{\partial r^2} + \frac{1}{r}\frac{\partial A}{\partial r} + \frac{\partial^2 A}{\partial z^2} - \frac{A}{r^2} = -4\pi\delta_{20} - 4\pi\sum_1^\infty \delta_{2m}\cos k_m z. \quad (32)$$

Let

$$A = \frac{-4\pi}{3}\delta_{20} r^2 + fr + \frac{g}{r} + \sum_1^\infty M_m(r)\cos k_m z \quad \ldots \quad (33)$$

be the solution. Then we have

$$\sum_1^\infty \left[M_m''(r) + \frac{1}{r}M_m'(r) - \frac{1}{r^2}(1 + k_m^2 r^2) M_m(r) \right] \cos k_m z - 4\pi\delta_{20}$$

$$= -4\pi\delta_{20} - \sum_1^\infty 4\pi\delta_{2m}\cos k_m z. \quad \ldots \quad (34)$$

Therefore

$$M_m''(r) + \frac{1}{r} M_m'(r) - \frac{1}{r^2}(1 - k_m^2 r^2) M_m(r) = -4\pi\delta_{2m}. \quad (35)$$

and the solution of this equation by the method of the variation of constants is

$$M_m = -4\pi\delta_{2m}\{Z_1(k_m r) - f_m\} I_1(k_m r) - 4\pi\delta_{2m}\{X_1(k_m r) - g_m\} K_1(k_m r), \quad (36)$$

where

$$Z_1(k_m r) = -\int_{k_m r}^{\infty} r K_1(k_m r)\, dr \quad (37)$$

and

$$X_1(k_m r) = \int_0^{k_m r} r I_1(k_m r)\, dr. \quad (38)$$

The solution of the differential equation in region III is therefore

$$A = fr + \frac{g}{r} - \frac{4\pi}{3}\delta_{20} r^2 - \sum_1^{\infty} 4\pi\delta_{2m}[\{Z_1(k_m r) - f_m\} I_1(k_m r) - \{X_1(k_m r) - g_m\} K_1(k_m r) \cos k_m z. \quad (39)$$

The solutions suitable for the seven regions are as follows:—

Region I :

Since $r = 0$ in this region, we have

$$A^{I} = ar + \sum_1^{\infty}[\cos k_m z \{a_m I_1(k_m r)\}], \quad (40)$$

$$B_r^{I} = \sum_1^{\infty}[k_m \sin k_m z \{a_m I_1(k_m r)\}], \quad (41)$$

$$B_z^{I} = 2a + \sum_1^{\infty}[k_m \cos k_m z \{a_m I_0(k_m r)\}]. \quad (42)$$

Region II:

$$A^{II} = cr + \frac{d}{r} + \sum_1^{\infty}[\cos k_m z \{c_m I_1(k_m r) - d_m K_1(k_m r)\}], \quad (43)$$

$$B_r^{II} = \sum_1^{\infty}[k_m \sin k_m z \{c_m I_1(k_m r) + d_m K_1(k_m r)\}], \quad (44)$$

$$B_z^{II} = 2c + \sum_1^{\infty}[k_m \cos k_m z \{c_m I_0(k_m r) - d_m K_0(k_m r)\}]. \quad (45)$$

Region III:

$$A^{III}=fr+\frac{g}{r}\frac{-4\pi}{3}\delta_{20}r^2-\sum_1^\infty 4\pi\delta_{2m}\cos k_mz$$
$$\times[\{Z_1(k_mr)-f_m\}I_1(k_mr)-\{X_1(k_mr)-g_m\}K_1(k_mr)], \quad (46)$$

$$B_r^{III}=-\sum_1^\infty 4\pi\delta_{2m}k_m\sin k_mz[\{Z_1(k_mr)-f_m\}I_1(k_mr)$$
$$-\{X_1(k_mr)-g_m\}K_1(k_mr)], \quad (47)$$

$$B_z^{III}=2f-4\pi\delta_{20}r-\sum_1^\infty 4\pi\delta_{2m}k_m\cos k_mz$$
$$\times[\{Z_1(k_mr)-f_m\}I_0(k_mr)+\{X_1(k_mr)-g_m\}K_0(k_mr)]. \quad (48)$$

Region IV:

$$A^{IV}=hr+\frac{j}{r}+\sum_1^\infty\cos k_mz\{h_mI_1(k_mr)+j_mK_1(kr_m)\}, \quad (49)$$

$$B_r^{IV}=\sum_1^\infty k_m\sin k_mz\{h_mI_1(k_mr)+j_mK_1(k_mr)\}, \quad (50)$$

$$B_z^{IV}=2h+\sum_1^\infty k_m\cos k_mz\{h_mI_0(k_mr)-j_mK_0(k_mr)\}. \quad (51)$$

Region V:

$$A^V=pr+\frac{q}{r}+\frac{4\pi}{3}\delta_{10}r^2+\sum_1^\infty 4\pi\delta_{1m}\cos k_mz$$
$$\times[Z_1(k_mr)-p_m]I_1(k_mr)-\{X_1(k_mr)-q_m\}K_1(k_mr)], \quad (52)$$

$$B_r^V=\sum_1^\infty 4\pi\delta_{1m}k_m\sin k_mz[\{Z_1(k_mr)-p_m\}I_1(k_mr)$$
$$-\{X_1(k_mr)-q_m\}K_1(k_mr)]. \quad (53)$$

$$B_z^V=2p+4\pi\delta_{10}r+\sum_1^\infty 4\pi\delta_{1m}k_m\cos k_mz$$
$$\times[\{Z_1(k_mr)-p_m\}I_0(k_mr)+\{X_1(k_mr)-q_m\}K_0(k_mr)]. \quad (54)$$

Region VI:

$$A^{VI}=sr+\frac{t}{r}+\sum_1^\infty\cos k_mz\{s_mI_1(k_mr)+t_mK_1(k_mr)\}, \quad (55)$$

$$B_r^{VI}=\sum_1^\infty k_m\sin k_mz\{s_mI_1(k_mr)+t_mK_1(k_mr)\}. \quad (56)$$

$$B_r^{VI}=2s+\sum_1^\infty k_m\cos k_mz\{s_mI_0(k_mr)-t_mK_0(k_mr)\}. \quad (57)$$

Region VII:

Since the outside yokes are assumed to extend to infinity, and since B_r and B_z must be finite, we have

$$A^{VII}=\frac{v}{r}+\sum_1^\infty \cos k_m z\{v_m K_1(k_m r)\}, \quad . \quad . \quad (58)$$

$$B_r^{VII}=\sum_1^\infty k_m \sin k_m z\{v_m K_1(k_m r)\}, \quad . \quad . \quad . \quad (59)$$

$$B_z^{VII}=-\sum_1^\infty k_m \cos k_m z\{v_m K_0(k_m r)\}. \quad . \quad . \quad (60)$$

On using the boundary conditions, eqs. (7) and (8), we get the necessary equations which enable us to determine the constants a_m, b_m, etc. On solving these equations we get

$$a_m=c_m+d_m\frac{K_1(k_m r_1)}{I_1(k_m r_1)}, \quad . \quad . \quad . \quad . \quad . \quad . \quad . \quad . \quad . \quad . \quad (61)$$

$$c_m=-4\pi\delta_{2m}\{Z_1(k_m r_2)-f_m\}, \quad . \quad . \quad . \quad . \quad . \quad . \quad . \quad . \quad . \quad (62)$$

$$d_m=4\pi\delta_{2m}\{X_1(k_m r_2)-g_m\}, \quad . \quad . \quad . \quad . \quad . \quad . \quad . \quad . \quad . \quad (63)$$

$$f_m=\frac{h_m}{4\pi\delta_{2m}}+Z_1(k_m r_3), \quad . \quad . \quad . \quad . \quad . \quad . \quad . \quad . \quad . \quad (64)$$

$$g_m=\frac{-j_m}{4\pi\delta_{2m}}+X_1(k_m r_3). \quad . \quad . \quad . \quad . \quad . \quad . \quad . \quad . \quad . \quad (65)$$

$$h_m=4\pi\delta_{1m}\{Z_1(k_m r_4)-p_m\}, \quad . \quad . \quad . \quad . \quad . \quad . \quad . \quad . \quad . \quad (66)$$

$$j_m=-4\pi\delta_{1m}\{X_1(k_m r_4)-q_m\}, \quad . \quad . \quad . \quad . \quad . \quad . \quad . \quad . \quad . \quad (67)$$

$$p_m=\frac{-s_m}{4\pi\delta_{1m}}+Z_1(k_m r_5), \quad . \quad . \quad . \quad . \quad . \quad . \quad . \quad . \quad . \quad (68)$$

$$q_m=\frac{t_m}{4\pi\delta_{1m}}+X_1(k_m r_5), \quad . \quad . \quad . \quad . \quad . \quad . \quad . \quad . \quad . \quad (69)$$

$$s_m=k_m r_6\left\{K_1(k_m r_6)K_0(k_m r_6)-\frac{K_1(k_m r_6)K_0(k_m r_6)}{\mu}\right\}v_m=S_m v_m, \quad (70)$$

$$t_m=k_m r_6\left\{K_1(k_m r_6)I_0(k_m r_6)+\frac{K_0(k_m r_6)I_1(k_m r_6)}{\mu}\right\}v_m=T_m v_m, \quad (71)$$

$$v_m = \left.\begin{array}{l} \mathrm{H}_m\mathrm{I}_1(k_m r_1)\mathrm{I}_0(k_m r_1)\left\{\dfrac{1}{\mu}-1\right\} \\ \qquad -\mathrm{M}_m\{\mathrm{K}_1(k_m r_1)\mathrm{I}_0(k_m r_1)+\mathrm{K}_0(k_m r_1)\mathrm{I}_1(k_m r_1)\} \\ \hline \mathrm{S}_m\mathrm{I}_1(k_m r_1)\mathrm{I}_0(k_m r_1)\left\{\dfrac{1}{\mu}-1\right\} \\ \qquad +\mathrm{T}_m\left\{\dfrac{\mathrm{K}_1(k_m r_1)\mathrm{I}_0(k_m r_1)}{\mu}+\mathrm{K}_0(k_m r_1)\mathrm{I}_1(k_m r_1)\right\} \end{array}\right\}, \quad (72)$$

$$v_m = \frac{\mathrm{H}_m\mathrm{I}_0(k_m r_1)+\mathrm{M}_m\mathrm{K}_0(k_m r_1)}{\mathrm{S}_m\mathrm{I}_0(k_m r_1)-\mathrm{T}_m\mathrm{K}_0(k_m r_1)}, \quad . \quad . \quad . \quad . \quad . \quad . \quad . \quad (73)$$

when μ is large.

$$\mathrm{H}_m = 4\pi\delta_{2m}\left[\{\mathrm{Z}_1(k_m r_2)-\mathrm{Z}_1(k_m r_3)\} - \frac{\delta_{1m}}{\delta_{2m}}\{\mathrm{Z}_1(k_m r_4)-\mathrm{Z}_1(k_m r_5)\}\right], \quad (74)$$

$$\mathrm{M}_m = 4\pi\delta_{2m}\left[\{\mathrm{X}_1(k_m r_2)-\mathrm{X}_1(k_m r_3)\} - \frac{\delta_{1m}}{\delta_{2m}}\{\mathrm{X}_1(k_m r_4)-\mathrm{X}_1(k_m r_5)\}\right]. \quad (75)$$

$$\left.\begin{array}{l} s=0, \\ p=-2\pi\delta_{10}r_5, \\ h=-2\pi\delta_{10}(r_5-r_4), \\ f=2\pi\delta_{20}r_3-2\pi\delta_{10}(r_5-r_4), \\ c=2\pi\delta_{20}(r_3-r_2)-2\pi\delta_{10}(r_5-r_4)=0, \\ a=0. \end{array}\right\} \quad . \quad . \quad (76)$$

A, B_r, and B_z can now be calculated in terms of the known proportions of the windings and core.

The curves $r\mathrm{A}=\psi=$constant will give the flux-lines, and we will then be able to determine the positions and the types of transformations to be used in reducing the eddy-current losses in large stranded conductors.

Since

$$\tfrac{1}{2}\mathrm{L}\mathrm{I}^2 = \iiint_{\mathrm{vol}} \frac{\mathrm{H}\,.\,\mathrm{B}}{8\pi}\,dv. \quad . \quad . \quad . \quad . \quad . \quad (77)$$

and

$$\mathrm{H}\,.\,\mathrm{B} = \mathrm{H}_r\mathrm{B}_r+\mathrm{H}_z\mathrm{B}_z = \frac{\mathrm{B}_r^2}{\mu}+\frac{\mathrm{B}_z^2}{\mu}, \quad . \quad . \quad (78)$$

we have

$$L=\frac{1}{\mu 4\pi I^2}\int_0^{\infty}\int_0^{z_3}\int_0^{2\pi}(B_r^2+B_z^2)\,r\,dr\,dz\,d\phi, \quad . \quad (79)$$

and since B_r and B_z are independent of ϕ, we have for all regions

$$L=\frac{1}{2\mu I^2}\int_0^{\infty}\int_0^{z_3}(B_r^2+B_z^2)\,r\,dr\,dz. \quad . \quad . \quad . \quad (80)$$

We also have

$$\int_0^{z_3}\cos k_m z\,dz=0, \quad . \quad . \quad . \quad . \quad (81)$$

$$\int_0^{z_3}\sin k_m z\sin k_n z\,dz=0=\int_0^{z_3}\cos k_m z\cos k_n z\,dz\;;\; m\neq n,$$

$$. \quad . \quad . \quad (82)$$

$$\int_0^{z_3}\sin^2 k_m z\,dz=\frac{z_3}{2}=\int_0^{z_3}\cos^2 k_m z\,dz, \quad . \quad (83)$$

and on using these results the following values for the inductance of the various regions were obtained:

$$L_I=\frac{z_3}{4\mu I^2}\int_0^{r_1}\sum_1^{\infty}k_m^2a_m^2\{I_1^2(k_mr)+I_0^2(k_mr)\}r\,dr. \quad . \quad (84)$$

When μ is large L_I is small when compared with L_{II}, L_{III}, etc., and can be neglected.

$$\begin{aligned}L_{II}=\frac{z_3}{4I^2}\int_{r_1}^{r_2}\sum_1^{\infty}k_m^2[&c_m^2\{I_1^2(k_mr)+I_0^2(k_mr)\}\\&+2c_md_m\{I_1(k_mr)K_1(k_mr)-I_0(k_mr)K_0(k_mr)\}\\&+d_m^2\{K_1^2(k_mr)+K_0^2(k_mr)\}]r\,dr. \quad . \quad . \quad . \quad (85)\end{aligned}$$

$$\begin{aligned}L_{III}=\frac{z_3}{4I^2}[&4f^2(r_3^2-r_2^2)+8\pi\delta_{20}^2(r_3^4-r_2^4)-\frac{32\pi}{3}f\delta_{20}\\&\times(r_3^3-r_2^3)+\int_{r_2}^{r_3}\sum_1^{\infty}16\pi^2\delta_{2m}^2k_m^2\big|\{Z_1(k_mr)-f_m\}^2\\&\times\{I_1^2(k_mr)+I_0^2(k_mr)\}+\{X_1(k_mr)-g_m\}^2\{K_1^2(k_mr)+K_0^2(k_mr)\}\\&-2\{Z_1(k_mr)-f_m\}\{X_1(k_mr)-g_m\}\{K_1(k_mr)I_1(k_mr)\\&-K_0(k_mr)I_0(k_mr)\}\big|r\,dr. \quad . \quad . \quad . \quad . \quad . \quad . \quad . \quad . \quad (86)\end{aligned}$$

$$\begin{aligned}L_{IV}=\frac{z_3}{4I^2}[&4h^2(r_4^2-r_3^2)+\int_{r_3}^{r_4}\sum_1^{\infty}k_m^2\big|h_m^2\{I_1^2(k_mr)\\&+I_0^2(k_mr)\}+2h_mj_m\{I_1(k_mr)K_1(k_mr)-I_0(k_mr)K_0(k_mr)\}\\&+j_m^2\{K_1^2(k_mr)+K_0^2(k_mr)\}\big|r\,dr]. \quad . \quad . \quad . \quad . \quad . \quad . \quad (87)\end{aligned}$$

$$L_V = \frac{z_3}{4I^2} 4p^2(r_5^2 - r_4^2) + 8\pi^2\delta_{10}^2(r_5^4 - r_4^4)$$

$$- \frac{32\pi}{3} p\delta_{10}(r_5^3 - r_4^3) + \int_{r_5}^{r_6} \sum_1^\infty 16\pi^2\delta_{1m}^2 k_m^2$$

$$\times \big| \{Z_1(k_m r) - p_m\}^2 \{I_1^2(k_m r) + I_0^2(k_m r)\} + \{X_1(k_m r) - q_m\}^2$$

$$\times \{K_1^2(k_m r) + K_0^2(k_m r)\} - 2\{Z_1(k_m r) - p_m\}\{X_1(k_m r) - q_m\}$$

$$\times \{I_1(k_m r)K_1(k_m r) - I_0(k_m r)K_0(k_m r)\} \big| r\, dr. \quad . \quad . \quad (88)$$

$$L_{VI} = \frac{z_3}{4I^2} \int_{r_5}^{r_6} \sum_1^\infty [s_m^2 \{I_1^2(k_m r) + I_0^2(k_m r)\}$$

$$+ 2s_m t_m \{I_1(k_m r)K_1(k_m r) - I_0(k_m r)K_0(k_m r)\}$$

$$+ t_m^2 \{K_1^2(k_m r) + K_0^2(k_m r)\}] r\, dr. \quad . \quad . \quad . \quad . \quad . \quad . \quad (89)$$

$$L_{VII} = \frac{z_3}{4I^2\mu} \int_{r_6}^{\infty} \sum_1^\infty k_m^2 v_m^2 \{K_1^2(k_m r) + K_0^2(k_m r)\} r\, dr. \quad . \quad . \quad (90)$$

When μ is large L_{VII} is small compared with L_{II}, L_{III}, etc., and can be neglected.

A typical example was worked out in order to determine the usefulness of the formulæ. The data are as follows :—

$r_1 = 3{\cdot}75$ cm.	$z_1 = 8$ cm.
$r_2 = 4{\cdot}00$,,	$z_2 = 8$,,
$r_3 = 4{\cdot}50$,,	$z_3 = 10$,,
$r_4 = 5{\cdot}50$,,	$N_1 = 400$ turns.
$r_5 = 6{\cdot}0$,,	$N_2 = 400$,,
$r_6 = 6{\cdot}35$,,	$I_1 = 1$ abampere.
$k_m = m\pi/10$	$I_2 = 1$,,

$a = c = s = 0.$

$p = -12\pi\delta_{10}.$

$h = -\pi\delta_{10}.$

$f = 9\pi\delta_{20} - \pi\delta_{10}.$

From the definitions of Z_1 and X_1 we get

$$Z_1(k_m r) = -\frac{rK_0(k_m r)}{k_m} - \frac{1}{k_m^2} \int_x^\infty K_0(x)\, dx, \quad . \quad (91)$$

$$X_1(k_m r) = \frac{rI_0(k_m r)}{k_m} - \frac{1}{k_m^2} \int_0^x I_0(x)\, dx, \quad . \quad . \quad . \quad (92)$$

where $$x = k_m r, \quad . \quad . \quad . \quad . \quad . \quad . \quad . \quad (93)$$

and Z_1 and X_1 were calculated using the tables given by V. Bursian and V. Fock *.

All the integrals were obtained by Simpson's Rule, using three ordinates. The final results are as follows :—

Fig. 1*a*.

$$L \text{ (total)} = 9{\cdot}3 \times 10^6 \text{ abhenries.} \quad . \quad . \quad . \quad (94)$$

Fig. 1*b*.

$$g_1 = 2 \text{ cm.}$$

$$L \text{ (total)} = 11{\cdot}1 \times 10^6 \text{ abhenries.} \quad . \quad . \quad (95)$$

Fig. 1*d*.

$$g_3 = 2 \text{ cm.}$$

$$L \text{ (total)} = 16{\cdot}6 \times 10^6 \text{ abhenries.} \quad . \quad . \quad (96)$$

XVIII. *Measurements on Photocathodes in Contact.* *By* P. Görlich, *Laboratory of Zeiss Ikon A.G., Dresden* †.

INVESTIGATIONS on photocathodes in contact suggest that the release of electrons by light does not take place only on the surface layer but that also deeper layers can make an essential contribution to the emission. This hypothesis led me to set up transparent Cs–Bi and Cs–Sb cathodes ‡ which, surprisingly, gave greater photocurrents in the short wave-length part of the visible region than hydrated K-cells. The condition for the high quantum efficiency is the small conductivity of the metal which is combined with the Cs. Applications of these cells have been discussed elsewhere §.

In the first experiments we did not vary the alkali metal, but used only Cs, because earlier experiments showed that the greatest sensitivity in the red was to be expected with this metal. The other metals are investigated here. The results obtained are unexpected.

As is well known, the alkali metals show a selective photoelectric effect. The selective or long wave-length maximum is denoted by λ_{max} in the following table :—

* 'Travaux de l'Institut Physico-Mathématique,' Stekloff, ii. pt. 1 (1931).

† Communicated by Prof. N. F. Mott, M.A., F.R.S.

‡ P. Görlich, *Zeits. f. Phys.* ci. p. 335 (1936).

§ P. Görlich and H. Sauer, *Zeits. f. Inst.-K.* lvi. p. 423 (1936); P. Görlich and W. Lang, *Zeits. f. Inst.-K.* lvii. p. 249 (1937).

TABLE I.

λ_{max} for massive alkali Cathodes and for Ag–M_2O–M Cathodes. (M=alkali metal.)

Cathode.	Cs.		Rb.		K.		Na.		Li.	
	λ_{max}.	Observer.	λ_{max}.	Observer.	λ_{max}.	Observer.	λ_{max}.	Observer.	λ_{max}.	Observer.
Massive ...	510	Braun.	480	Pohl and Pringsheim.	435	Pohl and Pringsheim.	340	Pohl and Pringsheim.	280	Pohl and Pringsheim.
	540	Kluge.	....		....		360	Compton and Richardson.	....	
Ag–M_2O–M.	730–850	Kluge.	620–680	Kluge.	460–520	Kluge.	....		....	
	750–850	Görlich.	....		....		....		....	

The position of λ_{max} corresponds to the position of the alkali metal in the periodic table, going to shorter wave-lengths from Cs onwards. The same type of variation remains when we use cathodes of the type $Ag—M_2O—M$, where M, as before, denotes the alkali metal. Further, one can say that current from the cathodes decreases as one goes from Cs to Rb, and so on.

We found that the transparent alloy cathodes do not show this regularity. The preparation of the cells can be carried out as already described, thin Sb or Bi layers being deposited on the alkali metal. The cells described

TABLE II.

λ_{max} for the transparent unsensitized Sb–M and Bi–M Cathodes.

Cathode.	Cs.	Rb.	K.	Na.	Li.
Sb–M	430	420	400	425	420
	460	450	..	400	430
	440	455	..	..	..
	440	460	..	..	..
Bi–M	430	440	400	420	445
		440	420	400	450

here are not sensitized with oxygen. We show the values of λ_{max} in Table II.

The selective maxima, therefore, lie between 400 and 460 mμ, independent of which alkali metal is used. A change in the maxima from Li to Cs does not occur; the λ_{max} values for Li are already at longer wave-lengths than those for Cs. A slight distortion of the selective maxima does not appear to have been caused through impurities of the materials used, since only pure materials were employed. The distortion appears to be dependent rather upon the thickness of the layer.

With the Rb–Sb and Cs–Sb layers the influence of the angle of incidence was investigated at angles of 20, 30,

and 60°. With the electric vector parallel and perpendicular to the plane of incidence a sharp maximum was found as with unpolarized light, only stronger in the first case.

As one goes from Cs to Rb, K and Na, the current becomes smaller ; with Li it is of the same order as for Rb. The influence of oxygen will be dealt with elsewhere.

I have to thank Mr. A. H. Wilson for showing me that an explanation of these results may be given in terms of wave mechanics ; this will be given elsewhere.

XIX. *Operational Systems.*

By N. W. McLachlan, *D.Sc.**

1. *Introduction.*

CONVERSATIONS from time to time with engineers and others associated with the application of mathematics to industrial and research problems, reveal that there is a feeling of uncertainty regarding solutions found by operational processes. This view is the direct outcome of ambiguities inherent in the Heaviside procedure. One engineer went as far as to say that he trusted operators only when the result could be checked by another method ! If so, why use operators at all ?

There are now several systems other than that of Heaviside, and since the symbol p is common to all, an operational process valid on one system may unwittingly be used on another system to which it is inapplicable. The purpose of this paper is to enumerate the principal systems and to show in some cases how errors may be avoided.

2. *Classification.*

Omitting the Heaviside system, which in part depends implicitly upon some of the other systems given below, we have the following, t being real throughout :—

A. Operators obtained from the Laplace integral, giving

$$\phi(p)=p\int_0^\infty e^{-pt}f(t)\,dt, \quad . \quad . \quad . \quad . \quad . \quad (1)$$

* Communicated by the Author.

the range of t being 0 to ∞. In some cases the origin may be moved to the point $t=a$ (real and finite), and (1) becomes

$$\phi(p)_a = p\int_0^\infty e^{-pt}f(t-a)\,dt = e^{-pa}p\int_0^\infty e^{-p\tau}f(\tau)\,d\tau,$$

$$= e^{-pa}\phi(p). \quad . \quad . \quad . \quad . \quad . \quad . \quad . \quad . \quad . \quad . \quad (2)$$

If desired, a finite interval $t=0$ to h may be used, implying that the function exists or is to be considered only when $0<t<h$. Here again the origin may be moved as at (2), the interval under consideration then being $a<t<h$. An example of the use of the former interval is given in § (6) formula (13).

B. Operators obtained from the integral

$$\phi(p) = p\int_{-\infty}^{\infty} e^{-pt}f(t)\,dt, \quad . \quad . \quad . \quad . \quad (3)$$

the range of t being $-\infty$ to ∞. In certain cases the limits may be finite, so that $f(t)$ is considered in the range $-h<t<h$ as illustrated in § 8 formula (34).

C. Operators obtained by inverting the integral equation

$$f(t) = \frac{1}{2\pi i}\int_{c-i\infty}^{c+i\infty} e^{zt}\phi(z)\frac{dz}{z}, \quad . \quad . \quad . \quad . \quad (4)$$

the range of t being 0 to ∞, and the O.F. $\phi(p)$. If $|\phi(z)/z| \to 0$ uniformly, with respect to phase z, as $|z| \to \infty$ in the angle range $-\frac{1}{2}\pi \leqslant$ phase $z \leqslant \frac{1}{2}\pi$, then (4) is zero when $t<0$*. The expansion of the O.F. does not have terms of the type p^ν, $R(\nu) \geqslant 1$, since the corresponding contour integrals are divergent.

D. Operators obtained by inverting the integral equation

$$f(t) = \frac{1}{2\pi i}\int_{-\infty}^{(0+)} e^{zt}\phi(z)\frac{dz}{z}. \quad . \quad . \quad . \quad . \quad (5)$$

If $\phi(z)$ has one branch point—with or without poles—the range of t is usually from 0 to ∞. When there are poles only or poles and two branch points †, the contour may usually be replaced by a circle about the origin, and then the range of t is $-\infty$ to ∞. In many cases the contour $c\pm i\infty$ is equivalent to $-\infty\,(0+)-\infty$, for $t>0$, so that

* It is possible to introduce another system in which this restriction is removed, as at (15) § 2 F.

† Reference is made here to singularities in the finite part of the z-plane.

operators on systems C and D are then identical [provided terms of the type p^n, n a positive integer $\geqslant 1$, are omitted from the latter (see (11)–(13))]. This equivalence happens when the integrals along the infinite arcs in the second and third quadrants of the z plane are zero. Sin $t \doteqdot p/(p^2+1)$ is a simple case, both contours mentioned above being equivalent to a circle about 0 enclosing the poles at $z=\pm i$. $J_0(t)=p/(p^2+1)^{\frac{1}{2}}$ is another instance, there being branch points at $z=\pm i$.

E. Operators which comply with a particular case of the Mellin inversion theorem, which is a combination of A and C. In reality there are two theorems which can be stated for our purpose as follows :

If

$$\phi(p)=p\int_0^\infty e^{-pt}f(t)\,dt, \quad . \quad . \quad . \quad . \quad . \quad (6)$$

then will

$$f(t)=\frac{1}{2\pi i}\int_{c-i\infty}^{c+i\infty} e^{zt}\phi(z)\frac{dz}{z}, \quad . \quad . \quad . \quad . \quad (7)$$

and *vice-versa*, provided :

(*a*) All the singularities of $\phi(z)$ lie to the left of $c\pm i\infty$, $c>0$;

(*b*) $\int_{c-i\infty}^{c+i\infty}\left|\frac{\phi(z)}{z}\right|dz=\int_{-\infty}^{\infty}\left|\frac{\phi(c+iy)}{c+iy}\right|dy$ converges * ;

(*c*) $R(p)>0$, t real and >0 ;

(*d*) Integral (6) is absolutely convergent ;

(*e*) $|\phi(p)/p|\to 0$ uniformly, with respect to phase p, as $|p|\to\infty$, in the angle range $-\frac{1}{2}\pi\leqslant$ phase $p\leqslant\frac{1}{2}\pi$, in other words $\int\frac{\phi(z)dz}{z(z-p)}=0$, C being an infinite semicircle on the right-hand side of $c\pm i\infty$. Integral (7) is then zero when $t<0$.

(*f*) Integral (7) represents a piecewise † continuous function of t, $t>0$.

* When z^ν, $0<R(\nu)<1$, is the highest power of z in the expansion of $\phi(z)$, this condition may be waived, *e. g.*,

$$\frac{1}{2\pi i}\int_{c-i\infty}^{c+i\infty} e^{zt}z^{\nu-x}dz=1/t^\nu\Gamma(1-\nu).$$

† Continuous between its discontinuities, finite in number in a finite interval, and at which points the function is finite. See, for instance, fig. 1 *a*, Phil. Mag. xxiv. p. 1057 (1937).

If the origin is moved to the point $t=a$, (6) and (7) become, respectively,

$$\phi(p)_a = p\int_a^\infty e^{-pt}f(t-a)\,dt = pe^{-pa}\int_0^\infty e^{-p\tau}f(\tau)\,d\tau. \quad . \quad (8)$$

$$= e^{-pa}\phi(p)\,; \quad . \quad . \quad . \quad . \quad . \quad . \quad . \quad . \quad . \quad . \quad (9)$$

$$f(t-a) = \frac{1}{2\pi i}\int_{c-i\infty}^{c+i\infty} e^{z(t-a)}\phi(z)\frac{dz}{z} \quad . \quad . \quad . \quad . \quad . \quad . \quad . \quad (10)$$

The range of t is from a to ∞, integral (10) being zero when $t<a$.

In many cases the O.F. of $f(t)$ is common to systems A, C, D, E, *e. g.*,

$$e^{-at} \doteq p/(p+a), \quad . \quad . \quad . \quad . \quad . \quad . \quad (11)$$

$t>0$. For system D, however,

$$\frac{1}{2\pi i}\int_{-\infty}^{(0+)} e^{zt}z^{n-1}\,dz = 0, \quad . \quad . \quad . \quad . \quad (12)$$

n being a positive integer $\geqslant 1$. Hence on this system, p^n is to be interpreted as zero, so that any number of terms of this type can be added * to the O.F., as, for example,

$$e^{-at} \doteq \sum_{n=0}^{\infty} a_n p^n + \frac{p}{(p+a)}. \quad . \quad . \quad . \quad . \quad . \quad (13)$$

This is explained by the fact that (5) considered as an integral equation for $\phi(z)$ has not a unique solution.

F. Operators which comply with the Mellin inversion theorem in which the lower limit of (6) is $-\infty$. In more general form this theorem is written :

If $$\phi(p) = \int_{-\infty}^{\infty} e^{-pt}f(t)\,dt, \quad . \quad . \quad . \quad . \quad . \quad (14)$$

then will

$$f(t) = \frac{1}{2\pi i}\int_{c-i\infty}^{c+i\infty} e^{zt}\phi(z)\,dz, \quad . \quad . \quad . \quad (15)$$

and *vice-versa*, provided :

(*a*) $\phi(z)$ is analytic in the strip $\alpha<x<\beta$, x being the real part of z ;

(*b*) $\int_{x-i\infty}^{x+i\infty} |\phi(z)|\,dz = \int_{-\infty}^{\infty} |\phi(x+iy|\,dy$ converges ;

* It is not usual to do so.

(*c*) $\phi(z) \to 0$ uniformly as $|y| \to \infty$ in the strip $(\alpha+\epsilon) \leqslant x \leqslant (\beta-\epsilon)$, $\epsilon > 0$ and arbitrary;

(*d*) integral (14) is absolutely convergent,

(*e*) $f(t)$ represents a piecewise continuous function of t (real, the range being $-\infty$ to $+\infty$).

Formulæ (14), (15) are obtained by substituting $x = e^{-t}$ in (1.5.1), (1.5.2), § 1·5, Titchmarsh, 'Theory of Fourier Integrals' (1937). In (*a*) the strip is not restricted to positive values of x, so c may be negative according to the values of z at which the singularities of $\phi(z)$ occur.

3. *Terminology.*

The terms "operator" and "operational form" used herein are inaccurate in a literal sense. In each of the five systems above, p is not an operator but an inversion or operational parameter. Whilst it would be preferable to use the terms "parameter" and "parametric" form in place of the foregoing, the terminology "operator" is of such long standing (about half a century) and widespread use, that an alteration now would probably lead to confusion.

4. *Interpretation of Operational Solution of a Problem.*

We assume that the system to which the operational solution $\phi(p)$ belongs is known. The problem is to find $f(t)$.

(*a*) For system A, (1) is solved as an integral equation for $f(t)$. This is facilitated by a list of O.F.'s of known functions. The solution can often be expressed in such a form that the interpretation is obtained in terms of functions from the list. If the O.F. complies with the restrictions in §2 E, $f(t)$ is found by evaluating a contour integral of the type at (7). The contour $c \pm i\infty$ or its equivalent may be used.

(*b*) For system B, see (*a*) above, excepting the last sentence but one. If the O.F. complies with the restrictions in §2 F, $f(t)$ is found by evaluating a contour integral of the type at (7) or (15), according as p is used outside (14) or not.

(*c*) For systems C, D, the contour integrals are evaluated. A list of O.F.'s can be used as in (*a*) above.

(*d*) For system E, see (*a*).

(*e*) For system F, see (*b*).

5. *Forms having Terms of the Type p^ν.*

When $R(\nu)>1$, but ν is otherwise unrestricted, the forms belong to D. In obtaining asymptotic formulæ Heaviside unwittingly used this system to interpret expansions in ascending powers of p. If ν is integral $\geqslant 1$, the forms may belong to A, B, or D. In the latter case p^n is interpreted as zero, an interpretation also used by Heaviside. Since

$$\frac{1}{2\pi i}\int_{c-i\infty}^{c+i\infty} e^{zt}z^{\nu-1}\,dz. \quad . \quad . \quad . \quad . \quad (16)$$

is divergent unless $R(\nu)<1$, forms of the type p^ν, $R(\nu)\geqslant 1$, are not associated with systems C and/or E.

When such forms occur in an expansion, $\phi(p)$ may belong to C and/or B, e. g., $e^{-p^{1/2}} \doteqdot 1-\mathrm{erf}\,(1/2t^{1/2})$. Terms of the type p^n are not to be interpreted individually in the expansion.

6. *The O.F. "p" referred to System A.*

Consider a disturbance whose wave form is an isolated Morse dot of height f_0, width h, and constant area $A=f_0h$, i. e., $f(t)=f_0$, $0<t<h$ and $\int_0^h f(t)dt=A$. Then the O.F.* is

$$\phi(p)=f_0p\int_0^h e^{-pt}\,dt=f_0(1-e^{-ph}), \quad . \quad . \quad . \quad (17)$$

$$=f_0\left(ph-\frac{p^2h^2}{2!}+\frac{p^3h^3}{3!}-\ldots\right), \quad . \quad (18)$$

$$=A\left(p-\frac{p^2h}{2!}+\ldots\right). \quad . \quad . \quad . \quad . \quad (19)$$

If $|p|$ is finite and $h\to 0$, $\phi(p)\to Ap$, so

$$f(t)\doteqdot Ap. \quad . \quad . \quad . \quad . \quad . \quad . \quad (20)$$

Let this "impulse" be applied to a pile of mass m driven

* The O.F. from h to ∞ is obviously zero, so in effect we obtain the O.F. for the range $t=0$ to ∞.

into the ground, the resistance to motion being r per unit velocity. The differential equation is

$$m\frac{dv}{dt}+rv=f(t), \quad . \quad . \quad . \quad . \quad . \quad . \quad (21)$$

and in operational form using system A,

$$(mp+r)v=\mathrm{A}p, \quad . \quad . \quad . \quad . \quad . \quad . \quad (22)$$

or the velocity

$$v=(\mathrm{A}/m)p/(p+r/m). \quad . \quad . \quad . \quad . \quad (23)$$

Since the O.F.'s in (22) are for system A, it appears that (23) should be interpreted thereon. But (23) conforms with the restrictions in E, so either A or E may be used for interpretational purposes, giving

$$v=\frac{\mathrm{A}}{m}e^{-rt/m} \quad . \quad . \quad . \quad . \quad . \quad . \quad (24)$$

Operators on system A having positive integral powers of p when expanded, will be found in papers by Dhar *, Lowry †, van der Pol ‡, and Varma §.

7. *O.F. of e^{-t^2} referred to System A.*

Expanding we have

$$e^{-t^2}=1-t^2+\frac{t^4}{2!}-\frac{t^6}{3!}+\cdots \quad . \quad . \quad . \quad (25)$$

Expressing each term operationally by aid of (1), we get

$$\phi(p)=1-\frac{2!}{1!\,p^2}+\frac{4!}{2!\,p^4}-\frac{6!}{3!\,p^6}+\ldots, \quad . \quad (26)$$

which is divergent, being, in fact, the asymptotic expansion of

$$p\int_{p/2}^{\infty}e^{\frac{p^2}{4}-x^2}dx. \quad . \quad . \quad . \quad . \quad . \quad (27)$$

This apparent anomaly can be explained in the following way :—

Let $$f(t)=\sum_{n=0}^{\infty}a_nt^n, \quad . \quad . \quad . \quad . \quad . \quad (28)$$

* Phil. Mag. xxi. p. 1082 (1936).
† Phil. Mag. xiii. p. 1033 (1932).
‡ Phil. Mag. viii. p. 861 (1929); and with K. F. Niessen, Phil. Mag. xiii. p. 537 (1932).
§ Bull. Calcutta Math. Soc. xxviii. p. 209 (1936); Proc. Camb. Phil. Soc. xxiii. p. 210 (1937); Proc. Lond. Math. Soc. xii. p. 26 (1937); Phil. Mag. xxiii. p. 926 (1937).

the series being absolutely convergent ; then if the O.F. is

$$\phi(p) = \sum_{n=0}^{\infty} \frac{a_n n!}{p^n}, \quad . \quad . \quad . \quad . \quad . \quad (29)$$

this series must also be absolutely convergent for p finite $R(p)>0$.

But (26) is divergent, so it does not represent the O.F. of e^{-t^2}.

Writing $x=(t+p/2)$ in (27), we get

$$p\int_0^{\infty} e^{-pt-t^2}\,dt = pe^{p^2/4}\int_0^{\infty} e^{-(t+p/2)^2}\,dt, \quad . \quad . \quad (30)$$

$$= \frac{\sqrt{\pi}}{2} pe^{p^2/4}(1-erf\, p/2), \quad . \quad . \quad (31)$$

which is the O.F. of e^{-t^2} referred to system A. This O.F. complies with neither C nor E. When expanded, (31) yields an infinite series in positive integral powers of p. It is not to be interpreted on system A term by term. If this were done, we should get an infinite series of impulse functions akin to that in §6. Interpretation on system D would yield zero.

8. *Operators on System B.*

The O.F. of e^{-t^2} is

$$\phi(p) = p\int_{-\infty}^{\infty} e^{-pt-t^2}\,dt = pe^{p^2/4}\int_{-\infty}^{\infty} e^{-(t+p/2)^2}\,dt, \quad . \quad (32)$$

$$= \sqrt{\pi}\, pe^{p^2/4}, \quad . \quad . \quad . \quad . \quad . \quad . \quad . \quad . \quad . \quad . \quad (33)$$

which should be compared with the O.F. (31) referred to system A. Formula (33) complies with the restrictions in §2 F, so

$$\frac{e^{-t^2}}{\sqrt{\pi}} = \frac{1}{2\pi i}\int_{c-i\infty}^{c+i\infty} e^{zt+z^2/4}\,dz, \quad . \quad . \quad . \quad . \quad (34)$$

so (33) is also the O.F. of e^{-t^2} on system C where t varies from $-\infty$ to $+\infty$ (see footnote to C).

As a second example, we take

$$\frac{p}{2}\int_{-\infty}^{\infty} e^{-pt-b\sqrt{t^2+a^2}}\,\frac{dt}{\sqrt{t^2+a^2}} = \frac{p}{2}\int_{-\infty}^{\infty} e^{-a(p\sinh\theta+b\cosh\theta)}\,d\theta,$$

$$. \quad . \quad . \quad (35)$$

which gives

$$\frac{e^{-b\sqrt{t^2+a^2}}}{2\sqrt{t^2+a^2}} \doteqdot p\mathrm{K}_0(a\sqrt{b^2-p^2}). \quad . \quad . \quad . \quad (36)$$

If both sides of (36) are differentiated with respect to b, we get

$$\frac{e^{-b\sqrt{t^2+a^2}}}{2ab} \doteqdot p\frac{\mathrm{K}_1(a\sqrt{b^2-p^2})}{\sqrt{b^2-p^2}}. \quad . \quad . \quad . \quad (37)$$

Operational forms of type B cannot generally be used in solving differential equations. Such forms are usually confined to functions of the above type which are symmetrical about some finite value of t. The lower limit $-\infty$ is useful in statistics.

As an example where the limits of the integral are $\pm h$ (finite), we may cite

$$p\int_{-h}^{h} e^{-pt}(h^2-t^2)^{n-1/2}\,dt = h^{2n}p\int_{-1}^{+1} e^{-hp\tau}(1-\tau^2)^{n-1/2}\,d\tau, \quad (38)$$

$$= (2h)^n\sqrt{\pi}\,\Gamma(n+\tfrac{1}{2})p^{1-n}\mathrm{I}_n(hp), \quad . \quad . \quad . \quad (39)$$

n being a positive integer. The r.h.s. of (39) is the O.F. of $f(t)=(h^2-t^2)^{n-\frac{1}{2}}$ over the range $-h<t<h$, i. e., where the function is real. It is, therefore, virtually the O.F. from $t=-\infty$ to ∞, since the O.F. in the ranges $t<-h$, $t>h$ does not exist.

A second example is

$$\frac{\cos(b\sqrt{a^2-t^2})}{\sqrt{a^2-t^2}} \doteqdot \pi p\mathrm{J}_0(a\sqrt{b^2-p^2}), \quad . \quad . \quad (40)$$

$-a<t<a$.

9. *O.F. of t^{-n} using System D.*

For all values of ν,

$$\frac{1}{2\pi i}\int_{-\infty}^{(0+)} e^{zt}\frac{dz}{z^{\nu+1}} = \frac{t^\nu}{\Gamma(1+\nu)}, \quad . \quad . \quad . \quad (41)$$

Differentiating both sides of (41) with respect to ν, we get

$$-\frac{1}{2\pi i}\int_{-\infty}^{(0+)} e^{zt}\log z\frac{dz}{z^{\nu+1}} = \frac{t^\nu}{\Gamma(1+\nu)}\left[\log t - \frac{\Gamma'(1+\nu)}{\Gamma(1+\nu)}\right]. \quad (42)$$

If $\nu=0$, (42) gives

$$-\frac{1}{2\pi i}\int_{-\infty}^{(0+)} e^{zt}\log z\,\frac{dz}{z}=\log t+\gamma, \quad . \quad . \quad (43)$$

where γ is Euler's constant. Differentiating (43), with respect to t, n times yields

$$\frac{1}{2\pi i}\int_{-\infty}^{(0+)} e^{zt}z^{n-1}\log z\,dz=(-1)^n\Gamma(n)t^{-n}, \quad . \quad (44)$$

n an integer >0, $t>0$. Thus we have

$$t^{-n}\doteqdot(-1)^n\frac{p^n\log p}{\Gamma(n)}, \quad . \quad . \quad . \quad . \quad (45)$$

and

$$(t+a)^{-n}\doteqdot(-1)^n\frac{e^{ap}p^n\log p}{\Gamma(n)} \quad . \quad . \quad . \quad . \quad (46)$$

These operators do not exist on other systems, *e. g.*, integral (44) diverges if the contour is $c\pm i\infty$.

10. *O.F. of $J_\nu(t)$ when* $\mathrm{R}(\nu)\leqslant -1$.

If $\mathrm{R}(\nu)>-1$, the O.F. of $\mathrm{J}_\nu(t)$ referred to systems A, C, E, is

$$\frac{p}{\sqrt{p^2+1}}\,\frac{1}{(p+\sqrt{p^2+1})^\nu} \quad . \quad . \quad . \quad . \quad (47)$$

When $\mathrm{R}(\nu)\leqslant -1$, the O.F. does not exist on these systems, but it exists on D for all ν. This applies to other Bessel functions, as shown in former papers by McLachlan and Meyers *.

11. *Conclusion.*

So far as general rules pertaining to operators are concerned, for instance those given by van der Pol and Niessen † relating to system A, these should be established independently for each system, although a number of rules are common to several systems. For instance, using system A

$$\int_0^t f(t)\,dt\doteqdot\int_0^\infty e^{-pt}f(t)\,dt. \quad . \quad . \quad . \quad . \quad (48)$$

* Phil. Mag. xxiii. p. 762 (1937); xxiii. p. 918 (1937).
† Phil. Mag. *loc. cit.*

Whilst this relationship is valid for other systems, it would be unwise to take it for granted, although this is often done ! On the whole, in using operational methods, it is preferable to adhere to one system for any particular problem. In certain cases, *e. g.*, §6 above, it is feasible to switch from one system to another, but before doing so the validity of procedure should be established. For general purposes in technical applications the Mellin inversion theorem (system E) seems to be very satisfactory. Approximations when t is small, and asymptotic formulæ when t is large are obtainable readily in many cases. This feature is of value when the solution for *any* t is particularly protracted and laborious.

XX. *On the Blocking Layer Photoelectric Effect of Cæsium Oxide. By* Horst Teichmann, *Physik. Institut. d. Techn. Hochschule, Dresden* *.

IN a previous paper † I have expressed the opinion that the intermediate layers of the composite cathodes of photocells act as semi-conductors. I believed it possible to explain in this way the position in the spectrum of the wave-length of the light for which the external photoelectric effect gave its maximum yield. My hypothesis was supported by observations on a thin potassium layer deposited on a selenium cell. The external photoelectric effect of such a cathode shows a selective maximum of the electron yield for the same wave-length of the incident light as that at which the selenium blocking layer photo-effect reaches its maximum value. It seems to me that the boundary layer between the potassium and the selenium acts as a " Sperrschicht " and that this blocking layer photo-effect causes an electron current in the direction of the potassium. These electrons can easily be freed by the external photoelectric effect.

It is clear that this description is a rough one, but I think that my assumption is useful as a working rule. It leads to the conclusion that, for instance, cæsium oxide layers, well known in the ordinary photo-cells, must show

* Communicated by Prof. N. F. Mott, M.A., F.R.S.
† H. Teichmann, *Ann. d. Phys.* (5) xiii. p. 649 (1932).

semi-conductive properties too. It must be possible to find a blocking layer photo-effect and a rectifying effect.

Indeed, P. Görlich * described some observations which can be explained by a blocking layer photo-effect of cæsium oxide with the boundary layer on the front wall. But his experiments have the disadvantage that the contact (caused by a movable positive electrode) is not clean enough to decide if the current measured is caused by an external photoelectric effect on the uncovered parts of the cathode.

Therefore, I have constructed a cell, shown in fig. 1, in which the surface is sufficiently clean. A glass disk

Fig. 1.

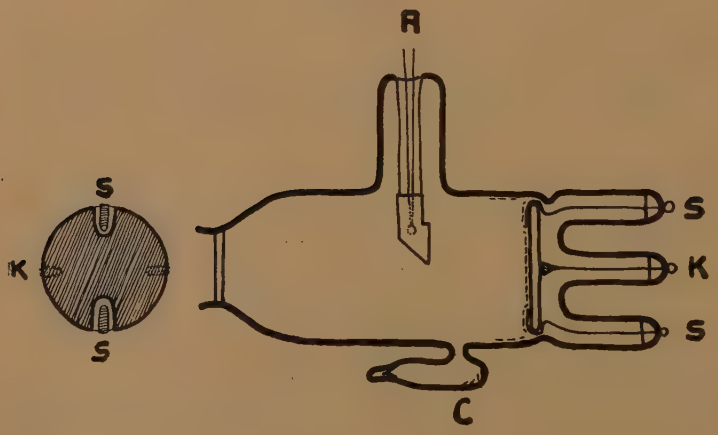

with two platinum electrodes on the front and two on the back is silvered by the solution method. On the front the silver layer is scratched away around the contacts (S). This disk is the cathode of our cell. The process used for the construction of the composite layer is the usual one for cæsium cells. After the last baking of the cell we get the usual external photoelectric effect between K and A. Now a thin silver layer ($\sim$50 μ thick) is deposited on the front of the composite electrode by evaporation of silver from a tungsten filament. The platinum electrodes S give the contact to this layer. The schemes of the

* P. Görlich, *Naturwiss.* xxii. p. 11 (1934).

arrangements for the measurement of the different photo-effects of this cathode are given in fig. 2. The arrangement I. permits the measurement of the external and the blocking layer photo-effect temporarily. In the case II. we measure the external effect, in case III. this of the blocking layer only. The measurement of the e.m.f.'s by a compensation method (not drawn in the figure) shows that we are measuring the sum of the two effects in the case I. Furthermore, we see that the current of the blocking layer photo-effect has such a direction that the electrons migrate in the direction of the incident light. The boundary layer is situated on the back wall. The

Fig. 2.

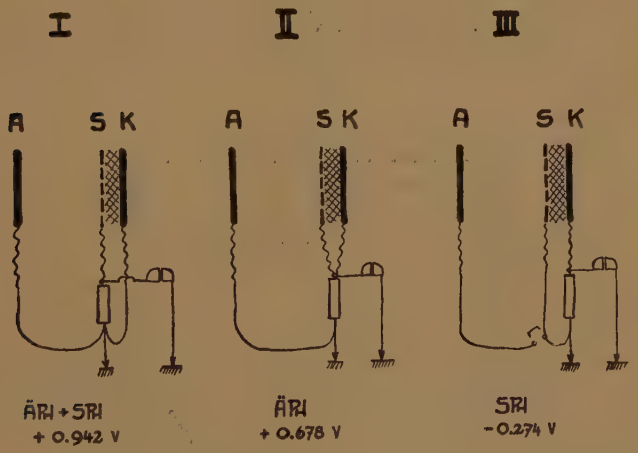

experiments show that the resistance of the intermediate layer of Cs_2O (including the high contact-resistance of the thin silver layer connecting the contact S, fig. 1, with the surface of the cathode) is about 10^9 ohm. Therefore it seems probable that a charging of the anode may have an influence on the magnitude of the e.m.f. of the blocking layer photo-effect. (The silver layer S acts as a grid in an ionization gauge.) The results of such an investigation are plotted in fig. 3.

Actually a great number of electrons which are available for the blocking layer effect leave the cathode as " external" photo-electrons, and cause in such manner a decrease of the e.m.f. of the blocking layer effect, if the electrode A has

Fig. 3.

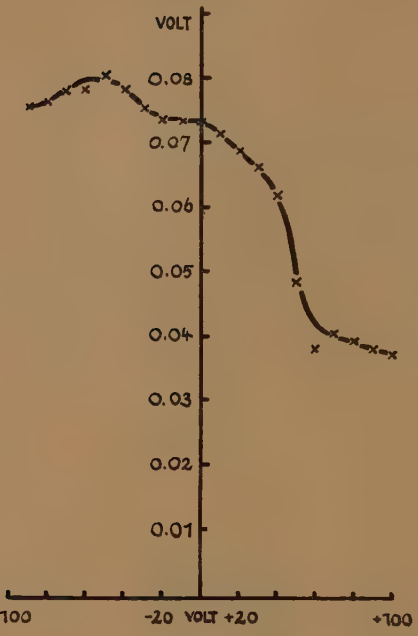
VOLT
0.08
0.07
0.06
0.05
0.04
0.03
0.02
0.01
-100
-20 VOLT +20
+100

Fig. 4.

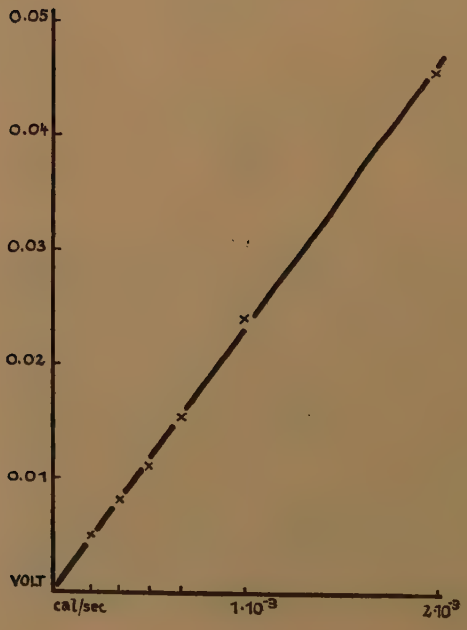
0.05
0.04
0.03
0.02
0.01
VOLT
cal/sec
1·10⁻³
2·10⁻³

positive potentials. Negative potentials cause a small change only.

The dependence of the blocking layer photo-effect described on the intensity of light (fig. 4) shows a strong linear character for light intensities in the order of 10^{-3} cal./sec. (100 watt lamp).

Further experiments will be made on the spectral distribution of both photo-effects and on the rectifying effect that has not yet been observed because of the small current density (high resistance of the cathode) available. We shall also attempt to get a boundary layer on the front wall in connexion with my previous assumptions cited above.

I have to thank the staff of the "Helmholtz-Gesellschaft," who have enabled me to carry out these experiments, and Prof. Tomaschell for valuable advice.

XXI. *The Radiation Integrals* $\int_x^\infty \frac{dx}{x^\alpha(e^x-1)}$.

By John R. Airey, *D.Sc., Sc.D.**

INTEGRALS of the type $\int_0^x \frac{x^n\,dx}{e^x-1}$ occur in a number of physical and astronomical problems, *e. g.*, when $n=1$, the X-ray analysis of crystal structure; when $n=2$, the radiative equilibrium of a planetary nebula and the temperatures of stars and novæ; and when $n=3$, temperature of the nuclei of planetary nebulæ and the exchange of energy between monatomic gases and solid surfaces.

The ascending series [1] for $\phi(x)=\frac{1}{x}\int_0^x \frac{x\,dx}{e^x-1}$, suitable for small values of x, is easily derived from the series involving the Bernoullian numbers, viz.,

$$\phi(x)=1-\frac{x}{4}+\frac{x^2}{36}-\frac{x^4}{3600}+\frac{x^6}{211680}-\frac{x^8}{10886400}+\ldots,$$

* Communicated by the Author.

and for large values of x,

$$\phi(x)=\frac{\pi^2}{6x}-e^{-x}\left(1+\frac{1}{x}\right)-e^{-2x}\left(\frac{1}{2}+\frac{1}{4x}\right)-e^{-3x}\left(\frac{1}{3}+\frac{1}{9x}\right)-\cdots$$

From these formulæ a table of $\phi(x)$ has been constructed [2]. Zanstra has given detailed methods of evaluating the integral $\int_x^\infty \frac{x^2\,dx}{e^x-1}$, which, having been already tabulated, greatly simplifies the computations. The integrals

$$\int_x^\infty \frac{dx}{x^\alpha(e^x-1)}, \quad 0\leqslant\alpha=2,$$

are derived as follows. By Planck's law, from a black body at temperature T, the radiation in the interval ν and $\nu+d\nu$ is $\frac{8\pi h\nu^3}{c^3}\cdot\frac{d\nu}{e^{h\nu/RT}-1}$, or proportional to $\frac{x^3\,dx}{e^x-1}$. Now suppose that the coefficient of absorption is proportional to ν^m. If m is assumed to be equal to -3 the amount of radiation absorbed per gram per sec. is proportional to $\int_x^\infty \frac{dx}{e^x-1}$, and, in general, if the absorption coefficient varies as ν^m, the integral becomes

$$\int_x^\infty \frac{x^{3+m}.dx}{e^x-1}.$$

There is some room for doubt about the value of m; Kramer's formula gives $m=-3$, which, according to Eddington, is a well-known experimental law in the X-ray region; no direct experiments have apparently been made in the optical region, but indirect experiments seem to support a law where the value of m lies between -3 and -5. On this assumption tables of the integral were constructed for

$$m=-3,\ -4,\ -5\ ;\ -3\tfrac{1}{4},\ -3\tfrac{1}{2},\ -3\tfrac{3}{4}.$$

(*a*) When $m=-3$, $\alpha=0$, and the integral is simply $-\log_e(1-e^{-x})$.

(*b*) When $m=-4$, $\alpha=1$; the exponential integral, negative argument is needed, since

$$\int_x^\infty \frac{dx}{x(e^x-1)}=-\sum_{n=1}^{\infty} Ei(-nx),$$

which is very convenient for $x=1{\cdot}0$ to $10{\cdot}0$. The table [3] of $Ei(-x)$ was extended from $x=15{\cdot}0$ to $20{\cdot}0$ by $0{\cdot}1$ intervals, the "Converging Factor" method [4] being used for this purpose; the integral could then be computed to twelve or more places of decimals. To complete the table for the interval $0{\cdot}1$ to $1{\cdot}0$ the first differences were found from

$$\int_{x_0}^{x_1} \frac{dx}{x(e^x-1)}$$

$$=\left|-\frac{1}{x}-\frac{1}{2}\log_e x+\frac{B_1}{2!}x-\frac{B_2}{4!}\cdot\frac{x^3}{3}+\frac{B^3}{6!}\cdot\frac{x^5}{5}-\ldots\right|_{x_0}^{x_1}.$$

For example, the first difference of this radiation integral for argument $1{\cdot}0$ to $0{\cdot}9$

$$=-0{\cdot}91712\ 31317+0{\cdot}98376\ 45035$$
$$=\ \ 0{\cdot}06664\ 13718.$$

The value of the integral,

$$\left.\begin{aligned} &x=1{\cdot}0 \text{ is } 0{\cdot}28679\ 24309, \\ \text{and}\quad &x=0{\cdot}9 \text{ is } 0{\cdot}35343\ 38027, \end{aligned}\right\}$$

and so on [5].

(*c*) When $m=-5$, $\alpha=2$; in this case, too, the exponential integral is required, since

$$\int_x^\infty \frac{dx}{x^2(e^x-1)}=\frac{1}{x(e^x-1)}+\sum_{n=1}^{\infty} n\,Ei(-nx).$$

This formula was used only for integer values of x from 1 to 10; for intermediate values of the argument first differences were derived from the differential coefficient

$$f'=\frac{1}{x^2(e^x-1)}$$

and

$$\Delta_{\frac{1}{2}}=\omega\left[1-\frac{1}{12}\mu\delta^2+\frac{11}{720}\mu\delta^4-\ldots\right]f'.$$

(*d*) When $m=-3\frac{1}{2}$, $\alpha=\frac{1}{2}$; if S_n is written for the series

$$1-\frac{1-r}{2nx}+\frac{(1-r)(2-r)}{(2nx)^2}-\frac{(1-r)(2-r)(3-r)}{(2nx)^3}+\ldots$$

and $1-\nu=\alpha=1/2$, then

$$\int_x^\infty \frac{dx}{x^{\frac{1}{2}}(e^x-1)} = x^{-\frac{1}{2}}e^{-x}S_1+(4x)^{-\frac{1}{2}}e^{-2x}.S_2+(9x)^{-\frac{1}{2}}e^{-3x}.S_3+\ldots$$

By the "Converging Factor" method S_1 can be calculated to about eight places of decimals, the C. F. being 0·4983847 when $x=4$. One or two decimal places only are obtained when the first five terms in the series are computed, *i.e.*, including the term $\frac{1.3.5.7}{8^4}$, which is equal to 0·0256 3476.

Finally

$$\begin{aligned} 4^{-\frac{1}{2}}e^{-4}S_1 &= 0{\cdot}0082\ 9107 \\ 16^{-\frac{1}{2}}e^{-8}S_2 &= 0{\cdot}\quad\ 7935 \\ 36^{-\frac{1}{2}}e^{-12}S_3 &= 0{\cdot}\quad\ \ 98: \\ 64^{-\frac{1}{2}}e^{-16}S_4 &= 0{\cdot}\quad\ \ \ 1: \\ \hline & 0{\cdot}0083\ 7142 \end{aligned}$$

The value of the integral when $x=4$ is 0·0083 7142
when $x=8$ is 0·0001 1323:

The colon (:) represents approximately half a unit in the last place of decimals.

For the range $x=1{\cdot}5$ to 10·0 by 0·1 intervals the first differences were obtained, as before, from the differential coefficients and their differences, and for the range 0·1 to 1·5 from the Bernoullian series.

$$\int_{x_0}^{x_1} \frac{dx}{x^{\frac{1}{2}}(e^x-1)}$$

$$= \left| -2x^{-\frac{1}{2}}\left(1+\frac{x}{2}-\frac{B_1}{2!}\frac{x^2}{3}+\frac{B_2}{4!}\cdot\frac{x^4}{7}-\frac{B_3}{6!}\cdot\frac{x^6}{11}+\ldots\right)\right|_{x_0}^{x_1}.$$

Since

$$\int_x^\infty \frac{dx}{x^{\frac{1}{2}}(e^x-1)} = \int_x^\infty x^{-\frac{1}{2}} \sum_{n=1}^{\infty} e^{-nx}dx = \sum_{n=1}^{\infty}\frac{1}{n^{\frac{1}{2}}}\int_x^\infty t^{-\frac{1}{2}}e^{-t}dt$$

use can be made of the tables of the Error Function [6].

$$\int_x^\infty t^{-\frac{1}{2}}e^{-t}dt = \sqrt{\pi}[1-H(\sqrt{x})] \text{ in Burgess's notation.}$$

$$\int_x^\infty \frac{dx}{x^\alpha(e^x-1)}.$$

x.	$\alpha=0$.	$\alpha=1$.	$\alpha=2$.
0·0	∞	∞	∞
·1	2·352168 :	8·210044	45·392542
·2	1·707771 :	3·548287 :	10·334801
·3	1·350225 :	2·076028 :	4·189935 :
0·4	1·109633	1·378220	2·152121 :
0·5	0·932752	0·981486 :	1·258588 :
·6	·795649	·731022 :	0·799026 :
·7	·686341	·561727 :	·536837
·8	·596618	·441666	·375939 :
0·9	0·521830 :	0·353434	0·271719
1·0	0·458675	0·286792 :	0·201339 :
·1	·404772	·235354 :	·152217
·2	·358382 :	·194947 :	·116998 :
·3	·318185	·162742	·91182 :
1·4	0·283155	0·136760 :	0·071903 :
1·5	0·252482 :	0·115583	0·057275 :
·6	·225517	· 98168	· 46024 :
·7	·201729	· 83737 :	· 37268
·8	·180681 :	· 71700	· 30382
1·9	0·162011 :	0·061600 :	0·024917
2·0	0·145413 :	0·053082 :	0·020544 :
·1	·130628 :	· 45865 :	· 17021
·2	·117436 :	· 39726	· 14163
·3	·105648	· 34483 :	· 11831 :
2·4	0·095100	0·029992 :	0·009919
2·5	0·085650 :	0·026133 :	0·008343
·6	· 77176 :	· 22809	· 7038 :
·7	· 69570 :	· 19937	· 5954
·8	· 62737 :	· 17451 :	· 5050
2·9	0·056595	0·015295 :	0·004293
3·0	0·051069	0·013421 :	0·003657 :
·1	· 46095 :	· 11790	· 3122 :
·2	· 41616	· 10367 :	· 2670 :
·3	· 37580 :	· 9125 :	· 2288
3·4	0·033943	0·008039	0·001963 :
3·5	0·030570	0·007088	0·001688
·6	· 27704	· 6254 :	· 1453
·7	· 25034 :	· 5523	· 1252 :
·8	· 22624 :	· 4880	· 1081
3·9	0·020449 :	0·004315	0·000934
4·0	0·018485 :	0·003817 :	0·000808
·1	· 16711 :	· 3379 :	· 700
·2	· 15109	· 2993	· 607
·3	· 13661 :	· 2652 :	· 526 :
4·4	0·012353 :	0·002351 :	0·000457 :

x.	$\alpha=0$.	$\alpha=1$.	$\alpha=2$.
4·5	0·011171	0·002086	0·000398
·6	· 10120 :	· 1851	· 346
·7	· 9137	· 1643 :	· 301 :
·8	· 8264	· 1459 :	· 263
4·9	0·007474 :	0·001296 :	0·000229
5·0	0·006761	0·001152 :	0·000200
·1	· 6115 :	· 1024 :	· 175
·2	· 5531 :	· 911 :	· 153
·3	· 5004	· 811	· 133 :
5·4	0·004527	0·000721 :	0·000117
5·5	0·004095	0·000642 :	0·000102 :
·6	· 3705	· 572	· 89 :
·7	· 3351 :	· 509 :	· 78 :
·8	· 3032	· 454	· 69
5·9	0·002743 :	0·000404 :	0·000060 :
6·0	0·002482	0·000360 :	0·000053
·1	· 2245 :	· 321 :	· 46 :
·2	· 2031 :	· 286 :	· 41
·3	· 1838	· 255 :	· 36
6·4	0·001663	0·000228	0·000031 :
6·5	0·001504 :	0·000203 :	0·000028
·6	· 1361 :	· 181 :	· 24 :
·7	· 1232	· 162	· 21 :
·8	· 1114 :	· 145	· 19
6·9	0·001008 :	0·000129 :	0·000017
7·0	0·000912 :	0·000115 :	0·000015
·1	· 825 :	· 103	· 13
·2	· 746 :	· 92	· 11 :
·3	· 676	· 82 :	· 10
7·4	0·000611 :	0·000073 :	0·000009
7·5	0·000553 :	0·000066	0·000008
·6	· 500 :	· 59	· 7
·7	· 453	· 52 :	· 6
·8	· 393 :	· 47	· 5 :
7·9	0·000371	0·000042	0·000005
8·0	0·000335 :	0·000037 :	0·000004 :
·1	· 303 :	· 33 :	· 4
·2	· 274 :	· 30	· 3 :
·3	· 248 :	· 27	· 3
8·4	0·000225	0·000024	0·000002 :
8·5	0·000203 :	0·000021 :	0·000002 :
·6	· 184	· 19 :	· 2
·7	· 166 :	· 17 :	· 2
·8	· 153	· 15 :	· 1 :
8·9	0·000136 :	0·000014	0·000001 :

x.	$\alpha=0$.	$\alpha=1$.	$\alpha=2$.
9·0	0·000123 :	0·000012 :	0·000001 :
·1	· 112	· 11	· 1
·2	· 101	· 10	· 1
·3	· 91 :	· 9	· 1
9·4	0·000083	0·000008	0·000001
9·5	0·000074 :	0·000007	0·000000 :
·6	· 67 :	· 6 :	· 0 :
·8	· 55 :	· 5	· 0 :
9·9	0·000050	0·000004 :	0·000000 :
10·0	0·000045 :	0·000004	0·000000 :

$$\int_x^\infty \frac{dx}{x^\alpha(e^x-1)}.$$

x.	$\alpha=\frac{1}{4}$.	$\alpha=\frac{1}{2}$.	$\alpha=\frac{3}{4}$.
0·0	∞	∞	∞
·1	3·013814 :	4·050615 :	5·670188
·2	1·960919	2·325971	2·838205
·3	1·452245 :	1·601072 :	1·805999
0·4	1·136006 :	1·192283 :	1·271628
0·5	0·922092 :	0·927516	0·947568
·6	·762933	·742420 :	·732273 :
·7	·640829 :	·606282 :	·580468 :
·8	·544342	·502512	·468854 :
0·9	0·466411 :	0·421294 :	0·384205 :
1·0	0·402404	0·356424 :	0·318457 :
·1	·349131 :	·303773	·266417 :
·2	·304318 :	·260481 :	·224594
·3	·266290	·224504	·190555 :
1·4	0·233783	0·194337	0·162559 :
1·5	0·205824 :	0·168851 :	0·139328
·6	·181652	·147182	·119902
·7	·160658 :	·128655	·103551 :
·8	·142356	·112738 :	· 89710
1·9	0·126344 :	0·099007 :	0·077933 :
2·0	0·112296 :	0·087117	0·067870
·1	· 99938 :	· 76788	· 59236
·2	· 89042 :	· 67788 :	· 51802 :
·3	· 79416	· 59927 :	· 45383
2·4	0·070895 :	0·053044 :	0·039823 :
2·5	0·063342	0·047006	0·034996 :
·6	· 56635 :	· 41698 :	· 30795 :
·7	· 50673 :	· 37025	· 27132
·8	· 45367	· 32904	· 23931 :
2·9	0·040638 :	0·029264 :	0·021130 :

x.	$\alpha-\frac{1}{4}$.	$\alpha-\frac{1}{2}$.	$\alpha-\frac{3}{4}$.
3·0	0·036422	0·026046 :	0·018675
·1	· 32658	· 23198 :	· 16519
·2	· 29295 :	· 20674	· 14624
·3	· 26289 :	· 18435	· 12956 :
3·4	0·023600 :	0·016447 :	0·011487
3·5	0·021193 :	0·014681	0·010191
·6	· 19038	· 13110 :	· 9047
·7	· 17106 :	· 11713	· 8035 :
·8	· 15375	· 10468 :	· 7141
3·9	0·013822	0·009360	0·006349 :
4·0	0·012428 :	0·008371 :	0·005648 :
·1	· 11178	· 7490	· 5027
·2	· 10055	· 6703	· 4476
·3	· 9047	· 6001	· 3986 :
4·4	0·008141	0·005373 :	0·003552 :
4·5	0·007327	0·004813	0·003166 :
·6	· 6595 :	· 4312	· 2823 :
·7	· 5937 :	· 3864	· 2518 :
·8	· 5346 :	· 3463 :	· 2247
4·9	0·004813 :	0·003105	0·002005 :
5·0	0·004336	0·002784 :	0·001790 :
·1	· 3905 :	· 2497	· 1598 :
·2	· 3518	· 2240	· 1428
·3	· 3169 :	· 2009 :	· 1276
5·4	0·002855 :	0·001803	0·001140
5·5	0·002573	0·001618 :	0·001019
·6	· 2318 :	· 1452 :	· 911
·7	· 2089 :	· 1304	· 814 :
·8	· 1883	· 1170 :	· 728 :
5·9	0·001697 :	0·001051 :	0·000652
6·0	0·001530	0·000944	0·000583
·1	· 1379	· 848	· 522
·2	· 1243	· 761 :	· 467
·3	· 1121	· 684 :	· 418
6·4	0·001011	0·000615	0·000374 :
6·5	0·000911 :	0·000552 :	0·000335:
·6	· 822	· 496 :	· 300
·7	· 741	· 446	· 269
·8	· 668 :	· 401	· 241
6·9	0·000602 :	0·000360 :	0·000216
7·0	0·000543 :	0·000324	0·000193
·1	· 490 :	· 291 :	· 173 :
·2	· 442 :	· 262	· 155 :
·3	· 399	· 235 :	· 139 :
7·4	0·000360	0·000212	0·000125

x.	$\alpha=\frac{1}{4}$.	$\alpha=\frac{1}{2}$.	$\alpha=\frac{3}{4}$.
7·5	0·000324 :	0·000190 :	0·000112
·6	· 293	· 171 :	· 100 :
·7	· 264	· 154	· 90
·8	· 238 :	· 138 :	· 81
7·9	0·000215	0·000125	0·000072 :
8·0	0·000194	0·000112	0·000065
·1	· 175	· 101	· 58 :
·2	· 158	· 91	· 52 :
·3	· 142 :	· 82	· 47
8·4	0·000128 :	0·000073 :	0·000042
8·5	0·000116	0·000066	0·000038
·6	· 105	· 59 :	· 34
·7	· 94 :	· 53 :	· 30 :
·8	· 85 :	· 48 :	· 27 :
8·9	0·000077	0·000043 :	0·000024 :
9·0	0·000069 :	0·000039	0·000022
·1	· 62 :	· 35	· 20
·2	· 56 :	· 31 :	· 18
·3	· 51	· 28 :	· 16
9·4	0·000046	0·000025 :	0·000014 :
9·5	0·000041 :	0·000023	0·000013
·6	· 37 :	· 21	· 11 :
·7	· 34	· 18 :	· 10 :
·8	· 30 :	· 17	· 9 :
9·9	0·000027 :	0·000015	0·000008 :
10·0	0·000025	0·000013 :	0·000007 :

By this means twelve or more decimal place tables can be obtained.

(*e*) $m=3\frac{1}{4}$, $3\frac{3}{4}$; since

$$\int_x^\infty \frac{dx}{x^{\frac{1}{2}}(e^x-1)} = \sum_{n=1}^{\infty}\int_x^\infty x^{-\frac{1}{2}}e^{-nx}dx = \sum_{n=1}^{\infty} n^{-\frac{1}{2}}\int_{nx}^\infty t^{-\frac{1}{2}}e^{-t}dt,$$

the construction of these tables required the values of the incomplete Γ function $\int_x^\infty t^{-p}e^{-t}dt$, when $p=\frac{1}{4}$ and $\frac{3}{4}$; in this case also the "Converging Factor" method gave several more decimal places than would have been obtained by stopping at the least term of the asymptotic series.

References.

(1) P. Debye, *Annalen d. Phys.* xliii. (1913–14).
(2) ' Reviews of Modern Physics ' (5), p. 175.
(3) J. R. Airey, Math. Tables Comm. Brit. Assoc. Report (1927).
(4) J. R. Airey, Phil. Mag. xxiv. p. 521 (1937).
(5) A. Pannekoek, Monthly Notices R. A. S. xcvi. pp. 789–792 (1936).
(6) J. Burgess, Trans. Roy. Soc. Edin. xxxix. pp. 257–321 (1898).

August 8th, 1937.

XXII. *The Potential Problem of a Sphere lying between Infinite Conducting Planes.* *By* C. Hurst, *Jesus College, Oxford* *.

Introduction.

THE electrical field produced by a distribution of charge on a conducting sphere lying between two parallel earthed planes has been investigated by Rigby [1] for the case in which the sphere is situated midway between the planes. In this paper the problem is considered more generally when the sphere is asymmetrically placed.

The method adopted is the usual one of combining a series of harmonic functions, each of which vanishes over the two planes, in such a way as to give the required value of the potential at the surface of the sphere. A suitable fundamental solution of Laplace's equation of this type is approached by way of the Green's function for the space between the planes rather than by the method of images used by Rigby. Additional harmonic functions are obtained from the fundamental one by successive differentiation. Arbitrary superposition of these functions, after their rearrangement in a form suitable to a spherical boundary, leads to an infinite system of linear equations. The successive approximation method used by Knight [2] in some analogous problems has been employed to solve numerically the system of equations obtained in the special case when the sphere is raised to unit potential and is off-centre by one-fifth the semi-distance between the planes.

* Communicated by the Author.

Potential Functions vanishing on the Planes.

Let us take rectangular Cartesian axes such that the equations of the two conducting planes are $z=\pm c$ and the centre of the sphere (of radius a) is the point $(0, 0, d)$ $(d+a<c)$. Consider throughout only the region lying between the planes. It is known [3] that

$$V_0=\int_0^\infty \left\{ e^{-\lambda|z-z'|} + \frac{e^{-2\lambda c}\cosh\lambda(z-z')-\cosh\lambda(z+z')}{\sinh 2\lambda c} \right\} J_0(\lambda\rho)\,d\lambda,$$

where $$\rho^2=x^2+y^2,$$

is a solution of Laplace's equation which satisfies the boundary conditions $V_0=0$ for $z=\pm c$, and is such that V_0-1/r (where r is the distance between (x, y, z) and (x', y', z')) is regular in the neighbourhood of the point P $(0, 0, z')$.

If the origin of coordinates is now transferred to the centre of the sphere it is seen that

$$V_0(z')=\frac{1}{r} + \int_0^\infty \left\{ \frac{e^{-2\lambda c}\cosh\lambda(z-z')-\cosh\lambda(z+z'+2d)}{\sinh 2\lambda c} \right\} J_0(\lambda\rho)\,d\lambda$$

satisfies Laplace's equation, vanishes identically on the planes $z=c-d$ and $z=-c-d$ for all values of z'; and is such that $V_0(z')-1/r$ is regular in the neighbourhood of P. This result follows since

$$\int_0^\infty e^{-\lambda|z-z'|}J_0(\lambda\rho)\,d\lambda=\frac{1}{r}.$$

The expressions obtained by differentiating $V_0(z')$ any number of times with respect to z' will have the same properties. In particular, putting $z'=0$ after differentiation, we are led to the following set of potential functions which vanish on the two planes and are regular between them except at the centre of the sphere:

$$V_{2n}=\frac{2n!\,P_{2n}(\cos\theta)}{r^{2n+1}} + \int_0^\infty \frac{\lambda^{2n}\{e^{-2\lambda c}\cosh\lambda z-\cosh\lambda(z+2d)\}}{\sinh 2\lambda c} J_0(\lambda\rho)\,d\lambda,$$

$$V_{2n+1} = -\frac{2n+1!\ P_{2n+1}(\cos\theta)}{r^{2n+2}} - \int_0^\infty \frac{\lambda^{2n+1}\{e^{-2\lambda c}\sinh\lambda z + \sinh\lambda(z+2d)\}}{\sinh 2\lambda c} J_0(\lambda\rho)\,d\lambda.$$

r now denotes distance measured from the centre of the sphere.

The next step is to transform these expressions into a form involving spherical harmonics. To do this the relation [4]

$$e^{r\cos\theta}J_0(r\sin\theta) = \sum_{m=0}^{\infty}\frac{r^m}{m!}P_m(\cos\theta)$$

is used. In it replace $r\cos\theta$ by $\pm\lambda z$ and $r\sin\theta$ by $\pm\lambda\rho$.

Then $$e^{\lambda z}J_0(\lambda\rho) = \sum_{m=0}^{\infty}\frac{r^m\lambda^m}{m!}P_m(\cos\theta)$$

and $$e^{-\lambda z}J_0(\lambda\rho) = \sum_{m=0}^{\infty}\frac{(-1)^m r^m\lambda^m}{m!}P_m(\cos\theta).$$

Substituting in the above expressions,

$$V_{2n} = \frac{2n!\ P_{2n}(\cos\theta)}{r^{2n+1}} + \sum_{m=0}^{\infty}\frac{r^m P_m(\cos\theta)}{m!} \times \int_0^\infty \frac{\lambda^{m+2n}[(e^{-2\lambda c}-e^{2\lambda d})+(-1)^m(e^{-2\lambda c}-e^{-2\lambda d})]}{2\sinh 2\lambda c}\,d\lambda$$

and

$$V_{2n+1} = -\frac{(2n+1)!\ P_{2n+1}(\cos\theta)}{r^{2n+2}} - \sum_{m=0}\frac{r^m P_m(\cos\theta)}{m!} \times \int_0^\infty \frac{\lambda^{m+2n+1}[(e^{-2\lambda c}+e^{2\lambda d})+(-1)^{m+1}(e^{-2\lambda c}+e^{-2\lambda d})]}{2\sinh 2\lambda c}\,d\lambda.$$

These harmonic functions are finally expressed in terms of the generalized Zeta-function by means of the identity

$$\int_0^\infty \frac{\lambda^p e^{\pm 2\lambda d}}{e^{2\lambda c}-e^{-2\lambda c}}\,d\lambda = \frac{p!}{(4c)^{p+1}}\zeta\left(p+1,\ \frac{c\mp d}{2c}\right),$$

valid so long as p is a positive integer and $0 < \frac{c\mp d}{2c} \leqslant 1$.

To reduce the coefficients of the spherical harmonics to tabulated functions it is necessary at this stage, however, to proceed by means of series-expansions in

powers of $d/2c$. We have, for example, under the same conditions as above,

$$I_p = \int_0^\infty \lambda^p \frac{[(e^{-2\lambda c} - e^{2\lambda d}) + (e^{-2\lambda c} - e^{-2\lambda d})]}{e^{2\lambda c} - e^{-2\lambda c}} \, d\lambda$$

$$= \frac{p!}{(4c)^{p+1}} \left[2\zeta(p+1) - \zeta\left(p+1, \frac{c+d}{2c}\right) - \zeta\left(p+1, \frac{c-d}{2c}\right) \right]$$

$$= \frac{2(p!)}{(4c)^{p+1}} \left[\zeta(p+1) - \zeta(p+1, \tfrac{1}{2}) - \left(\frac{d}{2c}\right)^2 \frac{\zeta''(p+1, \frac{1}{2})}{2!} - \left(\frac{d}{2c}\right)^4 \frac{\zeta^4(p+1, \frac{1}{2})}{4!} - \dots \right]$$

$$\left(\text{where } \zeta^n(s, a) \equiv \frac{\partial^n}{\partial a^n} \zeta(s, a) \right)$$

$$= \frac{2(p!)}{(4c)^{p+1}} \left[(2 - 2^{p+1})\zeta(p+1) - \left(\frac{d}{2c}\right)^2 \frac{(p+1)(p+2)}{2!} \zeta(p+3, \tfrac{1}{2}) - \left(\frac{d}{2c}\right)^4 \frac{(p+1)(p+2)(p+3)(p+4)}{4!} \zeta(p+5, \tfrac{1}{2}) - \dots \right]$$

$$= - \frac{2(p!)}{(4c)^{p+1}} \left[2^{p+1}\mu_{p+1} + \left(\frac{d}{2c}\right)^2 \frac{(p+1)(p+2)}{2!} (2^{p+3} - 1)\zeta(p+3) + \left(\frac{d}{2c}\right)^4 \frac{(p+1)(p+2)(p+3)(p+4)}{4!} \times (2^{p+5} - 1)\zeta(p+5) + \dots \right],$$

where μ_p denotes $-\sum_{n=1}^{\infty} \frac{(-1)^p}{n^p}$ and $\zeta(p)$ is the Zeta function of Riemann, *i. e.*,

$$\zeta(p) = \sum_{n=1}^{\infty} \frac{1}{n^p}.$$

These have been tabulated [5].

If similar transformations and expansions are performed for the other integrals occurring it is found that the set of potential functions to be combined can be taken as

$$V_n = \frac{c^{n+1} P_n(\cos\theta)}{r^{n+1}} + (-1)^{n+1} \sum_{m=0}^{\infty} {}_n a_m \frac{r^m}{c^m} . P_m(\cos\theta)$$

$$(n = 0,\ 1,\ 2,\ \ldots),$$

where

$${}_{2n}a_{2m} = \frac{(2m+2n)!}{2m!\ 2n!} \cdot \frac{1}{2^{2m+2n}} \Bigg[\mu_{2m+2n+1} + \frac{1}{2^{2m+2n+1}} \Bigg\{ \left(\frac{d}{2c}\right)^2 \frac{(2m+2n+1)(2m+2n+2)}{2!} \times (2^{2m+2n+3} - 1)\zeta(2m+2n+3) + \left(\frac{d}{2c}\right)^4 \frac{(2m+2n+1)(2m+2n+2)(2m+2n+3)(2m+2n+4)}{4!} \times (2^{2m+2n+5} - 1)\zeta(2m+2n+5) + \ldots \Bigg\} \Bigg],$$

$${}_{2n}a_{2m+1} = {}_{2m+1}a_{2n} = \frac{(2m+2n+1)!}{(2m+1)!\ 2n!} \frac{1}{2^{4m+4n+3}} \times \Bigg[\left(\frac{d}{2c}\right) \frac{(2m+2n+2)}{1!} (2^{2m+2n+3} - 1)\zeta(2m+2n+3) + \left(\frac{d}{2c}\right)^3 \frac{(2m+2n+2)(2m+2n+3)(2m+2n+4)}{3!} \times (2^{2m+2n+5} - 1)\zeta(2m+2n+5) + \ldots \Bigg]$$

and

$${}_{2n+1}a_{2m+1} = \frac{(2m+2n+2)!}{(2m+1)!\ (2n+1)!} \cdot \frac{1}{2^{2m+2n+2}} \Bigg[\zeta(2m+2n+3) + \frac{1}{2^{2m+2n+3}} \Bigg\{ \left(\frac{d}{2c}\right)^2 \frac{(2m+2n+3)(2m+2n+4)}{2!} \times (2^{2m+2n+5} - 1)\zeta(2m+2n+5) + \left(\frac{d}{2c}\right)^4 \frac{(2m+2n+3)(2m+2n+4)(2m+2n+5)(2m+2n+6)}{4!} \times (2^{2m+2n+7} - 1)\zeta(2m+2n+7) + \ldots \Bigg\} \Bigg].$$

(The evaluation of the integral I_p when $p=0$ needs separate consideration. However, using the relation

$$\int_0^\infty \frac{dx}{1+e^x} = \mu_1,$$

it is easy to show that

$$\int_0^\infty \frac{2e^{-2\lambda c} - e^{2\lambda d} - e^{-2\lambda d}}{e^{+2\lambda c} - e^{-2\lambda c}} d\lambda$$

$$= -\frac{1}{2c}\left[2\mu_1 + \left(\frac{d}{2c}\right)^2 \zeta(3, \tfrac{1}{2}) + \left(\frac{d}{2c}\right)^4 \zeta(5, \tfrac{1}{2}) + \dots \right],$$

whence the coefficient ${}_0a_0$ is obtained by putting $n=0$, $m=0$ in the expression given above for ${}_{2n}a_{2m}$.)

As the general potential function vanishing on $z=c-d$ and $z=-c-d$ and regular except at the centre of the sphere we have now

$$V = \sum_{n=0}^{\infty} A_n V_n$$

$$= \sum_{n=0}^{\infty} A_n \left\{ \frac{P_n(\cos\theta)}{\lambda^{n+1}} - (-1)^n \sum_{m=0}^{\infty} {}_na_m \lambda^m P_m(\cos\theta) \right\},$$

where $\lambda = \frac{r}{c}$ and the A's are arbitrary constants. This may be rewritten as

$$V = \sum_{m=0}^{\infty} \left\{ \frac{A_m}{\lambda^{m+1}} - \lambda^m \sum_{n=0}^{\infty} (-1)^n {}_na_m A_n \right\} P_m(\cos\theta).$$

The Evaluation of the Constants.

If the conditions on the sphere of radius a are such that its potential is representable as

$$V = \sum_{m=0}^{\infty} C_m P_m(\cos\theta),$$

then, when $\lambda = \frac{a}{c} = \mu$ (say), we must have

$$\sum_{m=0}^{\infty} \left\{ \frac{A_m}{\lambda^{m+1}} - \lambda^m \sum_{n=0}^{\infty} (-1)^n {}_na_m A_n \right\} P_m(\cos\theta)$$

$$= \sum_{m=0}^{\infty} C_m P_m(\cos\theta).$$

Hence

$$A_m\mu^{-m-1}-\mu^m \sum_{n=0}^{\infty}(-1)^n{}_na_mA_n=C_m \quad \text{for} \quad m \geqslant 0.$$

This infinite system of linear equations has been solved numerically for the case in which $\frac{d}{2c}=0{\cdot}1$ and the potential of the sphere is unity by the method of successive approximation used in like problems by Knight. Under these circumstances

$$C_0=1 \quad \text{and} \quad C_m\,(m \geqslant 1)=0$$

Let

$$A_m=\sum_{r=0}^{\infty}A_m^{(r)} \quad (m \geqslant 0),$$

TABLE I.

m.	0.	1.	2.	3.	4.	5.	6.	7.
${}_0a_m$	$7{\cdot}3689\times10^{-1}$	$2{\cdot}2739\times10^{-1}$	$2{\cdot}9214\times10^{-1}$	$1{\cdot}2291\times10^{-1}$	$1{\cdot}0620\times10^{-1}$	$5{\cdot}4391\times10^{-2}$	$3{\cdot}9318\times10^{-2}$	$2{\cdot}2375\times10^{-2}$
${}_1a_m$	$2{\cdot}2739\times10^{-1}$	$7{\cdot}3454\times10^{-1}$	$3{\cdot}6873\times10^{-1}$	$4{\cdot}4100\times10^{-1}$	$2{\cdot}7196\times10^{-1}$	$2{\cdot}3739\times10^{-1}$	$1{\cdot}5663\times10^{-1}$	$1{\cdot}1951\times10^{-1}$

m.	8.	9.	10.	11.	12.	13.	14.	15.
${}_0a_m$	$1{\cdot}4923\times10^{-2}$	$8{\cdot}9382\times10^{-3}$	$5{\cdot}7496\times10^{-3}$	$3{\cdot}5253\times10^{-3}$	$2{\cdot}2318\times10^{-3}$	$1{\cdot}3830\times10^{-3}$	$8{\cdot}6934\times10^{-4}$	$5{\cdot}4128\times10^{-4}$
${}_1a_m$	$8{\cdot}0444\times10^{-2}$	$5{\cdot}7506\times10^{-2}$	$3{\cdot}8778\times10^{-2}$	$2{\cdot}6783\times10^{-2}$	$1{\cdot}7979\times10^{-2}$	$1{\cdot}2171\times10^{-2}$	$8{\cdot}1191\times10^{-3}$	$5{\cdot}4265\times10^{-3}$

where

$$A_0^{(0)}=\mu, \quad A_m^{(0)}=0 \quad (m \geqslant 1),$$

$$A_m^{(r)}=\mu^{2m+1}\sum_{n=0}^{\infty}(-1)^n{}_na_mA_n^{(r-1)} \quad (r \geqslant 1).$$

From physical considerations we should expect convergence so long as the sphere lies between the planes, *i. e.*, so long as $d+a<c$. Any mathematical investigation would be difficult owing to the complexity of the coefficients ${}_na_m$, and hardly worth while, since it would lead to a much more restricted range of convergence

than that physically acceptable because of the crudeness of the inequalities which would have to be used.

The values of the coefficients ${}_0a_m$ and ${}_1a_m$ for $\frac{d}{c}=0{\cdot}2$ are given to five figures in Table I. for values of m from $m=0$ to $m=15$.

TABLE II.

Values of A_n.

μ.	0·1.	0·2.	0·3.	0·4.	0·5.	0·6.	0·7.
A_0	$1{\cdot}080\times10^{-1}$	$2{\cdot}345\times10^{-1}$	$3{\cdot}849\times10^{-1}$	$5{\cdot}664\times10^{-1}$	$7{\cdot}895\times10^{-1}$	$1{\cdot}071$	$1{\cdot}443$
A_1	$2{\cdot}45\times10^{-5}$	$4{\cdot}24\times10^{-4}$	$2{\cdot}32\times10^{-3}$	$7{\cdot}91\times10^{-3}$	$2{\cdot}08\times10^{-2}$	$4{\cdot}68\times10^{-2}$	$9{\cdot}58\times10^{-2}$
A_2	$3{\cdot}15\times10^{-7}$	$2{\cdot}19\times10^{-5}$	$2{\cdot}72\times10^{-4}$	$1{\cdot}67\times10^{-3}$	$7{\cdot}10\times10^{-3}$	$2{\cdot}41\times10^{-2}$	$7{\cdot}17\times10^{-2}$
A_3	..	$3{\cdot}67\times10^{-7}$	$1{\cdot}02\times10^{-5}$	$1{\cdot}10\times10^{-4}$	$7{\cdot}13\times10^{-4}$	$3{\cdot}42\times10^{-3}$	$1{\cdot}38\times10^{-2}$
A_4	..	..	$7{\cdot}95\times10^{-7}$	$1{\cdot}55\times10^{-5}$	$1{\cdot}60\times10^{-4}$	$1{\cdot}15\times10^{-3}$	$6{\cdot}62\times10^{-3}$
A_5	..	..	..	$1{\cdot}25\times10^{-6}$	$2{\cdot}00\times10^{-5}$	$2{\cdot}06\times10^{-4}$	$1{\cdot}66\times10^{-3}$
A_6	..	..	..	..	$3{\cdot}71\times10^{-6}$	$5{\cdot}67\times10^{-5}$	$6{\cdot}56\times10^{-4}$

Relations such as ${}_{2p}a_{2q}=\frac{(2p+2q)!}{2p!\,2q!}{}_0a_{2p+2q}$ allow other coefficients for which $m+n<15$ to be calculated from ${}_0a_m$ and ${}_1a_m$ with ease.

The values of the $A^{(r)}$'s were computed by using the equations of the approximation process, and thence the A_m's by summation, when the ratio $\frac{a}{c}$ assumed in turn the values 0·1, 0·2, ... 0·7. The results obtained are shown in Table II. as far as A_6.

The Capacity of the Condenser.

The capacity C of the condenser formed by the sphere and the two planes is readily seen to be $K\frac{A_0}{\mu}a$, where K

is the specific inductive capacity of the medium between them. It is interesting to compare the values of $\frac{C}{aK}$ obtained here with those calculated by Rigby for the case of the symmetrically situated sphere. This is done in Table III.

TABLE III.

Values of $\frac{C}{aK}$.

	$\mu=\frac{a}{c}$.	0·1.	0·2.	0·3.	0·4.	0·5.	0·6.	0·7.
$\frac{C}{aK}$	when $\frac{d}{c}=0{\cdot}2$	1·080	1·173	1·283	1·416	1·579	1·786	2·062
$\frac{C}{aK}$	when $d=0$	1·074	1·161	1·263	1·384	1·532	1·719	1·968

References.

(1) Proc. Lond. Math. Soc. (2) xxxiii. p. 525 (1932).
(2) *E. g.*, Quart. J. of Math. vii. p. 124 (1936).
(3) Fox, Phil. Mag. (7) vi. p. 994 (1928).
(4) Hobson, Proc. Lond. Math. Soc. (1) xxv. p. 66 (1893).
(5) Glaisher, Proc. Lond. Math. Soc. (1) iv. p. 56 (1872); Gram, *K. danske Videns. Selsk.* (*Nat. Math.*) (8) x. p. 318 (1926).

Jesus College,
Oxford.
September 25, 1937.

XXIII. *The Primary Standard of Mutual Inductance of the National Physical Laboratory.* *By* N. F. ASTBURY, *M.A.* (From the National Physical Laboratory.) *.

[Plate V.]

ABSTRACT.

THE experience gained in recent years in the construction of standards of mutual inductance showed that it would be possible to obtain increased accuracy with the Camp-

* Communicated by Prof. W. L. Bragg, F.R.S.

bell primary standard of mutual inductance by rewinding the secondary coil, so as to have a lower resistance, and to have a cross-section more nearly square. A new secondary coil possessing these features has been constructed. It has also been provided with auxiliary windings by means of which the mutual inductance may be varied continuously, without loss of accuracy, over a small range. This is achieved by having two additional windings, from one of which an integral number of turns may be selected, the other being in parallel with a small potentiometer, the potential circuit of which is put in series with the main secondary circuit. An interesting mechanical feature is that the adjusting and fixing screws for the new coil have been made from a synthetic resin.

The metrology of the standard is briefly described, and a new series of simplified formulæ for the computation of inductance and its derivatives is given, together with a formula giving explicitly the errors introduced by a displacement of the secondary coil.

The use of the standard is then discussed, and the importance of capacities to earth is pointed out. A simple method of eliminating the effect of these capacities at low frequencies is given. It is concluded that the unit of inductance is now usable with an accuracy approaching 1 part in 10^6.

---

1. *Introduction.*

THE standard of mutual inductance of ten millihenries designed by Albert Campbell in 1907, and built at the National Physical Laboratory in the following year, forms the basis of the whole system of audio-frequency alternating-current measurements made at the Laboratory. In particular it is the fundamental standard used in the absolute determination of the ohm by alternating current methods, and it is in connexion with this that the work described in this paper has been carried out. The details of the design of the standard are given in the original paper [(1)] and in two later papers [(2)], [(3)] describing similar standards presented to the Japanese Government, and it is not necessary to include here more than a brief note on the essential features of the instrument.

It consists of a primary winding and a secondary winding, the former consisting of two single-layer helices of 75 turns each, wound in screw-threads cut on a marble cylinder 30 cm. diameter, and separated by an interval (15 cm.) equal to twice the length of either. In a plane midway between these helices lies the secondary winding, a multi-layer coil of 484 turns lying in a channel cut in a marble ring. The mean circumference of this winding coincides with the neutral circle of the two primary helices. The inductance of the standard is calculated from its dimensions, and the characteristic feature of the design is that the responsibility for accuracy rests almost entirely on the dimensions of the primary windings, which can be determined with great precision.

The present paper does not deal with the general design of the standard, but rather with certain modifications which have increased the accuracy of working. The original standard provided a value of mutual inductance which could be varied only in steps of about $20\,\mu$h., corresponding to the addition of extra complete turns to the secondary winding. The value has now been made continuously adjustable over a range of $\pm 100\,\mu$h. by the addition of a potential divider to certain turns in such a way that any desired fraction of a turn is in effect obtainable. This device greatly simplifies the use of the instrument.

One of the main features of the original design is that corrections arising from the finite cross-section of the secondary coil are only of the second order of magnitude. Nevertheless these corrections are not negligible, and with the demand for increased accuracy in recent years it became worth while to consider how these corrections could be still further reduced. An obvious way is to make the cross-section of the winding more nearly square. This has now been done, and at the same time the resistance of the secondary winding has been reduced, and thereby the effects of capacitances associated with the instrument have been lessened.

The new coil is carried on a marble ring 45 cm. diameter and 4·5 cm. thick, and is in three sections. The main section, carrying 484 turns, is located in a channel cut midway in the cylindrical surface of the ring. There are two subsidiary sections, one consisting of two complete turns of heavy gauge eureka wire lying in a helical groove

of 0·125″ pitch, and the other consisting of a single turn of stranded copper wire lying in a circular groove. These subsidiary sections lie on either side of the main winding and about 1 cm. distant from it. The stranded wire is built up of four strands, brought out to a suitable switch, by means of which they may be so connected as to provide 1, 2, 3, or 4 complete turns in addition to the main winding. Leads from the eureka spiral are brought out to a small potentiometer, the potential circuit of which is connected in series with the turns from the stranded wire. The maximum potential difference obtainable from this potentiometer is slightly greater than that obtainable from one complete turn, so that by varying the potential tappings any desired fraction of a turn, from 0 to 1, is effectively made available, the adjustment being continuous throughout.

The new coil necessitated an improved form of mechanical mounting. The positional adjustments on this coil are those necessary to bring its axis into coincidence with that of the primary helices, and may conveniently be provided by three levelling screws and three circumferential thrust screws. It is clearly undesirable to use metal for these screws, although on the original standard some German silver was used. On the standards presented to Japan ebonite was used, but experience with such screws at this Laboratory has shown them to be unsatisfactory. Through the cooperation of the Chemical Research Laboratory it has been possible to use, in the mounting of the new ring, screws and fittings made from a synthetic resin, a polymeride of a condensation product of methyl ethyl ketone and formaldehyde [4]. This resin, which is colourless and transparent, possesses great mechanical strength, and can be machined to a finish comparable with that of a soft alloy like brass. The screws work in bushes cut from the same material, and, in order to avoid unnecessary attrition, thrust against small glass plates cemented to the marble. The base of the whole standard has also been fitted with three levelling screws, bearing on a glass "hole, slot, and plane" mounting.

The complete standard is shown in Pl. V., in which the adjusting screws, auxiliary secondary windings, and switch-blocks may be seen.

2. *Metrology of the Standard.*

The most important measurements on the dimensions of the standard are those of the diameter, length, and pitch of the primary helices. The methods used for the determination of these quantities have been fully dealt with elsewhere [(1), (2), (3)], together with the method of correcting for irregularities of pitch and diameter. The primary cylinder was completely remeasured in 1934, the previous series of measurements having been made in 1914. The dimensional changes recorded showed that the length of the cylinder had increased by 1 part in 300,000 and the diameter by a similar amount in this interval of 20 years. The computed change in inductance due to these changes was rather less than 5 parts in 10^6. During the recent measurements the primary cylinder was taken round a temperature cycle 12–31–12° C., and proved to be non-cyclic in its behaviour, for after this treatment a further increase in diameter and length were recorded, of the same order as the changes which had occurred since 1914, and, as far as evidence is available, the increased dimensions have persisted. The increases in diameter and length have, however, opposing effects on the value of mutual inductance, and when the final measurements, made after the temperature cycling in 1934, were completed, it was found that the changes from the 1914 dimensions represented a change of only 4 parts in 10^6 in mutual inductance. The long-period stability of the standard is therefore of a very high order.

It is unnecessary to determine the dimensions of the secondary windings with an accuracy greater than a few parts in ten thousand. The main winding lies in a channel about 0·55 cm. square, the dimensions having been chosen so that, when the coil was wound with no. 26 d.s.c. copper wire (overall diameter 0·02″), the mean diameter would be equal to that of the neutral circle. Preliminary experiments with wooden formers provided important information on the packing of the wire and probable values of space factor. The diameter of the bottom of the groove was measured on completion, and served as a base to which measurements on the successive layers of the winding could be referred. The actual winding was carried out on the lathe on which the ring was machined, the wire being maintained under a tension of two or three pounds weight, and the increase

in diameter for each layer read from a suitably mounted micrometer head. Twenty-three complete layers, containing alternately 21 and 20 turns, together with an incomplete layer of 12 turns, built up the 484 turns required for a mutual inductance of 10 mh. The ends of the windings were soldered into small brass nipples, made from no. 4 brass wood-screws *, accurately located in the same radial plane. The auxiliary windings were mounted with the ring still on the lathe and their ends similarly secured. It is very important, of course, that the subsidiary windings should start and finish in the same plane, and special attention was paid to securing this condition. The leads to the main and eureka windings were concentric: the leads to the stranded turn were formed by closely twisting the ends of the wire.

The standard is used with the mean circumference of the main secondary winding coincident with the neutral circle of the primary helices, a condition obtained by both mechanical and electrical adjustments. The subsidiary windings, therefore, cannot occupy this ideal position, and it was necessary, in order to compute their contributions to the inductance, to determine their positions relative to the neutral circle, *i. e.*, to the mean circumference of the main winding. The necessary measurements were carried out by the Metrology Department, the diameter and position of each winding being determined at a number of points round its circumference.

3. *Calculations of Inductance.*

The calculations are all based on the original formula due to J. Viriamu Jones [1], [2], [3]. It has been shown elsewhere [5] how this formula may be simplified by the use of scales of arithmeto-geometrical means [6], and we may recapitulate here the main formulæ required for the calculations. The formulæ refer to the mutual inductance, M, of a helix of N turns, length x, radius B, and a coaxial circle radius A, in the plane of one end. Let us define the quantities R_1 and R_2 by the relations

$$R_1^2=(A+B)^2+x^2, \quad . \quad . \quad . \quad . \quad (3.1)$$

$$R_2^2=(A-B)^2+x^2. \quad . \quad . \quad . \quad . \quad (3.2)$$

* To Mr. Cass, of the Metrology Workshop, who carried out the constructional work, is due the ingenious idea of making taps for threading the marble for these nipples from hardened steel wood-screws of the same size.

Now form the arithmetico-geometrical mean scales

$$a_0=R_1,\quad b_0=R_2,\qquad c_0=\sqrt{(R_1^2-R_2^2)}=\sqrt{4AB},$$

and $a_0'=R_1$, $b_0'=\sqrt{4AB}$, $c_0'=R_2$.

From the first scale derive the limit a_n, and the sum S_1 given by

$$S_1=\sum_{r=0} 2^r c_r^2. \quad . \quad . \quad . \quad . \quad . \quad . \quad (3.3)$$

In conjunction with the second scale use the recurrence formula

$$\tan(\phi'_{r+1}-\phi_r')=(b_r'/a_r')\tan\phi_r', \quad . \quad . \quad (3.4)$$

starting with

$$\tan\phi_0'=\frac{(A-B)R_1}{x\sqrt{4AB}} \quad . \quad . \quad . \quad . \quad (3.5)$$

and

$$\tan(\phi_1'-\phi_0')=\frac{A-B}{x}, \quad . \quad . \quad . \quad . \quad . \quad . \quad (3.6)$$

and hence find the limit Φ' to which $\phi_n'/2^n$ converges. Denoting by Ψ the complement, in degrees, of Φ', and forming the summation S_2 given by

$$S_2=\sum_{r=1} c_r'\sin\phi_r', \quad . \quad . \quad . \quad . \quad . \quad (3.7)$$

calculate the quantity u given by

$$u=\frac{\Psi}{90}-\frac{S_2}{a_n}. \quad . \quad . \quad . \quad . \quad . \quad (3.8)$$

Then the mutual inductance M and its derivatives are given by the following formulæ:

$$M=\pi^2N\left[\frac{1}{2}\frac{S_1}{a_n}-\frac{A^2-B^2}{x}u\right], \quad . \quad . \quad . \quad (3.9)$$

$$\frac{\partial M}{\partial x}=\frac{\pi^2N}{xa_n}[S_1-4AB]\,*, \quad . \quad . \quad . \quad . \quad . \quad (3.10)$$

$$\frac{\partial^2 M}{\partial x^2}=\frac{\pi^2N}{R_2^2a_n}\left[S_1\left(1-\frac{2AB}{R_1^2}\right)-4AB\right], \quad . \quad . \quad (3.11)$$

* This formula holds when the variation in x arises from a bodily displacement of the secondary coil. If, as when we are considering the temperature coefficient of the standard, the variation in x arises from an alteration in length, and so of pitch, of the primary helix, a term $-M/x$ must be added to this expression.

$$\frac{\partial M}{\partial A} = \frac{2\pi^2 NA}{x}\left[\frac{2B}{A+B}\cdot\frac{x}{a_n} - u\right], \quad . \quad . \quad . \quad . \quad (3.12)$$

$$\frac{\partial M}{\partial B} = \frac{2\pi^2 NA}{x}\left[\frac{2B}{A+B}\,\frac{x}{a_n} + u\right], \quad . \quad . \quad . \quad . \quad (3.13)$$

$$\frac{\partial^2 M}{\partial A^2} = \frac{1}{A}\frac{\partial M}{\partial A} - \frac{\partial^2 M}{\partial x^2}, \quad . \quad . \quad . \quad . \quad . \quad . \quad . \quad . \quad (3\ 14)$$

$$\frac{\partial^2 M}{\partial A\,\partial x} = \frac{2\pi^2 NA}{xa_n}\left[1 - \left(R_1^2 - \frac{S_1}{2}\right)\frac{x^2+A^2-B^2}{R_1^2 R_2^2}\right]. \quad (3.15)$$

Fig. 1.

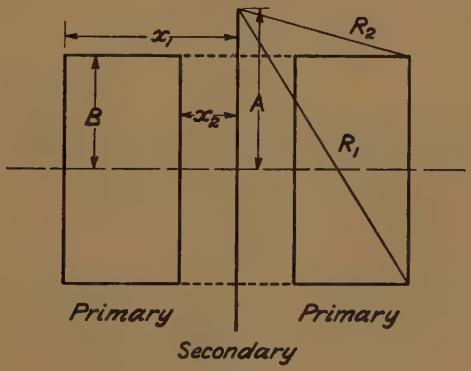

Diagram of Campbell standard.

In order to find the value for a standard of the Campbell form the values of M and its derivatives are calculated for helices of length x_1 and x_2 (see fig. 1), and the values for the whole standard are obtained by taking differences (remembering that there are two primary coils) and by multiplying by the number of turns in the secondary winding. In carrying out a calculation to eight significant figures by the above process it will be found that the arithmetico-geometrical mean scales converge in three or four terms and that the summations converge in two or three terms.

The calculations for the subsidiary windings may also be carried out using the above formulæ, but since these windings do not lie in the central plane four computations are necessary for each. Actually the mutual inductance

for these helices is more conveniently calculated using Butterworth's method of approximate integration [7], in which each primary helix is replaced by five circles distributed over its length, an appropriate number of turns being associated with every circle (see fig. 2). The mutual inductance between these circles and the secondary coil is calculated using Maxwell's well-known formula [8] for coaxial circles. These computations are greatly facilitated by the use of the tables of Nagaoka and Sakurai [9], which give the value of $M/\sqrt{AB}$ to argument $k^2=4AB/R_1^2$. The quantity k is the modulus of the elliptic integrals involved. The calculations involve the determination of R for every equivalent circle and the secondary coil,

Fig. 2.

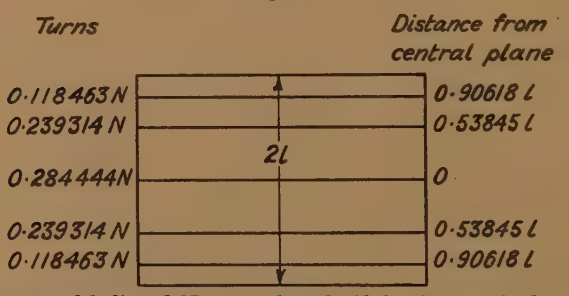

Replacement of helix of N turns, length 2*l*, by five equivalent circles (Butterworth).

and the addition of the individual values of M gives the required result. As the accuracy required is only of the order of parts in ten thousand very little labour is required.

(a) *Corrections for the Main Secondary Winding.*

Complete details of the main calculation have already been given in the papers quoted, and it is only necessary here to consider the additional calculations introduced by the finite size etc. of the secondary windings. The new secondary coil consists of 23 complete layers of d.s.c. copper wire, 0·02″ diameter, containing alternately 21 and 20 turns, and an incomplete layer of 12 turns, making 484 turns in all. The winding may therefore be considered as a " complete " coil of 23 layers to which 12 turns have been added, or as a " complete " coil of 24 layers from which 8 turns have been removed. If M is

the mutual inductance of the standard when the secondary turns are uniformly distributed over a rectangular section, radial depth 2P and axial length 2Q, and if M_0 is the mutual inductance when all the secondary turns are concentrated on a circle of radius A, then Searle [1], [2], [3] has shown that

$$M=M_0+\frac{1}{6}\left[\frac{Q^2}{A}\frac{\partial M}{\partial A}+(P^2-Q^2)\frac{\partial^2 M}{\partial A^2}\right]+\ldots \quad (3.16)$$

With this formula a correction for the " complete " section of the winding is determined. As far as the incomplete layer is concerned we can proceed as follows. Taking the centre of the section as origin of the coordinates,

Fig. 3.

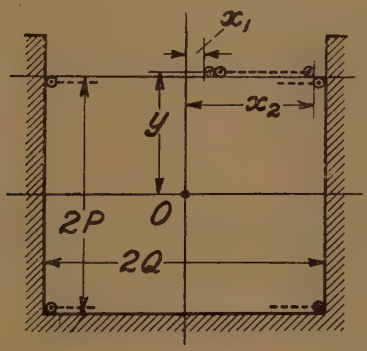

Diagrammatic section of secondary winding.

let the incomplete layer be bound by the lines $x=x_1$, $x=x_2$ (see fig. 3), and let the common ordinate of the centres of the wires be y. Then by integrating along the layer it can be shown that the contribution, m, to the total inductance made by this layer differs from the contribution m_0 to the same number of turns concentrated on a circle passing through the origin by an amount given by, as far as second order terms,

$$m-m_0=\frac{\partial M}{\partial A}\left[y+\frac{x_1^2+x_1x_2+x_2^2}{6A}\right]$$

$$-\frac{\partial^2 M}{\partial A^2}\left[\frac{x_1^2+x_1x_2+x_2^2-3y^2}{6}\right]. \quad (3.17)$$

According to the way in which the main winding is regarded the quantities A, P, and y may have one of two values. The uncertainty involved in the estimation of these quantities, particularly P and y, leads to a small difference in the values of the corrections completed by the two methods. The calculations are summarized in the following table :—

TABLE I.

Data for the Main Secondary Winding.

Mean radius (A) (cm.).		P (cm.).		Q (cm.).	M—M_0 (μh.).		$m-m_0$ (μh.).	
24 layers.	23 layers.	23 layers.	23 layers.		24 layers.	23 layers.	24 layers.	23 layers.
21·9039	21·8834	0·5456	0·5250	0·5568	0·103	0·297	−0·077	−0·142

Correction for difference in A = 0·019 μh.

Total correction for 24-layer coil = 0·103 − (−0·077)
= 0·180 μh.

Total correction for 23-layer coil = 0·297 − 0·142
+ 0·019 = 0·174 μh.

The difference of 0·006 μh., which arises largely from the uncertainty in determining y, represents only 6 parts in 10^7 of the total inductance, and is of no significance.

(b) *Corrections for the Irregularities etc. of the Subsidiary Windings.*

The inductance contributed by the subsidiary windings was obtained by regarding them as circles, the diameter and position of which coincided with the mean diameter and mean position of the windings deduced from the Metrology Reports. Departures from this condition were then dealt with in the following way.

Consider an arc, δs, of such a circle, and imagine it displaced radially and axially by amounts δA and δx respectively. Then its contribution to the total inductance will be altered by an amount $\delta(\Delta \mathrm{M})$ given by

$$\delta(\Delta \mathrm{M}) = \frac{\delta s}{2\pi \mathrm{A}}\left[\delta \mathrm{A}\frac{\partial \mathrm{M}}{\partial \mathrm{A}} + \delta x \frac{\partial \mathrm{M}}{\partial x} + \tfrac{1}{2}\delta \mathrm{A}^2 \frac{\partial^2 \mathrm{M}}{\partial \mathrm{A}^2} + \tfrac{1}{2}\delta x^2 \frac{\partial^2 \mathrm{M}}{\partial x^2} + \delta \mathrm{A}\,\delta x \frac{\partial^2 \mathrm{M}}{\partial \mathrm{A}\,\partial x} + \ldots\right]. \quad (3.18)$$

Since the irregularities, δA, δx, are not continuous functions of s, this expression cannot be integrated. If, however, we suppose the circle to be divided into n parts, so that $n\delta s = 2\pi A$, and we consider the mean displacements of every part, we may easily effect a summation, remembering that $\Sigma\delta A = 0 = \Sigma\,\delta x$. We then obtain

$$\Delta M = \frac{1}{2n}\left[\frac{\partial^2 M}{\partial A^2}\Sigma(\delta A)^2 + \frac{\partial^2 M}{\partial x^2}\Sigma(\delta x)^2\right] + \frac{1}{n}\frac{\partial^2 M}{\partial A\,\partial x}\Sigma(\delta A.\delta x) + \ldots \quad (3.19)$$

The quantities

$$\frac{1}{n}\Sigma(\delta A)^2, \quad \frac{1}{n}\Sigma(\delta x)^2, \text{ and } \frac{1}{n}\Sigma(\delta A\,\delta x)$$

are deducible directly from the measurements on the windings. Formula (3.19) is all that is necessary to correct for the irregularities of the single stranded turn. The eureka turns, however, form a helix and, quite apart from irregularities, it is necessary to calculate the difference between the mutual inductance into two turns concentrated on a circle and that into two turns developed into a helix symmetrical about that circle. Let p be the pitch of the helix, and consider an element $A\delta\theta$ at angular distance θ from the "start" of the mean turn. Then this element is displaced, relative to the mean plane, by an amount $\delta x = p\theta/2\pi$, so that its contribution to the total inductance is

$$\delta M = \frac{\delta\theta}{2\pi}\left[M_0 + \frac{p\theta}{2\pi}\frac{\partial M}{\partial x} + \frac{1}{2}\frac{p^2\theta^2}{4\pi^2}\frac{\partial^2 M}{\partial x^2} + \frac{1}{6}\frac{p^3\theta^3}{8\pi^3}\frac{\partial^3 M}{\partial x^3} + \ldots\right],$$

where M_0 is the inductance for one circular turn in the mean plane, the differential coefficients also referring to this turn. For a two-turn helix we have, therefore,

$$M = \frac{1}{2\pi}\int_{-2\pi}^{+2\pi}\left[M_0 + \frac{p\theta}{2\pi}\frac{\partial M}{\partial x} + \frac{1}{2}\frac{p^2\theta^2}{4\pi^2}\frac{\partial^2 M}{\partial x^2} + \frac{1}{6}\frac{p^3\theta^3}{8\pi^3}\frac{\partial^3 M}{\partial x^3} + \ldots\right]d\theta$$

$$= 2M_0 + \frac{p^2}{3}\frac{\partial^2 M}{\partial x^2} \quad (3.20)$$

To correct for the irregularities of the helix formula (3.19) is used, δx now representing departures from the true

helix. Both for the stranded turns and for the helix the irregularity correction amounted to $0{\cdot}000_1$ μh., which is quite negligible. In the helix $p = 0{\cdot}125'' = 0{\cdot}3175$ cm., and the correction computed from equation (3.20) amounted to $0{\cdot}003$ μh.

The values of mutual inductance and of its differential coefficients for the three secondary windings, including corrections for their irregularities etc. and for those of the primary windings, are given in Table II.

TABLE II.

Values of M and its Differentia Coefficients at 18° C.

Quantity.	Main winding (484 turns).	Stranded winding (per turn).	Eureka helix (two turns).
M.....	9997·27 μh.	$20{\cdot}68_8$ μh.	40·420 μh.
$\partial M/\partial A$	$-0{\cdot}38$ μh./cm. (A = 21·8834 cm.)	$-$ 0·07 μh./cm.	$-$ 0·14 μh./cm.
$\partial M/\partial B$	$1{\cdot}2 \times 10^3$ μh./cm.	3·1 ,,	6·2 ,,
$\partial M/\partial x$	$-5{\cdot}5 \times 10^2$*,,	0·11† ,,	0·20†,,
$\partial^2 M/\partial x^2$	52 μh./cm.^{2}	+ 0·09† μh./cm.^{2}	0·18† μh./cm.^{2}
$\partial^2 M/\partial A^2$	-52 ,,	$-$ 0·09 ,,	0·18 ,,
$\partial^2 M/\partial A\,\partial x$ ...	....	$-$ 0·03 ,,	$-$ 0·06 ,,

Temperature coefficient of mutual inductance = 6·3 parts per million per 1° C.

(c) *Correction for the Displacement of the Secondary Coil from its Ideal Position.*

A practical limit to the accuracy of the standard is set by the limits of adjustment of the secondary coil to its ideal position. Below is developed a formula giving explicitly the effect of a small displacement from its ideal position. For this purpose the coil will be regarded as a circle and the displacement will be considered as produced by an axial displacement α, a radial displacement β, and a rotation θ about a diameter making an angle ψ with the direction of radial displacement. Considering an element $\delta\phi$ at angular distance ϕ from this direction we have (fig. 4):

Total radial displacement $= \delta A = \beta \cos \phi - \frac{1}{2} A\theta^2 \cos^2(\phi - \psi)$.

Total axial displacement $= \delta x = \alpha + A\theta \cos(\phi - \psi)$.

* Referred to expansion of primary cylinder.

† Referred to displacement of secondary coil.

When the secondary coil is situated in its ideal position it is evident that coefficients like $\partial M/\partial x$ and $\partial^2 M/\partial A\,\partial x$ will be zero for the standard as a whole. The change in

Fig. 4.

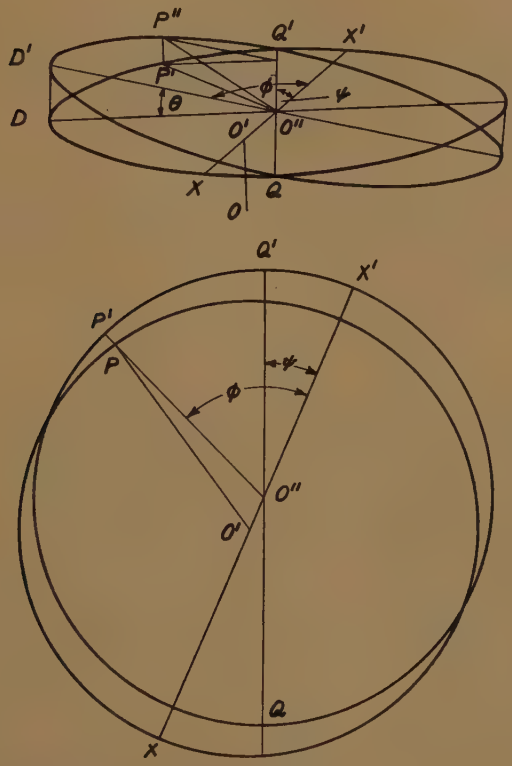

O is true position of centre of coil, $OO'=\alpha$, $O'O''=\beta$, $D\hat{O}''D=\theta$, $X\hat{O}''Q=\psi$, $X'\hat{O}''P'=\phi$.

Illustrating the displacement of the secondary winding.

mutual inductance caused by the above displacements will therefore be given by as far as second order terms,

$$\Delta M=\frac{1}{2\pi}\int_0^{2\pi}\left[\frac{\partial M}{\partial A}\{\beta\cos\phi-\tfrac{1}{2}A\theta^2\cos^2(\phi-\psi)\}\right.$$

$$\left.+\tfrac{1}{2}\beta^2\cos^2\phi\,\frac{\partial^2 M}{\partial A^2}+\tfrac{1}{2}\{\alpha+A\theta\cos(\phi-\psi)\}\,\frac{\partial^2 M}{\partial x^2}\right]d\phi$$

$$= \tfrac{1}{2}\alpha^2 \frac{\partial^2 M}{\partial x^2} + \tfrac{1}{4}\beta^2 \frac{\partial^2 M}{\partial A^2} + \tfrac{1}{4}\theta^2 A^2 \left(\frac{\partial^2 M}{\partial x^2} - \frac{1}{A} \frac{\partial M}{\partial A} \right)$$

$$= \tfrac{1}{2}\alpha^2 \frac{\partial^2 M}{\partial x^2} + \tfrac{1}{4}\beta^2 \frac{\partial^2 M}{\partial A^2} - \tfrac{1}{4}\theta^2 A^2 \frac{\partial^2 M}{\partial A^2}. \quad . \quad . \quad . \quad . \quad . \quad (3.21)$$

Inserting the values of the coefficients from Table II., and denoting by M_0 the value of the inductance when the ring is in its true position, we may write the value M, corresponding to the displaced position, as

$$M = M_0(1 + 0{\cdot}0026\,\alpha^2 - 0{\cdot}0013\,\beta^2 + 0{\cdot}62\,\theta^2). \quad . \quad (3.22)$$

If $\alpha = 0{\cdot}01$ cm. $= \beta$ and if $\theta = 0{\cdot}01/2A = 0{\cdot}00023$, then the error amounts to less than 2 parts in 10^7, so that if the adjustments can be made to a tenth of a millimetre no significant error will result.

4. *The Adjustable Secondary Windings.*

A brief description of the adjustable windings has already been given in the introductory section, and we have now to consider in more detail the method of connexion and use of these windings. The circuit of the whole instrument is shown diagrammatically in fig. 5 (*a*), from which it will be seen that the e.m.f. appearing at the secondary terminals is the sum of the voltages, (i.) induced in the main windings (ii.) induced in one or more complete turns of the stranded winding, and (iii.) appearing at the potential terminals of the potentiometer closing the eureka windings. The voltages induced in the main winding and in the complete single turns are, of course, deducible directly from the (calculated) mutual inductance associated with those windings, but in order to relate the voltage appearing at the potential terminals of the potentiometer to that induced in the eureka windings it is necessary to carry out an analysis of the circuit in the following manner. In fig. 5 (*a*) the coil A represents the main winding together with any added turns, B represents the eureka winding, and C_1C_2 the potentiometer. Let us now define

M = mutual inductance between primary winding and main secondary winding.

m_1 = mutual inductance between primary winding and eureka winding.

m_2 = mutual inductance between main secondary windings and potentiometer circuit.

R, L = total resistance and inductance respectively of the potentiometer circuit.

Fig. 5(*a*).

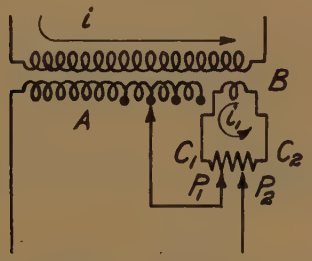

Circuit diagram of secondary winding.

Fig. 5(*b*).

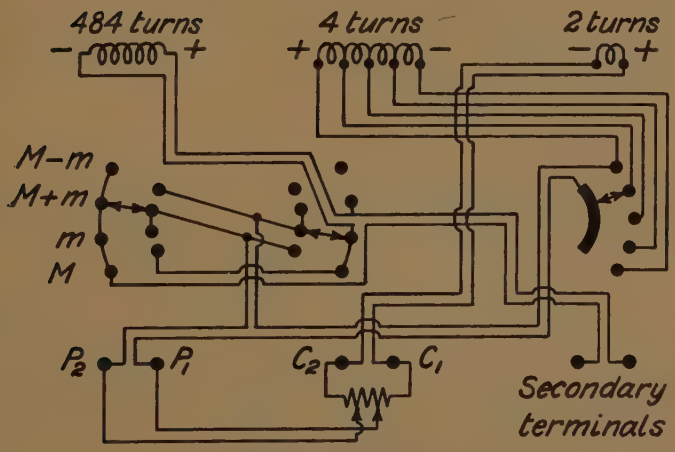

Secondary switch gear.

r, l^* = total resistance and inductance respectively of the part of the potentiometer between the tapping points.

V = voltage across secondary windings.

* l includes any mutual inductance between the closed circuit and the potential leads.

$\omega/2\pi$ =frequency of the currents i and i_1 circulating in the system.

$\alpha=\omega\sqrt{-1}$.

Then the following equations hold:

$$V=\alpha M i+\alpha m_2 i_1+(r+\alpha l)i,$$

$$\alpha m_1 i=(R+\alpha L)i_1,$$

from which we obtain

$$V=i\left[\alpha M+\alpha m_1 \frac{r}{R}(1+f)\right]+iS, \quad . \quad . \quad (4.1)$$

in which S represents a resistance the explicit value of which does not concern us here and f is a correcting factor given by

$$f=-\frac{\omega^2 L^2}{R^2}\left(1-\frac{R m_2}{rL}\right), \quad . \quad . \quad . \quad . \quad (4.2)$$

l being neglected in comparison with m_2, and higher powers of ω^2L^2/R^2 being omitted. We may determine the order of magnitude of f in the following way. The inductance L can be calculated by the following formula, due to Rayleigh and Nivens [10],

$$L=4\pi a n^2\left(\log\frac{8a}{b}-\frac{1}{2}\right), \quad . \quad . \quad . \quad . \quad (4.3)$$

in which n is the number of turns, a the radius, and b the axial length of the eureka helix. The value of m_2 may be estimated by Maxwell's approximate formula [11]

$$m_2=4\pi a n_1 n_2\left(\log\frac{8a}{d}-2\right), \quad . \quad . \quad . \quad (4.4)$$

which gives the mutual inductance between two coaxial circular coils of n_1 and n_2 turns respectively, radius a, and lying in planes distance d apart.

Substituting the known dimensions of the system, we find

$$L=6\times10^{-6}\text{ henry},$$

$$m_2=9\times10^{-4}\text{ henry}.$$

The resistance of the potentiometer circuit is approximately 2 ohms, so that, when the instrument is used with alternating current at a frequency of 10 c.p.s., we have

$$f=-3{\cdot}6\times10^{-8}\,(1-300/r),$$

or the effective contribution to the mutual inductance made by the potentiometer circuit is given by

$$\left.\begin{aligned} m' &= m_1\left[\frac{r}{\mathrm{R}}(1-3{\cdot}6\times10^{-8})+5{\cdot}4\times10^{-6}\right] \\ \text{or} \quad m' &= m_1\frac{r}{\mathrm{R}} \end{aligned}\right\} \quad . \quad (4.5)$$

for all practical purposes.

It appears then from equation (4.5) that the potentiometer circuit behaves like a small variable mutual inductance with a linear scale, and that in order to maintain a constant calibration the total resistance R should be steady. It was for this reason that eureka was chosen for this secondary winding, since it is an alloy of low temperature coefficient of resistance. Heavy gauge was selected because, in order to get the maximum variation of m', R must not greatly exceed the maximum value of r.

The potentiometer consists of a decade dial giving steps of 0·1 ohm and a slide wire of resistance 0·12 ohm, so that the maximum value of r is 1·12 ohm. The value of R is 2 ohms, so that the maximum available value of m' is (see Table II.)

$$m' = \frac{1{\cdot}12}{2}\times m_1 = \frac{1{\cdot}12}{2}\times 41{\cdot}41 \doteqdot 25\mu\text{h}.$$

A complete overlap with the discrete steps of 20·69 μh. given by the turns of the stranded coil is thus provided. To calibrate this variable part it was only necessary to determine the ratio r/R. This was done by inserting in the potentiometer circuit the current terminals of a Kelvin-Varley potential divider and obtaining two balances with direct current, first with a galvanometer connected between the sliding point of the potential divider and one of the potential terminals of the potentiometer circuit, and then with this latter connexion transferred to the other potential terminal (see fig. 6). Then if x and y be the two readings recorded on the potential divider for the two balances we have, P being the total resistance of the potential divider,

$$r/\mathrm{R} = (x-y)/\mathrm{P}. \quad . \quad . \quad . \quad . \quad . \quad (4.6)$$

The temperature coefficient of the ratio r/R appears to be of the order of parts in a hundred thousand per 1° C.,

and for normal ranges of temperature this is of no significance.

The main and subsidiary windings can be used separately * or together in series or in opposition, the switching arrangements being shown diagrammatically in fig. 5 (*b*). The actual switches and potentiometer are to be seen in the lower right-hand corner of Pl. V. The switches are about a metre distant from the standard, and tests have shown that the direct induction between the primary

Fig. 6.

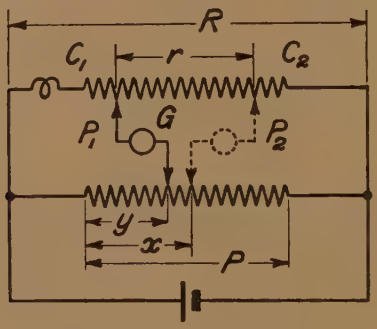

Measurement of r/R ratio.

helices and the unavoidable small loops in the switch-boxes does not amount to as much as 0·005 μh.

5. *The Effects of Capacitance.*

The mutual inductance of the standard calculated from its dimensions is only applicable to currents of zero frequency. The calculations take no account of the capacitances existing in the instrument, between the instrument and earth, and imposed on the instrument by external leads. When the instrument is used with alternating current these capacitances make definite contributions to its effective mutual impedance, and it is important to know the magnitude of these effects.

* When the main winding is used alone the potentiometer circuit may be opened, but at a frequency of 10 c.p.s. the correction on M due to the presence of the closed circuit does not amount to one part in ten million. Actually the correction on M, expressed as a fraction, is

$$\Delta M/M = \omega^2 L m_1 m_2 / M(R^2 + \omega^2 L^2).$$

The problem of the intrinsic capacitances of a mutual inductor has been dealt with by Butterworth [12] and by Hartshorn [13]. A mutual inductor is almost invariably used in practice with one end of the primary winding connected to one end of the secondary winding (see fig. 7). Then if L_1, R be the resistance and inductance of the primary winding, L_2, S those of the secondary winding, C_1 and C_2 the effective self-capacitances of the primary and secondary windings, and C_{12} the effective mutual capacitance between the windings, the effective mutual

Fig. 7.

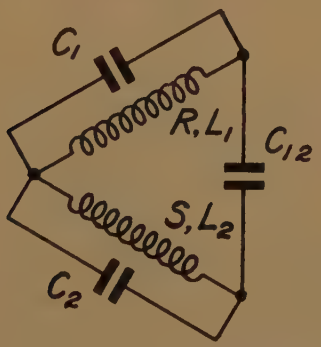

Equivalent circuit of mutual inductance.

inductance M at a frequency $\omega/2\pi$ is related to the true or geometrical inductance M_0 by the equation

$$M=M_0+C_{12}RS$$
$$+\omega^2\{C_1L_1M_0+C_2L_2M_0-C_{12}(L_1-M_0)(L_2-M_0)\}. \quad (5.1)$$

The terms additional to $M_0+C_{12}RS$ on the right-hand side of equation (5.1), expressed as a fraction of M_0, give the so-called "frequency coefficient" of the instrument, a quantity which is readily measurable by comparing the standard with a high-frequency standard [13] of special design. In the case of the Campbell standard used at a frequency of 10 c.p.s. this coefficient is less than one part in 10^6. The term $C_{12}RS$ may not, however, be so small. The effective value of C_{12} cannot be measured directly, but since it is not changed by reversing the sign of M, its magnitude may be estimated indirectly, since when M

is positive its effective value will be increased and when M is negative its effective value will be diminished by the term in question. The significance of this term in precision measurements will be discussed further below.

The addition of leads to the standard usually increases the effective value of all three capacitances associated with it. The standard is normally used with concentric leads in a bridge of the type shown in fig. 8. It will be clear that if the outer conductors of the leads all go to the common points no change in C_{12} will occur. The values of C_1 and C_2 will, however, be altered, and the effect may be calculated with great precision by regarding the leads as transmission lines of known constants. In

Fig. 8.

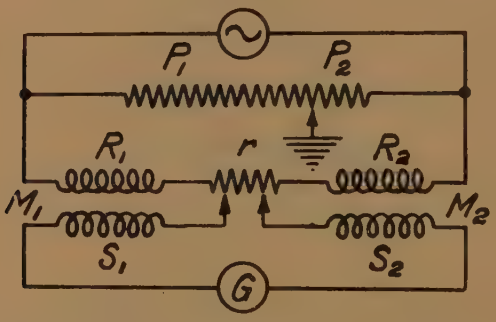

Mutual inductance comparison bridge (Hartshorn).

practice, however, it will generally be sufficiently accurate to regard C_1 and C_2 as each being augmented by the capacitance of the added leads. The correction is then very simply computed from (5.1).

We have now to consider the effect of capacitances to earth. The bridge network, with the addition of a resistance potentiometer across the supply, is as shown in fig. 8. If the tapping point of the potentiometer be connected to earth, and if the earth capacitances of the system may be regarded as replaceable by "lumped" capacitances between the ends of the coils and earth, the bridge may then be replaced by the equivalent self-contained system shown in fig. 9. Referring to the symbols shown in this figure, it can be shown (see Appendix) that if r is negligibly small and if C_3 and C_4 be for the

moment neglected, then at low frequencies one condition of balance is given by

$$M_1+M_2+(S_1C_1-S_2C_2)(R_1P_2-R_2P_1)/(P_1+P_2)=0, \quad (5.2)$$

from which it appears that the earth-capacitances of the detector arm may exercise a very significant influence on the balance-point, especially when, as is the case with standards of the Campbell form, the secondary resistances, S_1 and S_2, are high. However, by making $R_1P_2-R_2P_1=0$, which is easily done, it follows that the effect of C_1 and C_2 is completely wiped out, and, further,

Fig. 9.

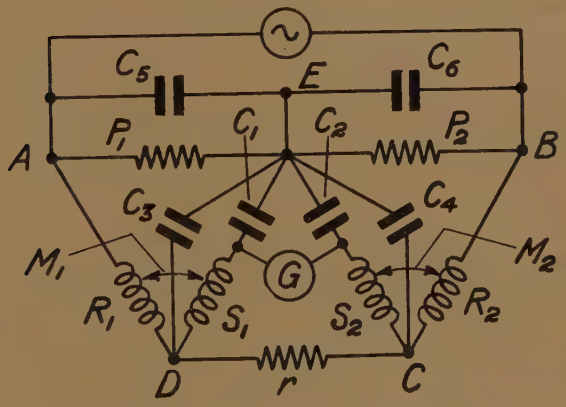

Circuit of fig. 8, showing earth capacitances.

when this is done the common points of the system are brought approximately to earth potential, so that the capacitances C_3 and C_4 will carry no current and therefore have no effect on the balance-point.

A number of measurements were carried out to test equation (5.2). The Campbell standard, with the new secondary coil, was compared against a sub-standard in which C_{12} was high but the product RS small, and the balance-points were plotted as a function of the ratio $P_2/(P_1+P_2)$.

The full lines, A, in fig. 10 represent the results of these measurements. The old secondary coil was then used, having a value of S roughly double that of the new coil,

and the broken lines, B, in fig. 10 were obtained. Finally, the value of S in the sub-standard was increased, and the broken lines, C, were obtained. In the first two cases it will be observed that the lines representing positive and negative connexions intersect at a point closely coincident with the observed balance-point of the potentiometer arm, and that the lines for the old coil have twice the slope of those for the new coil, results which are in complete accord with equation (5.2). Finally, lines C intersect at a point beyond the earth balance-point, the

Fig. 10.

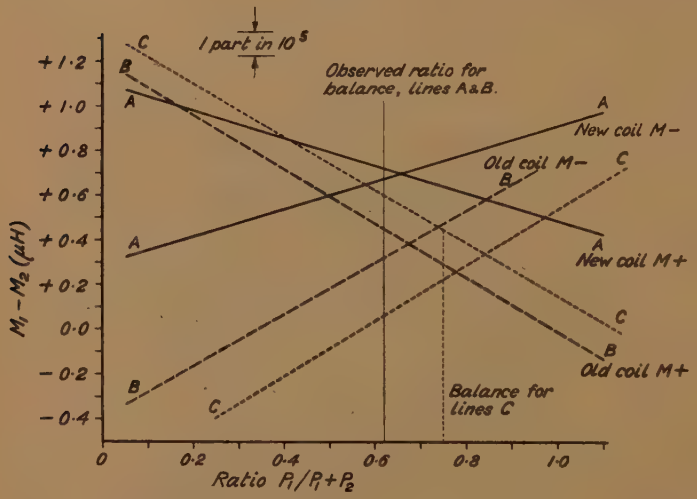

Illustrating effect of earthing arm balance.

difference in the effective values of M at this point being equal to $2C_{12}\,R_2S_2$.

The conditions under which a Campbell standard should be used to obtain the highest accuracy may now be conveniently summarized :—

(I.) Use a frequency not higher than 10 c.p.s.

(II.) Use concentric leads of as low capacitance and conductance as possible, the outer conductors being joined to the common point.

(III.) Use an earthing arm balanced so that the common points are at earth potential.

(IV.) Keep the earth-capacitances of the detector system low *—do not, for example, use any earth-connected screens in this circuit.

(V.) Take readings with M both positive and negative to test for the existence of the $C_{12}RS$ term.

The present Campbell standard seems to be free from any uncertainty as regards this last term, for it has been shown experimentally that screening the secondary coil does not alter its value. On the other hand, the much larger standard built up from the Lorenz coils, and described in the National Physical Laboratory Annual Report for 1934, p. 59, seems to possess a value of C_{12} of the order of 40 $\mu\mu$F, for its positive and negative values of inductance differ by 0·08 μh., and since for this standard RS = 1000 ohms[2], we have $2C_{12}RS = 2000\ C_{12} = 8 \times 10^{-8}$, whence $C_{12} = 40\ \mu\mu$F.

It is also worth while noting that the earth capacitances associated with the secondary windings and detector are of the order of 200 $\mu\mu$F according to the measurements recorded in fig. 10.

6. *Conclusion.*

The inductances of the separate turns and of the potentiometer circuit on the secondary coil have been checked against one another, and the measurements indicate an agreement of the order of 0·005 μh., which is practically beyond the limit of working. Numerous measurements made with the rebuilt standard have revealed no inconsistencies, and have shown that the modifications both of instrument and technique described above have materially improved the accuracy of working.

It remains now to consider the comparison between the standard in its present form and in its earlier form.

Following a redetermination of the dimensions of the primary cylinder in 1934 the recalculation of the inductance revealed a large divergence from the original figure than could be accounted for by the recorded dimensional changes, which, as pointed out in section 2, produce a change in inductance of only 4 parts in 10^6. It was concluded,

* For obvious reasons leads at least two or three metres long are inevitable in the detector circuit, so that the earth capacitances are always fairly large. It is important, however, not to enhance them by the use of earth-connected screens.

therefore, that the original value was probably in error by 3 or 4 parts in 10^5. Campbell himself actually stated that his value might be uncertain to this order. As far as the secondary coil is concerned it has not been possible to obtain any direct check on the dimensions of the original coil, but of course a direct electrical comparison between the two is easily made. The results of such a comparison are given below :—

$$\begin{aligned} \text{M (old)} - \text{M (new)} &= 0{\cdot}30\ \mu\text{h. measured,} \\ &= 0{\cdot}43\ \mu\text{h. calculated.} \end{aligned}$$

The difference of 13 parts in 10^6 is probably due to a change in the coil itself. The original coil was impregnated with wax, a procedure now known to be undesirable when permanence is a first consideration. Changes in dimensions and deterioration in insulation of this 25-year old coil are by no means unlikely in the light of our present knowledge.

The present position may be summarized by stating that the standard of inductance can be used for comparative measurements with an accuracy approaching 1 part in 10^6, and that any uncertainty in the values obtained is due only to dimensional instability of the standard. The use of the standard and maintenance of the unit really present two separate problems ; it is hoped that the work described in this paper has completely solved the former. The solution of the latter must await improvements in material, machines, and metrology.

7. *Acknowledgments.*

To Dr. L. Hartshorn for his continued advice and suggestions the writer owes his best thanks. To his colleague, Mr. P. Vigoureux he is indebted for many helpful discussions and for his assistance in checking some of the calculations by independent methods.

The cooperation of the Chemical Research Laboratory made it possible to use the synthetic resin described in the Introduction, and in this connexion thanks are due to the Director of the Chemical Research Laboratory, Sir Gilbert Morgan, F.R.S., and to Mr. E. L. Holmes.

The measurements of dimensions were made by the staff of the Metrology Department of the Laboratory, and the constructional work as carried out in the work-

shops of that Department. Special thanks are due to Mr. J. Cass for the skill and care with which he worked the resin and marble.

Appendix.

The Effect of Earth Capacitances on Mutual Inductance Comparisons.

Fig. 11 is derived from fig. 9 by the omission of C_5, C_6, C_3, and C_4. The first two capacitances are thrown in shunt with P_1 and P_2, and exert only a second-order effect in the balance, while C_3 and C_4, as we shall see later, carry no current when the final conditions are established.

Fig. 11.

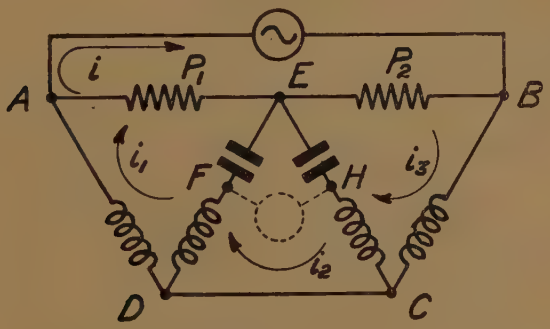

Illustrating Appendix.

Referring to fig. 11, the detector is connected between F and H, so that when the bridge is balanced F and H are the same potential.

Let ξ_1 ξ_2 be the impedance operators for arms AD, BC.

,, η_1 η_2 ,, ,, ,, ,, ,, DE, CE.

,, μ_1 μ_2 ,, mutual impedance operators for arms AD and DE and CB and CE.

,, γ_1 γ_2 ,, impedance operators of FE and EH.

,, ζ_1 ζ_2 ,, impedance operators of DF and CH.

,, ρ be the impedance operator of DC.

Thus any ξ is of the form $R+j\omega L$,

,, ,, ζ ,, ,, ,, ,, $S+j\omega N$,

,, ,, μ ,, ,, ,, ,, $\sigma+j\omega M$,

,, ,, γ ,, ,, ,, ,, $1/j\omega C$,

where R and L denote primary resistance and inductance respectively,
and S and N denote secondary resistance and inductance respectively.

Also we have $\eta_1-\zeta_1=\gamma_1$, $\eta_2-\zeta_2=\gamma_2$.

Writing down the mesh equations, we have

$$P(i_1-i)+\eta_1(i_1-i_2)-\mu_1 i_1+\xi_1 i_1-\mu_1(i_1-i_2)=0 \quad . \quad . \quad \text{(A 1)}$$

$$\eta_1(i_2-i_1)+\mu_1 i_1+\eta_2(i_2-i_3)+\mu_2 i_3+\rho i_2=0 \quad . \quad . \quad \text{(A 2)}$$

$$P_2(i_3-i_1)+\xi_2 i_3-\mu_2(i_3-i_2)+\eta_2(i_3-i_2)-\mu_2 i_3=0 \quad . \quad \text{(A 3)}$$

$$\zeta_1(i_2-i_1)+\zeta_2(i_2-i_3)+\mu_1 i_1+\mu_2 i_3+\rho i_2=0. \quad . \quad . \quad . \quad \text{(A 4)}$$

Put $$\phi_1=P_1+\eta_1+\xi_1-2\mu_1 \quad . \quad . \quad . \quad . \quad . \quad \text{(A 5)}$$

$$\phi_3=P_2+\eta_2+\xi_2-2\mu_2. \quad . \quad . \quad . \quad . \quad \text{(A 6)}$$

Then we may rearrange equations (A 1) to (A 4) in the following way :—

$$\phi_1 i_1-(\eta_1-\mu_1)i_2-P_1 i=0 \quad . \quad . \quad . \quad . \quad . \quad . \quad . \quad . \quad \text{(A 7)}$$

$$(\mu_1-\eta_1)i_1+(\eta_1+\eta_2+\rho)i_2+(\mu_2-\eta_2)i_3=0 \quad . \quad . \quad \text{(A 8)}$$

$$-(\eta_2-\mu_2)i_2+\phi_3 i_3-P_2 i=0 \quad . \quad . \quad \text{(A 9)}$$

$$(\mu_1-\zeta_1)i_1+(\zeta_1+\zeta_2+\rho)i_2+(\mu_2-\zeta_2)i_3=0 \quad . \quad . \quad \text{(A 10)}$$

Eliminating i_1, i_2, and i_3, we get

$$(\mu_1-\zeta_1)\begin{vmatrix} -(\eta_1-\mu_1) & 0 & P_1 \\ (\eta_1+\eta_2+\rho) & (\mu_2-\eta_3) & 0 \\ -(\eta_2-\mu_2) & \phi_3 & P_2 \end{vmatrix}$$

$$-(\zeta_1+\zeta_2+\rho)\begin{vmatrix} \phi_1 & 0 & P_1 \\ (\mu_1-\eta_1) & \mu_2-\eta_2 & 0 \\ 0 & \phi_2 & P_2 \end{vmatrix}$$

$$+(\mu_2-\zeta_2)\begin{vmatrix} \phi_1 & -(\eta_1-\mu_1) & P_1 \\ (\mu_1-\eta_1) & (\eta_1+\eta_2+\rho) & 0 \\ 0 & -(\eta_2-\mu_2) & P_2 \end{vmatrix}=0.$$

We may conveniently, for the present purpose, put $\rho=0$, and, remembering that $\eta_1-\zeta_1=\gamma_1$, $\eta_2-\zeta_2=\gamma_2$, we find

$$(\mu_1+\mu_2)[P_1P_2(\gamma_1+\gamma_2)+(P_1+P_2)\eta_1\eta_2]+\mu_1\mu_2[P_2(\eta_1+\zeta_1-2\gamma_2)$$
$$+P_1(\eta_2+\zeta_2-2\gamma_2)]$$

$$+\mu_1[P_1\xi_2(\gamma_1+\gamma_2)-P_1\zeta_1\eta_2-P_2\zeta_2\eta_1]+\mu_2[P_2\xi_1(\gamma_1+\gamma_2)-P_2\zeta_1\eta_2-P_1\zeta_2\eta_1)]$$

$$-(P_1\mu_2{}^2\gamma_1+P_2\mu_1{}^2\gamma_2)+(\zeta_1\eta_2-\zeta_2\eta_1)(P_2\xi_1-P_1\xi_2)=0 \quad . \quad (A\ 11)$$

Inserting the values for the operators, and neglecting terms like $LC\omega^2$ and $\omega^2C^2R^2$, we find

$$(M_1+M_2)(P_1+P_2)$$

$$-2\omega^2M_1M_2\left[P_2C_2\left(1-\frac{2C_1}{C_2}\right)-P_1C_1\left(1-\frac{2C_2}{C_1}\right)\right]$$

$$+\omega^2M_1[P_1N_1C_1+P_2N_2C_2-P_1L_2(C_1+C_2)]$$

$$+\omega^2M_2[P_2N_2C_2+P_1N_1C_2-P_2L_1(C_1+C_2)]$$

$$+\omega^2(P_1C_2M_2{}^2+P_2C_1M_1{}^2)+(C_1S_1-C_2S_2)(P_2R_1-P_1R_2)=0.$$

It is easily demonstrated that for $\omega=2\pi\times10$ cycles per second all the terms under ω^2 are negligibly small.

It follows, therefore, that we may write

$$M_1+M_2+(C_1S_1-C_2S_2)(P_2R_1-P_1R_2)/(P_1+P_2)=0, \quad (A\ 12)$$

which is identical with equation (5.2).

References.

(1) A. Campbell, Proc. Roy. Soc. A, lxxix. p. 428 (1907).
(2) D. W. Dye, Proc. Roy. Soc. A, ci. p. 315 (1922).
(3) D. W. Dye and L. Hartshorn, N. P. L. Collected Researches, xxi. p. 1 (1927).
(4) G. T. Morgan and E. L. Holmes, Brit. Pat. nos. 404317 ; 408063.
(5) N. F. Astbury, Proc. Phys. Soc. xlvii. p. 86 (1935).
(6) L. V. King, ' On the Direct Numerical Computation of Elliptic Functions,' C.U.P. (1924).
(7) Glazebrook's ' Dictionary of Applied Physics,' vol. 2, p. 387 (Macmillan, London, 1922).
(8) Rosa and Grover, Bull. Bur. Stds. viii. no. 1, p. 6 (1912).
(9) Nagaoka and Sakurai, Sci. Papers of the Inst. Phys. and Chem. Res., Tokyo, Table 2 (1927).
(10) Rosa and Grover, *loc. cit.* p. 116.
(11) Rosa and Grover, *loc. cit.* p. 13.
(12) S. Butterworth, Proc. Phys. Soc. xxxiii. p. 312 (1921).
(13) L. Hartshorn, Proc. Phys. Soc. xxxviii. p. 302 (1926).

February, 1937.

XXIV. *Lebesgue Complex Integration.*

By W. FABIAN, *M.A., Ph.D.**

1. *Introduction.*

IN the present paper we consider Lebesgue complex integration over fields which may be unbounded †.

Let L be a simple curve, bounded or unbounded, which is defined by

$$z=x+iy=x(t)+iy(t),$$

and which is such that it can be broken up into a finite number of simple curves for each of which $x(t)$ and $y(t)$ are continuous monotonic one-valued functions of the real parameter t.

Let E(L) be a set of points on L. Let $e_n(\mathrm{L})$ be a sequence of sets of points in E(L), each contained in the next, such that $e_n(\mathrm{L})\to\mathrm{E(L)}$ when $n\to\infty$. If such a sequence of sets $e_n(\mathrm{L})$ can be found such that each set of the sequence in the finite part of the plane is measurable ‡, then the set E(L) will be said to be measurable, and its measure $m[\mathrm{E(L)}]$ will be defined by

$$m[\mathrm{E(L)}]=\lim_{n\to\infty} m[e_n(\mathrm{L})],$$

where $m[e_n(\mathrm{L})]$ is the measure of $e_n(\mathrm{L})$ and $\lim_{n\to\infty} m[e_n(\mathrm{L})]$ may be finite or infinite.

Let $\mathrm{E}_1(\mathrm{L}),\ \mathrm{E}_2(\mathrm{L}),\ \ldots\ \mathrm{E}_r(\mathrm{L}),\ \ldots\ \mathrm{E}_N(\mathrm{L})$

be a finite number of measurable components into which the measurable set E(L) is divided, such that each of the components $\mathrm{E}_r(\mathrm{L})$ lies on an arc of L for which $x(t)$ and $y(t)$ are monotonic functions of t. A function $f(z)$ will be said to be measurable in E(L) if the real and imaginary parts of $f(z)$ are measurable in each of the sets of points on the x- and y-segments, which correspond to the components $\mathrm{E}_r(\mathrm{L})$.

Throughout this paper we shall suppose that the Lebesgue-Stieltjes integrals in our definition § of $\int_{\mathrm{E(L)}} f(z)\,dz$

* Communicated by the Author.

† Lebesgue integration examined in our previous papers was over bounded fields.

‡ Fabian, Phil. Mag. (7) xxii. pp. 523–534 (1936).

§ Fabian, Phil. Mag. (7) xxii. p. 525 (1936). The curve L was not restricted to be bounded in this definition.

converge absolutely if $\int_{E(L)} f(z)\,dz$ exists, whether the set E(L) is bounded or not.

We have, if $f(z)$ is integrable over the measurable set E(L), that

$$\int_{E(L)} f(z)\,dz = \sum_{r=1}^{N} \int_{E_r(L)} f(z)\,dz$$

and

$$\int_{E(L)} f(z)\,dz = \lim_{n=\infty} \int_{e_n(L)} f(z)\,dz,$$

where each of these integrals exists, and the measurable sets $E_r(L)$ and $e_n(L)$ are as defined in this paragraph.

It will be readily seen that a large part of our theory of Lebesgue complex integration over bounded fields * can be almost immediately extended to hold for unbounded fields.

2. *Inequalities.*

If $f(z)$ is measurable in a set of points E(L), and $\{f(z)\}^p$, where $p>0$, is integrable over E(L), then $f(z)$ will be said to belong to class L^p in E(L).

Theorem 1.—*If* $f(z)$ *belongs to class* L^p *and* $g(z)$ *to class* $L^{\frac{p}{p-1}}$ *in a measurable set of points* E(L), *where* $p>1$, *then* $f(z)g(z)$ *is integrable over* E(L), *and*

$$\int_{E(L)} |f(z)g(z)|\,|dz| \leqslant \left| \left\{ \int_{E(L)} |f(z)|^p |dz| \right\}^{p} \times \left\{ \int_{E(L)} |g(z)|^{\frac{p}{p-1}} |dz| \right\}^{1-\frac{1}{p}} \right|.$$

Proof.—Let z_1 be a fixed point on L, whose t-parameter is t_1. Let $|s|$ be the length of the arc $(z_1 z)$ of L, where $s>0$ when $t>t_1$, and $s<0$ when $t<t_1$. Let E_s be the set of points on this s-segment, which corresponds to E(L).

From the hypothesis and by previous theorems † it follows that $|f(z)|$ and $|g(z)|$ are measurable in the measurable set of points E_1, and $|f(z)|^p$ and $|g(z)|^{\frac{p}{p-1}}$ are integrable over E_s.

* Fabian, Phil. Mag. (7) xxii. pp. 523–534 (1936), 1117–1122; xxiv. pp. 256–262 (1937).

† *Loc. cit.*

Hence we can apply Hölder's inequality * to obtain

$$\int_{E_s} |f(z)g(z)|\,ds \leqslant \left| \left\{ \int_{E_s} |f(z)|^p\,ds \right\}^{\frac{1}{p}} \times \left\{ \int_{E_s} |g(z)|^{\frac{p}{p-1}} ds \right\}^{1-\frac{1}{p}} \right|,$$

where each of these integrals exists.

The conclusion follows immediately.

Theorem 2.—*If* $f(z)$ *and* $g(z)$ *belong to class* L^p *in a measurable set of points* E(L), *where* $p>1$, *then* $f(z)+g(z)$ *belongs to class* L^p *in* E(L), *and*

$$\left| \left[\int_{E(L)} |\{f(z)+g(z)\}^p|\,|dz| \right]^p \right| \leqslant \left| \left\{ \int_{E(L)} |f(z)|^p |dz| \right\}^{\frac{1}{p}} \right| + \left| \left\{ \int_{E(L)} |g(z)|^p |dz| \right\}^{\frac{1}{p}} \right|.$$

Proof.—For, using the same notation as in the proof of the last theorem, we have, from the hypothesis and by previous theorems †, that $|f(z)|$ and $|g(z)|$ are measurable in the measurable set of points E_s, and $|f(z)|^p$ and $|g(z)|^p$ are integrable over E_s. Hence we obtain, by Minkowski's inequality ‡,

$$\left| \left\{ \int_{E_s} (|f(z)|+|g(z)|)^p\,ds \right\}^{\frac{1}{p}} \right| \leqslant \left| \left\{ \int_{E_s} |f(z)|^p\,ds \right\}^{\frac{1}{p}} \right| + \left| \left\{ \int_{E_s} |g(z)|^p\,ds \right\}^{\frac{1}{p}} \right|, \quad . \quad (1)$$

where each of these integrals exists. Also

$$\left| \left\{ \int_{E_s} |f(z)+g(z)|^p\,ds \right\}^{\frac{1}{p}} \right| \leqslant \left| \left\{ \int_{E_s} (|f(z)|+|g(z)|)^p\,ds \right\}^{\frac{1}{p}} \right|, \quad . \quad (2)$$

where each of these integrals exists.

The conclusion follows by (1) and (2) and our theory of absolute convergence of integrals §.

* Titchmarsh, ' Theory of Functions,' p. 382 (1932).
† *Loc. cit.*
‡ Titchmarsh, ' Theory of Functions,' p. 384 (1932).
§ Fabian, Phil. Mag. (7) xxii. pp. 1117–1122 (1936).

XXV. *The Zeta-function of Riemann.*

By W. FABIAN, *M.A., Ph.D.**

IN a previous paper † we gave a relation between the Zeta-function of Riemann and the Weierstrass elliptic function. In the present paper we give relations between the Zeta-function of Riemann and Jacobian elliptic functions.

The Zeta-function of Riemann is defined ‡ when $R(s) \geqslant 1+\delta$, $\delta>0$, by

$$\zeta(s, z)=\sum_{n=0}^{\infty} \frac{1}{(z+n)^s}.$$

Let $\theta(z)$ be a function which is analytic in a region E except for poles at $0, -1, -2, \ldots\ldots -n, \ldots\ldots \infty$, at which the principal parts of $\theta(z)$ are

$$\frac{1}{z^\sigma}, \quad \frac{1}{(z+1)^\sigma}, \quad \frac{1}{(z+2)^\sigma}, \cdots \quad \frac{1}{(z+n)^\sigma} \cdots$$

respectively. Let C_n be a simple closed curve in E such that $\theta(z)$ is analytic on and within C_n except for poles *inside* C_n at $0, -1, -2, \ldots\ldots -n+1$. Let C_∞ denote the contour which C_n becomes ultimately when C_n increases indefinitely in size to enclose an infinite number of the points $0, -1, -2, \ldots\ldots -n, \ldots\ldots \infty$. Then§

$$\zeta(s, z)=\frac{(-1)^{\sigma-1}}{2\pi i}\,\Gamma(1-s).(\sigma-1)!\,D^{s-\sigma-\gamma}(C_\infty)\theta^{(\gamma)}(z),$$

$$R(s) \geqslant 1+\delta, \quad \delta>0,$$

where γ is the least integer greater than or equal to zero, such that $\sigma-R(s)+\gamma>0$; and this relation holds for no other values of s than those for which the series

$$\sum_{n=0}^{\infty} \frac{1}{(z+n)^s}$$

converges to $\zeta(s, z)$.

This formula gives us the following relations between

* Communicated by the Author.

† Fabian, Phil. Mag. (7) xxi. pp. 274–280 (1936).

‡ Whittaker and Watson, ' Modern Analysis,' p. 265 (1927).

§ Fabian, Phil. Mag. (7) xxi. pp. 278, 279 (1936). D stands for d/dz.

the Zeta-function of Riemann and Jacobian elliptic functions :

$$\zeta(s, z)=\frac{k}{2\pi i}\Gamma(1-s)\mathrm{D}^{s-1-\gamma}(\mathrm{C}_\infty)\mathrm{D}^\gamma \operatorname{sn}(z+i\mathrm{K}'),$$

$$\zeta(s, z)=-\frac{k}{2\pi i}\Gamma(1-s)\mathrm{D}^{s-1-\gamma}(\mathrm{C}_\infty)\mathrm{D}^\gamma \operatorname{sn}(z+2\mathrm{K}+i\mathrm{K}'),$$

$$\zeta(s, z)=\frac{k}{2\pi}\Gamma(1-s)\mathrm{D}^{s-1-\gamma}(\mathrm{C}_\infty)\mathrm{D}^\gamma \operatorname{cn}(z+i\mathrm{K}'),$$

$$\zeta(s, z)=-\frac{k}{2\pi}\Gamma(1-s)\mathrm{D}^{s-1-\gamma}(\mathrm{C}_\infty)\mathrm{D}^\gamma \operatorname{cn}(z+2\mathrm{K}+i\mathrm{K}'),$$

$$\zeta(s, z)=\frac{1}{2\pi}\Gamma(1-s)\mathrm{D}^{s-1-\gamma}(\mathrm{C}_\infty)\mathrm{D}^\gamma \operatorname{dn}(z+i\mathrm{K}'),$$

$$\zeta(s, z)=-\frac{1}{2\pi}\Gamma(1-s)\mathrm{D}^{s-1-\gamma}(\mathrm{C}_\infty)\mathrm{D}^\gamma \operatorname{dn}(z+3i\mathrm{K}'),$$

where* the Jacobian elliptic functions

$$\operatorname{sn}(z+i\mathrm{K}'),\ \operatorname{sn}(z+2\mathrm{K}+i\mathrm{K}'),\ \operatorname{cn}(z+i\mathrm{K}'),$$
$$\operatorname{cn}(z+2\mathrm{K}+i\mathrm{K}'),\ \operatorname{dn}(z+i\mathrm{K}'),\ \operatorname{dn}(z+3i\mathrm{K}'),$$

have unity for one of their periods and are analytic on and within C_∞ except for simple poles inside C_∞ at $z=0$, -1, -2, $\ldots -n$, $\ldots .\infty$; $\mathrm{R}(s)\geqslant 1+\delta$, $\delta>0$; D stands for d/dz, and γ is the least integer greater than or equal to zero, such that $1-\mathrm{R}(s)+\gamma>0$. These relations hold for no other values of s than those for which the series

$$\sum_{n=0}^{\infty}\frac{1}{(z+n)^s}$$

converges to $\zeta(s, z)$.

XXVI. *The Reflexion of β-Rays.* *By* J. Alan Chalmers, *M.A., Ph.D. (Cantab.), Lecturer in Physics in the Durham Colleges in the University of Durham* *.

1. *Introduction.*

RADIOACTIVE sources which emit β-rays are often obtained in the form of a deposit of the radioactive material on some solid base. The beam of β-rays

* The constants K, K′, and k are as defined in Whittaker and Watson's ' Modern Analysis ' (1927), chapter 22.

† Communicated by the Author.

emerging from the source will therefore contain some rays which have been reflected from the base. There are a number of instances where the interpretation of experimental results requires a separation of the effects of the direct and reflected β-rays ; as an example, measurements have been made by Emeléus [1] and Riehl [2] of the relative numbers of β-rays and α-rays emitted by a source of Radium E and Polonium in equilibrium, but reflected β-rays are included among those measured (very few α-rays are reflected) ; hence a knowledge of the fraction of β-rays reflected is needed in order to settle the question as to whether there is just one β-ray per disintegration of Radium E or more than one.

There are no experimental determinations of the reflected fraction under conditions corresponding to those of the problem under consideration. It is the object of the present work to relate the required reflexion coefficient with that obtainable experimentally under different conditions.

2. *Experiments on Reflexion.*

The experiments on reflexion consist of two types. Kovarik [3] and others have found the effect of a reflector on the ionization produced by a beam of β-rays. And Schonland [4] has measured the percentage reflected backwards of a beam of β-rays incident normally on a metal sheet.

The results obtained by the two methods do not agree, except in indicating that there is not much dependence of the reflexion coefficient on the velocity of the β-rays concerned. For aluminium, Kovarik's reflexion coefficient is 30 per cent. and Schonland's 13 per cent.

It is clear that there is a considerable difference between the geometrical conditions in the two cases, and this will be seen to account for the divergence between the results.

3. *Geometrical Conditions.*

In Kovarik's experiments the β-rays are incident on the reflector at various angles and emerge at various angles, the reflected fraction being the ratio of reflected to direct rays in the directions of emergence. In Schonland's experiments the β-rays are incident normally only, but

may be reflected to emerge at any angle. On the other hand, in the problem of reflexion of β-rays from a metal base (referred to, for convenience, as the case of Riehl's experiments) β-rays are incident at all angles, and the reflexion coefficient is the ratio of rays reflected so as to emerge in a small zone normal to the surface to those travelling directly into this cone. Since the angles in Kovarik's case are not definite, this cannot be considered further, and we are left with the comparison between the cases of Schonland and Riehl.

In order to contribute to the reflected rays in Schonland's case, a ray must be incident normally and be deflected to emerge backwards at any angle; whereas in Riehl's case, a ray may be incident at any angle but must emerge normally. At first sight, it might seem that the conditions are similar, for the rays travel in the same

Fig. 1.

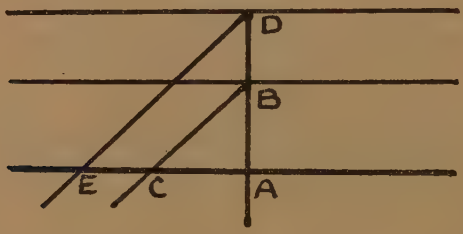

paths, but in opposite directions; however, we can see, in two ways, that the reflexion coefficient must be greater in Riehl's case than in Schonland's. Let us compare rays which follow the paths ABC and CBA, supposing we have equal numbers incident in the two cases. The two rays, on emerging, will have travelled the same distance, so that the chances of deflexions, other than at B, will be the same for both rays; thus the number of rays emerging as part of the reflected beam will depend on the chance of the appropriate deflexion at B. The ray CBA has a less velocity at B than the ray ABC, so that the chance of a deflexion at B is greater in this case, and hence we get a greater number of reflected rays in the case of Riehl's experiments (corresponding to CBA) than in the case of Schonland's (corresponding to ABC). Alternatively, we can compare the ray CBA with the ray ADE, where CB=AD, so that the velocities are the same at

the points of deflexion, and hence equal numbers of rays start on the journeys along DE and BA ; but the former, having a greater distance to travel, are more likely to be removed from the beam before emergence, and, also, as the distance CB is increased, the stage will be reached when AD+DE is greater than the total range of the incident rays, so that none can emerge, whereas CB+BA remains less than the range, and hence there is a contribution to the reflexion coefficient in Riehl's case that is lacking in Schonland's case.

The above arguments show that the reflexion coefficient is greater in Riehl's case than in Schonland's, but they are not quantitative, and in order to be able to obtain actual values for the reflexion coefficient in Riehl's case, it is necessary to make detailed calculations as to the ratio of the two coefficients. In order to do so, certain assumptions are needed, and deductions from these can then be made.

4. *Preliminary Assumptions and Deductions.*

We start with the assumption that the phenomena of β-ray reflexion can be discussed by considering the two processes of gradual loss of velocity and of single scattering ; the author [5] has shown that these two processes are adequate to account for the absorption of β-rays, and it seems probable that reflexion can equally adequately be considered.

Schonland's [4] experiments have shown that the reflexion coefficient is independent of the velocity of the β-rays, and therefore it is sufficient to calculate the reflexion coefficients for slow β-rays, for which the laws governing the processes at work are simple.

For the gradual loss of velocity in passing through matter, the law for slow β-rays is that of Whiddington [6] :

$$v_0^4 - v^4 = \frac{x}{\alpha}, \quad \ldots\ldots\ldots \quad (1)$$

where v_0, v are the velocities before and after travelling a distance x and α is a constant.

We can define the " range " D, where

$$v_0^4 = \frac{D}{\alpha} \quad \ldots\ldots\ldots \quad (2)$$

For single scattering, we can use Rutherford's [7] formula, which has been verified for β-rays by various experiments (*e.g.* [8]); this gives the chance of a deflexion through an angle between χ and $\chi+d\chi$ in a distance dx as

$$P(\chi)d\chi\,dx=\frac{A}{v^4}\cot\frac{\chi}{2}\operatorname{cosec}^2\frac{\chi}{2}d\chi dx \quad . \quad . \quad . \quad (3)$$

If we have a ray travelling in a direction at an angle θ to a given direction, and it is then deflected through an angle χ, considerations of solid geometry show that the chance that the resultant direction lies between ψ and $\psi+d\psi$ to the fixed direction is

$$\frac{1}{\pi}\frac{\sin\psi\,d\psi}{\sqrt{\{\cos(\theta-\chi)-\cos\psi\}\{\cos\psi-\cos(\theta+\chi)\}}} \quad . \quad . \quad (4)$$

We can now combine (3) and (4) and we find the chance that a ray at θ to the fixed direction shall, after travelling a distance dx, be deflected so as to be between ψ and $\psi+d\psi$ to the fixed direction.

This is

$$\int_{\theta-\psi}^{\theta+\psi}\frac{A}{v^4}\frac{1}{\pi}\frac{\sin\psi\,d\psi\cot\frac{\chi}{2}\operatorname{cosec}^2\frac{\chi}{2}d\chi\,dx}{\sqrt{\{\cos(\theta-\chi)-\cos\psi\}\{\cos\psi-\cos(\theta+\chi)\}}},$$

which gives:

$$\frac{2A}{v^4}\frac{\sin\psi\,d\psi\,(1-\cos\theta\cos\psi)}{(\cos\theta-\cos\psi)^3}dx \quad . \quad . \quad . \quad (5)$$

Similarly, the chance that a ray between θ and $\theta+d\theta$ to the fixed direction shall, after travelling dx, be moving at ψ to this direction is

$$\frac{2A}{v^4}\frac{\sin\theta\,d\theta\,(1-\cos\theta\cos\psi)}{(\cos\theta-\cos\psi)^3}dx \quad . \quad . \quad . \quad (6)$$

In order to proceed further, it is necessary to make some assumption in regard to the neglecting of certain small deflexions. There are two ways in which such assumptions can be made, and these will be considered in turn.

5. *Assumptions for First Method.*

We will assume that it is possible to choose a small angle ϵ such that we can neglect all deflexions which do

not alter the inclination to a fixed direction by more than ϵ. This is not the same as assuming that we neglect all deflexions of less than ϵ, for we may have a deflexion which does not change the inclination to the fixed direction, but which is still large (*i. e.*, a change which alters "longitude" without altering "latitude"). The assumption used is more convenient mathematically than the alternative assumption.

Then the chance of a deflexion which is not negligible in a distance dx is given by the integral of (5) outside the limits $\theta-\psi=\pm\epsilon$.

This gives

$$\frac{2A}{v^4}dx\left[\frac{1}{\epsilon^2}+\text{terms not involving }\epsilon\right]. \quad . \quad . \quad (7)$$

A difficulty arises in the particular case when the angle θ is zero, for then the integration must be from $\psi=\epsilon$ upwards, and this gives twice the above result. The difficulty can be got over provided we can assume that the angle θ is never exactly zero, but is always large compared with the small angle ϵ. Or else it is possible to say that we can neglect all deflexions such that the change in $\cos\theta$ is less than $\epsilon \sin\theta$; with this assumption, (7) becomes

$$\frac{2A}{v^4}dx\left[\frac{1}{\epsilon^2}+1\right] \quad . \quad . \quad . \quad . \quad . \quad . \quad (8)$$

Thus, after travelling a distance dx, the number N of β-rays in a beam will be altered by an amount

$$d\mathrm{N}=-\mathrm{N}.\frac{2A}{v^4}dx\left[\frac{1}{\epsilon^2}+1\right]. \quad . \quad . \quad . \quad . \quad (9)$$

Using (1) and (2), we get

$$d\mathrm{N}=-\mathrm{N}.\frac{2A\alpha}{(D-x)}dx\left[\frac{1}{\epsilon^2}+1\right], \quad . \quad . \quad . \quad (10)$$

where x is the distance already travelled by the beam.

If we put

$$2A\alpha\left[\frac{1}{\epsilon^2}+1\right]=n \quad . \quad . \quad . \quad . \quad . \quad (11)$$

we get

$$\mathrm{N}=\mathrm{N}_0\left(\frac{D-x}{D}\right)^n. \quad . \quad . \quad . \quad . \quad . \quad (12)$$

6. *Single Scattering.*

We can now discuss the reflexion coefficient due to single scattering in a reflector.

For the "fixed direction" of the preceding sections we will consider the normal to the reflector.

For reflexion by single scattering to occur, the β-ray must first travel from F to G, a distance $p \sec \phi$, without appreciable deflexion. From (12) the number doing so is

$$N=N_0\left(\frac{D-p \sec \phi}{D}\right)^n \quad . \quad . \quad . \quad . \quad . \quad (13)$$

Then there must be a deflexion in a thickness dp at G from an angle ϕ to the normal to an angle between

Fig. 2.

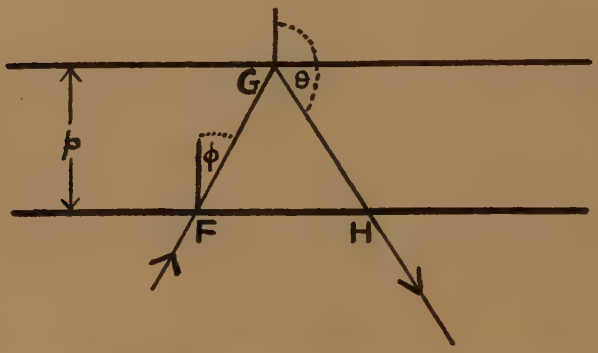

θ and $\theta+d\theta$ to the normal; the number so deflected is, from (5),

$$M=N\frac{2A}{v^4}\frac{\sin\theta\, d\theta\,(1-\cos\phi\cos\theta)}{(\cos\phi-\cos\theta)^3}dp \sec\phi. \quad . \quad (14)$$

Then the rays must travel from G to H, a distance of $-p \sec\theta$; the number so doing without deflexion is

$$P=M\left(\frac{D-p \sec\phi+p \sec\theta}{D-p \sec\theta}\right)^n \quad . \quad . \quad . \quad (15)$$

Using, from (1) and (2), $v^4=\frac{D-p \sec\phi}{\alpha}$, and (13), (14), and (15), we get

$$P=N_0\frac{2A\alpha}{D-p \sec\phi}\frac{\sin\theta\, d\theta\,(1-\cos\phi\cos\theta)}{(\cos\phi-\cos\theta)^3}dp \sec\phi \left(\frac{D-p \sec\phi+p \sec\theta}{D}\right)^n \quad . \quad . \quad (16)$$

This gives the contribution to the reflexion due to those β-rays deflected in a thickness dp at a depth p from a direction ϕ to a direction θ. To obtain the total reflexion coefficient this must be integrated for all values of p and all values of θ.

The integration with respect to p requires

$$\int\left(\frac{\mathrm{D}-p\sec\phi+p\sec\theta}{\mathrm{D}}\right)^n\frac{dp}{\mathrm{D}-p\sec\phi},$$

the limits for p being zero and such a distance that the total path of the β-rays is equal to its range, *i. e.*, such that $p\sec\phi-p\sec\theta=\mathrm{D}$.

Putting $\frac{p}{\mathrm{D}}=k$ we have

$$\int_0^{\frac{1}{\sec\phi-\sec\theta}}\frac{\{1-k(\sec\phi-\sec\theta)\}^n}{1-k\sec\phi}\,dk.$$

Now let $1-k(\sec\phi-\sec\theta)=y$

$$dk=-\frac{dy}{\sec\phi-\sec\theta},$$

and the limits for y are 1 and 0.

We have

$$\int_1^0\frac{-y^n\,dy}{(1-k\sec\phi)(\sec\phi-\sec\theta)}.$$

Integration by parts gives

$$-\left[\frac{y^{n+1}}{(n+1)(\sec\phi-\theta)(1-k\sec\phi)}\right]_1^0$$

$$-\int_1^0\frac{y^{n+1}\sec\phi\,dy}{(n+1)(\sec\phi-\sec\theta)^2(1-k\sec\phi)^2}. \quad . \quad . \quad (17)$$

It can easily be seen that successive integration by parts gives a series whose terms become successively smaller, and if n is large, each term is small compared with the preceding and can be neglected, leaving just the first term, which gives

$$\frac{1}{(n+1)(\sec\phi-\sec\theta)}. \quad . \quad . \quad . \quad . \quad (18)$$

In Schonland's case, we can put $\phi=0$ in (16) and (18) and the total reflected fraction becomes

$$\int_{\frac{\pi}{2}}^{\pi} 2A\alpha \frac{\sin\theta\, d\theta\,(1-\cos\theta)}{(1-\cos\theta)^3} \sec\phi \frac{1}{(n+1)(1-\sec\theta)}$$

$$=-\frac{2A\alpha}{n+1}\int_{\frac{\pi}{2}}^{\pi}\frac{\sin\theta\, d\theta\cos\theta}{(1-\cos\theta)^3}$$

which is

$$\frac{A\alpha}{4(n+1)}. \quad . \quad . \quad . \quad . \quad . \quad . \quad . \quad (19)$$

Or, using (11) and neglecting small terms, the reflected fraction due to single scattering in Schonland's case is

$$\frac{A\alpha}{4\frac{2A\alpha}{\epsilon^2}}=\frac{\epsilon^2}{8}. \quad . \quad . \quad . \quad . \quad . \quad . \quad . \quad (20)$$

Now, using (6) in place of (5) and putting $\theta=\pi$ for Riehl's case, we have

$$\int_0^{\frac{\pi}{2}} +2A\alpha \frac{\sin\phi\, d\phi(1+\cos\phi)\sec\phi}{(\cos\phi+1)^3(n+1)(1+\sec\phi)}$$

$$=+\frac{2A\alpha}{(n+1)}\int_0^{\frac{\pi}{2}}\frac{\sin\phi\, d\phi}{(1+\cos\phi)^3}. \quad . \quad . \quad . \quad . \quad . \quad (21)$$

$$=\frac{3A\alpha}{4(n+1)}=\frac{3\epsilon^2}{8}. \quad . \quad . \quad . \quad . \quad . \quad . \quad . \quad . \quad (22)$$

Comparing with (20), we see that Riehl's case gives a reflexion due to single scattering which is three times that of Schonland's case.

7. *Double and Multiple Scattering.*

It is clear that it is necessary to consider the cases in which there is more than one deflexion that cannot be neglected. If we consider the case of two deflexions, we can write down a result corresponding to (16), namely,

$$P=N_0\frac{2A\alpha}{D-p\sec\phi}$$

$$\cdot\frac{2A\alpha}{D-p\sec\phi-q\sec\psi}\frac{\sin\psi\, d\psi(1-\cos\phi\cos\psi)}{(\cos\phi-\cos\psi)^3}dp\sec\phi$$

$$\cdot \frac{\sin\theta\, d\theta(1-\cos\psi\cos\theta)}{(\cos\psi-\cos\theta)^3}\, dq \sec\psi$$

$$\cdot \left(\frac{D-p\sec\phi-q\sec\psi+(p+q)\sec\theta}{D}\right)^n \quad . \quad . \quad . \quad (23)$$

for the case where it is the second deflexion that alters the direction from forwards to backwards, and a somewhat similar expression for the case where ψ is greater than $\pi/2$. (23) can be integrated with respect to p and q by methods similar to those of the last section; then integration with respect to ψ from $\phi \pm \epsilon$ to 0 or $\pi/2$ gives a result which can be integrated with respect to θ or ϕ to give the results for the cases of Schonland and Riehl respectively.

Fig. 3.

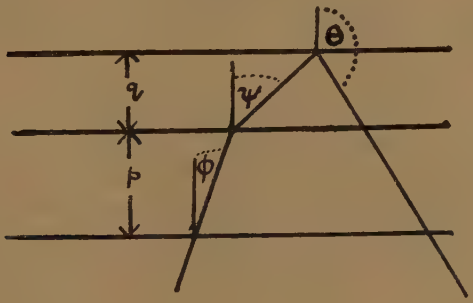

It is found that, considering together the two cases of ψ greater or less than $\pi/2$, the reflected fraction in either case for double scattering is just the same as for single scattering, namely $\epsilon^2/8$ for Schonland's case and $3\epsilon^2/8$ for Riehl's case.

The extension of the same principles to scatterings more than two-fold can be shown to give the same results, so that the total effect of reflexion in Schonland's case is the sum of a number of terms each $\epsilon^2/8$, while in Riehl's case the terms are $3\epsilon^2/8$. It does not seem possible to get a value for the actual reflexion coefficient, for the terms are all $\epsilon^2/8$, and it is not possible to determine where to stop the summation. Although the term $\epsilon^2/8$ is accurately true when ϵ is small, it may be that the next term, involving ϵ^4, may be important for many deflexions,

and perhaps the series to be summed may consist of terms not quite equal, and hence perhaps it may be possible to obtain a sum. Unfortunately it is not feasible to obtain the value of the second term except for single scattering, when it is $\epsilon^4\left[\frac{1}{8}-\frac{1}{24A\alpha}\right]$ in Schonland's case and $\epsilon^4\left[\frac{3}{8}-\frac{1}{24A\alpha}\right]$ in Riehl's case.

The only conclusion that can be reached is that the ratio of the reflexion coefficients must be very close to 1 : 3, and hence, if, for any base, Schonland's reflexion coefficient is known, then for Riehl's case it can be obtained and used.

It is, however, important to verify that the methods used in this calculation are suitable for the purpose and can give a reflexion coefficient of the same order of magnitude as the experimental values. Therefore an approximate method of calculation is considered in the next section.

8. *Second Method.*

We will now assume that it is possible to neglect all deflexions through less than $\pi/2$, and that a deflexion through more than $\pi/2$ removes the β-ray from the beam.

The chance of an appreciable deflexion then becomes

$$\frac{A}{v^4}dx=\frac{A\alpha}{(D-x)}dx. \quad . \quad . \quad . \quad . \quad (24)$$

Comparing with (10), we have to replace (11) by

$$A\alpha=n, \quad . \quad . \quad . \quad . \quad . \quad . \quad . \quad (25)$$

and now (12) still holds.

Single scattering can be discussed in a similar way to that of section 6, except that n is no longer large, and hence we cannot neglect the terms after the first in the integration (17). Instead we obtain the series

$$\frac{1}{(n+1)(\sec\phi-\sec\theta)}+\frac{\sec\phi}{(n+1)(n+2)(\sec\phi-\sec\theta)^2}$$
$$+\frac{2\sec^2\phi}{(n+1)(n+2)(n+3)(\sec\phi-\sec\theta)^3}$$
$$+\frac{6\sec^3\phi}{(n+1)(n+2)(n+3)(n+4)(\sec\phi-\sec\theta)^4}+\ldots \quad (26)$$

For Schonland's case $\phi=0$ and we have

$$-\int_{\frac{\pi}{2}}^{\pi} \frac{2A\alpha \sin\theta\, d\theta}{(1-\cos\theta)^2}\left[\frac{\cos\theta}{(n+1)(1-\cos\theta)}\right.$$

$$-\frac{\cos^2\theta}{(n+1)(n+2)(1-\cos\theta)^2}+\frac{2\cos^3\theta}{(n+1)(n+2)(n+3)(1-\cos\theta)^3}$$

$$\left.-\frac{6\cos^4\theta}{(n+)(n+2)(n+3)(1-\cos\theta)^4}\cdots\right], \quad \ldots \quad (27)$$

which gives

$$\frac{2A\alpha}{(A\alpha+1)}\left[\frac{1}{8}+\frac{1}{(A\alpha+2)24}+\frac{1}{(A\alpha+2)(A\alpha+3)64}\right.$$

$$\left.+\frac{1}{(A\alpha+2)(A\alpha+3)(A\alpha+4)160}+\ldots\right]. \quad (28)$$

In the same way, Riehl's case gives

$$\frac{2A\alpha}{(A\alpha+1)}\left[\frac{3}{8}+\frac{7}{(A\alpha+2)24}+\frac{15}{(A\alpha+2)(A\alpha+3)64}\right.$$

$$\left.+\frac{31}{(A\alpha+2)(A\alpha+3)(A\alpha+4)160}+\ldots\right]. \quad (29)$$

We see that if $A\alpha$ is large the reflexion coefficient in Schonland's case comes to 25 per cent. and in Riehl's case to 75 per cent., while for smaller values of $A\alpha$ the coefficients are smaller. If $A\alpha$ is very small, the ratio is the ratio of the series

$$\frac{1}{8}+\frac{1}{48}+\frac{1}{6.64}+\frac{1}{24\,.\,160}$$

and

$$\frac{3}{8}+\frac{7}{48}+\frac{15}{6\,.\,64}+\frac{31}{24\,.\,160}+\ldots,$$

which gives a ratio of 3·8 for the two coefficients. Thus it seems that this approximate method of calculation gives a ratio for all metals not very far from 3.

To carry out calculations in a particular case it is necessary to obtain values for A and α. A can be obtained from Rutherford's formula and is given by

$$A=\frac{\pi n Z^2 e^4}{m}, \quad \ldots \quad (30)$$

where n is the number of atoms per c.c. in the metal, Z the atomic number, e the electronic charge, and m the electronic mass. For aluminium, $A = 2{\cdot}04 \times 10^{42}$.

For the constant α, the experiments of Terrill [9] give $\alpha = 1{\cdot}4 \times 10^{-43}$ for aluminium, and other results agree with this; so that for aluminium the product $A\alpha$ is about ·28.

We thus get, for Schonland's case, a reflexion coefficient of ·064 = 6·4 per cent., or one-half of the experimental value. For Riehl's case the result is ·206 = 20·6 per cent.

It is clear that this method must be expected to give results which are less than the correct result, for we have neglected all deflexions except those due to one scattering of over $\pi/2$; neglected deflexions and effects due to more than one scattering must contribute appreciably, and hence it is not surprising that the result obtained is less than the true result.

7. *Conclusion.*

Experimentally, Schonland has found that the reflexion coefficient for aluminium under his conditions is 13 per cent. The above results show that the reflexion coefficient in Riehl's case must be about three times this, possibly slightly more, so that we can state that the reflexion coefficient is probably about 40 per cent. It may be pointed out that the use of this coefficient with the results of Riehl [2] gives a value of less than one recorded β-ray per disintegration, as might be expected, since some β-ray will be missed.

The author wishes to express his thanks to Dr. C. D. Ellis, F.R.S., whose interest in the problem first suggested the investigation; and to Mr. J. L. Burchnell and Dr. H. P. Mulholland, who have given help in some of the mathematical points.

References.

(1) Emeléus, Proc. Camb. Phil. Soc. xxii, p. 300 (1924).
(2) Riehl, *Zeit. fur. Phys.* xlvi. p. 479 (1928).
(3) Kovarik, Phil. Mag. xx. p. 849 (1910).
(4) Schonland, Proc. Roy. Soc. cviii. p. 187 (1925).
(5) Chalmers, Proc. Camb. Phil. Soc. xxvi. p. 252 (1930).
(6) Whiddington, Proc. Roy. Soc. lxxxix. p. 554 (1918).
(7) Rutherford, Phil. Mag. xxi. p. 669 (1911).
(8) Schonland, Proc. Roy. Soc. cxiii. p. 87 (1926).
(9) Terrill, Phys. Rev. xxii. p. 101 (1923).

XXVII. *On the Nature of Intermetallic Compounds of the Type Mg_2Sn. By* William Hume-Rothery, *D.Sc., F.R.S., and* Geoffrey Vincent Raynor, *B.A., B.Sc.**

IT is well known that, when alloyed with the metalloid elements of Groups IV B, V B, and VI B, many metals form intermetallic compounds with the formulæ to be expected from the normal valencies—*e. g.*, Mg_2Si, Mg_3Sb_2. In general the stability of such compounds is greater the more electro-positive the metal and the more electro-negative the metalloid. The form of the equilibrium diagrams is in agreement with the view that compounds of the above type are an extension of normal valency compounds (ionic or co-valent) into the region of the weakly electro-negative elements, of which the negative ions or co-valent bonds are comparatively unstable [1]. More recently Mott and Jones [2] have suggested that compounds of the type Mg_2Sn, Mg_2Pb, Mg_2Si, Mg_2Ge, with the fluor-spar structure, are better regarded, not as ionic compounds, but as electron compounds † characterized by a completely filled first Brillouin zone, which contains 8/3 electron states per atom. The high electrical resistance of these compounds is considered to be due to a completed zone with no unoccupied states. This is regarded as shown by the fact that the molten alloy for which the zone structure would be destroyed has about the same conductivity as molten tin. The conductivity of the molten alloy would, however, be equally in agreement with the conception of an ionic or co-valent compound which broke down on melting with the liberation of free electrons. We shall accept here the point of view that all compounds and crystals are examples of the general process of binding atoms together, and that the different types, ionic, co-valent, metallic etc., represent extremes in which one factor predominates, and so enables the mathematical treatment to be simplified. Great interest attaches to compounds of the type Mg_2Sn, which may be regarded from different points of view, and

* Communicated by the Authors.

† The term "electron compound" is used to denote a phase the structure of which is determined mainly by the ratio of valency electrons to atoms.

it seemed of value to investigate whether the compound Mg_2Sn would give rise to homogeneous ternary alloys of the same electron concentration. It is well known that in copper and silver alloys ternary electron compounds can be obtained provided that the atomic diameters of the various atoms do not differ too widely. Thus Bradley and Gregory [3] were able to obtain homogeneous copper-aluminium-tin γ-phases provided that the proportions of the constituents were adjusted to maintain the valency-electron/atom ratio of approximately 21/13, which is the characteristic of the γ-structure ; similar phenomena have been found in other ternary alloys. For the compound Mg_2Sn aluminium and indium are suitable for this investigation. The atomic diameters are such that indium is well within and aluminium on the border-line of the zone of favourable size-factor * for magnesium. In the binary systems magnesium-indium and magnesium-aluminium wide solid solutions are formed in magnesium, and, since intermediate phases of variable composition exist, the replacement of atoms of magnesium by those of indium or aluminium is clearly possible under some conditions.

Ternary Magnesium-Tin-Aluminium Alloys.

Alloys of the compositions shown in Table I. were prepared by melting the constituent metals under flux in alumina crucibles. They were cast into heavy copper moulds bored with 3/8″ diameter holes, and in this way a very fine microstructure was obtained. In the cast state all the alloys were two-phase. Owing to the presence of a low melting eutectic, annealing cannot be carried out at high temperatures, and the alloys were therefore annealed in evacuated sealed tubes for $4\frac{1}{2}$ weeks at 176° C., after which they were rapidly cooled in a blast of cold air, examined microscopically, and submitted to chemical analysis. All the alloys were clearly two-phase, and on etching with very dilute alcoholic nitric acid they were shown to contain small particles of a light etching constituent embedded in a ground-mass

* In general, if the atomic diameters of two metals differ by more than about 14–15 per cent., substitutional solid solutions are very restricted. If the atomic diameters are within those limits, the size-factor is said to be favourable, and solid solutions may be formed if other factors are favourable. See reference (1), page 52.

of dark etching Mg_2Sn, and the relative amounts of the second constituent were not in the same order as the divergence of the electron concentration, from the ratio 8/3.

It will be noted that the electron concentration of alloys 2 and 3 is 2·669, and this is very near to the value 8/3=2·667. Additional alloys were prepared containing approximately 4 and 6 atomic per cent. of aluminium, with an electron concentration of 8/3. After annealing, these were also two-phase, and the relative amount of the light etching constituent increased with increasing aluminium content. These alloys were not analysed, since the results for the alloys given in Table I. show clearly that the compound Mg_2Sn does not give

TABLE I.

No. of alloy.	Composition in atomic (%)			Electron concentration.
	Sn.	Mg.	Al.	
1	33·07	64·66	2·27	2·684
2	32·35	65·37	2·28	2·669
3	32·24	65·34	2·42	2·669

The analyses were carried out by Messrs. Johnson, Matthey & Co., Ltd. All three metals were determined, and the totals of the percentages found experimentally lay between the limits 99·95 and 99·97.

rise to any appreciable ternary magnesium-aluminium-tin solid solution even though the composition is adjusted to maintain an electron concentration 8/3.

Ternary Magnesium-Tin-Indium Alloys.

Alloys of the compositions shown in Table II. were prepared in the same way as the magnesium-tin-aluminium alloys, and were annealed for six weeks at 186°. All the alloys were two-phase, both in the "as cast" state and after annealing, the second constituent appearing as small white particles in a ground-mass of Mg_2Sn. Alloys nos. 1 and 2 have very nearly the required electron concentration of 2·667.

From the above experiments it is clear that, in marked contrast to the β- and γ-phases of copper, silver, and gold

alloys, the compound Mg_2Sn forms little or no ternary solid solution with indium or aluminium, even though the compositions are adjusted so that an electron concentration of approximately 8/3 is maintained. We have also failed to prepare homogeneous alloys of the type $Mg[SnPb]_2$, using similar methods to the above.

The crystal structures of these compounds are also of interest. The compounds MgS and MgSe have the sodium chloride type of crystal structure, whilst MgTe has the Wurtzite structure. The crystal structures of the compounds Mg_2Si, Mg_2Ge, Mg_2Sn, and Mg_2Pb are anti-isomorphous with that of fluor-spar CaF_2. The structures of the compounds Mg_3P_2 and Mg_3As_2 are anti-isomorphous with that of Sc_2O_3, whilst those of Mg_3Sb_2 and Mg_3Bi_2 are anti-isomorphous with that of

TABLE II.

No. of alloy.	Composition in atomic (%).			Electron concentration.
	Sn.	Mg.	In.	
1	32·90	65·14	1·96	2·676
2	32·93	65·13	1·95	2·678
3	35·06	62·85	2·09	2·722
4	36·84	61·10	2·06	2·757

The analyses were carried out by Messrs. Johnson, Matthey & Co., Ltd. All three metals were determined, and the totals of the percentages found experimentally lay between 99·96 and 100·02.

La_2O_3. In general, therefore, the types of structure * formed by these compounds are in agreement with the view that they are an extension of normal valency-compounds into the region of weakly electro-negative elements, and this is supported by many regularities in the melting points, heats of formation, and the relative stabilities of the compounds. In any case the experiments described above indicate that as regards its capability of forming ternary solid solutions of approximately constant electron concentrations the compound Mg_2Sn has entirely different properties from the electron compounds of copper and silver alloys.

* In the theoretical work of Mott and Jones the type of crystal structure is not predicted, but is assumed as the basis of the calculations.

Acknowledgements.

The authors must express their gratitude to Professor C. N. Hinshelwood, F.R.S., for his kindness in giving them laboratory accommodation and many other facilities which have encouraged them in this work. One author (W. H.-R.) must thank the Royal Society for election to a Research Fellowship, whilst thanks are also due to the Department of Scientific and Industrial Research and the British Non-Ferrous Metals Research Association for generous grants made to the authors individually to assist their research work Grateful acknowledgement is also made to Mr. A. R. Powell of Messrs. Johnson, Matthey & Co., Ltd., for his skill in connexion with the chemical analysis.

References.

1) See W. Hume-Rothery, 'The Structure of Metals and Alloys,' London, Institute of Metals (1936).
(2) W. P. Mott and H. Jones, 'The Theory of Metals and Alloys.' Oxford, 1936, p. 170.
(3) A. J. Bradley and C. H. Gregory, Proc. Manchester Phil. Soc. lxxii. p. 91 (1927–8).

The Old Chemistry Department,
The University Museum, Oxford.
September, 1937.

XXVIII. *Capacitance at Ultra-High Frequencies* *. *By* Ronold King, *A.B., M.S., Ph.D., John Simon Guggenheim Fellow, Berlin,* 1937 ; *Cruft Laboratory, Harvard University, Cambridge, Massachusetts, U.S.A.,* 1938 †.

Summary.

An approximate formula is derived from the Maxwell equations for the input admittance of a circular parallel-plate condenser as a function of frequency. A simple equivalent circuit is shown which represents well the input admittance down to centimetre waves. Restrictions on the dimensions of the plates and on the properties of the dielectric medium between them are considered, and reference is made to the measurement of dielectric

* Presented in part at the meeting of the U. R. S. I. and I. R. E. Washington, D.C., April 30, 1937.
† Communicated by the Author.

constants by the condenser method. An approximate expression is derived for predetermining the input reactance of a multiple-plate condenser from its static characteristics. Computed results for a General Radio Precision condenser and for a specially designed tuning unit are compared with the corresponding experimental ones measured at several ultra-high frequencies.

IN a recent paper [1] the properties of a variable air condenser were studied at radio frequencies. It is the purpose of this paper to extend the investigation to ultra-high frequencies. This will be done by examining the input admittance, first, of a circular parallel-plate condenser as a function of frequency and dimensions, second, of a number of such condensers joined to form a variable condenser. The analysis is concluded by computing the reactance curves of a General Radio Precision condenser and of a specially designed tuning unit at ultra-high frequencies, and by comparing these with experimentally measured curves.

A. *The Input Admittance of a Circular Condenser.*

Consider the problem of the input admittance, Y, as a function of the angular frequency, $\omega=2\pi f$, and as defined by the relation

$$Y=I(\omega)/V(\omega) \quad . \quad . \quad . \quad . \quad . \quad . \quad (1)$$

for a circular parallel-plate condenser. Let the following notation be introduced :

a=radius, d=separation of the condenser plates ;

c=velocity of light ; $\beta=\omega/c=2\pi/\lambda$;

$\mu=1$ throughout all material involved ;

$\epsilon=\epsilon'-j\sigma/\omega$=effective complex dielectric constant [2] ;

$\sigma=\sigma_1+\omega\epsilon''$=effective conductivity ;

$n=\sqrt{\epsilon}$; $n'=\sqrt{\epsilon'}$.

If it is assumed that voltage and current are both sinusoidal functions of the time, the instantaneous values of the electric intensity, $\underline{E}$, and of the magnetic flux density, $\underline{B}$, are given by the real parts of

$$\underline{E}_i=\underline{E}e^{j\omega t}; \quad \underline{B}_i=\underline{B}e^{j\omega t}. \quad . \quad . \quad . \quad . \quad (2)$$

For this sinusoidal dependence upon time two of the Maxwell equations may be written in the form [3]

$$\text{curl } \underline{B} = j\omega\epsilon\underline{E}/c, \quad . \quad . \quad . \quad . \quad . \quad . \quad (3)$$

$$\text{curl } \underline{E} = -j\omega\underline{B}/c. \quad . \quad . \quad . \quad . \quad . \quad (4)$$

Let the condenser be oriented with respect to a system of cylindrical coordinates, r, θ, z, so that the positive z-axis is directed down through the centres of the circular plates (fig. 1). The expressions for the z-components of (3) and (4) are respectively

$$\text{curl}_z\underline{B} = (1/r)(\partial r B_\theta/\partial r - \partial B_r/\partial\theta) = j\omega\epsilon E_z/c, \quad . \quad . \quad . \quad (5)$$

$$\text{curl}_\theta\underline{E} = (\partial E_r/\partial z - \partial E_z/\partial r) = -j\omega B_\theta/c. \quad . \quad . \quad . \quad (6)$$

Fig. 1.

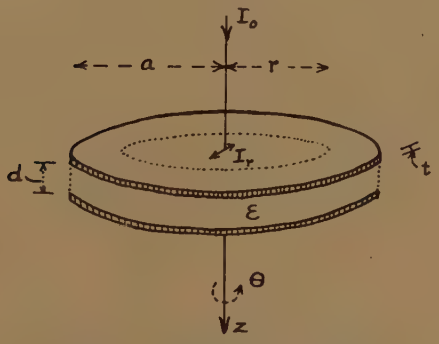

Diagram of parallel-plate condenser.

With cylindrical symmetry B_r is independent of θ. Let it be assumed that the condenser plates are such good conductors that the approximation, $E_r = 0$, is a good one. This reduces (5) and (6) to

$$dE_z/dr = j\omega B_\theta/c, \quad . \quad . \quad . \quad . \quad . \quad . \quad (7)$$

$$d/dr(rB_\theta) = j\omega\epsilon rE_z/c. \quad . \quad . \quad . \quad . \quad . \quad (8)$$

Upon combining (7) with (8), and introducing the new independent variable,

$$x = \omega r\sqrt{\epsilon}/c = \beta nr, \quad . \quad . \quad . \quad . \quad . \quad (9)$$

one obtains the Legendre equation,

$$d^2E_z/dx^2 + 1/x dE_z/dx + E_z = 0, \quad . \quad . \quad . \quad (10)$$

which has the solution

$$E_z = E_0 J_0(x). \quad . \quad . \quad . \quad . \quad . \quad . \quad . \quad (11)$$

The amplitude, E_0, is evaluated by noting that the Bessel's function, $J_0(x)=1$ at $x=r=0$, so that E_0 is the value of E_z at the centre of the condenser.

In order to derive an expression for the amplitude of the current flowing down into the centre of the upper condenser plate one proceeds from the Maxwell equation,

$$\text{div}\,\epsilon\underline{E} = 0. \quad . \quad . \quad . \quad . \quad . \quad . \quad . \quad (12)$$

With the aid of the divergence theorem [4], this becomes

$$\int \text{div}\,\epsilon\underline{E}\,dv = \int \epsilon E_n\,da = 0. \quad . \quad . \quad . \quad . \quad (13)$$

Here dv is an element of volume, da is an element of the surface enclosing the volume, E_n is the component of $\underline{E}$ along the exterior normal to the surface. Let this surface be a flat cylinder enclosing a circular section of radius, r, of the lower surface of the upper condenser plate. Let it be assumed that the current flows in a very thin layer along the surface of the conductor, so that current enters the thin cylinder of integration only radially [5]. Integration over this surface then includes the following terms :

$$\int_0^{2\pi} \epsilon E_r t r\,d\theta + \int_0^r \epsilon(-E_z) 2\pi r\,dr + \int_0^r \epsilon E_z 2\pi r\,dr = 0. \quad (14)$$

Here the first integral is extended over the thin sides of thickness, t, of the surface of integration, the second integral is in the condenser plate, the third is in the dielectric just below the plate [6]. In each integral the appropriate values of ϵ (*i. e.*, of σ and ϵ') must, of course, be used, depending upon whether the medium concerned is copper, air, or the dielectric between the plates.

Since the conductivity of copper is large it follows that in the plates $\epsilon \doteq -j\sigma_c/\omega$. The first integral in (14) then becomes

$$\int_0^{2\pi} \sigma_c E_r t r\,d\theta/c = I_r, \quad . \quad . \quad . \quad . \quad . \quad (15)$$

where I_r is the total outward current traversing radially any circumference-section of the plate.

Since the current is assumed to flow only in a thin layer on the surface of the conductor, the second integral will vanish with $E_z \doteq 0$ in the copper plates.

Upon combining (14) and (15) one has

$$I_r = j\omega/c \int_0^r \epsilon E_z 2\pi r\, dr. \quad . \quad . \quad . \quad . \quad . \quad (16)$$

By now introducing the value of E_z from (11), and making use of the relation [7]

$$\int_0^x x J_0(x)\, dx = x J_1(x), \quad . \quad . \quad . \quad . \quad (17)$$

one obtains, with (9),

$$I_r = (2\pi j\omega\epsilon E_0/c\beta n) r J_1(\beta n r). \quad . \quad . \quad . \quad . \quad (18)$$

At the edge of the plate, where $r=a$, $I_r = I_a = 0$. Hence

$$I_0 = (j\omega S\epsilon E_0/c)(2/\beta n a) J_1(\beta n a). \quad . \quad . \quad . \quad (19)$$

Here I_0 is the current amplitude entering the centre of the plates, $S = \pi a^2$ is the area of the plate, and ϵ is the value in the dielectric [8].

The general expression for E_z in terms of the scalar potential, V, and the vector potential, $\underline{A}$, is [9]

$$E_z = -\partial V/\partial z - j\omega A_z/c. \quad . \quad . \quad . \quad . \quad (20)$$

It can be shown [10] that

$$E_z \doteq -\partial V/\partial z \quad . \quad . \quad . \quad . \quad . \quad (21)$$

is a good approximation, provided that

$$(\omega d/c)^2 << 1. \quad . \quad . \quad . \quad . \quad . \quad . \quad (22)$$

Assuming this relation to be satisfied, the potential difference, V_a, between the plates at their outer edges where $r=a$ is given by

$$V_a = (V_0 - V_d) = \int_0^d E_z dz = E_z d. \quad . \quad . \quad (23)$$

Upon using (11) written for $r=a$, one has

$$V_a = E_0 d J_0(\beta n a). \quad . \quad . \quad . \quad . \quad . \quad (24)$$

Now let the input admittance, Y, of the condenser be defined to be the ratio of the current entering at the centre to the voltage difference between the plates at the edge, *i. e.* [11],

$$Y = cI_0/V_a. \quad . \quad . \quad . \quad . \quad . \quad . \quad (25)$$

Using (19) and (24) one obtains [12]

$$Y = j\omega\epsilon(S/d)(2/\beta na)J_1(\beta na)/J_0(\beta na). \quad . \quad . \quad (26)$$

Let a frequency factor, α, be defined by the relations

$$\alpha = \alpha_r - j(\sigma/\omega\epsilon')\alpha_i = (\epsilon/\epsilon')(2/\beta na)J_1(\beta na)/J_0(\beta na) \quad . \quad . \quad (27)$$

By a rather tedious manipulation of the Bessel's functions of complex argument it can be shown that the factors, α_r and α_i, assume the following values in terms of Bessel's functions of the real argument, $X = \beta n' a$. These are shown plotted in fig. 2.

$$\alpha_i = (2/X)J_1^2(X)/J_0^2(X) - J_1(X)/J_0(X) + 1, \quad . \quad . \quad (28)$$

$$\alpha_r = (2/X)J_1(X)/J_0(X), \quad . \quad . \quad . \quad . \quad . \quad . \quad . \quad . \quad . \quad (29)$$

Fig. 2.

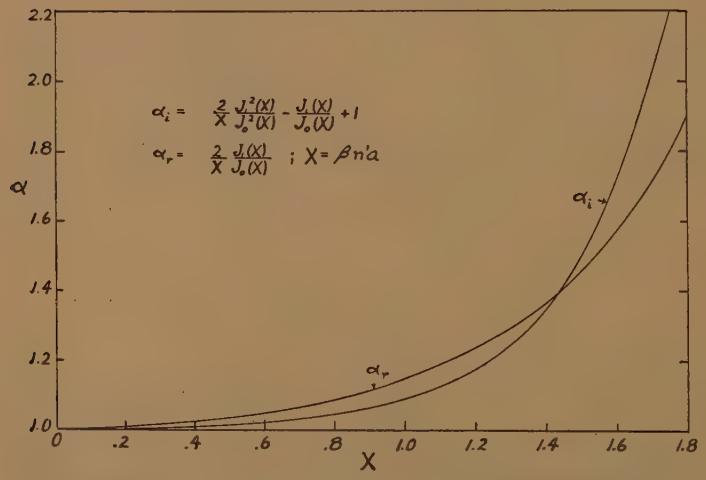

Components of the frequency factor of a circular parallel-plate condenser : $\alpha = \alpha_r - j(\sigma/\omega\epsilon')\alpha_i$.

provided that

$$(\sigma/\omega\epsilon')^2 J_1(X)/J_0(X) << 1. \quad . \quad . \quad . \quad . \quad . \quad (30)$$

Using this notation, and assuming that (30) is satisfied, (26) becomes

$$Y = g - jb = G\alpha_i - j\omega C\alpha_r \quad . \quad . \quad . \quad . \quad . \quad (31)$$

with

$$G = \sigma S/d \; ; \; C = \epsilon' S/d. \quad . \quad . \quad . \quad . \quad . \quad (32)$$

In (32) Y, G, and C are in rational electromagnetic units. Since the α's are numerical factors it is now easy

to change these three quantities to practical units by means of the following relations between quantities expressed in the two systems :—

$$Y, G, C \text{ (rat. units)} = (4\pi c^2/10^9)\ Y, G, C \text{ (prac. units)}. \quad (33)$$

with Y and G in mhos and C in farads. In particular

$$C(\text{farads}) = (\epsilon' S/d)(10^9/4\pi c^2). \quad (34)$$

Upon expanding (28) and (29) it can be shown that if

$$X^4 \ll 192, \text{ or } a \leq \lambda/5n' \quad (35)$$

one has

$$\alpha_i \doteq 1/(1+X^3/16), \quad (36)$$

$$\alpha_r \doteq 1/(1-X^2/8). \quad (37)$$

Continuing entirely in practical units, it is now readily verified that (37) leads to

$$\alpha = 1/(1-\omega^2 LC). \quad (38)$$

Here L, the inductance due to skin effect in the plates, is given by the simple formula

$$L = (d/2) \times 10^{-9} \text{ henries}. \quad (39)$$

Hence the input admittance, Y, of the condenser is given by

$$Y = g + j\omega C/(1-\omega^2 LC) \text{ mhos}. \quad (40)$$

This is exactly the input admittance of the circuit of fig. 3. In (40) C is defined by the static formula (34), L by (39), and g by

$$g = G/[1+\tfrac{1}{2}(\pi n' a/\lambda)^3] \text{ mhos} \quad (41)$$

with

$$G = \sigma(S/d)(10^9/4\pi c^2) \text{ mhos}. \quad (42)$$

In (42) σ is in mho-cm. The restrictions imposed include (23), (35), and (30). If (35) is satisfied (30) reduces to

$$(\sigma/\omega\epsilon')(4\pi c^2/10^9) \ll 1, \quad (43)$$

where σ is in mho-cm. and ϵ' is the value relative to vacuum.

To illustrate the nature of these restrictions let $\omega = 3 \times 10^9$ or $\lambda = 63$ cm. Then (23) requires $d \leqq 1$ cm.; (35) requires $a \leqq 12{\cdot}6$ cm. for $\epsilon' = 1$ (air), $a \leqq 1{\cdot}4$ cm. for $\epsilon' = 80$ (water); (43) requires $\sigma \leqq 3 \times 10^{-6}$ for $\epsilon' = 1$, $\sigma \leqq 2{\cdot}4 \times 10^{-4}$ for $\epsilon' = 80$. Evidently these restrictions

are not severe even at this high frequency, and (40), or its diagrammatic equivalent (fig. 3), is a widely useful approximation. Thus, at frequencies which are sufficiently high to make the static representation of a condenser as a pure capacitance inadequate, it may be treated as a capacitance in series with an inductance. In any case the error introduced by neglecting the inductance due to skin-effect in the plates is easily evaluated using (40) and (39).

Fig. 3.

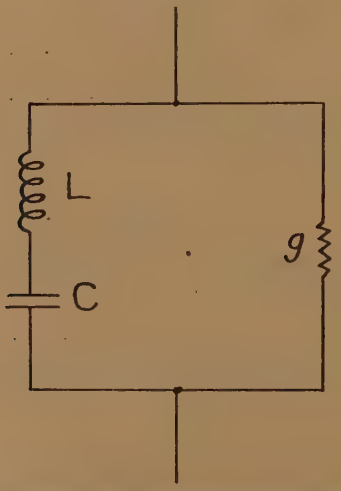

Equivalent circuit of the circular parallel-plate condenser.

B. *Application to the Measurement of Dielectric Constants.*

A common method for measuring dielectric constants is that in which the capacitance of a parallel plate condenser is measured both with and without the medium of unknown dielectric constant between its plates. Using circular plates this method may be extended to ultra-high frequencies if the input susceptance, b, of the condenser is measured with and without the medium in question between its plates. If C_0 is the statical capacitance in air, then the susceptances, respectively, in air and in the medium of dielectric constant, ϵ, are

$$b_0 = -\omega C_0/(1-\omega^2 L C_0), \quad . \quad . \quad . \quad . \quad (44)$$

$$b_\epsilon = -\omega \epsilon' C_0/(1-\omega^2 L \epsilon' C_0). \quad . \quad . \quad . \quad (45)$$

The ratio, b_ϵ/b_0, leads to a simple equation which may be solved for ϵ'. The solution is

$$\epsilon' = A/[1-\omega^2 LC_0(A-1)], \quad . \quad . \quad . \quad . \quad (46)$$

where $A = b_\epsilon/b_0$. The susceptances, b_0 and b_ϵ, must be measured between the centres of the condenser plates. This may be done using a parallel wire system [13] provided the input reactance of the leads to the condenser plates is first determined.

C. *The Input Reactance of Multiple-Plate Condensers.*

The multiple-plate condenser resembles a pile of two-plate condensers. The plates are, however, usually not circular, and stack and rotor rods are provided for connecting them in two parallel groups. In attempting to predict the input characteristics of tuning units of this kind from their dimensions and static characteristics two types of effect must be considered. The first of these is associated with a skin-effect phenomenon resembling that already discussed for circular plates; the second is related to the enormous change in the relative orders of magnitude of inductive reactance (due largely to stack and rotor rods and connecting leads) and capacitive reactance of the condenser proper as the frequency is increased. At sufficiently high frequencies the low-frequency concepts of lumped circuit parameters and of series circuits become quite meaningless. This effect is illustrated in fig. 4, which shows the measured input susceptance of a small five-plate, 15 mmf. condenser [13] compared with the calculated static susceptance, ωC_0.

The equivalent circuit diagram of an idealized multiple-plate condenser is that of a recurrent network, as illustrated in fig. 5, *a*. Following the method of Ollendorf [14], it is easily shown that the characteristic impedance of the network of fig. 5, *a*, is given by

$$N = \sqrt{z/y}. \quad . \quad . \quad . \quad . \quad . \quad . \quad . \quad (47)$$

This is precisely the same in form as the characteristic impedance of a parallel line with impedance, z, along, and admittance, y, between the lines per loop unit length (fig. 5, *a'*). The input impedance of such a line, open at both ends, is given by Cohen [15] to be

$$Z_i = N \coth Ks, \quad . \quad . \quad . \quad . \quad . \quad (48)$$

Fig. 4.

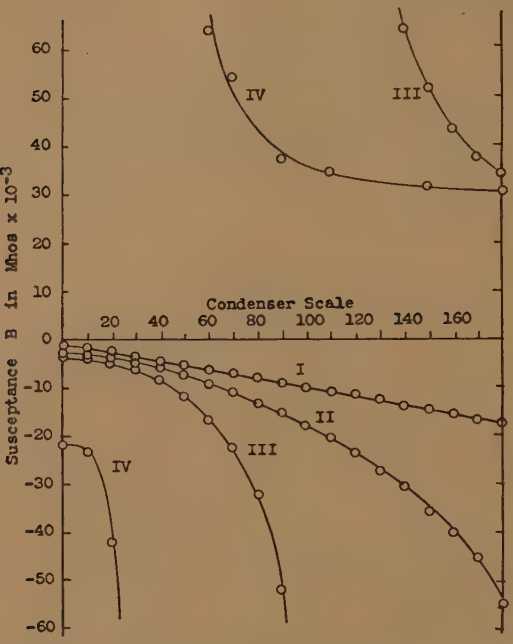

Susceptance of five-plate variable condenser (15 mmf.):

I. $B_0=\omega C_0$; C_0 measured at 750 k.c.
II. B measured at $\omega=10^9$ with shortest possible leads.
III. B measured at $\omega=10^9$ with 3·5 cm. leads.
IV. B measured at $\omega=2{\cdot}38\times10^9$ with shortest leads.

Fig. 5.

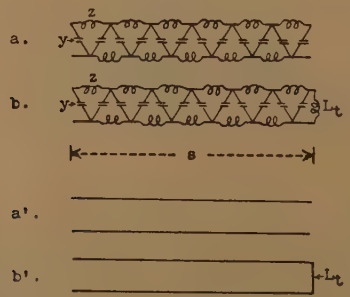

a. Equivalent network of multiple-plate condenser.
b. Equivalent network with terminal inductance.
a', *b'*. Corresponding parallel lines.

with $N=\sqrt{z/y}$, and $K=\sqrt{zy}$;

s is the length of the line.

If there are m spaces between the $m+1$ condenser plates, and if the length from the first to the last plate is s, the impedance per unit length of stator and rotor rods is approximately

$$z_1 \doteq nz/s.$$

Similarly the admittance between the rods (due to the condenser plates) per unit length is

$$y_1 \doteq my/s.$$

For negligible losses one has, from (40),

$$z_1 \doteq x_1 \doteq m\omega l_m/s = \omega l/s,$$

$$y_1 \doteq b_1 \doteq m/s[\omega C_m/(1-\omega^2 L_m C_m)] = \omega C/s(1-\omega^2 L_m C_m).$$

Here C_m is the static capacitance per single condenser, C is the static capacitance of the entire condenser; L_m is the inductance due to skin-effect per single condenser as given by (39); l_m is the inductance of stack and rotor rods per single condenser, l is the inductance of the stack and rotor rods of the entire condenser. Using this notation, the input reactance of the condenser is

$$X_i = -\sqrt{l/C - \omega^2 l_m L_m}\cot \omega\sqrt{lC/(1-\omega^2 L_m C_m)}. \quad . \quad (49)$$

This expression is complicated by the appearance of L_m, the inductance due to skin-effect in the plates. For condensers with large plates (49) cannot be further simplified for use at high frequencies; but if the plates are small, or if the frequency is not too high, the terms in L_m may become negligibly small. This will be true if in (37) $X^2/8 \ll 1$, or $a \leqq 0{\cdot}045\ \lambda/n'$. By satisfying this inequality it is possible to design tuning units for use at ultra-high frequencies in which the inductance due to skin effect in the plates is completely negligible. If this is true (49) reduces to the convenient and simple form

$$X_i = -\sqrt{l/C}\cot \omega\sqrt{lC} = -\sqrt{l_1/C_1}\cot \omega s\sqrt{l_1 C_1}.$$

Or, upon introducing the velocity of propagation of the electromagnetic waves along the stack and rotor rods, viz.,

$$v = 1/\sqrt{l_1 C_1},$$

one has

$$X_i = -l_1 v \cot \omega s/v. \quad . \quad . \quad . \quad . \quad . \quad (50)$$

The subscript, 1, refers to quantities per loop unit length; the ratio, c/v, is commonly called the index of refraction and denoted by n; the quantity, $l_1 c = \mathrm{N}$, is the characteristic impedance of the stack and rotor rods alone; $\beta = \omega/c$ is the propagation constant. With this notation (50) becomes

$$\mathrm{X}_i = -\mathrm{N}/n \cot n\beta s. \quad . \quad . \quad . \quad . \quad . \quad (51)$$

As before, s is the length of the unit between top and bottom plates. This formula is like that for a parallel line (fig. 5, a') for $n=1$. Thus the fundamental factors in determining the input reactance of a condenser tuning unit are the two constants, N and s, and the variable index of refraction, n. This last depends upon the static capacitance of the condenser which varies with the dial setting. It is, of course, entirely possible to write (51) without introducing the index of refraction of the tuning unit; but this would conceal the electromagnetic nature of the problem and its intimate relation to the measurement of dielectric constants [16]. The index of refraction of a condenser tuning unit is a measure of the velocity of propagation of electromagnetic waves along the stack and rotor rods for a given dial setting, compared with the velocity which would obtain if the condenser plates were completely removed (neglecting resistance, this is the velocity of light).

At low frequencies

$$\cot n\beta s = 1/\tan n\beta s \doteq 1/n\beta s,$$

so that (51) becomes, written for the susceptance, $\mathrm{B} \doteq 1/\mathrm{X}$,

$$\mathrm{B}_i = \omega \mathrm{C} \doteq n^2 \beta s/\mathrm{N}.$$

Solving this for the index, n, gives

$$n = \sqrt{(\mathrm{N}c/s)\mathrm{C}}. \quad . \quad . \quad . \quad . \quad . \quad . \quad (52)$$

From (52) the index of refraction of a condenser may be calculated for any dial setting in terms of the constants, N, c, s, and the variable static capacitance, C. With n so determined, (51) gives at once the input reactance of the unit at any desired frequency and dial setting.

If the stator and rotor rods are joined at the bottom by a bar of inductance, L_i (fig. 5, b), it is not difficult to show that the input reactance is

$$\mathrm{X}_i = (\mathrm{N}/n) \tan n\beta(s+k), \quad . \quad . \quad . \quad . \quad (53)$$

where $k=L_t/l_1$(*cf.* ref. (16), p. 202, eq. 6). This arrangement, often useful at ultra-high frequencies, is of no value at low frequencies, since for these (53) reduces to the usually very small quantity

$$X_i=\omega(L_t+l_1 s).$$

D. *Application of the Theory ; Experimental Results.*

In attempting to predict the reactance characteristics of a condenser such as the General Radio Precision, Type 222, considerable difficulty arises from the obvious fact that it is not constructed in a way to be well represented by a recurrent network. A rather rough approximation may be made by treating the condenser as an inductance, L (consisting largely of the two long and irregular connexions from the tips of the binding posts to the first condenser plates), in series with a recurrent network. The formula for the input reactance then takes the form

$$X_i=\omega L-N/n \cot n\beta s. \quad . \quad . \quad . \quad . \quad (54)$$

The inductance, L, was computed from the dimensions to be about 60 millihenries. This value was verified experimentally by measuring the reactance of rods of the same diameter at $\omega=10^9$. It was also in close agreement with the value of residual inductance obtained by Field and Sinclair [1]. The characteristic impedance of the stack and rotor rods was computed to be approximately 135 ohms. With these numerical values (54) becomes

$$X_i=6\times10^{-8}\,\omega-135/n \cot 7\beta n. \quad . \quad . \quad (54\,a)$$

The index of refraction, n, as a function of the static capacitance of the condenser was calculated from (52) to be :

$$n=\sqrt{(Nc/s)C}=\sqrt{0{\cdot}58C}. \quad . \quad . \quad . \quad . \quad (52\,a)$$

Fig. 6 shows n plotted both against C and the condenser scale. Upon now substituting the appropriate values of n in (54 *a*) the theoretical curves of fig. 7 were obtained for the angular frequencies indicated. The corresponding experimental curves, measured directly on a parallel wire system [17] are reproduced in fig. 8. The agreement is qualitatively good, but, as was to be expected, quantitatively only approximate. This is better illustrated in

Fig. 6.

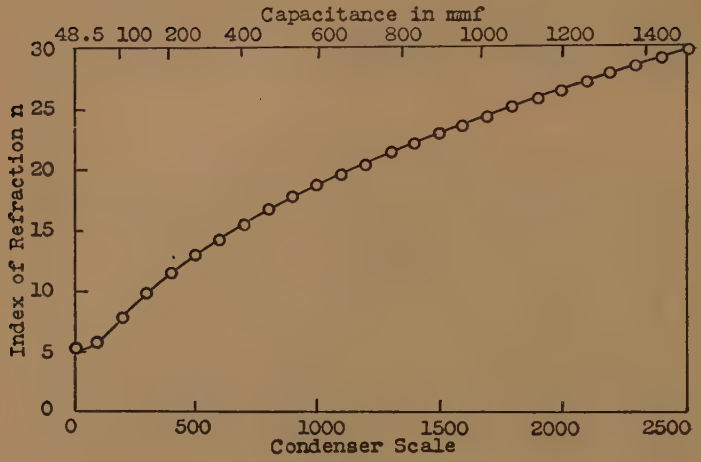

Index of refraction of general radio precision condenser, type 222.

Fig. 7.

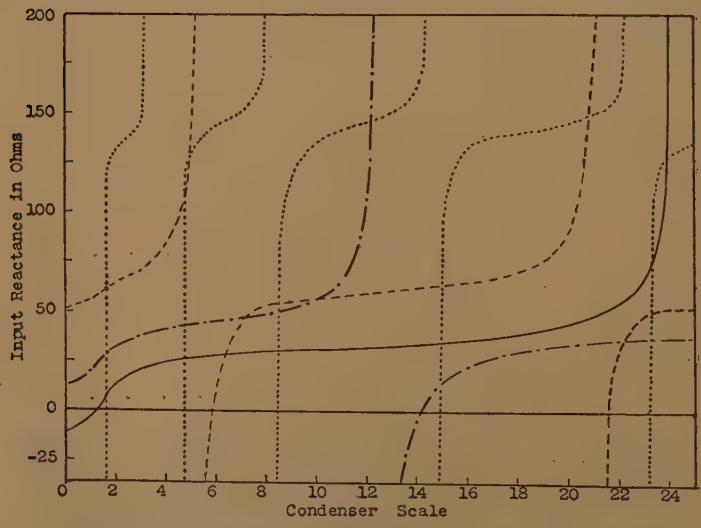

Calculated input reactance of general radio precision condenser.

Solid curve: $\omega = 4{\cdot}6 \times 10^8$; $\lambda = 409$ cm.
Dot dashed; $\omega = 6{\cdot}38 \times 10^8$, $\lambda = 295$ cm.
Dashed: $\omega = 10^9$; $\lambda = 188{\cdot}8$ cm.
Dotted: $\omega = 2{\cdot}38 \times 10^9$; $\lambda = 79{\cdot}1$ cm.

fig. 9, which shows one of the theoretical curves and the corresponding experimental one, together with the static value, ωC_0.

Fig. 8.

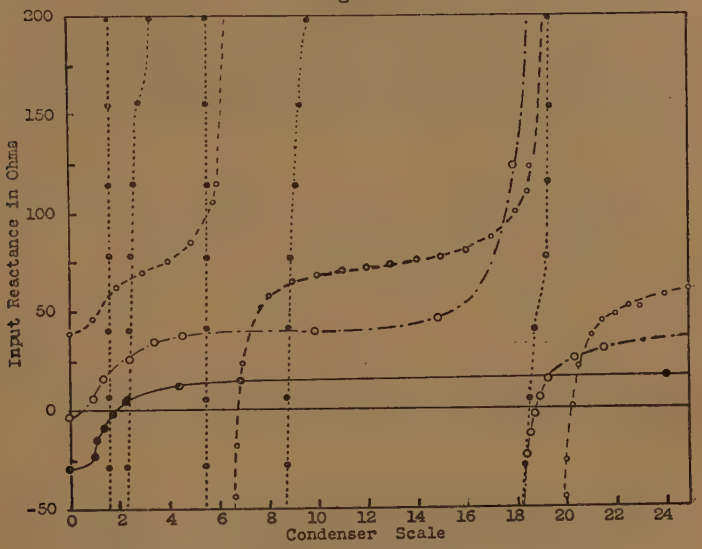

Measured input reactance of general radio condenser at angular frequencies given in fig. 7.

Fig. 9.

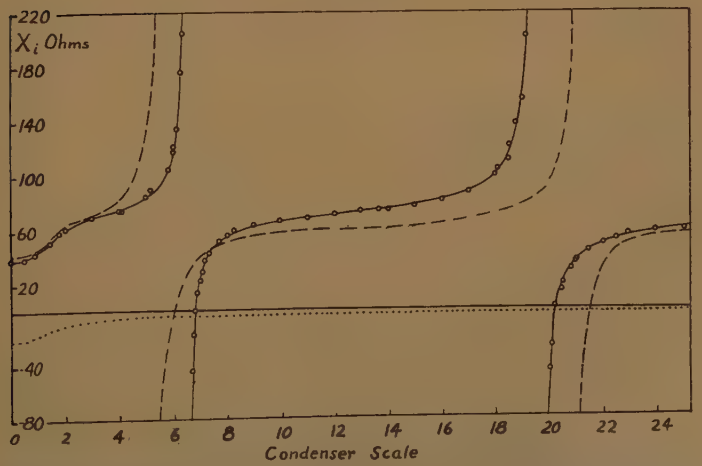

Calculated (dashed line) and measured (solid line) input reactance of general radio condenser at $\omega = 10^9$. Dotted curve is $X_i = -1/\omega C_0$ for the same ω.

Fig. 10.

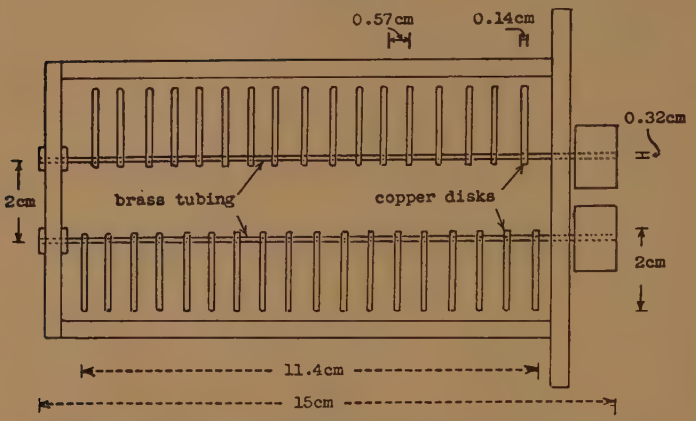

Construction diagram of variable tuner, top view. The copper plates are in the position for minimum capacitance.

Fig. 11.

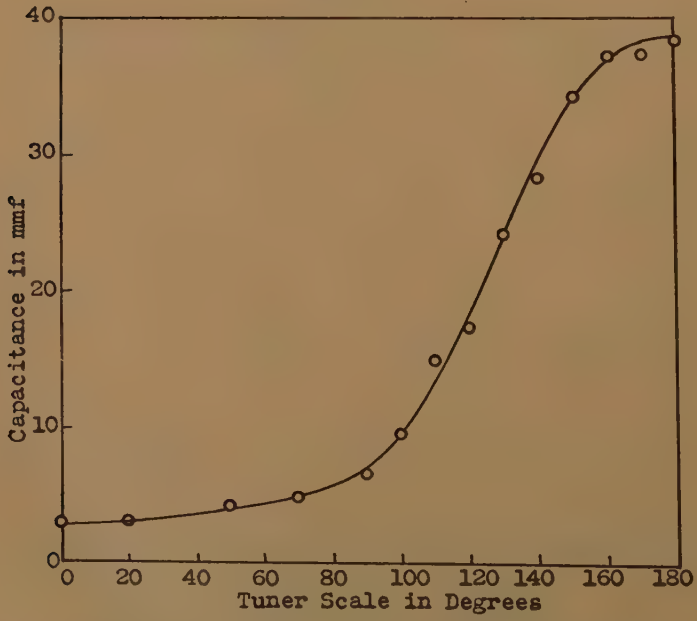

Capacitance of variable tuner as measured at 170 metres.

In order to obtain a better verification of the recurrent network analysis, and at the same time study the design of tuning units of predictable characteristics at any desired frequency, including the ultra-high, a small variable tuner was built, using copper coins of such dimensions that inductance due to skin-effect would be negligible for $\lambda \geqq 50$ cm. The construction of this unit is shown in fig. 10. Both sets of plates were movable, and the scale

Fig. 12.

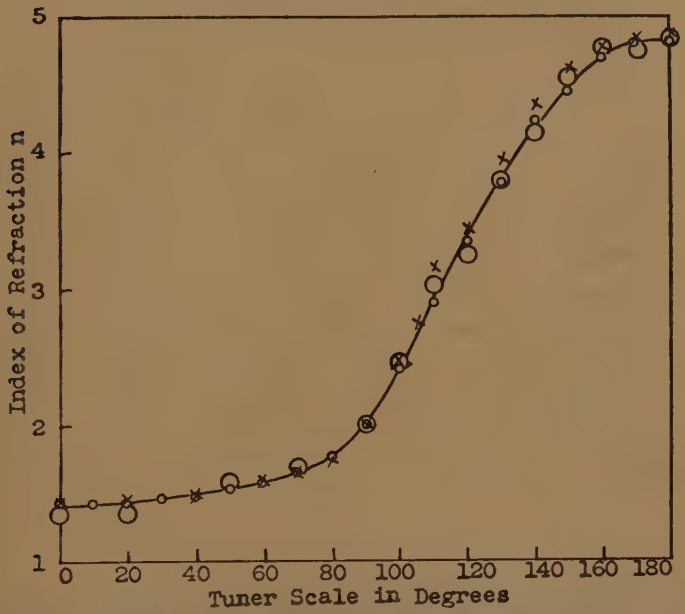

Index of refraction of variable tuner. Large circles, calculated from capacitance. Small circles, measured directly at 188·8 cm. Crosses, measured directly at 73·6 cm.

was calibrated by moving each set 10 degrees at a time. Unfortunately this special unit was not quite so well designed as it might have been; it would have been more convenient and accurate for purposes of calculation to have cut the rotor rods off flush with the end-plates, and so have avoided the perplexing difficulty of determining the length, s, of the unit. Thus, with the plates closely meshed the short ends of the rods projecting beyond them were relatively negligible. On the other

hand, when the plates were turned out (minimum capacitance) the rod ends were a significant part of the whole length. It was therefore necessary to choose this over-all length, although a not inappreciable error was so introduced; this will appear in the figures below.

The static capacitance of the tuner was measured with fair accuracy at 170 metres by substituting against a rather large precision condenser. The capacitance so

Fig. 13.

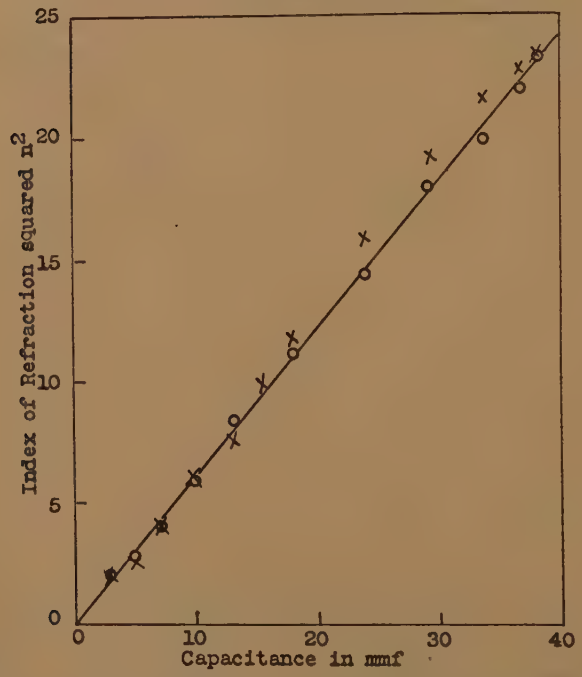

Index of refraction squared as a function of the capacitance of the variable tuner. Solid line, calculated from capacitance. Small circles, measured directly at 188·8 cm. Crosses, measured directly at 73·6 cm.

measured is shown in fig. 11. Using this capacitance, the readily computed characteristic impedance of the rotor rods, and the length of the tuner as explained above, the index of refraction of the unit was calculated from (52) as a function of the dial setting. This curve is shown in fig. 12. The index of refraction of the unit was

then measured directly at ultra-high frequencies by precisely the same method as was used for measuring the index of refraction of solids and liquids [18]. These results are also shown in fig. 12. They are seen to be in excellent agreement with the values computed from the dimensions and static capacitance. This agreement is further illustrated in fig. 13, in which n^2 is plotted against

Fig. 14.

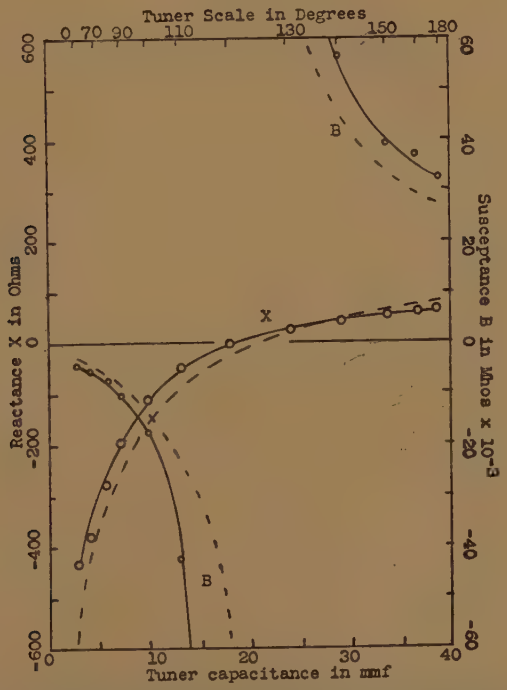

Reactance and susceptance of variable tuner at $\lambda = 188{\cdot}8$ cm.; open end. Dashed lines calculated; solid lines measured directly. $B = 1/X$.

the measured capacitance. The experimental points measured at ultra-high frequencies are seen to follow the theoretical straight line closely. This agreement between the computed and measured values of n is in itself excellent evidence that the input reactance of a condenser can be calculated at any frequency if the index of refraction over the dial range is known, and if the unit is designed

to be well represented by a recurrent network; for the reactance is readily computed from the same experimental data used to obtain n. However, in order to obtain a further, more direct check, the input reactance of the tuner was calculated for both open and bridged rotor ends using (51) and (53) and the computed index of refraction. The input reactance for each case was then

Fig. 15.

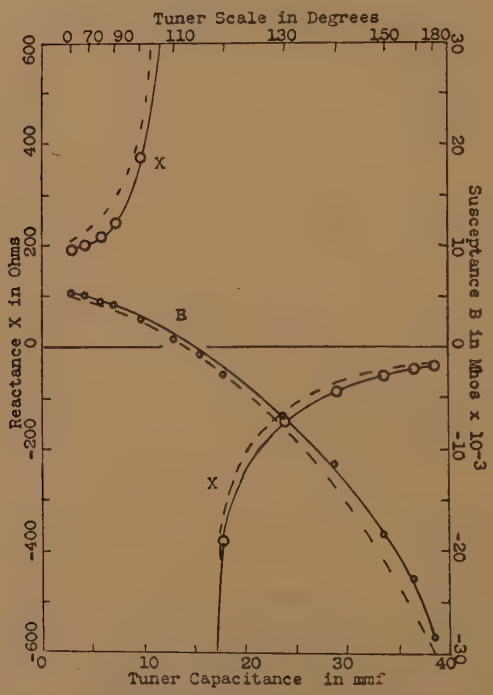
Tuner Scale in Degrees
0 70 90 110 130 150 180
600 400 200 0 -200 -400 -600
Reactance X in Ohms
30 20 10 0 -10 -20 -30
Susceptance B in Mhos x 10-3
X
B
X
0 10 20 30 40
Tuner Capacitance in mmf

Like fig. 14, but with tuner rotor rods bridged.

directly measured on the parallel wires at the same ultra-high frequencies used in the calculations. The results are shown in figs. 14–17. The agreement is seen to be not only qualitatively, but also quantitatively surprisingly good, especially if the ambiguity about the length is remembered; for a difference of half a centimetre in the length used in the calculations leads to a significant difference at critical resonance points. Thus the curves

definitely verify the theory, and indicate that it should be quite possible to predict the input characteristics of a condenser tuning unit of proper design at any desired ultra-high frequency. The constants which must be known, and which are usually easily obtained, are the tuner length, s, and the characteristic impedance of the rotor rods, N. The convenient variable is the index of refraction, n, as a function of the dial setting.

Fig. 16.

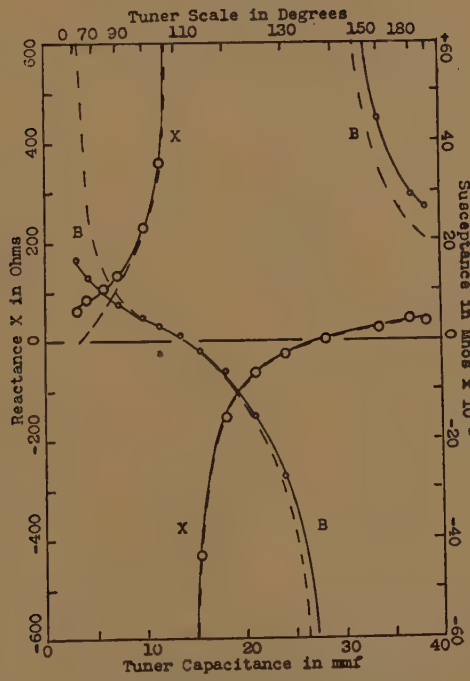

Like fig. 14, but determined at $\lambda = 73{\cdot}6$ cm.

Appendix I.

The general vector relation of which (20) is one component is

$$\mathrm{E} = -\nabla \mathrm{V} - \dot{\underline{\mathrm{A}}}/c. \quad . \quad . \quad . \quad \text{(I–1)}$$

A second relation which must be satisfied is [19]

$$\mathrm{div}\, \underline{\mathrm{A}} = -\dot{\mathrm{V}}/c. \quad . \quad . \quad . \quad . \quad . \quad \text{(I–2)}$$

Upon combining these two equations, by taking the divergence of the first and the time derivative of the second, one obtains

$$\text{div } \underline{E} = -\nabla^2 V + \ddot{V}/c^2. \quad . \quad . \quad . \quad \text{(I–3)}$$

But by (12) div $\underline{E}=0$. Hence, for sinusoidal time dependence one has

$$\nabla^2 V + \beta^2 V = 0 \quad (\beta = \omega/c \text{ as before}). \quad . \quad . \quad \text{(I–4)}$$

Fig. 17.

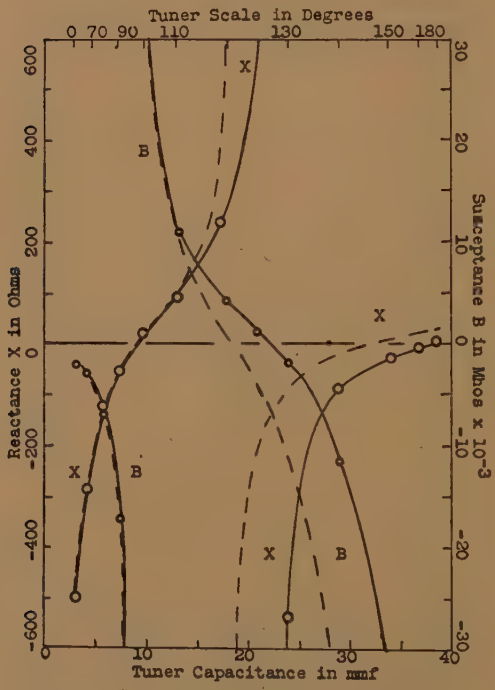

Like fig. 15, but determined at $\lambda = 73{\cdot}6$ cm.

Since $E_r \doteq 0$ and V is independent of θ, this reduces to the following, after changing to cylindrical coordinates,

$$\partial^2 V/\partial z^2 + \beta^2 V = 0. \quad . \quad . \quad . \quad . \quad \text{(I–5)}$$

The solution of this is

$$V = V_0 \cos \beta z + (V_1/\beta) \sin \beta z. \quad . \quad . \quad \text{(I–6)}$$

Upon expanding the trigonometric functions in power series, and retaining only the leading terms, one has

$$V \doteq V_0 + V_1 z, \quad . \quad . \quad . \quad . \quad . \quad . \quad (I\text{–}7)$$

subject to the condition, $\beta^2 z^2 << 1$. Hence

$$\partial V / \partial z \doteq E_z \doteq V_1 \quad . \quad . \quad . \quad . \quad (I\text{–}8)$$

if $\beta^2 d^2 << 1$, since d is the largest value of z.

Appendix II.*

The index of refraction, n, of the tuning unit was measured by precisely the method used for determining the index of refraction of a solid slab. Thus in fig. 2* the slab of thickness, s_1, must be replaced by the tuning unit of length, s. Experimentally this was possible because the rotor rods of the unit were of brass tubing so arranged that they could be slipped over a pair of parallel wires. A shift curve corresponding to those of fig. 8* might then have been plotted for each value of n obtained by changing the dial settings of the tuner plates. Actually only the maximum shifts had to be measured. The value of n in each case was computed by solving the equation

$$\tan \tfrac{1}{2}\beta(s' - s_2) = (l_2/l_1) n \tan \tfrac{1}{2} n \beta s, \quad . \quad . \quad . \quad (II\text{–}1)$$

using the experimentally observed values of $(s' - s_2)$, which by (18)* are the same as (shift$+s$). (II–1) corresponds to (14)* written for a solid (Nb=0) with the added factor, l_2/l_1. This is the ratio of the inductances respectively of the parallel wires and the rotor rods of the tuner. (In 14* $l_2 = l_1$.) For the equipment used $s = 15$ cm. and $l_2/l_1 = 1{\cdot}46$. The solution of (II–1) is carried out most conveniently by plotting curves like those of fig. 7*, showing n as a function of $\frac{1}{2}\beta(s' - s_2)$ for each frequency. Fig. 18 shows the curves which were computed for determining n for figs. 12 and 13. It is to be noted that, since all effects on the parallel wire system are repeated at intervals of a half wave-length, (II–1) is directly useful only up to that value of n (for a given $\frac{1}{2}\beta s$) which makes $(s' - s_2) = \lambda/2$. Let this value (which makes $\tan \frac{1}{2} n \beta s = \pi/2$) be noted by n_r. Then when $n = n_r$ a half wave-length is contained in the tuner; when $n = 2n_r$ a whole wave-length is contained, etc. For

* Starred figure and equation references are to R. King, Rev. Sci. Inst. viii. p. 201 (June 1937).

values of n greater than n_r, or $2n_r$, one proceeds as from $n=0$. Experimentally this is equivalent to moving the tuner back to zero shift when the shift becomes a half wave-length. In general there is no direct way of distinguishing the shifts for values of n differing by integral multiples of n_r. In the case of the tuner under discussion it was obvious from the construction that much less than a half wave-length must be contained in the tuner when the plates were turned for minimum capacitance. Any ambiguity is, of course, easily eliminated if n is also determined statically from (52). The ultra-high fre-

Fig. 18.

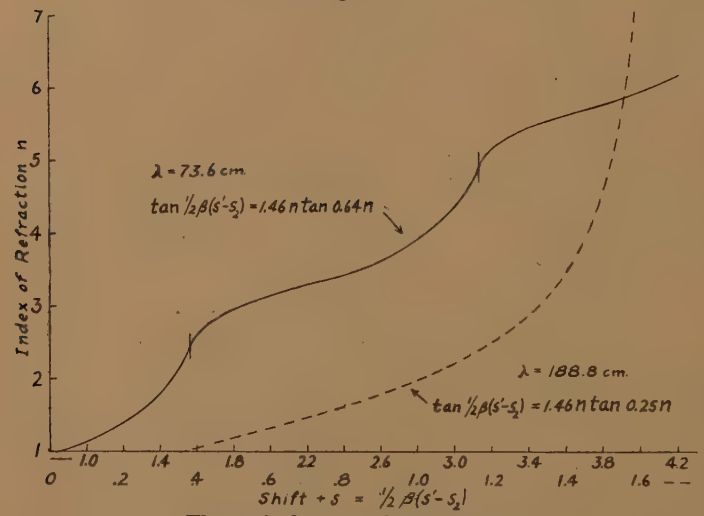

Theoretical curve of the equation

$\tan \frac{1}{2}\beta(s'-s_2)=(l_2/l_1)n \tan \frac{1}{2}n\beta s$

for the variable tuner at two wave-lengths.

quency check upon (52) may, of course, be obtained using (51) or (53) and calculating reactance curves like those of figs. 14–17. But since the shift method is more accurate it is to be preferred where the design of the condenser unit makes it available.

References.

(1) Field and Sinclair, Proc. I. R. E. xxiv. p. 255 (February, 1936).

(2) In the notation of Debye (' Polar Molecules,' pp. 91–94: Chemical Catalogue Company, New York, 1929) one has

$\epsilon'=\epsilon_0+(\epsilon_1-\epsilon_0)/(1+x^2)$; $\epsilon''=x(\epsilon_1+\epsilon_0)/(1+x^2)$; $x=\omega T(\epsilon_1+2)/(\epsilon_0+2)$,

where ϵ_1 is the statical dielectric constant at zero frequency, ϵ_0 is the optical dielectric constant, T is the relaxation time of the molecules.

(3) Mason and Weaver, the ' Electromagnetic Field,' p. 264, eqs. 180, 181 (Chicago University Press, 1932). This book uses Heaviside-Lorentz rational units throughout. Since frequent reference will be made to it, this system of units will be retained in the theoretical discussion. Final results will be written in practical units.

(4) Mason and Weaver, p. 348.

(5) In copper the skin thickness, $s=c/\sqrt{\omega\sigma c}$, is of the order of magnitude of 10^{-4} cm. at frequencies of 10^8 to 10^9 cycles per second.

(6) The assumption previously made that E_r be negligibly small assumed likewise that the conductivity of the plates be correspondingly great. Hence the condition for smallness imposed upon E_r imposes no such condition upon ϵE_r, since ϵ includes the conductivity as a term.

(7) Byerly, ' Fourier Series and Spherical Harmonics,' p. 224, eq. 9 (Ginn & Co., New York).

(8) It is easily verified that one obtains the same formula (19) if one assumes a total current, I_r, flowing radially outward in the upper plate and chooses a surface of integration completely enclosing a section of radius, r, of the upper plate. In either case (19) depends upon the assumption that the current distribution is such that the values of $\underline{E}$ and $\underline{B}$ at any point along the plate, due to the moving charge at all points, are determined by instantaneous current elements which all had the same amplitude at the retarded time, $t-x/c$. Here x is the distance between the point at which $\underline{E}$ and $\underline{B}$ are calculated and the instantaneous current element. This is the same assumption made in deriving the telegraphist's equations (see reference (5), R. King, Rev. Sci. Inst. viii. p. 203 (June 1937)), but is in this case not easily justified. No justification is attempted, however, since the solution obtained will be used only for plates of such dimensions compared with the wave-length that retardation is not very significant.

(9) Mason and Weaver, p. 280, eq. 194.

(10) Appendix I.

(11) The rational units used by Mason and Weaver follow the Gaussian system of expressing electromagnetic quantities (such as currents in electromagnetic units, the electrostatic quantities (such a) potential difference) in electrostatic units. In defining admittance at this point it is convenient to express it as the ratio between quantities in electromagnetic units, hence the factor, c, in (25).

(12) A formula corresponding to this is given by Ollendorf, ' Grundlagen der Hochfrequenztechnik,' p. 47, eq. 65 (Springer, 1928).

(13) R. King, Proc. I. R. E. xxiii. p. 905 (August 1935).

(14) *Loc. cit.* p. 423.

(15) Cohen, ' Heaviside's Electrical Circuit Theory,' p. 110 (McGraw-Hill).

(16) R. King, Rev. Sci. Inst. viii. p. 201 (June 1937).

(17) R. King, Proc. I. R. E. xxiii. p. 910 (August 1935).

(18) Appendix II.

(19) Mason and Weaver, p. 280, eq. 197.

XXIX. *The Frequency of Longitudinal and Torsional Vibration of Unloaded and Loaded Bars.* *By* R. M. Davies, *D.Sc., F.Inst.P., Lecturer in Physics, University College of Wales, Aberystwyth* *.

Contents.

	Page
I. Longitudinal Vibration of Infinitely Thin, Loaded, Fixed-Free Bars	365
II. Longitudinal Vibration of Bars of Finite Lateral Dimensions	369
III. Torsional Vibration of Infinitely Thin, Loaded, Fixed-Free Bars	376
IV. Torsional Vibration of Bars of Finite Lateral Dimensions.	379

Notation and Assumptions.

THE bar is assumed to be of uniform section and to be straight when in equilibrium. The line passing through the centres of inertia of the normal sections of the bar is taken as the axis of z, whilst the axes of x and y are the principal axes of inertia at the origin. The component displacements of the point (x, y, z) at time t will be denoted by u, v, w, parallel respectively to the axes of x, y, and z. Let

ρ=Density of the bar.
E=Young's modulus of the material of the bar.
G=Rigidity modulus of the material of the bar.
σ=Poisson's ratio of the material of the bar.
l=Length of the bar.
A=Area of cross-section of the bar.
$M'=\rho Al$=Mass of the bar.
M=Mass of the load fixed to the free end of the bar.
$c=M/M'$.
K=Radius of gyration of the cross-section of the bar about Oz.
$I'=\rho AlK^2$=Moment of inertia of the bar about Oz.
I=Moment of inertia of the load about Oz.
$d=I/I'$.
n_0, n=Natural frequency of vibration of the bar.
ω_0, ω=Natural pulsatance of vibration of the bar.
$(\omega_0=2\pi n_0\ ;\ \omega=2\pi n)$.

* Communicated by the Author.

$U=(E/\rho)^{\frac{1}{2}}$=Velocity of propagation of longitudinal waves in an infinitely thin bar.

$V=(G/\rho)^{\frac{1}{2}}$=Velocity of propagation of torsiona waves in an infinitely thin bar of circular cross-section.

I. *Longitudinal Vibration of Infinitely Thin, Loaded, Fixed-Free Bars.*

When longitudinal vibrations occur in infinitely thin bars the displacement is in the direction of the Oz axis only, and the differential equation governing the motion is the well-known equation

$$\frac{\partial^2 w}{\partial t^2}=\frac{E}{\rho}\frac{\partial^2 w}{\partial z^2}=U^2\frac{\partial^2 w}{\partial z^2}. \quad . \quad . \quad . \quad (1.1)$$

The boundary conditions appropriate to different end conditions are :—

(*a*) At a fixed end $w=0$ for all values of t.

(*b*) At a free, unloaded end the strain $\partial w/\partial z$ is zero for all values of t.

(*c*) At a free end, loaded with a point mass M, the restoring force due to the strain is equal to the product of M into its acceleration, *i. e.*,

$$M\frac{\partial^2 w}{\partial t^2}=-EA\frac{\partial w}{\partial z}. \quad . \quad . \quad . \quad . \quad (1.2)$$

The frequency of longitudinal vibration of thin, loaded, fixed-free bars was investigated by Rayleigh [1], using an energy method ; Rayleigh's results are approximations which are accurate in the two extreme cases of small and large values of c.

In the present notation Rayleigh's result for the natural pulsatance of vibration, ω_0, *for small values of* c, may be written

$$\omega_0=\frac{\pi(2m+1)U(1-c)}{2l}, \quad . \quad . \quad . \quad (1.3)$$

where m is an integer determined by the mode of vibration, m is zero for the fundamental mode, unity for the first overtone, etc.

If, on the other hand, c *is large*, it is usually only possible to set the bar in vibration in its fundamental

mode, and it is therefore sufficient to consider this mode only. For this mode, and for large values of c, Rayleigh's result for the natural pulsatance of vibration, ω_0, is

$$\omega_0 = \frac{U}{l}\left(\frac{3}{1+3c}\right)^{\frac{1}{2}} . \quad . \quad . \quad . \quad . \quad (1.4)$$

An alternative method of determining the frequency is to form the exact frequency equation, using the general equation (1.1) and the boundary conditions at the ends of the bar; this procedure gives a result whose accuracy is equal to the accuracy of the original equation (1.1). This investigation was first carried out by Donkin [2]; the problem is also considered by Prescott [3] and by Timoshenko [4]. The case considered by Donkin is that of a bar of mass M' and of length l, carrying a mass M_0 at the end $z=0$ and a mass M_1 at the end $z=l$. If $c_0=M_0/M'$ and $c_1=M_1/M'$, the frequency equation is

$$(1-c_0c_1\alpha^2l^2)\tan\alpha l+(c_0+c_1)\alpha l=0,$$

where

$$\alpha=\omega_0/U, \quad . \quad . \quad . \quad . \quad . \quad . \quad (1.5)$$

ω_0 being the pulsatance of vibration of the loaded bar.

The equation for a rod fixed at the end $z=0$ and carrying a load M at the end $z=l$ is obtained by putting $M_0=c_0=\infty$ and $M_1=M$ and $c_1=c$ in equation (1.5); this leads to the frequency equation

$$\alpha l \tan \alpha l = \frac{1}{c} . \quad . \quad . \quad . \quad . \quad . \quad (1.6)$$

In practice it is desirable to express the pulsatance ω_0 in terms of U, l, and c, and it is thus necessary to obtain an explicit solution of equation (1.6). It is impossible to give a solution which is valid for all values of the parameter c, but approximate solutions of reasonable accuracy can be obtained for small and for large values of c.

Considering first the approximate solutions *for small values of* c, Donkin has shown that the Rayleigh result of equation (1.3) can be derived from equation (1.6) as a first approximation. This result, together with a second approximation, can best be derived by noting that if the bar be unloaded, *i. e.*, if $c=0$, $\alpha l=(2m+1)\pi/2$, whilst for small values of c the value of αl is in the neighbourhood of $(2m+1)\pi/2$.

Equation (1.6) may be written

$$\alpha l = \tan^{-1}\left(\frac{1}{\alpha l c}\right),$$

and if $\left(\frac{1}{\alpha l c}\right)^2 > 1$,

$$\tan^{-1}\left(\frac{1}{\alpha l c}\right) = \frac{(2m+1)\pi}{2} - \alpha l c + \tfrac{1}{3}\alpha^3 l^3 c^3 - \tfrac{1}{5}\alpha^5 l^5 c^5 + \ldots .$$

Thus

$$\alpha l = \frac{(2m+1)\pi}{2} - \alpha l c + \tfrac{1}{3}\alpha^3 l^3 c^3 - \ldots . \quad . \quad . \quad (1.7)$$

The first approximation for α is obtained by terminating this series with the term $\alpha l c$, and this gives

$$\alpha l = \frac{(2m+1)\pi}{2(1+c)}, \quad . \quad . \quad . \quad . \quad . \quad (1.8)$$

which for small values of c is equivalent to equation (1.3).

A second approximation for α is obtained by terminating the series of equation (1·7) with the $\frac{1}{3}\alpha^3 l^3 c^3$ term. This gives

$$\alpha l(1+c) = \frac{(2m+1)\pi}{2}\left[1 + \frac{(2m+1)^2\pi^2}{12} \cdot \frac{c^3}{(1+c)^3}\right] \quad (1.9)$$

if the value of αl given by equation (1.8) is substituted in the small term $\frac{1}{3}\alpha^3 l^3 c^3$. From equation (1.9)

$$\omega_0 = \frac{(2m+1)\pi U}{2l(1+c)}\left[1 + \frac{(2m+1)^2\pi^2}{12} \cdot \frac{c^3}{(1+c)^3}\right]. \quad (1.10)$$

It should be added that Donkin also gives (without proof) a second approximation for ω_0 similar in form to that given in equation (1.10); his expression is, however, incorrect, in that the index of $(1+c)$ in the denominator of the last term in square brackets is given as 2 instead of 3.

As regards the accuracy of the solutions given in equations (1.8) and (1.10), calculation shows that the simpler solution (1.8) is accurate to within one in a thousand for values of c up to 0·12, whilst equation (1.10) has the same accuracy for values of c up to 0·4; when $c = 0{\cdot}4$ the simpler solution is about two per cent. in error.

Considering next the solutions appropriate to *large values of* c, Timoshenko [4] has shown that the Rayleigh

approximation of equation (1.4) can be derived from equation (1.6) by expanding $\alpha l \tan \alpha l$ in powers of αl and terminating the expansion at the $(\alpha l)^4$ term. Calculation shows that the error in the value of ω_0 given by equation (1.4) is accurate to within one in a thousand for values of c exceeding about 4, and to within one per cent. for values of c exceeding unity.

A better approximation for large values of c may be obtained by expanding $\alpha l \tan \alpha l$ in powers of αl and including terms in αl whose powers exceed the fourth. It is found that

$$\frac{1}{c} = \alpha l \tan \alpha l = (\alpha l)^2 + \frac{(\alpha l)^4}{3} + \frac{2(\alpha l)^6}{15} + \frac{17(\alpha l)^8}{315} + \frac{62(\alpha l)^{10}}{2835} + \ldots . \quad (1.11)$$

This series may be regarded as a series in ascending powers of $(\alpha l)^2$, and if the series be reversed we obtain

$$(\alpha l)^2 = \frac{1}{c}\left[1 - \frac{1}{3c} + \frac{4}{45c^2} - \frac{16}{945c^3} + \frac{16}{14{,}175c^4} + \ldots .\right],$$

giving

$$\omega_0 = \frac{U}{l\sqrt{c}}\left[1 - \frac{1}{3c} + \frac{4}{45c^2} - \frac{16}{945c^3} + \frac{16}{14{,}175c^4} + \ldots .\right]^{\frac{1}{2}}. \quad (1.12)$$

Considering next the accuracy of this equation, it is seen that the error will increase as c decreases. Taking all five terms in the square brackets the error is less than one in a thousand for values of c exceeding 0·8; if we take only the first four terms the equation is accurate to within one in a thousand for values of c greater than unity.

Thus, for values of c less than 0·4, ω_0 can be calculated to within one in a thousand by means of equation (1.10); the same accuracy can be obtained for values of c exceeding 0·8 by means of equation (1.12). When c is less than 0·12 or greater than 4 the same accuracy can be obtained more simply by means of equations (1.8) and (1.4) respectively. For values of c lying between 0·4 and 1 no explicit approximation appears possible, and it becomes necessary to find αl (or ω_0) either graphically or by interpolation from tables [5] giving $\alpha l \tan \alpha l$ for various values of αl.

II. *Longitudinal Vibration of Bars of Finite Lateral Dimensions.*

The differential equation (1.1) is valid only when the lateral dimensions of the bar are infinitely small in comparison with the wave-length λ of the vibration. When the lateral dimensions become finite the displacement of a point in the bar will, in general, have components in the directions of x and y in addition to the main component in the direction of z, and the differential equation requires modification on this account.

The effect of lateral motion on the frequency of an unloaded free-free bar of circular cross-section has been investigated by Rayleigh [6], using an energy method. In the present notation Rayleigh's approximation for a bar of radius r vibrating in the mth mode may be written

$$\frac{\omega}{\omega_0}=1-\frac{\pi^2}{4}.m^2\sigma^2.\frac{r^2}{l^2} \quad (m=1, 2, 3 \ldots.), \quad . \quad (2.1)$$

where ω_0 is the pulsatance of vibration when lateral motion is neglected and ω is the pulsatance, allowing for lateral motion. Using the same method, Rayleigh's result has been extended [7] to the case of a non-isotropic bar of rectangular cross-section.

An alternative method of calculating the ratio ω/ω_0 is to form a more accurate differential equation of motion of the bar, and to solve this equation, inserting the boundary conditions appropriate to the ends of the bar. The differential equation, allowing for lateral motion, is given by Love [8], and in the present notation it may be written

$$\frac{\partial^2 w}{\partial t^2}-\sigma^2\mathrm{K}^2\frac{\partial^4 w}{\partial z^2\partial t^2}=\mathrm{U}^2\frac{\partial^2 w}{\partial z^2}. \quad . \quad . \quad . \quad (2.2)$$

In this equation the effect of lateral motion is represented by the term involving $(\sigma^2\mathrm{K}^2)$ on the left-hand side. This equation is valid for bars whose lateral dimensions are finite ; it must, however, break down when the lateral dimensions become comparable with the length (or wave-length λ), since the bar then becomes a plate. We may estimate the accuracy of equation (2.2) by comparing the results which it gives with the more general results, obtained for certain simple cases of unloaded bars from

the general equations of motion of elastic solids by Pochammer [9] and by Chree [10]. Such a comparison shows that equation (2.2) is accurate provided that the ratio (K^4/λ^4) is small in comparison with unity; we may thus conclude that our results will probably be accurate to one in a thousand provided that (K^2/λ^2) is less than about 0·03.

The solution of equation (2.2) for a simple harmonic vibration of pulsatance ω is of the form

$$w=Ze^{i\omega t}; \quad i=\sqrt{-1}, \quad . \quad . \quad . \quad . \quad (2.3)$$

where Z, the normal or characteristic function, is a function of z only.

This leads to the following differential equation for Z:

$$\frac{\partial^2 Z}{\partial z^2}+\beta^2 Z=0,$$

writing

$$\beta^2=\frac{\omega^2}{U^2-\sigma^2K^2\omega^2}=\frac{\omega^2}{U^2}\cdot\frac{1}{1-\delta}, \text{ where } \delta=\frac{\sigma^2K^2\omega^2}{U^2}, \quad . \quad (2.4)$$

and thus

$$Z=B\cos\beta z+B'\sin\beta z, \quad . \quad . \quad . \quad . \quad (2.5)$$

where B and B′ are constants of integration determined by the boundary conditions. If lateral motion is neglected, δ vanishes, ω becomes equal to the pulsatance ω_0 in the absence of lateral motion, and β becomes equal to the parameter α of Section I.

As to the order of magnitude of δ, $\omega\lambda=2\pi U$, and thus $\delta=4\pi^2\sigma^2K^2/\lambda^2$. σ is of the order of 0·3, and $\pi^2\sigma^2$ may therefore be taken as unity. δ is thus of the order of K^2/λ^2, and, in view of the above restriction as to the accuracy of equation (2.2), δ must be regarded as a small quantity whose square is negligible in comparison with unity.

(a) *Unloaded Bars.*

Considering first the case of a *free-free* bar of length l, the boundary conditions lead to the frequency equation

$$\beta=\frac{m\pi}{l} \quad (m=1, 2, 3\ldots.). \quad . \quad . \quad . \quad (2.6)$$

From equation (2.4)

$$\omega^2 = \frac{\beta^2 U^2}{1+\beta^2\sigma^2 K^2}, \quad . \quad . \quad . \quad . \quad . \quad . \quad (2.7)$$

which gives

$$\frac{{\omega_0}^2}{\omega^2} = 1+m^2\pi^2\sigma^2 . \frac{K^2}{l^2} . \quad . \quad . \quad . \quad . \quad . \quad (2.8)$$

In the particular case of a bar of circular cross-section of radius r, $K^2=\frac{1}{2}r^2$, and, since $m^2\pi^2\sigma^2 . K^2/l^2$ is small in comparison with unity, equation (2.8) reduces to the Rayleigh result of equation (2.1).

For a *fixed-free* bar of length l it is found that

$$\beta l = (m+\tfrac{1}{2})\pi \quad (m=0, 1, 2, \ldots), \quad . \quad . \quad (2.9)$$

giving

$$\frac{{\omega_0}^2}{\omega^2} = 1+(m+\tfrac{1}{2})^2\pi^2\sigma^2 . \frac{K^2}{l^2} . \quad . \quad . \quad (2.10)$$

Finally, for a *fixed-fixed* bar of length l,

$$\beta l = m\pi \quad (m=1, 2, \ldots), \quad . \quad . \quad . \quad (2.11)$$

giving, as for a free-free bar,

$$\frac{{\omega_0}^2}{\omega^2} = 1+m^2\pi^2\sigma^2 . \frac{K^2}{l^2} . \quad . \quad . \quad . \quad . \quad (2.12)$$

(b) *Loaded Fixed-Free Bars.*

The effect of lateral motion on the frequency of loaded bars does not seem to have been investigated in any single instance. If necessary the investigation could be carried out by Rayleigh's method, but it is equally simple to solve the differential equation (2.2), using the boundary conditions given in Section I.

The only case likely to be of practical interest is that of a fixed-free bar, which is fixed at the end $z=0$, and which is loaded with a mass M at the free end, $z=l$.

At the fixed end $w=0$ for all values of t, and thus $B=0$. Hence $Z=B' \sin \beta z$.

At the free end (*v.* equation (1.2))

$$M\frac{\partial^2 w}{\partial t^2} = -EA\frac{\partial w}{\partial z},$$

which gives the frequency equation

$$\tan \beta l = \frac{EA\beta}{M\omega^2}.$$

This equation can be rewritten

$$\left.\begin{aligned} \beta l \tan \beta l = \frac{\beta^2 U^2}{c\omega^2} = \frac{1}{\gamma} = \frac{1+\beta^2\sigma^2 K^2}{c}, \\ \text{where } \gamma = c\omega^2/\beta^2 U^2 = c(1-\delta) \text{ from eq. (2.4).} \end{aligned}\right\} \quad . \quad . \quad (2.13)$$

If lateral motion is negligibly small $\beta^2\sigma^2K^2$ and δ vanish, β becomes equal to α of Section I., γ becomes equal to c, and equation (2.13) reduces to equation (1.6) of Section I.

As in Section I., approximate solutions for the frequency (or pulsatance) can be obtained from equation (2.13) in the two extreme cases of small values and large values of c.

Considering first the approximate solutions for *small values of* c, we obtain from equation (2.13) that

$$\beta l = \tan^{-1}\frac{1}{\gamma\beta l} = (m+\tfrac{1}{2})\pi - \gamma\beta l + \tfrac{1}{3}(\gamma\beta l)^3 - \ldots \quad (2.14)$$

(*cf.* equation (1.7) in Section I.).

The first approximation for the pulsatance is obtained by terminating this series at the term $\gamma\beta l$, and we thus obtain

$$\beta l = \frac{(2m+1)\pi}{2(1+\gamma)} \quad (m=0, 1, 2, \ldots). \quad . \quad . \quad (2.15)$$

Inserting the values of β and γ from equations (2.4) and (2.13), we obtain from equation (2.15)

$$\omega = \frac{(2m+1)\pi U}{2l(1+c)}\left[1 - \frac{\delta(1-c)}{2(1+c)}\right], \quad . \quad . \quad (2.16)$$

neglecting squares and higher powers of δ.

When considering δ no appreciable error will be committed if we write (ω/U) equal to β, and, in addition, for this purpose we may take β to be equal to its value when lateral motion is neglected. Since this value of β is equal to the value of α given by equation (1.8) we obtain

$$\delta = \sigma^2K^2\beta^2 = \frac{(2m+1)^2}{4}.\pi^2\sigma^2.\frac{K^2}{l^2}.\frac{1}{(1+c)^2}. \quad (2.17)$$

We thus obtain

$$\omega=\frac{(2m+1)\pi U}{2l(1+c)}\left[1-\frac{(2m+1)^2}{8}.\pi^2\sigma^2\frac{K^2}{l^2}.\frac{(1-c)}{(1+c)^3}\right], \quad (2.18)$$

or, if ω_0 be the pulsatance when lateral motion is neglected, the value of ω_0 corresponding to equation (2.18) is obtained from equation (1.8) or by putting $\sigma^2K^2=0$ in equation (2.18), and this gives

$$\frac{\omega_0}{\omega}=1+\frac{(2m+1)^2}{8}.\pi^2\sigma^2.\frac{K^2}{l^2}.\frac{(1-c)}{(1+c)^3}. \quad (2.19)$$

If $c=0$ equation (2.19) reduces to equation (2.10), and it is seen that, to the present degree of approximation, the effect of the load is to reduce the correction for lateral motion in the ratio $(1-c)/(1+c)^3$.

A second approximation for the pulsatance for small values of c may be obtained by including the $\frac{1}{3}(\gamma\beta l)^3$ term in equation (2.14). This equation may be written

$$\beta l(1+\gamma)=(2m+1)\frac{\pi}{2}+\frac{(\gamma\beta l)^3}{3},$$

and, since $\frac{1}{3}(\gamma\beta l)^3$ will be small if c is small, we may substitute in it the first approximation for βl given by equation (2.15). This gives first

$$\beta=\frac{(2m+1)\pi}{2l(1+\gamma)}\left\{1+(2m+1)^2.\frac{\pi^2}{12}.\frac{\gamma^3}{(1+\gamma)^3}\right\},$$

and then, using equations (2.4) and (2.13) and neglecting squares and higher powers of δ,

$$\omega=\frac{(2m+1)\pi U}{2l(1+c)}.\left\{1-\frac{\delta(1-c)}{2(1+c)}\right\}\left\{1+(2m+1)^2.\frac{\pi^2}{12}.\frac{c^3}{(1+c)^3}\right\}.$$

As before, we may use the value of δ given in equation (2.17), and, neglecting squares and higher powers of δ, we obtain finally

$$\omega=\frac{(2m+1)\pi U}{2l(1+c)}\left\{1-\frac{(2m+1)^2\pi^2}{4(1+c)^3}\left[\frac{\sigma^2K^2}{2l^2}(1-c)-\frac{c^3}{3}\right]\right\}. \quad (2.20)$$

If c is small this equation reduces to equation (2.18), and if c vanishes it reduces further to equation (2.10).

If lateral motion is negligibly small, ω becomes ω_0, the pulsatance in the absence of lateral motion, and equation (2.20) reduces to equation (1.10). To the present degree of approximation the ratio (ω_0/ω) becomes

$$\frac{\omega_0}{\omega} = 1 + \frac{(2m+1)^2}{8} \cdot \pi^2\sigma^2 \cdot \frac{K^2}{l^2} \cdot \frac{(1-c)}{(1+c)^3},$$

which agrees with equation (2.19) above.

Turning next to the case of *large values of* c, and confining our attention to the fundamental mode of vibration, a first approximation is obtained by equating $\tan \beta l$ to βl. From equation (2.13) we thus obtain

$$(\beta l)^2 = \frac{1}{\gamma}. \quad . \quad . \quad . \quad . \quad . \quad (2.21)$$

For a second approximation, corresponding to equation (1.4) of Section I., we include the second term in the expansion of $\tan \beta l$ in terms of ascending powers of βl. Thus

$$(\beta l)^2 \left[1 + \frac{(\beta l)^2}{3}\right] = \frac{1}{\gamma}. \quad . \quad . \quad . \quad (2.22)$$

In this equation the $\frac{1}{3}(\beta l)^2$ term in square brackets can be regarded as a small correction term if c or γ be large, and it is therefore permissible to replace it by $(1/3\,\gamma)$ from equation (2.21). Doing this, using equations (2.4) and (2.13), and neglecting terms involving squares and higher powers of δ, we obtain

$$\omega^2 = \frac{U^2}{l^2} \cdot \frac{3}{1+3c} \cdot \left(1 - \frac{\delta}{1+3c}\right). \quad . \quad . \quad (2.23)$$

Following the approximation used above, we equate δ to $\sigma^2 K^2 \beta^2$, and we replace β^2 by its value when lateral motion is negligibly small, *i. e.*, by $3/l^2(1+3c)$ from equation (1.4). Thus

$$\delta = \sigma^2 \frac{K^2}{l^2} \cdot \frac{3}{(1+3c)}. \quad . \quad . \quad . \quad . \quad (2.24)$$

Inserting this value of δ in equation (2.23), we obtain

$$\omega = \frac{U}{l}\left[\frac{3}{(1+3c)}\right]^{\frac{1}{2}} \cdot \left\{1 - \frac{\sigma^2}{2} \cdot \frac{K^2}{l^2} \cdot \frac{3}{(1+3c)^2}\right\}. \quad (2.25)$$

If lateral motion is neglected ω becomes ω_0 and equation (2.25) reduces to equation (1.4); the ratio (ω_0/ω) is

$$\frac{\omega_0}{\omega} = 1 + \frac{\sigma^2}{2} \cdot \frac{K^2}{l^2} \cdot \frac{3}{(1+3c)^2} \cdot \quad . \quad . \quad (2.26)$$

We may obtain a better approximation for ω in the present case by following the procedure of reversal of series, which in the case of negligible lateral motion leads to equation (1.12) of Section I. The required result can be obtained from equation (1.12), noting that αl and c of Section I. are to be replaced by βl and γ respectively. Thus

$$(\beta l)^2 = \frac{1}{\gamma}\left\{1 - \frac{1}{3\gamma} + \frac{4}{45\gamma^2} - \frac{16}{945\gamma^3} + \frac{16}{14{,}175\gamma^4} + \cdots\right\},$$

which, in conjunction with equations (2.4) and (2.13), gives

$$\omega = \frac{U}{l\sqrt{c}}\left\{1 - \frac{(1+\delta)}{3c} + \frac{4(1+2\delta)}{45c^2} - \frac{16(1+3\delta)}{945c^3} + \frac{16(1+4\delta)}{14{,}175c^4} - \cdots\right\}^{\frac{1}{2}} \quad (2.27)$$

to the present degree of approximation; the value of δ is given to sufficient accuracy by equation (2.24). Equation (2.27) reduces to equation (1.12) when δ is zero.

As regards the accuracy of equations (2.8), (2.10), (2.12), (2.18), (2.20), (2.25), and (2.27), all the equations are subject to the restriction that (K^4/λ^4) is small in comparison with unity; the equations relating to small and large values of c are in addition subject to the restrictions which apply to the corresponding solutions when lateral motion is negligible (*v.* Section I.).

Considering next the numerical magnitude of the effect of lateral motion, we may assume $\pi^2\sigma^2$ to be unity as before. Taking first the case of unloaded bars vibrating in the fundamental mode, for a free-free or a fixed-fixed bar, ω differs from ω_0 by one per cent. when l becomes approximately equal to 7 K; for a fixed-free bar the same difference is obtained when l becomes approximately equal to 3·5 K. For bars of circular cross-section this would imply that the length is five times the radius for free-free and fixed-fixed bars, and two and a half times the radius for a fixed-free bar.

Taking next the case of loaded fixed-free bars vibrating in the fundamental mode, we shall assume that $l=3{\cdot}5$ K, so that (ω_0/ω) for an unloaded bar is approximately equal to 1·01. The values of (ω_0/ω) for typical values of c are then as follows :—

TABLE I.

c.	ω_0/ω.
0·00	1·0102
0·01	1·0096
0·10	1·0068
0·50	1·0015
1·00	1·0008
10·00	1·0004

It is interesting to note that as c increases the ratio ω_0/ω approaches unity.

III. *Torsional Vibration of Infinitely Thin, Loaded, Fixed-Free Bars.*

There exists a very close analogy between the longitudinal and torsional vibrations of bars, and, as will be shown below, the various results given above for longitudinal vibrations yield similar results for torsional vibrations.

In the case of infinitely thin bars in torsional vibration it is legitimate to assume that the normal sections of the bar remain plane and undistorted, *i. e.*, that the displacement of a point in any normal section of the bar is confined to that section. If ψ be the angular displacement at time t at a normal section at distance z from the origin, then the differential equation of motion (Love, *op. cit.* p. 429) is

$$\rho \mathrm{AK}^2 \frac{\partial^2 \psi}{\partial t^2} = \mathrm{C} \frac{\partial^2 \psi}{\partial z^2}, \quad . \quad . \quad . \quad . \quad (3.1)$$

where C denotes the torsional rigidity of the bar, *i. e.*, the couple required to produce unit twist in unit length of the bar. The value of C is determined by the rigidity

modulus G of the material of the bar and by the size and shape of its cross-section. The evaluation of C for various cross-sections is due to Saint-Venant, and the results are given in a number of text-books on elasticity (*vide* Prescott, *op. cit.* ch. vii.; Love, *op. cit.* ch. xiv.). In general C can be written in the form

$$C=k^2GAK^2, \quad . \quad . \quad . \quad . \quad . \quad . \quad (3.2)$$

where k^2 is a dimensionless quantity determined by the shape of the cross-section.

For an elliptic cross-section, with semi-axes a and b,

$$k^2=\frac{4a^2b^2}{(a^2+b^2)^2}, \quad . \quad . \quad . \quad . \quad . \quad . \quad (3.3)$$

from which it follows that for a circular cross-section $k^2=1$.

If the cross-section is a rectangle with sides $2a$ and $2b$, $(a>b)$, and if $s=a/b$,

$$k^2=\frac{3}{4(1+s^2)}\left\{\frac{16}{3}-\left(\frac{4}{\pi}\right)^5\cdot\frac{1}{s}\right.$$
$$\left.\cdot\sum_{p=0}^{\infty}\frac{1}{(2p+1)^5}\cdot\tanh(2p+1)\frac{\pi s}{2}\right\}. \quad (3.4)$$

The value of the summation in equation (3.4) has been evaluated for a number of values of the parameter s; the variation of k^2 with s is given by curve (A) in figure, k^2 being plotted as ordinate and s as abscissa. In the particular case of a square $(s=1)$, $k^2=0{\cdot}8435$. If $a>3b$, the value of k^2 is given to an accuracy exceeding 1 in 10,000 by the expression

$$k^2=\frac{4}{1+s^2}\left(1-\frac{0{\cdot}63025}{s}\right). \quad . \quad . \quad . \quad (3.5)$$

Reverting to equations (3.1) and (3.2), it is possible to write

$$\frac{\partial^2\psi}{\partial t^2}=\frac{k^2G}{\rho}\cdot\frac{\partial^2\psi}{\partial z^2}=k^2V^2\frac{\partial^2\psi}{\partial z^2}, \quad . \quad . \quad . \quad (3.6)$$

and thus the velocity of propagation of torsional waves in an infinitely thin bar is equal to kV.

The boundary conditions appropriate to different end conditions are

(i.) At a fixed end $\psi=0$ for all values of t.

(ii.) At a free, unloaded end the strain $(\partial\psi/\partial z)$ is zero for all values of t.

(iii.) At a free end, carrying a laminar load of moment of inertia I about Oz, the restoring couple due to the strain is equal to the product of I into its angular acceleration, *i. e.*,

$$I\frac{\partial^2\psi}{\partial t^2} = -C\frac{\partial\psi}{\partial z}. \quad . \quad . \quad . \quad . \quad . \quad (3.7)$$

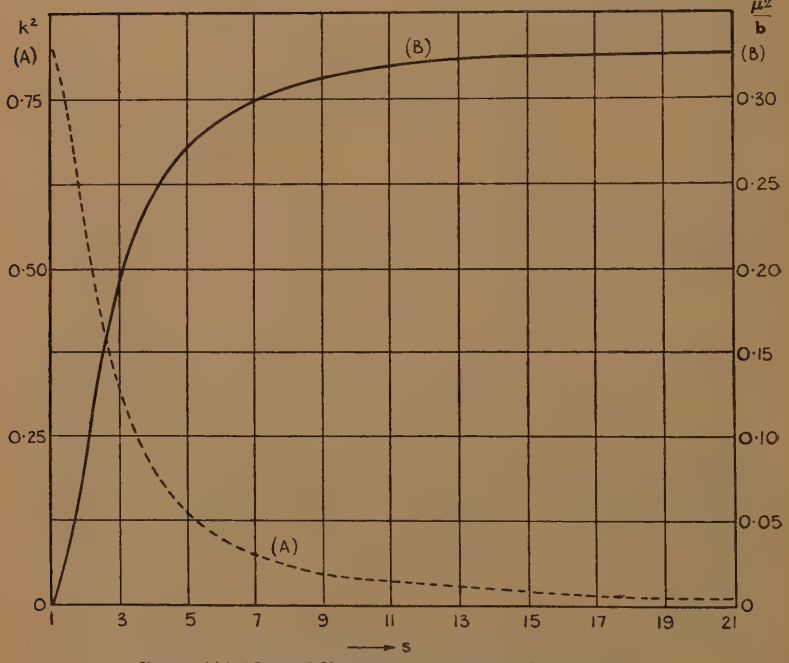

Curve (A) (dotted-line curve): graph of k^2 against s.
Curve (B) (full-line curve): graph of (μ^2/b^2) against s.

On account of the close analogy between the boundary conditions and equations (3.6) and (3.7), and the corresponding equations (equations (1.1) and (1.2)) for longitudinal vibration, it becomes possible to write down the frequency equations for the torsional vibration of unloaded and loaded bars. The results for unloaded bars have been given by Schulze [11]. The case of a bar of length l, fixed at the end $z=0$ and carrying at $z=l$ a laminar load of moment of inertia I about Oz, is analogous

to the case of longitudinal vibration treated in Section I. If necessary the required results could be obtained by Rayleigh's method (*cf.* equations (1.3) and (1.4)), but it is equally simple to write down the exact frequency equation (*cf.* equation (1.6)) and to derive the various approximate solutions from this, as in Section I. If ω_0 be the natural pulsatance of vibration in the present case, and if $\alpha'=\omega_0/k\mathrm{V}$, then the required frequency equation is

$$\alpha' l \tan \alpha' l = \frac{1}{d}, \quad . \quad . \quad . \quad . \quad . \quad (3.8)$$

where $d=\mathrm{I}/\mathrm{I}'$.

This equation is of the same form as equation (1.6), and it therefore follows that the explicit expressions derived in Section I. for longitudinal vibration for large and for small values of c (equations (1.3), (1.10), (1.4), and (1.12)) can be extended to the present case of torsional vibration by replacing c by d and U by kV respectively.

IV. *Torsional Vibration of Bars of Finite Lateral Dimensions.*

The validity of equation (3.1) is confined to cases where the lateral dimensions of the bar are infinitely small in comparison with the wave-length λ of the vibration. When the lateral dimensions become finite the normal sections of the bar no longer remain plane and the torsional displacement of a point, parallel to the plane of xy, is accompanied by a longitudinal displacement parallel to Oz. The effect of this longitudinal displacement on the pulsatance could, if necessary, be found by Rayleigh's method, but it is equally simple to use a modified differential equation and to proceed as in Section II. The necessary modification in the differential equation has been given by Love (*op. cit.* p. 429); in the present notation the modified equation may be written

$$\rho \mathrm{A} \mathrm{K}^2 \frac{\partial^2 \psi}{\partial t^2} - \rho \left(\int \phi^2 d\mathrm{A} \right) \frac{\partial^4 \psi}{\partial z^2 \, \partial t^2} = \mathrm{C} \frac{\partial^2 \psi}{\partial z^2}, \quad . \quad (4.1)$$

where ϕ is the torsion function for the section, *i. e.*, the displacement parallel to Oz per unit twist per unit length; the integral of ϕ^2 is to be taken over all the elements dA of the cross-section.

This equation may be rewritten

$$\frac{\partial^2\psi}{\partial t^2}-\mu^2\frac{\partial^4\psi}{\partial z^2\,\partial t^2}=k^2V^2\frac{\partial^2\psi}{\partial z^2}, \quad . \quad . \quad . \quad (4.2)$$

where $$\mu^2=\frac{\int\phi^2 dA}{AK^2}.$$

This equation is of the same form as equation (2.2); the second differentials with respect to t and z have unity and wave-velocity respectively as coefficients, whilst the term involving $(\partial^4\psi/\partial z^2\,\partial t^2)$ represents the effect of the warping of the normal sections when the lateral dimensions are not infinitely small. The accuracy of equation (4.2) is of the same order as that of equation (2.2), and it is thus accurate only when K^4/λ^4 is small in comparison with unity.

The similarity between equations (4.2) and (2.2) and between the boundary conditions for longitudinal and torsional vibrations enables us to write down the frequency equations appropriate to various cases of torsional vibrations. In the following equations ω is used to denote the pulsatance when allowance is made for warping of the cross-sections, whilst ω_0 denotes the pulsatance when warping of the cross-sections is neglected.

(a) *Unloaded Bars of length l.*

(i.) *Free-free bars* (*cf.* equation (2.8)).

$$\frac{\omega_0^2}{\omega^2}=1+\frac{m^2\pi^2\mu^2}{l^2} \quad (m=1, 2, \ldots). \quad . \quad . \quad (4.3)$$

(ii.) *Fixed-free bars* (*cf.* equation (2.10)).

$$\frac{\omega_0^2}{\omega^2}=1+(m+\tfrac{1}{2})^2\frac{\pi^2\mu^2}{l^2} \quad (m=0, 1, \ldots). \quad . \quad (4.4)$$

(iii.) *Fixed-fixed bars* (*cf.* equation (2.12)).

$$\frac{\omega_0^2}{\omega^2}=1+\frac{m^2\pi^2\mu^2}{l^2} \quad (m=1, 2, \ldots). \quad . \quad . \quad (4.5)$$

(b) *Loaded, Fixed-Free Bars of length l.*

The frequency equation (*cf.* equation (2.13)) is

$$\left.\begin{aligned}&\beta' l\tan\beta' l=\frac{\beta'^2k^2V^2}{\omega^2 d}=\frac{1}{\gamma'}=\frac{1+\beta^2\mu^2}{d},\\ &\text{where}\quad \beta'^2=\frac{\omega^2}{k^2V^2-\mu^2\omega^2}=\frac{\omega^2}{k^2V^2}\cdot\frac{1}{1-\delta'};\quad \delta'=\frac{\mu^2\omega^2}{k^2V^2},\\ &\qquad \gamma'=d(1-\delta').\end{aligned}\right\}. \quad (4.6)$$

For small values of d the ratio (ω_0/ω) can be written (*cf.* equation (2.19))

$$\frac{\omega_0}{\omega}=1+\frac{(2m+1)^2}{8}\cdot\frac{\pi^2\mu^2}{l^2}\cdot\frac{1-d}{(1+d)^3} \quad (m=0, 1, \ldots). \quad (4.7)$$

Similarly, for *large values of* d (*cf.* equation (2.26)), for the fundamental mode

$$\frac{\omega_0}{\omega}=1+\frac{\mu^2}{2l^2}\cdot\frac{3}{(1+3d)^2} \quad . \quad . \quad . \quad . \quad (4.8)$$

to a first approximation, whilst to a better degree of approximation (*cf.* equation (2.27))

$$\omega=\frac{kV}{l\sqrt{d}}\left\{1-\frac{1}{3d(1-\delta')}+\frac{4}{45d^2(1-\delta')^2}-\frac{16}{945d^3(1-\delta')^3}+\frac{16}{14{,}175d^4(1-\delta')^4}\cdots\right\}. \quad (4.9)$$

These solutions are naturally subject to the same restrictions as regards accuracy as the corresponding equations in Section II.

We have next to evaluate the parameter μ^2 of equation (4.2) for various cross-sections.

Taking first the case of an elliptic cross-section with semi-axes a and b, the appropriate form of the torsion function (Love, *op. cit.* p. 317) is

$$\phi=-\frac{a^2-b^2}{a^2+b^2}.xy.$$

Now $\iint x^2y^2dx.dy$, taken over the cross-section of the ellipse, can be shown to be $\pi a^3b^3/24$, and hence

$$\mu^2=\frac{a^2b^2}{6}\cdot\frac{(a^2-b^2)^2}{(a^2+b^2)^3}\cdot \quad . \quad . \quad . \quad . \quad (4.10)$$

It is interesting to note that μ^2, and therefore the correction under discussion, vanishes for a circular cross-section.

Considering next the case of a rectangular cross-section whose sides parallel to Ox and Oy are $2a$ and $2b$ respectively $(a>b)$,

$$\phi=-xy+4b^2\left(\frac{2}{\pi}\right)^3\sum_{p=0}^{\infty}\frac{(-)^p}{(2p+1)^3}\cdot\frac{\sinh\frac{(2p+1)\pi x}{2b}}{\cosh\frac{(2p+1)\pi a}{2b}}.\sin\frac{(2p+1)\pi y}{2b}. \quad (4.11)$$

(Love, *op. cit.* p. 318), or if we write

$$q_p=(2p+1)\pi/2,\ s=a/b,$$

$$\phi=-xy+\frac{32b^2}{\pi^3}\sum_0^\infty \frac{(-)^p}{(2p+1)^3}\cdot\frac{\sinh\frac{q_px}{b}\sin\frac{q_py}{b}}{\cosh q_ps}. \quad (4.12)$$

Thus μ^2 can be written as the sum of μ_1^2, μ_2^2, and μ_3^2, where

$$AK^2\mu_1^2=\int_{-a}^{a}\int_{-b}^{b}x^2y^2\,dx\,dy,$$

$$AK^2\mu_2^2=-\frac{64b^2}{\pi^3}\int_{-a}^{a}\int_{-b}^{b}\sum_0^\infty\frac{(-)^p}{(2p+1)^3}.xy \cdot\frac{\sinh\frac{q_px}{b}.\sin\frac{q_py}{b}}{\cosh q_ps}.dx\,dy,$$

$$AK^2\mu_3^2=\frac{1024b^4}{\pi^6}\int_{-a}^{a}\int_{-b}^{b}\left[\sum_0^\infty\frac{(-)^p}{(2p+1)^3}\cdot\frac{\sinh\frac{q_px}{b}.\sin\frac{q_py}{b}}{\cosh q_ps}\right]^2.dx\,dy. \quad (4.13)$$

The value of μ_1^2 is found to be

$$\mu_1^2=\frac{a^2b^2}{3(a^2+b^2)}=\frac{a^2}{3(1+s^2)}. \quad . \quad . \quad . \quad (4.14)$$

Turning next to the evaluation of μ_2^2, and taking the pth term of the series, we have to evaluate

$$-\frac{64b^2}{\pi^3AK^2}\cdot\frac{(-)^p}{(2p+1)^3} \cdot\ .\ .\ .\ .\operatorname{sech} q_ps\int_{-a}^{a}\int_{-b}^{b}xy\sinh\frac{q_px}{b}.\sin\frac{q_py}{b}\,dx\,dy.$$

Now $$\int_{-a}^{a}x\sinh\frac{q_px}{b}\,dx=\frac{2b^2}{q_p^2}(q_ps\cosh q_ps-\sinh q_ps),$$

$$\int_{-b}^{b}y\sin\frac{q_py}{b}\,dy=\frac{2b^2}{q_p^2}.(-)^p.$$

Hence the term in question becomes

$$-\frac{256b^2}{\pi^3 \mathrm{AK}^2}\frac{1}{(2p+1)^3}\cdot\frac{b^4}{q_p{}^4}(q_p s-\tanh q_p s)$$

or $$-\frac{192}{\pi^3}\cdot\frac{b^4}{(a^2+b^2)}\cdot\frac{1}{(2p+1)^3}\cdot\frac{1}{q_p{}^3}\left(1-\frac{\tanh q_p s}{q_p s}\right).$$

Thus

$$\mu_2{}^2=-\frac{1536}{\pi^6}\cdot\frac{b^2}{1+s^2}\sum_0^\infty\frac{1}{(2p+1)^6}\left(1-\frac{\tanh q_p s}{q_p s}\right). \quad (4.15)$$

Finally, considering the value of $\mu_3{}^2$, the square of the summation in the integral is equal to

$$\sum_0^\infty\frac{1}{(2p+1)^6}\cdot\frac{\sinh^2\frac{q_p x}{b}\sin^2\frac{q_p y}{b}}{\cosh^2 q_p s}$$

$$+\frac{2}{1^3}\frac{\sinh\frac{q_0 x}{b}\sin\frac{q_0 y}{b}}{\cosh q_0 s}\sum_1^\infty\frac{(-)^p}{(2p+1)^3}\cdot\frac{\sinh\frac{q_p x}{b}\sin\frac{q_p y}{b}}{\cosh q_p s}$$

$$-\frac{2}{3^3}\cdot\frac{\sinh\frac{q_1 x}{b}\sin\frac{q_1 y}{b}}{\cosh q_1 s}\sum_2^\infty\frac{(-)^p}{(2p+1)^3}\cdot\frac{\sinh\frac{q_p x}{b}\sin\frac{q_p y}{b}}{\cosh q_p s}+\ldots$$

. . . (4.16)

Now the integrands are either of the form

$$\sinh^2\frac{q_p x}{b}\sin^2\frac{q_p y}{b}$$

or $$\sinh\frac{q_p x}{b}.\sinh\frac{q_r x}{b}.\sin\frac{q_p y}{b}\sin\frac{q_r y}{b} \quad (p\neq r),$$

the former corresponding to the first summation in (4.16) and the latter to the second and subsequent summations. The former, when integrated over the cross-section, gives

$$\frac{b^2}{2q_p}(\sinh 2q_p s-2q_p s),$$

whilst the integral of the latter over the cross-section vanishes.

Thus

$$\mu_3{}^2=\frac{1024\,b^4}{\pi^6 \mathrm{AK}^2}\int_{-a}^{a}\int_{-b}^{b}\sum_{0}^{\infty}\frac{1}{(2p+1)^6}\cdot\frac{\sinh^2\frac{q_p x}{b}\sin^2\frac{q_p y}{b}}{\cosh^2 q_p s}\,.dx\,dy$$

$$=\frac{768}{\pi^6}\cdot\frac{b^2}{1+s^2}\sum_{0}^{\infty}\frac{1}{(2p+1)^6}\left(\frac{\tanh q_p s}{q_p s}-\operatorname{sech}^2 q_p s\right). \quad (4.17)$$

From equations (4.14), (4.15), and (4.17) it follows that

$$\mu^2=\mu_1{}^2+\mu_2{}^2+\mu_3{}^2$$

$$=\frac{b^2}{1+s^2}\left\{\frac{s^2}{3}+\frac{768}{\pi^6}\sum_{0}^{\infty}\frac{1}{(2p+1)^6}\left(\frac{3\tanh q_p s}{q_p s}+\tanh^2 q_p s-3\right)\right\}. \quad (4.18)$$

The expression for μ^2 given in equation (4.18) can be simplified, since $\tanh q_p s$ can always be identified with unity when $p\geqslant 1$. This can be seen when it is remembered that $s\geqslant 1$ and that $\tanh q_p s$ approaches unity as the argument increases. In the most unfavourable case of $s=1$, $q_0 s=\frac{\pi}{2}$, $q_1 s=\frac{3\pi}{2}$, . . . ; now $\tanh\frac{\pi}{2}=0{\cdot}9172$, whilst $\tanh\frac{3\pi}{2}$ differs from unity by less than 2 in 10,000. When s is unity, since we are dealing with a correction term, it is therefore justifiable to identify $\tanh q_p s$ with unity for $p\geqslant 1$. When $s\geqslant 3$, $q_0 s\geqslant\frac{3\pi}{2}$, and in this case $\tanh q_0 s$ also can be written as unity.

Thus, for $1\leqslant s\leqslant 3$,

$$\mu^2=\frac{b^2}{1+s^2}\left\{\frac{s^2}{3}+\frac{768}{\pi^6}\left(\frac{6\tanh\frac{\pi s}{2}}{\pi s}+\tanh^2\frac{\pi s}{2}-3\right)\right.$$

$$\left.+\frac{768}{\pi^6}\sum_{1}^{\infty}\left(\frac{6}{(2p+1)^7\pi s}-\frac{2}{(2p+1)^6}\right)\right\}. \quad (4.19)$$

Now

$$\sum_{1}^{\infty}\frac{1}{(2p+1)^7}=0{\cdot}0004715,$$

$$\sum_{1}^{\infty}\frac{1}{(2p+1)^6}=0{\cdot}001447$$

(Dale, Five-figure Tables, p. 92),

and these summations may thus be neglected in comparison with $\frac{6}{\pi s}\tanh\frac{\pi s}{2}$ and $(\tanh^2\frac{\pi s}{2}-3)$ without committing an error greater than about 2 in 1,000, which is negligible in a correction term.

Equation (4.19) may thus be written

$$\frac{\mu^2}{b^2}=\frac{1}{1+s^2}\left\{\frac{s^2}{3}+\frac{768}{\pi^6}\left(\frac{6\tanh\frac{\pi s}{2}}{\pi s}+\tanh^2\frac{\pi s}{2}-3\right)\right\}$$

$$=\frac{1}{3(1+s^2)}\left\{s^2+\frac{4{\cdot}577}{s}\tanh\frac{\pi s}{2}+2{\cdot}397\tanh^2\frac{\pi s}{2}-7{\cdot}190\right\}. \quad . \quad (4.20)$$

In the particular case of a square cross-section ($s=1$)

$$\frac{\mu^2}{b^2}=0{\cdot}0034_5.$$

If $s\geqslant 3$, μ^2 is given with sufficient accuracy by the expression

$$\frac{\mu^2}{b^2}=\frac{1}{3(1+s^2)}\left\{s^2+\frac{4{\cdot}577}{s}-4{\cdot}793\right\}. \quad . \quad (4.21)$$

The value of (μ^2/b^2) increases as s increases, and as s becomes infinite (μ^2/b^2) asymptotically approaches 1/3. The relation between (μ^2/b^2) and s is shown in curve B of the figure; in this figure s is plotted as abscissa and (μ^2/b^2) as ordinate.

We have next to consider the order of magnitude of the correction under discussion, and, following the procedure used in connexion with the correction for lateral motion in longitudinal vibrations, it is convenient to find the value of the ratio l/b which makes ω_0 differ from ω by one per cent. for the fundamental mode. The values of this ratio for different values of s are shown in Table II. for unloaded free-free and fixed-fixed bars, and in Table III. for unloaded fixed-free bars.

It is clear from the above tables that the correction is more important when s is large, and that the correction is greater for given free-free and fixed-fixed bars than

it is for a fixed-free bar of identical length and cross-section.

The magnitude of the correction for a loaded fixed-free bar vibrating in the fundamental mode can be seen from Table I., since it is permissible to replace c by d (see equations (4.6) to (4.9)). The table is, of course, applicable to those pairs of values of s and l/b, given in Table III., for which ω_0 differs from ω by one per cent. when the bar is unloaded.

TABLE II.

Free-Free and Fixed-Fixed Bars.

s	1	2	5	10
l/b	1·31	6·94	11·6	12·5

TABLE III.

Fixed-Free Bars.

s	1	2	5	10
l/b	0·65	3·47	5·80	6·25

In conclusion, the author desires to thank Mr. Thomas Lewis, Head of the Applied Mathematics Department, for discussing the results, and Mr. G. E. Bennett for checking them.

References.

(1) Lord Rayleigh, ' Theory of Sound,' vol. i. p. 249 (London, 1894).
(2) Donkin, ' Acoustics,' p. 156 (Oxford, 1870).
(3) Prescott, 'Applied Elasticity,' p. 263 (London, 1924).
(4) Timoshenko, ' Vibration Problems in Engineering,' p. 209 (New York, 1928).
(5) Jahnke-Emde, *Funktionentafeln*, p. 32 (Berlin, 1933).
(6) Lord Rayleigh, *op. cit.* p. 251.
(7) Davies, Phil. Mag. xvi. p. 97 (1933).
(8) Love, ' Theory of Elasticity,' p. 428 (Cambridge, 1934).
(9) Pochammer, *J. f. Math.* (*Crelle*), lxxxi. p. 324 (1876).
(10) Chree, Quart. J. of Math. xxi. (1886) and xxiv. (1890).
(11) Schulze, *Ann. der Phys.* xiii. p. 583 (1904).

XXX. *Note on the Paper "A Note on the Vibrations of a Rotating Rope*." By* C. E. Wright †.

THE following remarks are offered:—

1. The equations for the steady state of the rope yield the solution

$$T=\tfrac{1}{2}m\omega^2(l^2-x^2),\quad y=A\frac{x}{l},\quad z=\frac{2g}{\omega^2}\log\left(1+\frac{x}{l}\right),$$

when the rope is assumed to lie nearly along the (rotating) x-axis. The constant A is really unrestricted, but no loss of generality occurs by making it zero, which is done in what follows.

2. For small oscillations the changes in tension in the string are not necessarily negligible. Let $x+\xi$, η, $z+\zeta$ correspond in a small oscillation to x, 0, z in the steady state. When the arc-elements are identified $\dfrac{d\xi}{dx}$ is seen to be of the second order in $\dfrac{dz}{dx}$, $\dfrac{d\zeta}{dx}$, $\dfrac{d\eta}{dx}$; if it is put zero ξ, a function of t at most, must vanish identically, since it vanishes at $x=0$. Let the tension be $T+T'$. The equations reduce to

$$-2m\dot{\eta}\omega=dT'/dx, \quad . \quad . \quad . \quad . \quad . \quad . \quad (1)$$

$$m(\ddot{\eta}-\eta\omega^2)=\frac{d}{dx}\left[(T+T')\frac{d\eta}{dx}\right], \quad . \quad . \quad . \quad (2)$$

$$m\ddot{\zeta}=\frac{d}{dx}\left[T'\frac{dz}{dx}+(T+T')\frac{d\zeta}{dx}\right]. \quad . \quad . \quad . \quad (3)$$

If T' is neglected in comparison with T equations (2) (3) reduce to those in the original paper, and it is readily verified that ζ may involve *any* odd Legendre coefficient, η any odd coefficient except the first, the exception, with $\eta \propto P_1\left(\dfrac{x}{l}\right).e^{0\cdot t}$ corresponding merely to a

* Phil. Mag., Aug. 1937, pp. 293–299.
† Communicated by the Author.

constant displacement of the x-axis, which has been already provided for in the solution for the steady state.

3. The extra tension $T' = -2m\omega\int\dot{\eta}\,dx$ rises in importance with the frequency. If it is retained in eq. (2) (3), by use of (1), (2) gives $u=\int\eta\,dx$ by means of a non-linear equation of order 3 in x. η is still to this approximation entirely independent of the equation in ζ.

If values of η can be obtained from this equation corresponding values of ζ can be obtained from (3), which remains linear.

Bexley Heath.
19th August, 1937.

XXXI. *Supplementary Note to the Paper "The Propagation of Electromagnetic Waves in an Ionized Atmosphere"* *. *By* L. G. H. Huxley, *M.A.*, *D.Phil.* †

IN the above paper the quantities s, d, and g, which appear in the complex expression for the current density, were incorrectly prefixed with positive instead of negative signs. Consequently the symbols A, B, and C which appear in the general formulæ should now be interpreted as follows :—

$$A=-\frac{\sigma}{2p}(s+jS)\,;\quad B=-\frac{\sigma}{2p}(D-jd)\,;$$

$$C=-\frac{\sigma}{p}(g+jG). \qquad (8)$$

The formula for the complex refractive index for the case of propagation along the applied magnetic field becomes :—

$$\frac{c}{v^2}=(\mu-jk)^2=1-\frac{2\pi\sigma}{p}[(s\pm d)+j(S\pm D)].$$

* Communicated by the Author.
† Phil. Mag. (7) xxv. p. 148 (1938).

XXXII. *Notices respecting New Books.*

Mathematical Analysis. Volumes I. and II. By J. H. Michell and M. H. Belz. [Pp. 1087+xxiii+xi.] (MacMillan. Price 42*s.* each volume.)

In preparing this very attractive course of mathematical analysis the authors have determined that the treatment should differ from that found in other works of intermediate standard in that it should be rigorous. Little previous knowledge is assumed; indeed, in the differential calculus only the idea of rate of change is presupposed. The subject is expounded on the basis of the theory of real numbers, geometrical methods being employed only in an illustrative manner, and not as a means of replacing abstract discussions. The desirability of the book forming a working text is met by including many examples worked at length, and by suggesting problems to be worked by the student.

The authors have been aware of the possible detrimental effect which such a text-book, consisting largely of formal deductions, may have on the reader, and have attempted to foster his inventiveness and spirit of exploration by including sections entitled "working notions," in which results obtained in the text by formal methods are obtained rapidly by informal and intuitive processes. There is no doubt that these volumes will be especially welcomed by mathematics students. While an adequate mathematical equipment is essential to the understanding of recent developments in physical science, the desirability of replacing the present expositions by such a rigorous treatment as is offered here for the *average* science or engineering student (for whom this course is apparently intended) is debatable.

It is unfortunate that these excellent volumes are so highly priced.

Lectures on the Mathematical Theory of Electricity. By F. B. Pidduck. [Pp. 110+viii.] (Oxford University Press. Price 7*s.* 6*d.*)

This book, which is based upon a series of lectures delivered to mathematical students, does not aim at giving a complete or balanced treatment of the subject, but should be regarded as a supplement to the standard text-books, of which the author's 'Treatise on Electricity' may be cited. The following selection illustrates the variety in the topics discussed —the quadrant electrometer, the theory of the mass spectro-

graph, the calculation of mutual and self inductances, the oscillations of a triode, the application of the laws of reflexion and transmission of electric waves in the Lummer-Gehrcke interferometer—and indicates that the volume will be of considerable interest to physics students. The value of this excellent book is enhanced by the inclusion of eight useful exercises for the consideration of the reader.

Plane Trigonometry. By EDWARD S. ALLEN, Associate Professor of Mathematics in Iowa State College. (McGraw-Hill Publishing Co., Ltd.)

THE present reviewer regrets his inability to give a very favourable notice to this text-book, as it seems to him that the author has not realized that talking round and round mathematical difficulties has never yet cleared them up in pupils' minds. (A coordinate distance with its algebraic sign is not made easier to understand by calling it a "leg.") It would seem that the order in which the subject-matter is taken must be an almost impossible one for a beginner, for the results of addition formulæ, inverse functions, solution of trigonometrical equations all precede the solution of triangles. As a book for beginners it could not be a success; as part of a mathematical training it is inadequate and often misleading. The book compares unfavourably with the standard English Trigonometry text-books used in schools.

Hydrostatics. By A. S. RAMSEY, President of Magdalen College, Cambridge. (Cambridge University Press. Price 7*s.* 6*d.*)

WE have in this volume a most welcome addition to the stock of good text-books for good sixth form pupils and first year University students. The book is not a weakened version of the first volume of the 'Hydromechanics' of Besant and Ramsey; it is a new piece of work undertaken with its special *clientele* of sixth-formers clearly in view. In present days, when text-books so frequently reflect a vast collection of teaching devices, it is pleasant to find a book ignoring such devices, and building itself up upon a plain statement of physical and mathematical thought. Yet the level of difficulty of presentation throughout the book is admirably suited to those for whom it is intended.

The subject is developed along customary lines—pressure, resultant thrust, centres of pressure, metacentre, rotating fluids,—and then, in the closing chapters, the author turns to

pressure of gases and capillarity, matters which are all too often squeezed right out of the Hydrostatics course. There is an extremely interesting and simply written chapter on hydrostatic machines. Throughout the book will be found an admirable supply of figures and examples. The figures are well chosen, clearly printed and placed; the examples strike a happy balance between the heavy arithmetic of numerical work on the one hand, and the very rarefied hypothetical case on the other.

Anyone who has lectured on hydrostatics will be ready to recommend this book. It will be of great assistance to those who have previously taught without the aid of a text-book, and should also produce a spread of the subject amongst students in preliminary stages. The book is a product of the Cambridge first year mathematical school and of the Cambridge Press; both are seen to their usual advantage.

Electron Tubes in Industry. By K. Henney. [Pp. 539.] (McGraw Hill Publishing Co., Ltd.)

The first edition of this book appeared in 1934 under the same title; in this, the second edition, the subject-matter covers substantially the same field as before, with additions and revisions corresponding to inventive progress in three years. The author states in the preface that the purpose of the book is to acquaint industrial engineers, teachers, and students with the many applications of amplifiers, oscillators, photo-tubes, rectifiers, thyratrons, grid-glow tubes, and cathode-ray tubes to non-communication industries. The book is not therefore to be regarded as a text-book of instruction—Chapter I., which deals with Ohm's law and similar elements of electric theory, might well be omitted,—but as a manual of achievement of the "electronic art." In this it succeeds admirably, and there is no doubt it will be well received both by engineers, who will find an encyclopædic record of new tricks for performing industrial operations, and also by experimenters, who will find an equally complete description of new measuring devices.

Chapter II. describes—rather too briefly—the different types of valve or tube, and English readers will find helpful the list of American trade names for various genera. Actually three types are of major importance and occupy, with their applications, nearly the whole of the text. Chapter III. deals with applications of vacuum triodes or hard valves; Chapter IV. with gaseous triodes, perhaps more commonly known now as thyratrons. Chapters V. and VI. deal with

photo-electric cells, and the last chapter with miscellaneous tubes. Very few known applications of valves can have been omitted, and the book will therefore make an excellent manual of reference in the laboratory.

The Fundamentals of Vacuum Tubes. By A. V. Eastman. [Pp. 438.] (McGraw Hill Publishing Co., Ltd.)

The title of this book gives a wrong impression of its contents. The author in the preface states that it has been his intent to combine in a single text the basic theory underlying the operation of all types of modern vacuum tubes, both radio and industrial, together with their more common applications. In fact, however, the emphasis of the book is very largely on a few rather specialized, though important, applications in the communication field ; so that 117 pages are devoted to amplifiers and 93 to oscillators and modulation. On the other hand, physical phenomena underlying the tube characteristics receive scarcely any treatment, and even the " three-halves-power " law is given as a bald statement without derivation. The book is designed for senior electrical students in an engineering college, and the author is apparently reluctant to make too much use of the calculus.

Included under the heading of vacuum tubes are gas-filled tubes and photo-electric cells. The former are considered for 28 pages under diodes and for 20 pages under triodes, and thus in a sense take an adequate share of the text, while the chapter on photo-sensitive tubes contains good description of the characteristics.

It is to be hoped that in another edition a better balance will be kept between the various items of material which make up the scope of the book, but this criticism having been made, the treatment of the problems of amplifiers and oscillators is good. In particular the portion of Chapter IV. dealing with rectifier filter design is a welcome inclusion.

[*The Editors do not hold themselves responsible for the views expressed by their correspondents.*]

The primary standard of mutual inductance of the National Physical Laboratory.

THE

LONDON, EDINBURGH, AND DUBLIN

PHILOSOPHICAL MAGAZINE

AND

JOURNAL OF SCIENCE.

[SEVENTH SERIES.]

MARCH 1938.

XXXIII. *The Complete Detection of Beta-particles.* By SAMUEL C. CURRAN, *M.A., B.Sc., Ph.D., Carnegie Research Scholar, University of Glasgow* *.

Introduction.

IN the present paper the conditions under which the complete detection of α- and, in particular, of β-particles is possible are investigated. A comparison of the performance of the Geiger point counter[1] with reversed potentials is made, and it is shown that when it is desirable to count all the entering β-rays it is preferable to work with the case at a negative potential with respect to the point. The form and magnitude of the impulses, the variation in efficiency with the pressure and the path of the ray in the counter, and the shape of the count-voltage characteristic curve for different tubes are analyzed. From a discussion of the difference in the two methods of operating the tubes the conditions to be fulfilled for high efficiency in detection are deduced. Finally, the mode of action of the tube is discussed, and the explanation offered supported by some experimental results.

In many experiments with β-particles it is necessary to measure the absolute intensity of the radiation, and the

* Communicated by Prof. E. Taylor Jones.

only instrument available for this purpose is some form of counting tube. For work with relative values various methods, such as the ionization chamber, the cloud chamber, or the photographic plate, may be employed. It would appear that under certain well-defined conditions the Geiger point counter responds to every β-particle entering it. The writer finds that in many cases these conditions are difficult to fulfil, and normally a fraction of the β-rays are registered. It is usual practice to have the Geiger counter with the case at a positive potential relative to the point, but it is shown that it is much more readily possible to detect every β-particle with the potential reversed.

The Form of the Impulse.

In order that the form and magnitude of the impulse from the counter might be conveniently studied an

Fig. 1.

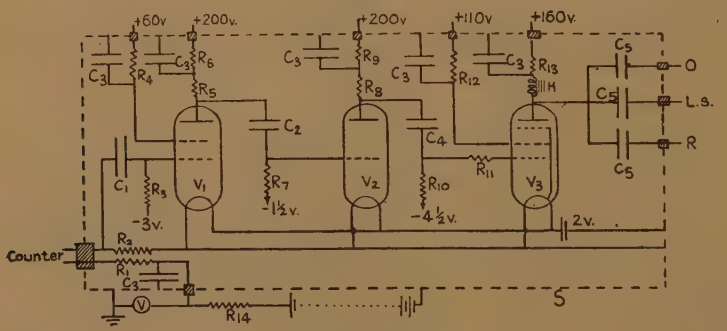

The amplifier.

$R_1=3.10^9\ \omega$, $R_2=1{\cdot}4\ .\ 10^7\ \omega$, $R_{3,\ 7,\ 10}=5\ .\ 10^4\ \omega$, $R_{4,\ 8}=5.10^4\ \omega$, $R_5=10^5\ \omega$, $R_6=1{\cdot}2.10^4\ \omega$, $R_{9,\ 12}=5.10^3\ \omega$, $R_{17}=10^3\ \omega$, $R_{13}=10^4\ \omega$, $R_{14}=2.10^6\ \omega$; $C_1=0{\cdot}0001\ \mu F$, $C_2=0{\cdot}001\ \mu F$, $C_3=2\mu F$, $C_4=0{\cdot}01\ \mu F$, $C_5=0{\cdot}1\ \mu F$; $V_1=$Osram VS 24, $V_2=$Cossor 210 HF, $V_3=$Cossor 220 HPT; H=L. F. choke; O, L.S., R=leads to C.R. oscillograph, loud-speaker, register resp.; V=electrostatic voltmeter; S=earthed metal shield.

amplifier of high voltage magnification was constructed. With this amplifier, shown in fig. 1, coupled to the counter, the impulses in the voltage region at which counting commenced could be more carefully analyzed. The amplifier actuated three systems—a loud-speaker, a cathode-ray oscillograph, and an automatic recording device [2]. The cathode-ray oscillograph showed that the impulses

produced by α- and β-rays in the region of the threshold voltage varied considerably for different tubes. The exact manner in which counting commenced seemed to depend to a large extent on the shape of the point, the pressure and nature of the filling gas, etc. The general behaviour of the tubes was somewhat as follows :—With the point negative the α-rays began by producing a small impulse, which gradually increased in magnitude as the voltage was raised. At a somewhat higher voltage the impulse produced by β-rays began to appear, and they rapidly approached in magnitude those produced by α-particles as the potential was still further increased. Finally, the impulses produced by both particles became more or less alike in form and magnitude. With some tubes the initial separation of α- and β-particle impulses was clearly defined, while in others it was very slight. When the point was positive the results were generally similar in nature to those obtained with a negative point,

TABLE I.

Voltage on tube	592	595	598	601	603
Per cent. change in α count	−1·3	−0·9	−0·5	−0·2	+1·2

except that the initial separation of the α and β impulses was more clearly defined and the magnitudes of the impulses produced by β-particles were much more variable. However, at sufficiently high potentials the impulses produced by both particles became the same in size. This initial separation of α- and β-particles makes it possible to count α-particles as distinct from β-particles, but it is not usually practicable to detect all the α-rays without counting β-rays. With some tubes, however, it is possible to do so, especially at lower gas pressures.

Table I. shows the effect on the α count for a very weak source when 1 mg. of radium was placed at 3 cm. from the counter, which was filled with air at 2·1 cm. pressure, the point being negative. The effect of the radium was likewise very small when the point was positive. These results are similar to those obtained by Rutherford and Geiger [3] with a tube counter, as examination of the working of such a tube showed. It is to be noted that the

point counter does not, when used in this manner, produce impulses proportional to the primary ionization of the particles.

This work on the magnitude of the impulses in the neighbourhood of the threshold voltage was really incidental to the investigation of the efficiencies of the tube, and it was carried out to determine whether the magnitude of the impulse had much effect on the number of particles registered. It was found that there was more difficulty in ensuring that all the particles produced impulses large enough to work the recording instrument when the point was positive than when it was negative. In all cases, however, if the point was positive and the impulses were of sufficient magnitude all the particles were detected. On the other hand, the point being negative, the impulses could be very much more than sufficient to actuate the relay while only a fraction of the entering β-particles were causing impulses. As the positive voltage on the case was raised the number of full-sized impulses increased without any of intermediate magnitude being produced. This is in agreement with the work of Geiger & Klemperer[4], who showed that when the point is positive the impulse produced may be continuously increased from that of the primary ionization to one characteristic simply of the applied potential, while for negative points the impulse passes abruptly from that due to the primary ionization without any magnification to one characteristic of the discharge through the tube at the applied voltage. Thus, if particles are missed when the point is negative it is because the primary ionization has failed to initiate a discharge. This is not incompatible with the above results, where it was shown that α- and β-rays could produce different impulses in a counter whose point was negative, the voltage being near the threshold value. The difference is not due to the fact that the α- and β-particles have produced different currents through the tube under the action of collision-ionization. It is due to the fact that the magnitude of the discharge near the starting potential is dependent on the number of ions initially formed in the tube as well as on other factors, such as the capacity of the system, etc. Larger over-voltages remove this dependence of the magnitude on the initial ionization, and then the initial ionization either brings about a discharge or it

produces no impulse at all. Thus above a certain positive case potential it is impossible that a particle shall enter the tube and cause a discharge whose impulse will be so different from the others that it may be missed. This point was investigated to ensure against the possibility that the low values of efficiency found with a negative point might be due to this cause.

Experimental.

The arrangement adopted for most of the work on α- and β-rays was that shown in fig. 2. A pyrex-glass tube T was closed at both ends by ebonite disks with central apertures which were sealed with thin mica films. The source S on the axis of the tube was formed from parts of three-years-old glass radon capillaries mounted on a

Fig. 2.

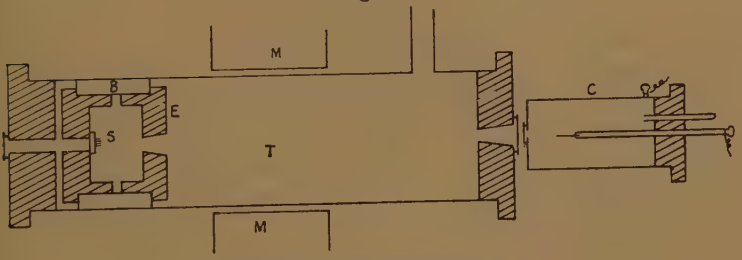

Arrangement of source and counter.

glass plate and supported in the cavity enclosed by the ebonite plugs E and the brass tube B. A small powerful electromagnet could be placed round the tube as indicated by M. The apparatus could be exhausted to a high vacuum. The counter C was placed so that its window was on the axis of the tube T. The air equivalent of the mica films between the source and counter was less than 2·5 cm. The source was R*a* (D+E+F) in equilibrium, and the counter detected the α-rays of R*a*F and the β-rays of R*a*E. The counters were constructed along the usual lines, the points being usually of steel or platinum. The filling gas, air, or argon was dried by phosphorus pentoxide or liquid air.

The Pressure in the Counter.

The number of ions formed by an ionizing particle in its passage through a gas depends on the pressure of

the gas. Experiments were carried out to determine how the number of particles detected varied with the pressure in the counting chamber. A point counter was set directly opposite a source of *Ra*E. The β-rays passed through 10 cm. of air on their way to the counter. The point was negative, and the results are shown in curve A of fig. 3. The different voltages applied to the tube at the various pressures are shown by curve B, fig. 3. The potentials were adjusted to values just below those

Fig. 3.

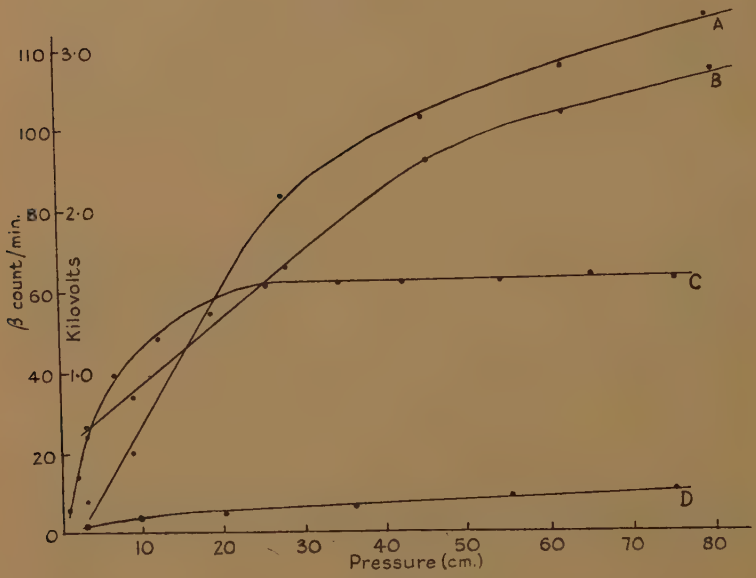

at which the tube passed spurious discharges. It is seen that the number of β-rays detected rises continuously with increasing pressure, and there is no evidence of saturation at 76 cm. A direct comparison of the two methods of using the tube was next made. The filling gas in this case was argon. The β-ray source was R*a*E at 20 cm. distance in air. The results are shown in curves C and D of fig. 3. The corresponding positive case potentials are graphed in fig. 4. Curve A_1 is the starting potential for β-ray counting and curve B_1 the actual potential on the tube. The working potentials were not adjusted to near the steady discharge values, but they represent normal

over-voltages. It was found that with the counter used here the count of β-rays increased continuously with the positive voltage on the case, while a constant counting range of voltage was obtained with the point positive, and readings were taken with the voltage within this range. Curve C, for a point positive, shows a rapid rise in β detection with increasing pressure, and saturation is reached between 30 and 40 cm. Curve D, for a point negative, shows a fairly rapid increase in the β count at first and a more gradual increase at higher pressures.

Fig. 4.

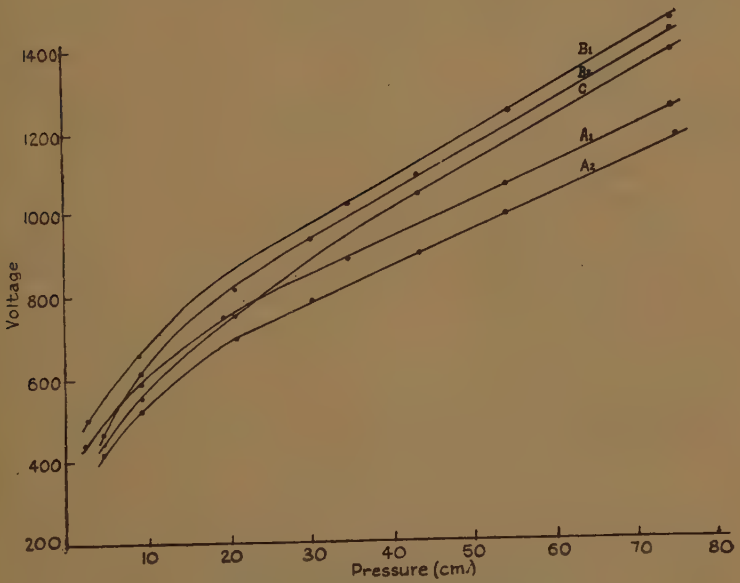

Working and starting potentials.

Saturation is not obtained in this case. Moreover, at 76 cm. pressure the efficiency of the tube with the point negative is only 0·14 of that with the point positive.

For comparison of the performance of the tube with α- and β-particles the arrangement of fig. 2 was adopted. The normal procedure was to take a count with no magnet present. This gave $N_1+N_2+N_0$, where $N_1=\alpha$-rays, $N_2=\beta$-rays, $N_0=$background count due to other agencies. With the magnet in position the β-rays were deviated in the magnetic field and N_1+N_0 was obtained. Finally

a thin mica sheet was put in front of the counter to absorb the α-rays, and N_0 was found. Thus N_1 and N_2 were evaluated. The counter was filled with air at different pressures up to atmospheric. The straight line B of fig. 5 gives the number of α-rays for both the point positive and negative. Curve A gives the β count with a positive point and curve C the β count for a negative point. In the curve A we again find saturation in the β count between 30 and 40 cm., with no saturation in curve C. The highest value of the ratio of the efficiencies is only 0·38, the value at 76 cm. The positive case voltages were adjusted to near the breakdown points in

Fig. 5.

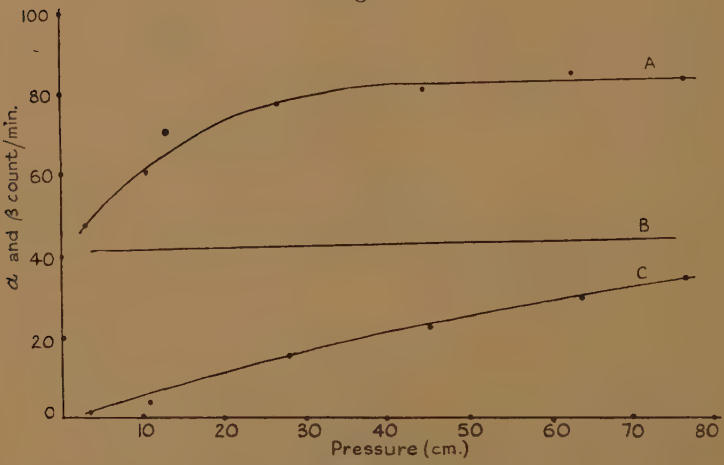

Results with air in counter.

obtaining these results. A further set of results was taken in a similar manner with a much smaller counter, argon being the filling gas. The results are given in fig. 6. The starting and working potentials in this instance are shown by curves A_2 and B_2 respectively in fig. 4. These potentials are for the point negative. Curve C of fig. 4 gives the voltages applied when the point was positive. The results shown in fig. 6 are substantially the same as those of fig. 5. The β detection is again complete for a positive point from 30 cm. upwards, but for a negative point the maximum efficiency is 0·32. Curve B shows that α detection is complete for both methods of working from 2 cm. to 76 cm.

The Path of the Ray within the Tube.

From figs. 5 and 6 it appears obvious that only at extremely high pressures would complete detection of β-rays with a negative point be attained. Indeed, the large differences in efficiency cannot be attributed to pressure values, since with the point positive it is apparent that with pressures above $\frac{1}{2}$ atmosphere almost all the β-rays form ions in the tube in sufficient quantity to be detected. It might be possible, however, that the point or points of formation of the ions in the tube are more critical when the point is negative, and some experiments were carried out to test this. In the first experiment a large brass counter was used, the diameter being 4·5 cm.,

Fig. 6.

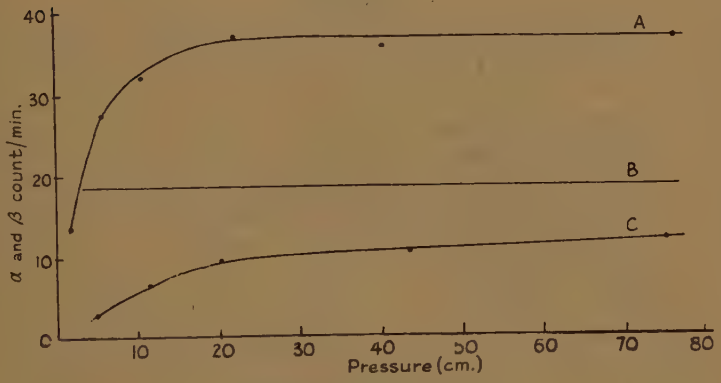

Results with argon filling.

the distance of the point from the face 1·8 cm. Three windows were pierced in the face of the tube—one on its axis and two others on a radius, each being 2·6 mm. in diameter and 6 mm. apart. All were sealed with the same mica film, and readings were taken with three different sources. The counter was filled with argon at atmospheric pressure. Table II. gives the results. The negative potential on the case was 1590 volts, the positive potential was 1880 volts, some 400 volts above the starting potential. Source 1 was R*a*E at 20 cm. distance in air, source 2 a deposit of R*a*E on a large plate at 7·5 cm. in air, and source 3 the arrangement of fig. 2. The numbers in brackets for source 3 refer to α-particle counts. We see that the α count disappears completely at 6 mm. in one

case, but it is complete up to 6 mm. in the other. The β count falls off with radial displacement in both instances, but more rapidly with the point negative.

The slower rate of diminution in the case of source 2 is due to the geometry of the arrangement of source and aperture. For the axial aperture the α-ray detection is complete in both cases, but for β-rays it varies between 0·07 and 0·15 for the point negative. The highest efficiencies are, of course, obtained when the rays enter the axial aperture.

Next a counter of diameter 3·5 cm., with the point at 2·5 cm. from the face, was used. This meant that the field of force was strongest between the point and the

TABLE II.

Radial displacement.		0·0 mm.	6·0 mm.	12·0 mm.
−1590 volts on case.	Source 1	58·9	6·4	0·3
	Source 2	100·8	15·1	5·0
	Source 3	42·1 (19·6)	5·5 (19·8)	0·8 (0·4)
+1880 volts on case.	Source 1	4·0	0·1	0·0
	Source 2	12·1	0·7	0·0
	Source 3	6·5 (21·0)	0·3 (0·0)	0·0 (0·0)

cylinder, while before it was strongest between the point and the face. A radial slit was cut in the face of the tube. and a moving aperture made it possible to expose different parts of the face in turn. A source of R*a*E at 5 cm. served as source. The positive case potential was 1880 volts, the negative potential 1572 volts. The results are shown in fig. 7. The abscissæ represent the distance of the aperture from the axis of the tube, the ordinates give the β counts per minute. The β detection does not fall off very rapidly here, and the maximum ratio of the efficiencies is 0·28. The arrangement of fig. 2 was used to determine the results entered in fig. 8. For the positive point the α count is complete over a considerable area of the face (curve B), the β count complete over a slightly smaller zone (curve A). The α count diminishes more rapidly with the displacement when the point is negative

(curve C), the β count more slowly (curve D), and both are nearly zero at 8 mm. The results here are somewhat different from those of Table II., the different disposition of the electrodes being the most probable cause of this change. The general inference to be drawn from the results is that, although radial displacement of the aperture is important in complete counting, particularly when the

Fig. 7.

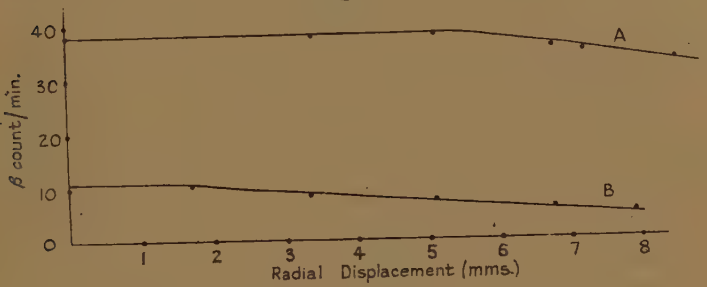

Curve A, point positive; curve B, point negative.

Fig. 8.

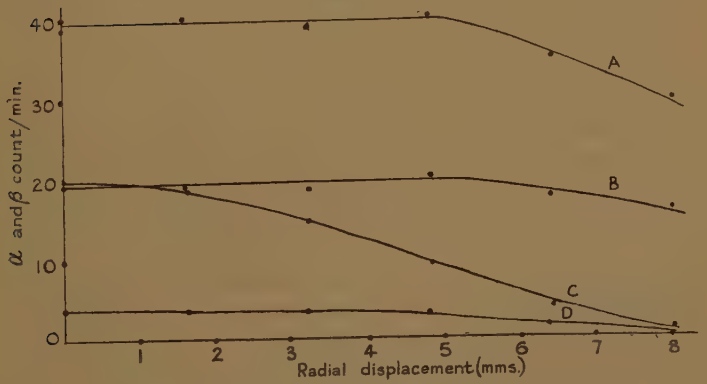

Curves B and C, α-rays; curves A and D, β-rays.

point is negative, it is not extremely critical, and would not cause any considerable loss in β detection if reasonable care is taken in fixing the aperture and point on the axis of the tube.

Test for Complete Detection of Beta-rays.

In the case of α-rays the action of the counter in detecting each entering particle can be checked by the method of

coincidences in two counters [5], or by comparison with the scintillation method [6], but a direct means of testing the efficiency to β-rays is not readily available. Kovarik [7] compared the number of β-rays from a source R*a*E as determined by a Geiger point counter with the number as determined by the electrical charge method, and found agreement. In the case of R*a*D he was unsuccessful. Emeléus [8] and Riehl [9] indirectly checked the efficiency in finding the number of β-particles emitted from a disintegrating atom of R*a*E. The arrangement they used was similar to that shown in fig. 2. Thus Emeléus found 1·43 β-particles to each α-particle liberated from a source of R*a*(D+E+F) in equilibrium. Correction for reflexion at the source reduced this to about 1·04 β-particles per disintegration [10]. From this result we must conclude that Emeléus had complete detection with his tube at 76 cm. pressure, while Riehl found it necessary to use

Table III.

Air equivalent in cm. . . .	2·5	3·9	5·3
Number of β-rays/min. .	35·0 (33·0)	28·5	21·5

pressures above 100 cm. to obtain the same result. Now from figs. 5 and 6 it is seen that about twice as many β-particles as α-particles are detected. In the above work, however, it was possible for β-rays to leave the source and reach the counter, while α-rays from the same parts of the source were absorbed in the glass of the capillaries. The source was therefore altered, and a small conical glass source used, so that α-rays passed freely from any active part of the surface to the counter. With a counter filled with argon to 50 cm. pressure, the point being positive, the results of Table III. were obtained. The table shows the variation in the number of β-rays of R*a*E with different amounts of absorbing film between source and counter. The number of α-rays at 2·5 cm. air equivalent is, as shown in brackets, 33·0. By extrapolation the number of β-rays at zero air equivalent is found to be 47·0 per minute. Thus the ratio of β-rays of R*a*E to α-rays of R*a*F=47·0/33·0=1·42. This may be regarded either as a further determination of the number of β-particles liberated per disintegration from R*a*E or

it can be taken as satisfactory evidence of the quantitative counting of the tube with its point positive. On the same basis the efficiency of the tubes used above had various values less than 0·50 when the point was negative, even though considerable over-voltages were used, and the rays entered the tube through a small axial aperture, so that they had a maximum opportunity of being recorded [11]. Bothe [11] used a small ball electrode supported on a metal cushion as the positive electrode, and found that the effective zone consisted of a cone with its apex at the ball and its base on the face of the tube. It is interesting to note that Bothe found in one test with the ball negative that the β count was $\frac{1}{4}$ of that with the ball positive. He suggested that the voltage on the tube might not have been pushed to its maximum. Now in the above work the over-voltage was often near the limit, and values of β efficiency less than 0·50 were obtained. It has been shown that neither pressure deficiency nor displacement of the aperture accounts for this failure of the tube to give complete detection with the point negative, and so we must seek for the explanation in some other factor in the working of the tube.

The Counts-Volts Characteristic Curve.

From a consideration of the form of the curve connecting the number of β-rays detected with different applied voltages much information about the mode of action of the tube may be obtained. Generally speaking it is much more difficult to obtain a satisfactory curve with β-rays than with α-rays or other strongly ionizing particles. As the voltage increases the number of particles recorded often increases steadily, and no constant count region is reached before the steady discharge sets in. In other cases a range of voltage over which the count remains almost steady is obtained, and for quantitative counting the voltage is adjusted to be at the upper end of this range. The form of the curve was not investigated for all the tubes used in the above work, but it was found that generally a region in which the count remained constant was not obtained. These remarks apply to tubes with the point negative. Curves A and D of fig. 9 might be taken as representative of their kind. In curve A the β counting started at just over 1300 volts, and the

number detected rose with increasing voltage till the state of spurious discharge was reached. Curves B, C, D show the effect of different values of resistance in series with the tube, the point being negative. For B, C, D the resistances were $1{\cdot}4 \cdot 10^7$, $3{\cdot}0 \cdot 10^8$, $3{\cdot}0 \cdot 10^9$ ohms respectively. It is seen that the counter tends to break down at lower voltages with lower values of series resistance. With $1{\cdot}4 \cdot 10^7$ ohms the counter worked from 1230 to 1450 volts approximately, with $3{\cdot}0 \cdot 10^8$ ohms it worked from 1230 volts to about 1750 volts, while with $3{\cdot}0 \cdot 10^9$ ohms the range extended from 1230 to more than 2100 volts. (All the work given above was carried out with $3 \cdot 10^9$ ohms in circuit.) We can compare with these results those obtained when the point was positive. Curves E and F correspond to curves C and D. The β count here remains quite constant over ranges of some 150 and 250 volts, these ranges being for series resistances of $3 \cdot 10^8$ and $3 \cdot 10^9$ ohms respectively. The α-ray constant counting ranges were somewhat longer. These results are similar to those of Henning and Schade [12] for tube counters with clean electrodes. Curve F was that for the tube used in the evaluation of the number of β-rays emitted per disintegrating atom of R*a*E. It was experimentally proved that the number of β-particles detected by the counter working at a positive case voltage of 2100 volts (curve D) was $\frac{1}{4}$ of that detected at a negative case voltage of 1660 volts (curve F). Thus, with the point negative and an over-voltage of nearly 900 volts the efficiency was only 0·25. It should be remarked here that the curves of fig. 9 were not taken in all cases with the same source under the same conditions. Thus, for curve D the source was stronger than for curve F. Consider next the curves X, Y, Z obtained with the point negative. The point was of steel, the radius being about 0·03 mm., and argon at 76 cm. was the filling gas. The counter did not pass a steady discharge at extremely high over-voltages. Curve X was taken with weak β irradiation and curve Z in its absence, while curve Y represents the difference curve. It is seen that the background count, shown by curve Z, has attained abnormally high values at the high operating potentials, but curve Y shows a flat region around 3000 volts, the count being about 74 per minute. The corresponding curve with the point positive, curve G, taken under the

same conditions as curve X, gives a β count of 86 per minute, the natural count being 2 per minute. The ratio of the efficiencies is therefore $74/84=0{\cdot}88$. A more significant result is that shown in curve W, taken with a counter with a platinum point of radius $a=0{\cdot}09$ mm., and argon at 50 cm. as the filling gas. The counter was stable to over 3000 volts, and discharge set in above 3500 volts. It was found that with the arrangement of fig. 2 the ratio of β-particles to α-particles was between 1·4 and 1·5, this proving that quantitative counting was obtained with the point at nearly 3000 volts negative potential. These last results suggest that with the high fields of force in the tube secured by the use of abnormally large over-voltages quantitative counting may be attained in place of the low efficiencies under more normal circumstances, provided, of course, the counter does not break down.

The Mode of Action.

Consider now the action of the counter in the two different methods of working. We will take first the case where the voltages applied between the point and the cylinder are not sufficiently high to cause a discharge. When this is so, if the point is positive and ions are formed within the tube by some ionizing agent, the negative ions or electrons will move towards the point. They must therefore pass through the strong field of force in its neighbourhood, and at certain applied voltages the electrons will produce much ionization by collision in the gas. The region in which the collision-ionization takes place is confined to a small volume surrounding the point. The positive ions so formed will be drawn to the case, and as we have assumed that a discharge does not take place these positive ions do not produce electrons either by collisions in the gas or by impact at the electrode. It is possible for electrons to act in circumstances in which positive ions fail to act because (1) $\beta<\alpha$ where α=the average number of molecules ionized by an electron in moving through one cm. of a gas, and β=the average number ionized per cm. of the gas by a positive ion moving under the same force. (2) Positive ions of low energy are inefficient agents in the production of secondary emission at an electrode. Thus it is in accordance with theory that when the point is positive a region of applied

voltage should be obtained in which magnification of the primary ionization by collision of electrons in the gas occurs.

Consider next a tube in which the point is negative. The positive ions formed by the external ionizing agent are now attracted towards the point, and they pass through the strong field of force existing in its vicinity. The electrons, on the other hand, pass through a weak field to the case, and they can therefore be left out of consideration, since it is unlikely that they will have any secondary action. If the positive ions move through the gas under a strong field and impinge on the point they may produce ions by collision in the gas round the point or they may bring about secondary emission at the electrode. Any electrons so formed will move in their turn through the strong field and cause the production of numerous positive ions. This increased number of positive ions will be much more certain to do what the single or few original positive ions did, and they in their turn will produce electrons, so that a discharge will be brought about. It is seen then that when the point is negative the impulse must pass abruptly from the stage at which the primary ions produced in the counter are gathered at the electrodes to the stage at which a discharge passes—in other words, when the point is positive we can, by increasing the applied voltage, pass continuously from a voltage at which the primary ions are gathered at the electrodes to a potential at which discharge takes place through the action of the positive ions, but, on the other hand, when the point is negative there is a definite abrupt increase from the primary ionization impulse to a discharge impulse.

When the voltage applied to a tube is in the discharge régime, as it is in normal use, it is difficult to say exactly what action takes place, since it is possible that space-charge effects etc. considerably influence the process. Let us consider, for the sake of argument, that the ionizing agent, a β-particle say, produces a single pair of ions somewhere in the tube between the point and the walls of the counting vessel. (We could, of course, in the same way consider the action of a small finite number of pairs of ions.) Then when the point is positive we know that a very large number of positive ions (and negative ions) are produced in the tube by the electron moving towards

the point ; but when the point is negative any increase in the number of positive ions in the tube must be brought about in the first place through the action of the positive ion itself, since the electron will usually move through a low field of force to the case. We might express the difference in the two cases thus : when the point is positive the initial process depends on the action of the electron, when the point is negative it depends on the action of the positive ion. The initial action of the electron is to produce many positive ions, so that in one case we have many positive ions in the tube as compared with the single positive ion present in the other case. Thus, whatever the action of the positive ions may be in bringing about a discharge, whether it is through collision-ionization in the gas or secondary emission at an electrode, it would appear that there is a much greater possibility of discharge occurring when the point is positive than when the point is negative, because of the much greater number of positive ions present in the tube—in other words, the low efficiency of the process by which the positive ions act is compensated by a large increase in the number of the ions available. We should expect, therefore, that it should be much more readily possible to obtain a quantitative counting state when the point is positive, and we have shown above that this is verified experimentally.

When the point is negative to attain to a state of quantitative counting we must have fulfilled the conditions under which a single positive ion (or at most a very few) can bring about a discharge without fail. Now, whether the positive ion produces collision-ionization in the gas or secondary emission at the electrode in initiating the discharge, we know that its efficiency of action depends on the energy of the ion, increasing with increasing energy. Indeed for secondary emission it has been expressed in the form of the equation [13] $N=N_0+AV$, where N is the number of secondary electrons due to each ion. This dependence on energy is clearly illustrated by curve W of fig. 9. The field at the point at normal over-voltages is insufficient to bring about a discharge on the entry of each particle, but at higher fields produced by abnormally high over-voltages we reach a stage at which complete detection takes place. Curve W should be contrasted with its counterpart for the point positive, curve G, fig. 9.

We see that quantitative counting is much more definitely obtainable at low over-voltages—in other words, when the point is negative the lack of positive ions in the tube as compared with those present when the point is positive is compensated for by producing a higher value of the field of force near the point. This explains the marked difference in the forms of the curves G and W.

Most of the counters used in this research had points which were less sharp than those used by some other writers who report quantitative counting (many of them had a radius of about 0·03 mm.). This points to a very potent reason for loss of efficiency. Thus, if we consider

Fig. 9.

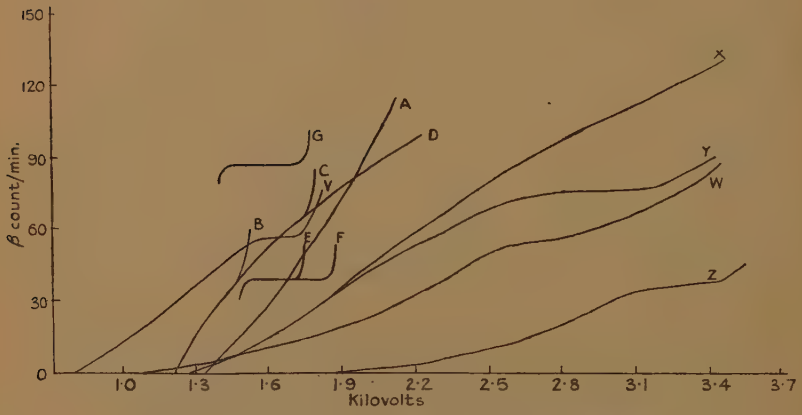

Characteristic curves for point negative and positive.

the formula due to Edmunds [14] for discharges in air at atmospheric pressure between a point and a plane, viz.,

$$E_0 = 30 + 18/\sqrt{a} \text{ kilovolts/cm.},$$

where E_0 is the critical stress at the point and a the radius of the point, we find that E_0 increases rapidly with decreasing a. This means that strong fields of force exist at the surface of finer points when the state of discharge is just reached. But on the above view of the action this implies the possibility of complete detection being more readily obtained with finer points, or higher efficiencies of tubes with negative points should be more easily secured if very sharp points are used. Curve

V of fig. 9 was taken to illustrate this effect; it was taken with the same tube as that which gave curve W of the same figure, the only difference being that for W the point had a radius $a=0{\cdot}09$ mm., while for V the radius was $a=0{\cdot}02$ mm. The β-rays were those from a source of RaE at 17 cm. in air in both instances. It is seen that both curves show a plateau at about 55 counts per minute, but an increase of voltage in V from 800 to 1650 volts corresponds to a rise in W from 1120 to 2700 volts. Thus with the finer point an over-voltage of 850 volts suffices in place of an over-voltage of 1680 volts required with the blunter point. By using a tube with a positive point it was verified that 55 counts per minute was a measure

Fig. 10.

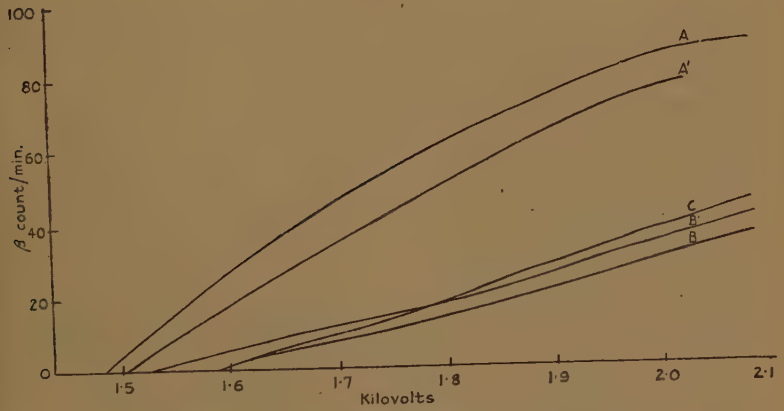

Variation in count with different point surfaces.

of all the entering β-particles, which was correct within the limits of the experimental error. Curve A, fig. 10, was for a fine steel point, $a=0{\cdot}008$ mm., in air at atmospheric pressure. A state approaching complete detection is reached at an over-voltage of 550 volts. We can conclude that the starting potential is not really important in determining the required over-voltage, but the point sharpness is. The field strength at the point depends to a great extent on the sharpness, and the counting action is dependent on the field strength. Indeed, the condition for quantitative counting might be conveniently expressed in terms of the field strength at the surface of the point.

From the equations given by Edmunds [14] for the point to plane discharge in air at atmospheric pressure we have

$$X = 30 + 18/\sqrt{a}, \quad . \quad . \quad . \quad . \quad . \quad (1)$$

$$V = \tfrac{1}{4}\, aX \log_e 8d/a, \quad . \quad . \quad . \quad . \quad . \quad (2)$$

where a=radius of point in cm. (as defined for a paraboloid of revolution), d=distance from point to plane in cm., X=critical force in kilovolts/cm. at the vertex of the point, and V=discharge potential in kilovolts. We shall regard equation (2), however, as the expression of a general relationship between the force at the point and the potential difference between the point and the plane. Let us take a definite value of $a=a_1$, and find $X=X_1$ for $a=a_1$ by equation (1). For this value of X there is a value of $V=V_1$ given by equation (2), d being known. We shall regard V_1 as the starting potential for counting. Now the counter can withstand over-voltages, and V_2, where $V_2>V_1$, may be applied to the tube, V_2-V_1 being the over-voltage. From equation (2) we can find X_2 corresponding to V_2. Thus for $a=0{\cdot}005$ mm., $d=1$ cm., we have $X_1=835$ kv./cm. and $V_1=1010$ volts. Now suppose an over-voltage $V_2-V_1=200$ volts is sufficient in this case to give a state of quantitative counting of β-rays. Then $V_2=1210$ volts and $X_2=1000$ kv./cm. by equation (2). So for $a=0{\cdot}01$ mm., $X_1=599$ kv./cm., and $V_1=1347$ volts. Moreover, if we wish to increase the field X_1 for $a=0{\cdot}01$ mm. to $X_2=1000$ kv./cm., we must now apply $V_2=2249$ volts to the tube according to equation (2). This means that an over-voltage $V_2-V_1=902$ volts is required in this case to produce a field of 1000 kv./cm. at the point. We can calculate in the same way for different points X_1, V_1, and V_2, where in each instance V_2 is the potential difference for $X_2=1000$ kv./cm. On the basis therefore that complete detection depends on the production of a minimum field of force, here taken as 1000 kv./cm., we find the over-voltage V_2-V_1 required for each point. The results of some calculations of this type are entered in Table IV. It can be seen that V_2-V_1 increases very rapidly for increasing point diameter. This agrees with the observations of the writer as given above, which suggest that V_2-V_1 varies with a in a manner given approximately by Table IV.

There are, unfortunately, no systematic observations available for purposes of comparison of the conditions

required in quantitative counting of β-rays in air at atmospheric pressure. The condition outlined above can be expressed in the form

$$V_2-V_1=\tfrac{1}{4}a(X_2-X_1)\log_e 8d/a$$
$$=\tfrac{1}{4}a(1000-30-18/\sqrt{a})\log_e 8d/a,$$

i. e.,

$$V_2-V_1\doteq\tfrac{1}{4}a\ (1000-18/\sqrt{a})\log_e 8d/a). \quad . \quad . \quad (3)$$

The condition expressed in equation (3) is obviously of a more or less empirical nature, since if it were possible

TABLE IV.

I.—Point Counter. II.—Wire Counter.

mm. a.	kv./cm. X_1.	Volts.			kv./cm. X_1.	Volts.		
		V_1.	V_2.	V_2-V_1.		V_1.	V_2.	V_2-V_1.
0·00125	—	—	—	—	835	938	1123	185
0·002	—	—	—	—	666	1136	1703	567
0·004	—	—	—	—	480	1503	3130	1627
0·005	835	1010	1210	200	432	1646	4852	3206
0·010	599	1347	2249	902	315	2194	6965	4771
0·020	433	1798	4158	2360	231	2873	12430	9557
0·050	285	2624	9212	6588	157	4160	26500	22340

to use a fine enough point V_2-V_1 would become negative according to this result.

If we use the equations [15] for a wire-cylinder system we have, corresponding to equations (1) and (2),

$$X=30+9/\sqrt{a}, \quad . \quad . \quad . \quad . \quad . \quad . \quad (4)$$

$$V=aX\log_e A/a. \quad . \quad . \quad . \quad . \quad . \quad (5)$$

Calculations based on these equations for the tube counter are shown in part II. of Table IV., and V_2 is expressed as before for $X_2=1000$ kv./cm. in air at atmospheric pressure. It is seen that the general nature of the results is similar to that for the point-plane system, but the wire requires to be extremely fine to obtain conditions corresponding to those for a point. Thus at normal wire

diameters, the radius a being about 0·05 mm. say, the value of $V_2 - V_1$ is in excess of 20,000 volts. This is supported by the very low values of efficiency of a tube counter with a negative wire found by Cowie [16] working with γ-rays. Here the γ efficiency with negative points was found in some experiments to be nearly the same as the β efficiency as given above, and generally much higher than those obtained by Cowie. The calculations of Table IV. show that this difference in the action of the wire-cylinder and the point counters is to be expected.

We have not so far attempted to determine whether in a counter at high pressures the action of the positive ions consists mainly in the production of ions by collision in the gas or in the production of secondary emission by impact at the electrodes. It is now generally agreed that positive ions can produce secondary emission at a surface, and that the mechanism by which it is produced resembles that suggested by Holst and Oosterhuis [17], who stated the condition $V_I > 2\phi$, where V_I is the ionization potential of the gas and ϕ the metallic work function. It has been shown that (1) in many cases the emission increases linearly with the primary energy of the ions [13]; (2) the emission is connected intimately with the nature of the emitting surface. We have already seen that the count obtained with a negative point depended to a large extent on the field at the point in agreement with statement (1), and it is shown by the following experiments that the count depends to a large extent on the nature of the point surface also, in agreement with (2). This last result indicates that the mode of action of the counter is to be explained mainly in terms of secondary emission rather than collision-ionization. It is well known that a point requires to be in a " sensitive " state [18] for counting purposes, but the following results prove further that the efficiency of a tube with a negative point depends on the condition of the surface of the " sensitive " point. Thus under otherwise exactly the same conditions one point with a certain type of surface may give a count different from that obtained with another point with a different surface, the difference being due to the fact that the two surfaces have not the same efficiency of production of electrons on impact by positive ions. In fig. 10 characteristic curves for a counter filled with air at atmospheric pressure are given. The β-rays were from a source of

R*a*E at 10 cm. in air. Curve A gives the results for a fine steel needle-point with a very smooth clean surface. This point, heated to oxidation in a Bunsen flame, gave the results of curve B under precisely the same conditions as those giving curve A previously. It is seen that heating has caused a rise in the starting potential due to blunting of the point, but the important thing is that the efficiency of the tube with the clean point is higher than the efficiency of the tube with the oxidized point, other things being the same. With another similar needle the experiment was repeated with less heating of the point, and curves A′ and B′ were obtained in place of A and B. Again the efficiency is lower for the oxidized point. Finally a similar clean steel needle was taken, and a fine layer of silver deposited electrolytically on its surface. The results for this kind of point are given by curve C. These experiments form definite evidence of the fact that the action of the counter with the point negative is to be explained in terms of secondary emission rather than the production of ionization by collision in the gas.

It has been shown that for quantitative counting of β-particles it is in general better to use a point counter with the point positive with respect to the case. Of the difficulties encountered in this arrangement perhaps the most serious are the smallness and variable magnitude of the impulses. Smallness can be allowed for by the use of a sensitive amplifier, and the variable magnitude can be eliminated by constructing it on the lines recommended by Barasch [19].

The writer is much indebted to Professor E. Taylor Jones for his valuable help and interest in the work. He wishes also to thank Dr. John Thomson for many helpful discussions. The research was performed in the Research Laboratories of the Natural Philosophy Department at Glasgow University. The author expresses his thanks to the Carnegie Trust for a scholarship which enabled him to devote his time to the investigation.

References.

(1) Geiger, *Verh. d. d. Phys. Ges.* xv. p. 534 (1913); *Phys. Zeit.* xiv. p. 1129 (1913).
(2) Wynn-Williams, Proc. Roy. Soc. A, cxxxii. p. 295 (1931).
(3) Rutherford and Geiger, Proc. Roy. Soc. A, lxxxi. p. 141 (1908).
(4) Geiger and Klemperer, *Zeit. f. Phys.* xlix. p. 753 (1928).

(5) Geiger, *Ann. d. Phys.* xliv. p. 813 (1914).
(6) Geiger, *Verh. d. d. Phys. Ges.* Jhrg. v. p. 12 (1924).
(7) Kovarik, Phys. Rev. xiii. p. 272 (1919).
(8) Emeléus, Proc. Camb. Phil. Soc. xxii. p. 400 (1923–25).
(9) Riehl, *Zeit. f. Phys.* xlviii. p. 478 1928).
(10) ' Radiations from Radioactive Substances,' Rutherford, Chadwick, and Ellis, p. 392.
(11) Kutzner, *Zeit. f. Phys.* xxiii. p. 117 (1924); Bothe, *Zeit. f. Phys.* xxxvii. p. 547 (1926).
(12) Henning and Schade, *Zeit. f. Phys.* xc. p. 597 (1934). See also Werner, *Zeit. f. Phys.* xc. p. 384 (1934); and xcii. p. 705 (1934).
(13) Penning, *Proc. Akad. Amsterdam*, xxxi. p. 14 (1928); and xxxiii. p. 841 (1930).
(14) Edmunds, Phil. Mag. (6) xxviii. p. 234 (1914).
(15) Townsend, ' Electricity in Gases,' pp. 360–370.
(16) Cowie, Phys. Rev. xlviii. p. 883 (1935).
(17) Holst and Oosterhuis, ' Physica,' i. p. 78 (1921).
(18) See *Handbuch der Physik*, xxiv. p. 138, and xiv. p. 149.
(19) Barasch, Proc. Phys. Soc. xlvii. p. 824 (1935).

XXXIV. *On the Operational Representation of M-functions of the Confluent Hypergeometric Type* *. *By* S. C. Dhar, *D.Sc. (Cal. & Edin.), F.R.S.E., Professor of Mathematics, Nagpur, India* †.

Introduction.

THE symbolic calculus is now being developed by various writers. Carson ‡ gave some fundamental rules of the calculus, which have since been added by various other writers. Levy § studied them from a different point of view and obtained some rules of the calculus. Pol ‖ has given a method by which linear differential equations with variable coefficients can be solved by the symbolic calculus.

In a recent paper ¶ I had occasion to apply Pol's method to study the properties of Whittaker and other functions and obtained some new relations and integrals. In this paper I obtain the operational representation of M-functions of the confluent hypergeometric type in the form of hypergeometric functions, and from the known

* Read before the Indian Science Congress, January 1937.
† Communicated by the Author.
‡ Carson, ' Electric Circuit Theory and the Operational Calculus ' (1926).
§ Levy, " Le Calcul symbolique d'Heaviside," *Bull. Sc. Math.* 2e série, *t. c.* 1926.
‖ Van der Pol, Phil. Mag. viii. pp. 103–125 (1929).
¶ S. C. Dhar, Phil. Mag. xxi. pp. 1082–1096 (1936).

properties of the latter deduce several relations and integrals of the former.

1. A given function $h(x)$ is said to be operationally represented by another function $f(p)$, called the "image," if they satisfy the Carson's integral *

$$f(p)=p\int_0^\infty e^{-px}h(x)\,dx, \quad . \quad . \quad . \quad . \quad (1)$$

provided the integral converges.

The relation (1) between $h(x)$ and $f(p)$ may be denoted as

$$f(p)\doteqdot h(x) \quad \text{or} \quad h(x)\doteqdot f(p),$$

both meaning that $h(x)$ transformed operationally gives $f(p)$ and $f(p)$ interpreted backwards gives $h(x)$.

When $f(p)$ is known and $f(p)/p$ is an analytic function of the complex variable p, by means of Bromwich-Wagner theorem we get back $h(x)$ as

$$h(x)=\frac{1}{2\pi i}\int_{c-i\infty}^{c+i\infty} e^{p(x)}\frac{f(p)}{p}\,dp, \quad . \quad . \quad . \quad . \quad (2)$$

where $c>0$. The above is obtained from the Mellin-Fourier theorem †.

Thus if $h(x)=x$, then $f(p)=1/p$, which will be represented operationally by

$$\frac{1}{p}\doteqdot x \quad \text{or} \quad x\doteqdot\frac{1}{p}.$$

In fact, we have the relation

$$\frac{1}{p^n}\doteqdot\frac{x^n}{\Gamma(1+n)}. \quad . \quad . \quad . \quad . \quad . \quad . \quad . \quad (3)$$

From the above definition of operational representation, a set of theorems has been derived by Carson, and a few more have been added later on by Van der Pol and K. F. Nissen ‡. As we shall make frequent use of some of them, they are given below.

* Carson, 'Electric Circuit Theory and the Operational Calculus' (1926).

† Courant and Hilbert, 'Methoden der Mathematischen Physik,' i. p. 90.

‡ Van der Pol and Nissen, Phil. Mag. xiii. pp. 537–577 (1932).

If $f(p) \doteqdot h(x)$, then we shall have

$$f\left(\frac{p}{s}\right) \doteqdot h(sx), \text{ if } s \text{ is constant, and } >0. \quad . \quad . \quad (4)$$

$$pf(p) \doteqdot \frac{d}{dx}h(x), \quad \text{if } h(0)=0. \quad . \quad . \quad . \quad (5)$$

$$\left(-p\frac{d}{dp}\right)^n f(p) \doteqdot \left(x\frac{d}{dx}\right)^n h(x), \quad n>0. \quad . \quad . \quad (6)$$

$$p\left(-\frac{d}{dx}\right)^n \left\{\frac{f(p)}{p}\right\} \doteqdot x^n . h(x), \quad n>0. \quad . \quad . \quad (7)$$

$$\frac{p}{p+\alpha} f(p+\alpha) \doteqdot e^{-\alpha x}h(x). \quad . \quad . \quad . \quad . \quad (8)$$

2. Consider the well-known differential equation

$$\frac{d^2y}{dx^2} + \frac{dy}{dx} + \left(\frac{k}{x} + \frac{\frac{1}{4}-m^2}{x^2}\right)y = 0, \quad . \quad . \quad . \quad (9)$$

whose solution we proceed to obtain.

Transform it by the substitution

$$u = x^{l-1}y,$$

and we obtain

$$x^2\frac{d^2u}{dx^2} + \{x - 2(l-1)\}x\frac{du}{dx}$$

$$+ \{l(l-1) + (k-l+1)x + (\tfrac{1}{4}-m^2)\}u = 0. \quad (10)$$

Multiply by e^{-px} and integrate between 0 and ∞. If now we put

$$X = \int_0^\infty e^{-px}u(x)\,dx,$$

we get, on integrating by parts,

$$p(p+1)\frac{d^2X}{dp^2} + \{(l-k+1) + 2(l+1)p\}\frac{dX}{dp}$$

$$+ \{l^2 + t + \tfrac{1}{4} - m^2\}X = 0. \quad (11)$$

This equation is of the hypergeometric type, whose solutions are given by

$$\left.\begin{aligned}(\alpha)\quad & P\equiv {}_2F_1(l+m+\tfrac{1}{2},\ l-m+\tfrac{1}{2};\ l-k+1;\ -p),\\ & Q\equiv(-p)^{(k-l)}{}_2F_1(m+k+\tfrac{1}{2},\ k-m+\tfrac{1}{2};\ k-l+1;\ -p).\end{aligned}\right\} \quad \ldots \quad (12)$$

valid near the origin.

$$\left.\begin{aligned}(\beta)\quad & R\equiv(-p)^{-(l+m+\frac{1}{2})}{}_2F_1\left(l+m+\tfrac{1}{2},\ k+m+\tfrac{1}{2};\ 2m+1;\ -\frac{1}{p}\right),\\ & S\equiv(-p)^{-(l-m+\frac{1}{2})}{}_2F_1\left(l-m+\tfrac{1}{2},\ k-m+\tfrac{1}{2};\ -2m+1;\ -\frac{1}{p}\right),\end{aligned}\right\} \quad \ldots \quad (13)$$

valid at infinity.

In a recent paper * I have examined the solutions given by (12) and arrived at the operational representation of the W functions. Here I study in detail the solutions (13).

If we denote the solutions of the differential equation (9) by $M_{k,\pm m}(x)$ †, it is easy to see from (3) that

$$\frac{x^{l-1}e^{-\frac{1}{2}x}M_{-k,m}(-x)}{(-)^{l+2m+1}\Gamma(l+m+\frac{1}{2})} \doteqdot p(-p)^{-(l+m+\frac{1}{2})}{}_2F_1\left(l+m+\tfrac{1}{2},\ k+m+\tfrac{1}{2};\ 2m+1;\ -\frac{1}{p}\right), \quad \ldots \quad (14)$$

and

$$\frac{x^{l-1}e^{-\frac{1}{2}x}M_{-k,-m}(-x)}{(-)^{l-2m+1}\Gamma(l-m+\frac{1}{2})} \doteqdot p(-p)^{-(l-m+\frac{1}{2})}{}_2F_1\left(l-m+\tfrac{1}{2},\ k-m+\tfrac{1}{2};\ -2m+1;\ -\frac{1}{p}\right). \quad \ldots \quad (15)$$

* Dhar, *loc. cit.*

† $M_{k,m}(x)$ is defined in 'Modern Analysis,' by Whittaker & Watson, pp. 338–339 (1927). This work will in future be referred to as M.A.

3. It is easy to see that the above two operational forms can be replaced by the following one form, viz.,

$$x^{l-1}e^{\frac{1}{2}x}\mathrm{M}_{k,m}(x) \doteqdot \Gamma(l+m+\tfrac{1}{2})p(p)^{-(l+m+\frac{1}{2})} \times {}_2\mathrm{F}_1\left(l+m+\tfrac{1}{2},\ -k+m+\tfrac{1}{2};\ 2m+1;\ \frac{1}{p}\right). \quad (16)$$

By (8) we can transform it into the form

$$x^{l-1}e^{-\frac{1}{2}x}\mathrm{M}_{k,m}(x) \doteqdot \Gamma(l+m+\tfrac{1}{2})p(p+1)^{-(l+m+\frac{1}{2})} \times {}_2\mathrm{F}_1\left(l+m+\tfrac{1}{2},\ -k+m+\tfrac{1}{2};\ 2m+1;\ \frac{1}{p+1}\right). \quad (17)$$

Now it is known * that

$$(1-z)^{-a}{}_2\mathrm{F}_1\left(a, b;\ c;\ \frac{-z}{1-z}\right) = {}_2\mathrm{F}_1(a, c-b;\ c;\ z),$$

so that

$$(1+p)^{-(l+m+\frac{1}{2})}{}_2\mathrm{F}_1\left(l+m+\tfrac{1}{2},\ -k+m+\tfrac{1}{2};\ 2m+1;\ \frac{1}{p+1}\right) = (p)^{-(l+m+\frac{1}{2})}{}_2\mathrm{F}_1\left(l+m+\tfrac{1}{2}, k+m+\tfrac{1}{2};\ 2m+1;\ -\frac{1}{p}\right). \quad . \quad . \quad . \quad (18)$$

Hence, from (17) we get by the help of (18) and (14),

$$x^{-\frac{1}{2}-m}\mathrm{M}_{k,m}(x) = (-x)^{-\frac{1}{2}-m}\mathrm{M}_{-k,m}(-x), \quad . \quad (19)$$

the well-known *Kummer's first formula* †.

Hence from (19) and (14) we obtain

$$x^{l-1}e^{-\frac{1}{2}x}\mathrm{M}_{k,m}(x) \doteqdot \Gamma(l+m+\tfrac{1}{2})p(p)^{-(l+m+\frac{1}{2})} \times {}_2\mathrm{F}_1\left(l+m+\tfrac{1}{2}, k+m+\tfrac{1}{2};\ 2m+1;\ -\frac{1}{p}\right). \quad (20)$$

Therefore from (16) and (20) we obtain the following integrals :—

$$\int_0^\infty x^{l-1}e^{x(\frac{1}{2}-\alpha)}\mathrm{M}_{k,m}(x)\,dx = \Gamma(l+m+\tfrac{1}{2})\alpha^{-(l+m+\frac{1}{2})} \times {}_2\mathrm{F}_1\left(l+m+\tfrac{1}{2},\ -k+m+\tfrac{1}{2};\ 2m+1;\ \frac{1}{\alpha}\right), \quad (21)$$

* Bailey, ' Generalized Hypergeometric Series ' (Cambridge Tract No. 32), 10.

† M.A., p. 338.

$$\int_0^\infty x^{l-1}e^{-x(\frac{1}{2}-\alpha)}\mathrm{M}_{k,m}(x)\,dx = \Gamma(l+m+\tfrac{1}{2})\alpha^{-(l+m+\frac{1}{2})} \times {}_2\mathrm{F}_1\left(l+m+\tfrac{1}{2},\ k+m+\tfrac{1}{2};\ 2m+1;\ -\frac{1}{\alpha}\right), \quad (22)$$

when $(2m+1)>0$ and the integrals are convergent.

It is worth while to note some more new forms for $\mathrm{M}_{k,m}(x)$ which are easily obtained by the transformation of the hypergeometric function. They are

$$x^{l-1}e^{\frac{1}{2}x}\mathrm{M}_{k,m}(x) \doteqdot \Gamma(l+m+\tfrac{1}{2})(p-1)^{k-l}p^{-m-k-\frac{1}{2}} \times {}_2\mathrm{F}_1\left(m-l+\tfrac{1}{2},\ k+m+\tfrac{1}{2};\ 2m+1;\ \frac{1}{p}\right), \quad (23)$$

and

$$x^{l-1}e^{-\frac{1}{2}x}\mathrm{M}_{k,m}(x) \doteqdot \Gamma(l+m+\tfrac{1}{2})p^{k-m-\frac{1}{2}}(p+1)^{-k-l} \times {}_2\mathrm{F}_1\left(m-l+\tfrac{1}{2},\ -k+m+\tfrac{1}{2};\ 2m+1;\ -\frac{1}{p}\right). \quad (24)$$

4. By the help of the rules of the calculus given above, it is now easy to investigate the properties of the function. We obtain the recurrence formulæ thus :—

Apply (6) when $n=1$ to (16) and we obtain on simplification

$$\begin{aligned} x\frac{d}{dx}\{x^{l-1}e^{\frac{1}{2}x}\mathrm{M}_{k,m}(x)\} &\doteqdot \Gamma(l+m+\tfrac{1}{2})\left\{(l+m-\tfrac{1}{2})p^{-(l+m+\frac{1}{2})} \times {}_2\mathrm{F}_1\left(l+m-\tfrac{1}{2},\ -k+m+\tfrac{1}{2};\ 2m+1;\ \frac{1}{p}\right)\right\} \\ &\quad + \frac{(l+m+\frac{1}{2})(-k+m+\frac{1}{2})}{2m+1}p^{-(l+m+\frac{1}{2})} \times {}_2\mathrm{F}_1\left(l+m+\tfrac{3}{2},\ -k+m+\tfrac{3}{2};\ 2m+1;\ \frac{1}{p}\right) \\ &= (l+m-\tfrac{1}{2})x^{l-1}e^{\frac{1}{2}x}\mathrm{M}_{k,m}(x) \\ &\quad + \frac{(-k+m+\frac{1}{2})}{2m+1}x^{l-\frac{1}{2}}e^{\frac{1}{2}x}\mathrm{M}_{k-\frac{1}{2},m+\frac{1}{2}}(x), \end{aligned}$$

whence we get

$$x\mathrm{M}'_{k,m}(x)=(m+\tfrac{1}{2}-\tfrac{1}{2}x)\mathrm{M}_{k,m}(x) + \frac{(-k+m+\frac{1}{2})}{2m+1}x^{\frac{1}{2}}\mathrm{M}_{k-\frac{1}{2},m+\frac{1}{2}}(x). \quad . \quad (25)$$

If instead we apply (6) when $n=1$ to (20) we obtain in the same way

$$x\mathrm{M}'_{k,m}(x)=(m+\tfrac{1}{2}+\tfrac{1}{2}x)\mathrm{M}_{k,m}(x) - \frac{(k+m+\frac{1}{2})}{2m+1}x^{\frac{1}{2}}\mathrm{M}_{k+\frac{1}{2},m+\frac{1}{2}}(x). \quad . \quad . \quad (26)$$

From (25) and (26) it is easy to obtain

$$(2m+1)x^{\frac{1}{2}}\mathrm{M}_{k,m}(x)=(k+m+\tfrac{1}{2})\mathrm{M}_{k+\frac{1}{2},m+\frac{1}{2}}(x) +(-k+m+\tfrac{1}{2})\mathrm{M}_{k-\frac{1}{2},m+\frac{1}{2}}(x). \quad . \quad (27)$$

Relations (25), (26), and (27) thus constitute the well-known recurrence formulæ of the functions.

5. If we apply Bromwich-Wagner theorem (2) to the relation (20) we obtain

$$x^{l-1}e^{-\frac{1}{2}x}\mathrm{M}_{k,m}(x)=\frac{\Gamma(l+m+\frac{1}{2})}{2\pi i}\int_{c-i\infty}^{c+i\infty}e^{px}p^{-(l+m+\frac{1}{2})} \times {}_2\mathrm{F}_1\left(l+m+\tfrac{1}{2},\ k+m+\tfrac{1}{2};\ 2m+1;\ \frac{1}{p}\right)dp. \quad (28)$$

By Barnes's integral* for the hypergeometric function, the above is transformed into

$$x^{l-1}e^{-\frac{1}{2}x}\mathrm{M}_{k,m}(x) = \frac{\Gamma(2m+1)}{\Gamma(k+m+\frac{1}{2})}\frac{-1}{2\pi i}\int_{c-i\infty}^{c+i\infty}\int_{-\infty i}^{\infty i}e^{px}p^{-(l+m+\frac{1}{2}+s)} \times\frac{\Gamma(l+m+\frac{1}{2}+s)\Gamma(k+m+\frac{1}{2}+s)\Gamma(-s)}{\Gamma(2m+1+s)}\,ds\,dp,$$

where p can always be properly chosen and the path of integration of the latter integral is curved if necessary to separate the poles $s=-(l+m+\frac{1}{2})-n$, $s=-(k+m+\frac{1}{2})-n$, $(n=0, 1, 2, \ldots)$ from the poles $s=0, 1, 2, \ldots$

* Barnes, Proc. London Math. Soc. (2) vi. p. 146 (1907–8).

Hence from the known relation

$$-\frac{1}{2\pi i}\int_{c-i\infty}^{c+i\infty} e^{px}p^{-(l+m+\frac{1}{2}+s)}\,dp=\frac{x^{(l+m-\frac{1}{2}+s)}}{\Gamma(l+m+\frac{1}{2}+s)}.$$

We obtain, on inverting the order of integration,

$$\mathrm{M}_{k,m}(x)$$
$$=\frac{\Gamma(2m+1)e^{\frac{1}{2}x}x^{m+\frac{1}{2}}}{\Gamma(k+m+\frac{1}{2})}\int_{-\infty i}^{\infty i}\frac{\Gamma(k+m+\frac{1}{2}+s)\Gamma(-s)}{\Gamma(2m+1+s)}x^s\,ds, \qquad \ldots \quad (29)$$

the path of integration being chosen as stated before.

Again, from (16) we get

$$x^{l-1}e^{\frac{1}{2}x}\mathrm{M}_{k,m}=\frac{\Gamma(l+m+\frac{1}{2})}{2\pi i}\int_{c-i\infty}^{c+i\infty}e^{px}p^{-(l+m+\frac{1}{2})}$$
$$\times\,{}_2\mathrm{F}_1\left(l+m+\tfrac{1}{2},\ -k+m+\tfrac{1}{2};\ 2m+1;\ \frac{1}{p}\right)dp.$$

Now we find that

$${}_2\mathrm{F}_1\left(l+m+\tfrac{1}{2},\ -k+m+\tfrac{1}{2};\ 2m+1;\ \frac{1}{p}\right)$$
$$=\frac{-\Gamma(2m+1)}{\Gamma(-k+m+\frac{1}{2})\Gamma(k+m+\frac{1}{2})}$$
$$\times\int_0^1 t^{-k+m-\frac{1}{2}}(1-t)^{m+k-\frac{1}{2}}\left(1-\frac{t}{p}\right)^{-(l+m+\frac{1}{2})}dt,$$

where $(\pm k+m+\frac{1}{2})>0$.

Hence the above relation becomes

$$x^{l-1}e^{\frac{1}{2}x}\mathrm{M}_{k,m}(x)=\frac{\Gamma(2m+1)\Gamma(l+m+\frac{1}{2})}{\Gamma(k+m+\frac{1}{2})\Gamma(-k+m+\frac{1}{2})}\cdot\frac{-1}{2\pi i}$$
$$\times\int_{c-i\infty}^{c+i\infty}\int_0^1 e^{px}(p-t)^{-(l+m+\frac{1}{2})}t^{-(k+m+\frac{1}{2})}(1-t)^{m+k-\frac{1}{2}}\,dt\,dp.$$

Now changing the order of integration, we obtain from the known relation

$$-\frac{1}{2\pi i}\int_{c-i\infty}^{c+i\infty}e^{px}(p-t)^{-(l+m+\frac{1}{2})}\,dp=\frac{e^{xt}x^{l+m-\frac{1}{2}}}{\Gamma(l+m+\frac{1}{2})},$$

the integral

$$x^{l-\frac{1}{2}}e^{\frac{1}{2}x}\mathrm{M}_{k,m}(x)=\frac{\Gamma(2m+1)x^{l+m-\frac{1}{2}}}{\Gamma(k+m+\frac{1}{2})\Gamma(-k+m+\frac{1}{2})}\times\int_0^1 e^{xt}t^{-k+m-\frac{1}{2}}(1-t)^{m+k-\frac{1}{2}}\,dt,$$

which becomes on simplification

$$\mathrm{M}_{k,m}(x)=\frac{\Gamma(2m+1)^{m+\frac{1}{2}}.2^{-2m}}{\Gamma(-k+m+\frac{1}{2})\Gamma(k+m+\frac{1}{2})}\times\int_{-1}^1(1+u)^{-k+m-\frac{1}{2}}(1-u)^{m+k-\frac{1}{2}}e^{\frac{1}{2}xu}\,du, \quad (30)$$

when the integral is convergent (*cf.* M.A., p. 352).

6. We proceed to consider a few particular forms of the operational representations given above.

(i.) From (16) we obtain when $l=m+\frac{1}{2}$,

$$x^{m-\frac{1}{2}}e^{\frac{1}{2}x}\mathrm{M}_{k,m}(x)\doteqdot\Gamma(2m+1)p^{-2m}\left(1-\frac{1}{p}\right)^{k-m-\frac{1}{2}}. \quad (31)$$

Further, take $k=s+m+\frac{1}{2}$, and we get

$$x^{m-\frac{1}{2}}e^{\frac{1}{2}x}\mathrm{M}_{s+m+\frac{1}{2},m}(x)\doteqdot\Gamma(2m+1)p^{-2m}\left(1-\frac{1}{p}\right)^{s}. \quad (32)$$

Hence

$$\sum_{s=0}^{\infty}\frac{\mathrm{M}_{s+m+\frac{1}{2},m}(x)}{\Gamma(s+1)}\doteqdot x^{-m+\frac{1}{2}}e^{-\frac{1}{2}x}\Gamma(2m+1)p^{-2m}e^{1-\frac{1}{p}}$$
$$=\Gamma(2m+1)x^{\frac{1}{2}}e^{-\frac{1}{2}x+1}\mathrm{J}_{2m}(2\sqrt{x}) \quad . \quad . \quad . \quad (33)$$

It can be easily shown that the series on the left-hand side is absolutely convergent. For when $2m$ is not an integer, the two integrals $\mathrm{M}_{k,m}(z)$, regular near 0, are valid for all finite values of z. Now applying D'Alembert's Ratio test, we get

$$\left|\frac{u_{s+1}}{u_s}\right|=\left|\frac{1}{s+1}\right|\left|\frac{\mathrm{M}_{s+m+\frac{3}{2},m}(x)}{\mathrm{M}_{s+m+\frac{1}{2},m}(x)}\right|,$$

and hence

$$\lim_{s\to\infty}\left|\frac{u_{s+1}}{u_s}\right|=0.$$

Similarly we obtain

$$\sum_{s=0}^{\infty}(-)^s\frac{\mathrm{M}_{s+m+\frac{1}{2},\,m}(x)}{\Gamma(s+1)}=\Gamma(2m+1)x\,e^{-\frac{1}{2}x-1}\mathrm{I}_{2m}(2\sqrt{x}). \quad (34)$$

Here also the series is convergent.

(ii.) Again when $m=0$, we get from (32)

$$x^{-\frac{1}{2}}e^{\frac{1}{2}x}\mathrm{M}_{s+\frac{1}{2},\,0}(x)\doteq\left(1-\frac{1}{p}\right)^s.$$

But if $\mathrm{L}_s(x)$ is the Laguerre polynomial defined by *

$$\mathrm{L}_s(x)=e^x\left(\frac{d}{dx}\right)^s(x^se^{-x}),$$

we obtain $$\mathrm{L}_s(x)\doteq s!\left(1-\frac{1}{p}\right)^s$$

and hence

$$x^{-\frac{1}{2}}e^{\frac{1}{2}x}\mathrm{M}_{s+\frac{1}{2},\,0}(x)=\mathrm{L}_s(x)/\Gamma(s+1). \quad . \quad . \quad (35)$$

Apply (4) to (31). We obtain, when $u>0$,

$$\left(\frac{x}{u}\right)^{m-\frac{1}{2}}e^{\frac{1}{2}\frac{x}{u}}\mathrm{M}_{k,\,m}\left(\frac{x}{u}\right)\doteq\frac{\Gamma(2m+1)}{u^{2m}p^{2m}}\left(1-\frac{1}{pu}\right)^{k-m-\frac{1}{2}},$$

from which we can get

$$u^ke^{\frac{1}{2}x\left(\frac{1}{u}-1\right)}\mathrm{M}_{k,\,m}\left(\frac{x}{u}\right)$$

$$=\mathrm{M}_{k,\,m}(x)+\sum_{r=1}^{\infty}\frac{(k-m-\frac{1}{2})\ldots(k-m-r+\frac{1}{2})}{r!}$$

$$(u-1)^r\mathrm{M}_{k-r,\,m}(x), \quad . \quad (36)$$

when the series is convergent.

If we apply (4) to (20) and put $l=m+\frac{1}{2}$, we obtain in the same way as above,

$$u^{-k}e^{\frac{1}{2}x\left(1-\frac{1}{u}\right)}\mathrm{M}_{k,\,m}\left(\frac{x}{u}\right)$$

$$=\mathrm{M}_{k,\,m}(x)+\sum_{r=1}^{\infty}\frac{(k+m+\frac{1}{2})\ldots(k+m+r-\frac{1}{2})}{r!}$$

$$\times(1-u)^r\mathrm{M}_{k+r,\,m}(x), \quad . \quad (37)$$

when the series is convergent.

Many more examples showing the application of the rules of the calculus can be multiplied.

* Courant and Hilbert, *loc. cit.* p. 77 (1924).

XXXV. *Charged Colloid Particles in an Ultrasonic Field.* *By* Dr. J. J. Hermans *.

§ 1.

A few years ago Debye [1] pointed out the possibility of determining the inertia of ions in an electrolytic solution by their behaviour in an ultrasonic field. Owing to their inertia the ions lag slightly behind the solvent, and, as this effect of inertia varies with different ions, a charge density S is generated, thus an electric field X which conforms to the equation of Poisson : div $X = 4\pi S/D$. If at a certain moment an ion with charge e_K and mass m_K has a velocity v_K in the sonic field, and if v_0 is the velocity of the solvent, the ion undergoes a certain friction $\rho_K(v_K - v_0)$, in which ρ_K is a frictional factor. If the force $e_K X$ which the ion experiences by the electric field X is added, the equation of motion becomes

$$e_K X - \rho_K(v_K - v_0) = m_K \frac{dv_K}{dt} \quad . \quad . \quad . \quad . \quad . \quad (1)$$

The frictional factor ρ_K is in inverse ratio to the mobility l_K of the ion [2] :

$$\rho_K = \frac{15.10^{-8}}{l_K} \simeq 2.10^{-9}.$$

If there are f_K ions of the kth species per unit of volume, the equation of continuity

$$\frac{\partial f_K}{\partial t} + \mathrm{div}\,(f_K v_K) = 0 \quad . \quad . \quad . \quad . \quad . \quad (2)$$

has to be met, while X conforms to the equation of Poisson :

$$\mathrm{div}\, X = \frac{4\pi}{D} \Sigma_K f_K e_K \quad . \quad . \quad . \quad . \quad . \quad (3)$$

Debye set himself the task of computing the field X. Integrating the result for a quarter of the length of the sonic wave one finds the amplitude of the electric potential, which in favourable cases proves to be of the order of 10^{-5} volts.

Hitherto it has apparently not been possible to measure this effect. Consequently the calculations of Oka [3], who

* Communicated by the Author.

adds the electrophoretic force and the force of relaxation of the surrounding ion sphere to the equations of motion, are at present only of theoretic interest.

It may be added that Oka, like Debye, ignores the diffusion. It will readily be seen that the relative error thereby made in the equations of motion amounts to about 1 per cent., for, if with Debye one takes a plane sonic wave moving in the direction of the axis x at the rate of g cm. per sec., then the velocity v_0 of the solvent is

$$v_0 = a_0 e^{i\omega(t-x/g)}.$$

The concentration f_K in (2) and (3) can only slightly diverge from the average concentration n_K, so that the quantities $\nu_K = f_K - n_K$ can be treated as small ones. Both Debye and Oka only retain the terms that are linear in ν_K, v_K and their derivatives in the equations (1), (2), (3). For instance, (2) becomes

$$\frac{\partial \nu_K}{\partial t} + n_K \frac{\partial v_K}{\partial x} = 0. \quad . \quad . \quad . \quad . \quad . \quad . \quad . \quad (4)$$

It is not difficult to show from the result of the calculations that these approximations are certainly permissible. Writing ν_K and v_K as periodic functions

$$\nu_K = \alpha_K e^{i\omega(t-x/g)}; \qquad v_K = a_K e^{i\omega(t-x/g)},$$

α_K becomes $a_K n_K/g$ according to (4). If now the diffusion is also taken into account, a force $-kT/f_K \cdot \partial f_K/\partial x$ must be added to the left-hand side of the equation (1). The relative error made by omitting this term is

$$\phi = \frac{-\frac{kT}{f_K}\frac{\partial f_K}{\partial x}}{m_K \frac{dv_K}{dt}} = \frac{-\frac{kT}{n_K}\frac{\partial \nu_K}{\partial x}}{m_K \frac{\partial v_K}{\partial t}} = \frac{kT}{m_K g^2}.$$

If M is the molecular weight of the ion under consideration, $m_K = 1{\cdot}6.10^{-24}$ M gram. Furthermore, the velocity g of sound in water is $1{\cdot}4.10^5$ cm. per sec., and $k = 1{\cdot}4.10^{-16}$ erg per degree, so that at room-temperature $\phi \cong 1{\cdot}3/M$. As the molecular weight of a hydrated ion has the order of magnitude 100, ϕ becomes about 1 per cent.

This error is unimportant in Debye's calculations. On the other hand, the force of relaxation and the electrophoretic force occur in Oka's calculations. The expressions used for these only apply to low electrolytic concentrations, where moreover they stand for corrections of merely a few parts per cent. A calculation claiming such accuracy must therefore also take the diffusion into account. We shall, however, defer discussing the matter further until the uncorrected theory has been compared with experiment.

A force is lacking in equation (1) which is far more important than the diffusion term or that which is caused by the ion sphere; for in equation (1) there is nothing to show that the effect of inertia must vanish as soon as the density of the ion in question is equal to that of the solvent. Debye[4] suggested replacing m_K by the so-called apparent mass $m_K - s_0 V_K$ (V_K = volume of the ion, s_0 = density of the solvent). This is correct so long as v_K

differs only slightly from v_0. Consequently an error of a higher order is made in Debye's theory when the mass is corrected in this way. If, however, v_K differs considerably from v_0—as may be the case with particles of colloidal dimensions—one may best reason as follows. What is actually missing in (1) is the force $-V_K \partial p/\partial x$ which acts upon the ion as a result of the gradient of pressure in the sonic wave. This gradient of pressure is found by remembering that the solvent is accelerated by it in the following way :

$$\frac{dv_0}{dt} = -\frac{1}{s_0}\frac{\partial p}{\partial x}.$$

The complete equation of motion then becomes

$$e_K X - \rho_K(v_K - v_0) = m_K \frac{dv_K}{dt} - V_K s_0 \frac{dv_0}{dt}. \quad . \quad . \quad . \quad (5)$$

Where the particle considered is of lower density than the solvent, the effect is reversed. The particle then overtakes the solvent in the sonic field.

Debye's result for the amplitude of potential reads

$$\phi_0 = g a_0 \frac{\frac{4\pi}{D\omega}\Sigma\frac{n_K e_K m_K}{\rho_K}}{\sqrt{1+\left(\frac{4\pi}{D\omega}\Sigma\frac{n_K e_K^2}{\rho_K}\right)^2}}. \quad . \quad . \quad . \quad . \quad (6)$$

If we abbreviate

$$\eta = \frac{4\pi}{D\omega}\Sigma\frac{n_K e_K^2}{\rho_K},$$

this becomes

$$\phi_0 = g a_0 \frac{\Sigma\frac{n_K e_K m_K}{\rho_K}}{\Sigma\frac{n_K e_K^2}{\rho_K}} \cdot \frac{\eta}{\sqrt{1+\eta^2}}. \quad . \quad . \quad . \quad . \quad . \quad (7)$$

To get a high figure, ω must be so chosen that η is at least of the order of unity ; when ϕ_0 becomes of the order of $g a_0 m/e$. Applying Debye's reasoning without more ado to colloidal solutions *, effects may be expected

* The author has been privately informed that Prof. A. J. Rutgers (Ghent) has been considering the application to colloids for some time, and is also making preparations for experimental investigations.

of a considerably higher order than those in electrolytic solutions. The value of m/e for heavy ions is in the neighbourhood of $5 \cdot 10^{-11}$ (m in grams, e in e.s.u.). This ratio may amount to 10^{-8} for a colloidal particle with a charge of between 10 and 100 elementary charges and a radius of 10^{-6} cm.

It remains to be seen, however, whether Debye's theory may be applied to colloidal solutions without material alteration. The structure at present accepted is that in which the charged colloidal particles in an electrolytic solution are surrounded by an electric double layer. This double layer may partly be rigidly attached to the particle (Helmholtz) and may partly be distributed diffusedly in the solution (Gouy). In the majority of cases, however, the electrolytic concentration is so large that the dimensions of the diffuse double layer are small as compared with the colloidal particle [5]. The particle will then carry along its double layer almost entirely, which will considerably reduce the amplitude of potential. On the other hand, larger particles will lag much more behind the solvent and may carry a very large electrical charge. Both theory and experiment must decide whether these factors will result in a decrease or an increase of the effect considered.

By taking an extremely low electrolytic concentration the dimensions of the double layer become large with respect to the particle. This more closely approximates to the model of a simple electrolytic solution with very large ions. Nevertheless, the treatment best adapted to this model will be to take each colloidal particle with its double layer as an individual system, and only subsequently to sum up all the particles. The ensuing sections are concerned with this problem. The author later hopes to publish calculations dealing with the other extreme case, *i. e.*, a double layer that is small as compared with the particles. Intermediate cases will probably be very difficult to deal with theoretically, but it may be inferred at this stage that very special conditions will have to be chosen to measure the effect in colloidal solutions.

§ 2.

Imagine an electrically charged spherical particle in a mixture of electrolytes. Let the charge e of the particle

be uniformly distributed on the surface. The charges of the gegen ions are divided diffusedly in the solvent. In other words, where gegen ions occur in a Helmholtz double layer around the particle, it is assumed that they completely follow the motion of the particle. When the particle is at rest with respect to the solvent, the ions around the particle form an ion sphere of spherical symmetry. The Debye-Hückel approximation

$$\psi_0 = A\frac{e^{-\chi r}}{r}; \quad A = \frac{e}{D}\frac{e^{\chi R}}{1+\chi R} \quad * \quad . \quad . \quad . \quad (8)$$

is used for the potential. Here R is the radius of the particle, $1/\chi$ is the characteristic length of Debye-Hückel's theory :

$$\chi^2 = \frac{4\pi}{DkT}\Sigma_K n_K e_K^2.$$

As soon as the particle acquires a velocity with respect to the solvent, the potential loses its spherical symmetry. The ions try to restore that symmetry, but only partly succeed : there is a final time of relaxation. The inertia of the ions is neglected compared with that of the colloidal particles.

Now let a plane sonic wave move in the direction of the axis x. For definiteness suppose x to be vertical. The velocity of the solvent is

$$v_0 = a_0 \cos\left(\frac{\omega}{g}x\right).e^{i\omega t}.$$

At a certain point at the level of x this becomes

$$v_0 = b_0 e^{i\omega t}; \quad b_0 = a_0 \cos\left(\frac{\omega}{g}x\right).$$

A colloid particle at this level acquires a velocity

$$v = be^{i\omega t}.$$

As a rule b will be complex, showing that the velocities v_0 and v are not in phase. Indeed, actually the sonic wave is disturbed by the presence of the colloid particle, but we assume that the wave-length of sound is large

* If the colloid particle carries a large electric charge, and if it is surrounded by a rather concentrated electrolytic solution, the expression (8) may be only a rough approximation. It may be pointed out, however, that we shall only apply our results to the case of very small electrolytic concentrations.

with respect to the radius of the particle, so that this disturbance may be ignored. Further, we shall always neglect products of the velocities or their derivatives, which means that dv/dt may be replaced by $\partial v/\partial t$.

Before proceeding to calculate b we shall find out to what distribution of potential round the particle a certain $(b-b_0)$ value gives rise. The method we shall follow resembles that developed by Falkenhagen [6] for calculating the effect of relaxation in electrolytic solutions. But in our case we may disregard the Brownian movement of the particle itself [7], as this is negligible as compared with that of the ions. Thus the relaxation may be dealt with in the same way as that originally indicated by Debye and Hückel [8], with this difference, however, that we are now concerned with a high frequency vibration and not with a stationary movement.

Let f_K be the number of ions with e_K charge in a unit of volume in the neighbourhood of the particle, and let the potential be ψ. In coordinates X, Y, Z, which are attached to the solvent, the equations of motion of the ions are

$$\rho_K \frac{\partial f_K}{\partial t'} = \text{Div}\,(k\text{T Grad}\, f_K + f_K e_K \text{ Grad}\, \psi), \quad . \quad . \quad (9)$$

$$\text{Div Grad}\, \psi = -\frac{4\pi}{D} \Sigma_K f_K e_K. \quad . \quad . \quad . \quad . \quad (10)$$

Div and Grad refer to the XYZ system, ρ_K is a factor of friction. To find the equations of motion in an xyz system attached to the colloid particle, it should be borne in mind that this particle has a velocity $(b-b_0)e^{i\omega t'}$ with respect to the surrounding liquid. We therefore substitute

$$t=t'; \quad z=\text{Z}; \quad y=\text{Y}; \quad x=\text{X}-\frac{b-b_0}{i\omega} e^{i\omega t'}.$$

If we abbreviate divgrad $= \triangle$, we get

$$\rho_K \frac{\partial f_K}{\partial t} - \rho_K (b-b_0) e^{i\omega t} \frac{\partial f_K}{\partial x} = k\text{T}\triangle f_K + e_K \text{ div}\,(f_K \text{ grad}\, \psi),$$

$$. \quad . \quad . \quad (11)$$

$$\triangle\psi = -\frac{4\pi}{D} \Sigma_K f_K e_K. \quad . \quad . \quad . \quad . \quad . \quad . \quad (12)$$

div and grad now refer to the xyz system.

In reality the hydrodynamic flow of the medium should be taken into account. The velocity in the immediate vicinity of the particle is $be^{i\omega t}$, and only at a greater distance becomes $b_0 e^{i\omega t}$. Obviously the foregoing is not exact reasoning, and the more slowly the velocity decreases as the distance r to the centre of the particle increases, the greater will be the error. Now Stokes's equations for the flow of liquid certainly lead to slow decrease of velocity, viz., as $1/r$. It is a fortunate circumstance, however, that the divergence of the flow of liquid round the particle is zero. This flow necessitates the addition of a term $-\rho_K \mathrm{Div}(f_K q)$ in (9), q being the velocity. In first approximation f_K may be replaced by the average concentration n_K, and the result is then zero. Corrections will become necessary in higher approximation if the rate at which the electric potential decreases with increasing r is greater than that at which the velocity decreases. It should be added that this velocity decreases as $1/r$ only in Stokes's approximation, whereas in reality it does so far more rapidly [9].

In (11) we replace f_K grad ψ by n_K grad ψ, a customary approximation in the theory of electrolytes. Now, if the particles were at rest with respect to the solvent (*i. e.*, if the left side of (11) were zero) the solution would read

$$\psi=\psi_0=A\frac{e^{-\chi r}}{r}; \quad f_K=f_{K,0}=n_K\left(1-\frac{e_K}{kT}\psi_0\right).$$

We now add periodic functions :

$$\psi=\psi_0+\phi e^{i\omega t}; \quad f_K=f_{K,0}+\nu_K e^{i\omega t}. \quad . \quad . \quad . \quad (13)$$

Furthermore, we restrict ourselves to terms that are linear in $b-b_0$, so that (11), (12) become

$$kT\Delta\nu_K+e_K n_K\Delta\phi-i\omega\rho_K\nu_K=\rho_K(b-b_0)\frac{n_K e_K A}{kT}\frac{\partial}{\partial x}\left(\frac{e^{-\chi r}}{r}\right), \quad (14)$$

$$\Delta\phi=-\frac{4\pi}{D}\Sigma_K e_K\nu_K. \quad . \quad . \quad . \quad . \quad . \quad (15)$$

The value (15) for $\Delta\phi$ can be substituted in (14). If there are s ion species, (14) becomes a system of s differential equations for the s quantities ν_K. Onsager and Fuoss [10] have developed methods of matrix calculation for a set of this kind, but the solution is still very complicated. We shall go no further than to solve it for a specially simple case, viz., that in which all the ρ_K are equal, say ρ. This condition is met approximately for most mixtures of electrolytes if the concentration of H-ions or OH-ions can be left out of consideration. This condition is also met approximately in the special case where only H-ions and OH-ions are present, *e. g.*, a colloidal solution of arabinic acid in water.

When all ρ_κ are equal to ρ, a differential equation for ϕ can easily be deduced from (14) (15); to which end multiply (14) by $\frac{-4\pi e_\kappa}{DkT}$, and sum up. Abbreviating

$$K^2=\chi^2+\frac{i\omega\rho}{kT}, \quad . \quad . \quad . \quad . \quad . \quad (16)$$

we get $$\Delta\Delta\phi-K^2\Delta\phi=-\rho(b-b_0)\frac{A\chi^2}{kT}\frac{\partial}{\partial x}\left(\frac{e^{-\chi r}}{r}\right). \quad . \quad (17)$$

According to the nature of our problem the solution of (17) may be written as $f(r)x$. Remembering that at infinity ϕ vanishes, one finds

$$\phi=-\frac{\rho(b-b_0)A}{kT(\chi^2-K^2)}\frac{\partial}{\partial x}\left(\frac{e^{-\chi r}}{r}\right)+P\frac{\partial}{\partial x}\left(\frac{e^{-Kr}}{r}\right)+Q\frac{x}{r^3}. \quad (18)$$

The constants P and Q are determined by the condition that ϕ and $\Delta\phi$ shall remain finite when r becomes zero. This gives us

$$P=\frac{\chi^2}{K^2}\frac{\rho(b-b_0)A}{kT(\chi^2-K^2)}; \quad Q=\frac{\rho(b-b_0)A}{kTK^2}. \quad . \quad (19)$$

The first two terms in (18) soon become zero at large distances from the particle. The last term expresses the fact that the system "particle with surroundings" behaves like a dipole of the following magnitude:

$$\mu=Qe^{i\omega t}=\frac{\rho(b-b_0)A}{kTK^2}e^{i\omega t}. \quad . \quad . \quad . \quad (20)$$

The smaller the concentration of the electrolyte the smaller the absolute value of K^2, and therefore the larger μ, for the ions have greater difficulty in following the particle when the diffuse double layer extends over larger distances. But mod K^2 has a lower limit, given it by the term $i\omega\rho/kT$. This is in accordance with the fact that increased frequency reduces the dipole, as was to be expected.

Finally, we have to determine the magnitude of the electric field in the centre of the particle. For this we find

$$X=-\frac{\lambda}{e}(b-b_0)e^{i\omega t}, \quad . \quad . \quad . \quad . \quad . \quad (21)$$

$$\lambda=\frac{\rho eA}{kT}\frac{\chi^2}{3(\chi+K)}. \quad . \quad . \quad . \quad . \quad . \quad (22)$$

An extra resistance eX (known as the force of relaxation) is exerted upon the particle by the field X. In the theory of electrolytes this force can be dealt with as a small correction of a few parts per cent. applied to the resistance. As, however, large charges may occur with colloidal particles, in our case the force of relaxation may become very considerable, and it depends upon the ratio between charge and size of the particle whether this force will be small or otherwise with respect to the friction. To be on the safe side we shall therefore include the force of relaxation eX in the equation of motion of the particle.

In conclusion, it should be pointed out that the calculation of relaxation is exactly the same as it would be when assuming the charge of the particle to be a point charge, which is only permissible if the dimensions of the diffuse double layer are large with respect to the particle.

Hitherto we have calculated the electric field for an assumed value of $b-b_0$. We have yet to determine b for known b_0. For this we will turn back to equation (5), in which, to avoid confusion, we shall now write W instead of ρ for the resistance of the colloid particle. Let R be the radius of the particle and η the coefficient of internal friction; then $W \cong 6\pi\eta R$.

Remembering that $v = be^{i\omega t}$, $v_0 = b_0 e^{i\omega t}$, and substituting the value (21) for X, (5) becomes

$$-(\lambda+W)(b-b_0)=i\omega(mb-Vs_0b_0),$$

where m is the mass of the particle, V its volume, s_0 the density of the solvent. So

$$b=\frac{\lambda W+i\omega V s_0}{\lambda+W+i\omega m}\, b_0. \quad . \quad . \quad . \quad . \quad (23)$$

This expression determines the amplitude of velocity of the particle and also the difference in phase between the velocity of the particle and its surroundings. The dipolar moment (20) is determined by this value of b to be

$$\mu=\frac{i\omega(Vs_0-m)}{\lambda+W+i\omega m}\,\frac{\rho A}{kTK^2}\, b_0 e^{i\omega t}.$$

Now A is determined by the charge and m by the mass of the particle. Assuming that all the particles have the same mass and charge, they all give rise to the same dipole. If there are n particles per unit of volume, the

potential difference between the levels x and $x+dx$ is $4\pi\mu ndx$. This is readily integrated for a quarter of the wave-length Λ if one remembers that $b_0=a_0\cos(\omega/g.x)$. A potential difference

$$\phi=2n\frac{i\omega(\mathrm{V}s_0-m)}{\lambda+\mathrm{W}+i\omega m}\frac{\rho\mathrm{A}}{k\mathrm{TK}^2}\Lambda a_0e^{i\omega t} \quad . \quad . \quad (24)$$

results.

§ 3.

The calculated effect is zero when the colloidal particles have the same density as the surrounding electrolytic solution, which is, of course, as it should be. We shall now proceed to examine the order of magnitude in a few special cases.

Let the charge e of the particle amount to α elementary charges, so $e=4{\cdot}8.10^{-10}\ \alpha$ e.s.u., and let the radius R of the particle be 10^{-6} cm.; then the resistance W will be of the order of $6\pi\eta\mathrm{R}=2\ .\ 10^{-7}$. In these circumstances ωm can be neglected compared with W; for, if s is the density of the particle,

$$\frac{\omega m}{\mathrm{W}}=\frac{4/3.\pi\mathrm{R}^3s\omega}{6\pi\eta\mathrm{R}}=2.10^{-10}\ s\omega.$$

This is a small fraction even when $\omega=10^8$. The nature of our calculations requires that $1/\chi$ shall be at least 10 R. We therefore suppose that $\chi=10^5$ cm.$^{-1}$. In the case of univalent ions this corresponds to an electrolytic concentration of $1{\cdot}5.10^{-5}$ grmol per litre. Abbreviating $nm=\mathrm{M}=$ mass of suspended colloid per unit of volume, and remembering that $\omega\Lambda=2\pi g$, ϕ has the order of magnitude

$$4\pi ga_0\frac{\mathrm{M}}{\lambda+\mathrm{W}}\frac{\rho\mathrm{A}}{k\mathrm{TK}^2}. \quad . \quad . \quad . \quad . \quad . \quad (25)$$

We shall first consider the case of small frequencies, viz., $\omega\rho/k\mathrm{T}\leqq\chi^2$, *i. e.*, $\omega\leqq1{\cdot}5.10^5$ sec^{-1}. In that case K has the same order of magnitude as χ, and that of λ becomes

$$\rho\frac{e\mathrm{A}}{k\mathrm{T}}\frac{\chi}{6}\simeqq\tfrac{1}{6}\rho\frac{e^2\chi}{\mathrm{D}k\mathrm{T}}=2{\cdot}5.10^{-12}\alpha^2.$$

Now with a particle radius of 10^{-6} cm. it is unlikely that the number of elementary charges will far exceed

100. λ is therefore at most of the same order as W, and (25) then becomes of the order

$$\phi \cong 4\pi g a_0 \frac{M}{W} \frac{\rho A}{kT\chi^2} \cong \frac{4\pi}{D} g a_0 \frac{M}{W} \frac{\rho e}{kT\chi^2}.$$

Substituting $g = 1{\cdot}4 . 10^5$ cm. per sec., $W = 2{\cdot}10^{-7}$, $\rho = 2{\cdot}10^{-9}$, $e = 4{\cdot}8 . 10^{-10}\,\alpha$, $\chi = 10^5$, $D = 80$, ϕ becomes

$$\phi \cong 10^{-3} a_0 M \alpha \text{ volt.}$$

Amplitudes of velocity of some 10 cm. per sec. are easily attained. The mass M per unit of volume is limited by the condition that the average distance between the particles must amount to at least ten times their radius if our considerations are to hold good. If one chooses particles of high density one may go as far as, say, $M = 10^{-2}$ gram per cubic cm. With α at 100, ϕ becomes several hundredths of a volt.

Let us now consider the case of higher frequencies, where $\omega\rho/kT >> \chi^2$, *i. e.*, $\omega >> 1{\cdot}5 . 10^5\,\text{sec}^{-1}$. The absolute value of K in (16) is then chiefly determined by the second term, *i. e.*, $K = \sqrt{\omega\rho/kT} = 3 . 10^3 \sqrt{\omega}$. Furthermore, the absolute value of λ becomes negligible as compared with W, so that

$$\phi \cong \frac{4\pi}{D\omega} g a_0 \frac{M}{W} \frac{\rho e}{kT}. \quad 10^{-7} \text{ e.s.u.}$$

This has the order of 10^{-6} volt for $\omega = 10^6$; so the effect becomes very small with high frequencies.

There is no difficulty in applying similar reasoning to particles of another size.

§ 4.

We should like to revert for a moment to the formula for the resistance of the colloid particle. Stokes's formula applies only to stationary motion and to low velocities. Actually we are dealing with vibrations of high frequency.

As regards the velocity, the utility of the formula is governed by Reynolds's number $s_0(v - v_0)R/\eta$. To determine its magnitude we may substitute $b - b_0$ for $v - v_0$, and then, with the assistance of (23), find

$$s_0 \frac{R}{\eta} \frac{\omega m}{W} b_0 \cong s_0 \frac{R}{\eta} \frac{\omega m}{W} a_0.$$

Assuming R to be 10^{-6} cm. and $\omega = 1{\cdot}5.10^5$, this becomes $3{\cdot}10^{-9}\ a_0$, so very far below 1. This condition is amply satisfied in other cases too (*e. g.*, larger R).

It remains for us to investigate the importance of the non-stationary character of the motion. According to Boussinesq [11] the resistance of a sphere with radius R, which has a velocity U in a liquid of s_0 density, U being a function of t, amounts to

$$6\pi\eta R\left[U+\frac{R}{\sqrt{\pi}}\sqrt{\frac{s_0}{\eta}}\int_0^t \frac{dU}{d\tau}\frac{d\tau}{\sqrt{t-\tau}}\right]+\tfrac{2}{3}\pi s_0 R^3\frac{dU}{dt}. \quad (26)$$

In the case of water $s_0=1$ and $\eta=0{\cdot}01$, while U is a periodic function: $U=U_0e^{i\omega t}$. The last term in (26) is to the first as

$$\frac{\frac{2}{3}.\pi R^3\omega}{6\pi\eta R}=\frac{R^2\omega}{9\eta}\cong 10R^2\omega.$$

The second term is to the first as

$$\frac{R}{\sqrt{\pi\eta}}\omega e^{-i\omega t}\int_0^t e^{i\omega\tau}\frac{d\tau}{\sqrt{t-\tau}}=2R\sqrt{\frac{\omega}{\pi\eta}}\int_0^{\sqrt{\omega t}} e^{-i\zeta^2}d\zeta.$$

We have here used the substitution $\omega(t-\tau)=\zeta^2$. Apparently the result is a periodic function of the order of $2R\sqrt{\omega/\pi\eta}\cong\sqrt{R^2\omega}$. In both cases, therefore, the important point is the magnitude of $R^2\omega$. In the foregoing cases this magnitude is considerably below unity. This sufficiently justifies the use of Stokes's formula.

Summary.

If a plane sonic wave moves in the solution of colloid particles, these particles will lag behind their surroundings because of their inertia. The diffuse double layer round a particle loses its spherical symmetry, and so gives rise to a dipolar moment. Summing up these dipolar moments for all the particles we get a potential difference ϕ between a node and an antinode of the sonic wave.

Two extreme cases may be distinguished: (1) The dimensions of the diffuse double layer are large as compared with the radius of the particle, and (2) these dimensions are small as compared with the particle. In this paper only the first case has been considered. The resulting potential difference ϕ, which proves to be proportional

to the apparent mass $m - Vs_0$ of the particles and to their charge e, may amount to about 0·01 volt. It seems to us that a potential difference which has this order of magnitude may easily be measured, thus leading to interesting information about mass and charge of colloidal particles.

References.

(1) P. Debye, Chem. Physics, i. p. 13 (1933).
(2) J. J. Hermans, Rec. Trav. Chim. lvi. p. 654 (1937).
(3) S. Oka, Proc. Phys. Math. Soc. Japan (3) xv. pp. 247, 413 (1933).
(4) Private communication.
(5) A. Voet, *Koll. Z.* lxxix. p. 15 (1937).
(6) H. Falkenhagen, ' Electrolytes,' p. 189 *et seq.* (Paris, 1934).
(7) L. Onsager, *Physikal. Z.* xxvii. p. 388 (1926) ; xxviii. p. 285 (1927).
(8) P. Debye and E. Hückel, *Physikal. Z.* xxiv. p. 305 (1923).
(9) C. W. Oseen, ' Hydrodynamik,' p. 166 *et seq.* (Leipzig, 1927).
(10) L. Onsager and R. Fuoss, J. Phys. Chem. xxxvi. p. 2689 (1932).
(11) J. Boussinesq, *Theorie anal. Chaleur*, II, p. 224 (Paris, 1903) ; C. W. Oseen, ' Hydrodynamik,' p. 134 (Leipzig, 1927).

The Sir William Ramsay Laboratories
of Inorganic and Physical Chemistry.
University College, London.

XXXVI. *The Gradient Diagram.*

By Harold Ward Gardner, *M.S.*, *LL.B.**

MANY different statements of Bernoulli's theorem may be found in scientific literature, but few of them are complete. They invariably omit to mention the effect of atmospheric pressure. Though this effect in the case of most hydraulic systems is so small that it may be neglected, still the law of the conservation of energy requires † that it be included in a consideration of the theorem. A simple statement of the theorem is that

> *During steady discharge the amount of energy displayed at any vertical section of an hydraulic system is equal to the amount displayed at any other vertical section.*

* Communicated by the Author.

† W. F. Durand, ' Hydraulics of Pipelines ' (1921 ed.), p. 36, D. Van Nostrand Co., New York.

The completeness of this statement can be illustrated by a gradient diagram.

As is usual, let abscissæ represent distances along an hydraulic system ; let ordinates represent head in linear units or in unit pressure units. Head, in linear units, is also equal to amount of energy per unit weight of liquid traversing a system since, in dimensional units,

$$\frac{\text{energy}}{\text{force}} = \frac{\text{L} \times \text{MLT}^{-2}}{\text{MLT}^{-2}} = \text{L}.$$

But head may represent five manifestations of energy. These manifestations include, from top to bottom, atmospheric pressure, heat, kinetic energy, pressure

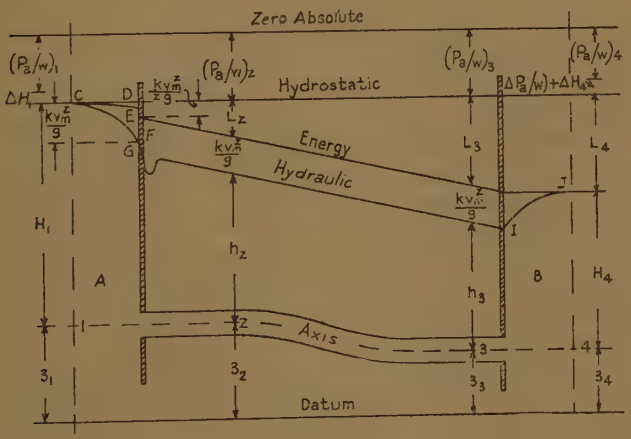

energy, and potential energy—that is to say, that every ordinate erected at any vertical section of any hydraulic system transporting liquid represents these five manifestations in the order mentioned heretofore. If, as is usual, several such ordinates be erected along an hydraulic system and the junctions representing the various manifestations of energy be joined by horizontal or inclined lines, then these lines represent gradients the vertical intercepts between which represent the amounts of the various manifestations of energy at the vertical sections at which intercepts are erected.

Thus, let the accompanying figure represent an hydraulic system consisting of an inclined tube that is delivering

liquid from reservoir A into reservoir B. The system may represent a viscometer, a plastometer, or an ordinary pipeline, of which the diameter is d and the length is l. The value of the mean velocity in the pipe is represented by v_m. The movement of liquid in the tube is unrestricted by valves or bends. The manifestations of energy are shown in their proper order from top to bottom as (1) atmospheric pressure, P_a/w; (2) heat energy, L; (3) kinetic energy or velocity head, kv_m^2/g; (4) hydrostatic pressure, h; and (5) potential head, z. The zones representing these five manifestations of energy are set apart by the six lines or gradients known from top to bottom as (1) the zero absolute; (2) the hydrostatic; (3) the energy; (4) the hydraulic; (5) the axis; and (6) the datum gradients.

The portion of an ordinate extending above the energy gradient represents neutral or dissipated head or energy that is unavailable; the portion below that gradient represents available head or energy. The zero absolute, the hydrostatic, and the datum gradients are level and parallel, but not horizontal. This is the basic condition on which Bernoulli's theorem is supported, for this theorem recites the fact that any vertical ordinate between the zero absolute and datum gradients is equal to any other vertical ordinate between those gradients.

The zero absolute gradient represents the elevation at which the pressure measures absolute zero. In fact, this condition prevails at the top surface of the atmosphere. Were the earth's atmosphere composed of water the elevation of this gradient should, at sea-level, be located P_a/w, or 33·9 feet above the surface of the liquid in the supply reservoir, A, if P_a and w represent respectively atmospheric pressure in pounds per square foot and unit weight of water in pounds per cubic foot. The hydrostatic gradient represents the elevation to which liquid will rise to every part of an installation when the liquid in it is stationary.

As soon as the liquid has developed steady motion through a tube the surface of the liquid will rise in piezometers only to the hydraulic gradient. The position of this gradient can be observed as menisci in the piezometers. At some distance kv_m^2/g, above it, one can only imagine the existence of the energy gradient. The value of k and the length of the vertical intercept between

these two gradients will depend on the regime of movement of the liquid in the tube. Since its value depends on the shape of the velocity gradient in a tube it is a function of Stokes's, usually called Reynolds's, criterion. During the turbulent regime its value approximates $\frac{1}{2}$. The energy gradient always slopes downward downstream. The hydraulic gradient usually slopes downward downstream, but it may slope upward as it progresses downstream. This situation always occurs when the diameter of a tube increases; it always occurs in the receiving or downstream reservoir. The slopes of both the energy and hydraulic gradients are usually assumed to be uniform, but they may deviate from uniformity on account of bends, ellipticity of bore, changing rugosity along a tube or on account of other factors.

Next in order below the hydraulic gradient is the axis of a tube. Its slope in large installations is usually variable, + or −. In small installations, such as viscometers or plastometers, in which the axes are straight, its slope is uniform and frequently horizontal. Naturally the hydrostatic pressure in a conduit will depend on its vertical alignment. A positive rule of design and construction, occasionally overlooked, is that the axis should always be placed below the hydraulic gradient in a gravity system. When the axis is placed above this gradient in a system of this kind the system may become a siphon temporarily; but because of an accumulation of air dissolved from the liquid the gradient will rise to the elevation of the surface of the water at a summit. This situation naturally diminishes the time rate of discharge from the tube, because of the diminished slope of the hydraulic gradient.

Finally, the lowest gradient of a complete diagram is the datum. Its location may, usually, be selected to suit convenience. In inland districts sea-level is often employed; but sea-level as a datum is disadvantageous in coastal regions. The reason for this statement is that datum should always be selected so that it will be below or at the same elevation as the lowest part of a system. If the axis be straight and horizontal the datum may coincide with it. At all events the datum and zero absolute gradients are parallel and level lines, with respect to which Bernoulli's theorem merely recites that the lengths of all vertical intercepts between them are

equal. Hence one may write for any two vertical sections through a system

$$(P_a/w)_2+L_2+\frac{kv_m^2}{g}+h_2+z_2=(P_a/w)_3+L_3+\frac{kv_m^2}{g}+h_3+z_3. \quad . \quad . \quad . \quad (1)$$

Thus far the discussion has progressed on the assumption that air and water are incompressible and that the atmospheric pressure on the surface of one reservoir is equal to that on the surface of the other; and in most instances the diminutive sizes of installations prevent compressibility and unequal atmospheric pressures on the surfaces of the two reservoirs from becoming measurable factors. With respect to viscometers and plastometers these factors are immaterial, but with respect to some large installations, when the difference between the elevations of the surfaces is large or when the submergence of either or both ends of a tube is comparatively large, compressibility of liquid and the additional column of air on the surface of the downstream reservoir may become material factors. The compressibility of liquid has the effect of increasing H_1, the hydrostatic head on the intake, by the amount ΔH_1. The large column of air, L_4, and a deep submergence, H_4, of the outlet end of a conduit both tend to increase the head, H_4, on an outlet by the amount $\Delta H_4+\Delta(P_a/w)_4$. To be sure the compressibility effect, ΔH_1, in the upstream reservoir tends to neutralize the compressibility effect in and the additional atmospheric pressure exerted on the surface of the downstream reservoir; but the effect of the unbalanced column of air $\Delta(P_a/w)_4$ will always be comparatively large when L_4 is large, whereas ΔH_1 and ΔH_4 may be comparatively small, or either may be small and the other large. A study of all three effects may be advantageous in a particular instance. The effect of ΔH_1 is to increase the time rate of discharge from a system by increasing the effective head causing discharge; the effect of ΔH_4 and of $\Delta(P/W)_4$ is to decrease time rate of discharge by increasing back pressure, and consequently decreasing effective head. A statement of Bernoulli's theorem when the two ends of a system are compared is, therefore,

$$(P_a/w)_1+\Delta H_1+H_1+z_1=(P_a/w)_4+\Delta(P_a/w)_4+\Delta H_4+L_4+H_4+z_4. \quad . \quad . \quad (2)$$

XXXVII. *The Ultra-Violet Absorption Bands of Ethyl Alcohol, n-Propyl Alcohol, and n-Butyl Alcohol in relation to Magneto-optical Dispersion.*

By W. J. G. Beynon, *B.Sc., Physics Department, University College, Swansea*.*

THE magneto-optical dispersions of these three alcohols in the region of spectrum ·44 μ to about ·29 μ have already been examined in these laboratories. The results of the investigations were published in this Journal [1]. Briefly, the investigation of each liquid consisted in measuring the magneto-optical rotation at some 15 to 20 ultra-violet wave-lengths and then relating the results to a formula of the type

$$\phi \equiv n\delta\lambda^2 = K_1\left[\frac{\lambda^2}{\lambda^2-\lambda_1^2}\right]^2,$$

n being the refractive index of the liquid for wave-length λ, δ being Verdet's Constant for wave-length λ, and K_1, λ_1 constants.

It was always found possible to represent the results, within experimental error, by a formula of this type, involving only a single characteristic wave-length. It is probable that had it been possible to extend the observations further into the ultra-violet, a simple formula of this type would have proved inadequate for the representation of the results.

In the present work an attempt has been made to photograph the ultra-violet absorption spectra of the liquids when in the vapour state, and then to relate the results to the magneto-optical work which has been done on them. A similar investigation upon two other alcohols has already been carried out, and the results recently published in this periodical.

Experimental Procedure.

The apparatus employed for this work was described in the previous publication (referred to above), so that it will suffice now merely to give a brief outline of the experimental procedure.

The vacuum spectrograph used was of the normal incidence type. It contained a one-metre concave speculum

* Communicated by Prof. E. J. Evans, D.Sc.

metal grating which gave a dispersion in the first order of about 17·5 Å.U. per mm. The spectrograph was evacuated by means of a large capacity mercury vapour pump, backed by a two-stage rotary oil pump. The vapour of the liquid was allowed into the main body of the spectrograph, the path-length in which absorption occurred being about two metres. The pressure of the vapour in the spectrograph was indicated on a McLeod mercury gauge. The continuum against which absorption was observed was produced by means of a condensed discharge in hydrogen. (A full description of the discharge-tube employed has already been published.) An excellent continuum down to 750 Å.U. was easily obtained, but the small reflecting power of the grating for very short wave-lengths incident normally on it made it impossible to photograph clearly absorption below this wave-length. The liquids examined, which were already in a fairly pure state, were subjected to a further process of careful fractional distillation before use.

It is to be noted that the absorption photographs have been obtained for the alcohols in the vapour state, whereas the magnetic rotation experiments were made with them in the liquid state. The possibility of a shift occurring in the absorption bands in changing the physical state was mentioned in the recent article by Beynon and Evans on the absorption of methyl and allyl alcohols. Up to the present time most of the work on the influence of physical state on the position of absorption bands indicates that the bands shift towards the red in passing from the vapour to more dense states. In the case of extreme ultra-violet bands the magnitude of this shift is not known, and hence this factor could not be considered when calculating suitable magneto-optical dispersion formulæ for the liquids. Although this possible shift was neglected, the formulæ obtained fit the experimental observations with considerable accuracy.

Experimental Results.

The Absorption Photographs.

The setting of the grating permitted photographs to be taken over the approximate range of spectrum ·20 μ to ·06 μ.

Victor Henri [2] found absorption bands in the region

·22 μ to ·23 μ for each of these alcohols. Henri states that these bands are very weak, and it is probable that their effect on magneto-optical and natural dispersion in the visible and near ultra-violet is very slight. Consequently no account has been taken of them in this investigation.

The spectrograms of all three alcohols are similar in that they each exhibit one rather diffuse absorption band in the region 1500 to 1600 Å.U., with further regions of absorption very low down in the spectrum (below 700 Å.U.). The absorption bands are in all cases broader and more diffuse than those found for methyl alcohol, and consequently they could not be fixed with the precision possible for the bands of that vapour. The wave-lengths of the absorption bands used in the formulæ are the mean values of several observations and are considered to be accurate within a few Å.U. Since the formulæ are being applied to magneto-optical measurements made in the visible and near ultra-violet, errors of several Å.U. in the wave-lengths of these bands will not seriously affect the results. Some of the photographs of ethyl alcohol exhibit a series of faint absorption bands above 1600 Å.U. The wave-lengths of these bands (which were extremely faint and narrow) are 1633, 1611, and 1602 Å.U. respectively. In the magneto-optical dispersion formula, instead of inserting a term for each of these bands, only a single wave-length has been employed in the calculation. This approximation greatly simplifies the formula and does not affect the calculated values at wave-lengths remote from the region of absorption. For the bands at 1633, 1611, and 1602 a mean value of 1618 Å.U. has been employed. In the case of *n*-propyl alcohol the diffuse absorption band has a wave-length of 1565 Å.U. In many of the spectrograms, however, especially those for heavy vapour pressures, the continuum ended abruptly at about 1648 Å.U., and gave some indication that there existed in the region of 1650 Å.U. another absorption band. For *n*-butyl alcohol only one diffuse band of wave-length 1577 Å.U. was observed in this region.

Apart from a single band, for each liquid in the region 1500 to 1600 Å.U. no further evidence of absorption was found until continuous absorption set in at approximately 700 Å.U. As has already been explained, the continuum in this region becomes very weak, and evidence of absorption could only be obtained with difficulty. However, even

comparatively large errors in fixing the absorption bands of very short wave-length will only slightly affect the natural and magneto-optical dispersion in the visible and ultra-violet regions of the spectrum, and it was found that sufficiently accurate formulæ could be obtained if the lower band of each liquid had a wave-length of 650 Å.U. It is probable, of course, that the wave-lengths of these extremely short wave-length bands increase with increasing molecular weight in the same manner as those of higher wave-length, but in each of the three magneto-optical dispersion formulæ given in this paper the same value (650 Å.U.) has been used.

The following are the estimated wave-lengths of the higher absorption bands of the three alcohols in the vapour states :—

Ethyl alcohol	1518, 1633, 1611, 1602 Å.U.
n-Propyl alcohol	1565 Å.U.
n-Butyl alcohol	1577 Å.U.

Using the values of the absorption bands given above, it was found that for each liquid the magneto-optical dispersion over a large range of spectrum can be represented by formulæ of the type

$$\phi \equiv n\delta\lambda^2 = K_1\left[\frac{\lambda^2}{\lambda^2-\lambda_1^2}\right]^2 + K_2\left[\frac{\lambda^2}{\lambda^2-\lambda_2^2}\right]^2 + \ldots,$$

where for

Ethyl alcohol	$\lambda_1=650$ Å.U., $\lambda_2=1518$ Å.U., $\lambda_3=1618$ Å.U.
n-Propyl alcohol	$\lambda_1=650$ Å.U., $\lambda_2=1565$ Å.U.
n-Butyl alcohol	$\lambda_1=650$ Å.U., $\lambda_2=1577$ Å.U.

Values of the constants K_1, K_2, etc., were calculated from the magneto-optical results after insertion of the respective values of λ_1 and λ_2.

The Magneto-Optical Dispersion Formulæ.

Ethyl Alcohol.

Measurements of the magnetic rotation of ethyl alcohol in the ultra-violet were first made by Stephens and Evans [1] in 1927. These measurements have recently been accurately repeated in these laboratories, and are

now given in this paper. Stephens and Evans represented their results by the formula

$$\phi \equiv n\delta\lambda^2 = 1{\cdot}4441\left[\frac{\lambda^2}{\lambda^2-(\cdot 1114)^2}\right]^2 . \quad . \quad . \quad . \quad (1)$$

for δ in circular measure,

or $$\phi = n\delta\lambda^2 = {\cdot}00496_5\left[\frac{\lambda^2}{\lambda^2-(\cdot 1114)^2}\right]^2 . \quad . \quad . \quad (2)$$

for δ in mins. per cm. gauss.

These observers, in their calculations, employed values of the refractive index determined by Seegert (Landolt and Bornstein's Tables, p. 969). The refractive indices of ethyl alcohol at many wave-lengths in both the visible and ultra-violet have since been accurately determined in these laboratories, and these values are employed in the present calculations. The formula now obtained for the magneto-optical dispersion of ethyl alcohol is

$$\phi \equiv n\delta\lambda^2 = {\cdot}00355_2\left[\frac{\lambda^2}{\lambda^2-(\cdot 065)^2}\right]^2 + {\cdot}00134_0\left[\frac{\lambda^2}{\lambda^2-(\cdot 1518)^2}\right]^2$$

$$+ {\cdot}000150_4\left[\frac{\lambda^2}{\lambda^2-(\cdot 1618)^2}\right]^2 . \quad . \quad . \quad . \quad (3)$$

In Table I. a comparison is given between values of δ calculated from this formula and the actual experimental values. The values of the refractive index used in the calculations are also included in this table.

Lowry and Dickson[4] measured the ratio $\delta/\delta_{\cdot 5461\,\mu}$ for seven wave-lengths in the visible spectrum. Table II. compares their values with those calculated from formula (3).

n-*Propyl Alcohol.*

The magneto-optical dispersion of *n*-propyl alcohol was measured by Jones and Evans[1], the formula deduced by them being

$$\phi \equiv n\delta\lambda^2 = 1{\cdot}553\left[\frac{\lambda^2}{\lambda^2-(\cdot 1138)^2}\right]^2 , \quad . \quad . \quad . \quad (4)$$

TABLE I.

Temperature 15° C.

Wave-length in microns.	Refractive index.	Verdet's Constant calculated.	Verdet's Constant observed.
·5893	1·3638	$·0113_0$	*
·46	1·3697	$·0192_6$	$·0192_4$
·45	1·3704	$·0201_5$	$·0201_5$
·44	1·3712	$·0212_4$	$·0212_2$
·43	1·3719	$·0223_7$	$·0223_3$
·42	1·3727	$·0235_8$	$·0235_7$
·41	1·3737	$·0248_8$	$·0248_9$
·40	1·3747	$·0263_2$	$·0263_3$
·39	1·3757	$·0279_1$	$·0279_3$
·38	1·3769	$·0296_1$	$·0296_0$
·37	1·3783	$·0315_3$	$·0315_3$
·36	1·3797	$·0336_2$	$·0337_3$
·35	1·3813	$·0359_7$	$·0361_0$
·34	1·3832	$·0385_7$	$·0387_0$
·33	1·3851	$·0415_1$	$·0416_4$
·32	1·3873	$·0448_0$	$·0449_5$
·31	1·3897	$·0485_7$	$·0487_0$
·30	1·3922	$·0529_1$	$·0529_5$
·29	1·3952	$·0579_1$	$·0579_4$
·28	1·3986	$·0637_3$	$·0637_6$

TABLE II.

Wave-length in microns.	$\delta/\delta_{\cdot5461\,\mu}$ calculated from formula (3).	$\delta/\delta_{\cdot5461\,\mu}$ observed by Lowry and Dickson.
·6708	·648	·638
·6438	·706	·708
·5893	·849	·849
·5086	1·164	1·166
·4800	1·321	1·318
·4678	1·398	1·393
·4359	1·633	1·626

* Perkin's results [3] corrected to 15° C. give $\delta_{\cdot5893\,\mu}=·0113_3$.
Lowry's results [5] corrected to 15° C. give $\delta_{\cdot5893\,\mu}=·0112_4$.

δ given in circular measure, or

$$\phi \equiv n\delta\lambda^2 = \cdot 00533_8 \left[\frac{\lambda^2}{\lambda^2 - (\cdot 1138)^2}\right]^2, \quad . \quad . \quad (5)$$

δ given in mins. per cm. gauss.

The formula derived from the present work is

$$\phi \equiv n\delta\lambda^2 = \cdot 00374_8 \left[\frac{\lambda^2}{\lambda^2 - (\cdot 065)^2}\right]^2 + \cdot 00164_9 \left[\frac{\lambda^2}{\lambda^2 - (\cdot 1565)^2}\right]^2 \quad . \quad . \quad . \quad (6)$$

Earlier in this paper it was mentioned that there is evidence for a third absorption band of wave-length

TABLE III.

Refractive Index of *n*-Propyl Alcohol in Visible Spectrum.

Temperature 19·5° C.

Wave-length in microns.	Refractive index.
·6678	$1\cdot 3834_3$
·5876	$1\cdot 3857_2$
·5016	$1\cdot 3894_7$
·4922	$1\cdot 3900_0$
·4713	$1\cdot 3912_5$
·4472	$1\cdot 3930_4$

about 1648 Å.U. (the actual value may be lower than this). If this band is taken into consideration, then the following formula will represent the magneto-optical dispersion

$$\phi \equiv n\delta\lambda^2 = \cdot 00377_4 \left[\frac{\lambda^2}{\lambda^2 - (\cdot 065)^2}\right]^2 + \cdot 00148_4 \left[\frac{\lambda^2}{\lambda^2 - (\cdot 1565)^2}\right]^2 + \cdot 00013_9 \left[\frac{\lambda^2}{\lambda^2 - (\cdot 1648)^2}\right]^2 \quad . \quad . \quad . \quad (6a)$$

Jones and Evans also employed values of the refractive index given by Victor Henri. The refractive indices of this liquid (needed for the calculations) have now been determined by the author for both the visible and ultra-violet, and are given in Tables III. and IV.

Verdet's constants of *n*-propyl alcohol have recently been measured by the author at a number of ultra-violet wave-lengths, and these observations are in good relative agreement with those made previously by Jones and Evans. Table V. gives the values of δ calculated from formula (6), together with those deduced from the observations. The values of the refractive index as required for the

TABLE IV.

Ultra-Violet Determinations at 23·6° C.

Wave-length in microns.	Refractive index.
·4063	1·3952
·3689	1·4000
·3656	1·4006
·3599	1·4014
·3534	1·4025
·3349	1·4062
·3337	1·4064
·3126	1·4112
·3064	1·4129
·3034	1·4137
·3012	1·4143
·2961	1·4159
·2883	1·4186
·2825	1·4208
·2767	1·4234

evaluation of Verdet's Constant were deduced from those given in Table IV. on the assumption that $\frac{dn}{dt} = -\cdot0004$.

It will be seen that the calculated and observed values agree within experimental error even at ·29 μ. The calculated value of δ at the wave-length ·5893 μ is between the values observed by Perkin and Lowry.

The calculated values of $\delta/\delta_{\cdot5461\,\mu}$, together with the observed values of Lowry and Dickson, are given in Table VI.

TABLE V.

Temperature 13·8° C.

Wave-length in microns.	Verdet's Constant calculated.	Verdet's Constant observed.
·5893	$·0119_3$	*
·43	$·0236_7$	$·0236_2$
·42	$·0249_6$	$·0249_5$
·41	$·0263_6$	$·0263_6$
·40	$·0278_9$	$·0278_6$
·39	$·0295_8$	$·0296_1$
·38	$·0314_3$	$·0314_6$
·37	$·0334_9$	$·0335_1$
·36	$·0357_5$	$·0357_6$
·35	$·0382_7$	$·0382_8$
·34	$·0410_8$	$·0411_1$
·33	$·0442_7$	$·0442_6$
·32	$·0478_6$	$·0478_5$
·31	$·0519_6$	$·0519_0$
·30	$·0567_1$	$·0567_5$
·29	$·0621_8$	$·0622_4$

TABLE VI.

Wave-length in microns.	$\delta/\delta_{\cdot 5461\,\mu}$ calculated from formula (6).	$\delta/\delta_{\cdot 5461\,\mu}$ observed by Lowry and Dickson.
·6708	·647	·642
·6438	·706	·713
·5893	·851	·850
·5086	1·165	1·163
·4800	1·323	1·321
·4359	1·638	1·635

n-*Butyl Alcohol.*

The magneto-optical dispersion (and the natural dispersion) of *n*-butyl alcohol was measured by Stephens (E.)

* $·0119_7$ Perkin [3] corrected to 13·8° C.
$·0118_8$ Lowry [5] corrected to 13·8° C.

and Evans [1]. They represented their results by the formula

$$\phi \equiv n\delta\lambda^2 = \cdot 005516\left[\frac{\lambda^2}{\lambda^2-(\cdot 1149)^2}\right]^2 . \quad . \quad . \quad (7)$$

The formula now given is

$$\phi \equiv n\delta\lambda^2 = \cdot 00389_7\left[\frac{\lambda^2}{\lambda^2-(\cdot 065)^2}\right]^2 + \cdot 00173_9\left[\frac{\lambda^2}{\lambda^2-(.1577)^2}\right]^2 . \quad . \quad . \quad (8)$$

TABLE VII.

Temperature 13° C.

Wave-length in microns.	Refractive index.	Verdet's Constant calculated from formula (8).	Verdet's Constant observed.
·5893	1·4024	$\cdot 0123_5$	*
·45	1·4096	$\cdot 0221_7$	$\cdot 0221_7$
·44	1·4105	$\cdot 0233_0$	$\cdot 0229_6$
·43	1·4115	$\cdot 0245_4$	$\cdot 0245_3$
·42	1·4124	$\cdot 0259_0$	$\cdot 0259_0$
·41	1·4135	$\cdot 0273_5$	$\cdot 0273_2$
·40	1·4146	$\cdot 0289_4$	$\cdot 0289_0$
·39	1·4158	$\cdot 0307_0$	$\cdot 0306_8$
·38	1·4171	$\cdot 0326_1$	$\cdot 0326_7$
·37	1·4185	$\cdot 0347_5$	$\cdot 0347_9$
·36	1·4200	$\cdot 0371_1$	$\cdot 0371_4$
·35	1·4218	$\cdot 0397_3$	$\cdot 0397_3$
·34	1·4237	$\cdot 0426_7$	$\cdot 0426_5$
·33	1·4261	$\cdot 0459_7$	$\cdot 0459_9$

The calculated and observed values are shown in Table VII. The values of the refractive index required for the calculations have been deduced from those given by Stephens and Evans in their paper.

The agreement between observed and calculated values is in this case particularly good, but it must be noted that the observations do not extend as far into the ultra-violet as for ethyl and propyl alcohols. Had observations

* Lowry [5] gives the "water ratio" for *n*-butyl alcohol at 20° C. to be ·931. Corrected to 13° C. this ratio would be ·937. Assuming δ for water to be ·0131, the calculated value for this ratio comes out as ·943.

of the magnetic rotation of butyl alcohol at shorter wave-lengths been available, it is possible that such good agreement could not then have been obtained.

The calculated values of $\delta/\delta_{5461\,\mu}$ and the observed values of Lowry and Dickson[4] are given in Table VIII.

TABLE VIII.

Wave-length in microns.	$\delta/\delta_{\cdot 5461\,\mu}$ calculated from formula (8).	$\delta/\delta_{\cdot 5461\,\mu}$ observed by Lowry and Dickson.
·6708	·647	·649
·6438	·705	·707
·5893	·850	·849
·5086	1·165	1·168
·4800	1·322	1·328
·4359	1·639	1·637

It will be seen that the calculated values of the ratios $\delta/\delta_{\cdot 5461\,\mu}$ are practically the same for *n*-propyl and *n*-butyl alcohols.

Range of Wave-lengths over which the Formulæ apply.

It is clear that the formulæ given will account quite well for the magnetic rotation of these alcohols over the range of spectrum ·67μ to ·30μ. It will be of interest to examine the extent to which they can be applied for longer wave-lengths.

Ingersoll[6] has measured Verdet's Constant in the near infra-red for a number of organic liquids, including two of the three liquids considered in this paper, viz., ethyl alcohol and *n*-butyl alcohol. Table IX. compares calculated and observed values of δ for these two liquids. The refractive indices quoted in the table are those measured by Ingersoll at 23° C., and given in the publication referred to above.

An interesting feature of this table is the fact that there is good agreement up to 1·0μ, but that above this wave-length the calculated values are too low.

It is probable that above $1{\cdot}0\,\mu$ the magnetic rotation is being influenced by infra-red absorption bands and that a third term, representative of these bands, must be included in the dispersion formulæ to account for the observed rotation. It appears, however, that the effect of infra-red absorption bands, even up to $2{\cdot}0\,\mu$, is very slight, and that in this region the extreme ultra-violet bands still practically control the magnetic rotation.

TABLE IX.

Values of Verdet's Constant in the near Infra-red.
Temperature 23° C.

	Ethyl alcohol.			*n*-butyl alcohol.		
Wave-length in microns.	Refractive index.	Verd. Const. calc.	Verd. Const. obs.	Refractive index.	Verd. Const. calc.	Verd. Const. obs.
·6	1·3609	·0111	·0111	1·3992	·0119	·012
·8	1·3566	·0060	·0060	1·3950	·0065	·0067
1·0	1·3542	·0038	·0038	1·3928	·0041	·0043
1·5	1·3506	$\cdot 0016_7$	·0019	1·3896	·0018	·0018
2·0	1·3470	$\cdot 0009_4$	·0010	1·3860*	·0011	·0014

Summary.

(1) The absorption spectra of ethyl alcohol, *n*-propyl alcohol, and *n*-butyl alcohol in the vapour state have been photographed in the ultra-violet down to approximately 650 Å.U.

(2) The vapours of all three liquids exhibit one diffuse band, together with a region of absorption below 700 Å.U. The wave-lengths of the higher bands are :—

Ethyl alcohol ..... 1518, 1633, 1611, 1602 Å.U.
n-Propyl alcohol.... 1565 Å.U.
n-Butyl alcohol .... 1577 Å.U.

* This value is not given by Ingersoll, but for the purpose of calculating δ has been extrapolated from the others.

(3) The magneto-optical dispersions of these three liquids can be represented from ·67 to approximately ·30 μ by the following formulæ involving the absorption bands given above :—

Ethyl alcohol :

$$\phi \equiv n\delta\lambda^2 = \cdot 00355_2 \left[\frac{\lambda^2}{\lambda^2-(\cdot 065)^2}\right]^2 + \cdot 00134_0 \left[\frac{\lambda^2}{\lambda^2-(\cdot 1518)^2}\right]^2 + \cdot 000150_4 \left[\frac{\lambda^2}{\lambda^2-(\cdot 1618)^2}\right]^2.$$

n-Propyl alcohol :

$$\phi \equiv n\delta\lambda^2 = \cdot 00374_8 \left[\frac{\lambda^2}{\lambda^2-(\cdot 065)^2}\right]^2 + \cdot 00164_9 \left[\frac{\lambda^2}{\lambda^2-(\cdot 1565)^2}\right]^2.$$

n-Butyl alcohol :

$$\phi \equiv n\delta\lambda^2 = \cdot 00389_7 \left[\frac{\lambda^2}{\lambda^2-(\cdot 065)^2}\right]^2 + \cdot 00173_9 \left[\frac{\lambda^2}{\lambda^2-(\cdot 1577)^2}\right]^2$$

(4) In the case of ethyl alcohol and *n*-butyl alcohol the formulæ apply up to the wave-length 1·0 μ; but it appears that above this wave-length the magnetic rotation is influenced by infra-red absorption bands. The influence of infra-red bands, however, is very slight compared with that of the extreme ultra-violet bands even up to 2·0 μ.

The author desires to thank Professor E. J. Evans, D.Sc., for suggesting this research, and for his continued help and advice during its progress.

References.

(1) D. J. Stephens and E. J. Evans, Phil. Mag. iii. p. 546 (March 1927); D. O. Jones and E. J. Evans, Phil. Mag. v. p. 593 (March 1928); E. Stephens and E. J. Evans, Phil. Mag. x. p. 759 (Nov. 1930).
(2) Victor Henri, ' Études de Photochemie,' pp. 41–64.
(3) Perkin, Journ. Chem. Soc. xlv. p. 466 (1884).
(4) Lowry and Dickson, Journ. Chem. Soc. i. p. 1072 (1913).
(5) Lowry, Journ. Chem. Soc. i. p. 91 (1914).
(6) Ingersoll, Journ. Optical Soc. Am. vi. p. 663 (Sept. 1922).

XXXVIII. *Integral Representations for Products of Weber's Parabolic Cylinder Functions.* By W. T. Howell, *M.Sc.**

IT is well known that Weber's parabolic cylinder functions are expressible in terms of the Laguerre polynomials of order $\pm\frac{1}{2}$, and it is natural to enquire whether it is possible to obtain a definite integral for products of these functions of a similar character to that for products of Laguerre polynomials [1] of integral order m, viz.,

$$\frac{n!}{(n+m!)}(x\sqrt{ab})^m \mathrm{L}_n^m(ax)\,\mathrm{L}_n^m(bx) = \frac{1}{2\pi}\int_0^{2\pi} e^{-im\gamma+x\sqrt{ab}\,e^{i\gamma}}\mathrm{L}_n^0\{x(a+b-2\sqrt{ab}\cos\gamma)\}d\gamma.$$

In this note I give a method of obtaining such a definite integral for the square of Weber's parabolic cylinder function. The same method also yields representations of certain products of parabolic cylinder functions in terms of contour integrals. The representation of these products by infinite integrals may be dealt with in a second paper.

§1. *A Definite Integral for the Square of Weber's Parabolic Cylinder Function.*

When n is integral we have the formula

$$\int_0^\infty e^{-sx}x^{-\frac{1}{2}}\mathrm{D}_n(2\sqrt{\lambda x})\,\mathrm{D}_n(2\sqrt{\mu x})\,dx = n!\sqrt{\pi}\frac{(\lambda+\mu-s)^{\frac{n}{2}}}{(\lambda+\mu+s)^{\frac{n+1}{2}}}\mathrm{P}_n\left\{\sqrt{\frac{4\lambda\mu}{(\lambda+\mu)^2-s^2}}\right\}. \quad (1.1)$$

The conditions of the Mellin [2] inversion theorem being satisfied, we may write

$$x^{-\frac{1}{2}}\mathrm{D}_n(2\sqrt{\lambda x})\,\mathrm{D}_n(2\sqrt{\mu x}) = \frac{n!\sqrt{\pi}}{2\pi i}\int_{c-i\infty}^{c+i\infty} e^{sx}\frac{(\lambda+\mu-s)^{\frac{n}{2}}}{(\lambda+\mu+s)^{\frac{n+1}{2}}}\mathrm{P}_n\left\{\sqrt{\frac{4\lambda\mu}{(\lambda+\mu)^2-s^2}}\right\}ds. \quad . \quad . \quad . \quad (1.2)$$

* Communicated by the Author.

Replacing the Legendre polynomial in (1.2) by Laplace's first integral [3], we have, on assuming that the inversion of the order of integration is allowable,

$$x^{-\frac{1}{2}}\,\mathrm{D}_n(2\sqrt{\lambda x})\,\mathrm{D}_n(2\sqrt{\mu x})$$
$$=\frac{n!}{\sqrt{\pi}}\int_0^{\pi}d\phi\cdot\frac{1}{2\pi i}\int_{c-i\infty}^{c+i\infty}e^{sx}(s+\lambda+\mu)^{-\frac{1}{2}-n}$$
$$\times\{\sqrt{4\lambda\mu}+\sqrt{s^2-(\lambda-\mu)^2}\cos\phi\}^n\,ds. \quad . \quad . \quad (1.3)$$

If we write $\lambda=\mu=\frac{1}{2}$, (1·3) becomes

$$x^{-\frac{1}{2}}\{\mathrm{D}_n(\sqrt{2x})\}^2$$
$$=\frac{n!}{\sqrt{\pi}}\int_0^{\pi}d\phi\cdot\frac{1}{2\pi i}\int_{c-i\infty}^{c+i\infty}e^{sx}(1+s)^{-\frac{1}{2}-n}(1+s\cos\phi)^n\,ds.$$
$$. \quad . \quad . \quad (1.4)$$

Using the known relation

$$\frac{1}{2\pi i}\int_{c-i\infty}^{c+i\infty}e^{sx}(1-s)^n(1+s)^{-n-\frac{1}{2}}\,ds=\frac{2^n n!}{\sqrt{\pi}(2n)!}\,x^{-\frac{1}{2}}\mathrm{D}_{2n}(2\sqrt{x}),$$

we have, after a few elementary manipulations,

$$\mathrm{D}_n^2(\sqrt{2x})=\frac{(-)^n 2^n(n!)^2}{\pi(2n)!}$$
$$\times\int_0^{\pi}e^{-\frac{x}{2}(1+\sec\phi)}\,\mathrm{D}_{2n}\{\sqrt{2x(1-\sec\phi)}\}\cos^n\phi\,d\phi,$$

or

$$\mathrm{D}_n^2(x)=\frac{(-)^n 2^n(n!)^2}{\pi(2n)!}$$
$$\times\int_0^{\pi}e^{-\frac{x^2}{4}(1+\sec\phi)}\,\mathrm{D}_{2n}\{x\sqrt{(1-\sec\phi)}\}\cos^n\phi\,d\phi;\ |\arg x|<\frac{\pi}{4}.$$
$$. \quad . \quad . \quad (1.6)$$

Dr. W. N. Bailey has remarked to me that the formula (1.6) is improved if Hermite polynomials are used instead of parabolic cylinder functions.

If $\mathrm{H}_n(x)$ is defined by

$$e^{xt-\frac{1}{2}t^2}=\sum_{n=0}^{\infty}\frac{t^n}{n!}\mathrm{H}_n(x),$$

then $$\mathrm{D}_n(x)=e^{-\frac{1}{4}x^2}\mathrm{H}_n(x),$$

so that (1.6) becomes

$$H_n^2(x)=\frac{(-)^n 2^n(n!)^2}{\pi(2n)!}\int_0^{\pi} H_{2n}\{x\sqrt{(1-\sec\phi)}\}\cos^n\phi\,d\phi.$$

§2. *Contour Integrals for Products of Weber's Parabolic Cylinder Functions.*

The fundamental formula of this section, which is due to Bateman [4], is

$$P_n(y)=\frac{2^n}{\pi}\int_c\frac{(y+it)^n}{(1+t^2)^{n+1}}\,dt \quad n>-1, \quad . \quad . \quad (2.1)$$

the contour c being a closed curve in the complex t-plane. If we write $\lambda=e^{\frac{1}{2}\pi i}$, $\mu=e^{-\frac{1}{2}\pi i}$ in (1.2) and use (2.1), we have, after inverting the order of integration,

$$x^{-\frac{1}{2}}D_n(2e^{\frac{1}{2}\pi i}\sqrt{x})\,D_n(2e^{-\frac{1}{2}\pi i}\sqrt{x})=\frac{2^n n!}{\sqrt{\pi}}\int_c(1+t^2)^{-n-1}t^n \cdot\frac{1}{2\pi i}\int_{c-i\infty}^{c+i\infty}e^{sx}s^{-\frac{1}{2}-n}\left(\frac{2}{t}-s\right)^n ds\,dt\,; \quad (2.2)$$

and evaluating the integral with respect to s, we have

$$D_n(2e^{\frac{1}{2}\pi i}\sqrt{x})\,D_n(2e^{-\frac{1}{2}\pi i}\sqrt{x})=\frac{2^{2n}(n!)^2}{\pi(2n)!}\int_c(1+t^2)^{-n-1}t^n e^{\frac{x}{t}}D_{2n}\left(2\sqrt{\frac{x}{t}}\right)dt,$$

or

$$D_n(ze^{\frac{1}{2}\pi i})\,D_n(ze^{-\frac{1}{2}\pi i})=\frac{2^{2n}(n!)^2}{\pi(2n)!}\int_c(1+t^2)^{-n-1}t^n e^{\frac{z^2}{4t}}D_{2n}\left(\frac{z}{\sqrt{t}}\right)dt. \quad (2.3)$$

Similarly we have

$$D_n(z)\,D_n(ze^{\frac{1}{2}\pi i})=\frac{2^{2n}(n!)^2}{\pi(2n)!}\int_c(1+t^2)^{-n-1}t^n e^{\frac{iz^2}{4t}}D_{2n}\left(\frac{ze^{\frac{i\pi}{4}}}{\sqrt{t}}\right)dt. \quad . \quad . \quad . \quad (2.4)$$

References.

(1) Bateman, ' Electrical and Optical Wave Motion,' equation (209), p. 100 (Cambridge, 1915).
(2) Courant and Hilbert, ' Methoden der Mathematischen Physik,' pp. 87–88 (1931).
(3) Whittaker and Watson, ' Modern Analysis ' (Third Edit.) §§15–23.
(4) Bateman, ' Partial Differential Equations,' p. 396 (Cambridge, 1932).

XXXIX. *Diffusion of Electrons in a Magnetic Field.* By J. S. Townsend, *M.A., F.R.S., Wykeham Professor of Physics, Oxford* *.

1. THE method of determining the effect of a magnetic field on the rate of diffusion of electrons in a gas which I gave some years ago has recently been criticized by Tonks † in the 'Physical Review,' and he finds it difficult to reconcile my explanation of diffusion in a magnetic field with some properties of large currents in a mercury rectifier.

In his description of the theory of diffusion Tonks limits himself to a survey of formulæ where the motion is treated as a drift of the electrons throughout the space occupied by the gas. In this method of investigating the motion certain small velocities, u, v, and w in the directions of the axes x, y, and z are attributed to all electrons in an element of the space depending on inequalities in the number n of electrons in unit volume of the gas. These velocities are mathematical quantities which satisfy the condition that the change in the distribution of electrons throughout the gas which would be obtained if all the electrons in an element of the space had the velocities u, v, and w, and no other motion, should be the same as the actual change in the distribution due to the motion of agitation. This method of indicating movements which affect the distribution of electrons in a current is convenient for some purposes on account of the simplicity of the notation, but it is only when the velocities u, v, and w are eliminated that any useful equation for the distribution is obtained. It would, of course, be impossible to represent completely the actual motion by any set of values of the velocities u, v, and w.

When there is no electric force acting on the electrons, all directions of motion of an electron are equally probable, and in most experiments the mean velocity of agitation is of a much higher order than the velocities u, v, and w. In a magnetic field the electrons move in spirals about axes parallel to the magnetic force. This has the effect of retarding the general motion of translation which tends

* Communicated by the Author.

† Lewis Tonks, 'Physical Review,' li. p. 744 (May 1937).

to equalize the distribution of electrons throughout the gas, and, in addition, a vortex motion or an angular velocity is established which does not affect the distribution. The two effects may be treated separately, and since diffusion depends only on motions which tend to equalize the distribution of electrons, it is unnecessary to consider this angular velocity in a theory of diffusion.

Thus the simplest set of velocities u, v, and w to represent the motion of translation in a magnetic field are those that I have given *, since the expressions for these velocities do not contain unnecessary terms representing rotations.

2. The methods I have adopted to determine the effect of a magnetic force H on the motion of translation takes fully into consideration the fact that the electrons rotate with an angular velocity He/m about axes in the direction of the magnetic force.

Tonks does not seem to have noticed this, and he adopts another set of expressions for the velocities, which includes terms to represent the motion of rotation by cross-drifts.

It may be mentioned that the equation for the distribution of electrons in a current deduced from the equation of continuity by eliminating the velocities u, v, and w adopted by Tonks is exactly the same as the equation for the distribution obtained by eliminating the velocities u, v, and w which I have adopted.

Thus all the difficulties he has encountered in reconciling my expression for the coefficient of diffusion with his observations on large currents in mercury vapour rectifiers would have been just the same if he tried to explain the properties of the currents by his system of cross-drifts.

It is well known that in all discharges the general distribution of the current and the electric force required to maintain it depend on the space-charges. Even with currents of the order of one-tenth or one hundredth of an ampere there are appreciable forces in the positive column of a uniform discharge due to differences of the order of one per cent. in the numbers of positive ions and electrons in the column.

The principal difficulty in arriving at a satisfactory explanation of the properties of discharges in gases

* Proc. Roy. Soc. A, lxxxvi. p. 571 (1912).

depends on the determination of the space-charges, and this difficulty would be much greater for fluctuating currents of the order of 2500 amperes in rectifiers than for small direct-current discharges. For this reason the conclusions arrived at by Tonks without considering the effect of space-charges cannot be regarded as evidence of any inaccuracy in equations of motion.

He also arrives at a remarkable conclusion by applying his own equations to discover the distribution of electrons moving under the action of an electric force R in directions perpendicular to the axis of z and a magnetic force H in the same direction. He assumes that in the symmetrical cylindrical distribution about the axis there is a steady state where both the radial velocities u_r and the velocities u_θ perpendicular to the radius are zero at all points of the field, and finds that this is in agreement with his set of values of u and v, but not in agreement with mine, and he concludes that this demonstrates the validity of his equations and exposes the fallacy of mine.

I do not consider that agreement or disagreement with the hypothesis of a state in which the velocities are zero is a test of the validity of my theory of the motion, since terms representing rotations are disregarded in the equations for the velocities u, v, and w, but this does not apply to Tonks's theory, where such terms are included in the equations for the velocities. One objection to his argument is that if the velocities u and v were zero the angular velocity of electrons at a point $(du/dy - dv/dx)/2$ would also be zero, which is inconsistent with the fact that all the electrons rotate with the angular velocity $\mathrm{H}e/m$ about axes in the direction of the force. The fallacy, therefore, is in the hypothesis that the velocities u and v are zero. Another objection to his views on cylindrical distributions is that u_r being zero, the value of n should be given by the equation $-dn/dr + ne\mathrm{R}/k\mathrm{T} = 0$ when there is no magnetic force, and it comes as a surprise to be told that this is Boltzmann's equation. If the electric force be towards the axis, the electrons moving by diffusion from the space inside a cylinder of radius r to the space outside lose energy by moving against the force, and the same number moving from the space outside to the space inside acquire energy by moving with the force; thus the mean energy E of the electrons diminishes as the distance from the axis increases.

In this case the expression for n should be

$$-(1/\mathrm{E})\,d(n\mathrm{E})\,dr+ne\mathrm{R}/k\mathrm{T}=0.$$

3. It may be stated that the principal objects of my investigations have been to determine the coefficient of diffusion K from experiments on the distribution of electrons in a current and to find an expression for K in terms of the mean free path and the mean velocity of agitation of the electrons. The method * of investigation depends on considerations of the actual motion of electrons in the free paths between collisions, and it may be seen from the following general description of the principle on which the calculations are based that it provides a simple and reliable method of determining not only the rates of diffusion of electrons in a magnetic field, but also the angular velocities which do not disturb the distribution.

Also, since the velocities u, v, and w are not the actual velocities of the electrons, and the equations involving these velocities are frequently misunderstood, it is of interest to show to what extent they contribute to the theory of the motion.

For these purposes it is necessary to consider the usual definition of the coefficient of diffusion in terms of changes in the distribution of electrons due to the motion of agitation †. If the number of electrons n_1 per cubic centimetre at any point P in the gas be greater than the number n_2 at another point Q, the number of electrons that flow per second from a small volume at P to a similar volume at Q is greater than the number that flow in the opposite direction, and the difference is proportional to (n_1-n_2) if the mean energy of agitation E be the same at all points of the gas. It must also be assumed that the points P and Q are not near the walls of the vessel containing the gas. From these elementary considerations the motions of the electrons in the directions of the axes are given by expressions of the form $-\mathrm{K}dn/dx$ when the number of electrons n per c.c. varies continuously throughout the gas.

The expression $-\mathrm{K}dn/dx$ may be defined as the difference between the number $(\mathrm{N}_1\bar{u})$ that pass per second from left to right, through unit area of a plane (yz), and

* ' Electricity in Gases,' Chapter III.
† ' Electricity in Gases,' p. 85.

the number ($N_2\bar{u}$) that pass from right to left. The mean velocity $\bar{u}$ is approximately $U/\sqrt{3}$, U being the mean velocity of agitation of the electrons. The sum of the numbers N_1 and N_2 is n, and in most experiments the difference (N_1-N_2) is very small compared with n.

The motion through unit area of the plane (yz) may therefore be represented by the equation

$$(N_1-N_2)\bar{u}=-K\,dn/dx. \quad . \quad . \quad . \quad . \quad (1)$$

The differential equation giving n in terms of K may be deduced from the equation of continuity, and in order to simplify the notation the flow (N_1-N_2) $\bar{u}$ through unit area of the plane (yz) is represented in that equation by the product of the number n and a small velocity u, and the corresponding flows through the unit areas of the co-ordinate planes (xz) and (xy) by the products nv and nw.

Thus in the ordinary notation the equation of continuity is

$$dn/dt+d(nu)/dx+d(nv)/dy+d(nw)/dz=0, \quad . \quad . \quad (2)$$

and the differential equation for n in terms of K is

$$\frac{dn}{dt}=K\left(\frac{d^2n}{dx^2}+\frac{d^2n}{dy^2}+\frac{d^2n}{dz^2}\right). \quad . \quad . \quad . \quad . \quad (3)$$

In this notation the definition of the velocity u is given by the equation

$$nu=-K\,(dn/dx). \quad . \quad . \quad . \quad . \quad . \quad (4)$$

This equation of motion and the corresponding equations for nv and nw state that the actual changes in the distribution of electrons due to diffusion is the same as the changes that would be obtained if all the n electrons at a point in the gas had the small velocities u, v, and w and no other motion. Much of the misunderstanding of the kinetic theory of electrons is due to this notation. It should be realized that the velocities u, v, and w in these equations are mathematical quantities, and there is no such motion as a general drift of all the electrons at a point with the small velocities u, v, and w due to inequalities in the values of n at different points of the gas.

4. In this respect these velocities differ from the mean velocity W due to an electric force Z in the direction

of the axis of z, which is a general drift of all the electrons with velocities distributed about the mean velocity W.

In the steady motion under the action of an electric force, where the mean energy of agitation of the electrons E is the same at all points, the velocity W is of the order $U \times 10^{-2}$. In a field where the electric force Z acts on the electrons the motion due to the force is superimposed on the motion due to diffusion, and the equation of continuity for n becomes

$$\frac{dn}{dt} = K\left(\frac{d^2n}{dx^2} + \frac{d^2n}{dy^2} + \frac{d^2n}{dz^2}\right) - W\frac{dn}{dz}. \quad . \quad . \quad (5)$$

In the case of a steady current where dn/dt is zero the value of n at any point is given in terms of W/K by the integral of equation (5).

The theory has thus been tested experimentally, and the values of W/K have been found by comparing the values of n given by the solution of equation (5) with the results of experiments on the lateral diffusion of a stream of electrons *. Also the velocity W has been found from observations of the deflexion θ of a stream by a magnetic force H ($W = z \tan \theta/H$, approx.).

It will be observed that neither equation (5) nor the values of W/K as found experimentally involve the velocities u, v, and w.

5. The method of finding the mean velocity W and the deflexion θ, taking into consideration the distribution of the free paths about the mean free path l and the distribution of the energies of agitation about the mean energy $mU^2/2$, has already been explained †, so that it remains to show how the coefficient of diffusion is determined by a method which is easily applied to the motion in a magnetic field.

If $q\,dx$ be the number of electrons at any time t in the space between two parallel planes at distances x and $x+dx$ from the coordinate plane (yz), the sum of the squares of the distances of a large number N of electrons from the coordinate plane (yz) is $\int qx^2 dx$, and the rate of increase of the mean square $d(x^2)/dt$ is $(1/N)\int x^2(dn/dt)\,dx$. The function $x^2(dn/dt)\,dx$ is integrated by substituting for

* ' Motion of Electrons in Gases,' Clarendon Press, Oxford, 1925.
† Phil. Mag. xxii. p. 145 (July 1936); xxiii. p. 880 (May 1937).

(dq/dt) the expression given by the equation of continuity for q, which is

$$dq/dt = -\mathrm{K}d^2q/dx^2, \quad . \quad . \quad . \quad . \quad . \quad (6)$$

and the integral is thus found to be 2NK, which is $\mathrm{N}d\bar{x}^2/dt$.

When there is no magnetic force the rate of change of the mean square of the distance from any axis $d\bar{r}^2/dt$ is 4K, and the rate of change of the mean square of the distance from any point $d\bar{\mathrm{R}}^2/dt$ is 6K.

An expression for $d\bar{\mathrm{R}}^2dt$ may easily be found in terms of the mean free path l and the mean velocity of agitation by considering the positions of a large group of electrons at any time t after starting from a small space near a fixed point P with the same velocity of agitation U *.

6. The same principle may be used to determine the coefficients of diffusion in a magnetic field. In this case it is necessary to take into consideration the curvature of the free paths, since the electrons move with an angular velocity $\mathrm{H}e/m$ about the axes in the direction of the magnetic force H. If the force be in the direction of the axis of y, the projections of the free paths on the plane (xz) are circles of different radii depending on the velocity of the electrons V in directions perpendicular to the axis of y. The velocity V is the component of the velocity of agitation U, the mean value of V^2 being $2\mathrm{U}^2/3$.

The projections of the paths of electrons starting from a point P, with the same velocities V and U, are shown in the figure by the circles passing through the point P. If there were no magnetic force the electrons would be at the distance $l_1\mathrm{V}/\mathrm{U}$ from the axis of y at the ends of the free paths of length l_1, but in the magnetic field the lengths of the arcs of the circles through P are $l_1\mathrm{V}/\mathrm{U}$, and at the time l_1/U required to traverse the free path the electrons are at points on a circle of radius r_1 less than l_1. Thus the rate of diffusion in directions perpendicular to the axis of y is diminished by the action of the electric force.

The rate of diffusion in these directions and the distribution about the axis of y is obtained by calculating the rate of change of mean square $\bar{r}^2$ of the distances of the electrons from the axis of y, for the general case where

* ' Electricity in Gases,' p. 87.

all directions of motion from the point P are equally probable.

The motion of rotation about the axis of y through P, which does not disturb the distribution, may also be determined.

In order to obtain results in accordance with the actual motions it is necessary to take into consideration the inequalities in the free paths of the electrons. A method of calculating the coefficients of diffusion under these conditions has already been given, and the same method may be used to determine the rotation about the axis of y, which does not disturb the distribution. But the following adaptation of the method, which is of a less

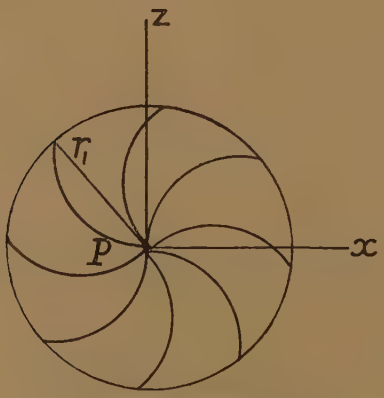

Free paths in magnetic field.

general character than the original *, is perhaps more easy to follow.

7. The free paths are widely distributed about the mean free path l, and if the electrons traverse a large number c of free paths, the number that exceed the length x is $c.\epsilon^{-x/l}$. The number of paths of lengths between x and $x+dx$ is $c\epsilon^{-x/l}\,dx/l$, and the sum of the squares of the free paths $c\int_0^\infty x^2\epsilon^{-x/l}\,dx/l$ is $2cl^2$. A similar calculation shows that the sum of the cubes of the free paths is $2.3.cl^3$ and the sum of the fourth powers $2.3.4.cl^4$, etc.

* Proc. Roy. Soc. A, lxxxvi. p. 576 (1912).

Thus if an electron traverses a large number of free paths of lengths ($l_1, l_2 \ldots l_c$) it is necessary to assume that the sum of the squares ($l_1^2+l_2^2+\ldots l_c^2$) is $2cl^2$, the sum of the cubes ($l_1^3+l_2^3+\ldots .l_c^3$) is $6cl^3$, etc.

In order to determine the changes in the positions of electrons moving with the same velocity V in directions perpendicular to the axis of y, the starting-point may be taken to be at P, as in the figure. The electrons may be supposed to traverse the free paths $l_1, l_2, \ldots l_c$ in the same order with the same velocity of agitation U, and all directions of motion perpendicular to the axis of y may be taken to be equally probable in moving from the point P and after the collisions which terminate the free paths.

If x and z be the distances of an electron from the coordinate planes through P, the velocities at any time t less than l_1/U are given by the equations

$$\left.\begin{aligned} dx/dt &= \mathrm{A}\cos\omega t + \mathrm{C}\sin\omega t, \\ \text{and} \qquad dz/dt &= \mathrm{C}\cos\omega t - \mathrm{A}\sin\omega t, \end{aligned}\right\} \quad \ldots \quad (7)$$

A being the velocity in the direction of the axis of x and C in the direction of z at the origin P, and $\omega = \mathrm{H}e/m$.

The distances x and z are given by the equations

$$\left.\begin{aligned} \omega x &= \mathrm{A}\sin\omega t - \mathrm{C}(\cos\omega t - 1), \\ \text{and} \qquad \omega z &= \mathrm{C}\sin\omega t + \mathrm{A}(\cos\omega t - 1). \end{aligned}\right\} \quad \ldots \quad (8)$$

At the time $t_1 = l_1/\mathrm{U}$, when the electrons arrive at the ends of the free paths of length l_1, the square of the distance from the axis of y, r_1^2 is

$$r_1^2 = 2(\mathrm{A}^2+\mathrm{C}^2)(1-\cos\omega t_1)/\omega^2. \quad \ldots \quad (9)$$

Since all directions of motion in the plane (xz) are equally probable when the electrons start from the point P, the centre of gravity of the group is at rest, and the increase in the mean square of the distances from any axis parallel to the axis of y is given by equation (9).

The motions represented by equations (7) and (8) are repeated about axes parallel to the axis of y when the electrons traverse the second set of free paths of length l_2, and at the time (t_1+t_2) when these free paths are terminated the mean square of the distance of the electrons from the axis through P is $2(\mathrm{A}^2+\mathrm{C}^2)(2-\cos\omega t_1-\cos\omega t_2)$. At the time lc/U when all the free paths have been traversed,

the mean square $\overline{r^2}$ of the distance of the electrons from the axis through P is given by the equation

$$\omega^2\overline{r^2}=2(A^2+C^2)(c-\cos\omega t_1-\cos\omega t_2, \text{ etc.}). \quad . \quad (10)$$

In order to evaluate this expression the cosines may be expanded in ascending powers of ωt_1, ωt_2, etc., and on substituting l_1/U, l_2/U, etc., for t_1, t_2, etc., the sum of the cosines becomes

$$c-\frac{\omega^2}{2U^2}(l_1^2+l_2^2\ldots l_c^2)+\frac{\omega^4}{2.3.4.U^4}.(l_1^4+l_2^4\ldots l_c^4), \text{ etc.},$$

and since the sum of the squares of the free paths is $2cl^2$ and the sum of the fourth powers $2.3.4.cl^4$, this expression reduces to

$$c(1-\omega^2T^2+\omega^4T^4, \text{ etc.}),$$

T being the mean interval between collisions l/U. This series is convergent and equal to $c/(1+\omega^2T^2)$ for small values of ωT, but by the more general method * of taking into account the distribution of the free paths the sum of the cosines in equation (10) was found to be $c/(1+\omega^2T^2)$ for all values of ωT. Equation (10) for $\overline{r^2}$ thus reduces to

$$\overline{r^2}=2c(A^2+C^2)T^2/(1+\omega^2T^2). \quad . \quad . \quad . \quad (11)$$

The mean value of (A^2+C^2) is $2U^2/3$, so that the mean square $\overline{r^2}$ of the distances of all the electrons from the axis of y, at the time lc/U is $4cU^2T^2/3(1+\omega^2T^2)$, and the rate of increase in the mean square of the distances $d\overline{r^2}/dt$ is $4lU/3(1+\omega^2T^2)$.

8. Thus the coefficient of diffusion K_h in the directions perpendicular to the axis of y is $K/(1+\omega^2T^2)$, K being the coefficient of diffusion $lU/3$ in the direction of the axis of y, and the actual changes in the distribution are the same as if the electrons had the velocities given by the equations

$$\left.\begin{aligned} &nu=-K_h\,dn/dx, \quad nv=-K\,dn/dy, \\ \text{and} \quad &nw=-K_h\,dn/dz. \end{aligned}\right\} \quad . \quad . \quad (12)$$

The electrons are distributed symmetrically about the axis of y, and if $2\pi\rho r\,dr$ be the number between two cylinders of radii r and $(r+dr)$, the equation of continuity for ρ is

$$K_h\frac{d}{dr}\left(r\frac{d\rho}{dr}\right)=r\frac{d\rho}{dt}, \quad . \quad . \quad . \quad . \quad . \quad (13)$$

* Proc. Roy. Soc. A, lxxxvi. p. 571 (1912).

and the solution satisfying the condition that all the electrons N should be very near the axis at the time $t=0$ is

$$\rho=N/4\pi K_h t\epsilon^{r^2/4K_h t}. \quad . \quad . \quad . \quad . \quad . \quad (14)$$

The distribution at any time t is given by this equation.

9. The motion of rotation may also be determined by considering the motion in a series of free paths of different lengths. Each electron moves with an angular velocity $He/2m$ about an axis through the free path, but in general the free paths do not intersect a given axis, and the most convenient method of investigating the angular motion about a fixed axis which does not disturb the distribution is to determine the mean moment of momentum of an electron about the axis. When a large number of electrons start from a point P (as in the figure), and all directions of motion are equally probable, the centre of gravity of all the electrons remains at rest, and the moment of momentum is the same about all axes parallel to the axis of y. This also applies to any large group of electrons after collisions with molecules. The moment of momentum M, $m(zdx/dt-x\,dz/dt)$, of an electron about the axis of y at any time t less than l_1/U, as given by equations (7) and (8), is $m(A^2+C^2)(1-\cos\omega t)/\omega$, and the mean moment of momentum M_1, during the time t_1, $(1/t_1\int_0^{t_1} M\,dt)$ is

$$M_1=m(A^2+C^2)(1-(\sin\omega t_1)/\omega t_1)/\omega. \quad . \quad . \quad (15)$$

The mean moment of momentum M_2 about the axis of y while the electrons are traversing the second free path in the time t_2 is $m(A^2+C^2)(1-(\sin\omega t_2)/\omega t_2)/\omega$, and while traversing a large number c of free paths in the time lc/U the mean moment of momentum

$$(M_1t_1+M_2t_2+\ldots M_ct_c)/cT$$

is

$$\bar{M}=2mU^2(cT\omega-\sin\omega t_1-\sin\omega t_2\ldots\sin\omega t_c)/3cT\omega^2. \quad (16)$$

Expanding the sines in ascending powers of ωt_1, ωt_2, etc., and substituting for the sums of the powers of the lengths l_1, l_2, etc., their values in terms of the powers of the mean free path l, as in the calculation of the mean square $\bar{r}^2$, the expression for $\bar{M}$ is reduced to

$$\bar{M}=2mU^2\omega T^2/3(1+\omega^2T^2), \quad . \quad . \quad . \quad . \quad (17)$$

which may be written in the form

$$\left.\begin{aligned} \bar{M} &= 2mlU\omega T/3(1+\omega^2T^2), \\ \text{or} \qquad \bar{M} &= 2m\omega TK_h. \end{aligned}\right\} \quad . \quad . \quad . \quad (18)$$

Thus there is a maximum value of $\bar{M}$ corresponding to the value U/l of the angular velocity ω.

10. Equations (18), together with the expression

$$4lU/3(1+\omega^2T^2)$$

for the rate of change of the mean square of the distance from an axis, completely represent the mean effects of the action of the magnetic force. There does not seem to be any reason for attempting to represent the motion given by equations (18) by additional terms of the form $d\phi/dz$ to the expression for nu and $-d\phi/dx$ to the expression for nw in equations (12). The angular velocities represented by these terms do not contribute to any change in the space distribution of the electrons, and disappear from the expression for dn/dt given by the equation of continuity.

Also from a practical point of view it is the motion represented by equations (12) that tends to bring the electrons from points in the gas towards electrodes or the boundaries of the gas, and can easily be tested by measurements of the lateral diffusion of a stream, but the motion represented by equations (18) is purely rotational, and cannot be deduced from measurements of the distribution n.

11. Equations of the form of equations (12) have been tested by Bailey * by experiments on the lateral diffusion of a stream of electrons moving under the action of a uniform electric force Z and a magnetic force H in the same direction. It was thus found experimentally that the lateral diffusion was reduced by the action of the force by an amount corresponding to a reduction of the coefficient of diffusion from K to $K/(1+\omega^2T^2)$, in good agreement with the theory. In these experiments the currents were very small photoelectric currents, so that there was no appreciable force due to space-charges.

* V. A. Bailey, Phil. Mag. (7) ix. pp. 560 & 625 (April 1930).

XL. *Some Aspects of Active Nitrogen.* *By* D. B. McNeill, *Ph.D., Queen's University, Belfast* *.

THE work of Lewis, Lord Rayleigh, Willey, Kaplan [1], and others has shown that active nitrogen and nitrogen afterglows present problems of great complexity. However, they certainly involve nitrogen atoms and the $A^3\Sigma$ metastable nitrogen molecule, and the discharge conditions required to produce them are fairly well known. In addition, impurities must be present if the Lewis-Rayleigh form of afterglow from a condensed discharge is to be produced with much intensity, and must be absent to obtain Kaplan's auroral afterglow from an uncondensed discharge. In the former case the impurities are supposed to act as negative wall catalysts which prevent the nitrogen atoms from recombining, a hypothesis made plausible by the recent discussion of atom recombination by Rabinowitch [2].

Some aspects of these problems are reported in this paper. In the experiments great care was taken in the preparation of the discharge-tubes. All were made entirely of soda or pyrex glass and metal, and were baked out under high vacuum, and the electrodes degassed by eddy currents. Liquid air-cooled traps protected the tubes from mercury vapour, and any condensible impurities arising from the action of stray discharges or active nitrogen on Apiezon grease, which was used for lubrication of traps and ground-joints. In spite of these precautions traces of impurity produced in the tubes were found to have a marked effect.

Special attention has been paid to (1) the consequences of the presence of traces of hydrogen, (2) the conditions favouring the excitation of the NH spectrum, and (3) Kaplan's auroral afterglow.

1. *Coloration of Halides in Nitrogen Discharge-tubes.*

Frerichs [3] found that the production of the spectrum of neutral oxygen was facilitated if an oxygen discharge was run in narrow capillary tubes with walls coated internally with alkali halide. It was thought that a discharge run under similar conditions in nitrogen might be

* Communicated by Professor K. G. Emeléus.

a strong source of the spectrum of neutral nitrogen atoms, which is difficult to produce by regular methods. Some π-shaped tubes were constructed with this aim. In the first set the inside of the horizontal arm (1 cm. diameter) was filled with quill-tubes coated with sodium chloride, deposited from solution before the tube was assembled and degassed. Nitrogen, prepared from Kahlbaum sodium azide, was admitted to a pressure of about 0·03 mm., and excited by a current of 50 milliamp. It was found that the nitrogen arc spectrum did not appear, but the sodium chloride became coloured, turning first blue and then almost black. The discharge did not go through all the quills at the same time, but flickered from one to another, avoiding some altogether. In the second set of tubes the horizontal arm was made of a single quill (0·3 cm. diameter) coated internally as before. The coloration was again observed. Where it was most pronounced the sodium arc spectrum was excited strongly. The chlorides of lithium and potassium were affected in the same way.

Microscopic examination of the coloured halides showed that the effect was almost completely confined to the surface. It disappeared if the tube was exhausted after passing the discharge and water vapour admitted. An aqueous solution of the salt had an alkaline reaction, which blank tests showed had been produced in the discharge. These observations indicate that the halides may have been reduced to metal. The colour was destroyed by heating *in vacuo*, although no deposit of metal could be detected on a nearby liquid air-cooled surface. If not treated in one of these ways the coloration in a sealed tube appeared permanent, showing no obvious change after six months.

Although it was found that similar coloration of sodium chloride took place in a hydrogen discharge-tube, particularly where the Balmer lines were strong, no trace of the Balmer lines was observed with the nitrogen tubes. Since these discharges were run with either alternating current or intermittent direct current, the supposed reduction was at first therefore attributed to active nitrogen. Careful examination of the spectrograms of the discharge showed, however, the presence of the 3360 A band of NH, so evidently hydrogen was present in some form in spite of the failure of its atomic spectrum

to appear. Since a likely source of hydrogen was water persistently occluded in the sodium chloride an attempt was made to eliminate it entirely by synthesising dry sodium chloride *in situ*. Metallic sodium, obtained by exploding sodium azide *in vacuo*, was distilled into the horizontal section of a clean degassed discharge-tube until an opaque mirror had been formed. Chlorine was prepared by heating gold chloride *in vacuo*, drying the gas evolved over phosphorus pentoxide, and storing it over freshly prepared sodium. The dry chlorine was passed into the evacuated discharge-tube, and made to react with the sodium there by warming the tube and touching the walls with a Tesla coil until the metallic mirror had disappeared. The residual chlorine was then pumped out and the tube again degassed and the electrodes glowed out. On passing a discharge through nitrogen in this tube the coloration of the halide was faint, and there was only a barely detectable trace of the NH band. This provides evidence that hydrogen, either free or combined, may be responsible for producing the coloration.

Since Gaviola and Wood [4] have found that water vapour is dissociated into H and OH by the action of active nitrogen, a mechanism for the reaction consistent with the observations is

$$N_2(A^3\Sigma)+H_2O=N_2(X'\Sigma)+OH+H$$

$$H+NaCl=HCl+Na.$$

If this occurs HCl and OH should be present. The 3064 A band of OH was identified on the spectrograms of the discharge, but no spectrum of HCl^+ was observed; no electronic spectra of HCl are known [5]. If the excitation is due to active nitrogen this is to be expected, since the maximum energy available from it is 10 volts [6], which is not sufficient to ionize and excite HCl or to excite the Balmer lines of hydrogen. Chlorine bands would be masked by the nitrogen bands. It is, however, not essential to invoke the action of active nitrogen at all, as direct dissociation of water vapour could take place in the discharge.

These experiments have been described in some detail, because they seem to raise the question of whether the impurities may not play a more active part than that mentioned in the introduction in the Lewis-Rayleigh

afterglow and in some of the chemical reactions of active nitrogen.

2. *The* 3360 A NH *Band.*

This band also appears with considerable intensity when a trace of nitrogen is admitted to a hydrogen discharge-tube. The delicacy of this test for hydrogen in nitrogen and nitrogen in hydrogen may be due to the fact that the NH molecule is capable of forming the negative ion [7] NH^-. Such ions will be repelled from the walls of the tube, which are negatively charged, and will tend to congregate in the centre. The molecule and its constituents will thus remain in the gas phase longer than if NH^- did not exist, since there will not be the same chance of the molecule being lost to the discharge by diffusion to the walls. The persistence of hydrogen in an iodine discharge-tube has been explained tentatively in a similar way [8].

3. *Kaplan's Auroral Afterglow.*

The spectrum of this afterglow, unlike that of the Lewis-Rayleigh form, includes the intercombination (Vegard-Kaplan) bands of the neutral molecule N_2 and the negative bands of the ion N_2^+. The range of excitation energies is thus wide, from 6–20 volts, and it is of interest to consider if the spectra could not arise in some way other than that suggested by Kaplan. The usual ways of obtaining the negative bands are from cathode ray excitation in a negative glow, and from a positive column in which the electron energy is large because there is a large ratio of electric field to gas pressure. The light from these sources includes bands of N_2, generally without the intercombination band.

It may be significant that the construction of Kaplan's tubes and the treatment to which they were subjected were such as might render them liable to exhibit the phenomenon of pseudo-high vacuum [9]. This consists essentially in a rise in the striking potential of gas-filled tubes, particularly those with shielded anodes, when a discharge has been passing for a long time. It is believed to be due to anomalous wall electrification, and does not occur in presence of at least some of the impurities which

inhibit the auroral afterglow. Kaplan's tubes were bulbs with the electrodes in side arms, and were conditioned by passing an intermittent current for some weeks. It seems possible that the negative bands may have been excited by the release of electric charges from the walls in the off phase which had accumulated there whilst the main discharge was passing or at the instant when it stopped. The intercombination bands may have been produced in true afterglows of the main discharge or of the feeble wall discharges, or in the wall discharges themselves. Déjardin [10] has described effects due to frictional electricity similar to those postulated here.

Summary.

Some experiments with nitrogen discharge-tubes are described which illustrate the large effect that can be produced by traces of impurity. The bearing of these observations on the problem of active nitrogen is mentioned. The persistence of the NH band spectrum is correlated tentatively with the existence of a stable ion NH^-. An electrical mechanism is suggested for the production of the negative nitrogen bands in the auroral nitrogen afterglow.

The writer wishes to thank Dr. R. W. Lunt and Dr. J. Kaplan for their criticisms of this work.

References.

(1) Kaplan, Phys. Rev. li. p. 143 (1937); Pub. Astron. Soc. Pacific, xlvii. p. 257 (1935).
(2) Rabinowitch, Trans. Faraday Soc. xxxiii. p. 283 (1937).
(3) Frerichs, Phys. Rev. xxxiv. p. 1239 (1929).
(4) Gaviola and Wood, Phil. Mag. vi. p. 1191 (1928).
(5) Sponer, *Molekülspektren*, vol. i. p. 27.
(6) Okubo and Hamada, Phil. Mag. v. p. 372 (1928).
(7) Bradbury, J. Chem. Phys. ii. p. 827 (1934).
(8) Emeléus, Cathcart, and Minnis, Proc. Roy. Irish Acad. lxiv. p. 11 (1937).
(9) Sir J. J. Thomson and G. P. Thomson, ' Conduction of Electricity through Gases,' vol. ii. p. 456.
(10) Déjardin, Rev. Mod. Physics, viii. p. 20 (1936).

XLI. *The Ultra-Violet Absorption Bands of Methyl Alcohol and Allyl Alcohol and their Relation to Magneto-Optical Dispersion.* *By* W. J. G. Beynon, *B.Sc.*, *and Professor* E. J. Evans, *D.Sc.*, *Physics Department, University College of Swansea* *.

DURING the last ten years an extensive systematic study has been made in these laboratories of the magneto-optical and natural dispersions of organic liquids. The results of these investigations have from time to time been published in this Journal[1], [2]. In the case of each liquid investigated, the magneto-optical dispersion has been measured on the average over the range of wave-lengths ·44 μ to ·30 μ. The results have been related to the usual theory of dispersion which, on the assumption of a formula of the Ketteler-Helmholtz type,

$$n^2-1=b_0+\sum_r \frac{b_r}{\lambda^2-\lambda_r^2}, \quad \ldots \quad (1)$$

for the natural dispersion, leads to the formula

$$\phi \equiv n\delta\lambda^2 = \sum_r \mathrm{K}_r\left[\frac{\lambda^2}{\lambda^2-\lambda_r^2}\right]^2. \quad \ldots \quad (2)$$

for the magneto-optical dispersion, In the above formulæ n is the refractive index for wave-length λ; δ is Verdet's Constant for wave-length λ; b_0, b_r, K_r are constants; and λ_r are the wave-lengths of the absorption bands of the substance.

If we assume that the dispersions are controlled by a single absorption band, then equation (2) reduces to

$$\phi \equiv n\delta\lambda^2 = \mathrm{K}_1\left[\frac{\lambda^2}{\lambda^2-\lambda_1^2}\right]^2. \quad \ldots \quad (3)$$

One feature of the researches referred to was the calculation of this wave-length λ_1. In all cases its existence was predicted to be in the Schumann-Lyman region of the spectrum.

It was not to be expected that there was in the case of any liquid just a single resonant frequency, but in the absence of more accurate and extensive data the

* Communicated by Prof. E. J. Evans, D.Sc.

use of formulæ involving two or more characteristic frequencies was not deemed to be justifiable. The predicted values of the absorption bands can thus only be regarded in the sense of " single equivalent absorption bands," *i. e.*, that the net effect on the natural and magneto optical dispersions of two or more absorption bands would be the same as that of a single band of the wave-length calculated.

In the present investigation an attempt has been made to photograph the absorption spectra of some of these organic liquids in the vapour state, and then to relate the results to previous magneto-optical work on them The liquids selected for this first investigation were methyl alcohol and allyl alcohol. The magneto-optical dispersions of these two liquids had been measured in these laboratories previously, the results being published in the ' Philosophical Magazine ' [2].

Experimental Procedure.

The vacuum spectrograph used in this work was of the normal incidence type. It contained a one-metre concave speculum metal grating having a ruled surface of 7 by 5 cm. with approximately 600 ruled lines per millimetre, the dispersion in the first order being about 17·5 Å.U. per millimetre. The slit, the film-holder, and the grating were fixed on the circumference of the usual circle of diameter equal to the radius of curvature of the grating. The path-length in which absorption occurred was about 2 metres.

The spectrograph was evacuated by means of a large-capacity Pfeiffer mercury vapour pump backed by a two-stage Pfeiffer oil pump, there being the usual liquid air traps in the system. The vapour of the liquid under investigation was allowed into the main body of the spectrograph and pumped out by means of the main pumps. The liquid itself was contained in a glass bulb attached to the centre portion of the spectrograph, and connexion with the evacuated apparatus was effected through a small bore glass tap. Different vapour pressures were obtained by varying the temperature of the small store of liquid contained in the glass bulb. Very slight vapour pressures were sufficient to produce the necessary absorption—the low temperatures of the supply bulb (down to $-70°$ C.) being obtained by surrounding it

with solid carbon dioxide or mixtures of solid carbon dioxide and methylated spirits. The pressure of the vapour in the spectrograph was indicated on a McLeod mercury gauge.

The source of the continuum against which absorption was observed was a condensed discharge in hydrogen. The arrangement of the discharge-tube itself is shown in the figure.

The tube, which was made throughout of pyrex glass, consisted of two parts, and each part carried a hollow aluminium electrode E. The outer tube A fitted on to the main body of the spectrograph, the joint being made vacuum tight by means of picein wax. The inner tube B

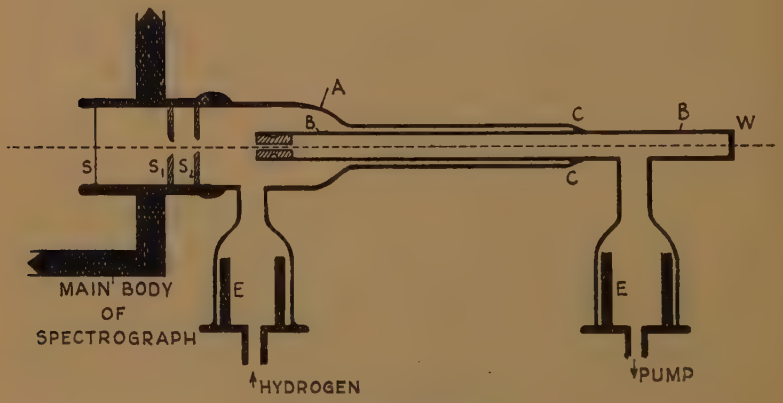

The discharge-tube.

fitted closely into A. Slipped into one end of B was a short length of pyrex capillary (about 1·5 cm. long and 1 mm. bore), and this was tightly packed with glass wool to prevent the discharge passing between it and the surrounding tube. Sealed to the other end of B was a glass window W. The electrodes EE (which also served as inlet and outlet tubes for hydrogen) were waxed with picein to the rest of the tube. The overall length of the tube was about 15 cm. and the distance from capillary to slit about 4·5 cm.

The hydrogen was generated electrolytically and dried by passing over calcium chloride and phosphorus pentoxide. After passing through a fine capillary it was allowed in at the electrode nearer the slit and pumped out at the

other electrode. The alignment of the capillary and the slit was effected by placing a small source of light in the position of the central image produced by the grating and adjusting the discharge-tube until the image of this source could clearly be seen when viewed through the capillary and the window W. The flow of hydrogen was adjusted so as to give an average pressure of about ·1 mm. of mercury in the discharge-tube. The pressure on the other side of the narrow slit was always much lower than this.

Two metal shields, S_1 and S_2, were found sufficient to prevent clogging of the slit by particles of glass torn from the inside of the capillary by the heavy discharges. After 15 to 20 photographs (involving a couple of thousand discharges) the bore of the capillary had increased to an extent that rendered it of no further use. The wax at C was then softened, the inner tube B removed, and a new capillary inserted.

During the discharges a considerable amount of heat was generated in and around the capillary and, to a lesser extent, in the neighbourhood of the electrodes. Although there was a space of a centimetre or so around the capillary end of the tube B, the generation of heat was sometimes great enough to cause slight softening of the wax, with a consequent danger of sagging of the tube. It was found that a small jet of cold water poured continuously over the waxed joints was sufficient to guard against this trouble.

The discharge was obtained from two ·5 m.f.d. T.C.C. condensers arranged in parallel. These could be charged to a maximum of 30,000 volts using a transformer and Philips' "Metalix" rectifying valve. By means of a metal slug attached to a rotating wooden wheel the condensers could be discharged through the tube at a rate which could be varied from 50 to 90 discharges per minute. The quality of the continuum depended upon the potential applied to the condensers and upon the diameter of the capillary, but with a new capillary a potential of less than 10,000 volts was found adequate to produce a satisfactory continuum. This problem has been considered by Anderson [3].

The photographs were made on Eastman Kodak X-ray films coated with a thin layer of fluorescent oil. Six photographs were taken on each film, a normal

exposure being about two minutes. No difficulty was experienced in obtaining a good continuum from 1900 Å.U. to about 750 Å.U. Below this wave-length the continuum was, however, rather weak, due to the small reflecting power of the grating for very short wave-lengths incident normally on it, and also due to the considerable absorption of hydrogen gas for wave-lengths in the neighbourhood of 800 Å.U. Consequently absorption photographs below this wave-length could only be obtained by delicate control of the hydrogen stream through the discharge-tube and of the vapour-pressure in the main body of the spectrograph. The bands of wave-length less than 750 Å.U. were not shown very clearly on the films.

In the preliminary evacuation of the apparatus the last traces of water-vapour were removed by connecting the spectrograph through large glass stop-cocks to three separate glass bulbs each containing phosphorus pentoxide.

Experimental Results.

In this attempt to relate the absorption bands to the magneto-optical dispersion, it must be pointed out that the absorption photographs have been obtained for the alcohols in the vapour state, whereas the experiments on magnetic rotation were made with the substances in the liquid state. The possibility of a shift occurring in the absorption bands in passing from one state to the other has therefore to be recognized. Seshan [4] compared the absorption spectra of certain organic substances when in different physical states. The substances examined had strong absorption bands in the region $\cdot 36\,\mu$ to $\cdot 30\,\mu$. The absorption spectrum of one of these substances, viz., fluorene, was examined in the vapour state, the molten liquid state and in the solid state. It was observed that in passing from the vapour to the liquid and thence to the solid state the absorption bands were shifted by about 100 Å.U. towards the red end of the spectrum. Measurements of infra-red absorption spectra of organic substances in the liquid and vapour states have been made by Purvis [5] and by Dreisch [6]. Purvis could not detect any shift in the bands of benzene situated around $3 \cdot 5\,\mu$. Dreisch, working with water, benzene and chloroform, detected a very slight shift of the absorption bands in passing from the liquid to the vapour state—the liquid band appearing at the higher wave-length.

It is probable that the wave-lengths of the far ultra-violet bands of the two alcohols here investigated change in passing from the vapour to the more dense state, but in the absence of any indication of its magnitude we have not taken this factor into account in our examination of magneto-optical dispersion formulæ for the liquids.

Methyl Alcohol.

The spectrograms of methyl alcohol exhibit two distinct band systems situated in the regions 1590 Å.U. and 1470 Å.U. In addition, certain of the photographs give some evidence of a region of absorption below 700 Å.U. The bands at the two higher wave-lengths show a fine structure. Thus around 1590 Å.U. we have three bands centred at 1607 Å.U., 1588 Å.U., and 1565 Å.U., and around 1470 Å.U. three bands centred at 1492 Å.U., 1470 Å.U., and 1445 Å.U. Each of the six bands has a width of some 10 to 12 Å.U. Owing to the difficulty, already stated, of obtaining good absorption photographs at short wave-lengths, the absorption below 700 Å.U. could not be fixed with great precision, but a certain amount of help in doing so can be obtained from the magneto-optical results for the liquid. In evolving a dispersion formula the two groups of three bands have each been replaced by a single band of wave-lengths 1588 Å.U. and 1470 Å.U. respectively (these are the central bands of the systems). This approximation results in a formula quite as efficient, yet far less unwieldy than a more complete formula involving a characteristic frequency for each of the six bands. It was then found that the existence of bands at 1588 Å.U. and at 1470 Å.U., together with one at about 650 Å.U., will satisfactorily explain the magneto-optical dispersion of methyl alcohol over the range of wave-lengths $\cdot 67\,\mu$ to $\cdot 26\,\mu$.

The measurements by Jones and Evans [2] on the magneto-optical dispersion of methyl alcohol in the ultra-violet were amongst the earliest made in these laboratories. These experiments have been carefully repeated by the present authors over the range $\cdot 44\,\mu$ to $\cdot 26\,\mu$, and the values given in this paper are those actually determined by us for a very pure sample of the liquid. By combining these results with those published by Lowry [8] for the visible spectrum, and also by Perkin [7]

for sodium light, a complete curve for the magnetic rotation from ·67 μ to ·26 μ can thus be obtained.

Jones and Evans were concerned with the evaluation of the "single equivalent absorption band," and consequently only needed ratios of the refractive index at different wave-lengths for their calculation of λ_1. In their calculations the values of the refractive indices determined by Victor Henri [9] in the neighbourhood of 20° C. were used, although the magneto-optical measurements were carried out at about 9° C. We have now determined the values of the refractive index in the visible and ultra-violet for the sample of methyl alcohol used in our magnetic rotation experiments. The values obtained for a few lines in the visible spectrum are given

Table I.

Refractive Indices of Methyl Alcohol.

Wave-length in microns.	$n_{20\cdot7°\text{ C.}}$	$*n_{16\cdot4°\text{ C.}}$
·6678	1·3274	1·3289
·5875	1·3293	1·3308
.5015	1·3323	1·3338
·4713	1·3337	1·3352
·4472	1·3348	1·3363

in Table I., and those for the ultra-violet spectrum are included in Table II.

The formula given by Jones and Evans [2] for the magneto-optical dispersion on the assumption of one absorption band was

$$\phi \equiv n\delta\lambda^2 = 1\cdot190\left[\frac{\lambda^2}{\lambda^2-(\cdot1100)^2}\right]^2. \quad . \quad . \quad . \quad (4)$$

The formula derived from the present investigations is

$$\phi \equiv n\delta\lambda^2 = \cdot92_2\left[\frac{\lambda^2}{\lambda^2-(\cdot065)^2}\right]^2 + \cdot266\left[\frac{\lambda^2}{\lambda^2-(\cdot1470)^2}\right]^2 + \cdot030_1\left[\frac{\lambda^2}{\lambda^2-(\cdot1588)^2}\right]^2. \quad (5)$$

* Corrected to the temperature of the magneto-optical experiments on the assumption that $\frac{dn}{dt} = -\cdot00036$.

The satisfactory agreement between the observed values of Verdet's Constant and those calculated from this formula is seen from Table II. Formulæ (4) and (5) give values of δ in circular measure. Values of δ in minutes per cm. gauss are given by the formula

$$\phi \equiv n\delta\lambda^2 = \cdot 00317_1\left[\frac{\lambda^2}{\lambda^2-(\cdot 065)^2}\right]^2 + \cdot 000913_2\left[\frac{\lambda^2}{\lambda^2-(\cdot 1470)^2}\right]^2 + \cdot 000103_4\left[\frac{\lambda^2}{\lambda^2-(\cdot 1588)^2}\right]^2 . \quad . \quad . \quad (6)$$

TABLE II.

Wave-length in microns.	$n_{16\cdot4^\circ\,C.}$	Verdet's Constant δ in min. per cm. gauss (observed at 16·4° C.)	δ calculated.
·5893	1·3306	$\cdot 00958_7$*	$\cdot 00954_1$
·4407	1·3365	$\cdot 0177_2$	$\cdot 0177_5$
·4184	1·3380	$\cdot 0199_4$	$\cdot 0198_9$
·3985	1·3397	$\cdot 0221_6$	$\cdot 0221_8$
·3825	1·3413	$\cdot 0243_7$	$\cdot 0243_1$
·3677	1·3432	$\cdot 0265_9$	$\cdot 0265_9$
·3555	1·3447	$\cdot 0288_0$	$\cdot 0287_4$
·3441	1·3464	$\cdot 0310_1$	$\cdot 0310_3$
·3342	1·3482	$\cdot 0332_3$	$\cdot 0332_1$
·3174	1·3514	$\cdot 0376_7$	$\cdot 0377_1$
·3100	1·3531	$\cdot 0398_9$	$\cdot 0398_3$
·3031	1·3548	$\cdot 0421_0$	$\cdot 0421_1$
·2972	1·3561	$\cdot 0443_3$	$\cdot 0442_6$
·2916	1·3578	$\cdot 0465_4$	$\cdot 0464_2$
·2815	1·3604	$\cdot 0509_8$	$\cdot 0510_0$
·2770	1·3616	$\cdot 0532_2$	$\cdot 0531_5$
·2687	1·3643	$\cdot 0576_7$	$\cdot 0576_8$

We estimate that our absolute values of Verdet's Constant are accurate to within 1/2 per cent. on the average. Hence the values calculated above differ from the observed values by an amount which is certainly less than the experimental error of the observations.

Lowry and Dickson [8] experimentally determined the ratio $\delta/\delta_{\cdot 5461\,\mu}$ for seven wave-lengths in the visible region of the spectrum. Table III. gives a comparison

* Value at 18·7° C. calculated from Perkin's results [7].

between the values of these ratios as observed by Lowry and Dickson, and values calculated from formula (6).

Lowry obtained the value ·714 for the " water ratio " of methyl alcohol at 20° C. Assuming $\delta_{\cdot 5893\,\mu}$ for water to be ·01309, Lowry's value for methyl alcohol at this wave-length and temperature is $\cdot 00934_6$. The value of $\delta_{\cdot 5893\,\mu}$ calculated from our formula is thus intermediate between the observed values of Perkin and Lowry, but nearer to Perkin's value.

TABLE III.

Wave-length in microns.	$\delta/\delta_{\cdot 5461\,\mu}$ observed by Lowry and Dickson.	$\delta/\delta_{\cdot 5461\,\mu}$ calculated from formula (6).
·6708	·645	·651
·6438	·707	·709
·5893	·851	·852
·5086	1·164	1·162
·4800	1·315	1·316
·4678	1·386	1·392
·4359	1·624	1·624

Allyl Alcohol.

The absorption photographs of allyl alcohol vapour exhibit two very broad diffuse bands centred at about 1650 Å.U. and 750 Å.U. respectively. Owing to the diffuse nature of the bands, and owing also to their width, the centres could not be fixed with the precision possible in the case of methyl alcohol. Nevertheless, it is readily seen from Table V. that a satisfactory magneto-optical dispersion formula can be obtained on the assumption that the liquid has these two absorption bands.

Measurements of both the natural and magneto-optical dispersion have again been made by the present authors, and the values given in the following tables are those actually determined by us.

Evans and Evans [2] obtained the formula

$$\phi \equiv n\delta\lambda^2 = \cdot 00724 \left[\frac{\lambda^2}{\lambda^2 - (\cdot 1372)^2}\right]^2 \quad . \quad . \quad . \quad (7)$$

for this liquid. The formula resulting from the present investigations is

$$\phi \equiv n\delta\lambda^2 = \cdot 00375_5 \left[\frac{\lambda^2}{\lambda^2-(\cdot 075)^2}\right]^2 + \cdot 00350 \left[\frac{\lambda^2}{\lambda^2-(\cdot 1650)^2}\right]^2. \quad (8)$$

TABLE IV.

Refractive Indices of Allyl Alcohol.

Wave-length in microns.	Refractive index $n_{17\cdot 8^\circ\,C.}$
·6678	1·4111
·5875	1·4144
·5015	1·4196
·4922	1·4203
·4713	1·4223
·4472	1·4249

TABLE V.

Wave-length in microns.	$n_{17.8^\circ\,C.}$	Verdet's Constant observed at 17·8° C.	Verdet's Constant calculated from formula (8).
·5893	1·4143	$\cdot 0163_0$*	$\cdot 0162_9$
·4400	1·4257	$\cdot 0317_3$	$\cdot 0316_2$
·4200	1·4284	$\cdot 0354_0$	$\cdot 0353_2$
·4000	1·4316	$\cdot 0398_4$	$\cdot 0398_6$
·3900	1·4334	$\cdot 0424_5$	$\cdot 0424_4$
·3800	1·4354	$\cdot 0453_2$	$\cdot 0452_7$
·3700	1·4376	$\cdot 0484_9$	$\cdot 0484_8$
·3600	1·4400	$\cdot 0521_2$	$\cdot 0520_3$
·3500	1·4427	$\cdot 0561_4$	$\cdot 0560_8$
·3400	1·4457	$\cdot 0606_5$	$\cdot 0606_7$
·3300	1·4489	$\cdot 0658_5$	$\cdot 0659_1$
·3200	1·4525	$\cdot 0718_8$	$\cdot 0719_4$
·3100	1·4567	$\cdot 0788_3$	$\cdot 0789_2$
·3000	1·4614	$\cdot 0871_0$	$\cdot 0872_4$
·2900	1·4666	$\cdot 0969_7$	$\cdot 0970_7$

* Value at 17·8° C. calculated from Perkin's results[7].

The calculated and observed values again agree to within the experimental error.

Lowry and Dickson [8] determined the magnetic rotation of allyl alcohol at six wave-lengths in the visible spectrum and, expressing their results in the form $\alpha = \frac{k}{\lambda^2 - \lambda_0^2}$, found λ_0^2 to have the value ·0293, giving the absorption band λ_0 a wave-length of 1710 Å.U. Comparison of Lowry and Dickson's values for the ratios $\frac{\delta}{\delta_{\cdot 5461\,\mu}}$ with the values calculated from formula (8) is given in Table VI.

TABLE VI.

Wave-length in microns.	$\delta/\delta_{\cdot 5461\,\mu}$ observed by Lowry and Dickson.	$\delta/\delta_{\cdot 5461\,\mu}$ calculated from formula (8).
·6708	·641	·639
·6438	·700	·699
·5893	·847	·846
·5086	1·177	1·173
·4800	1·332	1·339
·4359	1·672	1·677

Lowry's value for $\delta_{\cdot 5893\,\mu}$ at 20° C. comes out to be $\cdot 0162_2$ (taking the "water ratio" to be 1·239 and $\delta_{\cdot 5893\,\mu}$ (water) = ·01309).

Evans and Evans [2] found that their results could be represented within experimental error by a formula involving only one absorption band. Allyl alcohol produces a large magnetic rotation (*e. g.*, on the average it is double that of methyl alcohol), and it was thought that this liquid would be a very suitable one on which to conduct accurate magneto-optical observations, with a view to determining whether the results could really be represented by a simple formula involving just one absorption band. The magnetic rotation of allyl alcohol was therefore very carefully redetermined. The results of the investigation definitely showed that the magnetic rotation could not be represented by such a simple

formula. Attempts were then made to represent the results by a formula of the type

$$\phi \equiv n\delta\lambda^2 = K_0 + K_1\left[\frac{\lambda^2}{\lambda^2 - \lambda_1^2}\right]^2,$$

involving two absorption bands, one of very short wave-length and the other of wave-length λ_1. The best formula of this type was

$$\phi \equiv n\delta\lambda^2 = \cdot00312 + \cdot00427\left[\frac{\lambda^2}{\lambda^2 - (\cdot1591)^2}\right]^2.$$

This formula was found to fit the observations to a much closer degree than the simpler formula involving λ_1 only, but was not as accurate as formula (8).

It is of interest to note that Victor Henri[9] from his measurements of natural dispersion predicted an absorbtion band of wave-length 1588 Å.U. for allyl alcohol. This value is remarkably near that given by the formula above.

Summary of Results.

(*a*) The absorption spectra of methyl alcohol and allyl alcohol in the vapour state have been photographed over the region of spectrum 1850 Å.U. to about 600 Å.U.

(*b*) Methyl alcohol exhibits absorption bands centred at 1588 Å.U. and 1470 Å.U., with a further region of absorption low down in the spectrum around 650 Å.U.

Allyl alcohol exhibits two broad absorption bands centred approximately at 1650 Å.U. and 750 Å.U.

(*c*) The magneto-optical dispersion of methyl alcohol and allyl alcohol can be represented by the following formulæ, involving the absorption bands given above.

Methyl alcohol:

$$\phi \equiv n\delta\lambda^2 = \cdot00317_1\left[\frac{\lambda^2}{\lambda^2 - (\cdot065)^2}\right]^2 + \cdot000913_2\left[\frac{\lambda^2}{\lambda^2 - (\cdot1470)^2}\right]^2 + \cdot000103_4\left[\frac{\lambda^2}{\lambda^2 - (\cdot1588)^2}\right]^2.$$

Allyl alcohol:

$$\phi \equiv n\delta\lambda^2 = \cdot00375_5\left[\frac{\lambda^2}{\lambda^2 - (\cdot075)^2}\right]^2 + \cdot00350\left[\frac{\lambda^2}{\lambda^2 - (\cdot1650)^2}\right]^2.$$

The authors accord their thanks to Dr. W. M. Evans, who was responsible for the absorption photographs of allyl alcohol, and to Dr. W. C. Price and Mr. Eric Homeyard for considerable help in the design and construction of the apparatus.

References.

(1) D. J. Stephens and E. J. Evans, Phil. Mag. iii. p. 546 (March 1927), *et seq.*
(2) D. O Jones and E. J. Evans, Phil. Mag. v. p. 593 (March 1928); C. C. Evans and E. J. Evans, Phil. Mag. viii. p. 137 (August 1929).
(3) J. A. Anderson, Astrophys. Journ. lxxv. p. 394 (1932).
(4) P. K. Seshan, Trans. Faraday Soc. p. 689 (April 1936).
(5) Purvis, Proc. Camb. Phil. Soc. xxi. p. 556 (1923).
(6) Dreisch, *Zeits. f. Phys.* xxx. p. 200 (1924).
(7) Perkin, Journ. Chem. Soc. xlv. p. 466 (1884).
(8) Lowry and Dickson, Journ. Chem. Soc. i. p. 1072 (1913); Lowry, Journ. Chem. Soc. i. p. 91 (1914).
(9) Victor Henri, 'Études de Photochemie,' pp. 41–64.

Physics Department,
University College, Swansea.

XLII. *Wave Functions and Permeabilities for a new type of Potential Barrier.* *By* R. P. Bell *.

AMONG the various one-dimensional curves used in quantum mechanical problems to represent potential barriers only one has so far been treated which is without discontinuities in slope and at the same time admits of an exact solution of the wave equation. This is the so-called " Eckart barrier," † defined by the equation

$$V=\frac{4Ee^{2\pi x/a}}{(1+e^{2\pi x/a})^2}, \quad \ldots\ldots (1)$$

where E is the maximum value of the potential energy and $2a$ the width of the barrier. It is therefore of interest to point out that an exact solution can also be obtained for the continuous curve defined by

$$V=E\cos^2\frac{\pi x}{2a} \quad (|x|<a), \quad V=0 \quad (|x|>a). \quad \ldots (2)$$

Moreover, the barrier represented by equation (2) is considerably flatter at the top than the Eckart barrier,

* Communicated by the Author.

† Phys. Rev. xxxv. p. 1303 (1930); *cf.* Bell, Proc. Roy. Soc. A, cxxxix. p. 466 (1933).

and thus resembles more closely the potential energy curves met with in chemical problems. The exact expressions for the permeability of such barriers to light particles might therefore be of some interest.

The wave equation for the region $|x|<a$ is

$$\frac{d^2\psi_{II}}{dx^2}+\frac{8\pi^2 m}{h^2}\left\{W-E\cos^2\frac{\pi x}{2a}\right\}\psi_{II}=0, \quad . \quad . \quad (3)$$

or, introducing the abbreviations

$$z=\frac{\pi x}{2a}, \quad \lambda=\frac{32ma^2W}{h^2}, \quad \beta=\frac{32ma^2E}{h^2}, \quad . \quad . \quad (4)$$

$$\frac{d^2\psi_{II}}{dz^2}+(\lambda-\beta\cos^2 z)\psi_{II}=0, \quad . \quad . \quad . \quad . \quad (5)$$

which is the standard form of Mathieu's differential equation. The Mathieu functions, as usually defined, are completely periodic functions corresponding to particular values of the parameters λ and β; however, the more general solution applicable to the present problem has been given by Lindemann * and by Stieltjes †. Their solution may be written

$$\psi_{II}=\{F(\cos^2 z)\}^{\frac{1}{2}}\left[A\exp.\left\{i\alpha\int_0^z\frac{dz}{F(\cos^2 z)}\right\}\right.$$
$$\left.+B\exp.\left\{-i\alpha\int_0^z\frac{dz}{F(\cos^2 z)}\right\}\right], \quad . \quad (6)$$

where A and B are constants and $F(\cos^2 z)$ and α are defined by the following equations :—

$$F(\cos^2 z)=\sum_{n=0}^{\infty}c_n\cos^{2n}z, \quad \alpha^2=\lambda+c_1. \quad . \quad . \quad (7)$$

$$\left.\begin{aligned} &c_0=1,\\ &\frac{1}{c_1}=\lim_{m\to\infty}\left(u_0+\frac{v_1}{u_1}+\frac{v_2}{u_2}+\cdots\frac{v_m}{u_m}\right),\\ &c_{n+2}=\frac{u_n c_{n+1}+c}{v_{n+1}}. \end{aligned}\right\} \quad . \quad . \quad . \quad (8)$$

$$u_n=\frac{2(n+1)\{(n+1)^2-\lambda\}}{\beta(2n+1)}, \quad v_n=\frac{n(n+1)(2n+1)}{\beta(2n-1)}. \quad (9)$$

If we are considering a stream of particles approaching from the negative direction, then the wave functions in

* *Math. Ann.* xxii. p. 117 (1883).
† *Astr. Nach.* cix. pp. 145, 261 (1884).

the regions $-\infty < x < -a$ and $+a < x < +\infty$ are respectively

$$\left.\begin{aligned}\psi_{\mathrm{I}} &= \exp.\left\{\frac{2\pi i}{n}\sqrt{2m\mathrm{W}}x\right\} + \mathrm{C}\exp.\left\{-\frac{2\pi i}{n}\sqrt{2m\mathrm{W}}x\right\} \\ &= e^{i\sqrt{\lambda}z} + \mathrm{C}e^{-i\sqrt{\lambda}z}, \\ \psi_{\mathrm{III}} &= \mathrm{D}e^{i\sqrt{\lambda}z},\end{aligned}\right\} \quad . \quad . \quad . \quad (10)$$

where C and D are constants. The conditions of continuity of ψ and $d\psi/dz$ at $z = \pm\pi/2$ (*i. e.*, $x = \pm a$) are now sufficient to determine the constants in equations (6) and (10).

Introducing the abbreviations

$$w = \int_0^{\frac{\pi}{2}} \frac{dz}{\mathrm{F}(\cos^2 z)}, \quad \Phi = \mathrm{F}(1) = \sum_{n=0}^{\infty} c_n, \quad . \quad . \quad (11)$$

the equations of continuity are

$$\left.\begin{aligned} e^{-\frac{1}{2}\pi i\sqrt{\lambda}} + \mathrm{C}e^{\frac{1}{2}\pi i\sqrt{\lambda}} &= \Phi^{\frac{1}{2}}(\mathrm{A}e^{-i\alpha w} + \mathrm{B}e^{i\alpha w}), \\ i\sqrt{\lambda}e^{-\frac{1}{2}\pi i\sqrt{\lambda}} - \mathrm{C}i\sqrt{\lambda}e^{\frac{1}{2}\pi i\sqrt{\lambda}} &= i\alpha\Phi^{-\frac{1}{2}}(\mathrm{A}e^{-i\alpha w} - \mathrm{B}e^{i\alpha w}), \\ \mathrm{D}e^{\frac{1}{2}\pi i\sqrt{\lambda}} &= \Phi^{\frac{1}{2}}(\mathrm{A}e^{i\alpha w} + \mathrm{B}e^{-1i\alpha w}), \\ \mathrm{D}i\sqrt{\lambda}e^{\frac{1}{2}\pi i\sqrt{\lambda}} &= i\alpha\Phi^{-\frac{1}{2}}(\mathrm{A}e^{i\alpha w} - \mathrm{B}e^{-i\alpha w}).\end{aligned}\right\} \quad . \quad (12)$$

By eliminating A, B, and C we obtain

$$\mathrm{D} = \frac{-2i\alpha\sqrt{\lambda}\Phi e^{-\pi i\lambda}}{(\alpha^2 + \lambda\Phi^2)\cos 2\alpha w + 2i\alpha\sqrt{\lambda}\Phi \sin 2\alpha w}. \quad (13)$$

The permeability (*i. e.*, the ratio of the forward amplitudes in regions III and I) is then given by the value of $|\mathrm{D}|^2$. Provided that α is real (which will nearly always be the case in physical applications), this gives

$$\mathrm{G} = |\mathrm{D}|^2 = \frac{4\alpha^2\lambda\Phi^2}{(\alpha^2 + \lambda\Phi^2)^2\cos^2 2\alpha w + 4\alpha^2\lambda\Phi^2 \sin^2 2\alpha w}. \quad (14)$$

Equation (14) gives an exact expression for the permeability of the barrier defined by equation (2). However, when applied to chemical problems it is ill-suited to numerical computation, since for relevant values of λ and β the series $\mathrm{F}(\cos^2 z)$ consists of very large terms alternately positive and negative. Any extensive calculations would be prohibitively laborious, though the ex-

pression might be used in cases where it was particularly important to have an exact solution, *e. g.*, when $W \sim E$ *. It has not so far proved possible to find a more convenient summation for $F(\cos^2 z)$ or Φ.

Balliol College,
Oxford.

XLIII. *On Whittaker's Confluent Hypergeometric Function.*

By J. L. Sharma †.

1. *Introduction.*

VARIOUS properties of Whittaker's confluent hypergeometric function are given in 'Modern Analysis' ‡, and a number of new ones have been discovered by Goldstein § and a few other researchers on the subject. The object of the present paper is to investigate several new properties of Whittaker's function.

2. *Integrals Involving Confluent Hypergeometric Functions.*

2.1. Let us consider

$$I_1 = \int_0 W_{k,m}(z) W_{k+2,m'}(z)\, dz.$$

Since §

$$W_{k,m}(z) = e^{-\frac{1}{2}z} \cdot \frac{1}{2\pi i} \int_{-\infty i}^{\infty i} \frac{\Gamma(s-k)\Gamma(-s-m+\frac{1}{2})\Gamma(-s+m+\frac{1}{2})}{\Gamma(-k+m+\frac{1}{2})\Gamma(-k-m+\frac{1}{2})} z^s\, ds,$$

we get

$$I_1 = \int_0^\infty \left\{ e^{-z} \cdot \frac{1}{2\pi i} \int_{-\infty i}^{\infty i} \frac{\Gamma(s-k)\Gamma(-s-m+\frac{1}{2})\Gamma(-s+m+\frac{1}{2})}{\Gamma(-k-m+\frac{1}{2})\Gamma(-k+m+\frac{1}{2})} z^s\, ds, \right.$$
$$\left. \times \frac{1}{2\pi i} \int_{-\infty i}^{\infty i} \frac{\Gamma(t-k-2)\Gamma(-t-m'+\frac{1}{2})\Gamma(-t+m'+\frac{1}{2})}{\Gamma(-k-m'-\frac{3}{2})\Gamma(-k+m'-\frac{3}{2})} z^t\, dt \right\} dz$$

* *Cf.* Bell, Proc. Roy. Soc. A, clviii. p. 128 (1936).

† Communicated by the Author.

‡ Whittaker and Watson, 'Modern Analysis,' ch. xvi. This work will be referred to as M.A.

§ S. Goldstein, "Operational Representations, of Whittaker's Confluent Hypergeometric Function and Weber's Parabolic Cylinder Function." Proc. Lond. Math. Soc. (2) xxxiv. pp. 103–125 (1932).

‖ See M.A. p. 345.

$$=-\frac{1}{4\pi^2}\int_{-\infty i}^{\infty i}\frac{\Gamma(s-k)\Gamma(-s-m+\frac{1}{2})\Gamma(-s+m+\frac{1}{2})}{\Gamma(-k-m+\frac{1}{2})\Gamma(-k+m+\frac{1}{2})}\,ds$$

$$\times\int_{-\infty i}^{\infty i}\frac{\Gamma(t-k-2)\Gamma(-t-m'+\frac{1}{2})\Gamma(-t+m'+\frac{1}{2})}{\Gamma(-k-m'-\frac{3}{2})\Gamma(-k+m'-\frac{3}{2})}\,dt\int_0^\infty z^{s+t}e^{-z}\,dz, \quad \ldots \quad (1)$$

assuming the change in the order of integration which is justified, if $R(2\mp m\mp m')>0$, as proved below.

Hence

$$I_1=-\frac{1}{4\pi^2}\int_{-\infty i}^{\infty i}\frac{\Gamma(s-k)\Gamma(-s-m+\frac{1}{2})\Gamma(-s+m+\frac{1}{2})}{\Gamma(-k-m+\frac{1}{2})\Gamma(-k+m+\frac{1}{2})}\,ds$$

$$\times\int_{-\infty i}^{\infty i}\frac{\Gamma(t-k-2)\,\Gamma(-t-m'+\frac{1}{2})\Gamma(-t+m'+\frac{1}{2})\Gamma(s+t+1)}{\Gamma(-k-m'-\frac{3}{2})\Gamma(-k+m'-\frac{3}{2})}\,dt$$

$$=\frac{1}{2\pi i}\int_{-\infty i}^{\infty i}\frac{\Gamma(-s-m+\frac{1}{2})\Gamma(-s+m+\frac{1}{2})\Gamma(s+m'+\frac{3}{2})\Gamma(s-m'+\frac{3}{2})}{\Gamma(-k+m+\frac{1}{2})\Gamma(-k-m+\frac{1}{2})}\,ds$$

$$=\frac{\Gamma(2+m+m')\Gamma(2+m-m')\Gamma(2-m+m')\Gamma(2-m-m')}{6\Gamma(-k+m+\frac{1}{2})\Gamma(-k-m+\frac{1}{2})}.$$

It remains to justify the various processes used above.

To justify the inversion in step (1) suppose

$$\theta(z)=-e^{-z}.\frac{1}{4\pi^2}\int_{-\infty i}^{\infty i}\frac{\Gamma(s-k)\Gamma(-s-m+\frac{1}{2})\Gamma(-s+m+\frac{1}{2})}{\Gamma(-k+m+\frac{1}{2})\Gamma(-k-m+\frac{1}{2})}z^s\,ds$$

$$\times\int_{-\infty i}^{\infty i}\frac{\Gamma(t-k-2)\Gamma(-t-m'+\frac{1}{2})\Gamma(-t+m'+\frac{1}{2})}{\Gamma(-k-m'-\frac{3}{2})\Gamma(-k+m'-\frac{3}{2})}z^t\,dt$$

$$=W_{k,m}(z)W_{k+2,m'}(z),$$

$$\phi(s)=-\frac{1}{4\pi^2}\int_0^\infty e^{-z}\frac{\Gamma(s-k)\Gamma(-s-m+\frac{1}{2})\Gamma(-s+m+\frac{1}{2})}{\Gamma(-k+m+\frac{1}{2})\Gamma(-k-m+\frac{1}{2})}z^s\,dz$$

$$\times\int_{-\infty i}^{\infty i}\frac{\Gamma(t-k-2)\Gamma(-t-m'+\frac{1}{2})\Gamma(-t+m'+\frac{1}{2})}{\Gamma(-k-m'-\frac{3}{2})\Gamma(-k+m'-\frac{3}{2})}z^t\,dt,$$

$$(t)=-\frac{1}{4\pi^2}\int_0^\infty\frac{\Gamma(t-k-2)\Gamma(-t-m'+\frac{1}{2})\Gamma(-t+m'+\frac{1}{2})}{\Gamma(-k+m'-\frac{3}{2})\Gamma(-k-m'-\frac{3}{2})}z^t\,dz$$

$$\times\int_{-\infty i}^{\infty i}\frac{\Gamma(s-k)\Gamma(-s-m+\frac{1}{2})\Gamma(-s+m+\frac{1}{2})}{\Gamma(-k-m+\frac{1}{2})\Gamma(-k+m'+\frac{1}{2})}z^s\,ds.$$

Now $\theta(z)$ is uniformly and absolutely convergent if $R(1\pm m\pm m')>0$ in the unlimited range $z\geqslant 0$.

To prove the convergence of $\phi(s)$, let

$$\chi(s,z)=\frac{e^{-z}}{2\pi i}z^s\frac{\Gamma(s-k)\Gamma(-s-m+\frac{1}{2})\Gamma(-s+m+\frac{1}{2})}{\Gamma(-k+m+\frac{1}{2})\Gamma(-k-m+\frac{1}{2})}$$

$$\cdot\frac{1}{2\pi i}\int_{-\infty i}^{\infty i}\frac{\Gamma(t-k-2)\Gamma(-t-m'+\frac{1}{2})\Gamma(-t+m'+\frac{1}{2})}{\Gamma(-k-m'-\frac{3}{2})\Gamma(-k+m'-\frac{3}{2})}z^t\,dt$$

$$=e^{-\frac{1}{2}z}\cdot z^s\cdot\frac{1}{2\pi i}\frac{\Gamma(s-k)\Gamma(-s-m+\frac{1}{2})\Gamma(-s+m+\frac{1}{2})}{\Gamma(-k+m+\frac{1}{2})\Gamma(-k-m+\frac{1}{2})}W_{k+2,m'}(z).$$

$$\eta(t,s)=\frac{\Gamma(s-k)\Gamma(-s-m+\frac{1}{2})\Gamma(-s+m+\frac{1}{2})}{\Gamma(-k+m+\frac{1}{2})\Gamma(-k-m+\frac{1}{2})}\times\Gamma(t-k-2)\Gamma(-t+m'+\frac{1}{2})\Gamma(-t-m'+\frac{1}{2})\int_0^\infty e^{-z}z^{s+t}\,dz$$

$$\times\Gamma(-k-m'-\frac{3}{2})\Gamma(-k+m'-\frac{3}{2})$$

$$=\frac{\Gamma(s-k)\Gamma(-s-m+\frac{1}{2})\Gamma(-s+m+\frac{1}{2})\Gamma(t-k-2)}{\Gamma(-k+m+\frac{1}{2})\Gamma(-k-m+\frac{1}{2})\Gamma(-k-m'-\frac{3}{2})\Gamma(-k+m'-\frac{3}{2})}\times\Gamma(-t+m'+\frac{1}{2})\Gamma(-t-m'+\frac{1}{2})\Gamma(s+t+1).$$

It is easy to see that $\chi(s,z)$ and $\eta(t,s)$ converge uniformly and absolutely if $\mathrm{R}(\frac{1}{2}\mp m')>0$ in the unlimited ranges of integration of z, s, t. Hence, inverting the order of integration in $\phi(s)$, we get

$$\phi(s)=\frac{1}{4\pi^2}\frac{\Gamma(s-k)\Gamma(-s-m+\frac{1}{2})\Gamma(-s+m+\frac{1}{2})}{\Gamma(-k+m+\frac{1}{2})\Gamma(-k-m+\frac{1}{2})}$$

$$\times\int_{\infty i}^{\infty i}\frac{\Gamma(t-k-2)\Gamma(-t+m'+\frac{1}{2})\Gamma(-t-m'+\frac{1}{2})}{k-k--\Gamma(m'-\frac{3}{2})\Gamma(+m'-\frac{3}{2})}dt\int_0^\infty e^{-z}z^{s+t}\,dz$$

$$=\frac{1}{2\pi i}\frac{\Gamma(-s-m+\frac{1}{2})\Gamma(-s+m+\frac{1}{2})\Gamma(s+m'+\frac{3}{2})\Gamma(s-m'+\frac{3}{2})}{\Gamma(-k+m+\frac{1}{2})\Gamma(-k-m+\frac{1}{2})}.$$

From this it can be seen that $\phi(s)$ is also uniformly and absolutely convergent. Similarly we can show that $\psi(t)$ is uniformly and absolutely convergent. Thus the inversion of the order of integration in the step (1) and also in the succeeding steps is justifiable under the conditions stated above. But by the theory of analytic continuation the range can be extended to $\mathrm{R}(2\pm m\pm m')>0$.

2.2. Particular cases of the integral I_1. Putting $m=-\frac{1}{4}$ and

$$\mathrm{D}_m(\sqrt{2z})=2^{\frac{1}{2}m+\frac{1}{4}}(2z)^{-\frac{1}{4}}\mathrm{W}_{\frac{1}{2}m+\frac{1}{4},-\frac{1}{4}}(z),$$

we get

$$\int_0^\infty (z)^{\frac{1}{2}}\mathrm{D}_m(\sqrt{2}z)\mathrm{W}_{\frac{1}{2}m+\frac{2}{4},\,m'}(z)\,dz = \frac{\sqrt{\pi}\,\Gamma(\frac{7}{2}-2m')\Gamma(\frac{7}{2}+2m')}{3\,.\,2^{7+\frac{1}{2}m}\Gamma(-m)}.$$

Again putting $m=\frac{1}{4}$ and $k=-\frac{1}{4}$, and since

$$\mathrm{W}_{-\frac{1}{4},\,\frac{1}{4}}(z)=2\mathrm{E}rfc(\sqrt{z})z^{\frac{1}{4}}e^{\frac{1}{2}z},$$

we get

$$\int_0^\infty \mathrm{E}rfc(\sqrt{z})z^{\frac{1}{4}}e^{\frac{1}{2}z}\mathrm{W}_{\frac{1}{4},\,m'}(z)\,dz = \frac{\sqrt{\pi}\Gamma(\frac{7}{2}-2m')\Gamma(\frac{7}{2}+2m')}{3\,.\,2^7}.$$

2.3. Let us consider

$$\mathrm{I}_2=\int_0^\infty z^{n-2k-2}\mathrm{W}_{k,\,m}\left(\frac{z^2}{2}\right)\mathrm{D}_n(z)\,dz.$$

Using again Barnes's * type of integral for $\mathrm{W}_{k,\,m}(z)$, we get

$$\mathrm{I}_2=\int_0^\infty z^{n-2k-2}\mathrm{D}_n(z)e^{-\frac{z^2}{4}} \cdot \frac{1}{2\pi i}\int_{-\infty i}^{\infty i}\frac{\Gamma(s-k)\Gamma(-s+m+\frac{1}{2})\Gamma(-s-m+\frac{1}{2})}{\Gamma(-k+m+\frac{1}{2})\Gamma(-k-m+\frac{1}{2})}\left(\frac{z^2}{2}\right)^s ds$$

$$= \frac{1}{2\pi i}\int_{-\infty i}^{\infty i}\frac{\Gamma(s-k)\Gamma(-s+m+\frac{1}{2})\Gamma(-s-m+\frac{1}{2})}{\Gamma(-k+m+\frac{1}{2})\Gamma(-k-m+\frac{1}{2})2^s}\,ds \times \int_0^\infty z^{n-2k+2s-2}e^{-\frac{1}{2}z^2}\mathrm{D}_n(z)\,dz.$$

The inversion in the order of integration being easily justifiable, if $\mathrm{R}(n-2k\pm 2m)>0$, moreover †

$$\int_0^\infty e^{-\frac{1}{2}z^2}z^m\mathrm{D}_n(z)\,dz=\frac{\sqrt{\pi}\,2^{\frac{1}{2}n-\frac{1}{2}m-\frac{1}{2}}\Gamma(m+1)}{\Gamma(\frac{1}{2}m-\frac{1}{2}n+1)}.$$

Therefore

$$\mathrm{I}_2=\frac{1}{2\pi i}\int_{-\infty i}^{\infty i}\frac{\Gamma(-s+m+\frac{1}{2})\Gamma(-s-m+\frac{1}{2})\sqrt{\pi}\,2^{k-s+\frac{1}{2}}\Gamma(n-2k+2s-1)}{\Gamma(-k+m+\frac{1}{2})\Gamma(-k-m+\frac{1}{2})\,.\,2^s}\,ds$$

* See M.A., *loc. cit.*

† G. N. Watson, "The Harmonic Functions associated with the Parabolic Cylinder," Proc. Lond. Math. Soc. (2) viii. p. 400 (1910).

$$= \frac{1}{2\pi i}\int_{-\infty i}^{\infty i} \frac{\Gamma(-s+m+\frac{1}{2})\Gamma(-s-m+\frac{1}{2})2^{n-k+s-\frac{3}{2}}\Gamma(\frac{1}{2}n-k+s-\frac{1}{2}) \times \Gamma(\frac{1}{2}n-k+s)}{\Gamma(-k+m+\frac{1}{2})\Gamma(-k-m+\frac{1}{2})2^s}\,ds$$

$$= 2^{n-k-\frac{1}{2}} \frac{\Gamma\left(\frac{n}{2}-k+m\right)\Gamma(\frac{1}{2}n-k+\frac{1}{2}-m)\Gamma(\frac{1}{2}n-k-m) \times \Gamma(\frac{1}{2}n-k+m+\frac{1}{2})}{\Gamma(-k+m+\frac{1}{2})\Gamma(-k-m+\frac{1}{2})\Gamma(n-2k+\frac{1}{2})}$$

$$= \frac{\pi \cdot 2^{3k-n+\frac{1}{2}}\Gamma(n-2k+2m)\,\Gamma(n-2k-2m)}{\Gamma(-k+m+\frac{1}{2})\Gamma(-k-m+\frac{1}{2})\Gamma(n-2k+\frac{1}{2})}.$$

2.4. Let

$$I_3 = \int_0^\infty z^\lambda e^{-\frac{1}{2}z} P_n(z) W_{k,m}(z)\,dz.$$

Substituting again for $W_{k,m}(z)$, we get

$$I_3 = \int_0^\infty z^\lambda e^{-\frac{1}{2}z} P_n(z) e^{-\frac{1}{2}z} \times \frac{1}{2\pi i}\int_{-\infty i}^{\infty i} \frac{\Gamma(s-k)\Gamma(-s-m+\frac{1}{2})\Gamma(-s+m+\frac{1}{2})}{\Gamma(-k+m+\frac{1}{2})\Gamma(-k-m+\frac{1}{2})} z^s\,ds$$

$$= \frac{1}{2\pi i}\int_{-\infty i}^{\infty i} \frac{\Gamma(s-k)\Gamma(-s+m+\frac{1}{2})\Gamma(-s-m+\frac{1}{2})}{\Gamma(-k+m+\frac{1}{2})\Gamma(-k-m+\frac{1}{2})}\,ds \times \int_0^\infty z^{\lambda+s}e^{-z}P_n(z)\,dz.$$

It is a simple process in this case to justify the inversion. Hence

$$I_3 = \frac{1}{2\pi i}\int_{-\infty i}^{\infty i} \frac{\Gamma(s-k)\Gamma(-s+m+\frac{1}{2})\Gamma(-s-m+\frac{1}{2})}{\Gamma(-k+m+\frac{1}{2})\Gamma(-k-m+\frac{1}{2})}\,ds \times \int_0^\infty z^{\lambda+s}e^{-z} \sum_{r=0}^{p} \frac{(-1)^r z^{n-2r}\lfloor 2n-2r}{2^n \lfloor r \rfloor n-r \rfloor n-2r}\,dz,$$

where $p = \frac{1}{2}n$ or $\frac{1}{2}(n-1)$.

Integrating term by term, since $P_n(z)$ is a finite series, we get

$$I_3 = \sum_{r=0}^{p} \frac{(-1)^r \lfloor 2n-2r}{2^n \cdot 2\pi i \lfloor r \rfloor n-r \rfloor n-2r} \times \int_{-\infty i}^{\infty i} \frac{\Gamma(s-k)\Gamma(-s-m+\frac{1}{2})\Gamma(-s+m+\frac{1}{2})}{\Gamma(-k+m+\frac{1}{2})\Gamma(-k-m+\frac{1}{2})}\,ds \int_0^\infty z^{s+\lambda+n-2r}e^{-z}\,dz$$

$$= \sum_{r=0}^{p} \frac{(-1)^r \lfloor 2n-2r}{2^n \cdot 2\pi \cdot \lfloor r \lfloor n-r \lfloor n-2r} \times \int_{-\infty i}^{\infty i} \frac{\Gamma(s-k)\Gamma(-s-m+\frac{1}{2})\Gamma(-s+m+\frac{1}{2})\Gamma(s+\lambda+n-2r+1)}{\Gamma(-k+m+\frac{1}{2})\Gamma(-k-m+\frac{1}{2})} ds$$

$$= \sum_{r=0}^{p} \frac{(-1)^r \lfloor 2n-2r \, \Gamma(\lambda+n+m+\frac{3}{2}-2r)\Gamma(\lambda+n-m-2r+\frac{3}{2})}{2^n \lfloor r \lfloor n-r \lfloor n-2r \, \Gamma(\lambda+n-2r-k+2)},$$

which is expressible in ${}_4F_5$ also.

3. *Some Properties deduced by Operational Methods.*

3.1. We shall use the following theorems of operational calculus. If

$$f(p) \doteqdot h(t),$$

then

$$(a) \qquad \frac{f(p)}{p} \doteqdot \int_0^t h(t)\, dt,$$

$$(b) \qquad pf(p) \doteqdot \frac{d}{dt} h(t), \quad \text{provided } h(0)=0,$$

$$(c) \quad p\left(-\frac{d}{dp}\right)^n \frac{f(p)}{p} \doteqdot t^n h(t), \quad n>0.$$

The first two are due to Carson * and the last due to van der Pol †. Goldstein ‡ has shown that

$$(qr)^{\mu} K_{\nu}(qr) \doteqdot (4x)^k \cdot e^{-\frac{1}{2}x} W_{k,m}(x), \quad . \quad . \quad . \quad (2)$$

where $q^2=p$, $x=\dfrac{r^2}{4t}$, $k=\frac{1}{2}\mu-\frac{1}{2}$, and $m=\frac{1}{2}\nu$.

Putting $k=\frac{1}{2}$ and $\nu=0$ in (2), we get

$$(qr)^2 K_0(qr) \doteqdot (4x)^{\frac{1}{2}} e^{-\frac{1}{2}x} W_{\frac{1}{2},0}(x).$$

Using (*c*) we get

$$q^2r^2\left(-\frac{d}{dp}\right)^{\nu} K_0(qr) \doteqdot t^{\nu}(4x)^{\frac{1}{2}} e^{-\frac{1}{2}x} W_{\frac{1}{2},0}(x).$$

But

$$K_{\nu}(qr) = 2^{\nu}\left(\frac{q}{r}\right)^{\nu} \frac{d^{\nu}}{d(q^2)^{\nu}} K_0(qr);$$

* Carson, 'Electric Circuit Theory and the Operational Calculus' (McGraw-Hill, New York, 1926).

† Balth. van der Pol, Phil. Mag. viii. pp. 861–898 (1929).

‡ Goldstein, *loc. cit.*

therefore

$$t^{\nu}(4x)^{\frac{1}{2}}e^{-\frac{1}{2}x}W_{\frac{1}{2},0}(x) \doteq \frac{q^2r^2}{(-2)^{\nu}}\left(\frac{r}{q}\right)^{\nu} K_{\nu}(qr). \quad . \quad . \quad (3)$$

Using (*b*) we get (provided m is an integer)

$$\frac{d^{\nu/2}}{d(t)^{\frac{1}{2}\nu}}\{t^{\nu}(4x)^{\frac{1}{2}}e^{-\frac{1}{2}x}W_{\frac{1}{2},0}(x)\} \doteq \frac{q^2r^2}{2^{\nu}} r^{\nu}K_{\nu}(qr)$$

$$\doteq \frac{r^{\nu}}{2^{\nu}} W_{\frac{1}{2},m}(x) . (4x)^{\frac{1}{2}} . e^{-\frac{1}{2}x}.$$

Therefore

$$e^{-\frac{1}{2}x}(4x)^{\frac{1}{2}}W_{\frac{1}{2},m}(x) = \left(\frac{2}{r}\right)^{\nu}\left(\frac{d}{dt}\right)^{m}\{(4x)^{\frac{1}{2}-\nu} . r^{2\nu} . e^{-\frac{1}{2}x}W_{\frac{1}{2},0}(x)\},$$

or $$W_{\frac{1}{2},m}(x) = x^{-\frac{1}{2}}e^{\frac{1}{2}x}\left(-x^2\frac{d}{dx}\right)^{m}\{x^{1-2m}e^{-x}\}.$$

Using (*b*) in (3) we get (provided $(m+k-\frac{1}{2})$ is a positive integer)

$$\left(\frac{d}{dt}\right)^{\frac{1}{2}(\mu+\nu)-1}\{t^{\nu}(4x)^{\frac{1}{2}}e^{-\frac{1}{2}x}W_{\frac{1}{2},0}(x)\}$$

$$\doteq q^{\mu} . \frac{r^{\nu+2}}{(-2)^{\nu}} K_{\nu}(qr)$$

$$= \frac{r^{\nu-\mu+2}}{(-2)^{\nu}} (qr)^{\mu}K_{\nu}(qr)$$

$$\doteq \frac{r^{\nu-\mu+2}}{(-2)^{\nu}} (4x)^{k} . e^{-\frac{1}{2}x}W_{k,m}(x).$$

Therefore

$$W_{k,m}(x) = e^{\frac{1}{2}x} . (4x)^{-k}\frac{(-2)^{\nu}}{r^{\nu-\mu+2}}\left(\frac{d}{dt}\right)^{k+m-\frac{1}{2}}\{t^{\nu}(4x)^{\frac{1}{2}}e^{-\frac{1}{2}x}W_{\frac{1}{2},0}(x)\}$$

$$= e^{\frac{1}{2}x} . (x)^{-k}(-)^{k-m-\frac{1}{2}}\left(x^2\frac{d}{dx}\right)^{k+m-\frac{1}{2}}(x^{1-2m}e^{-x}).$$

3.2. Using (*a*) in

$$r^{\mu}q^{\mu+\nu-2}q^{-\nu+2}K_{\nu}(qr) \doteq (4x)^{k}e^{-\frac{1}{2}x}W_{k,m}(x) \equiv h(x),$$

we get

$$r^{\mu}q^{2-\nu}K_{\nu}(qr) \doteq \int_0^t\int_0^t\int_0^t \ldots h(x)\,(dt)^{\frac{1}{2}(\mu+\nu)-1},$$

or

$$r^{\mu}p\left(-\frac{d}{dp}\right)^{2s}\{q^{-\nu}\mathrm{K}_{\nu}(qr)\} \doteqdot t^{2s}\int_0^t\int_0^t\int_0^t \ldots h(x)\,(dt)^{\frac{1}{2}(\mu+\nu)-1}.$$

But

$$\frac{d^{2s}}{d(q^2)}\,q^{-\nu}\mathrm{K}_{\nu}(qr) = \frac{r^{2s}}{2^{2s}q^{\nu+2s}}\,\mathrm{K}_{\nu+2s}(qr)\ ;$$

hence

$$r^{\mu}p\left(\frac{r}{2}\right)^{2s} q^{-\nu-2s}\mathrm{K}_{\nu+2s}(qr) \doteqdot t^{2s}\int_0^t\int_0^t \ldots h(x)\ (dt)^{\frac{1}{2}(\mu+\nu)-1}$$

$$\doteqdot \frac{r^{\mu+2s}}{2^{2s}}\,q^{-\nu-2s+2}\mathrm{K}_{\nu+2s}(qr).$$

Using (*b*) we get

$$\frac{r^{\mu+2s}}{2^{2s}}\,q^{\mu}\mathrm{K}_{\nu+2s}(qr)$$

$$\doteqdot \left(\frac{d}{dt}\right)^{\frac{1}{2}(\mu+\nu)-1+s}\left\{t^{2s}\int_0^t\int_0^t \ldots h(x)\,(dt)^{\frac{1}{2}(\mu+\nu)-1}\right\}.$$

Therefore, interpreting the left-hand side we get

$$\left(\frac{r}{2}\right)^{2s} e^{-\frac{1}{2}x}(4x)^{k}\mathrm{W}_{k,\,m+s}(x)$$

$$= \left(\frac{d}{dt}\right)^{\frac{1}{2}(\mu+\nu)+s-1}\left\{t^{2s}\int_0^t\int_0^t \ldots h(x)\,(dt)^{\frac{1}{2}(\mu+\nu)-1}\right\}$$

$$= \left(\frac{d}{dt}\right)^{s}\sum_{l=0}^{\frac{1}{2}(\mu+\nu)-1} \frac{(\frac{1}{2}\mu+\frac{1}{2}\nu-1)!\,(2s)!}{l!\,(\frac{1}{2}\mu+\frac{1}{2}\nu-1-l)!\,(2s-l)!}$$

$$\times t^{2s-l}\int_0^t\int_0^t \ldots h(x)\,(dt)^{l}.$$

Since

$$r^{2l}(qr)^{\mu-2l}\mathrm{K}_{\nu}(qr) \doteqdot \int_0^t\int_0^t \ldots h(x)\,(dt)^{l}$$

and also

$$\doteqdot r^{2l}(4x)^{k-l}e^{-\frac{1}{2}x}\mathrm{W}_{k-l,\,m}(x).$$

Therefore

$$\frac{r^{2s}}{2^{2s}}\,e^{-\frac{1}{2}x}(4x)^{k}\mathrm{W}_{k,\,m+s}(x) = \sum_{l=0}^{k+m-\frac{1}{2}} \frac{(k+m-\frac{1}{2})!\,(2s)!}{l!\,(k+m-\frac{1}{2}-l)!\,(2s-l)!}$$

$$\times\left(\frac{d}{dt}\right)^{s}\left[t^{2s-l}\,.\,r^{2l}e^{-\frac{1}{2}x}(4x)^{k-l}\mathrm{W}_{k-l,\,m}(x)\right].$$

Hence, after simplifying, we get

$$e^{-\frac{1}{2}x}(x)^k \mathrm{W}_{k,\,m+s}(x) = \sum_{l=0}^{k+m-\frac{1}{2}} \frac{(k+m-\frac{1}{2})!\,(2s)}{l!\,(k+m-\frac{1}{2}-l)!\,(2s-l)!} \times \left(-x^2\frac{d}{dx}\right)^s e^{-\frac{1}{2}x}x^{k-2}\mathrm{W}_{k-l,\,m}(x)$$

Similarly it can be proved that

$$e^{-\frac{1}{2}x}(x)^{k+s}\mathrm{W}_{k+s,\,m+s}(x) = \sum_{l=0}^{k+m-\frac{1}{2}} \frac{(k+m-\frac{1}{2})!\,(2s)!}{l!\,(k+m-\frac{1}{2}-l)!\,(2s-l)!} \times \left(-x^2\frac{d}{dx}\right)^{2s} [e^{-\frac{1}{2}x}x^{k-2s}\mathrm{W}_{k-l,\,m}(x)].$$

4. *Summation of Series.*

4.1. Since *

$$\mathrm{M}_{k,\,m}(x) = x^{m+\frac{1}{2}}e^{-\frac{1}{2}x}{}_1\mathrm{F}_1(\tfrac{1}{2}+m-k\;\; 2m+1;\; x)$$

and

$$\mathrm{M}_{k,\,m}(y) = y^{m+\frac{1}{2}}e^{-\frac{1}{2}x}{}_1\mathrm{F}_1(\tfrac{1}{2}+m-k,\; 2m+1;\; y),$$

therefore

$$\mathrm{M}_{k,\,m}(x)\mathrm{M}_{k,\,m}(y) = (xy)^{m+\frac{1}{2}}e^{-\frac{1}{2}(x+y)}{}_1\mathrm{F}_1(\tfrac{1}{2}+m-k,\; 2m+1;\; x) \times {}_1\mathrm{F}_1(\tfrac{1}{2}+m-k,\; 2m+1;\; y).$$

But

$${}_1\mathrm{F}_1(\alpha,\beta;\; x)\times {}_1\mathrm{F}_1(\alpha,\beta;\; y) = \sum_{r=0}^{\infty} \frac{(-1)^r(\alpha)_r(\beta-\alpha)_r}{\lfloor r\,(\beta)_r(\beta)_{2r}}\,(xy)^r\,{}_1\mathrm{F}_1(\alpha+r,\beta+2r;\; x+y),$$

where

$$(\alpha)_r = \alpha(\alpha+1)\ldots(\alpha+r-1).$$

Hence

$$\mathrm{M}_{k,\,m}(x)\mathrm{M}_{k,\,m}(y) = (xy)^{m+\frac{1}{2}}e^{-\frac{1}{2}(x+y)} \sum_{r=0}^{\infty} \frac{(-1)^r(\frac{1}{2}+m-k)_r(\frac{1}{2}+m+k)_r}{\lfloor r\,(2m+1)_r(2m+1)_{2r}} \times (xy)^r\,{}_1\mathrm{F}_1(\tfrac{1}{2}+m-k+r,\; 2m+1+2r;\; x+y)$$

$$= \sum_{r=0}^{\infty} \frac{(-1)^r(\frac{1}{2}+m-k)_r(\frac{1}{2}+m+k)_r}{\lfloor r\,(2m+1)_r(2m+1)_{2r}} \times \left(\frac{xy}{x+y}\right)^{m+r-\frac{1}{2}} \mathrm{M}^{k,\,m+r}(x+y).$$

* See M.A. p. 337.

Putting $x=y$, we get

$$[\mathrm{M}_{k,\,m}(x)]^2 = \sum_{r=0}^{\infty} \frac{(-1)^r(\frac{1}{2}+m-k)_r(\frac{1}{2}+m+k)^r}{\lfloor r\,(2m+1)_r(2m+1)_{2r}} \times \left(\frac{x}{2}\right)^{m+r+\frac{1}{2}} \mathrm{M}_{k,\,m+r}(2x).$$

4.2. Since *

$$\frac{1}{\Gamma(k+\frac{1}{2}-m-s)} \cdot \mathrm{W}_{k,\,m+s}(z)$$

$$= -e^{-\frac{1}{2}z} z^k \cdot \frac{1}{2\pi i} \int_{\infty}^{(0+)} (-t)^{-\frac{1}{2}-k+m+s} \left(1+\frac{t}{z}\right)^{-\frac{1}{2}+k+s+m} e^{-t}\,dt,$$

provided $\mathrm{R}(k-\frac{1}{2}-m)$ is not a negative integer,

$$= -e^{-\frac{1}{2}z} z^{\frac{1}{2}-m-s} \frac{1}{2\pi i} \int_{\infty}^{(0+)} (-t)^{-\frac{1}{2}-k+m} (-t-z+z)^s \times (z+t)^{-\frac{1}{2}+k+m+s} e^{-t}\,dt$$

$$= -\sum_{r=0}^{s} \left[e^{-\frac{1}{2}z} z^{\frac{1}{2}-m-s+r} \frac{(-1)^{s-r}\lfloor s}{\lfloor r \lfloor s-r} \cdot \frac{1}{2\pi i} \int_{\infty}^{(0+)} (-t)^{-\frac{1}{2}-k+m} (z+t)^{-\frac{1}{2}+k+m+2s-r} e^{-t}\,dt \right]$$

$$= -\sum_{r=0}^{s} \left[e^{-\frac{1}{2}z} z^{k+s} \frac{(-1)^{s-r}\lfloor s}{\lfloor r \lfloor s-r} \cdot \frac{1}{2\pi i} \int_{\infty}^{(0+)} t^{-\frac{1}{2}-k+m} \left(1+\frac{t}{z}\right)^{-\frac{1}{2}+k+m+2s-r} e^{-t}\,dt \right].$$

Hence

$$\frac{\Gamma(k+\frac{1}{2}-m)}{\Gamma(k+\frac{1}{2}-m-s)} \mathrm{W}_{k,\,m+s}(z) = \sum_{r=0}^{s} \frac{(-1)^{s-r}\lfloor s}{\lfloor r \lfloor s-r} z^{\frac{r}{2}} \mathrm{W}_{k+s-\frac{r}{2},\,m+s-\frac{r}{2}}(z).$$

4.3. It has been shown by Goldstein that

$$\frac{1}{(1-h)^{n+1}} e^{-\frac{hx}{(1-h)}} = x^{-\frac{1}{2}(n+1)} e^{\frac{1}{2}x} \sum_{s=0}^{\infty} \frac{(-h)^s}{\lfloor s} \mathrm{W}_{\frac{1}{2}n+s+\frac{1}{2},\,\frac{1}{2}n}(x), \quad \ldots \quad (4)$$

where n and s are integers.

* See M.A. p. 330.

Thererefore

$$\sum_{n=0}^{\infty} [e^{\frac{1}{2}x}x^{-\frac{1}{2}(n+1)}W_{\frac{1}{2}n+s+\frac{1}{2},\frac{1}{2}n}(x)]$$

$$= \text{coefficient of } \frac{(-h)^s}{\lfloor s} \text{ in } \sum_{n=0}^{\infty}\left\{e^{\frac{-hx}{1-h}}\cdot\frac{1}{(1-h)^{n+1}}\right\}$$

$$= \text{coefficient of } \frac{(-h)^s}{\lfloor s} \text{ in } \left(1-\frac{1}{h}\right)\cdot\frac{1}{1-h}\cdot e^{\frac{-hx}{1-h}}$$

$$= e^{\frac{1}{2}x}x^{-\frac{1}{2}}\left\{W_{s+\frac{1}{2},0}(x)+\frac{1}{s+1}W_{s+\frac{3}{2},0}(x)\right\}.$$

Therefore

$$\sum_{n=0}^{\infty}\left(x^{-\frac{n}{2}}W_{\frac{n}{2}+s+\frac{1}{2},\frac{n}{2}}(x)\right) = W_{s+\frac{1}{2},0}(x)+\frac{1}{s+1}W_{s+\frac{3}{2},0}(x).$$

4.4. Multiplying (4) by $\dfrac{(-t)^n x^{\frac{1}{2}(n+1)}}{\lfloor n}$, and adding similar terms, we find that

$$\frac{\sqrt{x}}{1-h}e^{-\frac{\sqrt{x}t+hx}{1-h}} = e^{\frac{1}{2}x}\sum_{n=0}^{\infty}\sum_{s=0}^{\infty}\frac{(-t)^n(-h)^s}{\lfloor n \lfloor s}W_{\frac{n}{2}+s+\frac{1}{2},\frac{n}{2}}(x). \quad \ldots \quad (5)$$

Thus $e^{\frac{1}{2}x}W_{\frac{1}{2}n+s+\frac{1}{2},n/2}(x)$ is the coefficient of $\dfrac{(-h)^s(-t)^n}{\underline{s}\,\lfloor n}$ in the expansion of $\dfrac{\sqrt{x}}{1-h}\exp.\left(-\dfrac{\sqrt{x}t+hx}{1-h}\right)$.

5. *Recurrence Relations.*

5.1. Since

$$W_{k,m}(z) = e^{-\frac{1}{2}z}\cdot\frac{1}{2\pi i}\int_{-\infty i}^{\infty i}\frac{\Gamma(s-k)\Gamma(-s-m+\frac{1}{2})\Gamma(-s+m+\frac{1}{2})}{\Gamma(-k-m+\frac{1}{2})\Gamma(-k+m+\frac{1}{2})}z^s\,ds,$$

differentiating with respect to z, we get

$$zW'_{k,m}(z) = -\tfrac{1}{2}zW_{k,m}(z) + e^{-\frac{1}{2}z}\cdot\frac{1}{2\pi i}\int_{-\infty i}^{\infty i}\frac{\Gamma(s-k)\Gamma(-s-m+\frac{1}{2})\Gamma(-s+m+\frac{1}{2})}{\Gamma(-k-m+\frac{1}{2})\Gamma(-k+m+\frac{1}{2})}sz^s\,ds.$$

In the same way, writing the values of $W_{k,m+1}(z)$ and $W'_{k,m+1}(z)$, and substituting them in

$$I \equiv [(m+\tfrac{1}{2}-\tfrac{1}{2}z)W_{k,m}(z)-zW'_{k,m}(z)](k+m+\tfrac{1}{2})$$
$$+(k-m-\tfrac{1}{2})[(m+\tfrac{1}{2}+\tfrac{1}{2}z)W_{k,m+1}(z)+zW'_{k,m+1}(z)],$$

we get

$$I = e^{-\frac{1}{2}z}\cdot\frac{1}{2\pi i}\int_{-\infty i}^{\infty i} z^s \frac{\Gamma(s-k)\Gamma(-s+m+\frac{1}{2})\Gamma(-s-m-\frac{1}{2})}{\Gamma(-k+m+\frac{1}{2})\Gamma(-k-m-\frac{1}{2})}$$
$$\times[(m+\tfrac{1}{2})\{-s-m-\tfrac{1}{2}\}-s(-s-m-\tfrac{1}{2})$$
$$+(m+\tfrac{1}{2})(-s+m+\tfrac{1}{2})+s(-s+m+\tfrac{1}{2})]\,ds.$$

The expression within the square brackets is identically zero, hence

$$[(m+\tfrac{1}{2}-\tfrac{1}{2}z)W_{k,m}(z)-zW'_{k,m}(z)](k+m+\tfrac{1}{2})$$
$$+(k-m-\tfrac{1}{2})[(m+\tfrac{1}{2}+\tfrac{1}{2}z)W_{k,m+1}(z)+zW'_{k,m+1}(z)]=0. \quad \ldots \quad (6)$$

This relation connects $W_{k,m}(z)$ with $W_{k,m+1}(z)$.

5.2. Since

$$\frac{1}{\Gamma(k+\frac{1}{2}-m)}W_{k,m}(z)$$
$$=-\frac{1}{2\pi i}e^{-\frac{1}{2}z}\cdot z^k\int_{\infty}^{(0+)}(-t)^{-\frac{1}{2}-k+m}\left(1+\frac{t}{z}\right)^{-\frac{1}{2}+m+k}e^{-t}\,dt,$$

therefore

$$\frac{1}{\Gamma(k+\frac{1}{2}-m)}e^{\frac{1}{2}z}z^{-\frac{1}{2}+m+s}W_{k+s,m+s}(z)$$
$$=-\frac{1}{2\pi i}\int_{\infty}^{(0+)}(-t)^{-\frac{1}{2}-k+m}(z+t)^{-\frac{1}{2}+k+m+2s}e^{-t}\,dt.$$

Differentiating both the sides we get

$$\left(\frac{d}{dz}\right)^{2s}[e^{\frac{1}{2}z}z^{-\frac{1}{2}+m+s}W_{k+s,m+s}(z)]$$
$$=\frac{\binom{-\frac{1}{2}+k+m+2s}{2s}\Gamma(k-m+\frac{1}{2})}{2\pi i}\int_{\infty}^{(0+)}(-t)^{\frac{1}{2}-k+m}$$
$$\times(z+t)^{-\frac{1}{2}+k+m}e^{-t}dt$$
$$=\binom{-\frac{1}{2}+k+m+2s}{2s}e^{\frac{1}{2}z}\cdot z^{-\frac{1}{2}+m}W_{k,m}(z),$$

where $\binom{\alpha}{p}=\alpha(\alpha-1)(\alpha-2)\ldots(\alpha-p+1).$

Putting $s=1$, and simplifying, we get

$$(\tfrac{3}{2}+k+m)(\tfrac{1}{2}+k+m)z\,.\,W_{k,m}(z)$$
$$=z^2W''_{k+1,m+1}(z)+W'_{k+1,m+1}(z)\{z^2+z(2m+1)\}$$
$$+W_{k+1,m+1}(z)\{\tfrac{1}{4}z^2+(m+\tfrac{1}{2})z+m^2-\tfrac{1}{4}\}.$$

But $z^2W''_{k+1,m+1}(z)$

$$=-\left(-\frac{z^2}{4}+(k+1)z+\tfrac{1}{4}-(m+1)^2\right)W_{k+1,m+1}(z);$$

therefore we have

$$(\tfrac{3}{2}+k+m)(\tfrac{1}{2}+k+m)zW_{k,m}(z)$$
$$=z(z+2m+1)W'_{k+1,m+1}(z)+\{\tfrac{1}{2}z^2+(m-k-\tfrac{1}{2})z$$
$$+m^2+(m+1)^2-\tfrac{1}{2}\}W_{k+1,m+1}(z). \quad (7)$$

This relation connects $W_{k,m}(z)$ with $W_{k+1,m+1}(z)$.

6. *Zeros of Whittaker's Function.*

Theorem I.—$W_{k,m}(z)$ and $W_{k,m+1}(z)$ cannot have a common root.

To prove this theorem we require the following Lemma. All roots of $W_{k,m}(z)$ are simple.

Suppose $W_{k,m}(z)$ has a root which is repeated, then at this point $W'_{k,m}(z)$ will also vanish. Further, from the relations

$$W''+\left(-\tfrac{1}{4}+\frac{k}{z}+\frac{\frac{1}{4}-m^2}{z^2}\right)W=0$$

and $z^2W'''+(-\tfrac{1}{4}z^2+kz+\tfrac{1}{4}-m^2)W'+(-\tfrac{1}{2}z+k)W=0$

we conclude that $W''_{k,m}(z)$ and $W'''_{k,m}(z)$ also vanish at that point, and consequently all derivatives vanish. Hence $W_{k,m}(z)$ is identically zero, which it is not. Therefore no two roots of $W_{k,m}(z)$ are equal.

Now suppose $W_{k,m}(z)$ and $W_{k,m+1}(z)$ have a common root different from zero, then, from the differential equation, we find that

$$W''_{k,m}(z)=0$$

and

$$W''_{k,m+1}(z)=0.$$

Now, substituting these in the recurrence relation given above, we find

$$(k+m+\tfrac{1}{2})W'_{k,m}(z)-(k-m-\tfrac{1}{2})W'_{k,m+1}(z)=0. \quad (8)$$

Differentiate (6), and substitute the values of $W''_{k,m}(z)$ and $W''_{k,m+1}(z)$, we find

$$(m-\tfrac{1}{2})(k+m+\tfrac{1}{2})W'_{k,m}(z) + (m+\tfrac{3}{2})(k-m-\tfrac{1}{2})W'_{k,m+1}(z)=0. \quad (9)$$

From (8) and (9) we find

$$W'_{k,m}(z)=0$$

and

$$W'_{k,m+1}(z)=0.$$

Therefore $W_{k,m}(z)$ and $W'_{k,m}(z)$ vanish at the same point, which is impossible.

Hence $W_{k,m}(z)$ and $W_{k,m+1}(z)$ cannot have a common root.

6.2. Similarly we can prove the

Theorem II.—$W_{k,m}(z)$ and $W_{k+1,m}(z)$ cannot have a common root with the possible exception of zero, if at all.

This can be established from the known recurrence relation *

$$zW'_{k,m}(z)=(k-\tfrac{1}{2}z)W_{k,m}(z)-\{m^2-(k-\tfrac{1}{2})^2\}W_{k-1,m}(z).$$

Again, starting from the recurrence relation

$$W_{k,m}(z)=z^{\frac{1}{2}}W_{k-\frac{1}{2},m-\frac{1}{2}}(z)+(\tfrac{1}{2}-k+m)W_{k-1,m}(z),$$

we can prove another property, namely

Theorem III.—$W_{k,m}(z)$ and $W_{k\pm\frac{1}{2},m\pm\frac{1}{2}}(z)$ cannot have a common root.

From the relation (7) we can prove

Theorem IV.—$W_{k,m}(z)$ and $W_{k+1,m+1}(z)$ cannot have a common root with the possible exception of zero, if at all.

Goldstein † has shown that

$$\frac{d}{dx}\{x^{m-\frac{1}{2}}e^{-\frac{1}{2}x}W_{k,m}(x)\}=x^{m-1}e^{-\frac{1}{2}x}W_{k+\frac{1}{2},m-\frac{1}{2}}(x)$$

and

$$\frac{d}{dx}\{x^k e^{-\frac{1}{2}x}W_{k,m}(x)\}=-x^{k-1}e^{-\frac{1}{2}x}W_{k+1,m}(x).$$

From these we can prove the following

Theorem V.—Between any two consecutive zeros of $W_{k,m}(z)$ lies one and only one zero of $W_{k+\frac{1}{2},m-\frac{1}{2}}(z)$ as well as of $W_{k+1,m}(z)$.

Christ Church College,
Cawnpore, India.

* See M.A. p. 352.
† Goldstein, *loc. cit.*

XLIV. *A Method of Harmonic Analysis.—A Study of the Rotational Frequencies of Screw Propellers.* By G. F. Partridge, *B.Sc., F.Inst.P.**

[Plates VI.–VIII.]

§ I. Harmonic Analyser.

1. *Introduction.*

In alternating current work distorted current and voltage wave forms frequently occur, and the problem of deriving a harmonic analysis of such wave forms is of considerable importance.

The method of taking a graphical record of the wave form, either by means of an oscillograph or by Joubert's method [1], and then deriving the harmonics by analytical methods is well known. Although a record of the wave form is useful it does not form a suitable basis for accurate harmonic analysis, in that the accuracy of the recording process is not very high, while the calculation of the harmonics is very tedious.

Numerous methods have been devised whereby the magnitude of the various harmonics can be determined more directly by means of a suitable measuring instrument. These are of particular interest in the study of distortion in amplifiers and similar apparatus, and in acoustic work. Of the many methods developed the more accurate are of the following three forms :—

(1) Rectifier methods [2].
(2) Valve voltmeter methods [3].
(3) Dynamometer methods [4].

In the rectifier method the alternating current undergoing analysis is passed through a direct current meter *via* a motor-driven interrupter. As the interrupter runs up in speed rectification of the fundamental and the various harmonics in turn occurs. The order of the harmonic is thus determined in terms of the speed of the interrupter, while the magnitude of the harmonic is dependent upon the value of the maximum reading of the ammeter as the interrupter passes into synchronism with the respective harmonics. Owing to the fact that sub-harmonic responses occur the reading corresponding to

* Communicated by Sir Frank Smith, K.C.B., Sec.R.S.

any component depends upon the magnitude of this component, and also of the later harmonics, so that the magnitudes of the harmonics cannot be read off directly from the reading of the ammeter, but can only be derived after a certain amount of calculation. This is one of the disadvantages of the rectifier method.

In the second method the alternating current to be analysed is mixed with alternating current free from harmonics, and then applied to the grid of a valve. The source of applied alternating current may be a valve oscillator or other suitable generator provided the frequency can be varied continuously as desired. By virtue of the asymmetric nature of the valve characteristic a product term is introduced so that the current in the plate circuit of the valve contains difference terms such as $I \cos 2\pi(n-n_1)t$, where n is the frequency of the source and n_1 the frequency of a component of the complex A.C. As the frequency of the generator is varied the D.C. meter in the plate circuit exhibits slow oscillations, and when the frequency of the generator synchronizes with each respective harmonic a steady deflexion on the meter is obtained. The magnitude of the harmonic depends upon this deflexion, but, as in the case of the rectifier method, a certain amount of adjustment is necessary before the absolute value of the harmonic can be determined.

In the third method the dynamometer principle is used. The instrument may be a moving coil dynamometer as originally suggested or, as in the experiments to be described later, a string electrometer. In both cases we have a fixed member and a moving member. The complex wave form is applied to the moving part and an alternating e.m.f. is applied to the fixed part. As is well known, the force on the moving member is proportional to the product of the applied e.m.f.'s, so that the moving member is deflected by an amount proportional to a difference term of the form

$$k \cos 2\pi(n-n_1)t,$$

where n and n_1 have the same significance as above. If now the generator is allowed to pass through the frequency n the movement oscillates with the frequency $n-n_1$, and at synchronism shows a steady deflexion. Provided the e.m.f. supplied by the generator is free from

harmonics this deflexion is directly proportional to the magnitude of the harmonic n.

The dynamometer method has, therefore, the advantage over other methods of being direct reading. An instrument of this form is essentially less sensitive than a D.C. instrument such as can be used in the other methods, but in general this is not a serious disadvantage.

2. *Method of Analysis.*

The harmonic analyser described in this paper was developed with the object of providing a rapid method of analysis at acoustic frequencies. For this reason the dynamometer principle has been adopted, a string electrometer being employed so as to be able to record the responses at the various harmonics.

The e.m.f. of complex wave form is applied to the string of the electrometer. A sinusoidal e.m.f. of definite frequency f_2 is then applied to the plates of the electrometer from a suitable A.C. generator.

Let us consider one of the components of the complex wave form which acting alone would produce a voltage v on the string

where $$v = v_1 \sin [2\pi f_1 t + \phi].$$

Let the voltage between the plates be

$$V = V_1 \sin 2\pi f_2 t$$

where $$f_2 < f_1.$$

The force tending to move the string is proportional to the product of these two, so that

$$\begin{aligned} \text{Force} &\propto v.V \\ &\propto v_1 V_1 \sin [2\pi f_1 t + \phi] . \sin 2\pi f_2 t \\ &\propto v_1 V_1 \{\cos [2\pi (f_1 - f_2) t + \phi] - \cos [2\pi (f_1 + f_2) t + \phi]\}. \end{aligned}$$

The force on the string thus breaks up into two separate components, one tending to move the string at a frequency $f_1 - f_2$, and the other at a frequency $f_1 + f_2$. If the natural frequency of the string is far removed from either of these frequencies the string will be unaffected. The natural frequency of the string is usually low, and in the analyses given later is less than 10 p.p.s.

Consider now the effect of varying the frequency f_2. As this frequency increases the frequency $f_1 - f_2$ approaches the natural frequency of the string, and the latter tends to move in synchronism with the low frequency component of the force, still being unaffected by the higher frequency component. As f_2 increases and passes through the frequency f_1 the movement becomes slower and then faster again. At exact synchronism there is a steady deflexion of the string equal to $k.v_1V_1 \cos \phi$, where $2k$ is the constant of the electrometer.

The deflexion at synchronism is dependent upon the value of ϕ, and one method of determining the value of v_1 is to adjust the phase of the applied e.m.f., meanwhile keeping the frequency of the analysing e.m.f. constant, until there is a maximum deflexion which is then equal to $k.v_1V_1$. This of necessity is a slow process, and there is also the difficulty of keeping the frequency of the analyser constant while adjusting the phase.

In the method adopted a photographic record is taken of the movement of the string as the frequency of the e.m.f. applied to the plate is varied. In the records reproduced it will be noticed that the response of the string is of a definite character so that it is not difficult to pick out the point of exact synchronism. In this way a frequency analysis is obtained.

The maximum amplitude of the deflexion near synchronism has been taken as equal to kv_1V_1. (The conditions under which this is sufficiently accurate will be discussed in the next section.) Knowing the values of k and V_1 the value of the particular harmonic v_1 can be determined.

When a rapid analysis is being made over a range of frequencies it is not convenient to determine k at every response. Thus in the photographic method of recording described later a calibration run to determine k is made at one frequency, and then assumed to hold at all other points.

3. *Effect of making the Frequency continuously variable.*

When the frequency on the plates varies continuously the vibration of the string depends upon the rate at which this frequency changes. Thus if f is the change of frequency per second, and the time is measured from the

exact point of synchronism, the amplitude of the vibrations of the string is given by

$$y = kv_1 V_1 \cos [2\pi(f_1 - f_2)t + \phi]$$
$$= k.v_1 V_1 \cos [2\pi f t^2 + \phi],$$

so that the string moves at a much lower frequency than the difference frequency $(f_1 - f_2)$.

The type of response also depends upon the value of ϕ. In fig. 1 are given the responses for various values of ϕ as

Fig. 1.

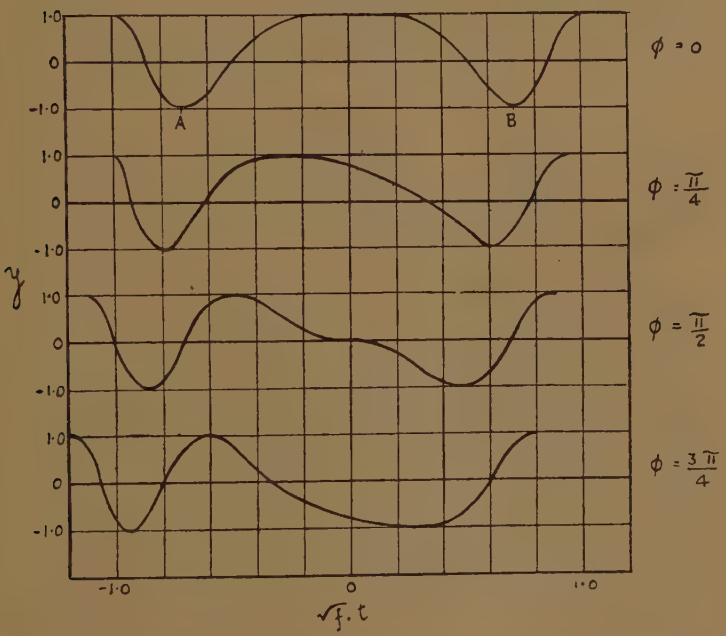

calculated from the above expression for y. Responses of these various types occur in the records reproduced.

The time taken for a complete oscillation of the string during a response, *i. e.*, the time represented by A.B. in fig. 1 is $\sqrt{2}/f$ and the mean frequency of the response, which the string must faithfully record, is $\sqrt{f}/2$.

It is shown in § IV. that the string under the conditions of sensitivity used in these measurements has a natural frequency of the order of 6 p.p.s. and is almost critically dead beat. If, therefore, the rate at which the

frequency on the plate is varied is always adjusted so that the mean frequency of response does not exceed 6 p.p.s., the string will be able to follow the variations of the force acting on it, and the amplitude of vibration will be given by

$$y=kv_1V_1 \cos (2\pi ft^2+\phi].$$

Two records are shown in No. 1 (Pl. VII.) which have been taken at two different rates, and it will be seen that the amplitude of response in each case is of the same order.

Referring again to the shape of the various responses (see fig. 1) it will be noticed that the maximum deflexion of the string is independent of ϕ, its value being in all cases

$$y_{max}=kv_1V_1.$$

Thus by varying the frequency continuously at the appropriate speed and recording the movement of the string we avoid the necessity for determining ϕ. This is one of the novel features of the present method.

4. *The Effect of Harmonics in the Analysing Voltage.*

The above results have been obtained by considering the effect of imposing a single frequency e.m.f. on the plates. Should there be any harmonics of this frequency present an error may be introduced into the determination of v_1.

Thus, suppose the analysis is of a harmonic series

$$v=v_1 \sin \omega_1 t+v_2 \sin 2\omega_1 t+\ldots v_n \sin n\omega_1 t\ldots,$$

and that the e.m.f. applied to the plates also contains harmonics, thus

$$V=V_1 \sin \omega_2 t+V_2 \sin 2\omega_2 t+\ldots V_n \sin \omega_2 t+\ldots$$

If phase differences are ignored we shall arrive at the maximum possible error.

The deflexion of the string is therefore given by the "effective" terms of the following series:—

$$y_2=2k[\Sigma v_nV_n \sin n\omega_1 t \,.\, \sin n\omega_2 t + \Sigma v_nV_m \sin n\omega_1 t \,.\, \sin m\omega_2 t], \quad m\neq n.$$

Under practical conditions the maximum error will

occur when determining the fundamental, *i. e.*, let $\omega_1=\omega_2$, then

$$y_2=2k[\Sigma v_n V_n \sin^2 n\omega_1 t+\Sigma v_n V_m \sin n\omega_1 t \,.\, \sin m\omega_1 t]$$
$$=k[\Sigma\{v_n V_n[1-\cos 2n\omega_1 t]+v_n V_m \cos \overline{n-m}\,\omega_1 t + v_n V_m \cos \overline{n+m}\,\omega_1 t\}$$
$$=k\sum_{n=1}^{n=\infty} v_n V_n,$$

since the other terms are too high a frequency to affect the string.

In the absence of harmonics in the analysing e.m.f. the deflexion of the string is $y_1=kv_1V_1$, so that the relative error σ is given by the following

$$\sigma=\frac{y_2-y_1}{y_1}$$
$$=\frac{v_2}{v_1}\cdot\frac{V_2}{V_1}+\frac{v_3}{v_1}\cdot\frac{V_3}{V_1}+\cdots\frac{v_n}{v_1}\cdot\frac{V_n}{V_1}.$$

This infinite series, representing the error, thus depends upon the ratios $\frac{V_n}{V_1}$ etc., which may be regarded as an index of the impurity of the analysing e.m.f. and upon the ratios $\frac{v_n}{v_1}$, *i. e.*, upon the relative magnitude of the harmonics in the e.m.f. being analysed. In general the latter will be of descending order of magnitude, so that the error in determining v_1 will be less than the impurity of the analysing e.m.f. In the exceptional case when the harmonics in the e.m.f. under analysis are greater than the fundamental the error will be greater than the impurity of the analysing e.m.f.

It is essential, therefore, to use for the plate supply a source of e.m.f. as free from harmonics as possible, and more particularly when analysing a wave form in which the harmonics are of greater magnitude than the fundamental.

5. *Variable Frequency Generator.*

As a means of supplying the plates of the electrometer with alternating voltage of continuously variable frequency a valve oscillator is obviously the most suitable form of generator. The frequency may be varied either (i.) by

varying the capacity, or (ii.) by varying the inductance, in the oscillatory circuit.

In order to obtain a continuous variation of frequency over the complete range of audible frequencies, the first method may be used. It is necessary in this case to employ the " beat tone " form of oscillator so that a vane condenser will give a sufficiently large variation of frequency. Here two high frequency circuits are used, one of fixed frequency, the frequency of the second circuit being varied by means of a vane condenser. By coupling the two circuits a " beat tone " of variable audible frequency can be obtained.

Fig. 2.

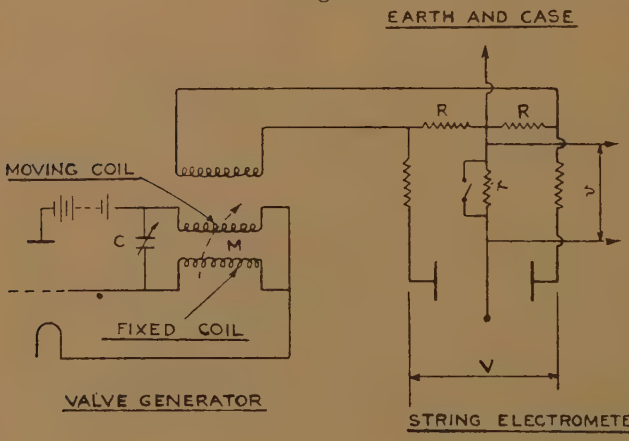

Some preliminary experiments were made using this method of frequency variation. It was apparent that in order to maintain a constant frequency calibration the valve circuits would need to be very carefully screened and the worm drive to the variable condenser very accurately made. Furthermore, it was found difficult to obtain a pure wave form with a simple form of apparatus. In view of these results it was decided to employ the second method of varying the frequency using a single audio valve oscillator.

The circuit which was adopted is the " Hartley Circuit " having capacity and inductive coupling between anode and grid (see fig. 2). The anode coil rotates inside the grid coil, thus varying the total inductance L in the

circuit, and hence the frequency. The voltage induced in the secondary coil is determined by the value of $MI/\sqrt{L}$, where M is the mutual between L and the secondary coil and I is the current in the oscillatory circuit LC. It is a matter of design to find values for the grid, anode, and secondary coils, such that the value of $MI/\sqrt{L}$ is approximately constant for all positions of the anode coil. The range of frequency covered by the rotation of the coil depends upon the value of the condenser C, and by selecting suitable values a series of overlapping ranges can be obtained.

The arrangement of the coils is shown in fig. 3 (Pl. VI.). The rotating coil is driven through a worm gear at a maximum speed of 7·5 r.p.m. Difficulty was found at first in obtaining satisfactory contact between the brushes and slip rings to which the ends of the anode coil are connected. This has been overcome, however, by using soft gauze loops held down by light spiral springs.

6. *Camera.*

To facilitate analysis a special camera has been designed (see fig. 3, Pl. VI.) by means of which, if necessary, eight ranges of frequency can be recorded on one film 55 cm. in length in such a way that the frequency of any response is known provided the condenser value is known.

The film is carried on a rotating drum 5 cm. wide and 18 cm. diameter driven by a shaft which can be coupled up to that of the rotating coil. On this shaft is a loose sleeve in the form of a three start screw of 1 cm. pitch carrying a nut. The film drum fits on an extension of this nut. Normally the drum with the screw and nut rotate together, but on locking the screwed sleeve by means of a cam shown at C, the film drum travels along the shaft while rotating. The lens aperture is 1 cm., so that a spiral record of 1 cm. width is traced out on the film for four revolutions of the drum.

Since the position of the drum bears a definite relation to the position of the moving coil, the frequency at any point of the record can be determined in terms of the lowest frequency of the range, by measuring the distance of this point from the point of lowest frequency. In one complete revolution the frequency passes twice through the range of frequency, so that a response occurs twice.

It is arranged that the shutter opens near the point of highest frequency, so that the point of lowest frequency is about the centre of the record and exactly midway between two corresponding responses. This provides a means of determining the point of lowest frequency with an accuracy depending only on the accuracy with which one can determine the centre of each response. As an example we may take record No. 4, in which the centre point of each range has been determined in this way, and these are consistent to less than 0·5 mm. The maximum possible error in frequency due to an error of 0·5 mm. in the fixing of the centre point is 0·1 per cent.

The shutter is operated mechanically by means of a system of levers. Just below the drum carrier are two rockers which can be set in one of four positions. As the drum travels out along the screw a projection in the carrier displaces the first rocker and opens the shutter. After one or more revolutions of the drum the second rocker is displaced and the shutter closes. The film can thus be exposed in sections as desired.

A special feature of the camera is that it does not require to be used in a dark room, since the light tight case in which the drum revolves can be slipped off the sleeve when the film has been exposed and taken into the dark room for reloading.

7. *String Electrometer.*

In this form of instrument a fine gold sputtered quartz fibre is stretched in a frame in such a manner that it lies between two parallel plates. These are insulated from one another and from the fibre.

If two equal and opposite potentials are applied to the plates, and the fibre is at earth potential it will remain undisturbed provided the fibre lies exactly midway between the plates.

If now a small potential is applied to the fibre it is deflected from this position, the amount of movement depending upon the potentials applied to the plates and to the fibre, and also upon the tension in the fibre.

The form of instrument used in these measurements is shown in fig. 4. The plates are fixed relative to one another, but can be adjusted so as to bring the fibre into a central position with respect to them. The method

by which this is done will be apparent from the figure, as also the method of adjusting the tension of the fibre.

Connexions from each of the plates and from the fibre are brought out to three terminals. An earth terminal is also provided on the case of the instrument. The method of connecting the instrument will be apparent from the circuit of fig. 2. The resistances R are of the order of 100,000 ohm, and form a potential divider so that one end of the string is initially connected to the mid

Fig. 4.

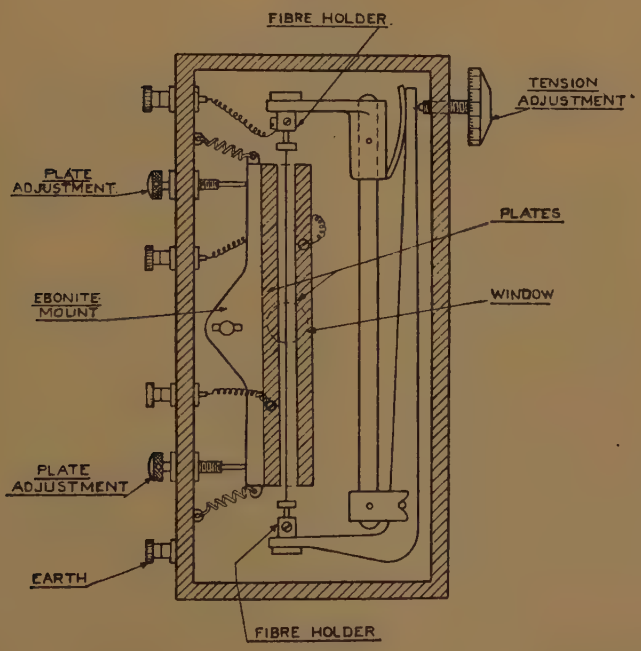

potential of the plates. The potential v is applied to the string across a suitable resistance r.

Further details of the electrometer are given in § IV.

In fig. 5 curves are given showing the relationship between deflexion and the product $v.\mathrm{V}$. It will be seen that the variation of deflexion with the product $v.\mathrm{V}$ is linear up to values of $v.\mathrm{V}=60$ volt.[2] Beyond this value the string is unstable.

Curve (a) shows the variation of deflexion for V constant at 30 volts r.m.s. and curve (b) for v constant at 2·4 volts

r.m.s. The slight difference in slope is due to a slight change in tension between the two sets of observations. Similar curves were obtained for steady voltages.

The relationship between deflexion and $v.\mathrm{V}$ is therefore

$$y=2kv\mathrm{V} \text{ where } k \text{ is a constant.}$$

With alternating voltages we have, as shown previously,

$$y=kv_1\mathrm{V}_1[\cos(\omega_1-\omega_2)t-\cos(\omega_1+\omega_2)t]$$
$$=2kv_\mathrm{R}\mathrm{V}_\mathrm{R}\cos(\omega_1-\omega_2)t,$$

Fig. 5.

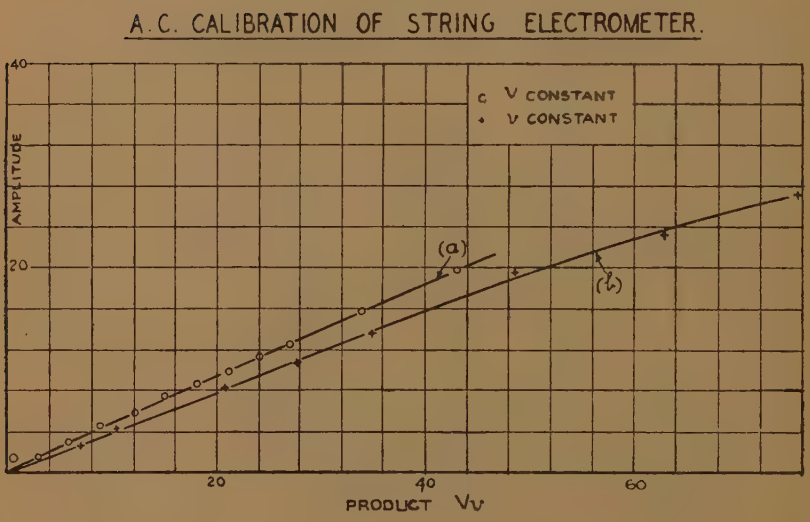

where v_1, V_1 are instantaneous voltages and v_R, V_R are the r.m.s. voltages.

The method of obtaining the values shown in fig. 5 is as follows :—

The frequencies applied to the plates and the fibre respectively are adjusted until there is a slow oscillation of the string corresponding to the term $\cos(\omega_1-\omega_2)t$, the term $\cos(\omega_1+\omega_2)t$ being ineffective. Half the double amplitude of oscillation has then been observed and plotted against the product of the values of v_R and V_R.

8. *Various Analyses.*

(i.) *Analysis of Square Top Wave.*

In this case the harmonics are of descending order of magnitude.

The square top wave form was produced by making and breaking the current in a circuit by means of a motor driven interrupter. Since the width of the brushes was commensurate with the width of the segments the ratio of make to the whole period was determined by current measurements.

Current at make $=\cdot 036$.
Interrupted current $=\cdot 012$.
R.M.S. current $=\cdot 021$.

These give a ratio 1 : 3.

The Fourier series for such a wave form is

$$f(t)=k\,.\,a+\sum_{n=1}^{n=\infty}\frac{a}{n\,.\,\pi}\sqrt{[2-2\cos 2\pi nk]}\sin(nt+\phi_n),$$

where k is the above ratio and a is the value of the current at "make."

For the particular value of k the periodic term vanishes when $n=3$, so that, omitting phases, we have

$$f(t)=\frac{a}{3}+\frac{\sqrt{3}\,.\,a}{\pi}[\sin t+\tfrac{1}{2}\sin 2t+\tfrac{1}{4}\sin 4t+\ldots].$$

A reproduction of the photographic record of the analysis is given in No. 5 (Pl. VIII.).

Four ranges of frequency are shown from about 550 p.p.s. to 3500 p.p.s. The number of interruptions per second was 615 per second ± 1 per cent.

The voltage applied to the string of the electrometer was taken from a potentiometer, and in order to obtain a reasonable deflexion, this voltage was increased for the higher ranges of frequency, as indicated by the voltage factor given in the Table I. The fundamental frequency as shown by the record is 618, and it will be noticed that the harmonic corresponding to $n=3$ is missing, as indicated by theory.

(ii.) *Analysis of a Series of Damped Oscillations.*

This is a very searching test of the method, for, as shown in § III., the analysis gives a series of harmonics whose

amplitude increases up to a certain frequency and then decreases.

The oscillations were produced by discharging a condenser C through a circuit (see fig. 6) containing a suitable inductance L and resistance R. The condenser was charged about 100 times per second by means of two contacts on a rotating drum, which was motor driven, the time of contact being ·012 of the whole period of charge and discharge. A suitable tapping r was made on

TABLE I.

	1.	2.	3.	4.
Frequency of response	618	1220	—	2460
Voltage factor	1	2	—	3
Voltage on string from deflexion	0·35	0·35	—	0·25
Amplitude of harmonic ...	0·35	0·175	—	0·083

Calibration 0·50 volt per mm. deflexion.

Fig. 6.

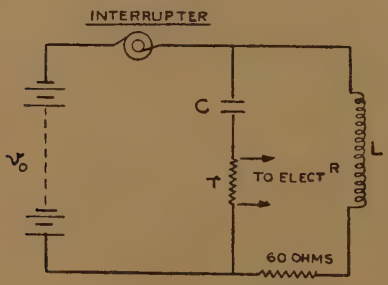

the resistance, and the voltage across this was applied to the string of the electrometer.

The values of L, C, and R are as follows :—R = 122 ohms, this includes the resistance of L measured at the frequency of the ensuing oscillations, r = 40 ohms, L = 0·125 henry, and C = 0·6 m.f.

The condition for oscillations, *i. e.*, $R^2 < \frac{4L}{C}$, is thus satisfied, and in the initial stage the voltage across the condenser is given by

$$v = v_0 e^{-at} \cdot \cos pt,$$

where $$p=\sqrt{\left[\frac{1}{LC}-\frac{R^2}{4L^2}\right]}=\frac{1}{\sqrt{LC}}$$ very nearly;

since $\frac{R^2}{4L^2}$ is small compared with $\frac{1}{LC}$.

v_0=applied voltage=48 volts,

and a=decay coefficient=$\frac{R}{2L}$=488.

The current in the circuit is therefore given by

$$i=v_0\sqrt{\frac{C}{L}}.e^{-at}.\sin pt,$$

so that the voltage across the tapping r is

$$E=v_0 r\sqrt{\frac{C}{L}}.e^{-at}\sin pt.$$

These are the initial conditions, so that to apply the results of § III. we must replace B in (3) by $v_0 r\sqrt{\frac{C}{L}}$. In doing so we ignore the small interval of time for charging the condenser.

Since a=488 and τ=0·01 nearly, giving $a\tau$=4·88, we can use the simpler expression for the amplitude of the harmonics, *i. e.*,

$$A_n=\frac{B\omega}{\pi}.\frac{p}{\sqrt{[(a^2+\omega^2n^2-p^2)^2+4a^2p^2]}},$$

where $$p=\frac{1}{\sqrt{LC}}=3650$$

B=4·18 volts,

and $\omega=\frac{2\pi}{\tau}=2\pi\times$ frequency at which condenser is charged.

As shown in § III., the value of the harmonics varies very rapidly with any change in the frequency of charge. The speed of the motor driving the contacts was therefore maintained as constant as possible. A variation of ±1·5 per cent. was obtained by a special control, as will be seen from the frequencies given in the record. The average frequency obtained from the record is 101 p.p.s., giving ω=634.

The photographic record is reproduced in No. 4 (Pl. VII.). The string sensitivity as measured at the time was 0·42 volt per mm. deflexion. The frequencies and voltages corresponding to the various responses are given in Table II., as also the theoretical values calculated from the expression given above.

Considering the restricted amplitude required to obtain a complete record on a narrow film the results are in good agreement with theory. A visual analysis would not have given greater accuracy here, since it would have been a slower process, and the amplitudes of the harmonics would have varied considerably due to changes of frequency of the applied charge.

TABLE II.

	3.	4.	5.	6.	7.	8.
Frequency of response.....	305	412	505	612	695	800
A_n from record..	0·31	0·38	0·67	0·80	0·42	0·21
A_n from theory .	0·305	0·408	0·658	0·805	0·410	0·234

(iii.) *Distortion in Amplifiers.*

It is well known that audio frequency transformer amplifiers produce frequency distortion at low frequencies, and an example is given here showing how the present method of analysis may be applied.

Records of two sinusoidal wave forms after amplification by means of a transformer amplifier are given in Nos. 2 and 3 (Pl. VII.). It will be seen that at a frequency of 720 p.p.s. there is practically no distortion, whereas at a frequency of 97 p.p.s. there is considerable distortion.

The conditions lend themselves to a visual analysis, and this was employed in determining the fundamental and harmonics of the distorted wave form. The e.m.f. after amplification was applied to the string of the electrometer and then analysed by adjusting the frequency on the plates until there were slow oscillations of the string. The amplitude of these oscillations was measured by means of a microscope focussed on the string.

The sensitivity as measured was 0·025 volt r.m.s. per division in the microscope. The harmonics beyond the

second were found to be negligibly small. The results of the analysis are given below.

An attempt was made to determine the relative phases by the method suggested in section (2), but the results were not sufficiently accurate. The phases were therefore determined by taking the relative amplitudes as given by the above analysis and applying Gauss's method to the record of the wave form, assuming that all harmonics higher than the second can be neglected. This gives the following expression for the amplitude in mm. on the record taking the zero as the lowest point of the record

$$y=6{\cdot}98-4{\cdot}9\sin x+2{\cdot}7\sin(2x+10)+4{\cdot}46\sin(3x+82).$$

TABLE III.

Analysis of Distorted Wave Form.

Component.	Fundamental.	First harmonic.	Second harmonic.
Deflexion divisions in microscope	27·5	14·6	25·0
Amplitude relative to fundamental.... ..	1·0	0·53	0·91

This expression was found to fit the curve very well at all points.

(iv.) *Analysis of Damped Sound Waves.*

In order to produce the damped waves vibrations in a brass plate were excited by means of a mechanical tapper. This was placed in water along with a distortionless receiver. The e.m.f. after three valve amplification was then applied to the string of the electrometer.

The frequency of the vibrations was 250 p.p.s., and damped trains of these vibrations were excited at the rate of 10 per second. The record is given in No. 6 (Pl. VIII.). Since the fundamental frequency of the series is 10 p.p.s. a response occurs at every multiple of 10 and these rapidly follow one another. The resulting record is rather confused, due to the fact that the frequency of the tapper was not under control. The amplitude of the responses, however, definitely reaches a maximum in the neighbourhood of 250 p.p.s. The whole effect is practically over

in the range of frequency 210 p.p.s.–300 p.p.s. Other ranges were recorded, but no definite responses were observed. Several similar records of the same range have been taken on the one film, and it will be noticed how the frequency of the maximum is increasing with time. This is due to a gradual increase in the frequency of the tapper.

The theory of § III. can be applied to the results provided we can determine a (the decay coefficient). This has been determined indirectly from the ratio of the maximum voltage v_n as given on the record and the r.m.s. voltage v_r applied to the string when the record was taken.

By direct integration of the series given in § III. it can be shown that the r.m.s. value of such a series is given very nearly by

$$A_r = \frac{B}{2\sqrt{a\tau}},$$

provided $a\tau > 3{\cdot}0$.

Also we have found that if $a\tau > 3{\cdot}0$

$$A_n = \frac{\frac{B.\omega.p}{\pi}}{\sqrt{[(a^2+\omega^2n^2-p^2)^2+4a^2p^2]}}.$$

So that the *maximum* amplitude on a record where the impulsing frequency is varying continuously will be given by

$$A_n = \frac{B.\omega.p}{2\pi ap} = \frac{B}{a\tau}.$$

The ratio of maximum voltage recorded to measured r.m.s. voltage will therefore be given by

$$\frac{v_n}{v_r} = \frac{2}{\sqrt{a\tau}}.$$

From the record v_n is found to be 0·85 volt. The r.m.s. voltage measured at the time of the experiment was 1·40 volt giving $a\tau = 10$ and $a = 100$.

Taking this value of a the amplitude of the various harmonics can be evaluated from the equation for A_n given above. A few of these are given in Table IV., and it will be noticed that they are in good agreement with the record. The amplitude of the maximum has been taken as unity.

§ II. Analysis of Propeller Sounds.

The theoretical analysis which is given in § III. has an important bearing on the subject of the frequencies emitted by a screw propeller. From experimental investigations carried out by Barlow and Keene[5] in connexion with under-water propellers and by Fage[6] on the vibrations of airscrews, it appears that the frequencies emitted by propellers exhibit a harmonic series.

It has been suggested that the sounds of rotation emitted from a propeller are due to cavitation effects, which produce fluctuations of pressure as each blade passes through the medium in which the propeller is rotating. In accordance with this, it has been found that the fundamental of the series of frequencies is the product of the frequency of rotation of the shaft into

Table IV.

Relative Amplitude of Harmonics.

Frequency	210	220	240	250	260	280	300
Amplitude	0·4	0·49	0·85	1·0	0·83	0·45	0·28

the number of blades of the propeller. This may be termed the " propeller frequency " and is the characteristic rhythm observed when listening to the propeller sound.

In both the investigations referred to above, it has been observed that the character of the series as shown by the relative magnitude of the harmonics varies with the speed of the propeller. As no adequate explanation has been given for this variation of character with speed, some of the results will be considered here in the light of the theory developed in § III. In the paper by Barlow and Keene it is stated that "it has not been possible to explain the variation completely, but it is partly due to the change in motor frequency." In the paper by Fage it is attributed to the fact that a resonator instrument was used to measure the amplitude of the harmonics so that measurements "are not necessarily representative of the intensity of the note." A resonator instrument is not the ideal instrument for the purpose of these measurements, as is shown in Barlow and Keene's results,

where the effect of resonance has been to introduce progressive distortion in the measurement of amplitude throughout the series. In Fage's results, however, which are reproduced in fig. 7, it is apparent that the resonant instrument which has been employed has not introduced progressive distortion, so that it is reasonable to assume that the relative magnitude of the harmonics are as given. If we make this assumption it is possible to explain the results obtained with varying speed remarkably well from the theory.

Before considering these results in detail it will be necessary to see how the case of the rotating propeller is

Fig. 7.

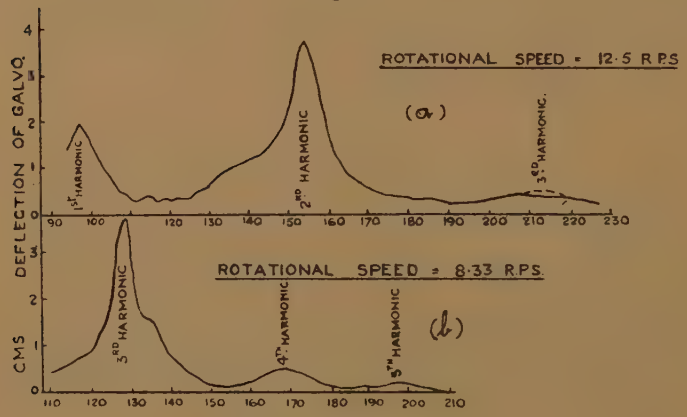

analogous to that of the electrical circuit taken in the theoretical analysis. Assuming that cavitation occurs near the blade as the propeller rotates, it will be realized that the fluctuations of pressure tend to force a blade into one or other of its natural modes of vibration. The forcing frequency will thus be the "propeller frequency," and will correspond to $f=1/\tau$, the frequency at which the condenser is charged in the electrical case. Also the natural frequency and the mechanical damping of the blade will have their counterparts in F the natural frequency and a the decay coefficient of the oscillations in the electrical circuit.

The figures we take from the paper by Fage are for a four bladed airscrew at speeds of rotation of 12·5, 15·95, and 8·33 r.p.s. As will appear later, the damping is not

excessive, so that the simpler expression (3) for the amplitude of the component frequencies can be used.

We have

$$A_n = \frac{\frac{B\omega p}{\pi}}{\sqrt{[(a^2+\omega^2 n^2-p^2)^2+4a^2p^2]}}$$

$$= \frac{\frac{B}{\pi}\cdot\frac{f}{F}}{\sqrt{\left[\left(\frac{a^2}{4\pi^2F^2}+\frac{f^2}{F^2}\cdot n^2-1\right)^2+\frac{4.a^2}{4\pi^2F^2}\right]}}$$

$$= \frac{Q.f}{\sqrt{[(S+Rn^2-1)^2+4S]}},$$

where Q=constant,

R=square of ratio $\frac{\text{propeller frequency}}{\text{blade frequency}}=\frac{f^2}{F^2}$,

and S depends upon damping and is also assumed constant over the range of measurements.

In fig. 7 the upper curve (*a*) shows the observed amplitudes of the first, second, and third harmonics at a speed of rotation of 12·5 r.p.s., *i. e.*, a propeller frequency of 50 p.p.s. From these values the appropriate values of Q, R, and S have been calculated which give the nearest approximation to the measured values. Thus we find that the amplitude in cm. in the figure is given by

$$A_n = \frac{0{\cdot}0188f}{\sqrt{[(0{\cdot}006+0{\cdot}132\,n^2-1)^2+0{\cdot}024]}}.$$

From these figures it will be seen that the simpler expression for A_n is sufficiently accurate to give the amplitudes of the component frequencies within 2 per cent.

A comparison between the calculated and the measured values is given in Table V.

Now it will be shown that the theory is capable of explaining the variation of amplitude obtained on varying the speed of rotation. If the airscrew speed is varied Q and S remain constant, but R varies according to the square of the ratio of the new speed to the original speed of 12·5 r.p.s. Taking the appropriate value for R in each case the amplitudes of certain of the harmonics

have been calculated for rotational speeds of 8·33 r.p.s. and 15·95 r.p.s. respectively. These are given in Tables VI. and VII.

The measured values at 8·33 r.p.s. are taken from fig. 7 (*b*). No measured values are given in the paper by Fage for

TABLE V.

$f=4\times12{\cdot}5$ p.p.s.

Amplitude of Harmonics.

Harmonic.	First. $n=2$.	Second. $n=3$.	Third. $n=4$.
A_n calculated	1·92	3·80	0·84
A_n measured.....	1·90	3·80	0·60

TABLE VI.

$f=4\times8{\cdot}33$.

Amplitude of Harmonics.

Harmonic.	Second.	Third.	Fourth.	Fifth.
A_n theory	1·27	3·80	1·27	0·56
A_n measured.....	—	3·80	0·70	0·40

TABLE VII.

$f=4\times15{\cdot}95$.

Amplitude of Harmonics.

Harmonic.	First.	Second.	Third.
A_n theory	5·90	1·26	0·49

15.95 r.p.s., but it is observed that "at 12·5 r.p.s. the second harmonic is more pronounced than the first although the reverse was the case at 15·95 r.p.s."

It will be seen from the above that there is nothing anomalous in the first harmonic becoming more pronounced than the second for the particular change of speed, but is to be expected from theory.

The theory thus provides a means of calculating the values of the various harmonics knowing the propeller

frequency and the natural frequency of the blade. Alternatively if the relative amplitudes of the harmonics can be measured accurately at a given rotational speed, the theory is capable of determining the natural frequency of the blade.

Thus for the measured values given in fig. 7 (*a*) we have found that

$$\left(\frac{f}{F}\right)^2 = 0{\cdot}132 \text{ at } 12{\cdot}5 \text{ r.p.s.},$$

from which we find that

$$F = 138 \text{ p.p.s.}$$

In the paper by Fage the frequency of lateral vibration of the blade of the airscrew used in the above measurements has been determined theoretically. Since the measured values of the modulus of elasticity of the material of the propeller were found to vary by 10 per cent. the theoretical value for the natural frequency of the blade was found to lie between 129 p.p.s. and 135·5 p.p.s. Under these conditions the value derived above may be regarded as in good agreement.

The experiments of Barlow and Keene were made with an Evinrude motor boat at a rotational speed of about 10 p.p.s. With an outboard engine such as was employed, the frequencies reaching the receiver were not entirely rotational, but partly due to direct vibrations of the motor. For this reason the results observed on analysis consist of a harmonic series whose fundamental has a frequency corresponding to the speed of the motor. Since the rectifier method of analysis was used the fundamental and early harmonics are also considerably enhanced due to subharmonic responses.

But if we ignore these the remainder of the harmonic series definitely exhibits the same behaviour as found with the airscrew. Two sets of analyses are given at speeds approximately of 10·2 r.p.s. and 11·4 r.p.s., and in each case three analyses are given using a resonant receiver tuned respectively to 40 p.p.s., 78 p.p.s., and 120 p.p.s. By comparing the results the approximate effect of resonance has been determined, and on making allowance for this the amplitudes of the harmonics beyond the third have been adjusted appropriately. The results are given in fig. 8.

The amplitudes thus determined for the three analyses at each speed lie between the broken lines, and it will be seen that qualitatively they show the same character as given more exactly in the case of the airscrew. Thus on reducing the speed from 11·4 r.p.s. to 10.2 r.p.s. the fifth harmonic is depressed and the sixth raised in value, thus indicating a natural frequency in the propeller system of about 70 p.p.s.

In conclusion it will be noted that the theory indicates certain differences in type between the sound spectrum from an airscrew and that from an under-water propeller.

Fig. 8.

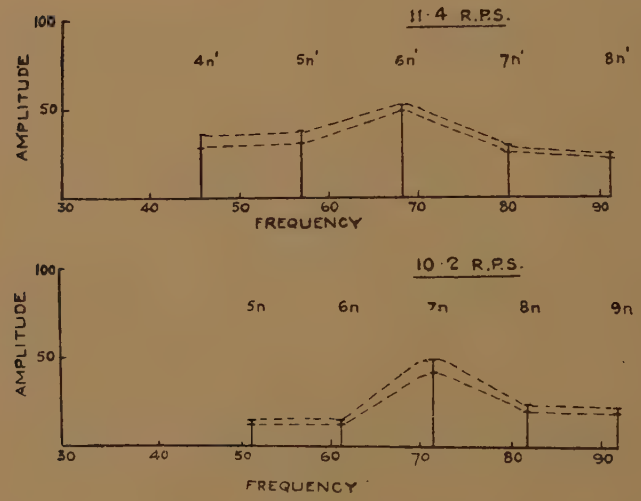

The speed of rotation of the latter is much lower, a propeller frequency from 5–10 p.p.s. being usual. A closer line spectrum is therefore to be anticipated. Also the damping in the case of water is heavier, and, as can be seen from the theoretical formula, this has the effect of reducing the relative magnitude of the maximum harmonic. This point is illustrated in the two examples given, the maximum in the case of the motor boat being only slightly greater than adjacent harmonics. With larger under-water propellers this effect is more marked, and many experiments made by the author have shown the absence of any frequency or region of maximum energy emission.

This is in agreement with the conclusion drawn from their experimental evidence by Barlow and Keene.

§ III. Theoretical Investigation of the Analysis of a Series of Damped Waves.

1. If a system whose natural frequency is $\frac{p}{2\pi}$ is set into vibration by an external stimulus applied momentarily at intervals of time τ, a series of free damped vibrations repeated at the regular intervals of time τ will be produced, of which the initial form is

$$f(t) = Ae^{-at} \sin pt,$$

where a is the decay coefficient of the system.

On analysis this leads to a harmonic series in which the amplitudes of the harmonics exhibit a maximum.

The case which will be considered here is that of a circuit containing inductance, resistance and capacity set into oscillation by a voltage applied at regular intervals to the condenser, but the results will be equally applicable to the analogous case of a mechanical system capable of sustaining vibrations.

2. As is well known, if a condenser is charged to a potential V_0 and then connected to a circuit containing inductance L and resistance R, oscillations are produced provided $R^2 < \frac{4L}{C}$. We will consider the case of moderate damping when R^2 is small compared with $\frac{4L}{C}$. In this case the variation of voltage across the condenser and of the current in the circuit are given by

$$V = V_0 e^{-at} \cos pt$$

and

$$i = V_0 \cdot \sqrt{\frac{C}{L}}\, e^{-at} \cdot \sin pt,$$

where $a = \frac{R}{2L}$ and $p = \frac{1}{\sqrt{LC}} = 2\pi . F$ (natural frequency of circuit).

When the voltage V_0 is applied at intervals of time τ the steady conditions finally attained will depend upon the relative values of p and τ. In general the frequency F of the oscillations in the circuit will not be an exact multiple

of the frequency at which the voltage V_0 is applied to the condenser.

We therefore put

$$p = \frac{2\pi N}{\tau} + \epsilon,$$

where $0 < \epsilon\tau < 2\pi$ and N is an integer.

Under these conditions it can be shown that the ensuing oscillations are eventually given by

$$V = \frac{V_0}{1 - e^{-a\tau} \cdot \cos \epsilon\tau} \cdot e^{-at} \cos pt$$

$$= V_0 \cdot \psi \cdot e^{-at} \cos pt$$

$$i = V_0 \cdot \psi \cdot \sqrt{\frac{C}{L}} \cdot e^{-at} \sin pt. \quad . \quad . \quad . \quad (1)$$

Both of these expressions can be represented as a Fourier Series of fundamental frequency

$$f = \frac{1}{\tau} = \frac{\omega}{2\pi};$$

thus

$$f(t) = a_0 + a_1 \cos \omega t + a_2 \cos 2\omega t + \ldots + a_n \cos n\omega t \ldots$$
$$+ b_1 \sin \omega t + b_2 \sin 2\omega t + \ldots + b_n \sin n\omega t \ldots$$
$$= A_0 + A_1 \sin (\omega t + \phi_1) + A_2 \sin (2\omega t + \phi_2)$$
$$\ldots + A_n \sin (n\omega t + \phi^n) \ldots$$

where $A_n^2 = a_n^2 + b_n^2$.

The expression (1) for the current i is of immediate interest and will be considered here.

In this case

$$a_0 = \frac{B \cdot \psi}{\tau} \int_0^\tau e^{-at} \sin pt \cdot dt,$$

$$a_n = \frac{2B\psi}{\tau} \int_0^\tau e^{-at} \sin pt \cdot \cos \omega nt \cdot dt,$$

and

$$b^n = \frac{2B\psi}{\tau} \int_0^\tau e^{-at} \sin pt \cdot \sin \omega nt \cdot dt,$$

where

$$B = V_0 \sqrt{\frac{C}{L}}.$$

Evaluating these integrals we find that

$$A_0 = \frac{B\omega}{\pi} \cdot \left[\frac{p - a\phi}{p^2 + a^2}\right],$$

$$A_n = \frac{B\omega}{\pi} \cdot \sqrt{\left[\frac{kp^2}{(a^2+\omega^2n^2-p^2)^2+4a^2p^2}\right]}, \quad . \quad (2)$$

where $$k = 1 - 2\frac{a}{p} \cdot \phi + \frac{a^2+\omega^2n^2}{p^2} \cdot \phi^2$$

and $$\phi = \frac{e^{-a\tau} \cdot \sin \epsilon\tau}{1 - e^{-a\tau} \cdot \cos \epsilon\tau}.$$

For any given value of $a\tau$, ϕ has a maximum value. These have been calculated for a few values of $a\tau$ and are as follows :—

Values of ϕ.

ϕ	∞	2·94	1·44	0·9	0·5	0·22	0·13	0·05	0·08
$a\tau$	0	0·1	0·2	0·4	0·8	1·6	2·0	3·0	4·0

Assuming $\frac{a}{p}$ to have a value 0·1 which corresponds to moderate damping we see that $k=1$ within an error of one per cent. provided $a\tau > 3{\cdot}0$, *i. e.*, $p\tau > 30$. The amplitude of the harmonics is then given by

$$A_n = \frac{\frac{B\omega p}{\pi}}{\sqrt{[(a^2+\omega^2n^2-p^2)^2+4a^2p^2]}}. \quad . \quad . \quad (3)$$

It will be seen from (3) that the amplitude A_n approaches a maximum as $\omega^2n^2 - p^2$ approaches zero.

The above expression is also obtained if we put $\epsilon = 0$ or $\phi = 0$ in (2), that is, if the natural frequency of the oscillations is an exact multiple of the frequency at which the voltage V_0 is applied to the condenser, in which case $\omega n = p$ and the harmonic of maximum amplitude is that having a frequency equal to the natural frequency of the oscillations.

The analysis of the vibrations of such a system will therefore present a harmonic series of which the fundamental frequency will be that at which the external

force is applied, and the term of greatest amplitude will be the harmonic whose frequency is nearest to the natural frequency of the system.

3. These results will also apply if the frequency $\frac{\omega}{2\pi}$ is subject to slow changes in value, the effect being to move the maximum amplitude from one harmonic to another. This is best seen by an example. If we take $p=4000$, $a=300$, and calculate the values of $\frac{A_n}{B}$ for various values of $\frac{p}{\omega}$ we get the following :—

Values of $\frac{A_n}{B}$.

	1.	2.	3.	4.	5.	6.	7.	8.	9.
$\frac{p}{\omega}=6{\cdot}0$	·054	·059	·069	·093	·154	·331	·134	·067	·042
$\frac{p}{\omega}=6{\cdot}37$	·050	·055	·063	·080	·121	·260	·188	·082	·058
$\frac{p}{\omega}=6{\cdot}44$	·048	·051	·057	·070	·118	·218	·224	·094	·06
$\frac{p}{\omega}=7{\cdot}0$	·046	·049	·055	·066	·089	·145	·274	·125	·064

These are shown graphically in fig. 9. No meaning is to be attached to the curves other than that they connect points representing the values obtained for one set of conditions. It is apparent that as ω is reduced from $\frac{p}{6}$ to $\frac{p}{7}$ the sixth harmonic is depressed and the seventh raised.

Curves are given in fig. 10 which show the continued change of amplitude of the sixth and seventh harmonic respectively with the frequency $\frac{\omega}{2\pi}$. It will be noticed that the amplitude changes most rapidly when ω has a value intermediate between those required to give a maximum amplitude to the sixth and seventh harmonic respectively.

Fig. 9.

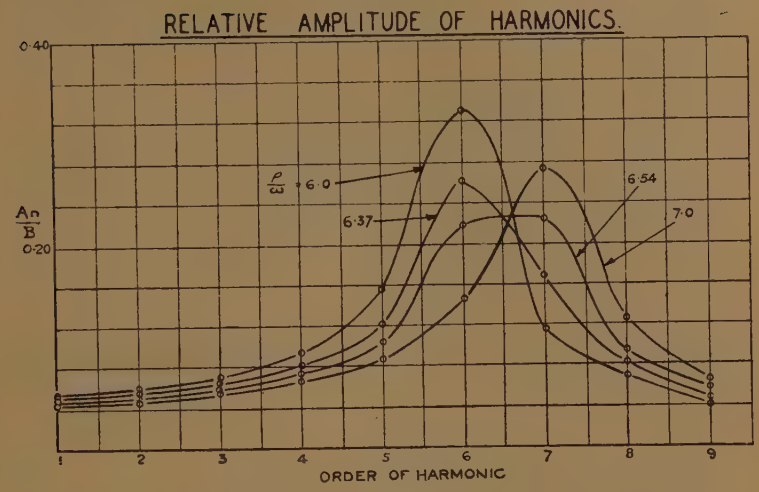

Fig. 10.

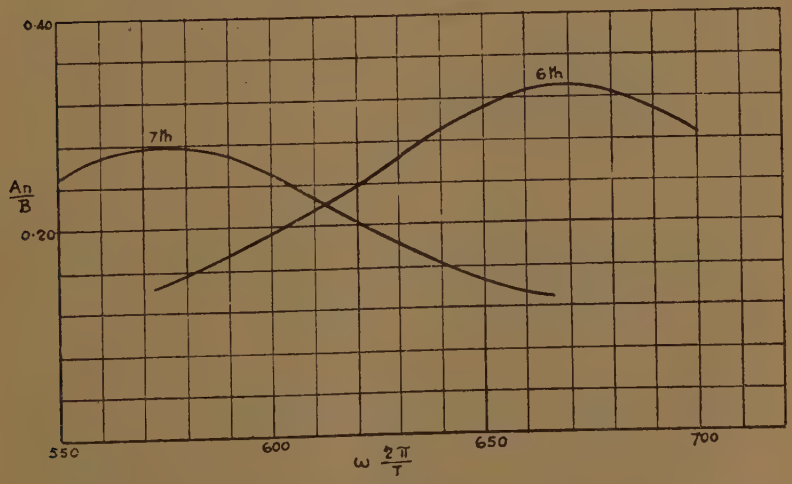

§ IV. String Electrometer.

Force on the String.

The force acting on the string can be determined from fundamental energy considerations.

It is assumed that the string is initially at earth potential and the plates respectively at $\frac{V}{2}$ and $-\frac{V}{2}$. On applying a potential v to the string there is a deflexion of the string towards one of the plates.

This has the effect of increasing the capacity between the string and one plate and reducing the capacity between the string and the other plate by an equal amount. Energy is therefore stored in the string and we have an increase in energy in moving towards one plate

$$E_1 = \tfrac{1}{2}\, dC\left(\frac{V}{2}+v\right)^2,$$

and a decrease in energy in moving away from the other plate

$$E_2 = \tfrac{1}{2}\, dC\left(\frac{V}{2}-v\right)^2,$$

where dC is taken as the change of capacity between unit length of string at the centre and the respective plate.

Hence the nett energy per unit length of string is

$$E = V v\,.\,dC. \quad . \quad . \quad . \quad . \quad . \quad . \quad (1)$$

Now assuming that the restoring force acting on unit length of the string is proportional to deflexion, we have work done in deflecting string

$$= \int_0^{\Delta} R\,.\,x\,.\,dx = \frac{R\Delta^2}{2} \text{ ergs},$$

where R=restoring force per unit length per unit deflexion in dynes/cm. (this may be assumed constant for a given tension of the string) and Δ=deflexion in cm.

Also if v and V are in volts and dC in cm. we have

$$E = \frac{V\,.\,v\,dC}{9\times 10^4} \text{ ergs.} \quad . \quad . \quad . \quad . \quad . \quad (2)$$

For a string of such small diameter, the capacity between unit length and one of the plates will be given very nearly by the expression for the capacity between a cylinder and an infinite plate, *i. e.*,

$$C = \frac{1}{2\log_e \frac{2h}{r}} \text{ cm.},$$

where h=distance between string and plate in cm. and r=radius of string in cm.

By differentiation

$$\frac{\partial C}{\partial h}=\frac{1}{2h\left(\log_e\frac{2h}{r}\right)^2},$$

so that for a deflexion of Δ cm. we have

$$dC=\frac{\Delta}{2h\left(\log_e\frac{2h}{r}\right)^2}. \quad . \quad . \quad . \quad . \quad . \quad (3)$$

From the equations (1), (2), and (3) we obtain R in terms of known quantities as follows :—

$$R=\frac{1{\cdot}11\times10^{-5}\,\frac{Vv}{\Delta}}{h\left(\log_e\frac{2h}{r}\right)^2}\text{ dynes/cm.}^2 \quad . \quad . \quad . \quad (4)$$

It has been found by measurement that Δ=K vV, where K is a constant, from which it follows that the assumption that R is constant for a given string tension is justified. The value of the constant K is therefore

$$K=\frac{1{\cdot}11\times10^{-5}}{R\,.\,h\left(\log_e\frac{2h}{r}\right)^2}. \quad . \quad . \quad . \quad . \quad . \quad (5)$$

Damping of the String.

The equation of motion of the string when damping is present is

$$m\ddot{x}+N\dot{x}+Rx=F, \quad . \quad . \quad . \quad . \quad . \quad (6)$$

where

m=mass per unit length in gm.

R=restoring force per unit length in dynes/cm.

and

N=damping factor.

In fig. 11 is given the deflexion of the string as measured from a record, due to a voltage suddenly applied to the string. It will be seen that the string is heavily damped. A similar record is obtained, but in the reverse order if, with the string deflected, the voltage on the plates is

suddenly removed, showing that the damping must be air damping.

The appropriate solution of the equation of motion in this case is

$$x = \mathrm{X}\left[1 - e^{-at}\left(\cos pt + \frac{a}{p}\sin pt\right)\right],$$

where

$$a = \frac{\mathrm{N}}{2m},$$

$$\mathrm{X} = \frac{\mathrm{F}}{\mathrm{R}},$$

Fig. 11.

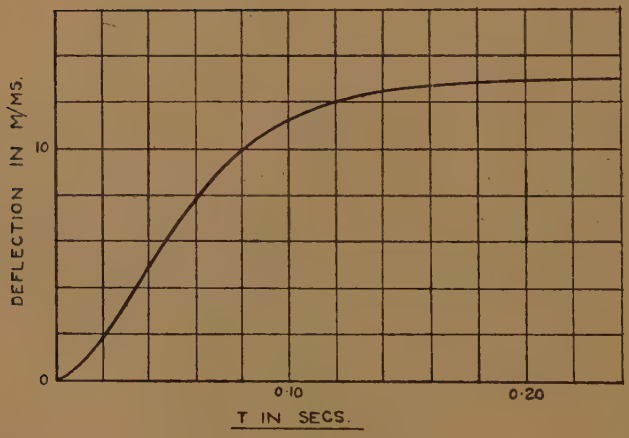

and

$$p = \sqrt{\left[\frac{\mathrm{R}}{m} - a^2\right]}.$$

From the record it is found that $a=29$ and $p=13$.

It can be assumed that the motion of the string is at its fundamental frequency, so that the natural undamped frequency of the string is given by

$$\omega = 2\pi f,$$

where

$$\omega^2 = \frac{\mathrm{R}}{m} = p^2 + a^2$$

$$= 1013,$$

$$\omega = 31{\cdot}8.$$

We see that the string is very nearly critically dead beat, the condition for this being $\frac{N}{m}=2\omega$.

Values of Constants.

The values of the constants for the particular string used in these measurements have been derived as follows:—

Determination of m.

Measured resistance of gold sputtered quartz fibre= 2000 ohms/cm.

Measured radius of fibre$=3{\cdot}5\times10^{-4}$ cm.

Resistance of fibre$=\frac{\phi}{\pi\, dt}$ per unit length,

where

ϕ=sp. resist. of gold$=2{\cdot}42\times10^{-6}$ ohm

and

t=thickness of gold.

Hence

$$\pi\, dt=\frac{\phi}{2000}=1{\cdot}21\times10^{-9}.$$

Also mass of fibre

$$m=\pi r^2\rho_1+\pi\, dt\,\rho_2,$$

where

ρ_1=density of quartz$=2{\cdot}66$

and

ρ_2=density of gold$=19{\cdot}32$,

so that

$m=1{\cdot}025\times10^{-6}$ gm./cm.

Determination of R, K, and ω.

For the record of deflexion shown

V$=32{\cdot}5$ volts $v=1{\cdot}1$ volt

and

Δ=deflexion$=2{\cdot}95\times10^{-2}$ cm.

Also

$h=0{\cdot}25$ cm., $r=3{\cdot}5\times10^{-4}$ cm.,

so that

$$\mathrm{R}=1{\cdot}11\times10^{-5}\frac{\mathrm{V}v}{\Delta h\left(\log_e\frac{2h}{r}\right)^2}\text{ dynes/cm.}^2$$

$$=1{\cdot}01\times10^{-3}\text{ dynes/cm.}$$

$$K = 8{\cdot}26 \times 10^{-4} \text{ cm./volt.}^2$$

and $$\omega = \sqrt{\frac{R}{m}} = 31{\cdot}4.$$

Determination of Damping Factor N.

The second term in equation (4) is the resistance per unit length due to air damping.

Lamb has given a formula for determining the resistance per unit length for uniform flow of a medium past a circular cylinder which is of interest[7].

The formula reduces to

$$\text{resistance per unit length} = \frac{4\pi\mu \,.\, U}{2 - \log_e R},$$

where U=velocity of medium.

μ=viscosity of medium.

$R = \text{Reynolds number} = \frac{Ud}{\nu}$.

d=diameter of cylinder.

ν=kinematic viscosity of medium.

The formula is valid only when R is small.

Assuming that the formula can be applied to the case of a string vibrating in air we see that the damping factor in this case is given by

$$N = \frac{4\pi\mu}{2 - \log_e R}.$$

For sinusoidal vibrations it can be shown that the second term of the denominator is very nearly constant for small values of R, the value of R used being that for the maximum velocity.

In the present case we have

$$R = 4{\cdot}7 \times 10^{-3}.$$

$$U = \omega \,.\, \Delta = 0{\cdot}94 \text{ cm./sec.}$$

$$\mu = 1{\cdot}81 \times 10^{-3} \text{ dynes/cm.}^2 \text{ sec.}$$

so that $$N = 3{\cdot}1 \times 10^{-4} \text{ dynes/cm.}^2 \text{ sec.}$$

From measurements on the record we have found that $a = 29$, so that

$$N = 2\,m \,.\, a = 0{\cdot}6 \times 10^{-4} \text{ dynes/cm.}^2 \text{ sec.}$$

The value determined by measurement is thus of the same order, but of much lower value than that given by the formula. This is in general agreement with experi-

ment, for from measurements on the drag of wires it appears that values deduced from the formula for Reynolds numbers from 0·5–2·0 are about twice the measured values. No measurements at Reynolds numbers of the order of 10^{-3} are available for comparison, but as the resistance values are increasing asymptotically in this region it is probable that the measured value is more correct than the calculated.

Summary.

A method of harmonic analysis of the dynamometer type is described. A string electrometer is employed, the e.m.f. to be analysed being applied to the string, while an analysing e.m.f. of variable frequency is applied to the plates. The frequency of this analysing e.m.f. is varied continuously, and the ensuing deflexions of the string, corresponding to the various component frequencies of the e.m.f. under examination, are recorded photographically. In this way an automatic frequency calibration of the record is obtained, and the amplitudes of the various components can be measured directly from the record without the necessity for determining their phase differences.

The method of analysis is applied to various electric and acoustic problems, in particular to the analysis of a series of electrical impulses.

A general theoretical analysis for a series of impulses is given, and this is applied to the explanation of the results obtained on analysing the sounds of rotation from screw propellers.

Formulæ are derived for determining the constants of a string electrometer.

Acknowledgment.

The author is indebted to the Admiralty for permission to publish this paper.

References.

(1) Duncan, Trans. Amer. Inst. El. Engs. ix. p. 179 (1892).
(2) Lyle, Phil. Mag. vi. p. 549 (1903).
(3) Greenwood, Wireless Eng. ix. p. 301 (June 1932).
(4) Nicholson and Perkins, Proc. Inst. Rad. Engs. xx. p. 734 (April 1932).
(5) Barlow and Keehne, Phil. Trans. Roy. Soc. p. 155 (1932).
(6) Fage, Proc. Roy. Soc. A, cvii. p. 451 (1925).
(7) Lamb, Phil. Mag. p. 120 (1911).

XLV. *On Fractional Differentials.* *By* ANDREW GEMANT. (Communicated from the Imperial College of Science and Technology, University of London.) *.

1. THE following note is concerned with the half-differential quotients of a few well-known functions, the result being presented by means of curves, constructed by numerical evaluation. The purpose of the presentation is to illustrate the main features of fractional differential quotients.

Generalized differentials have originally been dealt with by Riemann [1] and by Liouville [2]; but it was Heaviside [3] who has made a more extensive use of them in his operational calculus for the solution of electrical transient problems. Among more recent contributions those by J. R. Wilton [4], E. L. Post [5], A. Zygmund [6], and W. Fabian [7] should be mentioned.

There are several mathematical possibilities to establish a generalized differential and integral calculus of any fractional order, and, indeed, the papers quoted above contain several different propositions. From a purely mathematical standpoint they are more or less equally justified. From a physical standpoint, however, preference ought to be given to that system which is capable of physical applications. This is the case with the system used among others by Heaviside, and which therefore should also be considered in the following note. Two of the possible physical applications will be quoted at the end of this paper.

2. In order to give the basic definition utilized in this system let us consider a function

$$y=f(x) \quad . \quad . \quad . \quad . \quad . \quad . \quad (1)$$

which can be expanded into a power series with positive exponents, thus:

$$y=a+bx+cx^2+ \ldots \quad . \quad . \quad . \quad . \quad . \quad . \quad (2)$$

If a rule can be found to deal with the general term hx^n, any such function could be treated accordingly. Now the general rule for differentiating $y=hx^n$ gives for the qth differential quotient (q any integer):

$$y^{(q)}=h.n(n-1)\ldots(n-q+1).x^{n-q}.$$

* Communicated by Prof. A. C. Egerton, M.A., F.R.S.

This may be written :

$$y^{(q)}=h\frac{n!}{(n-q)!}x^{n-q}. \quad . \quad . \quad . \quad . \quad (3)$$

There is, however, no restriction in applying eq. (3) to any value of q, whether integer or fraction, since the factorial has not only a meaning for integers, but—by introducing the Legendre Γ-functions or Gauss Π-functions—for any value of the argument q. Thus eq. (3) is a possible definition for generalized differentials, and should be used as a basis for the following.

Negative values of q refer to integrals instead of differentials, which, however, should not be dealt with here.

Our definition involves that the general operator q is of an additive character. In order to show this let us differentiate the function hx^n to the qth order, where q is any number, thus obtaining (3). With this function $y^{(q)}$ a second differentiation should be performed, say to the q_1th order. The result is

$$(y^{(q)})^{(q_1)}=h\frac{n!}{(n-q)!}\frac{(n-q)!}{(n-q-q_1)!}x^{n-q-q_1}$$

$$=h\frac{n!}{[n-(q+q_1)]!}x^{n-(q+q_1)}.$$

But the last expression can be obtained more directly by carrying out the $(q+q_1)$th differentiation with the original function. Thus we have the result

$$(y^{(q)})^{(q_1)}=y^{(q+q_1)}.$$

A half-differential, or integral, for instance, is an operation, which, performed twice, leads to the first differential or integral.

It should be recalled that (3) is only applicable for positive exponents n. If function (1) is expanded into a series with negative exponents another rule is valid instead of (3). Having

$$y=hx^{-n}$$

(n positive), we obtain

$$y^{(q)}=hj^{2q}\frac{(n+q-1)!}{(n-1)!}x^{-(n+q)}, \quad . \quad . \quad . \quad (5)$$

involving complex values for fractional q. With

$$y=\frac{1}{x}$$

for instance we have

$$y^{(0\cdot5)} = j\frac{0\cdot886}{x^{1\cdot5}}.$$

Fig. 1.

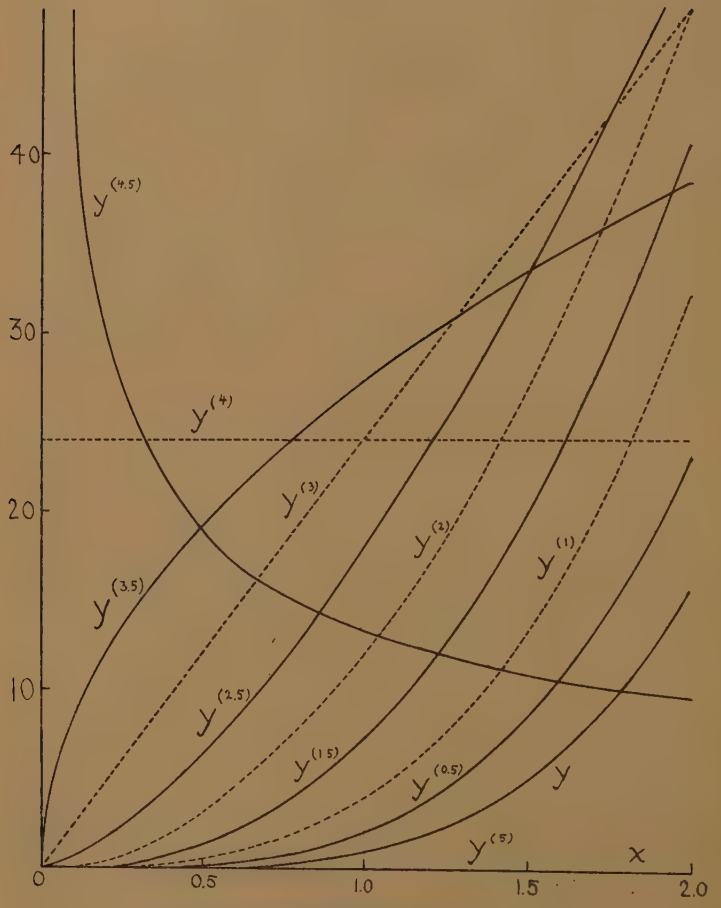

Fractional differential quotients for $y=x^4$.

3. First an elementary application of (3) should be given, starting from the equation

$$y=x^4.$$

In fig. 1 a series of fractional differential quotients is plotted as full lines against the variable x between $x=0$

and 2·0. The intermediate differentials of integer order are plotted as dotted curves, and it can be seen that the fractional functions are a sort of interpolation between the integer ones; $y^{(0\cdot5)}$, for instance, is given by

$$y^{(0\cdot5)} = \frac{4!}{3\cdot5!}x^{3\cdot5} = 2\cdot062x^{3\cdot5}.$$

Note that $y^{(3\cdot5)}$ passes, somewhat unexpectedly, above the crossing point of $y^{(3)}$, and $y^{(4)}$. $y^{(4\cdot5)}$ is represented by

$$y^{(4\cdot5)} = \frac{4!}{(-0\cdot5)!}\frac{1}{\sqrt{x}} = \frac{13\cdot53}{\sqrt{x}},$$

Fig. 2.

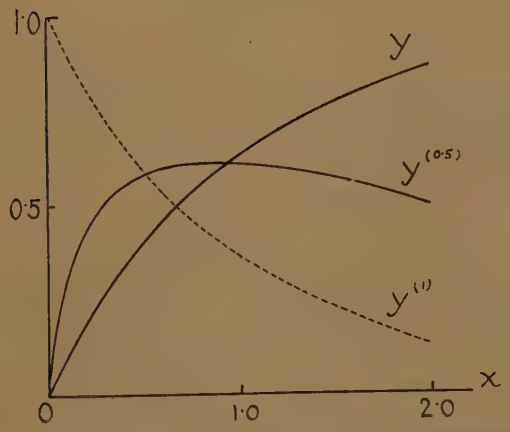

Half differential quotient of the negative exponential function.

starting with ∞ for $x=0$, crossing $y^{(4)}$ at $x=\frac{1}{\sqrt{\pi}}$, and reaching $y^{(5)}$ asymptotically.

It will be seen from the equations that the continuation of the fractional curves for negative values of the variable x will lie on complex planes.

Next the negative exponential function

$$y = 1 - e^{-x}$$

should be chosen, shown in fig. 2. The first differential quotient

$$y^{(1)} = e^{-x}$$

is shown too. In order to calculate the half-differential y has to be expanded into a power series :

$$y=x-\frac{x^2}{2}+\frac{x^3}{6}-\cdots$$

Applying (3) the half-differential will be

$$y^{(0\cdot5)}=\frac{x^{0\cdot5}}{0\cdot5\,!}-\frac{x^{1\cdot5}}{1\cdot5\,!}+\frac{x^{2\cdot5}}{2\cdot5\,!}-\cdots$$

This function, as shown on the figure, is a kind of interpolation between the two others. It is worth mentioning that the last series can be expressed by means of a finite integral which is tabulated [8]. It is

$$(1-e^{-x})^{(0\cdot5)}=\frac{2e^{-x}}{\sqrt{\pi}}\int_0^{\sqrt{x}}e^{x^2}\,dx. \quad . \quad . \quad . \quad (6)$$

Whereas the half-differential of the negative exponential can be expressed by means of the finite integral in eq. (6), that of the positive exponential is an analogous function of the error-integral Φ:

$$(e^x-1)^{(0\cdot5)}=e^x\Phi\sqrt{x}. \quad . \quad . \quad . \quad . \quad . \quad (7)$$

One could object to our system of generalized differentiation in pointing out that, while each integer differential quotient of e^x is again e^x, the fractional ones have a different value. This is, however, not a serious disadvantage. Differentiating to the qth order, we obtain

$$(e^x)^{(q)}=\frac{x^{-q}}{(-q)\,!}+\frac{x^{1-q}}{(1-q)\,!}+\frac{x^{2-q}}{(2-q)\,!}+\cdots \quad . \quad (8)$$

In fig. 3 eq. (8) is represented for the parameter $x=1\cdot0$ and $0\cdot5$ as a function of q from $q=0$ to $4\cdot0$. It can be seen that they are oscillatory functions, possessing the same value (e^x) for any integer value of the abscissa, and there seems to be no reason for objecting to the definition (3) because of this periodicity.

4. A further interesting series can be obtained by half-differentiating the circular function. Fig. 4 shows

$$y=\sin x$$

with

$$y^{(1)}=\cos x.$$

From the expansion

$$y=x-\frac{x^3}{3\,!}+\frac{x^5}{5\,!}-\cdots$$

Fig. 3.

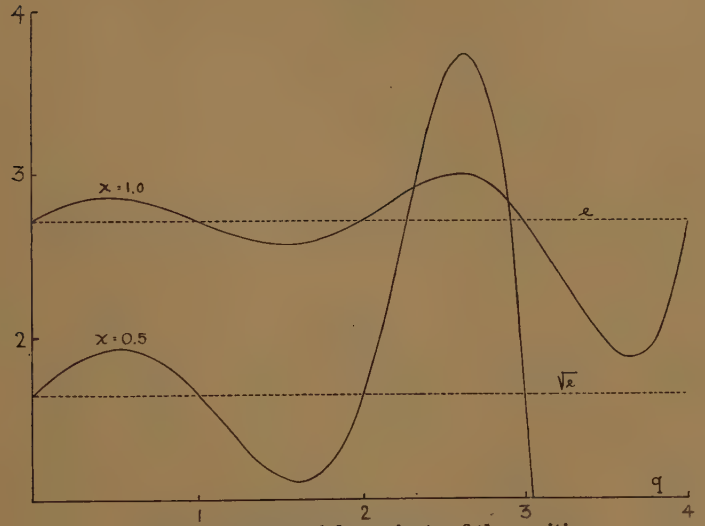

Fractional differential quotients of the positive exponential function.

Fig. 4.

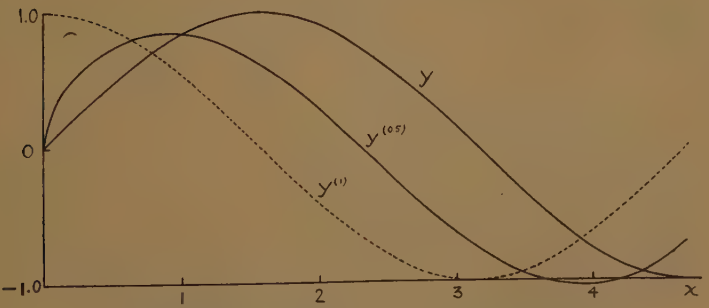

Half-differential quotient of the circular function.

one obtains

$$(\sin x)^{(0\cdot5)}=\frac{x^{0\cdot5}}{(0\cdot5)\,!}-\frac{x^{2\cdot5}}{2\cdot5\,!}+\frac{x^{4\cdot5}}{4\cdot5\,!}-\cdots \quad . \quad (9)$$

shown in the diagram *. There is the impression as if the

* The curve from $x=\pi$ onward is perhaps not quite exact, since too many terms had to be considered.

curve would reach the function sin $(x+\pi/4)$ asymptotically, shifted by the phase angle $\pi/4$ against both the sine and cosine curves. But this had to be proved more rigorously.

Fig. 5.

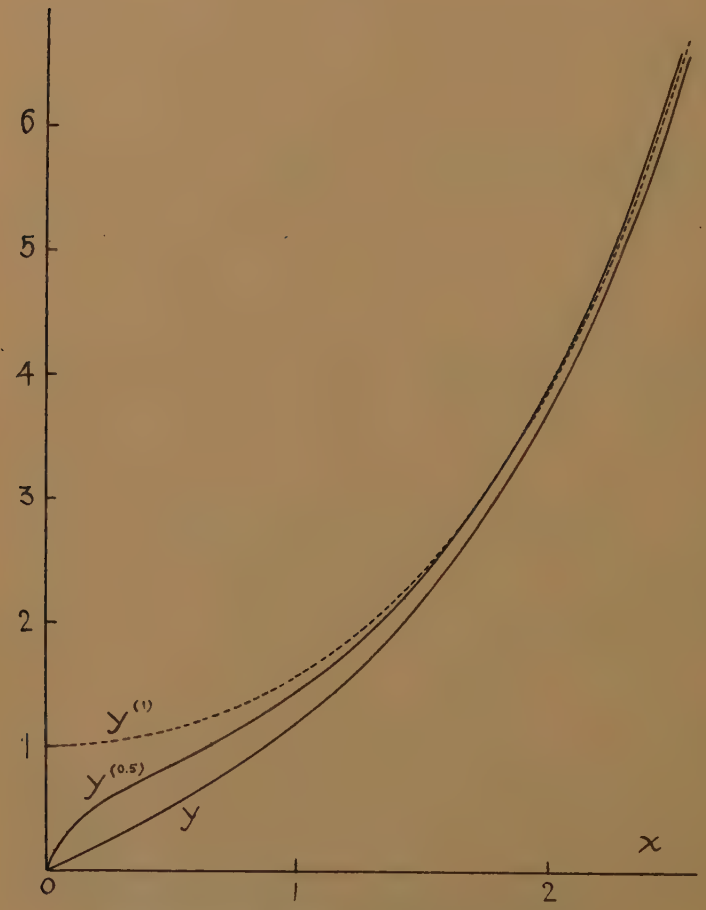

Half-differential quotient of a hyperbolic function.

In fig. 5 a hyperbolic function is dealt with. The hyperbolic sine can be expanded into

$$\sinh x = x + \frac{x^3}{3!} + \frac{x^5}{5!} + \dots$$

Accordingly the half-differential is

$$(\sinh x)^{(0\cdot5)} = \frac{x^{0\cdot5}}{0\cdot5\,!} + \frac{x^{2\cdot5}}{2\cdot5\,!} + \frac{x^{4\cdot5}}{4\cdot5\,!} + \ldots \quad . \quad (10)$$

Fig. 6.

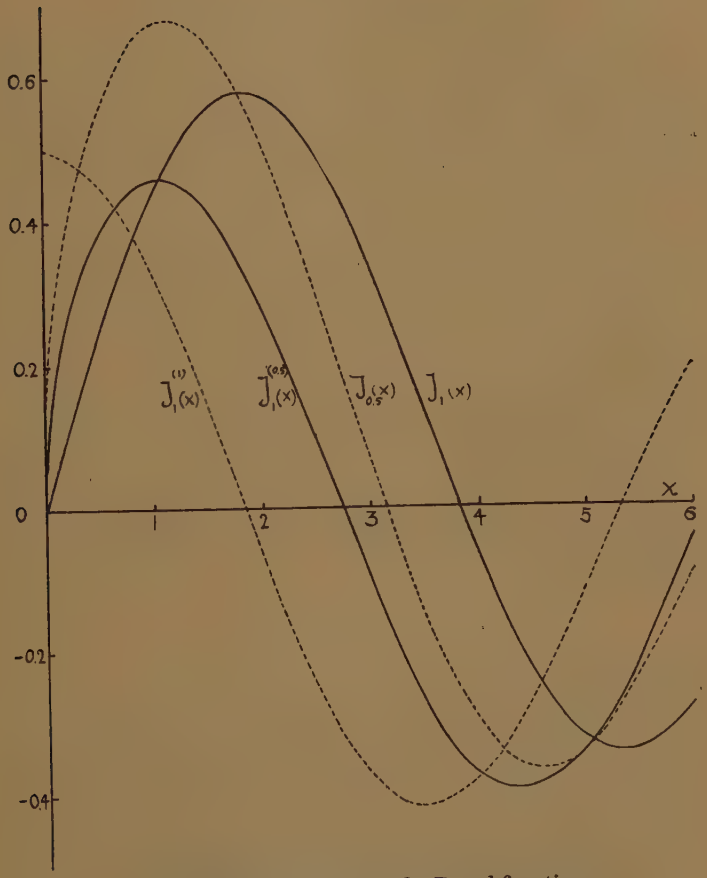

Half-differential quotient of a Bessel function.

The figure shows $\sinh x$, $\cosh x$, together with the half-differential, represented by eq (10).

The last diagram is concerned with Bessel functions. In fig. 6 are indicated $J_1(x)$, the Bessel function of the first kind and of first order, between $x=0$ and 6·0; further,

$J_1^{(1)}(x)$, the first differential quotient, and $J_1^{(0\cdot5)}(x)$, the half-differential quotient, $J_1(x)$ being given by

$$J_1(x) = \frac{(\frac{1}{2}x)}{1} - \frac{(\frac{1}{2}x)^3}{2\,!} + \frac{(\frac{1}{2}x)^5}{2\,!\,3\,!} - \cdots$$

and $J_1^{(0\cdot5)}(x)$ by

$$J_1^{(0\cdot5)}(x) = \frac{\frac{1}{2}x^{0\cdot5}}{0\cdot5\,!} - \frac{(\frac{1}{2})^3\,3\,!\,x^{2\cdot5}}{2\,!\,2\cdot5\,!} + \frac{(\frac{1}{2})^5\,5\,!\,x^{4\cdot5}}{2\,!\,3\,!\,4\cdot5\,!} - \cdots \quad (11)$$

For comparison $J_{0\cdot5}(x)$, the Bessel function of the half-order, is shown on the graph as well, and it appears, in analogy to the circular functions, as if the half-differential would reach $J_{0\cdot5}(x)$ asymptotically for large values of the argument.

5. Considering finally some physical applications, one has to bear in mind that the fractional differential quotients have only the meaning of a shorthand symbol for the corresponding mathematical operations expressed by eq. (3) or (5). In other words, they have a more formal character, and will therefore not generally occur in primary differential equations expressing basic physical laws, but only in secondary deduced equations.

Heaviside, for instance, obtains for the current J and the voltage V at the origin of an infinite cable with resistance R and capacitance C per unit length the relation

$$J = \sqrt{\frac{C}{R}}\, V^{(0\cdot5)}(t)$$

if the voltage is known as a function of the time t. In order to solve this problem evidently the unit element of the cable, with its basic differential equations, has to be considered; integration over the whole cable will then yield the relation valid at the origin, which, as it happens, can be represented by a half-differential quotient.

By deduction from experimental results on vibrational processes the author has obtained [9] for the strain S in an elasto-viscous body of a certain type, with viscosity η and shear elasticity modulus E, the relation

$$\frac{dS}{dt} = \frac{F}{\eta} + \frac{1}{\sqrt{\eta E}}\, F^{(0\cdot5)}(t),$$

if the stress F as a function of time is known. In this equation, relating to the body as a whole, the half-differential only occurs as a useful mathematical symbol, whereas the underlying elementary process, whatever it may be, will probably contain differential quotients of an integer order.

6. *Summary.*

The purpose of the paper is to illustrate the characteristic behaviour of fractional differential quotients. After a short introduction into their computation, whenever the functions involved can be expanded into power series, the fractional, especially half-differential quotients of the exponential, circular, hyperbolic, and Bessel functions, are given by means of graphical representation.

The application to physical problems of the conception is shown in two special cases.

References.

(1) B. Riemann, ' Gesammelte Werke,' Leipzig, p. 331.
(2) R. Liouville, *Journ. de l'École Polytechn.* xiii. p. 1 (1882).
(3) O. Heaviside, Electromagn. Theory, ii. p. 434 (London, 1922).
(4) J. R. Wilton, Proc. Roy. Soc. A, cxx. p. 358 (1928).
(5) E. L. Post, Trans. Amer. Mathem. Soc. xxxii. p. 723 (1930).
(6) A. Zygmund, Trigonometric Series, p. 224 (Warszawa, 1935).
(7) W. Fabian, Phil. Mag. xx. p. 781 (1935); Math. Gazette, xxi. p. 216 (1937).
(8) E. Jahnke a. F. Emde, ' Tables of Functions,' p. 106 (Leipzig, 1933).
(9) A. Gemant, ' Physics,' vii. p. 311 (1936).

XLVI. *Application of Derivatives of Line Integrals.* By W. S. Kimball, *Ph.D., Michigan State College, East Lansing, Michigan* *.

Introduction.

THE new derivative formulæ for line integrals † are applied to various special cases, including one where the vector integrand involves y' as in the Calculus of

* Communicated by the Author.

† Kimball, W. S., " Differentiation of Line Integrals by Parallel Displacement," Phil. Mag. xxv. p. 1 (1938).

Variations proper. They are best adapted to applications when adjusted to give the rates of change of that part of the dependent variable (the integral J) included between a variable point and a fixed limit along the path of integration:

$$\left.\begin{aligned}\frac{\partial J_i^n}{\partial x} = \frac{\partial J}{\partial dx} &= M(x, y) + \int_{xy}^{ab} M_x\,dx + N_x\,dy - M(a, b)\\ &\equiv \int_y^b (N_x - M_y)\,dy = \int_y^b \left(\frac{d}{dx} f_{y'} - f_y\right) dy,\\ \frac{\partial J_i^n}{\partial y} = \frac{\partial J}{\partial dy} &= N(x, y) + \int_{xy}^{ab} M_y\,dx + N_y\,dy - N(a, b)\\ &\equiv \int_x^a (M_y - N_x)\,dx = \int_x^a \left(f_y - \frac{d}{dx} f_{y'}\right) dx.\end{aligned}\right\} \quad . \quad (5)$$

Along extremal arcs these derivatives are ordinarily zero, and become identically so for integrals independent of the integration path. The second partials $\frac{\partial^2 J}{\partial x^2}$ and $\frac{\partial^2 J}{\partial y^2}$ always have the same sign along extremal arcs, being plus for relative minima and minus for relative maxima. The second partials with respect to both x and y are always equal if, and only if, J is taken along an extremal arc $\frac{\partial^2 J}{\partial x\,\partial y} = \frac{\partial^2 J}{\partial y\,\partial x}$, being of opposite sign from $\frac{\partial^2 J}{\partial x^2}$ and $\frac{\partial^2 J}{\partial y^2}$ when y' is plus and of the same sign when y' is minus. Along the extremal arcs the integrands of the second derivatives are related by

$$N_{xx} - M_{xy} = y'(M_{yy} - N_{xy}) = \text{curl } R_x = -y' \text{ curl } R_y, \quad . \quad (9)$$

where $R = iM + jN$ is the vector integrand of the integral J.

When y' is absent from this vector integrand the extremal arc is uniquely determined regardless of the limits of integration. Together with a family of null lines (curves along which $J = 0$) they constitute a characteristic pattern of extremal arcs and null lines associated with each line integral.

The line integral equal to the Calculus of Variations

integral of the type $\int g(x, y)\,ds$ along its extremal arc according to the Corollary of Theorem II. of the previous* article, and with equal vanishing derivatives on this path, is always less in magnitude than this Calculus of Variations integral along any other path than the extremal arc. Hence sufficiency conditions for a minimum of the line integral (such as positive second partial derivatives) are also sufficiency conditions for the minimum of the corresponding Calculus of Variations integral of this type.

The Calculus of Variations integral $\int(x-y)^{\frac{1}{3}}\,ds$ is shown to have infinite first partial and area derivatives for the extremal arc path $y=x$, indicating an exception to the applicability of those critical conditions that represent the vanishing of these derivatives such as the Euler and the Du Bois Raymond equations.

§ 1. *When a line integral is independent of its integration path its derivatives are identically zero.*

We consider a line integral

$$\mathrm{J}=\int_{x_0y_0}^{a,\,b}\mathrm{M}\,dx+\mathrm{N}\,dy\,;\ \text{with area derivative}\ \frac{d\mathrm{J}}{d\sigma}=\mathrm{N}_x-\mathrm{M}_y, \qquad (1)$$

whose first derivatives are given by

$$\left.\begin{aligned}\frac{\partial \mathrm{J}_i^k}{\partial x}&=\mathrm{M}(x_iy_i)+\int_{x_iy_i}^{x_ky_k}\mathrm{M}_x\,dx+\mathrm{N}_x\,dy-\mathrm{M}(x_ky_k)\\&\equiv\int_{y_i}^{y_k}(\mathrm{N}_x-\mathrm{M}_y)dy,\\ \frac{\partial \mathrm{J}_i^k}{\partial y}&=\mathrm{N}(x_iy_i)+\int_{x_iy_i}^{x_ky_k}\mathrm{M}_y\,dx+\mathrm{N}_y\,dy-\mathrm{N}(x_ky_k)\\&\equiv\int_{x_i}^{x_k}(\mathrm{M}_y-\mathrm{N}_x)\,dx,\end{aligned}\right\} \qquad (2)$$

* Kimball, W. S., *loc. cit.* § 22.

and whose second derivatives are given by

$$\left.\begin{aligned}
\frac{\partial^2 J_i^k}{\partial x^2} &= M_x(x_iy_i) + \int_{x_iy_i}^{x_ky_k} M_{xx}\,dx + N_{xx}\,dy - M_x(x_ky_k) \\
&\equiv \int_{y_i}^{y_k} (N_{xx} - M_{xy})\,dy, \\
\frac{\partial^2 J_i^k}{\partial y^2} &= N_y(x_iy_i) + \int_{x_iy_i}^{x_ky_k} M_{yy}\,dx + N_{yy}\,dy - N_y(x_ky_k) \\
&\equiv \int_{x_i}^{x_k} (M_{yy} - N_{xy})\,dx, \\
\frac{\partial}{\partial x}\left(\frac{\partial J_i^k}{\partial y}\right) &= N_x(x_iy_i) + \int_{x_iy_i}^{x_ky_k} M_{xy}\,dx + N_{xy}\,dy - N_x(x_ky_k) \\
&\equiv \int_{x_i}^{x_k} (M_{xy} - N_{xx})\,dx \equiv \int_{y_i}^{y_k} \frac{(M_{xy} - N_{xx})}{y'}\,dy, \\
\frac{\partial}{\partial y}\left(\frac{\partial J_i^k}{\partial x}\right) &= M_y(x_iy_i) + \int_{x_iy_i}^{x_ky_k} M_{xy}\,dx + N_{xy}\,dy - M_y(x_ky_k) \\
&\equiv \int_{y_i}^{y_k} (N_{xy} - M_{yy})\,dy \equiv \int_{x_i}^{x_k} (N_{xy} - M_{yy})y'\,dx.
\end{aligned}\right\} \quad . \quad . \quad . \quad (3)$$

The well-known condition that a line integral shall be independent of its path of integration is that the curl of its vector integrand shall be identically zero, which for the integral (1) becomes

$$N_x - M_y \equiv 0. \quad . \quad . \quad . \quad . \quad . \quad . \quad . \quad (4)$$

This shows by (2) that the derivatives of any part of it, such as from (x_iy_i) to (x_ky_k), are identically zero, *i. e.*, it takes on no change in case of displacement in either the x or y direction. Also the second derivatives (3) will be dientically zero, and so with higher derivatives.

§ 2. *Relative maxima and minima of line integrals are determined by the vanishing of their derivatives, whereby also the curl of the vector integrand is zero along the path of integration.*

A part of a line integral from (x_iy_i) to (x_ky_k) will ordinarily * have its extremum value when its derivatives (2)

* An exceptional case occurs when the derivatives of the integrand are discontinuous, as is the case with $\frac{dz}{dx}$ at the cusp of $z^3 = x^2$. See § 9 below.

vanish, as is the case with any ordinary function of x and y. If the integral over its entire path length is to be maximized or minimized, then the same must be true for the part of it between each and every pair of points $(x_i y_i)$ and $(x_k y_k)$ along its path, and the condition for this is given by (2) if we take $(x_i y_i)=(x, y)$ and $(x_k y_k)=(a, b)$, where (x, y) is a variable point :

$$\left.\begin{aligned} \frac{\partial \mathrm{J}}{\partial x} &= \mathrm{M}(x, y)+\int_{xy}^{ab} \mathrm{M}_x\,dx+\mathrm{N}_x\,dy-\mathrm{M}(a, b) \\ &\equiv \int_y^b (\mathrm{N}_x-\mathrm{M}_y)\,dy=0, \\ \frac{\partial \mathrm{J}}{\partial y} &= \mathrm{N}(x, y)+\int_{xy}^{a, b} \mathrm{M}_y\,dx+\mathrm{N}_y\,dy-\mathrm{N}(a, b) \\ &\equiv \int_x^a (\mathrm{M}_y-\mathrm{N}_x)\,dx=0. \end{aligned}\right\} \quad (5)$$

Here the fact that (5) is a condition upon the *variables* (x, y) is indicated by dropping the subscripts, and it will readily be seen that (5) includes every case of (2). (Use first $(x_i y_i)$ for (x, y) in (5) and then $(x_k y_k)$, and subtract, to get (2).) Also note that we could equally well have left $(x_k y_k)$ for the constant limit, or taken it as the lower limit $(x_0 y_0)$.

This variable limit feature of (5), which represents, as we see here, arbitrary limits for (2), is significant, and marks a distinction between (5) and the corresponding condition obtained by setting (62) of the previous article, or Volterra's differential (63) equal to zero, in that these latter maintain the fixed integration limits of the original integral.

Note that the vanishing of (5) implies the vanishing of the curl of the vector integrand $\mathrm{R}=i\mathrm{M}+j\mathrm{N}$ everywhere along the integration path :

$$\mathrm{N}_x-\mathrm{M}_y=0. \quad . \quad . \quad . \quad . \quad . \quad . \quad (6)$$

Eq. (5) and (6) hold everywhere along an extremal arc, but are *not* identities. This is in contrast to (4), which is identically zero where the line integral is independent of the integration path.

§ 3. *When* (1) *is a relative extremum, then* $\frac{\partial^2 J}{\partial x^2}$ *and* $\frac{\partial^2 J}{\partial y^2}$ *always have the same sign and are ordinarily* * *each minus or plus everywhere along the extremal arc according to whether* (1) *is maximum or minimum, and* $\frac{\partial^2 J}{\partial x \partial y} = \frac{\partial^2 J}{\partial y \partial x}$ *has the same or opposite sign according to whether* y' *is minus or plus.*

Like the second derivatives of an elementary function the first two of the second derivatives (3) are minus or plus ordinarily * when the integral is a relative maximum or minimum respectively along the indicated interval. As with (5), we get this condition for every interval when we take the upper limit as the constant (a, b) and the lower as the variable (x, y):

$$\left.\begin{aligned} \frac{\partial^2 J}{\partial x^2} &= M_x(x, y) + \int_{xy}^{a, b} M_{xx}\,dx + N_{xx}\,dy - M_x(a, b) \\ &\equiv \int_x^a (N_{xx} - M_{xy})y'\,dx \lesseqgtr 0, \\ \frac{\partial^2 J}{\partial y^2} &= N_y(x, y) + \int_{xy}^{a, b} M_{yy}\,dx + N_{yy}\,dy - N_y(a, b) \\ &\equiv \int_x^a (M_{yy} - N_{xy})\,dx \lesseqgtr 0, \end{aligned}\right\} \quad (7)$$

where the upper and lower inequalities on the right refer to maxima and minima respectively. The right members come from introducing the curls of the vector integrands $R_x = iM_x + jN$ and $R_y = iM_y + jN_y$ respectively, as in (3).

If we use (6) in the *last* two derivatives (3) between the limits (x, y) to (a, b), as before, we see that they are *equal* along *every* interval of the extremal arc.

$$\frac{\partial^2 J}{\partial x \partial y} = \frac{\partial^2 J}{\partial y \partial x} = \int_y^b \frac{M_{xy} - N_{xx}}{y'}\,dy$$

$$\equiv \int_x^a (M_{xy} - N_{xx})\,dx = \int_x^a (N_{xy} - M_{yy})y'\,dx. \quad (8)$$

Since the two right members are equal for every interval

* Various exceptional cases occur, as when the derivatives are discontinuous (see § 9 below) or non-existent. Exhaustive treatment of the sufficiency aspect of these conditions is outside the scope of the present article.

$(x_i y_i)$ to $(x_k y_k)$ along the path of integration, the integrands must be equal :

$$\left.\begin{aligned} &N_{xx}-M_{xy}=y'(M_{yy}-N_{xy})=\text{curl } R_x=-y'\text{ curl } R_y\,; \\ &\text{or} \\ &\frac{d}{dx}\text{curl } R=N_{xx}+y'N_{xy}-(M_{xy}+y'M_{yy}) \\ &\qquad\qquad =\text{curl } R_x+y'\text{ curl } R_y=0, \end{aligned}\right\} \quad (9)$$

since by (6) curl R=0=constant along the extremal arc, and hence the integrand of the first of (7) is y'^2 times the integrand of the second everywhere along the extremal arc, indicating that eq. (7) always have equal signs and that this sign is the same or the reverse of (8) according as y' is minus or plus.

§ 4. *Illustrations of derivatives of a line integral along an extremal arc.*

Consider the line integral

$$J=\int_{0,0}^{1,1} x^2y\,dx+xy\,dy, \quad . \quad . \quad . \quad . \quad (10)$$

for which the critical equations (5) become

$$\left.\begin{aligned} &\frac{\partial J}{\partial x}=x^2y+\int_{xy}^{1,1} 2xy\,dx+y\,dy-1\equiv\int_y^1 (y-x^2)\,dy=0, \\ &\frac{\partial J}{\partial y}=xy+\int_{xy}^{1,1} x^2\,dx+x\,dy-1\equiv\int_x^1 (x^2-y)\,dx=0. \end{aligned}\right\} \quad (11)$$

These equations are evidently satisfied by the parabola $y=x^2$ shown in fig. 1. Using this path $y=x^2$, we may show that J becomes a relative maximum for which the second derivatives (7) are negative :

$$\left.\begin{aligned} &\frac{\partial^2 J}{\partial x^2}=2xy+\int_x^1 2y\,dx-2\equiv\int_y^1 (-2x)\,dy=\frac{4}{3}(x^3-1)<0, \\ &\frac{\partial^2 J}{\partial y^2}=x+0-1\equiv\int_x^1 (-dx)=x-1<0, \end{aligned}\right\} \quad . \quad . \quad . \quad (12)$$

which indicate a negative value for x less than 1, which is the condition for a relative maximum J_i^k for every interval along the path from 0 to 1.

For the derivatives (8) we have

$$\frac{\partial^2 J}{\partial x\,\partial y} = \frac{\partial^2 J}{\partial y\,\partial x} = \int_x^1 2x\,dx = 1-x^2 = \int_x^1 y'\,dx = 1-y. \quad (13)$$

Note that these are equal along the parabolic arc and positive, being of opposite sign from (12) since y' is plus, as pointed out in connexion with (9). This it will be observed squares well with the geometry of the situation indicated by fig. 1.

Fig. 1.

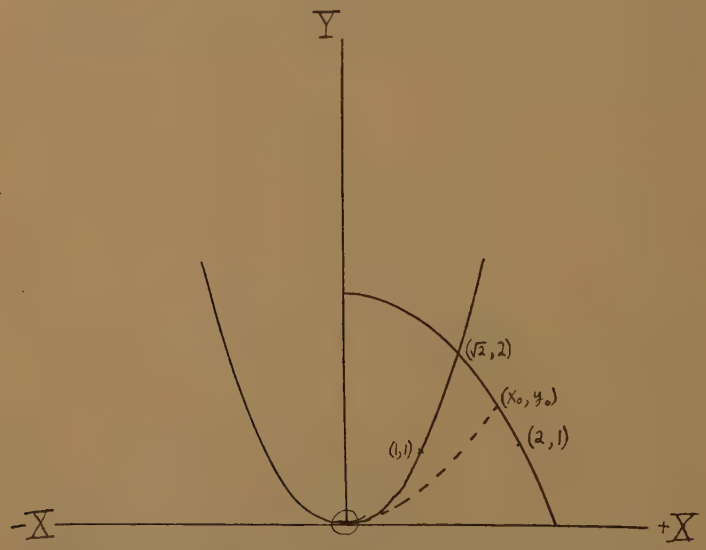

The extremal arc $y=x^2$ and the null curve $x^2+2y-6=0$.

This maximum J along $y=x^2$ is 3/5, which is greater than J along other neighbouring paths through (0, 0) and (1, 1) such as $y=x$ or $y=x^3$.

If the upper limit of (10) were taken as (2, 1), which is not on $y=x^2$, then the maximum would not exist in the above sense :

$$J = \int_{0,\,0}^{2,\,1} x^2y\,dx + xy\,dy. \quad . \quad . \quad . \quad . \quad (14)$$

The derivatives of (14), however, vanish along $y=x^2$ (that is, when upper and lower limits of (2) are both on

$y=x^2$), and the part between points $(x_i\, y_i)$ and $(x_k y_k)$ along it would still be a relative maximum like (10). Hence (14) may be taken along two sections of path shown in fig. 1 from (0, 0) to $(\sqrt{2},\ 2)$ along $y=x^2$ and from $(\sqrt{2},\ 2)$ to (2, 1) along the "null" path, $x^2+2y-6=0$ (to get it drop the integral signs and set (14) equal to zero and integrate). Then J is (1/5) $12\sqrt{2}$. This is a maximum compared with neighbouring paths such as from (0, 0) to $(x_0 y_0)$ along the dotted line and then $(x_0 y_0)$ to (2, 1) along the null path as can readily be seen. The integral becomes *indefinitely* large, however, if the part along $y=x^2$ is extended indefinitely beyond the null path $x^2+2y-6=0$, and then return made to (2, 1) along other null paths like the above on which the integrand of (14) is everywhere zero, such as $x=0$ and $y=0$.

§ 5. *Derivatives of a line integral whose integration path is not an extremal arc.*

The derivatives (11) of (10) will not be zero where the path is $y=x$ or $y=x^3$ which also include the limits of (10). Thus for $y=x$ the left members of (11) become

$$\left.\begin{aligned} \frac{\partial J}{\partial x} &= x^3+\int_x^1 2x^2\,dx+x\,dx-1 \\ &\equiv \int_x^1 (x-x^2)\,dx=\frac{1}{6}+\frac{x^3}{3}-\frac{x^2}{2}>0, \\ \frac{\partial J}{\partial y} &= x^2+\int_x^1 x^2\,dx+x\,dx-1 \\ &\equiv \int_x^1 (x^2-x)\,dx=\frac{x^2}{2}-\frac{x^3}{3}-\frac{1}{6}<0. \end{aligned}\right\} \tag{15}$$

Likewise, along $y=x^3$, the left members of (11) become

$$\left.\begin{aligned} \frac{\partial J}{\partial x} &= x^5+\int_x^1 2x^4\,dx+3x^5\,dx-1 \\ &\equiv \int_x^1 (x^3-x^2)3x^2\,dx=\frac{3}{5}x^5-\frac{x^3}{2}-\frac{1}{10}<0, \\ \frac{\partial J}{\partial y} &= x^4+\int_x^1 x^2\,dx+3x^3\,dx-1 \\ &\equiv \int_x^1 (x^2-x^3)\,dx=\frac{1}{12}+\frac{x^4}{4}-\frac{x^3}{3}>0. \end{aligned}\right\} \tag{16}$$

These derivatives give the rates of change (2) of that part of (10) between (x, y) and (1, 1) along the paths $y=x$ and $y=x^3$. Note how they square with the geometry of the situation indicated by fig. 1, which shows the path $y=x^2$ where these derivatives are zero. Thus $\frac{\partial J}{\partial x}$ is by (15) and (16) positive above $y=x^2$ and minus below it, and *vice versa* with $\frac{\partial J}{\partial y}$; and the constant fractions give the derivatives or rates of change of the entire integral (10), using the limit $x=0$ in (15) and (16).

§ 6. *The line integral whose vector integrand $R=iM+jN$ is a function of x and y only, being free from y', has a characteristic pattern of extremal arcs and null curves.*

When we drop the integral signs and set (10) equal to zero and integrate we obtain the family of parabolas $x^2+2y=\beta$ indicated by fig. 2, along which the line integral (10) is zero. Likewise the coordinate axes are seen to be lines along which (10) becomes zero. Note also that if we choose different limits in (10):

$$J=\int_{x_iy_i}^{x_ky_k} x^2y\,dx+xy\,dy, \quad . \quad . \quad . \quad (17)$$

and take (x_iy_i) and (x_ky_k) on the extremal arc $y=x^2$, then (17) is a maximum or minimum according as the path of integration is taken in the same or opposite directions respectively from that of the arrow along the path $y=x^2$. Thus for the limits $(x_iy_i)=(0, 0)$ and $(x_ky_k)=(-1, 1)$, we have instead of (12):

$$\left.\begin{aligned} \frac{\partial^2 J}{\partial x^2} &= 2xy+\int_x^{-1} 2y\,dx+2 \\ &\equiv \int_y^1 (-2x)\,dy=\frac{4}{3}(x^3+1)>0, \\ \frac{\partial^2 J}{\partial y^2} &= x+1\equiv\int_{-1}^{-1}(-dx)>0; \end{aligned}\right\} \quad (18)$$

indicating positive second derivatives, and hence a minimum dependent variable J_i^k given by (17) for the limits in question.

Note that both (12) and (18), as illustrations of (7), show an integrand in the first equation which is $y'^2=4x^2$ times

the integrand in the second equation (along the extremal arc, where $dy=y'dx$) according to (9) above.

Fig. 2.

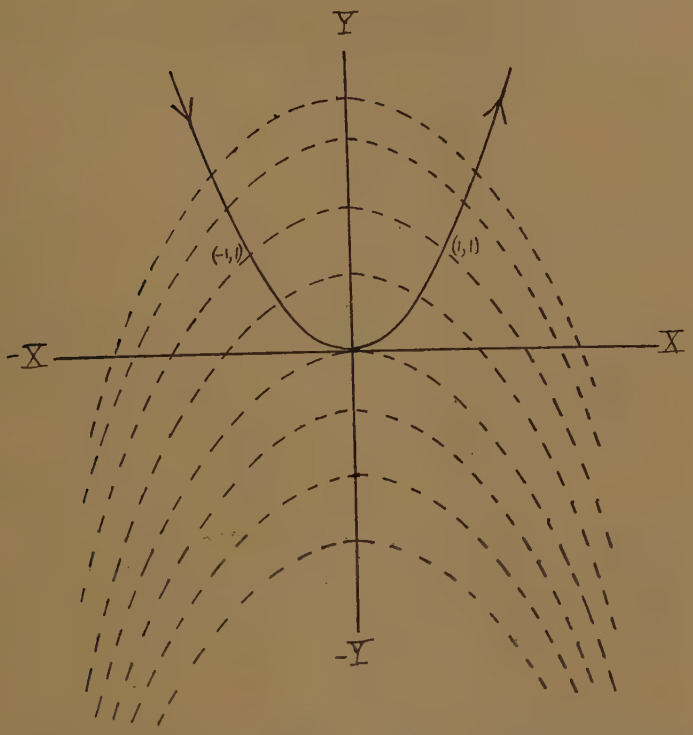

The extremal arc $y=x^2$ and null curves $x=0$, $y=0$, and $x^2+2y=\beta$ which make up the characteristic pattern of the line integral (17).

§ 7. *The derivative of a line integral along its null lines includes only the integral term.*

We may refer (10) to the curvilinear coordinates α, β given in terms of x and y by

$$\left.\begin{array}{ll} y=\alpha x^2\,; & d\alpha=\dfrac{-2y\,dx}{x^3}+\dfrac{dy}{x^2}\,, \\ \beta=x^2+2y\,; & d\beta=2(x\,dx+dy), \\ x=\sqrt{\dfrac{\beta}{1+2\alpha}}\,; & y=\dfrac{\alpha\beta}{1+2\alpha}\,. \end{array}\right\} \quad . \quad (19)$$

Then (10) becomes

$$J=\frac{1}{2}\int_0^3 \frac{\alpha\beta^{\frac{3}{2}}\,d\beta}{(1+2\alpha)^{\frac{3}{2}}}=\int M(\alpha,\beta)\,d\alpha+N(\alpha,\beta)\,d\beta, \quad . \quad (20)$$

whereby $M(\alpha, \beta)$ equals zero. For the partial derivatives

Fig. 3.

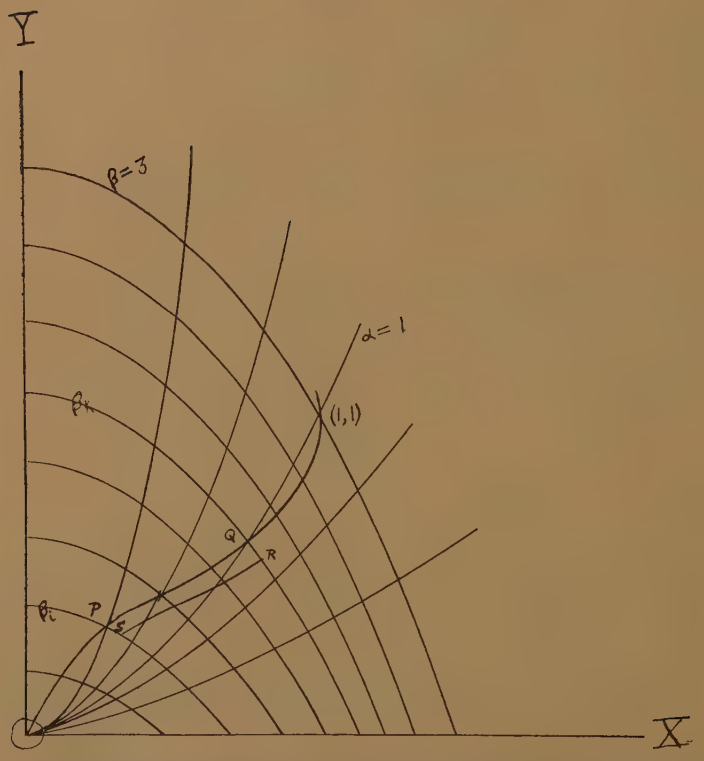

The closed differential circuit in curvilinear coordinates PSRQ taking $\delta\beta=0$, and $\delta\alpha$ is constant for this parallel displacement in the $\alpha\beta$ plane. PS and QR are given by $ds=hd\alpha$, where the variable h is the reciprocal of the gradient of α.

of (20) along the null lines β=constant we have, instead of (11) and (12),

$$\frac{\partial J_i^k}{\partial\alpha}=\frac{1}{2}\int_{\beta_i}^{\beta_k}\frac{(1-\alpha)\beta^{\frac{3}{2}}}{1+2\alpha)^{\frac{5}{2}}}\,d\beta=\int_{\beta_i}^{\beta_k}N_\alpha\,d\beta, \quad . \quad . \quad (21)$$

$$\frac{\partial^2 J_i^k}{\partial\alpha^2}=\frac{3}{2}\int_{\beta_i}^{\beta_k}\frac{\beta^{\frac{3}{2}}(\alpha-2)}{(1+2\alpha)^{\frac{7}{2}}}\,d\beta=\int_{\beta_i}^{\beta_k}N_{\alpha\alpha}\,d\beta. \quad . \quad (22)$$

An examination of fig. 3 shows why the integral term is the only one that appears in the derivatives (21) and (22), even though they represent, like all line integral derivatives here discussed, line integrals around the indicated closed differential circuit. The part of the line integral (21) along the curves $\beta=\beta_i$ and $\beta=\beta_k$ (along PS and RQ) is zero because these are null lines. The corresponding analytic fact is that $M(\alpha, \beta)$ is identically zero, being the integral (10) along a null line per unit change in α in the calculus sense of a rate of change. Thus our choice of curvilinear coordinates α and β is such that our closed circuit integral (the derivative (21)) has a zero value along the end pieces, and this is the part given by application of Working Rule I for differentiation with respect to differentials as shown in § 20 of the previous * paper. The non-vanishing part of (21) is hence the difference (in the calculus sense of a rate) between the integral (20) along the two curves PQ and SR, the latter being obtained from PQ by unit " parallel " displacement $\delta\alpha=1$. Note that this means parallel displacement in the α, β plane and that the two curves will not generally be parallel on the XY plane.

We obtain the extremal arc by setting (21) equal to zero, whereby $N^\alpha=0$ and $\alpha=1$, and hence by (19) $y=x^2$. Note also that when $\alpha=1$ $N_{\alpha\alpha}<0$, and likewise with the derivative (22), indicating that (20) is then a maximum rather than a minimum.

§ 8. *Characteristic patterns of certain line integrals.*

(*a*) Consider the integral

$$J=\int (xy)^n\,dx+(xy)^n\,dy, \quad . \quad . \quad . \quad . \quad (23)$$

where n=constant.

The extremal arcs are given by setting the area derivative (1) equal to zero :

$$\frac{dJ}{d\sigma}=N_x-M_y=n(xy)^{n-1}(y-x)=0, \quad . \quad . \quad (24)$$

or $y=x$.

* See also §14 of " Differentiation of Line Integrals by Parallel Displacement," Kimball, *loc. cit.*

And the null lines come from setting the integrand equal to zero :

$$x=0\,;\ y=0\,;\quad \text{and}\quad x+y=c. \quad . \quad . \quad . \quad (25)$$

(*b*) For the integral

$$J=\int (xy)^n\,dx-(xy)^n\,dy \quad . \quad . \quad . \quad . \quad (26)$$

Fig. 4.

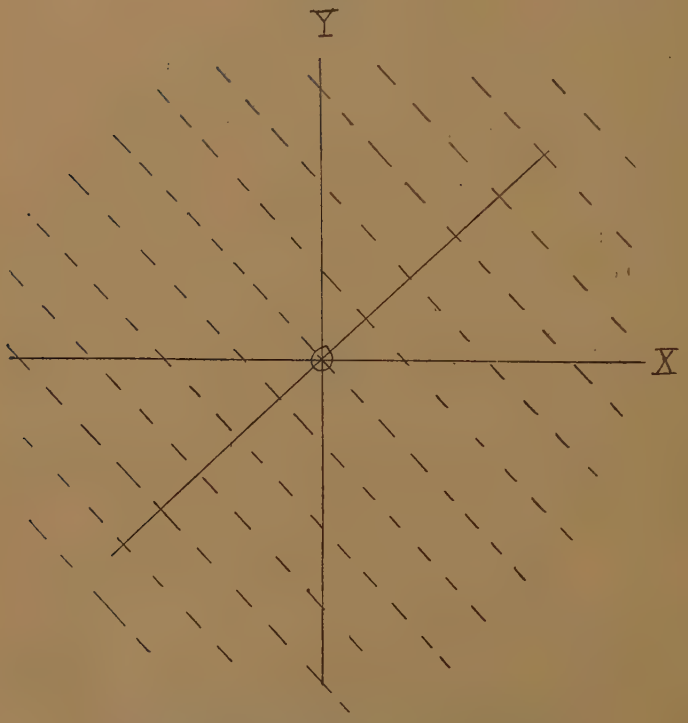

The extremal line and null lines for (23).

the equation of the extremal line is $y=-x$, and the null lines have a slope of 1 instead of -1 as in fig. 4.

(*c*) Consider, where $n=$constant

$$J=\int \frac{x\,dy-y\,dx}{(x^2+y^2)^n} \quad . \quad . \quad . \quad . \quad . \quad . \quad (27)$$

The null lines, obtained by solving the differential equation obtained when (27) without the integral sign

is set equal to zero, are evidently the straight lines $y=cx$.

The area derivative is

$$\frac{dJ}{d\sigma}=\frac{2(1-n)}{(x^2+y^2)^n}=N_x-M_y. \quad . \quad . \quad . \quad (28)$$

Since there is no relation between x and y that causes the vanishing of (28), we see that there are no extremal arcs for (27) no matter what value is taken for n.

Fig. 5.

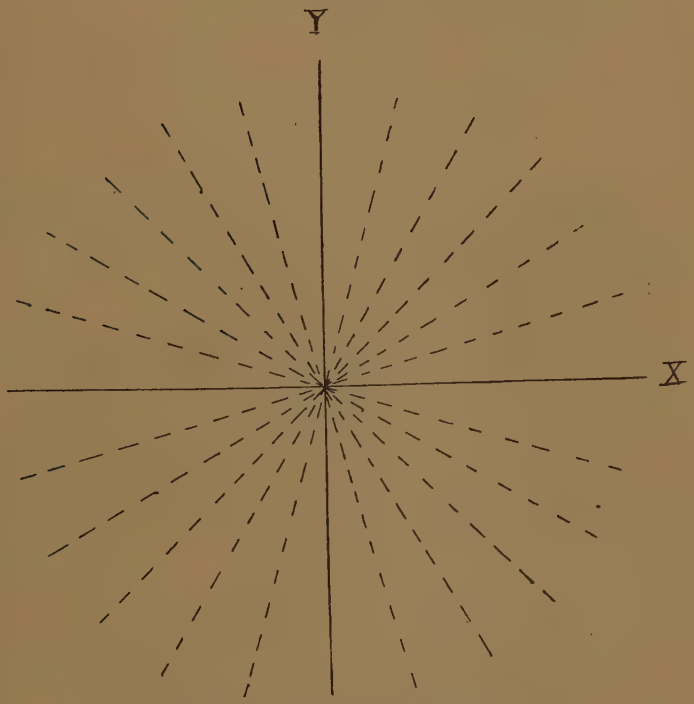

The null lines for the integral (27).

When $n=0$ the right member becomes 2 and checks the familiar fact that (27) taken around a closed circuit (with $n=0$) equals twice the enclosed area.

When $n=\frac{1}{2}$ (28) gives $1/r$, where $r=\sqrt{x^2+y^2}$ for the line integral per unit area or area derivative.

When $n=1$ (28) becomes identically zero, indicating (27) as independent of the integration path, and zero

around every closed circuit not including the origin, in which case it becomes 2π.

For all other values of n we note that the area derivative or line integral per unit enclosed area is given in terms of some power of the radial distance from the origin, $\sqrt{x^2+y^2}$.

§ 9. *Extremal arcs where the first partials and area derivatives do not vanish.*

The value of z for the surface $z=(x-y)^{2/3}$ shown in fig. 6 has its minimum value $z=0$ along the trough $x=y$. The integral

$$J=\int_{0,\,0}^{1,\,1}(x-y)^{\frac{2}{3}}\sqrt{(1+y'^2)}\,dx=\int f(xy\,y')\,dx\ . \quad (29)$$

is evidently the part included between $z=0$ and $z=(x-y)^{2/3}$ of the ruled surface generated by a line parallel to the z axis as the point where it cuts the xy plane moves along the path of integration in the xy plane.

The area derivative is given by

$$\frac{dJ}{d\sigma}=\frac{d}{dx}f_{y'}-f_y=\frac{y''(x-y)+\frac{2}{3}(1+y')(1+y'^2)}{(x-y)^{\frac{1}{3}}(1+y'^2)^{\frac{3}{2}}}, \quad (30)$$

which evidently becomes infinity along the minimizing arc $x=y$, where the slope $y'=1$. Thus Euler's equations are not satisfied even though (29) has its minimum value zero for this integration path. Likewise the partials with respect to x and y become infinity for this minimizing arc $y=x$:

$$\left.\begin{aligned}\frac{\partial J}{\partial x}=\frac{\partial J}{\partial\,dx}&=\frac{(x-y)^{\frac{2}{3}}}{\sqrt{1+y'^2}}+\frac{2}{3}\int_{x,\,y}^{1,\,1}\frac{dx+y'\,dy}{(x-y)^{\frac{1}{3}}\sqrt{1+y'^2}},\\ \frac{\partial J}{\partial y}=\frac{\partial J}{\partial\,dy}&=\frac{(x-y)^{\frac{2}{3}}y'}{\sqrt{1+y'^2}}-\frac{2}{3}\int_{xy}^{1,\,1}\frac{dx+y'\,dy}{(x-y)^{\frac{1}{3}}\sqrt{1+y'^2}}.\end{aligned}\right\} \quad (31)$$

Note that $M(1,\,1)=N(1,\,1)=0$, and hence the abbreviated form shown by (31). Each of (31) becomes infinite along the extremal arc $y=x$, indicating that the rate of change of that part of (29) included between (xy) and $(1,\,1)$ (the vertical ruled surface in question) increases indefinitely as points on the line $x=y$ are approached. Eq. (31) constitute exceptions to (5) above in that here is a mini-

Fig. 6.

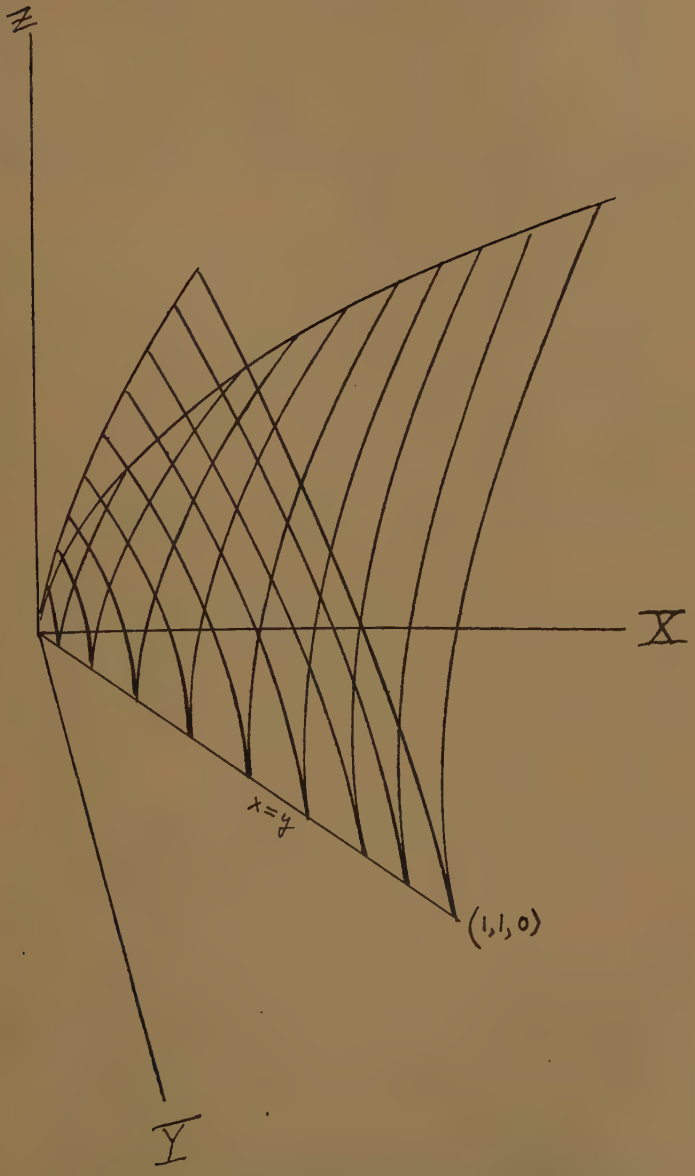

The surface $z=(x-y)^{\frac{5}{2}}$ and the minimizing arc $x=y$ for the integrals (29) and (32).

mizing arc for which the derivatives of the integral with respect to differentials * are not zero but infinite.

The associated † line integral given by taking $y'=1$:

$$J=\frac{1}{\sqrt{2}}\int_{0,0}^{1,1}(x-y)^{\frac{1}{3}}(dx+dy), \quad . \quad . \quad (32)$$

also has infinite first partial and area derivatives along its extremal arc $x=y$, instead of zero as ordinarily as in the corollary of Theorem II.

§ 10. *Theorem III.—Calculus of variations integrals of the type* $\int g(x, y)\,ds$ *are always greater in magnitude than the associated line integral for extremal arcs along any path other than the extremal arc itself whose slope is used for* y' *to give the line integral.*

Consider an integral of the form

$$J=\int g(x, y)\,ds\equiv\int_{x_0y_0}^{a,b} g(x, y)\left(\frac{dx}{\sqrt{1+y'^2}}+\frac{y'\,dy}{\sqrt{1+y'^2}}\right)$$

$$\equiv\int(f-y'f_{y'})\,dx+f_{y'}\,dy. \quad . \quad (33)$$

Let $y=\phi(x)$ be its extremal arc, having slope $y'=\phi'(x)$, which is also ordinarily expressible in terms of y only, or of both x and y. Substitute above in (33) to obtain the line integral referred to by the corollary of Theorem II. of the previous ‡ article.

$$J_b=\int_{x_0y_0}^{a,b} g(x, y)\left(\frac{dx+\phi'\,dy}{\sqrt{1+\phi'^2}}\right)\equiv\int g(x, y)\,ds\left(\frac{dx+\phi'\,dy}{ds\sqrt{1+\phi'^2}}\right)$$

$$\equiv\int g(x, y)\,ds\cos\theta, \quad . \quad (34)$$

where

$$\cos\theta=\cos(\alpha-\beta)=\cos\alpha\cos\beta+\sin\alpha\sin\beta$$

$$=\frac{dx}{ds}\frac{1}{\sqrt{1+\phi'^2}}+\frac{dy}{ds}\frac{\phi'}{\sqrt{1+\phi'^2}}.$$

* Note this exception to the critical equations (48) in the " Calculus of Variations," Kimball, *loc. cit.*

† See Theorem II. of section 22 of the paper on " Differentiation of Line Integrals by Parallel Displacement," Kimball, *loc. cit.*

‡ Kimball, *loc. cit.* § 22.

Here $\alpha = \arctan\left(\frac{dy}{dx}\right)$ is the angle of inclination of the path of integration, and $\beta = \arctan(\phi')$ is the angle of inclination of the extremal arc. Since (33) and (34) each have the same limits, it is clear that $\cos\theta$ cannot be unity along the entire integration path unless $y' = \phi'$ everywhere, *i. e.*, the path of integration is the extremal arc. In all other cases $\cos\theta$ will be occasionally (at least) smaller than one, and hence the integral (34) will be smaller than (33).

The advantage of this theorem lies in that it helps to establish (33) as a relative minimum, since, whenever the second partial derivatives $\frac{\partial^2 J}{\partial x^2}$ and $\frac{\partial^2 J}{\partial y^2}$ of (34) according to (7) are positive everywhere along the integration path, and are sufficient to show that (34) is a minimum, then also by the present theorem they furnish sufficiency conditions for the relative minimum of (33), the two integrals being equal along the extremal arc.

The integrals (29) and (32) above afford an illustration of this theorem. Thus (29) is greater than (32) except when equal (along the extremal arc, $y = x$), since the integrals are the same except for the extra factor $\cos\theta = \cos\left(\alpha - \frac{\pi}{4}\right) = \frac{dx+dy}{\sqrt{2}ds}$ under the integral sign of (32)

XLVII. *Note on the Equilibrium of a Vortex maintained in a sudden Expanding Stream.* *By* Atsushi Miyadzu, *Assistant Professor of Hydraulics and Hydrodynamics, Tohoku Imperial University, Sendai, Japan.**

I. *Introduction.*

According to the previous theory in the ordinary method of treatment the positions of equilibrium of a vortex maintained in a sudden expanding stream have been given by two curves † starting at a concave and a convex corner and tending to infinity. In the

* Communicated by the Author.

† A. Miyadzu, "Path and Stability of a Local Vortex moving round a Corner" (third paper), Phil. Mag. xix. p. 652 (March 1935).

actual state of the flow there appears, however, a single or a single principal vortex at a definite position in the channel. This discrepancy between theory and practice is chiefly the result of a deficient method of treatment. In this paper the writer presents a method of analytical treatment to decide uniquely the position of equilibrium in accordance with the actual condition of the flow.

II. *Method of Treatment.*

Whenever a fluid, such as water or air, moves in a moderate speed along a boundary with corners it always moves, in a curve round any sharp corner, with a stream-line tangential to the boundary. The present writer's idea is to take up and satisfy this fact in the process of treatment. The method consists in assuming the original

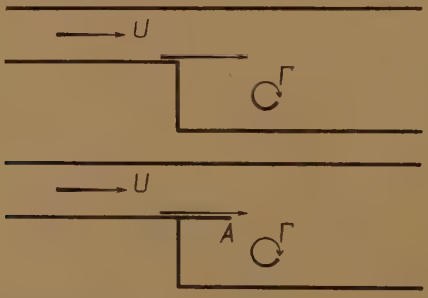

Fig. 1 (*a*).

Fig. 1 (*b*).

channel, for instance, as shown in fig. 1 (*a*) to be fitted with a salient wall as shown in fig. 1 (*b*), and finding out a position of equilibrium with the condition of a tangential flow at its end A, since this condition can always be satisfied regarding such a salient corner. The result may give a solution more in accordance with the actual flow in relation to the original channel. The difficult thing in practical application is to estimate a reasonable length of the virtual wall by experimental verification.

III. *Conditions of Equilibrium of a Vortex maintained in a sudden Expanding Stream.*

The correspondence between the planes of t and z in fig. 2 is given by

$$\frac{dz}{dt} = \frac{mH}{\pi} \frac{t+b+\epsilon}{t^{\frac{n-1}{n}}(t+a)(t+b)^n}, \quad \ldots \quad (1)$$

$$m=\frac{a^{\frac{n-1}{n}}(a-b)^{\frac{1}{n}}}{a-(b+\epsilon)}, \quad \ldots\ldots\ldots \quad (2)$$

where a, b, and ϵ are positive real constants, a being greater than b and ϵ such as $b+\epsilon<a$, H is a smaller breadth, and m the ratio of divergence.

Putting $n=2$ for the sudden expanding passage, and integrating (1), we have

$$z=\frac{m\mathrm{H}}{\pi}\left[\log\left\{t+\frac{b}{2}+t^{\frac{1}{2}}(t+b)^{\frac{1}{2}}\right\}\right.$$
$$\left.-\frac{1}{m}\log\frac{[a(t+b)]^{\frac{1}{2}}+[(a-b)t]^{\frac{1}{2}}}{[a(t+b)]^{\frac{1}{2}}-[(a-b)t]^{\frac{1}{2}}}-\log\frac{b}{2}\right], \quad . \quad (3)$$

Fig. 2.

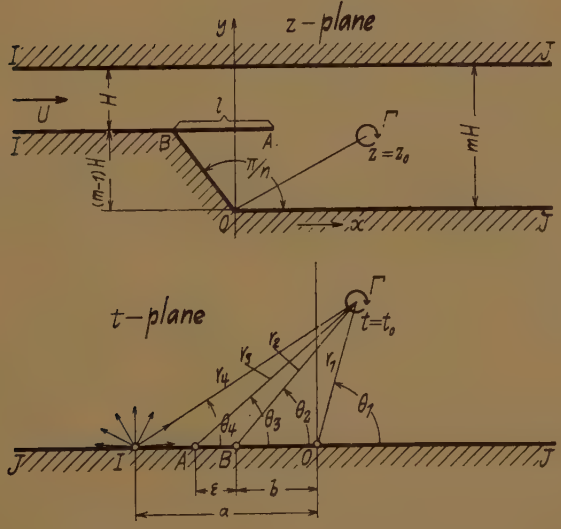

$t=0$ being correspondent to $z=0$, as is shown in fig. 2. Since

$$z=l+i(m-1)\mathrm{H} \quad \text{for} \quad t=-(b+\epsilon),$$

it follows that

$$\frac{l}{\mathrm{H}}=\frac{m}{\pi}\left[\log\left\{\epsilon+\frac{b}{2}+\sqrt{\epsilon(b+\epsilon)}\right\}\right.$$
$$\left.-\frac{1}{m}\log\frac{\sqrt{(a-b)(b+\epsilon)}+\sqrt{a\epsilon}}{\sqrt{(a-b)(b+\epsilon)}-\sqrt{a\epsilon}}-\log\frac{b}{2}\right]; \quad (4)$$

and equation (2) now becomes

$$a=\frac{2m^2(b+\epsilon)-b\pm\sqrt{4m^2\epsilon(b+\epsilon)+b^2}}{2(m^2-1)}. \quad . \quad . \quad (2')$$

By the same treatment in the writer's former paper, we have

$$w=-\frac{HU}{\pi}\log(t+a)-\frac{i\Gamma}{2\pi}\log\frac{t-t_0}{t-\bar{t}_0}, \quad . \quad . \quad (5)$$

$$\left.\begin{aligned}-u_t+iv_t&=\left[\frac{d}{dt}\left\{w+\frac{i\Gamma}{2\pi}\log(z-z_0)\right\}\right]_{\substack{t=t_0\\z=z_0}}\\&=-\frac{HU}{\pi}\frac{1}{t_0+a}+\frac{i\Gamma}{2\pi}\frac{1}{t_0-\bar{t}_0}+\frac{i\Gamma}{2\pi}\left[\frac{d^2z}{dt^2}\Big/2\,\frac{dz}{dt}\right]_{\substack{t=t_0\\z=z_0}},\\-u_z+iv_z&=(-u_t+iv_t)\left[\frac{dt}{dz}\right]_{t=t_0,\,z=z_0}.\end{aligned}\right\} \quad . \quad . \quad . \quad (6)$$

Then, putting

$$t_0=r_1e^{i\theta_1}, \quad t_0+b=r_2e^{i\theta_2}, \quad t_0+b+\epsilon=r_3e^{i\theta_3}, \quad t_0+a=r_4e^{i\theta_4},$$

and splitting (6) into the real and imaginary parts, we get

$$\left.\begin{aligned}u_t&=\frac{HU}{\pi r_4}\cos\theta_4+\frac{\Gamma}{4\pi}\left[\frac{1}{r_4}\sin\theta_4+\frac{1}{2}\frac{b}{r_1r_2}\sin(\theta_1+\theta_2)\right.\\&\qquad\left.+\frac{\epsilon}{r_2r_3}\sin(\theta_2+\theta_3)-\frac{1}{r_1\sin\theta_1}\right],\\v_t&=\frac{HU}{\pi r_4}\sin\theta_4-\frac{\Gamma}{4\pi}\left[\frac{1}{r_4}\cos\theta_4+\frac{1}{2}\frac{b}{r_1r_2}\cos(\theta_1+\theta_2)\right.\\&\qquad\left.+\frac{\epsilon}{r_2r_3}\cos(\theta_2+\theta_3)\right],\end{aligned}\right\} \quad . \quad (6')$$

from which the conditions of equilibrium of a vortex are obtained as

$$br_3\cos(\theta_1+\theta_2-\theta_4)-2\epsilon r_1\cos(\theta_2+\theta_3-\theta_4)=0, \quad . \quad (7)$$

$$\frac{\Gamma}{HU}=\frac{4\sin\theta_4}{\cos\theta_4+\frac{b}{2}\frac{r_4}{r_1r_2}\cos(\theta_1+\theta_2)+\epsilon\frac{r_4}{r_2r_3}\cos(\theta_2+\theta_3)}. \quad (8)$$

When $\epsilon=0$, as an extreme case, the results coincide with those already dealt with in the paper cited.

Now let us put $m=3$, $b=2$ in what follows, as in the former example; then

$$a=\frac{9\epsilon+17+\sqrt{9\epsilon(\epsilon+2)+1}}{8}, \quad . \quad . \quad . \quad (2'')$$

$$\frac{l}{\mathrm{H}}=\frac{3}{\pi}\Big[\log\{\epsilon+1+\sqrt{\epsilon(\epsilon+2)}\}$$

$$-\frac{1}{3}\log\frac{\sqrt{(a-2)(\epsilon+2)}+\sqrt{a\epsilon}}{\sqrt{(a-2)(\epsilon+2)}-\sqrt{a\epsilon}}\Big]. \quad (4')$$

The negative sign before the square root is rejected, as it is not fit for this example. The changes of a and l/H with ϵ are shown in the table; and (7) and (8) are reduced to

$$r_3\cos(\theta_1+\theta_2-\theta_4)+\epsilon r_1\cos(\theta_2+\theta_3-\theta_4)=0, \quad . \quad (7')$$

$$\frac{\Gamma}{\mathrm{HU}}=\frac{4\sin\theta_4}{\cos\theta_4+\dfrac{r_4}{r_1r_2}\cos(\theta_1+\theta_2)+\epsilon\dfrac{r_4}{r_2r_3}\cos(\theta_2+\theta_3)}, \quad (8')$$

which depend, of course, directly on ϵ and indirectly on l/H.

ϵ	0	0·5	1	2	3
a	2·25	3·125	3·911	5·443	6·958
l/H	0	0·3063	0·5095	0·7810	0·9685

IV. *Equilibrium of a Vortex not subjected to a special Condition.*

For further treatment we examine (7′) and (8′), assuming $\epsilon=0{\cdot}5$, $a=3{\cdot}125$ (accordingly $l/\mathrm{H}=0{\cdot}3063$) *. (7′) gives the position of equilibrium and (8′) the strength of circulation. As solutions of (7′) three θ-r curves in fig. 3 (*a*), (*b*), and (*c*) have been obtained, for which Γ/HU from (8′) is shown by curve I. Transforming these to the z-plane we have three curves, 1, 2, and 3 in fig. 4. Since Γ/HU due to (8′) is positive, then only a vortex with a clockwise

* This is due to the experimental verification for the flow of water. The details will be described in Technol. Rep. Tôhoku Imp. Univ., Sendai, Japan.

circulation can be in equilibrium when the main flow is divergent. Curves 1 and 2 correspond to those already

Fig. 3 (*a*).

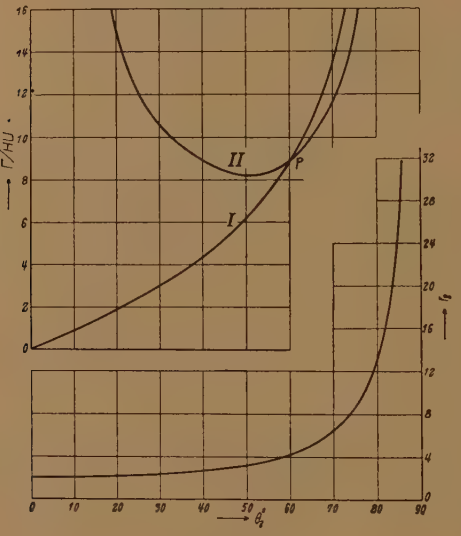

Fig. 3 (*b*).

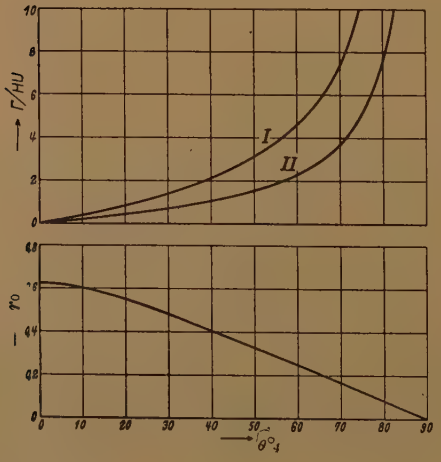

deduced regarding the original channel in the previous paper. On these curves the strength of circulation for equilibrium increases from 0 at the corners to ∞ at an

infinite distance. Curve 3 is peculiar to the present channel with a salient wall. The stength of circulation on this curve is zero at B ($\theta_2=90°$) and C ($\theta_2=0°$), and

Fig. 3 (*c*).

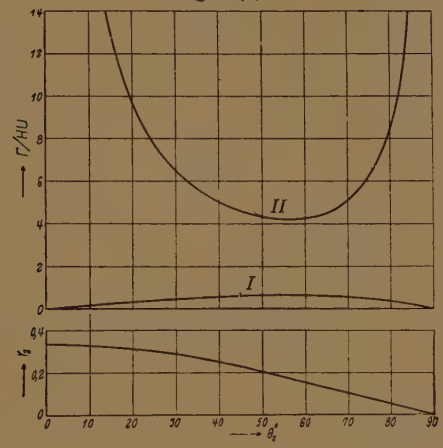

Fig. 3 (*d*).

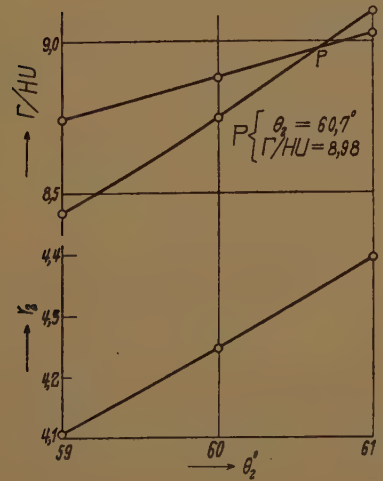

between them has the positive value, the greatest being $\Gamma/\mathrm{HU}=0{\cdot}666$ at M. Then we may conclude that :

(1) When a strength of clockwise circulation is less than $\Gamma/\mathrm{HU}=0{\cdot}666$ it can be in equilibrium at four points, two on curve 3 and one by one on curves 1 and 2.

(2) When the strength of circulation is greater than $\Gamma/\mathrm{HU}=0{\cdot}666$ two positions for equilibrium exist, one by one on curves 1 and 2.

Curve 2 has a practical meaning only when the sense of flow is reversed as a convergent flow, and is thus out of the question in the present investigation. Curve 1 lies in the upper position as compared with that for the original channel without the salient wall, but they coincide appreciably in this small figure.

Fig. 4.

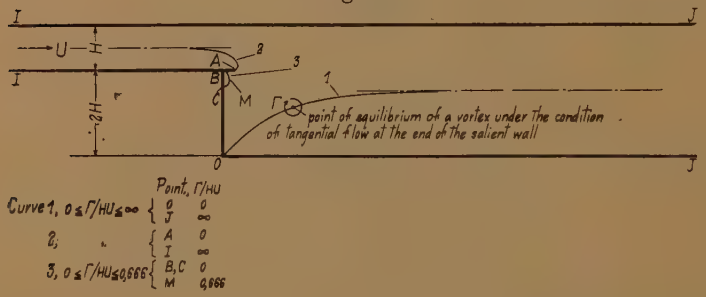
I
J
U
H
2H
A
B
C
M
Γ
0
point of equilibrium of a vortex under the condition of tangential flow at the end of the salient wall
Point, Γ/HU
Curve 1, 0 ≤ Γ/HU ≤ ∞ { 0 0 ; J ∞
2, " { A 0 ; I ∞
3, 0 ≤ Γ/HU ≤ 0.666 { B,C 0 ; M 0.666

V. *Equilibrium of a Vortex subjected to a Condition at a Salient Corner.*

The condition for the main flow to have a finite velocity at the end of the wall is given by

$$\left(\frac{dw}{dt}\right)_{t=-(b+\epsilon)}=0,$$

which, with eq. (5), gives

$$\frac{i\Gamma}{2\pi}=\frac{\mathrm{HU}}{\pi}\frac{(t_0+b+\epsilon)(\bar{t}_0+b+\epsilon)}{(\bar{t}_0-t_0)(a-b-\epsilon)}, \quad . \quad . \quad . \quad (9)$$

or

$$\frac{\Gamma}{\mathrm{HU}}=\frac{r_3}{[a-(b+\epsilon)]\sin\theta_3}=\frac{r_3}{0{\cdot}625\sin\theta_3}. \quad . \quad . \quad (9')$$

Let V_x, V_y denote the component velocities of the main flow at the corner A; they are evaluated as

$$-\mathrm{V}_x+i\mathrm{V}_y=\left[\left(\frac{dw}{dt}\right)\left(\frac{dt}{dz}\right)\right]_{t=-(b+\epsilon)}$$

$$=-\mathrm{U}\frac{\sqrt{\epsilon(b+\epsilon)}}{m[a-(b+\epsilon)]}\frac{t_0\bar{t}_0+a(t_0+b+\epsilon)+a(\bar{t}_0+b+\epsilon)-(b+\epsilon)^2}{(t_0+b+\epsilon)(\bar{t}_0+b+\varepsilon)},$$

from which we have

$$\left.\begin{aligned} V_x &= U\frac{\sqrt{\epsilon(b+\epsilon)}}{m[a-(b+\epsilon)]}\frac{r_3+2(a-b-\epsilon)\cos\theta_3}{r_3} \\ &= \frac{4\sqrt{5}}{15}\frac{r_3+1{\cdot}25\cos\theta_3}{r_3}U, \\ V_y &= 0. \end{aligned}\right\} \quad (10)$$

Obviously the flow is tangential to the wall and has a finite velocity, which depends on the velocity of the main stream, the length of the salient wall, and the position of the vortex.

Provided the tangential condition of the main flow is premised, the strength of a vortex must always be defined by (9′) whether it may be free or fixed. We examine first whether and where a vortex can be in equilibrium under this condition. For this purpose we have only to examine which point on curve, 1, 2, and 3 in fig. 4 satisfies both (8) and (9′). The calculated results from (9′) are shown by curve II in figs. 3 (*a*), (*b*), and (*c*). We see that at any point on curves 1 and 2 a free vortex cannot be in equilibrium. For only a point on curve 1 (*i. e.*, P in fig. 3 (*a*)) (8) is satisfied together with (9′); on this point only a free vortex can be in equilibrium in the condition under consideration, the coordinates of which have been obtained from fig. 3 (*d*) and eq. (3), as

$$\theta_2 = 60{\cdot}68^\circ, \qquad r_2 = 4.346,$$
$$x/H = 1{\cdot}61, \qquad y/H = 1{\cdot}11,$$

and the strength of circulation as

$$\frac{\Gamma}{HU} = 8{\cdot}98.$$

This position is marked with a circle on curve 1 in fig. 4.

The tangential velocity of the main flow is obtained from (10) as follows:

$$V_x = 0{\cdot}688\,U.$$

Even when the direction of the main stream is reversed the position of equilibrium and the magnitude of Γ/HU remain unchanged, while the rotational direction of the vortex becomes counter-clockwise. The result cannot, however, be considered as applicable also to the con-

vergent flow of an actual fluid, for the virtual wall can never be assumed to be common for the reversed flow of an actual fluid.

Leaving out the adoption or rejection of the result for the cases unexpected in the beginning, a unique position for equilibrium of a free vortex has first been given theoretically by the proposed method of treatment based on the actual condition of the main stream.

In conclusion, the writer wishes to express his sincere thanks to Prof. O. Miyagi for his guidance and encouragement, and also to Messrs T. Tanabe and T. Suzuki for their help in numerical calculations.

Institute of Mechanical Engineering,
Tohoku Imperial University,
Sendai, Japan.

XLVIII. *Equilibrium of a thin Plate, symmetrically loaded, resting on an Elastic Foundation of Infinite Depth.* *By* A. H. A. Hogg, *M.A.**

(1) *Summary.*

THE problem considered is that of a symmetrically loaded thin plate of infinite size, resting on the plane surface of a semi-infinite elastic solid. Expressions are obtained for the curvature and normal displacement of the plate with the load concentrated at a point, and for the curvature at the centre of a circular area over which the load is uniformly distributed.

The problem is of some interest in connexion with the design of concrete road slabs, and its investigation was undertaken as part of the writer's work at the Road Research Laboratory.

A similar problem has been investigated by Professor H. M. Westergaard [1], but on the assumption that the normal displacement of the surface of the foundation at any point is proportional to the normal pressure at that point.

The writer is greatly indebted to Dr. F. Garwood, of the Road Research Laboratory, for much valuable assistance and advice.

* Communicated by the Director of Road Research.

(2) *Symbols.*

w=Vertical downward displacement of plate and surface of foundation.

$\widehat{zz}$=Tensile stress on surface of foundation.

r=Distance of point on slab from centre of loaded area.

R=Constant depending on elastic properties of foundation.

k, α=Quantities involved in the integrations.

W (k)=Function of k depending on the form of the displaced surface.

$p=f(r)$=Normal load per unit area on surface of plate.

P (k)=Function of k depending on $f(r)$.

Π=Total load on plate.

a=Radius of area over which load is uniformly distributed.

$$b=r\left(\frac{\mathrm{R}}{\mathrm{D}}\right)^{\frac{1}{4}}.$$

$$c=a\left(\frac{\mathrm{R}}{\mathrm{D}}\right)^{\frac{1}{4}}.$$

t=Thickness of plate.

E, σ=Elastic constants of plate.

C, σ, λ, μ=Elastic constants of foundation.

D=Flexural rigidity of plate=$\dfrac{\mathrm{E}t^3}{12(1-\sigma^2)}$.

γ=Euler's constant, 0·5772.

$$\psi(r+1)=\frac{1}{1}+\frac{1}{2}+\frac{1}{3}+\ldots+\frac{1}{r}-\gamma.$$

$\Gamma(\ )$=The Gamma Function.

The notation of the Bessel Functions is that used in Watson's 'Bessel Functions' [2] and of the elastic constants that used in Love's 'Elasticity' [3].

(3) *Analysis.*

Use is made of K. Terazawa's [4] general solution in terms of Bessel Functions of Boussinesq's Problem for a normal load symmetrical about a point. It was shown that if the deflexion w of the surface of the elastic foundation

at a distance r from the centre of symmetry can be expressed as

$$w=\int_0^\infty \mathrm{W}(k)\mathrm{J}_0(kr)dk \quad . \quad . \quad . \quad . \quad . \quad (1)$$

then the surface tensile stress necessary to maintain this deflexion is

$$\widehat{zz}=-\mathrm{R}\int_0^\infty k\mathrm{W}(k)\,\mathrm{J}_0(kr)\,dk \quad . \quad . \quad . \quad . \quad (2)$$

If it is assumed that there is no radial displacement of the surface of the foundation,

$$\mathrm{R}=\frac{2\mu(\lambda+2\mu)}{\lambda+3\mu}=\frac{4\,(1-\sigma)}{(3-4\sigma)}\mathrm{C};$$

or if there is no shearing force on the surface,

$$\mathrm{R}=\frac{2\mu(\lambda+\mu)}{\lambda+2\mu}=\frac{\mathrm{C}}{1-\sigma}.$$

From the usual formula for a thin plate symmetrically loaded

$$\frac{p+\widehat{zz}}{\mathrm{D}}=\frac{1}{r}\frac{d}{dr}\left[r\frac{d}{dr}\left\{\frac{1}{r}\frac{d}{dr}\left(r\frac{dw}{dr}\right)\right\}\right]. \quad . \quad . \quad (3$$

Substituting for w

$$\frac{p+\widehat{zz}}{\mathrm{D}}=\int_0^\infty k^4\mathrm{W}(k)\mathrm{J}_0(kr)\,dk, \quad . \quad . \quad . \quad (4)$$

and hence, substituting for $\widehat{zz}$

$$p=\int_0^\infty (\mathrm{D}k^4+\mathrm{R}k)\mathrm{W}(k)\mathrm{J}_0(kr)\,dk. \quad . \quad . \quad . \quad (5)$$

If $p=f(r)$ is expressed in terms of Bessel Functions as

then *

$$\left.\begin{aligned} p&=\int_0^\infty \mathrm{P}(k)\mathrm{J}_0(kr)\,dk,\\ \mathrm{P}(k)&=k\int_0^\infty \alpha f(\alpha)\mathrm{J}_0(k\alpha)\,d\alpha. \end{aligned}\right\} \quad . \quad . \quad . \quad (6)$$

Hence

$$\mathrm{W}(k)=\frac{\mathrm{P}(k)}{\mathrm{D}k^4+\mathrm{R}k}. \quad . \quad . \quad . \quad . \quad . \quad (7)$$

* See (4) p. 453.

For a load Π uniformly distributed over a circular area of radius a,

$$P(k) = \frac{\Pi}{\pi a} J_1(ka), \quad \ldots \ldots \quad (8)$$

and for a load M concentrated at a point

$$P(k) = \frac{\Pi}{2\pi} k. \quad \ldots \ldots \quad (9)$$

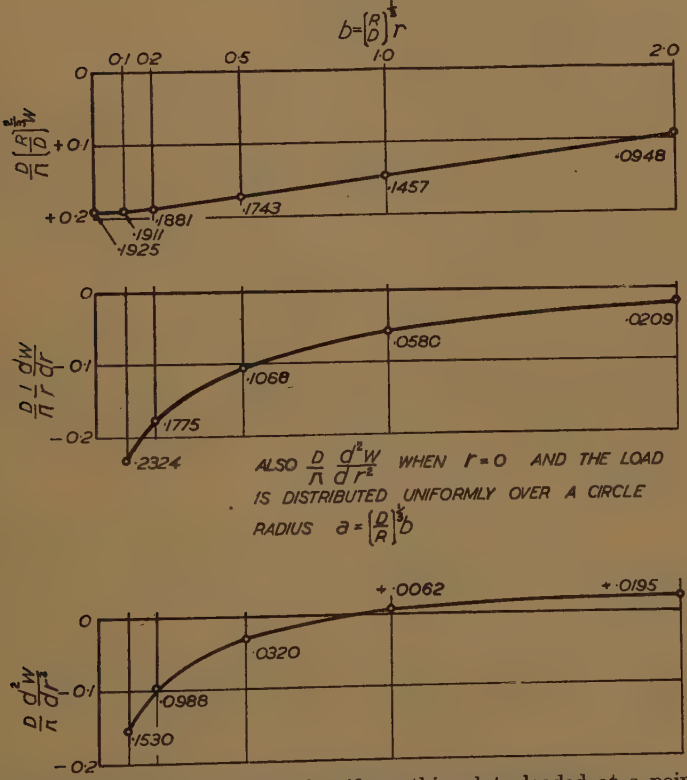

Displacement and curvature of uniform thin plate loaded at a point and resting on a semi-infinite perfectly elastic foundation.

So for a point load

$$\left.\begin{aligned} w &= \frac{\Pi}{2\pi}\int_0^\infty \frac{J_0(kr)\,dk}{Dk^3+R} = \frac{\Pi}{(DR^2)^{\frac{1}{3}}}\frac{b^2}{2\pi}\int_0^\infty \frac{J_0(x)\,dx}{x^3+b^3}, \\ \frac{dw}{dr} &= -\frac{\Pi}{2\pi}\int_0^\infty \frac{kJ_1(kr)\,dk}{Dk^3+R} = -\frac{\Pi}{(RD^2)^{\frac{1}{3}}}\frac{b}{2\pi}\int_0^\infty \frac{xJ_1(x)\,dx}{x^2+b^3}, \end{aligned}\right\} \quad \ldots \quad (10)$$

where $$b^3 = \frac{Rr^3}{D}.$$

For a load uniformly distributed over a circular area of radius a,

$$\frac{d^2w}{dr^2} = -\frac{\Pi}{2\pi a}\int_0^\infty \frac{kJ_1(ka)\,dk}{Dk^3+R} = -\frac{\Pi}{2\pi D}\int_0^\infty \frac{xJ_1(x)\,dx}{x^3+c^3} \quad (11)$$

at $r=0$, where $$c^3 = \frac{Ra^3}{D};$$

this is similar to the expression for $\frac{dw}{dr}$ under a point load.

For a point load, w will clearly be a function of b, and $\frac{dw}{dr}$ and $\frac{d^2w}{dr^2}$ can be found at once by direct differentiation, since

$$\frac{d}{dr} = \frac{(R)^{\frac{1}{3}}}{(D)}\frac{d}{db}.$$

It is unnecessary to give in full the details of the integration of these quantities. The method used will be outlined. The references are to pages in Watson's 'Bessel Functions.'

On p. 425

$$\int_0^\infty \frac{xJ_0(x)\,dx}{x^2+k^2} = K_0(k), \quad . \quad . \quad . \quad . \quad . \quad (12.1)$$

and $$\int_0^\infty \frac{J_0(x)\,dx}{x^2+k^2} = \frac{\pi}{2k}\{I_0(k)-L_0(k)\}. \quad . \quad (12.2)$$

Using the power series for $J_0(x)$,

$$\int_0^z \frac{xJ_0(x)\,dx}{x^2+k^2} \quad \text{and} \quad \int_0^z \frac{J_0(u)\,dx}{x^2+k^2}$$

can be expressed in powers of k and z, and hence, by substituting power series for K (k) (p. 80, eqn. 14), T (k) (p. 77, eqn. 2), and L (k) (p. 329, eqn. 11),

$$\int_z^\infty \frac{xJ_0(x)\,dx}{x^2+k^2} \quad \text{and} \quad \int_z^\infty \frac{J_0(x)\,dx}{x^2+k^2}$$

can be obtained as series.

Provided $k<z$, $\frac{1}{x^2+k^2}$ can be expanded in powers of k,

and equating the coefficients of k then gives the following expressions :—

$$\int_z^\infty \frac{J_0(x)\,dx}{x^{2r+1}} = (-)^r \left[\frac{1}{2^{2r}(\underline{|r})^2} \left\{ \psi(r+1) - \log_e \frac{z}{2} \right\} - \sum_{n=1}^{\infty} \frac{(-)^n z^{2n}}{2n 2^{2r+2n} (\underline{|r+n})^2} + \sum_{n=1}^{r} \frac{(-)^n z^{-2n}}{2n 2^{2r-2n} (\underline{|r-n})^2} \right] \quad (12.3)$$

and

$$\int_z^\infty \frac{J_0(x)\,dx}{x^{2r+2}} = (-)^{r+1} \left[\frac{\pi}{2^{2r+2}\{(\Gamma(r+\tfrac{3}{2})\}^2} + \sum_{n=1}^{\infty} \left\{ \frac{(-)^n z^{2n-1}}{(2n-1) 2^{2r+2n} (\underline{|r+n})^2} \right\} + \sum_{n=1}^{r+1} \left\{ \frac{(-)^n z^{-2n+1}}{(2n-1) 2^{2r-2n+2} (\underline{|r-n+1})^2} \right\} \right]. \quad (12.4)$$

Then $$\int_0^z \frac{J_0(x)\,dx}{x^3+b^3}$$

can be obtained by substituting the power series for $J_0(x)$ and provided $b<z$,

$$\int_z^\infty \frac{J_0(x)\,dx}{x^3+b^3} = \int_z^\infty \left\{ 1 - \frac{b^3}{x^3} + \frac{b^6}{x^6} - \dots \right\} \frac{J_0(x)\,dx}{x^3}.$$

Adding, the terms in z either cancel or tend to zero as z tends to infinity, giving finally :—

$$b^2 \int_0^\infty \frac{J_0(x)\,dx}{x^3+b^3} = \sum_{m=0}^{\infty} (-)^m \left[\frac{\left(\frac{b}{2}\right)^{6m+2} \cdot \log_e \left(\frac{b}{2}\right) - \left(\frac{b}{2}\right)^{6m+2} \cdot \psi(3m+2)}{(\underline{|3m+1})^2} + \frac{2\pi}{3\sqrt{3}} \cdot \frac{\left(\frac{b}{2}\right)^{6m}}{(\underline{|3m})^2} - \frac{2\pi}{3\sqrt{3}} \cdot \frac{\left(\frac{b}{2}\right)^{6m+4}}{(\underline{|3m+2})^2} + \frac{\pi}{2} \cdot \frac{\left(\frac{b}{2}\right)^{6m+5}}{\{\Gamma(3m+\frac{7}{2})\}^2} \right]. \quad \dots \quad (13)$$

Expressing the first few terms with numerical coefficients :—

$$\frac{D}{\Pi}\left(\frac{R}{D}\right)^{\frac{3}{2}} w = \{0{\cdot}03979\,b^2 - 0{\cdot}00001079\,b^8 + \ldots\}\log_e \frac{b}{2}$$
$$+ 0{\cdot}1925 - 0{\cdot}01682\,b^2$$
$$- 0{\cdot}003007\,b^4 + 0{\cdot}0007074\,b^5$$
$$- 0{\cdot}00008353\,b^6 + 0{\cdot}00001626\,b^8 + \ldots$$

$$\frac{D}{\Pi}\frac{1}{r}\frac{dw}{dr} = \{0{\cdot}07958 - 0{\cdot}00008635\,b^5 + \ldots\}\log_e \frac{b}{2}$$
$$+ 0{\cdot}006145 - 0{\cdot}01203\,b^2$$
$$+ 0{\cdot}003537\,b^3 - 0{\cdot}0005012\,b^4$$
$$+ 0{\cdot}00001193\,b^6 + 0{\cdot}0000001305\,b^8 + \ldots$$

$$\frac{D}{\Pi}\frac{d^2w}{dr^2} = \{0{\cdot}07958 - 0{\cdot}00006044\,b^6 + \ldots\}\log_e \frac{b}{2}$$
$$+ 0{\cdot}08572 - 0{\cdot}03608\,b^2$$
$$+ 0{\cdot}01415\,b^3 - 0{\cdot}002506\,b^4$$
$$+ 0{\cdot}00007484\,b^6 + 0{\cdot}000001175\,b^8 + \ldots$$

Curves are given showing the form of these functions for values of $b < 2$.

It has been verified by approximate numerical integration that for values of a of the same order as t the deflexion under the centre of the distributed load differs only slightly from the deflexion under the same total load applied at a point.

References.

(1) H. M. Westergaard, ' Public Roads,' vii. p. 31 (1926-7).
(2) G. N. Watson, ' Treatise on the Theory of Bessel Functions,' Cambridge, 1922.
(3) A. H. E. Love, ' Treatise on the Mathematical Theory of Elasticity,' 4th ed., Cambridge, 1927.
(4) K. Terazawa, ' On the Elastic Equilibrium of a Semi-Infinite Solid,' Journ. Coll. Science, Imp. Univ. of Tokyo, xxxvii. Art. 7 (Dec. 1916). See also H. Lamb, London Math. Soc. Proc. xxxiv. p. 276 (1902).

XLIX. *Notices respecting New Books.*

Random Variables and Probability Distributions. By HARALD CRAMÉR. [Pp. 121.] (Cambridge Tracts in Mathematics and Mathematical Physics: Cambridge University Press, 1937. Price 6*s.* 6*d.*)

THE mathematical theory of probability has had a long and interesting life before attaining to anything like a satisfactory definition of its subject-matter and method. As it arises out of the observation that, in assigned conditions which are insufficient for complete determination, the relative frequency of occurrence of an event often seems to indicate the existence of a characteristic proportion, two possible ways of defining this proportion suggest themselves :—(i.) as a limiting value of the relative frequency when the number of trials increases without limit, (ii.) as a property of the governing conditions. The first, or "frequency," theory requires as its basis a description of the series of trials which will account for its observed properties, and it is not generally agreed that any such description has yet been found. The second, or "classical," theory sets up a model or "constitution" which may be compared with those used in physical theories; but the aspect of observations dealt with is so general that the model becomes completely abstract and is expressed in terms of sets of points.

This is clearly and concisely explained in the opening chapter of this tract, which then proceeds to develop the foundations of the classical theory in its modern form.

Part I. (Chaps. 1, 2) gives the axioms and the required properties of point sets and Stieltjes integrals. Part II. (Chaps. 3 to 8) develops the theory of frequency distributions in terms of characteristic functions, examines the nature of stochastic or "probability" convergence, discusses the normal distribution and its relation to the distribution of a sum (theory of elementary errors), and then goes on to more recent developments of these fundamental principles. In Part III. (Chaps. 9, 10) is given an introduction to multivariate distributions.

There is a limited bibliography.

Though by no means elementary, the account thus given is easy to read by reason of the clear set-out and good exposition, and can be strongly recommended to anyone desirous of being able to read critically the frequent memoirs now being published on probability theory and its applications.

A Comprehensive Treatise on Inorganic and Theoretical Chemistry.—Vol. XVI. *Pt. and General Index.* By J. W. Mellor, D.Sc., F.R.S. [Pp. x+811.] (Price £3 3*s*.)

The appearance of this volume marks the completion of the original scheme of this vast work, but the indefatigable author is not yet content with his achievement, for we are informed in the Preface that three supplementary volumes are to be prepared, of which two will deal with recent work, more particularly on the subjects of the earlier volumes, whilst the third is to cover the "ill-defined borderland" between organic and inorganic chemistry.

The style and arrangement of the present volume conform closely to the model with which we have become familiar, and require no special comment. In addition, however, to the material dealing specifically with platinum the volume includes topics which concern the group of the platinum metals as a whole, such as their history and the analytical methods for their separation. Although the other metals of the group were included in the previous volume, this seems a very appropriate place for such topics, since platinum is the longest-known and most abundant member of the group to which its name has been given. There are also, as in the earlier volumes, short but comprehensive discussions of more general topics where relevant: on heterogeneous catalysis, and, in connexion with the platinum ammines, on the application of the electronic theory of valency to coordination compounds.

The general index (compiled by Miss E. M. Rigby) occupies very nearly four hundred pages, and to dip into it in the hope of finding some omission is a fascinating but completely disappointing pastime, and gives one a real impression of the tremendous scale of the work.

To congratulate the author would be an impertinence: rather is the Inorganic Chemist to be congratulated on having at last a really exhaustive summary of the immense literature of his subject.

[*The Editors do not hold themselves responsible for the views expressed by their correspondents.*]

FIG. 3.

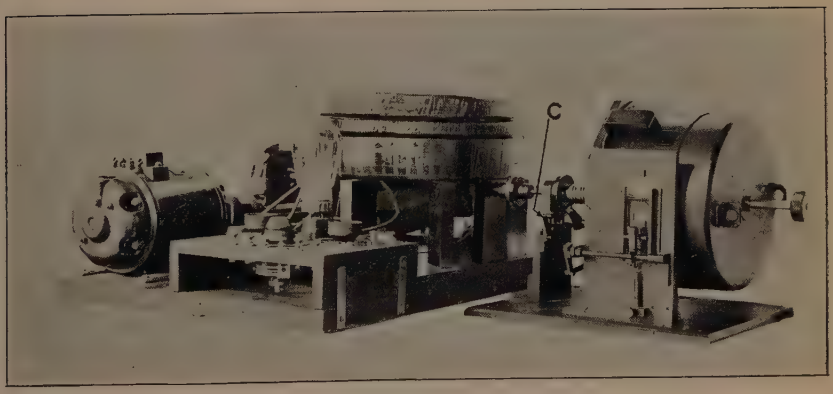

Harmonic analyses.

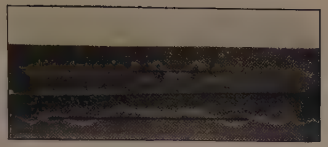

No. 1.

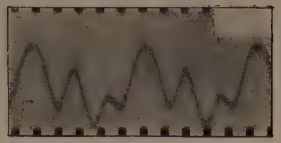

No. 2.

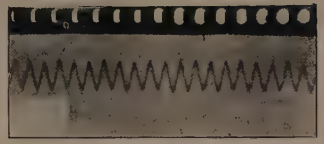

No. 3.

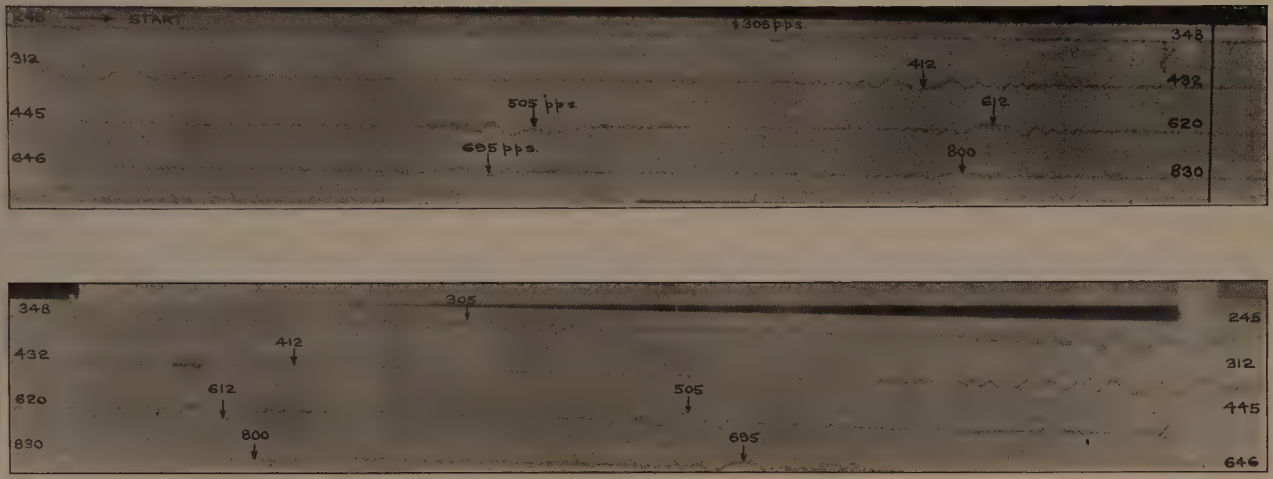

No. 4.

Harmonic analysis records.

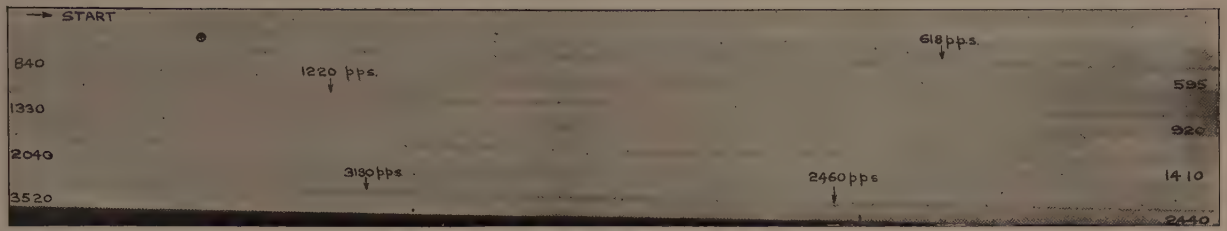

No. 5.

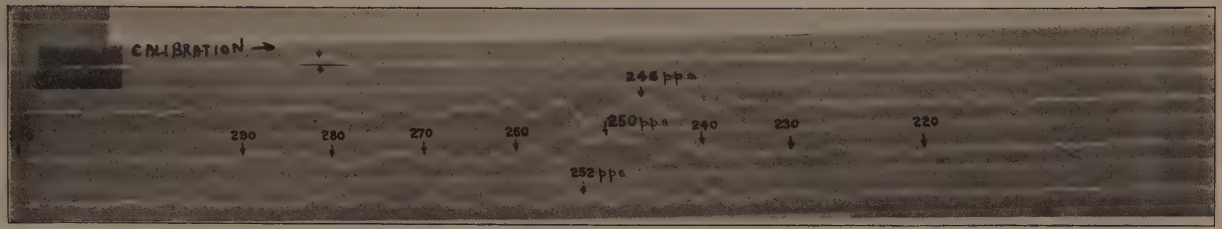

No. 6.

Harmonic analysis records.

THE

LONDON, EDINBURGH, AND DUBLIN

PHILOSOPHICAL MAGAZINE

AND

JOURNAL OF SCIENCE.

[SEVENTH SERIES.]

APRIL 1938.

L. *Operational and Matrix Methods in Linear Variable Networks.* *By* Louis A. Pipes, *Ph.D., Alumni Research Fellow, The University of Wisconsin* *.

Introduction.

IT is the purpose of this paper to present a general method for the solution of problems arising in the analysis of linear circuits whose parameters vary with the time. The first part of the paper will be devoted to a discussion of circuits in which the parameters vary continuously with the time in a known manner. This variation is assumed to be a variation which is smaller in absolute value than the constant part of the variable parameter. Circuits of practical importance that come under this category are, for example, the microphone transmitter, the condenser transmitter, and the induction generator. The latter may be regarded as a system with variable mutual inductance between primary and secondary. Many mechanical problems of variable stiffness or mass also come under this general class.

The second part of the paper is devoted to a discussion of linear lumped circuits whose parameters are fixed throughout definite time intervals, but are then abruptly changed to new values at certain definite times. Such a

* Communicated by the Author.

discussion covers general switching operations. By means of matrix notation and the Laplacian transform or operational method, general formulas will be established that are applicable to special cases.

I. *The Most General Linear Lumped Circuit.*

The discussion will begin with a consideration of the problem of the most general linear lumped series network whose parameters vary with the time. The variation of the parameters will be assumed to be a variation around a certain fixed value. That is, if $R(t)$, $L(t)$, and $S(t)$ be the resistance, inductance, and elastance of the circuit, we will suppose that

$$\left.\begin{aligned} R(t)&=R_0+r(t),\\ L(t)&=L_0+f(t),\\ S(t)&=S_0+s(t),\end{aligned}\right\} \quad \text{where} \quad \left.\begin{aligned} |s|&<S,\\ |r|&<R\\ |f|&<L,\end{aligned}\right\} \quad \text{throughout the range in } t.$$

If these three variable elements are connected in series with an electromotive force $e(t)$, the equation satisfied by the charge on the elastance element is

$$\frac{d}{dt}\left(L\frac{dQ}{dt}\right)+R\frac{dQ}{dt}+SQ=e(t), \quad . \quad . \quad . \quad (1)$$

or

$$D^2Q+\frac{(DL+R)}{L}DQ+\frac{SQ}{L}=\frac{e(t)}{L}, \quad . \quad . \quad . \quad (2)$$

where $$D=\frac{d}{dt}.$$

Now let

$$P(t)=\frac{DL+R}{L}, \quad . \quad . \quad . \quad . \quad . \quad . \quad (3)$$

and make the transformation

$$Q=v(t)e^{-\frac{1}{2}\int P dt}. \quad . \quad . \quad . \quad . \quad . \quad . \quad (4)$$

A substitution in (2) shows that $v(t)$ must satisfy

$$D^2v+A(t)v=B(t), \quad . \quad . \quad . \quad . \quad . \quad (5)$$

where

$$A(t)=\frac{S}{L}-\frac{1}{2}DP-\frac{1}{4}P^2. \quad . \quad . \quad . \quad . \quad (6)$$

$$B(t)=\frac{E}{L}e^{\frac{1}{2}\int P dt} \quad . \quad . \quad . \quad . \quad . \quad . \quad . \quad (7)$$

This equation is simpler than (2) in that it does not contain the first derivative. Let us now suppose that originally at $t=0$ we have specified the charge Q on the condenser and also the current flowing in the circuit, and that the source of e.m.f. is applied at the instant $t=0$.

We must translate these initial conditions as boundary conditions on v.

From (4) we obtain,

$$(\mathrm{Q})_{t=0}=\mathrm{Q}_0=v(0), \quad . \quad . \quad . \quad . \quad . \quad . \quad . \quad . \quad (8)$$

$$(\mathrm{DQ})_{t=0}=\mathrm{Q}_1=(\mathrm{D}v)_{t=0}-\tfrac{1}{2}\mathrm{P}(0)v(0) \quad . \quad . \quad . \quad (9)$$

The boundary conditions on v are, hence :

$$(v)_{t=0}=\mathrm{Q}_0, \quad (\mathrm{D}v)_{t=0}=\mathrm{Q}_1+\tfrac{1}{2}\mathrm{P}(0)\mathrm{Q}_0=x, \text{ say.} \quad (10)$$

II. *The Solution of the Equation.*

The problem has reduced to solving (5),

$$\mathrm{D}^2v+\mathrm{A}(t)v=\mathrm{B}(t),$$

subject to $v=\mathrm{Q}_0$, $\mathrm{D}v=x$ at $t=0$.

In the usual problem of practical importance, because of the original restrictions on R, L, and S, it happens that the coefficient $\mathrm{A}(t)$ may be decomposed into two parts, one which varies with the time and one that is constant.

Accordingly let us write

$$\mathrm{A}(t)=a^2+b(t), \quad . \quad . \quad . \quad . \quad . \quad (11)$$

a^2 being the constant part and $b(t)$ being the variable part of $\mathrm{A}(t)$. If, as is supposed, the variation of the circuit elements be small in comparison with their invariable part, then we can say

$$|b(t)|<a^2. \quad . \quad . \quad . \quad . \quad . \quad . \quad (12)$$

Let the equation (5) be multiplied through by $pe^{-pt}dt$ and integrated from 0 to infinity with the restriction that the real part of p is greater than zero.

We thus obtain

$$p\int_0^\infty e^{-pt}\mathrm{D}^2v\,dt+a^2p\int_0^\infty e^{-pt}v\,dt+p\int_0^\infty e^{-pt}b(t)v\,dt$$

$$=p\int_0^\infty e^{-pt}\mathrm{B}(t)\,dt \quad . \quad (13)$$

if we let

$$p\int_0^\infty e^{-pt}v(t)\,dt=\mathrm{V}(p), \quad . \quad . \quad . \quad . \quad (14)$$

or, more briefly, $\mathrm{V}\doteqdot v$, that is, $\mathrm{V}(p)$ be the operational or Laplacian transform of $v(t)$, and let

$$p\int_0^\infty e^{-pt}\mathrm{B}(t)\,dt=\mathrm{G}(p), \quad . \quad . \quad . \quad . \quad (15)$$

or $$\mathrm{B}(t)\doteqdot\mathrm{G}(p).$$

By integrating the equation (13) by parts and making use of the boundary conditions (10) we obtain

$$(p^2+a^2)\mathrm{V}+p\int_0^\infty e^{-pt}b(t)v\,dt=\mathrm{G}(p)+p^2\mathrm{Q}_0+px \quad (16)$$

or

$$\mathrm{V}=\frac{1}{p^2+a^2}\left(\mathrm{G}+p^2\mathrm{Q}_0+px-p\int_0^\infty e^{-pt}b(t)v\,dt\right). \quad (17)$$

We note that in the absence of $b(t)$, or of any variation in the circuit constants, we would have immediately the solution:

$$v=\frac{1}{2\pi j}\int_{c-j\infty}^{c+j\infty}\frac{e^{pt}\mathrm{V}(p)\,dp}{p}, \quad j=\sqrt{-1}. \quad . \quad . \quad (18)$$

By the inversion of the Laplacian transform period, C is such a constant that all the singularities of the integrand lie to the left of the path of integration, and V in this case is given by

$$\mathrm{V}(p)=\frac{1}{p^2+a^2}(\mathrm{G}+p^2\mathrm{Q}_0+px). \quad . \quad . \quad . \quad (19)$$

III. *The Successive Approximations.*

To solve equation (17) when $b(t)$ is not zero let us assume

$$\mathrm{V}=\sum_{n=0}^{\infty}\mathrm{V}_n \quad \text{and} \quad v=\sum_0^\infty v_n. \quad . \quad . \quad . \quad . \quad (20)$$

Now since $\mathrm{V}\doteqdot v$, this relation may be satisfied if we place $v_i\doteqdot\mathrm{V}_i$, or, that is, each of the v_i quantities is placed in operational equivalence with the V_i quantity.

Substituting the relations (20) into the equation (17), we obtain

$$\sum_{n=0}^{\infty} V_n = \frac{1}{p^2+a^2} \times \left(G+p^2Q_0+px-p\int_0^{\infty} e^{-pt}b(t) \sum_{n=0}^{\infty} v_n d_t\right). \quad (21)$$

Now let

$$\left.\begin{aligned} V_0 &= \frac{1}{p^2+a^2}(G+p^2Q_0+px) \doteqdot v_0, \\ V_1 &= \frac{-p}{p^2+a^2}\int_0^{\infty} e^{-pt}b(t)v_0\,dt \doteqdot v_1, \\ &\cdots\cdots\cdots\cdots \\ V_n &= \frac{-p}{p^2+a^2}\int_0^{\infty} e^{-p(t)t}\,bv_{n-1}\,dt \doteqdot v_n. \end{aligned}\right\} \quad (22)$$

That is, V_0 is the operational solution if there were no variable coefficient $b(t)$. V_1 is the operational equivalent of the first correction term, etc.

IV. *The Convergence.*

To establish the convergence of the process we employ the following theorem:

If $$g_1(p) \doteqdot h_1(i), \quad (23)$$

and $$g_2(p) \doteqdot h_2(t),$$

then

$$\frac{g_1g_2}{p} \doteqdot \int_0^t h_1(u)h_2(t-u)\,du, \quad (24)$$

a well-known theorem in the operational calculus.

Now

$$\frac{G(p)}{p^2+a^2} = \frac{1}{p}\cdot\frac{p}{p^2+a^2}G(p) \quad (25)$$

and

$$\frac{p}{p^2+a^2} \doteqdot \frac{\sin at}{a}; \quad G(p) \doteqdot B(t). \quad (26)$$

Hence

$$\frac{G(p)}{p^2+a^2} = \frac{1}{a}\int_0^t \sin a(t-y)B(y)\,dy, \quad (27)$$

and

$$\left.\begin{aligned} \frac{p^2 Q_0}{p^2+a^2} &\doteqdot Q_0 \cos at, \\ \frac{px}{p^2+a^2} &\doteqdot \frac{x \sin at}{a}. \end{aligned}\right\} \quad . \quad . \quad . \quad . \quad . \quad (28)$$

Therefore

$$V_0 \doteqdot v_0 = 1/a \int_0^t \sin a(t-y) B(y)\, dy + \cos at + \frac{x \sin at}{a}. \quad (29)$$

Now

$$\left| 1/a \int_0^t \sin a(t-y) B(y)\, dy \right| \leqslant 1/a \int_0^t |\sin a(t-y)| \,.\, |B(y)|\, dy. \quad . \quad . \quad . \quad (30)$$

Let $|B(y)| \leqslant M$, then

$$\left| 1/a \int_0^t \sin a(t-y) B(y)\, dy \right| \leqslant 1/a \int_0^t M\, dy = Mt/a. \quad (31)$$

Therefore

$$|v_0| < Mt/a + |Q_0| + |x/a|. \quad . \quad . \quad . \quad (32)$$

Now

$$V_1 = -p/(p^2+a^2) \int_0^\infty e^{-pt} b(t) v_0\, dt. \quad . \quad . \quad (33)$$

Let

$$G_1 = p \int_0^\infty e^{-pt} b(t) v_0\, dt \doteqdot b(t) v_0, \quad . \quad . \quad . \quad (34)$$

then

$$v_1 \doteqdot -\frac{p}{(p^2+a^2)} G_1(p). \quad . \quad . \quad . \quad . \quad (35)$$

Hence by (24)

$$v_1 = -1/a \int_0^t \sin a(t-y) b(y) v_0(y)\, dy. \quad . \quad . \quad (36)$$

Let $|b(t)| \leqslant M_1$.

Therefore

$$\left.\begin{aligned} |v_1| &\leqslant 1/a \int_0^t |\sin a(t-y)|\, |b(y)|\, |v_0(y)|\, dy, \\ |v_1| &\leqslant 1/a \int_0^t M_1 (My/a + Q_0 + x/a)\, dy, \\ |v_1| &\leqslant \frac{M_1 M t^2}{2a^2} + \frac{M_1 |Q_0| t}{a} + \frac{M_1 |x| t}{a^2}. \end{aligned}\right\} \quad . \quad (37)$$

Continuing the process, we can say

$$|v_n| \leqslant \frac{MM_1^n t^{n+1}}{a^{n+1}(n+1)!} + \frac{M_1^n |Q_0| t^n}{a^n n!} + \frac{M_1^n |x| t^n}{a^{n+1} n!} \quad . \quad (38)$$

Now, since $v = \sum_{n=0}^{\infty} v_n$, and if we let $h = M_1/a$, we obtain, on comparing with the exponential series e^{ht},

$$|v| \leqslant \frac{M}{M_1}(e^{ht}-1) + |Q_0| e^{ht} + |x/a| e^{ht}, \quad . \quad (39)$$

and hence the solution thus obtained converges absolutely. The limitations imposed on $b(t)$ and $B(t)$, namely, that they be bounded throughout the interval under consideration, are met in the type of physical system which we are considering. We note here that if $|b(t)|, < a^2$, then h is small and the series converges most rapidly. This means that the system is only slightly perturbed from the invariable state. The special merit of this form of solution is that the effect of each initial condition is clearly noted, and in practical problems operational processes may be used to great advantage in shortening the computations.

V. *Special Case. Variable Elastance.*

As an illustration of the general method, let us consider the case of a circuit having negligible resistance and a condenser and inductance in series. Let the elastance of the circuit vary in the following manner :

$$S = S_0 + s \cos wt, \quad \text{where} \quad |s| < S_0. \quad . \quad . \quad (40)$$

In the absence of any impressed electromotive force the equation for the charge is

$$D^2Q + S_0 Q/L + \frac{s}{L} \cos wt\, Q = 0, \quad D = \frac{d}{dt}. \quad . \quad (41)$$

Let $S_0/L = a^2$, $s/L = b$.

We shall suppose the boundary conditions

$$\left.\begin{aligned} DQ &= 0, \\ Q &= x \end{aligned}\right\} \text{ at } t = 0. \quad . \quad . \quad . \quad . \quad . \quad (42)$$

If we carry out the general process given in section III. we let

$$Q = V, \quad . \quad . \quad . \quad . \quad . \quad . \quad (43)$$

and we obtain

$$V_0 = \frac{p^2 x}{p^2+a^2} = x \cos at = Q_0, \quad . \quad . \quad . \quad (44)$$

the first approximation, and

$$V_1 = \frac{-pbx}{p^2+a^2}\int_0^\infty e^{-pt} \cos wt \cos(at)\, dt \doteqdot Q_1. \quad . \quad (45)$$

Now

$$\cos(wt)\cos(at) = \frac{\cos(w+a)t + \cos(w-a)t}{2} \quad . \quad (46)$$

and

$$\cos(mt) \doteqdot \frac{p^2}{p^2+m^2}. \quad . \quad . \quad . \quad . \quad . \quad (47)$$

Now to shorten the writing let us introduce the notation

$$T(a) = \frac{1}{p^2-a^2}. \quad . \quad . \quad . \quad . \quad . \quad (48)$$

Then we have the operational equivalents

$$\tfrac{1}{2}[T(a+b)p^2 + T(a-b)p^2] \doteqdot \cos(at)\cos(bt), \quad (49)$$

$$T(a)T(b)p^2 \doteqdot \frac{\cos(at)-\cos(bt)}{b^2-a^2}. \quad . \quad . \quad (50)$$

$$T^2(a) \doteqdot \frac{t \sin(at)}{2a}. \quad . \quad . \quad . \quad . \quad . \quad (51)$$

Equipped with these well-known operational equivalents we proceed to determine the various terms in the series for Q.

In this notation we have

$$Q_1 \doteqdot \frac{-xb}{2} T(a)[T(w+a)p^2 + T(w-a)p^2] \text{ if } w \neq a; \quad (52)$$

therefore

$$Q_1 = \frac{-xb}{2}\frac{[\cos(at)-\cos(w+a)t]}{(w+a)^2-a^2} + \frac{-xb}{2}\frac{[\cos(at)-\cos(w-a)t]}{(w-a)^2-a^2} \quad \text{if } w \neq \pm 2a, \quad (53)$$

and

$$Q_2 = \frac{b^2x}{4}\frac{[T(w+a)p^2+T(w-a)p^2-T(2w+a)p^2-T(-a)p^2]}{w(w+2a)}T(a)$$
$$+\frac{b^2x}{4}T(a)\frac{[T(w+a)p^2+T(w-a)p^2-T(2w-a)p^2-p^2T(a)]}{w(w-2a)}, \quad \ldots \quad (54)$$

and

$$Q_2 = \frac{b^2x}{4w(w+2a)}$$
$$\times\left[\frac{\cos(at)-\cos(w+a)t}{w(w+2a)}+\frac{\cos(at)-\cos(w-a)t}{w(w-2a)}\right.$$
$$\left.-\frac{\cos(at)-\cos(2w+a)t}{4w(w+a)}-\frac{t\sin(at)}{2a}\right]+\frac{b^2x}{4w(w-2a)}$$
$$\times\left[\frac{\cos(at)-\cos(w+a)t}{w(w+2a)}+\frac{\cos(at)-\cos(w-a)t}{w(w-2a)}\right.$$
$$\left.-\frac{\cos(at)-\cos(2w-a)t}{2w(w-a)}-\frac{t\sin(at)}{2a}\right]. \quad \ldots \quad (55)$$

We have here supposed that w is not an integral multiple of a. If b is small and w is large, the series converges very rapidly. The treatment when w is a rational integral multiple of a follows the same lines, but the operational expressions are somewhat more complicated. It may be noted that in this example the various terms may be written down at once when the operational expressions (49), (50), and (51) are used.

VI. *Special Case. Variable Resistance.*

We shall next consider a case which we can solve in finite form in order to bring out some points of interest in the method.

Consider a series circuit containing fixed inductance but variable resistance. The equation satisfied by the current in such a circuit is given by

$$Di+Ai+\frac{r(t)i}{L}=0, \quad D=\frac{d}{dt}, \quad A=R/L. \quad \ldots \quad (56)$$

We are here supposing that the resistance in the circuit

has a fixed part R and a variable component $r(t)$. Let the variation of the resistance be given by

$$r(t)=a\cos(wt) \quad |a|<\mathrm{R}, \quad . \quad . \quad . \quad (57)$$

and let us suppose that at $t=0$ we have the initial current $i=x$.

Carrying out our general process, we obtain the following equations :

$$i \doteqdot \mathrm{V}, \quad . \quad . \quad . \quad . \quad . \quad . \quad . \quad (58)$$

$$(p+\mathrm{A})\mathrm{V}=px-p\int_0^{\infty} e^{-pt}a\cos(wt)i\,dt, \quad . \quad (59)$$

$$\mathrm{V}_0=\frac{px}{p+\mathrm{A}} \doteqdot xe^{-\mathrm{A}t}, \quad . \quad . \quad . \quad . \quad (60)$$

$$\mathrm{V}_1=\frac{-pxa}{p+\mathrm{A}}\int_0^{\infty} e^{-pt}e^{-\mathrm{A}t}\cos(wt)\,dt. \quad . \quad . \quad (61)$$

Now

$$\frac{p(p+\mathrm{A})}{(p+\mathrm{A})^2+w^2} \doteqdot e^{-\mathrm{A}t}\cos wt\,; \quad . \quad . \quad . \quad (62)$$

therefore

$$\mathrm{V}_1=\frac{-xa}{(p+\mathrm{A})}\frac{p(p+\mathrm{A})}{(p+\mathrm{A})^2+w^2}=\frac{-xap}{(p+\mathrm{A})^2+w^2}. \quad . \quad (63)$$

But

$$\frac{p}{(p+\mathrm{A})^2+w^2} \doteqdot \frac{e^{-\mathrm{A}t}\sin(wt)}{w}\,; \quad . \quad . \quad . \quad (64)$$

therefore

$$i_1=\frac{-xa}{w}e^{-\mathrm{A}t}\sin(wt). \quad . \quad . \quad . \quad . \quad (65)$$

Carrying out the process, we obtain the solution

$$i=xe^{-\mathrm{A}t}\left(1-\frac{a\sin(wt)}{w}+\frac{a^2\sin^2(wt)}{w^2 2\,!}-\frac{a^3\sin^3(wt)}{w^3 3\,!}\right). \quad (66)$$

Now by elementary methods we can obtain the solution in finite form :

$$i=xe^{-\mathrm{A}t}\exp\left[\frac{(-a\sin wt)}{w}\right]. \quad . \quad . \quad . \quad (67)$$

The term $\exp\left[\frac{(-a\sin wt)}{w}\right]$ is the sum of the series in the

bracket term of (66), and the solutions are seen to be identical. Since the equation (56) is a linear equation of the first order, we can write down its solution in finite form. For second-order equations we must in general resort to series methods. The illustration here given shows in what relation the series solution obtained operationally stands with the solution in finite form.

VII. *The Effect of Switching Operations.*

In a great many problems of technical interest the circuit parameters are constant throughout certain intervals of time, but because of switching operations they are abruptly changed to new values at the instant of switching. It will now be shown how the effect of such abrupt changes in circuit parameters may be readily handled by the use of the Laplacian transform theory and matrix notation.

Let us consider the most general linear network with lumped invariable parameters. The well-known canonical equations of such a network may be written in the form

$$[Z]\,[i]=[e] \text{ (see reference (1))}, \quad . \quad . \quad . \quad (68)$$

where

$$Z_{ij}=L_{ij}\frac{d}{dt}+R_{ij}+S_{ij}\int_{-\infty}^{t}(\,)\,dt. \quad . \quad . \quad . \quad (69)$$

If we now multiply this matrix equation by $pe^{-pt}dt$ and integrate from 0 to infinity we then obtain

$$p\int_0^\infty e^{-pt}[Z][i]\,dt=p\int_0^\infty e^{-pt}[e]\,dt]. \quad . \quad . \quad (70)$$

(see reference (1) for the meaning of this process).

Now let

$$[E]=p\int_0^\infty e^{-pt}[e]\,dt, \quad . \quad . \quad . \quad . \quad (71)$$

$$[I]=p\int_0^\infty e^{-pt}[i]\,dt, \quad . \quad . \quad . \quad . \quad (72)$$

or $$[E]\doteqdot[e] \quad \text{and} \quad [I]\doteqdot[i]; \quad . \quad . \quad (73)$$

that is, the matrix [E] is the operational equivalent of the matrix [e], and similarly the matrix [I] is the operational equivalent of the matrix [i] (see reference (2)).

If we assume that the initial values of the currents at $t=0$ are given by the matrix [i^0] and the initial charges

on the condensers are given by $[Q^0]$ our equation (70) transforms into

$$[Z(p)][I]=[E]+p[L][i^0]-[S][Q^0], \quad . \quad . \quad (74)$$

where $$Z_{rs}=L_{rs}p+R_{rs}+S_{rs}/p. \quad . \quad . \quad . \quad . \quad (75)$$

Now

$$[I]=[Z(p)]^{-1}([E]+p[L][i^0]-[S][Q^0]) \quad . \quad (76)$$

and the n mesh currents are given explicitly by the expression

$$[i(t)]=\frac{1}{2\pi j}\int_{c-j\infty}^{c+j\infty}\frac{e^{pt}[I]\,dp}{p} \quad j=\sqrt{-1} \quad . \quad . \quad (77)$$

(see reference [2]).

We have, then, an explicit solution for the most general linear, lumped, invariable network satisfying specified initial conditions, and on which are impressed arbitrary e.m.f.s.

Case I.

Sudden Insertion of Electromotive Forces.

If the network is not altered, but an electromotive force is changed in some branch at $t=t_1$ then we have

$$[e]=[e^0]+[e'] \quad . \quad . \quad . \quad . \quad . \quad . \quad (78)$$

where $[e^0]$ is the matrix of electromotive forces at $t=0$, and $[e']$ takes into account the change in the electromotive forces at $t=t_1$. That is,

$$[e^1]=[0] \text{ at } 0<t<t_1 \quad . \quad . \quad . \quad . \quad . \quad (79)$$

Now if

$$[E^0]\doteq[e^0] \text{ and } [E']=[e']. \quad . \quad . \quad . \quad (80)$$

then $$[E]\doteq[E^0]+[E']. \quad . \quad . \quad . \quad . \quad . \quad . \quad (81)$$

If the e.m.f.s are changed at t_i $i=1, 2, 3, \ldots, n$, the matrix $[E]$ contains as many parts as there are operational equivalents to the e.m.f.'s added. The solution is given by (77).

Case II.

Change in Circuit Parameters.

Let us suppose that at $t=t_i$ the circuit parameters are changed by switching operations:

We have the fundamental boundary conditions that the currents and charges at the end of the nth interval must equal the currents and charges at the beginning of the $(n+1)$th interval.

Let

$(Z)_1$ be the operational impedance matrix throughout the interval $0<t<t_1$;

$[Z]_n$ be the operational impedance matrix throughout the interval $t_n<t<t_{n+1}$;

$$[E]_n \doteqdot [e(t_n+t)] \quad t_n<t<t_{n+1};$$

$$[I]_n \doteqdot [i(t)]_n \quad t_n<t<t_{n+};$$

$$[i^0]_n = [i] \quad \text{at } t=t_n;$$

$$[Q^0]_n = [Q] \quad \text{at } t=t_n.$$

Then

$$[I]_n=[Z]_n^{-1}([E]_n+p[L]_n[i^0]_n-[S]_n[Q^0]_n), \quad . \quad (82)$$

and in the interval $i_n<t<t_{n+1}$

$$[i(t)]_n \doteqdot [I]_n. \quad . \quad . \quad . \quad . \quad . \quad . \quad (83)$$

We have, therefore, a very convenient chain process by which the effect of the switching operations may be determined.

The systematizing of the work by the use of matrix notation results in a great saving of labour and effort in a numerical case.

VIII. *Systems of Equations with Variable Coefficients.*

The paper will be concluded with a consideration of a system of linear equations with variable coefficients. To illustrate the method, let us consider the following problem, which in a general form includes the problem of the induction generator.

Given an invariable primary and secondary circuit with a variable mutual inductance $M_{12}=M_{21}$, which is a specified function of the time. In this particular case let M_{12} be composed of an invariable part $L_{12}=L_{21}$, and a variable component $b_{12}(t)=b_{21}(t)$.

The fundamental equations for such a circuit are

$$\left.\begin{aligned} Z_{11}i_1+D(M_{12}i_2)&=e_1(t),\\ D(M_{21}i_1)-Z_{22}i_2&=0,\end{aligned}\right\} \quad . \quad . \quad . \quad . \quad (84)$$

where

$$Z_{11}=R_{11}+L_{11}\frac{d}{dt}+S_{11}\int_{-\infty}^{t}(\ )\,dt. \quad . \quad . \quad (85)$$

$e_1(t)$ is the impressed primary voltage.

$$M_{12}=L_{12}+b_{12}(t), \qquad M_{21}=L_{21}+b_{21}(t), \quad . \quad (86)$$

where $L_{12}=L_{21}$, $b_{12}=b_{21}$.

Let us multiply the equations (84) by $pe^{-pt}dt$ and integrate from 0 to infinity.

Let $$I_1 \doteqdot i, \quad . \quad . \quad . \quad . \quad . \quad . \quad . \quad (87)$$

$$E_1 \doteqdot e_1. \quad . \quad . \quad . \quad . \quad . \quad . \quad (88)$$

The equations transform as follows :

$$\left.\begin{aligned} &Z_{11}(p)I_1-pL_{11}i_1^0+S_{11}q_1^0+p\int_0^{\infty}e^{-pt}\frac{d}{dt}(M_{12}i_2)\,dt=E_1,\\ &p\int_0^{\infty}e^{-pt}\frac{d}{dt}(M_{21}i_1)\,dt+Z_{22}(p)I_2-pL_{22}i_2^0+S_{22}q_2^0=0, \end{aligned}\right\} \quad (89)$$

where $Z_{11}(p)=pL_{11}+R_{11}+S_{11}/p$ and i_1^0, i_2^0 are the initial currents at $t=0$ and q_1^0 q_2^0 are the charges at $t=0$.

By an integration by parts we obtain

$$p\int_0^{\infty}e^{-pt}\frac{d}{dt}(M_{12}i_2)\,dt=-pL_{12}i_2^0-pb_{12}^0i_2^0+pL_{12}I_2 \\ +p^2\int_0^{\infty}e^{-pt}b_{12}i_2\,dt, \quad (90)$$

where

$$b_{12}^0=b_{12}(0).$$

Transforming the other integral in (89) in a similar manner and employing similar notations, the two equations (89) may be written in the matrix form

$$\left.\begin{aligned} &\begin{pmatrix} Z_{11} & pL_{12}\\ pL_{21} & Z_{22}\end{pmatrix}\begin{pmatrix} I_1\\ I_2\end{pmatrix}=p\begin{pmatrix} L_{11} & (L_{12}+b_{12}^0)\\ (L_{21}+b_{21}^0) & L_{22}\end{pmatrix}\begin{pmatrix} i_1^0\\ i_2^0\end{pmatrix},\\ &-\begin{pmatrix} S_{11} & 0\\ 0 & S_{22}\end{pmatrix}\begin{pmatrix} q_1^0\\ q_2^0\end{pmatrix}+\begin{pmatrix} E_1\\ 0\end{pmatrix}-p\begin{pmatrix} T_1\\ T_2\end{pmatrix}, \end{aligned}\right\} \quad . \quad (91)$$

where

$$T_1 \doteqdot b_{12}i_2, \quad T_2 \doteqdot b_{21}i_1\,;$$

or, more briefly,

$$[Z][I]=p[L][i^0]-[S][q^0]+[E]-p[T] \quad . \quad . \quad (92)$$

or

$$[I]=[Z]^{-1}(p)[L][i^0]-[S][q^0]+[E]-p[T]. \quad . \quad (93)$$

Now let

$$[I] =[I]_n, \quad . \quad . \quad . \quad . \quad . \quad . \quad . \quad . \quad . \quad (94)$$

$$[I]_n=\begin{pmatrix} I_{1n} \\ I_{2n} \end{pmatrix} \quad [I] \doteq [i]_n=\begin{pmatrix} i_{1n} \\ i_{2n} \end{pmatrix}, \quad . \quad . \quad (95)$$

and let

$$[I]_0=[Z]^{-1}(p[L][i^0]-[S][q^0]+[E]). \quad . \quad . \quad . \quad (96)$$

This is the operational representation of the currents if there were no variable element in the coupling coefficient.

Now let

$$[I]_1=-p[Z]^{-1}[T]_0,$$

where

$$[T]_0 \doteq \begin{pmatrix} b_{12}i_{20} \\ b_{21}i_{10} \end{pmatrix}, \quad . \quad . \quad . \quad . \quad . \quad (97)$$

$$[I]_n =-p[Z]^{-1}[T]_{n-1}, \quad . \quad . \quad . \quad (98)$$

$$[T]_n \doteq \begin{pmatrix} b_{12}i_{2n} \\ b_{21}i_{1n} \end{pmatrix}. \quad . \quad . \quad . \quad . \quad . \quad (99)$$

The operational equivalent of the solution is given by

$$[I]=\sum_{n=0}^{\infty}[I]_n, \quad . \quad . \quad . \quad . \quad . \quad (100)$$

and the solution is

$$[I] \doteq [i]. \quad . \quad . \quad . \quad . \quad . \quad . \quad (101)$$

The fact that the series of matrices satisfies the equation shows that it is a solution if it converges. The proof of the convergence for cases where $| b_{12} | < L_{12}$ follows the same lines as the proof for the convergence given in the first part of the paper. If $b_{12}(t)$ is a function of trigonometric form, this method gives a quick and simple way of obtaining the higher order correction terms which must be added to the solution of the unvaried system. More general problems may be similarly treated.

Conclusion.

It has been shown in this paper how the Laplacian Transformation or Operational method of solving differential equations encountered in circuit theory may be

extended to the solution of systems with parameters varying with the independent variable subject to certain limitations. The use of matrix notation combined with the Laplacian Transformation has been shown to possess many advantages because of the symmetry and convenient arrangement of the operations. It is hoped that this exposition will give an impetus to these methods.

Bibliography.

(1) Pipes, "Matrices in Engineering," Elect. Eng., Sept. 1937, pp. 1177–1190.
(2) Pipes, "Laplacian Transform Circuit Analysis," Phil. Mag. xxiv. pp. 502–510 (Sept. 1937).

LI. *A Note on Hermite Polynomials.*

By W. T. Howell, *M.Sc.**

IT is well known that when n is a positive integer Weber's parabolic cylinder function $D_n(z)$ is expressible in terms of Hermite's polynomial $H_n\left(\frac{z}{\sqrt{2}}\right)$ as follows:

$$D_n(z)=(-)^n e^{\frac{1}{4}z^2}\frac{d^n}{dz^n}(e^{-\frac{1}{4}z^2})=2^{-\frac{1}{2}n}e^{-\frac{1}{4}z^2}H_n\left(\frac{z}{\sqrt{2}}\right);$$

and further,

$$e^{-\frac{1}{2}(x^2+t^2)+xt\sqrt{2}}=\sum_{n=0}^{\infty}\frac{t^n}{n!}D_n(x\sqrt{2}).$$

In this note I use the Fourier transform of the product of two Hermite polynomials to deduce a formula expressing this product as a sum of Hermite polynomials.

In a previous paper† I derived the formula

$$\int_{-\infty}^{\infty}e^{i2ax}D_n(x\sqrt{2})\,D_m(x\sqrt{2})\,dx$$
$$=\sqrt{\pi}\,n!\,(ia\sqrt{2})^{m-n}e^{-a^2}L_n^{m-n}(2a^2), \quad (1)$$

where n and m are positive integers and $L_n^{\alpha}(x)$ denotes the Laguerre polynomial. By interchanging n and m we have

$$n!\,L_n^{m-n}(x)=(-)^{n-m}m!\,L_m^{n-m}(x),$$

* Communicated by the Author.
† Phil. Mag. (7) xxiv. p. 1082 (1937).

a result which can be proved more easily by other means.

Fourier inversion of the result (1) gives

$$D_n(x)D_m(x)=\frac{n!}{\sqrt{2\pi}}\int_{-\infty}^{\infty}(iv)^{m-n}e^{-\frac{v^2}{2}}L_n^{m-n}(v^2)e^{-ixv}dv.$$

Since

$$L_n^{\alpha}(x)=\sum_{r=0}^{n}\binom{n+\alpha}{n-r}\frac{(-x)^r}{r!}$$

and

$$\frac{1}{\sqrt{2\pi}}\int_{-\infty}^{\infty}(iv)^n\exp(-\rho v^2)e^{-ivy}dv=\frac{\exp\left(-\frac{g^2}{4\rho}\right)}{(2\rho)^{\frac{1}{2}n+\frac{1}{2}}}H_n\left(\frac{g}{\sqrt{2\rho}}\right),$$

we have at once

$$\frac{H_n(x)H_m(x)}{n!\,m!}=\sum_{s=0}^{\text{norm}}\frac{H_{n+m-2s}(x)}{s!\,(n-s)!\,(m-s)!}.$$

the summation being taken to n or m whichever is least.

LII. *The Development of the Minor Axis in a Foucault's Pendulum. By* B. Dasannacharya, *M.A., Ph.D., F.Inst.P., Professor of Physics, Benares Hindu University, Benares, India* *.

1. *Introduction.*

Dasannacharya and Hejmadi † showed that Foucault's pendulum can give a correct value for the rotation of the earth round its axis even with such small lengths of the pendulum as 95 cm., and that the use of the braided string overcomes many difficulties arising out of the rigidity of the string etc.

It was observed by them that the orbit of the pendulum bob showed a slight departure from the straight line path, although the Foucault rotation of the plane of oscillation was not thereby affected. Denoting the Foucault rotation developed in a time t by θ we get

$$\theta=-\omega t\sin\lambda. \quad \ldots\ldots (1)$$

* Communicated by the Author.

† B. Dasannacharya and D. Hejmadi, Phil. Mag. (7) xxiii. pp. 65–88 (1937).

Here λ is the latitude of the place of observation, ω the angular velocity of the rotation of the earth. The negative sign indicates that the rotation for an observer on the earth is clockwise in the northern hemisphere. The departure showed itself in such a way that the orbit became slightly elliptical with the ratio γ of the minor to the major axis increasing linearly with time; the orbit in the ellipse was anti-clockwise. The theory of the Foucault pendulum developed by Bromwich * in 1914, while it gave the correct value for the Foucault rotation, did not permit of any variation of γ with time. Dasannacharya and Hejmadi †, taking into consideration the damping introduced due to air resistance, obtained the following expression for γ:—

$$\gamma = \frac{n}{p}\left(1+\frac{kt}{2}\right), \quad . \quad . \quad . \quad . \quad . \quad . \quad (2)$$

where $n = \omega \sin \lambda$,

$p^2 = g/l$.

g is the acceleration due to gravity and l the length of the pendulum;

k is the damping constant.

The increase of γ permitted by this expression fell far short of the experimentally observed values. Based on observations, equations were developed which correctly reproduce the observed values of the minor axis 2Q in detail, and certain conclusions were made. Hence it becomes of the utmost importance to examine the development of the minor axis and of γ in greater detail.

Secondly, Dasannacharya and Hejmadi studied the irregularities of the pendulum which have been observed by almost all workers by means of a special type of pendulum with knot suspensions, in which case the irregularities were particularly accentuated. It was shown how these irregularities can be traced to the formation of a favoured direction of vibration caused in the process of fixing the thread at the top. In the present paper we shall consider the effect of favoured directions, when they are small, but not so small that they can be neglected. It is of importance, since it is very

* T. J. I'a Bromwich, Proc. Lond. Math. Soc. (2) xiii. p. 222 (1914).
† *Loc. cit.*

difficult to overcome the disturbances which, as we shall show, sometimes make observations of the Foucault rotation almost impossible. These difficulties increase as we go to smaller lengths of pendulums.

2. *Experimental Arrangement.*

The apparatus and the method of observation remained essentially the same as with the experiments of Dasannacharya and Hejmadi (D. & H.).

The bob was of brass of the same shape and size as that of the steel bob of 450 gm. used in experiments 1–6 by D. & H., but the weight is 377 gm. This bob was used throughout in the present series of experiments.

TABLE I.

Variation of γ with Amplitude.

$2P_0$ (cm.).	$2Q_{max.}$ (cm.).	γ in 90 min.	Direction.
15	0·68	·23	North–South.
10	0·53	·22	
5	0·32	·23	
2·6	0·17	·22	
15	−0·8	−0·26	East–West.
10	−0·65	−0·25	
5	−0·32	−0·26	
2·5	−0·16	−0·23	
2·6	−0·16	−0·24	

$2P_0$=initial major axis; $2Q_{max.}$=the maximum value of minor axis; γ_{90} is the ratio of the minor to the major axis at 90 minutes after start.

Two types of string were used. In series I. and II. angler's braided silk string of diameter 0·4 mm. was used. This was almost identical with the string used in experiments 1–6 by D. & H. The string in series III., IV., and V. was of silk of diameter about 1·0 mm., but not braided. The effective length of the pendulum in all cases except in series II. was 255·0 cm., while in II. it was 15 cm. less.

3. *γ is independent of the Initial Value of an Amplitude.*

With a braided string pendulum observations were made in two directions at right angles to each other. The initial amplitudes were varied within very wide limits in both directions. Table I., column 1, gives

double the values of initial amplitudes, *i. e.*, they would be the major axis of the slowly developing ellipse, to start with. The minor axis of the ellipse starts from a zero value, attains a maximum value in about an hour's time to the value shown in column 2. The variation of γ is strictly linear with time. Column 3 shows the value of γ in 90 minutes from start. γ is therefore independent of the initial values of the amplitude. The observations of D. & H., that γ varies linearly with time, is in keeping with the present more extended observations on the independence of γ of amplitude.

4. *The Variation of θ with Amplitude.*

Figs. 1 and 2 show curves for the values of θ with respect to time in the experiments discussed in Table I.

Fig. 1.

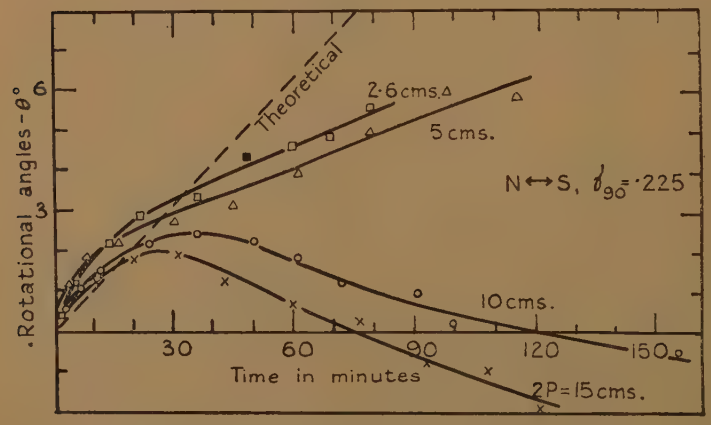

Variations of θ with varying initial amplitude P_0.

in the previous section. The values of $2P_0$ are marked against each curve. The values of θ that are to be expected on the basis of the simple theory as given in relation (1) are shown in dotted lines, namely, a line giving a change of $-6{\cdot}4°$ per hour for the latitude of Benares, namely, 25° 18′ N.

Considering fig. 1, with 15 cm. for initial major axis, θ proceeds with almost the correct value for about 15 minutes. The departure with further lapse of time becomes evident. At 28 minutes the maximum value

is reached, and at 76 minutes θ comes back to zero, the initial value, to develop on the opposite side. It was 2·0° at 122 minutes.

With 10 cm. the general course is the same as with the previous curve for 15 cm. However, up to 20 minutes θ has more than the expected values. The

Fig. 2.

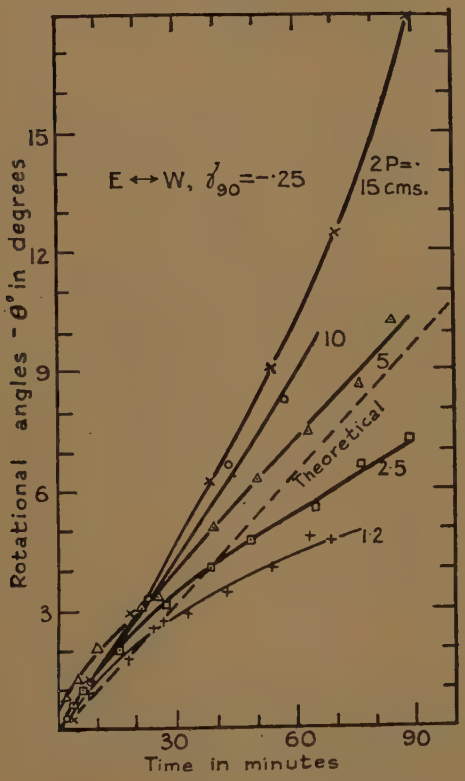

Variations of θ with varying amplitudes, direction normal to that in fig. 1.

maximum is reached at 35 minutes and zero at 125 minutes and 0·5 at 154 minutes.

With 5 cm. and 2·6 cm. as major axes θ increases as before, and with more than the expected values up to about 30 minutes, when the increase in θ takes place,

though the increase is less than the values to be expected theoretically.

The value of γ in the above cases is positive and the Foucault rotation is, however, always negative. Hence the anti-clockwise motion in the ellipse would tend to move the major axis in opposition to the Foucault rotation. The amount of this opposing rotation is an apsidal correction which is

$$\frac{3\pi PQ}{4l^2} \quad . \quad . \quad . \quad . \quad . \quad . \quad . \quad . \quad (3)$$

radians per period.

Fig. 3.

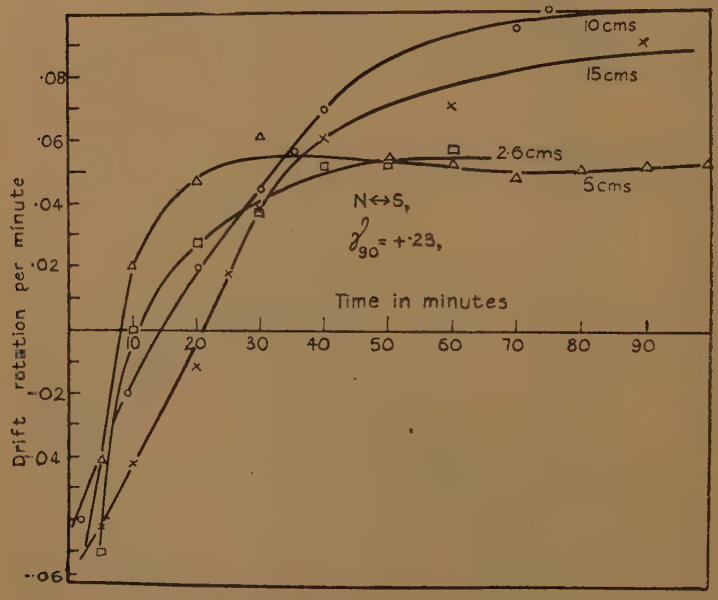

Dependence of drift with time and amplitude.
Pendulum I, N–S and γ_{90} +·23.

Since Q/P, namely γ is constant for a given period of time, the correction is proportional to the square of P. With diminution of the initial values of P the effect of the development of the minor axis should be to lessen this correction very rapidly.

This type of apsidal correction cannot explain the more than the expected initial values nor the less than the expected values at later stages for θ.

It would be clear therefore that the deviation of θ from the expected value, *when the amplitudes to start with are small*, would be a measure of some subsidiary force other than that considered above as giving the apsidal correction. Let us denote the subsidiary effect as a "drift."

That the "drift" effect exists can be derived from another consideration also. If the apsidal correction due to the minor axis were alone responsible the greatest deviation of θ should occur when PQ is a maximum, which

Fig. 4.

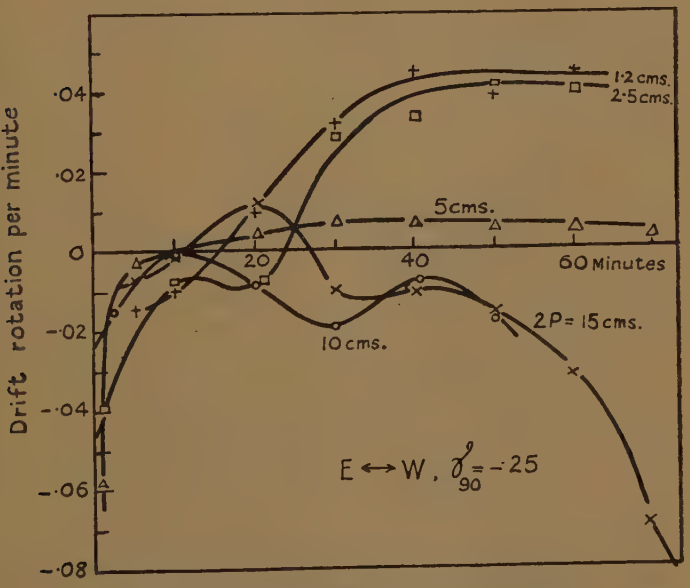

Dependence of drift with time and amplitude.
Pendulum I, E–W, $\gamma_{90} = -·25$.

occurs at about 30 minutes from the start in all the four cases. We can, however, see that θ goes on falling even up to more than 120 minutes with the initial values of 2P as 15 cm. and 10 cm.

More direct ideas on the drift effect can be seen from fig. 3. The ordinates represent the rate of change of θ per minute after allowing for the rate due to the development of the minor axis and for the theoretical value of the rate of change due to Foucault rotation. They

would therefore represent the " drift " effect per minute. The rate for the Foucault rotation may be taken as 0·1° per minute, and the effect of drift can be judged in comparison by looking at fig. 3. The positive value of drift would be a retardation of Foucault rotation, while a negative value would give an acceleration.

Fig. 5.

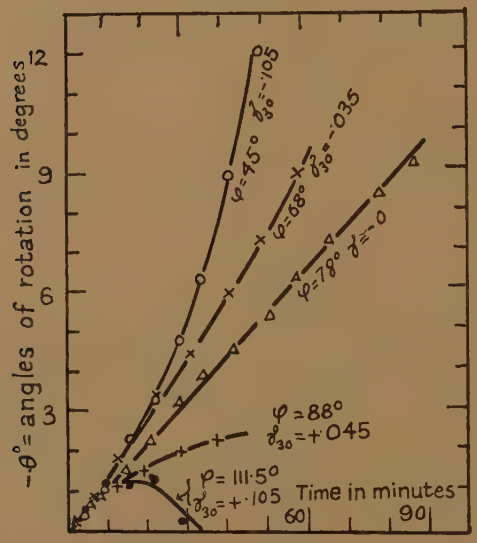

Variations of θ with initial directions ϕ and with the γ peculiar to those directions.

Variation of θ in the E.–W. Direction.

Here γ is negative; consequently the Foucault rotations are enhanced due to the clockwise orbit of the ellipse. The curves in fig. 2 bear this out. Drift is operative here too. Fig. 4 is similar to fig. 3, and is drawn for the observations contained in Table I. for the E.–W. direction. There is drift acceleration in the beginning as in the previous case, and, as before, a retardation in the end, however, only for less than a value of 10 cm. for initial 2P, while for 10 and 15 cm. the final drift is an acceleration within the period observed. As we shall see later on in section 10, the final shape of the 15 cm. curve will be clear as a possible retardation.

5. *Nature of θ in different Directions and the Values of γ in different Directions, and their Dependence on the Nature of the String and the Attachment at the Top.*

Fig. 5 shows the course of θ at various times for some typical directions ϕ, the γ for which are marked on the curves.

In fig. 6 are shown values of γ developed in the first thirty minutes from starting oscillations. As in the cases studied in the previous sections the dependence of γ

Fig. 6.

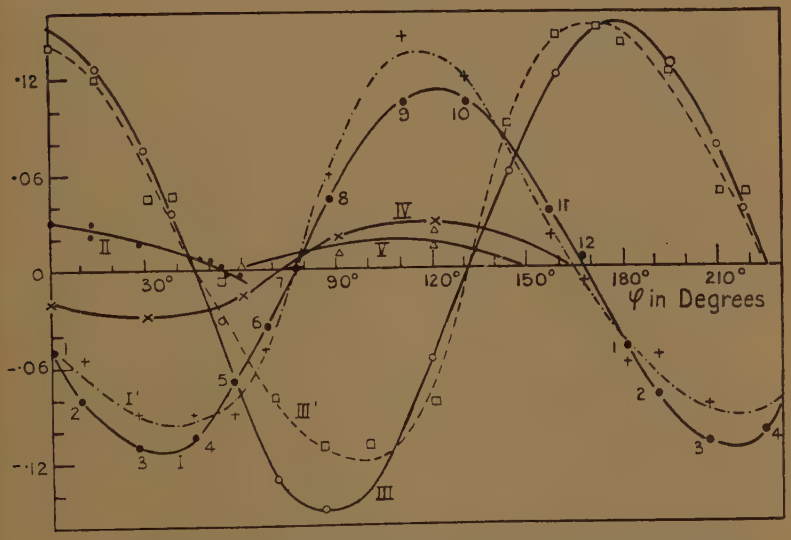

Variations of γ_{30} with initial directions ϕ; as also deviations of θ_{30} from theoretical values.

● ● ● Curve I. Braided string pendulum.
. . . II. Braided string pendulum readjusted at top fixing to give less γ.
O O O III. Non-braided string pendulum.
× × × IV. Non-braided string pendulum readjusted at top fixing to give less γ.
Δ Δ Δ V. Non-braided string pendulum readjusted at top fixing to give still less of γ.
+ + + I'. Being the deviation of θ from theoretical value, in expts. of Curve I, divided by 20.
□ □ □ III'. Being the deviation of θ from theoretical value, in expts. of Curve III, divided by 25.

on t is linear. The only exception to this would be when the γ reverses its sign within the period of observation

(see section 11). The linearity is very helpful, as otherwise it would be difficult to use it as an important characteristic of the pendulum. The ordinates give the values of γ. The abscissæ give the azimuth ϕ the direction of the initial oscillation.

Curves I and III refer to braided and non-braided strings respectively. The strings have been so fixed in the chuck jaws at the top that the string got a strong favoured direction of oscillation. In such cases the string under the jaws at the top when removed out of the chuck jaws showed the four-armed structure of a cross, due to the powerful pressing caused by the jaws. The formation of a favoured direction is seen in the large values of γ. Curves II, IV, and V are got by reducing the favoured direction. This is obtained by stiffening the portion of the string that is to go inside the jaws at the top, by slightly gluing the portion and drying it well before fixing. The fixing requires to be gentle. The success of the experiment in reducing the formation of the favoured direction consists in avoiding flattening or giving any kind of asymmetry to the string near about the position where the string hangs out of the jaws. The stiffened portion should never project outside of the chuck. Curves IV and V are for unbraided string. Perhaps due to its greater diameter or of its slight twist rotation of the bob about the string by about 10° in the most unfavourable cases gave slight fluctuations in the readings for the mean position of θ for any time. While this was inappreciable when the amplitudes were large, it could give considerable trouble when the periods of observation are extended till the amplitudes became rather small. It was found that the shadow of the string falling on the scale cut on the top part of the bob, in addition to slight creeping, sometimes in a clockwise, sometimes in an anti-clockwise direction, showed also fluctuations about a mean position by about 5° with a period roughly coinciding with the period of vibration of the bob about the string as axis. With the braided string the pendulum in only a few experiments showed a slight creeping in the beginning, but no fluctuations. Further, the non-braided string does not reproduce results as perfectly as the braided string pendulum does.

It may be pointed out that curve II is not the limit to which γ can be reduced; it is meant to show how and

on what lines reduction of γ can be achieved and completely estimated. The same remark holds also for curves IV and V. Experiments are being separately carried out to determine the utmost smaller limit to which γ can be reduced in all directions.

6. *The Zero Points of γ.*

These zero points on any one curve are almost exactly 90° apart. Those of one curve do not coincide with those of others. Curves I, III, and IV have been obtained with the position of the jaws of the supports at the top remaining unchanged in the sense that they are not rotated about the string as axis. The zero position of the scale for ϕ remained also the same. Now that the curves III and IV for the same non-braided string start with opposite signs of γ with a phase difference of nearly 55° shows that the fixing of the string at the top, which is different in the two cases, is responsible for the change. This is also meant to show that the zero directions and the signs need not be invariable with respect to the cross-slit spaces formed by the four jaws at the top. This fact is further supported by the curves I and III, where the phase difference is about 48°. It has been ascertained that the zero, when the top support is rotated, will also rotate by the same amount provided the fixing of the string to it is undisturbed.

7. *Representation of γ by a Sine Curve.*

All the curves of fig. 6 show that they can be represented by a sin 2ϕ curve. In fig. 7 points of curves I and II are drawn in polar coordinates with γ and ϕ. The zero points of the two curves have been made to coincide. On the same is also drawn a sin 2ϕ curve. It will be seen that the agreement is remarkably good. So the following

$$\gamma_t = \gamma_t^0 \sin 2\phi$$

may be taken as representing the azimuthal dependence of γ. Here γ_t^0 represents the maximum value of γ for the particular setting of the pendulum in a given period of time t.

In these curves of fig. 7 the direction of the arrows indicates the direction of vibration in the ellipse, clockwise or anti-clockwise, for the values of ϕ included in the

quadrant or loop. It is obvious that the major axis of the ellipse is impelled to move away from YOY′ to XOX′, due to the elliptical motion. This movement is due to the existence of γ. See also in this connexion the properties of favoured direction in D. & H., pp. 73 and 74. If both the axes are to be considered as favoured directions then an intermediate direction must exist for which the action of the two favoured directions would be equal and opposite, and for that direction γ

Fig. 7.

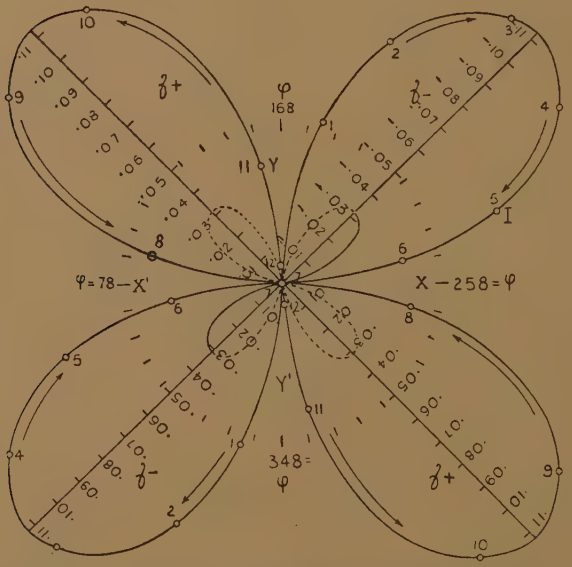

$\gamma=\gamma^{\circ}\sin 2\phi$ curve in full line against experimental values of γ_{30} of Curves I and II of fig. 6 in circles.

should be zero. The experimental curves are decidedly against such a conclusion.

8. *The Factor of Merit* F *of a Foucault Pendulum.*

F should give the efficiency with which the Foucault pendulum yields correct values for the rotation of the earth.

We shall define F as the ratio of the theoretical value

given in section 1 to the maximum value actually measured.

$$F = \frac{\gamma_t'}{\gamma_t^0} = \frac{n}{p}(1+kt/2)\Big/\frac{n}{p}(1+\sigma t) = \frac{1+kt/2}{1+\sigma t}.$$

Taking the values for the experimental curve II $\gamma^0_{30}=0{\cdot}03$ in 30 minutes and $n/p=1{\cdot}56.10^{-5}$, and $kt/2=0{\cdot}62$, so that $\sigma t=2{\cdot}10^3$ and $F={\cdot}0008$. F would be unity if the theoretical and experimental values should coincide.

What would be the value of F in our pendulum when the minor axis developed is just detectable, say 0·1 mm. This value would be reached in about an hour's time (see fig. 12, section 11) and would not increase any longer. γ^0_{60} would be $0{\cdot}01/4{\cdot}3=0{\cdot}0023$. Here 4·3 cm. is the value of the major axis at the end of an hour. Consequently $kt/2=ln.15/4{\cdot}3=1{\cdot}25$. The value of $\sigma t=0{\cdot}0023/n/p=153$. Hence $F=2{\cdot}25/154=0{\cdot}0146$. A pendulum of this efficiency or merit would be able, as we shall see in section 11, to give correct values for the Foucault rotation for at least the first three hours, *i. e.*, in the period usually convenient for observation. This being the lowest figure of merit for the particular setting there would be very large regions of ϕ where the performance of the pendulum would be much improved, as could be deduced from fig. 7.

9. γ *is a Measure of the Deviation of* θ *from the Correct Values of Foucault Rotation.*

In fig. 6 are drawn points which represent the deviation of θ at the end of thirty minutes from start from that due to Foucault rotation alone at that time. The deviations for convenience of representation have been reduced by a common factor to be able to bring them on the same scale as is used for γ. Deviations for curve I have been divided by 20, and those for III by 25. These deviation curves marked I′ and III′ appear as dot and dash curves.

The correlation is satisfactory. *We are therefore justified in concluding that the performance of the pendulum can be gauged from a study of the values of* γ.

10. *Drift in Different Directions* ϕ.

We have seen in section 4 how drift impulses work in two directions normal to each other and for different values of amplitude.

Fig. 8 has been drawn in the same way as were curves of figs. 3 and 4. The amplitudes in the present case remain the same initially in all the curves, namely, 15 cm. for 2 P.

Curves 1 to 12 represent the rate of change of θ due to drift. These curves refer to points marked 1 to 12 in figs. 6 and 7, and refer to a variation of γ from a nearly zero value to another zero at right angles, and then further

Fig. 8.

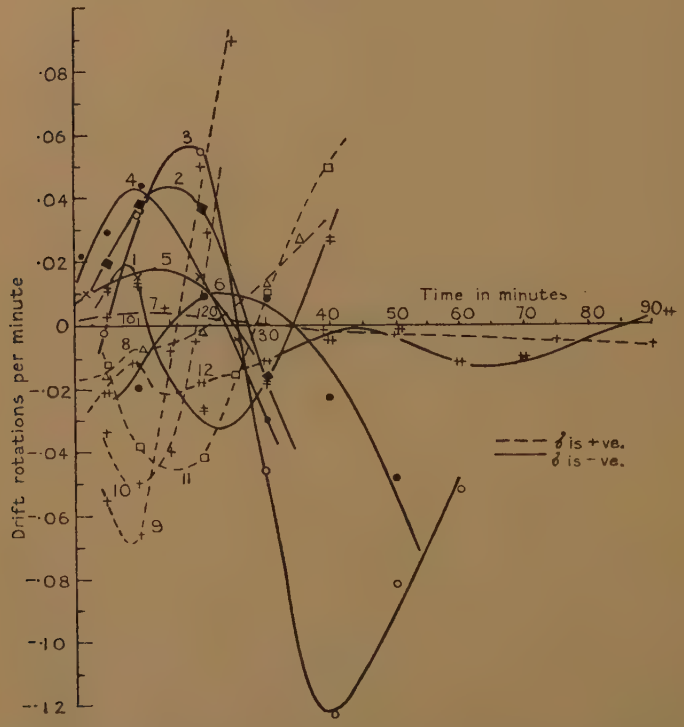

Dependence of drift with time and initial direction ϕ. The numbers on the curves refer to the points on Curve I in figs. 6 and 7.

on with increasing angles of ϕ till the original initial direction 180° apart is reached.

In the negative region of γ the drift is positive for about 30 minutes from start, *i. e.*, in that period it retards the Foucault rotation. In the positive region of γ, as in curves 8 to 12, it is negative, *i. e.*, it accelerates Foucault rotation.

There is clear indication, as in curve 3, that in the negative region of γ the retardation changes into an acceleration for times greater than 30 minutes. This acceleration, as can be seen in curves 12, 1, and 3, reaches a maximum at 40 minutes, and then diminishes in magnitude.

Similar conclusions have been drawn as regards drift in experiments of curve III of fig. 6 for the non-braided string pendulum. The drift is a consequence of the existence of the favoured direction of oscillation, and is an additional evidence for the presence of the favoured direction.

11. *Rotation when γ is small, as in Curve II of fig.* 6.

Table II. gives particulars regarding the points in curve II of fig. 6. Figs. 9, 10, 11, 12 refer respectively

TABLE II.

Pendulum with γ small.

Fig.	Initial direction (in degrees)	2P.2Q (in sq cm.).	Time (min.).	γ_{30}.	Time.	2Q.	Time.
9.....	47·2	·28	10	·0015	15	·25	18
		·00	100	·0022	30	·00	..
10.....	50·0	·18	25	·002	30	·2	30
		·00	60	·000	60	·0	60
		— ·04	80	—·004	90	— ·2	110
11.....	52·7	·23	8	·002	8	·1	8
		·00	14	·000	14	·0	14
		— ·15	30	—·006	60	— ·3	75
12.....	58·7	— ·425	32	—·007	30	— ·7	80
Nil	13·7	1·85	32	·029	30	2·8	32

to initial directions, namely, 47·2°, 50°, 52·7°, and 58·7°. The zero point for γ, as can be seen from curve II and in other ways too, is 53·2°. In all the curves the values of θ are indicated by $\times$, and are plotted against time in minutes as abscissæ; the theoretical values of θ are plotted in dotted lines. The values of 2 Q are indicated by Δ and of γ by circles. The values of 2P.2Q, to which correction due to the minor axis is proportional, are indicated by dots.

It may be seen from fig. 9 that Q is positive, and its influence in lessening θ is quite apparent till about 30 minutes. From that time onwards the correct value of Foucault rotation per minute is obtained. The inclination of the curve to the time axis is correct after the first thirty minutes. We would be justified in concluding that 2P . 2Q should not exceed the value attained at thirty minutes, namely, 0·1 square centimetres. As

Fig. 9.

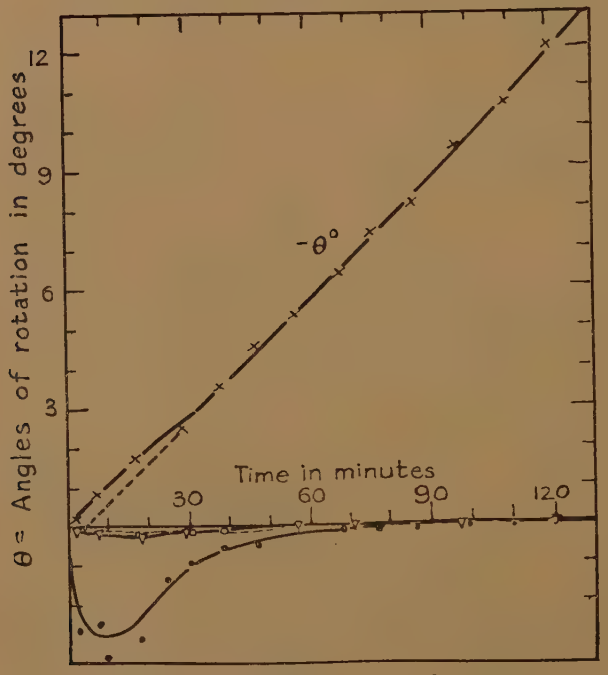

Variations of θ for Curve II, fig. 6. $\phi = 47{\cdot}2$.

the major axis in 30 minutes reduces to 7·5 cm., 2Q would be 0·13 mm. or $\gamma_{60} = 0{\cdot}0034$. We should, however, remember that this value may not hold for a pendulum with a heavier bob.

In fig. 10 we see the effect at a reversal of γ, and passing through from a positive to a negative value of γ. The maximum value of the minor axis developed at 30 minutes to the extent of only 0·2 mm., and γ reached the value of

0·003. The reversal of γ took place at 60 minutes, and γ increased linearly with sign reversed, up to 110 minutes, at $-0{\cdot}012$ per hour. After that there is seen a steeper rise of γ, a thing to be expected, because the plane of oscillation will then have rotated from 50° to about 63°, and the γ would be about 40 per cent. of the maximum value of the setting, namely $-0{\cdot}024$ per hour, and is

Fig. 10.

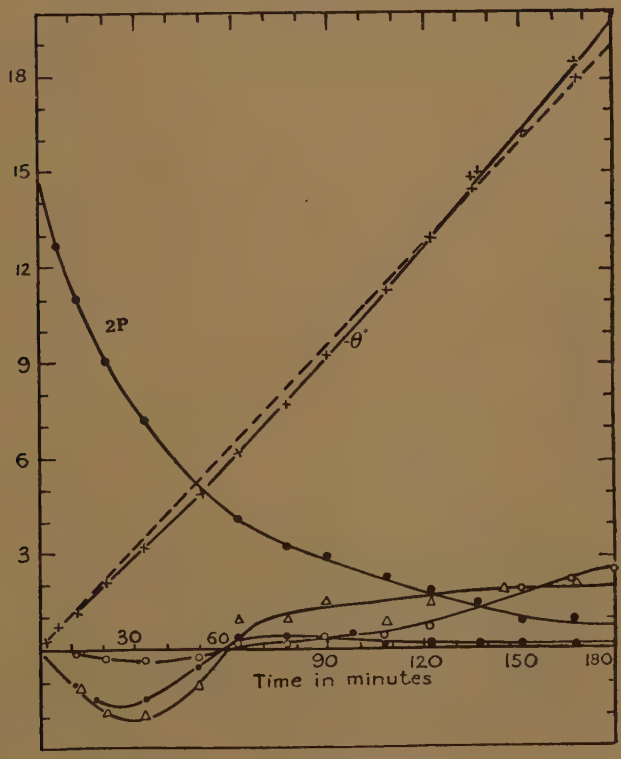

Variations of θ for Curve II, fig. 6. $\phi=50$.

exactly the amount that can be read off from the graph. The more than linear increase in γ is due to the very rapid change of γ near reversal, as would also follow from the $\sin 2\phi$ relation. The maximum value of 2Q after reversal does not exceed the small value of 0·2 mm.

At 120 minutes the corrections have cancelled themselves, and θ is the correct value, namely 12·8°. The total

correction up to any time is proportional to the area included by the 2P.2Q curve with the time axis. Considering the portions up to 120 minutes the positive and negative areas do not, however, balance, the positive being greater of the two. This leads to the presence of an accelerating drift which makes up for the deficiency of the negative area. In fig. 13 the drift curves are given for these sets of experiments. They are drawn similar

Fig. 11.

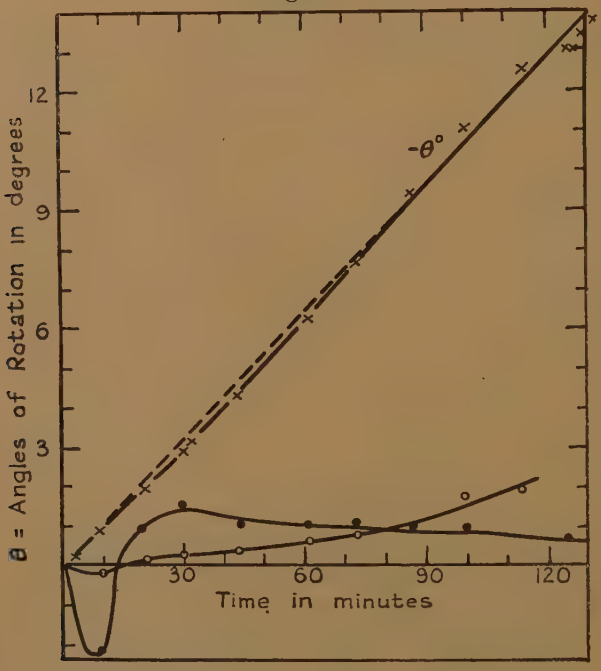

Variations of θ etc. for Cuve II, fig. 6. $\phi = 52{\cdot}7$.

to the curves in figs. 3, 4, and 8. In fig. 10 is shown the curve for 2P as a function of time; the initial amplitudes, excepting in sections 3 and 4, remained the same throughout the present series of experiments.

Fig. 11 refers to $\phi = 52{\cdot}7°$. The positive minor axis which reaches a maximum in 10 minutes reverses by about 15 minutes to develop on the negative side; the course and the magnitude of γ are the same as in fig. 10. The negative correction does not make up for the effect of the

earlier positive effect, although now the area included in the negative part of the 2P.2Q curve is greater. The drift curve in fig. 13 speaks for itself.

Fig. 12 refers to ϕ equal to 58·7°. Reference to fig. 6 shows that for this angle γ should be negative to start with, and no reversal for γ is to be expected, as actually is found to be the case. The drift curve gives the finer details.

Fig. 12.

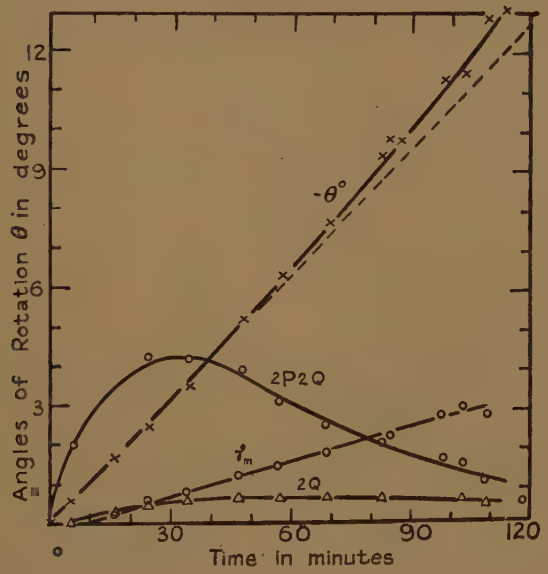

Variations of θ etc. for Curve II, fig. 6. $\phi = 58{\cdot}7$; $\gamma_{30} = -{\cdot}007$.

No figure has been given for $\gamma_{30} = 0{\cdot}029$, as it is in no way different essentially from similar curves in fig. 5. The drift curve is, however, included in fig. 13.

12. *Discussion of the Results of Dasannacharya and Hejmadi.*

In experiments 1 to 6 of D. & H. no. 2 gave a negative value for γ; so also did no. 21, and the Foucault angles were not different from those where positive values of γ were obtained. Further, the γ in these cases were as high as 0·03 per hour, although the deviations of θ were not considered appreciable. The reason most probably lies

in the much heavier steel bob (450 gm.) used in the experiments in 1 to 6, 8 to 10, where observations were extended up to about three hours. It would therefore be necessary to extend the work to study the influence of bobs of different weights later on. Now as regards the remainder of the experiments contained in Table III. of D. and H., we may note that the period of observation was only about an hour, as the bob was very light, and as the damping being considerable the vibrations die out quickly, and the small deviations in the Foucault rotation may have escaped observation.

Fig. 13.

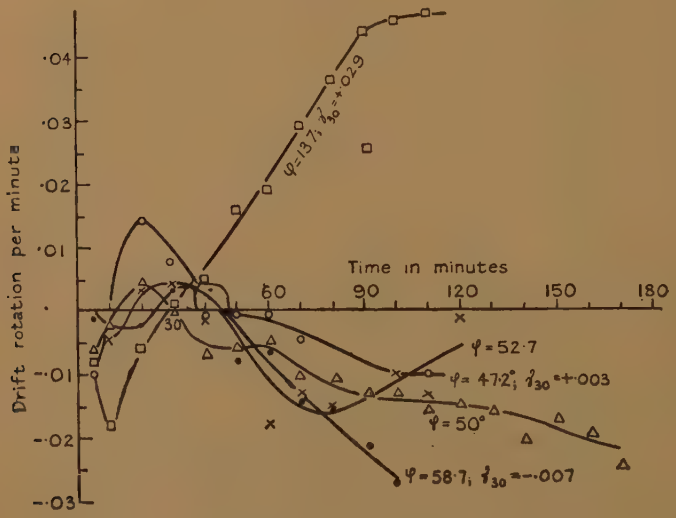

Dependence of drift with time for points in Curve II, fig. 6, and figs. 9, 10, 11, and 12.

The values of γ in two normal directions are not necessarily positive; but in cases where γ is so much reduced that it is very small all over it is possible to get γ positive in two directions normal to each other, provided we assume an error of not more than two degrees or less in the adjustment of normality.

The expressions derived by D. & H. for the growth of the minor axis etc. on p. 84 are quite correct provided γ does not pass through a zero value and reverse. The assumptions underlying the equations as regards independence of γ of amplitude are correct.

13. *Summary and Conclusion.*

The plane oscillations of the Foucault's pendulum change gradually with time into elliptical oscillations, in which the ratios of the minor to the major axes, called γ, is found to vary linearly with time. It is shown in section 3 that γ is independent of the initial values of the major axis within fairly wide limits. Section 4 shows that the Foucault rotation is less than the theoretically expected value if γ is positive, and more if it is negative, as illustrated in fig. 5 ; the greater the value of γ the more the deviation. In section 5 it is shown that γ is different in different directions ϕ of initial oscillation, and γ is shown to be correctly representable by a curve $\gamma_l^0 \sin 2\phi$. Consequently γ will pass through zero values in two definite directions normal to each other. These directions, as well as the maximum values of γ, namely γ_l^0, can be varied by manipulating the fixing of the string of the pendulum to its top support. By carefully avoiding any asymmetry being formed by the pressing of the jaws γ can be diminished to any extent desired or necessary. It is found that stiffening the part of the string going inside the jaws by means of gum and drying it before fixing, and further boring a small hole of nearly the size of the string at the meeting point of the jaws where the string is fixed, diminishes γ.

Fig. 6 shows the values of γ for different settings with the braided string, curve I with a large value for γ and curve II with about quarter of the value. In curves III, IV, and V values of γ for three different settings of the pendulum are shown where the string used was much coarser, and, in addition, unbraided. Non-braided string pendulums are not recommended for use, although good values for the Foucault rotation could be obtained.

It is also shown in fig. 6 for curves I and III that the values of γ correctly represent the deviations of the rotations of the pendulum from the theoretical values for the Foucault rotation brought about by the rotation or the spin of the earth. These curves are marked I′ and III′.

The efficiency of a given pendulum is defined in section 8 as a factor of merit and measured.

The origin of γ as actually observed lies in the polarization caused in fixing the string, by the excitation in it of favoured directions of oscillation. In addition to the effect of the minor axis in causing retardation or accelera-

tion to the rotation of the major axis, which can be calculated on the principle of the spherical pendulum and can be allowed for, there is an effect which is called " drift," and which is shown to be dependent on the values of γ for the directions concerned. The " drift " rotations explain the finer behaviour of the pendulum in its deviations from theoretical values.

Figs. 9, 10, 11, and 12 show the behaviour of the pendulum for some of the values of γ very near a reversing or zero point of γ for the case of curve II in fig. 6, and for which the maximum value of γ possible is itself extremely small. The response of the Foucault rotation to the presence of the minor axis is shown. The drift effect is shown in fig. 13 for curve II.

It is hoped to extend the work to pendulums of different dimensions, particularly in the direction of shortening the length to less than 95 cm. obtained by Dasannacharya and Hejmadi. Metallic wires would also be tried in place of the string.

Department of Physics,
Benares Hindu University, India.
August 23, 1937.

LIII. *On a Class of Functions which are Self-reciprocal in the Hankel Transform.* *By* W. T. Howell, *M.Sc.**

§ 1. THE object of this paper is to derive a general theorem relating to self-reciprocal functions, and to give a few examples.

In terms of the operational calculus, where

$$\phi(p)=p\int_0 e^{-px}f(x)\,dx \doteq f(x), \quad . \quad . \quad . \quad (1)$$

van der Pol and Niessen † have shown that

$$p^{1-\nu}\phi\left(\frac{1}{p}\right) \doteq x^{\frac{\nu}{2}}\int_0^\infty J_\nu(2\sqrt{xs})s^{-\frac{\nu}{2}}f(s)\,ds. \quad . \quad . \quad (2)$$

* Communicated by the Author.
† Phil. Mag. xiii. p. 537 (1932).

By the Mellin inversion theorem

$$x^{-\frac{\nu}{2}}f(x)=\frac{x^{-\frac{\nu}{2}}}{2\pi i}\int_{c-\infty i}^{c+\infty i}e^{sx}\phi(s)s^{-1}ds, \quad . \quad . \quad . \quad (3)$$

provided $|\phi(s)/s|\to 0$ uniformly with respect to phase s, as $|s|\to\infty$, $-\frac{\pi}{2}\leqslant$ phase $s\leqslant\frac{\pi}{2}$, all the singularities of $\phi(s)/s$ are on the left of the contour ($c>0$), and certain other conditions are fulfilled *.

Consequently if

$$p^{1-\nu}\phi\left(\frac{1}{p}\right)=\phi(p) \quad . \quad . \quad . \quad . \quad . \quad . \quad (4)$$

we have from (2), by interpretation of the left-hand side,

$$x^{-\frac{\nu}{2}}f(x)=\int_0^\infty J_\nu(2\sqrt{xs})s^{-\frac{\nu}{2}}f(s)\,ds,$$

i. e.,

$$\psi(x)=\frac{x^{\frac{1}{2}-\nu}}{2\pi i}\int_{c-i\infty}^{c+i\infty}e^{s\frac{x^2}{2}}\phi(s)s^{-1}ds \quad . \quad . \quad . \quad (5)$$

is self-reciprocal in the Hankel transform of order ν. This theorem was obtained by Titchmarsh † using a somewhat different procedure, without giving the restrictions which limit its applicability.

To exemplify the above take $\phi(s)=s^{\frac{1}{4}(1-\nu)}$, leading to the well-known result that $x^{-\frac{1}{2}}$ is self-reciprocal in the transform of order ν.

Taking $\phi(s)=\dfrac{s^{n+1}}{(s+1)^{2n+\nu+1}}$ leads to the result that the function

$$\psi(x)=e^{-\frac{x^2}{2}}x^{2n+\nu+\frac{1}{2}}L_n^{n+\nu}\left(\frac{x^2}{2}\right)$$

(where L_n^α is the usual Laguerre polynomial) is self-reciprocal in the transform of order ν.

Taking $\phi(s)=(as)^{\frac{1-\nu}{2}}\exp\left\{-a\left(s+\frac{1}{s}\right)\right\}$,

* See Courant and Hilbert, 'Methoden der Mathematischen Physik,' pp. 87–88.

† ' Theory of Fourier Integrals,' p. 248 (1937).

we get the result that

$$\psi(x)=x^{\frac{1}{2}-\nu}(x^2-a^2)^{\frac{1}{4}(\nu-1)}\mathrm{J}_{\frac{1}{2}(\nu-1)}\{a\sqrt{(x^2-a^2)}\}\,;\quad (x>a>0),$$

$$\psi(x)=0\,;\quad (0<x<a).$$

Taking $\phi(s)=\dfrac{s(s-1)^n}{(s+1)^{n+\nu+1}}$, we get the result that

$$\psi(x)=e^{-\frac{x^2}{2}}x^{\nu+\frac{1}{2}}\mathrm{L}_n^{\nu}(x^2)$$

is skew or self-reciprocal in the transform of order ν according as ν is odd or even.

Many more complicated self-reciprocal functions can be built up from those given above by superposition of a set of such functions. An example is afforded by Bateman's * polynomial

$$\mathrm{U}_n(x)=e^{-x}\sum_{m=0}^{n}a_{nm}\mathrm{L}_m(2x),$$

where a_{nm} is the coefficient in the series

$$\mathrm{P}_n(z)=\sum_{m=0}^{n}a_{nm}z^m,$$

which obviously satisfies a relation of the form

$$(-)^n\mathrm{U}_n(x)=\int_0^{\infty}\mathrm{J}_0(2\sqrt{xs})\mathrm{U}_n(s)\,ds.$$

§ 2. I now give a few further examples of the use of the above method of determining whether or not certain functions are self-reciprocal, incidentally evaluating some infinite integrals involving Bessel functions.

Consider the Laguerre polynomial $\mathrm{L}_n^{\alpha}(x)$, defined as usual as the coefficient of t^n in the expansion of

$$\exp\{-xt/(1-t)\}/(1-t)^{\alpha+1}$$

in ascending powers of t. Then it may be shown that

$$\int_0^{\infty}e^{-ps}s^{\alpha}\mathrm{L}_n^{\alpha}(s)\,ds=\frac{\Gamma(n+\alpha+1)}{n!}\,\frac{(p-1)^n}{p^{n+\alpha+1}},\quad p>0. \qquad (6)$$

Write $\beta+1/p$ for p throughout, multiply both sides by

* Duke, ' Mathematical Journal,' ii. no. 3, p. 570 (1936).

$p^{-\nu}$, and interpret the left-hand side regarding p as an operational parameter. Thus

$$x^{\frac{\nu}{2}}\int_0^\infty J_\nu(2\sqrt{xs})e^{-\beta s}s^{\alpha-\frac{\nu}{2}}L_n^\alpha(s)\,ds$$
$$\doteqdot \frac{\Gamma(n+\alpha+1)}{n!}\frac{\{(\beta-1)p+1\}^n}{(\beta p+1)^{n+\alpha+1}}p^{1-\nu+\alpha};\quad R(\nu)>-1. \quad (7)$$

To interpret the right-hand side of (7) suppose it is the operational representation of $f(x)$, so that

$$e^{-\frac{x}{1-\beta}}f(x)\doteqdot\frac{\Gamma(n+\alpha+1)}{n!}\frac{\{p\beta(1-\beta)\}^{n+1}}{\{p\beta(1-\beta)+1\}^{n+\nu+1}}$$
$$\times\left\{1-\frac{1-\beta}{p\beta(1-\beta)+1}\right\}^{\alpha-\nu}\frac{(\beta-1)^{n+\nu}}{\beta^{n+\alpha+1-\nu}}, \quad (8)$$

which is easily interpreted by (6) after expansion.

If in (7) ν is taken equal to α, we get at once from (8)

$$e^{-\frac{x}{1-\beta}}f(x)\doteqdot(-)^n\frac{\Gamma(n+\alpha+1)}{n!}\frac{\{p\beta(1-\beta)\}^{n+1}}{\{p\beta(1-\beta)+1\}^{n+\alpha+1}}$$
$$\times\frac{(1-\beta)^{n+\alpha}}{\beta^{n+1}}, \quad (9)$$

and since from (6)

$$e^{-\frac{x}{a}}\left(\frac{x}{a}\right)^\alpha L_n^\alpha\left(\frac{x}{a}\right)\doteqdot\frac{\Gamma(n+\alpha+1)}{n!}\frac{(pa)^{n+1}}{(pa+1)^{n+\alpha+1}},$$

we have

$$\int_0^\infty J_\alpha(2\sqrt{xs})e^{-\beta s}s^{\frac{\alpha}{2}}L_n^\alpha(s)\,ps$$
$$=\frac{(\beta-1)^n}{\beta^{n+\alpha+1}}e^{-\frac{x}{\beta}}x^{\frac{\alpha}{2}}L_n^\alpha\left\{\frac{x}{\beta(1-\beta)}\right\}, \quad (10)$$

which reduces for $\beta=\frac{1}{2}$ to Wilson's * theorem, which written more conventionally is

$$(-)^n e^{-\frac{x^2}{2}}x^{\alpha+\frac{1}{2}}L_n^\alpha(x^2)=\int_0^\infty J_\alpha(xs)\,(xs)^{\frac{1}{2}}e^{-\frac{s^2}{2}}s^{\alpha+\frac{1}{2}}L_n^\alpha(s^2)\,ds. \quad (11)$$

If in (7) we take $\beta=1$, we have

$$x^{\frac{\nu}{2}}\int_0^\infty e^{-s}s^{\alpha-\frac{\nu}{2}}J_\nu(2\sqrt{sx})L_n^\alpha(s)\,ds\doteqdot\frac{\Gamma(n+\alpha+1)}{n!}\frac{p^{\alpha+1-\nu}}{(p+1)^{n+\alpha+1}},$$

* Messenger of Math. liii. pp. 157–160 (1923–24).

so that, taking $\nu=\alpha-n$, we get

$$e^{-\frac{x^2}{2}}x^{n+\alpha+\frac{1}{2}}L_n^{\alpha}\left(\frac{x^2}{2}\right)=\int_0^{\infty}J_{\alpha-n}(xt)(xt)^{\frac{1}{2}}e^{-\frac{t^2}{2}}t^{n+\alpha+\frac{1}{2}}L_n^{\alpha}\left(\frac{t^2}{2}\right)dt;$$

$$\alpha-n>1. \quad (12)$$

If we use the known integral

$$\int_0^{\infty}e^{-at}J_{\nu}(bt)t^{\nu}\,dt=\frac{(2b)^{\nu}\Gamma(\nu+\frac{1}{2})}{\sqrt{\pi}(a^2+b^2)^{\nu+\frac{1}{2}}};\quad \mathrm{R}(\nu)>-\tfrac{1}{2},$$

together with the Hille-Hardy * generating function for products of Laguerre polynomials, we may readily prove that

$$\int_0^{\infty}e^{-qs}s^{2\alpha}e^{-s}\{L_n^{\alpha}(s)\}^2\,ds$$

$$=\frac{\Gamma(n+\alpha+1)}{2^{2n}n!}\sum_{l=0}^{n}\frac{\Gamma(2l+2\alpha+1)(2n-2l)!}{l!\,\Gamma(l+\alpha+1)[(n-l)!]^2\,l!}\frac{(q-1)^{2l}}{(q+1)^{2l+2\alpha+1}},$$

so that

$$\int_0^{\infty}e^{-qs}e^{-as}s^{2\alpha}\{L_n^{\alpha}(as)\}^2\,ds$$

$$=\frac{\Gamma(n+\alpha+1)}{2^{2n}n!}\sum_{l=0}^{n}\frac{\Gamma(2l+2\alpha+1)(2n-2l)!}{l!\,\Gamma(l+\alpha+1)\{(n-l)!\}^2\,l!}\frac{(q-a)^{2l}}{(q+a)^{2l+2\alpha+1}}.$$

Writing $q=\beta+\dfrac{1}{p}$, and proceeding as before, we find

$$x^{\alpha}\int_0^{\infty}e^{-\beta s}e^{-as}s^{\alpha}J_{2\alpha}(2\sqrt{xs})\{L_n^{\alpha}(as)\}^2\,ds$$

$$\doteq\frac{\Gamma(n+\alpha+1)}{2^{2n}n!}p\sum_{l=0}^{n}\frac{\Gamma(2l+2\alpha+1)(2n-2l)!}{l!\,\Gamma(l+\alpha+1)[(n-l)!]^2}$$

$$\times\frac{\{(\beta-a)p+1\}^{2l}}{\{(\beta+a)p+1\}^{2l+2\alpha+1}}. \quad (13)$$

Taking $\beta=0$ we get, by interpreting the right-hand side,

$$\int_0^{\infty}e^{-as}a^{\alpha+\frac{1}{2}}s^{\alpha}\{L_n^{\alpha}(as)\}^2J_{2\alpha}(2\sqrt{xs})\,ds$$

$$=e^{-\frac{x}{a}}a^{-(\alpha+\frac{1}{2})}x^{\alpha}\left\{L_n^{\alpha}\left(\frac{x}{a}\right)\right\}^2, \quad (14)$$

* Proc. Nat. Acad. of Sci. xii. pp. 261–265 (1926).

and changing a into $1/a$ and adding, we get the result that

$$e^{-\frac{x^2}{2a}}a^{-(\alpha+\frac{1}{2})}x^{2\alpha+\frac{1}{2}}\left\{\mathrm{L}_n^{\alpha}\left(\frac{x^2}{2a}\right)\right\}^2 + e^{-\frac{ax^2}{2}}a^{\alpha+\frac{1}{2}}x^{2\alpha+\frac{1}{2}}\left\{\mathrm{L}_n^{\alpha}\left(\frac{ax^2}{2}\right)\right\}^2$$

is self-reciprocal in the Hankel transform of order 2α, a result proved otherwise by Watson *.

Interpreting the right-hand side of (24) with $\beta>0$; $a>0$, we get

$$\int_0^{\infty} e^{-(\beta+a)s}s^{\alpha}\mathrm{J}_{2\alpha}(2\sqrt{xs})\{\mathrm{L}_n^{\alpha}(as)\}^2\,ds = \frac{\Gamma(n+\alpha+1)}{2^{2n}n!}x^{\alpha}e^{-\frac{x}{(\alpha+\beta)}}\sum_{l=0}^{n}\frac{(-)^l(2n-2l)!\,(2l)!}{l!\,\Gamma(l+\alpha+1)[(n-l)!]^2} \times\frac{(a-\beta)^{2l}}{(a+\beta)^{2l+2\alpha+1}}\mathrm{L}_{2l}^{2\alpha}\left(\frac{2ax}{a^2-\beta^2}\right). \quad (15)$$

Acknowledgment.—I am obliged to Dr. N. W. McLachlan for generous advice in connection with both paragraph 1 and the Appendix.

Appendix.

The Solution of a certain Integral Equation.

When $\left|s^{-\nu}\phi\left(\frac{1}{s}\right)\right| \to 0$ uniformly, with respect to phase s, as $|s| \to \infty$, $-\frac{1}{2}\pi \leqslant$ phase $s \leqslant \frac{\pi}{2}$, and the other conditions for the validity of the Mellin inversion theorem in the form

$$\mathrm{F}(x) = \frac{x^{-\frac{\nu}{2}}}{2\pi i}\int_{c-i\infty}^{c+i\infty} e^{sx}\phi\left(\frac{1}{s}\right)s^{-\nu}\,ds \quad . \quad . \quad . \quad (\mathrm{A})$$

$$p^{-\nu}\phi\left(\frac{1}{p}\right) = p^{-1}\int_0^{\infty} e^{-\frac{x}{p}}\mathrm{F}(x)x^{\frac{\nu}{2}}\,dx \quad . \quad . \quad (\mathrm{B})$$

are satisfied †, the right-hand side of (2) is given by A.

Here $$\mathrm{F}(x) = \int_0^{\infty} \mathrm{J}_{\nu}(2\sqrt{xs})\,s^{\frac{\nu}{2}}f(s)\,ds, \quad . \quad . \quad . \quad (\mathrm{C})$$

* Journal London Math. Soc. p. 256 (1936).

† See Courant and Hilbert, *loc. cit.*

so, by Hankel's inversion theorem, C yields

$$f(s)=s^{\frac{\nu}{2}}\int_0^\infty J_\nu(2\sqrt{xs})\,F(x)\,dx. \quad . \quad . \quad . \quad (D)$$

Hence A is the solution of D, regarded as an integral equation for $F(x)$.

LIV. *Note on Galerkin's Method for the Treatment of Problems concerning Elastic Bodies.* *By* W. J. Duncan, *D.Sc., A.M.I.Mech.E., F.R.Ae.S., Wakefield Professor of Aeronautics at University College, Hull* *.

1. *Introduction.*

THE method to be described here is attributed to the Russian engineer V. G. Galerkin, who gave it in a paper entitled "Rods and Plates" ('Vestnik Ingeneroff,' p. 897, 1915). This original description is inaccessible to the present writer, who owes his knowledge of the method to a paper by E. P. Grossman †. Grossman states that, so far as he knows, the first application of Galerkin's method to oscillation problems was made by V. P. Lyskov in 1932 when studying the problem of wing flutter. Grossman himself has pointed out the connexion of the method with the Lagrangian equations.

The method of Galerkin may be looked at from two distinct viewpoints :—

(*a*) As a process for the approximate solution of differential equations.

(*b*) As a means for quickly and easily applying Lagrange's principle of virtual work to problems in the statics and dynamics of elastic and other continuously deformable bodies.

The method is considered from both points of view in no. 1798 of the Reports and Memoranda of the Aeronautical Research Committee ‡, which also contains

* Communicated by E. F. Relf, F.R.S.

† "Oscillations of Tail Units of Aeroplanes," Transactions of the Central Aero-Hydrodynamical Institute, Moscow, no. 186.

‡ W. J. Duncan, 'Galerkin's Method in Mechanics and Differential Equations.'

numerous examples of its applications to such problems as the flexural and torsional oscillations of beams, the critical behaviour of struts, and the solution of linear ordinary and partial differential equations. In the present short note, however, attention will be mainly confined to the application of the method to the flexural motion of a cantilever, since this affords an excellent illustration of the principles involved.

2. *Flexural Motion of a Cantilever Beam.*

The differential equation governing the deflexion of a thin beam not subject to end load is

$$\frac{d^2}{dx^2}\left(\mathrm{EI}\frac{d^2y}{dx^2}\right)=w, \quad \ldots\ldots \quad (1)$$

where y=deflexion,
x=distance measured along the beam,
EI=flexural rigidity (a function of x),
and w=load per unit span (a function of x).

When the beam is in motion the same equation holds, but w must now be taken to include the reversed effective force (inertia force) per unit span, whose magnitude is $-m\frac{d^2y}{dt^2}$, where m is the mass per unit span. If the beam is placed in an airstream the aerodynamical forces will contribute to w, and these may be assumed to be expressed in terms of displacements and velocities by the help of "derivatives" in the usual way. Let w_i=inertia force per unit span and w_a=resultant external force per unit span. Then equation (1) becomes

$$\frac{d^2}{dx^2}\left(\mathrm{EI}\frac{d^2y}{dx^2}\right)=w_a+w_i,$$

which can be written still more simply as

$$w_a+w_i+w_e=0. \quad \ldots\ldots \quad (2)$$

where $$w_e=-\frac{d^2}{dx^2}\left(\mathrm{EI}\frac{d^2y}{dx^2}\right), \quad \ldots\ldots \quad (3)$$

and is the elastic force per unit span.

Now the deflexion y must satisfy the following boundary conditions :—

At the root $(x=0)$, $y=\frac{dy}{dx}=0$, $\ldots\ldots$ (4)

and at the tip

$$(x=l), \quad \mathrm{EI}\frac{d^2y}{dx^2}=\frac{d}{dx}\left(\mathrm{EI}\frac{d^2y}{dx^2}\right)=0, \quad . \quad . \quad . \quad (5)$$

where the equations (5) express the conditions that the shearing force and bending moment vanish at the tip. Suppose that Y_1, Y_2, Y_3, etc. are a sequence of linearly independent functions of x which all satisfy (4) and (5). Then we may write

$$y=\Sigma q_r \mathrm{Y}_r, \quad . \quad . \quad . \quad . \quad . \quad . \quad . \quad (6)$$

and regard the quantities q as the dynamical coordinates of the beam. For a strict treatment of the motion it would be necessary to employ an infinite number of coordinates, but it is evident that a good approximation may be obtained by the use of only a small number of coordinates provided that the functions Y are well chosen. They may with advantage correspond to the natural modes of oscillation of the beam *in vacuo*, when these are known *.

The Lagrangian dynamical equation corresponding to the coordinate q_r is the expression of the fact that the total work done by all the forces applied to the beam (including the inertia forces) in a virtual displacement corresponding to the increment δq_r vanishes. Hence

$$\int_0^l (w_a+w_i+w_e)\frac{\partial y}{\partial q_r}dx=0,$$

or

$$\int_0^l (w_a+w_i+w_e)\mathrm{Y}_r\,dx=0. \quad . \quad . \quad . \quad . \quad (7)$$

The identity of (7) with the usual Lagrangian equation

$$\frac{d}{dt}\left(\frac{\partial \mathrm{T}}{\partial \dot{q}_r}\right)-\frac{\partial \mathrm{T}}{\partial q_r}+\frac{\partial \mathrm{V}}{\partial q_r}=\mathrm{Q}_r \quad . \quad . \quad . \quad . \quad (8)$$

follows from

$$\mathrm{T}=\frac{1}{2}\int_0^l m\dot{y}^2\,dx \quad . \quad . \quad . \quad . \quad . \quad . \quad (9)$$

and

$$\mathrm{V}=\frac{1}{2}\int_0^l \mathrm{EI}\left(\frac{d^2y}{dx^2}\right)^2 dx. \quad . \quad . \quad . \quad . \quad (10)$$

* Approximations to these modes are easily found by the Galerkin method itself (see below).

It can be shown that

$$\frac{\partial V}{\partial q_r} = \int_0^l Y_r \frac{d^2}{dx^2}\left(EI\frac{d^2y}{dx^2}\right)dx \quad . \quad . \quad . \quad (11)$$

by integration by parts and use of the boundary conditions (4) and (5).

It will be seen that (7) is obtained from the original dynamical equation (2) by multiplication by Y_r and integration over the span. Hence the procedure in using the Galerkin method is as follows :—

Substitute the expression (6) (which already satisfies the boundary conditions) in the differential equation, and let the result be ϵ, which would of course be everywhere zero if the equation were exactly satisfied. Multiply ϵ by Y_1, Y_2, etc. in turn, integrate over the beam, and equate the results to zero. In this way as many dynamical equations are obtained as there are coordinates q in use, and the equations are linear in the coordinates and their time-rates of change. The further treatment of the dynamical equations proceeds in the usual manner.

It is evident that a procedure similar to that explained above can be applied to three-dimensional problems on the dynamics of an elastic body when the condition of support is zero displacement on a certain surface. Here we should write in general,

$$\left.\begin{aligned} u &= \Sigma q_r U_r(x, y, z), \\ v &= \Sigma q_r V_r(x, y, z), \\ w &= \Sigma q_r W_r(x, y, z), \end{aligned}\right\} \quad . \quad . \quad . \quad . \quad (12)$$

and choose the functions U, V, W to satisfy the given boundary conditions for displacement. The fundamental equations of motion are, in the case of an isotropic body,

$$(\lambda+\mu)\frac{\partial \Delta}{\partial x} + \mu\nabla^2 u - \rho\frac{\partial^2 u}{\partial t^2} + \rho X = 0, \quad . \quad . \quad (13)$$

together with two similar equations. This can be written

$$x_e + x_i + x_a = 0,$$

where x_e, x_i, and x_a are the x components of elastic force, inertia force, and external force respectively, all per unit volume. Hence the Lagrange or Galerkin equation corresponding to the coordinate q_r is

$$\iiint \left[\begin{aligned} U_r(x_e+x_i+x_a) + V_r(y_e+y_i+y_a) \\ + W_r(z_e+z_i+z_a) \end{aligned}\right] dx\,dy\,dz = 0. \quad (14)$$

If there are surface tractions at points where the displacements are not zero they may be supposed replaced by statically equivalent body forces acting on a thin surface layer in accordance with the Principle of St. Venant.

3. *Numerical Example. Free Flexural Oscillation of a Uniform Cantilever.*

The first step is to select a suitable set of functions Y_r, and it is clearly advantageous to employ rational integral functions, since the integrations are then greatly simplified. It will be found that the functions defined in equation (15) are suitable for the treatment of the flexural motion of any cantilever which does not taper to zero at the tip, for they satisfy the conditions

$$y=\frac{dy}{dx}=0 \quad \text{when } x=0,$$

and

$$\frac{d^2y}{dx^2}=\frac{d^3y}{dx^3}=0 \quad \text{when } x=l.$$

The functions are defined by

$$Y_r=(r+2)(r+3)\left(\frac{x}{l}\right)^{r+1}-2r(r+3)\left(\frac{x}{l}\right)^{r+2}+r(r+1)\left(\frac{x}{l}\right)^{r+3}, \quad . \quad (15)$$

where $r>0$. As a rule r will be an integer, but this is not necessary.

Let us employ the functions Y_1 and Y_2 in the present instance.

Then

$$y=q_1Y_1+q_2Y_2, \quad . \quad . \quad . \quad . \quad . \quad . \quad (16)$$

where

$$Y_1=12\xi^2-8\xi^3+2\xi^4,$$

$$Y_2=20\xi^3-20\xi^4+6\xi^5,$$

and

$$\xi=\left(\frac{x}{l}\right). \quad . \quad . \quad . \quad . \quad . \quad . \quad . \quad (17)$$

Suppose that the beam is oscillating in one mode with frequency $p/2\pi$. Then all displacements are proportional to $\sin pt$, and the equation of motion reduces to

$$EI\frac{d^4y}{dx^4}-mp^2y=0,$$

or
$$\frac{d^4y}{d\xi^4}-ky=0, \quad . \quad . \quad . \quad . \quad . \quad . \quad (18)$$

where
$$k=\frac{mp^2l^4}{EI}. \quad . \quad . \quad . \quad . \quad . \quad . \quad . \quad (19)$$

The result of substituting the expression (16) for y on the left-hand side of (18) is

$$\epsilon=q_1(48-k\,Y_1)+q_2(-480+720\xi-k\,Y_2),$$

and the two Galerkin equations are

$$\int_0^1 \epsilon Y_1\,d\xi=0$$

and
$$\int_0^1 \epsilon Y_2\,d\xi=0.$$

These reduce to

$$\left.\begin{aligned} q_1\left(\frac{18}{5}-\frac{13}{45}k\right)+q_2\left(3-\frac{163}{630}k\right)&=0,\\ q_1\left(3-\frac{163}{630}k\right)+q_2\left(\frac{30}{7}-\frac{163}{693}k\right)&=0.\end{aligned}\right\} \quad . \quad . \quad (20)$$

The condition of compatibility of the equations (20) is a quadratic equation for k whose roots are found to be 12·3625 and 515·86. In the following table the values of k for the fundamental mode and the corresponding modes of displacement, obtained by the use of Y_1 only, of Y_1 and Y_2, and of Y_1, Y_2, and Y_3, are compared with the true solution.

		Approximate solution obtained by the Galerkin method using the functions:			True solution.
		Y_1.	Y_1, Y_2.	Y_1, Y_2, Y_3.	
$k=\frac{mp^2l^4}{EI}$		12·46	12·3625	12·3624	12·3623 *
Mode. Value of y/y_1 for value of ξ stated.	0·25	0·1055	0·0972	0·0973	0·0973
	0·5	0·3542	0·3397	0·3395	0·3395
	0·75	0·6680	0·6580	0·6577	0·6577
	1·0	1·0	1·0	1·0	1·0

* Last figure doubtful.

LV. *Applications of the Galerkin Method to the Torsion and Flexure of Cylinders and Prisms.* *By* W. J. Duncan, *D.Sc., A.M.I.Mech.E., F.R.Ae.S., Wakefield Professor of Aeronautics at University College, Hull* *.

Summary.

The paper shows that the Galerkin method can be readily applied to the St. Venant torsion problem and to the St. Venant problem of the flexure of a cantilever under tip load. The following three cases of torsion are treated in detail :—(*a*) Cylinder of aerofoil section ; (*b*) cylinder of parabolic lenticular section ; (*c*) rectangular prism. It is shown that the solutions obtained by the Galerkin method agree closely with those obtained otherwise. A simple formula for the torsional stiffness of a cylinder whose section is narrow and symmetrical, but otherwise arbitrary, is obtained. This formula is accurate in the case of an elliptic cylinder. It is shown that the shearing stresses in the flexure problem and the position of the flexural centre can easily be found, and applications are made to the elliptic cylinder and to a cylinder of aerofoil profile.

Contents.

Page

§ 1. Introduction 634

Part I.—*Torsion.*

§ 2. General. 635
§ 3. Example 1. Cylinder of Aerofoil Section 637
§ 4. Example 2. Cylinder of Parabolic Lenticular Section 639
§ 5. Example 3. Rectangular Prism 641
§ 6. Example 4. Cylinder of Empirical Section 644

Part II.—*Flexure.*

§ 7. General 645
§ 8. Example 1. Elliptic Cylinder 646
§ 9. Example 2. Cylinder of Aerofoil Section 647
References 649

§ 1. *Introduction.*

THE object of this paper is to illustrate and test the application of the Galerkin method to the St. Venant problems of the torsion and flexure of cylindrical bodies. A general discussion of the basis of the

* Communicated by E. F. Relf, F.R.S.

Galerkin method has been given in recent papers [1], [2], and need not be further considered here.

Part I. is devoted to the torsion problem, and three cases are considered in detail. The first two are solved by the thickness parameter method [3] [4], and it is shown that the Galerkin process, with only two functions in use, leads to results which are in extremely close agreement. The third case is a rectangular prism. Here the results given by the Galerkin method are compared with the "exact" series solution obtained by St. Venant. The agreement is satisfactory, although not so good as in the other two instances. The Galerkin method is also applied to the torsion of a cylinder of arbitrary symmetrical section, and a very simple formula for the stiffness is obtained. This is exact for the case of an elliptic cylinder.

Part II. deals with the flexure of a cantilever under tip load. Use is made of the shearing stress function Ω introduced in R. & M. 1444 [4]. This is analogous to Prandtl's stress function Ψ for the torsion problem, for Ω also vanishes on the boundary, and like Ψ it satisfies a partial differential equation of the Poisson type. Approximations to Ω can be found by the Galerkin process, and from these the shearing stresses and the position of the flexural centre can be deduced. Applications are made to an elliptic cylinder, for which the exact solution is obtained immediately, and to the cylinder of aerofoil profile whose torsional properties are discussed in Part I.

Part I.—*Torsion.*

§ 2. *General.*

It is well known * that the torsion problem for a solid cylinder or prism can be reduced to the problem of finding a stress function Ψ, which vanishes on the boundary and which satisfies the differential equation

$$\nabla^2\Psi+2=0 \quad . \quad . \quad . \quad . \quad . \quad . \quad (1)$$

everywhere within the boundary. When this function has been found the components of shearing stress are given by

$$X_z=\mu\tau\frac{\partial\Psi}{\partial y}, \quad . \quad . \quad . \quad . \quad . \quad . \quad (2)$$

* For a demonstration see, for example, Love's 'Mathematical Theory of Elasticity,' chap. xiv.

$$Y_z = -\mu\tau \frac{\partial \Psi}{\partial x}, \quad . \quad . \quad . \quad . \quad . \quad (3)$$

where τ = twist of unit length (in radians)

and μ = modulus of rigidity of the homogeneous and isotropic material.

Also the torsional stiffness of unit length is given by

$$C = 2\mu \iint \Psi \, dx \, dy, \quad . \quad . \quad . \quad . \quad . \quad (4)$$

where the integral extends over the whole section. The function Ψ is proportional to the deflexion of the membrane in the familiar membrane analogy of torsion.

The Galerkin method provides a means for the approximate solution of the differential equation (1) with the assigned boundary condition. Let F_1, F_2, F_3, etc. be a sequence of linearly independent functions of x and y which all vanish on the boundary, and put as an approximation

$$\Psi = \sum_{r=1}^{n} c_r F_r. \quad . \quad . \quad . \quad . \quad . \quad . \quad (5)$$

Let the result of substituting this expression on the left-hand side of (1) be ϵ. Then ϵ is the error in the differential equation corresponding to the chosen function Ψ, and it is a linear function of the coefficients c. In accordance with the Galerkin method these coefficients are determined by the condition that the n equations typified by

$$\iint \epsilon F_r \, dx \, dy = 0 \quad . \quad . \quad . \quad . \quad . \quad . \quad (6)$$

must all be satisfied. This equation can easily be interpreted in relation to the membrane analogue. For if Ψ is proportional to the displacement of the membrane in a direction perpendicular to its undisturbed position, then ϵ is proportional to the external load per unit area which is left unbalanced by the tensions in the membrane, and equation (6) expresses the vanishing of the work done by the unbalanced loads in a virtual displacement of the membrane proportional to F_r. Thus the coefficients c may be regarded as generalized coordinates for the membrane, and the Lagrangian equations of equilibrium are then typified by (6).

It only remains to consider the choice of the functions

F. When the section is symmetrical about OX and has a smooth boundary given by

$$y=\pm t, \quad . \quad . \quad . \quad . \quad . \quad . \quad . \quad (7)$$

where t is a known function of x, the following functions, with p and q positive integers, will be suitable,

$$F_{pq}=(t^{2p}-y^{2p})x^q, \quad . \quad . \quad . \quad . \quad . \quad (8)$$

for these vanish all over the boundary. The same functions will serve if the boundary has a sharp corner or corners, except when part of the boundary is perpendicular to OX. Such cases require special treatment, but the simpler examples present no difficulty (see, for instance, the treatment of the rectangle in § 5).

It must be pointed out that an exact solution could in general only be reached by the employment of a doubly infinite set of functions F. But it is found that in most cases an excellent approximation is obtained by the use of only two or three functions, and as a rule it is sufficient to use only the functions which are of the second degree in y, at any rate for narrow sections.

§ 3. *Example* 1. *Cylinder of Aerofoil Section.*

Let the section of the cylinder be the cubic oval given by

$$t^2=\theta^2 cx\left(1-\frac{x}{c}\right)^2, \quad . \quad . \quad . \quad . \quad . \quad (9)$$

where c is the chord and θ is the thickness parameter. This boundary very closely resembles some of the symmetrical aerofoil sections in current use. The maximum thickness occurs at one-third of the chord from the nose, and its magnitude is $\frac{4c\theta}{\sqrt{27}}$.

This particular case has been worked out in detail by the thickness parameter method[3], [4]. The expression for the stiffness obtained in this way is

$$C=\frac{256\mu c^4\theta^3}{3465}\left(1-\frac{11}{13}\theta^2+\theta^4-\frac{379}{221}\theta^6\right), \quad . \quad . \quad (10)$$

correct to the 6th power of θ within the bracket.

In applying the Galerkin method the following approximation to the shearing stress function will be adopted :

$$\Psi=(t^2-y^2)\left[c_1+c_2\left(\frac{x}{c}\right)\right], \quad . \quad . \quad . \quad (11)$$

Hence $$\epsilon = \nabla^2\Psi + 2$$

$$= E_0 + E_1\left(\frac{x}{c}\right) + E_2\left(\frac{x}{c}\right)^2, \quad . \quad . \quad . \quad (12)$$

where $$E_0 = 2 - c_1(2+4\theta^2) + 2c_2\theta^2, \quad . \quad . \quad . \quad . \quad (13)$$

$$E_1 = 6c_1\theta^2 - c_2(2+12\theta^2), \quad . \quad . \quad . \quad . \quad (14)$$

and $$E_2 = 12c_2\theta^2. \quad . \quad . \quad . \quad . \quad . \quad . \quad . \quad . \quad (15)$$

The two Galerkin equations are

$$\iint \epsilon(t^2 - y^2)\, dx\, dy = 0 \quad . \quad . \quad . \quad . \quad (16)$$

and $$\iint \epsilon(t^2 - y^2)\left(\frac{x}{c}\right) dx\, dy = 0. \quad . \quad . \quad . \quad . \quad (17)$$

On substitution and reduction these become

$$c_1(13+11\theta^2) + c_2(5+3\theta^2) = 13 \quad . \quad . \quad (18)$$

and $$c_1(255+153\theta^2) + c_2(119+81\theta^2) = 255. \quad . \quad (19)$$

The last equations yield

$$c_1\triangle = 17 + 18\theta^2 \quad . \quad . \quad . \quad . \quad . \quad . \quad (20)$$

and $$c_2\triangle = 51\theta^2, \quad . \quad . \quad . \quad . \quad . \quad . \quad . \quad (21)$$

where $$\triangle = 17 + 52\theta^2 + 27\theta^4. \quad . \quad . \quad . \quad . \quad (22)$$

Hence by equation (4) the expression for the stiffness is

$$C = \frac{256\mu c^4\theta^3}{3465}\left(\frac{221+489\theta^2}{221+676\theta^2+351\theta^4}\right). \quad . \quad . \quad (23)$$

The fraction inside the bracket can be converted into an ascending power series in θ when θ is small. The expansion as far as the term in θ^6 is

$$1 - \frac{11}{13}\theta^2 + \theta^4 - \frac{379}{221}\theta^6,$$

and this is identical with the bracket in equation (10).

If the simpler approximation

$$\Psi = c_1(t^2 - y^2) \quad . \quad . \quad . \quad . \quad . \quad . \quad . \quad (24)$$

were employed, c_1 would be found from equation (18) by omission of the term in c_2. Hence

$$c_1 = \frac{13}{13+11\theta^2} \quad . \quad . \quad . \quad . \quad . \quad . \quad . \quad . \quad (25)$$

and $$C = \frac{256\mu c^4\theta^3}{3465}\left(\frac{13}{13+11\theta^2}\right). \quad . \quad . \quad . \quad . \quad (26)$$

A numerical comparison of the three formulæ for the stiffness for the case where θ is 0·2 is given in the following table :—

Method.	Value of $\frac{3465\ C.}{256\ \mu c^4\theta^3}$.
Galerkin (1 function)	0·967262
„ (2 functions)	0·967652
Thickness parameter	0·967644

§ 4. *Example* 2. *Cylinder of Parabolic Lenticular Section.*

It will be convenient to take the origin at the middle of the chord. Let $b=c/2$. Then the expression for t is

$$t = \frac{\theta}{2b}(b^2-x^2). \quad . \quad . \quad . \quad . \quad . \quad (27)$$

Thus the maximum value of t occurs when $x=0$, and the maximum total thickness $2t$ is θb.

The thickness parameter method will first be applied. In the standard notation [3], [4]

$$f_7(x) = \frac{\theta^2}{2b^2}(3x^2-b^2)+\frac{\theta^4}{8b^4}(45x^4-42b^2x^2+5b^4)$$

$$+\frac{\theta^6}{16b^6}(623x^6-975b^2x^4+393b^4x^2-25b^6), \quad (28)$$

and

$$\Psi_9=(t^2-y^2)f_7(x)$$

$$-(t^4-y^4)\left\{\frac{\theta^2}{4b^2}+\frac{\theta^4}{8b^4}(45x^2-7b^2)\right\}. \quad (29)$$

In the calculation of the torsional stiffness by the formula (4) it will be convenient to use the following results, which can be quickly verified :—

$$\iint (t^2-y^2)\left(\frac{x}{b}\right)^n dx\,dy = \frac{16b^4\theta^3}{(n+1)(n+3)(n+5)(n+7)}, \quad (30)$$

$$\iint (t^4-y^4)\,dx\,dy = \frac{128b^6\theta^5}{3465}, \quad . \quad . \quad . \quad . \quad . \quad . \quad (31)$$

$$\iint (t^4-y^4)\left(\frac{x}{b}\right)^2 dx\,dy = \frac{128b^6\theta^5}{3465\times 13}. \quad . \quad . \quad . \quad . \quad . \quad (32)$$

Hence $$C = \frac{2\mu c^4\theta^3}{105}\left(1-\frac{\theta^2}{3}+\frac{5\theta^4}{33}-\frac{17\theta^6}{143}\right). \quad . \quad . \quad (33)$$

In the application of the Galerkin method the following expression for the shearing stress function will be adopted:

$$\Psi = (t^2-y^2)\left[c_1+c_2\left(\frac{x}{b}\right)^2\right], \quad . \quad . \quad . \quad (34)$$

since Ψ is obviously an even function of x. Hence

$$\epsilon = E_0+E_2\left(\frac{x}{b}\right)^2+E_4\left(\frac{x}{b}\right)^4-2c_2\left(\frac{y}{b}\right)^2, \quad . \quad . \quad (35)$$

where $$E_0 = 2-c_1(2+\theta^2)+\tfrac{1}{2}c_2\theta^2, \quad . \quad . \quad . \quad . \quad (36)$$

$$E_2 = 3c_1\theta^2-c_2(2+6\theta^2), \quad . \quad . \quad . \quad . \quad . \quad (37)$$

and $$E_4 = \frac{15}{2}c_2\theta^2. \quad . \quad . \quad . \quad . \quad . \quad . \quad . \quad . \quad (38)$$

The Galerkin equations are

$$\iint (t^2-y^2)\epsilon\,dx\,dy = 0 \quad . \quad . \quad . \quad . \quad (39)$$

and $$\iint (t^2-y^2)\left(\frac{x}{b}\right)^2 \epsilon\,dx\,dy = 0, \quad . \quad . \quad . \quad . \quad (40)$$

which can be reduced to

$$c_1(99+33\theta^2)+c_2(11+\theta^2) = 99, \quad . \quad . \quad (41)$$

$$c_1(143+13\theta^2)+c_2(39+29\theta^2) = 143. \quad . \quad . \quad (42)$$

These yield

$$c_1\triangle = 286+341\theta^2 \quad . \quad . \quad . \quad . \quad . \quad . \quad (43)$$

and $$c_2\triangle = 429\theta^2, \quad . \quad . \quad . \quad . \quad . \quad . \quad . \quad (44)$$

where $$\triangle = 286+484\theta^2+118\theta^4. \quad . \quad . \quad . \quad (45)$$

Hence by equation (4) the torsional stiffness is

$$C = \frac{2\mu c^4\theta^3}{315}\left(\frac{858+1166\theta^2}{286+484\theta^2+118\theta^4}\right). \quad . \quad . \quad (46)$$

The expression inside the bracket can be converted into an ascending power series in θ, and is found to be

$$3-\theta^2+\frac{5}{11}\theta^4-\frac{51}{143}\theta^6+\text{ etc.}$$

Therefore (46) becomes

$$C=\frac{2\mu c^4\theta^3}{105}\left(1-\frac{\theta^2}{3}+\frac{5\theta^4}{33}-\frac{17\theta^6}{143}+\text{etc.}\right),$$

and this is identical with (33) up to the 6th power of θ within the bracket (compare example 1).

§ 5. *Example* 3. *Rectangular Prism.*

Suppose that the section of the prism is a rectangle of sides $2a$ and $2b$. Take the origin at the centre, and the axis OX parallel to the longer side $2a$. Then the following functions are even in both x and y, as is clearly necessary, and vanish on the boundary

$$f_r=(b^2-y^2)\left[1-\left(\frac{x}{a}\right)^{2r}\right] \quad . \quad . \quad . \quad . \quad . \quad (47)$$

To obtain a very accurate approximation which should hold even in the extreme case of a square it would be necessary to introduce functions of a similar form, but involving the fourth and higher even powers of y. However, it has not been considered necessary to explore this refinement.

Let

$$\Psi=c_1f_1+c_2f_2+c_3f_3 \quad . \quad . \quad . \quad . \quad (48)$$

and

$$\beta=\frac{b^2}{a^2} \quad . \quad . \quad . \quad . \quad . \quad . \quad . \quad . \quad . \quad (49)$$

Then

$$\epsilon=E_0+E_2\left(\frac{x}{a}\right)^2+E_4\left(\frac{x}{a}\right)^4+E_6\left(\frac{x}{a}\right)^6 + \left(\frac{y}{a}\right)^2\left(F_0+F_2\left(\frac{x}{a}\right)^2+F_4\left(\frac{x}{a}\right)^4\right), \quad (50)$$

where

$$E_0=2-2(c_1+c_2+c_3)-2\beta c_1, \quad . \quad . \quad . \quad (51)$$

$$E_2=2c_1-12\beta c_2, \quad . \quad . \quad . \quad . \quad . \quad . \quad . \quad (52)$$

$$E_4=2c_2-30\beta c_3, \quad . \quad . \quad . \quad . \quad . \quad . \quad . \quad (53)$$

$$E_6=2c_3, \quad . \quad . \quad . \quad . \quad . \quad . \quad . \quad . \quad . \quad (54)$$

$$F_0=2c_1, \quad . \quad . \quad . \quad . \quad . \quad . \quad . \quad . \quad . \quad (55)$$

$$F_2=12c_2, \quad . \quad . \quad . \quad . \quad . \quad . \quad . \quad . \quad . \quad (56)$$

and

$$F_4=30c_3. \quad . \quad . \quad . \quad . \quad . \quad . \quad . \quad . \quad . \quad (57)$$

The Galerkin equations are

$$\iint \epsilon f_r \, dx \, dy = 0, \quad . \quad . \quad . \quad . \quad . \quad (58)$$

with r taken as 1, 2, and 3 in succession.

These equations, when reduced and cleared of fractions, become *

$$420\,(1+\beta)c_1+24\,(20+21\beta)\,c_2+20\,(25+27\beta)\,c_3=525, \quad . \quad . \quad . \quad (59)$$

$$132\,(20+21\beta)\,c_1+440\,(7+9\beta)\,c_2+60\,(54+77\beta)\,c_3=3465, \quad . \quad . \quad . \quad (60)$$

and

$$2860\,(25+27\beta)\,c_1+1560\,(54+77\beta)\,c_2+1620\,(55+91\,\beta)\,c_3 = 96{,}525. \quad . \quad . \quad (61)$$

The solution of this set is

$$c_1\Delta = 135\,(4576\,\beta^2-440\beta+25), \quad . \quad . \quad . \quad . \quad (62)$$

$$c_2\Delta = 2475\,(52\beta-5), \quad . \quad . \quad . \quad . \quad . \quad . \quad . \quad (63)$$

$$c_3\Delta = 10725, \quad . \quad . \quad . \quad . \quad . \quad . \quad . \quad . \quad . \quad (64)$$

where $$\Delta = 64\,(7722\,\beta^3+8910\beta^2+1125\beta+25) \quad . \quad (65)$$

By equation (4) the stiffness is

$$C = 32\mu ab^3\left(\frac{c_1}{9}+\frac{2c_2}{15}+\frac{c_3}{7}\right)$$

$$= \frac{4\mu ab^3(60060\beta^2+9240\beta+225)}{7(7722\beta^3+8910\beta^2+1125\beta+25)} \quad . \quad . \quad . \quad (66)$$

It may be added that when the functions f_1 and f_2 only are employed the formula for the stiffness is

$$C = \frac{1120\mu ab^3(1+9\beta)}{9[28(1+\beta)(1+9\beta)-3]}, \quad . \quad . \quad . \quad (67)$$

and when f_2 and f_3 only are used the formula is

$$C = \frac{1056\mu ab^3(559\beta+35)}{35(4004\beta^2+3960\beta+207)} \quad . \quad . \quad . \quad . \quad (68)$$

In all of these formulæ $\beta \geqslant 1$, *i. e.*, $2b$ is the lesser side of the rectangle.

In the following table the results obtained from the formulæ (66), (67), and (68) are compared with the

* The array of coefficients in this and other similar sets of equations is symmetrical before fractions are cleared. Preservation of the symmetry in the final equations would require the introduction of redundant numerical factors.

true solution obtained by St. Venant *. The quantity tabulated is

$$\gamma = \frac{C}{16\mu a b^3} \quad . \quad . \quad . \quad . \quad . \quad . \quad . \quad (69)$$

$\frac{b}{a}$	β.	Values of γ.			
		By Galerkin using the functions f_1 and f_2.	f_2 and f_3.	f_1, f_2, and f_3.	By St. Venant.
0	0	0·3111	0·3188	0·3214	0·333
$\frac{1}{10}$	$\frac{1}{100}$	0·3047	0·3099	0·3109	0·312
$\frac{1}{4}$	$\frac{1}{16}$	0·2795	0·2805	0·2806	0·281
$\frac{1}{3}$	$\frac{1}{9}$	0·2627	0·2629	0·2631	0·263
$\frac{1}{2}$	$\frac{1}{4}$	0·2282	0·2277	0·2283	0·229
$\frac{2}{3}$	$\frac{4}{9}$	0·1952	0·1938	0·1952	0·196
1	1	0·1396	0·1371	0·1396	0·141

It will be seen that the results obtained by the Galerkin method with the functions f_r in use are least accurate for the two extreme forms of section, namely, the very attenuated rectangle and the square. This is not difficult to explain, for in the case of the attenuated rectangle the true stress function is independent of x except quite close to the ends of the section, and a linear combination of a *small* number of rational integral functions of the type f_r is clearly not well adapted to represent a function of this kind † unless the indices r are large. And, on the other hand, it is not to be expected that an approximation to Ψ which is parabolic in y will fit the true solution closely when the section of the prism is square or nearly square.

The table shows that the error in the result obtained by the use of f_2 and f_3 only is less than that obtained with f_1 and f_2 only for low values of β, but greater for values of β near 1. This can be explained on the ground

* The figures for the St. Venant solution are taken from 'Applied Elasticity' by Timoshenko and Lessells.

† Compare the representation of a stepped line by Fourier series.

that the higher the index r the more nearly does f_r become independent of x near the middle of the section.

§ 6. *Example* 4. *Cylinder of Empirical Section.*

Suppose that the boundary of the section is an arbitrary curve having OX as an axis of symmetry. The curve may be defined graphically or by an equation, and it will be assumed that the slope of the boundary is everywhere finite (except at the end points, where the tangent may be perpendicular to OX, but end walls of finite length perpendicular to OX are excluded).

Let the boundary be given by (7), and assume the approximation

$$\Psi = k(t^2 - y^2). \quad . \quad . \quad . \quad . \quad . \quad . \quad (70)$$

Then $$\epsilon = 2 - 2k + k\frac{d^2t^2}{dx^2},$$

and the Galerkin equation is

$$\iint (t^2 - y^2)\left(2 - 2k + k\frac{d^2t^2}{dx^2}\right) dx\, dy = 0,$$

or $$\int t^3\left(2 - 2k + k\frac{d^2t^2}{dx^2}\right) dx = 0. \quad . \quad . \quad . \quad (71)$$

The coefficient of k in this is

$$\int t^3\left(-2 + \frac{d^2t^2}{dx^2}\right) dx$$

$$= -2\int t^3\, dx + \left[t^3\frac{dt^2}{dx}\right] - 6\int t^3\left(\frac{dt}{dx}\right)^2 dx$$

$$= -2\int t^3\, dx - 6\int t^3\left(\frac{dt}{dx}\right)^2 dx, \quad . \quad . \quad . \quad . \quad (72)$$

since t is zero at both ends of the section.

Hence (71) yields

$$k = \frac{\int t^3\, dx}{\int t^3\, dx + 3\int t^3\left(\frac{dt}{dx}\right)^2 dx} \quad . \quad . \quad . \quad . \quad (73)$$

The torsional stiffness is

$$C = 2\mu \iint \Psi\, dx\, dy$$

$$= 2\mu k \iint (t^2 - y^2)\, dx\, dy$$

$$= \frac{8}{3}\mu k \int t^3\,dx$$

$$= \frac{8\mu \int t^3\,dx)}{3(1+3\mathrm{K})}, \quad \ldots\ldots\ldots \quad (74)$$

where $$\mathrm{K} = \frac{\int t^3 \left(\frac{dt}{dx}\right)^2 dx}{\int t^3\,dx} \quad \ldots\ldots\ldots \quad (75)$$

When $\left(\frac{dt}{dx}\right)$ is obtained graphically it should be checked by the relation

$$\int \left(\frac{dt}{dx}\right) dx = 0, \quad \ldots\ldots\ldots \quad (76)$$

since t vanishes at the two ends of the section.

By way of example the formulæ will be applied to an ellipse of semi-axes a and b. Then

$$t = \frac{b}{a}\sqrt{a^2 - x^2},$$

so that $$\int t^3\,dx = \frac{3\pi}{8} ab^3$$

and $$\int t^3 \left(\frac{dt}{dx}\right)^2 dx = \frac{\pi b^5}{8a}.$$

Hence (75) gives $\mathrm{K} = \frac{1}{3}\left(\frac{b}{a}\right)^2$, and by (74)

$$\mathrm{C} = \frac{\pi\mu a^3 b^3}{a^2 + b^2}.$$

Thus the formulæ are exact in the case of an elliptic cylinder.

Part II.—*Flexure.*

§ 7. *General.*

The problem to which the method will now be applied is that of the flexure of a cantilever under tip load. St. Venant obtained a particular solution to the problem which exactly satisfies the equations of the mathematical theory of elasticity. This solution leads to the determination of the shearing stresses on a normal section

of the beam, and the position of the flexural centre can be deduced from it.

Attention will be confined to the case where OX is an axis of symmetry of the section and the load W is applied downwards at right angles to OX. It can be shown[4] that the solution of the physical problem can be made to depend on the following formal problem:

Find a function Ω which vanishes on the boundary of the section given by $y=\pm t$, and which satisfies the differential equation

$$\nabla^2\Omega+\frac{1}{2}\frac{dt^2}{dx}-\frac{\sigma x}{1+\sigma}=0 \quad . \quad . \quad . \quad . \quad (77)$$

everywhere within the section. Here x is measured from the centroid and σ is Poisson's ratio.

When Ω has been found the components of shearing stress are obtained from

$$X_z=\frac{W}{I}\frac{\partial\Omega}{\partial y}, \quad . \quad . \quad . \quad . \quad . \quad . \quad . \quad . \quad (78)$$

$$Y_z=-\frac{W}{2I}\left(t^2-y^2+2\frac{\partial\Omega}{\partial x}\right), \quad . \quad . \quad . \quad (79)$$

where I is the moment of inertia of the section about OX. Also the abscissa of the flexural centre is

$$\bar{\bar{x}}=\frac{\int xt^3.dx-3\iint\Omega\,dx\,dy}{\int t^3\,dx}, \quad . \quad . \quad . \quad (80)$$

where the integrals extend over the entire section.

In the application of the Galerkin method to this problem it will be convenient to employ the functions defined by equation (8), and it will usually suffice to take two or three functions with $p=1$ and $q=0$, 1, 2, etc.

§ 8. *Example* 1. *Elliptic Cylinder.*

When the origin is the centroid the equation to the boundary is

$$t^2=\frac{b^2}{a^2}(a^2-x^2).$$

Hence (77) becomes

$$\nabla^2\Omega-x\left(\frac{b^2}{a^2}+\frac{\sigma}{1+\sigma}\right)=0. \quad . \quad . \quad . \quad (81)$$

Assume

$$\Omega = c_1(t^2-y^2)+c_2x(t^2-y^2). \quad . \quad . \quad . \quad (82)$$

Then

$$\epsilon = \nabla^2\Omega - x\left(\frac{b^2}{a^2}+\frac{\sigma}{1+\sigma}\right)$$

$$= -2c_1\left(\frac{b^2+a^2}{a^2}\right)$$

$$-x\left\{c_2\left(\frac{6b^2+2a^2}{a^2}\right)+\left(\frac{b^2}{a^2}+\frac{\sigma}{1+\sigma}\right)\right\},$$

and this obviously vanishes when

$$c_1 = 0$$

and

$$c_2 = -\frac{b^2+\dfrac{\sigma a^2}{1+\sigma}}{6b^2+2a^2}.$$

Hence the exact solution is at once found to be

$$\Omega = -x\left(\frac{b^2}{a^2}+\frac{\sigma}{1+\sigma}\right)\left(\frac{a^2b^2-b^2x^2-a^2y^2}{2a^2+6b^2}\right). \quad . \quad (83)$$

This agrees with equation (306) of R. & M. 1444[4].

§ 9. *Example* 2. *Cylinder of Aerofoil Section.*

The centroid of the cubic oval (9) is at the distance $3c/7$ from the origin. To allow for this the differential equation (77) must be rewritten

$$\nabla^2\Omega + \frac{1}{2}\frac{dt^2}{dx} - \frac{\sigma x}{1+\sigma} + \frac{3\sigma c}{7(1+\sigma)} = 0,$$

and on substitution of the expression for t this becomes

$$\nabla^2\Omega + \frac{3\sigma c}{7(1+\sigma)} + \frac{1}{2}\theta^2 c - x\left(\frac{\sigma}{1+\sigma}+2\theta^2\right) + \frac{3}{2}\frac{\theta^2x^2}{c} = 0. \quad (84)$$

Assume

$$\Omega = (t^2-y^2)\left[c_1+c_2\left(\frac{x}{c}\right)\right]. \quad . \quad . \quad . \quad . \quad (85)$$

Then

$$\epsilon = \mathrm{E}_0+\mathrm{E}_1\left(\frac{x}{c}\right)+\mathrm{E}_2\left(\frac{x}{c}\right)^2, \quad . \quad . \quad . \quad (86)$$

where

$$\mathrm{E}_0 = 2\theta^2c_2 - c_1(2+4^2)\theta + \frac{1}{2}c\theta^2 + \frac{3\sigma c}{7(1+\sigma)}, \quad . \quad (87)$$

$$E_1 = -\frac{\sigma c}{1+\sigma} - 2\theta^2 c + 6c_1\theta^2 - c_2(2+12\theta^2), \quad . \quad (88)$$

and $$E_2 = \frac{3}{2}\theta^2 c + 12c_2\theta^2. \quad . \quad . \quad . \quad . \quad . \quad . \quad . \quad . \quad (89)$$

The Galerkin equations when reduced become *

$$c_1(13+11\theta^2)+c_2(5+3\theta^2) = \frac{2\sigma c}{7(1+\sigma)}, \quad . \quad . \quad . \quad (90)$$

and

$$c_1(255+153\theta^2)+c_2(119+81\theta^2 = -\frac{34\sigma c}{7(1+\sigma)} - 8\theta^2 c. \quad (91)$$

These yield

$$c_1\triangle = \frac{c}{14(1+\sigma)}[51\sigma+\theta^2(35+68\sigma)+21(1+\sigma)\theta^4], \quad . \quad (92)$$

$$c_2\triangle = \frac{-c}{14(1+\sigma)}[119\sigma+\theta^2(91+176\sigma)+77(1+\sigma)\theta^4], \quad (93)$$

where $\triangle$ is given by equation (22). Hence (80) and (85) give after some reduction

$$\bar{\bar{x}} = -\frac{4c\{17(1+3\sigma)+\theta^2(52+54\sigma)-29(1+\sigma)\theta^4\}}{91(1+\sigma)(17+52\theta^2+27\theta^4)}. \quad (94)$$

When θ is so small that its square can be neglected this becomes

$$\bar{\bar{x}} = -\frac{4c(1+3\sigma)}{91(1+\sigma)}, \quad . \quad . \quad . \quad . \quad . \quad (95)$$

and this is identical with the result given by equation (316) of R. & M. 1444[4] when θ^2 is neglected. As a further comparison with the thickness parameter method take the case where $\theta = 0{\cdot}2$ and $\sigma = 0{\cdot}28$ (steel). It is found that (94) gives

$$-\frac{91\bar{\bar{x}}}{4c} = 1{\cdot}385,$$

whereas the thickness parameter method yields 1·370 (see table 4 of chapter iv. of R. & M. 1444)[4]. The difference of these corresponds to an error of about 1 per cent. in the separation of the flexural centre and centroid, but this only amounts to about 0·05 per cent. of the chord of the section.

* The array of coefficients on the left is naturally the same as in equations (18) and (19).

Acknowledgment.

The author is indebted to the Aeronautical Research Committee for permission to publish this paper.

References.

(1) Duncan, "Galerkin's Method in Mechanics and Differential Equations," Reports and Memoranda of the Aeronautical Research Committee, no. 1798 (1937).
(2) Duncan, "Note on Galerkin's Method for the Treatment of Problems concerning Elastic Bodies," Phil. Mag. xxv. p. 628 (1938).
(3) Duncan, "On the Torsion of Cylinders of Symmetrical Section," Proc. Roy. Soc. A, vol. cxxxvi. (1932).
(4) Duncan, "Torsion and Flexure of Cylinders and Tubes," Reports and Memoranda of the Aeronautical Research Committee, no. 1444 (1932).

LVI. *Pre-striking Currents in a Thyratron.* *By* Professor E. L. E. Wheatcroft, R. B. Smith, *Ph.D.*, *and* J. Metcalfe, *B.Sc.**

THYRATRON is a generic name † for a gas- (or vapour-) filled thermionic triode. The chief operating characteristic of these valves is a relation between positive anode potential (relative to the cathode) and a critical negative grid potential at which the tube "strikes." After striking, the anode potential is necessarily low and the current is limited by the impedance of the external circuit; at the same time the grid is surrounded by a plasma and can no longer act as a controlling electrode, but only after the manner of a Langmuir probe. The critical relation between grid and anode potentials is called the grid control curve; it depends upon the geometrical arrangement of the electrodes and upon the density of gas or vapour in the tube.

Empirical development of thyratrons has run ahead of any theory as to their operation, and discussions as to the mechanism of striking have usually been of a somewhat speculative nature, such as: "it is essential to the successful operation of the tube that the grid so completely shield the cathode from the anode that,

* Communicated by Prof. E. L. E. Wheatcroft.

† Actually the name Thyratron is the registered trade mark of the British Thomson-Houston Co.; however, the word is now in common use (with a small "t") to denote all valves of this type.

with the grid more negative than the starting voltage, no electrons can reach the cathode." Kirchstein *, however, realized that the phenomenon of striking represented the passage of the current I from a stable to an unstable region, which could be expressed in the form

$$\frac{dI}{dV}=\infty \quad \text{or} \quad \frac{dV}{dI}=0,$$

where V is the controlled potential.

The experiments discussed here were undertaken in the hope of elucidating the mechanism of striking and of arriving at a theory which could be used for quantitative

Fig. 1.

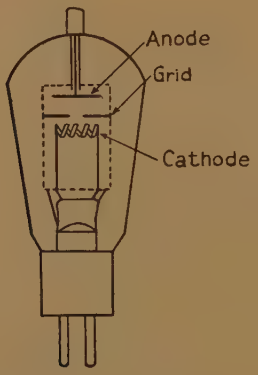

Cross-section of BT 1 thyratron.

results. The course of the measurements was guided by a tentative theory proposed by Wheatcroft † and reproduced here in explanation.

Fig. 1 shows a section of the Mazda BT 1 thyratron, on which most of the tests were made. After evacuation and before sealing, a little mercury is introduced into the tube, and the discharge takes place in mercury vapour at a pressure dependent on the temperature of the valve. The electrode arrangement is clear from the figure; part of the grid structure is a perforated metal cylinder which shields the interelectrode space from charges on

* *Arch. f. Elekt.* xxvii. p. 785 (1933).
† Leeds Phil. Soc. iii. p. 396 (1937).

the walls of the glass bulb, while the operative part of the grid is in the form of a washer with a central hole. The area of the hole is about 1/40th of that of the washer.

Theory.

Before the tube strikes, the electron current which escapes from the neighbourhood of the cathode is comparatively small. There must therefore be a potential minimum returning most of the emitted electrons to the cathode. In this respect the gas-filled tube resembles a vacuum triode when the grid of the triode is sufficiently negative. The potential minimum is then produced by the negative surface charges on the grid, and not, as in the region of higher currents, by the negative space charge of the electrons themselves. This condition is illustrated in fig. 2. The potential distribution in front of the grid hole can be compared to a mountain pass, the junction of the 1·5 volt lines in the figure being a minimum longitudinally and a maximum transversely. We may conveniently describe this, therefore, as the potential "pass."

Consider first in the light of fig. 2 the state of affairs in a *vacuum* triode when the grid is sufficiently negative. The electron current flowing from cathode to anode will be a minute fraction of the working current, and will therefore be a still smaller fraction of the total emission of the cathode. This can only happen by virtue of the existence of the pass, by which all except those electrons which leave the cathode with high velocities are turned back. Let the potential at the pass be V_m volts below the potential of the cathode. The fraction of electrons which have sufficient energy to pass through is then

$$e^{-\frac{V_m}{kT}}.$$

where T is the emission temperature in degrees K, k is Boltzmann's constant, and e the electronic charge.

If the hole in the grid were so large that practically all the emitted electrons proceeded in the direction of the pass we might write the current

$$I_e = I_s\, e^{-\frac{V_m e}{kT}},$$

where I_c is the cathode current and I_s is the total emission of the cathode. In general we may write

$$I_c = \eta I_s \, e^{-\frac{V_m e}{kT}}, \quad . \quad . \quad . \quad . \quad . \quad . \quad . \quad (1)$$

Fig. 2.

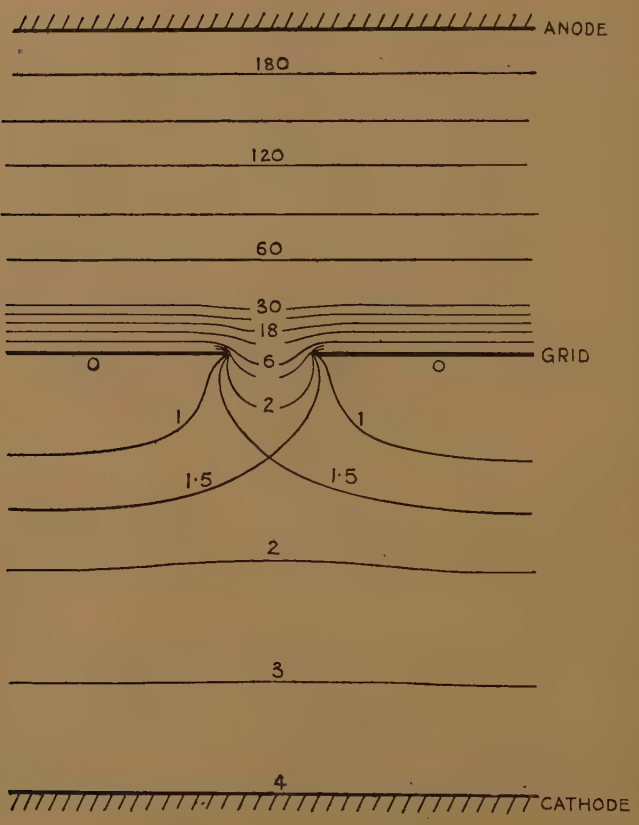

Potential distribution in valve.

where η is a factor which should depend chiefly on the electrode geometry. We should have then

$$\log I_c = \log \eta I_s - \frac{e}{kT} V_m.$$

We should expect $\log \eta I_s$ to be nearly independent of the applied potentials. Now in this region, where the current is very small, the magnitude of V_m is determined not by

the electron space charge but by the electrode potentials. We should therefore expect V_m to be a function of $V_a+\mu V_g$, where these quantities have the usual meanings, and the function would be nearly that of a simple proportion. In general, therefore, we should expect, for the vacuum triode, to be able to write

$$\log I_c = f(V_a+\mu V_g), \quad . \quad . \quad . \quad . \quad . \quad (2)$$

where the function *f approximates to a straight line.*

Fig. 3.

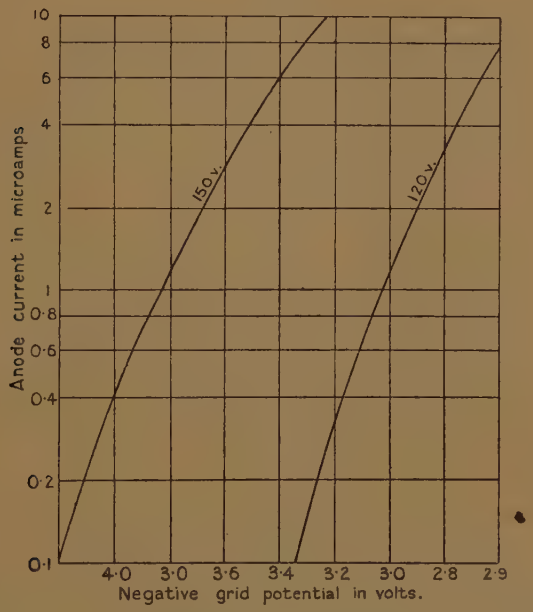

Current in vacuum triode.

The form of the function as found experimentally for a typical small receiving triode confirms this view, as shown in fig. 3. The curves are actually slightly concave downwards, and μ is not quite independent of the current.

We now consider in the light of fig. 2 and equation (2) the case of the *gas-filled* valve when the anode is at a high positive potential and the grid more negative than the critical striking point. There is still a pass over which only the fastest electrons can go. These electrons

proceed through the hole in the grid, and there are rapidly accelerated on their way to the anode. Now, however, they make a number of ionizing collisions between grid and anode, the resulting electrons being also swept away to the anode. The positive ions travel slowly to the grid, and so form a positive space charge on the anode side of the grid. This has the effect of changing the

Fig. 4.

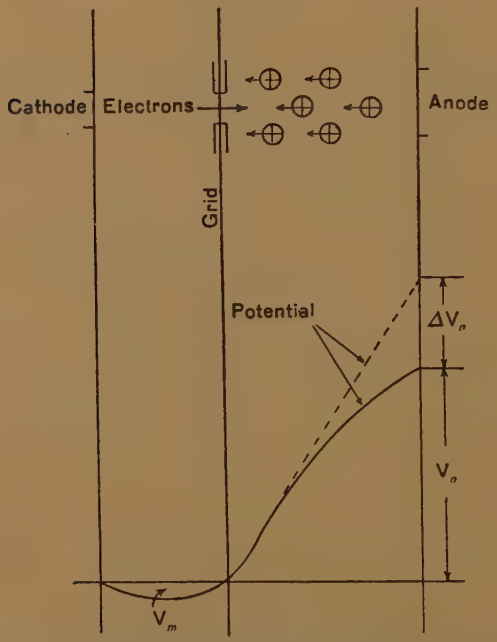

Change of potential distribution due to positive space charge.
[From Proc. Leeds Phil. Soc. (Scientific Section) vol. iii. pt. 6.]

potential distribution between grid and anode, making it concave downwards as shown by the full line in fig. 4.

It is now necessary to consider how equation (2) will be modified by the effect of the positive ions. This may be done by noting the potential distribution shown in fig. 2, where we see that as a first approximation the magnitude of V_m must be uniquely determined by V_g and by the *potential gradient on the anode side of the grid*, provided that, as in the BT 1 Thyratron, the washer

surface is large compared with that of the hole. Thus the dotted and full line curves in fig. 4 will both correspond to the same value of V_m (for the same grid potential), and the effect of the positive space charge may be met by substituting $V_a + \Delta V_a$ for V_a in equation (2). Moreover under given ionizing conditions we may expect ΔV_a to

Fig. 5.

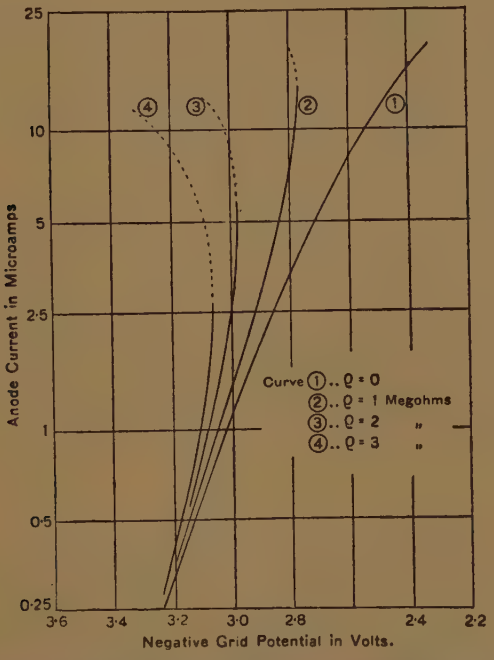

Theoretical effect of "negative resistance due to ionization."
[From Proc. Leeds Phil. Soc. (Scientific Section) vol. iii. pt. 6.]

be proportional to I_c, so that we may now write as a general equation

$$\log I_c = f(V_a + \mu V_g + \rho I_c), \quad . \quad . \quad . \quad . \quad (3)$$

where ρ is a constant, independent of I_c.

Fig. 5 shows the form taken by equation (3) for a function similar to that of the vacuum valve, and the theoretical effect of different values of ρ in modifying the current-voltage relation. It shows clearly that here is a possible explanation of striking, since on each curve

there is a point where $\frac{dV_g}{dI_c}=0$, and the dotted portions are obviously unstable. If then it can be shown experimentally that ρ, which may be called the "negative resistance due to ionization," is independent of I_c for given gas pressure and anode voltage, the formula will give a good basis for quantitative study.

In considering the plausibility of the assumptions leading to equation (3) it is important to realize that at the highest temperature at which the tubes were operated 135° C.) the density of the vapour is still comparatively (ow, viz., ·004 mm., and that at anode potentials of over 200 volts almost all the electrons making a collision will have adequate energy to ionize. Under these conditions the number of ions created by each electron should be a small fraction which should be proportional to the vapour density and nearly independent of the anode voltage, as in the Dushman and Found ionization gauge *. Preliminary calculation from the data of Compton and Van Voorhis † indicates that the number of ions created per electron will be less than 1/10 at 35° C. We may therefore take it that the ionizing conditions are unaffected by the magnitude of ΔV_a, at any rate if the latter is small compared with V_a.

Experiments.

The object of this paper is to describe in greater detail the experiments by which the validity of equation (3) was established for the Mazda BT 1 and BT 5 ‡ thyratrons.

Fig. 6 shows the electrical connexions for the tests. The anode voltage (up to about 450 volts) was supplied by a "battery eliminator" containing a Westinghouse rectifier, connected to the 200 volt A.C. mains. The grid voltage (up to about 10 volts negative) was supplied by a secondary battery. The cathode-heating current (about 6·5 amps at 2·8 volts) was supplied generally from a large main battery in another part of the building, but

* Phys. Rev. xvii. p. 7 (1921) ; and xxiii. p. 734 (1924).

† Phys. Rev. xxvi. p. 436 (1925) ; and xxvii. p. 724 (1926).

‡ The BT 5 is larger than the BT 1 and has an indirectly heated cathode of the "Hull" type, where the emitting surface is located within a cylindrical metal box, the electrons escaping through a hole in the end of the box towards the anode.

in special cases a small portable battery was used when a high insulation resistance to earth was necessary.

The resistances R_1 and R_2 are safety resistances to limit the current after the thyratron strikes; before striking the potential drop across either of them is negligible. R_3 is used in conjunction with a valve-voltmeter to measure the anode current. The full range of the valve voltmeter was about 1 volt, and R_3 was chosen to give a suitable current range. For this purpose a series of Dubilier metallized resistance units, calibrated by Wheatstone bridge, were used in a "grid leak holder" for easy substitution; the maximum was 2 megohms. The valve-voltmeter was employed because there seemed

Fig. 6.

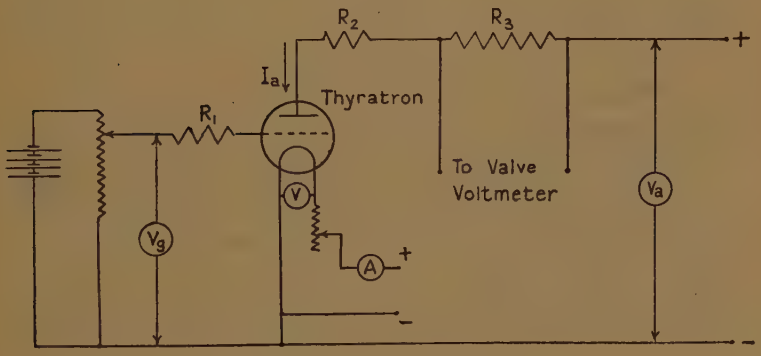

Electrical connexions for tests.

to be no way of avoiding damage to a sensitive galvanometer when the current suddenly increased a thousandfold on striking, whereas the valve automatically protects the microammeter used as indicator in its own anode circuit. The other currents and voltages were measured by Weston moving coil instruments.

The aim of the experiments was naturally to make two or more tests of the variation of I_c with $(V_a+\mu V_g)$ under such conditions that f was constant and ρ had a different but constant value for each test. Since ρ is dependent upon the presence of ions there is clearly a possibility of achieving the purpose by varying the vapour pressure in the valve. It was at the time considered unsafe to assume that ρ would not depend somewhat on the value

of V_a. The anode voltage was therefore held constant in any one test and the variation of I_c obtained by varying V_g. To particularize, for any given value of V_a and I_c let two measurements of V^g be made, one at pressure p_1 and the other at pressure p_2. Assuming that f does not vary with pressure, we may write

$$\log I_c = f(V_a + \mu V_{g1} + \rho_1 I_c)$$
$$= f(V_a + \mu V_{g2} + \rho_2 I_c),$$

where the suffixes denote the respective tests.

Hence

$$\mu(V_{g1} - V_{g2}) = I_c(\rho_2 - \rho_1).$$

ρ, however, according to the theory, depends only on V_a and p, and not on either V_g or I_c. The theory is therefore confirmed if it is found that for given values of V_a, p_1, and p_2

$$\mu(V_{g1} - V_{g2})/I_c = \text{constant}$$

for all values of I_c.

The valves being mercury filled, the variation of pressure was conveniently made by varying the condensing temperature of the glass walls. After their end-caps had been removed, they were placed in oil, which was continually stirred. The oil-bath was surrounded by another bath which could be filled with ice, hot water, etc. to give a temperature control of the oil between $-8°$ C. and 30° C.

Leakage.

Preliminary tests were made to determine the magnitude of the leakage currents in and across the valve. These showed that the leakage at the anode terminal at the usual anode voltages (200 to 300 volts) was of the order of 10^{-7} amperes * ; this therefore represented a lower limit of accurate measurement of any electron current to the anode. Measurement of electron current from the cathode was even more difficult on account of the leakage between the eliminator and the heating battery. For this reason in nearly all cases measure-

* In later experiments this value was improved. The oil, however, always deteriorated badly after solid CO_2 had been used as a cooling substance, even though every precaution was adopted to prevent contamination.

ments were all made of the anode current, I_a. The justification for using this quantity to establish equation (3) lies in the fact that the grid current was experimentally found to be small compared with the anode current, and thus I_a and I_c are nearly equal. Even were this not the case, however, there is reason to suppose that, on the analogy of the ionization gauge, the grid current will be proportional to the anode current at any given pressure, so that ρ will still appear constant and independent of I, although its absolute magnitude may be in error.

Determination of μ.

In a second preliminary experiment the BT 1 thyratron was immersed in liquid air (in place of the oil) and variation of anode current with grid potential at various values of anode potential was measured, exactly as for a vacuum valve. In this and all subsequent experiments anode leakage current was determined by making the grid more and more negative until the anode current became independent of any further variation of grid potential. This value of the current was then called the anode leakage. In fact it would include any current due to electron emission from the grid, but there was no point in attempting to separate these two effects provided that the apparent leakage was measured in the way mentioned above at every pressure and every anode potential—in any case it was small compared with the actual measured currents used to establish the equation.

Curves of anode current (corrected for leakage) were plotted semilogarithmically against grid potential and were in every way similar to those of fig. 3. μ varied slightly with current as in the receiving valve.

Experimental Proof of the Constancy of ρ.

The object of the main series of experiments was to obtain curves of the type shown in fig. 5, each corresponding to a different vapour pressure. Here we anticipated considerable difficutly. It is obvious from equation (1) that an increase in the total emission I_s will move any of the curves parallel to the current axis, while a change of contact potential difference will move the curve parallel to the potential axis. It seemed too much

to hope that both these quantities would be independent of oil temperature. Moreover with a directly heated cathode, as in the BT 1, there is an unknown potential difference between the negative cathode terminal (from which V_g is measured) and the emitting part of the cathode. We were prepared therefore to take this bull by the horns and shift the experimental curves bodily parallel to themselves to make them meet at the low current ends, and if after this adjustment ρ was shown to be constant to assert a *prima facie* proof of equation (3). In fact we have not had to adopt this expedient except in one or two cases. In the large majority of tests, both on the BT 1 and BT 5 tubes, we were able, by adopting the procedure set out below, to obtain directly experimental curves which yielded a constant value of ρ over the whole range of current. The procedure was as follows. The cathode-heating current was set at a given value (6·50 amps for the BT 1) which was held constant throughout all the tests. After a few minutes the cathode-heating voltage became steady at a value ($2{\cdot}28 \pm {\cdot}01$ volts for the BT 1) which was found to be independent of the oil temperature. However, the total emission (or perhaps the contact potential, for it is not easy to distinguish these two effects) continued to change in that the low-current end of the curve (10^{-7} amps) was still shifting. After about $1\frac{1}{2}$ hours, however, any further shift became negligible. Meanwhile the oil temperature had been adjusted to a convenient lower value, *e. g.*, 12° C. for most of the tests. The readings corresponding to this temperature were then determined, the time of reading occupying some 10 to 20 minutes. *As quickly as possible* after this the oil temperature was raised, by substituting warm water for ice, to the selected higher temperature, and the readings for the second curve obtained. This usually completed the procedure for that day.

In fig. 7 are plotted semilogarithmically the results of two tests, nos. 13 and 18. In no. 13 the lower temperature was 12° C. and the second temperature 25° C. ; in no. 18 the first temperature was −8° C. and the second 12° C. The dots represent plots of the experimental readings while the curves are drawn in such a way as would represent constant values of ρ while keeping as near to the experimental points as possible. In test no. 13 the agreement is clearly very good and is typical of most

of the twenty-six tests of this kind. Test no. 18 is not so good, and is included partly for that reason and partly because it includes the lowest oil temperature, at which ρ was probably nearly zero. The two curves for 12° C. do not coincide for reasons discussed above, but they are parallel. The displacement between them appears to agree better with a change of potential rather than of total emission.

Fig. 7.

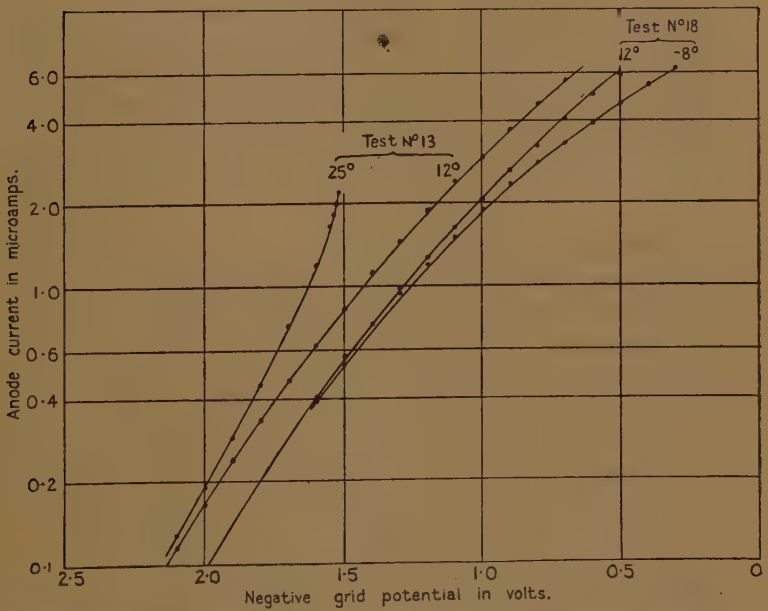

Pre-striking currents of BT 1 thyratron at 270 volts anode potential.

Fig. 7 must be considered in the light of the probable experimental accuracy of the readings. The first likely source of error is variation of vapour pressure during a set of readings, particularly at the higher temperature, where less time had been taken to attain steady conditions. Actually the thermometer reading often varied by half a degree, while of course the variation of average temperature inside the valve might be greater. A change of 1 degree corresponds to about 15 per cent. change in ρ. The valve-voltmeter accuracy varied from about 5 or 6 per cent. down to about 2 per cent. The poorer value

applies in fig. 7 to the current range between 0·6 and 1·0 microamps, where the resistance R_3 was changed from 2 megohms to 0·2 megohms and the sensitivity was small. The grid potential could be read as accurately as it can be plotted in the figure.

Fig. 8.

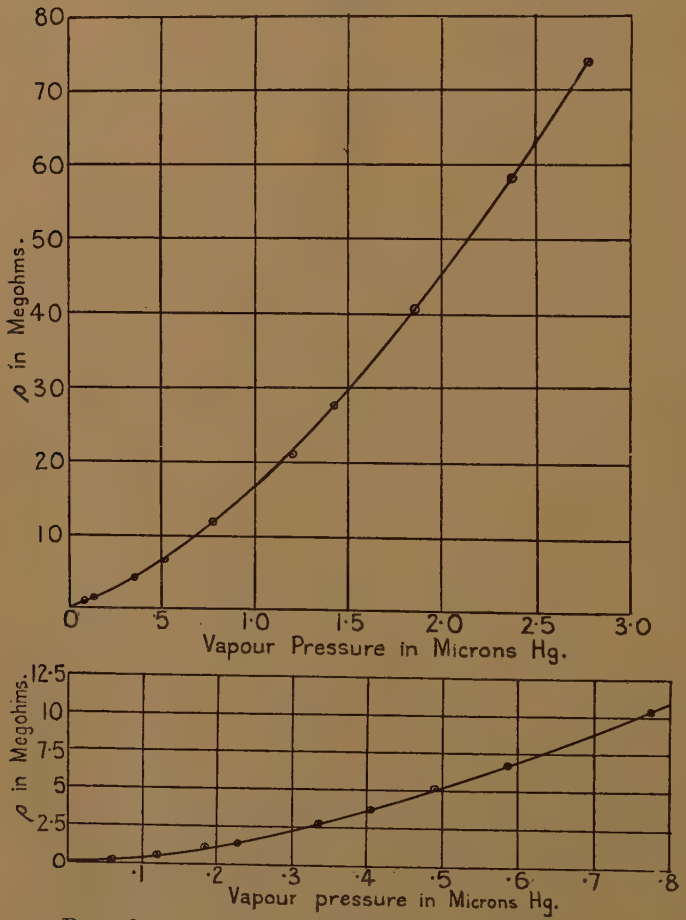

Dependence of "negative resistance due to ionization" on vapour pressure.

Variation of ρ with Vapour Pressure.

Each set of results gives the difference between two values of ρ. We had no method of measuring directly the average value of the vapour pressure in the ionizing

space of the valve. In fig. 8 therefore the measured differences of ρ are plotted as ordinate against "condensing vapour pressure," *i. e.*, the pressure given in Physical Tables as corresponding to the oil temperature. The fact that all the differences with one exception could be fitted on to a single curve is evidence that there was no great random discrepancy between the effective vapour pressure for ionization and the calculated condensing pressure; there may, however, be a systematic discrepancy, since presumably there is a greater temperature gradient the cooler the oil. We think nevertheless that the temperature difference across the walls of the glass bulb is comparatively small, and that, since ρ must be zero at zero vapour pressure, the origin of the curve cannot be far from that found by extrapolation as in the lower part of fig. 8. This particular point will, however, require further investigation.

Conclusion.

We are satisfied that the validity of equation (3) has been established for the BT 1 and BT 5 Mazda thyratrons. For other types of mercury-filled triode where the grid is an open spiral it will probably require modification. We have not yet, however, been able to obtain consistent pre-striking currents for tubes of this type, presumably due to the effect of charges on the glass bulb.

LVII. *On an Extension of Thévénin's Theorem.* By Hikosaburo Ataka, *Meidi College of Technology, Tobata, Japan* *.

THIS note deals with some properties of electrical circuits, consisting of any number of linear impedances and any number of generators of the same frequency, connected in any manner whatsoever.

Theorem.—A current $\dot{I}_m$ through any branch m (say) is equal to the sum of a current $\dot{I}_{m0}$ through the branch m when any branch n (say) is open-circuited, and a current $\dot{I}'_m$ through the branch m when an open-circuited E.M.F.

* Communicated by the Author.

$\dot{E}_{n0}$ acts in the branch n and all other E.M.F.'s in the circuit are replaced by their internal impedances.

If the theorem is expressed by the formula, then we shall have

$$\left.\begin{aligned} \dot{I}_m &= \dot{I}_{m0} + \dot{I}'_m, \\ \text{or} \quad \dot{I}_m &= \dot{I}_{m0} + \frac{\dot{E}_{n0}}{\dot{Z}_t} \end{aligned}\right\} \quad \ldots\ldots\ldots \quad (1)$$

where $\dot{Z}_t$ is the transfer impedance between the branch m and the branch n.

Proof.—The branches m and n are supposed to be drawn out of the circuit, then will be formed an active four-terminal circuit, as represented in fig. 1.

Fig. 1.

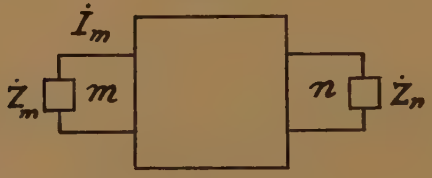

Fig. 2.

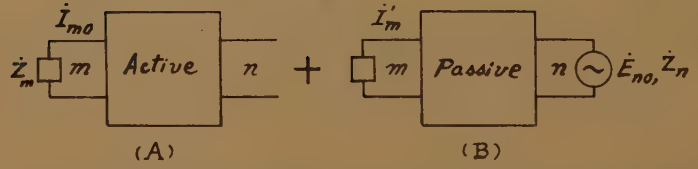

Let $\dot{Z}_m$ and $\dot{Z}_n$ be the impedances of the branches m and n respectively, and $\dot{E}_{n0}$ be the open-circuited E.M.F. of the branch n. Two E.M.F.'s are supposed to be placed oppositely in series in the branch n. Then by the principle of superposition the current $\dot{I}_m$ can be considered as being made up of two parts :

(A) A current $\dot{I}_{m0}$, when the branch n is open-circuited and all E.M.F.'s in the circuit are present ;

(B) A current $\dot{I}'_m$, when the E.M.F. $\dot{E}_{n0}$ is placed in the branch n and all other E.M.F.'s in the circuit are absent.

The conditions are shown diagrammatically in fig. 2.

In the case (B) all E.M.F.'s are absent in the rectangular frame, and it may be taken to be a passive four-terminal circuit. Denoting constants of the four-terminal circuit by $\dot{A}$, $\dot{B}$, $\dot{C}$, and $\dot{D}$, we have

$$\left.\begin{aligned}\dot{V}_1&=\dot{A}\dot{V}_2+\dot{B}\dot{I}_2,\\ \dot{I}_1&=\dot{C}\dot{V}_2+\dot{D}\dot{I}_2,\end{aligned}\right\},$$

where $\dot{V}_1$ and $\dot{I}_1$ are the voltage and the current at the branch m and $\dot{V}_2$ and $\dot{I}_2$ those at the branch n.

The transfer impedance between the branches m and n can easily be calculated :

$$\dot{Z}_t=\dot{C}\dot{Z}_m\dot{Z}_n+\dot{A}\dot{Z}_n+\dot{D}\dot{Z}_m+\dot{B} \quad . \quad . \quad . \quad . \quad (2)$$

Thus we have

$$\dot{I}_m=\dot{I}_{m0}+\frac{\dot{E}_{n0}}{\dot{Z}_t}.$$

The theorem which is expressed by (1) will be found to be an extension of Thévénin's theorem. Two special cases may be of some interest.

Case I. : $m=n$.

The four-terminal circuit will degenerate into a two-terminal circuit.

$$\left.\begin{aligned}\dot{I}_{m0}&=0,\\ \dot{C}\dot{Z}_n+\dot{D}&=1,\end{aligned}\right\} \quad . \quad . \quad . \quad . \quad . \quad (3)$$

and $$\dot{Z}_t=\dot{Z}m+\dot{A}\dot{Z}_n+\dot{B}=\dot{Z}_m+\dot{Z}_{m0}$$

where $\dot{Z}_{m0}$ is the impedance of the circuit, as considered at the branch m.

$$\dot{I}_m=\dot{I}_n=\frac{\dot{E}_{n0}}{\dot{Z}_m+\dot{Z}_{m0}} \quad . \quad . \quad . \quad . \quad . \quad . \quad (4)$$

Thévénin's Theorem.—A current through any branch is equal to a current through the same branch when an open-circuited E.M.F. acts in the same branch and all other E.M.F.'s are replaced by their internal impedances.

Case II. : $\dot{Z}_n \rightarrow \dot{Z}_n + \delta\dot{Z}_n$.

Let the impedance $\dot{Z}_n$ of the branch n be varied by an amount $\delta\dot{Z}_n$ and the variation of current $\dot{I}_m$ due to $\delta\dot{Z}_n$ be $\delta\dot{I}_m$.

From (1) and (2)

$$\dot{I}_m = \dot{I}_{m0} + \frac{\dot{E}_{n0}}{(\dot{C}\dot{Z}_m + \dot{A})\dot{Z}_n + (\dot{D}\dot{Z}_m + \dot{B})},$$

and

$$\dot{I}_m + \delta\dot{I}_m = \dot{I}_{m0} + \frac{\dot{E}_{m0}}{(\dot{C}\dot{Z}_m + \dot{A})(\dot{Z}_n + \delta\dot{Z}_n) + (\dot{D}\dot{Z}_m + \dot{B})}. \quad (5)$$

Hence we get

$$\delta\dot{I}_m = \frac{-\dot{E}_{n0}(\dot{C}\dot{Z}_m + \dot{A})\delta\dot{Z}_n}{\{(\dot{C}\dot{Z}_m + \dot{A})(\dot{Z}_n + \delta\dot{Z}_n) + \dot{D}\dot{Z}_n + \dot{B}\}\{(\dot{C}\dot{Z}_m + \dot{A})\dot{Z}_n + \dot{D}\dot{Z}_m + \dot{B}\}} \quad (6)$$

On the other hand, by Thévénin's theorem,

$$\dot{I}_n = \frac{\dot{E}_{n0}}{\dot{Z}_n + \dfrac{\dot{D}\dot{Z}_m + \dot{B}}{\dot{C}\dot{Z} + \dot{A}}} = \frac{\dot{E}_{n0}(\dot{C}\dot{Z}_m + \dot{A})}{(\dot{C}\dot{Z}_m + \dot{A})\dot{Z}_n + \dot{D}\dot{Z}_m + \dot{B}}. \quad (7)$$

Substituting (7) in (6), we get finally

$$\dot{I}_m = \frac{-\dot{I}_n\delta\dot{Z}_n}{(\dot{C}\dot{Z}_m + \dot{A})(\dot{Z}_n + \delta\dot{Z}_n) + (\dot{D}\dot{Z}_m + \dot{B})} = \frac{-\dot{I}_n\delta\dot{Z}_n}{\dot{Z}'_t}, \quad (8)$$

where $\dot{Z}'_t = (\dot{C}\dot{Z}_m + \dot{A})(\dot{Z}_n + \delta\dot{Z}_n) + (\dot{D}\dot{Z}_m + \dot{B})$,

and $\dot{Z}'_t$ is the transfer impedance between m and n in the modified circuit.

The equation (8) is expressed as follows :

Compensation theorem.—If the circuit is altered by making a change $\delta\dot{Z}_n$ in the impedance $\dot{Z}_n$ of a branch n (say), the change in the current $\delta\dot{I}_m$ in the branch m (say) is equal to that which would be produced by an E.M.F. $-\dot{I}_n\delta\dot{Z}_n$ acting in series with the modified branch where $\dot{I}_n$ is the current in the same branch.

Thus it will be found that Thévénin's theorem and the compensation theorem, which are treated hitherto almost independently, can be wholly covered by the extension of Thévénin's theorem.

LVIII. *Note on Numerical Valency in Polyatomic Molecules.* *By* H. Lessheim, *Lahore* (*India*), *and* R. Samuel, *Haifa* (*Palestine*) *.

I.

In his original paper on the number of valencies exhibited by the atoms of the various groups of the periodic table London [1] assumed all the higher states of valency of the free atoms to be brought about by excitation. The sulphur atom, to take this as an example, in its ground state ^3P is divalent, only two unpaired spin vectors being present in the electron configuration $3s^2 3p^4$; the tetravalent state is represented by the excited configuration $3s^2 3p^3 3d$, and hexavalency is said to obtain in the configuration $3s 3p^3 3d^2$. This is due to the condition of electron pairing, the essential feature of the Heitler-London pair bond theory of valency [2], which makes the unpairing of the electrons and the uncoupling of the spin vectors of the configuration $s^2 p^4$ indispensable for the exhibition of higher valencies. It is quite true that in the ^3P state two of the four p electrons form a complete λ group with neutralized spin and only two have parallel spin vectors. Nevertheless, in this publication it is intended to show that tetravalency obtains from the ground level without any excitation at all of the p electrons, and hexavalency by excitation of one of the s electrons to the p shell without invoking the d orbital. London's statement as to the numerical valency of unexcited atoms is necessary and valid only for diatomic molecules, while in polyatomic ones, when the field possesses more than one preferential direction, Pauli's exclusion principle imposes different rules and affords an enhanced number of possibilities for uncoupled spin vectors. This has not yet been considered in detail †. It is remarkable that indeed valencies higher than three are never exhibited in diatomic molecules, but are met with only in polyatomic ones. The activation of the $\dot{s}$ electrons by excitation remains of course necessary, and this has been

* Communicated by the Authors.

† This conception has already been made use of some time ago without detailed explanation, *cf.* reference (3).

supported experimentally likewise for di- and polyatomic molecules; but also in this case the d shell need not be invoked, and the sulphur atom in polyatomic molecules is hexavalent with an electron configuration $3s3p^5$. Hence there exists no exception for the atoms of the second period, which do not possess a low d shell, and in polyatomic molecules nitrogen, for instance, may exhibit pentavalency with an electron configuration $2s2p^4$. This is in accord with the experimental fact that nitrogen can display a decided penta-covalency, *e. g.*, in N_2O_5, in nitro compounds and in nitrates in the vapour state.

II.

It is sufficient to confine oneself here to a consideration of the s and p electrons. The d electrons of the transition elements, such as the atoms from Sc to Ni, are of secondary importance. The results obtained for p electrons are easily applicable to d electrons as well.

There is only one s orbital and three possible types of p orbitals, *i. e.*, $p\sigma$, $p\pi_+$, and $p\pi_-$. According to Pauli's principle the maximal population of any such orbital is two. The state of maximal valency is therefore obtained when an atom possesses one electron only in each of these four orbitals. It is capable of exhibiting tetravalency when each of these four unpaired spins is neutralized by coupling itself with an electron from another atom. Any increase in the number of electrons, *i. e.*, the introduction of additional ones into any of these orbitals, reduces the number of free valencies, because a second electron in an orbital will cancel the spin of the first one. But even the tetravalent configuration sp^3 belongs to an excited atom, the highest number of free valencies of an unexcited atom being three and belonging to the electron configuration s^2p^3 in ^4S. This mechanism is valid for diatomic molecules, and therefore the maximum number of valencies theoretically possible in diatomic molecules without previous excitation is three. At the same time this is the highest valency number which chemistry knows in individual diatomic molecules.

III.

It is well known that neither strict localization nor strict non-localization describes in an entirely accurate

manner the conditions prevailing in a polyatomic molecule. In such molecules, however, which possess a central atom like IF_7, IF_5, ICl_3, SO_2, $SOCl_2$, SO_2Cl_2, etc. for all practical purposes each bond can be considered as localized between the central atom and a particular one of the other partners. The non-localizing influence of a bond on another one linking a different atom to the same central atom is reduced to a simple screening effect. This is borne out by spectroscopical evidence. In SeO_2, *e.g.*, the harmonic valence vibration has almost exactly the same value as the vibrational frequency of SeO both in the excited and the unexcited states of these molecules, and the atomic energy of dissociation of SeO_2 is about twice that of SeO[4]. The same relation[5] prevails in SO_2 and SO, and the energy of the S=O bond remains constant even in $SOCl_2$. Again, that of the S—Cl bond is approximately equal in SCl_2 and $SOCl_2$, that of the Se—Cl bond in $SeCl_2$, Se_2Cl_2, $SeOCl_2$, and $SeCl_4$, and many other similar examples are available[6]. This could hardly be understood if, *e. g.*, the ground-level of SO involved an S atom in the s^2p^4 and that of SO_2 one in the s^2p^3d state.

IV.

In order to discuss the formation of a polyatomic molecule let us consider an atom A with four or five p electrons, such as S or Cl with the configuration s^2p^4 or s^2p^5 respectively. In its ground state two or one electron respectively will be unpaired and will be ready to undergo a linkage with a di- or a monovalent partner B, as the case may be. The remaining two or four electrons are paired in fully occupied orbitals, which may be called σ or π orbitals according to their relation to the molecule axis of AB. It must be distinctly understood that both the σ, π property of these electrons and a statement as to the parallelism or antiparallelism of their spins have a meaning only with respect to a definite axis.

A third atom C, which is divalent, but which may also be replaced by two monovalent atoms, may now approach the molecule AB. It is the fundamental idea of localization of the bonds that such an approach, though slightly modifying the energy of the existing bond AB, does not essentially alter the bond. With the exception of a screening effect those electrons which form the bonding pair or pairs between A and B remain undisturbed.

Not so, however, those electrons of A which, owing to pairing among themselves, did not take part in the linkage between A and B. Their σ, π property with respect to the axis AB is lost with respect to the axis AC, now created afresh on account of the approach of the third atom, and with respect to it they may or may not be paired. In those terms, in which they are paired—singlet terms—AB repels C and no new combination is formed, whereas in the triplet terms arising from the same combination two free valencies are offered to C and a new molecule BAC is formed. If there is still a pair of p electrons left or, more correctly expressed, such a pair of electrons which on adiabatic dissociation will become p electrons of the A atom, the process may be repeated with yet another divalent atom D. After all those electrons have been used up only the s electrons are available to form additional bonds. The two s electrons form a closed shell of spherical symmetry, *i. e.*, with respect to any axis, and thus have a repulsive effect on any atom that may approach them. Therefore in this case one or both of them must be excited to p orbitals, or rather to orbitals which will become p orbitals of A on adiabatic dissociation. After this also they may be employed to link one more divalent atom to A. An excitation to the d orbital is not necessary.

This procedure, though extremely plausible in itself, appears at the first glance like a violation of Pauli's principle. It seems as if by and by more groups of p electrons are created than are admissible, and that, *e. g.*, in a molecule like IF_7 a set of 14 p electrons is accommodated in one shell. It can, however, be seen that this is indeed not so.

Firstly, there are no p electrons in the molecule ; the l property is already lost on formation of the first link AB, and only a λ property remains. At the same time the number of orbitals is doubled in accordance with Pauli's principle, the number of orbitals in the outside shell of the molecule AB—and it is only this that we are interested in—being equal to the sum of the numbers of outside orbitals of A and B. Again, the λ property is lost when C is attached to AB, and again the number of possible orbitals is increased, Finally, when the poly-atomic molecule is completed, its wave-function will exhibit a certain symmetry property which corresponds

to the geometric configuration of the molecule and is such as leaves room for exactly as many electrons as would be present if all the constituents were rare gas atoms, which is at least eight more than the number of electrons actually present in the shell. This is, of course, the same whether the bonds are localized or not, but the description in terms of localized pair bonds facilitates the consideration in so far as the discussions of the various linkages can be separated from each other, and in the discussion of each internuclear connexion the electrons particularly concerned can be described by means of a λ symmetry, while all the others can be considered as not quantized at all.

This may be described in a simple way considering a particular case. An S atom, as stated above, has four outside p electrons. The ground state ^{3}P indicates that two of these p electrons are paired with one another, while the two remaining ones have parallel spins. Thus the S atom is initially divalent and can undergo a double bond, *e. g.*, with an oxygen atom, whose ground state is also ^{3}P. The resulting SO molecule has singlet, triplet, and quintet terms. The singlet terms belong to a saturated SO molecule, which is incapable of contracting any further linkages, all the remaining electrons being paired among themselves with respect to the axis of reference. The triplet terms correspond to states in which two former p electrons are not paired with respect to the axis, and in particular the ground state of the SO molecule is a certain $^3\Sigma$ term, in which the two electrons with now parallel spins belonged formerly to the S atom. Those triplet terms in which former O electrons play this part and the quintet terms in which this is the case with both the O electrons and S electrons, are higher excited and are of no interest for the present consideration. Thus the ground-level of SO is $^3\Sigma$, which exhibits now *a posteriori* two more free valencies, although it is correlated to the ground state of S, which is initially divalent and whose two free valencies have been saturated by an O atom. In this way SO_2 may be formed without any excitation of the S atom. For the last two valencies excitation is indispensable. The only valence electrons left with the S atom in a molecule like SO_2 are the two which originally have formed the group $3s^2$. This closed shell has a repulsive effect in any direction, and only after it is

Group of the periodic table.	Configuration of electrons.	Numerical valency.	Remarks.	Examples.
I. (Li, Na, etc.) Sub-group (Cu, Ag, Au)	s $d^{10}s$	1 1, 2, 3	The s-electron produces monovalency. The atoms of the sub-group with low d-terms can exhibit higher valencies on excitation of a d-electron.	LiF, LiC_2H_5.
II. (Be, Mg, ... Zn, Cd, etc.)	s^2 sp } p^2 }	0 2	The two electrons are chemically inert as long as they form a closed s shell; by excitation two free valencies are created.	BeO, $Zn(C_2H_5)_2$.
III. (B, Al, etc.)	s^2p sp^2	1 3	. . . .	TlCl. $AlCl_3$, $Tl(C_2H_5)_3$.

IV. (C, Si, etc.)	s^2p^2 sp^3 p_4	2 4 2(+2)	"Tetrahedral" configuration. *A priori* two valencies only; but after these two are saturated, two more valencies can be exhibited *a posteriori*.	CO, $SnCl_2$, $Sn(C_2H_5)_2$. CCl_4, $SnCl_4$, $Sn(C_2H_5)_4$. =CO (carbonyl), CO_2.
V. (N, P, etc.)	s^2p^3	3 (+2)	The configuration $s^2p^3\ ^4S$ gives trivalency only. When the s^2 group is fissured, after the first three valencies have been saturated, two valencies become available.	NCl^3, nitroso-compounds. N_2O_5, nitro-compounds.
VI. (O, S, etc.).	sp^5	2 (+2+2)	After the two valencies have been saturated, two additional ones are liberated *a posteriori*; after also these have been saturated fissure of the *s*-shell produces another two more valencies, bringing the total to six.	SO, $SeCl_2$, $TeCl_2$. SO_2, $SeCl_4$, $TeCl_4$. SO_3, SF_6.
VII. (F, Cl, etc.)	s^2p^5	1 (+2+2+2)	After the single valency has been saturated two additional ones becomes available *a posteriori*, making a total of three. These also having been saturated, again two more valencies appear. After all these five have been saturated the s^2 group may undergo fissure, thus bringing about a total of seven valencies.	ICl, KO—Cl. ICl_3, KO—Cl=O. IF_5, KO—ClO_2. IF_7, KO—ClO_3.

fissured the two electrons become unpaired and available for chemical reactions. If one of them is excited to an orbital of the molecule which on adiabatic dissociation would become a p orbit of the S atom, two more free valencies are produced, which then may link two monovalent atoms as in SO_2Cl_2, or one divalent one as in SO_3.

V.

In the preceding table the possible numerical valencies for atoms with normal configurations are summarized. In the last column examples are given which establish those results as experimental facts. Although there is no fundamental difference between electrovalent and covalent molecules as far as numerical valency is concerned[7], care was taken to add also such molecules as from measurements of conductivity, boiling-point, etc. are obviously covalent. Not all the valency states possible have been obtained for every atom of the respective groups. Numerical valency indicates the possibility of formation of a molecule; whether or not it is actually formed depends on energetic considerations, *i. e.*, on whether the molecule in question or another combination of the same constituent atoms (*e. g.*, the elementary molecules) represent the lower state of energy.

VI.

The above considerations are confirmed not only by the examples of molecule formation as shown in the last column of the table but also by an experimental fact which, although it is well known, has escaped attention in this connexion. Every atom in its ground state and—as far as the first four groups of the periodic system are concerned—in certain excited states has one and only one definite numerical valency for combination with a single other partner, which is identical with the number of unpaired electrons in that particular state. Only after these valencies are saturated further bonds become available in pairs, which then are attached either to divalent or pairs of monovalent atoms, and the higher valency numbers appear only as the sum of several valencies exhibited in separate links. This will become clearer from an example.

The chlorine atom has two s electrons and five p electrons in its outer shell. The maximum valency is therefore seven, but, on account of the electron pairing on the s and two of the three p orbits, only one p electron remains unpaired and ready to form a bond. Therefore ordinarily chlorine is monovalent. Thus, *e. g.*, KO—Cl is formed. If further valencies are exhibited, they are naturally developed in pairs, because they are due to a pair of electrons being fissured, but the remarkable fact about it is that each of these pairs undergoes linkages to separate partners. Thus

$$KO{-}Cl{=}O,\quad KO{-}Cl\begin{matrix}=O\\=O\end{matrix},\quad KO{-}Cl\begin{matrix}=O\\=O\\=O\end{matrix}$$

are obtained, but combinations like

$$KO{-}Cl\begin{matrix}\equiv N\\=N\end{matrix},\quad N{\equiv}Cl,\quad N{\equiv}Cl{=}O,\quad Cl{-}S{\equiv}N$$

are not formed, although they do not contradict the simple valency rules. Of course when an atom like N is trivalent and another one like Al or C can become tri- or tetravalent on excitation there is no reason why they should not form AlN or —CN. But Cl, *e. g.*, is not trivalent, but exclusively monovalent. Only after this single valency is saturated, *e. g.*, with a KO— group, two more valencies may become available in directions different from the direction of the first valency, and may be attached to an oxygen atom (KO—Cl=O); but it is impossible to form molecules like N≡Cl, because no three valencies of chlorine are ever available at the same time.

On the other hand, a theory which assumes that the pairs of p electrons undergo a fissure by previous excitation to the d shell necessarily fails to explain the non-occurrence of those combinations.

VII.

In addition to the above confirmation of the present view by chemical evidence further corroboration is forthcoming by spectroscopical evidence. We have

already mentioned that in diatomic molecules the highest number of valencies attained by atoms with normal electron configuration is three, as in N_2, three being one half of the maximal population of the p shell. It is also significant that the radical CN appears to contain only a double bond in its ground state according to the configuration s^2p^2 of unexcited C. The chemical formula therefore is C=N—, *i. e.*, the isonitrile radical. The radical —C≡N forms apparently an excited level of C=N—, because only in the excited configuration sp^3 the carbon atom is tetravalent. For the isoelectronic N_2^+ the configuration corresponding to the formula N^+=N— has been made probable from band spectra, and it was also shown that the unpaired electron belongs essentially to the neutral N atom[8]. The splitting of the s^2 shell for the purpose of obtaining free valencies has been established by the band spectra of the oxides and halides of the atoms of the second group[9]. For polyatomic molecules it finds its experimental expression in the fact that the photo-dissociation process follows directly the energy difference between the atomic energies of formation of the molecule with maximal valency of the central atom and that of the next lower valency state. Thus the beginning of continuous absorption of SO_3 agrees with the value of $D(SO_3)$–$D(SO_2)$; the molecule is broken up by excitation from the stable ground-level of SO_3 to the excited repulsive level SO_2 (singlet term)+O(^{3}P). In SO_2, however, the energy of the S=O bond is exactly similar to that in SO, and the photo-dissociation of such molecules, whose central atom is in a lower state of valency, follows therefore the bond energies. This has been discussed elsewhere at greater length[10].

VIII.

In conclusion, attention may be drawn to the following significant fact. The ground-level of a molecule like SO_3 or SO_2Cl_2 involves an excited S atom, and therefore its adiabatic dissociation leads to a level considerably higher than that of the unexcited constituent atoms. The bond energies are in general only slightly increased, and although the ground-level of SO_3 or SO_2Cl_2 lies lower than that of SO_2, the energy differences $D(SO_3)-D(SO_2)$ or $D(SO_2Cl_2)-D(SO_2)$ are considerably smaller than

$D(SO_2)-D(SO)$, because the adiabatic formation of the molecules SO_3 and SO_2Cl_2 begins at an excited level of the system, and therefore does not reach such a low level as it would otherwise. The rupture of the bonds, however, will not follow the course of adiabatic dissociation, but is already obtained when the comparatively low singlet level of SO_2 is reached. Thus chemical reaction produces the impression that the bonds of the atoms added last, as, *e. g.*, the two last Cl atoms in PCl_5, are bound with less energy. In reality their bond energy is rather increased, but the reaction does not break up the bonds adiabatically. It appears that these circumstances are responsible for the introduction of conceptions like the semipolar double bond or the singlet link, which essentially mean a second variety of covalent linkage with decreased bond energy. The true explanation, however, of the apparently weakened bond has to be found in the fact that the ground state of a polyatomic molecule, in which the central atom exhibits its maximal valency, is adiabatically correlated to an excited level of the constituent molecule of lower valency state, while decomposition concerns the ground-level of that molecule. This has been discussed at greater length elsewhere [10].

References.

(1) F. London, *Zeits. f. Phys.* xlvi. p. 455 (1928).
(2) *Cf.* the report of J. H. Van Vleck and A. Sherman, Rev. of Mod. Phys. vii. p. 168 (1935), and the literature quoted there.
(3) H. Lessheim and R. Samuel, Proc. Ind. Ac. Sci. (Bangalore), i. p. 623 (1935), particularly Section XIV.
(4) R. K. Asundi, Mohd Jan Khan, and R. Samuel, 'Nature,' cxxxvi. p. 642 (1935); Proc. Roy. Soc. A, clvii. p. 28 (1936).
(5) R. K. Asundi and R. Samuel, Proc. Ind. Ac. Sci. (Bangalore), ii. p. 30 (1935).
(6) *Cf.* R. K. Asundi and R. Samuel, Proc. Phys. Soc. (Lond.), xlviii. p. 28 (1936); R. Samuel and Mohd Jan Khan, *ibid.* xlviii. p. 626 (1936); R. Samuel and S. L. Hussain, *ibid.* xlix. p. 679 (1937); Y. P. Parti and R. Samuel, *ibid.* xlix. p. 568 (1937).
(7) *Cf.* ref. (3) or R. F. Hunter and R. Samuel, Chem. and Ind. p. 733 (1936), and literature mentioned there.
(8) R. K. Asundi and R. Samuel, Proc. Ind. Ac. Sci. (Bangalore).
(9) H. Lessheim and R. Samuel, Phil. Mag. xxi. p. 41 (1936).
(10) R. Samuel, Proc. Ind. Ac. Sci. (Bangalore), vi. p. 257 (1937).

The University Chemical Laboratory, Lahore.
The Hebrew Technical Institute, Haifa.
July 1937.

LIX. *Remarks on the more Accurate Calculation of the Deflexion of Beams and Struts.* *By* Th. Pöschl, *Karlsruhe* *.

REGARDING the paper of Mr. H. H. Jeffcott on the same subject published in the 'Philosophical Magazine' (7) xiii. pp. 310–322 (1932), I will only give here some short remarks for a possible simplification of the calculation. Firstly, the praxis shows in many cases that the expansion of the solution in series after a parameter can often be more clearly arranged as the successive-approximation-method of Picard, used in the paper mentioned. Then for the more accurate calculation of elastic problems of this kind it seems to be more advantageous to take as independent variable the arc-lengths of the neutral axis of the beam, and not the abscissa x; for in the deflected state the length of the beam is given, and not the position of its ends. By this modification the curvature is

$$\frac{1}{\rho}=\frac{\ddot{y}}{\sqrt{1-\dot{y}^2}} \quad . \quad . \quad . \quad . \quad . \quad . \quad (1)$$

(a dot signifies differentiation with respect to s). The results follow then more directly.

I will restrict myself here to the solution of the two examples treated by Mr. Jeffcott (in reversed order), the notations being nearly the same as in his paper. I intend to publish some more examples on elastic stability and on other related subjects elsewhere.

1. A long, thin, straight beam AB is clamped horizontally at one end B, and subjected to a single vertical load P at the other end A, the weight of the beam being negligible. Take axes of x and y horizontally and vertically through the loaded end A of the beam, x_B, y_B being the coordinates of the clamped end B. Let, further, s be the length of the arc of the neutral axis from the origin A to the point x, y, and let the whole length of the beam be l.

* Communicated by the Author.

The bending moment at the point x, y is Px, and accordingly the form of the neutral axis is given by

$$\frac{1}{\rho} \equiv \frac{\ddot{y}}{\sqrt{1-\dot{y}^2}} = -\frac{Px}{EI} = -\mu x, \quad \ldots \quad (2)$$

if $\mu = P/EI$.

We must differentiate the equation (2) eliminating x, and find

$$\frac{\dddot{y}}{\sqrt{1-\dot{y}^2}} + \frac{\dot{y}\ddot{y}^2}{\sqrt{1-\dot{y}^2}^3} = -\mu \frac{dx}{ds} = -\mu\sqrt{1-\dot{y}^2},$$

or approximately

$$\dddot{y} = -\mu(1-\dot{y}^2) - \dot{y}\ddot{y}^2(1+\dot{y}^2+\ldots). \quad \ldots \quad (3)$$

For integration of this equation we may put

$$y(s) = \mu y_1(s) + \mu^3 y_3(s) + \ldots, \quad \ldots \quad (4)$$

where $y_1(s)$, $y_2(2)$, ... are unknown functions. Putting this series in equation (3) we get, by comparing the successive powers of μ, exactly as many equations as functions $y_i(s)$ were introduced.

The members with μ give

$$\dddot{y}_1 = -1, \quad \ldots \quad (5)$$

and by integration with the conditions at the ends,

$$\begin{cases} y = \ddot{y} = 0, & \text{for } s = 0, \\ \dot{y} = 0, & \text{for } s = l, \end{cases}$$

we obtain

$$y_1(s) = \frac{l^2 s}{2} - \frac{s^3}{6}. \quad \ldots \quad (6)$$

For $s = l$ we have

$$y_1(l) = \frac{l^3}{3}, \quad \text{therefore } y_B = \mu y_1(l) = \frac{Pl^3}{3EI}. \quad \ldots \quad (7)$$

The members with μ^3 give the equation

$$\dddot{y}_3 = \dot{y}_1^2 - \dot{y}_1\ddot{y}_1^2, \quad \ldots \quad (8)$$

and putting in this y_1 as found before we have

$$\ddot{y}_3 = \tfrac{1}{4}(l^4 - 4l^2s^2 + 3s^4).$$

By integration under the same conditions at the ends as before we obtain

$$y_3(s) = \frac{1}{4}\left(\frac{l^4 s^3}{6} - \frac{l^2 s^5}{15} + \frac{s^7}{75}\right) - \frac{l^6 s}{15}. \quad \ldots \quad (9)$$

Finally we find y by equation (4), and especially for the coordinates of the clamped end B :

$$\left.\begin{aligned} y_B &= \frac{Pl^3}{3EI} - \frac{4}{105}\frac{P^3l^7}{E^2I^3} + \dots, \\ x_B &= l - \frac{1}{15}\frac{P^2l^5}{E^2I^2} + \dots . \end{aligned}\right\} \quad . \quad . \quad . \quad (10)$$

In the paper mentioned y_B shall be found by eliminating x between the two equations for y and s. The result is the same.

2. The other example is in common sense a "propre-value-problem." A long, thin, straight rod AB clamped vertically at its lower end A is subjected to a vertical load P at its upper, free end B. It is required to study the deflexion of the rod, its weight being negligible. Take axes of x and y vertically and horizontally through the lower end A of the rod as origin, and let x_B and y_B be the coordinates of the upper or free end B. Let s be the length measured along the neutral axis of the rod from the origin A to the point x, y, and let the whole length of the rod be l.

The bending moment at the point x, y is $-P\,(f-y)$, $f \equiv y_B$ being the unknown deflexion of the upper end B. The form of the neutral axis in its deflected state is defined by

$$\frac{1}{\rho} \equiv \frac{\ddot{y}}{\sqrt{1-\dot{y}^2}} = \frac{P(f-y)}{EI} = k^2(f-y), \quad \left(\frac{P}{EI} = k^2\right), \quad (11)$$

or approximately by

$$\ddot{y} = k^2(f-y)(1-\tfrac{1}{2}\dot{y}^2+\dots). \quad . \quad . \quad . \quad (12)$$

We solve this equation putting

$$y(s) = fy_1(s) + f^3y_3(s) + \dots . \quad . \quad . \quad . \quad (13)$$

f is first an arbitrary parameter, we may take for it immediately the deflexion at the upper end.

Putting in equation (12) for y the form (13), we get for the members with f

$$\ddot{y}_1 + k^2y_1 = k^2, \quad . \quad . \quad . \quad . \quad . \quad . \quad (14)$$

with the solution

$$y_1(s) = 1 - \cos ks, \quad . \quad . \quad . \quad . \quad . \quad (15)$$

satisfying the end-conditions

$$y=\dot{y}=0, \quad \text{for } s=0.$$

The geometrical condition for the free end $s=l$ being

$$f=y_1(l)=f(1-\cos kl)$$

can only be satisfied by putting

$$kl=\frac{\pi}{2}, \quad \text{or } \mathrm{P}\equiv\mathrm{P_E}=\frac{\pi^2\mathrm{EI}}{4l^2}; \quad . \quad . \quad . \quad (16)$$

this is the Eulerian load in the case treated; the deflexion f remains indeterminate.

The members with f^3 in equation (12) give

$$\ddot{y}_3=k^2y_3=-\frac{k^2}{2}(1-y_1)\dot{y}_1{}^2=-\frac{k^4}{2}\sin^2 ks\cos ks; \quad (17)$$

the solution of this equation with the same conditions as above $y=\dot{y}=0$ for $s=0$ is

$$y_3(s)=-\frac{k^2}{8}\sin ks\left\{\frac{ks}{2}-\frac{\sin 2ks}{4}\right\}, \quad . \quad . \quad (18)$$

and therefore is the complete solution corresponding to the first two members in (13):

$$y(s)=f(1-\cos ks)-f^3\frac{k^2}{32}\sin ks\{2ks-\sin 2ks\}. \quad (19)$$

Satisfying the geometrical condition $y=f$ for $s=l$, we get

$$\frac{f^2}{l^2}=-\frac{32\cos kl}{k^2l^2\{2kl-\sin 2kl\}}. \quad . \quad . \quad . \quad . \quad (20)$$

The denominator is always positive, the numerator only if $kl>\pi/2$. If therefore $kl\leqq\pi/2$, the load P thus under the Eulerian load, we have the unique solution $f\equiv 0$: in this case the straight line is the sole equilibrium-form of the rod. If, on the contrary, $kl>\pi/2$, the deflexion of the free end is given by (19).

Assuming that P exceeds the Eulerian load $\mathrm{P_E}$ only by a small amount, we may put

$$kl=\frac{\pi}{2}+\xi.$$

Considering then ξ as a small quantity, putting this in equation (20), expanding the trigonometrical functions,

and retaining only the members of the first order, we get, finally,

$$\frac{f}{l}=\frac{8}{\pi}\sqrt{\sqrt{\frac{P}{P_E}}-1}, \quad . \quad . \quad . \quad . \quad (21)$$

an approximate formulæ for calculating the deflexion of the free end.

LX. *Magnetism and the Vibratory Electron.* *By* E. Taylor Jones, *D.Sc., Professor of Natural Philosophy in the University of Glasgow* *.

IT has been shown in two recent papers † that in a great many electrostatic systems the mutual energy of the parts, and the electrostatic forces between them, can be accounted for on the assumption that the electrons of which their charges are composed form systems of coupled vibrators, difference of phase of their vibrations corresponding to difference of sign of their charges. In a third paper ‡ this vibrational theory of the electron was shown to lead very naturally to a theory of the photon, a particle which when moving freely possesses energy only when moving with the velocity of light, and has also other properties identical with those well known to be possessed by light.

In the present communication the question will be considered whether the magnetic forces between moving electrons can be accounted for in a similar way, *i. e.*, by assuming that the common frequency of two coupled electrons depends not only upon the distance between them, but also upon their velocities. In accordance with this assumption, the equations for the vibratory movement of two electrons in presence of each other must be supposed to contain terms the coefficients of which depend upon the translational velocities of the electrons and may be called the " magnetic coupling " between them. Bearing in mind the close relationship which exists between

* Communicated by the Author.
† Phil. Mag. xxi. p. 337, and xxii. p. 921 (1936).
‡ Phil. Mag. xxiv. p. 458 (1937).

electrical and magnetic effects, we shall further suppose that the magnetic terms are, as in electrostatics, proportional to the displacements rather than to the accelerations in the vibratory movements *.

We have already found † that for two stationary electrons of similar kind at distance r apart the square of the periodicity $n^2(=4\pi^2\nu^2)$ is given by

$$n^2=a+b, \quad . \quad . \quad . \quad . \quad . \quad . \quad . \quad (1)$$

a being the value of $n^2(=4\pi^2\nu_0{}^2)$ for a single electron far removed from other electrons, and b the electrostatic coupling k/r. If the two electrons are moving with uniform velocity v in the same direction at right angles to the line joining them, the value of n^2 will be affected in two ways by this motion, viz. :—(1) to a stationary observer the frequency will be increased by the motion, (2) the frequency will be diminished in consequence of the magnetic coupling between the electrons. The magnetic coupling being represented by $-b'v^2$, the equation for n^2 now becomes

$$n^2=\frac{a+b}{1-v^2/c^2}-b'v^2, \quad . \quad . \quad . \quad . \quad . \quad (2)$$

the magnetic term in which, $-b'v^2$, changes sign with reversal of the direction of motion and also with change of kind of one of the electrons. Hence

$$n=\sqrt{\frac{a}{1-v^2/c^2}}\left\{1+\frac{b}{a}-\frac{b'v^2(1-v^2/c^2)}{a}\right\}^{1/2}. \quad (3)$$

Now $v^2\left(1-\frac{v^2}{c^2}\right)$ cannot be greater than $c^2/4$, and at moderate or great distances b and b' will be small in comparison with the large quantity a ‡. Approximately therefore, at such distances,

$$n=2\pi\nu$$

$$=\sqrt{\frac{a}{1-v^2/c^2}}+\frac{b}{2\sqrt{a}}\frac{1}{\sqrt{1-v^2/c^2}}-\frac{b'v^2\sqrt{1-v^2/c^2}}{2\sqrt{a}} \quad . \quad . \quad (4)$$

* See *loc. cit.* p. 338.
† *Loc. cit.* p. 339.
‡ The value of a is $6{\cdot}07.10^{41}$ sec.$^{-2}$.

If the electrons were infinitely far apart b and b' would be zero, and the value of n would be

$$n_1 = 2\pi\nu_1 = \sqrt{\frac{a}{1-v^2/c^2}} \quad . \quad . \quad . \quad . \quad . \quad (5)$$

Consequently their mutual energy at distance r is

$$2h(\nu-\nu_1) = \frac{hb}{2\pi\sqrt{a}} \frac{1}{\sqrt{1-v^2/c^2}} - \frac{hb'v^2\sqrt{1-v^2/c^2}}{2\pi\sqrt{a}}, \quad (6)$$

the first term representing the electrical, the second the magnetic energy. Since $b = k/r$ and $e^2 = hk/2\pi\sqrt{a}$, the first term in the expression (6) agrees with the value $e^2/r\sqrt{1-v^2/c^2}$ given by electromagnetic theory for the mutual electrical energy of two moving charged particles.

Also according to electromagnetic theory the magnetic attraction of the two moving electrons is $e^2v^2/r^2c^2\sqrt{1-v^2/c^2}$, corresponding to the value $-e^2v^2/rc^2\sqrt{1-v^2/c^2}$ * for their mutual magnetic energy. Equating this expression to the second term in (6) we find for the magnetic coupling at moderate or great distances

$$b'v^2 = \frac{bv^2/c^2}{1-v^2/c^2} \quad . \quad . \quad . \quad . \quad . \quad . \quad . \quad (7)$$

The complete expression for the energy of two similar electrons moving abreast with velocity v at a moderate or great distance apart is therefore

$$2h\nu = \frac{h}{\pi}\sqrt{\frac{a}{1-v^2/c^2}} + \frac{hb}{2\pi\sqrt{a}}\sqrt{1-v^2/c^2} \quad . \quad . \quad . \quad (8)$$

If the two electrons are moving with different speeds and in different directions their common frequency is to be found from the group formula given in a former paper †, viz :—

$$n^2 = \frac{a_1+a_2}{2} + \tfrac{1}{2}\sqrt{(a_1-a_2)^2+4b_1b_2}, \quad . \quad . \quad . \quad (9)$$

where a_1, a_2 are the values of n^2 for the two electrons when uncoupled ($b=0$), and b_1, b_2 are the values of the coupling (electrical and magnetic) of the second electron

* This expression for the mutual magnetic energy is equivalent to $-Aev/c$, where A is the vector potential due to one of the moving particles in the position of the other, and e is the charge of each in electrostatic units.

† *Loc. cit.* p. 923.

on the first, and the first on the second, respectively. Thus

$$a_1=\frac{a}{1-v_1^2/c^2},\quad a_2=\frac{a}{1-v_2^2/c^2},\quad .\quad .\quad . \quad (10)$$

and b_1, b_2 are to be found, if possible, from known facts regarding the action of one moving electron upon another. If the velocities v_1, v_2 are in the same plane through r, and the angles which their directions make with that of r are θ and θ' respectively, an apparently suitable value for b_2, suggested by electromagnetic theory and by the special case in which v_1 and v_2 are equal and parallel, is

$$b_2=b.\frac{\sqrt{1-v_1^2/c^2}}{(1-v_1^2\sin^2\theta/c^2)^{3/2}}-\frac{bv_1v_2\sin\theta/c^2}{(1-v_1^2/c^2)^{1/2}(1-v_1^2\sin^2\theta/c^2)^{1/2}},$$

$$.\quad .\quad . \quad (11)$$

the first term representing the electrical, the second the magnetic, coupling. The value of b_1 is found from (11) by interchanging v_1 and v_2 and substituting θ' for θ. The very complicated expression for n^2 derived by substituting for b_1 and b_2 in (9) becomes much simplified if $v_1=v_2=v$ and $\theta'=\theta$, that is, if the two electrons are moving with the same velocity in parallel directions but not necessarily at right angles to the line joining them. In this case we have

$$\left.\begin{aligned} a_1=a_2&=\frac{a}{1-v^2/c^2}\\ b_2=b_1&=b\frac{\sqrt{1-v^2/c^2}}{(1-v^2\sin^2\theta/c^2)^{3/2}}-\frac{bv^2\sin\theta/c^2}{(1-v^2/c^2)^{1/2}(1-v^2\sin^2\theta/c^2)^{1/2}}\end{aligned}\right\},$$

$$.\quad .\quad . \quad (12)$$

and

$$n^2=\frac{a}{1-v^2/c^2}+b_1.\quad .\quad .\quad .\quad .\quad .\quad .\quad (13)$$

If, further, $\theta=\pi/2$, the expression for n^2 becomes

$$n^2=\frac{a+b-bv^2/c^2}{1-v^2/c^2}$$

in agreement with (2) and (7).

Finally, if v_1 and v_2 are not in the same plane through the line joining the two electrons, the value of v_1 in the expressions for b_1 and b_2 is to be taken as the component of v_1 in the plane containing r and v_2, and the value of v_2

as the component of v_2 in the plane of r and v_1: also, if the two electrons are of different kinds the sign before b in all the above expressions, and the sign before the square root in (9), must be changed.

As an application of the above formulæ we shall consider a problem which leads to an expression for the magnetic moment of a system containing revolving electrons in terms of the vibrational coefficients. A system suitable for this purpose is that consisting of two pairs of electrons revolving, at diametrically opposite points, in coaxial circles about central fixed positive charges (fig. 1). The central particles will be taken as each consisting of two positive electrons within the critical distance r_0 of each other, so that the pair at each centre have the limiting

Fig. 1.

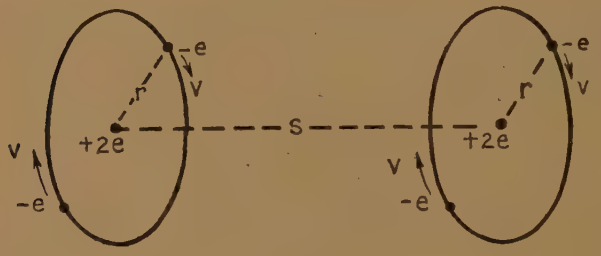

coupling a and do not repel each other. The radii of the circles in which the negative electrons revolve being each r, the velocity of each electron v, the distance between the planes of the circles being s, and the two pairs of electrons being on parallel diameters (*i. e.*, in the same phase in their revolutions), the system may clearly be divided into two groups for the purpose of applying the formula (9) for the common frequency of the whole. The four central electrons being taken as group I., the four revolving electrons as group II., we have

$$\left.\begin{aligned} a_1 &= 2a+2k/s, \\ a_2 &= \frac{a+k/2r+k/s+k/y}{1-v^2/c^2}+(b'-b''+b''')v^2, \end{aligned}\right\} \quad . \quad (14)$$

$$\left.\begin{aligned} b_1 &= \frac{2k/r+2k/x}{1-v^2/c^2}, \\ b_2 &= 2k/r+2k/x, \end{aligned}\right\} \quad . \quad . \quad . \quad . \quad (15)$$

where
$$x=\sqrt{s^2+r^2},$$
$$y=\sqrt{s^2+4r^2},$$

and $b'v^2$, $b''v^2$, $b'''v^2$, are the magnetic couplings of two electrons (each moving with velocity v at right angles to the line joining them) at distances $2r$, s, and y respectively. We shall now suppose that the radii of the two orbits are so small in comparison with the distance between them that higher powers than the square of r/s may be neglected. The second and third magnetic terms in a_2 therefore become, on substitution from (9),

$$-b''v^2+b'''v^2=-\left(\frac{k}{s}-\frac{k}{y}\right)\frac{v^2/c^2}{1-v^2/c^2}$$
$$=-\frac{2kr^2}{s^3}\cdot\frac{v^2/c^2}{1-v^2/c^2}$$
$$=-Bv^2, \text{ say.} \quad . \quad . \quad . \quad . \quad . \quad . \quad (16)$$

We shall further suppose that the radius r of each orbit is large in comparison with the critical distance $r_0(=k/a)$, so that quantities of the order k^2/a^2r^2 may be neglected. In these circumstances it is clear from (14) and (15) that the quantity $4b_1b_2$ is small in comparison with $(a_1-a_2)^2$. Now by the group formula (9), when this is the case, and $a_1>a_2$, the expression for n^2 becomes

$$n^2=a_2-\frac{b_1b_2}{a_1-a_2}, \quad . \quad . \quad . \quad . \quad . \quad . \quad (17)$$

so that, to the order of magnitude stated, we have

$$n^2-a_2=0. \quad . \quad . \quad . \quad . \quad . \quad . \quad . \quad (18)$$

Hence, by (14),

$$n^2=\frac{a+k/2r+k/s+k/y}{1-v^2/c^2}+b'v^2-Bv^2. \quad . \quad . \quad (19)$$

In this expression for n^2 the first term $a/(1-v^2/c^2)$ is much greater than the others, and therefore,

$$n=\frac{\sqrt{a}+\frac{k}{\sqrt{a}}\left(\frac{1}{4r}+\frac{1}{2s}+\frac{1}{2y}\right)}{1-v^2/c^2}+\frac{b'v^2}{2\sqrt{a}}-\frac{Bv^2}{2\sqrt{a}}. \quad (20)$$
$$=2\pi\nu,$$

where ν is the common frequency of all the eight electrons,

If s is infinite the terms containing the factors $1/s$, $1/y$ and B all vanish and we have

$$n_1=2\pi\nu_1=\frac{\sqrt{a}+k/4r\sqrt{a}}{\sqrt{1-v^2/c^2}}+\frac{b'v^2}{2\sqrt{a}}. \quad . \quad . \quad (21)$$

Consequently the mutual energy of the two revolving systems, if all the electrons are oscillating with the frequency ν, is

$$8h(\nu-\nu_1)=\frac{2hk}{\pi\sqrt{a}}\frac{1/s+1/y}{\sqrt{1-v^2/c^2}}-\frac{2h\mathrm{B}v^2}{\pi\sqrt{a}}. \quad . \quad . \quad (22)$$

The ratio of the amplitudes of vibration A_1 and A_2 of the first and second groups is, however,

$$\frac{\mathrm{A}_1}{\mathrm{A}_2}=\frac{n^2-a_2^*}{b_2}, \quad . \quad . \quad . \quad . \quad . \quad (23)$$

and in the present problem this is zero so long as quantities of the order k^2/a^2r^2 and higher orders are neglected in comparison with unity †. It appears, therefore, that the central particles do not take part in the oscillation of frequency ν, but instead oscillate as an independent system in their own mode, and being stationary they do not contribute to the magnetic energy. So far as the common frequency ν is concerned the mutual energy of the two revolving systems depends upon four electrons instead of eight, and is equal to

$$4h(\nu-\nu_1)=\frac{hk}{\pi\sqrt{a}}\cdot\frac{1/s+1/y}{\sqrt{1-v^2/c^2}}-\frac{h\mathrm{B}v^2}{\pi\sqrt{a}}, \quad . \quad . \quad (24)$$

in which expression the second term represents the mutual magnetic energy, which we will denote by E_m.

Hence

$$\mathrm{E}_m=-\frac{h\mathrm{B}v^2}{\pi\sqrt{a}}$$

$$=-\frac{2hkr^2}{\pi s^3\sqrt{a}}\cdot\frac{v^2}{c^2}, \quad . \quad . \quad . \quad . \quad . \quad (25)$$

by (16) since v^4/c^4 is neglected.

* *Loc. cit.* p. 923.

† If higher order terms are retained, so that $\mathrm{A}_1/\mathrm{A}_2$ is very small, this is to be interpreted as meaning that the whole system oscillates with the common frequency for only a very small fraction of the time (see *loc. cit.* p. 936).

Since $e^2 = hk/2\pi\sqrt{a}$ the expression for the mutual magnetic energy becomes

$$E_m = -\frac{4e^2r^2v^2}{s^3}, \quad \ldots\ldots \quad (26)$$

e being here the charge for an electron in electromagnetic units. The mutual magnetic attraction of the two revolving systems is therefore

$$F_m = -\frac{dE_m}{ds} = \frac{12e^2r^2v^2}{s^4} \quad \ldots\ldots \quad (27)$$

Now the mutual attraction of two small magnets or electrical circuits, each of magnetic moment M, placed coaxially at distance s apart, is $6M^2/s^4$. Hence the equivalent magnetic moment of each of the two revolving systems of fig. 1, deduced from their magnetic attraction, is

$$M = \sqrt{2}erv, \quad \ldots\ldots \quad (28)$$

or since *

$$e(\text{in e m.u.}) = \frac{}{2\pi c^2}\sqrt{\frac{k}{m_0}}, \quad \ldots \quad (29)$$

m_0 being the mass of an electron at rest,

$$M = \frac{hrv}{\sqrt{2}.\pi c^2}\sqrt{\frac{k}{m_0}} \quad \ldots\ldots \quad (3)$$

Calculated from the ordinary expression for the magnetic attraction of two electrons moving in parallel directions at right angles to the line joining them, the mutual attraction of the two revolving systems is

$$F_m = \frac{2e^2v^2}{s^2} - \frac{2e^2v^2s}{(s^2+4r^2)^{3/2}} \quad \ldots\ldots \quad (29)$$

$$= \frac{12e^2v^2r^2}{s^4},$$

the fourth and higher powers of r/s being neglected. This agrees with (27) and leads again to the value $\sqrt{2}\,erv$ for the magnetic moment. The result given by the vibrational theory thus coincides with that given by the elementary formula.

* *Loc. cit.* p. 340.

The formula generally employed, however, for the "magnetic moment" of revolving electron systems is that which represents the current multiplied by the area of the orbit in which the electrons revolve. In the present instance the current × area of one of the revolving systems of fig. 1 is simply *evr*, which does not agree with the value given by the vibrational theory and by the ordinary formula for the mutual force of moving electrons. It appears, therefore, that the value of the magnetic moment of such a system depends greatly upon the nature of the magnetic effect which is employed in its estimation. A still greater discrepancy is found if we base the calculation upon the value of the couple acting upon a system tending to turn its axis into the direction

Fig. 2.

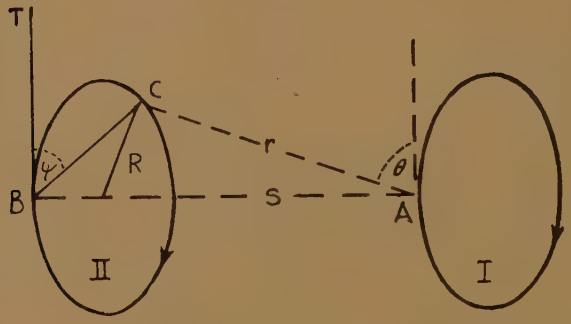

of the magnetic field in which it is placed. According to this method of calculation the magnetic moment of a system of electrons revolving under the influence of a central attracting force is approximately zero, since no such aligning couple exists, except perhaps as a secondary effect, in systems of this kind, the main effect of the application of the magnetic field being to cause the orbit to rotate round the direction of the field *.

The conditions are very different if the system consists of a large number of electrons moving round a circular turn of thin wire and forming a conduction current. The mutual magnetic energy of a pair of such circular currents arranged coaxially, and their mutual attraction, may be found from the vibrational theory as follows.

* See Larmor, 'Aether and Matter,' p. 341 (1900).

Referring to fig. 2 let the two circuits be represented by the circles I and II, each of radius R supposed small in comparison with the distance s between their planes. The number of electrons in motion in each circuit is N, all moving with velocity v the same way round in both circuits. It is supposed that v/c is so small that the factor $1/(1-v^2/c^2)$ in the expression for the coupling is sensibly equal to unity, and, further, that the moving electrons are so intermingled with the fixed positive charges in the atoms of the wires that all electrical couplings between pairs of electrons are neutralised and only the magnetic coupling need be considered.

Let A be an element of circuit I and B the element in circuit II which is parallel to A and similarly situated in its circuit. Let C be any other element of circuit II, the angle CBT between the chord BC and the tangent at B being denoted by ψ. Then taking circuits I and II as the two groups for the purpose of applying equation (9), and first estimating the effect on an electron at B of all the moving electrons in circuit II, we have, from the magnetic term in (11),

$$\begin{aligned} a_1 = a_2 &= a + \Sigma b' v^2 \\ &= a + \frac{v^2}{c^2} \Sigma \frac{k \sin\psi}{\mathrm{BC}} \\ &= a + \frac{kv^2}{c^2} \Sigma \frac{\sin\psi}{2\mathrm{R}\sin\psi} \\ &= a + \frac{\mathrm{N}kv^2}{2\mathrm{R}c^2} \quad \ldots\ldots\ldots \quad (30) \end{aligned}$$

Similarly, the effect of all the moving electrons in circuit I on one of those in circuit II (*e. g.*, the one situated at B) is represented by

$$b_1 = b_2 = -\frac{kv^2}{c^2} \frac{\mathrm{N}}{2\pi\mathrm{R}} \int_0^{\pi} \frac{2\mathrm{R}\, d\psi \cos 2\psi \sin\theta}{r},$$

where r denotes the distance AC and θ the angle between AC and the element at A, *i. e.*,

$$r = \sqrt{s^2 + 4\mathrm{R}^2 \sin^2\psi}, \quad \text{and} \quad \sin\theta = \sqrt{1 - \frac{\mathrm{R}^2 \sin^2 2\psi}{s^2}},$$

since the fourth power of R/s is neglected.

Hence

$$b_1 = b_2$$

$$= -\frac{\mathrm{N}kv^2}{\pi s c^2}\int_0^{\pi}\left(1-\frac{\mathrm{R}^2}{s^2}\sin^2 2\psi-\frac{2\mathrm{R}^2}{s^2}\sin^2\psi\right)\cos 2\psi\, d\psi$$

$$= -\frac{\mathrm{N}k\mathrm{R}^2v^2}{2s^3c^2}. \quad . \quad . \quad . \quad . \quad . \quad . \quad . \quad . \quad . \quad . \quad . \quad . \quad (31)$$

On substitution in (9) we have

$$n^2 = a+\frac{\mathrm{N}kv^2}{2\mathrm{R}c^2}-\frac{\mathrm{N}k\mathrm{R}^2v^2}{2s^3c^2}. \quad . \quad . \quad . \quad . \quad (32)$$

If s is infinite the periodicity n_1 of each of the two circuits separately is given by

$$n_1^2 = a+\frac{\mathrm{N}kv^2}{2\mathrm{R}c^2}, \quad . \quad . \quad . \quad . \quad . \quad . \quad (33)$$

so that

$$n^2 = n_1^2-\frac{\mathrm{N}k\mathrm{R}^2v^2}{2s^3c^2},$$

and

$$n = n_1-\frac{\mathrm{N}k\mathrm{R}^2v^2}{4s^3c^2n_1}$$

$$= n_1-\frac{\mathrm{N}k\mathrm{R}^2v^2}{4s^3c^2\sqrt{a}}, \quad . \quad . \quad . \quad . \quad . \quad . \quad (34)$$

approximately, since the fourth power of v/c is neglected.

The mutual magnetic energy of the two circuits is therefore

$$2\mathrm{N}h(\nu-\nu_1) = \frac{\mathrm{N}h}{\pi}(n-n_1)$$

$$= -\frac{\mathrm{N}^2hk\mathrm{R}^2v^2}{4\pi s^3c^2\sqrt{a}}$$

$$= -\frac{\mathrm{N}^2\mathrm{R}^2v^2e^2}{2s^3c^2}, \quad . \quad . \quad . \quad . \quad . \quad (35)$$

since $e^2 = hk/2\pi\sqrt{a}$, e being in electrostatic units. With e in electromagnetic units the mutual energy becomes

$$-\frac{\mathrm{N}^2\mathrm{R}^2v^2e^2}{2s^3},$$

and the mutual attraction of the circuits is

$$\frac{3N^2R^2v^2e^2}{2s^4} \quad . \quad . \quad . \quad . \quad . \quad . \quad . \quad . \quad (36)$$

If this is equated to $6M^2/s^4$ we have, for the magnetic moment of each circuit,

$$M=\tfrac{1}{2}NRve \quad . \quad . \quad . \quad . \quad . \quad . \quad (37)$$

The current in each circuit is $Nve/2\pi R$, and the current multiplied by the area of the circuit is $\frac{1}{2}NRve$, so that the value (37) given by the vibrational theory for the magnetic moment agrees in this case with that given by Ampère's theorem of the equivalence of an electric circuit and a magnetic shell of the same area.

It is evident from the above examples that magnetic energy due to electrons in translational motion can be satisfactorily accounted for on the vibrational theory, that is, on the view that this energy is represented by the change in the vibrational energy of moving electrons due to the influence which they exert upon one another in accordance with the laws of coupled vibratory systems. The magnetic forces between moving electrons are the space variations of these energy changes. In previous papers it has been shown that the electrostatic energy and the mutual electric forces of stationary electrons can be accounted for in a similar way.

According to the vibrational theory an isolated electron at rest or in motion has neither electrical nor magnetic energy, but it acquires one or both when its frequency is changed by the coupling effect of other electrons upon it, the quantity of energy so acquired being equal to the frequency change multiplied by Planck's constant. Also in this theory an electromagnetic field contains only one kind of energy, and it is unnecessary to regard space as filled with three kinds, electrical, magnetic, and vibrational, the first two kinds being merely changes in amount of the third.

Natural Philosophy Department,
The University, Glasgow.

LXI. *A Relativistic Study of Joule-Thomson Effect and Adiabatic Processes in a Gas.*—Part I. *By* D. V. Gogate, *M.Sc., Physics Department, King's College, London* *.

Introduction.

THE application of Fermi-Dirac statistics has proved increasingly useful in the solution of problems relating to the internal constitution of stars and has led to some very striking results during the last few years. As a result of the researches of Prof. R. H. Fowler [1] and their important developments by Milne [2], Kothari [3], and others, it has now been definitely established that the theory of the degenerate electron-gas, degenerate in the sense of Fermi-Dirac statistics, can explain, fairly satisfactorily, the internal constitution of the white dwarf stars (stars characterized by a high effective temperature, a low value of luminosity, and a large mean density). By working out the degree of ionization in degenerate matter in terms of its density or pressure and applying the usual theory of the white dwarf stars, Kothari [4] and Majumdar have established the very interesting result that there exists a maximum radius—of the order of the radius of Jupiter, the largest planet in the solar system—for every cold † body, *i. e.*, for a body in which the free electrons form a degenerate gas in the sense of Fermi-Dirac statistics. As degenerate matter possibly exists in all the stars, an investigation of its various properties is naturally attracting the attention of many physicists. Recently, Kothari [5] has studied the Joule-Thomson effect and adiabatic change in a gas obeying Fermi-Dirac statistics. He has shown that during a Joule-Thomson expansion a degenerate gas is heated (and not cooled) and the amount of heating per unit fall of pressure increases with the degree of degeneracy which is measured by the degeneracy-discriminant

$$A_0 = \frac{nh^3}{2(2\pi mkT)^{3/2}},$$

where n is the free electron concentration, T, the temperature, m, the mass of the electron and k and h are Boltz-

* Communicated by Prof. O. W. Richardson, F.R.S.

† The planets and the white dwarf stars may be regarded as cold bodies in this technical sense of the word.

mann's and Planck's constants respectively. From this it follows that as the Joule-Thomson expansion proceeds, the rate of heating of a degenerate gas will continuously go on falling till finally the gas becomes non-degenerate and behaves very nearly like a classical perfect gas, exhibiting no further rise of temperature with more Joule-Thomson expansion. He has further shown that during an adiabatic process the degree of degeneracy always remains constant, which means that a degenerate gas will continue to remain degenerate and a non-degenerate gas will remain non-degenerate in any adiabatic change.

In view of the growing importance of the physics of " degenerate matter " it may be of interest to study the Joule-Thomson effect and adiabatic processes in a Fermi-Dirac gas on a relativistic * basis. The relativistic cases are also likely to occur in the stellar interiors. In fact, Kothari[6] has recently shown that relativistic degeneracy occurs in white dwarf stars above a certain mass—very nearly equal to the mass of the Sun (to be more accurate, above the mass $4\odot/\mu^2$ where $\odot$ is the mass of the Sun and μ is the mean molecular weight per free electron). For the sake of completeness and clarity it may be worth while to give here the physical meaning of the limiting states of a gas obeying Fermi-Dirac statistics.

Limiting states of a gas obeying Fermi-Dirac statistics :—

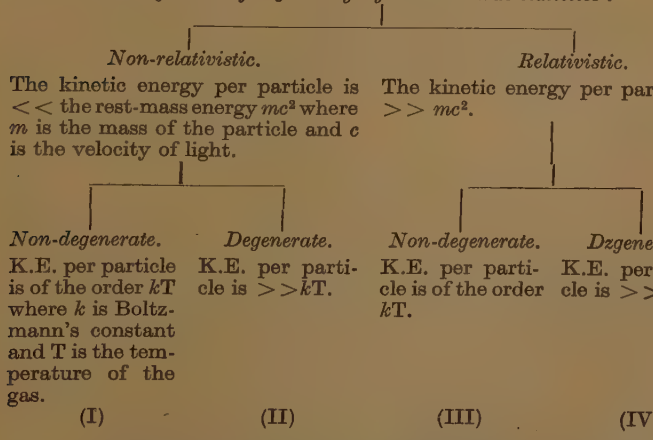

* Kothari has not taken into account the effect of relativity-mechanics and the expressions for energy, pressure, and Joule-Thomson effect given in his paper refer to the non-relativistic case.

Our investigation will be confined only to the cases (III) and (IV). The non-relativistic cases have been, as already mentioned, fully discussed elsewhere by Kothari[7]. In the present paper we propose to study the case (III) relating to the relativistic non-degenerate gas. The investigation of Joule-Thomson effect and adiabatic changes for the case (IV), *i. e.*, for the relativistic degenerate gas will be given in part II. which will appear shortly.

In section 1, we shall derive in an elementary way and in a form suited to our purpose, the expressions for the energy E^r, pressure p^r, etc. (the suffix "r" in these symbols indicates that the latter refer to the relativistic case), which * are required in the investigation of the Joule-Thomson effect discussed in section 2. The adiabatic changes occurring in a relativistic non-degenerate gas will then be discussed in section 3.

1. *An Elementary Derivation of Formulæ for Energy, Pressure, etc.*

We know that in an enclosure of volume V, the number of wave-functions for which the momentum s lies between the values s and $s+ds$ is given by

$$4\pi s^2 ds . V/h^3. \quad . \quad . \quad . \quad . \quad . \quad . \quad (1)$$

In the case of an electron we have,

$$\text{momentum } s = \frac{m\beta c}{\sqrt{1-\beta^2}} \quad . \quad . \quad . \quad . \quad (2)$$

and kinetic energy

$$\epsilon = mc^2\left[\frac{1}{\sqrt{1-\beta^2}} - 1\right] \quad . \quad . \quad . \quad . \quad (3)$$

where m is the rest-mass of the electron, c is the velocity of light and $\beta = v/c$, v being the velocity of the electron. From (2) and (3) we get,

$$m^2c^2 + s^2 = \frac{(\epsilon + mc^2)^2}{c^2}$$

* These expressions are implicitly contained in the results of investigations of Fowler, Majumdar, and others (see Fowler, ' Statistical Mechanics,' 2nd ed., p. 650 ; also Majumdar, *Astro. Nachr.* p. 246 (Dec. 1932)). They have, however, not been so far explicitly given in the form in which they appear in this paper.

or $$s\,ds=\frac{(\epsilon+mc^2)\,d\epsilon}{c^2}$$

and $$S^2=\frac{(\epsilon+mc^2)^2}{c^2}-m^2c^2=\frac{1}{c^2}(\epsilon+2mc^2)\epsilon. \quad . \quad . \quad (4)$$

Hence the number of wave-functions lying within the energy-range ϵ to $\epsilon+d\epsilon$ will be

$$a(\epsilon)\,d\epsilon=g.\frac{4\pi V}{c^3h^3}(\epsilon^2+2mc^2\epsilon)^{\frac{1}{2}}.(\epsilon+mc^2)\,d\epsilon, \quad . \quad (5)$$

where g is the weight factor equal to 2 for an electron. Now, according to the Fermi-Dirac distribution law, the number of electrons having kinetic energies in the range ϵ to $\epsilon+d\epsilon$ is

$$N(\epsilon)\,d\epsilon=\frac{a(\epsilon)\,d\epsilon}{1/A.e^{\epsilon/kT}+\beta}, \quad . \quad . \quad . \quad . \quad (6)$$

where $\beta=+1$ and A is independent of ϵ. (β assumes the value -1 in the case of Bose-Einstein statistics).

Let $n(\epsilon)d\epsilon$ denote the number of electrons per unit volume lying within the energy-range ϵ, $\epsilon+d\epsilon$.

Then, $$n(\epsilon)\,d\epsilon=\frac{4\pi g}{c^3h^3}\frac{(\epsilon^2+2mc^2\epsilon)^{\frac{1}{2}}.(\epsilon+mc^2)\,d\epsilon}{1/A.e^{\epsilon/kT}+\beta}. \quad . \quad (7)$$

Since n is the total number of electrons per unit volume,

$$n=\int_0^\infty n(\epsilon)\,d\epsilon=\frac{D}{V}\int_0^\infty\frac{(u^2+2yu)^{\frac{1}{2}}.(u+y)\,du}{1/A.e^u+\beta}, \quad . \quad (8)$$

and the total energy

$$E=\int_0^\infty n(\epsilon)\,d\epsilon.\epsilon=DkT\int_0^\infty\frac{u(u^2+2yu)^{\frac{1}{2}}.(u+y)}{1/A.e^u+\beta}\,du, \quad (9)$$

where $$y=\frac{mc^2}{kT}, \quad u=\frac{\epsilon}{kT}, \quad \text{and} \quad D=4\pi g\left(\frac{kT}{ch}\right)^3.V. \quad (10)$$

k being the Boltzmann constant and T the temperature. We now proceed to derive an expression for the pressure p. From elementary kinetic theory we know

$$p=\frac{1}{3}\int_0^\infty n(\epsilon)\,d\epsilon.v.s, \quad . \quad . \quad . \quad . \quad (11)$$

where s is the momentum and v the velocity of a particle with energy ϵ.

From (2) we have

$$v=\frac{sc}{(m^2c^2+s^2)^{\frac{1}{2}}} \quad . \quad . \quad . \quad . \quad . \quad (12)$$

or

$$vs=\frac{cs^2}{(m^2c^2+s^2)^{\frac{1}{2}}}.$$

Now expressing s in terms of ϵ with the help of equation (4), we get

$$vs=\frac{\epsilon^2+2mc^2\epsilon}{(mc^2+\epsilon)}. \quad . \quad . \quad . \quad . \quad . \quad (13)$$

Substituting (7) and (13) in equation (11), we obtain

$$p=\frac{\mathrm{D}k\mathrm{T}}{3\mathrm{V}}\int_0^\infty \frac{(u^2+2yu)^{\frac{3}{2}}}{1/\mathrm{A}.e^u+\beta}\,du, \quad . \quad . \quad . \quad (14)$$

where the symbols y, u, and D are defined by (10).

The integrals (8), (9), and (14) cannot be evaluated in finite terms. We shall, therefore, deal only with the important limiting cases. Here we are concerned with the relativistic case, *i. e.*, the case in which the kinetic energy is much greater than the rest-mass energy; or

$$mc^2/\epsilon<<1\,; \quad i.\,e.,\ y/u<<1. \quad . \quad . \quad . \quad (15)$$

(In the non-relativistic case the condition is $u/y<<1$.)

Since in the case we are dealing with, y is very small compared to u, equations (8), (9), and (14) reduce to

$$n=\frac{\mathrm{D}}{\mathrm{V}}\int_0^\infty \frac{u^2\,du}{1/\mathrm{A}.e^u+\beta}. \quad . \quad . \quad . \quad . \quad . \quad (16)$$

$$\mathrm{E}^r=\mathrm{D}k\mathrm{T}\int_0^\infty \frac{u^3\,du}{1/\mathrm{A}.e^u+\beta}. \quad . \quad . \quad . \quad . \quad (17)$$

$$p^r=\frac{\mathrm{D}k\mathrm{T}}{3\mathrm{V}}\int_0^\infty \frac{u^3\,du}{1/\mathrm{A}.e^u+\beta}. \quad . \quad . \quad . \quad . \quad (18)$$

Comparing (17) and (18) we get,

$$p^r=\frac{1}{3}\frac{\mathrm{E}^r}{\mathrm{V}}, \quad . \quad . \quad . \quad . \quad . \quad (19)$$

where $\frac{\mathrm{E}^r}{\mathrm{V}}$ is the energy per unit volume. (In the non-relativistic case $p=\frac{2}{3}\cdot\frac{\mathrm{E}}{\mathrm{V}}$.)

Let us now apply these results to a non-degenerate gas. In the case of non-degeneracy $\mathrm{A}<<1$.

We then have

$$n=\frac{D}{V}\int_0^\infty \frac{u^2\,du}{1/A.e^u+\beta}=\frac{D}{V}\int_0^\infty u^2\,du.Ae^{-u}.(1+\beta Ae^{-u})^{-1}$$

$$=\frac{AD}{V}\int_0^\infty u^2\,du.e^{-u}(1-\beta Ae^{-u}),$$

neglecting terms containing higher powers of A than 1.

Hence,

$$n=A.8\pi g\left(\frac{kT}{ch}\right)^3\left(1-\frac{\beta A}{8}\right)$$

or

$$A=\frac{n}{8\pi g}\left(\frac{ch}{kT}\right)^3\left(1-\frac{\beta A}{8}\right)^{-1}.$$

Let us now put

$$A_0^r=\frac{n}{8\pi g}\left(\frac{ch}{kT}\right)^3.$$

Then to the approximation we are considering,

$$A=A_0^r[1+\beta A_0^r/8]. \quad . \quad . \quad . \quad . \quad . \quad (20)$$

A_0^r is known as the degeneracy discriminant and is $<<1$ for a non-degenerate system and $>>1$ for a degenerate system. The expression for E^r may be derived in a similar manner. Thus, we have

$$E^r=DkT\int_0^\infty \frac{u^3\,du}{1/A.e^u+\beta}$$

$$=V.4\pi g.\left(\frac{kT}{ch}\right)^3.kT\int_0^\infty u^3\,du.Ae^{-u}(1-\beta Ae^{-u})$$

$$=3nkTV.\left[1+\frac{\beta A_0^r}{16}\right]=3RT\left[1+\frac{\beta A_0^r}{16}\right]. \quad . \quad . \quad (21)$$

to the first approximation.

Again,

$$p^r=\frac{E^r}{3V}=nkT\left[1+\frac{\beta A_0^r}{16}\right]. \quad . \quad . \quad . \quad (22)$$

2. *Joule-Thomson Effect in a Relativistic Non-degenerate Gas.*

The Joule-Thomson effect is given by the well-known expression

$$\Delta T=\frac{T\left(\frac{dV}{dT}\right)_p-V}{C_p}\Delta p, \quad . \quad . \quad . \quad . \quad (23)$$

where ΔT is the fall in temperature of a gas when its pressure is diminished by Δp and C_p is the specific heat per Avogadro number (N) at constant pressure.

The relativistic expression for the internal energy of a non-degenerate gas is according to (21),

$$E^r = 3RT\left[1+\frac{\beta}{16}A_0^r\right].$$

We now have, for the specific heat per Avogadro number of free electrons, at constant volume,

$$C_V = \left(\frac{dE^r}{dT}\right)_V = 3Nk\left(1-\frac{\beta}{8}A_0^r\right)$$

$$= 3R\left(1-\frac{\beta}{8}A_0\right), \quad . \quad . \quad . \quad (24)$$

where $R(=Nk)$ is the gas constant.

β, as we have already remarked, assumes the value $+1$ for Fermi-Dirac statistics and -1 for Bose-Einstein statistics. Electrons obey Fermi-Dirac statistics and hence for them β is always equal to $+1$ (Nuclei of even mass number obey Bose-Einstein statistics and those of odd mass number obey Fermi-Dirac statistics.)

We know from the well-known thermodynamical relations that the difference between the two specific heats of a gas is given by

$$C_p - C_V = T\left(\frac{dp}{dT}\right)_V\left(\frac{dV}{dT}\right)_p \quad . \quad . \quad . \quad . \quad (25)$$

and remembering that $p^r = E^r/3V$, in the relativistic case we are considering, we get,

$$\left(\frac{dp^r}{dT}\right)_V = nk\left(1-\frac{\beta}{8}A_0^r\right) \quad . \quad . \quad . \quad . \quad (26)$$

$$-V\left(\frac{dp^r}{dV}\right)_T = nkT\left(1+\frac{\beta A_0^r}{8}\right), \quad . \quad . \quad . \quad (27)$$

and since $$\left(\frac{dV}{dT}\right)_p = -\left(\frac{dp}{dT}\right)_v\left(\frac{dp}{dv}\right)_T,$$

$$\left(\frac{dV}{dT}\right)_p = \frac{\left(1-\frac{\beta}{8}A_0^r\right)}{\left(1+\frac{\beta}{8}A_0^r\right)}\cdot\frac{V}{T} \quad . \quad . \quad . \quad . \quad . \quad (28)$$

Substituting the above values of $\left(\frac{dp^r}{dT}\right)_v$ and $\left(\frac{dV}{dT}\right)_p$ in (25), we get

$$C_p - C_V = Nk \frac{\left(1-\frac{\beta}{8}A_0^r\right)^2}{\left(1+\frac{\beta}{8}A_0^r\right)}, \quad . \quad . \quad . \quad . \quad (29)$$

$$\doteqdot R\left[1-\frac{3}{8}\beta A_0^r\right], \quad . \quad . \quad . \quad . \quad (30)$$

since A_0^r is $<<1$ for a non-degenerate gas.

Hence

$$C_p = 3Nk\left(1-\frac{\beta}{8}A_0^r\right)\left[1+\frac{1}{3}\cdot\frac{1-\frac{\beta}{8}A_0^r}{1+\frac{\beta}{8}A_0^r}\right] \quad . \quad . \quad (31)$$

$$\doteqdot 4R\left[1-\frac{3}{16}\beta A_0^r\right]. \quad . \quad . \quad . \quad . \quad . \quad . \quad . \quad (32)$$

We can now substitute the values of $\left(\frac{dV}{dT}\right)_p$ and C_p from equations (28) and (31) in equation (23) to evaluate ΔT. We then get, after a little algebraical simplification, the following expression for the Joule-Thomson effect

$$\Delta T = -\frac{1}{16kn}\cdot\left(\frac{\beta A_0^r}{1-\frac{3}{16}\beta A_0^r}\right)\Delta p \doteqdot -\frac{\beta A_0^r}{16kn}\Delta p. \quad (33)$$

It is obvious from the above equation that, during a Joule-Thomson expansion, a relativistic non-degenerate gas obeying Fermi-Dirac statistics ($\beta=+1$) will always be heated while a gas obeying Bose-Einstein statistics ($\beta=-1$) will always experience a fall in temperature, the change in temperature being, in either case, proportional to the value of A_0^r.

3. *Adiabatic Changes.*

The relativistic expression for the entropy of a non-degenerate system is

$$S = R\log\left[8\pi g\left(\frac{kT}{ch}\right)^3\cdot\frac{e^4}{n}\right]. \quad . \quad . \quad . \quad (34)$$

where e is the exponential base.

As entropy S remains constant during an adiabatic process, we have from the above equation

$$\frac{n}{T^3} = \text{constant},$$

and therefore the degeneracy discriminant

$$A_0^r = \frac{n}{8\pi g}\left(\frac{ch}{RT}\right)^3$$

also remains constant, *i. e.*, a non-degenerate gas remains non-degenerate in an adiabatic process.

The pressure of a relativistic non-degenerate gas is given by $p^r = nkT$ and therefore, during an adiabatic change,

$$\frac{p^r}{T^4} = \text{constant}.$$

Again we know that for an adiabatic process,

$$T\,dS = dE + p\,dV = 0,$$

and since, in the relativistic case,

$$p^r = \frac{1}{3}\frac{E^r}{V}$$

we get, by eliminating E from the above two equations,

$$p^r V^{4/3} = \text{constant}.$$

In conclusion I wish to express my sincere thanks to Prof. O. W. Richardson, F.R.S., for his useful suggestions and advice.

References.

(1) Mon. Not. R. Astr. Soc. lxxxvii. p. 121 (1926).
(2) Mon. Not. R. Astr. Soc. xcii. p. 611 (1932).
(3) Phil. Mag. xii. p. 665 (1931); Mon. Not. R. Astr. Soc. xciii. p. 61 (1932); xcvi. p. 833 (1936).
(4) 'Nature,' cxxxvii. p. 157 (1936 *a*).
(5) Proc. Nat. Inst. Sci. (India) iv. no. 1 (1938).
(6) Proc. Roy. Soc. A, clxii. p. 521 (Oct. 1937).
(7) Proc. Nat. Inst. Sci. (India), iv. no. 1 (1938); 'Nature,' cxl. p. 970 (Dec. 1937).

LXII. *Notices respecting New Books.*

Measurement of Radiant Energy. Edited by L. E. Forsythe. [Pp. 452+xiv.] (McGraw-Hill Publishing Company, Ltd. Price 30*s.*)

THIS book consists mainly of a collection of articles by a number of practising physicists on those aspects of radiometry in which they are expert. It does not, as the title might imply, cover the whole field of radiation, but deals only with heat and light.

The material falls into sections on fundamental concepts and laws, sources, analysis, measurement and special problems. The treatment is uneven, some of the articles being quite exhaustive while others are so inadequate as to cause wonder at their inclusion. The chapter on photographic radiometry contains a most thorough and valuable discussion of the many sources of variation of density with condition of exposure and development, and should be read by anyone using or contemplating the use of this method of measurement. In the section on light filters less than justice is done to the Christiansen filter, while there is no mention of the very useful set of filters designed by Bowen. There is a wealth of figures and illustrations, but many of these are too small to be of real value.

Undoubtedly the book will prove in many respects a valuable source of reference to those engaged in the measurement of heat and light radiation—yet it may perhaps be hoped that it is as yet a first draft of a more balanced and comprehensive survey.

Atomic Spectra and Atomic Structure. By Gerhard Herzberg. Translated by J. W. T. Spinks. [Pp. xvi+257.] (London and Glasgow: Blackie & Son, 1937. Price 18*s.* 6*d.*)

The general subject-matter of this book is necessarily much the same as that of several others which have recently appeared. After an account of the simpler types of line spectra, and of multiplet structure, considered in relation to the Zeeman and Stark effects, a survey is given of the up-building principle and the periodic system of the elements. More specialized topics are then taken up, including intensity and interval rules, and hyperfine structure, and in the final chapter some chemical and magnetic applications are given.

In spite of, or perhaps because of, the familiarity of the general scheme, the book is admirably adapted to the purpose for which it is intended, which is to serve as an introduction

to the beginner in the field and as a sufficient survey for those primarily interested in applications in other fields. It bridges the gap between the one or two chapters devoted to the subject in more general text-books and the detailed accounts in more special treatises. In keeping with the general aims the mathematical side is reduced to a minimum, and extensive tables of wave-lengths, term values, etc. are not included.

A particularly valuable feature is that sections dealing with the wave mechanical treatment are included in connexion with each of the topics discussed, these being adequate to give the student a clear idea of what it is all about.

The author is particularly to be congratulated on having withstood the temptation to include much more. He has attempted the harder task of selecting significant illustrative material, and the selection is admirably made. The book is well produced, and it includes a series of excellent diagrams. A fully representative but not too detailed bibliography of books, as well as of papers, will be of great assistance to the student who wishes to proceed further with the subject.

Differential Systems. By J. M. Thomas. [Pp. ix+118.] (American Mathematical Society, New York, 1937. Price $2.00.)

The American Mathematical Society has again placed mathematicians in its debt by an addition to its admirable series of colloquium publications. While the appeal of the present work is less general than that of some of its predecessors, all interested in modern algebra and the theory of differential equations will welcome it. It is devoted to the theory of Pfaffian systems treated from the algebraic standpoint, a method which essentially originated with Grassmann. The earlier chapters develop from its postulates an algebra based on the non-commutative units of Grassmann, which, by the introduction of differential and integral elements, is fitted for the manipulation of differential systems so as not only to discover when solutions exist, but also to provide canonical forms and, as interesting chapters of examples show, actually to determine the solutions.

The author expresses his debt to Riquier and others, but the pure algebraic treatment is his own, and embodies results which have previously been accessible only in the proceedings of various societies. The excellent and accurate printing adds to the pleasure of reading this valuable monograph.

[*The Editors do not hold themselves responsible for the views expressed by their correspondents.*]

THE

LONDON, EDINBURGH, AND DUBLIN

PHILOSOPHICAL MAGAZINE

AND

JOURNAL OF SCIENCE.

[SEVENTH SERIES.]

MAY 1938.

LXIII. *On the Hydration and Denaturation of Proteins.*

By D. M. WRINCH, *M.A., D.Sc. Oxon, D.Sc. Lond., Mathematical Institute, Oxford* *.

[Plate IX.]

SUMMARY.

THE cyclol theory of protein structure is further developed with special reference to the hydration and denaturation of the globular proteins. The hydration of protein crystals, it is suggested, comprises intra- and intermolecular water, and, in addition, water directly associated with the fabric of the molecule. As an example, the hydration of egg albumin is considered: on the hypothesis of the 288 residue structure for the 35,000 class of proteins put forward by the present writer in 1936, hydration of 27 per cent. is deduced from the molecular weight for egg albumin put forward by Svedberg in 1937, a figure which may be compared with hydration values of 22 and 32·4 per cent. found by Adair and Adair for egg albumin crystals.

It is further suggested that some types of denaturation, in particular film-denaturation, consists in the opening or fragmenting of cyclol cage structures. This view emphasizes the contrast between the unique configuration

* Communicated by the Author.

of the native protein and the vast variety of structures characteristic of denatured proteins. Its implications with respect to the structure of protein films are explored and compared with experiment.

I. *Introduction.*

IN previous communications (Wrinch, 1937 *a–f*, 1938 *a*, *b*), the implications of the cyclol hypothesis regarding the molecular weights to be expected for the globular proteins, the shapes of the molecules, and the existence of compound structures have been developed. It is now found (Wrinch, 1938 *b*) that all the molecular weight classes given by Svedberg in his review in 'Nature' (1937) are covered by the structures predicted, that the compound structures explain and interpret certain behaviour traits of proteins discovered by the ultracentrifuge, and that in the cases of insulin and pepsin (the only proteins for which X-ray measurements of the lattice have so far been published) the proposed cyclol structure fits adequately into the crystal lattice. In this communication further fundamental aspects of the globular proteins are discussed in detail, namely hydration and denaturation.

II. *The Hydration of Cyclol Cages.*

One of the striking points about the present state of protein chemistry resides in the fact, so far unexplained on the polypeptide chain hypothesis, that Svedberg's results strongly suggest that proteins of definite chemical structure, with definite molecular weights, exist ; also that in a certain sense these proteins are "globular." It has not yet proved possible to deduce from Svedberg's experiments and analyses any information regarding the geometrical sense in which the term "globular" is used.

On the cyclol hypothesis the essential entity in proteins is a fabric or two-dimensional atomic network, which is a surface polycondensation of amino acid (and imino acid) residues (fig. 1). It proves possible geometrically to build from this network space-enclosing structures. There is a definite number of such structures in any given range of molecular weights. The polyhedral shape of these structures and the chemical nature of the network make it possible to construct compound structures. All

these deductions are in accord with Svedberg's requirements. They also offer a precise interpretation of the sense in which the molecules are "globular." On this theory globular molecules of two types can be constructed: the "simple" ones consist of single closed cyclols, the "compound" ones of a number of such structures in association.

We consider first a simple globular protein consisting of a single cage-like structure (Pl. IX. figs. 2 & 3). The material of the cage is a lamina of amino acid residues, a fabric therefore which is one residue thick. This fabric is

Fig. 1.

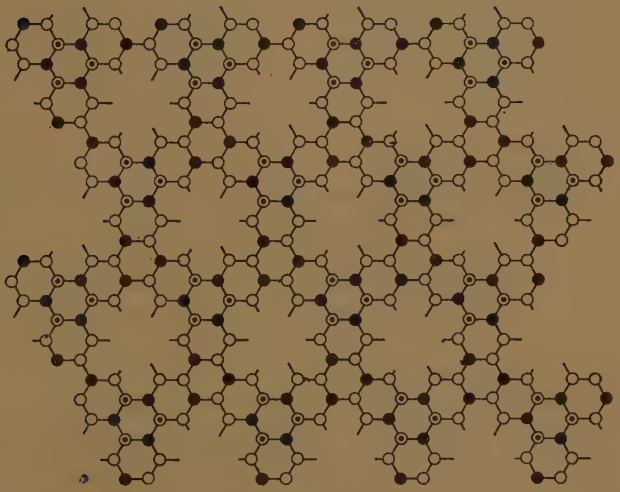

The cyclol fabric. The median plane of the lamina is the plane of the paper. The lamina has its "front" surface above and its "back" surface below the paper.—[From Proc. Roy. Soc. A, clx. p. 69, fig. 9.]

● =N.
⊙ =C(OH), peptide hydroxyl upwards.
⊙ =C(OH), peptide hydroxyl downwards.
○— =CHR, direction of side chain initially outwards.
○– =CHR, direction of side chain initially upwards.

dorsiventral, since all the amino acids obtained from proteins have the same configuration (fig. 4). When arranged with the "front" surface outwards all the C_β atoms lie outside the median framework and the molecule

is of " extravert " type ; when arranged with the " back " surface outwards all the C_β atoms lie inside the median network and the molecule is of " introvert " type. With both types there are trios of hydroxyls carried by the peptide carbons pointing alternatingly inwards and outwards. It is possible in the case of an extravert that some small proportion of the R groups whose initial direction is outwards from the median plane of the network may curve round and enter the interior through the lacunæ which are characteristic of the cyclol fabric. Similarly, some small proportion of the R groups of an introvert may emerge.

In the case of an extravert structure there is, therefore, a considerable space within the cage which is not occupied by any atoms belonging to the amino acid residues. This space must, presumably, be tenanted. Thus the

Fig. 4.

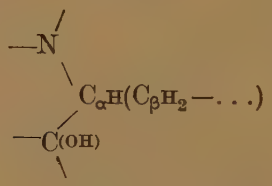

An amino acid residue.

first deduction from the theory is that a globular protein of extravert type must have foreign molecules or ions associated with it. If only water molecules are involved an estimate as to their number can be obtained. For suppose a C_n cyclol of extravert type contains water molecules in orderly array. The polyhedral framework of C_n (Wrinch, 1937 *d*) is obtained by cutting from a tetrahedron of side $(p+2q_n)$ four tetrahedra of side q_n, where $q_n=(4n-1)p$ and $p=\sqrt{6}a$, a being a mean value between the length of C—C and C—N links, say 1·5 Å. Thus the volume enclosed by the C_n framework is

$$V_n=[(p+2q_n)^3-4q_n^3]\sqrt{2}/12$$
$$=[(8n-1)^3-4(4n-1)^3]\sqrt{3}a^3.$$

Assuming that on the average the atoms of the network and the inward pointing hydroxyls occupy a layer of

thickness 3 Å., the net volume available for water molecules (since the distance between parallel C_n faces is $8na = 12n$ Å.) is

$$v_n = V_n(1-6/12n)^3,$$

giving $$v_1, v_2, v_3 \ldots = \sqrt{3}a^3(29, 845, 3963 \ldots).$$

An interesting precedent for a mass consisting of a considerable number of water molecules is afforded by the case of phosphotungstic acid (Bradley and Illingworth, 1935), where massive cations $(H_3.29\,H_2O)^{+3}$ alternate with anions $(PW_{12}O_{40})^{-3}$ in two interpenetrating diamond lattices. (It may be noticed also that phosphotungstic acid can exist as a 5-hydrate (Keggin, 1933, 1934).) Here it was necessary to find an arrangement of twenty-nine water molecules to fill a polyhedral space. An arrangement satisfying the necessary conditions was found ; a central molecule is in contact with four molecules at the corners of a tetrahedron, and twelve molecules are strung out in pairs along fourfold cube axes to link together six anions ; midway between two such blocks, comprising seventeen water molecules, six water molecules form a puckered hexagonal ring and link together six anions. The full complement of water molecules is then represented by one block of seventeen and two hexagonal rings, giving in all twenty-nine molecules. The waters are arranged for the most part with four nearest neighbours ; the distances between oxygens all lie between 2·84 Å. and 2·9 Å., so that the volume per water is about 28 Å.^{3}. The shape of each individual mass of waters is a truncated octahedron of volume about 800 Å.^{3}. Important features of this structure, which (presumably) may be used as a guide to the anatomy of water masses in general, are three—the very small variation in the inter-water distances, the fact that the geometry allows them to pack into the interior of a polyhedron, and the fact that a certain proportion of them are linked with the non-water components of the crystal.

The problem of filling the interior of a C_n is similar to the problem solved in the case of phosphotungstic acid in several respects. For all the C_n extraverts the space to be filled is a polyhedron which differs from the polyhedron in phosphotungstic acid only by a parallel displacement of the faces. Furthermore, the inner surface of a C_n extravert carries trios of inward-pointing

hydroxyls (one hydroxyl per two residues), which, we suggest, form hydroxyl links (Bernal and Megaw, 1935; Huggins, 1936) with the water molecules on the periphery of the water masses. There is also a large number of nitrogens (one per two residues), each with a lone pair of electrons on the inner surface of the structure, which may also link to the water molecules on the periphery (Hendricks et al., 1936). If we assume 28 Å.^{2} as the volume of each water molecule, the number is then $v_n/28$, giving six water molecules for a C_1 interior, 176 for a C_2 interior, 827 for a C_3 interior, and so on. It will be seen that the number of water molecules in C_n interiors increases a little more rapidly than n^3, whereas the number of residues is proportional to n^2. Thus the number of water molecules per residue increases with n. If the stability of the water mass is dependent on the number of links with the fabric of the molecule, then it is possible that the higher cyclols when filled with water become increasingly unstable as n increases.

It has already been pointed out (Wrinch, 1938 *b*) that, so far as a rough and necessarily tentative investigation of Svedberg's molecular weight classes is concerned, it is only necessary to assume the existence of C_1 units. Again, it was noticed that C_2 units alone can account for all proteins except the 17,600 class and gliadin (26,000) and yellow ferment (77,800). Svedberg himself favours very considerable economy in the number of different units to be postulated. If therefore there is any difficulty about the higher cyclols, structures based upon C_1 or upon C_1 and C_2 units alone can be devised.

The water complements of C_n introverts may be considered on the same lines. They will be lower than those of the extraverts owing to the room occupied in the interior by R groups. It is evident from the dimensions of the C_1 molecule (*e. g.*, the distance between parallel faces is 12 Å.) that a C_1 introvert can only exist when the side-chains are sufficiently short. A C_1 molecule consisting of (say) equal numbers of glycine and alanine residues may be a possibility. For the proteins whose chemical composition is known the average length of the R groups suggests C_1 extravert structures rather than introverts. In the case of a C_n introvert it should be noticed that there must be enough glycine residues to fill the congested situations at the six slits. There are two

such positions at each slit, so that a minimum of 12 glycines per molecule is required. With a mean residue weight of 120 the residue weight of 57 for glycine implies that a complement of 12 glycines per $72n^2$ residues is equivalent to $7{\cdot}9/n^2$ per cent. of glycine. Thus a C_2 introvert needs a minimum of (say) 2 per cent. glycine. These deductions make it possible to decide whether a certain structure can be of introvert type. (It is of interest to notice that edestin contains 3·8 per cent. of glycine, and so may be made up of C_2 or higher C_n introverts.)

III. *The Hydration of Cyclol Networks.*

It has been suggested that the tertiary nitrogens and peptide hydroxyls on the inner surfaces of C_n structures are linked to water molecules in the interior. In the case of the other half of the nitrogens and peptide hydroxyls which lie on the outside of the median framework we may also presume that links are formed to water molecules if available. We anticipate, then, that a cyclol cage is capable of holding a number of water molecules on each of its surfaces. The upper limit is one per residue, since there is on each surface one nitrogen and one hydroxyl per two residues. Mention should be made here of the suggestion of Frank (1936) that it is necessary for the stability of the network that all the peptide hydroxyls be hydrated.

The question of the water content of protein lattices can also be considered on the same lines. The cyclol cages, owing to the fact that they are truncated tetrahedra, are not capable of filling space in the sense in which cubes (for example) can fill space. Hence even a cyclol molecule made entirely of glycine residues cannot form a lattice without considerable intermolecular spaces. In the case of a protein with a variety of R groups of different lengths and of different types, some capable of forming ionic linkages, others capable of forming hydrogen or hydroxyl links and so on, the intermolecular spaces are necessarily still bigger. We presume that these spaces are tenanted and that water molecules can be used for this purpose. If this is the case, a protein lattice will then be hydrated in three different ways—there will be intramolecular water, water linked to the cages themselves, and, finally, intermolecular water. In view

of the precedent afforded by phosphotungstic acid, which exists both as a 5-hydrate and as a 29-hydrate, with the same phosphotungstic anions in both cases, it is possible that one and the same protein can form lattices by different packings with vastly different complements of intermolecular water.

So far we have pictured the cyclol structures in the case when all the foreign molecules associated with them are water molecules; but other possibilities present themselves for consideration.

The idea of a cage-like molecule, which has spontaneously arisen in the course of developing the implications of the cyclol hypothesis, is not new *. Large classes of silicates are cage structures (Bragg, 1937). These include the felspars: sodalite, helvite, the ultramarines, and the scapolites; and the zeolites. The cages of the ultramarines (Jaeger, Westenbrink and van Mille, 1927; Jaeger, 1930) have the shape of truncated octahedra, with six square faces and eight hexagonal faces. The cyclol cages, which can be obtained by giving the faces of these silicate cages a parallel displacement, are of a very similar type. The six square faces become the six slits and the eight hexagonal faces become four hexagonal and four triangular faces. An interesting feature of these related silicates is that each type of hole in the structure is filled with foreign molecules or ions of appropriate type, and that there is a considerable degree of interchangeability in the occupants of each type. Many contain water molecules and cations (Hey and Bannister, 1932; Taylor, Meek, and Jackson, 1933). Thus in analcite (Taylor, 1930) Na ions are present in the spaces; each lies between two water molecules. In natrolite also Na ions and water molecules, are present; in scolecite there are Ca ions and water molecules; in thomsonite Na and Ca ions and water molecules, and so on. Other cage silicates contain cations and anions alone. Thus (Pauling, 1930; Barth, 1932) sodalite has Cl surrounded tetrahedrally by Na, noselite Na and SO_4, and haüynite Na, Ca, and SO_4 ions. Sodalite can be converted into noselite by heating in fused sodium sulphate and haüynite into sodalite by heating in fused sodium chloride.

* The author is greatly indebted to Professor H. S. Taylor for valuable suggestions as to the relations between the proteins and the silicates (*cf.* Taylor, 1937).

These well-established structures thus suggest that globular proteins may contain in their interiors water molecules with or without suitable ions and that there may on occasion also be local sets of cations and anions without water molecules. Intermolecular spaces may also be tenanted in the same way. We anticipate that some protein crystals may possibly under favourable conditions be " pure " in the sense that they contain nothing except frameworks comprising amino acid condensations and water molecules within and between the frameworks. The water complement can then be predicted within limits if the molecular weight and dissociation properties of the protein molecules are known. But it appears likely that many protein crystals will contain foreign ions. The particular nature and arrangement of the R groups on the framework will largely determine what complements of foreign ions are appropriate. It is therefore to be expected that individual proteins will exhibit specific requirements as regards crystallizing media. It will be noticed that this discussion strongly suggests throughout that the crystallizability of proteins carries with it no implication of " purity ", nor any implication regarding the size of the protein molecules. Such implications, which may perhaps be justifiable in some cases, lose all justification when polyhedral cage-like structures are under consideration. The considerable area of the individual faces of the polyhedra, in which the atoms of the amino acids are localized, suggests that the formation of adequate numbers of intermolecular links is not dependent upon the smallness of the molecules. The considerable volumes within and between the polyhedral frameworks implies the possibility that large numbers of foreign molecules and ions may be present.

The interchangeability of occupants of cages of the silicates further suggests that this may also be a characteristic of proteins. We may then expect that one and the same protein may be able to form crystals with vastly different complements of foreign ions, and in particular that the hydration terms will vary enormously with different crystallizing media. Very different water contents will also result when, as may sometimes be the case, the cyclol cages of one and the same protein exhibit more than one type of packing.

IV. *The Experimental Facts relating to the Hydration of Protein Crystals.*

A large number of the deductions from the cyclol hypothesis in the present phase of development can be tested by means of experimental facts which are either known already or could be ascertained by experiments following the lines of others already performed. The first prediction that protein crystals must contain considerable numbers of foreign molecules is amply substantiated by innumerable facts. No protein crystal is known which does not contain numbers of water molecules. Many estimates of the water in protein crystals have been given by Adair and Adair (1936), which amply bear out the suggested picture of a protein as a molecule having in the crystal lattice varying degrees of hydration. Thus the figures for egg albumin give 32·4 per cent. and 22 per cent. respectively for the water for crystals obtained from two different media. This enormous relative difference in the amount of water is very striking. The first figure gives 2·16 water molecules per residue of weight (say) 120, the second 1·47. Corresponding figures for a number of other proteins are of the same order of magnitude. Thus for horse hæmoglobin they are 16·6 to 34·4 per cent., for sheep hæmoglobin 18·3 to 33·8, and for serum albumin 18·2 to 34·4. The figures for edestin are lower, namely 6·3 to 14·3 per cent.; this result is interesting in view of the high content of glycine, to which attention has already been directed.

It is of great interest to compare the two hydration values obtained by Adair and Adair for egg albumin with the hydration values which would be deduced on the cyclol theory from Svedberg's molecular weight determination. The molecular weight given by Svedberg for egg albumin (1937) is $M_s=43{,}800$. We will suppose that the molecule consists of $72k$ residues and γ water molecules per residue. It then follows that if w is the hydration and r the average residue weight

$$M=72k(r+18\gamma)=72kr(1+w)=72kr_a,$$

where r_a may be called the "apparent residue weight." Now $M/72=608{\cdot}33$. Thus, if the molecule consists of 3, 4, or 5 times 72 residues, the corresponding values of r_a are 202·77, 153·08, and 121·66. It may be presumed

that apparent residue weights greater or less than these are out of the question. If we now assume that R is (say) 120, it follows that the values of w for $k=3$, 4, and 5, are respectively ·69, ·27, and ·01. Only the value for $k=4$ appears plausible in the light of the figures of Adair and Adair. We then again repeat the suggestion, which we first put forward in 1936, that egg albumin is a 288 amino acid residue structure *, a suggestion which, assuming Svedberg's figure, implies that the molecule, as it existed in the centrifuge, had a hydration of about 27 per cent., giving $\gamma=1{\cdot}77$.

V. *The Stability of Cyclol Cages.*

The precedent afforded by the general cage structure of the silicates is interesting, but it must be noted that they differ in several important respects from the cyclol structures. The silicates consist of cage colonies, in which great numbers of cages are juxtaposed, and each piece of the network functions as the boundary of two cages. The network in this case consists simply of oxygen and silicon (or possibly aluminium), and there is no sense in which the network has two sides which may be differentiated. In the cyclol structures, on the other hand, the network is essentially dorsiventral. In the compound cyclol (Wrinch, 1938 *b*) we postulate the apposition of slits, of edges, or of faces, but even in the last case there is no question of a network functioning as a part of two cages. The presence of the R groups carried by the cyclol network, which may be of considerable size (*e. g.*, in the case of arginine and tyrosine), makes the unit in cyclol structures essentially a single cage, though these may be interlinked at shorter or longer distances and in various ways in the compound structures. There is, therefore, an immense difference, from the point of view of the geometry alone, which goes far in itself to explain the difference in stability between the minerals and the proteins. The stability of an indefinitely continued colony of cages offers a striking contrast with the stability of a certain number of separate cages more or less closely and more or less firmly linked, still more with that of a single cage existing in isolation.

* Reference may also be made to the paper by Bergmann and Niemann (1937), in which it is stated that the chemical analysis of egg albumin allows the deduction that each molecule contains 288 residues.

We may first consider the stability characteristics to be expected of a single closed cyclol molecule. This molecule consists of a portion of the cyclol fabric which is bent about a series of lines in such a way that it forms a cage-like space-enclosing structure. The C_n cyclols in particular are cages in which the fabric is bent round so that considerable parts of it are plane in the sense that they have a single median plane (see Pl. IX. figs. 2 & 3). The whole fabric, in fact, has eight median planes, namely the eight faces of the polyhedral framework of the molecule shown in fig. 5, and so comprises eight plane pieces of fabric. Four of these lie on the hexagonal faces of the polyhedral framework; the other four lie on the triangular faces of the polyhedral framework. The detailed structures of these

Fig. 5.

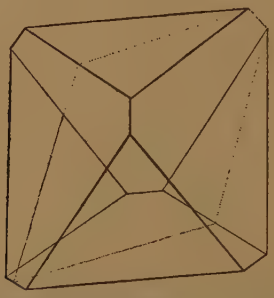

The polyhedral frame of the C_2 molecule.—['Transactions of the Faraday Society,' xxxiii. 1368 (October 1937), p. 1373.]

are shown in fig. 6 for C_1, in fig. 7 for C_2. The C_n cyclols thus possess eight different median planes which abut in twelve edges, over which the fabric is bent. These plane pieces of fabric abut four at a time in six special lacunæ of standard type and size which occur in all the C_n molecules, independently of the value of n.

Treating the problem of closed cyclols in terms of the concept of three-way graphs (König, 1936), it was found that any closed cyclol whatever must possess some type of lacuna other than that found in open cyclols (Wrinch, 1937 *d*). In the case of the C_n cyclols this lacuna is of the type shown in Pl. IX. figs. 2 & 3, and arguments of a purely topological nature show that there can be six and only six of them. The problems of constructing

closed cyclols, indeed, resolves itself into the problem of possible types of lacunæ. The C_n series follows at once when the lacunal type shown in Pl. IX. figs. 2 & 3 is postulated.

Fig. 6.

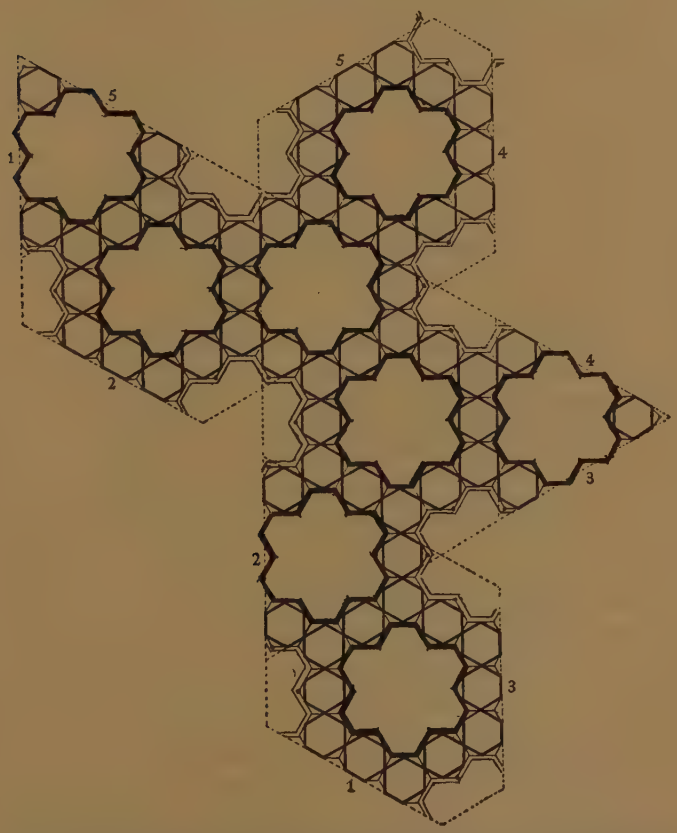

The complete fabric of a C_1 structure. It is shown fragmented into eight hexapeptide anhydrides and six tetrapeptide anhydrides, by means of $\overset{\downarrow}{N}-C(OH)\rightarrow NH$, CO changes.

The essential difference between any closed cyclol and an open cyclol thus resides in the fact that an open cyclol may or may not have a single median plane, whereas a closed cyclol must have a number of median planes and, in addition, a definite number of special regions or slits,

representing new types of lacunæ in the fabric. Evidently therefore a closed cyclol has faces which have the same order of stability as an open plane cyclol. We presume for the moment that the edges are less stable, and the slits even less so.

Fig. 7.

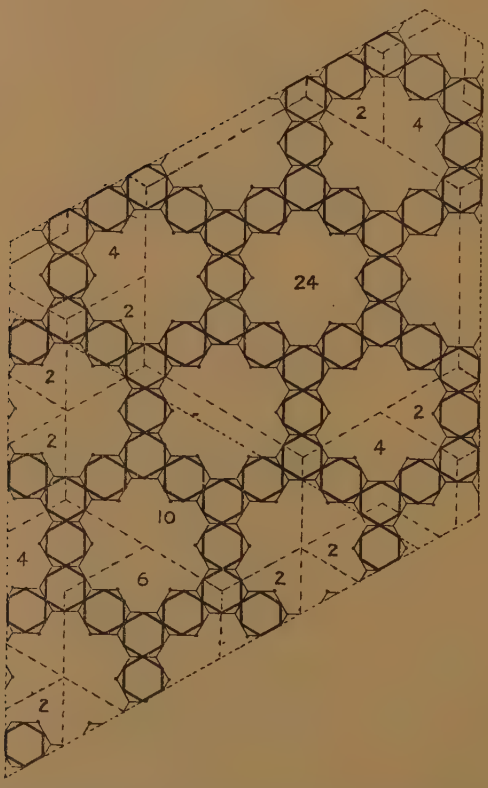

One-quarter of the fabric of a C_2 structure. It is shown fragmented into one 24 residue structure, one 10 residue structure, one 6 residue structure, four 4 residue structures, and eight 2 residue structures.

We suppose now that at any point in the closed cyclol molecule one or more of the links are broken. We may visualize an isomeric break which replaces an $\diagdown\!\!\diagup N-(HO)C\diagdown\!\!\diagup$ link by $\diagdown\!\!\diagup NH\ OC\diagdown\!\!\diagup$ groups. The linked N—C atoms are

at a distance apart of say 1·5 Å.; the unlinked NC atoms will push apart until they are at least 2·8 Å. to 4·2 Å. apart. In consequence no break can occur in isolation. Either it is repaired or a number of neighbouring breaks will occur. This may be accompanied by the formation of new links as indicated in fig. 8.

If, as presumed, the slits are regions of weakness in the cyclol structures, then breaks will in general be initiated at

Fig. 8.

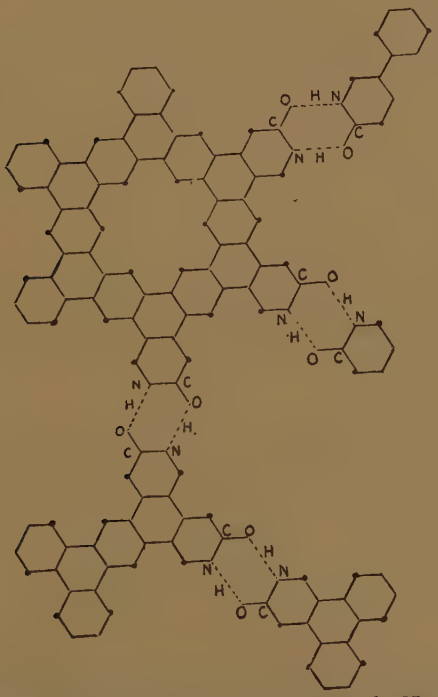

Some of the fragments obtainable from a C_2 structure by N—C(OH)→NH, CO changes, as shown in fig. 7. Dotted lines indicate the possibility of the interlinking of fragments by means of N . . H . . O hydrogen bonds.

a slit. Such a break may initiate a ripping of the network along edges contiguous to it. The process of ripping may result in a partially opened cyclol cage. Ripping may, on the other hand, proceed until the cyclol cage is broken up into a number of larger or smaller plane fragments.

If we take the C_2 structures as an example, the plane fragments (which presumably come from pieces of the cyclol fabric lying on a single face) can include diketopiperazines and cyclols comprising 4, 6, 10, 24 residues (figs. 7 & 8). For cyclol C_3 we add cyclols comprising as many as forty-two residues, and so on.

All these fragments are of cyclol type with a distribution of CO–NH groups round the periphery. It is also possible by breaking $\diagdown\!\!\diagup N-(HO)C\diagdown\!\!\diagup$ links to get polypeptide anhydrides. Thus the fabric of a C_n molecule can yield (as is shown in fig. 6 for the C_1 fabric) closed polypeptides consisting of four and six residues, *i. e.*, tetrapeptide anhydrides and hexapeptide anhydrides. Products combining both types of structure are also possible. In all these cases fragments are formed by replacing $\diagdown\!\!\diagup N-(HO)C\diagdown\!\!\diagup$ situations by new $\diagdown\!\!\diagup NH,\ OC\diagdown\!\!\diagup$ groups.

Hydrolytic breaking of certain —NH—CO— links in these products already discussed will give open polypeptides, partially or completely uncyclized, and products in which such open polypeptides are linked by cyclol links.

We have here given some indication of the different types of product (which, though large in number, are mathematically determinate) which can result from the breaking of N—C(OH) links. Evidently permissible paths along which fragmentation can take place must to some extent be conditioned by the nature and arrangement of R groups which give to each protein its specific character. It is possible that, in certain cases, only a few products will be formed. Thus a C_n structure, which is made up of six tetrapeptide anhydrides and $(12n^2-4)$ hexapeptide anhydrides, linked back to back by cyclol links (see fig. 6 for the case of C_1), may fall solely into these two products. Alternatively it may fall into these $(12n^2-4)$ cyclol structures and 12 diketopiperazines, or any C_n structure ($n>1$) may fall into 8 fragments by breaking along its edges, and so on. In the case of each type of fragmentation the number of breaks due to the replacement of N—C(OH) situations by NH CO situations can be calculated.

The testing of these predictions as to possible types of

degradation products of proteins would be a matter of great interest from the point of view of protein structure in general. The cyclol theory, originally devised with a view to explaining the very small number of free-amino groups in proteins (Wrinch, 1936), interprets this fact to mean that there are in proteins few if any open polypeptides, but instead polypeptide anhydrides interlinked by $\rangle N-(HO)C\langle$ bonds. The fact that (open) polypeptides are found when proteins are treated with aqueous solvents is perfectly consistent with this view, and there is little possibility on these lines of deciding between the polypeptide hypothesis in its original form and as modified by the introduction of multiple peptide links. We anticipate, however, that products of cyclol type may appear when the intact protein is treated with anhydrous solvents *, particularly solvents whose molecules contain hydroxyls. Even then the existence of considerable numbers of water molecules in the intact protein may lead to some hydrolysis, and thus to the appearance of products which are only partially cyclized.

So far we have considered only the stability of the single closed cyclols proposed as the structure of certain globular proteins. For globular proteins which manifest the phenomenon of reversible dissociation a compound structure consisting of a few, or even many, closed cyclols in association has been proposed (Wrinch, 1938 *b*). The fact that closed cyclols presumably have a certain number of regions which are less stable than open cyclols gives to the compound structures a considerable significance in terms of stability considerations. Thus in the case of a compound cyclol, such as that shown in fig. 9, two units are linked by a slit. The compound structure has ten slits, whereas the single cyclols have six slits each;

* In this connexion reference may be made to a series of papers of Fodor and his collaborators (*Zeits. f. Phys. Chem.* clxxi. p. 222 (1927); Kolloid, *Zeits. f. phys. Chem.* lxiii. p. 203 (1933), *Biochem. Zeit.* cclxii. p. 69 (1933); Kolloid, *Zeits. f. phys. Chem.* lxxiv. p. 66 (1936); *Enzymologia*, i. p. 311 (1936), iv. p. 36 (1937)) in which products have been obtained from proteins, by the use of anhydrous solvents, which are not polypeptides. Attention is also called to the fact that the existence of $\rangle N-(HO)C\langle$ links in proteins, which is postulated in the cyclol theory of protein structure (Wrinch, 1936), was already suggested in 1927 by Fodor and Epstein in a paper in the *Zeit. f. phys. Chem.* clxxi. p. 222.

Fig. 9.

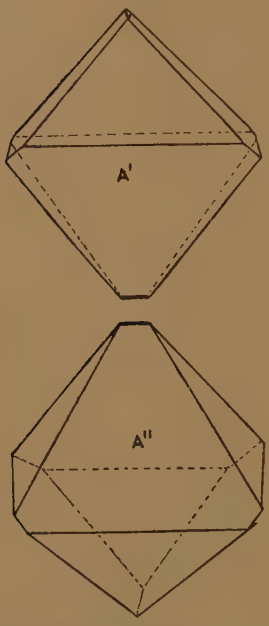

A compound structure consisting of A and A′, a pair of C_n units (drawn for $n=2$). The units have one slit apposed.

Fig. 10.

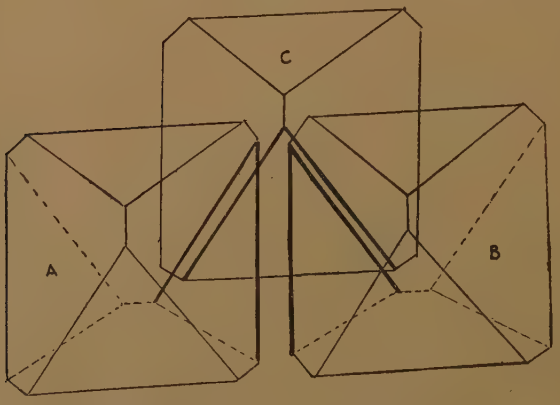

A compound structure consisting of A ,B, C, a trio of C_n units (drawn for $n=2$). A and B, B and C, C dna A have one edge apposed.

the number of slits per residue is thus reduced in the ratio 6 to 5. In the case of such a structure as that shown in fig. 10 the slits are partially apposed, and the ratio of unassociated slits is reduced from 6 per $72n^2$ residues to 10 per $3\times72n^2$ residues, *i. e.*, in the ratio 9 to 5. The number of unassociated slits per residue offers in fact a convenient way of characterizing compound structures. In an earlier communication (Wrinch, 1937 *a*) the idea of an index for open cyclols, defined as the number of CO—NH groups per residue, was introduced. A polypeptide anhydride has index unity, the cyclol 6 molecule index 1/2, cyclol 18 index 1/3, and so on. This index, worked out for a number of closed cyclols, was as small as 1/6 for a certain 162 residue structure. It was found that any index, however small, can be attained in an open cyclol provided a minimum number of residues is present. The idea of a closed cyclol falls into line when it is noticed that closed cyclols may be defined as structures with zero index. This zero index is, however, only attained at the cost of the existence of a certain number of regions (six for C_n cyclols) which are presumably less stable than the open cyclols.

In the same kind of way therefore we may define the "slit" index as the number of slits per residue. Then C_1 has index 1/12, C_2 index 1/48, and C_n index $1/12n^2$. This gives a measure of the number of regions of maximum instability per residue. Any association of C_n units, where slits are juxtaposed, has then a smaller index than C_n and so a smaller proportion of specially unstable regions. Just as cyclols reduce their CO NH index by polymerization, so single cyclol cages reduce their slit index by association.

VI. *Protein Denaturation.*

There can be no doubt, as Wu (1931) says, that the liability to denaturation of proteins is associated with some peculiarity in the structure of their molecules, since no other class of substance possesses this property. It has already been suggested that the cage-like structures, which have been deduced for the globular proteins, will on occasion exhibit characteristic behaviour due to the opening of these cages, and we suggest, as a basis for discussion, that the "peculiarity" about proteins is the

cage-like structure, and that the essential feature of many different types of denaturation may consist simply in the opening or breaking up of cages. Since the cages can open in many different ways the denatured protein, on this theory, provides a striking contrast to the native protein, whose configuration is perfectly definite. The cyclol hypothesis thus leads to the view to which Mirsky and Pauling (1936) have been led by a consideration of energy data that " the characteristic specific properties of native proteins " are to be attributed to their " uniquely defined configurations," whereas the denatured protein is characterized by the absence of a " uniquely defined configuration." As Wu (1931) has pointed out, " the compact and orderly structure of the native protein is disorganized on denaturation." There is, we presume, general agreement on this aspect of the difference between the structure of native and denatured protein. The form of the " uniquely defined configuration " of native proteins, therefore, remains the outstanding question.

As Wu was perhaps the first writer to point out explicitly, " the crystallizability of the natural and soluble proteins indicates that their molecule is not an open and flexible chain, but a more or less rigid structure." This conclusion is amply confirmed by Svedberg's findings, which attribute to these proteins structures of " globular " type. " What kind of structure," asks Wu, " can there be in the natural protein molecule and not in the denatured protein or in the polypeptide ? " " All the amino acid radicals in the natural protein molecule," he continues, " are in the molecule of the denatured protein or polypeptide." And he draws the conclusion that there is some interlinking of amino acid radicals in the intact protein which is absent in the denatured protein.

The logical procedure is therefore to consider in turn all types of link and to investigate the deductions to be drawn from those which pass the qualifying test of being geometrically feasible. It appears that any proposed structure for the globular proteins must satisfy three conditions : it must explain the non-random distribution of the molecular weights of proteins established by Svedberg ; it must interpret the nature of the " globularity " which Svedberg attributes to them ; and it must explain the spontaneous formation of protein films from proteins in solution, and give for these films structures which

are in accordance with their known mechanical properties.

Among the links so far proposed are (*a*) hydrogen and hydroxyl bonds and (*b*) cyclol links. In a number of communications (Jordan Lloyd, 1932; Astbury and Woods, 1933; Wrinch, 1936; Wrinch and Jordan Lloyd, 1936; Mirsky and Pauling, 1936; Huggins, 1937) suggestions which fall into the category (*a*) have been partially developed. It is not yet known whether it is possible to devise structures on these lines which satisfy the three conditions formulated. In the hope of settling this point the line of investigation indicated by Wrinch and Jordan Lloyd (1936) is being continued. Meanwhile the cyclol hypothesis (which, in addition to hydrogen and hydroxyl bonds, postulates also the existence of cyclol links (Astbury, 1936 *a*, *b*) in the native protein), is being further developed, since this hypothesis yields, by straight deductions from its premises, structures for the globular proteins which satisfy the conditions. Its implications with regard to protein denaturation, interpreted as a set of phenomena concerned with the opening or fragmentation of cage will now be considered.

The cyclol cage may, we presume, be broken open or caused to fragment by many different agencies, in particular when linkages with foreign molecules such as waters are broken and the covering of the cyclol fabric is disturbed asymmetrically. Denaturation, on this view, requires a certain minimum number of breaks. The number may be considerable, since otherwise the breaks may be repaired and denaturation will not result. The necessary minimum of breaks depends to some extent upon the specific character of the protein, since the R groups no doubt play a part in determining at what point the disturbance of the fabric by individual breaks is sufficient to lead to further tearing. The tearing open of a cyclol fabric may be, but need not be, reversible (Anson and Mirsky, 1934). It will be apparent that a C_n structure, containing $144n^2$ $\diagdown N-(HO)C\diagup\diagdown$ links can be torn open in a vast number of ways, dependent upon which set of links is broken. The cyclol links, say of length 1·5 Å., on breaking give instead an equal number of $\diagdown NH$, $OC\diagup\diagdown$ groups. Thus denaturation may also be accompanied by the formation

of hydrogen bonds (*cf.* fig. 8) between the newly occurring $\diagdown$NH, OC$\diagup$ groups.

The number of different configurations geometrically available for a denatured protein on the present hypothesis is therefore enormous. This is in accordance with the fact that in the case of trypsin (Northrop, 1930, 1932), for example, the entropy of denatured protein is very much greater than that of native protein. In calling attention to the big difference in entropy of denatured and native trypsin, and pointing out that it implies an enormous number of different configurations for the denatured protein, Mirsky and Pauling estimate the number to be as high as 10^{20}, a number which may not be impossible on the present hypothesis, which gives trypsin (say) 576 N—C(OH) links per molecule. Energy data for proteins have also been discussed by Stearn and Eyring (1937), who point out that the bonds broken in denaturation must be such as to provide a degree of randomness in the activated molecule unusual in chemical reactions. The present picture of denaturation as essentially a tearing open or fragmentation of a closed fabric which can happen in vast numbers of different ways is not inconsistent with this conclusion ; on the contrary, it offers a precise interpretation in geometrical terms of the " unusual degree of randomness," and shows how it may be interpretable by the structure of the two-dimensional network which on the present theory is the essential entity in proteins.

Many other facts regarding proteins can also be interpreted on the present theory. Denatured protein, consisting of partially opened or fragmented cages, will have an increased viscosity (Loughlin and Lewis, 1932 ; Astbury, Dickenson, and Bailey, 1935) ; the variety of its forms will inhibit crystallization. Changes in the immunological properties may also occur. On the view that a protein is characterized by a special type of fabric the specific character of an individual protein is located in the specific nature and arrangement of R groups carried by the fabric. Immunological reactions, remarkable for their high degree of specificity, presumably are concerned with the " front " surfaces of proteins (Wrinch, 1936). On fragmentation it may happen that some essential constellation of R groups is broken up. In such a case the original specificity of the protein will be destroyed, and possibly a new specificity

may be created, as has been shown to be the case for egg albumin by Wu, Tenbroeck, and Li (1927). The interesting finding by these authors that egg albumin denatured by heat, by alcohol, and by alkali are closely related immunologically is also interpretable in terms of the suggestion made earlier that permissible paths of fragmentation are dependent essentially on the arrangement of the R groups, *i. e.*, upon the specificity of the individual protein.

We may also anticipate that a globular protein molecule in solution may break open and so denature if one of its slits momentarily reaches the surface. Molecules of the solvent, for example, are presumably linked to nitrogens and/or peptide hydroxyls of the fabric of a protein molecule in the body of the solution, and form a covering for the molecule. Withdrawing some of these foreign molecules asymmetrically may then cause the cage to break open and fragment. We suggest that protein films can be formed in this way, a view in line with those of Gorter (1934) and Neurath (1936). Evidently on this view the activity of enzymes such as pepsin and urease may or may not be affected by surface denaturation. In cases where activity is still present (Langmuir and Schaefer, 1938) the interpretation offered is that some at least of the essential complex of groups involved have not been disturbed by fragmentation.

VII. *Structures proposed for Protein Films.*

It has often been emphasized that, owing to the uniform configuration of the amino acids obtained from proteins, the cyclol fabric is dorsiventral in the sense that the C_β atoms emerge from the "front" of the fabric and none emerges from the "back" (Wrinch, 1936). The moment a cage opens this essential characteristic becomes relevant in the sense that the broken cage may allow itself to be flattened out on to the surface with the front surface of the fabric (carrying all the $C_\beta H_2$ groups) out of the water phase. The splitting of only slightly opened cages can no doubt be inhibited by sufficiently high pressures, but under appropriate conditions (and these include a low enough surface pressure) the cages, we presume, break down into plane fragments. We suggest that fairly uniform protein monolayers under low pressures are formed from plane fragments carrying R groups sufficiently non-hydrophilic to allow them to float in the surface, and

that these fragments are interlinked either by hydrogen bonds or by salt linkages between R^+ and R^- groups, or by the formation of new cyclol links. An essential step in film denaturation (probably in denaturation in general) may thus consist in the formation of new links. In view of the types of fragment, a protein monolayer can never form a complete cyclol fabric. The last type of interlinking consists essentially in the polymerization of cyclol fragments, and some of the possibilities with regard to this type of structure and the corresponding surface densities have already been worked out (Wrinch, 1937 *a*). Thus for a polymer of cyclol 18 the density is $1{\cdot}425\times10^{-7}$ g./cm.^{2} for an average residue weight of 120. Similarly, a cyclol 66 polymer can be constructed with density $1{\cdot}16\times10^{-7}$ g./cm.^{2}. For polymers of higher cyclols the densities are correspondingly lower.

The first type of interlinking has been worked out for the particular case of cyclol 6 by Wrinch and Jordan Lloyd (1936), and yields, for an average residue weight of 120, a surface density of $\cdot76\times10^{-7}$ g./cm.^{2}. The corresponding structure with cyclol 18 gives a density of $\cdot73\times10^{-7}$ g./cm.^{2} The interlinking by means of R^+ and R^- groups depends essentially upon the specificity of the protein and upon the electrolytes present, and can be worked out for any particular case.

In the case of a protein film formed by interlinking of cyclol fragments considerable variation in thickness may be anticipated. To find the minimum thickness we consider the case when the fragments are interlinked in such a way that the ionized R groups which emerge from the upper surfaces are curved round so that the carboxyl or guanidine or amino groups lie in the water phase. The thickness of the film is then determined by the length of the hydrocarbon side chains. For glycine for which R is H, for alanine for which R is CH_3, for valine for which R is $CH(CH_3)_2$, for leucine for which R is $CH_2{-}CH(CH_3)_2$, and for phenylalanine for which R is $CH_2{-}C_6H_5$, the maximum thicknesses of HO . . . . .C are roughly 1·87 Å., 3·41 Å., 3·92 Å., 5·46 Å., 5·78 Å., as shown in fig. 11. (We have taken C—OH as 1·36 Å., as in resorcinol (Robertson, 1936), and C—C as 1·54 Å. and C=C as 1·41 Å.). Suppose now that such a film is used to form built-up protein films of AB type (Langmuir, Schaefer, and Wrinch, 1937). If the phenylalanine R groups of consecutive layers are

apposed we may allow 3·60 Å. for the distance CH . . .CH, as in naphthalene (Robertson, 1933 *b*). If methyl groups of consecutive layers are apposed we may allow 3·87 Å. for the $CH_3 \ldots CH_3$ distance, as in durene (Robertson, 1933 *a*). For the distance between hydroxyl of consecutive layers we may take (say) 2·8 Å. in view of the dimensions of kaolinite given by Pauling (1934) and the "effective radius of hydroxyl towards hydroxyl" given by Bernal and Megaw (1935). The layer thicknesses (see fig. 11) when phenylalanines are apposed is then 5·78+(2·8+3·6)/2=8·98 Å.; when leucines are apposed it is 5·46+(2·8+3·87)/2=8·80 Å.; when alanines are apposed 3·41+(2·8+3·87)/2=6·745 Å.; when leucines or phenyl-

Fig. 11.

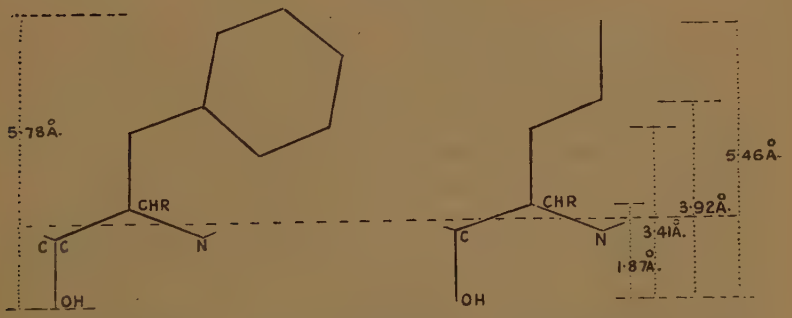

The orientation of various residues $\rangle N-CHR-C(OH)\langle$ in the cyclol fabric, indicating the thicknesses to be expected of protein monolayers containing glycine, alanine, valine, leucine, tyrosine. The position of the median plane of the fabric is indicated by long dashes.

alanines are apposed to alanines, say [6·745+8·89]/2=7·82Å. Roughly, thicknesses from about 6·75 Å. upwards seem to be indicated. Evidently such thin films can only be formed when the pressure is sufficiently small (*cf.* Neurath, 1937) and allows the R^+ and R^- groups to curve round so that ionized groups lie in the water phase, and when the *p*H is appropriate to the chemical composition of the individual protein.

Thicker films of protein are also to be expected under appropriate circumstances. For suppose that the cages are only partially opened; the dorsiventrality of the cyclol fabric even then has its effect, and a collection of very

partially opened cages held in the surface of the solution by hydrocarbon R groups will give layers of considerable thickness when used for built-up films. Thus a single layer of partially opened C_2 structures may have a very considerable thickness, comparable with their longest diameters (say) 48 Å., and interlinking at different levels of such structures may indeed yield layers several times as thick.

It may be presumed that there is the same variety in types of interlinking for partially opened cages as has been postulated for the same plane cyclol fragments discussed earlier. Further, an essential condition for maintaining the stability of a thick film is, we presume, a high enough

Fig. 12.

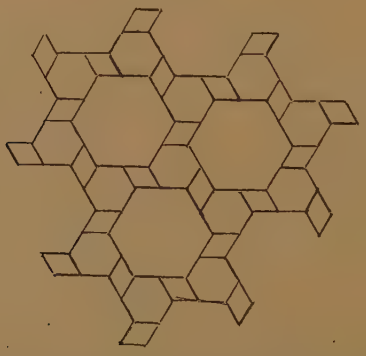

A fragment of cyclol fabric, in which the diazine hexagons have their median planes at the tetrahedral angle to the median plane of the triazine hexagons.

pressure. A progressive splitting into plane fragments, which are geometrically capable of forming uniform thin films, may take place when the pressure is reduced.

Dependent upon changes of pressure, different types of interlinking entail very considerable changes in the thickness: these intermolecular changes are apparently reversible, resulting in a high degree of elasticity.

Protein films may also exhibit elasticity due to intramolecular adjustments. For consider the area per residue *within* any cyclol fragment. When it has one median plane the area per residue is $B=10{\cdot}4$ Å^2. But it is also capable geometrically of assuming the position shown in fig. 12, in which the area per residue is 7 B/12,

and, indeed, of assuming still more contracted positions. The essential point about the cyclol fabric is involved in this transition, namely, the fact that two hexagons sharing two atoms can stand in only one of two relations to one another. They may share a median plane, as is the case with all the hexagons in fig. 1, or they may have median planes abutting at the tetrahedral angle of 109° 28′ 16″. It is possible that "switching" between such positions as those indicated in figs. 1 & 12 (as Langmuir has called it) may occur very readily, and that a cyclol fragment in the surface of a solution may change reversibly between such configurations. This suggestion gains plausibility when it is noticed that the cyclol fabric has hydroxyl groups on both sides, front and back, so that a certain degree of waviness may be expected.

VIII. *Experimental Facts relating to Protein Films.*

It is claimed that the structures proposed for protein films give a picture which in general terms fits the facts.

(1) It has been suggested by Bernal (1937) that it is improbable that polypeptide chains give surface films at all, "because owing to their flexibility the hydrophilic groups would be equally available on all sides, and true solution rather than surface adsorption would take place." Whether this is so or not, it appears to be well established by a considerable number of experiments that the essential unit in protein films is a two-dimensional dorsiventral network of atoms. This view, implicit in much of the work on protein films during the past ten years, was directly tested in a series of experiments by Langmuir, Schaefer, and Wrinch (1937), who concluded that "the properties of protein films as shown in the experiments seem to be in accord with the view that the protein monolayer is a two-dimensional network held together by strong elastic springs, and are not in accord with a structure consisting of polypeptide chains." In this research monolayers of protein from a water surface were transferred on to solid surfaces. A single monolayer can be transferred to a prepared plate, covered with 37–49 layers of barum stearate, in two different ways. In the first method, which we denoted as method A, the plate, held in a vertical plane, is lowered into the water. The plate is then kept immersed in the water while the protein film is removed from the surface by scraping and by blowing any residual film to

the other end of the tray, where it may be confined behind a barrier. The plate when raised out of the water comes out wet, whereas if the protein film had not been placed upon the plate the plate would have shed water when it was withdrawn. The second method of applying the protein film, which we called method B, consists in lowering the prepared plate vertically through a clean water surface, then applying the protein film as before, and raising the plate out through the film. The plate comes out wet and only shows interference colours after the water dries. Multiple films were also constructed. Several experiments were performed which allowed direct deductions as to the nature of A and B layers to be made. Thus A and B layers were partly covered by petrolatum; a drop of water was placed on an adjacent place on the layer, and on tilting the plate it was found that the water displaces the hydrocarbon to some extent in both cases, more with an A film than with a B film. We concluded that there are hydrophilic groups on both surfaces (the peptide hydroxyls), but that there is a preponderance of hydrophobic groups (belonging to R groups which are dorsiventrally arranged) on the outer surface of a B film. Striking evidence that the outer surface of A and the inner surface of B are predominantly hydrophilic was given by the ejection on to the water of a B layer which rests upon an A layer. This action is undoubtedly due to the affinity of this hydrophilic interface for water.

Further evidence for the essential dorsiventrality of protein films is afforded by recent experiments on urease (Langmuir and Schaefer, 1938). Urease, it is found, may be built up as A or B films. Urease films can also be built on conditioned surfaces. There is some evidence for the view that individual films of urease can turn inside out. This behaviour allows of interpretation in terms of the cyclol fabric. For by means of $N-C(OH) \rightarrow NH\ CO \rightarrow N-C(OH)$ tautomeric changes, the units (which polymerized constitute the cyclol fragments) can turn through 180°. This change cannot be confined to, but may well be initiated by, one single unit, say a two residue unit. When one unit has turned neighbouring units presumably follow suit, so that the whole cyclol fragment turns inside out. It is found that a film can be placed on a thorium-conditioned surface and held with its hydrophobic side outside, and that a film can be placed on a desoxycholate

surface and held with its hydrophobic side inside. When the activity of the urease film is tested by immersion in urea solution it is found that only the film with its hydrophobic surface outside is active. This experiment clearly indicates that the two sides of the urease fabric differ and that the activity of urease is associated with its hydrophobic side only. Evidently, therefore, the globular urease molecule is an extravert, and its enzymatic activity is dependent upon some complex of R groups, that is, upon the particular nature and arrangement of some of the amino acid residues in the molecule. In the cyclol hypothesis the uniform configuration of all the amino acids obtained from proteins is interpreted to mean that the specific character of a protein (which is manifested in reactions of an enzymatic or immunological character and in other ways) can be associated with one side only of the protein fabric (Wrinch, 1936). It is of interest to find that this prediction is now confirmed for urease.

(2) It is well established that uniform films give surface densities which vary from protein to protein within limits (owing, *inter alia*, to variations in the length and number of R^+ and R^- groups), and for one and the same protein vary with pressure, owing we suggest to differences in interlinking and intramolecular modifications. The various figures given earlier are to be regarded simply as rough estimates of the order of magnitude of the surface densities which protein films would have on the cyclol hypothesis. Actual figures obtained from protein, especially as monolayers of gliadin, glutenin, egg albumin, zein, serum albumin, and serum globulin range from $1{\cdot}724 \times 10^{-7}$ g./cm.^{2} for serum globulin to $1{\cdot}111 \times 10^{-7}$ g./cm.^{2} for serum albumin (Schulman and Rideal, 1933; Gorter, 1934; Gorter and van Ormondt, 1935). The rough estimates given above are evidently satisfactory in their order of magnitude.

In the studies of protein films by the methods of Langmuir and Blodgett direct optical measurements of layer thicknesses have been made for the first time. Thicknesses as small as 6 Å. for egg albumin, gliadin, and zein, and 9 Å. for pepsin at zero pressure have been deduced (Langmuir and Schaefer, 1938). These we interpret in terms of cyclol fragments, as shown in fig. 8, which can give thicknesses ranging from (say) 6·75 Å., to 9·0 Å., as shown in fig. 11. On the other hand, enormously

greater thicknesses have also been found which allow of interpretation on the cyclol hypothesis in terms of the interlinking at different levels of partially opened cyclol cages. The extremely high elasticity expected with these structures has long been known to be a property of proteins. The most mild type of "switching," shown in fig. 12, entails a contraction factor of 7/12. To test the view that the contraction of protein films is due to differences in interlinking of cyclol fragments and to intramolecular modifications of the type shown in fig. 12, formaldehyde was added to the water under a protein film (Langmuir, Schaefer, and Wrinch, 1937). It was found that the compressibility was greatly reduced, presumably owing to links (possibly methylene bridges) being formed by the formaldehyde molecules between cyclol fragments; this restricts their freedom as regards "switching" and as regards changes in interlinking.

The highly hydrophilic nature of the cyclol fabric, which carries one peptide hydroxyl per residue, appears to be to some extent confirmed. As suggested earlier, it is to be expected that such a fabric will whenever possible be highly hydrated. Figures for the hydration of egg albumin films have been given by Neurath and Bull (1936). These authors claim to have demonstrated that there is 19–20 per cent. hydration "in the film," which means 1·27 to 1·33 water molecules per residue of weight 120. The estimates given earlier suggested a maximum of two water molecules per residue for an indefinitely extended cyclol network, and a somewhat smaller number for cyclol fragments.

(3) The postulated existence of compound cyclol structures for certain of the proteins suggests that there should be a considerable difference in the circumstances in which film formation takes place for the simple and the compound globular proteins. It has been pointed out by Philippi (1936) that certain proteins only spread at the values of the *p*H which lie outside the isoelectric zone of the individual protein. We suggest that in such cases the structure is compound, and that the division of the compound structure into single cyclol units is necessary before the cages are broken open. It should be emphasized that the breakdown of a compound structure into sub-groups of units, or even into single units, does not necessarily involve any breaking of cages.

IX. *The Interrelations of Film and Globular Proteins.*

The figures quoted from Neurath and Bull were obtained in a research on the relation between egg albumin in solution and when film-denatured. Striking differences in hydration were found. Thus in solution the figure was 36 per cent. This represents 2·4 water molecules per residue of weight 120, as contrasted with 1·27 to 1·33 in the film, *i. e.*, an increase of about one water molecule per residue.

We consider that much can be deduced as to the structures of the "globular" egg albumin molecule from this figure alone. We have already pointed out that, while Svedberg's results indicate clearly that egg albumin (and many other proteins) in appropriate solutions are "globular" in some sense, so far nothing has been deducible from their results as to the geometrical nature of this globularity. It can, perhaps, be the type of globularity possessed by a lump of matter, where the atoms are distributed throughout a three-dimensional space, or it can perhaps be the type possessed by a hollow body, where the atoms are distributed on a space-enclosing surface, or it can perhaps be of the type possessed by a number of space-enclosing surfaces juxtaposed. On the cyclol theory an interpretation in line with the second and third types is offered. A crucial test for the theory therefore (in so far as it implies cage-like structures for the globular proteins) is to discover whether or not there is any evidence that globular proteins have associated with them in solution, and lose when film-denatured, the considerable numbers of foreign molecules necessary to tenant these spaces which lie within single cyclols and within and between associated cyclols. The figure quoted above answers this question in the affirmative for egg albumin, since it indicates that about one water molecule per residue is lost when the cages are broken, a figure of the order of magnitude required by the cyclol hypothesis. It may be pointed out that the fact that denaturation is associated with loss of water molecules does not on the cyclol hypothesis carry with it the implication that denaturation is a process of condensation. Also, on this hypothesis there is no contradiction in a decrease of hydration being associated with an increased viscosity.

The cyclol hypothesis, as is shown in this and other communications, lends itself to development by means

of purely mathematical arguments. It yields in this way numbers of predictions, many of which are difficult to test. However, the most fundamental of its implications is that the essential unit in proteins is a characteristic fabric or two-dimensional network, dorsiventral in character. This implication, we claim, is already to some extent confirmed. The fact that a protein in solution readily forms a monolayer lends support to the view that the globular proteins are essentially surface distributions of atoms or cages made of a characteristic dorsiventral fabric, the rupture of which yields fragments of the fabric capable (in virtue of their dorsiventral character) of forming monolayers. It is difficult to see how a three-dimensional or volume distribution of amino acid residues could form monolayers spontaneously in this way, and still more difficult to understand how such a metamorphosis, if it were accomplished, would be reversible, as is claimed to be the case for certain proteins.

X. *Conclusions.*

The function of a hypothesis is to link together into a single consistent scheme the largest possible number of experimental facts. We claim that the cyclol hypothesis, in suggesting a cage-like structure for globular proteins, links together many facts which appear to be rather remote from one another, notably those relating to hydration and denaturation. This treatment emphasizes the unique character of proteins among all chemical substances. The cage structure is capable, geometrically speaking, of isomerism on the grand scale. Thus, to take the example of a C_2 structure, 288 residues can be arranged on a polyhedral surface, and again without any change whatsoever of chemical composition (*i. e.*, no question of hydrolysis or its converse is involved) can be arranged in a number of plane fragments. Such an isomerism draws attention to the striking extent to which substances in protein chemistry can differ in viscosity, in capacity for hydration, in their response to changes of temperature, in their immunological reactions and enzymatic activity, and in other respects, without any difference in chemical composition. The nearest approach to such a deep-seated many-sidedness consistent with unchanged chemical composition is, perhaps, the case of the diamond and

graphite. Here we have identical chemical compositions and yet fundamentally different properties. There is, perhaps, a hint of resemblance between proteins and graphite. Although, as we have stressed, the proteins occupy a unique position among chemical substances, it is of interest to notice that practically every characteristic of the structures here suggested for them can be found in some other class of substance. It is the complex of all these characteristics together which defines the protein situation.

The cage structure, for example, is not without precedent. Many different silicates have a cage structure which so far as the individual cage is concerned closely resembles the cyclol cages in their geometry. The important aspect of the protein situation which resides in the hydration of the cyclol network is, however, absent in the silicates. On the other hand, hydrated atomic fabrics are a common feature of the clay minerals. Large masses of water, which we suggest may on occasion tenant the cyclol cages, again, are not without precedent. They are characteristic of the crystals of phosphotungstic acid. But here they are not associated with enclosing networks. The list can be continued. The cyclol picture of protein structure need not, therefore, be considered to be unacceptable because of the novelty of the structures proposed. Practically every aspect of them can be linked to precedents among well-known structures.

The type of argument used in establishing structures of molecules with only a few atoms can, we believe, also be used with profit in an enquiry into the structure of proteins. Thus it will be noticed that many of the arguments used in this communication are based upon the arrangement of hydroxyls and tertiary nitrogens and of water molecules in structures already established on the basis of X-ray analysis. A mass of water molecules in the crystal of phosphotungstic acid is arranged in a certain way ; perhaps therefore masses of water molecules can exist also in other crystals, arranged somewhat in the same manner. If all the oxgyens of these waters in phosphotungstic acid lie at distances apart of 2·84 Å. to 2·90 Å., then perhaps water molecules in protein crystals will arrange themselves at distances apart which are not very different. In certain crystals tertiary nitrogens form hydrogen bonds of definite length with hydroxyl

groups; in protein crystals also such groups, if they are present, may be linked in the same manner. These are examples of the type of argument used. We consider them to be justified. Tables have been published giving measurements for a number of different bond lengths. The implication is that a C—N bond (for example) has a certain autonomy; in the same way measurements of hydrogen and hydroxyl bonds give standard lengths under standard circumstances. It is, indeed, only on assumptions of this type that it has proved possible to make this tremendous progress in analyzing crystal structures of molecules containing numbers of atoms. This procedure has passed the pragmatic test. It is our hope and expectation that its application to the case of the proteins will prove its own justification. We take the view, indeed, that an insulin crystal, for example, which is pure in the sense that it contains only amino acid residues, water molecules, and (say) the correct complement of zinc ions, represents an arrangement in space of atoms which within very narrow limits is just as determinate as the arrangement of atoms in a crystal of phosphotungstic acid. If this is so, its structure is mathematically determinate, and will, we claim, prove mathematically determinable when the requisite number of experimental facts is available.

The thanks of the author are offered to Professor H. S. Taylor, M. L. Anson, and H. Eyring, to Dr. Irving Langmuir, C. P. Haskins, and V. Schaefer, to Professor E. H. Neville, to Professor H. T. Clarke, to M. F. Howson, to Professor Cohn and Dr. Vickery, to Professor Gorter, Dr. J. van Ormondt, and Dr. G. F. Adair, to Professor McBain, to Professor Pauling, and to many American colleagues.

References.

Adair and Adair, Proc. Roy. Soc. B, 819, p. 422 (1936).
Anson and Mirsky, J. Gen. Physiol. xvii. pp. 393 & 399 (1934).
Astbury, J. Text. Inst. xxvii. p. 281 (1936 *a*).
Astbury, *Chemisch. Weekblad*, cxxxiii. p. 778 (1936 *b*).
Astbury and Woods, Phil. Trans. Roy. Soc. p. 817 (1933).
Astbury, Dickinson, and Bailey, Biochem. J. xxix. p. 2351 (1935).
Barth, *Zeit. f. Krist.* lxxxiii. p. 405 (1932).
Bergmann and Niemann, J. Biol. Chem. cxviii. p. 301 (1937).
Bernal, Trans. Faraday Soc. xxxiii. p. 1143 (1937).
Bernal and Megaw, Proc. Roy. Soc. A, cli. p. 384 (1935).
Bradley and Illingworth, Proc. Roy. Soc. A, clvii. p. 113 (1935).

Bragg, ' Atomic Structure of Minerals,' Cornell Univ. Press (1937).
Fischer, *Z. physik. Chem. A.*, clxxvi. p. 260 (1936).
Frank, ' Nature,' cxxxviii. p. 242 (1936).
Gorter, Am. J. of Diseases of Children, xlvii. p. 945 (1934).
Gorter, J. Gen. Physiol. xviii. p. 421 (1935).
Gorter and van Ormondt, Biochem. J. xxix. p. 48 (1935).
Hendriks, Wulf, Hilbert, and Liddel, J. Am. Chem. Soc. lviii. p. 1991 (1936).
Hey and Bannister, Mineral Mag. xxv. pp. 51 & 243 (1932).
Huggins, J. Organic Chem. i. p. 407 (1936).
Huggins, ' Nature,' cxxxix. p. 550 (1937).
Keggin, ' Nature,' cxxxii. p. 351 (1933).
Keggin, Proc. Roy. Soc. A, cxliv. p. 75 (1934).
Konig, ' Theorie der endlichen und unendlichen Graphen ' (Leipzig, 1936).
Jaeger, Westenbrink, and van Melle, Proc. Acad. Amsterdam, xxx. p. 249 (1927).
Jaeger, Baker Lectures, Cornell University, New York (1930).
Jordan Lloyd, Biol. Rev. vii. p. 254 (1932).
Langmuir and Schaefer, J. Amer. Chem. Soc. lix. pp. 1406 & 1762 (1937).
Langmuir and Schaefer, private communication (1938).
Langmuir, Schaefer, and Wrinch, ' Science,' lxxxv. p. 76 (1937).
Loughlin and Lewis, Biochem. J. xxvi. p. 476 (1932).
Mirsky and Pauling, Proc. Nat. Ac. Sci., Washington, xxii. p. 439 (1936).
Neurath, J. Physic. Chem. xl. p. 361 (1936).
Neurath, ' Science,' lxxxv. p. 289 (1937).
Neurath and Bull, J. Biol. Chem. cxv. p. 519 (1936).
Northrop, J. Gen. Physiol. xiii. p. 756 (1930).
Northrop, J. Gen. Physiol. xvi. pp. 33 & 323 (1932).
Pauling, Proc. Nat. Acad. Sci. Washington, xvi. p. 453 ; *Zeit. f. Krist.* lxxiv. p. 2 (1930 *a*).
Pauling, Proc. Nat. Acad. Sci. Washington, xvi. p. 578 (1930 *b*).
Philippi, ' On the Nature of Proteins ' Amsterdam (Doctor's dissertation) (1936).
Robertson, Proc. Roy. Soc. A, cxli. p. 549 (1933 *a*) ; *ibid*, pp. 142 & 674 (1933 *b*).
Schulman and Rideal, Biochem. J. xxvii. p. 1581 (1933).
Stearn and Eyring, J. Chem. Phys. v. p. 113 (1937).
Svedberg, ' Nature,' cxxxix. p. 1051 (1937).
H. S. Taylor, ' Science,' lxxxv. p. 299 (1937).
H. S. Taylor, *Zeit. f. Krist.* lxxiv. p. 1 (1930).
W. H. Taylor, Proc. Roy. Soc. A, cxlv. p. 80 (1934).
W. H. Taylor, Meek, and Jackson, *Zeit. f. Krist.* lxxxiv. p. 373 (1933).
Wrinch, ' Nature,' cxxxvii. p. 411 (1936).
Wrinch, Proc. Roy. Soc. A, clx. p. 59 (1937 *a*).
Wrinch, ' Nature,' cxxxix. p. 972 (1937 *b*).
Wrinch, ' Science,' lxxxv. p. 566 (1937 *c*).
Wrinch, Proc. Roy. Soc. A, clxi. p. 505 (1937 *d*).
Wrinch, Trans. Faraday Soc. xxxiii. p. 1368 (1937 *e*).
Wrinch, Phil. Mag. xxiv. p. 940 (1937 *f*).
Wrinch, Proc. Phys. Soc. l. p. 141 (1938 *a*).
Wrinch (in course of publication) (1938 *b*).
Wu, Chinese J. Physiol. v. p. 321 (1931).
Wu, Tenbroek, and Li, Chinese J. Physiol. i. p. 277 (1927).

Schenectady.
March 1938.

LXIV. *Note on Approximations to Functions and to Solutions of Differential Equations.* *By* R. A. Frazer, *B.A.*, *D.Sc.*, *F.R.Ae.S.*, W. P. Jones, *B.A.*, *and* Sylvia W. Skan, *of the Aerodynamics Department, National Physical Laboratory* *.

1. *Introductory Remarks.*

THE present brief paper gives some comparisons between three known methods of approximation, which will be referred to as (i.) collocation, (ii.) least squares, (iii.) Galerkin's method. A fuller account, with numerical examples, is given in No. 1799 of the Reports and Memoranda of the Aeronautical Research Committee [1].

The term *collocation* is here used in connexion with approximations to mean the act of assigning the error at one or more given points or stations. For example, when a polynomial approximation to a given function is constructed by Lagrange's interpolation formula, the errors are made zero at specified points, and the approximation is accordingly collocated in the sense just defined. In relation to differential equations an approximation will be understood to be collocated if given errors (usually zero errors) in the differential equations are assigned at given stations.

The solution of differential equations by methods (ii.) and (iii.), which depend on the minimization of average errors, has been considered recently by W. J. Duncan [2]. The original papers by V. G. Galerkin, describing method (iii.), do not appear to be available in this country, but accounts with references are given in two papers by E. P. Grossman [3], [4]. Galerkin's method reduces to the method of least squares when it is applied to obtain approximate representations of functions.

2. *Approximations to Functions by Collocation and Least Squares.*

Suppose $X_1(x)$, $X_2(x)$, etc., to denote any functions chosen at convenience, and let $f(x)$ be the function to be represented approximately. It is assumed that $f(x)$ is

* Communicated by E. F. Relf, F.R.S. The writers are indebted to the Aeronautical Research Committee for permission to publish the paper.

continuous and single-valued in the interval (a_1, a_2) of the real variable x, and the sth approximation to $f(x)$ is taken to be

$$\mathrm{F}(x)=c_1\mathrm{X}_1(x)+c_2\mathrm{X}_2(x)+\ \ldots\ +c_s\mathrm{X}_s(x)\,, \qquad (1)$$

where c_1, c_2, etc., are constants left free for choice. Then, if the method of collocation is used, and if the errors are made zero at s given points, $x_1, x_2, \ldots x_s$, of (a_1, a_2), the equations for the constants will be

$$\sum_{j=1}^{s} \mathrm{X}_j(x_i)c_j=f(x_i), \qquad (2)$$

for $i=1, 2, \ldots s$. The corresponding equations in the case of least squares are

$$\frac{\partial}{\partial c_i}\int_{a_1}^{a_2}[\mathrm{F}(x)-f(x)]^2\,dx=0$$

for $i=1, 2, \ldots s$, or explicitly

$$\sum_{j=1}^{s} u_{ij}c_j=h_i, \qquad (3)$$

in which

$$u_{ij}=u_{ji}=\int_{a_1}^{a_2}\mathrm{X}_i(x)\mathrm{X}_j(x)\,dx,$$

$$h_i=\int_{a_1}^{a_2}\mathrm{X}_i(x)f(x)\,dx.$$

The foregoing formulæ are expressible concisely by matrices. Let $\mathrm{X}(x)$ denote the row matrix of the s functions $\mathrm{X}_i(x)$, and c be the column of the s constants c_i. Then, if $\theta_{ij}=\mathrm{X}_j(x_i)$, equations (2) can be written

$$\theta c=\{f(x_i)\}, \qquad (4)$$

where the braces, as usual, indicate a column. The approximation given by collocation is accordingly

$$\mathrm{F}(x)\equiv\mathrm{X}(x)c=\mathrm{X}(x)\theta^{-1}\{f(x_i)\}.$$

Similarly, with least squares, the constants are given by the equation $uc=h$, so that

$$\mathrm{F}(x)=\mathrm{X}(x)u^{-1}h.$$

When s is large the values of the constants given by (2) tend to equality with those given by (3). This is readily proved as follows. An axisymmetrical system of equations equivalent to (2) or (4) is

$$(\theta' d\theta)c=(\theta' d)\{f(x_i)\}\,,$$

where θ' denotes the transposed of θ, and d is any non-singular diagonal matrix of order s. Now divide the total interval (a_1, a_2) into s steps of (not necessarily equal) lengths $l_1, l_2, \ldots l_s$, and let the point x_i be assumed situated in l_i. Then if d is chosen to be the diagonal matrix of the lengths l, the (i, j)th element of $\theta' d\theta$ is readily seen to be

$$\sum_{k=1}^{s} d_k \mathrm{X}_i(x_k)\mathrm{X}_j(x_k),$$

while the ith element of $\theta' d\{f(x_i)\}$ is

$$\sum_{k=1}^{s} d_k \mathrm{X}_i(x_k) f(x_k).$$

When s becomes large these last two summations tend to equality with the integrals u_{ij} and h_i.

The preceding argument shows that, as s is increased indefinitely, the two sequences of representations $\mathrm{F}(x)$ derived by collocation and by least squares will either both converge to the same limit or else will both diverge. Cases of failure may occur if the interval of representation is chosen too large *.

3. *Approximate Solutions of Linear Ordinary Differential Equations.*

For simplicity only a single differential equation will be considered. This will be denoted by

$$\phi_0(x)\frac{d^n y}{dx^n} + \phi_1(x)\frac{d^{n-1}y}{dx^{n-1}} + \ldots + \phi_{n-1}(x)\frac{dy}{dx} + \phi_n(x)y - f(x) = 0,$$

or more briefly by

$$\phi(\mathrm{D})y - f(x) = 0 \quad \ldots\ldots\ldots \quad (5)$$

where D denotes the differential operator d/dx and

$$\phi(\mathrm{D}) \equiv \phi_0 \mathrm{D}^n + \phi_1 \mathrm{D}^{n-1} + \ldots + \phi_{n-1}\mathrm{D} + \phi_n.$$

It will be supposed that an approximate solution is required in the interval (a_1, a_2) of x. The boundary conditions may be of general type and consist of n relations

$$\mathrm{B}_i = b_i \quad \ldots\ldots\ldots \quad (6)$$

for $i = 1, 2, \ldots, n$, in which the expressions B_i are linear and homogeneous in the values of y (and possibly deriva-

* See, for instance, p. 74 of Ref. (5).

tives of y) appropriate to specified points of (a_1, a_2), and b_i are constants which are not all zero.

Assume an approximate solution to be

$$Y(x)=X_0(x)+\sum_{j=1}^{s} X_j(x)c_j, \quad . \quad . \quad . \quad . \quad (7)$$

where $X_0(x)$ is any function which satisfies the conditions (6), and $X_1(x)$, $X_2(x)$, etc., are functions each of which satisfies the simpler conditions $B_i=0$ for $i=1, 2, \ldots n$. When the functions X are chosen in this way Y necessarily satisfies conditions (6) for all constants c_j. Lastly, let $\epsilon(x)$ denote the function obtained when $Y(x)$ is substituted for y in the left-hand side of (5), so that

$$\epsilon(x)\equiv\sum_{j=1}^{s} Z_j(x)c_j+Z_0(x)-f(x),$$

where $Z_j(x)\equiv\phi(D)X_j(x)$ for $j=0, 1, 2, \ldots s$.

The three methods may now be stated.

(i.) *Collocation.*—In the normal application of this method the constants c are chosen so that $\epsilon(x)=0$ for s given points $x_1, x_2, \ldots x_s$ of (a_1, a_2). The equations for the constants are then

$$\sum_{j=1}^{s} Z_j(x_i)c_j=f(x_i)-Z_0(x_i). \quad . \quad . \quad . \quad . \quad (8)$$

(ii.) *Least Squares.*—The conditions satisfied are here

$$\frac{\partial}{\partial c_i}\int_{a_1}^{a_2}\epsilon^2\,dx=0,$$

or explicitly

$$\sum_{j=1}^{s} U_{ij}c_j=H_i, \quad . \quad . \quad . \quad . \quad . \quad . \quad (9)$$

where $$U_{ij}=U_{ji}=\int_{a_1}^{a_2} Z_i(x)Z_j(x)\,dx$$

and $$H_i=\int_{a_1}^{a_2} Z_i(x)\{f(x)-Z_0(x)\}\,dx$$

(iii.) *Galerkin's Method.*—In this case the equations for the constants are taken to be

$$\sum_{j=i}^{s} W_{ij}c_j=L_i, \quad . \quad . \quad . \quad . \quad . \quad . \quad (10)$$

in which $$W_{ij}=\int_{a_1}^{a_2} X_i(x)Z_j(x)\,dx$$

and $$L_i=\int_{a_1}^{a_2} X_i(x)\{f(x)-Z_0(x)\}\,dx.$$

By an argument similar to that given in § 2 it can be proved that, as s is increased indefinitely, the sequences of functions $Y(x)$ derived by the three methods will either all converge to the same limit or else will all diverge. Generally the methods may be expected to be successful if the interval (a_1, a_2) is not taken too large. From numerical examples it appears that Galerkin's method usually offers the advantage of rapid convergence. On the other hand, the method of collocation avoids the evaluation of integrals, and is, therefore, simple to apply.

4. *Problems involving Characteristic Numbers.*

An important field of application is the determination of characteristic numbers. With such problems the differential equation is homogeneous and contains a parameter (say K), and the boundary conditions also are homogeneous, so that $b_i=0$ in (6). In this case $f(x)=0$, and X_0 will be absent from (7), so that also $Z_0(x)=0$. The terms on the right of equations (8), (9), (10) then all vanish, and approximations for characteristic numbers are given by the condition of compatibility of s homogeneous linear equations. It is to be noted that, even when the true characteristic numbers are wholly real, the earlier approximations may sometimes be complex.

The problem of the transverse vibrations of a uniform stretched string provides a simple illustration. In this case the equation of motion is

$$\frac{\partial^2 z}{\partial x^2}=a^2\frac{\partial^2 z}{\partial t^2},$$

where a^2 denotes the ratio of mass per unit length to the tension. If a normal mode is assumed to be

$$z=y\sin(\omega t/a),$$

the differential equation for y is

$$\frac{d^2y}{dx^2}+Ky=0, \quad \ldots\ldots \quad (11)$$

where $K=\omega^2$. Moreover, y must vanish at the ends, say $x=0$ and $x=1$. The exact values of the first three characteristic numbers are here

$$K_1=\pi^2=9{\cdot}8696 \text{ (fundamental)},$$
$$K_2=4\pi^2=39{\cdot}478 \text{ (first overtone)},$$
$$K_3=9\pi^2=88{\cdot}826 \text{ (second overtone)}.$$

For the approximate solution of (11) it may be assumed that

$$X_0(x)=0 \quad \text{and} \quad X_j(x)=x^j(x-1)$$

in (7), so that

$$Y(x)=x(x-1)(c_1+c_2x+\ \ldots\ +c_sx^{s-1}).$$

If, as a rough approximation, only three unknown constants are retained, equations (8) reduce to

$$2c_1-2c_2=0,$$
$$\left(2-\frac{K}{4}\right)c_1+\left(1-\frac{K}{8}\right)c_2-\frac{K}{16}c_3=0,$$
$$2c_1+4c_2+6c_3=0.$$

The positions for collocation are here chosen to be $x=0$, $x=0{\cdot}5$, and $x=1$. The condition of compatibility yields $K_1=9{\cdot}6$ for the fundamental: the next approximation by the same method leads to $K_1=9{\cdot}82$ and $K_2=36{\cdot}0$, and one further approximation yields $K_1=9{\cdot}872$, $K_2=38{\cdot}40$, $K_3=75{\cdot}3$.

With the other two methods the convergence is more rapid, but the earlier approximations by least squares are complex. The details of the calculations will be omitted, and only the final results will be compared.

TABLE I.

Characteristic Numbers for Vibrating String.

Method.		K_1.	K_2.	K_3.
Exact solution.....		9·8696	39·478	88·826
Collocation	$s=3$..	9·6	—	—
	$s=4$..	9·82	36·0	—
	$s=5$..	9·872	38·40	75·3
Least squares ..	$s=2$..	$10{\cdot}0\pm4{\cdot}47\,i$	$42\pm27{\cdot}5\,i$	—
	$s=3$..	$9{\cdot}870\pm0{\cdot}230\,i$	$42\pm27{\cdot}5\,i$	$102\pm8{\cdot}3\,i$
Galerkin	$s=2$..	10·0	42·0	—
	$s=3$..	9·870	42·0	102

A further example, discussed in Ref. (1), relates to the transverse symmetrical vibrations of an annular membrane. The true characteristic numbers in this case are given by the roots of the transcendental equation

$$J_0(\sqrt{K})Y_0(2\sqrt{K}) - J_0(2\sqrt{K})Y_0(\sqrt{K}) = 0,$$

where J_0 and Y_0 denote the Bessel functions of zero order. The corresponding values calculated by the use of approximating polynomials compare as follows :—

TABLE II.

Characteristic Numbers for Vibrating Membrane.

Method.		K_1.	K_2.	K_3.
Exact solution		9·753	39·35	88·72
Collocation	$s=3$	9·51	—	—
	$s=4$	9·721	36·1	—
Least squares	$s=2$	$9·86 \pm 3·71\,i$	$41·7 \pm 26·8\,i$	—
Galerkin	$s=2$	9·88	41·6	—
	$s=3$	9·733	41·74	101·8

References.

(1) Frazer, R. A., Jones, W. P., and Skan, S. W., " Approximations to Functions and to the Solutions of Differential Equations." R. & M. 1799 *.
(2) Duncan, W. J., " Galerkin's Method in Mechanics and Differential Equations." R. & M. 1798.
(3) Grossman, E. P., " Oscillations of Tail Units of Aeroplanes." Transactions of the Central Aero-Hydrodynamical Institute, Moscow, no. 186.
(4) Grossman, E. P. ," The Twist of a Monoplane Wing." *Ibid.* no. 253.
(5) Borel, E., " Leçons sur les Fonctions de Variables Réeles." Monograph on the Theory of Functions (Paris, 1928).

LXV. *The Secondary Flow due to a Sphere rotating in a Viscous Fluid. By* W. G. BICKLEY, *D.Sc., Imperial College of Science and Technology* †.

THE approximate solution of the problem of the steady motion induced in an infinite incompressible viscous fluid by the slow rotation of an immersed solid sphere about a diameter is well known. Neglecting the

* R. & M. denotes Reports and Memoranda of the Aeronautical Research Committee.

† Communicated by the Author.

"convection" terms in the full Navier-Stokes equations the motion is found to be such that a concentric spherical shell of fluid of radius r rotates with an angular velocity $\Omega a^3/r^3$, where Ω is the angular velocity of the solid sphere and a its radius. In giving the solution Lamb *, quoting Stokes †, remarks that when the second order terms are taken into account no such steady motion is possible, since the sphere behaves as a centrifugal fan, causing an inflow parallel to the axis and an outflow parallel to the equatorial plane. So far as I am aware, this phenomenon has not been investigated, and the present paper gives a second approximation based upon the one above quoted as a first.

1. It is convenient first to throw the equations into non-dimensional form. Taking the radius a of the sphere as a characteristic length, we write for the coordinates of any point, relative to perpendicular axes through the centre of the sphere, of which the z-axis is the axis of rotation (ax, ay, az), so that x, y, and z are non-dimensional. Further, taking the equatorial velocity of the sphere, Ωa, as a characteristic velocity, we write for the components of the fluid velocity parallel to the axes $\Omega a(u_x, u_y, u_z)$, so that u_x, u_y, and u_z are also non-dimensional. For the pressure we write $\rho\Omega^2a^2p$, where ρ is the density and p is non-dimensional. We also form the Reynolds number R from the length a, the velocity Ωa and the kinematic viscosity ν, so that

$$\mathrm{R}=\Omega a^2/\nu. \quad . \quad . \quad . \quad . \quad . \quad . \quad (1.1)$$

The Navier-Stokes equations for steady motion then become

$$u.\frac{\partial u_x}{\partial x}+u_y\frac{\partial u_x}{\partial y}+u_z.\frac{\partial u_x}{\partial z}=-\frac{\partial p}{\partial x}+\mathrm{R}^{-1}\nabla^2u_x, \quad (1.2)$$

with similar equations for u_y and u_z, taken along with the equation of continuity

$$\frac{\partial u_x}{\partial x}+\frac{\partial u_y}{\partial y}+\frac{\partial u_z}{\partial z}=0. \quad . \quad . \quad . \quad . \quad (1.3)$$

* Lamb, 'Hydrodynamics,' § 334.
† Stokes, 'Scientific Papers,' i. p. 103.

In terms of the above variables the well-known first approximation distinguished by the affix $^{(1)}$ can be written

$$\left.\begin{aligned}(u_x^{(1)},\ u_y^{(1)},\ u_z^{(1)} &= r^{-3}(-y,\ x,\ 0),\\ p^{(1)} &= 0,\end{aligned}\right\} \quad . \quad . \quad (1.4)$$

where $r^2=x^2+y^2+z^2$.

We now assume that the exact solution can be expanded in powers of R, writing

$$u_x=u_x^{(1)}+\mathrm{R}u_x^{(2)}+\mathrm{R}^2u_x^{(3)}+\ldots \quad . \quad . \quad (1.51)$$

with similar expansions for u_y and u_z, and

$$p=p^{(2)}+\mathrm{R}p^{(3)}+\ldots \quad . \quad . \quad . \quad . \quad (1.52)$$

Inserting these in the equations (1.2) and taking into account the values of $u_x^{(1)}$, $u_y^{(1)}$, $u_z^{(1)}$ given above, the terms of the lowest degree in R which survive are

$$\nabla^2u_x^{(2)}=\frac{\partial p^{(2)}}{\partial x}-\frac{x}{r^6}=\frac{\partial}{\partial x}\left(p+\frac{1}{4r^4}\right), \quad . \quad (1.61)$$

$$\nabla^2u_y^{(2)}=\frac{\partial p^{(2)}}{\partial x}-\frac{y}{r^6}=\frac{\partial}{\partial y}\left(p+\frac{1}{4r^4}\right), \quad . \quad (1.62)$$

$$\nabla^2u_z^{(2)}=\frac{\partial p^{(2)}}{\partial z}=\frac{\partial}{\partial z}\left(p+\frac{1}{4r^4}\right)-\frac{\partial}{\partial z}\left(\frac{1}{4r^4}\right), \quad (1.63)$$

and

$$\frac{\partial u_x^{(2)}}{\partial x}+\frac{\partial u_y^{(2)}}{\partial y}+\frac{\partial u_z^{(2)}}{\partial z}=0. \quad . \quad . \quad . \quad (1.64)$$

The boundary conditions to be satisfied are that $u_x^{(2)}$, $u_y^{(2)}$, and $u_z^{(2)}$ vanish on the surface of the sphere ($r=1$) and at infinity. In what follows we drop the affix $^{(2)}$.

2. *Solution of the Equations.*—Differentiating (1.61), (1.62), and (1.63) with respect to x, y, and z respectively and adding, and taking (1.64) into account, we obtain

$$\nabla^2\left(p+\frac{1}{4r^4}\right)=\frac{\partial^2}{\partial z^2}\left(\frac{1}{4r^4}\right). \quad . \quad . \quad . \quad (2.1)$$

A particular integral of this equation is p', given by

$$p'+\frac{1}{4r^4}=\frac{1}{8}\frac{\partial^2}{\partial z^2}\left(\frac{1}{r^2}\right) \quad . \quad . \quad . \quad . \quad (2.2)$$

and the complementary function is harmonic.

Corresponding to the particular integral for the pressure there is evidently a particular integral for the velocity components which may be written

$$(u_x', u_y', u_z') = \left(\frac{\partial}{\partial x}, \frac{\partial}{\partial y}, \frac{\partial}{\partial z}\right)\phi + (0, 0, u_z''), \quad . \quad (2.3)$$

for which

$$\text{(i.)} \quad \nabla^2\phi = p' + \frac{1}{4r^4} = \frac{1}{8}\frac{\partial^2}{\partial z^2}\left(\frac{1}{r^2}\right),$$

so that

$$\phi = \frac{1}{8}\frac{\partial^2}{\partial z^2}(\log r); \quad . \quad . \quad . \quad . \quad . \quad (2.4)$$

$$\text{(ii.)} \quad \nabla^2 u_z'' = -\frac{1}{4}\frac{\partial}{\partial z}\left(\frac{1}{r^4}\right),$$

so that

$$u_z'' = -\frac{1}{8}\frac{\partial}{\partial z}\left(\frac{1}{r^2}\right). \quad . \quad . \quad . \quad . \quad . \quad (2.5)$$

To complete the solution we must add a solution of the equations *

$$\left.\begin{aligned} \nabla^2 u_\alpha &= \frac{\partial p''}{\partial \alpha}, \quad (u = x, y, z), \\ \frac{\partial u_x}{\partial x} + \frac{\partial u_y}{\partial y} + \frac{\partial u_z}{\partial z} &= 0, \end{aligned}\right\} \quad . \quad . \quad (2.6)$$

where p'' is the (harmonic) complementary function for equation (2.1). A particular solution is

$$u_\alpha''' = \tfrac{1}{2}\alpha p''. \quad . \quad . \quad . \quad . \quad . \quad . \quad (2.7)$$

Noting that on the boundary $r=1$ the solution given by (2.4) and (2.5) reduces to

$$u_\alpha' = \alpha(\mathrm{L} + \mathrm{M}z^2),$$

where L and M are constants, not the same for z as for x and y, we assume

$$p'' = \mathrm{A}\frac{\partial^2}{\partial z^2}\left(\frac{1}{r}\right),$$

and find that the components given by (2.7) satisfy the second of (2.6). Finally, to complete the solution we

* The general solution in spherical harmonics of equations (2.6) is given by Lamb (*loc. cit.*, §336), but the present instance is so simple that it was thought preferable to give the details.

may add the gradient of a harmonic function ϕ'', and again taking the boundary conditions into account we assume

$$\phi'' = \frac{B}{r} + C\frac{\partial^2}{\partial z^2}\left(\frac{1}{r}\right).$$

To make the complete solution satisfy the boundary conditions at $r=1$ we find that we must have

$$A=-\tfrac{1}{4}, \quad B=0, \quad \text{and} \quad C=\frac{1}{24}.$$

We thus obtain the velocity components

$$\left.\begin{aligned} u_x &= \frac{1}{8}\frac{x(r-1)}{r^7}\{r^2(r-1)-z^2(3r-5)\}, \\ u_y &= \frac{1}{8}\frac{y(r-1)}{r^7}\{r^2(r-1)-z^2(3r-5)\}, \\ u_z &= \frac{1}{8}\frac{z(r-1)}{r^7}\{r^2(r-3)-z^2(3r-5)\}, \end{aligned}\right\} \quad . \quad (2.8)$$

and the pressure

$$p = \frac{r^2(r-2)-z^2(3r-4)}{r^5}. \quad . \quad . \quad . \quad . \quad (2.9)$$

3. *Discussion of the Solution.*—Since the solution found is symmetrical about the z-axis, there is a current function ψ corresponding to it. Denoting $\sqrt{(x^2+y^2)}$ by ϖ, we easily find that

$$\psi = \frac{1}{8}\frac{z\varpi^2(r-1)^2}{r^5}, \quad . \quad . \quad . \quad . \quad . \quad . \quad (3.1)$$

or, if θ is the angle made by the radius vector with the z-axis,

$$\psi = \tfrac{1}{8}\sin^2\theta\cos\theta\left(1-\frac{1}{r}\right)^2. \quad . \quad . \quad . \quad (3.2)$$

The maximum value of ψ occurs at infinity where $\cos\theta = 1/\sqrt{3}$, and $\psi_{\max} = \sqrt{3}/36$, $2\pi\psi_{\max}$ represents the total (volume) inflow in the axial direction, or the total outflow parallel to the equatorial plane. Restoring the dimensional variables, this outflow (or inflow) is at the rate (volume per unit time) of

$$\frac{\pi\sqrt{3}}{36}\frac{\Omega^2 a^5}{\nu}. \quad . \quad . \quad . \quad . \quad . \quad . \quad . \quad (3.3)$$

A drawing of the stream-lines in a meridional plane which illustrates the flow is given in the figure, at interval $0{\cdot}1\psi_{max.}$

It is interesting, and at first sight surprising, to note that the secondary flow (to this order of approximation) adds nothing to the torque resisting the rotation of the sphere. On general dynamical grounds it is clear that energy must be supplied to make good the dissipation

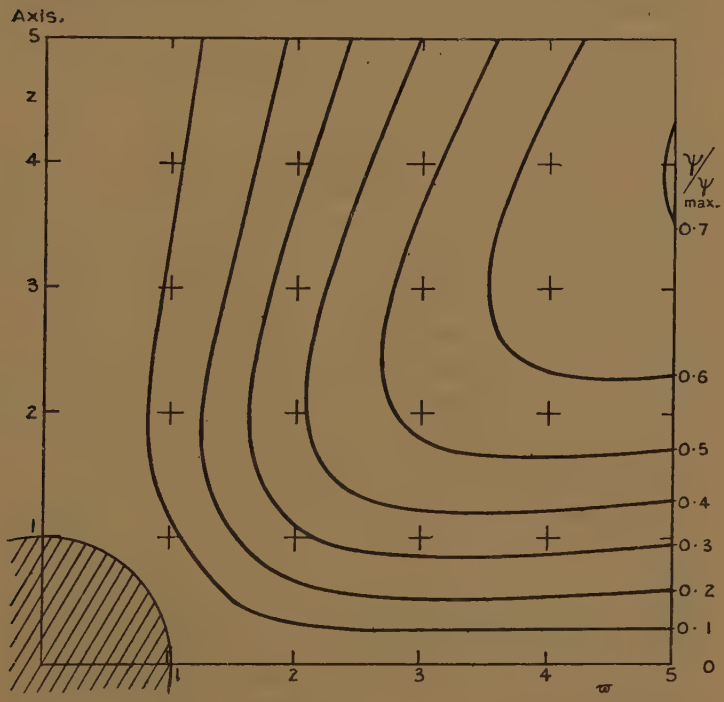

due to viscosity. The secondary flow, not being irrotational, will contribute to this dissipation, but since the only non-vanishing component of the deformation tensor of the primary flow is $e^{(1)}_{r\phi}$, and $e^{(2)}_{r\phi}$ vanishes identically, the coefficient of R in the dissipation function due to the combined motion will be zero. The additional dissipation is thus of order R^2, and, since the third approximation will (presumably) also contribute terms of this order, the effect cannot be calculated completely from the

results so far obtained. This does indicate, however, that the secondary torque is small, probably too small appreciably to affect experimental results, and this conclusion is likely still to be valid when the effect of outer boundaries is considered.

With regard to the pressure distribution, it is easy to verify that the greatest pressure defect occurs round the equator of the sphere, and its value is $\rho\Omega^2a^2/4$. It is also obvious from (2.9) that the sphere $r=4/3$ is a surface of constant pressure, the value being $-27\rho\Omega^2a^2/512$. The pressure gradient is thus small except in an equatorial belt between $r=1$ and $r=4/3$. Small positive pressures exist along the axis.

As far as these results—which take into account neither compressibility, temperature variation, nor an outer boundary—can be applied to the Earth's atmosphere, they indicate a low pressure belt round the equator, resulting in a circulation of the air which would rise at the equator and descend at the poles. The double circulation actually present, in which the air descends long before it reaches the poles, is an additional effect mainly due to temperature (and consequent density) variations.

I should like to thank Dr. R. J. Schmidt for reading my manuscript and for some valuable comments.

LXVI. *On the Calculation of Surface Tension from the Measurement of Sessile Drops.* *By* Alfred W. Porter, *D.Sc., F.R.S., Emeritus Professor in the University of London* *.

IN the 'Philosophical Magazine' for November 1937, p. 823, I published a preliminary note "On the Calculation of Surface Tension from the Measurement of Sessile Drops." In that paper it was shown that the values for the region of large drops can be derived from an important paper by C. H. Bosanquet in the 'Philosophical Magazine' for February 1928. Bosanquet employed a step-by-step method applicable from the point at which

* Communicated by the Author.

Bashforth and Adams's method becomes inapplicable and extending to the case of infinitely large drops, *i. e.*, to small values of h^2/r^2. To display these new results it is best to make use of non-dimensional quantities.

Let $$\beta^2 = \frac{\text{surface tension}}{g(\rho_1 - \rho_2)} ;$$

then β has the physical dimensions of a length and we may write

$$\frac{\beta^2}{r^2} = \frac{1}{2}\frac{h^2}{r^2} + \Delta_2,$$

where Δ_2 is a pure numeric.

Fig. 1.

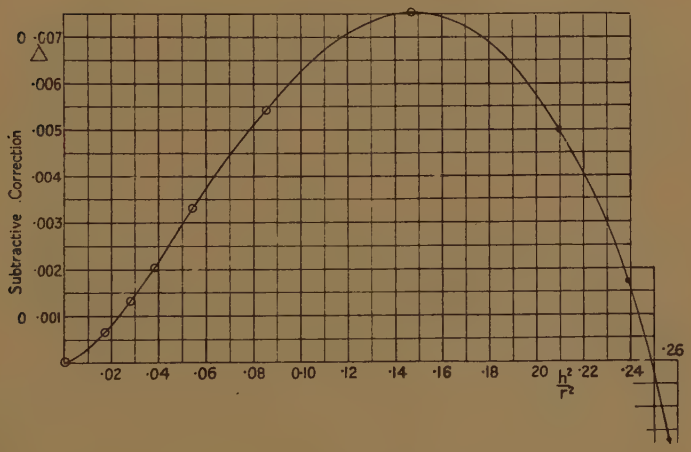

The values of Δ_2 are subtractive for values of h^2/r^2 less than about 0·248, after which they become additive.

The values of Δ_2 are shown plotted against h^2/r^2 in fig. 1. Those on the left-hand of the curve replace those of Rayleigh, Worthington, and Ferguson, to which they approximate (see Phil. Mag. (7) xv. p. 163 (1933)), while those on the right-hand of the summit correspond to the values based on Bashforth and Adams's Tables. It will be seen that this curve has a similar character to that given in the 1933 paper, the central portion of which was obtained by graphical interpolation. The present diagram, although not much different in general character, is based

on a secure foundation. It can be extended beyond $\frac{h^2}{r^2}=\cdot 25$ by employing the values given in the table (derived from Bashforth and Adams's data) as follows:—

$\frac{h^2}{r^2}$	$\frac{\beta^2}{r^2}-\frac{1}{2}\frac{h^2}{r^2}$
·257040	$+\cdot 00153_8$
·281426	$+\cdot 00666_6$
·313675	$+\cdot 01570_5$
·426071	$+\cdot 07331_4$
·538453	$+\cdot 19466_3$
.....	.....
·948341	7·8485

Thus the problem of the calculation of the surface tension from the measurement of the height and radius of drops is solved for drops of all sizes.

LXVII. *Experiments on Water Waves of Translation in Small Channels.* *By* J. Allen, *M.Sc., Assoc.M.Inst.C.E., Engineering Department, Manchester University* †.

I. *List of Symbols and Formulæ.*

V_p = velocity of propagation of wave-crest, relative to the fixed boundaries of the stream.

V_p' = velocity of propagation of wave-crest, relative to the stream.

v = velocity of stream itself.

h = depth of stream before the arrival of the wave.

k = height of wave-crest above surface of stream.

h_m = effective depth
b = bottom width
w = surface width
S = side-slope
Δ = area of cross-section
} in a trapezoidal channel.

† Communicated by the Author.

$$V_p' = \sqrt{\frac{2g(h+k)^2}{2h+k}} \quad \ldots\ldots\ldots\ldots \quad (1)$$

$$V_p' = \sqrt{\frac{g}{2}\frac{(h+k)(2h+k)}{h}} \quad \ldots\ldots\ldots\ldots \quad (2)$$

$$V_p' = \sqrt{g(h+k)} \quad \ldots\ldots\ldots\ldots \quad (3)$$

$$V_p' = \sqrt{gh} \quad \ldots\ldots\ldots\ldots \quad (4)$$

$$V_p = V_p' \pm v \quad \ldots\ldots\ldots\ldots \quad (5)$$

Concerning the different expressions for V_p' see § II.

Except where otherwise stated all dimensions quoted in this paper are expressed in cm. and all velocities in cm. per sec.

II. *Introduction.*

THE propagation of a "long wave" through a river or canal possesses considerable scientific and engineering importance. Such a wave may be generated by the admission of water through a quickly opened sluice-gate or as the result of sudden rainfall communicated to the upper reaches of the waterway. Another interesting example is provided by the phenomenon of the bore as found in many tidal rivers.

Not only is the phenomenon important as manifested in large canals or natural rivers, but also in small-scale models, since there is a growing tendency to apply the method of model investigation to the many complex problems of open channel flow.

Some few years ago Professor A. H. Gibson † studied the height and rate of travel of the bore in a model of the River Severn, and demonstrated that, despite the small dimensions of the model river, close agreement was to be found with the phenomena observed in the natural river. He concludes that "the speed of the bore depends on the depth of water, the height of the bore, and the velocity of the river current, as indicated by the theoretical formula

$$V_p = \sqrt{\frac{2g(h+k)^2}{2h+k}} - v \quad \text{ft. per sec.},$$

and that if h is taken as the depth of the deep water channel of the river, the actual velocity is approximately 95 per cent. of that given by the formula."

† 'Construction and Operation of a Tidal Model of the Severn Estuary,' Section IX. H.M. Stationery Office (1933).

The formula (1) differs from formula (2) by less than 1 per cent. for values of k/h up to 0·25 ; if $k=h$ (1) gives a velocity 6 per cent. less than (2) †.

Comparing formulæ (1) and (3), the former gives the higher values by 5, 10, and 15 per cent. respectively when $k/h=0{\cdot}25$, 0·50, and 1·00.

If k is very small compared with h all the formulæ reduce to (4).

Scott Russell ‡, in his classical investigation of waves propagated along straight channels of simple geometrical shape, found formula (3) to agree very closely with his experimental results. The maximum value of k/h used by Scott Russell, in channels of rectangular cross-section, appears to have been 0·326 ; in general his experiments were conducted with comparative wave heights not exceeding $0{\cdot}15\,h$.

The present investigation includes experiments on two small-scale river models, one (the Mersey) non-tidal but extremely tortuous, the other tidal (the Dee) ; the results are discussed in relation to theoretical considerations and to further experimental work on small, straight channels of rectangular, trapezoidal, and triangular cross-section. Certain of the observations have been made with wave-heights, k, as great as $0{\cdot}5\,h$.

III. *Experiments on a Model of the River Mersey.*

This model, constructed with horizontal and vertical scales of 1 : 800 and 1 : 120 respectively, embraces the stretch of the Mersey between Ashton-upon-Mersey and Irlam Weir, where the river falls into the Manchester Ship Canal. The special feature is the number of bends involved—no fewer than twenty-eight—making the length of channel some 8·3 miles as compared with the direct distance of 3·7 miles between its ends. Wave velocities were measured in the model over a length, AB, of 1510 cm., the upstream gauge-point (A) being some 105 cm. below the upper limit of the model, and the downstream gauge-point (B) some 55 cm. above Irlam Weir. The width

† For derivation of formula (1) see ' Hydraulics and its Applications,' Gibson, 3rd edn., p. 405 (1923).

Formula (2) is derived, by different reasoning, in Lamb's ' Hydrodynamics,' 4th edn., p. 272 (1916).

‡ Report on Waves, British Association, p. 311 (1844).

of the water surface averages about 2·18 cm. with the lowest river discharges and 4·55 cm. with the highest.

The experimental procedure adopted was as follows :—

(1) A steady stream of water was supplied at the upstream limit of the model. The corresponding rate of flow, q, was determined by timing the collection of a measured volume at the downstream end.

(2) A pointer-gauge erected over the station B was adjusted until the pointer stood 0·01 inch above the water surface.

(3) A quantity, x, of water was then poured into the model at its upstream end. This quantity produced a wave of translation superimposed upon the general flow of the stream.

(4) A stop-watch graduated in tenths of a second was started as the resulting wave passed station A, and was stopped when the wave arrived at B. The pointer-gauge greatly facilitated the latter observation, since the instant of the wave's rising into contact with the pointer was sharply defined.

In certain of the observations it was possible to detect the arrival of the wave by visual observation of the reduction of the 0·01″ gap between the pointer and the water surface, but the general method employed was to stop the watch when contact with the pointer was definitely established.

In many of the observations the quantity x of water poured into the top of the model to create a wave was 2000 c.c.; in others it was increased to 8000 c.c. The time of passage of the wave was sensibly unaltered by this change in value of x, although with 8000 c.c. it was easier to follow the progress of the wave in the lower stretches of the model. The reason for the agreement in times observed with the very different volumes of added water is evidently that, while the wave-height *near the point of its formation* was appreciable, the *average* height in either case was small compared with the depth of water in which the wave travelled.

Discussion of Results.

1. Assuming the wave-height to be negligible in comparison with the depth of the stream, and dividing the

whole length l into elements δl over which h is the approximately uniform depth, we have

$$V_p = V_p' + v$$
$$= \frac{l}{\Sigma\left(\frac{\delta l}{\sqrt{gh}}\right)} + v, \text{ from (4).}$$

For the purpose of this calculation the depth of stream previous to the passage of the wave was measured at twenty-four sections between A and B. It was thus possible to calculate $\frac{\delta l}{\sqrt{gh}}$ for the lengths δl between the respective sections, and, by simple addition, to obtain $\Sigma\frac{\delta l}{\sqrt{gh}}$.

TABLE I.

q	11·1	25·9	59·7	75·0	107*	126	161*	214*
v	5·21	8·32	11·7	13·0	13·5	15·5	15·0	15·8
Calculated V_p'	33·6	40·3	49·8	52·5	55·9	59·5	61·9	66·5
Calculated V_p	38·8	48·6	61·5	65·5	69·4	75·0	76·9	82·3
Measured V_p	36·9	43·6	48·6	54·0	54·2	58·0	57·2	63·5
Ratio of meas. : calc. V_p.	0·953	·898	·790	·824	·782	·773	·745	·772
Measured V_p : calculated V_p'.	1·10	1·08	·98	1·03	·97	·98	·92	·95
Mean h	1·24	1·73	2·54	2·78	3·18	3·56	3·92	4·62

The value of v was calculated from the measured areas of the cross-sections in conjunction with the known discharge, q, account being taken of the spacing of the sections along the river.

Table I. provides a summary of the observations and calculations.

In the above table q represents the rate of discharge in c.c. per second. 214 c.c. per second in the model is equivalent to 8000 cubic feet per second in nature. h is the average depth in cm., measured along the *deep water* channel, *i. e.*, the mean of the greatest depths at the several cross-sections.

The observations marked * were made after roughening the bed of the model river with coarse sand.

It will be seen from the results obtained that, except at very low discharges, the observed velocities of propagation are appreciably less than the calculated.

On the other hand, it appears that, with sufficient accuracy for practical purposes, the times of travel could be calculated as though the wave were moving in a channel containing *still* water of depth equal to that measured along the deep water channel of the river. Thus, the velocity scale of the model being $1 : \sqrt{120}$, or $1 : 10{\cdot}96$, a measured wave-velocity in the model of 36·9 cm. per sec. represents 13·3 ft. per sec. in nature, and the corresponding time of travel between stations A and B (39,600 feet apart in the actual river) would be 49·5 minutes,

TABLE II.

Rectangular Section.

v	7·30	0·0	0·74	3·96	0·0	0·0	0·0	0·32	1·34
Calculated V_p' ..	35·6	41·4	43·2	46·4	49·0	55·9	62·5	68·0	69·7
Calculated V_p ...	42·9	41·4	43·9	50·4	49·0	55·9	62·5	68·3	71·0
Measured V_p ...	43·0	40·8	41·0	49·6	48·4	54·0	62·7	68·0	71·0
Ratio of measured to calculated V_p	1·00	0·99	0·94	0·99	0·99	0·97	1·00	1·00	1·00
Mean h	1·09	1·54	1·70	1·98	2·26	2·97	3·76	4·52	4·55

whereas the time obtained from the calculated V_p' would be 54·4 minutes.

2. The question remains, however, as to how far the conclusion reached above is due to the tortuous nature and how far to the small cross-section of the model channel.

In order to study this point the author has made observations on a 5-foot length of straight channel having a nearly constant width of 2·03 cm. and a total length of 7 feet. The sides of this channel were of smooth cement, the bed moulded in fine sand. In these experiments a small wave was propagated by displacing water in a well or basin at the upstream end of the channel. The height of wave in no case exceeded 0·05 inch, or 0·127 cm. The results are summarized above.

In considering the results quoted above it is necessary to observe that :

(*a*) The calculated values of V_p are derived from formula (1), using the maximum value (0·127) of k. With the biggest four depths the result is not affected by more than 3 per cent. if k is treated as negligible. With the lowest depth the calculated V_p' would be 32·8 if k were taken as negligible.

(*b*) The channel-bed and water-surface levels were measured from time to time at six uniformly spaced cross-sections. The average values thus obtained are probably true within $\pm 0{\cdot}01$ inch. There is, accordingly, a possible error in the depths of 0·02 inch, or 0·05 cm., which is equivalent to approximately 5 per cent. of the smallest value of h, or $2\frac{1}{2}$ per cent. in the resulting calculated V_p'. With the higher values of h the possible error from this cause is less than 1 per cent.

(*c*) The values of v are obtained from the measured rate of discharge and the cross-sectional area of the stream before the passage of the wave.

(*d*) The observations quoted in Table II. were made with water temperatures ranging between 15·9 and 16·7° C., but no appreciable difference was detected when two of the still-water tests were repeated with average water temperatures as high as 24° C.

In view of these considerations it may be stated that, within the limits of observation, the results obtained confirm the theoretical formula (1).

3. Reverting now to the measurements made on the model of the River Mersey (Table I.), a further question arises, viz., as to the effect of the *shape* of the *cross-section* of the model. In order to investigate this question experiments have been made on still water contained in a 5-foot length of straight channel having a bottom width of 0·95 cm. and side slopes of 1 horizontal to 2 vertical. The overall length was 7 feet.

In this channel the ratio of the mean depth to the maximum depth is sensibly the same for a given maximum depth of water as in the Mersey model.

The results are summarized in the following table :—

TABLE III.

Trapezoidal Section—bottom width 0·95 cm.

h.	Observed V_p (0).	V_p calculated from $\sqrt{\bar{h}}$ (1).	$\sqrt{\bar{h}}$ (2).	$\sqrt{\bar{h}}$ (3).	Ratio (0) : (1).	(0) : (2).	$\bar{h} : h$.
1·35	33·0	36·6	30·8	29·5	·90	1·07	·71
1·52	34·9	38·8	32·4	30·8	·90	1·08	·70
1·83	38·4	42·5	34·8	33·3	·90	1·10	·67
2·28	41·6	47·4	38·2	36·4	·88	1·09	·65
2·82	45·4	52·9	41·9	39·7	·86	1·08	·63
3·54	49·1	59·0	46·1	43·6	·83	1·06	·61
4·17	53·0	64·1	49·5	46·6	·83	1·07	·60

In the above table the calculated velocities labelled (1), (2), (3) correspond respectively to $\sqrt{g\bar{h}}$, $\sqrt{g\bar{\bar{h}}}$, $\sqrt{g\bar{\bar{\bar{h}}}}$, where h = maximum depth of cross-section

$\bar{h}$ = mean ,, ,, ,,

= area ÷ surface width,

$\sqrt{\bar{h}}$ = mean square root of depth.

The observed values of V_p quoted in the table are less than those actually observed in the experiments, having been reduced to a basis of $k = 0$ by a correction appropriate to the observed maximum value (0·127) of k.

Inspection of the data quoted shows that

(*a*) there is an almost constant ratio, 1·08 : 1, between the observed velocity and that calculated on the basis of $\sqrt{\bar{h}}$;

(*b*) the observed values agree more closely with the square root of the mean than with the mean square root of depth ;

(*c*) with the smaller depths the observed velocities agree almost as well with $\sqrt{g\bar{h}}$ as with $\sqrt{g\bar{\bar{h}}}$.

It is important to note, however, that Scott Russell †, experimenting on *triangular* channels with 45° side slopes, discovered that "we may take the simple arithmetical mean depth as the depth of the rectangular channel of a wave of equal velocity." He says, further, that "no great number of experiments has been made on channels of other forms of variable depth, such as have been made coinciding with those in the triangular channel."

There is, accordingly, an apparent discrepancy between Scott Russell's findings and those of the author concerning trapezoidal sections. The author has, therefore, made a number of tests on waves propagated in

(i) a trapezoidal channel of bottom-width 1·29 cm., the side-slopes being 1 horizontal to 2 vertical;
(ii) a triangular channel with side-slopes of 1 horizontal to 2 vertical.

In each set of experiments the wave was timed over a central 5-foot length of a channel 7 feet long, containing still water at a temperature varying at different times between 13·2 and 18·9° C. The measurements were also repeated by timing the wave over a 4-foot length, one gauge-point being situated 2 feet from the end of the channel where the wave was generated. In no case did the height of wave exceed 5 per cent. of the depth of still water in the channel, and in assessing the results averages of a number of time-observations have been taken and curves drawn through the plotted points. From these curves the following values are obtained :—

TABLE IV.

Trapezoidal Channel—bottom width 1·29 cm.

h cm.	Ratio of observed velocity to $\sqrt{gh}$.
1·0	1·07
1·5	1·08
2·0	1·06
3·0	1·04
5·0	1·03
8·0	1·02

† *Loc. cit.*

On the other hand, the observations made with the triangular section agree in all cases with calculations based on the mean depth within ± 3 per cent., while in a number of cases the agreement is within 1 per cent. The present tests were made, incidentally, over a range of depths between 2·38 and 11·2 cm.; Scott Russell's triangular sections covered depths between 10·2 and 72·5 cm.

We are therefore led to the conclusion that, as stated by Scott Russell, a wave in a channel of triangular cross-section is propagated with a speed appropriate to the average depth of the cross-section. On the other hand, there is evidence to show that in trapezoidal sections the wave may advance with a velocity appreciably greater than would be expected from the average depth of the section.

If the bottom width of a trapezoidal section be represented by b and the side-slope by S, then the mean depth is

$$\bar{h} = \frac{bh + Sh^2}{b + 2Sh}.$$

Suppose now that the effective mean depth is

$$h_m = \frac{bh + \lambda Sh^2}{b + 2\lambda Sh}.$$

When $b=0$ the case of a triangular section is obtained and appropriately $h_m = \bar{h}$. Similarly, for a rectangular channel, $S=0$ and again $h_m = \bar{h}$.

For intermediate cases the maximum ratio of h_m to $\bar{h}$ becomes

$$\frac{2+(\lambda+2)\sqrt{\frac{1}{2\lambda}}}{2+(2\lambda+1)\sqrt{\frac{1}{2\lambda}}},$$

and occurs when $h = \frac{b}{S}\sqrt{\frac{1}{2\lambda}}$.

In particular, if $\lambda = \frac{1}{2}$,

$$\left(\frac{h_m}{\bar{h}}\right)_{\text{max.}} = 1{\cdot}125,$$

and this maximum ratio occurs when $h=b/S$, *i. e.*, when the water-surface width is three times the bottom width.

Adopting the formula

$$h_m=\text{effective depth}=\frac{bh+\frac{1}{2}Sh^2}{b+Sh},$$

the observed velocities in the trapezoidal section of bottom width 0·95 cm. are, on the average, 3 per cent. greater than given by $\sqrt{gh_m}$, the maximum excess being 4 per cent. and the minimum 2 per cent. In the case of the channel with bottom width 1·29 cm. the observed velocities agree with $\sqrt{gh_m}$ within $\pm 2{\cdot}5$ per cent.

4. Reverting now to a consideration of the results obtained on the Mersey model, suppose the form of the cross-sections with different depths of water to be reduced to analogous trapezoidal sections by calculating b and S from the equations

$$b=\frac{2\Delta}{h}-w,$$

$$S=\frac{w-b}{2h},$$

where Δ=area of cross-section,

w=surface width.

Next suppose the effective depth to be calculated as

$$h_m=\frac{bh+\frac{1}{2}Sh^2}{b+Sh}$$

and V_p' calculated as $\sqrt{gh_m}$.

It is then found that, except for the two smallest discharges (11·1 and 25·9 in Table I.), the measured V_p agrees closely with $\sqrt{gh_m}+\frac{1}{2}v$. When $q=11{\cdot}1$ the measured V_p is 9 per cent. greater, and when $q=25{\cdot}9$, 7 per cent. greater, than $\sqrt{gh_m}+\frac{1}{2}v$.

Apparently, therefore, unless the flow is very small, only about half of the steady velocity of the stream itself is superimposed upon the wave. This effect may be

attributed to the presence of transverse currents at the many bends in the river.

IV. *Experiments with Waves of appreciable Height.*

These tests have been made upon a tidal model of the Dee estuary (scales 1 : 5000 horizontal, 1 : 200 vertical). In this model a bore is frequently observed to form on the flood-tide some distance below Connah's Quay and to proceed upstream to Chester Weir. The height of the sudden rise due to this wave, and the speed of its translation, vary considerably according to the configuration of the sandbanks, the flow of water down the river, and the presence in the model of various proposed schemes of training walls. It is of special interest to note that in this model the bore is usually not in the form of a solitary wave, but appears as a train of waves in much the same fashion as Dr. Vaughan Cornish has described † in connexion with his observations of the Severn and the Trent. When the bed and the training walls in the model are adjusted to represent present-day conditions in the river, the time elapsing between the first sharp rise of the flood-tide at Connah's Quay and at a point near Chester Weir is 9·8 seconds. The distance between the points is 247 cm., so that the speed of propagation averages 25·2 cm. per sec. The velocity-scale of the model being $1 : \sqrt{200}$, this represents 355 cm. per sec., or 7·94 miles per hour in nature, a figure which is closely in agreement with that of 8 m.p.h. measured in the Dee itself by Mr. A. Caradoc Williams, Assoc.M.Inst.C.E., and Mr. Ll. E. Williams, Assoc.M.Inst.C.E., to whom the author is indebted for the information. It is further observed in the model that the surface current follows the bore at a speed of about 0·75 of that of the wave crest—this again being in agreement with nature. The average width of this channel in the model is approximately 2·5 cm.

The opportunity has also been taken to measure the height and speed of the bore under different conditions in the Dee model, and to compare the results with those calculated by Professor Gibson's formula

$$V_p = \sqrt{\frac{2g(h+k)^2}{2h+k}} - v.$$

† 'Ocean Waves,' 1934.

The method of measuring the height of the wave consisted of

(*a*) adjusting a pointer gauge to touch the water just before the arrival of the wave ;

(*b*) adjusting the gauge, by trial and error, so that the first sharp rise of the flood, due to the bore, just touched the pointer.

The difference in the gauge readings (*b*) and (*a*) gave the height of the bore.

In the first series of tests the observations were made on a length of model river containing one gradual bend but many irregularities in bed level in the form of sandbanks.

The results are tabulated below.

TABLE V.

Dee Tidal Model.

Mean h.	Mean k.	v.	Calculated V_p.	Measured V_p.	Ratio of measured to calculated.
0·64	0·31	0·8	32·6	30·8	0·94
·43	·16	1·4	24·5	21·5	0·88
·68	·25	8·6	23·9	22·2	0·93

In the second series observations were made in a channel of almost constant width 3·82 cm. bounded by gently curving training walls in the form of metal plates. Here the bed was of nearly uniform level, free from sandbank obstructions.

TABLE VI.

Dee Tidal Model.

Mean h.	Mean k.	v.	Calculated V_p.	Measured V_p.	Ratio of measured to calculated.
·36	·18	3·0	22·2	22·6	1·02
·53	·23	9·6	20·0	20·1	1·00

In the third series observations were made on a stretch of straight model river of approximately uniform width 2·00 cm. and bed level.

TABLE VII.

Dee Tidal Model.

Mean h.	Mean k.	v.	Calculated V_p.	Measured V_p.	Ratio of measured to calculated.
·56	·20	1·6	27·7	27·6	0·975

In all these calculations h is the depth of the *deep water channel*, which in the case of the tests of Table V. is appreciably greater than the average depth of water.

It should be remarked also that v has been taken as 2/3 of the central or maximum surface velocity of the stream previous to the arrival of the bore, *i. e.*, as 2/3 of the maximum velocity indicated by a shallow float. In general this would not differ greatly from the mean velocity over the whole cross-section †, at any rate in its proportional influence on the final calculated value V_p.

V. *Summary of Conclusions.*

(1) In an extremely tortuous channel such as the portion of the river Mersey at present under discussion a wave is propagated at a speed approximately as calculated from the depth of water measured along the *deepest* axis of the channel, and neglecting the speed of the stream in which the wave travels. This net result is brought about by the observed fact that, while the wave velocity itself is less than that corresponding to the greatest depth of water, it is greater than that due to the mean depth, and at the same time, presumably because of transverse currents at the bends of the river, only a portion of the velocity of the stream itself is superimposed upon the wave.

(2) The observations in the model indicate that if the river Mersey itself, discharging some 400 cubic feet per

† The basis for this argument is 'Hydraulics and its Applications,' A. H. Gibson, 3rd ed., p. 335.

second, receives flood-water from the reaches upstream of Ashton-upon-Mersey, this water will take approximately 50 minutes to reach the vicinity of Irlam Weir, where the river flows into the Manchester Ship Canal.

(3) In straight channels of triangular cross-section the wave-velocity is very closely equal to that calculated on the basis of the average depth. In trapezoidal channels, however, the effective depth is somewhat greater than the average, being approximately

$$h_m = \frac{bh + \frac{1}{2}Sh^2}{b + Sh}.$$

(4) In straight or comparatively straight and uniform channels a bore is propagated with velocity closely equal to

$$\sqrt{\frac{2g(h+k)^2}{2h+k}} - v,$$

where v is 2/3 of the maximum surface velocity indicated by a shallow float (or approximately the mean velocity over the cross-section) and h is the depth measured along the deep-water axis of the stream. (Both v and h are measured just previous to the arrival of the bore.)

Even when the bed of the channel is beset with sand-banks the velocity is only 10 or 15 per cent. less than that given by the formula.

(5) The speed of a bore in a tidal model represents the natural phenomenon with very remarkable accuracy, despite the small widths and depths involved in such a model.

The experiments described were made in the Whitworth Engineering Laboratory of Manchester University, and the author wishes to record his thanks to the Director, Professor A. H. Gibson, D.Sc., LL.D., for the facilities provided and for much helpful criticism. Also his thanks to Messrs. Z. W. Segal, M.Sc., and S. S. Surana, M.Sc., research students, for assistance in the experiments on the Mersey model.

LXVIII. *Studies on the Oxidation of Metals.*—Part V. *The Oxidation of Molten Lead.* *By* L. L. Bircumshaw, *M.A., D.Sc., University College, Exeter, and* G. D. Preston, *M.A., National Physical Laboratory* *.

IN a recent paper[1] we have discussed results obtained in an experimental study of the kinetics of the oxidation of molten tin at temperatures up to 800° C. The present communication deals with a similar investigation of molten lead. The technique employed was similar to that previously described (*loc. cit.*). The prepared metal, which nearly always showed very fine films of oxide, was heated in a current of pure hydrogen for one hour at 700° C. The specimen was then heated in argon in the apparatus to the required temperature, and when the latter had steadied up the argon was pumped off and oxygen admitted. The rate of oxidation was followed by measurement of the rate of fall of pressure of oxygen.

The results of a series of experiments carried out at 500° 600° and 700° C. are shown graphically in figs. 1 to 6 where p/p_0 is plotted against time, p_0 being the initial pressure at the time $t=0$. The different values of p_0 are indicated on each curve. At 500° C. the rate of fall of pressure is small but it increases rapidly as the temperature is raised. The divergence between duplicate experiments is much less than in the case of tin but still exceeds considerably the limits of experimental error. All the methods used in the previous work on tin were employed again to ascertain the cause of these differences, but without success. In spite of the failure to obtain reasonable agreement between repetitions of an experiment carried out under apparently identical conditions it appeared to be worth subjecting the data to numerical analysis, with a view to ascertaining whether the Tamman-Pilling-Bedworth parabolic law of oxidation applied to molten lead. This law is usually expressed in the form

$$w^2=2kt \quad . \quad . \quad . \quad . \quad . \quad . \quad . \quad (1)$$

where w is the weight of oxygen absorbed per unit area in time t. For the present purpose it is more convenient to use the differential form

$$w\frac{dw}{dt}=k. \quad . \quad . \quad . \quad . \quad . \quad . \quad (2)$$

* Communicated by C. H. Desch, F.R.S.

which expresses the fact that the rate of absorption of oxygen is inversely proportional to the thickness (which is assumed uniform and proportional to w) of the film. In a recent paper Krupkowski[2] has shown that in a series of experiments carried out at constant pressure the integral form (1) of the law held good. When experiments are carried out at constant volume and the weight increment measured by the fall of pressure it is necessary to make some assumption as to the dependence of k in (2) on the pressure p. The simplest assumption is that k is independent of p. We will start by considering the consequences of this assumption. Let v be the volume and T the temperature of the reaction vessel which initially ($t=0$) contains a mass m_0 of oxygen at pressure p_0 so that

$$p_0 v = m_0 \mathrm{RT}$$

R being the gas constant per gramme. At a subsequent instant t, the pressure has fallen to p and a mass m of gas remains in the vessel, so that

$$pv = m\mathrm{RT}$$

whence by subtraction

$$m_0 - m = (p_0 - p)\frac{v}{\mathrm{RT}}.$$

This difference represents the mass of oxygen absorbed by the metal in the interval 0 to t. The first pressure reading, p_0 at $t=0$, does not correspond to zero thickness film so we write

$$w = (p_0 - p)\ \frac{v}{\mathrm{RTA}} + w_0,$$

where w_0 is the weight of oxygen per sq. cm. already absorbed when the first observation, p_0, is recorded and A is the area of the metal surface. In any actual experiment it will not as a rule be possible to have the whole reaction vessel at the temperature T, so that the term $\frac{v}{\mathrm{T}}$ will have to be replaced by $\left(\frac{v_1}{\mathrm{T}} + \frac{v_2}{\mathrm{T}'}\right)$ where v_1 and v_2 are the volumes of the apparatus at temperatures T and T′. When this value of w is substituted in (2) and the integra-

tion is carried out treating k as constant we find an expression of the type

$$(p-a)^2=bt+c \quad . \quad . \quad . \quad . \quad . \quad . \quad (3)$$

where

$$\left.\begin{aligned} a&=p_0+\frac{w_0\mathrm{RTA}}{v},\\ b&=\frac{2\mathrm{R}^2\mathrm{T}^2\mathrm{A}^2}{v^2}\mathrm{K},\\ c&=\left(\frac{w_0\mathrm{RTA}}{v}\right)^2=(a-p_0)^2. \end{aligned}\right\} \quad . \quad . \quad . \quad (4)$$

TABLE I.

p_0.		500° C.	p_0.		600° C.	p_0.		700° C.
10·4	a	10·72	10·1	a	11·6	9·6	a	9·5
	b	0·097		b	3·94		b	1·35
	c	0·1		c	2·25		c	0·01
10·6	a	10·95	11·8	a	12·0	10·5	a	9·85
	b	0·235		b	2·76		b	0·73
	c	0·12		c	0·04		c	0·55
			20·6	a	20·5	20·0	a	18·8
				b	1·17		b	3·39
				c	0·01		c	1·44
			21·3	a	21·45	20·6	a	21·15
				b	1·76		b	1·99
				c	0·02		c	0·30
39·8	a	39·8	40·0	a	39·5	40·5	a	39·75
	b	0·075		b	0·75		b	2·09
	c	0·0		c	0·25		c	0·56
40·0	a	39·9	41·0	a	40·45	40·7	a	39·5
	b	0·012		b	0·41		b	2·22
	c	0·01		c	0·30		c	1·44

The parameters a, b, and c have been evaluated and the results are given in Table I. These values of a, b, and c give very reasonable agreement with the observational data over part of the range covered by experiment. It will be observed that the parameter a should always be greater than p_0 since all the quantities w_0, R, T, and v are essentially positive. This condition is violated in half the experiments, the reason being that the pressure drop in the first ten minutes is much faster than that

corresponding to the pressure drop occurring in the parabola which fits the observations in the period $t=10$ to $t=50$ minutes. We have been forced to the conclusion that the assumption that k, of equation (1) and (2), is independent of pressure is untenable. It will be noticed that the values of b at constant temperature, and therefore of k, show a tendency to diminish with increasing p_0 except for the low initial pressures at 700° C. which appear anomalous. The values of b must be divided by T^2 (*cf.* equation (4)) in order to obtain numbers proportional to k. When this is done the resulting numbers increase with T again with the exception of the low pressure observations at 700° C. In view of the lack of agreement between the theory and observations the figures are of little interest. The formula (3) can only be regarded as a very approximate expression of the observed pressure changes which represents the process empirically over a limited range.

The failure of the assumption $k=$constant to represent the facts makes it necessary to consider an alternative. We assume then that k of equation (2) is proportional to the pressure, so that (2) takes the form

$$w\frac{dw}{dt}=kp. \quad . \quad . \quad . \quad . \quad . \quad . \quad (5)$$

k having now a different significance, but being independent of w and p. We still assume

$$w=(p_0-p)\frac{v}{\mathrm{RTA}}+\mathrm{W}_0$$

to allow for the existence of a film of oxide when $p=p_0$. Making this substitution in (5) we find

$$\frac{p-p_0}{p_0}-\left(1+\frac{w_0\mathrm{RTA}}{p_0v}\right)\log_e\frac{p}{p_0}=\frac{\mathrm{R^2T^2A^2}}{p_0v^2}kt \quad . \quad (6)$$

An expression of this type, with $w_0=0$, has been used by Hinshelwood[3] to evaluate k in the oxidation of copper. We find that (6) gives a very good account of the pressure change observed in the early stages of oxidation. At the higher initial pressures during the first 50 minutes of oxidation the formula fits with $w_0=0$; at 600° and 700° C., the coefficient of $\log_e\frac{p}{p_0}$ is greater than unity at the lower

pressures. The values of the parameters of the equation are given in Table II. In fig. 1 the theoretical curves are shown as full lines with the experimental points obtained at 500° C. plotted for comparison. Within the first fifty minutes the experimental points fall on the curves within the limits of error and the agreement extends up to the end of the experiment in the lower curves obtained

TABLE II.

Values of a and b in the equation

$$\frac{p-p_0}{p_0} - a \log_e \frac{p}{p_0} = bt.$$

p_0.	500° C.	p_0.	600° C.	p_0.	700° C.
10·4	a 1·01	10·1	a 2·28	9·6	a 1·33
	b $3·7\times10^{-4}$		b $10·3\times10^{-2}$		b $27·6\times10^{-3}$
10·6	a 1·02	11·8	a 1·28	10·5	a 1·08
	b $10·8\times10^{-4}$		b $3·87\times10^{-2}$		b $9·5\times10^{-3}$
		20·6	a 1·04	20·0	a 1·08
			b $2·4\times10^{-3}$		b $11·5\times10^{-3}$
		21·3	a 1·085	20·6	a 1·08
			b $3·5\times10^{-3}$		b $3·8\times10^{-3}$
39·8	a 1·00	40·0	a 1·00	40·5	a 1·00
	b $27·5\times10^{-6}$		b $3·2\times10^{-4}$		b 9×10^{-4}
40·1	a 1·00	41·0	a 1·00	40·7	a 1·00
	b $4·35\times10^{-6}$		b $1·7\times10^{-4}$		b $11·5\times10^{-4}$

at 10·4 and 10·6 cm. initial pressure. The calculated curves and experimental points for 600° C. are shown in figs. 2 and 3. In fig. 2 the observed points on the curve $p_0=41$ cm. are only in fair agreement, discrepancies amounting to about 2 mm. occurring between the calculated and observed pressures. The other curve, $p_0=40·0$, gives very satisfactory agreement over the whole period of nearly 150 minutes during which observations were made. In fig. 3 for $p_0=21·3$ the agreement is again rather poor, but for $p_0=20·6$ is fairly good. In the same figure the results for the lower pressures are given on a reduced pressure and increased time scale. During the first ten minutes the pressure fall follows the calculated curve very exactly and then the observed points break away

suddenly. In the curve $p_0=11{\cdot}8$ the points after the break follow very accurately a law of the type

$$\log_{10} p_0/p = kt, \quad k = {\cdot}0205$$

Fig. 1.

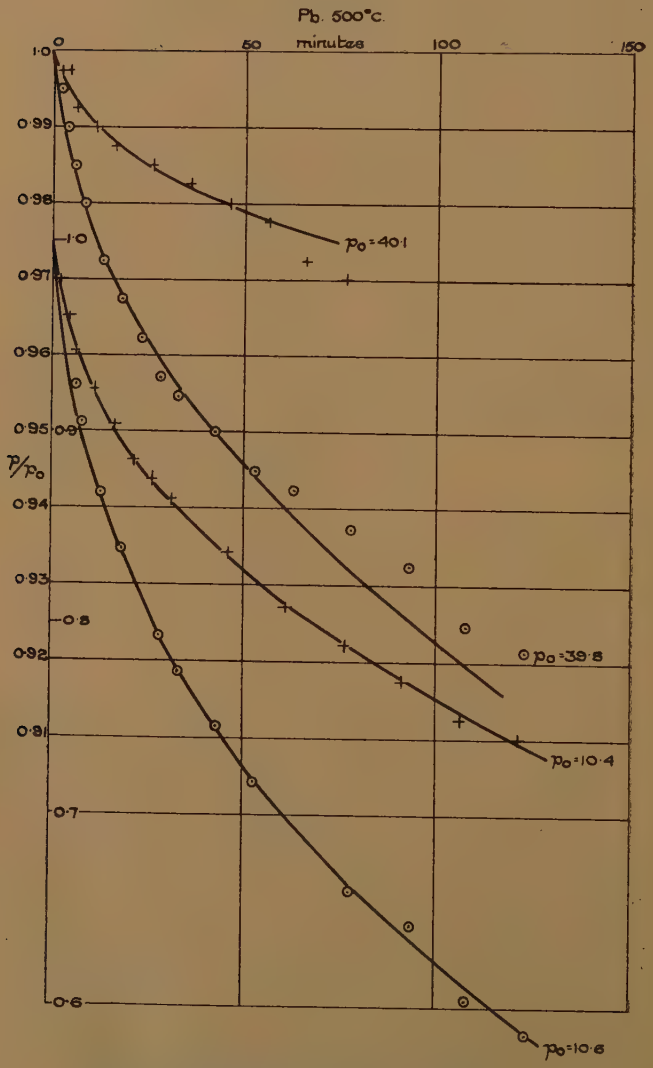

Experimental points ⊙ and +. The curves are calculated from equation (6).

Fig. 2.

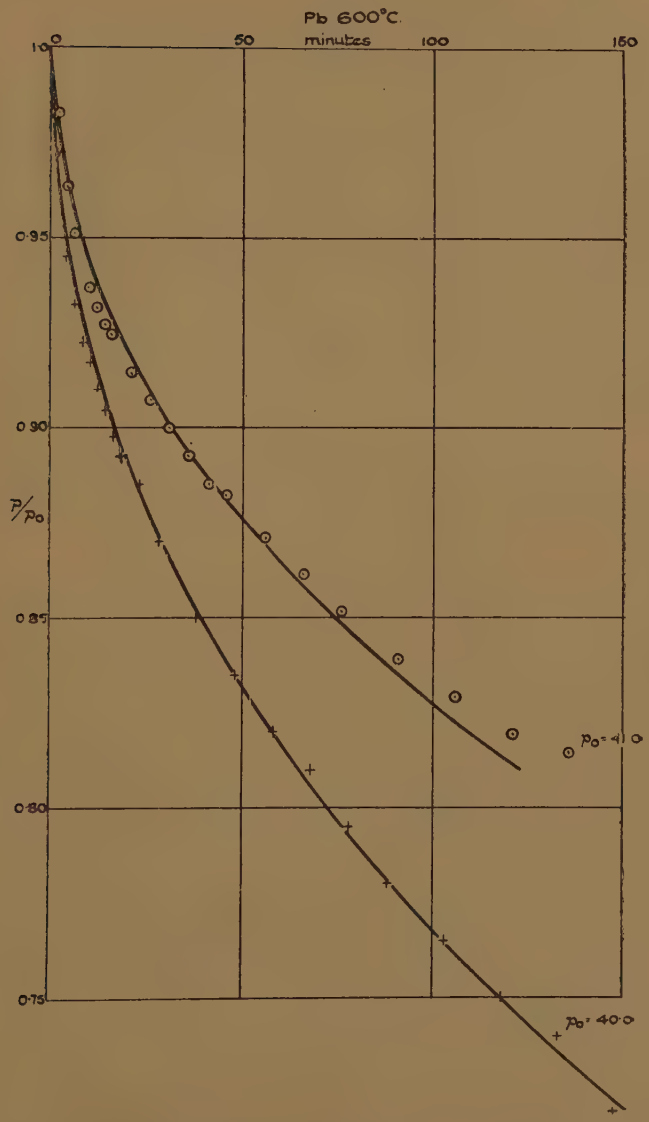

Experimental points ⊙ and +. The curves are calculated from equation (6).

in which p_0 is the initial pressure, 11·8 cm. of the whole series. In the other curve, $p_0=10{\cdot}1$, the points following the break are represented by

$$\log_{10} p=1{\cdot}302-{\cdot}0441t$$

which is of the same form as the last expression, but the origin of p and t no longer coincide with $p=p_0$ when $t=0$. At 700° C. the experimental points for the initial pressures 9·6 and 10·5 cm. fall very well on the calculated curve except for three points at the end of each series (fig. 4). The later portions of these curves can also be represented by a logarithmic pressure-time equation. At initial pressures of 20·0 and 20·6 cm. the early observations fit accurately on a curve of the form (6), but the later points require a logarithmic curve (fig. 5). For $p_0=20{\cdot}6$ the end of the curve is quite accurately represented by

$$\log_{10} p_0/p={\cdot}005t,$$

p_0 being the initial pressure 20·6 and t the same time scale as that used for the earlier observations. The curve $p_0=20{\cdot}0$ cm. requires a formula

$$\log_{10} p=\log_{10} 13{\cdot}87-{\cdot}0074t$$

to represent the final observations from $t=40$ to $t=125$ minutes. The observed points fall accurately on this curve.

The observations at 700° C. with initial pressures of 40·5 and 40·7 cm. are shown in fig. 6. The early part of the curves up to about $t=30$ mins. are quite well represented by equation (6). No satisfactory account of the later portion has been obtained.

The result of the numerical analysis of the data is thus to show that in all cases the early part of the pressure-time curves is represented by equation (6), a modified form of the type proposed by Hinshelwood. In four cases the later part of the curves is accurately represented by an equation of the type

$$\log p=\text{constant}-kt, \quad . \quad . \quad . \quad . \quad . \quad (7)$$

a form which has been used by Wilkins and Rideal[4] to account for the pressure fall during oxidation of copper at constant volume. The occurrence of this logarithmic type of pressure-time relation is not necessarily proof

Fig. 3.

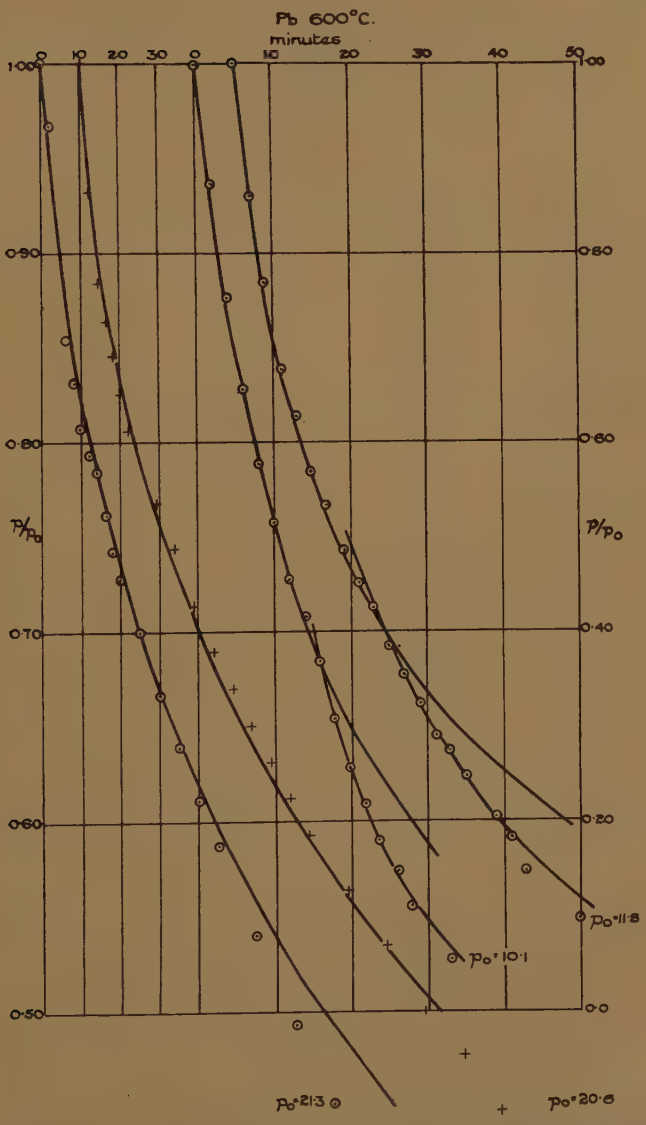

Experimental points ⊙ and +. The lower parts of the two curves on the right are calculated from equation (7), the remaining curves from equation (6).

of a failure of the parabolic law, that is to say the relation $w^2=kt$ may still be valid at constant pressure. It rather suggests that the quantity k, considered as a function of p,

Fig. 4.

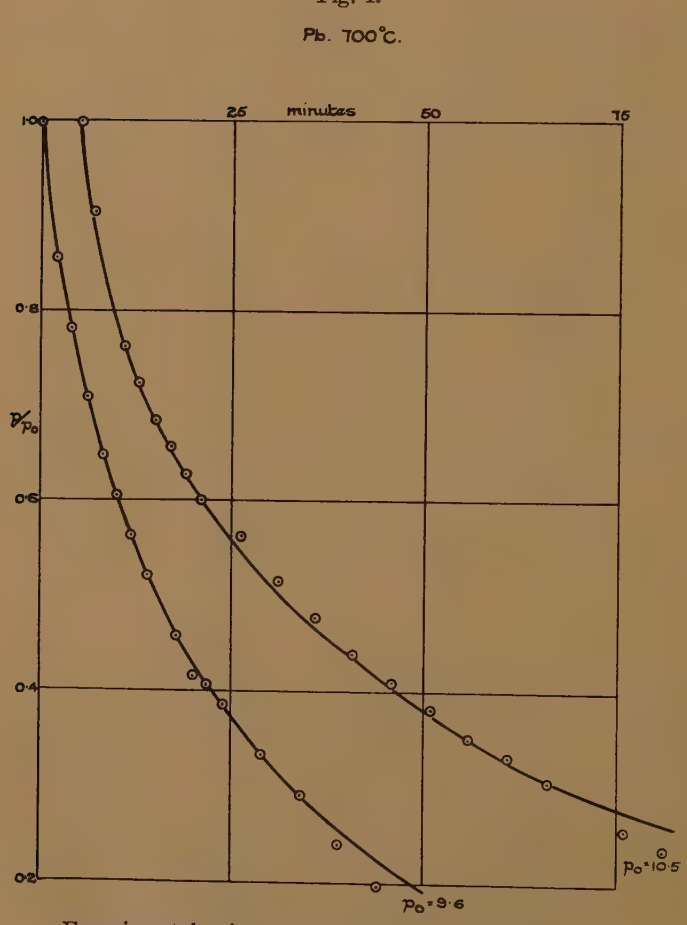

Experimental points ⊙. The curves are calculated from equation (6).

alters its form at some critical pressure or thickness of film.

The experiments on lead described in this paper show that the quantity k must depend on some factor which

is not as yet under control. Any particular specimen behaves as if the parabolic law were obeyed, but repetition

Fig. 5.

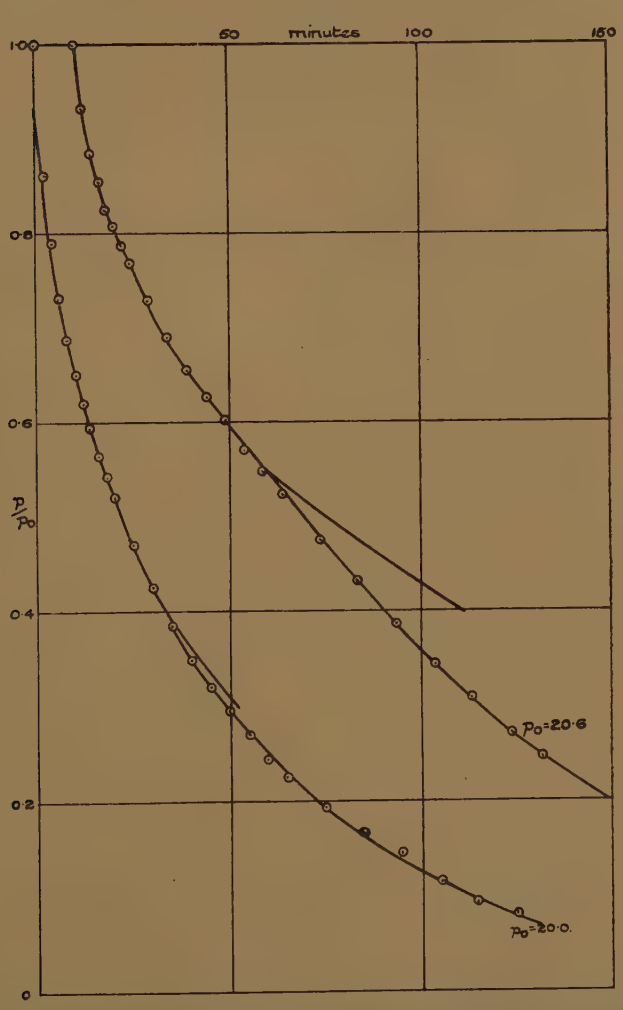

Experimental points ⊙. The upper parts of the curves are calculated from equation (6), the lower from equation (7).

on another specimen under apparently identical conditions gives a different value of the constant, k, in the equation.

The Hinshelwood relation, equation (6), represents the observations quite accurately during the first thirty or fifty minutes in all experiments, but the parameters of the equation differ from specimen to specimen. It

Fig. 6.

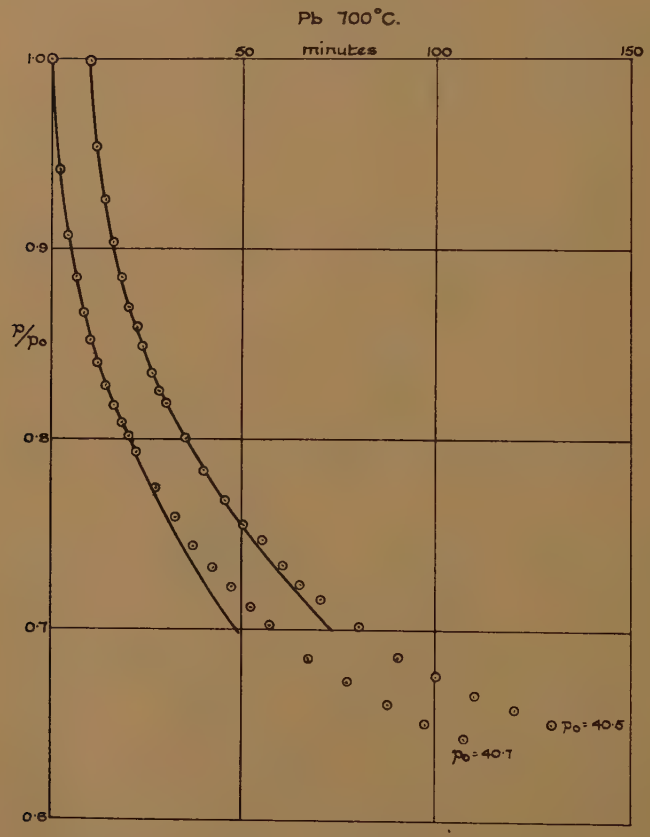

Experimental points ⊙. The curves are calculated from equation (6).

seems probable that the behaviour of any particular specimen is determined by some factor, such as the texture of the oxide film, which depends on the conditions existing at some very early stage of the oxidation process, possibly while the oxygen is being admitted to the system.

X-ray Investigation.

After cooling to room-temperature the oxide films on the specimens used in the oxidation experiments werd examined by X-rays. The investigation was facilitatee by the fact that during solidification the metal contracted and in places left hollows bridged over by films of oxide which could be removed and thus both sides of the film were available for examination. Several specimens, formed at different temperatures and at different initial oxygen pressures were examined, all giving similar results. The following account of the structure of a film taken from metal heated at 600° C. in an initial pressure of 10 cm. of oxygen is typical. The upper, oxygen-oxide, interface consists of yellow PbO, the orthorhombic modification, orientated with a (001) face parallel to the surface. The orientation is very strongly developed, some of the X-ray photographs suggesting that the material is a single crystal flake, distorted by the process of solidification and by the fact of its formation on the meniscus of molten metal. The lower, metal-oxide, interface consists of the red, tetragonal, modification of PbO. Orientation of this layer was not always observed, but in some specimens there were indications of a tendency for a (001) plane to lie parallel to the metal surface. It seems probable that any orientation existing when the metal was molten would be partly destroyed by rupture of the film when solidification was taking place and separation of the metal from the film occurred.

The above conclusions are in agreement with those already given [5] as a result of an electron diffraction examination of thin films on molten lead. The X-ray results here recorded are open to the objection that they have been obtained from specimens removed from the metal after it has cooled. The previous electron diffraction results, however, indicated the presence of the red-tetragonal, PbO in the thinnest films on the molten metal. The present investigation shows that the thicker films are composed of layers of the two modifications. Jenkins [6] in an electron diffraction examination of the oxide film on molten lead, concluded that the surface of the film was a thin single crystal of yellow, orthorhombic, PbO with a (001) plane parallel to the surface. From our own observations we must conclude that this film of yellow

PbO is separated from the metal by a layer of the red modification.

The existence of a layer of the red oxide in contact with the metal at temperatures as high as 600° C. is interesting because it is unstable and transforms to the yellow modification when heated in air to this temperature. A specimen on which, when separated from the metal on which it had been formed, the red oxide could be seen by visual inspection was examined before and after heating at 650° C. in air. Before this treatment the characteristic diffraction pattern of the red (tetragonal) oxide was obtained from the under surface, but after heating the originally red oxide had changed to yellow and the diffraction pattern to that of the orthorhombic variety of PbO.

Summary.

Experiments on the formation of oxide films on molten lead at 500°, 600°, and 700° C. show that the early part of the process is consistent with the "parabolic" law, the constant in the equation being proportional to the pressure. In several cases after the parabolic law has apparently ceased to be obeyed, the pressure falls in accordance with an equation of the type $\log p = kt + c$. An X-ray examination of the oxide film shows that it consists of two layers; red, tetragonal PbO next the metal and yellow, orthorhombic PbO at the oxygen-oxide surface. The latter oxide is very perfectly orientated with a (001) plane parallel to the metal surface: the photographs give the impression that this oxide is present as a thin single crystal film.

Acknowledgments.

The work has been carried out at the National Physical Laboratory for the Executive Committee in connexion with an investigation into the structure of oxide films and metal surfaces. We are indebted to Dr. C. H. Desch, F.R.S., Superintendent of the Department of Metallurgy and Chemistry, for his interest in the experiments.

References.

(1) Bircumshaw and Preston, Phil. Mag. xxxi. p. 686 (1936).
(2) Krupkowski, Int. Assoc. for Testing Materials, London, p. 38 (1937).
(3) Hinshelwood, Proc. Roy. Soc. A, cii. p. 318 (1922).
(4) Wilkins and Rideal, Proc. Roy. Soc. A, cxxviii. p. 394 (1930).
(5) Preston and Bircumshaw, Phil. Mag. xix. p. 160 (1935).
(6) Jenkins, Proc. Phys. Soc. xlvii. p. 109 (1935).

LXIX. *Potentials in Curved Surfaces.*

By G. R. Stibitz *.

ALTHOUGH most treatises on potentials devote considerable space to the discussion of two-dimensional potentials in the plane, few mention the corresponding problem for general curved surfaces. Such problems arise in the study of the flow of electric currents, heat, and fluids in thin curved shells.

It is the object of this note to derive the differential equations in curvilinear coordinates satisfied by two-dimensional electric potentials in isotropic surfaces.

We shall consider a surface at every point of which we may define a potential V. The properties of the surface as a conductor of electricity are completely described by two postulates :

(1) In any direction, s, at each point, there exists a current density I_s, which is related to the potential by the equation

$$\rho I_s = -\frac{\partial V}{\partial s},$$

where ρ is a function of position alone.

(2) The total normal current flow across any closed curve on the surface is zero.

Let any system of coordinates (u, v), not necessarily orthogonal, be drawn on the surface. It is well known that the intrinsic geometry of the surface is determined by the First Differential Form

$$ds^2 = g_{11}du^2 + 2g_{12}du\,dv + g_{22}\,dv^2,$$
$$g_{11} \neq 0,$$
$$g_{22} \neq 0,$$

where we assume the g_{jk} to possess derivatives with respect to u and v at every point.

We shall compute the current densities along the normals to the curves u=constant and to the curves v=constant, which densities by (1) are $1/\rho$ times the

* Communicated by the Author.

derivatives of V in these directions. The derivative of V in the direction normal to the curve u=constant is

$$\frac{1}{\sqrt{g_{22}}\sqrt{g}}\left(g_{22}\frac{\partial V}{\partial u}+g_{12}\frac{\partial V}{\partial v}\right),$$

while that normal to the curve v=constant is

$$\frac{1}{\sqrt{g_{11}}\sqrt{g}}\left(g_{11}\frac{\partial V}{\partial v}+g_{12}\frac{\partial V}{\partial v}\right),$$

where

$$g=\sqrt{g_{11}g_{22}-g_{12}^2}.$$

We apply postulate (2) to these current densities by computing the net current crossing the boundaries of an infinitesimal region bounded by the curves u, $u+du$, v, $v+dv$. The length of the arc v=constant is $\sqrt{g_{11}}\,du$, whence the total normal current flowing across this boundary is

$$-\frac{du}{\rho\sqrt{g}}\left(g_{11}\frac{\partial V}{\partial v}+g_{12}\frac{\partial V}{\partial u}\right).$$

The total normal current flowing across the two boundaries v=constant and $v+dv$=constant is therefore

$$+\frac{\partial}{\partial v}\left[\frac{1}{\rho\sqrt{g}}\left(g_{11}\frac{\partial V}{\partial v}+g_{12}\frac{\partial V}{\partial u}\right)\right]du\,dv.$$

A similar expression gives the total current across the remaining boundaries. By postulate (2), therefore, we have

$$\frac{\partial}{\partial u}\left[\frac{1}{\rho\sqrt{g}}\left(g_{22}\frac{\partial V}{\partial u}+g_{12}\frac{\partial V}{\partial v}\right)\right]+\frac{\partial}{\partial v}\left[\frac{1}{\rho\sqrt{g}}\left(g_{11}\frac{\partial V}{\partial v}+g_{12}\frac{\partial V}{\partial u}\right)\right]=0.$$

This is the differential equation which must be satisfied by the potential throughout any source-free region of a thin conducting surface of resistivity ρ.

When ρ is a constant the quantity which must vanish becomes the second differential parameter of the invariant V for curvilinear coordinates.

If u and v are chosen so as to be isometric coordinates for the given surface, we have

$$g_{12}=0,$$
$$g_{11}=g_{22}=\sqrt{g}.$$

Then, for constant resistivity, the potential equation reduces to

$$\frac{\partial^2 V}{\partial u^2} + \frac{\partial^2 V}{\partial v^2} = 0,$$

which is identical with that satisfied by the potential in plane Cartesian coordinates. In this case it is possible to translate any problem about potentials on curved surface into an analogous problem about potentials on a plane. In particular the method of conformal transformations may be applied to such potential distributions.

It is interesting to note, in particular, that the stereographic projection of a plane on a sphere is conformal. Hence any potential distribution on a sphere may be projected stereographically on to the plane.

Bell Telephone Laboratories.
September 30, 1937.

LXX. *Thermo-Electric Effects in Homogeneous Conductors.*

By Malcolm Fraser, *M.A., D.Phil., Trinity College. The University of Melbourne* *.

ON short circuiting the terminals of a sensitive galvanometer with a copper wire it was found that deflexions of the galvanometer were produced when the wire was warmed. This was in apparent disagreement with the Law of Magnus, which states that in a circuit composed of a homogeneous conductor no thermo-electric currents will be set up if various parts of the circuit are at different temperatures. It was in order to test this law that the present research was carried out.

If the wire is heated at a point so that the temperature gradients on both sides of the point are the same, it is obvious from the symmetry of the circuit that no thermo-electric current can be set up. If, however, the wire is heated asymmetrically, *i. e.*, the temperature gradients on each side of the hottest point are different, it might be possible to get thermo-electric currents providing the Law of Magnus were false.

* Communicated by W. Hume-Rothery, D.Sc., F.R.S.

A Broca galvanometer was used in all the experiments on account of its voltage sensitivity. The galvanometer was very nearly astatic—actually the suspension had to be remade for this to be so—with the result that it was not necessary to screen it with an iron shield. Care had to be taken, however, that there were no non-uniform variations in the external magnetic field caused by variations in magnitude and position of electric currents or by movements of iron in the neighbourhood of the galvanometer. The constancy of the galvanometer zero and the constancy of galvanometer readings in all experiments showed that external magnetic fields were not affecting readings. When the galvanometer coils were in series the galvanometer had a resistance of 10·6 ohm and a sensitivity of $2{\cdot}6 \times 10^{-8}$ volt per mm. deflexion. When in parallel the resistance was 2·65 ohm and the sensitivity $1{\cdot}3 \times 10^{-8}$ volt per mm. Readings could be taken to less than 0·5 mm.

Experiments with Copper.

A copper wire about 2 metres long had its two ends connected to the terminals of the galvanometer. The middle portion of the wire was subjected to asymmetrical heating by means of an electric heater, which could be moved along the wire. The heater (fig. 1) consisted of a glass tube, round the outside of which was wound nichrome wire. Through variations in the thickness of the glass and through variations in the closeness of the windings of the nichrome wire it was possible to get a large temperature gradient from A to B and a small gradient from A to C. In order to obtain some idea of the temperatures from B to C a thermocouple was used. The thermocouple was made by joining a constantan wire of diameter 0·3 mm. to a manganin wire of the same diameter, so as to form a straight wire of uniform diameter. Constantan and manganin were chosen because they possess nearly equal thermal conductivities. The thermocouple wire was slipped through the heater and the e.m.f. was observed with the constantan-manganin junction in various positions relative to the heater. Fig. 1 shows the result graphically. It must be noted, however, that this gives the temperature distribution along the thermocouple wire and not that along the copper wire, which has to be substituted for the constantan manganin wire.

A copper wire 0·21 mm. diameter was first used. The heater was moved along the middle 20 cm. of the wire and the galvanometer reading was noted for various fixed positions of the heater. At first e.m.f's. of the order of 15×10^{-6} volt were obtained, but it was found that these were due to the heater annealing the wire. The annealed wire and the unannealed behaved thermo-electrically as two different metals. The e.m.f. developed was 15×10^{-6} volt when the hot junction was at 300° C.

Fig. 1.

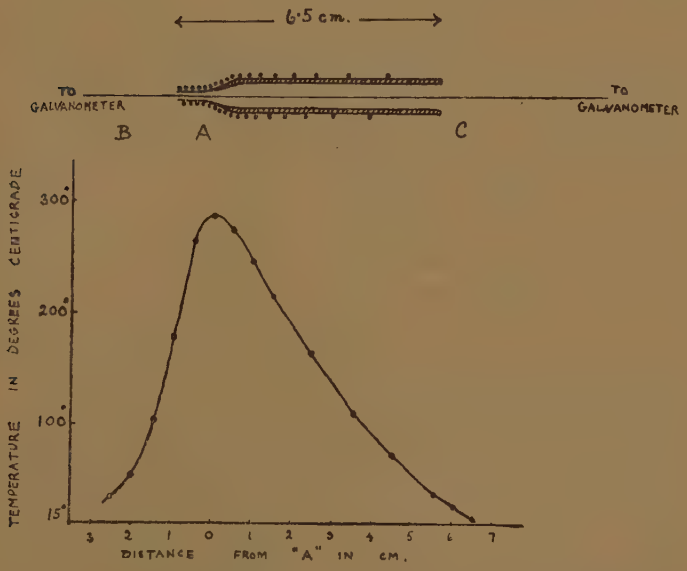

and the cold junction at 15° C.—the current flowing from the annealed to the unannealed at the hot junction. To avoid this e.m.f. 25 cm. of the mid-portion of the copper wire was annealed for 30 minutes at a temperature of 550° C. On proceeding with the experiment as before it was found that the galvanometer deflexion varied as the heater was moved relative to the wire. This is shown graphically by the continuous curve in fig. 2. It was found that the results were repeatable—the same deflexion always being obtained for the same position of the heater. It will be seen that the deflexions were both positive and negative, and that the maximum deflexion corresponds

to $1{\cdot}8 \times 10^{-7}$ volt. The heater was then reversed relative to the wire so as to reverse the temperature gradients and the procedure repeated. The results obtained are shown by the dotted curve in fig. 2. It will be noticed that its shape is similar to that of the continuous curve except that it lies to the left.

Another copper wire was taken, but of 0·07 mm. diameter. This had its mid-portion annealed at 450° C. for 30 minutes. The results with this wire are shown in fig. 3. Here, again, the dotted curve is similar to the

Fig. 2.

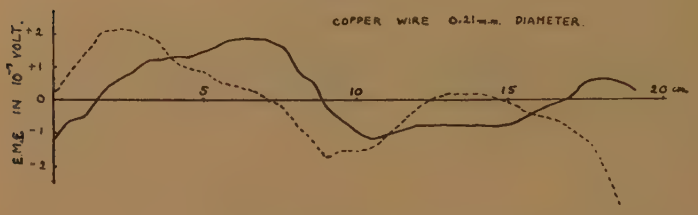

Fig. 3.

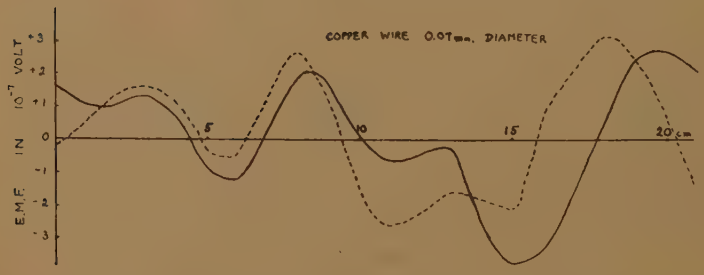

continuous curve. The maximum deflexion corresponds to an e.m.f. of $3{\cdot}7 \times 10^{-7}$ volt.

A third experiment was performed on a much purer copper wire. This was obtained by drawing down a Hilger spectroscopically pure copper rod to 0·23 mm. diameter. This had its mid-portion annealed at 400° C. for 90 minutes. The results are shown in fig. 4. It will be noticed that the e.m.f.'s are much smaller, the maximum being $0{\cdot}6 \times 10^{-7}$ volt.

From these experiments it will be seen that the e.m.f's. produced were not due to the asymmetric heating, otherwise they would not have changed sign on moving the

heater along the wire and they would have reversed in sign on reversing the heater. That the e.m.f. was due to inhomogenities in the wire is shown by the three facts :— (1) That the e.m.f. varies in both magnitude and sign for different positions of the heater relative to the wire. (2) That the shape of the continuous curve is similar to that of the dotted curve. Perfect agreement is not to be expected because the wire was heated over a portion of its length. Hence the e.m.f. is an integrated effect. (3) That the purer the wire the less the e.m.f.

Experiments were also performed using small gas jets to heat the copper wires instead of the electric heater. Similar results were obtained.

Fig. 4.

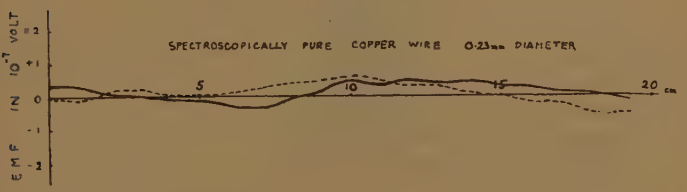

Experiments with Mercury.

A similar experiment was performed with mercury. The mercury was purified by twice warming with dilute nitric acid. It was then washed with water and dried by heating it near its boiling-point for about half an hour. The mercury, however, was not distilled, so it was not as pure as it might have been.

It was introduced into a glass capillary tube of the shape shown in fig. 5. PQR and STUV being respectively two vertical planes, and PRSU being in a horizontal plane. The total length of the capillary was 112 cm. Its mid-portion had an internal diameter of 0·15 mm. and an external diameter 0·3 mm. Dipping into the mercury at T was an iron wire 1 cm. long. Its other end was soldered to a copper wire which was connected to one terminal of the galvanometer. Similarly, the mercury at V was connected to the other terminal of the galvanometer. In some experiments the portion of the capillary to one side of Q was asymmetrically heated by means of a nichrome heater, which was placed about 1 cm. below

the capillary as shown in fig. 5. In other experiments the heating was by means of small gas-jets.

At first erratic results were obtained with this apparatus. They were traced to fluctuating temperature differences between the mercury-iron-copper junctions at T and V respectively. By placing the ends of the capillary ST

Fig. 5.

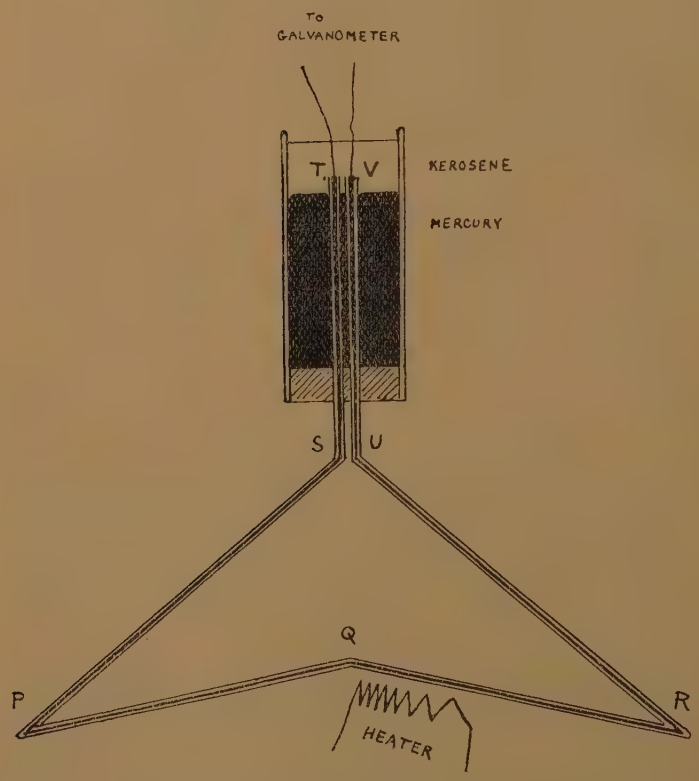

and UV respectively in a kerosene bath the trouble was only partially overcome. Eventually, however, when the lower portion of the bath was filled with mercury, as shown in fig. 5, constant galvanometer readings were obtained.

In all the experiments no deflexion was obtained even when the mercury was near its boiling-point. The experiment was repeated many times under varying conditions,

but no deflection could be obtained, *i. e.*, no e.m.f. greater than 10^{-8} volt was obtained. When, however, the mercury was heated so strongly that the thread of mercury in the capillary broke, a kick was obtained on the galvanometer but no permanent deflexion. On discontinuing heating another kick was obtained when the two threads reunited. The charge which caused the kick was found to be $1{\cdot}3 \times 10^{-7}$ coulomb. This charge corresponds to a passage of six electrons per mercury atom across the cross-section of the mercury thread. This effect, although interesting, has nothing to do with this investigation.

The experiments with mercury show that asymmetric heating produces no measurable e.m.f.

Discussion of Results.

The results with both copper and mercury are in disagreement with the results of Benedicks[1]. He states[2] "There is evidence that the e.m.f.'s which come into play when the thermal asymmetry is a pronounced one are of just the same order as the electromotive forces of the Seebeck effect." With the hot junction at 300° C. and the cold junction at 15° C. the electromotive forces of the Seebeck effect are of the order of 1000 microvolts. Yet in the experiments described, the author obtains no measurable e.m.f., *i. e.*, no e.m.f. greater than 0·01 microvolts. Benedicks' experiments with solid metals are open to criticism for the following reasons. Firstly, he subjects portion of his metal wire to strain either by varying its diameter or by fusing on to it beads of glass or quartz. Bridgman[3] has shown that a strained metal behaves thermoelectrically as a different metal. Secondly, he makes no mention of annealing his metals, which is essential, otherwise the heating will produce inhomogeneities.

The author's results with copper are in disagreement with those of Feng and Band[4]. These workers, however, make no mention of annealing their wires. Their results are similar both in sign and magnitude to those obtained by the author before he annealed his wires. It is essential for the wires to be annealed as the local heating would otherwise cause the wires to be heterogeneous. It seems, therefore, that Feng and Band's conclusion that the Law of Magnus does not hold for copper is wrong, the e.m.f.'s

which they obtained being due to inhomogeneities in their wires and not due to asymmetric temperature gradients. Band and his co-workers[5] have also worked with nickel, aluminium, and silver, but here again their results are open to the same criticism as those they obtained with copper. Ch'en and Band's[6] results with mercury are only in agreement with those of the author at temperatures above 150° C. when they get no measurable e.m.f. At temperatures below 100° C. they obtained e.m.f.'s of the order of 23×10^{-8} volt. This surprising result was not obtained by the author.

Bridgman[7], Benade[8], and Haga and Zernicke[9] get similar results to the author with mercury. Tsutsui [10] obtains fluctuating e.m.f.'s with mercury, but is unable to account for them. He shows, however, that they are independent of the temperature gradients. Terada, Tsutsui, and Tamana [11] get e.m.f.'s with asymmetrically heated wires of nickel, copper, silver, aluminium, and tungsten, but conclude that they are due to inhomogeneities in the wires, for they get similar effects with symmetrical heating.

Thus five different workers or groups of workers, including the author, obtain results which are in agreement with the Law of Magnus. The two groups of workers who have concluded that the Law of Magnus is false have in certain experiments not taken sufficient precautions to see that their wires are homogeneous. Thus it seems that accurate experimental results are in agreement with the Law of Magnus. This means, therefore, that the thermo-electric effect * (Benedicks effect) which Benedicks claims to have discovered is apparently non-existent.

The author's experiments are of importance in accurate thermo-electric thermometry. His results show that e.m.f.'s are to be expected when a wire consisting of one metal is not at a uniform temperature. This means that the e.m.f. of a thermocouple depends not only on the temperatures of the hot and cold junctions, but also on the temperatures of the wires themselves. This rather surprising result is due to the difficulty in obtaining thermo-electrically homogeneous wires.

* Not to be confused with the electro-thermic effect [12] (X-effect), which Benedicks claims to have discovered also.

In conclusion, I should like to thank Professor Laby for placing the resources of the Natural Philosophy Department of the University of Melbourne at my disposal. He and the members of his staff are to be thanked for the help they have given me. Dr. W. Hume-Rothery of Oxford must also be thanked, for it was partly through him that I decided to carry out this investigation.

References.

(1) Benedicks. Many papers, the principal of which are :—*Compte Rendus*, clxiii. p. 751 (1916) ; clxv. pp. 391, 426 (1917) ; clxix. p. 578 (1919). *Annalen d. Physik.* lv. pp. 1, 103 (1918) ; lxii. p. 185 (1920). Journal Institute Metals, xxiv. p. 7 (1920). *Ark. f. Mat. Astrom. Fysik.* xix b, p. 4 (1925).
(2) Benedicks, Journal Institute Metals, xxiv. p. 25 (1920).
(3) Bridgman, Proc. Amer. Acad. liii. p. 269 (1917–18).
(4) Feng and Band, Phys. Soc. Proc. xlvi. p. 515 (1934).
(5) Band, Phys. Soc. Proc. xlvii. pp. 852–909 (1935).
(6) Ch'en and Band, Phys. Soc. Proc. xlviii. p. 164 (1936).
(7) Bridgman, Proc. Amer. Acad. liii. p. 379 (1917–18).
(8) Benade, Phys. Review, xviii. p. 199 (1921).
(9) Haga and Zernicke, *Proc. K. Akad. Wet. Amst.* xxi. p. 1262 (1919).
(10) Tsutsui, Inst. Phys. & Chem. Research Tokyo, x. p. 19 (1929).
(11) Terada, Tsutsui, and Tamana, Inst. Phys. and Chem. Tokyo, vii. p. 201 (1927–28).
(12) Benedicks. Many papers, the principal of which are :—*Comptes Rendus*, clxvii. p. 296 (1918) ; clxx. p. 1382 (1920). *Ark. f. Mat. Astrom. Fysik*, xxiii. A, no. 27 ; xxiv. A, no. 1 ; xxiv. A, no. 7 (1933) ; xxv. A, no. 9 (1936) ; xxv. A, no. 20 (1937).

LXXI. *Direct Determination of the Electrical Constants of Soil at Ultra-high Radio-frequency.* *By* Manindra Kumar Chakravarty, *M.Sc.*, *and* S. R. Khastgir, *D.Sc.*, *Dacca University* *.

1. *Introduction.*

In connexion with our work on the ground attenuation of ultra-short waves recently carried out at Dacca, it has been considered desirable to obtain some detailed knowledge of the electrical properties of Dacca soil for ultra-high frequencies. Accordingly direct determinations of the electrical conductivity and of the dielectric constant of a specimen of Dacca soil have been undertaken for varying moisture-contents of the soil and for a certain range of ultra-high frequencies.

* Communicated by S. R. Khastgir, D.Sc.

Direct determinations of the electrical constants of soil for ultra-high radio frequencies have been attempted by Smith-Rose and McPetrie *, but in their investigations the values of the dielectric constant have been only conjectured. S. S. Banerjee and Joshi † have recently published some results by the laboratory method where the electrical constants have been evaluated for varying moisture-contents (6 to 14 per cent.) and for frequencies of the order of 50 to 70 megacycles per second.

We have followed the standard method of separating the electrical conductivity and the dielectric constant of the specimen by determining the attenuation constant of the Lecher-wire system immersed in it. The values of electrical conductivity and the dielectric constant have been obtained at a definite frequency (82 megacycles per sec.) for moisture-contents varying from 8 to 41 per cent. and for a definite moisture-content for 73 to 89 megacycles per sec.

2. *Theory of the Method.*

If V_x is the voltage at a distance x from the input end of a parallel wire transmission line and V_0 the input voltage to the line, then

$$V_x = V_0 \cdot e^{-(\alpha+j\beta)x},$$

where α and β are the attenuation and wave-length constants. The values of α and β are obtained from

$$\alpha^2 = \tfrac{1}{2}[\sqrt{\{(R^2+\omega^2L^2)(G^2+\omega^2C^2)\}}+(RG-\omega^2LC)], \quad (1)$$

$$\beta^2 = \tfrac{1}{2}[\sqrt{\{(R^2+\omega^2L^2)(G^2+\omega^2L^2)\}}-(RG-\omega^2LC)], \quad (2)$$

where R is the resistance, L the inductance, G the leakance, C the capacitance per unit length of the transmission lines, and ω the angular frequency of the waves. When the lines are immersed in a *pure* dielectric such as air or water, $G=0$, then if R is taken as zero, $\alpha=0$, $\beta=\omega\sqrt{LC}$.

If λ is the length of the standing wave set up on the wire-system,

$$\lambda_a = \frac{2\pi}{\beta} = \frac{2\pi}{\omega\sqrt{LC}}.$$

* Smith-Rose and McPetrie, Proc. Phys. Soc. xlvi. p. 6 (1934).
† S. S. Banerjee and Joshi, ' Science and Culture ' (May 1937).

When the wire-system is immersed in the medium of dielectric constant ϵ, the length of the standing wave in that medium is then λ_s, corresponding to λ_a in air.

Then
$$\frac{\lambda_a}{\lambda_s}=\frac{\sqrt{\mathrm{L}.\epsilon.\mathrm{C}}}{\sqrt{\mathrm{L}.\mathrm{C}}}$$

or
$$\left(\frac{\lambda_a}{\lambda_s}\right)^2=\epsilon.$$

If the medium possesses a conductivity σ, the leakance will no longer be zero, and the equations (1) and (2) will be reduced to

$$\alpha^2=\tfrac{1}{2}[\omega\mathrm{L}\sqrt{(\mathrm{G}^2+\omega^2\mathrm{C}^2)}-\omega^2\mathrm{LC}], \quad . \quad . \quad . \quad (3)$$

and
$$\beta^2=\tfrac{1}{2}[\omega\mathrm{L}\sqrt{(\mathrm{G}^2+\omega^2\mathrm{C}^2)}+\omega^2\mathrm{LC}]. \quad . \quad . \quad (4)$$

Now $\mathrm{G}=4\pi\mathrm{C}\sigma$,

C_s=capacitance per unit length of the Lecher-wire system immersed in the medium$=\epsilon.\mathrm{C}$.

Hence (3) and (4) would reduce to

$$\alpha=\sqrt{\{\tfrac{1}{2}\omega^2\mathrm{LC}(\epsilon'-\epsilon)\}}, \quad . \quad . \quad . \quad . \quad . \quad (5)$$

$$\beta=\sqrt{\{\tfrac{1}{2}\omega^2\mathrm{LC}(\epsilon'+\epsilon)\}}; \quad . \quad . \quad . \quad . \quad . \quad (6)$$

where
$$\epsilon'=\sqrt{\epsilon^2+\frac{4\sigma^2}{f^2}}.$$

Since
$$\omega^2\mathrm{LC}=\left(\frac{2\pi}{\lambda_a}\right)^2,$$

$$\alpha=\frac{2\pi}{\lambda_a}\sqrt{\frac{\epsilon'-\epsilon}{2}}, \quad . \quad . \quad . \quad . \quad . \quad (7)$$

and
$$\beta=\frac{2\pi}{\lambda_a}\sqrt{\frac{\epsilon'+\epsilon}{2}}. \quad . \quad . \quad . \quad . \quad . \quad (8)$$

Now
$$\lambda_s=\frac{2\pi}{\beta}=\lambda_a\sqrt{\frac{2}{\epsilon+\epsilon'}}$$

or
$$\left(\frac{\lambda_a}{\lambda_s}\right)^2=\frac{\epsilon'+\epsilon}{2}. \quad . \quad . \quad . \quad . \quad . \quad . \quad . \quad (9)$$

From (7) and (9)

$$\epsilon=\left(\frac{\lambda_a}{\lambda_s}\right)^2-\frac{\alpha^2\lambda_a^2}{4\pi^2}. \quad . \quad . \quad . \quad . \quad . \quad (10)$$

Remembering $$\epsilon' = \sqrt{\epsilon^2 + \frac{4\sigma^2}{f^2}},$$

we obtain from (8) and (10)

$$\sigma = \frac{\alpha f \lambda_a^2}{2\pi\lambda} = \frac{\alpha\omega\lambda_a^2}{4\pi^2\lambda_s} \quad . \quad . \quad . \quad . \quad . \quad . \quad (11)$$

In the experiments, the details of which are given in the next section, the Lecher-wires are immersed in the soil over a certain length beginning from the first potential node in air. The first potential node in the soil next to the first potential node in air is determined, and a resonance curve is then drawn showing galvanometer deflexions for either sides of this resonance point. The values of the dielectric constant ϵ and the electrical conductivity σ of the soil are determined easily from

Fig. 1.

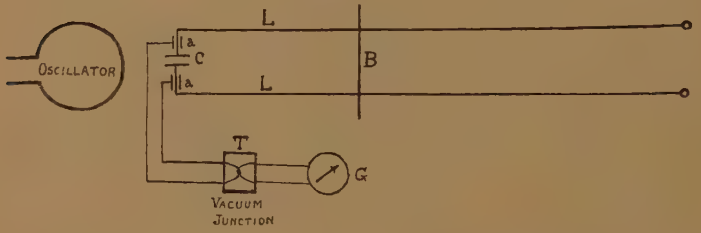

(10) and (11) by measuring λ_a and λ_s and by determining the attenuation constant α. This constant α is obtained by the measurement of the " half-width " of the resonance curve, *i. e.*, the distance between the points on either sides of the resonance curve when the deflexion of the galvanometer becomes half that at the resonance point. It can be shown that under the condition of the experiments α is given by

$$\alpha = \frac{2\pi . d}{\lambda_s^2\left(1 + \frac{\lambda_a}{\lambda_s}\right)},$$

where d is the " half-width."

3. *Experimental Arrangements.*

The experimental arrangements are shown in fig. 1.

Into the Lecher-wire system is induced a resonance radio-frequency e.m.f. from a neighbouring ultra-short

wave oscillator. LL are the Lecher-wires, C a very small air-condenser, and B a copper bridge for tuning.

The amplitudes of the oscillations induced in the Lecher system are measured in arbitrary units by means of a vacuum thermal junction T in conjunction with a mirror galvanometer G. The vacuum junction is coupled to the Lecher-wire system by means of two small condensers *aa*, consisting of short brass tubes insulated from the Lecher-wires by glass sleeves.

A large wooden rectangular box about 1·8 metres long, 15–20 cm. wide, 20–25 cm. high, has been taken through which are passed the Lecher-wires. First with the box empty the consecutive positions of the current antinodes (or potential nodes) are determined by short-circuiting the wires with the copper bridge. When the bridge is in the exact position of a current antinode the galvanometer gives a maximum deflexion. The box is now moved so that its forward end coincides with the first potential node. This ensures that there is no potential variation on the wires at this point, so that the effect of reflexion at the boundary between soil and air would be reduced to a minimum. The distance between the first two potential nodes gives $\lambda_a/2$. The soil is then introduced and rammed as much as possible to simulate the conditions prevailing in the field. The position of the second potential node (the first potential node in the soil) now comes nearer the first node—the distance between these successive nodes gives $\lambda_s/2$ for that particular soil. A resonance curve is then constructed. The attenuation constant α is determined from this resonance curve.

The copper bridge which is shown in fig. 2 (*a*) is fixed to an ebonite handle. The ebonite handle can be mounted vertically through a slit in a wooden frame with two supporting flanges falling over the two sides of the box and sliding along the edges of the long box (see fig. 2 (*b*)) A paper scale is attached lengthwise on one side of the box. A brass point attached to the flange on this side serves as the index on the scale.

4. *Experimental Results.*

For 82 megacycles/sec. frequency the values of ϵ, σ, and α of the specimen of Dacca soil are given for different values of the moisture-contents in Table I. In Table II. the

values of ϵ, σ, and α are given for different ultra-high frequencies for a particular moisture-content.

Fig. 2.

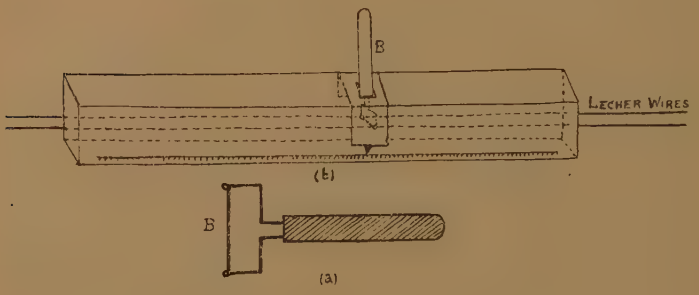

TABLE I.

$f=82$ megacycles/sec.

Moisture-content (per cent.).	λ_α (in metres).	λ_g (in metres).	α.	ϵ (e.s.u).	σ (e.m.u.).
7·78	3·66	1·84	$1·304\times10^{-3}$	3·95	$1·377\times10^{-14}$
19·9	,,	1·68	1·29 ,,	4·74	1·507 ,,
26·8	,,	1·60	1·68 ,,	5.23	2·039 ,,
32·1	,,	1·30	2·339 ,,	7·92	3·275 ,,
36·8	,,	·781	2·057 ,,	21·95	5·249 ,,
41·4	,,	·674	3·549 ,,	29·4	9.35 ,,

TABLE II.

Moisture-content 13·8 per cent.

Frequency in mega-cycles/sec.	λ_α (in metres).	λ_g (in metres).	α.	ϵ (e.s.u.).	σ (e.m.u.).
73·89	4·06	1·98	$·8145\times10^{-3}$	4·20	$·885\times10^{-14}$
77	3·88	1·96	1·263 ,,	3·91	1·12 ,,
78·9	3·80	1·93	1·704 ,,	3·87	1·75 ,,
81·08	3·70	1·89	1·39 ,,	3·83	1·79 ,,
88·7	3·38	1·80	1·146 ,,	3·52	1·135 ,,

The results are graphically shown in figs. 3 and 4 on the opposite page.

Fig. 3.

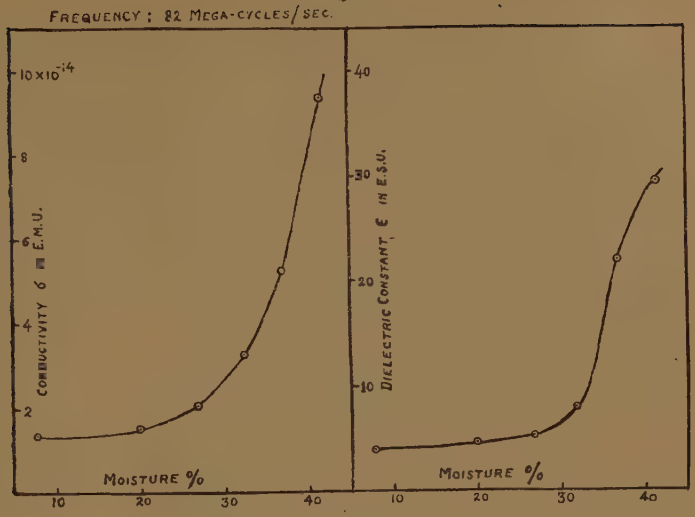
FREQUENCY : 82 MEGA-CYCLES/SEC.
10x10⁻¹⁴
8
6
4
2
CONDUCTIVITY σ IN E.M.U.
MOISTURE %
10
20
30
40
40
30
20
10
DIELECTRIC CONSTANT, ε IN E.S.U.
MOISTURE %
10
20
30
40

Fig. 4.

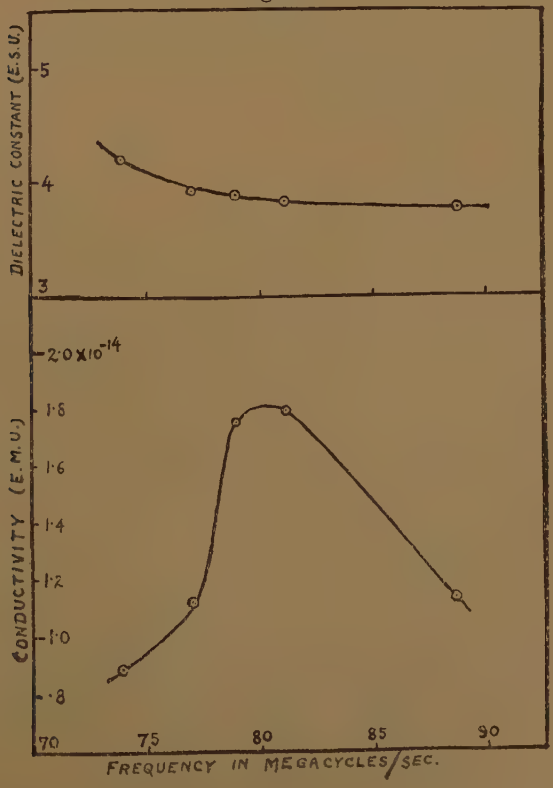
DIELECTRIC CONSTANT (E.S.U.)
5
4
3
CONDUCTIVITY (E.M.U.)
2·0x10⁻¹⁴
1·8
1·6
1·4
1·2
1·0
·8
70
75
80
85
90
FREQUENCY IN MEGACYCLES/SEC.

5. *Interpretation of Experimental Results.*

That the values of the dielectric constant ϵ and the electrical conductivity σ of the soil would increase with the increase of moisture-content needs no explanation. To interpret our experimental results showing the relation between ϵ or σ with frequency we should consider here Debye's treatment of dispersion in polar liquid under the influence of high radio-frequencies.

Taking ϵ to be the value of the dielectric constant for high radio-frequencies and ϵ_0 the statical dielectric constant of a polar liquid, Debye * has shown

$$r^2 = \frac{1}{2}\left[\sqrt{\frac{\epsilon_0^2+\epsilon^2x^2}{1+x^2}} + \frac{\epsilon_0+\epsilon x^2}{1+x^2}\right],$$

$$r^2k^2 = \frac{1}{2}\left[\sqrt{\frac{\epsilon_0^2+\epsilon^2x^2}{1+x^2}} - \frac{\epsilon_0+\epsilon.x^2}{1+x^2}\right],$$

where

r=ordinary refractive index,

k=absorption index,

$x = \frac{\epsilon_0+2}{\epsilon+2}.w.\tau.$,

τ=relaxation time,

and w=angular frequency.

The curve showing r against w according to Debye's formula clearly indicates that r diminishes with the increase of frequency. The soil contains water which is a polar liquid. Our result that the dielectric constant of the soil (with a certain percentage of moisture in it) diminishes with the increase of frequency is therefore in accord with Debye's formula.

In connexion with our measurements of electrical conductivity for different frequencies, much more comprehensive investigation is necessary before it is possible to give any theoretical interpretation.

6. *Summary and Conclusion.*

In the present investigation the attenuation of ultra-short waves travelling along a Lecher-wire system immersed in a specimen of Dacca soil has been determined

* Debye, 'Polar Molecules,' p. 91 (1929).

for a certain range of ultra-high frequencies (73 to 89 megacycles per sec.) and for varying moisture-contents from 8 to 41 per cent. The values of the electrical conductivity σ and the dielectric constant ϵ of the soil are then determined by the application of the standard formulæ.

The value of the dielectric constant of the specimen of the soil has varied from 3·95 e.s.u. at a moisture-content of 8 per cent. to 29·4 e.s.u. at a moisture-content of 41 per cent. The value of the electrical conductivity has been of the order of 10^{-14} e.m.u. It has increased with the increase of the moisture-content.

The value of the electrical conductivity of the soil has been found first to increase and subsequently to diminish with the increase of frequency. The dielectric constant of the soil has been found to diminish with the rise of frequency, as is expected from Debye's theory of dispersion in polar liquids for high frequencies.

It is to be noted that the values of the electrical conductivity and the dielectric constant of the soil obtained by the direct laboratory method agree well in their orders of magnitude with the values estimated from the attenuation measurements.

Physics Department,
Dacca University.
Nov. 10th, 1937.

LXXII. *Thick Lenses and Combinations of Thin Lenses.*

By Frederick Record, *B.Sc., The Technical College, Derby* *.

THE method described uses extrafocal distances and enables problems regarding thick lenses or combinations of thin lenses to be solved by the same procedure.

A coordinate system is used, the direction of travel of the light being regarded as positive, but the use of another convention only necessitates slight sign changes. As the method does not involve the finding of a square root there is no ambiguity with respect to the sign of the power of the equivalent system.

* Communicated by the Author.

A *spherical refracting surface* has one focal length, ϕ, in the first medium or object space, and another, f, in the second medium or image space. The relations between these focal lengths, the magnification, m, and the extra-focal distances, p and q, are

$$m=-\phi/p=-q/f, \quad \text{and} \quad pq=\phi f.$$

For unit magnification, *i. e.*, the position of the surface,

$$m=1, \quad p=-\phi, \quad q=-f.$$

Also
$$-\mu/\phi=\mu'/f=(\mu'-\mu)/r,$$

$$r=f+\phi,$$

and
$$\phi/f=-\mu/\mu',$$

μ and μ' being the refractive indices of the first and second media respectively, and r the radius of curvature of the surface. If F is the power of the surface,

$$\mathrm{F}=(\mu'-\mu)/r, \quad \phi=-\mu/\mathrm{F}, \quad \text{and} \quad f=\mu'/\mathrm{F}.$$

A *thin lens* may also be regarded as possessing two focal lengths, one, f, relating to the image space, and the other, ϕ, to the object space. The magnification, the focal lengths, and the extrafocal distances are connected by the expressions previously given. If F be the power of the lens, $-\phi=f=1/\mathrm{F}$, and $\phi/f=-1$.

As the relations between the magnification, the focal lengths, and the extrafocal distances are represented by the same equations for both surfaces and lenses, problems concerning combinations of such components may be solved by the same method if these quantities are employed. When a calculation shows that $\phi/f=-1$ it is concluded that the system behaves as a *lens*; if the ratio has some other value there is an equivalent *surface*.

The diagrams show the relative positions of the components and their foci for the case of a glass block bounded by convex spherical surfaces and surrounded by air, *i. e.*, for two separated surfaces. The fourth diagram shows the formation of the final image by the action of the components in turn. Diagrams drawn for large separations are most helpful.

In the calculations quantities without suffixes refer to the system as a whole, while those with suffixes relate to the respective components.

The distance between the components is indicated by d, and that between the second principal focus of the first component and the first principal focus of the second by k ('Geometrical Optics,' Blakesley, Whittaker, 1903).

The *first principal focus of the system* (fig. 2) is at a point distant a from the first principal focus of the first component, and therefore (ϕ_1+a) from the surface. As the emergent rays are parallel the intermediate image is formed at the first principal focus of the second component.

Hence $ak=\phi_1 f_1$, so that $a=\phi_1 f_1/k$.

Figs. 1–4.

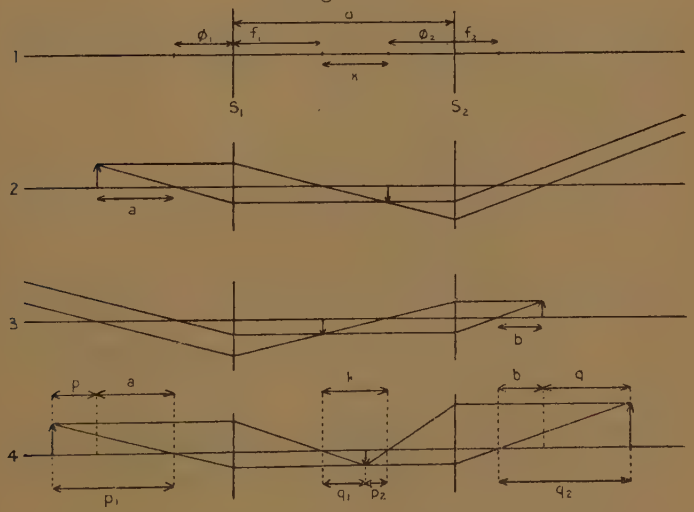

The *second principal focus of the system* (fig. 3) is at a point distant b from the second principal focus of the second component, and therefore (f_2+b) from the surface. For a reason similar to that stated in the preceding paragraph.

$$(-k)b=\phi_2 f_2, \quad \text{so that } b=-\phi_2 f_2/k.$$

The *focal length of the system for the object space*,

$$\phi=-mp, \quad \text{because } m=-\phi/p$$
$$=-m_1 m_2 p$$
$$=-\frac{\phi_1\phi_2 p}{p_1 p_2}.$$

The diagram shows that $p_2=q_1-k$ (fig. 4),

and that $$p=p_1-a=p_1-\phi_1 f_1/k.$$

Hence
$$\phi=-\frac{\phi_1\phi_2(p_1-\phi_1 f_1/k)}{p_1(q_1-k)}$$
$$=-\frac{\phi_1\phi_2(p_1k-\phi_1 f_1)}{k(p_1q_1-p_1k)}$$
$$=-\frac{\phi_1\phi_2(p_1k-\phi_1 f_1)}{k(\phi_1 f_1-p_1k)}$$
$$=\frac{\phi_1\phi_2}{k}.$$

For *the first principal or unit point* * $m=+1$, so that p becomes $-\phi$, and the distance of this point from the first component is $\phi_1+a-\phi$

$$=\phi_1+\phi_1 f_1/k-\phi_1\phi_2/k$$
$$=\phi_1(k+f_1-\phi_2)/k$$
$$=\frac{\phi_1 d}{k}, \quad \text{since } d=f_1+k-\phi_2 \text{ (fig. 1)}$$
$$=\frac{(\phi_1 d)\phi}{\phi_1\phi_2}$$
$$=\frac{d\phi}{\phi_2}.$$

The focal length of the system for the image space,

$$f=-q/m, \quad \text{because } m=-q/f$$
$$=-q/m_1m_2$$
$$=-\frac{qf_1f_2}{q_1q_2}.$$

The diagram shows that $q_1=p_2+k$ (fig. 4),

and that $$q=q_2-b=q_2+f_2\phi_2/k.$$

Hence
$$f=-\frac{f_1f_2(q_2+f_2\phi_2/k)}{q_2(p_2+k)}$$
$$=-\frac{f_1f_2(q_2k+f_2\phi_2)}{k(p_2q_2+q_2k)}$$

* Alternatively the equivalent lens or surface is at a distance $-\phi$ from its first principal focus, or of $-f$ from its second principal focus.

$$=-\frac{f_1f_2(q_2k+f_2\phi_2)}{k(f_2\phi_2+q_2k)}$$

$$=-\frac{f_1f_2}{k}.$$

For *the second principal or unit point* * $m=+1$, so that q becomes $-f$, and the distance of this point from the second component is f_2+b-f

$$=f_2-\phi_2f_2/k+f_1f_2/k$$
$$=f_2(k-\phi_2+f_1)/k$$
$$=\frac{f_2d}{k}$$
$$=\frac{(f_2d)(-f)}{f_1f_2}$$
$$=-\frac{df}{f_1}.$$

The *ratio of the focal lengths* is

$$\phi/f=-(\phi_1\phi_2)/(f_1f_2)$$
$$=-(\phi_1/f_1)(\phi_2/f_2).$$

The value of this ratio is

(1) for two thin separated lenses,

$$\phi/f=-(-1)(-1)=-1;$$

(2) for a thick lens of refractive index μ, between media of refractive indices μ_1 and μ_3,

$$\phi/f=-(-\mu_1/\mu)(-\mu/\mu_3)=-\mu_1/\mu_3;$$

(3) for a thick lens when the initial and final media are alike,

$$\phi/f=-\mu_1/\mu_3=-1.$$

Consequently, in cases (1) and (3) there is an *equivalent lens*, although this must be regarded as occupying one position (the first principal plane) for the object space, and another (the second principal plane) for the image space. In case (2) there is an *equivalent surface* which also has two positions, its radius being $r=(f+\phi)$.

The *power of the equivalent lens or surface* may be expressed in terms of that of the constituents.

* See footnote on preceding page.

For two thin separated lenses, $\phi/f=-1$, so that $-\frac{1}{\phi}=\frac{1}{f}$.

Either of the latter expressions gives the power, F, of the equivalent system.

$$\begin{aligned}
\mathrm{F}&=\frac{1}{f}\\
&=-\frac{k}{f_1f_2}\\
&=-\frac{\phi_2-f_1+d}{f_1f_2}, \quad \text{since } d=f_1+k-\phi_2\\
&=\frac{1}{f_1}+\frac{1}{f_2}-\frac{d}{f_1f_2}\\
&=\mathrm{F}_1+\mathrm{F}_2-d\mathrm{F}_1\mathrm{F}_2.
\end{aligned}$$

For a thick lens of refractive index μ, between media of refractive indices μ_1 and μ_3,

$$\frac{\phi}{f}=-\frac{\mu_1}{\mu_3}, \quad \text{so that } -\frac{\mu_1}{\phi}=\frac{\mu_3}{f}.$$

Either of the latter expressions indicates the power, F, of the equivalent surface in this case.

$$\begin{aligned}
\mathrm{F}&=\frac{\mu_3}{f}\\
&=\frac{-\mu_3 k}{f_1f_2}\\
&=\frac{-\mu_3(\phi_2-f_1+d)}{f_1f_2}.
\end{aligned}$$

But $\phi_2=-\mu/\mathrm{F}_2, \quad f_1=\mu/\mathrm{F}_1, \quad f_2=\mu_3/\mathrm{F}_2.$

On substitution of these values it is found that

$$\mathrm{F}=\mathrm{F}_1+\mathrm{F}_2-\frac{d}{\mu}\mathrm{F}_1\mathrm{F}_2.$$

When $\mu_1=\mu_3$, the same expression is obtained.

When the initial and final media are unlike each position of the equivalent surface has a corresponding centre of curvature at a distance of $r=\phi+f$. These centres are the *nodal points* of the equivalent surface.

The distance of the first nodal point from the first principal point is $(\phi+f)$, and that of the first principal focus is ϕ, so that the distance from the first principal focus of the system to the first nodal point is $\phi+f-\phi=f$. Similarly the distance from the second principal focus of the system to the second nodal point is $\phi+f-f=\phi$.

LXXIII. *Lebesgue Complex Integration and Generalized Differentiation.* *By* W. Fabian, *M.A., Ph.D.**

WE shall establish here further theorems on this subject †.

1. *Integration by Parts.*

Let l be a bounded simple curve, defined by

$$z=x+iy=x(t)+iy(t)$$

in the finite interval $(t_0 \leqslant t \leqslant \mathrm{T})$, such that $x(t)$ and $y(t)$ are monotonic in this interval.

Theorem 1.—*If $f(z)$ is an indefinite integral along l, and the measurable function $g(z)$ has an indefinite integral along l, then, everywhere on l,*

$$\int_a^z f(z)g(z)\,dz = \left[f(z)\int_b^z g(z)\,dz\right]_a^z - \int_a^z \left\{\frac{df(z)}{dz}\int_b^z g(z)\,dz\right\}dz,$$

where a and b are any two points on l, and the differentiation and integrations are along l.

Proof.—We have, almost everywhere on l,

$$\frac{d}{dz}\left\{f(z)\int_b^z g(z)\,dz\right\} = f(z)g(z)+\frac{df(z)}{dz}\int_b^z g(z)\,dz, \qquad (1)$$

where the integration and differentiations are along l.

* Communicated by the Author.

† Our previous papers on this subject were: Phil. Mag. ser. 7, vol. xxii. pp. 523–534, 1117–1122 (1936); ser. 7, vol. xxiv. pp. 256–262, 807–813 (1937); and ser. 7, vol. xxv. pp. 318–320 (1938).

The integral $\int_a^z f(z)g(z)\,dz$, taken along l, can be seen to exist everywhere on l from the inequalities

$$\left|\int_a^z f(z)g(z)\,dz\right| \leqslant \int_a^z \left|f(z)g(z)\right|\left|dz\right|$$

$$\leqslant M\int_a^z \left|g(z)\right|\left|dz\right|,$$

where M is the finite upper bound of $|f(z)|$ on l.

The integral $\int_a^z \left\{\frac{df(z)}{dz}\int_b^z g(z)dz\right\}dz$ (along l) can be seen to exist everywhere on l from the inequalities

$$\left|\int_a^z \left\{\frac{df(z)}{dz}\int_b^z g(z)\,dz\right\}dz\right| \leqslant \int_a^z \left|\frac{df(z)}{dz}\int_b^z g(z)\,dz\right|\left|dz\right|$$

$$\leqslant N\int_a^z \left|\frac{df(z)}{dz}\right|\left|dz\right|,$$

where N is the finite upper bound of $\left|\int_b g(z)dz\right|$ on l, and $\int_a^z \left|\frac{df(z)}{dz}\right|\left|dz\right|$ exists for all z on l, since $f(z)$ is an indefinite integral along l. Since $f(z)$ and $\int_b^z g(z)dz$ (along l) are indefinite integrals along l, therefore $f(z)$ and $\int_b^z g(z)dz$ (along l), and hence $f(z)\int_b^z g(z)dz$ (along l), are absolutely continuous * on l. Consequently,

$$\int_a^z \left[\frac{d}{dz}\left\{f(z)\int_b^z g(z)\,dz\right\}\right]dz = \left[f(z)\int_b^z g(z)\,dz\right]_a^z$$

everywhere on l, the differentiation and integrations being along l. The conclusion follows now on integrating (1) along l between the limits a and z.

Let $G(l)$ be a measurable set of points on l, and $E(l)$ that component which consists of all points of $G(l)$ on the arc corresponding to (t_0, t).

* Fabian, Phil. Mag. ser. 7, vol. xxiv. pp. 807–813 (1937).

Theorem 2.—If $\phi\{\mathrm{E}(l)\}$ is a generalized indefinite integral over $\mathrm{E}(l)$ in $\mathrm{G}(l)$, and the measurable function $g(z)$ has a generalized indefinite integral over $\mathrm{E}(l)$ in $\mathrm{G}(l)$, then

$$\int_{\mathrm{G}(l)} \phi\{\mathrm{E}(l)\}g(z)\,dz$$
$$=\phi\{\mathrm{G}(l)\}\int_{\mathrm{G}(l)} g(z)\,dz-\int_{\mathrm{G}(l)}\left[\mathrm{D}\phi\{\mathrm{E}(l)\}\int_{\mathrm{E}(l)} g(z)\,dz\right]dz.$$

Proof.—Let Ω be the curve traced out in the w-plane by the point

$$w=\pm m(\mathrm{E}_x)\pm im(\mathrm{E}_y)=m_0[\mathrm{E}(l)],$$

when $\mathrm{E}(l)$ varies simply * in $\mathrm{G}(l)$ with respect to t; where the sets E_x and E_y correspond to $\mathrm{E}(l)$ on the x- and y-segments respectively; and the positive or negative signs in $\pm m(\mathrm{E}_x)$ are taken, according as $x(t)$ is a non-diminishing or non-increasing function of t in (t_0, T), and the positive or negative signs in $\pm im(\mathrm{E}_y)$ are taken, according as $y(t)$ is a non-diminishing or non-increasing function of t in (t_0, T).

Under the conditions of the hypothesis we have, by theorem 1,

$$\int_\Omega \psi(w)\mathrm{F}(w)\,dw=\left\lfloor \psi(w)\int_0^w \mathrm{F}(w)\,dw\right\rfloor_0^{m_0\{\mathrm{G}(l)\}}$$
$$-\int_\Omega\left\{\frac{d\psi(w)}{dw}\int_0^w \mathrm{F}(w)\,dw\right\}dw,$$

where $\psi(w)=\phi\{\mathrm{E}(l)\}$, $\mathrm{F}(w)=g(z)$, and the differentiation and integrations are along Ω. The conclusion follows immediately, since †

$$\int_0^w \mathrm{F}(w)\,dw \text{ (along } \Omega) = \int_{\mathrm{E}(l)} g(z)\,dz,$$

and

$$\frac{d\psi(w)}{dw} \text{ (along } \Omega) = \mathrm{D}\phi\{\mathrm{E}(l)\}.$$

2. *Integration of Series.*

Let a simple curve, L, bounded or unbounded, and defined by

$$z=x+iy=x(t)+iy(t),$$

* Fabian, Phil. Mag. ser. 7, vol. xxii. p. 528 (1936).
† Fabian, Phil. Mag. ser. 7, vol. xxii. pp. 531, 532 (1936).

be such that it can be broken up into a finite number of simple curves, for each of which $x(t)$ and $y(t)$ are monotonic functions of t.

Theorem 3.—*Let the series* $\sum_{n=1}^{\infty} f_n(z)$ *converge to* $\mathrm{F}(z)$ *almost everywhere in a measurable set of points* $\mathrm{E(L)}$ *on* L, *of finite measure where the measurable functions* $f_n(z)$ *are integrable over* $\mathrm{E(L)}$. *Also let*

$$\left| \sum_{n=m}^{\infty} f_n(z) \right| < a \text{ finite constant } \mathrm{K}$$

for all m *and* z *in* $\mathrm{E(L)}$. *Then* $\mathrm{F}(z)$ *is integrable over* $\mathrm{E(L)}$ *and the series*

$$\sum_{n=1}^{\infty} \int_{\mathrm{E}_r(\mathrm{L})} f_n(z)\, dz$$

converges to $\int_{\mathrm{E}_r(\mathrm{L})} \mathrm{F}(z)\, dz$ *uniformly for all measurable sets of points* $\mathrm{E}_r(\mathrm{L})$ *in* $\mathrm{E(L)}$.

This theorem follows at once from the fact that * under the conditions of the hypothesis

$$\sum_{n=1}^{\infty} \int_{{}_r\mathrm{E}_t} \mathrm{P}_n(t)\, dx(t), \qquad \sum_{n=1}^{\infty} \int_{{}_r\mathrm{E}_t} \mathrm{Q}_n(t)\, dx(t),$$

$$\sum_{n=1}^{\infty} \int_{{}_r\mathrm{E}_t} \mathrm{P}_n(t)\, dy(t), \text{ and } \sum_{n=1}^{\infty} \int_{{}_r\mathrm{E}_t} \mathrm{Q}_n(t)\, dy(t),$$

converge to

$$\int_{{}_r\mathrm{E}_t} \mathrm{F}_1(t)\, dx(t), \qquad \int_{{}_r\mathrm{E}_t} \mathrm{F}_2(t)\, dx(t),$$

$$\int_{{}_r\mathrm{E}_t} \mathrm{F}_1(t)\, dy(t), \text{ and } \int_{{}_r\mathrm{E}_t} \mathrm{F}_2(t)\, dy(t)$$

respectively uniformly for all sets of points ${}_r\mathrm{E}_t$ on the t-segment, corresponding to the sets $\mathrm{E}_r(\mathrm{L})$; where $\mathrm{P}_n(t)$ and $\mathrm{Q}_u(t)$ are the real and imaginary parts of $f_n(z)$, and $\mathrm{F}_1(t)$ and $\mathrm{F}_2(t)$ the real and imaginary parts of $\mathrm{F}(z)$, respectively.

* Hobson, 'Theory of Functions of a Real Variable,' vol. ii. p. 291 (1926).

LXXIV. *Notices respecting New Books.*

Modern Theories of Integration. By H. KESTELMAN. (Oxford: University Press. Price 17*s.* 6*d.*)

THE principal object of this book is clearly to give an account of the Lebesgue Integral and its properties. An English text-book of this kind has been needed for many years, as is shown by Wiener's preface to his work 'The Fourier Integral' (1933), in which he laments the lack of knowledge of the Lebesgue Integral and finds it necessary to give a comprehensive list of Lebesgue Integral results in a long introductory chapter. The attitude of many English students of analysis has been that we can be grateful for the truth of certain results which hold for Lebesgue Integrals but not for Riemann Integrals, and we need not bother too much about the proofs. Such an attitude is not likely to produce a powerful grasp of the situation, and it is to be hoped that the arrival of this standard work will end this point of view.

The author says in his preface that the work is based upon postgraduate lectures given by Dr. Estermann in the University of London, but we can confidently assert that the book shows no uncomfortable signs of having been based upon lectures; indeed, if the author had not told us this secret we should not have discovered it for ourselves. The work is clearly cast for a body of students provided with adequate interest and grasp, and consequently does not undergo the contortions of a "teaching text-book"; on the other hand, it is no mere formal exposition of the subject, and one feels sure that Mr. Kestelman (and Dr. Estermann) pay great attention to their readers (and audience).

The work opens with a chapter on the theory of sets, and after a second chapter which surveys the Riemann Integral with its deficiencies well in mind, the book proceeds through a chapter on the theory of Lebesgue Measure to the structure of the Lebesgue Integral. No previous knowledge of the theory of sets is assumed, and the work is in this sense completely self-contained. The author clearly enjoys a very wide use of the symbolism of the theory of sets, and there will be readers who would prefer just a shade more use of the English language and a little less of the symbolism. References to the Axiom of Selection are kept down to a tactful bare mention.

Throughout the theory of sets and of measure the author is subject to no temptation to flaunt the abstract side of his subject before the reader's eyes, and, indeed, strikes a very

happy mean between set theory in its most abstract form on the one hand, and the mere handling of coordinate numbers on the other.

When the structure of the Lebesgue Integral has been set up, the author proceeds to a chapter dealing specially with the single-variable case, and contrives to include a very workmanlike account of the detailed integration theory involved in modern functional work. He begins with integration by parts for the Lebesgue Integral, and goes on to approximation by means of continuous functions, and the theory of absolute continuity. This chapter is a complete armoury of weapons for use in modern functional theory.

After a chapter on Multiple Lebesgue Integrals come two rather compact chapters upon extensions of Lebesgue theory and upon Fourier's Series respectively. The former gives a brief approach to the Denjoy Integral, while the latter sets out Fourier's Series results up to the Parseval and Riesz-Fischer theorems as a monument to the power of the Lebesgue Integral. If this last chapter appears condensed it is probably because of the ease with which results follow once the structure of the integral has been established.

Taking the book as a whole, as we have already indicated, the degree of abstraction is pitched at a very happy level, and the technical use of the notation of the theory of sets, if wide, is at any rate along the trend of recent analytical usage. The work is well conceived as an entity and has clearly been carefully made ready for press. Explanatory matter is never long-winded nor is it unduly curt. The use of sufficient pointed examples set out in the text to demonstrate the need for conditions, or the impossibility of more extended results, has been admirably managed. As one would expect from the Oxford Press the work is well printed and well set out. It is, in fact, a work helpfully constructed for students who have sufficient grasp to be able to approach the subject, whether those students specialize in a field of mathematical analysis or not.

Thermodynamics. By Enrico Fermi. [Pp. x+160.] (London and Glasgow: Blackie & Son, Ltd., 1938. Price 12*s.* 6*d.*)

This book originated in a course of lectures given at Columbia University during 1936. It presents a straightforward account of the first principles of thermodynamics, illustrated by applications to physics and chemistry.

After an explanation of the thermodynamic concept of the state of a system, and a brief discussion of transformations

and of the equation of state of a perfect gas, successive chapters deal with the first and second laws of thermodynamics, entropy, and the thermodynamic potentials. The main applications made are to gaseous reactions and to dilute solutions. In the last chapter the Nernst heat theorem is enunciated and applied, and application is made of the statistical results for the entropy constant of an ideal gas.

The treatment throughout is admirably clear. "The aim of the book," it is stated, "is to develop physical insight rather than to cultivate dexterity in mathematical manipulation," and it may be said that the aim is likely to be achieved. Considerable difficulty is undoubtedly encountered by most of those who take up the study of thermodynamics. It may be questioned whether this is entirely due to lack of appreciation of the basic ideas involved. It often arises from a failure to acquire sufficient familiarity with the subtle, rather than difficult, technique which enables the principles to be usefully applied to problems beyond those of an apparently trivial and academic character. In this direction the book will give little direct help, and owing to the absence of references it does not simplify the approach to the extensive literature of the subject. The unpretentious exposition of the basic principles, communicating the author's clear appreciation of essentials, should, however, be assured of a wide welcome.

Higher Algebra. By S. Barnard and J. M. Child. [Pp. xiv+585.] (Macmillan & Co., Ltd., London, 1936. Price 20*s*.)

This work is intended for students working for the Higher School Certificate, scholarship examinations, and other examinations of similar scope. It follows the traditional content of books with its title, as, for example, the one-time standard works by Todhunter and Chrystal. From early chapters on polynomials and symmetric functions the theory of equations is developed in a series of chapters which occur at intervals through the book. Partial fractions, determinants, the summation of series, the theory of numbers, and continued fractions are discussed with thoroughness and lucidity, and every teacher will be grateful for the large number of admirable examples which are given in, and at the end of, the various chapters.

With so much to praise it may seem invidious to criticize, but when an addition is at length made to the few modern text-books of algebra in English, one could have wished for a bold departure from tradition. It is now customary to confine the title algebra to the study of finite operations,

so that the authors might with advantage have excluded the chapters which deal with limiting operations, infinite series, and the elements of the calculus. This would have provided space for other topics, for example, the elements of matrix theory, which have an increasing importance in modern mathematics. It is perhaps due to the authors' adherence to tradition that they retain the old symbol for a factorial and that they have not used the customary $[x]$ for the integral part of x. The printing and freedom from observed errors are good.

Through Science to Philosophy. By HERBERT DINGLE. [Pp. viii+363.] (Oxford: at the Clarendon Press, 1937 Price 15*s*.)

THAT science is concerned with the rational correlation of experiences rather than with the discovery of fragments of absolute truth about an external world is a view which is now widely accepted. It is a view which Dingle has presented in his earlier writings, but in this book, based on his Lowell Lectures of 1936, the thorough analysis of scientific activity has resulted in a much more fundamental viewpoint, in the light of which discussions are given of many of the most puzzling problems raised by the present scheme of correlation.

The correlation, Dingle holds, is between atomic units of experience, as represented by memories, resolved by reason from the undifferentiated field of consciousness. Other "normal people," to whom the experiences are common, need not be assumed, as was previously supposed, as a prerequisite for the possibility of correlation. For interpretation, concepts are introduced, such as "molecules," or groupings of unitary experiences for purposes of correlation, "postulates," in terms of which logical connexions can be expressed, and "laws," including theories and working hypotheses. The "molecules" formed for different purposes are not necessarily, or even generally, the same. The scientific correlation, for example, may be quite independent of the "physical objects," which are prominent in the common-sense correlation, and much confusion has arisen simply from the attempted attribution to scientific concepts of characteristics similar to those of physical objects. The dualism in Dingle's scheme is that of reason and experience rather than of mind and matter. Knowledge becomes awareness of experience, and truth is relative to a scheme of correlation, connoting "that the experience is placed in the proper molecule according to the prevailing scheme of scientific correlation."

A clear distinction is made between subjective and physical time, and the arbitrary character of time measurement is emphasized. Apart from a discussion of the bearing of relativity Dingle introduces the novel point, which seems of particular importance, that the character of physical time is necessarily dependent on the kind of sequence arbitrarily adopted for its measurement. The law of entropy is dethroned from its exalted position, for it is suggested that its apparently objective indication of the " going on " of time arises simply from the conventional choice of a space-like measure ; with a suitable thermal measure the going on would no longer be indicated, at least by thermal laws.

The causality relation is regarded as essential in the common-sense correlation, but in the scientific correlation it becomes less and less prominent, being replaced by logical relations between concepts. The quantum theory is considered as " a legitimate but infelicitous process of correlating experience." With Dingle's stress on the view that an electron, say, is a creation of reason some of the difficulties of the theory do, however, appear to become much less fundamental.

The final chapter contains some penetrating comments on logical positivism and on the philosophical views of Eddington and Whitehead.

The book perhaps suffers from the fact that it is based on lectures, in which variety of emphasis may serve to focus attention more immediately on essential points. The book is long, and must be read with care and alertness if the essential ideas are to be clearly grasped. Philosophers have never realized the value of a summary, and Dingle here writes, perhaps, more as a philosopher than as a scientist. It is a full-dress performance, the presentation being elaborate rather than succinct. In themselves, however, the elaborations are often admirable, and none would wish to lose the literary allusions and witty asides which add much to the reader's enjoyment.

The general scheme is full of loose ends, which is, perhaps, as it should be. The replacement of mind and matter by reason and experience, for example, seems but a restatement of the fundamental metaphysical problem, and statements in terms of a field of consciousness, memories, and so on are the beginning, not the end of philosophy. For its profound analysis of the character of scientific activity, however, its constructive criticism and comment in the development of the theme, and its at least partial solution of many of the puzzling problems connected with the character of the present scientific scheme of correlation the book is an outstanding contribution to the philosophy of science. Most scientists

will welcome this statement of the nature of their activities and conclusions, and will feel that they are well represented when it is handed over to the philosopher and the layman; if rich and strange characterizations of science should persist, the fault is no longer with the scientist.

Analytic Geometry and Calculus. By Max Morris and O. E. Brown. [Pp. x+507.] (McGraw-Hill Publishing Co., Ltd., London, 1937.)

It is unusual in England to combine analytical geometry and the calculus in one volume, but there may be technological students to whom such a combined course would be useful and to whom this volume would appeal. Few mathematicians would agree with the opening statement of the preface that "analytic geometry has come to be regarded almost entirely as a preparation for the calculus," but in reviewing the book that attitude must be given due weight.

About one-hundred-and-forty pages are used in laying the foundations of the geometry and in discussing the form of the curves and surfaces of the second degree, but there is no real attempt to develop their properties; indeed, the tangent to a curve only emerges—and without emphasis—in the later chapter on derivatives. The first two chapters, however, discussing coordinates and loci, are particularly thorough and painstaking, a remark which may be applied to the teaching of fundamentals throughout the book.

The remaining three-hundred-and-sixty pages are concerned with the calculus. Chapters are devoted to derivatives, indefinite and definite integrals, and the usual applications. There follow chapters on partial derivatives, multiple integrals, expansions in series, and a final chapter on differential equations. The treatment is traditional and generally sound, but the work as a whole would benefit by the omission of attempts to supply "rigour," attempts which often fail due to loose and misleading statement. Such omission would give more space for the last chapter, in which the attempt to cover the solution of ordinary differential equations, including solution in series, in some fifty pages is too ambitious.

[*The Editors do not hold themselves responsible for the views expressed by their correspondents.*]

FIG. 2.

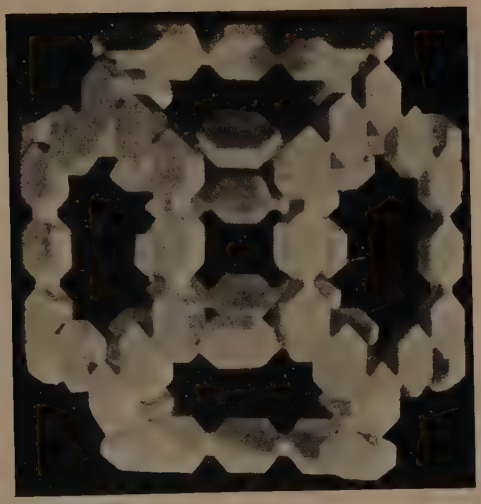

The C_1 molecule. The six characteristic lacunæ are shown, one in the centre in front, one in the centre at the back, and four round the edge.—[From Proc. Roy. Soc. A, clxi. pl. 15.]

FIG. 3.

The C_2 molecule. The six characteristic lacunæ are shown, one in the centre in front, one in the centre at the back, and four round the edge.—[From Proc. Roy. Soc. A, clxi. pl. 16.]

THE

LONDON, EDINBURGH, AND DUBLIN

PHILOSOPHICAL MAGAZINE

AND

JOURNAL OF SCIENCE.

[SEVENTH SERIES.]

SUPPLEMENT, JUNE 1938.

LXXV. *The Propagation of Radio Waves over a Finitely Conducting Spherical Earth.* *By* BALTH. VAN DER POL *and* H. BREMMER, *Natuurkundig Laboratorium der N. V. Philips' Gloeilampenfabrieken, Eindhoven, Holland**.

§1. *Introduction.*

IN two former papers †, which will here be referred to as I. and II., the general theory of the diffraction of electromagnetic waves from an electrical point source round a finitely conducting sphere was considered in detail. For the application to radio communication general formulæ for the field at any distance from the transmitter were derived. Special practical formulæ were given for two limiting cases: (*a*) total reflexion corresponding to an infinitely conducting sphere ($|k_2| \to \infty$) and (*b*) maximum absorption corresponding to

$$|\delta| = \left| \frac{i k_2^2/k_1^2}{z^{1/3}\sqrt{k_2^2/k_1^2 - 1}} \right| << 1,$$

where the same notation as in the former papers is used.

It is the purpose of the present paper, while making full use of our former results, to derive approximations

* Communicated by the Authors.

† Balth. van der Pol and H. Bremmer, Phil. Mag. xxiv. pp. 141 and 825 (1937).

suitable for numerical application for any arbitrary conductivity σ and dielectric constant ϵ of the earth and for any frequency. In order to simplify the problem we assume both sender and receiver to be situated on the earth's surface ($h_1=h_2=0$). While adhering to our former notations, the present investigation, moreover, will enable us to compare our numerical results with those of other writers.

The basis of our present investigation will, therefore, be the series I. (15) for the Hertzian vector Π_{tot}, but for $b=a$, which thus reduces to

$$\Pi_{\text{tot}} \sim \Pi_0 \sim \frac{2\sqrt{2\pi}\cdot e^{3/4\,i\pi}}{(k_1 a)^3\sqrt{\sin\vartheta}} \cdot \sum_{s=0}^{s=\infty} \frac{n_s^{1/2}}{\left(\frac{\partial N_{n-1/2}}{\partial n}\right)_{n=n_s}} \cdot e^{in_s\vartheta}, \quad (1)$$

where (see I. (6))

$$N_n(z, z') = \left[\frac{1}{z}\cdot\frac{d}{dz}\log\{z\zeta_n^{(1)}(z)\}\right]_{z=k_1 a} - \left[\frac{1}{z'}\cdot\frac{d}{dz'}\log\{z'\psi_n(z')\}\right]_{z'=k_2 a}. \quad (2)$$

In these formulæ n_s represents the zeros with positive imaginary part of $N_{n-1\,2}(z, z')$ considered as a function of n. Our problem, therefore, consists of a further numerical determination of the position of these zeros together with their corresponding residues.

§ 2. *The Zeros of* $N_{n-1/2}(z, z')$ *considered as a Function of* n.

In order to obtain a clear picture of the position of the individual zeros of $N_{n-1/2}$, we first decompose the outgoing wave $\zeta_{n-1/2}^{(1)}(z)$ occurring in $N_{n-1/2}$, as the complex sum of two standing waves $\psi_{-n-1/2}$ and $\psi_{n-1/2}$, according to the known formula

$$\zeta_{n-1,2}^{(1)}(z) = \frac{e^{-\frac{n}{2}\pi i}}{i\sin(n\pi)}\cdot\left\{e^{\frac{n}{2}\pi i}\cdot\psi_{-n-1/2}(z) - e^{-\frac{n}{2}\pi i}\cdot\psi_{n-1/2}(z)\right\}. \quad (3)$$

Substitution of (3) in $N_{n-1/2}=0$ leads to the following linear relation in $e^{n\pi i}$:

$$e^{n\pi i}=\frac{z'^2\psi_{n-1/2}(z')\cdot\frac{d}{dz}\{z\psi_{n-1/2}(z)\}-z^2\psi_{n-1/2}(z)\frac{d}{dz'}\{z'\psi_{n-1/2}(z')\}}{z'^2\psi_{n-1/2}(z')\cdot\frac{d}{dz}\{z\psi_{-n-1/2}(z)\}-z^2\psi_{-n-1/2}(z)\frac{d}{dz'}\{z'\psi_{n-1/2}(z')\}},$$

$$(z=k_1a\,;\ z'=k_2a), \quad . \quad (4)$$

which constitutes an equation in n. Now, in order to show clearly the position of the different roots $n=n_s$, we write (4) in the equivalent logarithmic form

$$(n_s-1)\pi i=\log\left\{\frac{\psi_{n_s-1/2}(z)}{\psi_{-n_s-1/2}(z)}\cdot R''_{(n_s-1/2)}\right\}+2\pi is, \quad (5)$$

where the logarithmic term is meant to represent the principal value, whereas the multiplicity of the logarithm is accounted for by the term $2\pi is$ $(s=0,\ 1,\ 2\ldots)$, and where in (5) we introduced a new reflexion coefficient

$$R''(n)=\frac{-\left[\frac{1}{z}\frac{d}{dz}\log\{z\psi_n(z)\}\right]_{z=k_1a}+\left[\frac{1}{z'}\frac{d}{dz'}\log\{z'\psi_n(z')\}\right]_{z'=k_2a}}{\left[\frac{1}{z}\frac{d}{dz}\log\{z\psi_{-n-1}(z)\}\right]_{z=k_1a}-\left[\frac{1}{z'}\frac{d}{dz'}\log\{z'\psi_n(z')\}\right]_{z'=k_2a}}. \quad (6)$$

It is worth noticing that this reflexion coefficient built up of ψ functions only, and therefore suggesting standing waves, is different from the R_{11} of II. (68 *a*), in which ζ functions (*i. e.*, progressing waves) occurred only. It also differs from R_n of I. (2) which was of a mixed type. In a later paper we hope to consider in more detail the physical character of these different reflexion coefficients which are closely related to the dual d'Alembert and Bernoulli solutions of the wave equation in one or more dimensions.

The expression (5) is still rigorous, but two approximations for the Bessel functions, already considered before, are available : I. (16) and I. (17) where, as shown in I., the

expression (17) leads to more accurate results. Considering the less accurate case I. (16) first and making use of

$$\psi_{n-1/2}(z)=\tfrac{1}{2}\{\zeta^{(1)}_{n-1/2}(z)+\zeta^{(2)}_{n-1/2}(z)\},$$
$$\psi_{-n-1/2}(z)=\tfrac{1}{2}\{e^{n\pi i}\zeta^{(1)}_{n-1/2}(z)+e^{-n\pi i}\zeta^{(2)}_{n-1/2}(z)\},$$

one finds for $I_m n>0$, $|n|$ and $|z|>>1$,

$$\frac{d}{dz}\log\{z\psi_{n-1/2}(z)\}\sim\sqrt{\frac{n^2}{z^2}-1},$$

$$\frac{d}{dz}\log\{z\psi_{-n-1/2}(z)\}\sim-\sqrt{\frac{n^2}{z^2}-1},$$

$$\frac{\psi_{n-1/2}(z)}{\psi_{-n-1/2}(z)}\sim e^{\pi i(n+1/2)+2n\int_1^{z/n}\sqrt{1-u^2}\frac{du}{u}}.$$

Substitution of these expressions in (5), and calling $n_s=a\lambda_s$, leads to

$$ia\lambda_s.\int_1^{k_1/\lambda_s}\sqrt{1-u^2}\frac{du}{u}+\frac{i}{2}.\log R(\lambda_s)=(s+\tfrac{1}{4})\pi, \quad . \quad (7)$$

where

$$R(\lambda_s)=\frac{k_2^2\sqrt{\lambda_s^2-k_1^2}-k_1^2\sqrt{\lambda_s^2-k_2^2}}{k_2^2\sqrt{\lambda_s^2-k_1^2}+k_1^2\sqrt{\lambda_s^2-k_2^2}}=\frac{tg(\vartheta'-\vartheta'')}{tg(\vartheta'+\vartheta'')},$$

and the spherical reflexion coefficient R'' thus degenerates to the Fresnel plane reflexion coefficient as occurring in the plane Sommerfeld problem. ϑ' and ϑ'' represent the angles of incidence and refraction according to the relations $\lambda=k_1\sin\vartheta'=k_2\sin\vartheta''$.

Our result (7) has the character of a phase-integral equation and is the same as that derived by T. L. Eckersley *. However, it should be noted that the term $\pi/4$ in the right-hand member of (7) appears here in a stringent way, whereas in Eckersley's considerations, which leave an absolute phase constant undetermined, this term is borrowed from Watson's analysis.

Returning to (7), it may be remarked that for practical purposes the roots n_0, n_1, n_2 of low order s are of dominating importance, because they are the roots with the smallest imaginary part, representing in the final expression the terms with the smallest attenuation. Thus

* T. L. Eckersley, Proc. Roy. Soc. London A, cxxxvi. p. 499 (1932), see pp. 520–523, where Eckersley's variable s should be replaced by $s-1$ for comparison with our notations.

considering (7) again as an equation in n, we obtain the approximation

$$n_s = z + z^{1/3}\tau_s,$$

where τ_s satisfies

$$-\tfrac{1}{3}(-2\tau_s)^{3/2} + \text{arc } tg(\delta\sqrt{-2\tau_s}) = (s+\tfrac{3}{4})\pi, \quad . \quad . \quad (8)$$

where

$$\delta = -\frac{i}{2z^{1/3}} \cdot \left(\frac{d\mathrm{R}}{d\vartheta'}\right)_{\vartheta'=\pi/2} = \frac{ik_2^2/k_1^2}{z^{1/3}\sqrt{k_2^2/k_1^2 - 1}}, \quad . \quad (9)$$

and

$$0 < \mathrm{Re}\{\text{arc } tg[\ \ ]\} < \pi,$$

$$-\pi/2 < \arg\sqrt{-2\tau} < 0.$$

Our present expression (8) fully confirms the two limiting cases of total reflexion and maximum absorption considered in I. and II., for, if in (8) we take $|k_2| \to \infty$ and therefore $|\delta| \to \infty$, it degenerates to

$$\tau_s \sim \tfrac{1}{2}\{3\pi(s+\tfrac{1}{4})\}^{2/3} e^{i\pi/3},$$

which is our old I. (40 *a*), whereas for $|\delta| << 1$, (8) degenerates to

$$\tau_s \sim \tfrac{1}{2}\{3\pi(s+\tfrac{3}{4})\}^{2/3} e^{i\pi/3} - \delta,$$

which is the other case already considered in II. (page 853).

The phase integral equation (7) and its approximation (8) for the zeros of low order s were derived with the aid of the approximations I. (16) for the Bessel functions. As already remarked, we gave in I. also another approximation for Bessel functions, viz., I. (17), which is considerably more accurate, especially in the neighbourhood of $n=z$, and therefore gives us a better approximation for the low order zeros n_s of $\mathrm{N}_{n-1/2}$. The numerical difference of these two approximations was already fully considered in I., page 163. The application of this better approximation to the Bessel functions occurring in the function $\mathrm{N}_{n-1/2}$, leads to

$$\mathrm{N}_{n-1/2} \sim \frac{e^{2/3 i\pi}}{z^{4/3}} \cdot \frac{\sqrt{-2\tau}\,\mathrm{H}^{(1)}_{2/3}\{\tfrac{1}{3}(-2\tau)^{3/2}\}}{\mathrm{H}^{(1)}_{1/3}\{\tfrac{1}{3}(-2\tau)^{3/2}\}} - \frac{1}{z^{4/3}\delta}, \quad (10\,b)$$

whereas the approximation I. (16) yields

$$\mathrm{N}_{n-1/2} \sim -\frac{\sqrt{-2\tau}}{z^{4/3}} \cdot tg\left\{\frac{\pi}{4} + \frac{(-2\tau)^{3/2}}{3}\right\} - \frac{1}{z^{4/3}\delta}. \quad (10\,a)$$

Hence we obtain as equations determining the zeros n

$$\frac{e^{-i\pi/3}H^{(1)}_{2/3}\{\frac{1}{3}(-2\tau_s)^{3/2}\}}{H^{(1)}_{1/3}\{\frac{1}{3}(-2\tau_s)^{3/2}\}} = -\frac{1}{\delta\sqrt{-2\tau_s}}, \quad . \quad (11b)$$

which equation we will call the *Hankel* approximation and which may be compared with the following inversion of (8),

$$tg\left\{\frac{\pi}{4}+\frac{(-2\tau_s)^{3/2}}{3}\right\} = -\frac{1}{\delta\sqrt{-2\tau_s}}, \quad . \quad (11a)$$

which we will call the *tang.* approximation. In order to obtain a clear distinction between expressions based on the *tang.* and *Hankel* approximation we shall also later on number the formulæ based on the first one with an a and those based on the second one with a b. It may be remarked that the older work of T. L. Eckersley * and also the more recent investigations of B. Wwedensky † are based on the *tang.* approximation. This was also the case in I. and II., but only when $|\delta| << 1$, where, as will be explained further on (see (14)), the error in τ is small and less than 1 per cent.

Having thus treated the general aspect of the approximations, we will in the next paragraph elaborate the numerical behaviour of the roots of (11).

§ 3. *The Numerical Values of the First Few Zeros of* $N_{n-1/2}(z, z')$.

The behaviour of (11) is completely determined by the numerical value of the δ of (9). This variable has in its denominator the great factor $z^{1/3}=(k_1 a)^{1/3}$, and $|\delta|$ may therefore in practice obtain values as low as 0·005. On the other hand, k_2/k_1 may reach such big values that it more than compensates the factor $z^{-1/3}$, so that then $|\delta|$ may be as high as 1000. We shall, therefore, have to evaluate the zeros of (11) for a great range of values of δ. As, moreover, we shall derive the zeros n_s of $N_{n-1/2}$ for finite values of δ from the two limiting cases $\delta=\infty$ and $\delta=0$, a very exact knowledge of the values of $n_s=z+z^{1/3}\tau_s$ for these limiting cases is necessary.

* T. L. Eckersley, *loc. cit.*

† B. Wwedensky, Techn. Phys. U.S.S.R. ii. p. 624 (1935); iii. p. 915 1936); and iv. p. 579 (1937).

It follows from (11) that the first case, corresponding to total reflexion, leads to

$$(-2\tau_s)^{3/2}=(3\pi)^{3/2}(s+\tfrac{1}{4})e^{-i\pi}, \quad . \quad . \quad . \quad (12a)$$

or $H^{(1)}_{2/3}\{\frac{1}{3}(-2\tau_s)^{3/2}\}=0$, which is equivalent to

$$J_{2/3}\{\tfrac{1}{3}(-2\tau_s)^{3/2}e^{i\pi}\}-J_{-2/3}\{\tfrac{1}{3}(-2\tau_s)^{3/2}e^{i\pi}\}=0, \quad (12b)$$

whose roots we shall call $\tau_{s,\infty}$, whereas the second case, corresponding to maximum absorption, leads to

$$(-2\tau_s)^{3/2}=(3\pi)^{3/2}(s+\tfrac{3}{4})e^{-i\pi}, \quad . \quad . \quad . \quad (13a)$$

or $H^{(1)}_{1/3}\{\frac{1}{3}(-2\tau_s)^{3/2}\}=0$, which is equivalent to

$$J_{1/3}\{\tfrac{1}{3}(-2\tau_s)^{3/2}e^{i\pi}\}+J_{-1/3}\{\tfrac{1}{3}(-2\tau_s)^{3/2}e^{i\pi}\}=0, \quad (13b)$$

with the roots $\tau_{s,0}$, say.

A careful numerical evaluation gave us :—

	Tang. approximation.	Hankel approximation.
$\delta=\infty$	$\tau_{0,\infty}=0{\cdot}885.e^{i\pi/3}$	$\tau_{0,\infty}=0{\cdot}808.e^{i\pi/3}$
	$\tau_{1,\infty}=2{\cdot}589\ e^{i\pi/3}$	$\tau_{1,\infty}=2{\cdot}577.e^{i\pi/3}$
	$\tau_{2,\infty}=3{\cdot}830\ e^{i\pi/3}$	$\tau_{2,\infty}=3{\cdot}824.e^{i\pi/3}$
	$\tau_{3,\infty}=4{\cdot}895.e^{i\pi/3}$	$\tau_{3,\infty}=4{\cdot}892.e^{i\pi/3}$
	$\tau_{4,\infty}=5{\cdot}853.e^{i\pi/3}$	$\tau_{4,\infty}=5{\cdot}851.e^{i\pi/3}$
	$\tau_{5,\infty}=6{\cdot}739.e^{i\pi/3}$	$\tau_{5,\infty}=6{\cdot}737.e^{i\pi/3}$
$\delta=0$	$\tau_{0,0}=1{\cdot}842.e^{i\pi/3}$	$\tau_{0,0}=1{\cdot}856.e^{i\pi/3}$
	$\tau_{1,0}=3{\cdot}240.e^{i\pi/3}$	$\tau_{1,0}=3{\cdot}245.e^{i\pi/3}$
	$\tau_{2,0}=4{\cdot}379.e^{i\pi/3}$	$\tau_{2,0}=4{\cdot}382.e^{i\pi/3}$
	$\tau_{3,0}=5{\cdot}384.e^{i\pi/3}$	$\tau_{3,0}=5{\cdot}386.e^{i\pi/3}$
	$\tau_{4,0}=6{\cdot}304.e^{i\pi/3}$	$\tau_{4,0}=6{\cdot}305.e^{i\pi/3}$
	$\tau_{5,0}=7{\cdot}161.e^{i\pi/3}$	$\tau_{5,0}=7{\cdot}161.e^{i\pi/3}$

Now, in order to deduce the τ_s's for any finite δ from these limiting values, we make use of the *Riccati* equations for τ as function of δ, which can be derived from (10),

using the known properties of the Hankel and the tang. functions respectively, viz. :

$$\frac{d\delta}{d\tau} - 2\delta^2\tau + 1 = -\frac{\delta}{2\tau}. \quad . \quad . \quad . \quad (14a)$$

$$\frac{d\delta}{d\tau} - 2\delta^2\tau + 1 = 0. \quad . \quad . \quad . \quad . \quad . \quad (14b)$$

(14 *b*) can also directly be derived for $|z| >> 1$ from

$$N_{n-1/2} \sim \frac{1}{z}\frac{d}{dz}\log\{z\zeta_n^{(1)}(z)\} - \frac{1}{z^{4/3}\delta} = 0,$$

with the aid of

$$\frac{d^2}{dz^2}\{z\zeta_n^{(1)}(z)\} + \left\{1 - \frac{n(n+1)}{z^2}\right\} z\zeta_n^{(1)}(z) = 0.$$

It also follows from a comparison of (14 *a*) and (14 *b*) that the error by using the *tang.* approximation is small only when $|\delta| << 2|\tau_s|$.

Now that the limiting values $\tau_{s,\infty}$ and $\tau_{s,0}$ are known, we can with the aid of (14 *b*) derive two series of asymptotic character, expressing τ_s as a function of δ^{-1} and of δ. These are easily found to be

$$\left.\begin{aligned}
\tau_s = \tau_{s,\infty} &- \frac{1}{2\tau_{s,\infty}\delta} - \frac{1}{8\tau_{s,\infty}^3\delta^2} - \frac{1}{12\tau_{s,\infty}^2}\left(1 + \frac{3}{4\tau_{s,\infty}^3}\right)\frac{1}{\delta^3} \\
&- \frac{1}{32\tau_{s,\infty}}\left(\frac{7}{3\tau_{s,\infty}^3} + \frac{5}{4\tau_{s,\infty}^6}\right)\frac{1}{\delta^4} \\
&- \frac{1}{40\tau_{s,\infty}^3}\left(1 + \frac{21}{8\tau_{s,\infty}^3} + \frac{35}{32\tau_{s,\infty}^6}\right)\frac{1}{\delta^5} \\
&- \frac{1}{48\tau_{s,\infty}^5}\left(\frac{29}{15} + \frac{231}{80\tau_{s,\infty}^3} + \frac{63}{64\tau_{s,\infty}^6}\right)\frac{1}{\delta^6} \cdots, \\
\tau_s = \tau_{s,0} - \delta &- \frac{2}{3}\tau_{s,0}\delta^3 + \frac{1}{2}\delta^4 - \frac{4}{5}\tau_{s,0}^2\delta^5 + \frac{14}{9}\tau_{s,0}\delta^6 \\
&- \frac{1}{7}(5 + 8\tau_{s,0}^3)\delta^7 + \frac{58}{15}\tau_{s,0}^2\delta^8 \cdots
\end{aligned}\right\} \quad . \quad . \quad . \quad (15b)$$

Fortunately the numerical values derived from the first series for $|\delta^2\tau| > \frac{1}{2}$ and from the second one for $|\delta^2\tau| < \frac{1}{2}$ yield a good fit even for complex values of δ. As, further,

the imaginary parts of the τ_s's will determine the attenuation of the different terms in our final expression for Π_{tot}, we add the corresponding series (17 *b*) (18 *b*) for the imaginary part of the more important τ_0 and τ_1. In these series we have also introduced δ by its modulus and argument as

$$\delta = K.e^{i(3/4\,\pi-\psi)}, \quad . \quad . \quad . \quad . \quad . \quad (16)$$

where the argument is taken as $\frac{3}{4}\pi-\psi$, because then the case often encountered in practice, where the conduction current is great in comparison with the dielectric current, we have $\psi=0$.

The two series referred to above are :—

$$\begin{aligned} Im\tau_0 = 0{\cdot}6996 &+ \frac{0{\cdot}6189\sin(\psi-15^\circ)}{K} + \frac{0{\cdot}2370\cos(2\psi)}{K^2} \\ &- \frac{0{\cdot}0539\sin(3\psi+15^\circ)}{K^3} + \frac{0{\cdot}00273\sin(4\psi-60^\circ)}{K^4} \\ &- \frac{0{\cdot}00211\sin(5\psi+45^\circ)}{K^5} + \frac{0{\cdot}00142\sin(6\psi-30^\circ)}{K^6} \ldots, \end{aligned}$$

$$\begin{aligned} Im\tau_0 = 1{\cdot}6070 &- \sin(\psi+45^\circ)K - 1{\cdot}237\sin(3\psi+75^\circ)K^3 \\ &+ \tfrac{1}{2}\sin(4\psi)K^4 + 2{\cdot}755\sin(5\psi-75^\circ)K^5 \\ &- 2{\cdot}887\sin(6\psi-150^\circ)K^6 - 6{\cdot}589\sin(7\psi+135^\circ)K^7 \\ &- 13{\cdot}32\sin(8\psi-120^\circ)K^8 \ldots, \end{aligned}$$

. . . (17 *b*)

and

$$\begin{aligned} Im\tau_1 = 2{\cdot}2317 &+ \frac{0{\cdot}1940\sin(\psi-15^\circ)}{K} + \frac{0{\cdot}0073\cos(2\psi)}{K^2} \\ &+ \frac{0{\cdot}0120\sin(3\psi+15^\circ)}{K^3} - \frac{0{\cdot}00160\sin(4\psi-60^\circ)}{K^4} \\ &+ \frac{0{\cdot}00124\sin(5\psi+45^\circ)}{K^5} - \frac{0{\cdot}000324\sin(6\psi-30^\circ)}{K^6} \ldots, \end{aligned}$$

$$\begin{aligned} Im\tau_1 = 2{\cdot}810 &- \sin(\psi+45^\circ)K - 2{\cdot}163\sin(3\psi+75^\circ)K^3 \\ &+ \tfrac{1}{2}\sin(4\psi)K^4 + 8{\cdot}422\sin(5\psi-75^\circ)K^5 \\ &- 5{\cdot}047\sin(6\psi-150^\circ)K^6 - 38{\cdot}32\sin(7\psi+135^\circ)K^7 \\ &- 40{\cdot}71\sin(8\psi-120^\circ)K^8 \ldots \end{aligned}$$

. . . (18 *b*)

These series are graphically represented in fig. 1, where the abscissæ represent $K = |\delta|$ and the ordinates $Im\tau_0$ and $Im\tau_1$, the parameter being the phase ψ of δ as defined in (16). As ψ varies between 0 and 45°, we

Fig. 1.

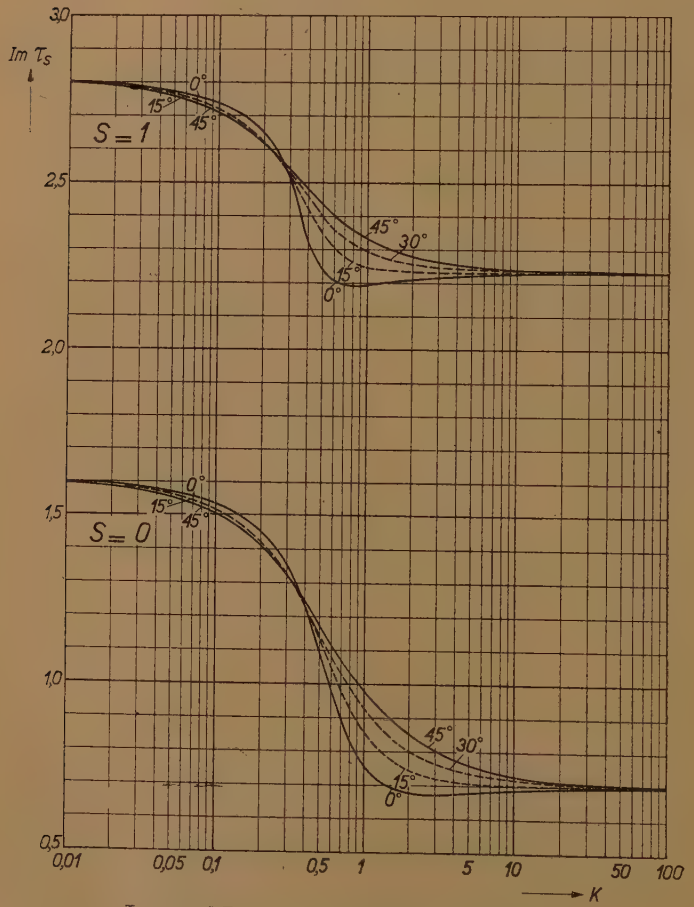

$Im\tau_0$ and $Im\tau_1$ as a function of $|\delta| = K$.

have chosen for this parameter the values 0, 15°, 30°, and 45° only.

From this figure it may be noted, as also follows from (17), that for $\psi = 0$, $Im\tau_s$ shows a minimum as function of $|\delta|$. This fact, as we shall see later on, has important

numerical consequences in the theory of radio propagation. However, it should be observed that this minimum disappears when $\psi > 15°$.

Fig. 2.

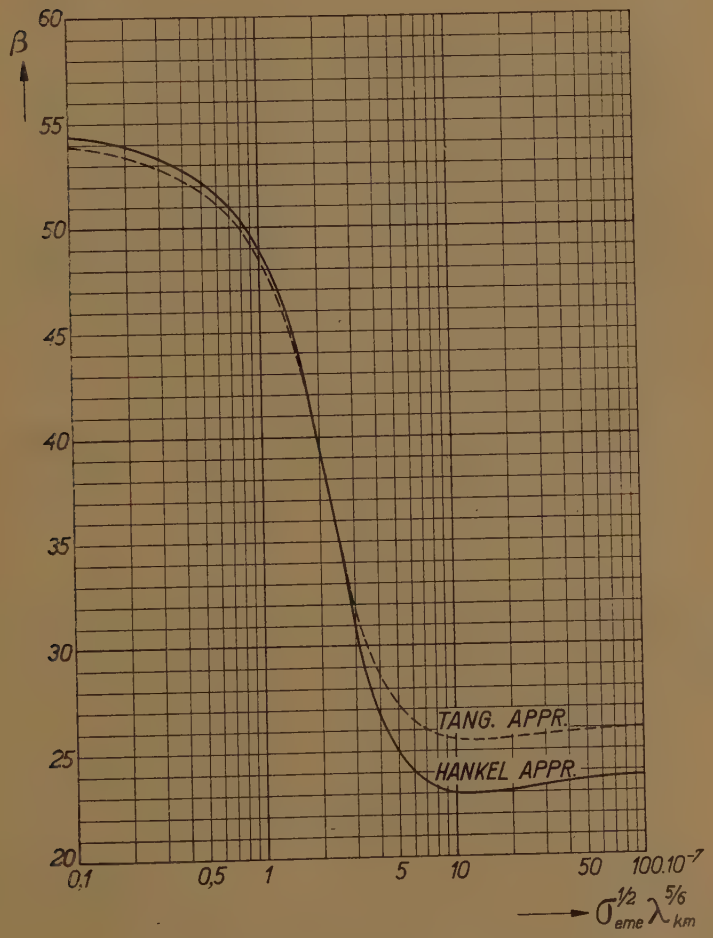

$\beta = \sqrt[3]{2\pi a_{\text{km.}}} \cdot Im\ \tau_0$ as a function of $\sigma^{1/2}_{\text{e.m.u.}} \lambda^{5/6}_{\text{km.}}$

We are now prepared to compare our result with a similar one obtained for $Im\tau_0$ only by Wwedensky *,

* B. Wwedensky, *loc. cit.* ii. pp. 633–635 (1935).

and we therefore replot the lower part of fig. 1 for $\psi=0$, but introduce the new, practical variables

$$\beta = \sqrt[3]{2\pi a_{\text{km.}}}.\,\text{Im}\tau_0 = 34{\cdot}20\,.\,\text{Im}\tau_0,$$

and

$$\sigma^{1/2}_{\text{e.m.u.}}\lambda^{5/6}_{\text{km.}} = \frac{\sqrt[3]{2\pi a_{\text{km.}}}}{\sqrt{2c_{\text{km.}}}}.10^{-5}.|\,\delta\,| = 4{\cdot}415.10^{-7}.|\,\delta\,|.$$

As, moreover, as stated above, Wwedensky used the *tang.* approximation, we also represent this approximation in fig. 2. It clearly follows from this figure that the two approximations practically coincide for $\sigma^{1/2}_{\text{e.m.u.}}\lambda^{5/6}_{\text{km.}}<2$, but that an appreciable difference remains when $\sigma^{1/2}_{\text{e.m.u}}\lambda^{5.6}_{\text{km.}}>5$. Again, the curves given by Wwedensky and Eckersley do not show the minimum obtained above, to which we will refer later on.

§ 4. *The Final Formulæ for the Hertzian Vector* Π_{tot}.

Returning to our basic formula (1) for Π_{tot}, the last necessary step is to investigate

$$\left(\frac{\partial \text{N}_{n-1/2}}{\partial n}\right)_{n=n_s} = \frac{1}{z^{1/3}}\left(\frac{\partial \text{N}}{\partial \tau}\right)_{\tau=\tau_s}.$$

This is easily done by differentiating (10 *a*) and (10 *b*) and applying known differential relations for the tang. and the H functions respectively together with (11). One thus obtains

$$\left(\frac{\partial \text{N}_{n-1/2}}{\partial n}\right)_{n=n_s} \sim \frac{1}{z^{5/3}}\left(-2\tau_s + \frac{1}{2\delta\tau_s} + \frac{1}{\delta^2}\right), \quad (19\,a)$$

$$\left(\frac{\partial \text{N}_{n-1/2}}{\partial n}\right)_{n=n_s} \sim \frac{1}{z^{5/3}}\left(-2\tau_s + \frac{1}{\delta^2}\right). \quad (19\,b)$$

Substituting these results in (1) and introducing the variable $\chi = z^{1/3}\vartheta = \sqrt[3]{2\pi}.\,\dfrac{\text{D}}{a^{2/3}\lambda^{1/3}}$ already considered in I. and II., we obtain as our final formulæ

$$\Pi_{\text{tot}} \sim 2\Pi_{pr}.\sqrt{2\pi i\chi}.\sum_{s=0}^{\infty}\frac{e^{i\tau_s\chi}}{\left(2\tau_s - \dfrac{1}{2\delta\tau_s} - \dfrac{1}{\delta^2}\right)}, \quad (20\,a)$$

$$\Pi_{\text{tot}} \sim 2\Pi_{pr} \cdot \sqrt{2\pi i\chi} \cdot \sum_{s=0}^{\infty} \frac{e^{i\tau_s \chi}}{\left(2\tau_s - \frac{1}{\delta^2}\right)} \quad . \quad . \quad (20\,b)$$

(20 *a*) is essentially the equivalent of Wwedensky's final expression *. However, apart from the fact that the τ_s's of our expression (20 *b*) are defined by (11 *b*), and not by (11 *a*) as is the case for (20 *a*), for the reasons given above *we consider* (20 *b*) *as the proper solution*, this being based on the *Hankel* approximation, which is accurate up to terms of the order $z^{-2/3}$.

A verification of (20 *b*) can be obtained by considering the two limiting cases (*a*) total reflexion $\delta \to \infty$ and (*b*) maximum absorption $\delta \to 0$, fully confirming our former expressions II. (100).

It can also be proved that, just as in I. (§ 5), the general rigorous formula for the plane boundary could be considered as a limiting case for $a \to \infty$ of the general rigorous expression I (1 *a*) of the spherical problem, so can the well-known approximate ρ formula of Sommerfeld † be derived as similar limiting case (for $a \to \infty$) of our final approximate formula (20 *b*). We hope to return to this question in a later note.

§ 5. *Numerical Results.*

Now that we have obtained our final expression (20 *b*) in a form readily adapted for numerical evaluation, it was a relatively simple matter to construct practical curves for the field at the earth's surface of an emitter also placed on the ground. For an emitter radiating P kilowatt we have for the field in practical units

$$E_{\mu v/m} = \frac{3 \cdot 10^5}{D_{\text{km.}}} \cdot \sqrt{P_{\text{kw.}}} \cdot \left| \frac{\Pi_{\text{tot}}}{2\Pi_{pr}} \right| .$$

With these units we have calculated the figs. 3, 4, 5, and 6 showing curves representing the field due to a sender radiating one kilowatt as a function of distance. Figs. 3 and 4 refer to a conductivity $\sigma = 4 \cdot 10^{-11}$ e.m.u. and

* B. Wwedensky, *loc. cit.* ii. p. 631, formula (6, 6), where it should be noted that Wwedensky uses instead of δ : $M = 1/(3^{1/3}K)$.

† See, *e. g.*, Balth. van der Pol, *Zeits. für Hochfreq. Techn.* xxxvii. p. 152 (1931).

dielectric constant $\epsilon=80$, corresponding to sea-water, whereas figs. 5 and 6 were calculated for $\sigma=10^{-13}$, $\epsilon=4$ corresponding to average soil. The different curves in each of these figures cover the frequency range from 15 kc./s. to 300 mc./s. ($\lambda=20$ kilometres to 1 metre). A new

Fig. 3.

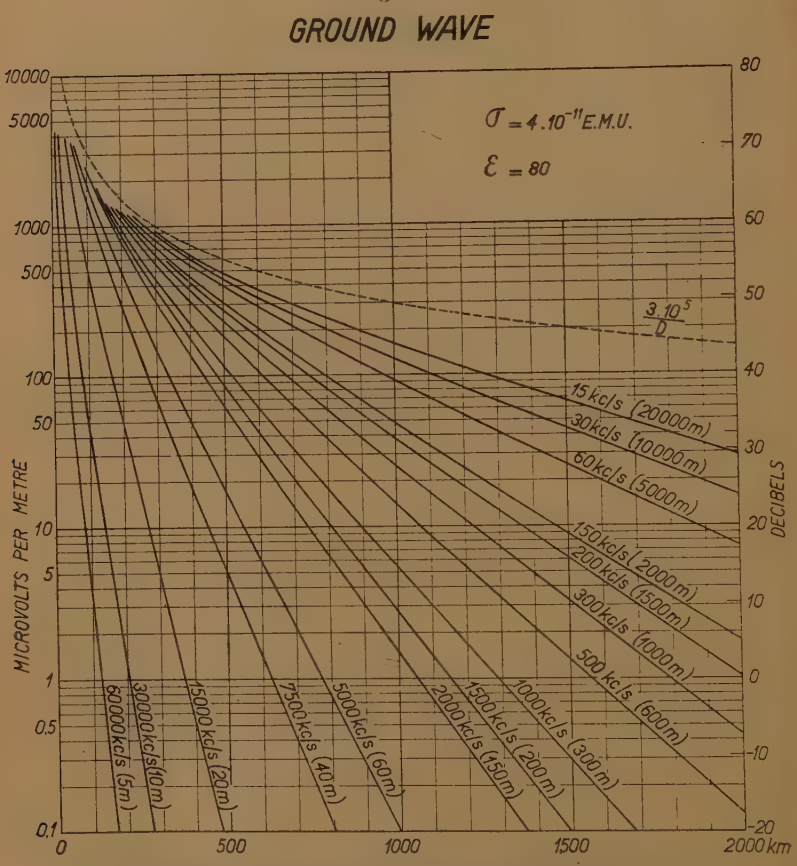

Field strength of the ground wave of a transmitter of 1 kw. for propagation over sea-water for distances to 2000 km.

interesting fact may be read off from these curves viz., that for long distances long waves are slightly better propagated over average soil than over sea-water, *e. g.*, at D=2000 km. the field of a wave $\lambda=20$ km. is 4 per cent. stronger over average soil than over sea-water. This

is a consequence of the minimum of $Im\tau_0$ as function of $|\delta|$ (fig. 2) already referred to above. It follows from fig. 2, that for a given wave-length, at least as long as the dielectric current is small compared with the conduction current, always a conductivity can be found for which

Fig. 4.

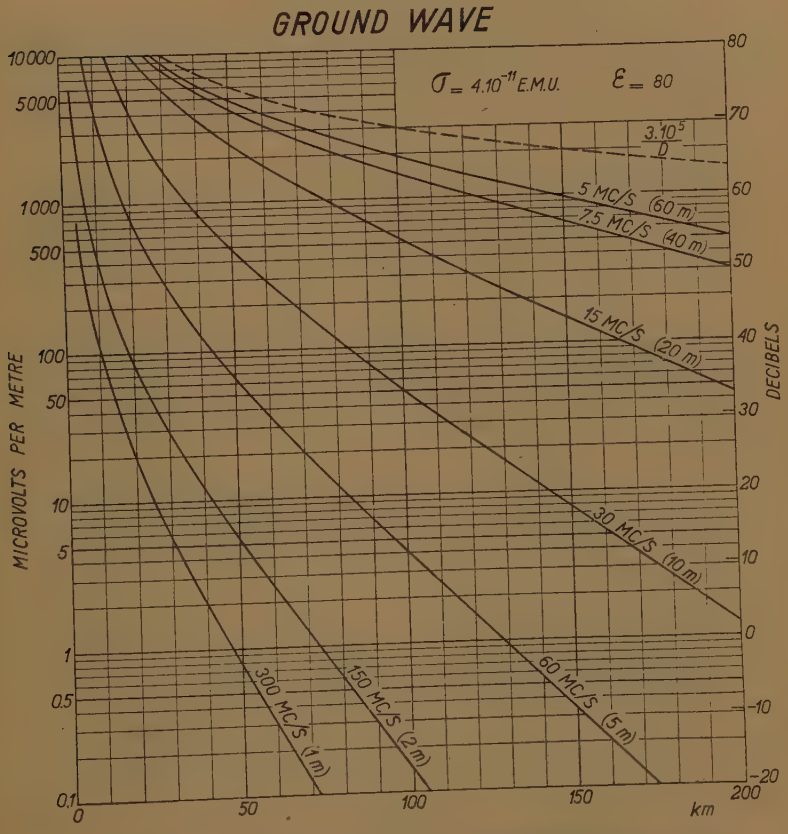

Field strength of the ground wave of a transmitter of 1 kw. for propagation over sea-water for distances to 200 km.

at long distances the propagation conditions are optimum. As this minimum of $Im\tau_0$ occurs near 15.10^{-7}, this optimum conductivity is given by

$$\sigma_{\text{e.m.u.}} = \frac{0{\cdot}225}{\lambda_{\text{km.}}^{5/3}} .10^{-11}.$$

Finally, it may be remarked that in constructing these curves the use of three terms only of the series (20 *b*) gives at shorter distances already a good transition to the values calculated with the aid of the ρ formula for the

Fig. 5.

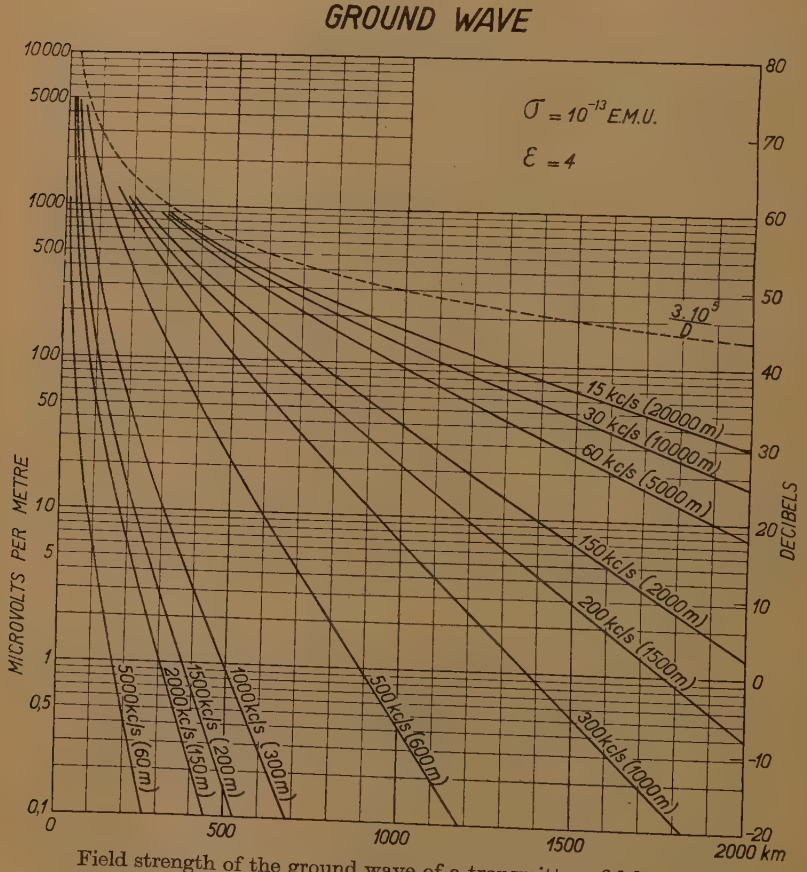

Field strength of the ground wave of a transmitter of 1 kw. for propagation over average soil for distances to 2000 km.

plane problem. Hence, the curves could be extended to short distances from the sender.

Summary.

An extension is given to the applications in the radio case of a general theory treated in two former papers

on the problem of diffraction of electro-magnetic waves round an absorbing sphere. Asymptotic series have been derived from which the numerical constants occurring in the final formula may be calculated for the field strength of a sender emitting waves over a homogeneous sphere

Fig. 6.

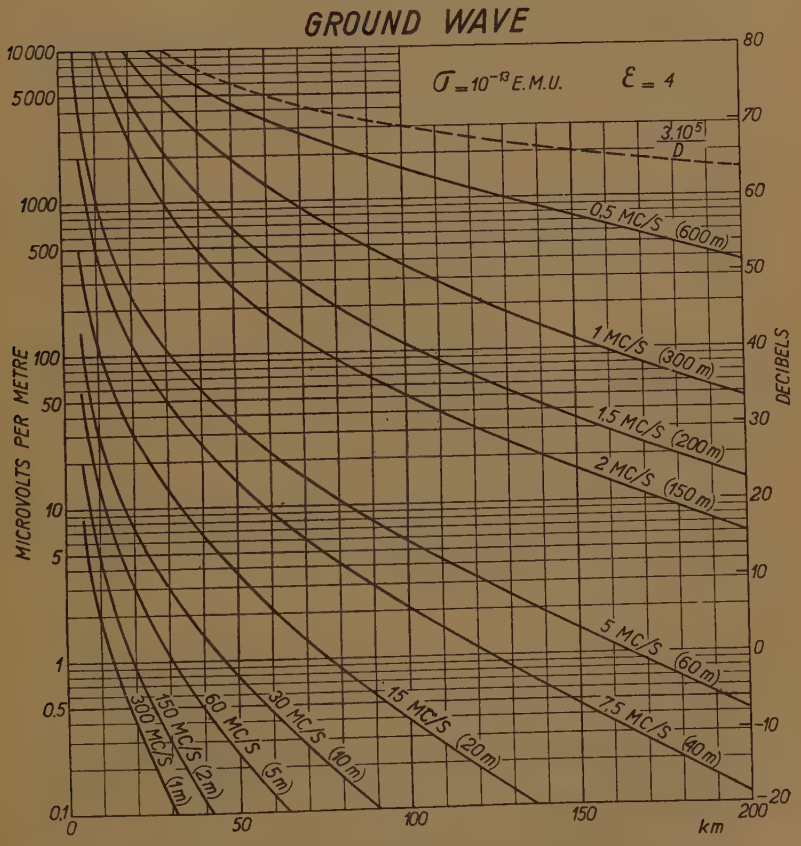

Field strength of the ground wave of a transmitter of 1 kw. for propagation over average soil for distances to 200 km.

with arbitrary electrical conductivity and dielectric constant; the sender and receiver are hereby supposed to be situated on the earth. The general results are compared with those of Eckersley and Wwedensky, treating the same problem. Finally, curves are given

showing the field strength as a function of the distance for propagation over sea-water and over average soil.

Postscript.

Hereby we call attention to the following errata in our former papers :—

(1) Page 151, in formula (18) *read* I *instead of* I_n.

(2) Page 164, line 6 from the top, read $z^{-5/3}$ instead of z^{-13}.

(3) Page 171, in formula (55) read z'/z instead of z/z'.

(4) Page 835, line 2 from the bottom, *read* $I^e_{-1,0}$ *instead of* $I^e_{1,0}$.

(5) Page 838, at the end of the first line of formula (81 *a*)' read τ_{2K+4} instead of τ_{2K+}.

(6) Page 838, in formula (81 *b*) *read*

$$\sum_{\nu=3}^{2K+4} \quad \textit{instead of} \quad \sum_{A=3}^{2K+4} .$$

(7) Page 854, in the denominator of the last line of formula (102), read τ'^2 instead of τ'^{22}.

(8) Page 860, in the second line of formula (109), *read* $P_n^{-1}(\cos\vartheta)$ *instead of* $P_n^1(\cos\vartheta)$.

(9) Page 861, line 7 from the top, *read* and *instead of* en.

(10) Page 863, in the formula of line 10 from the top, read 9/128 instead of $g/128$.

Eindhoven.
20th January, 1938.

LXXVI. *The Evaporation of Atoms, Ions and Electrons from Tungsten.* *By* A. L. Reimann, *Ph.D., D.Sc.** (Communication from the Research Staff of the M.O. Valve Co., Ltd., at the G.E.C. Research Laboratories, Wembley, England.)

Introduction.

THE Saha-Langmuir-Kingdon theory [1] of the equilibrium between neutral atoms, positive ions and electrons in a gaseous mixture at absolute temperature

* Communicated by C. C. Paterson.

T leads, when the electron spin is taken into account, to the equation

$$\log_\epsilon \frac{n_p n_e}{n_a} = -\frac{I}{kT} + \frac{3}{2}\log_\epsilon T + \log_\epsilon \left[\frac{2\sigma_p}{\sigma_a} \frac{(2\pi mk)^{3/2}}{h^3} \right], \quad (1)$$

where n_p, n_e, and n_a are the molecular concentrations of ions, electrons and atoms respectively, σ_p and σ_a are the ionic and atomic statistical weights, I is the work required to ionize an atom, m is the electronic mass, k Boltzmann's constant and h Planck's constant. Now in the case where the electrons are in equilibrium, not only with the ions and atoms, but also with a metal, we have, according to thermionic theory,

$$\log_\epsilon n_e = -\frac{\chi}{kT} + \frac{3}{2}\log_\epsilon T + \log_\epsilon \left[\frac{2(2\pi mk)^{3/2}}{h^3} \right], \quad (2)$$

where χ is the electron work function of the metal. Thus, substituting (2) in (1), we find that

$$\frac{n_p}{n} = \frac{\sigma_p}{\sigma_a} \epsilon^{\frac{\chi - I}{kT}} \quad (3)$$

Hence, if i_p and i_a are the rates of evaporation of ions and atoms, respectively, from the metal surface, and r_p and r_a are the corresponding mean reflexion coefficients, we have, finally,

$$\frac{i_p}{i_a} = \frac{\sigma_p}{\sigma_a} \frac{1 - \bar{r}_p}{1 - \bar{r}_a} \epsilon^{\frac{\chi - I}{kT}}. \quad (4)$$

Unfortunately we do not know anything about the mean reflexion coefficients. If, as seems not improbable, both are negligibly small, the right-hand side of (4) reduces to that of (3). But even if there is an appreciable reflexion of either kind of particle, neither reflexion coefficient is likely to vary sufficiently rapidly with temperature to have an important effect on the relative temperature variation of i_p/i_a.

Several experimental determinations of the variation of i_p with temperature have been made in the case of the metals tungsten and molybdenum, whose σ_p, σ_a, χ and I are sufficiently well known to make possible some sort of comparison between the experimental results and theoretical expectations. In none of the earlier work was the agreement between the two at all good, the

measured rate of variation of i_p with T being much too small. While the reason for this has not yet been found, the agreement in later work has been considerably better. Thus, in 1935, Wahlin and Reynolds [2] obtained i_p-T data for molybdenum which are in satisfactory theoretical agreement with the corresponding data for electron and atom evaporation. Somewhat earlier, Moon [3] had obtained results of the right order for tungsten, although there was a considerable spread in his i_p-T points. More consistent data for tungsten, also of the right order, have been obtained more recently by Wahlin and Whitney[4]. As we shall see, however, in neither case are the results quite what we should expect theoretically.

The present work had just been completed when the paper by Wahlin and Whitney appeared. While the agreement between theory and experiment here attained is no better than in the work of Moon or of Wahlin and Whitney, it has nevertheless seemed worth while to publish the results for what they may mean theoretically. In addition to the i_p-T data, independent determinations of the evaporation of atoms and electrons as a function of temperature have been made.

The Temperature Scale.

The true temperature, T, may be found either from the brightness temperature, T_b, and the spectral emissivity, or from the colour temperature, T_c, and the T_c-T relationship. Both the spectral emissivity and the T_c-T relationship over a wide range of temperatures have been given by Forsythe and Worthing [5], and it was decided to arrive at the true temperature as a function of the heating current in a long, well-aged wire by both of these methods.

A number of 20 cm. lengths of wire, having a diameter approximately 0·2 mm., and all cut from the same original spool, were each mounted as a freely-hanging U-shaped filament in a separate bulb, and on one of the supports of each filament there was also mounted a getter disk, holding a copper-clad barium getter pellet. After each tube had been baked on the pump, the getter was dispersed from disk the by high-frequency induction, forming a small patch on the bulb near the disk, and the tube was then sealed off. The tubes were now connected in series

and the filaments heated for 1 hour at 1870° K., then for 110 hours at 2400° K., next for 1 hour at 2600° K., and finally for 5 minutes at 2800° K.* The bulbs were not perceptibly blackened by this heat treatment. One tube was now broken open, and after discarding 2·5 cm. of " cold ends " adjacent to each support, and also the curved part of the filament, the two straight lengths remaining were measured and weighed, and, taking 19·35 g. per c.c. as the density, the wire diameter was calculated. It was found to be 0·2012 mm. Another tube was set aside for finding the temperature of the wire in terms of the current, and the remaining tubes were used for other purposes.

With the tube set aside for temperature calibration the brightness and colour temperatures were now found in terms of heating current, the former between T_b values of 1350° and 2127° K., and the latter between T_c values of 1858° and 2686° K. The results are represented by the curves labelled T_b and T in fig. 1. As basis for these measurements the temperature scale at present in use by the National Physical Laboratory was adopted. To facilitate the T_b measurements the filament of a tungsten strip lamp was used as background both for the experimental tungsten filament and for the pyrometer filament. By matching the pyrometer filament against the tungsten strip (kept at a constant temperature) with and without the experimental bulb interposed, it was easy to find the correction that should be made for absorption and reflexion by the wall of the experimental bulb between the filament and the pyrometer, and this correction was made at each temperature. Of course, a part of the filament was used for matching which was well removed from the supports, and therefore not cooled by conduction to them. For the colour-temperature measurements the cooled ends were screened off.

A difficulty now arises in determining the curve for true temperature from the T_b and T_c curves. According to Forsythe and Worthing, T is between T_b and T_c. Yet, using their T_b-T data and the measured T_b curve, values of T are obtained which are appreciably higher than the corresponding T_c. For example, Forsythe and

* These temperatures, which are approximate only, were arrived at subsequently from the heating currents employed.

Worthing state that T is 2000° when T_b is 1857° K. ($\lambda = 0{\cdot}665\,\mu$). But the measured T_c corresponding to a T_b of 1857° is only 1970° K., whereas, according to Forsythe and Worthing, it should be 2033° K. It seems out of the question that the combined errors of the T_b and T_c measurements can have been anything like great enough to account for this discrepancy. A similar difficulty is experienced in using the newer value for spec-

Fig. 1.

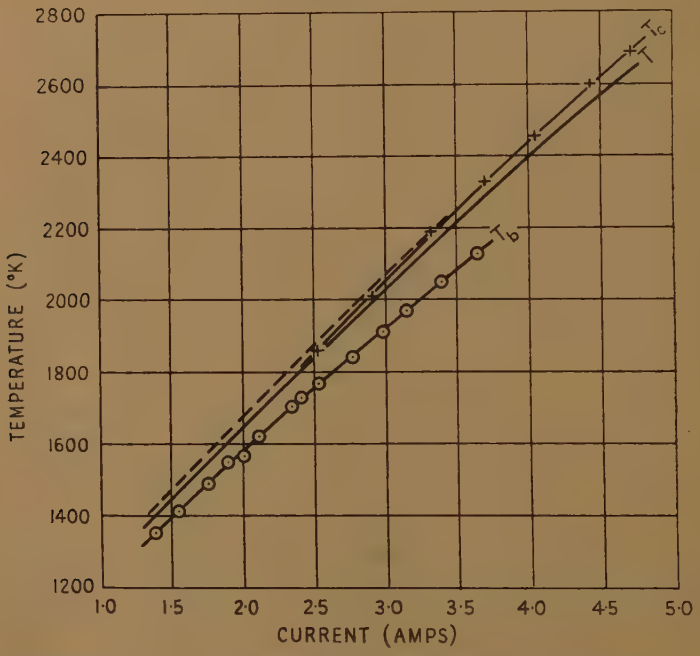

Brightness, colour, and assumed true temperature of a 0·2012 mm. diameter wire as a function of heating current.

tral emissivity found recently by Wahlin and Whitney [4]. The curve for T obtained by using this and the measured T_b is shown dashed, and this, too, is above the T_c curve at the lower temperatures.

It appears that the best way out of these difficulties is to assign equal weights to the T_b and T_c curves and assume that the true T curve divides the interval between them in the same ratio as is given by the data of Forsythe

and Worthing. It is in this way that the curve marked T has been arrived at. In obtaining the T curve for the interval covered by both T_b and T_c measurements, equal weights have been given not only to the positions of the T_b and T_c points, but also to the slopes of the corresponding curves. At higher temperatures the T curve has been continued by using Forsythe and Worthing's values of $T_r - T$ all reduced by the appropriate factor, and at lower temperatures the values of $T - T_b$ given by Forsythe and Worthing have been similarly reduced. The whole T curve thus obtained agrees closely with that obtained from the tables of Jones and Langmuir[6] (calculating temperatures from current and wire diameter), except for a slight difference in slope. Hence the Jones and Langmuir curve has been used as a basis for extrapolation to higher temperatures. The relation between the temperatures finally assumed in this work (T) and those calculated from Jones and Langmuir's tables on the basis of current and wire diameter (T_{JL}) is

$$T = 2{,}000 + 1{\cdot}024(T_{JL} - 2{,}000) \quad . \quad . \quad . \quad (5)$$

Thus at 2000° K. the two temperature scales agree, at 1650° K. (about the lowest temperature used in this work) T is 8° lower than T_{JL}, and at 3500° K. (the highest) T is 35° higher than T_{JL}.

Electron Emission.

A 20 cm. length of wire from the same spool as had been used before was bent into an elongated U and mounted on a pinch, together with two previously outgassed oval molybdenum electrodes of coarse mesh, surrounding the filament and placed end-to-end, 1 mm. apart. The part of the filament enclosed by the molybdenum electrode remote from the pinch was 9·9 cm. in length. A copper-clad barium getter pellet was attached to a nickel disk which was mounted on a wire held by a glass bead, so that it would be electrically floating during the operation of the tube. After the pinch was sealed in, the tube was pumped and baked in the usual manner, the molybdenum electrodes were heated to redness by high-frequency induction, the getter was dispersed, and finally, the tube was sealed off from the pump. The filament was then given the same heat

treatment as were the previous ones, including that used for temperature calibration, while an ionizing electron discharge was passed from it to the two molybdenum electrodes to assist in the clean-up of residual gases.

The tube was designed to operate with the filament hanging vertically downwards, the lower molybdenum electrode acting as electron collector, while the upper one served as guard electrode. These electrodes were made of mesh to facilitate the escape of radiant energy from the filament and render certainly negligible any "oven effect" of the electrodes on the filament. In order that the lower electrode should collect electrons only from that length of filament which hung below the centre of the gap separating the two molybdenum mesh electrodes from one another, the upper one was always held as much negative to the centre of the filament as the lower one was positive. The field at the surface of the filament thus changed from electron-retarding to electron-accelerating at the two points on the filament in the centre of the gap, or rather, on account of the potential drop along the filament, as much above this level in one limb as below it in the other.

The thermionic current from the part of the filament where the field was electron-accelerating was now measured at each of several temperatures for a number of values of this field, and the corresponding zero-field emissions then found by extrapolation, using Schottky's relation. Finally, zero-field emissions per apparent unit area of filament surface were calculated, allowance being made for thermal expansion. These emissions are plotted in the usual manner and the corresponding Richardson line drawn in fig. 2. If we denote the "roughness factor" for the filament by ρ, we find that the thermionic constants A and ψ in the emission formula

$$i = AT^2\epsilon^{-\psi/kT} \quad . \quad . \quad . \quad . \quad . \quad . \quad (6)$$

are given by

$$\rho A = 72 \text{ amp. cm.}^{-2} \text{ degree}^{-2}, \quad \psi = 4{\cdot}52 \text{ e.v.}$$

These are in good agreement with the values that have been found by other workers. Those obtained by Wahlin and Whitney were

$$\rho A = 75 \text{ amp. cm.}^{2} \text{ degree}^{-2}, \quad \psi = 4{\cdot}55 \text{ e.v.}$$

The value of ρ is probably about 1·3[7].

Evaporation of Atoms.

Straight lengths of well-aged wire were cut from the limbs of the U-shaped filaments of the tubes prepared at the same time as that used for temperature calibration. These were mounted each in a separate bulb, and provision was made for barium gettering. After pumping, baking, dispersal of the getter and sealing off, the tubes were ready for use. Each filament was burnt at constant

Fig. 2.

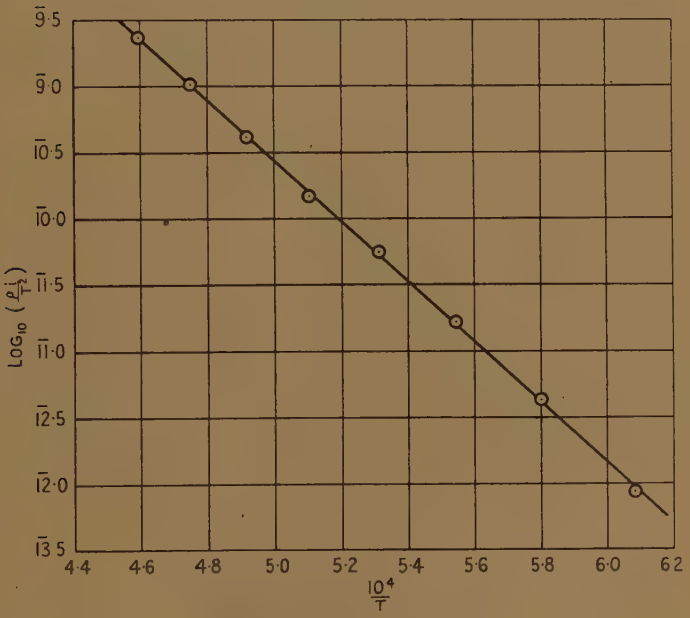

Richardson line for tungsten.

voltage for a sufficient length of time to ensure substantial evaporation, but not long enough to run the risk of the formation of "hot spots." It is a matter of experience that hot spots usually begin to develop in tungsten wires when the diameter has diminished by about 10 per cent., this, curiously enough, being true for all sizes of wire. Burning at constant voltage maintains the wire at an almost constant temperature throughout, and a rough estimate of the progress of evaporation could be obtained by watching the current. A record of the current was

kept throughout the period of burning, and from the initial and final diameters and currents the initial and final temperatures were calculated. As these never differed to an important extent it was legitimate to take the mean of the two as the constant temperature, which would have produced the same evaporation in the same time. The initial diameter was known to be 0·2012 mm. The final diameter was obtained by first discarding as much of each end of the filament as might conceivably have suffered appreciable cooling by conduction to the supports—Forsythe and Worthing's end-cooling tables[5] were used as a guide here—and measuring the length of and weighing the remainder. In arriving at the rate of evaporation per unit area, thermal expansion was allowed for in each case.

The results are plotted in fig. 3, together with the earlier results of Langmuir[8], Zwikker[9], and Wahlin and Whitney[4], for comparison. It is seen that there is fairly close agreement between the present results and those of Wahlin and Whitney. The agreement with the results of Langmuir and of Zwikker is somewhat less good. Incidentally, the closeness of the agreement between the present results and those of Wahlin and Whitney, as regards both evaporation and electron emission, indicates that over a very considerable temperature range there is a correspondingly close agreement in the temperature scales employed. The evaporation data obtained in the present work may be represented by the equation

$$\log_{10} m = 7{\cdot}814 - \frac{4{\cdot}188 \times 10^4}{T},$$

where m is the rate of evaporation in grams per cm.^{2} per sec.

Positive-ion Emission.

A straight 9 cm. length of 0·2012 mm. wire was cut from one of the aged U-shaped filaments and mounted on a fresh pinch. It was arranged to run along the centre of three previously outgassed molybdenum-sheet electrodes, of oval section, placed end-to-end with 1 mm. gaps separating them. The end electrodes were 2·5 cm. long and the central one 3·9 cm. Barium getter was not provided in this case, but, instead, a nickel ring coated

Fig. 3.

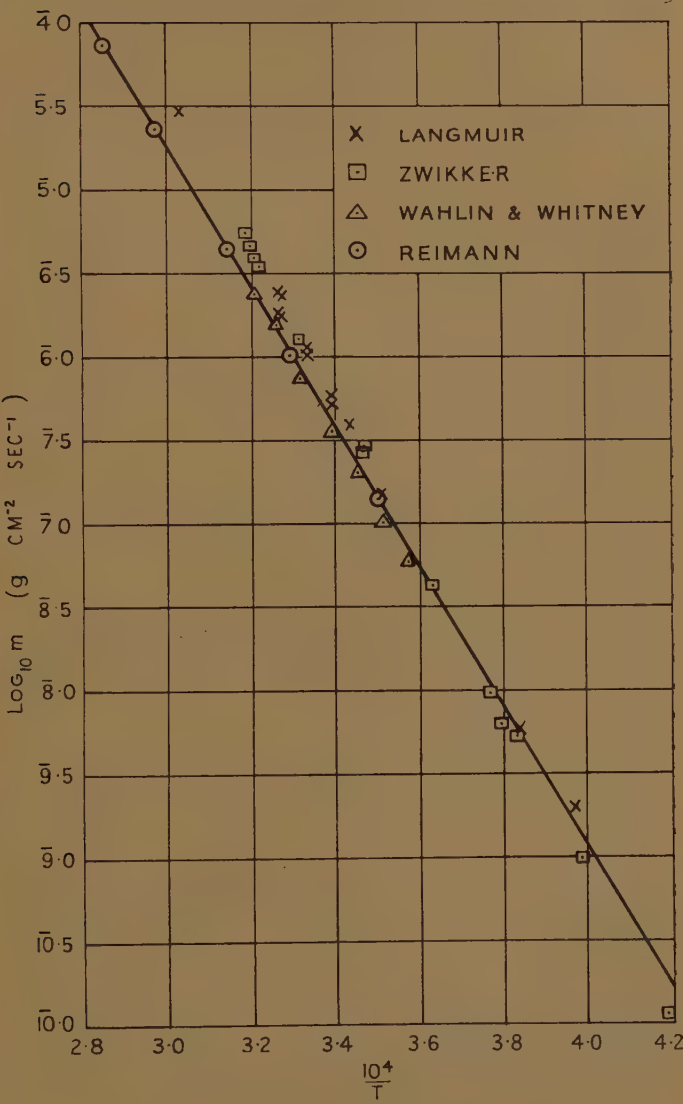

Evaporation data.

with calcium carbonate was attached to a glass bead mounted on the pinch. Alkaline-earth oxides have been

found to act as very efficient getters after they have been heated to redness in a vacuum. The reason for not employing the usual barium getter in this case was to avoid rendering the molybdenum electrodes photo-sensitive as a result of the deposition of a trace of barium on them.

After the pinch had been sealed in, the tube was baked on the pump in the usual manner, the molybdenum electrodes heated to redness by high-frequency induction, and then the getter ring was similarly heated to break down the carbonate to oxide. The bake, electrode heating, and getter ring heating were then repeated, and the tube was sealed off from the pump. Finally, the filament was heated at 2300° K. for 16 hours, while the molybdenum electrodes, held at 100 volts positive to it, collected an electron current of 15 *m*A from it. This was done to improve the vacuum by the clean-up of residual gases.

Positive-emission measurements were now made with the three molybdenum electrodes held at either 10 volts or 30 volts negative to the negative end of the filament, and an axial magnetic field of 50 gauss applied to the tube. Only the ion current collected by the central electrode was measured, the other two serving as guard electrodes. The magnetic field was to suppress electrons emitted photoelectrically from the molybdenum electrodes. The magnetic field made only a relatively small difference to the measured current, and was more than sufficient to suppress all electrons. From the previous work on rate of evaporation as a function of temperature, a rough estimate of the thinning suffered by the filament, and thus of the change in the current-temperature calibration, could be made. A more precise determination of this was made by means of frequent tests of the filament current required to give a standard electron emission per unit area, the above-mentioned rough estimate of thinning being used in this. A final check was obtained by breaking open the tube at the end of the positive-emission measurements, and finding the weight per unit length of the central region of the filament.

The results are plotted in fig. 4, together with those of Moon and of Wahlin and Whitney, for comparison. Moon's points are adjusted for the difference between T_{JL}, which he assumed for his temperatures, and T, according to equation (5). (It is to be assumed that Moon's T_{JL} would be the same as those for the wire used in the present

work. since his wire was obtained from these Laboratories.) It will be observed that there is no appreciable difference between the currents obtained at −10 V and at −30 V.

Fig. 4.

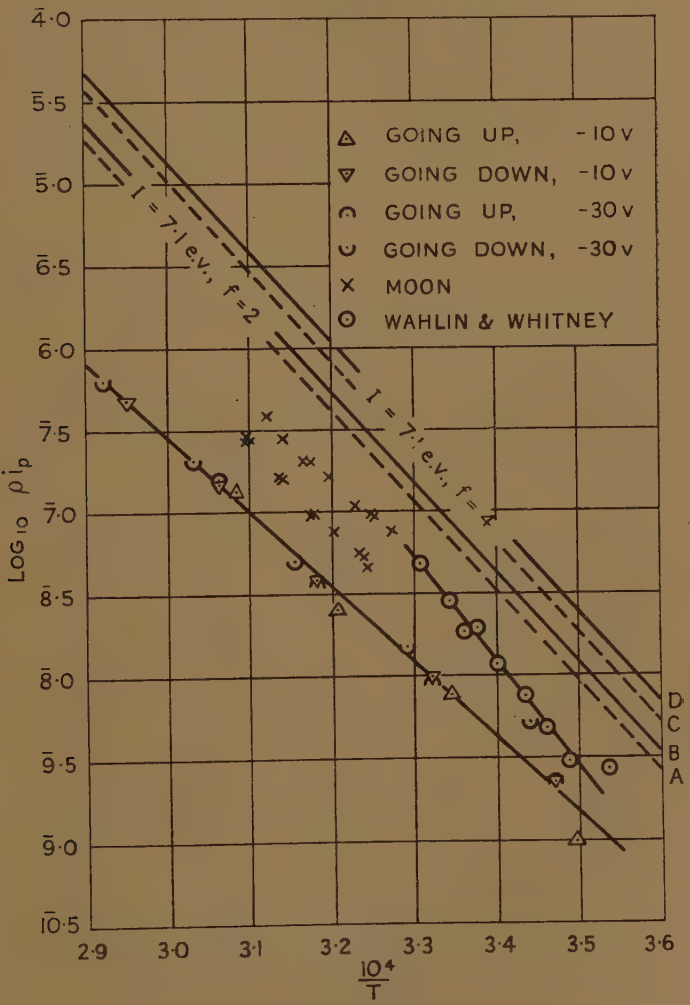

Positive-ion emission data.

To find the theoretical value of i_p/i_a at any temperature from equation (4) we need to know the weight factor

σ_p/σ_a (which is denoted by f in fig. 4), the reflexion coefficients $\bar{r}_p$ and $\bar{r}_a$, the work of ionization I, and the work function χ. The weight factor for tungsten is not known for certain, but it must be either 2 or 4 [10]. In the absence of positive knowledge concerning $\bar{r}_p$ and $\bar{r}_a$ it will be of interest to try the assumption that they are both negligibly small. The work of ionization for tungsten is believed to be about 7·1 e.v. As regards χ, we can calculate it for each temperature from the constants A and ψ of the empirical electron emission formula (6), the probable value of 1·3 being assumed for ρ, while it is further assumed that the transmission coefficient $\bar{D}$ in the theoretical equation

$$i = A_0 \bar{D} T^2 \epsilon^{-\chi/kT} \quad . \quad . \quad . \quad . \quad . \quad . \quad (7)$$

is practically unity, the discrepancy between A and A_0 (whose value is 120 amp. cm.$^{-2}$ deg.$^{-2}$) being due entirely to a temperature variation of the work function χ. There is considerable justification for these assumptions [11]. Thus, according to these assumptions and the electron emission data obtained in this work, the value of χ at 2800° K. would be $4{\cdot}71_7$ e.v., while at 3400° K. it would be $4{\cdot}75_7$ e.v.

A and B in fig. 4 are the theoretical lines obtained in this way, based on the electron emission and evaporation data obtained in this work, with the assumption that f is equal to 2. C and D are the corresponding lines for $f=4$. The upper (full) line of each pair corresponds to an effective roughness factor for positive ions the same as we have assumed for electrons, viz. 1·3. There appears to be no obvious reason why the positive-ion roughness factor should be much less than this. However, to cater for the possibility that it is less, the lines corresponding to the limiting case where the positive-ion roughness factor is equal to unity have also been drawn. These are the dashed lines A and C.

It is seen that the experimental points are in all cases considerably below the theoretical lines. It would be possible to bring the latter down to the region of the experimental points by assuming that $(1-\bar{r}_p)/(1-\bar{r}_a)$ is not, after all, equal to unity, but considerably less. This would not really help us, however, for it would only displace the theoretical lines parallel to themselves, and the difference between their slope and those of the experi-

mental lines would lead to a divergence in other temperature regions. Another possibility is that the work of ionization of tungsten is really somewhat greater than 7·1 e.v. This would both bring the theoretical lines downwards and increase their slope. If I were 7·6 e.v., the line D would come down to the region of Wahlin and Whitney's points, but the disagreement in slope would still be about two-thirds as bad as it is with I equal to 7·1 e.v. Thus, no adjustment of either the reflexion coefficients or I will bring the experimental data and theory into line, and the same is obviously true of the data obtained in the present work. To be sure, by taking the best line through Wahlin and Whitney's evaporation points instead of the one obtained here, and assuming a value of I of nearly 7·6 e.v., the line D could be brought into agreement with a possible (though not the best) line through their positive-emission points. This would hardly be fair, however, since their evaporation data are less consistent among themselves and cover a lesser temperature range than those obtained in the present work. Also, it would still leave unexplained the discrepancy between the two experimental lines. It seems clear that the present theory of positive-ion emission is too simple, and that there must be some variable surface condition that should be taken account of, which, while not affecting appreciably either electron emission or evaporation, does nevertheless have an important effect on the emission of ions.

In conclusion, the author wishes to tender his acknowledgments to the General Electric Company and the Marconi Company, on whose behalf the work was done which has led to this publication.

References.

(1) I. Langmuir and K. H. Kingdon, Proc. Roy. Soc. (A), cvii. p. 61 (1925).
(2) H. B. Wahlin and J. A. Reynolds, Phys. Rev. xlviii. p. 751 (1935).
(3) P. B. Moon, Proc. Camb. Phil. Soc. xxviii. p. 490 (1932).
(4) H. B. Wahlin and L. V. Whitney, Phys. Rev. l. p. 735 (1936).
(5) W. E. Forsythe and A. G. Worthing, Astrophys. J. lxi. p. 146 (1925).
(6) H. A. Jones and I. Langmuir, Gen. El. Rev. xxx. pp. 310, 354 and 408 (1927).
(7) See A. L. Reimann, Phil. Mag. xx. p. 594 (1935).
(8) I. Langmuir, Phys. Rev. ii. p. 450 (1913); H. A. Jones, I. Langmuir, and G. M. J. Mackay, Phys. Rev. xxx. p. 201 (1927).

(9) C. Zwikker, *Physica*, v. p. 249 (1925) ; Proc. Roy. Acad. Amsterdam, xxviii. p. 499 (1925).
(10) See A. L. Reimann, 'Thermionic Emission,' Chapman and Hall, Ltd., p. 308 (1934).
(11) A. L. Reimann, Sc. J. Roy. Coll. Sc., vi. p. 104 (1936) ; Proc. Roy. Soc. (A), clxiii. p. 499 (1937).

LXXVII. *A Proof by Induction of the Analytical Continuations of certain Generalized Hypergeometric Functions.* *By* T. M. MacRobert, *Professor of Mathematics in the University of Glasgow* †.

In a recent paper (Proc. Roy. Soc. Edin. lviii. pp. 1–13, 1937) a proof by induction was given of the relations between certain linear combinations of Generalized Hypergeometric Series and corresponding Asymptotic Expansions. If the usual notation,

$$ {}_pF_q(\alpha_r\,;\rho_s\,;z), \quad . \quad . \quad . \quad . \quad . \quad . \quad (1)$$

for the Generalized Hypergeometric Series is employed, these results hold when $p \leqq q$. If $p \geqq q+2$ the series are divergent, unless $z=0$. In such cases, however, the series may be regarded as asymptotic for z small ; or, if $z=1/\zeta$, for ζ large. The functions which they represent can then, by the method referred to above, be expressed as linear combinations of Generalized Hypergeometric Series in ζ, for which $p \leqq q$. In the remaining case, $p=q+1$, the series is convergent for $|z|<1$.

The differential equation satisfied by the function (1) is

$$\vartheta(\vartheta+\rho_1-1)(\vartheta+\rho_2-1)\ldots(\vartheta+\rho_q-1)w$$
$$-z(\vartheta+\alpha_1)(\vartheta+\alpha_2)\ldots(\vartheta+\alpha_p)w=0, \quad (2)$$

where ϑ denotes the operator zd/dz. For the case $q=p-1$ the equation possesses other $p-1$ solutions valid fo $|z|<1$, namely,

$$z^{1-\rho_s}\,{}_pF_{p-1}\left(\begin{matrix}\alpha_1-\rho_s+1,\ \alpha_2-\rho_s+1,\ \ldots,\ \alpha_p-\rho_s+1\,;\ z\\ 2-\rho_s,\ \rho_1-\rho_s+1,\ \ldots\ *\ \ldots,\ \rho_{p-1}-\rho_s+1\end{matrix}\right), \quad (3)$$

where $s=1, 2, \ldots, p-1$, and the * denotes that the

† Communicated by the Author.

expression $\rho_s - \rho_s + 1$ is omitted. It also has p solutions valid for $|z| > 1$. These are

$$z^{-\alpha_s}{}_pF_{p-1}\left(\begin{matrix}\alpha_s, \alpha_s-\rho_1+1, \alpha_s-\rho_2+1, \ldots, \alpha_s-\rho_{p-1}+1; \\ \alpha_s-\alpha_1+1, \ldots * \ldots, \alpha_s-\alpha_p+1\end{matrix} 1/z\right), \quad \ldots \quad (4)$$

where $s=1, 2, 3, \ldots, p$.

The formulæ which give the analytical continuation of any one of these solutions into the region external to its region of convergence were given by Thomae (*Math. Ann.* ii. pp. 427–444, 1870). The proof which follows is different from that of Thomae. It has been found advantageous to replace z by $-z$ in the formulæ, so that the singularities of the functions are at -1, 0, and infinity. The formula to be established can then be written

$$\sum_{r=1}^{p} F(p, \alpha_r; -z) = \frac{\Gamma(\alpha_1)\Gamma(\alpha_2)\ldots\Gamma(\alpha_p)}{\Gamma(\rho_1)\Gamma(\rho_2)\ldots\Gamma(\rho_{p-1})} \times {}_pF_{p-1}(\alpha_r; \rho_s; -1/z), \quad (5)$$

where

$$F(p, \alpha_r; -z) = \frac{\prod_{t=1}^{p}{}' \Gamma(\alpha_t-\alpha_r)}{\prod_{s=1}^{p-1} \Gamma(\rho_s-\alpha_r)} \Gamma(\alpha_r) z^{\alpha_r} \times {}_pF_{p-1}\left(\begin{matrix}\alpha_r, \alpha_r-\rho_1+1, \ldots, \alpha_r-\rho_{p-1}+1; \\ \alpha_r-\alpha_1+1, \ldots * \ldots, \alpha_r-\alpha_p+1\end{matrix} -z\right), \quad (6)$$

and $-\pi < \mathrm{amp}\, z < \pi$, the functions being made uniform by a cross-cut from the origin through -1 to $-\infty$.

The formula for the case, $p=2$, is well known, and will be here taken as proved. It can be written

$$P(\alpha; -z) + P(\beta; -z) = \frac{\Gamma(\alpha)\Gamma(\beta)}{\Gamma(\rho)} F(\alpha, \beta; \rho; -1/z), \quad (7)$$

where

$$P(\alpha; -z) = \frac{\Gamma(\beta-\alpha)}{\Gamma(\rho-\alpha)} \Gamma(\alpha) z^{\alpha} F\left(\begin{matrix}\alpha, \alpha-\rho+1; \\ \alpha-\beta+1\end{matrix} -z\right), \quad (8)$$

and $P(\beta\ ;\ -z)$ is the same function with α and β interchanged. The L.H.S. of formula (7) may also be written

$$\frac{\sin(\rho-\alpha)\pi}{\sin(\beta-\alpha)\pi}\frac{\Gamma(\alpha)}{\Gamma(\rho-\beta)}\int_0^1 \mu^{-\rho}(1-\mu)^{\rho-\beta-1}\left(1+\frac{1}{\mu z}\right)^{-\alpha} d\mu$$

$$+\text{ the same function with } \alpha \text{ and } \beta \text{ interchanged}, \quad (9)$$

provided that

$$0<\mathrm{R}(\rho-\alpha)<1,\ 0<\mathrm{R}(\rho-\beta)<1.$$

Now

$${}_pF_{p-1}(\alpha_r;\ \rho_s;-1/z)=\prod_{s=1}^{p-2}\frac{\int_0^1 \lambda_s^{\alpha_{s+1}-1}(1-\lambda_s)^{\rho_s-\alpha_{s+1}-1}\,d\lambda_s}{\mathrm{B}(\alpha_{s+1},\ \rho_s-\alpha_{s+1})}$$

$$\times\frac{\int_0^1 \lambda_{p-1}^{\alpha_p-1}(1-\lambda_{p-1})^{\rho_{p-1}-\alpha_p-1}\left(1+\frac{\lambda_1\lambda_2\ldots\lambda_{p-1}}{z}\right)^{-\alpha_1} d\lambda_{p-1}}{\mathrm{B}(\alpha_p,\ \rho_{p-1}-\alpha_p)},$$

$$\ldots\ldots \quad (10)$$

provided that $\mathrm{R}(\alpha_{s+1})>0$, $\mathrm{R}(\rho_s-\alpha_{s+1})>0$, where $s=1, 2, \ldots, p-1$.

Also if, in the integral

$$\int_0^1 \mu^{-\rho_p}(1-\mu)^{\rho_p-\alpha_{p+1}-1}F(p,\ \alpha_r\ ;\ -\mu z)\,d\mu,$$

where

$$\mathrm{R}(\alpha_r-\rho_p)>-1, \qquad \mathrm{R}(\rho_p-\alpha_{p+1})>0,$$

the series is expanded in powers of μz and integrated term by term, the integral is found to have the value

$$\mathrm{B}(\alpha_r-\rho_p+1,\ \rho_p-\alpha_{p+1})\frac{\prod_{t=1}^{p}{}' \Gamma(\alpha_t-\alpha_r)}{\prod_{s=1}^{p-1}\Gamma(\rho_s-\alpha_r)}\Gamma(\alpha_r)$$

$$\times z^{\alpha_r}{}_{p+1}F_p\left(\begin{matrix}\alpha_r,\ \alpha_r-\rho_1+1,\ \ldots,\ \alpha_r-\rho_p+1\ ;\ -z\\ \alpha_r-\alpha_1+1,\ \ldots\ *\ \ldots,\ \alpha_r-\alpha_{p+1}+1\end{matrix}\right)$$

$$=\Gamma(\rho_p-\alpha_{p+1})\frac{\sin(\alpha_{p+1}-\alpha_r)\pi}{\sin(\rho_p-\alpha_r)\pi}F(p+1,\ \alpha_r\ ;\ -z).$$

Hence, from (5) and (10), with suitable restrictions on the constants,

$$\sum_{r=1}^{p} \frac{\sin(\alpha_{p+1}-\alpha_r)\pi}{\sin(\rho_p-\alpha_r)\pi} \mathrm{F}(p+1,\ \alpha_r;\ -z)$$

$$= \prod_{s=1}^{p-1} \frac{\int_0^1 \lambda_s^{\alpha_{s+1}-1}(1-\lambda_s)^{\rho_s-\alpha_{s+1}-1}\, d\lambda_s}{\Gamma(\rho_s-\alpha_{s+1})}$$

$$\times \frac{\Gamma(\alpha_1)}{\Gamma(\rho_p-\alpha_{p+1})} \int_0^1 \mu^{-\rho_p}(1-\mu)^{\rho_p-\alpha_{p+1}-1}\left(1+\frac{\lambda_1\lambda_2\ldots\lambda_{p-1}}{\mu z}\right)^{-\alpha_1} d\mu.$$

Now multiply by

$$\frac{\sin(\rho_p-\alpha_1)\pi}{\sin(\alpha_{p+1}-\alpha_1)\pi},$$

interchange α_1 and α_{p+1}, and add the two equations so obtained. Then, noting that

$$\sin(\rho_p-\alpha_1)\pi \sin(\alpha_{p+1}-\alpha_r)\pi - \sin(\rho_p-\alpha_{p+1})\pi \sin(\alpha_1-\alpha_r)\pi$$

$$= \sin(\alpha_{p+1}-\alpha_1)\pi \sin(\rho_p-\alpha_r)\pi,$$

and applying (7) and (9) with ρ_p, α_1, α_{p+1} for ρ, α, β respectively and $z/(\lambda_1\lambda_2\ldots\lambda_{p-1})$ for z to the innermost integrals on the R.H.S., we get

$$\sum_{r=1}^{p+1} \mathrm{F}(p+1,\ \alpha_r;\ -z)$$

$$= \prod_{s=1}^{p-1} \frac{\int_0^1 \lambda_s^{\alpha_{s+1}-1}(1-\lambda_s)^{\rho_s-\alpha_{s+1}-1}\, d\lambda_s}{\Gamma(\rho_s-\alpha_{s+1})}$$

$$\times \frac{\Gamma(\alpha_1)\Gamma(\alpha_{p+1})}{\Gamma(\rho_p)} \mathrm{F}\left(\alpha_1,\ \alpha_{p+1};\ \rho_p;\ -\frac{\lambda_1\lambda_2\ldots\lambda_{p-1}}{z}\right)$$

$$= \frac{\Gamma(\alpha_1)\Gamma(\alpha_2)\ldots\Gamma(\alpha_{p+1})}{\Gamma(\rho_1)\Gamma(\rho_2)\ldots\Gamma(\rho_p)}\, {}_{p+1}\mathrm{F}_p(\alpha_r;\ \rho_s;\ -1/z).$$

The restrictions on the constants may now be removed by applying the method of analytical continuation. The formula just obtained is (5) with $p+1$ in place of p. Now the formula holds when $p=2$. Hence it holds for all positive integral values of p.

From (5) the analytical continuations of all the functions given by (3) and (4) can be deduced by replacing z by $-1/z$ and $-z$ respectively and suitably altering the constants.

LXXVIII. *New Forms of the Theorem of Three Moments.* *By* F. J. Turton, *B.Sc., A.R.C.S., City and Guilds College* *.

§ 1. *Introductory.*

In § 3 and § 6 of this paper are developed new forms of the "Theorem of Three Moments," giving in § 3 the relation between the bending moments at any three consecutive supports, A, B, C, from left to right, for a continuous beam having on AB *any* distributed load w per unit length at X from A, any number of concentrated loads W_1 at x_1, W_2 at x_2 etc. from A, and any applied couples M_1 at ξ_1, M_2 at ξ_2 etc. from A, with similar loads w' per unit length at Z from C, W_1' at z_1, W_2' at z_2 etc. from C, and couples M_1' at ζ_1, M_2' at ζ_2 etc. from C, on CB, together with couples m_A at A, m_B at B, m_C at C etc., whilst in § 6 axial thrust † is also included. The inclusion of couples at the points † A, B, C makes it necessary to distinguish the bending moment at B in AB (to be denoted by M_{BL}) from the bending moment at B in CB (denoted by M_{BR}). Evidently $M_{BR}=M_{BL}+m_B$.

In § 5 it is explained how the equations of § 3 may be used when the distributed loads give integrals which cannot be found by formal methods.

In § 2 is developed the usual form of the Theorem of Three Moments for a continuous beam with concentrated loads and couples only. The result is required for § 3, and possibly the method of proof, which is short, is new.

In § 4 the reaction R_B at the middle support is obtained in terms of the bending moments at A, B, and C for the loading of § 3, dealing with the distributed load on similar lines, and in § 7 thrust is included.

§ 2. Consider the continuous beam of the figure, having concentrated loads W_1 at x_1, W_2 at x_2 etc. on AB, W_1' at z_1, W_2' at z_2 etc. on CB, couples M_1 at ξ_1, M_2 at ξ_2 etc. on AB,

* Communicated by Dr. W. G. Bickley.

† Offset thrusts may be dealt with by replacing the offset thrusts by equivalent axial thrusts, together with couples of transference. The latter will be included in m_A, m_B etc. at the points A, B etc. They occur in aeroplane calculations due to the line of a flying wire and the mean line of a strut not meeting the axis of the spar at the same point. (See Pippard and Pritchard, 'Aeroplane Structures,' p. 77.)

M_1' at ζ_1, M_2' at ζ_2 etc. on CB, together with a couple m_B at B. For AB, let a be the length and I (constant) the second moment of the cross-section about its neutral axis; let c and I′ refer similarly to CB.

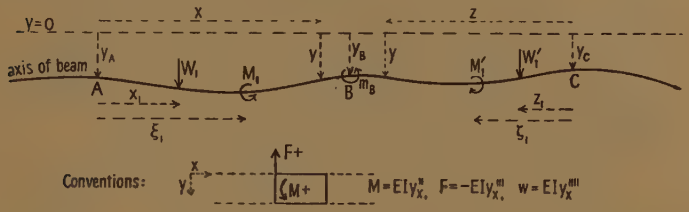

When "x" is to the right of x_1, x_2 etc., ξ_1, ξ_2 etc., but $\leqslant a$, we have, using accents on y to denote successive derivatives with respect to x,

$$EIy''' = -F_{AR} + \Sigma W_1, \quad \text{for the concentrated loads only,}$$

$$EIy'' = M_{AR} - xF_{AR} + \Sigma W_1(x-x_1) + \Sigma M_1,$$

adding in terms for the couples between A and B,

$$EIy' = EIy'_{AR} + xM_{AR} - \frac{x^2}{2}F_{AR} + \Sigma\frac{W_1(x-x_1)^2}{2} + \Sigma M_1(x-\xi_1),$$

$$EIy = EIy_A + xEIy'_{AR} + \frac{x^2}{2}M_{AR} - \frac{x^3}{6}F_{AR} + \Sigma\frac{W_1(x-x_1)^3}{6} + \Sigma\frac{M_1(x-\xi_1)^2}{2},$$

all the integrations being carried out on the system due to Macaulay.

At $x=a$ these give

$$EIy''_{BL} = M_{BL} = M_{AR} - aF_{AR} + \Sigma W_1(a-x_1) + \Sigma M_1, \quad . \quad . \quad (1)$$

$$EIy'_{BL} = EIy'_{AR} + aM_{AR} - \frac{a^2}{2}F_{AR} + \Sigma\frac{W_1(a-x_1)^2}{2} + \Sigma M_1(a-\xi_1), \quad . \quad (2)$$

$$EIy_B = EIy_A + aEIy'_{AR} + \frac{a^2}{2}M_{AR} - \frac{a^3}{6}F_{AR} + \Sigma\frac{W_1(a-x_1)^3}{6} + \Sigma\frac{M_1(a-\xi_1)^2}{2}. \quad (3)$$

To eliminate y'_{AR} and F_{AR} multiply (1) by $-a/3$, (2) by 1, and (3) by $-1/a$, and add; then

$$-\frac{a}{3}M_{BL}+EIy'_{BL}-EI\frac{y_B}{a}=-EI\frac{y_A}{a}+\frac{a}{6}M_{AR}$$
$$-\Sigma\frac{W_1x_1(a^2-x_1^2)}{6a}+\Sigma\frac{M_1(a^2-3\xi_1^2)}{6a}. \quad (4)$$

Similarly for the bay CB, y' being in this case the first derivative of y with respect to z,

$$-\frac{c}{3}M_{BR}+EI'y'_{BR}-EI'\frac{y_B}{c}=-EI'\frac{y_C}{c}+\frac{c}{6}M_{CL}$$
$$-\Sigma\frac{W_1'z_1(c^2-z_1^2)}{6c}+\Sigma\frac{M_1'(c^2-3\zeta_1^2)}{6c}. \quad (5)$$

But $y'_{BL}+y'_{BR}=\left(\frac{dy}{dx}\right)_{BL}+\left(\frac{dy}{dz}\right)_{BR}=0$, for these are of the same magnitude and opposite sign, since x and z are measured in opposite directions. Bending moments involve $\frac{d^2y}{dx^2}$ and $\frac{d^2y}{dz^2}$, however, so the same sign convention for bending moments applies to both bays. Hence, multiplying (4) by $\frac{6}{EI}$, (5) by $\frac{6}{EI'}$, adding corresponding sides together, and rearranging, we have

$$\frac{aM_{AR}}{EI}+\frac{2aM_{BL}}{EI}+\frac{2cM_{BR}}{EI'}+\frac{cM_{CL}}{EI'}$$
$$=6\frac{y_A-y_B}{a}+\Sigma\frac{W_1x_1(a^2-x_1^2)}{aEI}-\Sigma\frac{M_1(a^2-3\xi_1^2)}{aEI}$$
$$+6\frac{y_C-y_B}{c}+\Sigma\frac{W_1'z_1(c^2-z_1^2)}{cEI'}-\Sigma\frac{M_1'(c^2-3\zeta_1^2)}{cEI'},$$

where $M_{BR}=M_{BL}+m_B$.

§ 3. Suppose the beam of § 2 carry in addition *any* distributed load (not necessarily uniform or even continuous), w per unit length at X from A in the bay AB, and w' per unit length at Z from C in the bay CB.

These loads may be regarded as two series of concentrated loads, of type wdX at X, and $w'd$Z at Z, summed

throughout the bays. They contribute to the right-hand side of the result of § 2 the terms

$$\sum_{AB}\frac{w\,dX(a^2-X^2)X}{aEI}+\sum_{CB}\frac{w'\,dZ(c^2-Z^2)Z}{cEI'},$$

$$i.e.,\quad \int_0^a\frac{wX(a^2-X^2)\,dX}{aEI}+\int_0^c\frac{w'Z(c^2-Z^2)\,dZ}{cEI'}.$$

(When w and w' are constant, these reduce to the well-known value $\frac{wa^3}{4EI}+\frac{w'c^3}{4EI'}$.)

So we now have, for distributed loads, concentrated loads and couples

$$\frac{aM_{AR}}{EI}+\frac{2aM_{BL}}{EI}+\frac{2cM_{BR}}{EI'}+\frac{cM_{CL}}{EI'}$$
$$=6\frac{y_A-y_B}{a}+\Sigma\frac{W_1x_1(a^2-x_1^2)}{aEI}+\int_0^a\frac{wX(a^2-X^2)\,dX}{aEI}$$
$$-\Sigma\frac{M_1(a^2-3\xi_1^2)}{aEI}+6\frac{y_C-y_B}{c}+\Sigma\frac{W_1'z_1(c^2-z_1^2)}{cEI'}$$
$$+\int_0^c\frac{w'Z(c^2-Z^2)\,dZ}{cEI'}-\Sigma\frac{M_1'(c^2-3\zeta_1^2)}{cEI'},$$

where $M_{BR}=M_{BL}+m_B$.

When there are no couples at A, B, and C the left-hand side takes the simpler form

$$\frac{aM_A}{EI}+2\left(\frac{a}{EI}+\frac{c}{EI'}\right)M_B+\frac{cM_C}{EI'}.$$

It will be noticed that when w (or w') has to be represented by different functions of x (or z) in different ranges of the bay it is only necessary to split the definite integral into corresponding ranges.

§ 4. Adding terms for the distributed loads, EIy''' and EIy'' at x from A in AB, when x is greater than x_1, x_2 . . ., ξ_1, ξ_2 etc., but $\leqslant a$, are given by

$$EIy'''=-F_{AR}+\Sigma W_1+\int_0^x w\,dX,$$

$$EIy'' = M_{AR} - xF_{AR} + \Sigma W_1(x - x_1) + \Sigma M_1 + \int_0^x w'(x - X)\,dX\,*.$$

At $x = a$ these give

$$EIy'''_{BL} = -F_{AR} + \Sigma W_1 + \int_0^a w\,dX,$$

$$EIy''_{BL} = M_{BL} = M_{AR} - aF_{AR} + \Sigma W_1(a - x_1) + \Sigma M_1 + \int^a w(a - X)\,dX.$$

To eliminate F_{AR}, multiply the second by $-1/a$ and add to the first, and we have

$$EIy'''_{BL} - \frac{M_{BL}}{a} = -\frac{M_{AR}}{a} + \Sigma\frac{W_1 x_1}{a} + \frac{1}{a}\int_0^a wX\,dX - \frac{\Sigma M_1}{a},$$

y'''_{BL} denoting the third derivative with respect to x.

Similarly for CB we have

$$EI'y'''_{BR} - \frac{M_{BR}}{c} = -\frac{M_{CL}}{c} + \Sigma\frac{W_1' z_1}{c} + \frac{1}{c}\int_0^c w'Z\,dZ - \frac{\Sigma M_1'}{c},$$

y'''_{BR} denoting the third derivative with respect to z.

At B the shear force increases by R_B, hence EIy'''_x diminishes by R_B, and therefore

$$R_B = EI\left(\frac{d^3y}{dx^3}\right)_{BL} + EI'\left(\frac{d^3y}{dz^3}\right)_{BR}, \quad \text{for } \frac{d^3y}{dx^3} = -\frac{d^3y}{dz^3}$$

at the same point, z and x being in opposite senses. Thus

$$R_B = EIy'''_{BL} + EI'y'''_{BR};$$

hence, adding corresponding sides of the two equations and rearranging,

$$R_B = \frac{M_{BL} - M_{AR}}{a} + \Sigma\frac{W_1 x_1}{a} + \frac{1}{a}\int_0^a wX\,dX - \Sigma\frac{M_1}{a} + \frac{M_{BR} - M_{CL}}{c} + \Sigma\frac{W_1' z_1}{c} + \frac{1}{c}\int_0^c w'Z\,dZ - \Sigma\frac{M_1'}{c}.$$

(When w and w' are constant the integrals reduce to $\frac{wa}{2} + \frac{w'c}{2}$.)

* The moment of load $w dX$ at X from A, about a point distant x from A ($x > X$), is $w dX(x - X)$.

§ 5. When the integrals

$$\frac{1}{EI}\int_0^a \frac{wX(a^2-X^2)\,dX}{a} \quad \text{and} \quad \frac{1}{EI'}\int_0^c \frac{w'Z(c^2-Z^2)\,dZ}{c}$$

cannot be formally evaluated, we may evaluate them by numerical or graphical methods, *e. g.*, Simpson's Rule.

Alternatively, we note that

$$\int_0^a \frac{wX(a^2-X^2)\,dX}{a} = a\int_0^a wX\,dX - \frac{1}{a}\int_0^a wX^3\,dX$$

$=(a\times$ 1st moment $-\frac{1}{a}\times$ 3rd moment) of the distributed load diagram for AB, about an axis through A parallel to the y axis.

If 1st and 3rd derived figures be drawn, taking the "pole" at A and the "reference line" through B parallel to the y axis, and the areas of the 1st and 3rd derived figures be A_1 and A_3 respectively, then the 1st moment of the load diagram is aA_1 and the 3rd moment is a^3A_3, hence

$$\int_0^a \frac{wX(a^2-X^2)\,dX)}{a} = a^2(A_1-A_3).$$

§ 6. Let the continuous beam have concentrated loads W_1 at x_1, W_2 at x_2, . . . W_n at x_n from A on AB, couples M_1 at ξ_1, M_2 at ξ_2, . . . M_n at ξ_n from A on AB, also axial thrust P on AB; similar concentrated loads, W_1' at z_1 from C, etc., couples M_1' at ζ_1 from C etc., and axial thrust P'* on CB; and a couple m_B at B.

We shall suppose $o<x_1<\xi_1<x_2<\xi_2<\ldots<x_n<\xi_n<a$. This involves no lack of generality, for n is unlimited, and it will appear that the value of any W or M may be made zero if necessary.

Then, for the bay AB, using the convention that a term in brackets [ ] is only to be included when positive, we have for the bending moment at x from A,

$$EIy'' = M_{AR} - xF_{AR} - P(y-y_A) + \Sigma W_r[x-x_r] + \Sigma M_s\dagger[x-\xi_s]^0,$$

* In aeroplane structures the forces due to the flying wires attached at or near the points A, B, etc. will cause variation in the thrust from bay to bay.

† A well-known extension of the method of Macaulay.

$$EIy''+Py=Py_A+M_{AR}-xF_{AR}+\Sigma W_r[x-x_r]+\Sigma M_s[x-\xi_s]^0,$$

or

$$EI(y''+m^2y)=Py_A+M_{AR}-xF_{AR}+\Sigma W_r[x-x_r]+\Sigma M_s[x-\xi_s]^0,$$

where $m^2EI=P$.

The solution is of the form

$$y=A\cos mx+B\sin mx+\frac{1}{m^2EI}\{Py_A+M_{AR}-xF_{AR}+\Sigma W_r[x-x_r]+\Sigma M_s[x-\xi_s]^0\},$$

or, since $m^2EI=P$,

$$y=A\cos mx+B\sin mx+y_A+\frac{M_{AR}}{P}-\frac{xF_{AR}}{P}+\Sigma\frac{W_r[x-x_r]}{P}+\Sigma\frac{M_s[x-\xi_s]^0}{P},$$

where the constants A, B will be different in each of the $(2n+1)$ parts into which the bay is divided by n concentrated loads and n couples.

Taking the constants as A_0, B_0 from $x=0$ to x_1, A_0', B_0' from $x=x_1$ to ξ_1, A_1, B_1 from $x=\xi_1$ to x_2, and so on, then

$$0\leqslant x\leqslant x_1,$$

$$y=A_0\cos mx+B_0\sin mx+y_A+\frac{M_{AR}}{P}-\frac{xF_{AR}}{P},$$

$$x_1\leqslant x\leqslant \xi_1,$$

$$y=A_0'\cos mx+B_0'\sin mx+y_A+\frac{M_{AR}}{P}-\frac{xF_{AR}}{P}+\frac{W_1(x-x_1)}{P},$$

$$\xi_1\leqslant x\leqslant x_2,$$

$$y=A_1\cos mx+B_1\sin mx+y_A+\frac{M_{AR}}{P}-\frac{xF_{AR}}{P}+\frac{W_1(x-x_1)}{P}+\frac{M_1}{P},$$

$$x_2\leqslant x\leqslant \xi_2,$$

$$y=A_1'\cos mx+B_1'\sin mx+y_A+\frac{M_{AR}}{P}-\frac{xF_{AR}}{P}+\frac{W_1(x-x_1)}{P}+\frac{W_2(x-x_2)}{P}+\frac{M_1}{P},$$

$$\xi_2\leqslant x\leqslant x_3,$$

$$y=A_2\cos mx+B_2\sin mx+y_A+\frac{M_{AR}}{P}-\frac{xF_{AR}}{P}+\frac{W_1(x-x_1)}{P}+\frac{W_2(x-x_2)}{P}+\frac{M_1}{P}+\frac{M_2}{P},$$

and so on, to $\xi_n \leqslant x \leqslant a$,

$$y = A_n \cos mx + B_n \sin mx + y_A + \frac{M_{AR}}{P} - \frac{xF_{AR}}{P} + \sum_{r=1}^{n} \frac{W_r(x-x_r)}{P} + \sum_{s=1}^{n} \frac{M_s}{P}.$$

Also we have, $0 \leqslant x \leqslant x_1$,

$$y' = -mA_0 \sin mx + mB_0 \cos mx - \frac{F_{AR}}{P},$$

$x_1 \leqslant x \leqslant \xi_1$,

$$y' = -mA_0' \sin mx + mB_0' \cos mx - \frac{F_{AR}}{P} + \frac{W_1}{P},$$

$\xi_1 \leqslant x \leqslant x_2$,

$$y' = -mA_1 \sin mx + mB_1 \cos mx - \frac{F_{AR}}{P} + \frac{W_1}{P},$$

$x_2 \leqslant x \leqslant \xi_2$,

$$y' = -mA_1' \sin mx + mB_1' \cos mx - \frac{F_{AR}}{P} + \frac{W_1}{P} + \frac{W_2}{P},$$

$\xi_2 \leqslant x \leqslant x_3$,

$$y' = -mA_2 \sin mx + mB_2 \cos mx - \frac{F_{AR}}{P} + \frac{W_1}{P} + \frac{W_2}{P},$$

and so on, to $\xi_n \leqslant x \leqslant a$,

$$y' = -mA_n \sin mx + mB_n \cos mx - \frac{F_{AR}}{P} + \sum_{r=1}^{n} \frac{W_r}{P}.$$

At each of the points x_1, ξ_1, x_2, ξ_2, ... x_n, ξ_n we have the condition of continuity for y and for y' :

At $x = x_1$, y being continuous,

$$A_0 \cos mx_1 + B_0 \sin mx_1 = A_0' \cos mx_1 + B_0' \sin mx_1.$$

At $x = x_1$, y' being continuous,

$$-mA_0 \sin mx_1 + mB_0 \cos mx_1 = -mA_0' \sin mx_1 + mB_0' \cos mx_1 + W_1/P.$$

Multiply the first by $\cos mx_1$, the second by $-\frac{1}{m} \sin mx_1$ and add, giving

$$A_0' - A_0 = \frac{W_1 \sin mx_1}{mP}.$$

At $x = \xi_1$, y being continuous,

$$A_0' \cos m\xi_1 + B_0' \sin m\xi_1 = A_1 \cos m\xi_1 + B_1 \sin m\xi_1 + M_1/P.$$

At $x=\xi_1$, y' being continuous,

$$-mA_0' \sin m\xi_1 + mB_0' \cos m\xi_1 = -mA_1 \sin m\xi_1 + mB_1 \cos m\xi_1.$$

Multiply the first by $\cos m\xi_1$, the second by $-\frac{1}{m}\sin m\xi_1$, and add, giving

$$A_1 - A_0' = -\frac{M_1 \cos m\xi_1}{P}.$$

Thus

$$A_0' - A_0 = \frac{W_1 \sin mx_1}{mP},$$

$$A_1 - A_0' = -\frac{M_1 \cos m\xi_1}{P}.$$

Similarly

$$A_1' - A_1 = \frac{W_2 \sin mx_2}{mP},$$

$$A_2 - A_1' = -\frac{M_2 \cos m\xi_2}{P},$$

and so on, to

$$A_{n-1}' - A_{n-1} = \frac{W_n \sin mx_n}{mP},$$

$$A_n - A'_{n-1} = -\frac{M_n \cos m\xi_n}{P}.$$

On adding the columns

$$A_n - A_0 = \sum_{r=1}^{n} \frac{W_r \sin mx_r}{mP} - \sum_{s=1}^{n} \frac{M_s \cos m\xi_s}{P},$$

the summations now including all loads or couples. We revert to the notation $\Sigma \frac{M_1 \cos m\xi_1}{P}$ etc. of § 2.

It is evident that if any load or couple is zero, *e. g.*, W_2, then the constants for the sections on each side of it become the same, and the two sections coalesce into one. Thus the result for $A_n - A_0$ applies for any distribution of intermediate loads and couples on AB.

We now have, at $x=0$, $y=y_A$, so

$$y_A = A_0 + y_A + \frac{M_{AR}}{P} \quad \ldots\ldots \quad (6)$$

At $x=a$, $y=y_B$, so

$$y_B=A_n\cos ma+B_n\sin ma+y_A-\frac{aF_{AR}}{P}+\frac{M_{AR}}{P}+\Sigma\frac{W_1(a-x_1)}{P}+\Sigma\frac{M_1}{P}. \quad (7)$$

At $x=a$, $y'=y'_{BL}$, so

$$y'_{BL}=-mA_n\sin ma+mB_n\cos ma-\frac{F_{AR}}{P}+\Sigma\frac{W_1}{P}. \quad (8)$$

At $x=a$, $EIy''=M_{BL}$, so

$$M_{BL}=-PA_n\cos ma-PB_n\sin ma \quad \text{(using } m^2EI=P\text{)}, \quad (9)$$

and also

$$0=-A_0+A_n-\Sigma\frac{W_1\sin mx_1}{mP}+\Sigma\frac{M_1\cos m\xi_1}{P}. \quad (10)$$

To eliminate A_0, A_n, B_n, and F_{AR}, multiply (6) by m cosec ma (7) by $-1/a$ (8) by 1 (9) by $(ma\cot ma-1)/aP$ and (10) by m cosec ma, and add; then

$$y'_{BL}-\frac{y_B}{a}+\frac{ma\cot ma-1}{aP}M_{BL}=-\frac{y_A}{a}+\frac{ma\operatorname{cosec}ma-1}{aP}M_{AR}+\Sigma\frac{W_1}{P}\left(\frac{x_1}{a}-\frac{\sin mx_1}{\sin ma}\right)+\Sigma\frac{M_1}{P}\left(\frac{m\cos m\xi_1}{\sin ma}-\frac{1}{a}\right),$$

y' being the first derivative with respect to x.

Similarly for the bay CB,

$$y'_{BR}-\frac{y_B}{c}+\frac{m'c\cot m'c-1}{cP'}M_{BR}=-\frac{y_C}{c}+\frac{m'c\operatorname{cosec}m'c-1}{cP'}M_{CL}+\Sigma\frac{W_1'}{P'}\left(\frac{z_1}{c}-\frac{\sin m'z_1}{\sin m'c}\right)+\Sigma\frac{M_1'}{P'}\left(\frac{m'\cos m'\zeta_1}{\sin m'c}-\frac{1}{c}\right),$$

y' being the first derivative with respect to z.

Then, as in §2, $y'_{BL}+y'_{BR}=0$, giving

$$\frac{ma\operatorname{cosec}ma-1}{aP}M_{AR}+\frac{1-ma\cot ma}{aP}M_{BL}+\frac{1-m'c\cot m'c}{cP'}M_{BR}+\frac{m'c\operatorname{cosec}m'c-1}{cP'}M_{CL}$$

$$= \frac{y_A - y_B}{a} + \Sigma \frac{W_1}{P}\left(\frac{\sin mx_1}{\sin ma} - \frac{x_1}{a}\right)$$
$$- \Sigma \frac{M_1}{P}\left(\frac{m \cos m\xi_1}{\sin ma} - \frac{1}{a}\right)$$
$$+ \frac{y_C - y_B}{c} + \Sigma \frac{W_1'}{P'}\left(\frac{\sin m'z_1}{\sin m'c} - \frac{z_1}{c}\right)$$
$$- \Sigma \frac{M_1'}{P'}\left(\frac{m' \cos m'\zeta_1}{\sin m'c} - \frac{1}{c}\right),$$

where $m^2EI = P$, $m'^2EI' = P'$, and $M_{BR} = M_{BL} + m_B$.

If, in addition, there is a distributed load w per unit length at X from A on AB, and a similar one w' at Z from C in CB, we see as in § 3 that they will contribute

$$\int_0^a \frac{w}{P}\left(\frac{\sin mX}{\sin ma} - \frac{X}{a}\right) dX + \int_0^c \frac{w'}{P'}\left(\frac{\sin m'Z}{\sin m'c} - \frac{Z}{c}\right) dZ$$

to the right-hand side.

Hence, for *any* distributed loads, *any* concentrated loads, *any* applied couples, and axial thrust, we have

$$\frac{ma \operatorname{cosec} ma - 1}{aP} M_{AR} + \frac{1 - ma \cot ma}{aP} M_{BL}$$
$$+ \frac{1 - m'c \cot m'c}{cP'} M_{BR} + \frac{m'c \operatorname{cosec} m'c - 1}{cP'} M_{CL}$$
$$= \frac{y_A - y_B}{a} + \Sigma \frac{W_1}{P}\left(\frac{\sin mx_1}{\sin ma} - \frac{x_1}{a}\right)$$
$$+ \int_0^a \frac{w}{P}\left(\frac{\sin mX}{\sin ma} - \frac{X}{a}\right) dX *$$
$$- \Sigma \frac{M_1}{P}\left(\frac{m \cos m\xi_1}{\sin ma} - \frac{1}{a}\right)$$
$$+ \frac{y_C - y_B}{c} + \Sigma \frac{W_1'}{P'}\left(\frac{\sin m'z_1}{\sin m'c} - \frac{z_1}{c}\right)$$
$$+ \int_0^c \frac{w'}{P'}\left(\frac{\sin m'Z}{\sin m'c} - \frac{Z}{c}\right) dZ *$$
$$- \Sigma \frac{M_1'}{P'}\left(\frac{m' \cos m'\zeta_1}{\sin m'c} - \frac{1}{c}\right),$$

* When these integrals cannot be formally evaluated, we may evaluate them by numerical or graphical methods.

where

$$m^2\mathrm{EI}=\mathrm{P},\ m'^2\mathrm{EI}'=\mathrm{P}',\ \text{and}\ \mathrm{M_{BR}}=\mathrm{M_{BL}}+m_\mathrm{B}. \quad (11)$$

(When w and w' are constant, the integrals become

$$\frac{w}{m\mathrm{P}}\left(\tan\frac{ma}{2}-\frac{ma}{2}\right)\ \text{and}\ \frac{w'}{m'\mathrm{P}'}\left(\tan\frac{m'c}{2}-\frac{m'c}{2}\right);$$

functions arising from these, together with corresponding functions arising from the coefficients of $\mathrm{M_{AR}}$ and $\mathrm{M_{BL}}$, have been tabulated by Berry *.)

A similar expression involving hyperbolic functions may be obtained when tension replaces thrust.

The result of § 3 may be deduced by considering the limiting values of the terms of (11) as m and m' tend to zero.

§ 7. If $\tan\psi=\left(\frac{dy}{dx}\right)_\mathrm{B}$, then $\cos\psi=1$, $\sin\psi=\left(\frac{dy}{dx}\right)_\mathrm{B}$ to the first order. Equating to zero the vertical forces on an element of the beam containing B, $\mathrm{R_B}$ denoting the reaction there, and S true shear in contrast to apparent shear F in § 6,

$$\mathrm{P}\sin\psi-\mathrm{P}'\sin\psi-\mathrm{S_{BL}}\cos\psi+\mathrm{S_{BR}}\cos\psi-\mathrm{R_B}=0,$$

$$\mathrm{R_B}=\mathrm{P}\left(\frac{dy}{dx}\right)_\mathrm{B}-\mathrm{S_{BL}}-\mathrm{P}'\left(\frac{dy}{dx}\right)_\mathrm{B}+\mathrm{S_{BR}}$$

$$=\left(\mathrm{EI}\frac{d^3y}{dx^3}+\mathrm{P}\frac{dy}{dx}\right)_\mathrm{BL}-\left(\mathrm{EI}'\frac{d^3y}{dx^3}+\mathrm{P}'\frac{dy}{dx}\right)_\mathrm{BR}$$

$$=\left(\mathrm{EI}\frac{d^3y}{dx^3}+\mathrm{P}\frac{dy}{dx}\right)_\mathrm{BL}+\left(\mathrm{EI}'\frac{d^3y}{dz^3}+\mathrm{P}'\frac{dy}{dz}\right)_\mathrm{BR},$$

i. e., $\mathrm{R_B}$† $=\mathrm{EI}y'''_\mathrm{BL}+\mathrm{P}y'_\mathrm{BL}+\mathrm{EI}'y'''_\mathrm{BR}+\mathrm{P}'y'_\mathrm{BR}$ in the notation previously used.

For the bay AB, adding the term for the distributed load, we have

$$\xi_n\leqslant x\leqslant a,$$

$$\mathrm{EI}y''+\mathrm{P}y=\mathrm{P}y_\mathrm{A}+\mathrm{M_{AR}}-x\mathrm{F_{AR}}+\Sigma\mathrm{W}_1(x-x_1)+\Sigma\mathrm{M}_1+\int_0^x w(x-\mathrm{X})\,d\mathrm{X},$$

* "The Calculation of Stresses in Aeroplane Wing Spars," Transactions of the Royal Aeronautical Society, No. 1. The tables are reprinted by Pippard, *loc. cit.*

† This gives $\mathrm{R_B}=\mathrm{EI}y'''_\mathrm{BL}+\mathrm{EI}'y'''_\mathrm{BR}$ when $\mathrm{P}=\mathrm{P}'$, for $y'_\mathrm{BL}+y'_\mathrm{BR}$ is zero.

differentiating,

$$EIy''' + Py' = -F_{AR} + \Sigma W_1 + \int_0^x w\,dX$$

(w being independent of x).

At $x=a$, these give

$$EIy'''_{BL} + Py'_{BL} = -F_{AR} + \Sigma W_1 + \int_0^a w\,dX,$$

$$EIy''_{BL} = M_{BL} = P(y_A - y_B) + M_{AR} - aF_{AR} + \Sigma W_1(a - x_1) + \Sigma M_1 + \int_0^a w(x - X)\,dX.$$

To eliminate F_{AR}, multiply the second by $-1/a$ and add to the first, giving

$$EIy'''_{BL} + Py'_{BL} = \frac{M_{BL} - M_{AR}}{a} - P\frac{y_A - y_B}{a} + \Sigma\frac{W_1 x_1}{a} - \Sigma\frac{M_1}{a} + \int_0^a \frac{wX\,dX}{a},$$

accents on y denoting derivatives with respect to x.

Similarly, for the bay CB,

$$EI'y'''_{BR} + P'y'_{BR} = \frac{M_{BR} - M_{CL}}{c} - P'\frac{y_C - y_B}{c} + \Sigma\frac{W'_1 z_1}{c} - \Sigma\frac{M'_1}{c} + \int_0^c \frac{w'Z\,dZ}{c},$$

accents on y denoting derivatives with respect to z.

Adding,

$$R_B = \frac{M_{BL} - M_{AR}}{a} - P\frac{y_A - y_B}{a} + \Sigma\frac{W_1 x_1}{a} - \Sigma\frac{M_1}{a} + \int_0^a \frac{wX\,dX}{a} + \frac{M_{BR} - M_{CL}}{c} - P'\frac{y_C - y_B}{c} + \Sigma\frac{W'_1 z_1}{c} - \Sigma\frac{M'_1}{c} + \int_0^c \frac{w'Z\,dZ}{c}.$$

When w and w' are constant, the integrals reduce to $\frac{wa}{2} + \frac{w'c}{2}$. The result of § 4 is obtained when P and P' are made zero. The integrals in this paragraph (and in § 4) may also be obtained by considering the distributed load as a series of concentrated loads, as in § 3.

LXXIX. *Molecular Force and Viscosity of Gases.*

By Weng Wen-Po *.

(1) *Introduction.*

ACCORDING to Maxwell's † deduction in 1860 the coefficient of viscosity of a gas, or the coefficient of internal friction as it is called in the original paper, should be equal to $\frac{1}{3}\rho_g l\bar{v}$, where ρ_g is the density of the gas, l the mean free path, and $\bar{v}$ the mean velocity of the molecules. In spite of many corrections due to the distribution of velocity and mean free path by Tait, Jeans ‡, Chapman §, and others the proportionality of $\rho_g l\bar{v}$ to viscosity has not been altered. Viscosity will then be expected to be proportional to the square root of the absolute scale of temperature. The experimental results, however, revealed that the viscosity changes much more rapidly with temperature than is required by the above theory.

Molecular force was then brought in to attempt to overcome the difficulty. The original investigation by Maxwell ‖ applied only to molecules repelling each other as the inverse fifth power law. Sutherland ¶ introduced the conception of molecular attraction in 1893. His work has since been generalized by Chapman and Enskog**. Formulæ for the viscosity have been obtained for different models of molecular force, such as (1) a force of repulsion varying inversely as the λth power of the distance and (2) a weak attractive force superposed on perfectly elastic and rigid spheres. The last model, which is generally referred to as the Sutherland model, yields an expression for the coefficient of viscosity $\eta\alpha\frac{\sqrt{T}}{1+\frac{D}{T}}$, where D is a constant and T the temperature on the absolute

* Communicated by the Author.
† Phil. Mag. xix. p. 20 (1860).
‡ Jeans, ' Dynamical Theory of Gases ' (1921).
§ A series of papers appeared in Phil. Trans. Roy. Soc. (1912–1916).
‖ Maxwell, 'Scientific Papers,' ii. p. 26.
¶ Phil. Mag. xxxvi. p. 507 (1893).
** Enskog, ' Kinetishe theorie der Vorgänge in massig Verdünnten Gasen ' (1917).

scale. This expression was found to give good agreement between fact and theory. But the agreement was by no means perfect. Schmidt*, Bestelmeyer, Vögel †, and others pointed out that the divergences from the observed values were considerable at low temperatures. The experimental results of K. Onnes on helium and hydrogen showed still higher discrepancies, so much so that he had to abandon the use of the formula altogether.

Using the virial theorem Reinganum ‡ treated Sutherland's model and obtained for the temperature variation of the formula $\eta \propto T e^{-\frac{D'}{T}}$, in which D′ is another constant characteristic of each gas, and similar to the Sutherland constant. Lennard-Jones § assumed the molecules to repel according to an inverse λth-power law and to attract according to an inverse third-power law. The inverse third law of force was chosen only for the simplicity of calculation. He arrived at

$$\eta \propto \frac{T^{3/2}}{\left(T^{\frac{\lambda-3}{\lambda-1}} + D''\right)},$$

where D″ is a constant as before. Lennard-Jones's formula shows a remarkable improvement in agreement with experiment. He concluded that the index λ could be anything from 15 to 25. On the contrary, Massey and Mohr || gave another explanation of the temperature variation of viscosity by considering the problem using de Broglie's wave theory, and gave fairly coincident results for helium and hydrogen.

The connexion between viscosity and molecular force is indirectly suggested by the fact that the constant in the equations for η just mentioned, such as D and D′, were found to be closely related to other physical constants of the gas. Besides Rankine's empirical rule for Sutherland's constant the best-known rule is that of Vogel, which stated that Sutherland's constant D is proportional to the boiling-point of the substance on the absolute

* *Ann. d. Phys.* xxx. p. 399 (1909).
† Berlin Dissertation (1903).
‡ *Physik Z.* ii. p. 242 (1900).
§ Proc. Roy. Soc. Lond. cvi. p. 441 (1924).
|| Proc. Roy. Soc. Lond. cxli. p. 434 (1933); cxliv. p. 188 (1934).

scale of temperature. Recently Arnold * has shown this rule to be valid for many substances.

(2) *Molecular Force.*

In an investigation † dealing with atomic forces in solids some success has been obtained by assuming that the force is composed of two independent parts, namely, the repulsive and attractive forces. Each part of the force may be composed of forces of entirely different natures in which we are not for the moment interested. It was found that for a number of substances, including nearly all elements, both parts of the force can be represented by inverse power laws of the distances which separate the atoms, and that both the indices are constants, or nearly so, for one group of substances, such as metals, non-metals, etc. The above results are now applied to the gaseous states.

Let the force between two spherically symmetrical molecules be represented by

$$f(\gamma) = -\frac{d}{d\gamma}\mathrm{E}_p(\gamma) = \frac{\mathrm{A}}{\gamma^{\mu}} + \frac{\mathrm{B}}{\gamma^{\lambda}}, \quad . \quad . \quad . \quad (1)$$

where γ is the distance between the centres of the two molecules, $\mathrm{E}_p(\gamma)$ the mutual energy of the molecules at the separation γ, and A, B, λ, and μ are constants. When a pair of molecules of a substance in the gaseous state meet in a head-on collision the average kinetic energy of the molecules will be always great enough to ensure that the nearest distance of approach is comparable with the molecular spacing in the solid state. It is apparent that the same force which holds molecules together in solids governs the interaction during collisions in gases. Therefore the force $f(\gamma)$ has all the properties of the force in the solid state which we have discussed in previous papers. The exact definition of the force is, however, changed to suit the different conditions. In the solid state we dealt with the force due to an assembly of atoms, but $f(\gamma)$ in equation (1) is due only to one single molecule. Furthermore, we expressed the force in the solid state

* Journ. of Chem. Phys. i. p. 170 (1933).

† Phil. Mag. xii. p. 49 (1936); xxii. p. 281 (1936); xxiii. p. 33 (1937); xxiv. p. 466 (1937); xxv. p. 111 (1938).

as the inverse powers of the mean distance between two neighbouring molecules, which is in general slightly greater than the actual distance between the nearest neighbouring atoms. As a result the value of the constants will be numerically affected.

The main features of $f(\gamma)$ in equation (1) which we can easily derive from the study of solid state are worth stating briefly. They can be considered as the assumptions of the present investigation. In the first place, $f(\gamma)$ vanishes when γ is equal to the separation γ_0 between the nearest molecules in the solid state at absolute zero. The separation γ_0 is thus assumed to be the equilibrium position for $f(\gamma)$. In the second place μ and λ are common for a class of substances, for example, for all non-metallic elements. In the third place, the energy required to separate a pair of molecules from a separation γ_0 to infinity is proportional to the energy $\frac{\mathscr{L}_0 M}{N_0}$ required to separate one molecule from the interior of a solid mass to infinity at absolute zero. N_0 and M are respectively Avogadro's number and molecular weight, so that $\mathscr{L}_0$ refers to one gram of the substance. Symbolically we may write

$$\frac{\mathscr{L}_0 M}{N_0} = W E_p(\gamma) \Big]_{\gamma=\gamma_0}^{\gamma=\infty},$$

where W is a constant of proportionality and may be regarded as the effective number of neighbouring molecules. W was equal to 2 when we dealt with the atomic vibrational frequency in solids.

Since $f(\gamma)$ vanishes at $\gamma=\gamma_0$ we have

$$-\frac{A}{{\gamma_0}^{\mu}} = \frac{B}{{\gamma_0}^{\lambda}}$$

by definition of $E_p(\gamma)$ we have

$$E_p(\gamma) = -\int f(\gamma)\, d\gamma = \frac{A}{{\gamma_0}^{\mu-1}}\left[\frac{1}{(\mu-1)}\left(\frac{\gamma_0}{\gamma}\right)^{\mu-1} - \frac{1}{(\lambda-1)}\left(\frac{\gamma_0}{\gamma}\right)^{\lambda-1}\right].$$

$$\frac{\mathscr{L}_0 M}{W N_0} = -E(\gamma_0),$$

this simplifies to

$$E_p(\gamma) = -\frac{\mathscr{L}_0 M}{WN_0}\frac{(\mu-1)(\lambda-1)}{(\lambda-\mu)}\left[\frac{1}{(\mu-1)}\left(\frac{\gamma_0}{\gamma}\right)^{\mu-1} - \frac{1}{(\lambda-1)}\left(\frac{\gamma_0}{\gamma}\right)^{\lambda-1}\right]. \quad (2)$$

(3) *The Interaction between Molecules.*

In normal gaseous state of matter there is much evidence to show that the interaction between the molecules is a weak one—that is to say, the energy of an assembly of gaseous molecules is approximately the sum of the energies of the individual molecules. In treating the case of the molecular collision, for example, we have perfect justification for considering two molecules only. Of course, it is not impossible for a collision to take place in which three or even more molecules are involved at once, but it may be shown that such cases are extremely rare. To take advantage of this fact the process can be described statistically.

Let p_1, p_2, p_3, q_1, q_2, and q_3 be the momenta and space coordinates of the centre of a molecule with respect to that of another molecule which is at the origin of the p and q_j phase space, and let the mutual energy of the molecules be E. We can then express the probability of the molecule being in a state q_1 to $q_1+dq_1 \ldots . p_3$ to p_3+dp_3 by

$$P = \frac{1}{h^3 f_p} e^{-\frac{E}{k_0 T}} dp_1 \ldots . dq_3,$$

where T is the absolute temperature, k_0 Boltzmann's constant, h Planck's constant, and f_p the partition function of the molecule, or,

$$f_p = \frac{1}{h^3}\int \ldots \int e^{-\frac{E}{k_0 T}} dp_1 \ldots dq_3.$$

In the case when there is a continual and steady current of flow inside the gas there will be a part of momentum which is a function of q_1, q_2, and q_3 only superposed on the thermal agitation of the molecules. Then the total energy E will be composed of three parts, namely the mutual potential energy $E_p(q_1 q_2 q_3)$, the kinetic energy due to the thermal agitation, and a third energy $U(q_1 q_2 q_3)$

which is the energy due to the momentum of the steady flow. When the steady flow possesses relatively small amount of energy we can easily find the probability that the moving molecule has space coordinates between q_1 to q_1+dq_1, q_2 to q_2+dq_2, and q_3 to q_3+dq_3, as

$$P_q = \frac{1}{B(T)} e^{-\frac{1}{k_0 T}[E_p(q_1 q_2 q_3)+U(q_1 q_2 q_3)]} dq_1 dq_2 dq_3, \quad . \quad (3)$$

where the function B(T) is defined by

$$B(T) = \iiint^{\infty} e^{-\frac{1}{k_0 T}[E_{p'(q_1 q_2 q_3)}+U(q_1 q_2 q_3)]} dq_1 dq_2 dq_3. \quad . \quad (4)$$

These are the functions which determine all the equilibrium phenomena of collision of the molecules.

To study the phenomenon of viscosity it is sufficient for us to assume that the collision cross-section Q_η effective in the viscosity is one of the properties which are determined by the distribution functions mentioned above. Moreover Q_η is independent of $U(q_1 q_2 q_3)$ under normal conditions, otherwise the coefficient of viscosity no longer has a physical meaning, and in the expression for Q_η, q_1, q_2, and q_3 (as well as γ, which is one of the space coordinates) will appear only under definite integrals such as those in equation (4). It follows Q_η is determined in any case by the quantity

$$\frac{E_p(q_1 q_2 q_3)}{k_0 T}.$$

Taking polar coordinates, and measuring all lengths in units of γ_0, $E_p(q_1 q_2 q_3)$ becomes by equation (2) a product of $\frac{\mathscr{L}_0 M}{N_0}$ and a function of the relative radius vectors in a form common to all substances with same μ and λ. We conclude naturally that the quantity Q_η when measured in these relative dimensions shall be a common function of $\frac{\mathscr{L}_0 M}{RT}$, where $R = k_0 \times N_0$ is the gas constant. In symbols we may write

$$\frac{Q_\eta}{{\gamma_0}^2} = \phi\left(\frac{\mathscr{L}_0 M}{RT}\right) \quad . \quad . \quad . \quad . \quad . \quad . \quad (5)$$

for a group of substances of same μ and λ. ${\gamma^2}_0$ is put into the expression since Q_η has the dimension of an area.

Now $Q_\eta \propto \frac{\sqrt{MT}}{\eta}$, where M is the molecular weight and η the coefficient of viscosity in poises, and, $\gamma_0^2 \propto \left(\frac{M}{\rho_0}\right)^{\frac{2}{3}}$, where ρ_0 is the density of the substance in solid state at absolute zero. We obtain at once

$$\frac{\rho_0^{\frac{1}{3}} T^{\frac{1}{2}}}{\eta M^{\frac{1}{2}}} = \psi\left(\frac{\mathscr{L}_0 M}{T}\right), \quad \ldots \ldots \quad (6)$$

where ψ as ϕ is a common function for a group of substances at any temperature.

(4) *Application.*

Unless it is of theoretical importance we should naturally avoid using such quantities as $\mathscr{L}_0$, which cannot be obtained by a single experimental measurement. To get over this difficulty the following modification is introduced.

Let $\frac{\mathscr{L} M}{N_0}$ be the latent heat of evaporation in ergs per molecule at the normal boiling-point, and γ_l be a quantity having the dimensions of a length such that $(\gamma_l : \gamma_0)^3$ represents the ratio of the specific volume of the substance in liquid state at the boiling-point over that in solid state at absolute zero temperature. By neglecting the potential energy in the normal vapour state, by definition of $E_p(\gamma)$,

$$E_p(\gamma_l) = \frac{\mathscr{L} M}{W N_0}.$$

Therefore equation (2) can be put into the following form:

$$E_p(\gamma) = \frac{\mathscr{L} M}{W N_0} \left[\frac{\frac{1}{(\mu-1)}\left(\frac{\gamma_0}{\gamma}\right)^{\mu-1} - \frac{1}{(\lambda-1)}\left(\frac{\gamma_0}{\gamma}\right)^{\lambda-1}}{\frac{1}{(\mu-1)}\left(\frac{\gamma_0}{\gamma_l}\right)^{\mu-1} - \frac{1}{(\lambda-1)}\left(\frac{\gamma_0}{\gamma_l}\right)^{\lambda-1}} \right].$$

Assuming $\frac{\gamma_l - \gamma_0}{\gamma_0}$ to be small, we can express $E_p(\gamma)$ in a power series of $\gamma_1 - \gamma_0$ as

$$E_p(\gamma) = \frac{\mathscr{L} M}{W N_0} \times \frac{(\mu-1)(\lambda-1)}{(\lambda-\mu)} \left\{ \left[\frac{1}{(\mu-1)} \left(\frac{\gamma_l}{\gamma}\right)^{\mu-1} - \frac{1}{(\lambda-1)} \left(\frac{\gamma_l}{\gamma}\right)^{\lambda-1} \right] - \left[\left(\frac{\gamma_l}{\gamma}\right)^{\mu-1} - \left(\frac{\gamma_l}{\gamma}\right)^{\lambda-2} \right] \frac{\gamma_l - \gamma_0}{\gamma} + \ldots \right\}.$$

When $\gamma_l - \gamma_0$ is very small $E_p(\gamma)$ practically depends on $\mathscr{L}M$ and $\frac{\gamma_l}{\gamma}$ only; but when $\gamma_l - \gamma_0$ is only fairly small reliance has to be placed on an additional assumption that $\frac{\gamma_l - \gamma_0}{\gamma_0}$ is approximately a constant for the group of substances. For non-metallic elements, for example, the assumption can be justified to a certain extent. Under this additional assumption $E_p(\gamma)$ will vary with $\mathscr{L}M$ and $\frac{\gamma_l}{\gamma}$ as before. Thus equation (6) takes the form

$$\frac{\rho_l^{\frac{2}{3}} T^{\frac{1}{2}}}{\eta M^{\frac{1}{4}}} = \psi_1\left(\frac{\mathscr{L}M}{T}\right), \quad . \quad . \quad . \quad . \quad . \quad (7)$$

where ρ_l is the density of the substance in the liquid state at its normal boiling-point. There are definite advantages of equation (7) over equation (6) in practice. In equation (7) ρ_l and $\mathscr{L}$ are the results of direct measurement and are accurately known. Moreover the state of molecular chaos in the liquid state is a nearer approach to that in the gaseous state than the orderly packing in the crystalline state. Thus the complication due to crystalline structure will not be present in equation (7). On the other hand, equation (7) suffers the disadvantage of involving an extra assumption which can never be justified strictly. Using the data for the non-metallic elements taken from International Critical Tables and Tables Annuelles Internationales de Numériques constants et Données up to vol. x. $\frac{\rho_2^{\frac{2}{3}} T^{\frac{1}{2}}}{\eta M^{\frac{1}{4}}} \times 10^{-5}$ has been plotted against $\frac{\mathscr{L}M}{T} \times 10^{-7}$, where $\mathscr{L}$ is in units of ergs per gram. As shown in fig. 1, the function ψ_1 or equation (7) does exist beyond any doubt.

With the aid of the rough graph an empirical formula for η has been found without any difficulty. The form of the equation has been chosen only for the sake of convenience and simplicity. There is no physical significance attached to it. In addition, the formula is not expected to be valid beyond a certain range. The formula can be written as

$$\eta \times 10^6 = \left(\frac{\rho_l^{\frac{2}{3}}}{M^{\frac{1}{4}}}\right) \times \sqrt{T} \times 37{\cdot}00\left[1 - 0{\cdot}370 \log_{10} \frac{\mathscr{L}M}{T} \times 10^7\right]; \quad . \quad . \quad . \quad (8)$$

where η is the coefficient of viscosity in poises, ρ_l the density of the substance in liquid state at the normal boiling-point, M the molecular weight, T the absolute temperature, and $\mathscr{L}$ the latent heat of evaporation in ergs per gram. Equation (8) can be also written as

$$\eta \times 10^6 = \left(\frac{\rho_l^{\frac{2}{3}}}{M^{\frac{1}{3}}}\right) \times \sqrt{T} \times 37{\cdot}00 \left[0{\cdot}6596 - 0{\cdot}370 \log_{10} \frac{\mathscr{L}M}{RT}\right], \quad \ldots \quad (8)$$

Fig. 1.

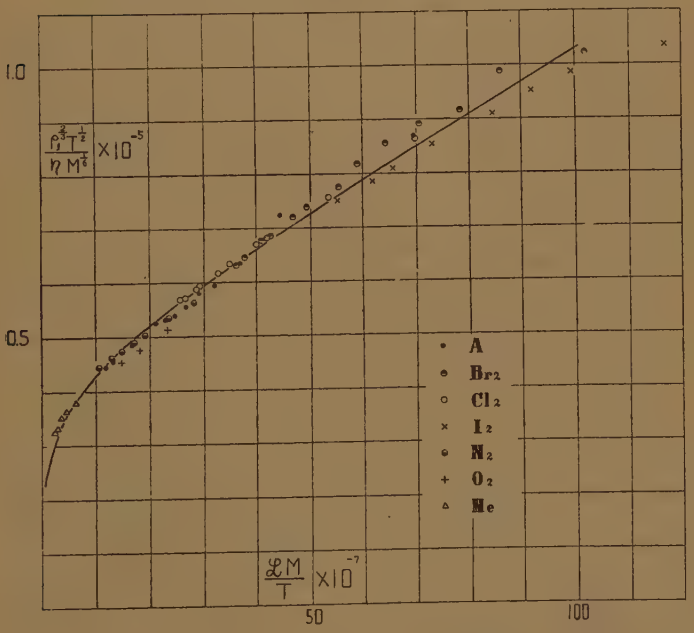

where R is the gas constant. The graph of equation (8) has been plotted in fig. 1 in a thick line. By means of equation (8) calculated and observed values of η in micropoises have been tabulated in Table I. In the last column the percentage deviation between the calculated and observed values of η have been given. The relative deviations were computed before the insignificant figures of the calculated value were rejected. It follows, therefore, that they are not the same as if the calculated values of η in the table had been used.

(5) *Discussion of the Relation.*

It is evident that equation (8) has a definite region of validity. The upper limit for $\frac{\mathscr{L}M}{T} \times 10^{-7}$ is about 100 joules per gram-mole per degree. Beyond this point we expect the equation to be meaningless. On the contrary,

TABLE I.

Argon.—M = 39·91. $\rho_l = 1{\cdot}402$. $\mathscr{L}M = 6{\cdot}30 \times 10^{10}$.

T °A.	$\eta \times 10^6$ obs.	$\eta \times 10^6$ calc.	Dev.	T °A.	$\eta \times 10^6$ obs.	$\eta \times 10^6$ calc.	Dev.
			%				%
90·0	73·6	75·4	2	273	209·6	205	−1·7
140·9	110·6	116	−4·5	296	221·0	219	−0·8
168·8	137·9	136	−1·4	373	269·5	264	−2·0
194·4	157·5	151	−4·7	473	322·3	318	−1·4
233·0	185·4	180	−3·0	523	346·4	344	−0·8
252·9	198·4	193	−3·0				

Bromine.—M = 159·83. $\rho_l = 2{\cdot}987$. $\mathscr{L}M = 29{\cdot}2 \times 10^{10}$.

T °A.	$\eta \times 10^6$ obs.	$\eta \times 10^6$ calc.	Dev.	T °A.	$\eta \times 10^6$ obs.	$\eta \times 10^6$ calc.	Dev.
			%				%
286·0	151	143	−5·1	683·0	347·6	341	−1·8
338·9	170	172	0·7	712·0	359·1	355	−1·2
372·9	188	190	1·3	789·1	396·7	389	−2·0
452·9	227	234	3·2	861·0	430·0	419	−2·5
524·2	269·8	267	−1·0	867·0	429·2	422	−1·8
589·0	299·9	298	−0·8				

Chlorine.—M = 70·92. $\rho_l = 1{\cdot}557$. $\mathscr{L}M = 20{\cdot}0 \times 10^{10}$.

T °A.	$\eta \times 10^6$ obs.	$\eta \times 10^6$ calc.	Dev.	T °A.	$\eta \times 10^6$ obs.	$\eta \times 10^6$ calc.	Dev.
			%				%
285·9	129	130	1·0	606·6	262·6	264	0·6
372·3	168	170	1·2	675·9	287·0	289	0·6
498·5	219·1	220	0·5	692·7	294·8	296	0·3
570·2	248·0	250	0·9	772·0	320·9	324	1·1

Hydrogen.—M = 2·016. $\rho_l = 0{\cdot}0709$. $\mathscr{L}M = 0{\cdot}900 \times 10^{10}$.

T °A.	$\eta \times 10^6$ obs.	$\eta \times 10^6$ calc.	Dev.	T °A.	$\eta \times 10^6$ obs.	$\eta \times 10^6$ calc.	Dev.
			%				%
15·5	5·7	7·6	—	323·2	93·7	95·9	2·3
20·1	10·6	9·8	—	373·2	102·9	103·8	0·9
71·0	31·9	28·2	—	423·2	112·4	109	−1·0
89·7	39·2	33·6	—	473	121·2	119	−5·6
170·3	60·93	67·3	—	523·2	129·7	128	−1·5
273·2	84·2	87·0	3·3				

Nitrogen.—M = 28·02. $\rho_l = 0{\cdot}808$. $\mathscr{L}M = 5{\cdot}60 \times 10^{10}$.

T °A.	$\eta \times 10^6$ obs.	$\eta \times 10^6$ calc.	Dev.	T °A.	$\eta \times 10^6$ obs.	$\eta \times 10^6$ calc.	Dev.
			%				%
196·9	127·5	119	−6·3	373·4	208·4	201	−2·0
235·3	146·5	139	−6·1	425·1	228·1	223	−1·8
289·3	172·8	164·0	−5·1	473·2	246·1	242	−1·7
296·2	176·5	167	−5·1	523·3	262·9	261	−0·7
324·8	188·0	180	−4·1				

Oxygen.—M = 32·00. $\rho_l = 1{\cdot}14$. $\mathscr{L}M = 6{\cdot}83 \times 10^{10}$.

T °A.	$\eta \times 10^6$ obs.	$\eta \times 10^6$ calc.	Dev.	T °A.	$\eta \times 10^6$ obs.	$\eta \times 10^6$ calc.	Dev.
			%				%
290·0	202·3	190	−6·1	459·0	288·5	275	−4·7
372·9	248·5	233	−6·1				

Xenon.—M = 131·3. $\rho_l = 3{\cdot}06$. $\mathscr{L}M = 13{\cdot}5^* \times 10^{10}$(?).

T °A.	$\eta \times 10^6$ obs.	$\eta \times 10^6$ calc.	Dev.	T °A.	$\eta \times 10^6$ obs.	$\eta \times 10^6$ calc.	Dev.
			%				%
289·7	225·0	225	−0	372·6	287·1	265	−8

* Calculated by periodic law of elements, taken from International Critical Tables, vol. i. p. 102.

Iodine.—M = 253·86. ρ_l = 3·75. $\mathscr{L}M = 44{\cdot}0 \times 10^{10}$.

T °A.	$\eta \times 10^6$ obs.	$\eta \times 10^6$ calc.	Dev.	T °A.	$\eta \times 10^6$ obs.	$\eta \times 10^6$ calc.	Dev.
			%				%
397·2	184	172	−6·5	602·1	274·8	270	−1·8
443·2	204	195	−4·5	669·7	306·5	300	−2·1
478·6	220	212	−3·6	710·7	325·0	318	−2·2
520·3	240	232	−3·7	795·8	360·4	355	−1·5

Krypton.—M = 82·9. ρ_l = 2·6. $\mathscr{L}M = 9{\cdot}4 \times 10^{10}$.

T °A.	$\eta \times 10^6$ obs.	$\eta \times 10^6$ calc.	Dev.	T °A.	$\eta \times 10^6$ obs.	$\eta \times 10^6$ calc.	Dev.
			%				%
288·4	243·6	251	3·0	372·6	306·2	311	1·7
273	232·7	239	2·8				

Neon.—M = 20·2. ρ_l = 1·204. $\mathscr{L}M = 1{\cdot}74 \times 10^{10}$.

T °A.	$\eta \times 10^6$ obs.	$\eta \times 10^6$ calc.	Dev.	T °A.	$\eta \times 10^6$ obs.	$\eta \times 10^6$ calc.	Dev.
			%				%
273	297·3	295	−0·9	523	453·2	468	3·3
373	364·6	369	1·1	572·2	490·1	498	1·7
473	424·8	436	2·6	717·7	558·4	583	4·5

Helium.—M = 4·00. ρ_l = 0·20. $\mathscr{L}M = 0{\cdot}10 \times 10^{10}$.

T °A.	$\eta \times 10^6$ obs.	$\eta \times 10^6$ calc.	Dev.	T °A.	$\eta \times 10^6$ obs.	$\eta \times 10^6$ calc.	Dev.
			%				%
15·1	29·5	27·2	−8	250·4	178·8	184	4
20·3	35·0	33·6	−4	296·2	196·2	203	3
75·2	81·5	81·7	0	373	228·1	235	3
88·8	91·9	93	1	473	267·2	267	0
170·6	139·2	143	3	523	285·3	292	2
203·2	156·4	163	4				

equation (8) may closely represent the true facts down to a low value of $\frac{\mathscr{L}M}{T} \times 10^{-7}$. The equation was made to fit the available data for seven gases, namely, A, Br_2, Cl_2, I_2, N_2, O_2, and Ne. The value of $\frac{\mathscr{L}M}{T} \times 10^{-7}$ covers a range approximately from 3 to 100 joules per gram-mole per degree. Working on the extrapolated part of the curve for hydrogen down to $\frac{\mathscr{L}M}{T} \times 10^{-7} = 1{\cdot}7$ joules per gram-mole per degree, the deviation is still of the order of one per cent. The available physical data for helium have not enough significant figures for the purpose of this investigation. Taking $\mathscr{L}M = 100 \times 10^7$ ergs per gram-mole, $\rho_l = 0{\cdot}20$ for liquid He*, equation (8) works fairly well to

$\frac{\mathscr{L}M}{T} \times 10^{-7} = 0{\cdot}2$ joules per gram-mole per degree. In the limiting case when $\frac{\mathscr{L}M}{T} = 0$ or the temperature is infinite the molecules possess such enormous kinetic energies that they can pass through the centres of one another if there is a limit to the potential energy. The cross-section effective in viscosity would therefore be zero. Equation (8) can be shown to fit this limiting condition.

The principal assumption that has been made for the derivation of equation (7) is that the molecules are spherically symmetrical. Naturally the inert gases fit this condition best. The wave mechanical solution of the hydrogen molecule makes the molecule nearer to the assumption, and the same will probably apply to other diatomic molecules, such as Br_2, O_2, etc. Another assumption is that the molecular force has only two dominant parts each of which is proportional to a definite inverse power of the distance. It is probable that the non-metallic elements will satisfy the condition best. As far as we are aware at present there are only two distinct types of force between those molecules. The overlap energy is responsible for the repulsion and the secondary polarization energy for the attraction. For molecules with a permanent dipole moment, such as NaCl etc., the force

* *Cf.* Rev. Mod. Phys. viii. p. 352 (1936).

between the molecules may not be of the same form as that for non-metallic elements. It would not be surprising if equation (8) does not hold for them. But for molecules such as NO and CO, which have only very weak permanent dipole moments, the molecular force should be similar in form to that for non-metallic elements. For CO it is found that equation (8) holds only approximately. In Table II. the calculated values of η for CO are compared with the observed ones. Although the percentage deviation is not particularly large the relative deviation changes constantly with temperature. If equation (8) does strictly hold this can only be explained if the value of the heat of evaporation is not correct. This is evidently not the case.

TABLE II.

Carbon Monoxide.—M $=28{\cdot}00$. $\rho_l=0{\cdot}8138$.
$\mathscr{L}M=5{\cdot}91\times10^{10}$.

T °A.	$\eta\times10^6$ obs.	$\eta\times10^6$ calc.	Dev.	T °A.	$\eta\times10^6$ obs.	$\eta\times10^6$ calc.	Dev.
			%				%
81·7	56·1	69	—	424·2	228·3	216	−6
194·7	127·5	117	−9	473·6	246·7	239	−3
273	166	155	−7	527·1	263·5	260	−1
373·1	210	199	−6				

The percentage deviation between the calculated and observed values of η for hydrogen at low temperatures is not given in Table I., since different determinations of η give widely different values. For example, the values of η at 20·7° A. 20·1° A., and 20·1° A. were given to be 8·5, 10·6, and 11·1 micropoise respectively by different experiments. It is quite possible that the calculated value $\eta=9{\cdot}82$ micropoise at 20·1° A. is nearly correct.

(6) *The Classical Theory.*

Equations (6) and (7) may be used to study the temperature variation of viscosity and molecular force. If equation (8), which is a special form of equation (7), is assumed to be true within the region $\frac{\mathscr{L}M}{T}\times10^{-7}=0{\cdot}2$ to 100 joules per gram-mole per degree, it is equivalent

to a complete set of data of η for helium from 1° A. to 500° A. or for iodine from 440° A. to 220,000° A. available for our investigation.

An attempt has been made to start the investigation from equation (6). By doing this the uncertainty discussed in section (4) is avoided.

In constructing the function indicated by equation (6) the density under 20° A. was taken for ρ_0, while for chlorine that at 78° A. was used. In this case a suitable compensation of $\mathscr{L}_0\mathrm{M}$ based on the principle outlined in section (4) has been effected. The values $\mathscr{L}_0\mathrm{M}$, *i. e.*, the total intermolecular potential energy in ergs per gram-mole in crystalline state at absolute zero, have been computed by summing up all the increases of potential energy from the crystalline state at absolute zero to the vapour state at normal boiling-point. The increase of potential energy between 0° A. to the melting-point in solid state and that from the melting-point to the normal boiling-point in liquid state have been supposed equal to half the integral of the specific heat with respect to temperature. In other words, it has been assumed that the molecules in solids and liquids are linear harmonic vibrators without rotation. As these quantities are small compared with $\mathscr{L}_0\mathrm{M}$, rough estimation is not particularly objectionable. Graphical integration has been applied for the actual evaluation. The main parts of $\mathscr{L}_0\mathrm{M}$ are the latent heat of fusion and latent heat of evaporation at the normal boiling-point. The values of $\mathscr{L}_0\mathrm{M}$ so calculated for several non-metallic elements are shown in Table III. In some cases the values have been compared with the latent heat of sublimation from the vapour pressure data. The density near to absolute zero is also tabulated.

With these constants $\frac{\mathscr{L}_0\mathrm{M}}{\mathrm{T}} \times 10^{-7}$ in joules per gram-mole per degree has been plotted against $\frac{\sqrt{\mathrm{T}}\rho_0^{\frac{2}{3}}}{\eta \mathrm{M}^{\frac{1}{3}}}$, as shown in fig. 2. By a similar procedure to that used before we get

$$\eta \times 10^6 = \left(\frac{\mathrm{R}}{\mathscr{L}_0\mathrm{M}}\right) \times \frac{\rho_0^{\frac{2}{3}}}{\mathrm{M}^{\frac{1}{3}}} \times 10^2 \times \frac{\mathrm{T}^{\frac{3}{2}}}{\left[3{\cdot}950\left(\frac{\mathrm{RT}}{\mathscr{L}_0\mathrm{M}}\right)^{0{\cdot}776} + 0{\cdot}242\right]} \quad . \quad . \quad . \quad (9)$$

where R is the gas constant. Comprehensive numerical tests which have not been presented in this paper reveal that the equation is at least as accurate as equation (8). Therefore the probable error of the constants given in the equation should not be greater than a few per cent.

The most general law of interaction for which exact classical calculation can be carried out is that given by Lennard-Jones *, in which he assumed μ to be 3 and λ any number. In addition to these assumptions his final conclusions are reached by making a further assumption of a weak attraction. This last assumption of a weak

TABLE III.

Elements.		A.	Br_2.	Cl_2.	I_2.	O_2.	N_2.
Increases of $E_p(\gamma)$ in kilo-joules per gram-mole.	0°A–M.P.	0·7	5·9	2·24	8·5	0·60	0·85
	Fusion	1·12	10·8	6·8	16·8	0·44	0·71
	M.P.–B.P.	0·08	2·4	2·3	2·4	0·61	0·42
	Evaporation	6·3	29·2	20·0	44	6·83	5·60
$\mathscr{L}_0 M \times 10^{-10}$		8·20	48·2	31·3	71·7	8·48	7·57
Heat of sublimation in kilo-joules per gram-mole		7·815	—	29·3	—	—	6·88
ρ_0 density at low temperature		1·645	4·14	2·121	5·052	1·46	1·0265
Temperature of the measurement in Å.		20	20	78	—	—	20·7

attraction has been removed by Hasse and Cook †, whose results are unfortunately very complicated.

If Lennard-Jones's condition of a weak attraction is expressed by means of equation (2) it can be seen that the condition is generally fulfilled. Therefore it will be expected that equation (9) corresponds to Lennard-Jones's equation, namely,

$$\eta \propto \frac{T^{\frac{3}{2}}}{T^{\frac{\lambda-3}{\lambda-1}} + D''}, \quad \ldots\ldots \quad (10)$$

* *Loc. cit.* 1924.

† Phil. Mag. iii. p. 977 (1927).

where D″ is a constant. By rewriting equation (9) as

$$\eta = \left(\frac{R}{\mathscr{L}_0 M}\right)^{0\cdot224} \times \left(\frac{\rho_0^{\frac{2}{3}}}{M^{\frac{1}{2}}}\right) \times 25\cdot3 \times \frac{T^{\frac{3}{2}}}{\left[T^{0\cdot776} + 0\cdot061\left(\frac{\mathscr{L}_0 M}{R}\right)^{0\cdot776}\right]} \quad . \quad . \quad . \quad . \quad (9')$$

it becomes analogous in form to Lennard-Jones's equation.

Equation (10) reduces to Sutherland's equation when λ approaches infinity. Equation (9), which represents the

Fig. 2.

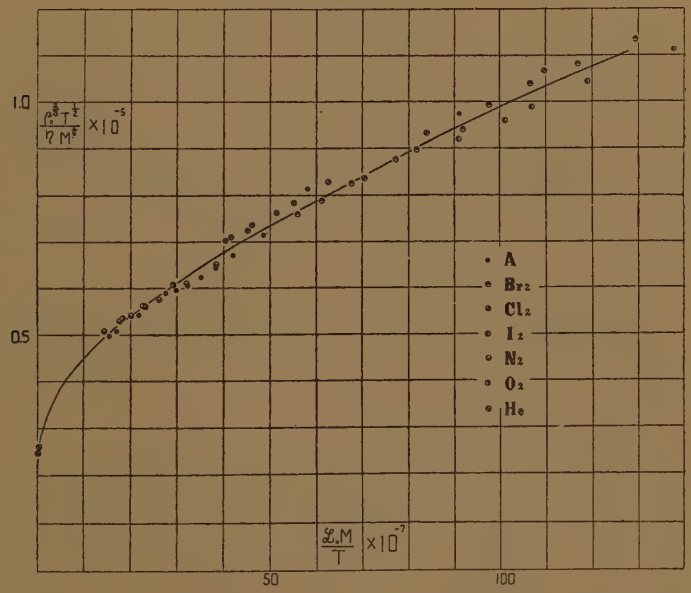

general experimental results, shows that for molecules of high $\mathscr{L}_0 M$ such as I_2, Br_2, etc. the Sutherland's equation is apparently valid in low temperature region. This corresponds to the case when the contribution of repulsion to the temperature variation of viscosity is negligible. Working on Sutherland's model, Enskog and James * have shown that D″ of equation (10) is proportional to the energy required to separate two molecules from contact to infinity. Equation (9′) gives an indirect verification of this statement.

* Proc. Camb. Phil. Soc. xx. 4, p. 447.

For molecules having low values of the latent heat $\mathscr{L}_0 M$, D'' becomes unimportant except at extremely low temperatures. It applies in the case of helium, neon, and hydrogen at moderately high temperatures. Equation (9) for these gases then reduces to $\eta \propto T^{0\cdot724}$. Kamerlingh-Onnes and Weber obtained $\eta \propto T^{0\cdot695}$ for helium and $\eta \propto T^{0\cdot647}$ for hydrogen.

Lennard-Jones inferred in his paper that the index in equation (10) would remain the same even when the attractive force is not an inverse third one. By equation (9') $\lambda = 10$ according to the inference.

(7) *The Wave Theory.*

Since Davison and Kunsman and G. P. Thomson discovered the diffraction of electrons the wave property of matter has been applied to many problems with uniform success. Massey and Mohr were the first to consider the scattering of molecules in transport phenomena. They showed that the cross-section effective in the viscosity Q_η is

$$Q_\eta = 2\pi \int_0^\pi I(\theta) \sin^3\theta \, d\theta.$$

The function $I(\theta)$ is the scattering function of a wave of the wave-length $\lambda_0 = \dfrac{h}{mv}$, where m is the effective mass and v the mean velocity.

They allowed for the symmetry of the system and the boundary conditions, and assumed molecules to be solid balls of diameter γ_0. Their results for viscosity can be summed up in Table IV., where the figures are the ratios of quantum theoretical to the classical cross-section effective in the viscosity.

As λ_0 is inversely proportional to $\sqrt{T}$, the effect of the scattering of particles is the increase of Q_η as temperature decreases. Massey and Mohr set reasonable values of $\gamma_0 = 2\cdot10$ A. for helium and $\gamma_0 = 2\cdot75$ A. for hydrogen, and obtained values of η reasonably close to those observed. A paradoxical conclusion was reached that viscosity is not related to molecular force.

If the question is studied more closely it will be found that there is no contradiction between classical mechanics and wave-theory. This is only a case of quantitative modification. It can be shown that in the case of helium

from 15° A. and of hydrogen from 100° A. onward the force of attraction does not contribute very much to the viscosity. In equation (9) the term 0·242 is comparatively small with its accompanying term. As a result the omission of the attractive force does not affect the result seriously. For hydrogen under 100° A. it is rather different, for here the attractive force comes into play. Massey and Mohr's results fail here. In their original paper the difference between the calculated and observed value for hydrogen rises to as much as 100 per cent. at 15·5 A.

TABLE IV.

$2\pi\gamma_0/\lambda_0$	0.	2.	3.	5.	10.	20.	30.	8
Ratio	16·00	2·28	1·76	1·47	1·23	1·11	1·07	1·00

As for the repulsive force Massey and Mohr's results show only that the index of the inverse distance is very high, being so great that the molecule behaves like a solid ball. Neglecting the scattering of the matter wave, we deduced that the index of the inverse distance for repulsion is about 10. Taking the scattering of the particles into consideration we shall conclude that the index for repulsion λ is larger than 10, probably by a considerable amount.

In conclusion, the author takes this opportunity of thanking Mr. K. H. Waters for his kind help.

LXXX. *Dielectric Constant of Ionized Gases.*—II. *By* SUKHAMAYA GANGOPADHYAYA, *M.Sc., and* S. R. KHASTGIR, *D.Sc.(Edin.), Dacca University* *.

1. *Introduction.*

IN a recent paper it has been shown by Khastgir and A. Imam † that with the condenser plates placed *outside* the discharge-tubes the values of the dielectric constant of ionized chlorine and thallium vapour decrease below unity almost proportionately with the increase of

* Communicated by S. R. Khastgir, D.Sc.

† Ali Imam & Khastgir, Phil. Mag. (May 1937).

the tube current. Appleton & Chapman * have also previously shown that when very short waves and external plates are used the reduction in the value of the dielectric constant of ionized air below unity increases steadily with the increase of the tube current. An abrupt increase in the value of the dielectric constant has, however, been observed in their experiments at a certain value of the tube-current ; but it has been shown to be possibly connected with the free period of the plasmoidal oscillations discussed by Tonks and Langmuir †. The object of the present paper is to describe further experiments performed with the condenser plates placed against the outside surface of a few discharge-tubes. These experiments show that for small ionization densities, the dielectric constant of air or nitrogen is less than unity and that as the ionization is increased by increasing the current through the tube, the dielectric constant at first decreases and then increases gradually and even becomes greater than unity. These experimental results obtained with external condenser plates are very similar to those obtained by Appleton and Childs ‡, who employed condenser plates *inside* the discharge-tube. The cause or causes giving rise to these anomalous results in the present experiments did not evidently exist in the chlorine and thallium discharge-tubes within the range of the tube currents in the experiments of Khastgir and A. Imam.

In the experiments with ionized air where the condenser plates are inside the discharge-tube, the observed anomalous increase in the value of the dielectric constant has been attributed by Appleton and Childs ‡ to the formation of positive ionic sheaths on the plates of the experimental condenser. Since the velocity of the positive ions is much lower than that of the electrons, the condenser plates inside the discharge-tube collect more electrons per second than positive ions and thus acquire a negative potential. The acquired negative potential produces a positive ion sheath round the surface of the condenser plates. The ionic sheath has the effect of reducing the distance between the plates, thereby increasing the effective capacity of the condenser.

* Appleton and Chapman, Proc. Phys. Soc. xliv. p. 246 (1932).
† Tonks and Langmuir, Phys. Review, xxxvii. p. 195 (Feb. 1929).
‡ Appleton and Childs, Phil. Mag. x. (Dec. 1930).

Gutton and Clement * have attempted to explain the increase of the dielectric constant above unity as due to the existence of quasi-elastically bound electrons in the ionized gas. According to them, the electric carriers in the ionized gas are not free and they possess a natural frequency due to quasi-electic forces.

Gutton † has shown that the dielectric constant of an ionized gas is given by

$$\epsilon = 1 + \frac{4\pi N e^2}{m(\omega_0^2 - \omega^2)}$$

and $\omega_0^2 = A.N^{\frac{2}{3}}$, where ω_0 is the natural frequency of the electrons, e and m are the charge and mass of each electron, ω the angular frequency of the radio-frequency oscillations, N the number of electrons per c.c., and A a constant. It is evident that for very large values of N when $\omega_0 > \omega$ the value of the dielectric constant can be greater than unity.

Pederson‡, on the other hand, considers that the increase in the value of the dielectric constant of the ionized gas may be an effect of the conductivity acquired by the ionized gas inside the discharge-tube. The conductivity effect can, however, be eliminated by obtaining the condition for *voltage resonance* in the measuring circuit; for it is known that the L—C value necessary for maximum voltage across the condenser is independent of the conductivity acquired by the ionized medium. If, however, the conductivity be not uniform the voltage resonance condition does not really eliminate the conductivity effect. Banerjee § has shown that the dispositions of the condenser system and the discharge-tube in the experiments on the dielectric constant of ionized media are usually such that even for measurements by voltage resonance the effect of conductivity is to increase the effective capacity of the condenser system. The anomalous increase in the dielectric constant of the ionized gas may therefore be caused by this conductivity effect. Van der Pol ‖ attributed the increase of the dielectric constant beyond unity to inhomogeneity in the ionized medium.

* Gutton and Clement, ' Comptes Rendus,' clxxxiv. (1927).
† Gutton, *Ann. de Physique*, xiii. p. 68 (1930).
‡ Pederson, ' The Propagation of Radio Waves.'
§ Banerjee, Phil. Mag. xvii. p. 834 (April 1934).
‖ Van der Pol, Thesis, University of Utrecht (1920).

Experiments have therefore been undertaken to investigate into the cause or causes of the anomalous variation in the value of the dielectric constant of an ionized gas. The results of these experiments are given in the present paper. Further experimental results on the variation of the dielectric constant of ionized air with the wave-length of the oscillation are also given. The method of measurement of the dielectric constant of the ionized gases has been different in these sets of experiments from that adopted in the experiments of Khastgir and A. Imam.

2. *Experimental Method and Arrangements.*

The discharge-tube A containing the gas under examination has been fixed in a vertical position between two thin cylindrical metal pieces CC held tightly round the outside of the discharge-tube. These pieces, which are placed symmetrically with regard to the discharge-tube, make up a condenser constituting the terminal capacity of a pair of Lecher wires. Ultra-high frequency oscillations have been induced in the Lecher system from a neighbouring oscillator, and resonance adjustments have been made by sliding a short circuiting bridge B across the wires. The resonance has been indicated by means of a sensitive vacuum junction in combination with a mirror galvanometer. The junction has been coupled to the Lecher wire system at the input end by means of two small condensers *aa* consisting of short brass tubes insulated from the Lecher wires by glass sleeves. A valve detector unit (consisting of an A.C. S_2 valve fed by D.C.), coupled to the Lecher wires in a similar way, has also been employed to indicate the tuning point of the bridge. The diagram of the arrangements is shown in fig. 1. The method of measuring the dielectric constant of the ionized gas consists in determining the tuning position of the short circuiting bridge when there is no discharge through the tube, and in noting the shift of the tuning position when the discharge is passed through the tube. If l be the length of the Lecher wire measured from the input end up to the first point of resonance when there is no discharge, l' the corresponding length when the discharge is passed, C and C′ be values of the capacity of the experimental condenser with the discharge current off and on

respectively, then the dielectric constant of the ionized gas is determined from

$$\epsilon = \frac{C'}{C} = \frac{\tan \frac{2\pi l}{\lambda}}{\tan \frac{2\pi l'}{\lambda}}.$$

3. *Experimental Details and Results.*

(a) *Variation of the Dielectric Constant of Ionized Gas with Tube Current.*

Experiments have been performed with air and nitrogen discharge-tubes. The air-discharge-tube has been 42 cm.

Fig. 1.

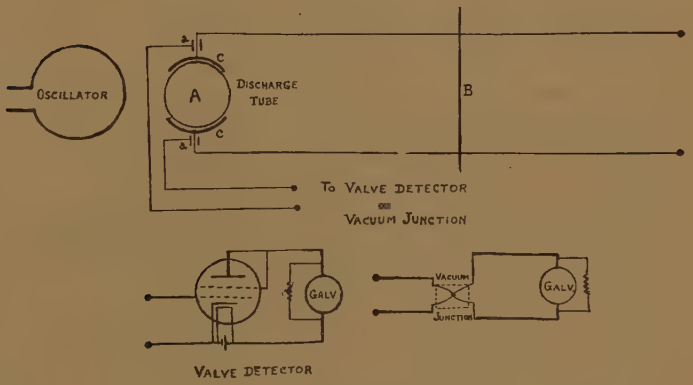

long and $2\frac{1}{2}$ cm. in diameter and fitted with aluminium electrodes $1\frac{1}{2}$ cm. in diameter. A cold cathode discharge has been passed between them by means of a large induction coil. The tube-current has been regulated by varying the current in the primary of the induction coil and by altering the speed of the mercury interrupter.

The outside condenser plates have been two cylindrical copper-foil sheets 15 cm. long and 4 cm. wide surrounding the middle of the air-discharge-tube. The narrow part of the nitrogen tube used has been 6 cm. long and about ·5 cm. in diameter, and the cylindrical condenser pieces have been 5 cm. long and about ·6 cm. wide Two bare copper wires of 18 S.W.G. about 6 metres long and 9 cm. apart have been used for the Lecher system. A third

parallel wire fitted with a long wooden scale running parallel to it has been fixed close to one of the two Lecher wires. A slider on the third wire can be fixed at the point where the pointer attached to the slider indicates the resonance point. The scale reading for the tuning position can then be noted. The short-circuiting bridge has been filed on two sides to give it a prismatic shape. The sharp edge of the prism touches the wires when the resonance adjustments are made.

Two sets of observations are given, one when the vacuum junction has been used in combination with a mirror

Fig. 2.

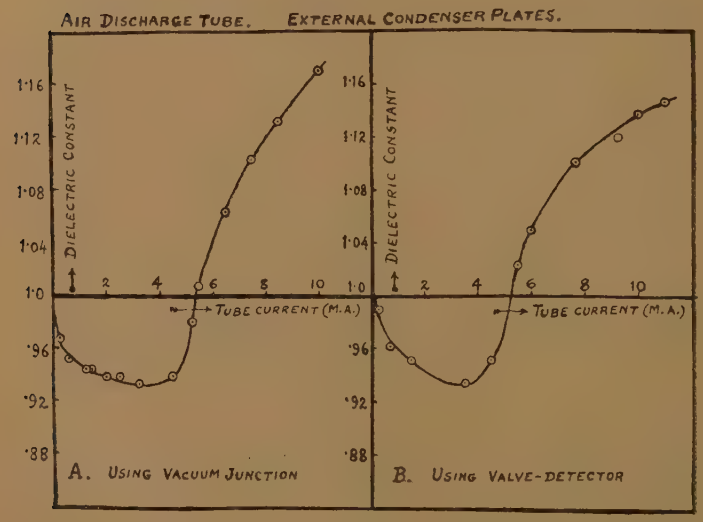

galvanometer and the other when a valve-detector unit with a mirror galvanometer in the anode circuit has been used as the resonance indicator. Both methods of determining the tuning position have given practically the same results. The value of the dielectric constant of the ionized air has been less than unity for small tube-currents. It decreases at first with the increase of the tube-current and then increases again and attains a value greater than one. The results are graphically represented in fig. 2.

Similar experimental results with external condenser plates round the nitrogen discharge-tube are shown in

fig. 3. The thermionic valve detector has been used to determine the resonance points.

In their experiments with internal condenser plates Appleton and Childs have attributed the anomalous effect to the formation of ionic sheaths round the condenser plates. If the theory of ionic sheaths is correct, this anomalous result is also expected in the experiments with external condenser plates; for the ionic sheaths can be formed in a similar way round the inside glass surface of the discharge-tube, at least for the larger values of the tube-current. It is to be observed that the dielectric constant of ionized air in our air-discharge-tube attains

Fig. 3.

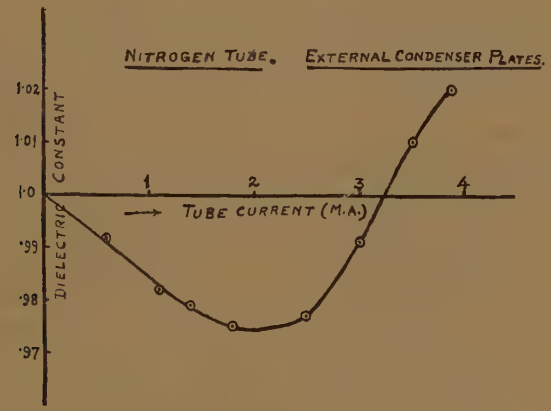

a value greater than one when the tube-current exceeds 5·5 ma. In the case of the nitrogen tube, which is much narrower than the air-discharge-tube, the corresponding tube-current above which the dielectric constant has a value greater than one is about 3·25 ma.

(b) *Experiments avoiding Ionic Sheath Formations*

According to Appleton and Childs the effect of the ionic sheath is to cause an increase of the effective capacity of the experimental condenser, and they have furnished experimental evidence in support of the theory To decide this question experiments have been performed with a discharge-tube where these ionic sheaths are not formed.

With this purpose in view a discharge-tube of length about 20 cm. and $2\frac{1}{2}$ cm. in diameter has been made with two coaxial cylindrical electrodes. The outer electrode is a cylinder of thin copper sheet just fitting into the discharge-tube and touching its side, and the inner one is an aluminium rod fixed along the axis of the discharge-tube (see fig. 4). A number of narrow slits has been cut on the outer copper cylinder and a small brass cylinder is coaxially fitted into the aluminium rod, so that when a discharge is passed between the electrodes

Fig. 4.

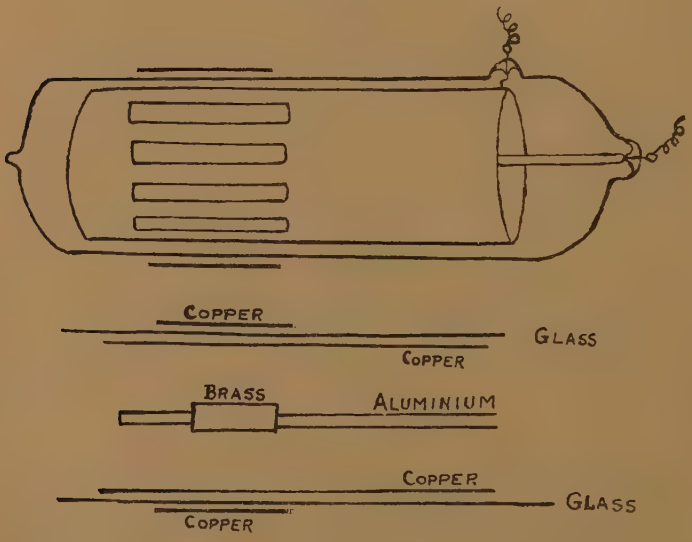

the discharge takes place radially between the small brass cylinder on the aluminium rod and the surrounding copper cylinder with a number of slits on it. The experimenting condenser is made up of two cylindrical brass pieces (4×4 cm.) which have been placed outside the discharge-tube pressing against its side. Two sets of experiments have been performed. In the first set the copper cylinder has been made the anode and the axial rod the cathode, and the anode has been earthed. In the second set the inner rod has been made the anode and earthed, the copper cylinder acting as the cathode. There is practically no possibility of any ionic sheath formation

on the inside of the discharge-tube. The slits have been cut to avoid the shielding effect of the copper cylinder inside the discharge-tube.

The values of the dielectric constant of the ionized air for different values of the tube-current are illustrated in fig. 5.

It is significant that in these experiments *the value of the dielectric constant of the ionized air never exceeds unity.*

Fig. 5.

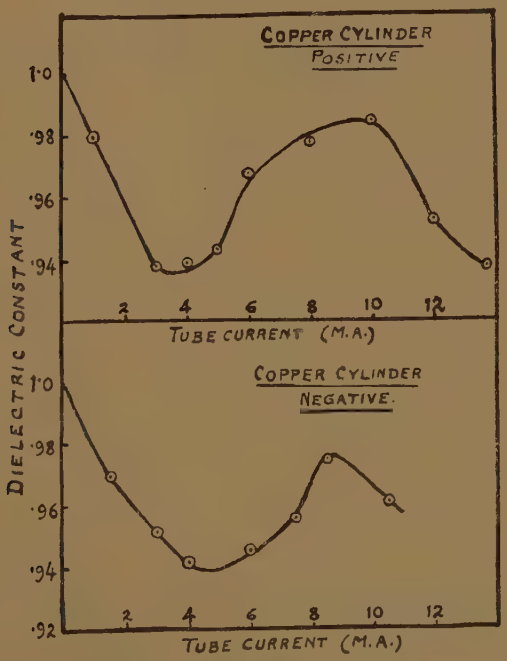

The dielectric constant decreases steadily in the beginning with the increase of the tube current. It, however, rises again and subsequently falls rapidly with increasing tube-currents.

4. *Discussion of the Experimental Results.*

A comparison of figs. 2 and 5 clearly shows that the formation of ionic sheaths round the surface of the discharge-tube plays an important part in increasing the effective capacity of the experimental condenser, thus giving an *apparent* increase in the value of the dielectric

constant of the ionized air which may even exceed the value of unity for large tube-currents. Gutton's explanation of the phenomenon as due to a quasi-resonance effect of the electrons in the discharge-tube cannot, however, be entertained, although such effect has been demonstrated by experimenters. If Gutton's explanation is correct, the value of the dielectric constant of the ionized air greater than unity would have been obtained in the experiments with the discharge-tube where there is practically no ionic sheath formation.

To explain the irregularity in the dielectric constant curve of fig. 5 which remains even after the elimination of the sheath effect, we can examine whether this is due to the plasma electronic resonance of Tonks and Langmuir. The frequency of the plasma electronic oscillation is given by $\nu = 8980.\sqrt{N}$, so that $N.\lambda^2 = 1{\cdot}12 \times 10^{13}$. The value of the electron content N can be approximately calculated (neglecting collision frequency) from the lowest value of the dielectric constant in the first part of the curve in fig. 5, using the Eccles-Larmor formula. On calculation $N = 4{\cdot}4 \times 10^6$ per c.c. and we know $\lambda = 390$ cm. The product $(N.\lambda^2)$ then comes out to be equal to $6{\cdot}7 \times 10^{11}$. We can therefore say that the observed irregularity is not due to the plasma electronic oscillations. It cannot also be attributed to the Gutton effect, for according to Gutton's formula the dielectric constant of the ionized gas should be greater than unity beyond the point of quasi-electric resonance.

The irregularity can perhaps be explained as due to the effect of non-uniform conductivity of the ionized gas in the condenser system of the arrangement. For small ionizations this effect of non-uniform conductivity is not perceptible. With increasing ionizations this effect asserts itself, while for still higher ionizations it appears that the Eccles-Larmor effect is predominant.

5. *Variation of Dielectric Constant of Ionized Air with the Wave-length of the Oscillation.*

The dielectric constants of ionized air have been measured for a certain range of wave-lengths (307 cm. to 541 cm.). The current through the tube has been kept sufficiently low so that the sheath effect may be neglected. The measurements have yielded results similar to those of the experiments of Khastgir and A. Imam where the

method was different. The reduction in the value of the dielectric constant below unity has been found, as before, to increase nearly proportionately with the square of the wave-length up to a certain wave-length where there is an unmistakable turning point in the dielectric constant curve. The dielectric constant then begins to increase and approaches the value of unity. The experimental results are illustrated in fig. 6.

The turning point of the dielectric constant curve appears at a wave-length of 400 cm.

This anomalous increase of the dielectric constant, which has also been observed by Mitra and Banerjee *

Fig. 6.

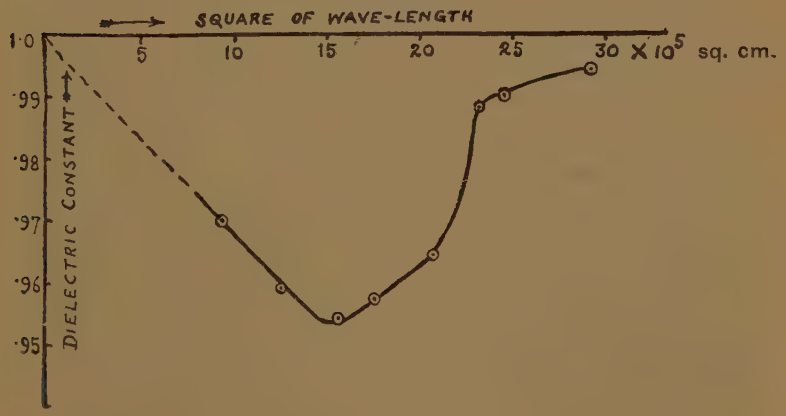

following a different method of measurement, has been explained as due to the conductivity acquired by the ionized gas. Khastgir and A. Imam † have suggested the possibility of a resonance effect. The effect, however, seems definitely unconnected with the plasma electronic oscillation. The value of $(N.\lambda^2)$ at the turning-point of the curve in these experiments is $5{\cdot}3\times10^{11}$ which is very different from what is expected from Tonks and Langmuir's calculation. According to Tonks and Langmuir the resonance effect should appear at a much higher wave-length, since the value of electron-current in our discharge-tubes is only of the order of 10^6 per c.c.

* Mitra and Banerjee, 'Nature,' cxxxvi. p. 512 (Sept. 28, 1935).

† Ali Imam and Khastgir, Phil. Mag. (May 1937) and Ind. Journ. Phys. xi. pt. 1 (Feb. 1937).

Further experiments are necessary to arrive at a definite conclusion.

6. *Summary.*

Measurements of the dielectric constant of ionized air and nitrogen have been made for ultra-high frequencies using condenser plates placed *outside* the discharge-tube. It has been found that the value of the dielectric constant which is less than unity decreases with the increase of the tube-current only up to a certain value of the latter. Beyond this value the dielectric constant gradually attains the value of unity and subsequently becomes greater than one for larger tube-currents. The results of our experiments have been explained as due to the formation of ionic sheaths round the inside surface of the discharge-tube. By practically eliminating the ionic sheath formation by using an earthed cylindrical copper anode (with slits) surrounding the inside of an air-discharge-tube and an aluminium cathode in the shape of a straight rod along the axis of the copper cylinder, it has been found that the dielectric constant of ionized air is always less than one. An irregularity in the curve showing the values of the dielectric constant of ionized air for different ionization values still remains after the elimination of the sheath effect. It has been shown that this is not connected with Tonks and Langmuir's plasma electronic oscillations. The irregularity can perhaps be explained as due to the effect of conductivity acquired by the ionized medium.

When wave-length has been changed keeping the tube-current constant, the dielectric constant of the ionized air has been found to decrease nearly proportionately with the square of the wave-length up to a certain wave-length, thus showing agreement with the Eccles-Larmor formula up to that point. Beyond this wave-length the dielectric constant has been found to increase. These results are similar to those of the earlier experiments of Khastgir and A. Imam using a different method. It has been shown that the turning-point in the dielectric constant curve is not due to the effect of plasma electronic resonance.

Supplementary Note.—Since writing the paper, Mitra and Roy ('Nature,' cxl. Oct. 2, 1937, p. 586,) have pointed out that the so-called anomalous dielectric constant of an

ionized gas in a discharge-tube is what is expected from the complete dispersion formula. The simpler formula $\epsilon=1-\frac{4\pi Ne^2}{m(p^2+\nu^2)}$ is accurate only when $\frac{c^2k^2}{p^2}$ can be neglected.

The collision frequency ν in the discharge-tubes employed in our experiments is of the order of 10^8. A little calculation will show that with such a value of ν and with a wave-length of about 3·8 metres used in our measurements of the dielectric constant for different tube-currents, the dielectric constant according to the complete dispersion formula decreases steadily with the increase of the electron density N up to $N=10^8$ per c.c. or more. It is to be noted that the maximum electron density in all our discharge-tubes has been within 10^7 per c.c. Calculation will also show that with $N=10^7$ per c.c. and $\nu=10^8$, when wave-length is varied, the value of the dielectric constant dimininishes steadily with the square of wave-length up to $\lambda=12$ m. when the dielectric constant begins to rise in value. In our measurements of dielectric constant for different wave-lengths of oscillations, the turning point in the dielectric constant curve appears at $\lambda=4$ m. In this experiment the tube-current has been kept sufficiently low.

The complete dispersion formula does not therefore explain these experimental results. An analysis of the complete dispersion formula and a fuller discussion has been published elsewhere *.

Physics Department,
Dacca University.

LXXXI. *Raman Effect in Solid Cyclohexane.*

By S. M. Mitra, *University of Dacca, Bengal* †.

[Plate X.]

Introduction.

THE Raman effect in liquid cyclohexane has been investigated by a large number of investigators—namely, Krishnamurty [1], Kohlrausch and Stockmair [2],

* 'Science and Culture,' iii. no. 6, p. 335 (Dec. 1937).

† Communicated by the Author.

Ananthakrishnan [3] and others, but the case of solid Cyclohexane has not yet been investigated by anyone. Recently in connexion with our investigation on the fluorescence of cyclohexane [4] we had an occasion to study its Raman spectra at low temperatures. The following gives a report of the same.

Experimental.

The accompanying figure 1 gives the experimental arrangements we adopted in our investigation. "C" is the tube containing pure cyclohexane. It was surrounded by a bath containing freezing mixture, and the

Fig. 1.

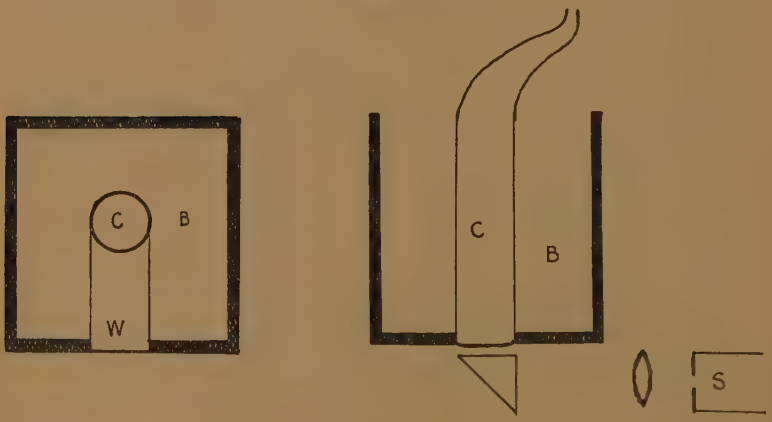

latter had a window "W" through which light from a vertical mercury arc was focussed on to "C." The scattered radiations were totally reflected by a right-angled prism and were focused on the slit of the spectrograph "S." The wave-lengths of the Raman lines were calculated with the help of the Hartmann's simplified formula, taking iron lines as standard. For making a comparative study another spectrogram at the ordinary temperature was also taken.

Results and Discussions.

The results of our measurements are given in the following Table I. The spectrogram due to solid cyclohexane (Pl. X. fig. 2) was compared with that due to liquid at the laboratory temperature, Table II.

Just as in the case of benzene [5], [6], two new lines at $\Delta\nu$ 60 and 105 cm.$^{-1}$ were observed in the neighbourhood of the Rayleigh lines. These two lines are characteristic of the solid state, and are probably due either to the vibrations in the polymerized groups, as suggested by

TABLE I.

Raman Spectrum in Solid Cyclohexane *.

No.	ν Raman.	$\Delta\nu$.	Assignment.
1	20001	2937	A
2	20018	2920	A
3	20049	2889	A
4	20088	2850	A
5	20276	2662	A
6	21490	1448	A
7	21498	1440	A
8	21579	2937	B
9	21594	1344	A
		2920	B
10	21666	2850	B
11	21670	1268	A
12	21678	1260	A
13	21768	2937	BI
14	21783	1155	A
		2922	BI
15	21855	2850	BI
16	21913	1025	A
17	22138	800	A
18	22513	425	A
19	22556	382	A
20	22833	105	A
21	22878	60	A
22	23257	1448	BI
23	23265	1440	BI
24	23436	1269	BI
25	23445	1260	BI
26	23905	800	BI
27	24451	2937	C
28	24468	2920	C
29	24600	105	BI
30	24694	61	BI

A = λ 4358·3 Å. = 22938 cm.$^{-1}$.
B = λ 4077·8 Å. = 24516 cm.$^{-1}$.
BI = λ 4046·5 Å. = 24705 cm.$^{-1}$.
C = λ 4650 Å. = 27388 cm.$^{-1}$.

Sarker, or to the lattice oscillations, as pointed out by Gross and others. As the whole theory of lattice oscillations and of vibrations in the polymerized groups are yet in their infancy, it is rather difficult to point which is

* Some lines were too faint to be measured.

responsible for the excitation of these two lines, at this stage of our investigation.

Another striking feature in our low-temperature measurements is that the line at 1266 cm.$^{-1}$ observed at the room-temperature becomes a little broad and when microphotometered shows two maxima at $\Delta\nu=1260$ and 1268 cm.$^{-1}$. The line at $\Delta\nu=2922$ cm.$^{-1}$ becomes also broader. This is perhaps due to the effect of the crystalline field on the antisymmetrical vibration of

TABLE II.

Cyclohexane $\Delta\nu$ in cm.$^{-1}$.

Liquid.	Solid.
	60
	105
384	382
425	425
800	800
1028	1025
1156	1155
1266	1260
	1268
1348	1348
1437	1440
	1448
2353	
2467	
2630	
2662	2662
2698	
2853	2850
2889	2889
2922	2921
2937	2937

the group CH_2. The line at $\Delta\nu$ 1437 cm.$^{-1}$ in the liquid is shifted to $\Delta\nu=1440$ and is accompaniou at $\Delta\nu=1448$.

It might be mentioned here in passing that Kohlrausch and Stockmair, from their studies on the Raman effect in cyclohexane and its mono derivatives, concluded that the symmetry of the molecule of cyclohexane to be S_{6u}. For this symmetry there must be four two-fold degenerate vibrations having frequencies less than 1500 cm.$^{-1}$; these vibrations according to them are 425, 1028, 1266, and 1437 cm.$^{-1}$. The splitting of the

lines into two at the low temperature gives an additional support to their contention.

Summary and Conclusion.

The paper describes the results obtained in the authors' investigation on the Raman effect in solid cyclohexane. Each of the lines at 1266, 1437 cm.$^{-1}$ in the case of liquid seems to split up into two in the case of the solid. The line at $\Delta\nu=2922$ cm.$^{-1}$ broadens, and the other lines found in the case of the liquid appear more or less in the same positions. Two new lines of $\Delta\nu=60$ and 105 cm.$^{-1}$ also appear in the solid state.

In conclusion the author thanks Prof. S. N. Bose for his kind interest in the work.

Note added in proof.—The Raman effect in cyclohexane at low temperature seems to have been investigated recently by Sarker and Gupta*. Their results are fairly in agreement with those reported above, excepting that they have failed to observe the low frequency shifts.

References.

(1) P. Krishnamurty, Ind. J. Phys. vi. p. 543 (1931).
(2) K. Kohlrausch ane Stockmair, *Zeit. f. Phys. Chem.* B 31, p. 382 (1936).
(3) R. Ananthakrishnan, Proc. Ind. Acad. Sci. 2 A, p. 452 (1936).
(4) S. M. Mitra, Phil. Mag. xxiii. p. 558 (1937).
(5) E. Gross and Vuks, 'Nature,' cxxxv. pp. 100, 431, 998 (1935).
(6) S. Sarker, Ind. J. Phys. x. p. 189 (1936).

LXXXII. *Collective Electron Energy and Specific Heat.*

By Edmund C. Stoner, F.R.S., *Reader in Physics at the University of Leeds* †.

1. *Introduction.*

At low temperatures the specific heat of solids associated with the lattice vibrations is proportional to $(T/\theta_D)^3$, where θ_D is the Debye characteristic temperature. Near absolute zero this becomes very small, and for metals the greater part of the specific heat is then due to

* Sarker and Gupta, Ind. J. Phy. xi. p. 55 (1937).
† Communicated by the Author.

electronic specific heat contributed by electrons in partially filled electron energy bands. The electronic specific heat gives rise to a term closely proportional (in this temperature range) to the absolute temperature. From its magnitude estimates may be made of the energy density of states in the band in the region corresponding to electrons of highest energy, that is at the top of the Fermi distribution, at absolute zero. It is usually difficult to make precise estimates from the experimental data of the electronic contribution to the specific heat at high temperatures, but the evidence indicates clearly that the electronic term is often comparable with the dilatation term (of the order 0·5 calories per degree per gram atom at 1000° K.), and that it is sometimes considerably greater. Unless proper allowance can be made for the electronic specific heat, therefore, the interpretation of the vibrational specific heat (say by the assignment of a particular θ_D) may be seriously in error. In this connexion a reasonably precise numerical treatment of the temperature variation of the electronic specific heat over a wide temperature range is clearly desirable. Such a treatment has a more direct value in opening up the possibility of deriving further information about the character of the electronic energy bands than can be obtained from the results at very low temperatures alone.

Whereas the low temperature specific heat can be expressed in terms of the density of states at the top of the Fermi distribution in the band, the variation over the whole temperature range can be treated only on the basis of a completely specified band form. The form which it is most appropriate to consider in detail, as providing a standard set of results, is that in which the energy density of states is proportional to the square root of the energy, measured from the bottom of the band. Such a distribution of states is appropriate for free electrons, and it often holds, to a fair approximation, over the relevant energy range, for electrons in metals. The results obtained, using Fermi-Dirac statistics, then pass over, in the high temperature limit, to those given by classical statistics. The distribution is most conveniently specified by a parameter ϵ_0, the Fermi zero energy, giving the width of the occupied portion of the band (or the maximum electron energy, measured from

the bottom of the band) at absolute zero. For N electrons in the band the reduced energy per electron, $E/N\epsilon_0$, is then a unique function of the reduced temperature, kT/ϵ_0.

In a previous paper (Stoner, 1936, 1) series expansions in powers of ϵ_0/kT and kT/ϵ_0 were obtained (from the basic expressions for the energy, involving Fermi-Dirac functions) appropriate for the representation of the energy and specific heat in the ranges $kT/\epsilon_0 > 1$ and $kT/\epsilon_0 \ll 1$. The low temperature series, an asymptotic series, is usefully applicable only up to about $kT/\epsilon_0 = 0{\cdot}3$. Computations of the energy and specific heat in the ranges for which the series are applicable were supplemented by estimates for the intermediate range, obtained by rough interpolation, based on the fact that the high temperature series can be used to determine upper and lower limits in the range $kT/\epsilon_0 < 1$ in which the series is not uniformly convergent. Although the error in these interpolated results for the energy, as given in the paper to about 1 part in 1000, is shown by the present work to be well within 1 per cent., the position was unsatisfactory in that no precise estimate of the uncertainty could be made. Improvement in certainty and precision is possible only through the evaluation of the basic Fermi-Dirac functions involved in the general formulæ. An extensive table of these functions is now available (McDougall and Stoner, 1938), and the present treatment of electronic energy and specific heat is based in the main, on the computational side, on the use of these tables.

After an account of the method of computation, tables of values of the energy and specific heat as functions of the reduced temperature are given which should be sufficiently complete and precise for most purposes. The series method is then considered in the light of these results, as series representations, if reasonably accurate, are often of considerable value. Since band widths are often given in electron volts, a corresponding form of presentation of the results is embodied in a shorter table which enables their numerical significance to be more readily appreciated. A number of conversion factors are also evaluated. Finally a brief discussion is given of the relevance of the present theoretical results in connexion with experimental material.

2. *Method of Computation and Results.*

(i) *Computation of* $E/N\epsilon_0$.

It is shown in the previous paper that the energy, E, of N electrons in an energy band of standard form (as described above) may be expressed by

$$\frac{E}{N\epsilon_0} = \frac{kT}{\epsilon_0} \cdot \frac{F_{3/2}(\eta)}{F_{1/2}(\eta)}, \quad . \quad . \quad . \quad . \quad . \quad (2.1)$$

where

$$F_k(\eta) = \int_0^\infty \frac{x^k\, dx}{e^{x-\eta}+1}, \quad . \quad . \quad . \quad . \quad . \quad (2.2)$$

and ϵ_0 is the width of the occupied portion of the band at absolute zero. (The treatment applies also to bands in which the density of states is proportional to the square root of the energy measured from the top of the band, N then representing the number of " holes " in the band, and ϵ_0 the width of the unoccupied portion.) The equation relating η and kT/ϵ_0 is

$$F_{1,2}(\eta) = \frac{2}{3}\left(\frac{\epsilon_0}{kT}\right)^{3/2}. \quad . \quad . \quad . \quad . \quad . \quad (2.3)$$

The paper on the computation of Fermi-Dirac functions (McDougall and Stoner, 1938) includes a table giving $\frac{2}{3}F_{3/2}(\eta)$ and $F_{1,2}(\eta)$ at intervals of 0·1 in η to six places of decimals for $-4{\cdot}0 \leqslant \eta \leqslant +4{\cdot}0$, and to five places of decimals for $+4{\cdot}0 \leqslant \eta \leqslant +20{\cdot}0$. The method of computation of $E/N\epsilon_0$ for a given value of kT/ϵ_0 from this table is most simply illustrated by an example :—

Evaluation of $E/N\epsilon_0$ *for* $kT/\epsilon_0 = 0{\cdot}3$.

From (2.3),

$$F_{1/2}(\eta) = \frac{2}{3}\left(\frac{\epsilon_0}{kT}\right)^{3/2} = 4{\cdot}05720.$$

By inverse interpolation in the η, $F_{1,2}(\eta)$ table,

$$\eta = 3{\cdot}04861.$$

By direct interpolation in the $\frac{2}{3}F_{3/2}(\eta)$ table,

$$\frac{2}{3}F_{3/2}(\eta) = 7{\cdot}09773.$$

Hence $F_{3/2}(\eta)/F_{1/2}(\eta) = 2{\cdot}62412,$

and $$\frac{E}{N\epsilon_0} = \frac{kT}{\epsilon_0} \cdot \frac{F_{3/2}(\eta)}{F_{1/2}(\eta)} = 0{\cdot}78724.$$

The inverse interpolations have been carried out by the two machine method of Comrie (1936). The use of this method in connexion with the η, $F_{1/2}(\eta)$ table is considered more fully in another paper (Stoner, 1938). The method is based on the use of the Bessel formula for interpolation, and the Besselian coefficients required, both for direct and inverse interpolation, have been obtained from Comrie's tables (1936).

The tables of Fermi-Dirac functions cover an η range corresponding to $11{\cdot}95519 \geqslant kT/\epsilon_0 \geqslant 0{\cdot}04990$. For $kT/\epsilon_0 \leqslant 0{\cdot}05$, values of $E/N\epsilon_0$ may be obtained by means of the asymptotic series given in the next section. The convergent series for $kT/\epsilon_0 > 1$, also given below, may be applied for the higher temperature range, the series method being in practice more convenient than that described above (for comparable accuracy) for values of kT/ϵ_0 greater than about 1·3.

Accuracy.—The Fermi-Dirac functions $F_{1/2}(\eta)$ and $F_{3/2}(\eta)$ are believed to be accurate to within 0·5 in units of the last decimal place tabulated. It is then readily shown—it is unnecessary to give details—that, using the tables, the attainable accuracy in $E/N\epsilon_0$ is within 1 unit in the fifth decimal place over the range considered (up to $kT/\epsilon_0 = 2{\cdot}0$). When the tables are supplemented by the use of the convergent series for the higher temperature range the uncertainty should not exceed 2 units in the sixth place. That the errors are within this estimated upper limit is indicated by a check by the method of differences of the numbers on which are based the values, rounded to five decimal places, given in Table I.

(ii) *Computation of* C_v/Nk.

From the tabulated values of the energy at equal intervals of temperature those of the specific heat (at constant volume) may be obtained by differentiation :—

$$\frac{C_v}{Nk} = \frac{1}{Nk} \cdot \frac{dE}{dT} = \frac{d(E/N\epsilon_0)}{d(kT/\epsilon_0)}. \quad . \quad . \quad . \quad (2.4)$$

The formula applied for obtaining derivatives f' of a function f tabulated at intervals w in the argument is

$$wf'_0=\delta^1_0-\frac{1}{6}\delta^3_0+\frac{1}{30}\delta^5_0\ldots, \quad . \quad . \quad . \quad (2.5)$$

where δ^1_0, δ^3_0, δ^5_0 ... are the first, third, fifth ... mean differences:

$$\delta^1_0=\tfrac{1}{2}(\delta^1_{-\frac{1}{2}}+\delta^1_{\frac{1}{2}}),$$

and correspondingly for δ^3_0, δ^5_0 ...

When the formula (2.5) is applied in calculating the derivatives of a tabulated function the ideally attainable relative accuracy in the derivatives is limited by the relative accuracy of the first differences of the function; alternatively expressed, the absolute accuracy in wf' cannot exceed the absolute accuracy of the tabulated functions. This ideally attainable accuracy is approached in practice if the contributions from differences of higher order than those considered may be treated as negligible. If the tabular interval is increased, so as to increase the relative accuracy of the first differences, the contributions from the higher order differences increase rapidly, and a limit to the attainable accuracy is ultimately set by the range of the table. These considerations are particularly relevant in connexion with the determination of the derivatives of the function $\mathrm{E}/\mathrm{N}\epsilon_0$ for the initial part of the $k\mathrm{T}/\epsilon_0$ range. Here the higher order central differences are not available, and the forward difference series for computing derivatives converges very slowly. With a tabular interval of 0·05 in $k\mathrm{T}/\epsilon_0$, the higher order differences remain large over a considerable range of $k\mathrm{T}/\epsilon_0$, so limiting the practically attainable accuracy in the derivatives. If further computations are made of $\mathrm{E}/\mathrm{N}\epsilon_0$ so as to reduce the tabular interval, the reduction in the higher order differences is accompanied by a reduction in the first order differences, so limiting the ideally attainable accuracy, but on the balance a considerable reduction of interval would be practically advantageous. The effect of such a reduction can be obtained, however, without additional computations of $\mathrm{E}/\mathrm{N}\epsilon_0$, by a modified method of computing the derivatives, which makes use of the already tabulated values of the derivatives (with respect to η) of $\mathrm{F}_{1\cdot2}(\eta)$. A derivation of the formula required follows.

Using the abbreviations

$$x = kT/\epsilon_0,$$

$$y = E/N\epsilon_0,$$

equation (2.4) may be written

$$\frac{C_v'}{Nk} = \frac{dy}{dx},$$

and, from (2.1),

$$y = xF_{3/2}(\eta)/F_{1/2}(\eta).$$

Thus,

$$\frac{dy}{dx} = \frac{F_{3/2}(\eta)}{F_{1/2}(\eta)} + \frac{x}{\{F_{1/2}(\eta)\}^2} \times \left[F_{1/2}(\eta) \frac{dF_{3/2}(\eta)}{d\eta} \cdot \frac{d\eta}{dF_{1/2}(\eta)} \cdot \frac{dF_{1/2}(\eta)}{dx} - F_{3/2}(\eta) \frac{dF_{1/2}(\eta)}{dx} \right].$$

Using (2.3) in the form

$$F_{1/2}(\eta) = \frac{2}{3} x^{-3/2},$$

and the recurrence relation,

$$\frac{dF_{3/2}(\eta)}{d\eta} = \frac{3}{2} F_{1/2}(\eta),$$

there results

$$\frac{C_v}{Nk} = \frac{dy}{dx} = \frac{5}{2} \cdot \frac{F_{3/2}(\eta)}{F_{1/2}(\eta)} - \frac{9}{4} \cdot \frac{F_{1/2}(\eta)}{F_{1/2}'(\eta)}. \quad . \quad (2.6)$$

The use of this equation in the computation of C_v/Nk may again be illustrated by an example.

Evaluation of C_v/Nk *for* $kT/\epsilon_0 = 0{\cdot}30$.

As in the example given above,

$$\eta = 3{\cdot}04861,$$

$$F_{1/2}(\eta) = 4{\cdot}05720,$$

$$F_{3/2}(\eta) = 7{\cdot}09773.$$

By interpolation in the η, $F_{1/2}'(\eta)$ table,

$$F_{1/2}'(\eta) = 1{\cdot}65803.$$

These values give

$$F_{3/2}(\eta)/F_{1,2}(\eta)=2\cdot62412, \quad F_{1/2}(\eta)/F'_{1/2}(\eta)=2\cdot44700,$$

and, using (2.6),

$$C_v/Nk=1\cdot05455.$$

It should be pointed out that the computation of the specific heat by the use of (2.6) does not enable a higher accuracy to be obtained than would be possible from a table of energy values, provided that these were obtained as accurately as possible at suitably small intervals of kT/ϵ_0. The method is, however, clearly advantageous from the point of view of convenience, as it makes unnecessary the numerous calculations of the energy which would otherwise be required. In the "awkward" ranges the intervals in the energy table cannot be reduced by interpolation without decrease of accuracy, for the accuracy of interpolation is limited by factors similar to those which limit the accuracy of derivatives.

The method of computation of the specific heat described above has been supplemented by the use of series methods described in the next section for the temperature ranges $kT/\epsilon_0<0\cdot05$ and $kT/\epsilon_0\geqslant1\cdot3$ as in the energy calculations. For the range $0\cdot05<kT/\epsilon_0<0\cdot1$ more accurate values of $F'_{1/2}(\eta)$ than those given in the tables may be obtained by means of an asymptotic series. The coefficients in this series are readily derived from those given for the series for $F_{1/2}(\eta)$ in the paper on the computation of the functions. The values of C_v/Nk over the kT/ϵ_0 range 0·05 to 0·09 have been obtained by using $F'_{1/2}(\eta)$ values calculated by this method, six terms of the series having been summed.

Accuracy.—In calculating specific heats by (2.6) the accuracy is limited by that of $F_{1/2}(\eta)$, the least accurately known of the functions entering into the formula. Usually the relative error in C_v/Nk will be considerably greater than the relative error in $F'_{1/2}(\eta)$, as will be clear from consideration of the formula and the example. The values of $wF'_{1\cdot2}(\eta)$ (where $w=0\cdot1$) are believed to be correct to within 1 unit of the last decimal place tabulated. An error of 1 unit in the fifth place for $kT/\epsilon_0=0\cdot10$ ($\eta=9\cdot91641$, $wF'_{1/2}(\eta)=0\cdot31351$) corresponds to an error of 5 in the fourth place in the value of C_v/Nk. This is an extreme example, and with the further figures available,

which were used in these calculations, the uncertainty is considerably reduced. Over the kT/ϵ_0 range from 0·10 to 0·20, however, there is an uncertainty of about 1 unit in the fourth place in the values given in Table I for C_v/Nk. Outside this range the uncertainty is considerably less, probably within 2 units in the fifth place throughout,

TABLE I*a*—Collective Electron Energy and Specific Heat as Functions of the Reduced Temperature.

kT/ϵ_0.	$E/N\epsilon_0$.	C_v/Nk.	kT/ϵ_0.	$E/N\epsilon_0$.	C_v/Nk.
0·00	0·60000	0·0000	1·00	1·69674	1·4056
0·05	0·60615	0·2449	1·05	1·76718	1·4119
0·10	0·62428	0·4772	1·10	1·83792	1·4176
0·15	0·65336	0·6793	1·15	1·90893	1·4227
0·20	0·69152	0·8400	1·20	1·98018	1·4273
0·25	0·73671	0·9622	1·25	2·05165	1·4314
0·30	0·78724	1·0546	1·30	2·12332	1·4352
0·35	0·84181	1·1251	1·35	2·19517	1·4386
0·40	0·89949	1·1798	1·40	2·26718	1·4418
0·45	0·95960	1·2230	1·45	2·33934	1·4447
0·50	1·02164	1·2576	1·50	2·41164	1·4473
0·55	1·08525	1·2858	1·55	2·48407	1·4498
0·60	1·15014	1·3090	1·60	2·55662	1·4521
0·65	1·21609	1·3285	1·65	2·62927	1·4542
0·70	1·28294	1·3449	1·70	2·70203	1·4561
0·75	1·35054	1·3589	1·75	2·77488	1·4579
0·80	1·41879	1·3709	1·80	2·84782	1·4596
0·85	1·48760	1·3814	1·85	2·92084	1·4612
0·90	1·55690	1·3905	1·90	2·99394	1·4627
0·95	1·62663	1·3985	1·95	3·06711	1·4641
1·00	1·69674	1·4056	2·00	3·14035	1·4654

N, number of electrons in band.
E, energy of N electrons.
ϵ_0, maximum electron energy (band width) at absolute zero.
C_v, electronic specific heat at constant volume for N electrons.
k, Boltzmann constant.

so that the four place values given are subject only to rounding errors.

In Table I*a* values of $E/N\epsilon_0$, to five places of decimals, and of C_v/Nk to four, are tabulated at intervals of 0·05 in kT/ϵ_0 over the range $0{\cdot}00 \leqslant kT/\epsilon_0 \leqslant 2{\cdot}00$. Apart from rounding errors the tabulated values are believed to be correct as given, except for possible errors of the order of 1 unit in the fourth place in C_v/Nk over the range

from 0·05 to 0·20. For values of kT/ϵ_0 greater than 0·4, the maximum contribution in interpolation from differences of higher order than the second, does not exceed 0·5 units in the fifth and fourth place for $E/N\epsilon_0$ and C_v/Nk respectively, so that interpolation is readily carried out. It becomes progressively more troublesome as kT/ϵ_0 decreases, and for this reason a supplementary table, I*b*, is given, covering the range $0{\cdot}00 \leqslant kT/\epsilon_0 \leqslant 0{\cdot}20$ at intervals of 0·01. Up to $kT/\epsilon_0 = 0{\cdot}04$, the values of $E/N\epsilon_0$ and C_v/Nk are given to a further place, as it seems desirable to retain four significant figures in C_v/Nk and in this range

Table I*b*—Collective Electron Energy and Specific Heat at Low Temperatures.

kT/ϵ_0.	$E/N\epsilon_0$.	C_v/Nk.	kT/ϵ_0.	$E/N\epsilon_0$.	C_v/Nk.
0·00	0·600000	0·00000	0·10	0·62428	0·4772
0·01	0·600247	0·04933	0·11	0·62928	0·5206
0·02	0·600986	0·09858	0·12	0·63469	0·5626
0·03	0·602218	0·14765	0·13	0·64052	0·6031
0·04	0·603938	0·19646	0·14	0·64675	0·6420
0·05	0·60615	0·2449	0·15	0·65336	0·6793
0·06	0·60883	0·2928	0·16	0·66033	0·7148
0·07	0·61200	0·3402	0·17	0·66765	0·7486
0·08	0·61564	0·3868	0·18	0·67530	0·7807
0·09	0·61973	0·4325	0·19	0·68326	0·8112
0·10	0·62428	0·4772	0·20	0·69152	0·8400

For symbols, see Table I*a*.

the uncertainty does not exceed 1 unit in the last place tabulated.

The variation of $E/N\epsilon_0$ and C_v/Nk with kT/ϵ_0 is shown graphically in fig. 1; the tangents to the curves at $kT/\epsilon_0 = 0$, and the asymptotes (approached as $kT/\epsilon_0 \to \infty$) are shown in order to bring out more clearly the character of the curves.

3. *Comparison with Series Method.*

The method of obtaining representations of $E/N\epsilon_0$ and C_v/Nk as power series in kT/ϵ_0 has been described in the earlier paper (Stoner, 1936, 1), to which reference may be made. The series are given below with more accurate numerical values of the coefficients. The series are based

on those for $F_k(\eta)$ appropriate for $\eta \gg 1$ and $\eta < 0$. By inverse interpolation in the η, $F_{1/2}(\eta)$ table, it is found, from (2.3), that the value $\eta = 0$ corresponds to $kT/\epsilon_0 = 0{\cdot}988734$. Sufficiently closely, therefore, the low and high temperature series may be taken as appropriate for $kT/\epsilon_0 \ll 1$ and $kT/\epsilon_0 > 1$.

Fig. 1.

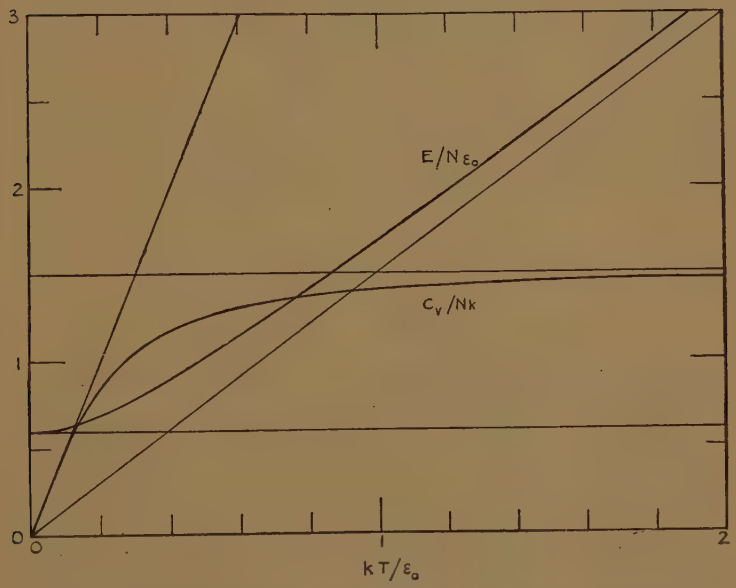

Variation with temperature of electronic energy and specific heat.

N, number of electrons in band.
E, energy of N electrons.
ϵ_0, maximum electron energy (band width) at absolute zero.
C_v, electronic specific heat at constant volume for N electrons.
k, Boltzmann constant.
The straight lines are the tangents at $kT/\epsilon_0 = 0$ and the asymptotes to the curves.

(i) *Low Temperatures.* $kT/\epsilon_0 \ll 1$.

The low temperature series expression for $E/N\epsilon_0$, based on the asymptotic series for $F_{3/2}(\eta)$ and $F_{1/2}(\eta)$ for $\eta \gg 1$, may be put in the form :

$$\frac{E}{N\epsilon_0} = \frac{3}{5}\left[1 + \sum_{r=1}^{n} a_{2r}\left(\frac{kT}{\epsilon_0}\right)^{2r}\right], \quad . \quad . \quad . \quad (3.1)$$

where
$$a_2 = +\frac{5\pi^2}{12} = +4{\cdot}112\ 335,$$
$$a_4 = -\frac{\pi^4}{16} = -6{\cdot}088\ 068,$$
$$a_6 = -\frac{1235\pi^6}{36288} = -32{\cdot}719\ 236.$$

The low temperature series for C_v/Nk may be obtained by differentiating the series (3.1) term by term.

$$\frac{C_v}{Nk} = \sum_{r=1}^{n} a'_{2r-1}\left(\frac{kT}{\epsilon_0}\right)^{2r-1}, \quad . \quad . \quad . \quad . \quad (3.2)$$

where
$$a'_1 = +\frac{\pi^2}{2} = +4{\cdot}934\ 802,$$
$$a'_3 = -\frac{3\pi^4}{20} = -14{\cdot}611\ 364,$$
$$a'_5 = -\frac{247\pi^6}{2016} = -117{\cdot}789\ 251.$$

A check on the coefficients in (3.2) has been obtained by developing the series from (2.6).

The low temperature series (3.1) and (3.2) are subject to limitations of the same kind as the asymptotic series from which they have been derived. A full discussion has previously been given of the asymptotic series for $F_{1/2}(\eta)$ (McDougall and Stoner, 1938) with particular reference to the limits of error resulting from the summation of a particular number of terms, and the number of terms to be summed to obtain a value of minimum uncertainty. Since this has made clear the essential points that arise, a correspondingly detailed discussion of the derived series is hardly necessary. It will be sufficient to give the actual errors made by summing the terms whose coefficients have been evaluated. These errors are given in Table II*a*.

The number of terms to be summed to obtain the best approximation to the functions decreases as kT/ϵ_0 increases. Since the further terms are negative, a slight improvement in accuracy could be made up to $kT/\epsilon_0 = 0{\cdot}15$ by including terms beyond those whose coefficients have been evaluated. The inaccuracy here, however, is relatively small, and no improvement would be made in

this way for the higher values of kT/ϵ_0. The smallest error at $kT/\epsilon_0=0{\cdot}20$ is obtained by using the L 4 and L′ 3 approximations, but at $kT/\epsilon_0=0{\cdot}30$ the error is decreased by dropping the last term. The calculable limit of error, using the asymptotic series, is considerably greater than the actual error as shown in Table II*a*; so that the errors there given represent a minimum uncertainty in the values of the functions when these are evaluated by the asymptotic series method alone. By a comparison with the values calculated by the present method, however,

TABLE II*a*—Errors in the values of $E/N\epsilon_0$, in units of the fifth decimal place, obtained by summing 4 and 3 terms of the series (3.1) (L 4 and L 3), and of C_v/Nk, in units of the fourth decimal place, by summing 3 and 2 terms of the series (3.2) (L′ 3 and L′ 2).

	$E/N\epsilon_0$.		C_v/Nk.	
kT/ϵ_0.	L 4.	L 3.	L′ 3.	L′ 2.
0·00	0·0	0·0	0·00	0·00
0·05	0·0	0·0	+ 0·02	+ 0·39
0·10	+ 0·6	+ 2·6	+ 4·8	+ 16·6
0·15	+ 8	+ 31	+ 26	+116
0·20	− 10	+115	− 76	+301
0·25	−155	+323	− 718	+432
0·30	−906	+524	−2549	+314

it may be said that the series (3.1) with four terms gives $E/N\epsilon_0$ correctly to within 0·001, 0·014, and 1·16 per cent. up to $kT/\epsilon_0=0{\cdot}1$, 0·2, and 0·3 respectively; the corresponding values for C_v/Nk using three terms are 0·1, 1·0, and 25 per cent., this last value becoming 3 per cent. if the two term formula is used. (In the previous paper the numerical value of the coefficient a_6 in (3.1) was given as 30·7 owing to an algebraical error in the derivation of the series; this, however, was without significant effect on the numerical values there given for E and C_v.)

(ii) *High Temperatures.* $kT/\epsilon_0>1$.

The high temperature series expression for $E/N\epsilon_0$, based on the convergent series for $F_{3/2}(\eta)$ and $F_{1/2}(\eta)$ for $\eta<0$, may be put in the form:

$$\frac{E}{N\epsilon_0}=\frac{kT}{\epsilon_0}\left[\frac{3}{2}+\sum_{r=1}^{\infty}b_r\left(\frac{\epsilon_0}{kT}\right)^{3r/2}\right], \quad . \quad . \quad (3.3)$$

where

$$b_1 = \frac{3}{2} \cdot \left(\frac{4}{3\sqrt{\pi}}\right) \times \frac{\sqrt{2}}{4} = +0{\cdot}199\ 471\ 14,$$

$$b_2 = \frac{3}{2} \cdot \left(\frac{4}{3\sqrt{\pi}}\right)^2 \times \left(\frac{1}{8} - \frac{2\sqrt{3}}{27}\right) = -0{\cdot}002\ 801\ 18,$$

$$b_3 = \frac{3}{2} \cdot \left(\frac{4}{3\sqrt{\pi}}\right)^3 \times \left(\frac{3}{32} + \frac{5\sqrt{2}}{64} - \frac{\sqrt{6}}{12}\right) = +0{\cdot}000\ 071\ 06.$$

The corresponding series expression for C_v/Nk is obtained by differentiating :

$$\frac{C_v}{Nk} = \frac{3}{2} + \sum_{r=1}^{\infty} b_r' \left(\frac{\epsilon_0}{kT}\right)^{3r/2}, \quad . \quad . \quad . \quad (3.4)$$

where

$$b_1' = -\frac{1}{2} b_1 = -0{\cdot}099\ 735\ 57,$$

$$b_2' = -\frac{4}{2} b_2 = +0{\cdot}005\ 602\ 36,$$

$$b_3' = -\frac{7}{2} b_3 = -0{\cdot}000\ 248\ 72.$$

A check has again been obtained by developing the series (3.4) from (2.6).

The series (3.3) and (3.4) are uniformly convergent for $kT/\epsilon_0 > 1$, and at $kT/\epsilon_0 = 1{\cdot}0$, the value obtained by summing four terms is correct to within 1 unit in the fifth decimal place. It is of interest to examine how far the series may be used in practice to obtain useful limits for the values of the functions in the range $kT/\epsilon_0 < 1$, as well as in the higher range. The series were previously used in this way to obtain estimates of the values of $E/N\epsilon_0$ and C_v/Nk ; apart from this, it is desirable to ascertain whether the numerical values of the functions can be at all closely reproduced by means of a relatively simple artificially terminated series. The errors in the values obtained by summing three and four terms of the series are given in Table II*b*.

A comparison of Tables II and I shows that for $kT/\epsilon_0 \leqslant 0{\cdot}2$ and $\geqslant 0{\cdot}3$ the values of $E/N\epsilon_0$ may be obtained by the use of the low and high temperature series respectively correctly to within 0·1 per cent., and those of C_v/Nk to within 1 per cent. Over the range $0{\cdot}2 < kT/\epsilon_0 < 0{\cdot}3$ the minimum uncertainties resulting from the use

of the series are considerably greater. The very much greater accuracy made possible through the evaluation of the basic Fermi-Dirac functions need not be stressed. The series do, however, retain their value for computational purposes for certain temperature ranges. More accurate values of $E/N\epsilon_0$ may be obtained by the series than by the use of the Fermi-Dirac table for kT/ϵ_0 greater than about 1·5, and of C_v/Nk for kT/ϵ_0 greater than 1·2; in the range covered by Table I (up to $kT/\epsilon_0=2·0$) it is unnecessary to make further use of them, as interpolation

TABLE II*b*—Errors in the values of $E/N\epsilon_0$, in units of the fifth decimal place, obtained by summing 4 and 3 terms of the series (3.3) (H 4 and H 3), and of C_v/Nk, in units of the fourth decimal place, by summing 4 and 3 terms of the series (3.4) (H′ 4 and H′ 3).

	$E/N\epsilon_0$.		C_v/Nk.	
kT/ϵ_0.	H 4.	H 3.	H′ 4.	H′ 3.
0·2	+435	−1552	−1023	+2453
0·3	63	418	101	460
0·4	16	160	19	135
0·6	2·1	40·5	1·8	23·0
0·8	0·5	15·1	0·3	6·5
1·0	0·2	7·0	0·1	2·4
1·2	0·1	3·7	0·03	1·06
1·4	0·0	2·8	0·01	0·53
1·6	0·0	2·2	0·00	0·30

is more convenient, but they could appropriately be applied if accurate values were required for $kT/\epsilon_0>2·0$. In the range $kT/\epsilon_0<0·05$, again, more accurate values of $E/N\epsilon_0$ or of C_v/Nk can be obtained by use of the low temperature series than by interpolation in Table I*b*. The series have a further value in providing a relatively simple approximate analytical representation of the functions, the use of which is much less unsatisfactory when precise information about the degree of numerical accuracy of the approximation is available.

4. *Supplementary Formulæ and Conversion Factors.*

The results given in Table I are so expressed that the numbers given do not involve the numerical values of any physical constants, as is clearly desirable in the primary

expression of the theoretical results. In applying them to experimental data a number of conversion factors are required, the values of which are subject to the uncertainties in the values of the physical constants involved. Before giving the formulæ appropriate to the expression of energies and band widths in units which are ordinarily used, an explicit statement of the values which have been adopted for the fundamental constants is almost indispensable, since there is at present no generally accepted set of most probable values. Those adopted are shown in Table III.

TABLE III.

Adopted Values of Physical Constants.

Fundamental constants.	
Velocity of light	$c = 2{\cdot}9978 \times 10^{10}$ cm. sec.$^{-1}$.
Electronic charge	$e = 4{\cdot}800 \times 10^{-10}$ e.s.u.
Specific electronic charge	$e/mc = 1{\cdot}7585 \times 10^{7}$ e.m.u. gm.$^{-1}$.
Planck's constant	$h = 6{\cdot}610 \times 10^{-27}$ erg. sec.
Faraday constant	$F = 9{\cdot}6511 \times 10^{3}$ emu. gm. equiv.$^{-1}$.
Gas constant	$R = 8{\cdot}3136 \times 10^{7}$ erg. deg.$^{-1}$ mole^{-1}.
Joule equivalent	$J_{15} = 4{\cdot}1852 \times 10^{7}$ erg. cal$_{15}^{-1}$.
Derived constants.	
Gas constant	$R' = 1{\cdot}9864$ cal$_{15}$.deg.$^{-1}$ mole^{-1}.
Avogadro's number	$L = Fc/e = 6{\cdot}0275 \times 10^{23}$ mole^{-1}.
Boltzmann's constant	$k = R/L = 1{\cdot}3793 \times 10^{-16}$ erg. deg.$^{-1}$.

The values adopted for the fundamental constants, except the last two, which are from Birge (1929), are those given by von Friesen (1937) as most probable as a result of a recent survey. It is unnecessary to discuss here the probable errors in these values, which are fully considered in the papers from which they are taken. Derived constants and conversion factors are obtained by treating the values as exact ; and although the probable error may be greater than 1 in 1000, the values are given uniformly to four decimal places to ensure that calculation errors shall not exceed errors due to uncertainties in the values of the basic constants. The symbol L has been used for Avogadro's number to avoid confusion with N, which has been used for the total number of electrons in an energy band.

Conversion Factors and Formulæ.—In Table I the reduced energy, $E/N\epsilon_0$, and specific heat, C_v/Nk, are given as functions of kT/ϵ_0. They may also be considered as functions of T/θ_F, where θ_F is a Fermi characteristic temperature, playing a part in the present treatment similar to that of θ_D in the Debye treatment of the specific heat associated with lattice vibrations, the relation between ϵ_0 and θ_F being

$$\epsilon_0 = k\theta_F. \quad . \quad . \quad . \quad . \quad . \quad . \quad (4.1)$$

Since band widths are often expressed in electron volts, the relation between the numerical measure of the energy width in ergs (ϵ_0) and volts (V_0) is also required.

$$\epsilon_0 = (e/c) \times 10^8 V_0. \quad . \quad . \quad . \quad . \quad . \quad (4.2)$$

TABLE IV.

Conversion Factors for energy expressed in ergs (ϵ), electron volts (V), and as a corresponding temperature (T). (See equation 4.3.)

ϵ	V	T
1	$6{\cdot}2454 \times 10^{11}$	$7{\cdot}2501 \times 10^{15}$
$1{\cdot}6012 \times 10^{-12}$	1	$1{\cdot}1609 \times 10^{4}$
$1{\cdot}3793 \times 10^{-16}$	$8{\cdot}6140 \times 10^{-5}$	1

More generally the relation between the numerical measures of an energy in ergs (ϵ), electron volts (V), and as a corresponding temperature (T) is given by

$$\epsilon = kT = (e/c) \times 10^8 \text{ V}. \quad . \quad . \quad . \quad . \quad (4.3)$$

The conversion factors calculated by using the values of the fundamental constants in Table III are given in Table IV.

As exemplifying the use of this table, a band width of 0·1 volt corresponds to a characteristic temperature $\theta_F = 1160{\cdot}9$, and $kT/\epsilon_0 = 1$ for $T = 1160{\cdot}9°$ K. It may be noted that the conversion factors from ϵ to T and ϵ to V are subject to the still considerable uncertainty in the value of the electronic charge, but the conversion factor from T to V involves only the " well-determined " con-

stants R and F, and the probable error is of the order of only 1 in 10^4. From (4.3),

$$V=(kc/e)\times 10^{-8}T,$$

and
$$(kc/e)=(Rc/Le)=R/F. \quad . \quad . \quad . \quad . \quad (4.4)$$

The columns $E/N\epsilon_0$ in Table I give the energy per electron as a multiple of ϵ_0. For practical purposes it is convenient to obtain the contribution to the energy per gram atom, most conveniently expressed in calories. Writing q for the number of electrons per atom in the band, the electronic contribution E′ to the gram atomic energy may be written in the form

$$E'=qL\epsilon_0(E/N\epsilon_0),$$

giving
$$(E'/q)/(E/N\epsilon_0)=Lk(\epsilon_0/k)=R\theta_F, \quad . \quad . \quad . \quad (4.5)$$

$$=R'(e/kc)V_0\times 10^8. \quad . \quad . \quad . \quad . \quad (4.6)$$

Inserting numerical values

$$\frac{E'}{q\theta_F}=1{\cdot}9864\left(\frac{E}{N\epsilon_0}\right) \text{ cal. mole}^{-1}, \quad . \quad . \quad . \quad (4.7)$$

$$\frac{E'}{q\sqrt{V_0}}\times 10^{-4}=2{\cdot}3060\left(\frac{E}{N\epsilon_0}\right) \text{ cal. mole}^{-1}. \quad . \quad (4.8)$$

Similarly, denoting the electronic contribution to the gram atomic heat by C_v',

$$C_v'=qLk(C_v/Nk)=qR'(C_v/Nk), \quad . \quad . \quad (4.9)$$

and numerically,

$$C_v'/q=1{\cdot}9864(C_v/Nk) \text{ cal. deg.}^{-1} \text{ mole}^{-1}. \quad . \quad (4.10)$$

In Table V are given the values of E'/qV_0 and C_v'/q at intervals of 0·1 in $T/V_0\times 10^{-4}$ over the range $0{\cdot}0 \leqslant T/V_0\times 10^{-4}\leqslant 2{\cdot}0$. From Table IV,

$$kT/\epsilon_0=0{\cdot}8614(T/V_0)\times 10^{-4}. \quad . \quad . \quad . \quad (4.11)$$

The values of $E/N\epsilon_0$ and C_v/Nk corresponding to a particular value of T/V_0 are found by interpolation in Table I, using (4.11), and are then converted to E′ and C_v' values by means of (4.8) and (4.10). The table serves to give an immediate indication of the magnitude of the electronic contribution to the gram atomic energy and

specific heat in the usual units (cal. mole^{-1} and cal. deg.$^{-1}$ mole^{-1}) for any value of the zero point width of the energy band expressed in electron volts over the whole temperature range.

For free electrons ϵ_0 is given by

$$\epsilon_0 = \frac{h^2}{2m} \cdot \left(\frac{3n_v}{8\pi}\right)^{2/3}, \quad . \quad . \quad . \quad (4.12)$$

where n_v is the number of electrons per unit volume. Inserting numerical values,

$$\epsilon_0/5{\cdot}8167 \times 10^{-27} = V_0/3{\cdot}6327 \times 10^{-15} = \theta_F/4{\cdot}2172 \times 10^{-11} = n_v^{2/3}. \quad . \quad . \quad . \quad (4.13)$$

With q as the number of free electrons per atom, A the atomic weight, ρ the density, some simple transformations, and the use of the values in Tables III and IV, lead to the following numerical formulæ for the energy width of the electron distribution at absolute zero, expressed in ergs, electron volts, and as a corresponding temperature:

$$\epsilon_0/4{\cdot}1505 \times 10^{-11} = V_0/2{\cdot}5921 \times 10 = \theta_F/3{\cdot}0092 \times 10^5 = (q\rho/A)^{2/3}. \quad . \quad (4.14)$$

Since the value of $(\rho/A)^{2/3}$ for metals ranges from about 0·06 to 0·3, it follows at once that for electrons in bands for which the energy distribution approaches that for free electrons only the first part of Table I*b* (say up to $kT/\epsilon_0 = T/\theta_F = 0{\cdot}1$) will be relevant for the experimental temperature range. The wider relevance of the tables will be conisdered in the next section.

Series Expansions for E'/qV_0 *and* C_v'/q.

In the previous paper (Stoner, 1936, 1) series expansions were given for E'/RqV_0 and C_v'/Rq, E' and C_v' being the electronic contributions to the gram atomic energy and specific heat, and q the number of electrons per atom in the band considered. For completeness these are repeated below, and more accurate values are given for the coefficients. With V_0 in electron volts, the expressions below give E' in cal. mole^{-1}, and C_v' in cal. deg.$^{-1}$ mole^{-1}.

(i) *Low Temperatures.* $(T/V_0)\times 10^{-4}=x \ll 1$.

The low temperature series are obtained from (3.1) and (3.2), using the conversion factors of (4.8), (4.10), and (4.11). Writing

$$x=(T/V_0)\times 10^{-4},$$

$$(E'/qV_0)\times 10^{-4}=a\left[1+\sum_{r=1}^{n}\alpha_{2r}x^{2r}\right], \quad . \quad (4.15)$$

where

$$a = +1{\cdot}3836,$$
$$\alpha_2=+3{\cdot}0514, \qquad a\alpha_2=+4{\cdot}2184,$$
$$\alpha_4=-3{\cdot}3520, \qquad a\alpha_4=-4{\cdot}6303,$$
$$\alpha_6=-1{\cdot}3367\times 10, \qquad a\alpha_6=-1{\cdot}8495\times 10.$$

Similarly,

$$C_v'/q=\sum_{r=1}^{n}\alpha'_{2r-1}x^{2r-1}, \quad . \quad . \quad . \quad . \quad (4.16)$$

where

$$\alpha_1'=+8{\cdot}4439,$$
$$\alpha_3'=-1{\cdot}8551\times 10,$$
$$\alpha_5'=-1{\cdot}1097\times 10^2.$$

(ii) *High Temperatures.* $(T/V_0)\times 10^{-4}=x>1{\cdot}1609$.

The high temperature series are obtained from (3.3) and (3.4), using the conversion factors of (4.8), (4.10), and (4.11).

$$(E'/qV_0)\times 10^{-4}=x\left[2{\cdot}9796+\sum_{r=1}^{\infty}\beta_r x^{-3r/2}\right], \quad (4.17)$$

where

$$\beta_1=+4{\cdot}9561\times 10^{-1},$$
$$\beta_2=-8{\cdot}7055\times 10^{-3},$$
$$\beta_3=+2{\cdot}7624\times 10^{-4}.$$

Similarly $$C_v'/q=2\ 9796+\sum_{r=1}^{\infty}\beta' x^{-3r/2}, \quad . \quad . \quad . \quad (4.18)$$

where

$$\beta_1'=-2{\cdot}4780\times 10^{-1},$$
$$\beta_2'=+1{\cdot}7411\times 10^{-2},$$
$$\beta_3'=-9{\cdot}6684\times 10^{-4}.$$

The discussion of the range of applicability of the series (3.1) to (3.4), and of the errors made by using them, applies at once to the series (4.15) to (4.18), on replacing kT/ϵ_0 values by x values 1·1609 times as great. Thus for $x \leqslant 0{\cdot}232$ and $\geqslant 0{\cdot}348$ the low and high temperature series respectively give E′ correctly to 0·1 per cent. and C'_v to 1 per cent.

TABLE V.

Electronic Contribution to the Gram-atomic Energy and Specific Heat.

$\frac{T}{V_0}\times 10^{-4}$	$\frac{E'}{qV_0}\times 10^{-4}$	$\frac{C'_v}{q}$	$\frac{T}{V_0}\times 10^{-4}$	$\frac{E'}{qV_0}\times 10^{-4}$	$\frac{C'_v}{q}$
0·0	1·3836	0·0000	1·0	3·4668	2·7483
0·1	1·4253	0·8244	1·1	3·7431	2·7773
0·2	1·5436	1·5019	1·2	4·0220	2·8008
0·3	1·7177	1·9459	1·3	4·3031	2·8201
0·4	1·9271	2·2214	1·4	4·5859	2·8361
0·5	2·1588	2·3985	1·5	4·8703	2·8497
0·6	2·4050	2·5182	1·6	5·1558	2·8613
0·7	2·6612	2·6028	1·7	5·4425	2·8713
0·8	2·9247	2·6648	1·8	5·7300	2·8799
0·9	3·1937	2·7118	1·9	6·0184	2·8875
1·0	3·4668	2·7483	2·0	6·3075	2·8941

Limit $(T/V_0) \to \infty$.
$(E'/qV_0) \to 2{\cdot}9796\ (T/V_0)$.
$(C'_v/q) \to 2{\cdot}9796$.

E', electronic contribution to the gram-atomic energy (cal. mole^{-1}).
C'_v, electronic contribution to the gram-atomic specific heat (cal. deg.$^{-1}$ mole^{-1}).
V_0, maximum electron energy (band width) at absolute zero in electron volts.
q, number of electrons per atom in electron energy band.

5. *Application to Experimenta Data.*

The nature of the problem of electronic specific heats in metals has been outlined in the introductory section. A detailed discussion of the experimental material is outside the scope of this paper, but in this section the relevance of the present treatment to the general specific heat problem will be briefly considered. If the energy distribution of the electronic states approaches that for

free electrons the energetic characteristics will be closely covered over the experimentally attainable temperature range by the formulæ appropriate for low temperatures (equations, (3.1), (3.2), or (4.15), (4.16)) and by the numerical results of the first part of Table I*b*. For almost any conceivable distribution of electronic states in metals the low temperature formulæ will apply in the liquid helium range, and it is from the results at these low temperatures that the most definite information about electronic specific heats has been obtained. For those metals (provided they are not supraconductors) which have been examined the electronic specific heat is proportional to the temperature in this range. The characteristic temperature, θ_F (or the effective band width, ϵ_0 or V_0) can immediately be found from the proportionality factor. Using the conversion factors of section 4,

$$\theta_F/q = 9{\cdot}8025\,(T/C_v')_{T\to 0}, \quad . \quad . \quad . \quad . \quad . \quad (5.1)$$

$$V_0/q = 8{\cdot}4439\times 10^{-4}\,(T/C_v')_{T\to 0}, \quad . \quad . \quad . \quad (5.2)$$

where C_v' is the electronic contribution to the gram atomic heat (cal. deg.$^{-1}$ mole^{-1}) and q is the number of electrons per atom in the band. The value of kT/ϵ_0 for a particular value of T is then given by

$$\frac{kT}{\epsilon_0} = \frac{T}{\theta_F} = 1{\cdot}02015\times 10^{-1}\left(\frac{T}{q}\right)\left(\frac{C_v'}{T}\right)_{T\to 0} \quad . \quad . \quad (5.3)$$

The corresponding value of C_v/Nk can be obtained by interpolation in Table I, and the value of C_v' by using (4.10):

$$C_v' = 1{\cdot}9864\,q\,(C_v/Nk). \quad . \quad . \quad . \quad . \quad (5.4)$$

Thus, if the value of q is known the value of C_v' can be found for the whole range of temperature with considerable precision from the low temperature value. The treatment, however, is strictly valid only if the bands are of the standard form assumed, with the density of states proportional to the square root of the energy.

The value of (C_v'/T) near absolute zero is strictly proportional to the density of electronic energy states at the top of the Fermi distribution, and expressions for the specific heat in the low temperature range may be developed involving this density and its derivatives with respect to the energy Stoner, 1936, 2). The value of

ϵ_0 or V_0 as derived from (5.2) has significance as representing the band width only if the band has the particular form assumed ; and only then is the characteristic temperature, θ_F, related to the band width by (4.1). The position is somewhat similar to that in connexion with the characteristic temperature θ_D in the Debye theory of specific heat. If q is known an effective θ_F can be found from the electronic specific heat at any temperature. If these values are approximately constant the indication is that the band form approximates to that assumed. It would not be profitable to pursue this particular question further until it becomes possible to obtain more reliable estimates from the experimental side of electronic specific heats over a wide temperature range, but the effect of different values of q for bands of standard form may appropriately be considered.

The electronic specific heat is due to electrons in incompletely filled bands. Reference may be made to the book of Mott and Jones (1936, pp. 178, 192) for a general account of the theory and a discussion of the experimental material. For the alkali metals, and for copper, silver, and gold, a single band is concerned, and q may be taken as unity ; for most metals, however, there is an overlapping of bands, and this often occurs in such a way that the main contribution to the specific heat may be formally treated as arising from the " holes " in a nearly full band. The number of holes is then N of the above treatment, and the energy ϵ_0 is to be measured from the top of the band. The metals nickel, palladium, and platinum, in particular, have been treated successfully on this basis by Mott (1935). The value of q corresponding to the effective N for these metals is less than unity ; an estimate of its magnitude may be made from a consideration of the magnetic properties.

For a band containing a fixed number, q, of electrons (or holes) per atom the temperature variation of the specific heat may be calculated as described above. The essential points are brought out by calculating the specific heat at a particular high temperature as a function of C'_0/T at very low temperatures for different values of q. A series of curves giving the electronic contribution to the gram atomic specific heat at 1000° K. are shown in illustration in fig. 2 for q=0·3, 0·5, 1·0, and 2·0.

The values of $(C_v'/T)_{T\to 0}$, which have hitherto been directly measured, range from 1·6 (Ag) to 31 (Pd) in 10^{-4} units. To the values recently collected by Jones and Mott (1937) may be added the value $3{\cdot}484\times10^{-4}$ for aluminium (Keesom and Kok, 1937). The experimentally relevant range is therefore covered by fig. 2. The greater q, the greater is ϵ_0 and the greater the range over which C_v' varies approximately linearly with temperature. (This is shown indirectly by the curves on the left of fig. 2 for $q=1$ and 2.) The asymptotic high temperature value

Fig. 2.

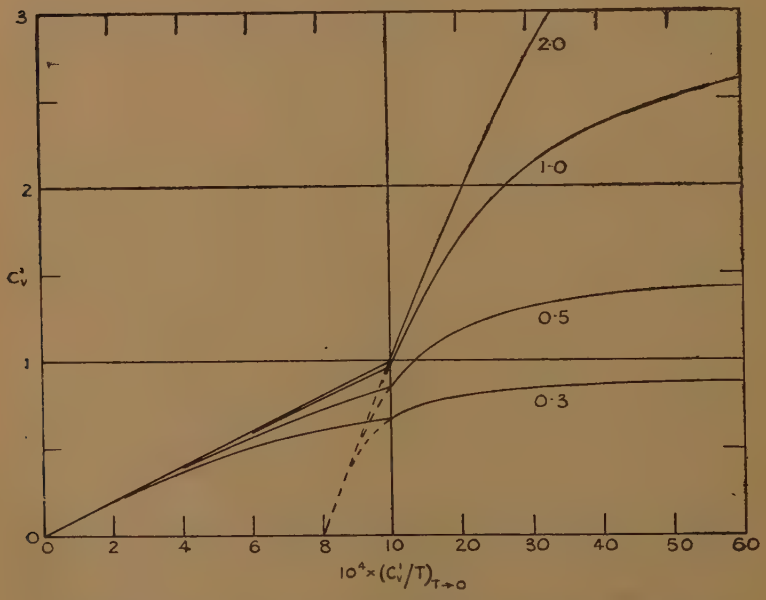

Electronic contribution, C_v', to the gram atomic specific heat (cal. deg.$^{-1}$ mole^{-1}) at 1000° K. as a function of the specific heat at low temperatures.

The numbers on the curves give the values of q, the number of electrons per atom in the band.

Note the change of scale. The curves on the right are continued to the left on the same scale by the broken curves.

of C_v' is $q\mathrm{R}'$, which is approached more nearly at a particular high temperature the higher the value of the low temperature C_v'/T, as shown by the curves.

In order to show the orders of magnitude involved

some typical specific heat values are given in the following table :—

TABLE VI.

Specific Heats at Low and High Temperatures.

	$T \to 0°$ K. $(C'_v/T) \times 10^4$.	$T = 1000°$ K. C'_p.	C'_v.	$C'_v - C'_D$.
Cu	1·777	6·847	6·30	0·37
Ni	17·44	8·17	7·61	1·70
Pd	31	7·36	6·66	0·73

C'_p = gram atomic specific heat at constant pressure.
C'_v = gram atomic specific heat at constant volume.
C'_D = specfic heat due to lattice vibrations.
Unit for C' = cal. deg.$^{-1}$ mole^{-1}.

The values for low temperatures for Cu, Ni, and Pd are due to Kok and Keesom (1936), Keesom and Clark (1934), and Pickard (1936); at high temperatures to Jaeger, Rosenbohm, and Bottema (1932), Klinkhardt (1927), and Jaeger and Veenstra (1934). The values at 1000° K. have been obtained by interpolation. The dilatation corrections to constant volume are semi-empirical, that for nickel having been discussed by Lapp (1929) and Stoner (1936, 3).

For copper $q = 1$. For nickel and palladium the effective q is the number of holes in the d electron band; the value estimated from the saturation magnetization of nickel is approximately 0·6, while the value for palladium is estimated by Mott (1935) from the magnetic moments of palladium alloys as about 0·55. By comparing Table VI with fig. 2 it is clear that, on the basis of these values of q, the value of the specific heat excess at 1000° K. is somewhat too high for copper and nickel and for palladium, as has been noted by Mott and Jones, too low. (The calculated values of C'_v at 1000° K. for Cu, Ni, and Pd are 0·1775, 1·476, and 1·42. For nickel, a ferromagnetic, a modified method of calculation has been used, as described in previous papers.) It is, of course, possible to choose a value of q to fit the results at low temperatures and at one particular high temperature (thus a value of

about 0·3 would be required for palladium), but such a procedure would not be justifiable in view of the uncertainties in the experimental values. The uncertainty is in part in the direct experimental values for C'_v (thus an error of 2 per cent. in the value for copper would result in an error of nearly 40 per cent. in $C'_v - C'_D$) and in part in the estimated dilatation correction.

The advantage of considering a fairly high temperature for making estimates of electronic specific heat is simply that the lattice vibration contribution is then practically constant and little affected by even considerable errors in the estimated Debye characteristic temperature, θ_D. A really satisfactory treatment, however, can be obtained only by a detailed analysis of the variation of the specific heat over the whole temperature range, of the kind which has been made for nickel * (Stoner, 1936, 3). The making of detailed analyses is outside the scope of the paper, and the aim in this section has simply been to indicate the manner in which the electronic contribution may be considered when such analyses are made. Essentially, if q is known, and the value of the electronic specific heat at any temperature, calculations of its value at any other temperature may be made. There are obvious directions in which the theoretical treatment can be extended, such as by more detailed consideration of the effect of overlapping of bands and of deviations from the standard band form ; such elaborations, however, will be more appropriately made in connexion with the detailed analysis of the experimental data on particular metals. The whole trend of the discussion has shown that the possibility of drawing significant conclusions from experimental results on specific heats depends critically on their degree of accuracy. The more immediate interpretation which can be given of low temperature specific heats has perhaps focussed attention unduly on them ; but it is clear that accurate results are desirable for the whole temperature range, and that the work which is being carried out in the higher temperature ranges is equally necessary for the more complete understanding of the electronic structure of metals.

* The provisional estimates of the electronic specific heat in the temperature range below the Curie point may require considerable modification in the light of further development of the collective electron treatment of ferromagnetism. The problem is now being investigated.

I have pleasure in acknowledging the loan of a Brunsviga calculating machine from the Government Grants Committee of the Royal Society.

Summary.

Calculations are made of the temperature variation of the energy and specific heat due to electrons in unfilled bands of the standard form. The theory has previously been developed, and calculations have been made by series methods which are accurate only for high and very low temperatures (for $kT/\epsilon_0 > 1$ and $kT/\epsilon_0 \ll 1$, where ϵ_0 is the energy width of the occupied part of the band at absolute zero). In the method developed here the computations are made with the aid of tables of the basic Fermi-Dirac functions (McDougall and Stoner), enabling a precision of within 1 in 10^5 to be attained in the value of the energy and within 3 in 10^4 in the value of the specific heat for the whole temperature range. A table is given of $E/N\epsilon_0$ and C_v/Nk (where E and C_v are the energy and specific heat for N electrons) at intervals of 0·05 in kT/ϵ_0 for the range $0{\cdot}0 \leqslant kT/\epsilon_0 \leqslant 2{\cdot}0$, and at intervals of 0·01 for $0{\cdot}00 \leqslant kT/\epsilon_0 \leqslant 0{\cdot}20$ (Tables I*a* and I*b*). A comparison is made between the results obtained by the present and the series methods (Tables II*a* and II*b*). Conversion factors required in the consideration of the experimental results are evaluated, and a supplementary table is given of E'/qV_0 and C_v/q, as functions of T/V_0, where E' and C_v' are the electronic contributions to the gram atomic energy in cal. mole^{-1} and specific heat in cal. deg. mole^{-1}, and V_0 is the energy width of the band in electron volts (Table V). Typical experimental results are considered, and the method of utilizing the present tables in the analysis of specific heat data is described. Attention is drawn to the potential value of accurate specific heat determinations over wide temperature ranges in enabling fuller information to be obtained about the characteristics of electron energy bands in metals.

References.

Birge, R. T., Phys. Rev. Supp. i. p. 1 (1929).

Comrie, L. J., 'Interpolation and Allied Tables,' reprinted from the 'Nautical Almanac' for 1937. (London: H.M. Stationery Office, 1936.)

Friesen, S. von, Proc. Roy. Soc. cxl. p. 424 (1937).

Jaeger, F. M., Rosenbohm, E., and Bottema, J. A., *Proc. Akad. Amst.* xxxv. p. 772 (1932).
Jaeger F. M., and Veenstra, W. A., *Proc. Akad. Amst.* xxxvii. p. 280 (1934).
Jones, H., and Mott, N. F., Proc. Roy. Soc. clxii. p. 49 (1937).
Keesom, W. H., and Clarke, C. W., *Physica*, ii. p. 513 (1935).
Keesom, W. H., and Kok, J. A., *Physica*, iii. p. 1035 (1936); iv. p. 835 (1937).
Klinkhardt, H., *Ann. Physik*, lxxxiv. p. 67 (1927).
Lapp, E., *Ann. de Physique*, xii. p. 442 (1929).
McDougall, J., and Stoner, E. C., Phil. Trans. Roy. Soc. ccxxxvii. p. 67 (1938).
Mott, N. F., Proc. Phys. Soc. xlvii. p. 571 (1935).
Mott, N. F., and Jones, H., 'The Theory of the Properties of Metals and Alloys.' (Oxford: Clarendon Press, 1936.)
Pickard, G. L., 'Nature,' cxxxviii. p. 123 (1936.)
Stoner, E. C., Phil. Mag. xxi. p. 145 (1936); Proc. Roy. Soc. cliv. p. 665 (1936); Phil. Mag. xxii. p. 81 (1936); Proc. Leeds Phil. Soc. iii. p. 403 (1938).

Physics Department,
University of Leeds.
February 1938.

LXXXIII. *Suggested Explanation of the Contradiction between the Rayleigh-Jeans Formula and Experiment.* *By* Preston B. Carwile, *Ph.D., Lehigh University, U.S.A.**

Abstract.

Reasons are advanced, on classical grounds, to show that modes of resonance do not exist for radiant energy in free space bounded by a material surface. This leads to the conclusion that the Rayleigh-Jeans formula is not theoretically applicable to the partition of energy between space and a material body.

THE distribution of energy in a wave-propagating medium, as developed by Rayleigh[1] and Jeans[2] on classical grounds, is given by

$$\psi_\lambda d\lambda = 8\pi k T \lambda^{-4} d\lambda, \quad . \quad . \quad . \quad . \quad . \quad . \quad (1)$$

where ψ_λ is the monochromatic energy per unit volume, λ the wave-length, k Boltzmann's constant, and T the absolute temperature. When this formula was applied to the partition of energy between space and a material

* Communicated by the Author.

body, it gave a result which was flatly contradicted[3] by experiment. Attacking the problem from a different point of view, Planck[4] proposed the radical concept of quanta, nearly four decades ago. Since that time the quantum theory has been reinforced by a great array of experimental data and theoretical correlation. Classical theory had been remarkably adequate up to the problem of the partition of radiant energy, but here it failed signally. So far as the writer is aware, no acceptable explanation of its failure has heretofore been found

We shall attempt to show that classical concepts are not at fault Briefly, the explanation is this. Boundary

Fig. 1.

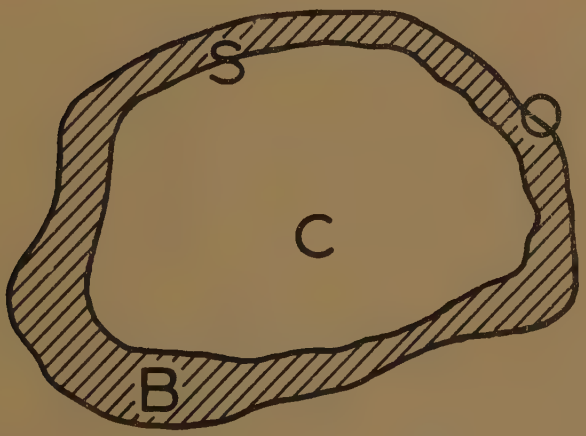

Free space C adjacent to a body B.

conditions, which were duly specified in the derivation of the Rayleigh-Jeans formula, were later disregarded in the application of the formula to the partition of energy between space and a material body.

Consider a free and structureless cavity C inside a material body B (fig. 1). Let the outer boundary O be a closed surface which is impervious to energy. Let the interior surface S be black. By this we mean that S completely absorbs all incident radiation and that emission from S, whatever its spectral distribution may be, is at every time and place independent of incident radiation as regards amplitude, direction, polarization, and phase.

These conditions are all quite in accord with classical concepts.

According to the usual treatment[5], space has $8\pi\lambda^{-4}d\lambda$ degrees of freedom (modes of resonance) per unit volume for wave-lengths between λ and $\lambda+d\lambda$. If the volume of the whole cavity is V, then its number of degrees of freedom in the same range of wave-length is $8\pi V\lambda^{-4}d\lambda$. For space, which is structureless, there is no lower limit[6] to λ. The total number of degrees of freedom, then, for all possible wave-lengths, is

$$\int_0^\infty 8\pi V\lambda^{-4}d\lambda=\infty \quad . \quad . \quad . \quad . \quad . \quad . \quad (2)$$

In the material body B the granular structure puts an effective lower limit[7] to the wave-length. Its total number of degrees of freedom is finite. Therefore, if we apply the principle of equipartition of energy among all the degrees of freedom in the combined system C and B, we should expect the space to absorb all the energy. Experimentally, the situation is more nearly the reverse.

But let us examine more carefully the number of degrees of freedom in C. These are considered to be the discrete modes of free vibration[8], *i. e.*, modes of resonance, for waves in the cavity. Each mode is based on the condition of perfect reflexion[9] at the boundary with respect to amplitude, direction, polarization, and phase. But the boundary S is black. There is no reflexion. There is no mode of resonance. Hence, *there are no degrees of freedom in C.* Or perhaps it would be better to say that only the preliminary stage—the first and only trip across the cavity—exists for any degree of freedom before the wave is absorbed and loses its identity.

Empirically a state of equilibrium is soon established when the average rate of emission is equal to the average rate of absorption. But the amplitude, direction, polarization, and phase of the emission at any point and instant are wholly unrelated to the amplitude, direction, polarization, and phase of the incident radiation. Obviously this state of affairs is not physically the same as perfect reflexion, and therefore the usual concept of degrees of freedom is not applicable. If we are still inclined to identify the behaviour of a black surface with

the action of a perfect reflector, let us consider whether we can replace the surface of any ordinary mirror by a perfectly black surface and still form the same images as before. We know that we cannot. Yet we should be able to if a black surface were physically the same as a perfect reflector.

In order to generalize our findings, let us replace the black surface S (fig. 1) by any material surface, keeping the temperature constant. By Kirchhoff's[10] law (classical theory) the energy density in C remains unchanged from its previous value which obtained when

Fig. 2.

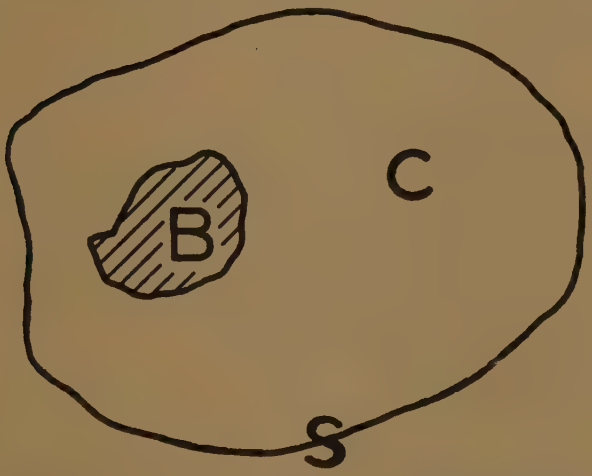

Free space C adjacent to a body B and to a reflecting surface S.

degrees of freedom had no meaning. Hence, degrees of freedom in the cavity still have no significance.

If we let the surface S become a perfect reflector, then we do have degrees of freedom in C, but we have no mechanism of transfer of energy between C and B. Hence, we cannot apply the principle of equipartition to the combined system.

What if we have a black body B (fig. 2) in a cavity C which is enclosed by a perfectly reflecting surface S? At first glance we seem to be right back in our original dilemma. But such is not the case. The cavity now has two boundaries, one being the outer surface S and

the other being the surface of the black body B. Any emergent radiation from B returns to B and is completely absorbed after a finite number of reflexions, whereas in a mode of resonance it would be reflected over and over indefinitely. Hence again, a mode of resonance, or degree of freedom, in C is meaningless. By Kirchhoff's law the situation remains unaltered by the substitution of any real surface in place of the black surface of B.

It appears that for any system including free space adjacent to a real body, the concept of degrees of freedom in the space fades to insignificance. Therefore the Rayleigh-Jeans formula, derived as it is on the basis of equipartition of energy among degrees of freedom, is not applicable to the partition of energy between space and a material body.

References.

(1) Phil. Mag. xlix. p. 539 (1900).
(2) Phil. Mag. x. p. 91 (1905).
(3) J. H. Jeans, ' Dynamical Theory of Gases,' section 472 (1921).
(4) *Verhand. Deutsch. Phys. Ges.* ii. p. 237 (1900). Also *Ann. d. Phys.* iv. p. 553 (1901).
(5) J. H. Jeans, ' Dynamical Theory of Gases,' ch. xvi. (1921); or almost any text-book on heat.
(6) J. H. Jeans, ' Dynamical Theory of Gases,' section 470 (1921).
(7) J. H. Jeans, *ibid.* section 469 (1921).
(8) J. H. Jeans, *ibid.* sections 456–465 (1921).
(9) J. H. Jeans, *ibid.* section 461 (1921).
(10) *Ann. d. Phys. u. Chem.* cix. p. 275 (1860).

Bethlehem, Pennsylvania.
December 10, 1937.

LXXXIV. *On Lommel Functions.* *By* N. A. Shastri, *Department of Mathematics, College of Science, Nagpur* *.

THE object of the present note is to establish some symbolic relations with Lommel functions as nucleus and derive some results from them.

I.

Lommel's function for the unrestricted values of n has been defined[1] as

$$U_n(w, z) = \sum_{m=0}^{\infty} (-)^m \left(\frac{w}{z}\right)^{n+2m} J_{n+2m}(z).$$

* Communicated by the Author.

Changing w into $2wx$ and z into $2\sqrt{zx}$, we get

$$U_n(2wx, 2\sqrt{zx}) = \sum_{m=0}^{\infty} (-)^m \left[w\sqrt{\frac{x}{z}}\right]^{n+2m} J_{n+2m}(2\sqrt{zx}).$$

But [2] $$x^{\frac{n}{2}} J_n(2\sqrt{x}) \doteqdot p^{-n} e^{-\frac{1}{p}},$$

$$\left(\frac{x}{z}\right)^{\frac{1}{2}n} J_n(2\sqrt{zx}) \doteqdot p^{-n} e^{-\frac{z}{p}} \quad \text{valid for } R(n) > -1.$$

Hence [3]

$$U_n(2wx, 2\sqrt{zx}) \doteqdot \sum_{m=0}^{\infty} (-)^m w^{n+2m} p^{-(n+2m)} e^{-\frac{z}{p}},$$

$$\doteqdot \frac{w^n e^{-\frac{z}{p}}}{p^{n-2}(p^2+w^2)}, \quad R(n) > -1. \quad . \quad (1)$$

Now from the operational calculus we have

$$f(p) = p\int_0^{\infty} e^{-px} h(x)\, dx,$$

if $$f(p) \doteqdot h(x).$$

Therefore $$pf\left(\frac{1}{p}\right) = \int_0^{\infty} e^{-\frac{s}{p}} h(s)\, ds,$$

and

$$\frac{w^n f\left(\frac{1}{p}\right)}{p^{n-3}(p^2+w^2)} = \int_0^{\infty} \frac{e^{-\frac{s}{p}} w^n}{p^{n-2}(p^2+w^2)} h(s)\, ds,$$

$$\doteqdot \int_0^{\infty} U_n(2wx, 2\sqrt{sx}) h(s)\, ds, \quad R(n) > -1,$$

$$. \quad . \quad . \quad (2)$$

using (1).

Again, $$\frac{p}{w} f\left(\frac{w}{p}\right) = \int_0^{\infty} e^{-\frac{sw}{p}} h(s)\, ds,$$

$$pf\left(\frac{w}{p}\right) = \int_0^{\infty} e^{-\frac{s}{p}} h\left(\frac{s}{w}\right) ds, \quad w \text{ +ve.}$$

Hence

$$\frac{w^n f\left(\frac{w}{p}\right)}{p^{n-3}(p^2+w^2)} = \int_0^\infty \frac{e^{-\frac{s}{p}} w^n}{p^{n-2}(p^2+w^2)} h\left(\frac{s}{w}\right) ds,$$

$$\doteqdot \int_0^\infty \mathrm{U}_n(2wx, 2\sqrt{sx}) h\left(\frac{s}{w}\right) ds, \quad \mathrm{R}(n) > -1. \quad \ldots \quad (3)$$

Relations (2) and (3) give two new operational formulæ.

II.

We will now evaluate certain integrals by choosing $h(x)$ in a suitable manner.

(i.) Let $h(x)=x^{r-1}$, so that $f(p) \doteqdot \frac{\Gamma(r)}{p^{r-1}}$.

Hence from (2)

$$\int_0^\infty \mathrm{U}_n(2wx, 2\sqrt{sx}) s^{r-1} ds \doteqdot \Gamma(r) w^n \frac{1}{p} \frac{1}{p^{n-r-1}} \cdot \frac{p^2}{p^2+w^2} \quad (4)$$

$$= \frac{\Gamma(r) w^n}{\Gamma(n-r)} \cdot \int_0^x (x-\xi)^{n-r-1} \cos w\xi \, d\xi, \quad \ldots \quad (5)$$

using $\frac{p^2}{p^2+w^2} \doteqdot \cos wx$ and the product theorem of the operational calculus.

Again,

$$\int_0^\infty \mathrm{U}_n(2wx, 2\sqrt{sx}) s^{r-1} ds \doteqdot \Gamma(r) w^{n-1} \frac{1}{p} \cdot \frac{1}{p^{n-r-2}} \frac{pw}{p^2+w^2}$$

from (4)

$$= \frac{\Gamma(r) w^{n-1}}{\Gamma(n-r-1)} \int_0^x (x-\xi)^{n-r-2} \sin w\xi \, d\xi, \quad (6)$$

using $\frac{pw}{p^2+w^2} \doteqdot \sin wx$ and the product theorem.

If we put $r=n-1$ in (5) we get

$$\int_0^\infty \mathrm{U}_n(2wx, 2\sqrt{sx}) s^{n-2} ds = \Gamma(n-1) w^n \int_0^x \cos w\xi \, d\xi$$

$$= \Gamma(n-1) w^{n-1} \sin wx. \quad \ldots \quad (7)$$

Put $r=n$ in (4), we have

$$\int_0^\infty \mathrm{U}_n(2wx,\ 2\sqrt{sx})s^{n-1}\,ds \doteqdot \Gamma(n)w^n\frac{p^2}{p^2+w^2}$$
$$=\Gamma(n)w^n\cos wx. \quad . \quad . \quad . \quad (8)$$

(ii.) Let $h(x)=\frac{x^2}{2}+w^2$, so that $f(p)=\frac{1}{p^2}+w^2$.

Hence from (2) we have

$$\int_0^\infty \mathrm{U}_n(2wx,\ 2\sqrt{sx})(s^2+2w^2)\,ds \doteqdot \frac{2w^n}{p^{n-3}}$$
$$=\frac{2w^nx^{n-3}}{\Gamma(n-2)} \quad \mathrm{R}(n)>2. \quad . \quad (9)$$

(iii.) Now $$x^2+w^2 \doteqdot \frac{2}{p^2}+w^2. \quad . \quad . \quad . \quad . \quad . \quad (10)$$

Apply Parsevals' theorem [4] as used in the operational calculus to (10) and (1), we get

$$\int_c^\infty \mathrm{U}_n(2wx,\ 2\sqrt{zx})\left(\frac{2}{x^2}+w^2\right)\frac{dx}{x}=w^n\int_0^\infty e^{-\frac{z}{x}}\left(\frac{1}{x}\right)^{n-1}dx$$
$$=w^nz^{-n+2}.\Gamma(n-2)$$
$$\mathrm{R}(n)>2. \quad . \quad (11)$$

(iv.) Let $h(x)=\cos\frac{x}{b}$, so that $f(p)=\frac{b^2p^2}{b^2p^2+1}$.

Hence from (2) we have

$$\int_0^\infty \mathrm{U}_n(2wx,\ 2\sqrt{sx})\cos\frac{s}{b}\,ds$$
$$\doteqdot \frac{w^nb^2}{p^{n-3}(p^2+w^2)(p^2+b^2)}$$
$$=\frac{b^2w^n}{b^2-w^2}\frac{1}{p}\left[\frac{1}{p^{n-2}}\left\{\frac{p^2}{p^2+w^2}-\frac{p^2}{p^2+b^2}\right\}\right]$$
$$\doteqdot \frac{b^2w^n}{(b^2-w^2)\Gamma(n-1)}\int_0^x(x-\xi)^{n-2}\{\cos w\xi-\cos b\xi\}\,d\xi$$
$$\mathrm{R}(n)>-1. \quad (12)$$

(v.) Let $h(x)=\sin\frac{x}{b}$, so that $f(p)=\frac{pb}{b^2p^2+1}$.

Hence

$$\int_0^\infty U_n(2wx,\ 2\sqrt{zx})\sin\frac{z}{b}\,dz$$

$$\doteqdot \frac{w^n b}{p^{n-4}(p^2+w^2)(p^2+b^2)}$$

$$= \frac{bw^n}{b^2-w^2}\cdot\frac{1}{p}\cdot\left[\frac{1}{p^{n-3}}\left\{\frac{p^2}{p^2+w^2}-\frac{p^2}{p^2+b^2}\right\}\right]$$

$$\doteqdot \frac{bw^n}{(b^2-w^2)\Gamma(n-2)}\int_0^x (x-\xi)^{n-3}(\cos w\xi-\cos b\xi)\,d\xi$$

$$\mathrm{R}(n)>2. \quad (13)$$

(vi.) Take $h(x)=\dfrac{\sqrt{\pi}}{2^m\Gamma(m+\frac{1}{2})}x^m J_m(x)$,

then [2] $$f(p)=\frac{p}{(1+p^2)^{m+\frac{1}{2}}}.$$

Therefore $$f\left(\frac{w}{p}\right)=\frac{wp^{2m}}{(p^2+w^2)^{m+\frac{1}{2}}}$$

and $$\frac{w^n f\left(\frac{w}{p}\right)}{p^{n-3}(p^2+w^2)}=\frac{w^{n+1}p^{2m-n+3}}{(p^2+w^2)^{m+\frac{3}{2}}}$$

$$=\frac{w^{n+1}p}{(p^2+w^2)^{\frac{n}{2}+\frac{1}{2}}}$$

by choosing $2m=n-2$.

But $$\frac{pw^{\frac{n}{2}}}{(p^2+w^2)^{\frac{n+1}{2}}}\doteqdot\frac{\sqrt{\pi}}{2^{\frac{n}{2}}\Gamma\left(\frac{n+1}{2}\right)}x^{\frac{n}{2}}J_{\frac{n}{2}}(wx).$$

Hence $$\frac{w^n f\left(\frac{w}{p}\right)}{p^{n-3}(p^2+w^2)}\doteqdot\frac{w^{\frac{n}{2}+1}\sqrt{\pi}}{2^{\frac{n}{2}}\Gamma\left(\frac{n+1}{2}\right)}x^{\frac{n}{2}}J_{\frac{n}{2}}(wx).$$

Using (3) we get

$$\int_0^\infty U_n(2wx,\ 2\sqrt{sx})s^{\frac{n}{2}-1}J_{\frac{n}{2}-1}\left(\frac{s}{w}\right)ds$$

$$= \frac{\Gamma\left(\frac{n-1}{2}\right)}{2\Gamma\left(\frac{n+1}{2}\right)} w^n x^{\frac{n}{2}} \mathrm{J}_{\frac{n}{2}}(wx)$$

$$= \frac{1}{n-1} w^n x^{\frac{n}{2}} \mathrm{J}_{\frac{n}{2}}(wx) \quad \mathrm{R}(n)>0. \quad . \quad (14)$$

(vii.) Take $h(x)=\mathrm{S}(x)$, where $\mathrm{S}(x)$ is a Fresnel Integral, so that [2]

$$f(p)=\frac{(\sqrt{p^2+1}-p)^{\frac{1}{2}}}{2\sqrt{p^2+1}}$$

$$f\left(\frac{w}{p}\right) = \sum_{r=0}^{\infty} \frac{(\frac{1}{2})_r(-)^r}{r!\ 2} \frac{\sqrt{p}w^r}{(p^2+w^2)^{\frac{r}{2}+\frac{1}{4}}}$$

and

$$\frac{w^n f\left(\frac{w}{p}\right)}{p^{n-3}(p^2+w^2)} = \sum_{r=0}^{\infty} \frac{(\frac{1}{2})_r(-)^r w^{n+r} p}{r!\ 2p^{n-\frac{5}{2}}(p^2+w^2)^{\frac{r}{2}+\frac{5}{4}}}.$$

Put $n=5/2$, we have

$$\frac{w^{\frac{5}{2}} f\left(\frac{w}{p}\right)\sqrt{p}}{p^2+w^2} = \sum_{r=0}^{\infty} \frac{(\frac{1}{2})_r(-)^r . w^{r+\frac{5}{2}}}{r!\ 2} \cdot \frac{p}{(p^2+w^2)^{\frac{r}{2}+\frac{5}{4}}}$$

$$\doteqdot \sum_{r=0}^{\infty} \frac{(\frac{1}{2})_r(-)^r w^{\frac{r}{2}+\frac{7}{4}} \sqrt{\pi}}{r!\ 2^{\frac{r}{2}+\frac{7}{4}}\Gamma\left(\frac{r}{2}+\frac{5}{4}\right)} x^{\frac{r}{2}+\frac{3}{4}} \mathrm{J}_{\frac{r}{2}+\frac{3}{4}}(wx).$$

Hence we get after using (3)

$$\int_0^{\infty} \mathrm{U}_{\frac{5}{2}}(2wx,\ 2\sqrt{sx})\mathrm{S}\left(\frac{s}{w}\right) ds$$

$$= \sum_{r=0}^{\infty} \frac{(\frac{1}{2})_r(-)^r \sqrt{\pi} w^{\frac{r}{2}+\frac{7}{4}}}{r!\ 2^{\frac{r}{2}+\frac{7}{4}}\Gamma\left(\frac{r}{2}+\frac{5}{4}\right)} x^{\frac{r}{2}+\frac{3}{4}} \mathrm{J}_{\frac{r}{2}+\frac{3}{4}}(wx). \quad (15)$$

(viii.) Now take $h(x)=\mathrm{C}(x)$, where $\mathrm{C}(x)$ is other Fresnel Integral, so that[2]

$$f(p)=\frac{(\sqrt{p^2+1}-p)^{-\frac{1}{2}}}{2\sqrt{p^2+1}}$$

$$f\left(\frac{w}{p}\right)=\sum_{r=0}^{\infty}\frac{(-)^r(-\tfrac{1}{2})_r p^{\frac{3}{2}}w^r}{r!\,2(w^2+p^2)^{\frac{3}{4}+\frac{r}{2}}},$$

and

$$\frac{w^n f\left(\frac{w}{p}\right)}{p^{n-3}(p^2+w^2)}=\sum_{r=0}^{\infty}\frac{(-)^r(-\tfrac{1}{2})_r w^{n+r}}{r!\,2p^{n-\frac{9}{2}}(p^2+w^2)^{\frac{7}{2}+\frac{r}{2}}}.$$

Choosing $n=7/2$, we have

$$\frac{w^{\frac{7}{2}}f\left(\frac{w}{p}\right)}{p^{\frac{1}{2}}(p^2+w^2)}=\sum_{r=0}^{\infty}\frac{(-)^r(-\tfrac{1}{2})_r w^{r+\frac{7}{2}}p}{r!\,2(p^2+w^2)^{\frac{7}{4}+\frac{r}{2}}}$$

$$=\sum_{r=0}^{\infty}\frac{(-)^r(-\tfrac{1}{2})_r w^{\frac{r}{2}+\frac{9}{4}}}{r!\,2}\cdot\frac{pw^{\frac{r}{2}+\frac{5}{4}}}{(p^2+w^2)^{\frac{7}{4}+\frac{r}{2}}}$$

$$\doteqdot\sum_{r=0}^{\infty}\frac{(-)^r(-\tfrac{1}{2})_r\sqrt{\pi}w^{\frac{r}{2}+\frac{9}{4}}}{r!\,2^{\frac{r}{2}+\frac{9}{4}}\Gamma\left(\frac{r}{2}+\frac{7}{4}\right)}x^{\frac{r}{2}+\frac{5}{4}}\mathrm{J}_{\frac{r}{2}+\frac{5}{4}}(wx).$$

Hence from (3) we get

$$\int_0^{\infty}\mathrm{U}_{\frac{7}{2}}(2wx,\,2\sqrt{sx})\mathrm{C}\left(\frac{s}{w}\right)ds$$

$$=\sum_{r=0}^{\infty}\frac{(-)^r(-\tfrac{1}{2})^r\sqrt{\pi}w^{\frac{r}{2}+\frac{9}{4}}}{r!\,2^{\frac{r}{2}+\frac{9}{4}}\Gamma\left(\frac{r}{2}+\frac{7}{4}\right)}x^{\frac{r}{2}+\frac{5}{4}}\mathrm{J}_{\frac{r}{2}+\frac{5}{4}}(wx),$$

which can be written as

$$\int_0^{\infty}\mathrm{U}_{\frac{7}{2}}(2wx,\,\sqrt{2wsx})\mathrm{C}\left(\frac{s}{2}\right)ds$$

$$=\sum_{r=0}^{\infty}\frac{(-)^r(-\tfrac{1}{2})_r\sqrt{\pi}}{r!\,\Gamma\left(\frac{r}{2}+\frac{7}{4}\right)}\left(\frac{wx}{2}\right)^{\frac{r}{2}+\frac{5}{4}}\mathrm{J}_{\frac{r}{2}+\frac{5}{4}}(wx). \quad (16)$$

(ix.) Let $h(x)=n/x\mathrm{J}_n(x)$, so that

$$f(p)=p[\sqrt{p^2+1}-p]^n,$$

$$f\left(\frac{w}{p}\right)=\sum_{r=0}^{\infty}(-)^r\binom{n}{r}\frac{w^{r+1}}{p^{n+1}(p^2+w^2)^{\frac{r-n}{2}}},$$

and

$$\frac{w^m f\left(\frac{w}{p}\right)}{p^{m-3}(p^2+w^2)}=\sum_{r=0}^{\infty}(-)^r\binom{n}{r}\frac{w^{m+r+1}}{p^{m+n-2}(p^2+w^2)^{\frac{r-n+2}{2}}}.$$

Choose $m=1-n$, we have

$$\frac{w^{1-n}f\left(\frac{w}{p}\right)}{p^{-n-2}(p^2+w^2)}=\sum_{r=0}^{\infty}(-)^r\binom{n}{r}.w^{\frac{r-n+3}{2}}\frac{p.w^{\frac{r-n+1}{2}}}{(p^2+w^2)^{\frac{r-n+2}{2}}}$$

$$\doteqdot\sum_{r=0}^{\infty}(-)^r\binom{n}{r}w^{\frac{r-n+3}{2}}\frac{\sqrt{\pi}}{2^{\frac{r-n+1}{2}}\Gamma\left(\frac{r-n+2}{2}\right)}$$

$$\times x^{\frac{r-n+1}{2}}\mathrm{J}_{\frac{r-n+1}{2}}(wx).$$

Therefore from (3) we get

$$\int_0^{\infty}\mathrm{U}_{1-n}(2wx,\ 2\sqrt{sx})\frac{nw}{s}\mathrm{J}_n\left(\frac{s}{w}\right)ds$$

$$=\sum_{r=0}^{\infty}(-)^r\binom{n}{r}\frac{\sqrt{\pi}\,w^{\frac{r-n+3}{2}}}{2^{\frac{r-n+1}{2}}\Gamma\left(\frac{r-n+2}{2}\right)}x^{\frac{r-n+1}{2}}\mathrm{J}_{\frac{r-n+1}{2}}(wx)$$

or

$$\int_0^{\infty}\mathrm{U}_{1-n}(2wx,\ 2\sqrt{sx})\mathrm{J}_n\left(\frac{s}{w}\right)\frac{ds}{s}$$

$$=\sum_{r=0}^{\infty}(-)^r\binom{n}{r}\frac{\sqrt{\pi}}{n\Gamma\left(\frac{r-n+2}{2}\right)}\left(\frac{xw}{2}\right)^{\frac{r-n+1}{2}}\mathrm{J}_{\frac{r-n+1}{2}}(wx)$$

$$0>\mathrm{R}(n). \quad . \quad (17)$$

(x.) Let $h(x)=\mathrm{J}_{i_0}(x)$, where $\mathrm{J}_{i_0}(x)$ is a Bessel Integral function, so that

$$f(p) = \log(\sqrt{1+p^2}-p),$$

$$f\left(\frac{w}{p}\right) = \tfrac{1}{2}\log\left(1+\frac{w^2}{p^2}\right) - \sum_{r=1}^{\infty}\frac{1}{r}\cdot\frac{w^r}{(w^2+p^2)^{\frac{r}{2}}},$$

and

$$\frac{w^n f\left(\frac{w}{p}\right)}{p^{n-3}(p^2+w^2)} = \frac{1}{2}\frac{w^n}{p^{n-3}}\frac{\log\left(1+\frac{w^2}{p^2}\right)}{p^2+w^2} - \sum_{r=1}^{\infty}\frac{1}{r}\cdot\frac{w^{n+r}}{p^{n-3}(p^2+w^2)^{\frac{r}{2}+1}}.$$

By putting $n=2$ this reduces to

$$\frac{w^2 p f\left(\frac{w}{p}\right)}{p^2+w^2} = \frac{w^2}{2}\frac{p}{p^2+w^2}\log\left(1+\frac{w^2}{p^2}\right) - \sum_{r-1}^{\infty}\frac{w^{r+2}p}{r(p^2+w^2)^{\frac{r}{2}+1}}. \quad . \quad . \quad . \quad (18)$$

But
$$\frac{pw}{2}\log\left(1+\frac{w^2}{p^2}\right) = -w\sum_{r=1}^{\infty}\frac{(-)^r w^{2r}}{2rp^{2r-1}}$$

$$\doteqdot -w\sum_{r=1}^{\infty}\frac{(-)^r w^{2r}x^{2r-1}}{2r\Gamma(2r)}$$

$$= -\frac{w}{x}\sum_{r=1}^{\infty}\frac{(-)^r(wx)^{2r}}{(2r)!}$$

$$= \frac{w}{x}(1-\cos wx).$$

The relation (18) can be written as

$$\frac{pw^2 f\left(\frac{w}{p}\right)}{p^2+w^2} = \frac{1}{p}\left[\frac{pw}{2}\log\left(1+\frac{w^2}{p^2}\right)\right]\frac{pw}{p^2+w^2} - \sum_{r=1}^{\infty}\frac{w^{\frac{r}{2}+\frac{3}{2}}}{r}\cdot\frac{pw^{\frac{r}{2}+\frac{1}{2}}}{(p^2+w^2)^{\frac{r}{2}+1}}$$

$$\doteqdot \int_0^x w\frac{(1-\cos w\xi)}{\xi}\sin w(x-\xi)\,d\xi - \sum_{r=1}^{\infty}\frac{1}{r}\cdot\frac{\sqrt{\pi}\,w^{\frac{r}{2}+\frac{3}{2}}}{2^{\frac{r+1}{2}}\Gamma\left(\frac{r}{2}+1\right)}x^{\frac{r+1}{2}}\mathrm{J}_{\frac{r+1}{2}}(wx).$$

Hence by using (3) we get

$$\int_0^\infty U_2(2wx,\ 2\sqrt{sx})J_{i_0}\left(\frac{s}{w}\right)ds$$

$$=\int_0^x \frac{w(1-\cos w\xi)}{\xi}\sin w(x-\xi)\,d\xi$$

$$-\sum_{r=1}^{\infty}\frac{1}{r}\cdot\frac{\sqrt{\pi}\,w^{r+\frac{3}{2}}}{2^{\frac{r+1}{2}}\Gamma\left(\frac{r}{2}+1\right)}x^{\frac{r+1}{2}}J_{\frac{r+1}{2}}(wx), \quad (19)$$

which can be written as

$$\int_0^\infty U_2(2wx,\ 2\sqrt{swx})J_{i_0}(s)\,ds$$

$$=\int_0^x \frac{1-\cos w\xi}{\xi}\sin\left[w(x-\xi)\right]d\xi$$

$$-\sum_{r=1}^{\infty}\frac{\sqrt{\pi}}{r\Gamma\left(\frac{r}{2}+1\right)}\left(\frac{wx}{2}\right)^{\frac{r+1}{2}}J_{\frac{r+1}{2}}(wx). \quad (20)$$

III.

(i.) Now

$$U_n(2wx,\ 2\sqrt{zx})\doteqdot\frac{e^{-\frac{z}{p}}w^n}{p^{n-2}(p^2+w^2)}.$$

Hence

$$\int_0^\infty U_n(2wx,\ 2\sqrt{zx})\frac{\cos rw}{w^n}dw\doteqdot\int_0^\infty\frac{e^{-\frac{z}{p}}}{p^{n-2}}\frac{\cos rw}{p^2+w^2}dw.$$

But
$$\int_0^\infty\frac{\cos rw}{p^2+w^2}dw=\frac{\pi}{2p}e^{-pr}.$$

Hence
$$\int_0^\infty U_n(2wx,\ 2\sqrt{zx})\frac{\cos rw}{w^n}dw\doteqdot\frac{\pi}{2}\frac{e^{-\frac{z}{p}}}{p^{n-1}}e^{-pr}$$

But
$$e^{-\frac{z}{p}}p^{-n+1}\doteqdot\left(\frac{x}{z}\right)^{\frac{n-1}{2}}J_{n-1}(2\sqrt{xz}),$$

so
$$e^{-pr}e^{-\frac{z}{p}}p^{-n+1}\doteqdot 0 \quad \text{if } x<r$$

$$\doteqdot\left(\frac{x-r}{z}\right)^{\frac{n-1}{2}}J_{n-1}(2\sqrt{z(x-r)}) \quad \text{if } x>r.$$

Therefore

$$\int_0^\infty \mathrm{U}_n(2wx,\ 2\sqrt{zx})\frac{\cos rw}{w^n}dw = 0 \quad \text{if } x<r$$

$$\text{or} \qquad = \frac{\pi}{2}\left[\frac{x-r}{z}\right]^{\frac{n-1}{2}} \mathrm{J}_{n-1}[2\sqrt{z(x-r)}]$$

$$\text{if } x>r. \quad . \quad . \quad (21)$$

(ii.) Similarly,

$$\int_0^\infty \mathrm{U}_n(2wx,\ 2\sqrt{zx})\frac{\sin rw}{w^{n-1}}dw \doteqdot \frac{e^{-\frac{z}{p}}}{p^{n-2}}\int_0^\infty \frac{w\sin rw}{p^2+w^2}dw$$

$$\doteqdot \frac{\pi}{2}\frac{e^{-\frac{z}{p}}}{p^{n-2}}e^{-rp} \quad \left\{\text{using } \int_0^\infty \frac{w\sin rw}{p^2+w^2}dw = \frac{\pi}{2}e^{-rp}\right\}$$

$$= 0 \quad \text{if } x<r$$

$$\text{or} \qquad = \frac{\pi}{2}\left(\frac{x-r}{z}\right)^{\frac{n-2}{2}} \mathrm{J}_{n-2}[2\sqrt{z(x-r)}] \quad \text{if } x>r. \quad . \quad (22)$$

(iii.) We have [5]

$$\int_0^\infty \frac{e^{-\frac{1}{4}w^2}w^n\mathrm{D}_n(w)\,dw}{w^2+p^2} = \sqrt{\frac{\pi}{2}}p^{n-1}e^{\frac{1}{4}p^2}\mathrm{D}_{-n-1}(p)\Gamma(n+1)$$

$$0<n<1.$$

Hence

$$\int_0^\infty \mathrm{U}_n(2wx,\ 2\sqrt{zx})w^m\mathrm{D}_{m+n}(w)e^{-\frac{1}{4}w^2}dw$$

$$\doteqdot \int_0^\infty \frac{e^{-\frac{z}{p}}}{p^{n-2}}\cdot\frac{w^{m+n}e^{-\frac{1}{4}w^2}\mathrm{D}_{m+n}(w)}{p^2+w^2}dw$$

$$\doteqdot \sqrt{\frac{\pi}{2}}\frac{1}{p}e^{-\frac{z}{p}}p^{m+1}pe^{\frac{1}{4}p^2}\mathrm{D}_{-m-n-1}(p)\Gamma(m+n+1)$$

$$0<m+n<1. \quad (23)$$

Let $m+1$ be negative. Then

$$p^{m+1}e^{-\frac{z}{p}} \doteqdot \left(\frac{x}{z}\right)^{-\frac{m+1}{2}} \mathrm{J}_{-m-1}(2\sqrt{zx}) \quad . \quad . \quad (24)$$

and [6] $$pe^{\frac{1}{4}p^2}\mathrm{D}_{-m-n-1}(p)\Gamma(m+n+1) \doteqdot x^{m+n}e^{-\frac{1}{4}x^2}. \quad . \quad (25)$$

Hence, using the product theorem, (23) can be transformed into

$$\int_0^\infty \mathrm{U}_n(2wx,\ 2\sqrt{zx})w^m\mathrm{D}_{m+n}(w)e^{-\frac{1}{4}w^2}\,dw$$

$$= \sqrt{\frac{\pi}{2}}\int_0^x \left(\frac{x-\xi}{z}\right)^{-\frac{m+1}{2}} \mathrm{J}_{-m-1}(2\sqrt{z(x-\xi)})\xi^{m+n}e^{-\frac{1}{4}\xi^2}\,d\xi,$$

or $$= \sqrt{\frac{\pi}{2}}\int_0^x \left(\frac{\xi}{z}\right)^{-\frac{m+1}{2}} \mathrm{J}_{-m-1}(2\sqrt{z\xi})(x-\xi)^{m+n}e^{-\frac{1}{4}(x-\xi)^2}\,d\xi \quad . \quad . \quad . \quad (26)$$

$$0<m+n<1 \text{ and } m+1 \text{ −ve.}$$

(26) can be further transformed by putting $m+1=-k$.

$$\int_0^\infty \mathrm{U}_n(2wx,\ 2\sqrt{zx})\mathrm{D}_{n-k-1}(w)e^{-\frac{1}{4}w^2}\frac{dw}{w^{k+1}}$$

$$= \sqrt{\frac{\pi}{2}}\int_0^x \left(\frac{x-\xi}{z}\right)^{\frac{k}{2}} \mathrm{J}_k(2\sqrt{z(x-\xi)})\xi^{n-k-1}e^{-\frac{1}{4}\xi}\,d\xi,$$

or $$= \sqrt{\frac{\pi}{2}}\int_0^x \left(\frac{\xi}{z}\right)^{\frac{k}{2}} \mathrm{J}_k(2\sqrt{z\xi})(x-\xi)^{n-k-1}e^{-\frac{1}{4}(x-\xi)^2}\,d\xi, \quad (27)$$

$$0<n-k-1<1 \text{ and } k \text{ is } +\text{ve.}$$

(iv.) Again we have [5]

$$\int_0^\infty \frac{e^{-\frac{1}{4}w^2}\mathrm{D}_m(w)}{w(p^2+w^2)}\,dw = (-)^{\frac{1}{2}(m-1)}2^{m+1}\sqrt{\frac{\pi}{2}}\frac{1}{p^2}$$

$$\times\left\{2^{-\frac{1}{2}(m+3)}\Gamma\left(\frac{m+1}{2}\right) - 2^{-m-1}e^{\frac{1}{4}p^2}\mathrm{D}_{-m-1}(p)\Gamma(m+1)\right\}, \quad . \quad . \quad . \quad (28)$$

m being an odd positive integer.

Hence

$$\int_0^\infty e^{-\frac{1}{4}w^2}\mathrm{D}_m(w)\mathrm{U}_n(2wx,\ 2\sqrt{zx})\frac{dw}{w^{n+1}}$$

$$\doteqdot \frac{e^{-\frac{z}{p}}}{p^{n-2}}\int_0^\infty \frac{e^{-\frac{1}{4}w^2}\mathrm{D}_m(w)}{w(p^2+w^2)}dw$$

$$\doteqdot (-)^{\frac{1}{2}(m-1)}2^{m+1}\sqrt{\frac{\pi}{2}}2^{-\frac{1}{2}(m+1)}\Gamma\left(\frac{m+1}{2}\right)e^{-\frac{z}{p}}p^{-n}$$

$$+(-)^{\frac{1}{2}(m+1)}\sqrt{\frac{\pi}{2}}\frac{1}{p}p^{-n}e^{-\frac{z}{p}}pe^{\frac{1}{4}p^2}\mathrm{D}_{-m-1}(p)\Gamma(m+1).$$

. . . (29)

Using (24) and (25) with the product theorem, the right-hand side can be interpreted as

$$(-)^{\frac{1}{2}(m-1)}2^{\frac{m-1}{2}}\sqrt{\frac{\pi}{2}}\Gamma\left(\frac{m+1}{2}\right)\left(\frac{x}{z}\right)^{\frac{n}{2}}\mathrm{J}_n(2\sqrt{xz})$$

$$+(-)^{\frac{1}{2}(m+1)}\sqrt{\frac{\pi}{2}}\int_0^x\left(\frac{x-\xi}{z}\right)^{\frac{n}{2}}\mathrm{J}_n(2\sqrt{z(x-\xi)})\xi^m e^{-\frac{1}{2}\xi^2}\,d\xi.$$

Therefore

$$\int_0^\infty e^{-\frac{1}{2}w^2}\mathrm{D}_m(w)\mathrm{U}_n(2wx,\ 2\sqrt{zx})\frac{dw}{w^{n+1}}$$

$$=(-2)^{\frac{m-1}{2}}\sqrt{\frac{\pi}{2}}\Gamma\left(\frac{m+1}{2}\right)\left(\frac{x}{z}\right)^{\frac{n}{2}}\mathrm{J}_n(2\sqrt{xz})$$

$$+(-)^{\frac{1}{2}(m+1)}\sqrt{\frac{\pi}{2}}\int_0^x\left(\frac{x-\xi}{z}\right)^{\frac{n}{2}}\mathrm{J}_n(2\sqrt{z(x-\xi)})\xi^m e^{-\frac{1}{2}\xi^2}\,d\xi,$$

or $$(-2)^{\frac{m-1}{2}}\sqrt{\frac{\pi}{2}}\Gamma\left(\frac{m+1}{2}\right)\left(\frac{x}{z}\right)^{\frac{n}{2}}\mathrm{J}_n(2\sqrt{xz})$$

$$+(-)^{\frac{1}{2}(m+1)}\sqrt{\frac{\pi}{2}}\int_0^x\left(\frac{\xi}{z}\right)^{\frac{n}{2}}\mathrm{J}_n(2\sqrt{z\xi})(x-\xi)^m e^{-\frac{1}{2}(x-\xi)^2}\,d\xi,$$

. . . (30)

where m is a positive odd integer and $\mathrm{R}(n)>-1$.

IV.

If we take the relation [7]

$$2\sum_{n=0}^{\infty}\frac{(2n+1)\mathrm{J}_{2n+1}(t)}{p^2+(2n+1)^2}$$

$$=\sum_{r=0}^{\infty}\frac{(-)^r t^{2r+1}}{(p^2+1^2)(p^2+3^2)\ldots[p^2+(2r+1)^2]}$$

and multiply both sides by $e^{-\frac{z}{p}} p^{-m+2}$ we get

$$2\sum_{n=0}^{\infty}\frac{(2n+1)e^{-\frac{z}{p}}J_{2n+1}(t)}{p^{m-2}[p^2+(2n+1)^2]}$$

$$=\sum_{r=0}^{\infty}\frac{(-)^r t^{2r+1}e^{-\frac{z}{p}}}{p^{m-2}(p^2+1^2)(p^2+3^2)\ldots[p^2+(2r+1)^2]}. \quad (31)$$

But
$$\frac{e^{-\frac{z}{p}}}{p^{m-2}[p^2+(2n+1)^2]} \doteqdot \frac{U_m[(4n+2)x,\ 2\sqrt{zx}]}{(2n+1)^m},$$

$$\frac{p}{(p^2+1^2)(p^2+3^2)\ldots[p^2+(2r+1)^2]} \doteqdot \frac{\sin^{2r+1}x}{\Gamma(2r+1)},$$

and
$$e^{-\frac{z}{p}}p^{-m+2} \doteqdot \left(\frac{x}{z}\right)^{\frac{m-2}{2}} J_{m-2}(2\sqrt{xz}).$$

. . . (32)

Interpreting the equation (31) with the help of these relations and the product theorem we get

$$2\sum_{n=0}^{\infty}\frac{(2n+1)J_{2n+1}(t)}{(2n+1)^m}U_m[(4n+2)x,\ 2\sqrt{zx}]$$

$$=\sum_{r=0}^{\infty}\int_0^x\left(\frac{x-\xi}{z}\right)^{\frac{m-2}{2}}J_{m-2}[2\sqrt{z(x-\xi)}](-)^r t^{2r+1}\frac{\sin^{2r+1}\xi}{2r!}\,d\xi$$

$$=\int_0^x\left(\frac{x-\xi}{z}\right)^{\frac{m-2}{2}}J_{m-2}[2\sqrt{z(x-\xi)}]t\sin\xi \times\left\{\sum_{r=0}^{\infty}\frac{(-)^r(t\sin\xi)^{2r}}{2r!}\right\}d\xi$$

$$=\int_0^x\left(\frac{x-\xi}{z}\right)^{\frac{m-2}{2}}J_{m-2}[2\sqrt{z(x-\xi)}]t\sin\xi\cos(t\sin\xi)\,d\xi.$$

. . . (33)

Now $\left(\frac{x-\xi}{z}\right)^{\frac{m-2}{2}} J_{m-2}[2\sqrt{z(x-\xi)}]t\sin\xi$ is finite for $0\leqslant\xi\leqslant x$, and $\sum_{r=0}^{\infty}\frac{(-)^r(t\sin\xi)^{2r}}{2r!}$ is a uniformly convergent series. Hence the term by term integration is justified.

Similarly, starting with the relation[7]

$$\frac{\mathrm{J}_0(t)}{p^2}+2\sum_{n=1}^{\infty}\frac{\mathrm{J}_{2n}(t)}{p^2+n^2}=\sum_{r=1}^{\infty}\frac{(-)^{r-1}(\frac{1}{2}t)^{2r-2}}{p^2(p^2+1^2)\ldots[p^2+(r-1)^2]},$$

we get

$$\frac{e^{-\frac{z}{p}}\mathrm{J}_0(t)}{p^{m+2}}+2\sum_{n=1}^{\infty}\frac{e^{-\frac{z}{p}}\mathrm{J}_{2n}(t)}{p^m(p^2+n^2)}$$

$$=\sum_{r=1}^{\infty}\frac{(-)^{r-1}(\frac{1}{2}t)^{2r-2}e^{-\frac{z}{p}}}{p^{m+2}(p^2+1^2)\ldots[p^2+(r-1)^2]},$$

and using the equations (32) and

$$\sin^{2n}\frac{x}{2}\doteqdot\frac{\Gamma(2n+1)}{2^{2n}(p^2+1^2)\ldots(p^2+n^2)}$$

and the product theorem, we have

$$\mathrm{J}_0(t)\left(\frac{x}{z}\right)^{\frac{m+2}{2}}\mathrm{J}_{m+2}(2\sqrt{xz})+2\sum_{n=1}^{\infty}\frac{1}{n^{m+2}}\mathrm{J}_{2n}(t)\mathrm{U}_{m+2}(2nx,\ 2\sqrt{zx})$$

$$=\sum_{r=1}^{\infty}(-)^{r-1}(\tfrac{1}{2}t)^{2r-2}\int_0^x\left(\frac{x-\xi}{z}\right)^{\frac{m+1}{2}}\mathrm{J}_{m+4}[2\sqrt{z(x-\xi)}]$$

$$\times\frac{2^{2r-2}\sin^{2r-2}\frac{\xi}{2}}{\Gamma(2r-1)}d\xi$$

$$=\int_0^x\left(\frac{x-\xi}{z}\right)^{\frac{m+1}{2}}\mathrm{J}_{m+1}(2\sqrt{z(x-\xi)})$$

$$\times\sum_{r=1}^{\infty}\frac{(-)^{r-1}t^{2r-2}\sin^{2r-2}\frac{\xi}{2}}{(2r-2)!}d\xi$$

$$=\int_0^x\left(\frac{x-\xi}{z}\right)^{\frac{m+1}{2}}\mathrm{J}_{m+1}(2\sqrt{z(x-\xi)})\sum_{r=0}^{\infty}\frac{(-)^rt^{2r}\sin^{2r}\frac{\xi}{2}}{2r!}d\xi$$

$$=\int_0^x\left(\frac{x-\xi}{z}\right)^{\frac{m+1}{2}}\mathrm{J}_{m+1}(2\sqrt{z(x-\xi)})\cos\left(t\sin\frac{\xi}{2}\right)d\xi. \quad . \quad (35)$$

The term by term integration can be easily justified.

V.

From the operational representations

$$\mathrm{U}_{n+1}(2wx,\ 2\sqrt{zx}) \doteqdot \frac{w^{n+1}e^{-\frac{z}{p}}}{p^{n-1}(p^2+w^2)}, \qquad \frac{1}{p} \doteqdot x,$$

$$\mathrm{U}_{m+1}(2wy,\ 2\sqrt{zy}) \doteqdot \frac{w^{m+1}e^{-\frac{z}{q}}}{q^{m-1}(q^2+w^2)}, \qquad \frac{1}{q} \doteqdot y,$$

we get

$$\frac{\mathrm{U}_{n+1}.\mathrm{U}_{m+1}}{w^{n+m+2}}dw \doteqdot \frac{e^{-z\left(\frac{1}{p}+\frac{1}{q}\right)}}{p^{n-1}q^{m-1}} \cdot \frac{1}{(p^2+w^2)(q^2+w^2)}.$$

Hence

$$\int_0^\infty \frac{\mathrm{U}_{n+1}.\mathrm{U}_{m+1}}{w^{n+m+2}}dw \doteqdot \frac{e^{-z\left(\frac{1}{p}+\frac{1}{q}\right)}}{p^{n-1}q^{m-1}} \cdot \int_0^\infty \frac{dw}{(p^2+w^2)(q^2+w^2)}$$

$$\doteqdot \frac{\pi}{2}\frac{e^{-z\left(\frac{1}{p}+\frac{1}{q}\right)}}{p^nq^m(p+q)}. \qquad \ldots\ldots \quad (36)$$

To interpret the right-hand side regard q as constant for a moment, and use

$$\frac{p}{p+q} \doteqdot e^{-qx}$$

and

$$p^{-n}e^{-\frac{z}{p}} \doteqdot \left(\frac{x}{z}\right)^{\frac{n}{2}}\mathrm{J}_n(2\sqrt{xz}).$$

We get

$$\frac{e^{-\frac{z}{p}}}{p^n(p+q)} = \frac{1}{p}.p^{-n}.e^{-\frac{z}{p}}\frac{p}{p+q}$$

$$\doteqdot \int_0^x e^{-qv}\left(\frac{x-v}{z}\right)^{\frac{n}{2}}\mathrm{J}_n[2\sqrt{z(x-v)}]\,dv, \quad \ldots \quad (37)$$

using the product theorem.

Therefore

$$\frac{e^{-z\left(\frac{1}{p}+\frac{1}{q}\right)}}{p^nq^m(p+q)} \doteqdot \int_0^x e^{-qv-\frac{z}{q}}q^{-m}\left(\frac{x-v}{z}\right)^{\frac{n}{2}}\mathrm{J}_n[2\sqrt{z(x-v)}]\,dv. \quad (38)$$

Again $$e^{-\frac{z}{q}}q^{-m} \doteqdot \left(\frac{y}{z}\right)^{\frac{m}{2}} J_m(2\sqrt{yz})$$

and

$$e^{-qv}e^{-\frac{z}{q}}q^{-m} \doteqdot 0 \quad \text{for } y<v$$

$$\doteqdot \left(\frac{y-v}{z}\right)^{\frac{m}{2}} J_m[2\sqrt{z(y-v)}] \quad \text{for } y>v.$$

Consider x greater than y, and break the interval $(0\ x)$ into $(0\ y)$ and $(y\ x)$, we have

$$\int_0^x e^{-qv-\frac{z}{q}} q^{-m}\left(\frac{x-v}{z}\right)^{\frac{n}{2}} J_n[2\sqrt{z(x-v)}]\,dv$$

$$=\left[\left\{\int_0^y + \int_y^x\right\} e^{-qv-\frac{z}{q}} q^{-m}\left(\frac{x-v}{z}\right)^{\frac{n}{2}} J_n[2\sqrt{z(x-v)}]\,dv\right]$$

$$=\int_0^y \left(\frac{y-v}{z}\right)^{\frac{m}{2}}\left(\frac{x-v}{z}\right)^{\frac{n}{2}} J_m[2\sqrt{z(y-v)}]\,.\,J_n[2\sqrt{z(x-v)}]\,dv$$

as the integrand in the second member vanishes after interpretation. Hence

$$\int_0^\infty U_{n+1}(2wx,\ 2\sqrt{zx})\,.\,U_{m+1}(2wy,\ 2\sqrt{zy})\,\frac{dw}{w^{m+n+2}}$$

$$=\frac{\pi}{2}\int_0^y \frac{(y-v)^{\frac{m}{2}}(x-v)^{\frac{n}{2}}}{z^{\frac{m+n}{2}}} J_m[2\sqrt{z(y-v)}]J_n[2\sqrt{z(x-v)}]\,dv$$

$$x>y. \quad . \quad . \quad . \quad (39)$$

Similarly for the case when x is less than y we have $v<x<y$, and hence

$$\int_0^x e^{-qv-\frac{z}{q}} q^{-m}\left(\frac{x-v}{z}\right)^{\frac{n}{2}} J_n[2\sqrt{z(x-v)}]\,dv$$

$$=\int_0^x \left(\frac{y-v}{z}\right)^{\frac{m}{2}}\left(\frac{x-v}{z}\right)^{\frac{n}{2}} J_m[2\sqrt{z(y-v)}]J_n[2\sqrt{z(x-v)}dv.$$

Therefore

$$\int_0^\infty U_{n+1}(2wx,\ 2\sqrt{zx})\,.\,U_{m+1}(2wy,\ 2\sqrt{2y})\,\frac{dw}{w^{n+m+2}}$$

$$=\frac{\pi}{2}\int_0^x \frac{(y-v)^{\frac{m}{2}}(x-v)^{\frac{n}{2}}}{z^{\frac{m+n}{2}}} J_m[2\sqrt{z(y-v)}]J_n[2\sqrt{z(x-v)}]\,dv.$$

$$x<y. \quad . \quad . \quad (40)$$

VI.

Let $$h(x)=\mathrm{U}_m(2wx,\ 2\sqrt{zx})$$

$$\doteqdot \frac{w^m e^{-\frac{z}{p}}}{p^{m-2}(p^2+w^2)} \qquad \mathrm{R}(m)>-1$$

$$=f(p), \quad \text{say.}$$

Therefore

$$\frac{1}{p^{n-1}}f\left(\frac{1}{p}\right)=w^{m-1}\frac{1}{p}\cdot\frac{1}{p^{n-m-1}}e^{-zp}\frac{pw}{1+p^2w^2}.$$

But $$\frac{pw}{1+p^2w^2}\doteqdot \sin\frac{x}{w}$$

and $$e^{-zp}\frac{pw}{1+p^2w^2}\doteqdot 0 \quad \text{if } x<z$$

$$\doteqdot \sin\frac{x-z}{w} \quad \text{if } x>z.$$

Hence

$$\frac{1}{p^{n-1}}f\left(\frac{1}{p}\right)\doteqdot \frac{w^{m-1}}{\Gamma(n-m)}\int_0^x (x-\xi)^{n-m-1}\sin\frac{\xi-z}{w}\,.d\xi \quad \text{if } x>z$$

$$\doteqdot 0 \quad \text{if } x<z.$$

We will now use the formula [8] of the operational calculus

$$\frac{1}{p^{n-1}}f\left(\frac{1}{p}\right)\doteqdot \int_0^\infty \left(\frac{x}{s}\right)^{\frac{n}{2}}\mathrm{J}_n(2\sqrt{xs})\bar{h}(s)\,ds. \quad . \quad (41)$$

Interpreting the left-hand side, and substituting for $h(s)$ its value, we get

$$\int_0^\infty \left(\frac{x}{s}\right)^{\frac{n}{2}}\mathrm{J}_n(2\sqrt{xs})\mathrm{U}_m(2ws,\ 2\sqrt{zs})\,ds$$

$$=\frac{w^{m-1}}{\Gamma(n-m)}\int_0^x (x-\xi)^{n-m-1}\sin\left(\frac{\xi-z}{w}\right)d\xi \quad x>z$$

$$\mathrm{R}(m)>-1, \quad . \quad . \quad (42)$$

or $$=0 \quad \text{if } x<z.$$

In the particular case when $n=m$ we have

$$\int_0^\infty \left(\frac{x}{s}\right)^{\frac{n}{2}} J_n(2\sqrt{xs})U_n(2ws, 2\sqrt{zs})\,ds$$

$$\doteqdot w^{n-1}e^{-zp}\frac{pw}{1+p^2w^2}$$

$$\doteqdot 0 \quad \text{if } x<z$$

or

$$\doteqdot w^{n-1}\sin\frac{x-z}{w} \quad \text{if } x>z \quad R(n)>-1.$$

Hence

$$\int_0^\infty \left(\frac{x}{s}\right)^{\frac{n}{2}} J_n(2\sqrt{xs})U_n(2ws, 2\sqrt{zs})\,ds=0 \quad \text{if } x<z$$

$$=w^{n-1}\sin\frac{x-z}{w} \quad \text{if } x>z.$$

. . . (43)

VII.

We have [8]

$$\frac{p}{\sqrt{1+p^2}}f(\sqrt{1+p^2})$$

$$\doteqdot h(x)-\int_0^x h(\sqrt{x^2-s^2})J_1(s)\,ds$$

$$\doteqdot h(x)-\int_0^x h(\xi)\frac{\xi}{\sqrt{x^2-\xi^2}}J_1(\sqrt{x^2-\xi^2})\,d\xi \quad . \quad (44)$$

if

$$f(p)\doteqdot h(x).$$

Let

$$h(x)=U_n(2wx, 2\sqrt{zx}).$$

Therefore

$$f(p)=\frac{w^n e^{-\frac{z}{p}}}{p^{n-2}(p^2+w^2)}.$$

Hence

$$\frac{p}{\sqrt{1+p^2}}f(\sqrt{1+p^2})=w^n e^{-\frac{z}{\sqrt{1+p^2}}}\cdot\frac{p}{(p^2+1)^{\frac{n-1}{2}}}\frac{1}{1+p^2+w^2}$$

$$=\sum_{r=0}^{\infty}\frac{w^n}{\sqrt{1+w^2}}\frac{(-z)^r}{r!}\frac{1}{p}\cdot\frac{p}{(1+p^2)^{\frac{r+n-1}{2}}}\cdot\frac{p\sqrt{1+w^2}}{1+p^2+w^2}.$$

But
$$\frac{p\sqrt{1+w^2}}{1+p^2+w^2} \doteq \sin(x\sqrt{1+w^2})$$

and
$$\frac{p}{(1+p^2)^{\frac{r+n-1}{2}}} \doteq \frac{\sqrt{\pi}}{2^{\frac{r+n-2}{2}}\Gamma\left(\frac{r+n-1}{2}\right)} x^{\frac{r+n-2}{2}} \mathrm{J}_{\frac{r+n-2}{2}}(x).$$

Hence, using these results and the product theorem we can interpret the formula (44) as

$$\mathrm{U}_n(2wx, 2\sqrt{zx}) - \int_0^x \mathrm{U}_n[2w\sqrt{x^2-s^2}, 2\sqrt{z\sqrt{x^2-s^2}}]\mathrm{J}_1(s)\,ds$$

$$= \mathrm{U}_n(2wx, 2\sqrt{zx}) - \int_0 \mathrm{U}_n(2w\xi, 2\sqrt{z\xi})\frac{\xi}{\sqrt{x^2-\xi^2}} \times \mathrm{J}_1(\sqrt{x^2-\xi^2})\,d\xi$$

$$= \sum_{r=0}^{\infty} \frac{\sqrt{\pi}w^n(-z)^r_{\mathrm{J}}}{2^{\frac{r+n-2}{2}}\Gamma\left(\frac{r+n-1}{2}\right).r!\sqrt{1+w^2}} \int_0^x \xi^{\frac{r+n-2}{2}} \times \mathrm{J}_{\frac{r+n-2}{2}}(\xi).\sin[\sqrt{1+w^2}(x-\xi)]\,d\xi. \quad (45)$$

VIII.

From the results
$$p^{-n}e^{-\frac{z}{p}} \doteq \left(\frac{x}{z}\right)^{\frac{n}{2}} \mathrm{J}_n(2\sqrt{zx}),$$

$$\frac{p}{(w^2+p^2)^m} \doteq \frac{\sqrt{\pi}}{\Gamma(m)}\left(\frac{x}{2w}\right)^{m-\frac{1}{2}} \mathrm{J}_{m-\frac{1}{2}}(wz),$$

we get with the help of the product theorem

$$\frac{\sqrt{\pi}}{\Gamma(m)z^{\frac{n}{2}}(2w)^{m-\frac{1}{2}}} \int_0^x (x-\xi)^{m-\frac{1}{2}}\xi^{\frac{n}{2}}\mathrm{J}_n(2\sqrt{z\xi})\mathrm{J}_{m-\frac{1}{2}}[w(x-\xi)]\,d\xi$$

$$\doteq \frac{e^{-\frac{z}{p}}}{(p^2+w^2)p^{2m+n-2}}\left(1+\frac{w^2}{p^2}\right)^{1-m}$$

$$= \frac{1}{w^{n+2m}} \sum_{r=0}^{\infty} \frac{(1-m)_r}{r!} \frac{w^{n+2m+2r}}{p^{n+2m+2r-2}} \frac{e^{-\frac{z}{p}}}{p^2+w^2}$$

$$\doteq \frac{1}{w^{n+2m}} \sum_{r=0}^{\infty} \frac{(1-m)_r}{r!} \mathrm{U}_{n+2m+2r}(2wx, 2\sqrt{2x})$$

after interpretation.

Therefore

$$\int_0^x \xi^{\frac{n}{2}} (x-\xi)^{m-\frac{1}{2}} J_n(2\sqrt{z\xi}) J_{m-\frac{1}{2}}[w(x-\xi)]\, d\xi$$

$$= \frac{z^{\frac{n}{2}} 2^m \Gamma(m)}{\sqrt{2\pi} w^{n+m+\frac{1}{2}}} \sum_{r=0}^{\infty} \frac{(1-m)_r}{r!} U_{n+2m+2r}(2wx, 2\sqrt{zx}). \quad (46)$$

References.

(1) Watson, ' Theory of Bessel Functions,' chap. xvi. p. 537.
(2) P. Humbert, ' Le Calcul Symbolique.'
(3) Mitra, Bull. Cal. Math. Soc. xxv. p. 175 (1933).
(4) Goldstein, Proc. Lond. Math. Soc. (2) xxxiv. (1932).
(5) Varma, Proc. Ben. Math. Soc. ix. (1927).
(6) Varma, Proc. Camb. Phil. Soc. xxxiii. (1937).
(7) Shastri, Proc. Physico-Math. Soc. Jap. (3) xvii. (1935).
(8) Niessen, Phil. Mag. (7) xx. (1935).

LXXXV. *The Operational Theory of Solid Friction.* By Louis A. Pipes, *Ph.D.*, *Alumni Research Fellow, The University of Wisconsin* *.

I. *Summary.*

It is the purpose of this paper to present a discussion of the interesting and important phenomenon of solid friction by the use of the Laplacian Transform or operational method of attack. The inherent simplicity of the approach to this non-linear problem makes it possible to obtain some interesting results most easily.

II. *Free Vibrations. No Viscous Damping.*

Let the mechanism shown schematically below be considered :

Fig. 1.

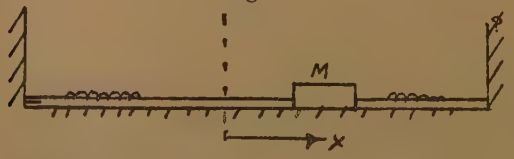

This system consists of a mass m, connected to rigid supports by means of springs of effective stiffness h.

* Communicated by the Author.

The mass is supposed to slide on a rough surface and hence experience a frictional force F, which is directed in a direction opposite to that of the velocity.

Let the motion start in such a manner that

$$\left.\begin{aligned} \text{at } t=0, \quad x&=a, \\ \dot{x}&=0, \end{aligned}\right\} \quad \ldots\ldots \quad (1)$$

That is, the mass is pulled out a distance a from its equilibrium position and released at $t=0$. The equation that is valid during motion, that is, when $\dot{x}=0$, is

$$\left.\begin{aligned} &m\ddot{x}+hx=\pm\mathrm{F}, \\ \text{or if} \quad &w^2=\frac{h}{m} \quad \text{and} \quad \mathrm{A}=\frac{\mathrm{F}}{m}, \end{aligned}\right\} \quad \ldots\ldots \quad (2)$$

then

$$\ddot{x}+w^2x=+\mathrm{A} \quad \ldots\ldots \quad (3)$$

during the interval $0<t<\pi/w$ when the force is acting in the positive x direction. It is expressly understood that this is true provided that the initial position $x=a$ is such that

$$w^2a>\mathrm{A}, \quad \ldots\ldots \quad (4)$$

so that the spring force is greater than the frictional force. That is, the initial displacement lies out of the so-called "dead region"

$$x=\pm\frac{\mathrm{A}}{w^2}. \quad \ldots\ldots \quad (5)$$

If motion is possible, and the first swing to the left is of such magnitude that it is still outside the "dead region," then

$$\ddot{x}+w^2x+-\mathrm{A}, \quad \ldots\ldots \quad (6)$$

for $$\frac{\pi}{w}<t<\frac{2}{w}.$$

We can thus write the equation of motion as

$$\ddot{x}+w^2x=\mathrm{A}(t), \quad \ldots\ldots \quad (7)$$

where A(t) is a discontinuous function of the "Meander type" and whose graph is

Fig. 2.

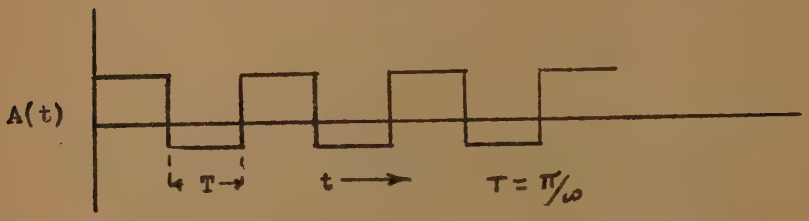

provided that $\dot{x}=0$, that is, the motion continues and that successive swings are of such amplitude that they lie outside the "dead region."

We now treat the equation operationally. We shall follow the notation of Van der Pol[1].

Let $$y \doteqdot x \quad . \quad . \quad . \quad . \quad . \quad . \quad . \quad (8)$$

and $$g(p) \doteqdot \mathrm{A}(t) \quad . \quad . \quad . \quad . \quad . \quad . \quad (9)$$

that is,

y is the operational equivalent of x,

$g(p)$ is the operational equivalent of A(t).

Under the boundary conditions

$$t=0, \quad \left.\begin{matrix} x=a \\ \dot{x}=0 \end{matrix}\right\} \quad . \quad . \quad . \quad . \quad . \quad (10)$$

we get, in the usual manner, the transformed equation

$$(p^2+w^2)y=p^2a+\mathrm{A}(1-2e^{-\mathrm{T}p}+2e^{-2\mathrm{T}p}-2e^{-3\mathrm{T}p}+\ldots). \quad (11)$$

$$\mathrm{T}=\frac{\pi}{w}.$$

But by a well-known result

$$\tanh\frac{\mathrm{T}p}{2}=1-2e^{-\mathrm{T}p}+2e^{-2\mathrm{T}p}-2e^{-3\mathrm{T}p}+\ldots \quad . \quad (12)$$

The transformed equation may be written in the form

$$y(p)=\frac{1}{p^2+w^2}\left(p^2a+\mathrm{A}\tanh\frac{\mathrm{T}p}{2}\right). \quad . \quad . \quad (13)$$

and we have the explicit solution

$$x(t)=\frac{1}{2wi}\int_{c-i\infty}^{c+i\infty}\frac{ye^{pt}dp}{p}, \quad i=\sqrt{-1}, \quad . \quad . \quad (14)$$

where c is such that all the singularities of the integrand are to the left of the path of integration.

This is a most concise result. For purposes of actual computation, however, it is preferable to resort to the following procedure :

Remembering the operational equivalents

$$\frac{p^2}{p^2+w^2} \doteq \cos(wt), \quad . \quad . \quad . \quad . \quad . \quad (15)$$

$$\frac{1}{p^2+w^2} \doteq \frac{1-\cos(wt)}{w^2}, \quad . \quad . \quad . \quad . \quad (16)$$

and the well-known operational theorem

$$\left.\begin{array}{ll} \text{if} & g(p) \doteq g(t) \\ \text{then} & e^{-pt}g(p) \doteq \begin{cases} 0 & t>\mathrm{T} \\ g(t-\mathrm{T}) & t>\mathrm{T} \end{cases} \end{array}\right\}, \quad . \quad . \quad (17)$$

and we have explicitly

$$x=a\cos(wt)+\frac{\mathrm{A}[1-\cos(wt)]}{w^2}, \quad 0<t<\mathrm{T}, \quad . \quad (18)$$

$$x=a\cos(wt)+\frac{\mathrm{A}}{w^2}[1-\cos(wt)]-\frac{2\mathrm{A}}{w^2}[1=\cos w(t-\mathrm{T})], \quad (19)$$

$$\mathrm{T}<t<2\mathrm{T},$$

and the solution for greater values of t may be similarly written down. We note that at

$$t=0, \quad x=-a+\frac{2\mathrm{A}}{w^2}, \quad . \quad . \quad . \quad . \quad (26)$$

$$t=2\mathrm{T}, \quad x=a-\frac{4\mathrm{A}}{w^2}, \text{ etc.} \quad . \quad . \quad . \quad (27)$$

The solution should be continued until one of the swings lies inside the "dead region." In such a case the motion stops.

III. *Combined Solid and Viscous Damping.*

If, besides experiencing solid friction, the mass also undergoes damping proportional to its velocity throughout its motion, then the equation of motion is

$$\ddot{x}+2k\dot{x}+w_0^2x=\mathrm{A}(t). \quad . \quad . \quad . \quad . \quad . \quad (22)$$

We shall in this case assume $w_0^2 < k^2$, so that the motion is not critically damped. Then if we place

$$w^2 = w_0^2 - k^2, \quad . \quad . \quad . \quad . \quad . \quad . \quad (23)$$

the motion reverses at

$$t = \frac{\pi}{w}, \quad t = \frac{2\pi}{w}, \text{ etc.}, \quad . \quad . \quad . \quad . \quad (24)$$

accordingly, we can again write

$$A(t) \doteqdot g(p) = A(1 - 2e^{-Tp} + 2e^{-2Tp} - 2e^{-3Tp} + \ldots), \quad (25)$$

where

$$T = \frac{\pi}{w}.$$

Again, let $x \doteqdot y$ and impress the boundary conditions

$$\text{at } t=0, \quad \begin{cases} x = a \\ \dot{x} = 0 \end{cases}, \quad . \quad . \quad . \quad . \quad . \quad (26)$$

the equation transforms to

$$p^2 y + 2kpy + w_0^2 y = p^2 a + 2pka + g(p), \quad . \quad . \quad (27)$$

or

$$y = \frac{p^2 a + 2pka + g(p)}{p^2 + 2kp + w_0^2}. \quad . \quad . \quad . \quad . \quad (28)$$

Now we have the operational equivalents

$$\frac{p^2}{p^2 + 2hp + w_0^2} \doteqdot \frac{-w_0}{w} e^{-kt} \sin(wt - b), \quad w^2 = w_0^2 - k^2,$$

$$b = \tan^{-1} \frac{w}{k}. \quad (29)$$

Since

$$\frac{p}{p^2 + 2kp + w_0^2} \doteqdot \frac{e^{-kt} \sin(wt)}{w}, \quad . \quad . \quad . \quad . \quad . \quad (30)$$

$$\frac{1}{p^2 + 2kp + w_0^2} \doteqdot \frac{1}{w_0^2}\left[1 - \frac{w_0}{w} e^{-kt} \sin(wt + b)\right]. \quad (31)$$

Now

$$g(p) = A[1 - 2e^{-Tp} + 2e^{-2Tp} - 2e^{-3Tp} + \ldots]. \quad . \quad (32)$$

Hence

$$x = -\left(\frac{aw_0}{w}\right) e^{-kt} \sin(wt - b) + \left(\frac{ka}{w}\right) e^{-kt} \sin(wt)$$

$$+ \left(\frac{A}{w_0^2}\right)\left[1 - \left(\frac{w_0}{w}\right) e^{-kt} \sin(wt + b)\right], \quad (33)$$

$$0 < t < T,$$

and

$$x=-\left(\frac{aw_0}{w}\right)e^{-kt}\sin(wt-b)+\left(\frac{ka}{w}\right)e^{-kt}\sin(wt)$$
$$+\left(\frac{A}{w_0^2}\right)\left[1-\left(\frac{w_0}{w}\right)e^{-kt}\sin(wt+b)\right]$$
$$-\left(\frac{2A}{w_0^2}\right)\left[1-\left(\frac{w_0}{w}\right)e^{-k(t-T)}\sin[]\,w(t-T)+b[]\right], \quad (34)$$
$$\text{for } T<t<2T,$$

as t continues to increase, more and more terms may be added in a routine manner. The solution should be tested to determine whether the maximum amplitude of successive swings falls within the "dead region." In such a case the motion ceases.

IV. *The Velocity.*

In some cases a knowledge of the velocity is desired. Rather than take the derivative of the displacement to determine the velocity it appears simpler to treat the velocity itself in an operational manner directly.

Considering the viscously damped case for generality, we return to the equation

$$\ddot{x}+2k\dot{x}+w_0^2x=A(t). \quad (35)$$

Let

$$x=\int_{-\infty}^{t}v\,dt, \quad x=v. \quad (36)$$

Hence the equation may be written as

$$\dot{v}+2kv+w^2\int_{-\infty}^{t}v\,dt=A(t). \quad (37)$$

Let

$$z\doteqdot v, \quad (38)$$

then $$\dot{v}\doteqdot pz-pv_0, \quad \text{where } v_0=v, \quad \text{at } t=0, \quad (39)$$

$$x=\int_{-\infty}^{t}v\,dt\doteqdot a+\left(\frac{1}{p}\right)z, \quad x=a, \quad \text{at } t=0. \quad (40)$$

Let $$g(p)=A(t). \quad (41)$$

Then the transformed equation is

$$pz+2kz+w^2\frac{z}{p}=g(p)-w_0^2a, \quad (42)$$

where use has been made of the initial boundary relations

$$v=0, \quad x=a, \quad \text{at } t=0. \quad . \quad . \quad . \quad . \quad . \quad (43)$$

Hence

$$z=-\frac{pw_0^2a}{(p+2kp+w_0^2)}+\frac{pg(p)}{(p+2kp+w_0^2)}, \quad . \quad . \quad (44)$$

and $$g(p)=\mathrm{A}[1-2e^{-\mathrm{T}p}+2e^{-2\mathrm{T}p}-2e^{-3\mathrm{T}p}+\ldots]. \quad . \quad (45)$$

Now using the operational equivalent

$$\frac{p}{(p^2+2kp+w_0^2)} \doteq \frac{e^{-pt}\sin(wt)}{w} \quad . \quad . \quad . \quad . \quad (46)$$

Hence

$$v=\frac{(\mathrm{A}-w_0^2a)}{w}e^{-kt}\sin(wt), \quad 0<t<\mathrm{T}, \quad . \quad . \quad (47)$$

and

$$v=(\mathrm{A}-w_0^2)e^{-kt}\sin(wt)-\frac{2\mathrm{A}}{w}e^{-k(t-\mathrm{T})}\sin[w(t-\mathrm{T})], \quad (48)$$

$$\mathrm{T}<t<2\mathrm{T},$$

and succeeding terms may be added as t increases.

V. *Forced Vibration.* (*Non-Resonant Case.*)

A. *The Velocity.*

If the mass experiences a sinusoidal driving force of magnitude M sin (nt), then the equation of motion is

$$m\ddot{x}+kx=\mathrm{F}+\mathrm{M}\sin(nt) \quad . \quad . \quad . \quad . \quad . \quad (49)$$

in the absence of viscous damping. Now let

$$\frac{k}{m}=w^2, \quad \mathrm{A}=\frac{\mathrm{F}}{m}, \quad \frac{\mathrm{M}}{m}=\mathrm{N}.$$

Then the equation may be written

$$\ddot{x}+w^2x=\mathrm{N}\sin(nt). \quad . \quad . \quad . \quad . \quad . \quad (50)$$

Let

$$\dot{x}=v, \quad x=\int_{-\infty}^{t} v\,dt; \quad . \quad . \quad . \quad . \quad (51)$$

therefore $$\dot{v}+w^2\int_{-\infty}^{t} v\,dt=\mathrm{A}+\mathrm{N}\sin(nt). \quad . \quad . \quad (52)$$

Let

$$z \doteqdot v, \quad \text{and at } t=0, \quad v=0 \quad \text{and} \quad x=a. \quad . \quad (53)$$

That is the motion is supposed to start from rest when the mass is at a distance a to the right. Then, since

$$\mathrm{N}\sin(ut) \doteqdot \frac{\mathrm{N}np}{(p^2+n^2)}, \quad . \quad . \quad . \quad . \quad . \quad (54)$$

the transformed equation is

$$pz+\frac{w^2z}{p}=g(p)-w^2a+\frac{\mathrm{N}np}{(p^2+n^2)}, \quad . \quad . \quad (55)$$

and in this case

$$g(p)=\mathrm{A}[1-2e^{-t_1p}+2e^{-t_2p}-2e^{-t_3p}+\ldots], \quad . \quad (56)$$

where t_1, t_2, t_3, etc. are the times of successive reversals of the motion. t_1, the time of the first reversal, may be found by equating $v=0$, as will be shown.

We have

$$z=\frac{pg(p)}{(p^2+w^2)}=\frac{pw^2a}{(p^2+w^2)}+\frac{\mathrm{N}np^2}{(p^2+w^2)(p^2+n^2)}. \quad (57)$$

Now we have the operational equivalents

$$\frac{p}{(p^2+w^2)} \doteqdot \frac{\sin(wt)}{w}, \quad . \quad . \quad . \quad . \quad . \quad . \quad (58)$$

$$\frac{p^2}{(p^2+w^2)(p^2+n^2)} \doteqdot \frac{1}{(w^2-n^2)}[\cos(nt)-\cos(wt)], \quad (59)$$

provided $w^2 \neq n^2$, the case of non-resonance.

Hence

$$v=\frac{\mathrm{N}n}{(w^2-n^2)}[\cos(nt)-\cos(wt)]+\frac{\sin(wt)}{w}(\mathrm{A}-w^2a) \quad (60)$$

$$\text{for } 0<t<t_1.$$

Now let

$$\mathrm{K}_1=\frac{(\mathrm{A}-w^2a)}{w}, \quad \mathrm{K}_2=\frac{\mathrm{N}n}{(m^2-w^2)}, \quad . \quad . \quad (61)$$

then $$v=(\sqrt{\mathrm{K}_1^2+\mathrm{K}_2^2})\sin(wt+b)-\mathrm{K}_2\cos(nt), \quad . \quad (62)$$

$$b=\tan^{-1}\left(\frac{\mathrm{K}_2}{\mathrm{K}_1}\right). \quad . \quad . \quad . \quad . \quad . \quad (63)$$

Now at $t=t_1$,

$$v=0, \quad . \quad . \quad . \quad . \quad . \quad . \quad . \quad (64)$$

or

$$\frac{\sin(wt_1+b)}{\cos mt_1}=\frac{K_2}{(K_1^2+K_2^2)} \quad . \quad . \quad . \quad . \quad (65)$$

This equation may be solved by the usual graphical method if numerical values are available and t_1 obtained.

Now for the interval $t_1<t<t_2$

$$v=\frac{Nn}{(w^2-m^2)}[\cos(nt)-\cos(wt)]+\frac{\sin(wt)}{w}(A-w^2a) - \frac{2A}{w}\sin w(t-t_1). \quad (66)$$

By again equating $v=0$ at $t=t_2$ an equation to determine the value of t_2 is obtained and a further term in the series determined. The process may be repeated as far as desired. It is seen that the case of forced solid friction is quite a complicated phenomenon in that the so-called "transient terms" persist.

B. *The Displacement.*

If (67) $y=x$, the equation $x+w^2x=A+N\sin(nt)$ is transformed to

$$(p^2+w^2)y=p^2a+A[1-2e^{-t_1p}+2e^{-t_2p}-2e^{-t_3p}+\ldots] + \frac{Nnp}{(p^2+n^2)}, \quad (68)$$

or

$$y=\frac{Nnp}{(p^2+w^2)(p^2+n^2)}+\frac{p^2a}{(p^2+w^2)}+\frac{A}{(p^2+w^2)} \times[1-2e^{-t_1p}+2e^{-t_2p}\ldots]. \quad (69)$$

Now we have the operational equivalents

$$\frac{p}{(p^2+w^2)(p^2+n^2)}-\frac{\sin(wt)}{w(n^2-w^2)}+\frac{\sin(nt)}{n(w^2-n^2)}, \quad (70)$$

$$n^2 \neq w^2.$$

Therefore

$$x=\frac{Nn\sin(wt)}{w(n^2-w^2)}+\frac{N\sin(nt)}{(w^2-n^2)}+a\cos(wt)+\frac{\left(\frac{A}{w^2}\right)}{[1-\cos(wt)]}, \quad 0<t<t_1, \quad . \quad . \quad . \quad (71)$$

and

$$x=\frac{\mathrm{N}n\sin(wt)}{w(n^2-w^2)}+\frac{\mathrm{N}\sin(nt)}{(w^2-n^2)}+a\cos(wt)+\frac{\left(\frac{\mathrm{A}}{w^2}\right)}{[1-\cos(wt)]}$$
$$-\left(\frac{2\mathrm{A}}{w^2}\right)[1-\cos w(t-t_1)]. \quad (72)$$
$$t_1<t_1<t_2.$$

VI. *Forced Vibration (Resonant Case).*

A. *The Velocity.*

In case of resonance, that is, $w=n$, the procedure is exactly as before except that some of the operational equivalents differ. In this case the operational equivalent for the velocity is

$$z=\frac{pg(p)}{(p^2+w^2)}-\frac{pw^2a}{(p^2+w^2)}+\frac{\mathrm{N}wp^2}{(p^2+w^2)^2}. \quad . \quad (73)$$

Now, we have the operational equivalents

$$\frac{p^2}{(p^2+w^2)^2}\doteq\frac{t\sin(wt)}{2w}, \quad . \quad . \quad . \quad . \quad . \quad (74)$$

and hence

$$v=\sin(wt)\left[\left(\frac{\mathrm{N}t}{2}\right)-\frac{\mathrm{A}}{w}-wa\right], \quad . \quad . \quad . \quad (75)$$
$$0<t<t_1.$$

Now, if

$$\frac{\pi}{w}<\left(\frac{2}{\mathrm{N}}\right)\left(wa-\frac{\mathrm{A}}{w}\right), \quad . \quad . \quad . \quad . \quad (76)$$

then

$$v=0 \quad \text{at} \quad t=t_1=\frac{\pi}{w}, \quad . \quad . \quad . \quad . \quad . \quad (77)$$

or if

$$\frac{\pi}{w}>\left(\frac{2}{\mathrm{N}}\right)\left(wa-\frac{\mathrm{A}}{w}\right), \quad . \quad . \quad . \quad . \quad (78)$$

then

$$t_1=\left(\frac{2}{\mathrm{N}}\right)\left(wa-\frac{\mathrm{A}}{w}\right). \quad . \quad . \quad . \quad . \quad . \quad (79)$$

In any case for the interval $t_1<t<t_2$ where t_2 is the time at which the velocity reverses direction the velocity is

$$v=\sin(wt)\left[\frac{\mathrm{N}t}{2}+\frac{\mathrm{A}}{w}-wa\right]-\left(\frac{2\mathrm{A}}{w}\right)\sin w(t-t_1), \quad (80)$$
$$\text{for } t_1<t<t_2,$$

and t_2 is obtained by equating v to zero. This leads to a rather complicated transcendental equation which may be solved if numerical values are available, and the solution continued for the next interval.

B. *The Displacement.*

In case of resonance the operational equivalent for the displacement is

$$y = \frac{Nwp}{(p^2+w^2)^2} + \frac{p^2 a}{(p^2+w^2)} + \left[\frac{A}{(p^2+w^2)}\right](1-2e^{-t_1 p}+\ldots). \quad . \quad . \quad . \quad (81)$$

Now

$$\frac{wp}{(p^2+w^2)^2} \doteqdot \frac{\sin(wt)}{2w^2} - \frac{t\cos(wt)}{2w}. \quad . \quad . \quad (82)$$

Hence

$$x = N\left[\frac{\sin(wt)}{2w^2} - \frac{t\cos(wt)}{2w}\right] + \cos(wt) + \frac{A[1-\cos(wt)]}{w^2}, \quad \text{for } 0<t<t_1, \quad . \quad . \quad . \quad (83)$$

and

$$x = N\left[\frac{\sin(wt)}{2w^2} - \frac{t\cos(wt)}{2w}\right] + a\cos(wt) + \frac{A[1-\cos(wt)]}{w^2}, \quad \text{for } t_1<t<t_2, \quad . \quad . \quad . \quad (84)$$

and the solution for larger values of t may be similarly obtained.

It is to be noted that because of the factor $t\cos(wt)$ the successive swings reach greater and greater amplitudes. In this respect the phenomenon of solid friction damping differs from that of viscous damping in that the amplitude in the case of resonance reaches an indefinitely great value.

Unfortunately because of the transcendental character of the equations for t_1, t_2, etc., the solution may only be performed in the presence of numerical values.

VII. *Conclusion.*

An explicit solution for the velocity and displacement of a mass-spring system undergoing solid friction has been given. The phenomenon is of such a nature that it lends itself very readily to an operational discussion,

because of the discontinuous character of the damping function. It is hoped that this presentation will give an impetus to the operational discussion of non-linear systems of this type.

VIII. *Bibliography.*

(1) Van der Pol, "A Simple Proof and an Extension of Heaviside's Operational Calculus for Invariable Systems," Phil. Mag. vii. pp. 1153–1162 (1929).
(2) Harry Bateman, 'Partial Differential Equations of Mathematical Physics,' p. 499, Cambridge.
(3) H. S. Rowell, Phil. Mag. (6) xliv. pp. 284, 951 (1922).
(4) L. S. Jacobsen, "Forced Vibration swith Combined Coulomb and Viscous Friction," Trans. A.S.M.E. Paper APM 53–9 (1931).

LXXXVI. *The Viscosity of Air, Oxygen, and Nitrogen.* *By* P. J. Rigden, *B.Sc., Senior Scholar of the University of Reading* *.

Introduction.

FOR many years the value of the electronic charge as obtained by Millikan has been in disagreement with values of e obtained by other methods. Millikan's value was $(4{\cdot}770 \pm {\cdot}005) \times 10^{-10}$ e.s.u., while other workers, using X-ray methods and recently electron diffraction, have obtained a value of about $4{\cdot}800 \times 10^{-10}$ e.s.u.

The only possibility of accounting for this discrepancy seemed to be an error in the value of the viscosity of air used by Millikan. Kellström † has recently redetermined the viscosity of air by a rotating cylinder method, and obtains a value of $(1834{\cdot}9 \pm 2{\cdot}7) \times 10^{-7}$ c.g.s., which inserted into Millikan's data yields $e = 4{\cdot}818 \times 10^{-10}$ e.s.u. In 1936 Bond ‡ made some preliminary experiments to redetermine η for air, using a new modification of the capillary flow method and obtained $(1834{\cdot}8 \pm 0{\cdot}8) \times 10^{-7}$, in good agreement with the value obtained by Kellström. This higher value of η, however, yields a value of e considerably higher than that obtained by X-ray methods. On the other hand, if this value of η is substituted in the

* Communicated by Prof. J. A. Crowther, M.A, Sc.D.
† G. Kellström, Phil. Mag. xxiii. p. 313 (1937).
‡ W. N. Bond, Proc. Phys. Soc. xlix. p. 205 (1937).

data recently obtained for e by Bäcklin and Flemberg * by an oil-drop method, a value of $4{\cdot}800 \times 10^{-10}$ e.s.u. is obtained, in good agreement with X-ray values.

The problem of the discrepancy in the values of e is not really solved then by this latest work on η unless the rather drastic step is taken of rejecting the results of Millikan's work. Houston † has recently determined η

Fig. 1.

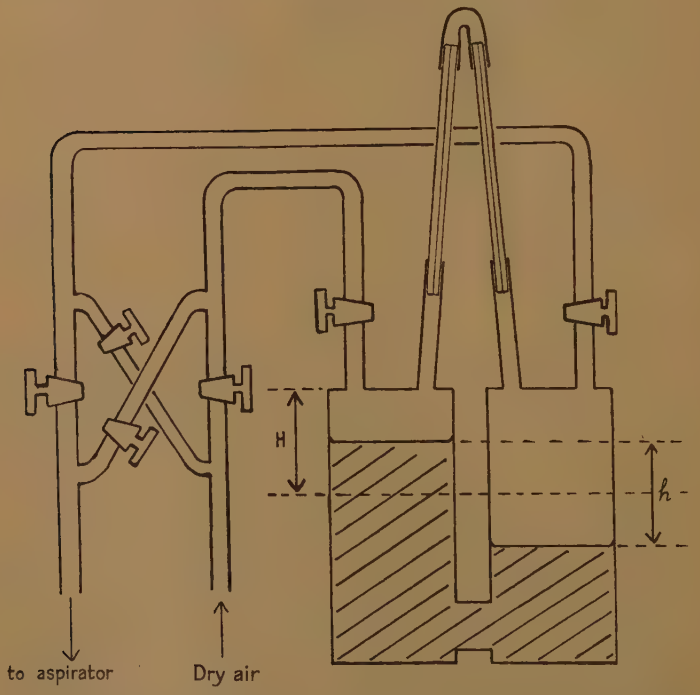

by the rotating cylinder method and obtains a much lower value than Kellström of $(1829{\cdot}2 \pm 4{\cdot}5) \times 10^{-7}$. Although current opinion seems to be that the rotating cylinder method for the viscosity of air is capable of giving the most accurate value, yet, if this were the case, it might be expected that the values obtained by Kellström and Houston would be in closer agreement. Bond's preliminary work on the value of η has shown that his

* Bäcklin and Flemberg, ' Nature,' cxxxvii. p. 656 (1936).
† Houston, Phys. Rev. liii. p. 751 (1937).

modification of the capillary flow method is capable of very considerable accuracy, and at his suggestion the present redetermination of η was carried out.

Method.

A full account of the theory of the experiment is given in Bond's paper and need not be reproduced here. Two capillary tubes in series are joined to the ends of a wide-limbed U-tube containing oil, the whole forming a closed system (fig. 1). The two oil-air surfaces are initially at different levels, and in proceeding towards the equilibrium position the air is forced round the capillaries.

Fig. 2.

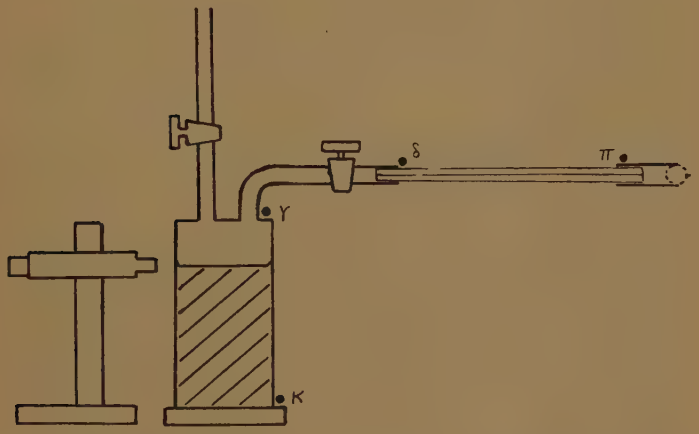

From measurements on the rate of movement of the oil the rate of flow of air can be found, and the difference in level of the oil surfaces determines the driving pressure. The final expression for η is

$$\eta=\frac{\pi g(\rho-\sigma)}{4a\Sigma\frac{l}{r^4}}\times\frac{[t]}{-[\log_e h]+\frac{\mathrm{H}g(\rho-\sigma)}{p_0}\left[\left(\frac{h}{2\mathrm{H}}\right)^2-\log_e h\right]},$$

where ρ=oil-density.

σ=air-density.

a=area of cross-section of U-tube.

h=difference of oil-levels.

l=length of capillaries.

r=radius of capillaries.

H=effective height of top of U-tube above zero oil-level.

Experimental Details.

Apparatus.

The apparatus used for this work has been an improvement in certain details on the apparatus used by Bond. The metal U-tube is the original one, but new plate-glass windows have been fitted, and it has been recalibrated entirely. The oil used by Bond was a light paraffin oil which must have given off a little vapour. In the present experiments Apiezon " A " has been used having a stated vapour pressure of only 10^{-5} mm. at 15° C. The apparatus has been completely enclosed in a plywood box, lined inside with tinplate, and outside with " Treetex" to protect it from local temperature fluctuations. It seemed undesirable to thermostat the apparatus, as the temperature inside the box was very steady during an experiment. It was thus possible to carry out determinations at different temperatures over a range of 15°–20° C., and so obtain an estimate of the temperature coefficient of viscosity. At the commencement of the work the possibility of using stainless steel capillaries was investigated, but preliminary measurements on the tubes showed them to be unsuitable for viscosity work owing to the inside surface being matt. In the present experiments three different sets of glass capillaries have been used with differing lengths and radii.

Oil-Density.

A large number of density determinations were made, using four different density bottles. Two were ordinary laboratory specific gravity bottles, one a 50 c.c. standard flask in which stood a thermometer, and the fourth a special bottle (Sprengel type) incorporating a thermometer. All four were calibrated with distilled water and gave consistent results. Measurements were made at various temperatures, including 25° C. and 31° C. Measurements over a period of several months did not reveal any systematic change of oil-density with time. The mean value of the oil-density at 17° C. was found to be $0{\cdot}8741_7 \pm 0{\cdot}00008$ gm./c.c. deduced from the determinations at different temperatures, the two extreme

values being $0{\cdot}8738_9$ and $0{\cdot}8750_3$ at 17° C. The higher temperature values at 25° C. and 31° C. were only used for determining the temperature coefficient accurately.

The area of cross-section of the U-tube was determined by introducing weighed quantities of this oil at known temperatures and measuring the rise in oil-level by means of the travelling microscope. The tube was found to be uniform to a fair degree of accuracy, and it was quite satisfactory to use the mean value of the cross-section of the whole tube in evaluating the viscosity. The mean value of the cross-section as determined by several experiments is 15·553 sq. cm. (with a probable error of $\pm 0{\cdot}01_9$ per cent.).

Oil Draining and Gas Absorption.

Experiments were made to find out if the amount of oil retained on the walls of the tube by viscosity, and subsequently drained down, was significant. The displaced oil was allowed suddenly to return to its equilibrium position and the oil-level read at subsequent time-intervals. A theoretical treatment of the problem has been made by Gaucher and Ward *, and experimental results agree fairly well with results predicted by their theory. Owing to the slow rate of movement of the oil, draining does not introduce any error into the final value for the viscosity comparable with the other errors of the experiments.

Experiments were also made to detect any absorption of the gases by the oil during a change of pressure of the gas. The oil surface was left for some time in contact with air and then the pressure suddenly diminished, but no effect could be observed. On one occasion the oil was kept displaced in the U-tube for over 48 hours and no change of level could be detected. Hence no apparent amount of gas was absorbed on the high pressure side, diffused through to the low pressure side and emitted there. It appears then that for the small pressure changes involved in the experiments there is no absorption effect of the oil.

Measurement of Temperature.

Four thermometers were used to determine temperature inside the apparatus—a fifth one being introduced when

* Gaucher and Ward, Proc. Camb. Phil. Soc. xxvi. p. 204 (1929); Phil. Mag. xliv. p. 1002 (1922).

the very long tubes were used. All temperatures were recorded a number of times during each run. The experiments were only carried out when temperature fluctuations were a minimum. All thermometers were checked against a standard at various temperatures. The thermometers were graduated in 1/10° and read to 1/100° by means of a lens.

Measurement of Time.

As described in Bond's paper, the time of passage of the meniscus is recorded with a calibrated stop-watch fitted with a "split" seconds hand. The watch was checked over several periods against Greenwich time signals, and no systematic variation could be detected over short periods. The watch was always wound fully at the commencement of each half of a run.

Data on Capillaries and Correction Terms.

As in the previous experiments, the capillaries were calibrated by filling completely with mercury and weighing the mercury. The ellipticities of the tubes were measured by a microscope at each of the ends of the tubes. The variation in cross-section along a tube was found by means of a short (5 cm.) column of mercury, whose length was measured at a number of equal intervals along the tube. The correction term $\left(\left[\frac{1}{q}\right]^2\left[q^2\right]\right)$ was evaluated as described in Bond's paper. The calculation of the other correction terms is also described, and need not be repeated here. Density determinations made on the mercury used in these experiments indicated that it could be regarded as pure to an accuracy very much greater than that required for calibrating the tubes. The table on p. 967 gives the data for all the capillaries used in the present experiments.

The final corrected values of $\Sigma l/r^4$ for the four sets of tubes used are as follows :—

Capillaries.	
1, 2	$22{\cdot}26_8 \times 10^7$ c.g.s.
5, 6, 7, 8,	$21{\cdot}803 \times 10^7$,,
1, 5, 7, 8,	$25{\cdot}76_3 \times 10^7$,,
11, 12	$17{\cdot}557 \times 10^7$,,

TABLE.

Capillary.	l (cm.).	r (cm.).	$\left[\frac{1}{q}\right]^2 [q^2]$.	Ellipticity.	Ellipticity correction.	End correction.	Slip correction.
				Per cent.	Per cent.	Per cent.	Per cent.
1.....	$37{\cdot}55_8$	$0{\cdot}02441_4$	1·00074	6·5	$0{\cdot}21_1$	0·073	0·13
2.....	$37{\cdot}39_8$	$0{\cdot}02380_1$	1·00000	7·2	$0{\cdot}25_9$		
5.....	$55{\cdot}22_3$	$0{\cdot}03058_5$	$1{\cdot}00000_5$	5·5	$0{\cdot}15_1$		
6.....	$54{\cdot}98_8$	$0{\cdot}03021_2$	1·00027	5·8	$0{\cdot}16_8$	0·069	$0{\cdot}10_5$
7.....	$54{\cdot}92_6$	$0{\cdot}03249_7$	1·00054	2·1	$0{\cdot}02_2$		
8.....	$45{\cdot}84_8$	$0{\cdot}03283_0$	$1{\cdot}00000_3$	2·0	$0{\cdot}02_0$		
11.....	$160{\cdot}39_1$	$0{\cdot}03413_1$	1·00683	—	—	0·024	$0{\cdot}09_7$
12.....	$159{\cdot}58_8$	$0{\cdot}04100_8$	1·0042	—	—	0·029	$0{\cdot}08_0$

Correction for Compressibility of the Gas in the U-tube.

This correction arises from the term

$$\frac{\mathrm{H}g(\rho-\sigma)}{p}\left[\left(\frac{h}{2\mathrm{H}}\right)^2-\log_e h\right]$$

in the final expression for viscosity. Data from a number of different runs were analysed in order to make a test of the validity of this correction. The value of η was evaluated at different values of $h/2\mathrm{H}$ during each run and the results all averaged. The values so obtained were then plotted (fig. 3) against $h/2\mathrm{H}$, and it was found that if no compressibility correction is applied the value of η deduced by this method increases as $h/2\mathrm{H}$ decreases. If now the appropriate correction term corresponding to each value of $h/2\mathrm{H}$ is subtracted from each of the uncorrected values of η a second line results (more nearly horizontal), showing that application of this correction has made η almost independent of $h/2\mathrm{H}$. In the experiments from which data for this graph were taken there was an average temperature rise of 0·13° C., which corresponds to an increase in η of 0·036 per cent. If the graph is corrected for this rise in temperature it becomes horizontal to within 0·05 per cent. of η. The possible error in the final average value of η deduced from any run after correction for compressibility has been made will only be a small fraction of 0·05 per cent., and is therefore negligible.

This analysis not only showed that the compressibility term was correct, but that there were probably no other similar terms which had been unaccounted for by the theory of the experiments. It also served as an indication of the general accuracy of the experiments themselves, since the compressibility term is only 0·23 per cent. on the final value of η, and this test shows it to be correct to less than 10 per cent. of itself.

The correction for " slip " varies with the radius of the tube, and is given by the factor

$$1+\frac{0{\cdot}000{,}033}{r}.$$

For the tubes used in the present experiments this is of the order of 0·1 per cent.

Drying the Air.

During the course of the experiments three different drying agents were used: sulphuric acid, soda lime, and calcium chloride. Changing the drying agent had no significant effect on the results.

Fig. 3.

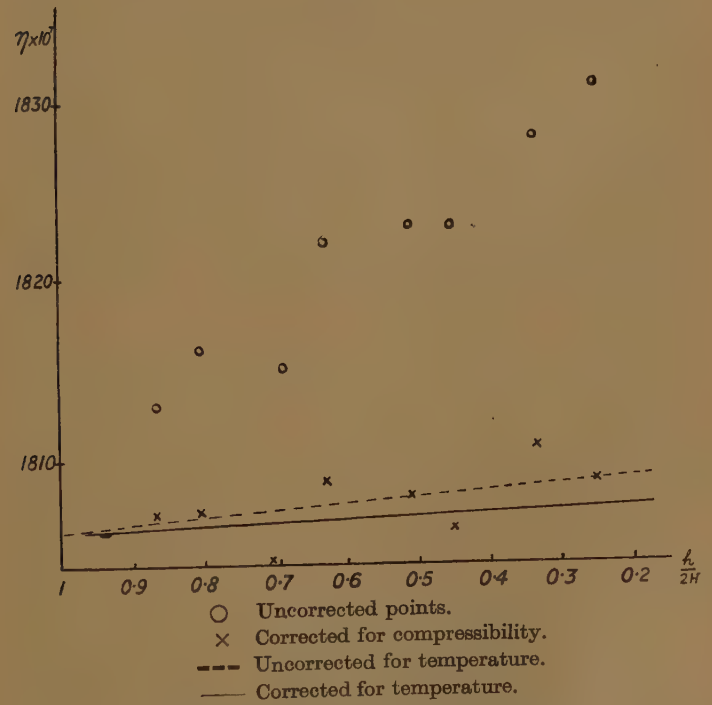

Details of Experimental Procedure.

A brief description of run No. 213 may suffice to indicate the experimental method more clearly. This run was a determination of the viscosity of air with tubes 11 and 12 in the apparatus. Taps were first opened in the inlet system (see fig. 1) to allow the oil-level to attain equilibrium if it had not already done so. The "zero" of oil-level is read on the microscope, 4·720 cm. The microscope is then set on the first timing-point, 9·500 cm. on the left-hand limb of the U-tube. Dry air is then drawn through the apparatus by means of an aspirator in order to displace the oil-levels until the oil on the left-hand side is above the 9·500 cm. mark. The

oil is maintained at this height for a minute or so in order to allow any oil retained on the walls of the right-hand tube to drain down. The stop-watch is fully wound, the taps to the supply system are closed, and the oil commences to fall. The stop-watch is started just before the high meniscus is about to pass the 9·500 cm. mark, and the reading of the watch is taken on the "split" seconds hand as the meniscus passes the cross-wire in the microscope. In this way the starting error of the watch is eliminated. The thermometers, κ, γ, δ, π, β, are all read (fig. 2), and then the microscope quickly set on the first setting on the "low" side (0·500 cm.), and the time taken when the rising meniscus passes this point. In this way the movement of the oil is timed alternately each side until nine readings have been taken and the high level has passed the 6·000 cm. mark. The following figures were obtained for this run :—

Left-hand side micr. settings.	Right-hand side micr. settings.	Time readings. mins.	Time readings. secs.	Thermometer readings (°C.). κ.	γ.	δ.	π.	β.
9·5		0	5·1	17·82	17·77	17·72	17·70	18·43
	0·5	1	36·8					
8·5		2	56·6					
	1·5	4	54·5					
7·5		6	41·8	·84	·78	·74	·71	·43
	2·5	9	26·4					
6·5		12	10·5					
	3·2	14	5·4					
6·0		16	13·8	·89	·80	·79	·72	·45°

The stop-watch is rewound, and then the oil displaced in the opposite sense, and the whole experiment repeated. The results are as follows :—

Left-hand side micr. settings.	Right-hand side micr. settings	Time readings. mins.	Time readings. secs.	Thermometer readings (°C.). κ.	γ.	δ.	π.	β.
	9·5	0	9·5	17·89	17·80	17·79	17·72	18·46
0·5		1	45·2					
	8·5	3	1·2					
1·5		5	3·1					
	7·5	6	47·0	·90	·83	·80	·74	·48
2·5		9	35·0					
	6·5	12	16·5					
3·2		14	13·8					
	6·0	16	19·1	·97	·89	·86	·78	·49

Taps are now opened to allow the oil to reach equilibrium at once, and the zero level read again, 4·720 cm. If the zero had changed slightly during an experiment the mean of the two readings is taken. The two thermometers κ and γ give the temperature of the U-tube, and the thermometers δ, π, β give the temperature along the capillaries. Applying the corrections to all the thermometers and taking mean values we have

Temperature of oil for first part of run, 17·81° C., temperature of air, 17·75° C.

Temperature of oil for second part of run, 17·87° C., temperature of air, 17·80° C.

The mean temperatures are taken as the correct temperatures for the run, viz. :—Oil, 17·84° C., air, 17·78° C. As in this case, there is often a small difference of temperature between the U-tube and the capillaries. However, the temperature at which the viscosity is measured is certainly that of the capillaries, and is taken as such. By means of logarithmic interpolation it is possible to find the position of one meniscus at the moment that the other is being timed. From these figures the difference of oil-level, h, can be found for each time recorded. The logarithms are then found and the compressibility correction added on. The tables of figures for the two halves of the run are on p. 972.

The mean of these two final values of $\frac{[t]}{[\log h]}$ is taken as the mean value of the whole run

$$\left.\begin{matrix}1686{\cdot}3\\1686{\cdot}8\end{matrix}\right\}\ \text{Mean, } 1686{\cdot}5_5.$$

The oil-density is determined from the graph of oil-densities, and at 17·84° C. is 0·87360 gm./c.c. Density of the air is 0·00121 gm./c.c. The final corrected value of $\Sigma \frac{l}{r^4}$ for tubes 11 and 12 is $17{\cdot}5572 \times 10^7$ c.g.s. The expression for η is

$$\eta = \frac{\pi g(\rho - \sigma)}{4a\,\Sigma \frac{l}{r^4}} \times 0{\cdot}43429 \times \frac{[t]}{[\log_{10} h]}.$$

Left.	Right.	t (secs.).	h.	log h.	Corrected log h.		[log h].	[t].	$\frac{[t]}{[\log h]}$.
9·500	0·064	5·1	9·564	0·9807	0·9810				
8·936	0·500	96·8	8·436	·9261	·9264	.....	0·3333	561·3	1684
8·500	0·936	176·6	7·564	·8787	·8790				
7·937	1·500	294·5	6·437	·8087	·8089	..	0·3763	633·7	1684
7·500	1·939	401·8	5·561	·7452	·7453				
6·945	2·500	566·4	4·445	·6479	·6477	..	0·3962	668·8	1689
6·500	2·946	730·5	3·554	·5507	·5501				
6·245	3·200	845·4	3·045	·4836	·4828	..	0·4027	679·3	1688
6·000	3·445	973·8	2·555	·4074	·4062				

The mean of the four values of $\frac{[t]}{[\log h]}$ in the last column is 1686·3.

For the second half of the run the figures are :—

Left.	Right.	t.	h.	log h.	Corrected log h.		[log h].	[t].	$\frac{[t]}{[\log h]}$.
0·084	9·500	9·5	9·584	0·9816	0·9819				
0·500	8·916	105·2	8·416	0·9251	·9254	.....	0·3352	565·5	1687
0·916	8·500	181·2	7·584	·8799	·8802				
1·500	7·922	303·1	6·422	·8076	·8078	..	0·3745	631·3	1686
1·929	7·500	407·0	5·571	·7460	·7461				
2·500	6·935	575·0	4·435	·6469	·6467	..	0·3985	672·6	1688
2·939	6·500	736·5	3·561	·5515	·5509				
3·200	6·238	853·8	3·038	·4825	·4817	..	0·4006	676·0	1688
3·439	6·000	979·1	2·561	·4084	·4072				

The mean of four values of $\frac{[t]}{[\log h]}$ in the last column is 1686·8,

a=area of cross-section of U-tube = 15·553 sq. cm. Thus we have

$$\eta = 1803{\cdot}5 \times 10^{-7} \text{ c.g.s. at } 17{\cdot}78^\circ \text{ C.}$$

Experimental Results.

Air.

The table gives the value obtained for air with tubes 1 and 2. Millikan's * temperature coefficient ($4{\cdot}93 \times 10^{-7}$/°C.) is used to reduce the values to 17° C. :—

Run no.	θ°.	η_θ.	η_{17°.
7	17·74	1804·9	1801·2
9	17·84	1805·2	1800·8
11	15·33	1793·4	1801·6
13	15·69	1793·1	1799·6
15	17·41	1804·0	1802·0
17	16·26	1797·3	1801·0
81	17·41	1803·1	1801·1
83	19·22	1811·8	1801·9
113	17·19	1802·9	1802·0
171	18·23	1808·4	1802·3
173	18·09	1807·3	1801·9
179	16·92	1800·8	1801·2

Arithmetic mean, $\eta_{17^\circ} = (1801{\cdot}3_8 \pm 0{\cdot}1_4) \times 10^{-7}$ c.g.s.

Results for tubes 5, 6, 7, 8 are :—

Run no.	θ°.	η_θ.	η_{17°.
35	17·03	1801·4	1801·3
37	15·81	1796·3	1802·2
39	17·22	1800·7	1799·6
41	15·69	1796·1	1802·6
43	15·26	1792·3	1800·9
45	16·55	1797·2	1799·4
47	18·72	1808·8	1800·3
49	18·45	1807·4	1800·3
75	17·27	1800·6	1799·3
77	17·86	1805·3	1801·1
79	17·22	1801·3	1800·2

Arithmetic mean, $\eta_{17^\circ} = (1800{\cdot}6_3 \pm 0{\cdot}2_1) \times 10^{-7}$ c.g.s.

* R. A. Millikan, *Ann. Phys.* xli. p. 759 (1913).

Results for tubes 1, 5, 7, 8:—

Run no.	$\theta°$.	η_θ.	$\eta_{17°}$.
93	16·28	1797·2	1800·8
95	15·92	1794·2	1799·6
97	17·21	1802·3	1801·3

Arithmetic mean, $\eta_{17°}=(1800{\cdot}5_9\pm0{\cdot}5_1)\times10^{-7}$ c.g.s.

Results for tubes 11 and 12:—

Run no.	θ.	η_θ.	$\eta_{17°}$.
207	19·48	1813·0	1800·8
211	18·51	1808·0	1800·6
213	17·78	1803·8	1799·9
215	16·67	1799·4	1801·0
217	15·96	1795·8	1800·9
219	15·25	1790·8	1799·4

Arithmetic mean, $\eta_{17°}=(1800{\cdot}4_3\pm0{\cdot}18)\times10^{-7}$ c.g.s.

The four values are:—

Tubes.	$\eta_{17°}\times10^7$.	Probable error.
1, 2	$1801{\cdot}3_8$	$\pm0{\cdot}1_4$
5, 6, 7, 8	$1800{\cdot}6_3$	$\pm0{\cdot}2_1$
1, 5, 7, 8	$1800{\cdot}5_7$	$\pm0{\cdot}5_1$
11, 12	$1800{\cdot}4_3$	$\pm0{\cdot}1_8$

These errors arise only from the scatter of the points on each viscosity-temperature line. The following table gives the calibration errors of the different tubes and the total probable error arising from calibration and scatter of points:—

Tubes.	Probable error of calibration.	Error in η.	Final probable error.
	Per cent.		
1, 2	0·066	$\pm1{\cdot}19$	$\pm1{\cdot}20$
5, 6, 7, 8	0·012	$\pm0{\cdot}22$	$\pm0{\cdot}30$
1, 5, 7, 8	0·027	$\pm0{\cdot}49$	$\pm0{\cdot}70$
11, 12	0·019	$\pm0{\cdot}34$	$\pm0{\cdot}39$

The four values now represent a self-consistent set of results :—

$$1801{\cdot}3_8 \pm 1{\cdot}20 \times 10^{-7} \text{ c.g.s.}$$
$$1800{\cdot}6_3 \pm 0{\cdot}30$$
$$1800{\cdot}5_9 \pm 0{\cdot}70$$
$$1800{\cdot}4_3 \pm 0{\cdot}39$$

It was considered that the best value would be obtained by taking the arithmetic mean. Thus we have

$$\eta_{17^\circ} = (1800{\cdot}7_6 \pm 0{\cdot}2_1) \times 10^{-7} \text{ c.g.s.}$$

Other Errors in the Experiments.

Temperature.

A thorough investigation was made of the possible error arising from unreliable temperature measurements. It was decided that the final error arising from temperature cannot have been more than $\pm 0{\cdot}05^\circ$ C. This introduces a possible error in the viscosity of $\pm 0{\cdot}014$ per cent.

Cross-section of U-tube.

The probable error deduced from all the measurements was $\pm 0{\cdot}019$ per cent.

Oil-Density.

The final probable error deduced from the mutual consistency of the determinations was $\pm 0{\cdot}013$ per cent. As the same oil was used to calibrate the U-tube this error will be introduced twice. Thus the probable error in the viscosity due to the oil-density is $\pm 0{\cdot}026$ per cent.

Microscope Scale.

This was checked against a standard steel scale and showed very little discrepancy. Analysis of the readings, however, suggested a probable error of $\pm 0{\cdot}010$ per cent. on the viscosity.

The final total of all these errors, including the error given in the previous section, is $\pm 0{\cdot}03_8$ per cent. Thus the viscosity of air at 17° C. is $(1800{\cdot}7_6 \pm 0{\cdot}6_9) \times 10^{-7}$ c.g.s.

Temperature Coefficient of Viscosity.

Since the sets of tubes do not yield identical values of viscosity it is not possible to use all the 32 points together

for evaluating the temperature coefficient. Any single set of points may be used. The points obtained with tubes 1 and 2 show the best mutual consistency, and this set was analysed by the method of least squares, and the resulting value of the temperature coefficient was $(4{\cdot}93 \pm 0{\cdot}11) \times 10^{-7}$ per degree Centigrade.

This value is identical with Millikan's value of $4{\cdot}93 \times 10^{-7}$ per degree Centigrade.

Using this coefficient the value of η at 23° C. becomes

$$\eta_{23^\circ} = (1830{\cdot}3_4 \pm 0{\cdot}6_9) \times 10^{-7} \text{ c.g.s.}$$

If this value of η is substituted in Millikan's data on e we have

$$4{\cdot}770 \times \left(\frac{1830{\cdot}3_4}{1822{\cdot}6}\right)^{3/2} \times 10^{-10} = 4{\cdot}800 \times 10^{-10} \text{ e.s.u.}$$

This value of e is in very good agreement with that deduced recently by von Friesen * from a survey of all the more recent determinations of e obtained by X-ray and electron diffraction methods. He quotes a final value for e as

$$e = (4{\cdot}800 \pm 0{\cdot}005) \times 10^{-10} \text{ e.s.u.}$$

Experimental Results for Nitrogen and Oxygen.

Experimental procedure was exactly the same as for air. The gases were not passed over any drying agent, but passed straight into the apparatus from the cylinders. Care was taken to ensure that the apparatus was completely full of the pure gas before any results obtained were used in evaluating the viscosity.

The manufacturer's analyses of the two gases are as follows :—

Nitrogen.

Impurities :

Water vapour	Traces
Oxygen	,,
Neon	Nil up to ·036 per cent. by vol.
Helium	,, ,, ·008 ,, ,,
Carbon monoxide	Approximately 5 parts/million.
Carbonaceous matter as CO_2	Approximately 40 parts/million.

The gas is free from argon, krypton, and xenon.

* von Friesen, Proc. Roy. Soc. clx. p. 424 (1937).

Oxygen.

Guaranteed to contain :

Oxygen	99·8 per cent.
Air	0·2 „

In neither case will the impurities affect the results to an amount comparable with the accuracy obtainable experimentally. The following values were obtained with nitrogen with tubes 1 and 2 :—

Run no.	$\theta°$.	η_θ.	$\eta_{17°}$.
19	14·68	1728·2	1739·2
21	14·71	1726·7	1737·6
23	15·90	1732·3	1737·5
25	14·51	1725·3	1737·1
27	19·14	1749·5	1739·3
29	18·35	1742·5	1736·1
109	19·34	1749·1	1738·0
111	15·61	1731·6	1738·2

Arithmetic mean, $\eta_{17°}=(1737{\cdot}8_8\pm0{\cdot}2_9)\times10^{-7}$ c.g.s.

For tubes 5, 6, 7, 8 :—

Run no.	$\theta°$.	η_θ.	$\eta_{17°}$.
59	17·84	1742·1	1738·1
61	14·53	1725·8	1737·6
63	16·39	1736·6	1739·5
65	16·83	1738·9	1739·7
67	17·93	1743·8	1739·4
69	17·75	1742·4	1736·8
73	15·89	1735·3	1740·6
141	18·59	1746·8	1739·2
143	18·66	1745·0	1737·1

Arithmetic mean, $\eta_{17°}=(1738{\cdot}6_7\pm0{\cdot}2_6)\times10^{-7}$ c.g.s.

and for tubes 1, 5, 7, 8 :—

Run no.	$\theta°$.	η_θ.	$\eta_{17°}$.
99	18·41	1746·9	1740·2
101	18·28	1740·1	1734·0
103	17·72	1742·6	1739·2
105	17·55	1741·5	1738·2
107	18·98	1747·0	1737·6

Arithmetic mean, $\eta_{17°}=(1737{\cdot}9_8\pm0{\cdot}7_3)\times10^{-7}$ c.g.s.

The three values are

$$1737{\cdot}8_8 \pm 0{\cdot}2_6 \times 10^{-7} \text{ c.g.s.}$$
$$1738{\cdot}6_7 \pm 0{\cdot}2_9$$
$$1737{\cdot}9_8 \pm 0{\cdot}7_2$$

The values, including errors of calibration as for air, are

$$1737{\cdot}8_8 \pm 1{\cdot}2_1 \times 10^{-7} \text{ c.g.s.}$$
$$1738{\cdot}6_7 \pm 0{\cdot}3_7$$
$$1737{\cdot}9_8 \pm 0{\cdot}9_1$$

The arithmetic mean of these is

$$(1738{\cdot}2 \pm 0{\cdot}2_0) \times 10^{-7} \text{ c.g.s.}$$

The temperature coefficient used in deducing the above results was $4{\cdot}76 \times 10^{-7}$ per degree Centigrade from the set of points obtained with tubes 1 and 2.

Including the remaining sources of error as for air the final value for nitrogen at 17° C. is

$$\eta_{17^\circ} = (1738{\cdot}2 \pm 0{\cdot}7_3) \times 10^{-7} \text{ c.g.s.}$$

The results for oxygen are as follows :—

With tubes 1 and 2 :—

Run no.	θ°.	$\eta\theta^\circ$.	η_{17°.
181	18·00	2017·9	2011·7
183	17·60	2015·4	2011·7
185	17·62	2015·6	2011·7
187	15·20	1999·8	2011·0
189	15·21	2000·8	2012·0
203	19·11	2023·4	2010·3
205	15·96	2004·9	2011·4

Arithmetic mean, $\eta_{17^\circ} = (2011{\cdot}3_7 \pm 0{\cdot}1_5) 10^{-7}$ c.g.s.

and with tubes 5, 6, 7, 8 :—

Run no.	θ.	η_θ.	η_{17°.
191	17·64	2014·3	2010·3
193	17·00	2010·1	2010·1
195	16·94	2008·3	2008·7

Arithmetic mean, $\eta_{17^\circ} = (2009{\cdot}6_6 \pm 0{\cdot}1_7) \times 10^{-7}$ c.g.s.

The two values are, with errors of calibration inserted,

$$2011{\cdot}3_7 \pm 1{\cdot}2_0 \times 10^{-7} \text{ c.g.s.}$$
$$2009{\cdot}6_6 \pm 0{\cdot}28$$

Arithmetic mean is $(2010{\cdot}5_2 \pm 0{\cdot}6) \times 10^{-7}$ c.g.s.

Introducing remaining errors as before, the final value for oxygen at 17° C. is

$$(2010{\cdot}5 \pm 0{\cdot}9) \times 10^{-7} \text{ c.g.s.}$$

The experimental temperature coefficient used for deducing these results was obtained from the values for tubes 1 and 2 and is $6{\cdot}23 \times 10^{-7}$ per degree Centigrade.

From these values for oxygen and nitrogen it is possible to predict a value for the viscosity of air (if the value for argon is known).

Assuming the analysis of air as given by Kaye and Laby in 'Tables of Physical Constants,' viz. :—

	N_2.	O_2.	A.
Percentage by volume	78·05	21·00	0·95

(traces of CO_2 and rare gases present will not affect this value to any appreciable extent). The viscosity of argon need not be known accurately and was taken as 2225×10^{-7} c.g.s. at 17° C. Then if the ordinary mixing law is valid calculation gives a value for the viscosity of air at 17° C. as

$$\eta_{17} = 1800{\cdot}0 \times 10^{-7} \text{ c.g.s.}$$

in good agreement with the value obtained by direct measurement.

Now if the values of η for the three component gases are first raised to 23° C. by the three temperature coefficients,

Nitrogen.....	$4{\cdot}76 \times 10$/°C.	(experimental values, Kaye and Laby),
Oxygen.....	$6{\cdot}23 \times 10$/°C.	
Argon	$7{\cdot}32 \times 10$/°C.	

they become

N_2	$1766{\cdot}8 \times 10^{-7}$ c.g.s.
O_2	2050·0
A	2268·6

and the value for air at 23° C. calculated from them is $1831{\cdot}1 \times 10^{-7}$ c.g.s., which again is in good agreement with the experimental value of $1830{\cdot}3 \times 10^{-7}$ c.g.s.

This agreement at both 17° C. and 23° C. indicates the accuracy of the three experimental temperature coefficients found for oxygen, nitrogen, and air.

Summary of Results.

The value of the viscosity of air at 17° C. is

$$\eta_{17}=(1800{\cdot}7_6\pm 0{\cdot}6_9)\times 10^{-7} \text{ c.g.s.}$$

The experimental temperature coefficient obtained from the data is $(4{\cdot}93\pm 0{\cdot}11)\times 10^{-7}$ per degree Centigrade, identical with the value obtained by Millikan.

Using this temperature coefficient the value obtained for air at 23° C. is

$$\eta_{23}=(1830{\cdot}3_4\pm 0{\cdot}6_9)\times 10^{-7} \text{ c.g.s.},$$

which introduced into Millikan's oil-drop data for the electronic charge yields

$$e=(4{\cdot}800\pm 0{\cdot}004)\times 10^{-10} \text{ e.s.u.}$$

The values obtained for the viscosities of pure oxygen and nitrogen at 17° C. are :—

Nitrogen .... $\eta_{17}=(1738{\cdot}2\pm 0{\cdot}7_3)\times 10^{-7}$ c.g.s.
Oxygen..... $\eta_{17}=(2010{\cdot}5\pm 0{\cdot}9)\times 10^{-7}$ c.g.s.

The values of the temperature coefficients found experimentally for these gases are :—

Nitrogen ..... $4{\cdot}76\times 10^{-7}$/degree C.
Oxygen..... $6{\cdot}23\times 10^{-7}$/degree C.

Acknowledgments.

I wish to thank Prof. J. A. Crowther, in whose laboratories the work was carried out, for his interest in the experiments. I had the advice of Dr. W. N. Bond during the major part of the work, and latterly of Dr. P. White, to whom I am indebted for much helpful criticism. I am also indebted to the Department of Scientific and Industrial Research for a maintenance grant which enabled me to carry out the work.

Additional Note on Errors.

Owing to the uncertainty of the meaning of the sign $\pm$ when used in much scientific literature the following note has been added in order to make clear its significance in the present paper.

In every case in this paper the figure following the sign $\pm$ is the *probable error* of the *mean* value of the quantity, *e. g.*, the oil-density is stated to be $0{\cdot}8741_7 \pm 0{\cdot}0000_8$ gm/c.c. The figure $\pm 0{\cdot}0000_8$ is derived solely from the mutual consistency of the determinations made, and is the probable error of the arithmetic mean as given by Bessel's formula,

$$\text{Probable error of mean} = 0{\cdot}6745 \sqrt{\frac{\Sigma(v^2)}{n(n-1)}},$$

where there are n readings differing from the mean value by amounts v_1, v_2, v_3, etc. Unless otherwise stated the error is arrived at in this way.

If the error refers to a quantity which is not measured directly but which is calculated from experimental values of several other quantities, the probable error quoted has been computed from the percentage probable errors associated with each of these quantities by the formula

$$\text{Percentage probable error} = \sqrt{r_1^2 + r_2^2 + \ldots},$$

where r_1, r_2, etc. . . are the individual *percentage* probable errors associated with each experimental quantity; *e. g.*, in the final value of the viscosity of air the term $\pm 0{\cdot}6_9 \times 10^{-7}$ is the probable error of η deduced from all known sources of error in the experiment.

LXXXVII. *Impedance Characteristics of Short-Wave Dipoles.* *By* T. Walmsley, *Ph.D., M.Inst.C.E.**

A TWO-WIRE transmission line conveying alternating-current energy behaves as a more or less effective radiator according to the extent of the separation between the two wires. If the ends of such a line are bent in a suitable manner, the bent termination becomes a very effective radiator. For example, if the ends of each of the two parallel wires of a transmission line are bent at right angles in opposite directions, a radiating termination of the feeder is formed, the effectiveness of the radiator being dependent upon the frequency of the received or transmitted radiation. Whereas the unbent

* Communicated by the Author.

line termination theoretically has an infinite impedance, the bent line termination comprising the two members of a dipole has a measurable but varying impedance depending upon the wave-length of the transmitted or received energy.

In a previous paper the author gave formulæ * and described a method of measuring the terminating impedance of a feeder by observing the adjacent maximum and minimum current values along the feeder. The formulæ are :

$$Z=Z_0 \frac{K+0{\cdot}5\,j(1-K^2)\sin\frac{4\pi d}{\lambda}}{K^2\sin^2\frac{2\pi d}{\lambda}+\cos^2\frac{2\pi d}{\lambda}}, \quad . \quad . \quad . \quad (I.)$$

$$\phi=\text{arc tan}\,\frac{1-K^2}{2K}\sin\frac{4\pi d}{\lambda}, \quad . \quad . \quad . \quad . \quad (II.)$$

where Z and ϕ are the modulus and phase-angle of the terminating impedance ; Z_0 is the characteristic impedance of the line ; K is the ratio maximum to the minimum current in the line measured at points separated a quarter of a wave-length ; and $\frac{\lambda}{4}-d$ is the distance from the terminating impedance to the point of maximum line current.

By applying the principles described in the previous paper, investigation has been made into the manner in which the impedance of the radiators as measured across the end of their feeder varies with frequency and the extent to which the radiators can be regarded as simply radiating extensions of their feeder.

For this purpose a vertical single-wire dipole connected at adjacent ends to a two-wire horizontal transmission line was suspended from insulators attached to a wooden pole. The wire of both the transmission line and the aerial was copper No. 14 S.W.G., the length of each of the two members of the dipole was 9 metres, and the centre of the dipole was 12 metres above earth. The tests were made in the intervals between the wet weather,

* T. Walmsley, " Characteristics of Transmission Lines at High Frequencies," Phil. Mag. ser. 7, vol. xxii. (Suppl., Nov. 1936).

Fig. 1.

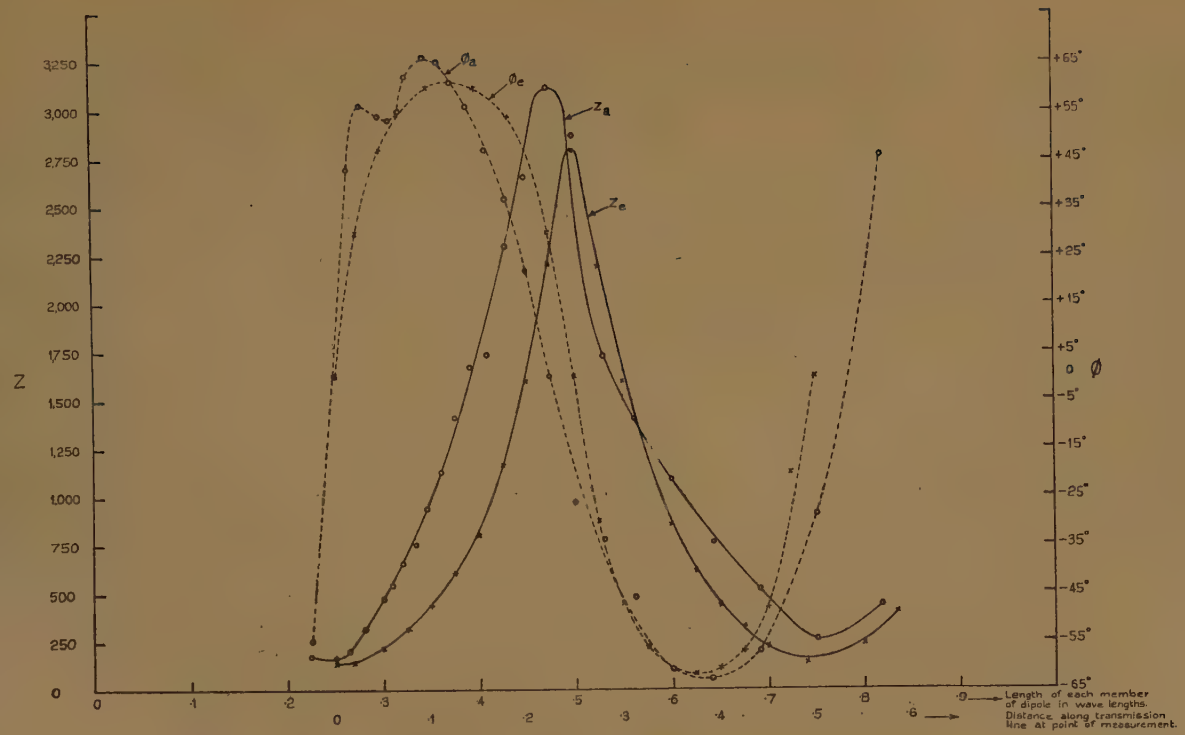

Z_a and ϕ_a.—Modulus and phase-angle of dipole impedance measured at the termination of the transmission line.

Z_e and ϕc.—Modulus and phase-angle of apparent impedance of transmission line terminated in 150 Ω.

so that the ground and the pole were damp, which fact would account for the high values of resistance observed when each of the dipoles was a quarter of a wave-length long. Adjacent maxima and minima values of current at points in the transmission line closest to the aerial and the distance of these points from the centre of the aerial were measured. By formulæ I. and II. the values of both the impedance modulus and phase-angle were calculated for various frequencies of supply.

The results are shown in fig. 1. There is a striking resemblance between this curve and that obtained when a transmission line is terminated in an impedance other than its characteristic impedance. To study this resemblance, suppose an open twin-wire transmission line is terminated in a resistance having a value equal to that of the dipole, when each of the members of the latter is one-quarter of a wave-length long. This value measured in the tests under consideration was 150 Ω, that is, rather less than one-quarter of the characteristic impedance of the transmission line. If, whilst a particular frequency was maintained, the impedance along the line were calculated, the value at various distances from the termination would be such as shown in the relevant curve of fig. 1. The same curve would be obtained if the frequency, instead of being fixed, were varied and the impedance of the line were calculated at a suitable fixed distance from the load. The general resemblance between the two pairs of curves of fig. 1 is at once apparent. Particular features of resemblance are as follows :—

(1) There is considerable agreement in the values of the maximum impedance and of the maximum positive and negative phase-angle.

(2) In the theoretical case of a transmission line terminated in a pure resistance, the maximum phase-angle occurs at a point along the line separated from the termination by distances equal in length to odd multiples of one-eighth of a wave-length. Although, in the case of the aerial, the ratio of length of each dipole to the wave-lengths at which the maximum phase-angle occurs is not well defined, there is a considerable degree of agreement with the line case.

(3) The characteristic impedance of a transmission line is a geometrical mean of the maximum and minimum

impedance of the line measured at points separated by a quarter of a wave-length, or $Z=\sqrt{Z_1 \times Z_2}$. The numeri-

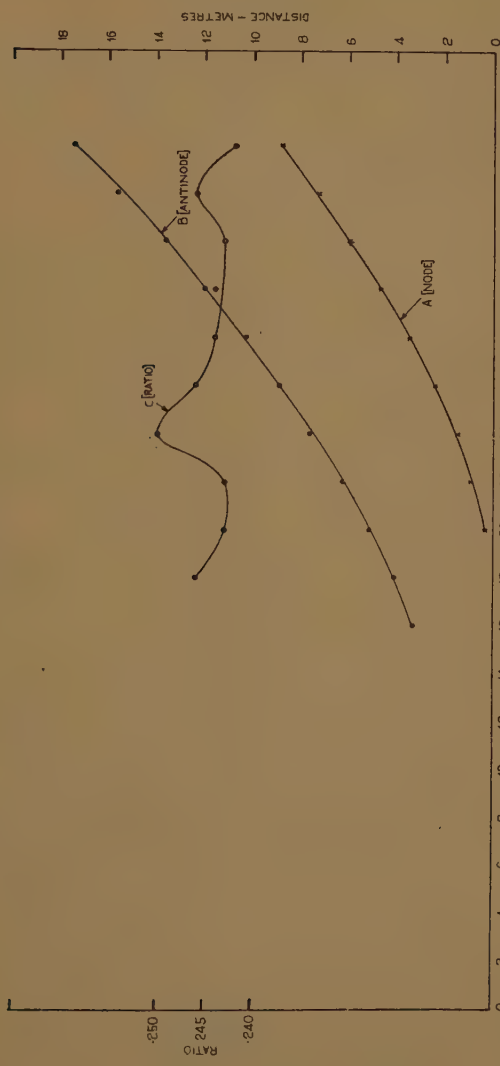

Fig. 2.

Location of nodes and antinodes of current in the transmission line feeding a single-wire vertical dipole. A and B, distance of node and antinode respectively from dipole ; C, ratio of distance between node and antinode to wave-length of supply.

cal value in the case considered was $650\,\Omega$. For the dipole the geometrical mean of the maximum and minimum impedance was $690\,\Omega$.

As already stated, the impedance of the aerial terminating the transmission line was obtained by supplying radio energy of varying frequency to the aerial and measuring the ratio of adjacent maximum and minimum values of the current in the line and the distances of the points of measurement from the load. It is interesting to examine how these distances change with frequency. The curves of fig. 2 have therefore been plotted to show these distances and also the separation between adjacent nodes and antinodes of current.

The first fact of interest is that, in accordance with expectations, the distance between points of maximum and minimum current is substantially one-quarter of a wave-length in all cases. The mean of all the readings taken at all wave-lengths is 98·0 per cent. of a quarter-wave-length, betokening an average velocity of propagation along the transmission line of 98·0 per cent. of the velocity of light. If attention is now focussed upon the curve of distance of the maximum line current from the aerial, it will be seen that when the wave-length was 36 metres, that is, when each dipole was one-quarter of a wave-length long, the distance of the point of maximum line current from the aerial was nearly half a wave-length. This, again, was in accordance with expectations, since the antinode of current distribution in an aerial comprising two quarter-wave-length dipoles occurs at the centre of the aerial, as shown in fig. 3 (*a*), and, therefore, an antinode of current in the transmission line should occur half a wave-length from the aerial along the line. In fig. 3 (*a*), (*b*), and (*c*) is shown the approximate position of this antinode of current as the frequency of supply is increased. It might be expected that, from theoretical considerations, the distance of this antinode in the aerial from the first antinode in the transmission line, *i. e.*, the distance PQR in fig. 3, would remain substantially half a wave-length. The departure from half a wave-length with varying frequencies is shown in fig. 4, the measured maximum departure being not more than 12·8 per cent.

The general conclusion, from the result of the foregoing investigations, is that dipoles consisting of wire similar to that of the transmission lines behave, as regards impedance presented to the transmission line, substantially the same as though the line were terminated in an

impedance equal to that of two quarter-wave dipoles, provided that this impedance is regarded as being located

Fig. 3.

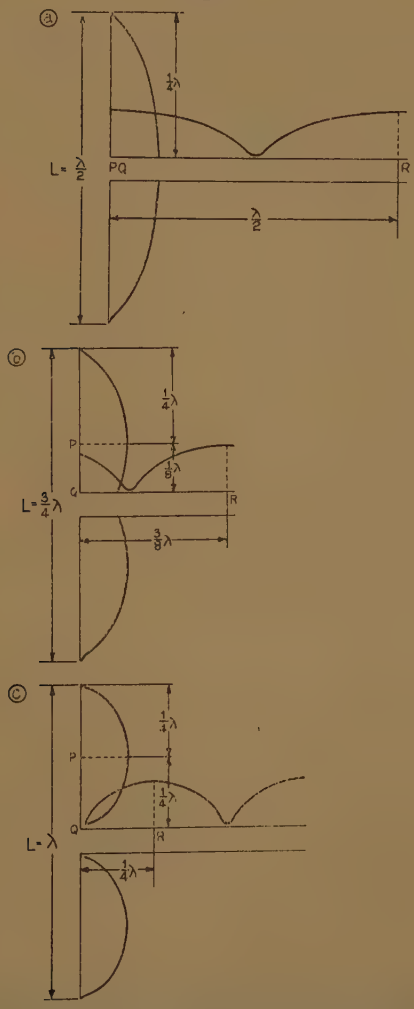

Distribution of current in dipole and transmission line at various wave-lengths.

at the point extending from the end of the transmission line a distance equal to that of the antinode of aerial current from the end of the transmission line. Further

deductions can be made and applied to practical problems of aerial design. For example, since the greater proportion of the resistance of a dipole comprising two

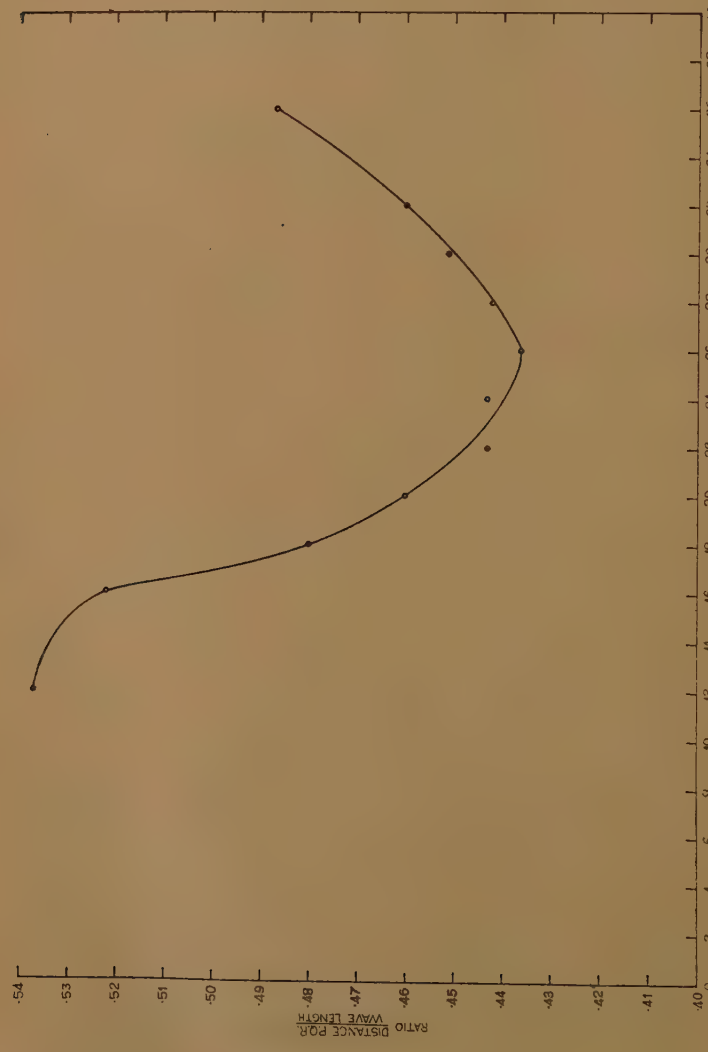

Fig. 4.

Distance of antinode of current in single-wire dipole from first antinode of current in feeder (PQR, fig. 3).

quarter-wave elements consists of radiation resistance. the total resistance of such a dipole is not greatly dependent upon and does not greatly vary with the material and

diameter of the wire of the aerial. Now the resistance of a dipole consisting of two half-wave elements is equal approximately to the square of the characteristic impedance of the aerial divided by the resistance of the quarter-wave dipole. Thus, since the latter value does not vary greatly with the diameter of the aerial, the former can be considerably reduced by reducing the characteristic impedance of the aerial, *i. e.*, by increasing the diameter of the aerial, which can conveniently be done by " cage " aerials. In consequence, the steep slope of the impedance-frequency characteristic curve of dipoles is greatly reduced.

An immediate practical result of the use of " cage " aerials is that the matching of such aerials to their transmission lines is more staple than in the case of single-wire dipoles. Further, since the impedance variations with changing frequency are relatively small, the " cage " type can more advantageously be used in those cases where an aperiodic type of aerial is required. To form some conception of the manner in which the impedance of " cage " aerials varies with frequency, several dipoles, each having the same length as a single-wire dipole in fig. 1, but consisting of several parallel wires, were built. These were suspended from a bracket on the same pole as was used previously for the single-wire tests already described. The source of radio-frequency energy was connected to the dipole by twin open-wire transmission lines similar to that used in the single-dipole tests. The results are shown in fig. 5. The eight-wire cage aerial is selected for detailed examination, and the relevant curve of fig. 5 shows both the modulus and phase-angle of the impedance in terms of wave-length of the radio-frequency energy. Comparison with the corresponding curves of fig. 1 relating to a single-wire dipole reveal many similarities. The slopes $\frac{\delta Z}{\delta f}$ and $\frac{\delta \phi}{\delta f}$, however, throughout the whole of the frequency range are less for the eight-wire dipole than for the single-wire dipole. When the impedance of the dipoles is approaching or receding from the highest values this contrast is accentuated. Again, in the case of the eight-wire dipole the extremes of phase-angle are not so great. The effect of phase-angle in producing standing waves and varying impedance along

Fig. 5.

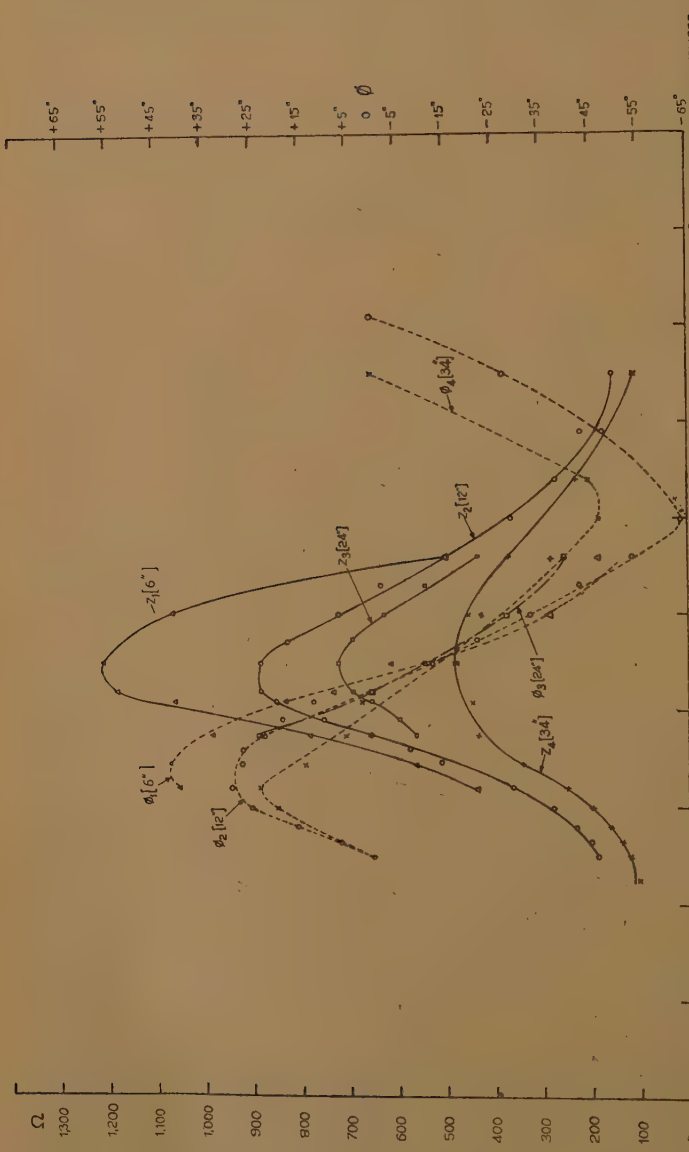

Impedance of vertical "cage" type dipoles. Z_1, Z_2, Z_3, and ϕ_1, ϕ_2, ϕ_3, refer to modulus and phase-angle of 4-wire aerials arranged at the corners of squares having 6", 12" and 24" sides respectively, thus : : Z_4 and ϕ_4 refer to modulus and phase-angle of 8-wire dipole arranged symmetrically on the circumference of a circle 34" diameter.

a transmission line is shown in fig. 6, the curves of which have been calculated from formula I. Here the modulus of the characteristic impedance of the line and of the terminating load are equal. If the phase-angle of the load were zero, a perfect match would be obtained and the effective impedance along the line would be constant. Such a condition, however, does not hold when the phase-angle is other than zero. The curves show how the impedance along the line varies for different values of the load phase-angle and emphasize the necessity of matching both the phase-angle and modulus of the load to reduce

Fig. 6.

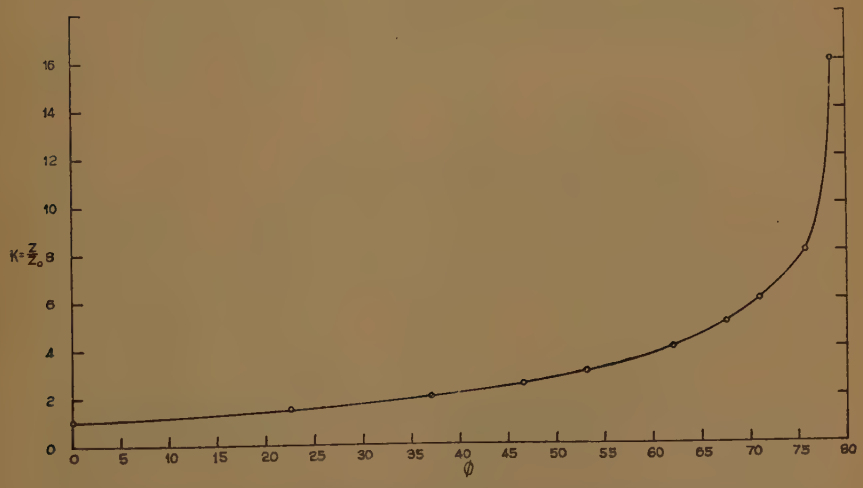

Ratio of maximum impedance Z measured along a transmission line to characteristic impedance Z_0 of the line for various values of the phase-angle ϕ of the terminating load, which has a modulus equal to the modulus of the characteristic impedance of the line.

standing waves and impedance variations along a transmission line to a minimum. Its frequency-impedance characteristics render the "cage" type dipole more suitable for the design of beam arrays that are required to function over a fairly broad band of wave-length. For example, if the type of array shown in fig. 7, utilizing dipoles having the characteristics of the eight-wire dipole shown in fig. 5, were correctly matched when each half dipole was equal approximately to half a wave-length,

the mis-match as the wave-length varied within the limits shown in fig. 5 would not be greater theoretically than about 4 : 1. In other words, the effective impedance at any point in the transmission line feeding the array cannot fall to a value less than one-quarter of the matched impedance. If, however, the array consisted of single-wire dipoles having the characteristics of the single-wire dipole shown in fig. 1, the possible variation in this effective impedance is 1 : 25. The important fact is that an aerial consisting of a number of similar symmetrically arranged elements presents an impedance to its feeder which varies with the wave-length of the

Fig. 7.

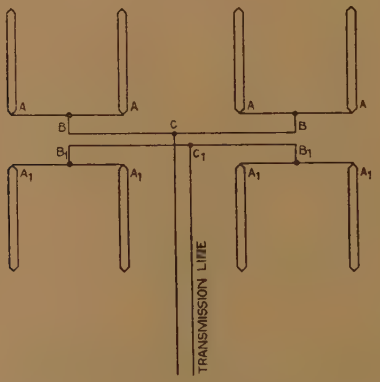

Vertical type array with fixed matching at AA_1, BB_1, and CC_1.

supplied energy between limits dependent upon the impedance limits of the individual elements.

The practical advantage of reducing the ratio of extreme value of impedances is considerable. For example, it may be required to use the same array for different wave-lengths. An array of the type shown in fig. 7, in which the radiators may be either vertical (as shown) or horizontal, gives a true beam effect for all wave-lengths, since the currents in all the radiators are synphased. Its impedance, however, as already stated, varies with the wave-length.

The problem of designing variable matching at the junction of the array feeders and the transmission line, or alternatively of providing suitable variable coupling

to the output circuit of the emitter or input circuit of the receiver, as the case may be, so that the best use can be made of the array, is much simplified when the variations of array impedance are not great.

The thanks of the author are due to Messrs. L. L. Hall and F. Anderson for their assistance in making tests.

LXXXVIII. *On the Trajectory of Ash Particles in Air and the Determination of their Size.* *By* K. Prosad, *M.Sc.* (*Cal.*), *B.A.* (*Cantab*), *Professor of Physics, and* D. N. Sen, *M.Sc.* (*Cal*), *B.A.* (*Cantab*), *Professor of Mathematics, Science College, Patna, India* *.

[Plate XI.]

Abstract.

The paper is concerned with the theoretical and experimental investigations of the trajectory of cigar ash particles shot out in a horizontal direction in air, from a narrow orifice by effluent air under a measured driving pressure in the form of a jet. The theoretical and experimental curves fit in very well.

From the investigations made, it has been found possible to determine the average size of the ash particles, assumed spherical, which, as a result of coagulation, must be growing in bulk rapidly during their flight. The experimental value of the radius has come out to be $2{\cdot}34 \times 10^{-3}$ cm., and is considered satisfactory.

The method is claimed to be a novel one and admits of extension and application to the study of the general problems of "smokes" and "aerosols" under different conditions.

The present study has suggested further extension of the problem by taking simultaneously into account (*a*) initial particles of different sizes, and (*b*) growth of the particles under flight in the same effluent jet These and other aspects noted in the body of the paper are under investigation now.

---

* Communicated by the Authors.

1. *Introduction.*

AS far as the authors are aware, there does not appear to have been any investigation so far recorded of the nature of the trajectory described when smoky and ash-laden air is blown under a steady difference of pressure in the form of a jet from a narrow orifice.

Helmholtz[1] was probably the first to study the colour changes in a jet of water vapour owing to the introduction of mist nuclei, but no attempt seems to have been made by him to estimate the size of the particles in these experiments. Tolman, Reyerson, Vliet, Gerke and Brooks[2] have studied the relation between the intensity of the Tyndall beam and the constants of the particles in a mist. Barus[3] estimated the size of smoke particles from the diameter of diffraction rings. Whytlaw-Gray and others[4] have studied finer smokes made up of several metallic oxides and ammonium chloride. They conclude that there is at first a rapid agglomeration of particles followed by a nearly steady state in which the smoke particles slowly settle down on the walls of the chamber. Other references to work on smokes can be found in advanced text-books of Physical Chemistry, but, as pointed out at the outset, they have hardly any bearing on the problem discussed in this paper.

The purpose of this paper is to describe the results of both experimental and theoretical investigations of the trajectory of tobacco smoke and ash issuing in the form of a jet in air. It will be clear from the following that the method of attack is not only novel, but that it is capable of extensions to problems of "smokes" and aerosols" under a variety of conditions.

2. *Apparatus—a Mechanical Smoker.*

The experimental arrangements with the "mechanical smoker" are shown in fig. 1. A lighted cigar (Hay's Burma cigars were used) is fixed to one end of a glass tube which fits air-tight into the neck of a glass flask by a ground joint. The other end of the glass tube has a T-piece attached for holding a water manometer and one end of a brass tube, by rubber tubing joints. A brass cap with a narrow aperture can be screwed to the other end of the brass tube. To the bent glass tube sealed into the wall of the glass flask is connected a long piece of

rubber tubing, the other end of which is connected to a short glass tube tightly fixed to a cork in the mouth of a large glass bottle of capacity about 4 litres. This is marked A in fig. 1. Into the side opening of the lower end of this bottle A is fixed a cork through which a short glass tubing passes. A long rubber tubing connects this glass tube to a similar glass tube fixed in the cork of the side opening of another large glass bottle B. This bottle B is filled with water, and if it is raised bodily up into the position B′ water flows from it into the bottle A, driving the air enclosed in it through the flask, so that the cigar burns and a jet of smoky and ash-laden air issues from the orifice of the brass cap. By lowering the

Fig. 1.

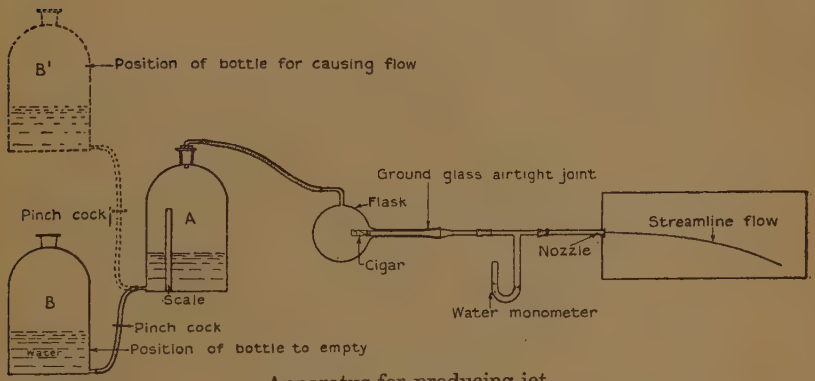

Apparatus for producing jet.

bottle B, after removing the glass tube with ground joint in the neck of the flask, water can be sucked back from A into B. In this way the operation of producing the experimental jet can be again and again repeated. Regulation of a pinch-cock attached to the rubber tubing connecting the two bottles A and B enables the rate of flow of water from B′ into A, and hence the driving pressure, to be maintained steady at any desired value.

3. *Photography of the Trajectory.*

In order to avoid effectively the disturbing effects of casual draughts and convection currents on the jet it was arranged to issue in a chamber made of wood, the top and the front sides of which were closed with glass

plates. The dimensions of the chamber were $64 \times 13 \times 13$ cm. A centimetre scale subdivided into millimetres was fixed lengthwise into the chamber, and the end of the brass tube from which the jet issued was so arranged through a small opening in one of the 13×13 cm. sides that the jet formed was in the plane of the scale. The jet was illuminated by two 100 c.p. bulbs from the top of the chamber and photographed from the front by scattered light. The position of the bulbs prevented any convection currents being set up inside the chamber, so fatal to the appearance to be photographed. The sharpness of the bounding lines of the trajectory reproduced in Pl. XI., as well as its smoothness, is sufficient proof of the steadiness of the appearance during the exposure.

4. *General Appearance of the Jet.*

Before proceeding further, it is advisable to describe the general appearance and the structure of the smoky jet under different driving pressures. With a very small driving pressure (less than 1 cm. of water) the length of the almost straight jet with sharp bounding sides is small, the end portion assuming a cone-shaped figure. With slight increase of pressure the length increases at first, and then decreases as the pressure is still further increased. In fact, with steadily increasing driving pressure the nearly straight portion of the jet is found to be periodically oscillating with diminishing length. This interesting property of the jet is being studied at present and will form the subject of future communications. It is well to remember here that the function of the smoke mixed with air is not only to make visible the whole of the path of the effluent gas, but also to reveal to the eye the effect of scattering of the jet as it collides against the gas in the experimental chamber. But the smoke actually does much more than is indicated above. It introduces particles of cigar ash, water vapour, and other products of combustion which form complex colloidal aggregates into the effluent air.

5. *Theory and Measurements.*

As pointed out above, the constitution of the jet is highly complex. For the sake of simplicity we shall

consider here the ideal jet composed of particles of ash only of a definite size. Let the ash particles be supposed spherical and of radius r. If x, y be the coordinates of one of these ash particles at any point of the trajectory at time t, where the pressure in the jet is p_x, then the horizontal force F acting on the particle is given by

$$F = p_x \pi r^2.$$

The pressure along the jet may be assumed to diminish with the horizontal distance x travelled according to some law

$$p_x = p_0 e^{-kx},$$

where p_0 is the initial pressure difference read from the water manometer at $x=0$ and k is a constant. In fact, it is easily shown [5] that $k = \frac{\gamma - 1}{\gamma}$, where γ is the ratio of the two specific heats for the mixture of materials composing the jet.

Assuming further that for the vertical motion of the ash particles, under gravity, Stokes's law holds good, it is possible to write down the differential equations determining the motion of the particles as follows :

$$m \frac{d^2x}{dt^2} = -p_0 e^{-kx} \cdot \pi r^2,$$

and

$$\frac{dy}{dt} = v = \frac{2}{9} \frac{r^2(\triangle - \rho)}{\xi} \cdot g,$$

where

$m = \frac{4}{3} \pi r^3 \triangle$, the mass of an ash particle,

$\triangle$ = density of cigar ash,

ρ = density of air,

ξ = viscosity of air.

From

$$\frac{d^2x}{dt^2} = -A p_0 . e^{-kx}, \quad \text{where} \quad A = \frac{3}{4r\triangle},$$

we get

$$\frac{dx}{dt} = \sqrt{B^{-kx} + \alpha^2},$$

where

$$B=\frac{2Ap_0}{k} \quad \text{and} \quad \alpha \text{ is a constant.}$$

Since $\frac{dy}{dt}=v$, which is constant,

$$dy=\frac{vdx}{\sqrt{\alpha^2+Be^{-kx}}},$$

which gives, on integration,

$$y=\frac{v}{\alpha k}\log\frac{z+\alpha}{z-\alpha}+D,$$

where

$$z^2=\alpha^2+Be^{-kx}.$$

From initial conditions, we have

$$0=\frac{v}{\alpha k}\log\frac{u_0+\alpha}{u_0-\alpha}+D,$$

so that

$$y=\frac{v}{\alpha k}\log\frac{z+\alpha}{z-\alpha}\cdot\frac{u_0-\alpha}{u_0+\alpha}$$

$$=2c_1.\log\left[c_2.\frac{\sqrt{\alpha^2+\zeta}+\alpha}{\sqrt{\zeta}}\right],$$

where

$$c_1=\frac{v}{\alpha k},\quad c_2{}^2=\frac{u_0-\alpha}{u_0+\alpha},\quad \text{and}\quad \zeta=Be^{-kx}.$$

We therefore have

$$e^{y/2c_1}.\frac{\sqrt{\zeta}}{c_2}=\sqrt{\alpha^2+\zeta}+\alpha.$$

$$\therefore\quad e^{-y/2c_1}.c_2\sqrt{\zeta}=\sqrt{\alpha^2+\zeta}-\alpha.$$

Hence

$$\frac{1}{c_2}.e^{y/2c_1}-c_2.e^{-y/2c_1}=\frac{2\alpha}{\sqrt{\zeta}}=\frac{2\alpha}{\sqrt{B}}.e^{kx/2},$$

which leads to the equation

$$\cosh\frac{y}{2c_1}+\frac{u_0}{\alpha}\sinh\frac{y}{2c_1}=e^{kx/2}. \quad . \quad . \quad . \quad . \quad \text{(A)}$$

This equation simplifies considerably if we take u to vanish finally. This assumption seems justified, as the

horizontal velocity must necessarily vanish when the excess of pressure p vanishes.

Making $\alpha \to 0$ in the equation (A), we get

$$y = \frac{v}{u_0} \cdot \frac{2}{k} (e^{kx/2} - 1). \quad . \quad . \quad . \quad . \quad . \quad . \quad \text{(B)}$$

Fig. 2.

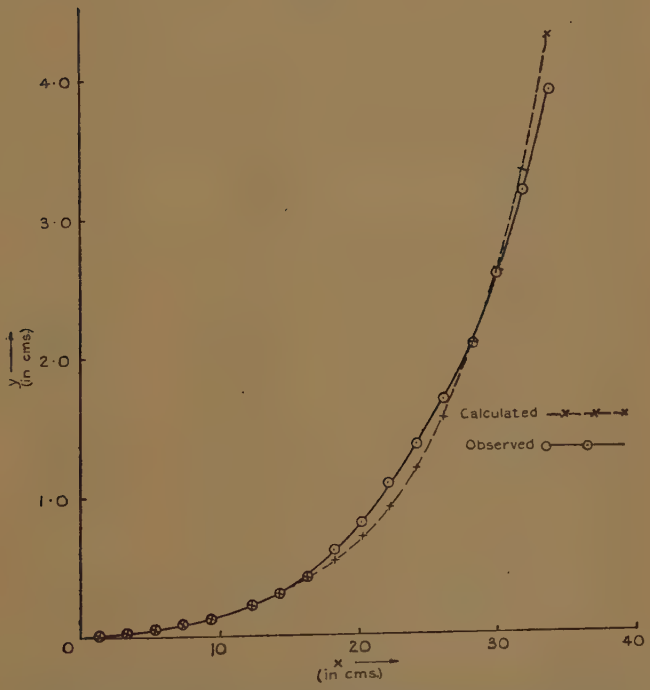

Theoretical and experimental trajectories of smoke particles.

From the graphical value of $\frac{y}{x}$ in fig. 2 near the origin we get $\frac{v}{u_0}$ equal to $\frac{\cdot 0100}{\cdot 1316}$ or $\frac{1}{132}$ nearly.

Equation (B) reduces to

$$66\,ky = e^{kx/2} - 1. \quad . \quad . \quad . \quad . \quad . \quad \text{(C)}$$

For different points on the curve we get the values of k satisfying this equation and an average is taken. A curve with this value of k is drawn with the help of equation (C).

This curve and the one plotted with x and y directly measured on the negative with a comparator are shown in fig. 2.

To determine the size of the particles we require to know ρ, $\triangle$, p_0, and ξ. We get u_0 from the formula $p_0=\frac{1}{2}\rho u_0^2$, and then v is obtained from the relation

TABLE.

x.	y.	k.	$\log_{10}(1+66ky)$.	$k\frac{x}{2}\log_{10}e$.
1·316	0·0100	[0·20]	0·0538	0·0571
7·296	0·0817	0·21	0·3288	0·3328
9·306	0·1205	·22	0·4392	0·4446
12·286	0·2068	·23	0·6169	0·6135
14·290	0·3043	·25	0·7797	0·7756
16·286	0·4133	·25	0·8932	0·8840
18·296	0·6115	·27	1·0754	1·0727
20·276	0·8027	·27	1·1847	1·1888
22·276	1·0837	·27	1·3077	1·3060
24·226	1·3737	·27	1·4062	1·4202
26·256	1·6937	·26	1·4780	1·4825
28·250	2·0787	·25	1·5478	1·5336
30·226	2·6097	·25	1·6441	1·6409
32·226	3·1857	·25	1·7289	1·7495
34·236	3·9122	·24	1·7992	1·7842

Average value of $k=\frac{3\cdot49}{14}=0\cdot2493$ or 0·25 approx.

$u_0=132\,v$. r, the radius of the particle, is then calculated from Stokes's formula

$$6\pi\xi rv=\frac{4}{3}\pi r^3(\triangle-\rho)g.$$

The following table gives the calculated values of k from equation (C), which is equivalent to

$$\log_{10}(1+66\,ky)=k\frac{x}{2}.\log_{10}e,$$

for different measured values of x and y for points lying on the axes of the trajectory in Pl. XI.

6. *Numerical Values of the Constants and the Size of Particles.*

The density of air was taken to be 0·0013 gm. cm.$^{-3}$. $\triangle$, the density of tobacco ash, was determined by a separate experiment with a specific gravity bottle. A large amount of cigar ash was collected and its density was determined with respect to kerosene oil of known density in the usual way. It was found to be 2·835 gm. cm.$^{-3}$. ξ, the viscosity of air, was assumed to be 181×10^{-6} gm. cm.$^{-1}$ sec.$^{-1}$, while p_0, the steady pressure difference maintained during the experiment, was 4·0 cm. of water.

These now enable the value of r, the radius of the tobacco-ash particle, to be determined thus :—

Since

$$u_0^2=\frac{2p_0}{\rho}=\frac{2\times4\times978}{\cdot0013}=601\cdot8\times10^4,$$

we have

$$u_0=24\cdot53\times10^2 \text{ cm./sec.}$$

and

$$v=\frac{u_0}{132}=\frac{1}{132}\times24\cdot53\times10^2=18\cdot58 \text{ cm./sec.}$$

$$\therefore\quad r=\sqrt{\frac{9}{2}\cdot\frac{\xi v}{(\triangle-\rho)g}}=2\cdot34\times10^{-3} \text{ cm.}$$

7. *Discussion of the Results.*

(1) Although there is no previous record of the sizes of the tobacco ash particles with which to compare our value recorded above, there seems to be little doubt that the magnitude is of the right order. Previous workers using "smoke particles" have estimated their initial size to be of the order 1×10^{-4} cm., but they have also laid emphasis on the rapid increase of their size due to coagulation. Our value may be taken to be the mean size of the ash particle during the time taken to describe the trajectory. It is to be noted that the density of the smoky air has been taken in the above calculation to be the same as for the ordinary clean air, namely, 0·0013. Actually the density must be higher. The effect of this would be to give a lower value to u_0, and hence to v, which would lead to a value of r smaller than recorded above—a change which is in the right direction.

(2) A reference to fig. 2, where the theoretical and the experimental trajectories are plotted together for the sake of comparison, will make it clear that the former fits the latter as well as can be expected considering the complexity of the constitution of the actual jet and the simplicity of the assumptions made. The extreme difficulty in entirely eliminating the disturbing effects of convection currents during the photographing of the jet is a point which has also to be borne in mind.

(3) There are certain features in the trajectory shown on Pl. XI. which invite attention :—

(*a*) The two bounding edges are sharp over a long distance, but the lower edge is more sharply defined than the upper one. Towards the end of the track the upper edge becomes much more fuzzy. These features appear to be due to the presence of particles of different size not only initially, but produced by rapid coagulation during their flight.

(*b*) The cross-section of the jet gradually expands as we move away from the aperture. This feature appears to be due both to the presence of particles of different size and to a velocity distribution of the issuing jet over the cross-section, symmetrical with respect to the axes of the jet according to a well-known parabolic relation.

These features require further study, and the equation of the trajectory taking into account presence of particles of different size and their growth during their flight must necessarily be a much more complex one. It is hoped to extend the scope of the present study by taking these factors into account.

(4) It seems interesting at this stage to examine a little further the information obtainable from the constant k. It has been pointed out that $k=\frac{\gamma-1}{\gamma}$ where γ is the ratio of the two specific heats of the materials of the jet.

Substituting the experimental value of k found in the present experiment, we have

$$0{\cdot}25=\frac{\gamma-1}{\gamma},$$

or $\gamma=1{\cdot}333$.

Now if we take $\gamma=1{\cdot}402$ for air and $\gamma=1{\cdot}300$ for CO_2 and consider the jet to be mainly composed of CO_2 and air, we can find the proportion by volume of CO_2 and air in the jet, assuming that the observed value of γ for the mixture obeys the law of proportional parts. This gives for the jet a percentage composition as below :—

CO_2	67·3 per cent.
Air	32·7 per cent.

These figures appear to be of the right order.

In conclusion, we would record with pleasure our thanks to Prof. P. B. Ganguly, of the Chemistry Department of the College, for supplying references to chemical literature, and to Mr. S. N. Chatterji, of the Physics Department, for drawing the diagram.

References.

(1) *Wied. Ann.* xxxii. p. 1 (1887) ; *ibid.* xl. p. 161 (1890).
(2) J. Amer. Chem. Soc. xli. p. 300 (1919).
(3) Phil. Mag. iv. p. 24 (1902). Amer. Journal of Science, xiii. p. 81 (1902) ; xv. p. 335 (1903) ; xxii. p. 342 (1906).
(4) Proc. Roy. Soc. cii. A, pp. 600, 615 (1923).
(5) Dict. of Applied Physics, i. pp. 774-75 ; 1922 Ed.

Physics and Mathematics Departments,
Science College, Patna, India.

LXXXIX. *Summation of the Series* $1+x^3/3!+x^6/6!+\ldots$

By Ludwik Silberstein, *Ph.D.**

THE function represented by the convergent series

$$y=1+\frac{x^3}{3!}+\frac{x^6}{6!}+\frac{x^9}{9!}+\cdots$$

is manifestly a particular integral of the differential equation

$$\frac{d^3y}{dx^3}=y,$$

namely, for the initial conditions $y_0=1$, $y_0'=y_0''=0$.

* Communicated by the Author.

Now, since the cube roots of unity are 1 and $-\frac{1}{2}(1\pm i\sqrt{3})$, the complete integral of this equation may be written

$$y=ae^{x}+e^{-\frac{x}{2}}\left(b\cos\frac{\sqrt{3}}{2}x+c\sin\frac{\sqrt{3}}{2}x\right),$$

where a, b, c are arbitrary constants. For $x=0$,

$$y_0=a+b+c,\ y_0'=a-\tfrac{1}{2}b+\frac{\sqrt{3}}{2}c,\ y_0''=a-\tfrac{1}{2}b-\frac{\sqrt{3}}{2}c,$$

so that to $y_0=1$, $y_0'=y_0''=0$ correspond $a=\frac{1}{3}$, $b=\frac{2}{3}$, $c=0$. Thus,

$$1+\frac{x^3}{3!}+\frac{x^6}{6!}+\ldots=\frac{1}{3}\left\{e^{x}+2e^{-\frac{x}{2}}\cos\frac{\sqrt{3}}{2}x\right\},$$

the required sum. Thus, also,

$$1-\frac{x^3}{3!}+\frac{x^6}{6!}-\ldots=\frac{1}{3}\left\{e^{-x}+2e^{\frac{x}{2}}\cos\frac{\sqrt{3}}{2}x\right\},$$

and, taking half the sum of the two expansions,

$$1+\frac{x^6}{6!}+\frac{x^{12}}{12!}+\ldots=\frac{1}{3}\left\{\cosh x+2\cosh\frac{x}{2}.\cos\frac{\sqrt{3}}{2}x\right\}.$$

Rochester, N.Y.
March 1938.

XC. *Notices respecting New Books.*

Factor Tables giving the Complete Decomposition into Prime Factors of all Numbers up to 256,000. By Dr. GEORGE KAVÁN. [Pp. 514.] (London: Macmillan and Co., Ltd. Price £2 2*s*. 0*d*.)

THESE tables were calculated by the late director of the State Observatory of Stará Dala, Czechoslovakia, and the English edition has been supervised by Dr. Bear of Cambridge. They offer greater completeness within their range than any other such tables, and cover a much greater range than the only comparable work—the recently published British Association tables for numbers up to 100,000.

Accuracy and easy reference are the chief requisites in a book of this character. Comparison with the B. A. tables in the earlier part of the work, and recalculation of selected blocks of numbers in the later pages, has not revealed any errors other than those noted in the page of errata at the end. The printing is good on the whole, though the impression of some pages is light, the indices are rather small, and some of the heavy numbers are slightly blurred. A distinct superiority over the B. A. tables is given by the larger page, which enables 1000 numbers to be consulted at each opening, and by the consecutive arrangement of the numbers, obviating the somewhat annoying backward and forward reference required in using the older work.

The book should be placed in all libraries, and should be bought by all calculators who can afford the heavy price—a price which is inevitable in an unsubsidized work of this character.

Advanced Algebra. Vols. II. and III. By C. V. Durell and A. Robson. [Pp. xlvi, 195–510.] (London: G. Bell & Sons, Ltd., 1937. Price 12*s.* 6*d.*)

This text-book is completed by the volumes under review. It is considerably in advance of any other school work on the subject which is known to the reviewer, and might well be used by university students as an introduction to the less elementary parts of algebra. The authors have made a successful effort to break with tradition, though, as they confess in the preface, the departure from it is not so complete as they could wish.

Commencing with a chapter on the summation of series, the first half of the book continues with chapters on difference equations, partial fractions, the theory of equations, and sequences; the second half has chapters on inequalities, determinants, matrices, probability, and the theory of numbers. In dealing with series, principal emphasis is laid on the method of differences, which furnishes a guiding principle in a theory which often appears as a collection of tricks. The H.C.F. process is given its rightful prominence in the chapter on partial fractions, and the chapter on inequalities directs attention to a subject which is of prime importance in modern analysis. Most welcome of all is the chapter on matrices, which will give the young student a first taste of a fascinating and essential branch of modern algebra.

The one chapter which appears out of place in a modern work on *algebra* is that on sequences. It is well done, but the work would gain in homogeneity if this excursion into

non-finite processes were omitted. Little use is made of it in the subsequent chapters, and its presence is probably one of those concessions to tradition which the authors thought it unwise to refuse.

A few criticisms of details may be added. It is now accepted that the accusation of plagiarism brought against Cardan is, if not proved false, at least rendered most improbable. The authors state that no general method exists for the solution of equations of degree greater than four, which is misleading; it should be emphasized that no *algebraic* method is possible in general. The ordinary equality sign is used for congruences in place of the customary three-line symbol; it is probably an advantage in practice to have the additional line, which draws immediate attention to the difference from an equation. The term "*dull set*" used in the chapter on inequalities is, it is believed, new; it appears to the reviewer neither necessary nor desirable.

The book may be strongly recommended. Such criticisms as are offered aim solely at still further improving an admirable book.

An Introduction to the Philosophy of Science. By A. Cornelius Benjamin, Assistant Professor of Philosophy, University of Chicago. [Pp. xvi+469.] (New York: The Macmillan Company, 1937. Price 16*s.* net.)

Science has studied nature; students now study science itself. The new discipline discusses the limits and interrelations of the sciences, examines scientific method critically, and analyses the basic scientific notions. This young Philosophy of Science requires text-books, and Professor Benjamin has provided one.

The text-book purpose need deter no one from reading this volume, for it can be read with both interest and profit. The author disclaims comprehensiveness—partly to avoid duplicating text-books on logic, and partly because the field is somewhat indeterminate. The descriptions inevitably involve comments, implicit or explicit, that will not please every one, but this does not impair the descriptive value of the book.

The Philosophy of Science has its more speculative problems: Benjamin discusses the classification of the sciences, human freedom, and the nature of reality. In one topical comment the mathematical nature of scientific symbols is said to lead Jeans to suppose that God is a mathematician and Eddington to presume that he is not. Benjamin notes in such speculative essays as Keyser's logical realism a tendency to discern in

" the realm of obvious data " hints of a realm beyond. Such speculative problems, he ends the book by insisting, must be based on the critical part of the Philosophy of Science.

Such problems as the criteria " of the real as opposed to the unreal or imaginary " and " the distinction between particular and universal " are reserved for philosophy proper. Such reservations, the recognition of speculative problems, and the avoidance of trespass on logic leave for the Philosophy of Science an abundance of more critical matter.

The Logic of Science, which includes the logical structure, the nature of symbols and interpretations of scientific concepts, is covered in 190 pages. In the section on the Analysis of Scientific Concepts, 151 pages include such items as order, time, force, and law.

The term *event* may startle when applied to " a pair of objects," and perplex when applied to " numbers." Benjamin accepts the modern adoption of this term to denote " the basic entity of science." It seems curious that each " symbol is an event " if " the realm of symbols is 'actually' more extensive than the realm of events."

Physics inevitably predominates in this valuable contribution to the Philosophy of Science. Benjamin suggests a " development of postulate systems " to secure the future of the biological and humanistic sciences. Woodger's 'The Axiomatic Method in Biology' seems to respond to the suggestion.

Philosophy and the Physicists. By L. Susan Stebbing, D.Lit., Professor of Philosophy in the University of London. [Pp. xvi+295.] (London: Methuen & Co., Ltd., 1937. Price 7*s.* 6*d.* net.)

Sir Arthur Eddington's elephant and Sir James Jeans's Mathematical God are now as famous as Laplace's supreme Calculator. All three recur with entertaining regularity when the relations between science and philosophy are discussed.

The elephant represents one incursion into philosophy by mathematical physics; the Divine Mathematician expresses a second. The spiritual idealism of Eddington and the mathematical idealism of Jeans might be dangerous to their authors in Soviet Russia; in Britain they have drawn severe reproof. The reprovers, the reading public, and even those who are impressed by these two idealisms should welcome Professor Stebbing's systematic discussion of the reproof. She confirms that reproof, and does not mitigate its severity, by an analysis both thorough and searching.

Philosophizing physicists often incline to idealism, as Professor Stebbing notes when she ends her book with an interesting discussion of the changed conceptions concerning matter and natural law that have prompted these inclinations. The idealistic ventures of Eddington and Jeans will rank as striking historical episodes, and presumably have their significances, but Professor Stebbing deals faithfully with their logic.

Beethoven would be transformed from a musician into a mathematician if the sounds of his sonatas were replaced by mathematical formulæ. So Jeans, Professor Stebbing urges, reduces final truth about phenomena to mathematical description, and the Author of these phenomena to a Mathematician. Some who agree that the universe becomes "God's pure thought" by somewhat unsophisticated metaphysical legerdemain may consider Professor Stebbing to be less happy with Jeans's more emotional or æsthetic moments. Thinking minds do feel awe, and even æsthetically realized terror, before the stupendous cosmos. The æsthetic use of "vast *meaningless* distances," for instance, is not successfully challenged by the logical query whether a distance can be *meaningful*. Neither is anthropomorphism successfully alleged against the æsthetically realized "hostility" of the universe.

Eddington's presumed reduction of stars, elephants, atoms, and other items to schedules of pointer readings exposes him to severe logical attack. Jeans relies on the mathematical formulation for insight; Eddington uses it to clear the way for introspective justification of a mental reality and mystical justification of a spiritual realm. Eddington's logic is fully and competently handled, though some readers may sense a too insistent polemic and, perhaps, suspect an excessive fuss over some details. Eddington, however, has to face Professor Stebbing's firmly pressed charge of constructing arguments out of parables.

The book discusses very clearly the vexed questions of determinism, indeterminism, and human freedom that have been so insistently raised by both Eddington and Jeans. A chapter is also devoted to Eddington's deductions from entropy.

[*The Editors do not hold themselves responsible for the views expressed by their correspondents.*]

Fig. 2.

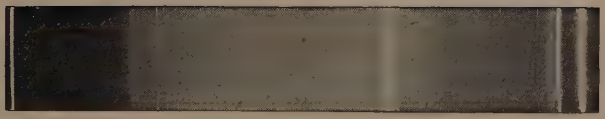

Raman spectrum in solid cyclohexane.

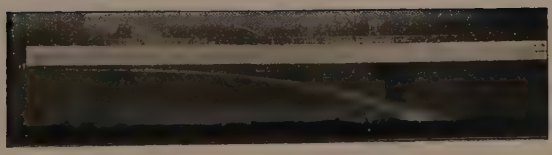

Trajectory of smoke particles.

THE

LONDON, EDINBURGH, AND DUBLIN

PHILOSOPHICAL MAGAZINE

AND

JOURNAL OF SCIENCE.

[SEVENTH SERIES.]

JUNE 1938.

XCI. *A Screened Sub-Standard Inductometer.*

By N. F. ASTBURY, *M.A.*, *and* L. H. FORD, *M.Sc.* (From the National Physical Laboratory *.)

ABSTRACT.

THE design and construction of a completely screened variable mutual inductance of high stability are described. The instrument has a range of 10,000 μH., and changes of 0·01 μH. can be read. Double screening renders the properties of the instrument independent of the circuit in which it is used. A novel method of adjustment of the sections is described, together with a novel form of inductance slide-wire. The instrument is compensated for phase defect, which even at 3000 cycles per second is only 0·0005 radian at the maximum setting. The variation of mutual inductance with frequency is also low, being less than 4 parts in 10^4 at 1000 cycles per second. The method of calibration is described, the limits of error being $\pm 0{\cdot}02\,\mu$H. throughout the range. The instrument is admirably suited for high precision a.c. bridge measurements of all kinds.

* Communicated by the Authors.

Introduction.

ALL measurements of capacitance and inductance at the National Physical Laboratory are based on the primary standard of mutual inductance, which was made at the Laboratory in 1907 to the design of Albert Campbell [1] and modified [2] in 1934–5. The design, construction and use of working substandards of mutual inductance thus form an essential part of the work of maintenance of laboratory standards and play a great part in meeting the growing requirements of industry for high precision tests on apparatus used in communication engineering. The form of working standard of mutual inductance most generally useful is one which is continuously variable from a value equal to that of the primary standard (10 mh.) down to zero, the variation being effected by decade dials and some small continuously variable part such as is provided by a moving coil or slide-wire.

For high precision a.c. bridge work an inductometer has to meet a number of exacting and often mutually conflicting requirements, and although existing instruments possessed some or other of the necessary qualities, none possessed all. The instrument must be stable (its maximum value should remain constant to ± 5 parts in 100,000 over a period of at least a year), must be so subdivided that a change of one hundred thousandth part of the maximum value can be easily and accurately read, the variation of mutual inductance with frequency must be small, the phase defect (which measures the departure from true quadrature of secondary e.m.f. and primary current) must be low, and the potential distribution of the instrument must be so controlled as to make its properties independent of the circuit in which it is used, that is, adequate screening must be provided. In the instrument described in this paper an attempt has been made to combine all these requirements, and it is believed that in the system of screening, in the design of the continuously variable scale, and in the method of adjustment, the instrument presents novel features *.

* Albert Campbell has described a simple form of inductance slide-wire (Campbell and Childs, 'The Measurement of Inductance, Capacitance and Frequency,' p, 162).

General Features of Design.

The question of long-period stability is one which experience has shown to be dependent almost entirely on the provision of a suitable former for the windings and on the removal of winding stresses from the coils by some "annealing" process. Selected marble, free from ferrous inclusions, has proved to be the best available material for the coil former. An "annealing" process[3] in which the completed windings are maintained at a temperature of 120° C. in transformer oil for twenty-four hours, has proved effective not only in removing winding stresses, but also in dehydrating the system, an essential prerequisite if the instrument is not to develop defects arising from dielectric failures.

The problem of subdivision is one which is intimately bound up with the variation with frequency of the inductance and phase defect of the instrument. In the early Campbell instruments[4] subdivision of the adjustable winding into decade dials was obtained by the use of cable of ten strands, which were connected in series. This arrangement imposes fairly large capacitances on the windings, and the frequency variations of the instrument may become very large. The Butterworth system[5] of providing coils in the ratio 6 : 3 : 1, which are combined in series or opposition as required, reduces the capacitance difficulty at the expense of the introduction of a fairly complex switching arrangement, which is liable to give trouble for purely mechanical reasons. In the present instance it was decided to make individually adjusted coils for all the subdivisions except the smallest, and although, on the face of it, this appears to be a formidable task, a comparatively simple practical solution was found. In this way the effects of winding capacitance were kept down and the switching arrangements were of the simplest.

Turning now to the problem of providing a final, small and continuous variation of mutual inductance by means of which changes equal to one hundred thousandth of the maximum may be read, it was felt that it would be desirable to break away from the tradition of using a small moving coil rotating about an eccentric axis in a plane approximately parallel to that of the main fixed winding. This system gives a non-linear scale, very open near the

zero region and closing in towards the maximum. By various devices the angular length of the scale can be extended and its law brought into close conformity with an exponential type of variation, which gives a constant percentage accuracy of reading over the range of the scale. This is thought by some workers to be an advantage, but the present writers feel that a linear scale is much more valuable in general practice as being easier to read (especially when interpolation is required) and easier to engrave in the first place. A novel form of slide-wire was therefore designed to give the final variation, providing a range of 12 μH. on a scale length of 330° and being strictly linear.

Finally, the problem of screening the instrument has to be considered. This presents a number of interesting features, since a mutual inductance as normally used in a bridge circuit is a three-terminal instrument in which the absolute potentials of the three terminals may differ in different circuits. The mere presence of screens will alter the electric fields of the windings and react on the frequency variations, while eddy-current losses in the screens will contribute to the phase defect of the instrument. The reconciliation of the conflicting requirements implied above proved impossible without an auxiliary compensating circuit, and with this the problem has been solved for all practical purposes.

Considering the screening first of all purely from the standpoint of providing a control on the electric field of the coil system, it seems desirable that each winding should have its own screen, preferably connected to one end of the winding, so that external capacitance effects associated with the instrument are immediately localized at definite points in the system. The position is still further simplified if the screen of one winding can be arranged to enclose the other winding and its screen. Since, as has already been pointed out, the absolute potentials of the terminals in the network may differ in different circuits, the final stage in the screening is clearly the provision of an earthed screen enclosing the whole instrument, thus fixing permanently the earth-capacitances of the system. Six possible ways of arranging the screens then arise when the mutual inductance is used with one point of the windings common. These are shown in fig. 1, in which AC and CB are the windings,

C being the common point. A brief consideration of the advantages and disadvantages of each arrangement will illustrate fairly well the principles involved. In every case the self-capacitance of each winding is augmented by the presence of the screens, but the effects of this can be made small by generous spacing between coils and screeens. In fig. 1 (*a*) the capacitance between the inner screens is thrown across the open ends of the system, and when the windings are connected, as is generally the case, so that the mutual inductance opposes the self-inductance, the effect of a capacitance in this position is relatively small[6]. In this respect this arrangement is superior to the other five, in which the inter-screen capacitance is thrown across one or other of the windings. The

Fig. 1.

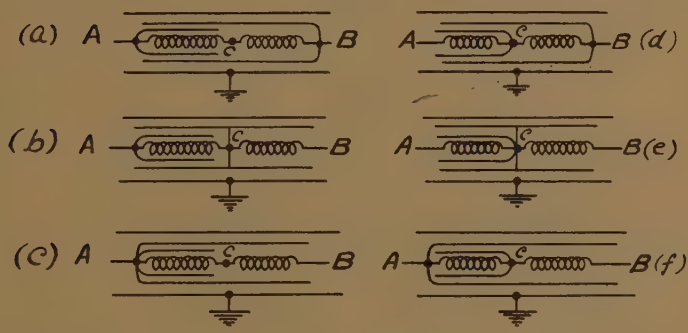

earth-capacitances of the system (arising almost entirely from the middle screen) are concentrated at one of the open ends, which facilitates their elimination or compensation in bridge circuits. This distinction is also shared by arrangements (*c*), (*d*), and (*f*). In arrangements (*b*) and (*e*) this earth capacitance is concentrated at the common point, C. This is a bad arrangement for many bridges, especially when a Wagner earthing arm is used, for the latter does not in general take account of such a capacitance *. The arrangement shown in fig. 1 (*a*) is therefore regarded as the most generally satisfactory, although in the complete instrument provision is made for all possible connections of the screens.

* An analysis of this problem will be given in the authors' paper on "The Precision Measurement of Capacitance."

The actual structure of the screen can be so designed as to minimize eddy-current losses without greatly impairing their efficiency as electrostatic screens. One simple way of doing this is to make the screen of thin tinfoil and to cut it, by a system of parallel slits, into the form of a comb. A practically complete equipotential surface is thus provided from the electrostatic point of view, while the actual geometry of the system makes the available eddy-current paths of very high resistance. A grille of fine wires, arranged without closed loops, is also very useful, and both types are used in the present instrument.

Construction.

A consideration of the many purposes for which the inductometer would be required led to the decision to

Fig. 2.

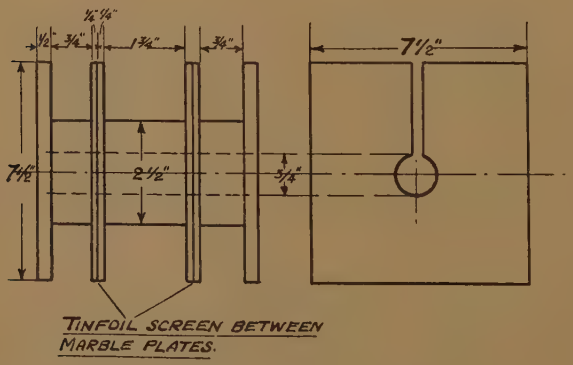

Marble bobbin.

construct the instrument with three decade dials, giving steps of 10×1, $10 \times 0{\cdot}1$, and $10 \times 0{\cdot}01$ mh. respectively, and a scale of rather more than $10\,\mu$H. The fixed winding (which will be described henceforward as the " secondary ") was first wound to have a self-inductance of just over 11 mh., this being a convenient value for bridge work, particularly for certain special circuits, and the resistance of the finished winding was approximately 1 ohm. The fixed and adjustable windings are carried on a marble bobbin, built up by cementing together plates and disks with a bakelite varnish. The bobbin (fig. 2) has three winding

spaces, the inner being occupied by the secondary winding. The marble plates on the outside are slotted for the passage of leads, while those bounding the inner section are double, sandwiched between each pair being a sheet of tin-foil, slit as already described, forming part of the screen of the secondary winding. The secondary winding itself consists of 352 turns of litz wire, made up of 81 strands of copper wire, 0·2 mm. diameter, each strand enamelled, with double silk insulation overall. The main primary (subdivided) windings occupy the outer spaces and are of

Fig. 3.

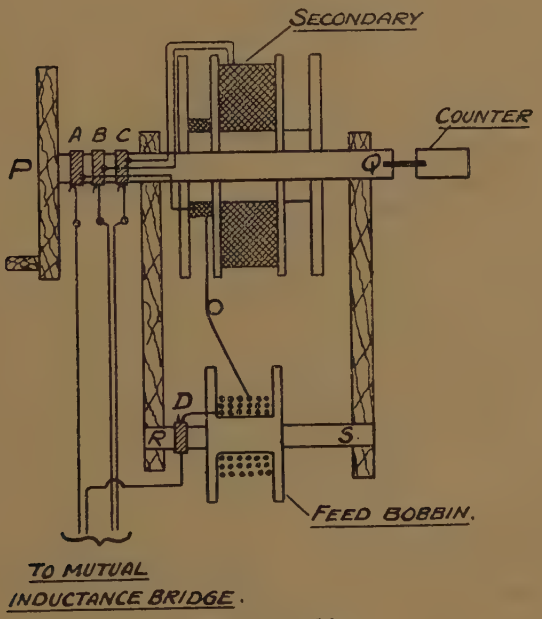

Winding machine.

litz wire of 27 strands of the same gauge as that used in the secondary windings. The secondary coil having been wound and adjusted to the nearest turn, the winding of the subdivided primary was then carried out on the machine shown diagrammatically in fig. 3. In this machine, constructed for obvious reasons largely of wood, the marble bobbin is clamped to a shaft PQ carrying three slip-rings A, B, and C, and a revolution counter. One of the rings, A, is connected to the inside end of the

primary winding, and the other two, B and C, to the completed secondary winding. The feed bobbin runs on a fixed shaft RS, carrying a contact ring D on which bears a brush connected to the inside end of the feed. Leads from this ring and from brushes bearing on A, B and C then pass to an inductance comparison bridge, so that the mutual inductance is continuously under observation as the primary sections are wound on. In this way the ten sections of 100 μH. each and the ten sections of 1000 μH. each were rapidly wound on, adjustment being made to the nearest turn. The windings were arranged so that in each outer section were five sections each of about 100 μH. nearest the core, and five sections each of 1000 μH. remote from the core. When these windings had been completed they were subjected to the annealing process already described.

The final adjustment of these sections was carried out using a system of adjusting turns, mounted on insulating material and bolted to each face of the marble bobbin. These turns, the optimum radii of which had been chosen after preliminary explorations of the field of the secondary winding, were made from copper wire of about 2 mm. diameter, rolled into thick strip, and were mounted edgewise in circular grooves milled in a plate of keramot. The open ends of the turns terminated by the edges of a slot cut radially in this plate to register with the corresponding slot in the cheek of the bobbin (see fig. 2) through which the ends of the primary sections passed. The arrangement is shown diagrammatically in fig. 4 (*b*). The open ends of the primary sections are completed through these turns in the manner indicated in fig. 4 (*a*), and clearly these turns may be added in series or in opposition to the windings as required. The contacts of the decade dial are brought to a group of ten soldering pins in the centre of the keramot plate, and from these pins radial wires are carried out to the adjusting turns. The position in which each radial wire has to be soldered to its corresponding turn to give the correct adjustment of any section is quickly determined on a bridge. The circuit arrangement is, as will be seen from fig. 4 (*a*), simply that of a number of preset slide-wires. The system provides a rapid method of adjusting every section and possesses one great advantage in that the adjustment is carried out with the switches in position

as actually used, so that any uncertainty which may arise from subsequent fitting of the switchgear is avoided. Two

Fig. 4.

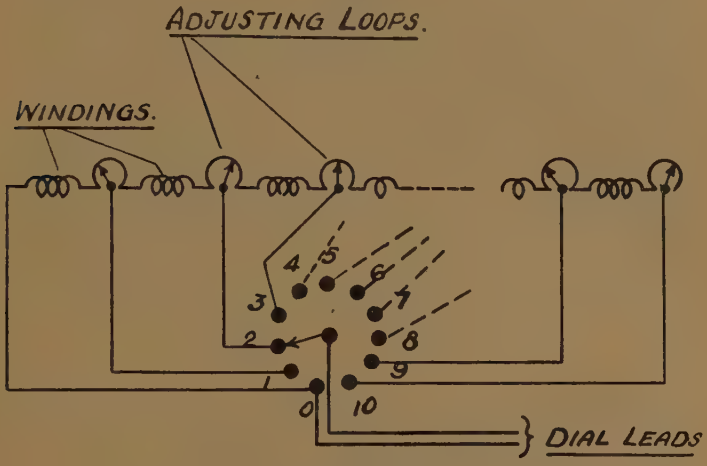

(*a*) Illustrating method of connecting series adjusting turns to the dial.

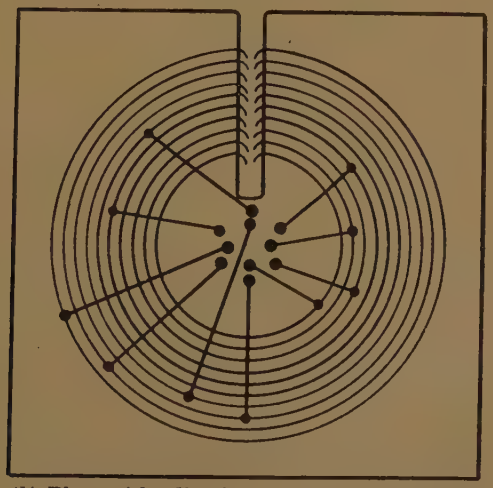

(*b*) Plate with adjusting turns and radial wires.

supernumerary adjusting turns were provided on each face, to be employed later in the compensating circuit (see below).

The smallest decade dial, that giving steps of 10 μH., was made using Campbell's stranding principle. This is permissible here, since the inductance of the section is very low and the capacitance effects will be correspondingly small. Four turns of a cable of 10 strands of litz wire (27/36) were wound on a keramot bobbin about 15 cm. diameter, threaded on to a keramot shaft, the axis of which was coincident with that of the main windings. The exact position of this coil could then be adjusted within very fine limits to give the required mutual inductance, and it was secured in its final position by locking nuts on either side.

The continuously variable part was made, as has already been indicated, on a slide-wire principle. If a circular coil of one turn be placed in a uniform magnetic field,

Fig. 5.

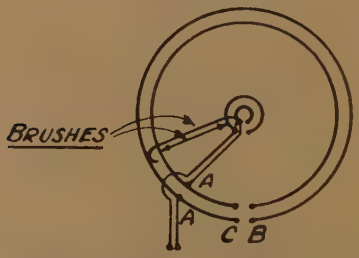

Double-loop series slider. M is zero when the brushes are at A, is positive in the arc AB, and negative in the arc AC.

perpendicular to its plane, then the flux through any sector is clearly proportional to the length of the arc of the sector. If the magnetic field alternates, then the e.m.f. developed between the ends of the arc will be proportional to the arc and will increase uniformly as the arc increases. The practical utilization of this idea depends on the use of radial collectors in which, if the assumptions as to uniformity of field are realized, no e.m.f. will be developed. A single turn, if kept within manageable size, may often prove too small to give the required variation. This was actually the case in the present instrument, but the range was doubled by the simple device of having a double loop with the turns connected in series. The method of construction will be apparent from figs. 5 and 6. The two loops were of brass strip, placed edgewise to the

magnetic field to reduce eddy-current losses, the double collector brush working in the annular space between them. The rings are about 9 and 10 cm. radius and give a variation in mutual inductance from -1 to $+12\,\mu$H. On the scale of the instrument a change of $0{\cdot}1\,\mu$H is represented by an arc of length 4·5 mm., so that actually it is easy to read to one millionth part of the total mutual inductance. The advantage of this is very great from the practical viewpoint, for it enormously extends the lower range of measurements which can be usefully made with the instrument.

The completion of the screening was the next stage in the construction. It will be clear from what has gone

Fig. 6.

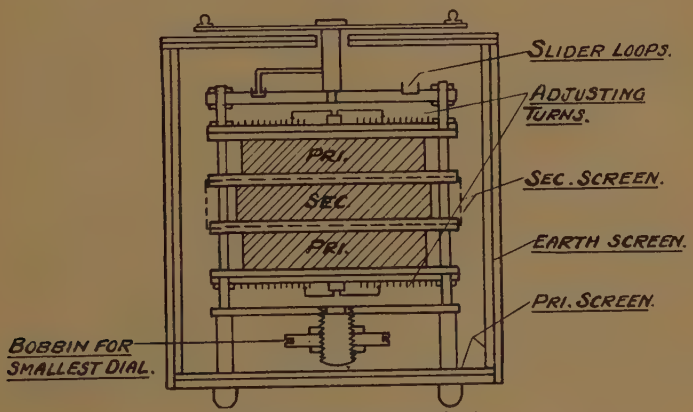

General assembly (section).

before that the primary screen had to enclose the whole instrument, even the switchgear and slider. This was done by fitting the primary screen, made of slit tin-foil in the manner already described, to the inside of the inner wall of a double-walled box designed for the instrument. The outside of this inner wall carries the earth screen. The roof of the box is of similar construction to the walls and base, but has holes through which the operating handles of the decade dial switches pass, and carries two small selector switches by means of which any of the six screening arrangements (see fig. 1) can be chosen at will. The whole box, a section of which is shown in fig. 6, was made of sheets of keramot, screwed together,

and sealed with a cellulose cement. The secondary screen is completed by a wire grille fitted round the periphery of the inner cheeks of the bobbin.

The inductometer at this stage possessed a fairly large impurity or phase defect, arising largely from the inevitable residual eddy-current losses in the screens, etc. The actual value of impurity at a frequency of 1000 cycles per second was about 0·05 ohm at the maximum setting of the instrument, corresponding to a phase defect of about 0·001 radian. This value, although by no means intolerable, was considered too large for a precision instrument of the type required, and it was therefore compensated by an auxiliary circuit in the manner described below.

The Compensating Circuit.

The principle of the compensating circuit is the very simple one of introducing a phase defect of the same mag-

Fig. 7.

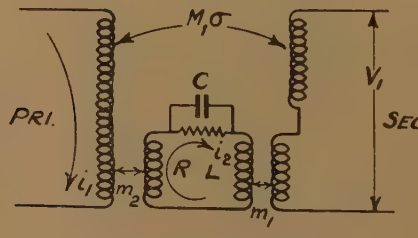

Compensating circuit.

nitude, but of opposite sign, to that already in existence. The practical difficulties lie in producing an "artificial" impurity which shall vary with inductometer setting and with frequency in the same way as the real impurity, and, further, shall have only a small effect on the value of mutual inductance. Consider a closed circuit, of total resistance R and total effective inductance L, coupled to both windings of the instrument as shown in fig. 7. Let M and σ be respectively the mutual inductance and impurity of the main windings. Then if m_1 and m_2 be the mutual inductances into the compensating circuit, as indicated in fig. 7, the effective values of mutual

inductance and impurity at a frequency of $\omega/2\pi$ cycles per second are given by

$$M_{eff.}=M+L\frac{\omega^2 m_1 m_2}{R^2+\omega^2 L^2} \quad . \quad . \quad . \quad . \quad . \quad (1)$$

$$\sigma_{eff.}=\sigma-R\frac{\omega^2 m_1 m_2}{R^2+\omega^2 L^2}. \quad . \quad . \quad . \quad . \quad . \quad (2)$$

If m_1 is fixed and m_2 varies as M, and if ωL is made small compared with R, then clearly the effect on M will be very small and proportional to M, and the effect on σ will be to add a term of opposite sign which varies approximately as M and as ω^2—*i. e.*, which behaves approximately in the same way as σ itself. These requirements are obtained by providing the mutual inductance m_1 from a small toroidal system of coils and the mutual inductance m_2 from two of the supernumerary turns (one from each group to preserve symmetry) on the plates carrying the adjusting turns. The mutual inductance into these turns varies in the same way as M. The condenser C, shunting the added resistance in the closed circuit, in effect helps to reduce L.

The constants of the circuit were determined partly by calculation and partly empirically. The toroid providing m_1 is about 10 cm. diameter, m_1 having a value of about 200 μh. One winding is put in series with the main secondary winding (and enclosed in a screen connected to the screen of that winding) and the other is closed through the two adjusting turns already mentioned and an added resistance of about 5 ohms, across which is a condenser of about 2·4 μF. capacitance. The windings are, of course, connected in the sense required to give a correction of the necessary sign. The effect of the compensating circuit is illustrated by the figures given in the following table,

TABLE.

Effect of Compensating Circuit.

Quantity.	Frequency. c.p.s.	No compensation.	With compensation.
Frequency change of M.	1000	3·1 parts in 10^4.	3·9 parts in 10^4.
	3000	30 parts in 10^4,	36 parts in 10^4.
Impurity	1000	0·05 ohm.	$<$0·001 ohm.
	3000	0·5 ohm.	$<$0·01 ohm.

referring to the maximum setting of the instrument for a positive mutual inductance.

The compensating circuit is enclosed in the instrument case and conforms to the same screening arrangements as the main windings.

On completion the case was filled with a mixture of equal parts of vaseline and transformer oil. This mixture, which is pasty at ordinary temperatures and liquefies at about 30° C., possesses all the good qualities of pure transformer oil. It is therefore admirable for sealing the windings against air and moisture, while it possesses none of the disadvantages attendant on the use of a mobile liquid.

Calibration and Performance.

The precision calibration of inductometers of the kind under discussion has been greatly facilitated by the modifications recently made to the primary standard. These are described in detail elsewhere[2], but a brief note here will help the discussion. Additional windings and circuits have been added to the standard, so that a continuous variation in mutual inductance of $\pm 100\ \mu$H. is now possible. Like the values for the main windings of the standard, those for the new windings are calculated from the geometry of the system. The technique of using the standard has been improved, so that errors arising from capacitance effects are entirely eliminated.

The method of calibration adopted involves the absolute determination of the value at any one setting on the inductometer and the subsequent relation of all other readings to this. By the use of an auxiliary uncalibrated instrument, the value at any one setting can be immediately related to those on either side of it by the addition or subtraction of a mutual inductance equal to the full setting on the next lower dial, and this process can be extended to cover the whole range. Analytically, the argument is as follows. Let the correction on the rth stud of the top dial (1000 μH. steps) be α_r, that on the corresponding stud of the middle dial be β_r, and that on the corresponding stud of the lowest dial be γ_r. Then we can determine experimentally quantities ζ_r, ξ_r, and η_r such that, the units being μH.,

$$\zeta_r=(1000r+\alpha_r)-\{1000(r-1)+\alpha_{r-1}+1000+\beta_{10}\} \quad . \quad . \quad (3)$$

$$\xi_r=(100r+\beta_r)-\{100(r-1)+\beta_{r-1}+100+\gamma_{10}\} \quad . \quad . \quad . \quad (4)$$

$$\eta_r=(10r+\gamma_r)-\{10(r-1)+\gamma_{r-1}+S_r\}, \quad . \quad . \quad . \quad . \quad . \quad . \quad . \quad (5)$$

where S_r is a scale reading of the instrument approximately equal to $10\,\mu$H. We thus find

$$\sum_1^{10}\zeta_r=\sum_1^{10}(\alpha_r-\alpha_{r-1})+10\beta_{10} \quad . \quad . \quad . \quad . \quad (6)$$

$$\sum_1^{10}\xi_r=\sum_1^{10}(\beta_r-\beta_{r-1})+10\gamma_{10} \quad . \quad . \quad . \quad . \quad (7)$$

$$\sum_1^{10}\eta_r=\sum_1^{10}(\gamma_r-\gamma_{r-1})+S_r \quad . \quad . \quad . \quad . \quad (8)$$

The quantities ζ, ξ, η, and S are experimentally observed. If *one* of the quantities α_r, β_r, γ_r is known, then the above system of equations is soluble (since, of course, $\alpha_0=\beta_0=\gamma_0=0$) and the corrections for every setting of the inductometer, even of the scale setting in the neighbourhood of the readings S, are determined. In practice, the value of α_{10}, the correction at the highest setting of the top dial, is determined by comparison against the primary standard. The scale of the instrument is compared directly with the continuously variable part of the primary standard, and it is very satisfactory to record that the corrections in the neighbourhood of the scale reading $10\,\mu$H. obtained by this direct method agree to within $0{\cdot}02\,\mu$H. with those obtained from the solution of equations (6), (7) and (8). The additional windings on the primary standard also make it possible for every setting of the lowest dial ($10\,\mu$H. steps) to be checked directly, and the corrections obtained in this way agree excellently with those deduced from equations (6), (7) and (8). In fact, in only one instance does the difference appear to be as big as $0{\cdot}02\,\mu$H., and the average difference is less than $0{\cdot}005\,\mu$H. This agreement, which falls below the lowest usable limit of the instrument, is a striking tribute not only to the precision of calculation of the additional windings to the primary standard, but also to the technique of the calibration.

It is, of course, much too early in the history of the instrument to attempt to assess its probable long-period stability. Actually, since its completion and first calibration in November 1937, until the time of writing (March 1938), the value at the maximum setting has increased by

5 parts in 10^5. This period is likely in any event to witness the most rapid changes, as experience has shown that inductances of this type "settle down" most quickly in the period immediately following the annealing process. The adjustment of the instrument is within 1 part in 10^4 of its nominal value at the maximum setting, on the second dial the mean correction is about $0{\cdot}1\,\mu$H., and on the third dial about $0{\cdot}05\,\mu$H.

The scale is engraved linearly in microhenries, but since the system cannot be absolutely symmetrical with regard to the secondary field, there are small corrections on the engraved divisions. These, as already indicated, are determined by reference to the primary standard, and range from $0{\cdot}02\,\mu$H on the first three cardinal points, $0{\cdot}05\,\mu$H. at 5 μH. and $0{\cdot}02\,\mu$H. at $10\,\mu$H.

The frequency coefficient and impurity of the instrument are of such an order that it is easily possible to use the instrument up to 3000 cycles per second, and even higher frequencies are quite manageable. The frequency coefficient and impurity vary somewhat with the setting of the instrument, as, indeed, is only to be expected from the nature of the subdivision. This is in accordance with Butterworth's analysis[6] of the equivalent circuit of mutual inductance, from which it would appear that the frequency coefficient of an inductometer of the present type should decrease as the setting increases when the coils are connected in the positive sense (*i. e.*, mutual inductance opposing self-inductance). The frequency coefficient at a frequency of 1000 cycles per second ranges from 5 parts in 10^4 at a setting of 200 μH to 4 parts in 10^4 at a setting of 10,000 μH. The frequency coefficient throughout is proportional to the square of the frequency. The impurity is negligibly small over the whole range at a frequency of 1000 cycles per second, and at 3000 cycles per second it varies by a few thousandths of an ohm over the range of the instrument. Actually, day-to-day variations in impurity arising from the effect of temperature changes on the resistance of the compensating circuit, and on the metal responsible for the eddy-current losses are of this order, and it is interesting to note that a limitation on performance should be set by an effect of this kind. Actually, it represents an uncertainty in phase defect at 3000 cycles per second of less than 10^{-5} radian, so that its practical importance is negligible.

The temperature coefficient of the instrument appears to be of the order of 7 parts in 10^6 for 1° C. This figure has been deduced from day-to-day observations when room-temperature has varied between 13° and 19° C., and appears to be well-substantiated by a number of subsequent tests. Any scheme of heating or cooling the whole instrument in order to discover this figure is clearly impracticable.

The inductometer is now in regular use and appears to represent a very fair realization of the original requirements. It will, however, be at least ten years before a final verdict can be given as to its performance.

In conclusion, the authors must acknowledge their indebtedness to Mr. W. G. Turl, of the Instrument Workshop of the Laboratory, whose skill and patience in surmounting the practical difficulties of construction have contributed so largely to the successful accomplishment of the work.

References.

(1) Campbell, Proc. Roy. Soc. A, lxxix. p. 428 (1907).
(2) Astbury, Phil. Mag. ser. 7, xxv. p. 290 (1938).
(3) Hartshorn and Astbury, Phil. Trans. Roy. Soc. A, no. 769, ccxxxvi. p. 442.
(4) Campbell, Proc. Phys. Soc. xxi. p. 69 (1907–09).
(5) Hartshorn, Proc. Phys. Soc. xxxviii. p. 302 (1926).
(6) Butterworth, Proc. Phys. Soc. xxxiii. p. 312 (1921).

XCII. *Dielectric Constant and Conductivity of Soil at High Radio Frequencies.*

By S. S. Banerjee, *D.Sc., and* R. D. Joshi, *M.Sc., A.M.I.R.E., Benares Hindu University* *.

Introduction.

TRANSMISSION of long distance messages by wireless and also their successful reception depend much on the conditions of the upper atmosphere. But the reception of the short distance messages by the ground-wave depends on the electrical properties of soil around the transmitter. In view of this, the field-strength survey around a broadcasting transmitter has been carried out

* Communicated by the Authors.

in many important cities of America [1], Australia [2], and England [3]. In India also such surveys have been made by Rakshit [4], Roy [5], and Khastgir [6]. Attenuation of the signal along the ground is obtained from the graphs computed from field-strength measurements as one goes away from the transmitter, and from these graphs it is possible to calculate the conductivity and the dielectric constant of the soil. This method of calculating the electrical constants of soil is a laborious process, and there has always been an attempt to determine these constants experimentally in the laboratory. Various investigators [7], [8], [9] have employed different methods at different frequencies for the determination of the above constants. It may be mentioned that, in order to determine the exact value of the conductivity of the soil, the knowledge of the attenuation constant of radio waves in the medium is necessary. In most of the methods employed so far, no account has been taken of the actual attenuation of the wave. In the present investigation we have observed the attenuation of the waves travelling through the soil under test and thence calculated its conductivity and dielectric constant. The attenuation constant has been measured by immersing a Lecher wire system in the soil and allowing the wave to travel along the system. The constants have been determined of different soils at different moisture contents and at frequencies of the order of 50 to 70 megacycles per second. The ultra-high frequency was adopted in the present case because, along with these measurements, simultaneous observations were being taken for the field-strength measurements around an ultra-short wave transmitter of low power. From these observations also the attenuation constant and conductivity were calculated, and the values obtained from this were found to be in close agreement with those obtained by the present method.

Theoretical Considerations.

The theory of the method consists in evaluating the value of the dielectric constant of a conducting medium and also its conductivity in terms of the attenuation constant of a radio wave travelling along the medium. By standard analysis of the propagation of alternating currents along a pair of parallel wire system, it has been

shown by Smith-Rose and McPetrie [9] that if the medium between the wires possesses conductivity then the following relations with the attenuation constant and dielectric constant can be obtained :—

$$\alpha = \frac{2\pi}{\lambda_a}\sqrt{\frac{K' - K}{2}} \quad . \quad . \quad . \quad . \quad . \quad . \quad (1)$$

$$\frac{\lambda_a}{\lambda_s} = \sqrt{\frac{K' + K}{2}} \quad . \quad . \quad . \quad . \quad . \quad . \quad (2)$$

and

$$K' = \sqrt{K^2 + \frac{16\pi^2\sigma^2}{\omega^2}} \quad . \quad . \quad . \quad . \quad (3)$$

where

α=attenuation constant ;

λ_a and λ_s=wave-lengths in air and soil respectively ;

K=dielectric constant of the soil ;

ω=angular frequency of the impressed waves ;

σ=conductivity of the soil.

Now from (1) and (2) it can be easily shown that

$$K' = \frac{\alpha^2\lambda_a^2}{4\pi^2} + \frac{\lambda_a^2}{\lambda_s^2} \quad . \quad . \quad . \quad . \quad . \quad (4)$$

and the dielectric constant of the soil,

$$K = \frac{\lambda_a^2}{\lambda_s^2} - \frac{\alpha^2\lambda_a^2}{4\pi^2} \quad . \quad . \quad . \quad . \quad (5)$$

By substituting the values of K and K′ in equation (3) it can be shown that the conductivity of the soil,

$$\sigma = \frac{\alpha\omega\lambda_a^2}{\lambda_s 4\pi^2} \quad . \quad . \quad . \quad . \quad . \quad . \quad (6)$$

From equations (5) and (6) the values of the dielectric constant and conductivity of the soil can be determined from the knowledge of the attenuation constant α, λ_a, and λ_s the wave-lengths in air and soil respectively. The attenuation constant is measured experimentally as described below. As the wave-length in soil, λ_s, cannot be measured without disturbing the soil the value of $\frac{\lambda_a}{\lambda_s}$ is determined by the "wave-shift" method employed by

Smith-Rose and McPetrie. This is obtained from the relation

$$\frac{\lambda_a}{\lambda_s} = \frac{N\lambda_a - l}{L}, \quad \ldots \ldots \ldots \ldots \quad (7)$$

where N is the total number of waves between the input end of the box, which is kept at a node, to the node next to the other end of the box outside it, l is the distance between the first node encountered after the soil away from the input end and the end of the soil nearest to it. L is the length of the soil along the parallel wires. By the substitution of the value of $\frac{\lambda_a}{\lambda_s}$ in equation (6) the conductivity of the soil can be determined.

The attenuation constant α is found by the "half-width" method after drawing the resonance curves along the parallel wire system. It is obtained from the relation $\alpha = \frac{2\pi d}{n\lambda_a^2}$, where d is the "half-width," that is, the distance on the wire between the points where the deflexion of the galvanometer is half that of the maximum deflexion at a node, n is the number of node from the input end. Thus by the substitution of the value of α in equations (5) and (6), conductivity and dielectric constant can be evaluated.

Experimental Arrangement and Observations.

Two hard drawn copper wires (LL) of 0·645 cm. in diameter each were stretched horizontally at 6 cm. apart. To make the resonance curves symmetrical the input end of the parallel wire system, instead of being connected with a loop of copper wire, was connected with a series of high value condensers (C_1, C_2, C_3 in fig. 1). Two ends of the central condenser were connected to a low resistance mirror galvanometer (G) through a Cambridge Vacuo-thermojunction (T.) This experimental arrangement of Lecher wire system is similar to that employed by Banerjee [10] for the measurement of the radiation resistance of the parallel wire transmission lines.

The soil for the experiment was kept in a wooden box of dimensions $130 \times 11 \times 10$ cm. Two slits were cut on either side of the box nearly to the bottom. The parallel

wires passed through these slits. This was done so that the box could be slid and shifted along the parallel wires. A retroaction type of valve generator (O) emitting waves of 3 to 5 metres long was used to energize the Lecher wire system.

The input end of the parallel wires was loosely coupled with the oscillator. When the waves meet the soil surface they are reflected back to some extent due to the conducting nature of the medium. To minimize this chance of the boundary reflexion of the waves at the surface of the soil, the box was shifted to such a position along the wires that its end nearer to the input end of the Lecher wires coincided with a potential node.

The box was now filled with soil and the positions of the nodes were noted. It was observed that as the

Fig. 1.

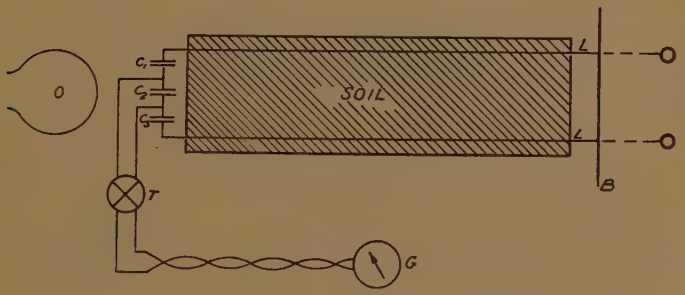

Illustrating the experimental arrangement.

soil was put gradually the shift of the nodes was towards the box. The wires were covered with soil and compressed, and the number of nodes shifted in the soil was counted. Lastly, the final node next to the end of the box was located and the distance of this node to the box was measured.

The resonance curves were drawn by plotting the distance along the parallel wires against the deflexions of the galvanometer as a short circuiting metal bridge (B, fig. 1) was gradually moved along the parallel wires. Similar readings were taken for the different frequencies and moisture contents.

To find the moisture content a weighed amount of soil was heated for twenty-four hours or more. After extracting all the moisture of the soil it was again weighed.

The moisture content of the soil was measured the same day as it was used for the experiment with the parallel wires.

Tables I. and II. give the values of dielectric constant and conductivity of a typical soil for different moisture

TABLE I.

Frequency 57·03 megacycles per second.

Moisture content in percentage.	Attenuation constant.	Dielectric constant.	Conductivity in e.s.u.
6·3	$2·12 \times 10^{-2}$	4·58	$1·53 \times 10^{6}$
6·8	2·99 „	6·50	2·58 „
7·6	2·53 „	6·95	2·91 „
8·8	3·43 „	10·25	5·09 „
9·2	3·32 „	11·01	4·67 „
13·9	5·16 „	17·33	7·17 „

TABLE II.

Frequency 70·92 megacycles per second.

Moisture content in percentage.	Attenuation constant.	Dielectric constant.	Conductivity in e.s.u.
6·3	$4·21 \times 10^{-2}$	3·22	$2·56 \times 10^{6}$
6·8	4·97 „	5·78	4·04 „
7·6	6·38 „	6·11	5·33 „
8·8	6·44 „	10·20	5·86 „
9·2	7·11 „	11·71	8·21 „
13·9	8·34 „	12·03	9·77 „

contents at two frequencies of 57·03 mc./sec. and 70·92 mc./sec. As the amount of soil necessary in this experimental arrangement was considerably high, a homogeneous mixture of artificial moisture was not possible, and thus the values of moisture contents of soil given in Tables I. and II. correspond to natural moisture content of the same soil obtained on different days. Figs. 2 and 3 show the variations of the conductivity and dielectric constant

with moisture content. It will be observed from these figures that conductivity and dielectric constant of the soil increase with moisture content and ultimately tend to become constant.

Fig. 2.

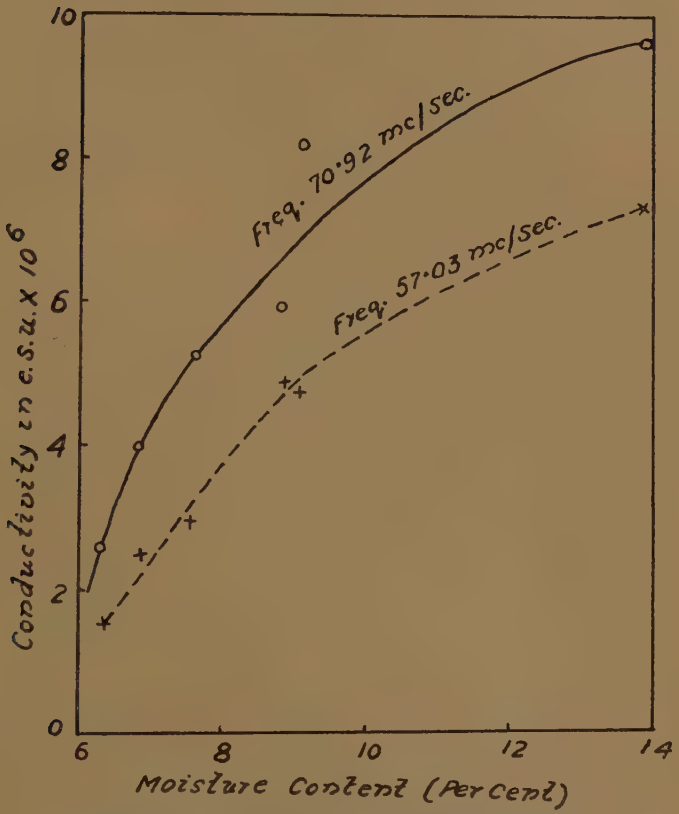

Variation of conductivity with moisture content.

Summary and Conclusion.

Conductivity and the dielectric constant of soil at ultra-high frequencies have been determined experimentally by measuring the actual attenuation of the waves in the soil. The soils tested were taken from different sites and depths. The above electrical constants are found at two different frequencies and different

moisture contents. The value of the conductivity measured was of the order of 10^6 e.s.u. The conductivity increases with the frequency as well as the moisture content. For dry soil or soil of less moisture content the conductivity increased from a value of $1{\cdot}5 \times 10^6$ e.s.u. to a value nearly equal to $2{\cdot}6 \times 10^6$ e.s.u.

Fig. 3.

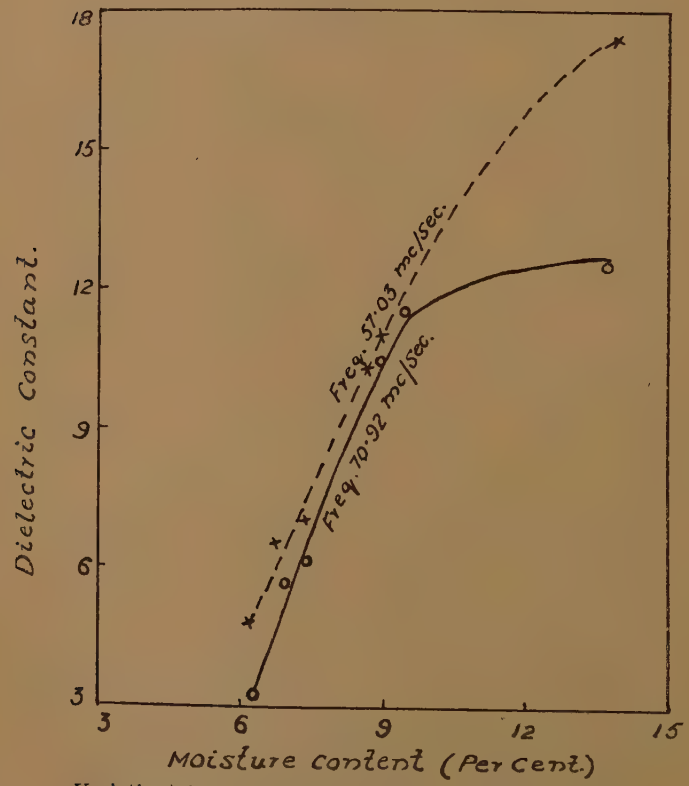

Variation of dielectric constant with moisture content.

Unlike the conductivity the dielectric constant diminishes with a rise of frequency, but it increases with moisture content. It varied from a value of nearly 4·5 at a moisture content of 6·3 per cent. to a value of 17·3 at a moisture content of 13·9 per cent. The variation of attenuation constant is not very regular. Generally it is higher for moist soil and high frequencies. The conductivity of

soil by the side of a river is not so high even at higher moisture content as other soils, which may be presumably due to the presence of sand in the soil near the river bank. The values of conductivity and dielectric constant obtained are small for Indian soil as compared to the values previously found in other countries.

In conclusion, we desire to record our sincere thanks to Professor P. Dutt, M.A.(Cantab.), for his helpful advice and continued interest in the present work. Further, we express our thanks to Mr. H. L. Kirke, Head of Research Department of the B.B.C., for his interesting discussions on the subject which he gave us during his visit to our laboratory.

References.

(1) Kirby, S. S., and Norton, R. A., ' Bureau of Standards Journal of Research,' viii. p. 463 (1932).
(2) Cherry, R. O., Proc. Phys. Soc. xlii. p. 192 (1930).
(3) Barfield, R. H., Jour. Inst. Elec. Eng. lxvi. p. 204 (1928).
(4) Rakshit, H., Phil. Mag. xi. p. 174 (1931).
(5) Roy, K. K., Ind. Jour. of Physics, x. p. 295 (1936).
(6) Khastgir, S. R., and Chowdhuri, D. N., Ind. Jour. of Physics, viii. p. 469 (1934).
(7) Ratcliffe, J. A., and White, F. G. W., Phil. Mag. x. p. 647 (1930).
(8) Strutt, M. J. O , *Elekt. Nach. Teck.* vii. p. 387 (1930).
(9) Smith-Rose, R. L., and McPetrie, J. S., Proc. Phys. Soc. xlvi. p. 649 (1934).
(10) Banerjee, S. S., Phil. Mag. xix. p. 787 (1935).

Physics Laboratory,
College of Science,
Benares Hindu University.
Jan. 27, 1938.

XCIII. *On the Nuclear Structure of Radioactive Substances.* *By* U. C. Bardhan †.

IT is well known that Gamow ‡, Sexl §, and others ‖ have theoretically studied the phenomenon of radioactive disintegration from the standpoint of wave theory.

† Communicated by Prof. K. C. Kar, D.Sc.

‡ G. Gamow, *Zeits. f. Phys.* li. p. 204 (1928); liii. p. 601 (1929); Gamow and Hautermans, *ibid.* lii. p. 496 (1928).

§ Sexl, *ibid.* liv. p. 445 (1929); lvi. p. 62 (1929).

‖ Gourney and Condon, ' Nature,' cxxii. p. 439 (1928); Phys. Rev. xxxiii. p. 127 (1929); Gupta, *Zeit. f. Phys.* lxix. p. 686 (1931); Laue, *Zeit. f. Phys.* clii. p. 726 (1928); Born, *ibid.* lviii. p. 306 (1929); Fowler and Wilson, Proc. Roy. Soc. cxxiv. p. 493 (1929); Kudar, *ibid.* liii. pp. 95, 134, 166 (1929).

Later on Sexl has pointed out that probably the phenomenon occurs on account of some form of damping within the nucleus. The above interpretation of the origin of spontaneous disintegration is obviously not as clear as it should be. This is probably due to the fact that the wave-mechanical interpretation of Schrödinger equation is still rather vague.

Recently, however, Kar † has developed a wave-statistical theory of the whole problem of spontaneous and artificial disintegration of atoms. The theory appears to be perfectly rigorous, and is based on the Rutherford model of the nucleus. According to this model a nucleus consists of a hard core encircled by a spherical shell filled with partially polarized circulating neutral helium atoms. The hard core is positively charged and the shell is electrically neutral. It may be mentioned that the idea of potential barrier used by Gamow and others bears a close resemblance to the above model of Rutherford. In developing wave-statistical theory it is assumed that the phase space for the hard core is compressible and also slightly viscous. This assumption would appear to be perfectly natural when it is remembered that the phase density within the core is very high. Thus in disintegrating, the α-particle crosses the surface of the hard core, overcoming the *surface potential*, and enters the shell where there is a strong Coulombian field. Under the action of the repulsive force the particle then moves towards the outer boundary of the shell, making its way through the large number of circulating helium atoms. Consequently a considerable part of its energy is lost in exciting the polarized helium atoms. It is evident that the particle becomes free on crossing the boundary of the shell.

The object of the present paper is to study the variation of the *surface potential* of the hard core of different radio-active elements belonging to the radium, thorium and actinium families.

It is shown by Kar that the wave-equations within and without the hard core are:

$$\frac{d^2\mathrm{D}'}{dt^2} + 2b\frac{d\mathrm{D}'}{dt} = v^2\Delta\mathrm{D}' \text{ (inside)}, \quad . \quad . \quad . \quad (1)$$

† K. C. Kar and A. Ganguly, Phil. Mag. xvi. p. 1097 (1933); K. C. Kar, Phil. Mag. xxi. p. 1067 (1936).

$$\frac{d^2D}{dt^2} = v^2 \Delta D \text{ (outside)}, \quad . \quad . \quad . \quad . \quad (2)$$

where $2b$ is evidently of the nature of the coefficient of viscosity.

On solving the above equations it may be found that

$$D' \sim \chi_1 \chi_2 e^{2\pi i \nu t} e^{-bt} \quad . \quad . \quad . \quad . \quad . \quad (3)$$

and

$$D \sim \chi_1 \chi_2 e^{2\pi i \nu t} \quad . \quad . \quad . \quad . \quad . \quad . \quad (4)$$

On eliminating time from equations (1) and (2) we have for the χ-equations inside and outside the hard core

$$\Delta\chi' + \frac{8\pi^2 mE}{h^2}\left(1 + \frac{b^2h^2}{16\pi^2E^2}\right)\chi' = 0, \quad . \quad . \quad . \quad (5)$$

$$\Delta\chi + \frac{8\pi^2 m}{h^2}(E + U_0 - V(r))\chi = 0, \quad . \quad . \quad . \quad (6)$$

where for the disintegrating α-particle $V(r) = \frac{2ez^*e}{r}$, z^* being the effective charge of the nucleus and U_0 the surface potential of the core.

The corresponding R-equations are

$$\frac{d^2R}{dr^2} + \frac{2}{r}\frac{dR}{dr} + \frac{8\pi^2 m}{h^2} E\left(1 + \frac{b^2h^2}{16\pi^2E^2}\right)R = 0 \text{ (inside)}, \quad (7)$$

$$\frac{d^2R}{dr^2} + \frac{2}{r}\frac{dR}{dr} + \frac{8\pi^2 m}{h^2}\left(E + U_0 - V(r)\right)R = 0 \text{ (outside)}. \quad (8)$$

The well-known solutions of (7) and (8) are

$$R = \text{const.}\frac{\sin \alpha r}{r}, \quad \alpha^2 = \frac{8\pi^2 mE}{h^2}\left(1 + \frac{b^2h^2}{16\pi^2E^2}\right), \quad . \quad (9)$$

$$R = \text{const.}\frac{\sqrt{\cot}\, u\, e^{k(2u - \sin 2u)}}{r}, \quad . \quad . \quad . \quad . \quad . \quad (10)$$

where

$$\cos^2 u = \frac{\rho}{4k}, \quad \rho = \frac{4\pi\sqrt{2m(E + U_0)}}{h} r$$

and

$$k = \frac{4\pi z^* e^2}{h\sqrt{2(E + U_0)/m}}.$$

Now it is evident that at the surface of the hard core the following boundary conditions should be satisfied:

$$R \text{ (inside)} = R \text{ (outside)},$$

$$\frac{dR}{dr}\text{(inside)} = \frac{dR}{dr}\text{(outside)}\Big|_{r = r_0};$$

on combining the two conditions into one we get

$$d \log \mathrm{R}\,(\text{inside}) = d \log \mathrm{R}\,(\text{outside}). \quad . \quad . \quad . \quad (11)$$

On substituting for R (inside) and R (outside) from (9) and (10), in (11), it may be found that

$$\frac{1}{r_0}\left\{-\frac{3}{4}-\frac{4\pi}{h}\sqrt{mz^*e^2r_0}\right\}=0 . \quad . \quad . \quad (12)$$

and $$-\frac{r_0}{3}\cdot\frac{8\pi^2 m\mathrm{E}}{h^2}\left(1+\frac{b^2h^2}{16\pi^2\mathrm{E}^2}\right)$$

$$=\frac{\pi\sqrt{2m(\mathrm{E}+\mathrm{U}_0)}}{2hk}\left\{\frac{1}{2}+\frac{4\pi}{h}\sqrt{mz^*e^2r_0}\right\}. \quad (13)$$

From (12) we easily get

$$r_0=\left(\frac{3}{16\pi}\right)^2\cdot\frac{h^2}{mz^*e^2}, \quad . \quad . \quad . \quad . \quad (14)$$

being the value of the radius of the hard core. Again, on equating terms of the same order in (13) we get

$$b^2=\frac{3}{8mz^*e^2r_0}\,\mathrm{U}_0\,\mathrm{E}. \quad . \quad . \quad . \quad . \quad (15)$$

Thus the linear damping coefficient becomes (*vide* (14))

$$\lambda_1=\frac{b}{4\pi}=\frac{a}{h}\sqrt{\mathrm{U}_0\,\mathrm{E}}, \quad . \quad . \quad . \quad . \quad (16)$$

where $a\sim 1$.

It should be noted here that the disintegration constant (λ) and the damping coefficient (λ_1) are not the same. They are defined as

$$\lambda=-\frac{1}{\mathrm{N}_a}\frac{d\mathrm{N}_a}{dt},\ \lambda_1=-\frac{1}{\mathrm{N}}\frac{d\mathrm{N}}{dt}, \quad . \quad . \quad . \quad (17)$$

where N_a is the effective number of particles within the core, *i. e.*, the number occupying a thin shell just inside the hard core, and N the total number within the core.

Since $\frac{d\mathrm{N}_a}{dt}=\frac{d\mathrm{N}}{dt}$, it follows immediately from (16) and (17) that

$$\lambda=\frac{a}{h}\sqrt{\mathrm{U}_0\,\mathrm{E}}\,\frac{\mathrm{N}}{\mathrm{N}_a} \quad . \quad . \quad . \quad . \quad . \quad . \quad (18)$$

Now from (9) and (10) we have

$$N_a = N \text{ const. } \frac{\sin^2 \alpha r_0}{r_0^2} . r_0^2 dr_0$$

$$= NA^2 \frac{\cot u_0}{r_0^2} e^{2k(2u_0 - \sin 2u_0)} r_0^2 dr_0, \quad . \quad (19)$$

where A is the averaging factor. On combining (18) and (19) we get

$$\lambda = \frac{\frac{a}{h}\sqrt{U_0 E}}{A^2 \cot u_0 dr_0} e^{-2k(2u_0 - \sin 2u_0)}, \quad . \quad . \quad . \quad (20)$$

which is the formulæ for the disintegration constant given by Kar.

In the above formula A^2, U_0, and dr_0 are unknown. They are usually combined into one constant (C) for a given family of radioactive substances. In verifying the formula usually the fitting value of the combined constant (C) is first determined for a given element of the family, *e. g.*, R_n in uranium-radium family, T_n in thorium family, and A_n in actinium family. The constant thus determined is then used to evaluate λ for other elements of the family. Consequently A^2 and U_0 are not separately known for the different elements.

We shall determine the averaging factor A by the graphical method. This will enable us to compare the surface potential (U_0) of the hard core for the different elements, assuming dr_0 to be the same for all and of the order 10^{-15} cm.

Now it is evident that the function (10) gives the phase density in the region where the potential field is Coulombian. The region evidently extends from $r = r_0$ to $r = \infty$. Therefore the averaging factor A may be obtained from the condition,

$$A^2 \int_{r_0}^{\infty} \cot u e^{2k(2u - \sin 2u)} dr = 1 \quad . \quad . \quad . \quad (21)$$

or $A^2 \times I = 1$, so that $A = \frac{1}{\sqrt{I}}$,

where the integral I is evaluated by a graphical method. The values of A^2 thus determined are given in Tables I., II., and III., column 5.

Table I.
Uranium-Radium Family.

Element.	Atomic number.	$v \times 10^{-9}$ cm. per sec.	$r_0 \times 10^{15}$ cm.	A^2.
U_1	92	1·41	1·122	$0·2830 \times 10^{-58}$
U_{11}	92	1·50	1·122	$0·1419 \times 10^{-54}$
Io	90	1·48	1·148	$0·4114 \times 10^{-53}$
Ra	88	1·51	1·174	$0·4312 \times 10^{-50}$
Rn	86	1·61	1·201	$0·1815 \times 10^{-44}$
RaA.....	84	1·69	1·231	$0·4139 \times 10^{-41}$
RaC.....	83	1·61	1·247	$0·2841 \times 10^{-42}$
RaC′	84	1·922	1·231	$0·3956 \times 10^{-33}$
Po	84	1·58	1·231	$0·3913 \times 10^{-44}$

Table II.
Thorium Family.

Element.	Atomic number.	$v \times 10^{-9}$ cm. per sec.	$r_0 \times 10^{15}$ cm.	A^2.
Th	90	1·390	1·48	$0·1218 \times 10^{-57}$
RdTh	90	1·600	1·48	$0·8215 \times 10^{-48}$
ThX	88	1·64	1·74	$0·9857 \times 10^{-46}$
Tn	86	1·73	1·201	$0·3619 \times 10^{-40}$
ThA	84	1·80	1·231	$0·1397 \times 10^{-36}$
ThC	83	1·70	1·247	$0·4559 \times 10^{-39}$

Table III.
Actinium Family.

Element.	Atomic number.	$v \times 10^{-9}$ cm. per sec.	$r_0 \times 10^{15}$ cm.	A^2.
PaC	91	1·55	1·134	$0·1191 \times 10^{-50}$
RdAc	90	1·68	1·148	$0·1183 \times 10^{-44}$
AcX	88	1·65	1·174	$0·2629 \times 10^{-44}$
An	86	1·81	1·201	$0·1592 \times 10^{-37}$
AcA	84	1·886	1·231	$0·4172 \times 10^{-34}$
AcC	83	1·73	1·247	$0·4348 \times 10^{-38}$
AcC′.....	84	1·90	1·231	$0·1917 \times 10^{-34}$

Again, since the combined constant

$$C=\frac{\sqrt{U_0}}{A^2 dr_0}, \quad \ldots\ldots\ldots \quad (22)$$

we have, $$U_0=(CA^2 dr_0)^2. \quad \ldots\ldots \quad (23)$$

As already explained the constant C may be evaluated for any element from (20) on using the experimental value of the disintegration constant (λ). Thus from (23) we get the corresponding value of U_0. The values of U_0 thus determined are given in the Tables IV., V., and VI., column 3. If, however, we use the average value of C

TABLE IV.

Uranium-Radium Family.

Element.	C (from (20))†.	U_0 (with different C).	U_0 (with mean C).
U_1	$1{\cdot}1161\times10^{32}$	$0{\cdot}9972\times10^{-83}$	$0{\cdot}1613\times10^{-85}$
U_{II}	$2{\cdot}6473\times10^{32}$	$0{\cdot}1512\times10^{-74}$	$0{\cdot}4056\times10^{-76}$
Io	$2{\cdot}3599\times10^{31}$	$0{\cdot}9423\times10^{-74}$	$3{\cdot}3778\times10^{-72}$
Ra	$1{\cdot}7506\times10^{30}$	$0{\cdot}5699\times10^{-70}$	$3{\cdot}4522\times10^{-54}$
Rn.....	$5{\cdot}3161\times10^{29}$	$0{\cdot}9305\times10^{-60}$	$0{\cdot}6631\times10^{-56}$
RaA	$3{\cdot}3397\times10^{28}$	$1{\cdot}9110\times10^{-56}$	$3{\cdot}4506\times10^{-48}$
RaC	$8{\cdot}8410\times10^{29}$	$6{\cdot}3080\times10^{-56}$	$0{\cdot}1625\times10^{-51}$
RaC′ ...	$7{\cdot}7679\times10^{29}$	$9{\cdot}4410\times10^{-88}$	$0{\cdot}3251\times10^{-33}$
Po	$6{\cdot}5524\times10^{27}$	$6{\cdot}4450\times10^{-64}$	$3{\cdot}0234\times10^{-54}$
Mean	$0{\cdot}44878\times10^{32}$		

for a given radioactive family we get a slightly different set of values for U_0. These modified values are given in Tables IV., V., and VI., column 4.

As already pointed out, in calculating the disintegration constant Kar and others have used the fitting value of C for an element occupying the middle position in a radioactive family. This evidently amounts to approximately taking the average value of C. But it appears that for a closer agreement the actual value of C is preferable.

It is evident from the tables that as U_0 increases the disintegration constant increases. Further, as we proceed higher up the series we find that in general U_0

† In calculating C, λ is taken per atom per second.

goes on increasing. However, the last elements, P_0 and ThC of uranium-radium and thorium family respectively, show a decrease in the value of U_0. In the actinium family, however, U_0 attains the maximum value for AcA. It becomes less for AcC and again for the last element of the series, namely AcC′, there is appreciable increase

TABLE V.

Thorium Family.

Element.	C (from (20)).	U_0 (with different C).	U_0 (with mean C).
Th	$7{\cdot}5700\times10^{30}$	$0{\cdot}8506\times10^{-84}$	$0{\cdot}1019\times10^{-84}$
RdTh ...	$7{\cdot}0517\times10^{30}$	$33{\cdot}5576\times-10^{66}$	$4{\cdot}6319\times10^{-66}$
ThX	$1{\cdot}0590\times10^{30}$	$1{\cdot}0874\times10^{-62}$	$6{\cdot}6558\times10^{-62}$
Tn	$1{\cdot}9788\times10^{28}$	$0{\cdot}5127\times10^{-54}$	$0{\cdot}8988\times10^{-50}$
ThA ...	$1{\cdot}9222\times10^{28}$	$0{\cdot}7203\times10^{-47}$	$0{\cdot}1338\times10^{-42}$
ThC.....	$1{\cdot}7026\times10^{26}$	$0{\cdot}6021\times10^{-56}$	$1{\cdot}4258\times10^{-48}$
Mean	$2{\cdot}61997\times10^{30}$		

TABLE VI.

Actinium Family.

Element.	C (from (20)).	U_0 (with different C).	U_0 (with mean C).
PaC	$7{\cdot}4766\times10^{29}$	$0{\cdot}8069\times10^{-72}$	$3{\cdot}0566\times10^{-52}$
RdAc ...	$5{\cdot}6911\times10^{29}$	$0{\cdot}4536\times10^{-60}$	$3{\cdot}0361\times10^{-45}$
AcX	$4{\cdot}3611\times10^{29}$	$1{\cdot}3165\times10^{-60}$	$6{\cdot}7180\times10^{-44}$
An	$1{\cdot}5944\times10^{28}$	$0{\cdot}6446\times10^{-49}$	$4{\cdot}0852\times10^{-39}$
AcA	$1{\cdot}0365\times10^{28}$	$0{\cdot}1871\times10^{-42}$	$0{\cdot}7050\times10^{-33}$
AcC	$1{\cdot}5790\times10^{27}$	$0{\cdot}4712\times10^{-52}$	$1{\cdot}1154\times10^{-39}$
AcC′ ...	$1{\cdot}5346\times10^{27}$	$0{\cdot}8655\times10^{-45}$	$4{\cdot}4183\times10^{-36}$
Mean	$2{\cdot}546147\times10^{29}$		

in the value of U_0. Thus the variation of U_0 is more or less similar in all the three radioactive families. This is rather interesting.

In conclusion, we may point out that in calculating graphically the value of the integral (I) in (21) between the limits r_0 and ∞ the maximum value of r used is $\sim6\times10^{-14}$ cm. (*vide* Tables I., II., and III., column 6). For greater values of r the integral becomes too small to affect the first four significant digits. This shows that

the nucleus, or rather the neutral shell, practically extends up to 6×10^{-14} cm. This is in general agreement with the conclusion arrived at by Kar and others.

Finally, I must acknowledge my indebtedness to Prof. K. C. Kar, D.Sc., for his kindly suggesting the problem and giving advice and help during my present investigation.

Science Laboratory, Vidyasagar College,
Calcutta, India, 15th July, 1937.

XCIV. *The Theory of Electrocapillarity.*—VII. *The Theory of Surface Films.* *By* S. R. Craxford, O. Gatty, *and* T. Teorell .

Introduction.

THE behaviour of substances in thin surface films has become of importance in a number of different industries, in biology, and in colloid chemisty. Any theory relating experimental observations with the molecular structure of the surface layers might therefore turn out to be useful. In the case of metal–solution interphases information of this kind has been obtained from measurements of surface tension and of surface differences of electrical potential. The experimental data have been interpreted by means of the thermodynamical theory of electrocapillarity as developed by Gibbs[1] and Lippmann[2]. A more detailed investigation of the theory by Craxford, Gatty, McKay, and Philpot[3] has shown that the systems considered have so many degrees of freedom that considerable care must be taken in choosing which variables are to be kept constant while differentiating the surface tension with respect to given intensive variables; otherwise the results do not yield the expected information about the structure and composition of the interphase. Many of these equations have also been deduced by Koenig[4], and their applications to experimental data are given by Craxford[5] and McKay[6].

† Communicated by Sir Harold Hartley, F.R.S.

A similar set of difficulties is liable to arise in the theory of surface films. The thermodynamical theories of surface films as given by Adam[7] and Guggenheim[8] neglect the gaseous phase above the film, which is treated as though it were completely insoluble, and the theory is developed for simple systems where the surface adsorption of different component molecules and ions of the liquid phase under the film can be neglected and Γ_{solvent} is set equal to zero by definition. For many systems this treatment seems a sufficiently good approximation, and it certainly gives the simplest picture of interfacial conditions where the component at the interphase does not occur in either of the bulk phases. A more satisfactory method for dealing with the complicated systems met with in actual practice would, however, be to develop a complete thermodynamical theory allowing for all components in both phases. The precise equations so developed would need simplification by means of certain approximations if they are to be applied to the degree of detail that existing experimental data provide about the given systems. These approximations have been treated for metal–solution interphases in paper IV. of reference (3). (These papers will be referred to as I., II., III., IV., etc. in the sequel.) The magnitude of the approximations involved needs to be investigated for surface films, and it is then for investigators to decide whether it is worth the trouble to obtain more extensive data so as to be able to apply the exact equations. It is important to realize that data suitable for evaluating individual $\mathcal{T}$ terms without the use of approximations are practically non-existent even for mercury–solution interphases.

Provided that exact equations are applied it is possible to use thermodynamical theory to relate observations on surface potential and surface tension to the molecular structure of the film. The present paper extends the thermodynamical theory of electrocapillarity to surface films, using the notation of IV.† and gives examples of how the theory can be both applied and misapplied. The theory is then extended to cover two or more surface phases, and the possibility of such a group of surface

† Note that in IV. p. 386 and 387 " D " is expressed in moles cm.$^{-2}$ of area of interphase cm.$^{-1}$ of depth across the interphase for all the chemical components of the system, and that " V " on p. 386 is in cm. across the interphase.

phases coexisting on a solution–metal interphase is discussed. This enables the theory to be linked with the theory of the electrode potentials of corroding metals[9]. Problems of surface pH can then be discussed as in the succeeding paper.

An Electrocapillary Apparatus for Surface Films.

The case where the solubility of one component is very low in both phases and it is strongly adsorbed at the interphase is mentioned in IV. (p. 397) in the discussion on capillary adsorption. Such a system can be, and was supposed to be, in an electrocapillary apparatus of the type discussed in III. (p. 973), so that the equations deduced in III. and IV. are valid for the special case of vanishingly low solubility in the two bulk phases.

Thermodynamically this apparatus has advantages over an idealized Langmuir trough. In the latter case, if complete thermodynamical equilibrium were to be set up, and if the surface phase were not completely insoluble in both bulk phases, it would not be possible to observe a change in surface tension due to the existence of a surface film, because there would be a film over the whole solution in the trough and there would be no clean surface against which to measure the surface tension of the film. Moreover the application of electrical fields across the interphase would be difficult to arrange satisfactorily owing to the difficulty of restricting and adapting the boundaries of the applied field to the surface film. The use of the apparatus described in III. permits of the treatment of surface films of all solubilities in the bulk phases.

In ordinary measurements of surface films the interphase is sensibly plane (curvature of earth due to gravity) so that p_1 sensibly equals p_2. This condition has already been used in III. and IV. to obtain information about the structure of the non-expanding or static interphase from equations that involve expansion terms. In the electrocapillary apparatus it merely means that the radius of the conical capillary is very great. If gravity is neglected, as it is in the idealized apparatus under consideration, the meniscus becomes part of a large spherical surface (for constant total curvature see V.). If gravitational effects were to be considered the meniscus would approximate to a plane surface except at regions

close to the conical tube. It is still possible to vary s at will, but variations in p_1-p_2 become very small ; these small variations must, however, be supposed to be capable of being observed, since the observed value for γ depends on observations of p_1-p_2. By reducing p_1-p_2 sufficiently it is possible to eliminate the effect of changes in p_1 during surface expansions at p_2 constant along the conical capillary, and thereby to eliminate the " volume correction " term

$$\left[\left(\frac{\partial p_1}{\partial \gamma}\right)_s \left(\frac{\partial V_1}{\partial s}\right)_{p_1} \left(\frac{\partial \gamma}{\partial E}\right)_s\right]_{X,\alpha,\beta-1}$$

in IV., equation (1). Since the suffix X implies constancy of p_2, it therefore, under the given conditions, implies also the constancy of p_1, and, in addition, large values for s do not increase

$$\left(\frac{\partial V_1}{\partial s}\right)_{p_1, X, \alpha, \beta-1}$$

in proportion to the radius of the capillary tube, which is the ratio in which $\left(\frac{\partial p_1}{\partial \gamma}\right)_{s\,X,\alpha,\beta-1}$ is reduced.

It follows that the electrocapillary equation for surface films is that given in IV., equation (2), viz.

$$\left[\left(\frac{\partial \gamma}{\partial E_s}\right) = -\sum_1^e \left(\frac{\partial q_r}{\partial s}\right)_{E_r} \left(\frac{\partial E_r}{\partial E}\right)_s\right]_{X',2,c-3} \quad . \quad . \quad (1)$$

For completely insoluble films a Langmuir trough is an alternative type of electrocapillary apparatus which however, can be shown to yield the same equation (1). Actually the trough leads to an equation for $\left(\frac{\partial(\gamma-\gamma_0)}{\partial E}\right)_s$, where γ_0 represents the surface tension of the pure phase 2 against the pure gaseous phase 1 without the film, and γ the tension with it. Similarly, on the right-hand side the $\left(\frac{\partial E_r}{\partial E}\right)_s$ terms can be assumed to be unaffected by the presence of a completely insoluble film (because the solution is the same whether it is underlying insoluble film or whether it underlies the clean surface. Thus all the electrodes in the solution are at one place only and take up a potential that depends on the composition of the bulk solution and not on their proximity to the film. There is only one electrode in the vapour phase, and in

both apparatuses this is above film covered surface), and all changes of surface area are conversions of an area with film to an equal area without, and *vice versa*. Thus the $\left(\frac{\partial q_r}{\partial s}\right)_{E_r}$ terms become $\left(\frac{\partial(q_r - q_{or})}{\partial s}\right)_{E_r}$ terms, where $\left(\frac{\partial q_{or}}{\partial s}\right)_{E_r}$ refers to the interphase with no film present. The ordinary electrocapillary equations show that an expression of type (1) holds between γ_0 and q_{or}; the trough shows by thermodynamical reasoning that a similar one holds between $(\gamma - \gamma_0)$ and $(q_r - q_{or})$, so that it follows that (1) itself is valid.

It is evident, therefore, that equation (1) is valid for surface films of substances of all varying degrees of solubility in the bulk phases, and that all the applications of this formula discussed in IV. can be applied in principle to interphases that include surface films. The results should be valid for a homogeneous surface film whether it is gaseous, liquid expanded, liquid condensed, or solid in its nature; other factors would have to be considered if the film is in a metastable state or at such a compression as to correspond to negative surface tension at the interphase containing the film. Negative surface tensions must be regarded as unstable, though not necessarily impossible of realization in practice. In a surface film the particles, owing to thermal motion, may be said to exert a pressure (internal pressure) in the surface, just as molecules of ether under a negative pressure still collide with the walls of the containing vessel. The field of force on the particles is such, however, that the surface tends to shink in spite of the thermal movement of the molecules. A very small increase of surface area in the case of a film with negative surface tension would, in general, be sufficient to render the surface tension positive at the reduced surface compression; it follows that indefinite surface expansion is no more to be expected of surface films, as opposed to film-free surfaces, with negative surface tension than indefinite contraction is to be expected of ether under negative pressure as it is allowed to contract. Recent experiments in Cambridge indicate that it might become possible to produce surface films with a spreading force greater than the corresponding surface tension of the solution on which the film is spread.

The results obtained by the use of equation (1) are indicated in the rest of this paper, using the notation of III. and IV. ; following IV. the units in which all T and Γ terms are expressed are moles cm.$^{-2}$ instead of grams cm^{-2}. as in III.

The Applications of the Electrocapillary Equation.

In order to illustrate the scope of the present treatment the system N_2 (gas ionized by Po radiations), Po/Fatty acid HA/H_2O, HCl, NaCl, Na_2HPO_4 will be dealt with. Let the system be subject to the condition that no nitrogen is added to it or subtracted from it, let the same be true for hydroxyl ion, and let the other chemical components be taken as H^+, Cl^-, Na^+, $HPO_4^=$, A^-, and Po, the latter being kept at a constant chemical potential as it is assumed to be a pure solid phase. The same would be true for the degradation products of polonium, but they will be neglected in the present treatment as also will the energy liberated in the form of heat by the radioactivity of the polonium. The two boundary conditions for the surface become $T_{N_2}=0$ and $T_{OH^-}=0$. If Y refers to constancy of s, p_2 (and sensibly $p_2-p_1=0$), T, s_k, W″, E_{Po}, q_{N_2}, and q_{OH^-}, and if the electrodes in the aqueous phase reversible to the ions H^+ to A^- above are numbered respectively 1 to 5, the equations, taking the metallic polonium-covered electrode in the gaseous phase as reference electrode, give

$$\left.\begin{aligned}
\left(\frac{\partial\gamma}{\partial E_1}\right)_{Y,\,E_2,\,E_3,\,E_4,\,E_5} &= z_1FT_1 = FT_1,\\
\left(\frac{\partial\gamma}{\partial E_2}\right)_{Y,\,E_3,\,E_4,\,E_5,\,E_1} &= z_2FT_2 = -FT_2,\\
\left(\frac{\partial\gamma}{\partial E_3}\right)_{Y,\,E_4,\,E_5,\,E_1,\,E_2} &= z_3FT_3 = FT_3,\\
\left(\frac{\partial\gamma}{\partial E_4}\right)_{Y,\,E_5,\,E_1,\,E_2,\,E_3} &= z_4FT_4 = -2FT_4,\\
\left(\frac{\partial\gamma}{\partial E_5}\right)_{Y,\,E_1,\,E_2,\,E_3,\,E_4} &= z_5FT_5 = -FT_5.
\end{aligned}\right\} \quad . \quad . \quad (2)$$

These equations give the amount of surface adsorption of a number of component ions of the system. They do not give information as to how those ions are adsorbed at the interphase. Thus adsorbed HA would count as

(adsorbed H^+ + adsorbed A^-), adsorbed $PO_4^{=}$ would count as (adsorbed $HPO_4^{=}$ − adsorbed H^+), and so on. A rearrangement of electrical circuits would lead to a different choice of chemical components, but would still leave unsolved the relative amounts of A^- and HA in the interphase (see for example, the case of C_2H_5OH worked out in IV., p. 365).

It was pointed out in I., p. 863, that the introduction of a gravitational field led to the necessity of considering pressures in layers very close to the interphase in order to define surface tension if the electrocapillary equations are to be valid for ordinary surface tension. This arose because in a gravitational field the pressure varies from one point in a bulk phase to another ; similar difficulties are encountered if inequalities of electrical potential are set up in a bulk phase, and for such cases the E_r terms in the electrocapillary equation should refer to electrodes close to the interphase. In thermodynamical equilibrium such inequalities of electrical potential only occur in insulating bulk phases. In the presence of small leakage currents across an interphase thermodynamical equations still hold to a good approximation, and in the case of electrocapillary data for aqueous solutions–metallic mercury interphases, the bulk phases conduct electricity so well that the ohmic drop of potential between the electrodes and the interphase can be neglected. Gases ionized by polonium do not conduct electricity so well, and it is possible that equations (2) would not hold with the E's uncorrected for ohmic drops of potential through the gas, because the electrode is too far away from the interphase. In consequence potentials in practice would have to be referred to an electrode in phase 2 as the reference electrode, and the data would have to be restricted to capillary phenomena where no polarizing potentials are applied by means of the polonium electrode. The question as to whether the relative electrical resistances of the ionized nitrogen and of the film are such that it should be possible to observe changes in surface tension due to applied electric fields can only be settled by experiment. If it is possible to consider the film as almost completely polarizable, it should be possible to observe electrocapillary curves with an electrode of large area, covered with polonium, in the gaseous phase, and from these curves to obtain data for the electrostatic capacity

of the interphase (see IV., p. 370). Under these conditions the applied voltage would be concentrated across the film and would produce an electrical field comparable to that produced by the oriented surface dipoles ; a few millivolts would alter the distribution of particles at the interphase, as in the case of electrocapillary curves, and would change the surface tension by an observable amount. If it is found, on the other hand, that the electrical resistance of the ionized gas is comparable to or greater than that of the film, even under experimental conditions most favourable for a low gaseous resistance, the problem is reduced to one of capillarity where it is possible also to measure surface potentials. The problem is in fact analogous to that of data from electrocapillary curves where the potential of the mercury is controlled by variations in mercurous ion activity in the solution. (Note that in presence of metallic mercury an equilibrium $Hg+Hg^{++}=Hg_2^{++}$ is set up. In IV. the Hg_2^{++} and Tl electrodes and all other electrodes should strictly be supposed to be of the idealized type discussed in III., p. 969.) This case is not dealt with in detail in IV., although it arises when considering system 2, p. 367.

If no charge is allowed to flow through the electrode in the gaseous phase, so that it is merely a measuring electrode, equations (2) have to be modified so that q_R is kept constant ; *i. e.*, $T_R=0$. It is convenient to work with circuits 2R, 12, 32, 42, 52, and the circuits $1-OH^-$ and $R-N_2$ (to introduce gas in an idealized electrochemical way, for FE_{RN_2} write μ_{N_2} and for q_{RN_2} write N_{N_2}, and use the equation in the form of II., equation (17) for N_2 ; see also IV., p. 368). The equations for the boundary conditions $T_R=0$ and $T_{OH^-}=0$ become :

$$\left.\begin{aligned}
\left(\frac{\partial\gamma}{\partial E_{12}}\right)_{Y',\,\mu_{N_2},\,E_{32},\,E_{42},\,E_{52}} &= z_{12}FT_{12},\\
\left(\frac{\partial\gamma}{\partial E_{32}}\right)_{Y',\,\mu_{N_2},\,E_{12},\,E_{42},\,E_{52}} &= z_{32}FT_{32},\\
\left(\frac{\partial\gamma}{\partial E_{42}}\right)_{Y',\,\mu_{N_2},\,E_{12},\,E_{32},\,E_{52}} &= z_{42}FT_{42},\\
\left(\frac{\partial\gamma}{\partial E_{52}}\right)_{Y',\,\mu_{N_2},\,E_{12},\,E_{32},\,E_{42}} &= z_{52}FT_{52},\\
\left(\frac{\partial\gamma}{\partial \mu_{N_2}}\right)_{Y',\,E_{12},\,E_{32},\,E_{42},\,E_{52}} &= T_{N_2},
\end{aligned}\right\} \quad . \quad . \quad (3)$$

where Y′ denotes constancy of s, p_2 (and also p_1), T, s_k, W″, E_{P_0}, q_{H_2O}, q_R; and where $z_{12}=1$, $z_{32}=1$, $z_{42}=-2$, $z_{52}=-1$, and $E_{rs}=E_r-E_s$ (as in IV., p. 363); Γ_{12}=surface adsorption of NaCl, Γ_{42}=surface adsorption of $(HPO_4^{=}-2Cl^-)$, Γ_{52}=surface adsorption of (A^--Cl^-), and Γ_{N_2} that of the nitrogen gas; the equations holding for $\Gamma_{H_2O}=0$, and $\Gamma_R=0$, R referring to the ionizing electrons in the nitrogen gas.

It is evident that adequate data are lacking for the use either of equations (2) or (3). The possibility of replacing E_{rs} suffixes by corresponding q_{rs} suffixes and the approximations involved are discussed in IV., pp. 375–378. But even when these substitutions have been made it is still found that adequate data are missing in the case of most systems of any interest to biologists and biochemists. The simplest possible case is the adsorption of one component in a three component system, and the theory of this is already given in IV., p. 399, for the case of a component that occurs only at the interphase. It is possible to simplify equations (3) above by neglecting circuits 2R, 32, 42, and 52, and for a boundary $\Gamma_{H_2O}=0$, and $\Gamma_{N_2}=0$ to write

$$\left(\frac{\partial\gamma}{\partial E_{12}}\right)_{s,\ p_2,\ (=p_1),\ T,\ s_k,\ W'',\ E_{P_0},\ q_{H_2O},\ q_{N_2}} = z_{12}F\Gamma_{12}.$$

This gives Γ_{12} for the given boundary conditions, and by interchanging the numbers 2 and 5 to denote A^- and Cl^- respectively instead of Cl^- and A^- the data even in the case where HA is soluble can still be made to give

$$\frac{\partial\gamma}{\partial E_{12}} = F\Gamma_{HA}. \quad . \quad . \quad . \quad . \quad . \quad . \quad . \quad (4)$$

Most of the commoner misapplications of equations (2) to (4) involve insufficient attention being paid to which factors are kept constant during differentiation. One example of a possible misapplication would be to take an ordinary surface tension–surface potential curve and differentiate it twice with respect to surface potential, and say that the resulting $\frac{\partial^2\gamma}{\partial E^2}$ was the electrostatic capacity of the interphase. The correct expression for capacity, if the interphase is sufficiently polarizable, is obtained by differentiation at constant surface area;

the curve discussed above, however, relates to measurements of surface tension and surface potential as the surface area is altered, and these curves when differentiated give no simple property of the system. They can be interpreted from the identity

$$\left(\frac{\partial\gamma}{\partial \mathrm{E}_r}\right)_{\mathrm{Z},\,s} = \left(\frac{\partial\gamma}{\partial \mathrm{E}_r}\right)_{\mathrm{Z},\,q_{15}} + \left(\frac{\partial\gamma}{\partial q_{15}}\right)_{\mathrm{Z},\mathrm{E}_r}\left(\frac{\partial q_{15}}{\partial \mathrm{E}_r}\right)_{\mathrm{Z},\,s},$$

where Z represents constancy of a suitable set of variables, but use of identities of this type leads to no simplification. In the observed curves breaks occur as changes in surface area lead to changes of state in the surface films. Equations (2) to (4) are not valid during the transition from one surface state to another ; if they were the equations would indicate infinite values for the capacity at the point of change of the surface phase of the film. The electrocapillary equation for systems containing two coexistent surface phases is examined in the next section.

Another difficulty arises about the particular choice of boundary or boundaries for the Γ and $\mathcal{T}$ terms which could be used in the electrocapillary equation. Guggenheim and Adam [10] show that Gibbs's method of selecting a boundary so that one term becomes zero can be extended to selecting a boundary so that any desired linear combination of Γ terms is zero. The picture of the interphase arrived at in their paper neglects entirely the gaseous phase above the film, and does not therefore give a satisfying picture for a liquid–liquid interphase even if their errors owing to neglect of the gaseous phase turn out to be inappreciable. In III., p. 986, it was shown that the general electrocapillary equation giving an expression for a single differential coefficient of the surface tension can be reduced to a sum of not fewer than 3 Γ terms if the Γ's refer to a boundary for which no single Γ term vanishes identically. By selecting a boundary in the interphase so that one Γ term vanishes, a single differential coefficient of the corresponding surface tension can be expressed as the sum of two Γ terms (III., p. 988). Thus the use of Γ terms in the sense of Gibbs never allows the values for individual Γ's to be determined from thermodynamical data. Guggenheim and Adam (*l. c.*) and Butler and Wightman [11] appear to get values for a single Γ term, but only do so because they have neglected Γ_{gas} for the gaseous phase above. This, and the neglect of vapour

molecules in the phase above may not introduce serious error, but it means that their equations are inexact. It was pointed out in III., p. 986, that $^{(ii)}\Gamma^*$ terms, corresponding to surface expansions at constant volume of both phases up to the boundary s (V_1 and V_2' constant), can be identified with Gibbs's Γ terms for the same boundary. For certain phase boundaries, expansions at V_1 and V_2' constant are also at constancy of one of the q_r's or of some linear combination of them. In III., p. 987, terms have been called $^{(iii)}\Gamma^*$ terms for which one q_r and V_2' are constant during surface expansions. For appropriate boundaries $^{(iii)}\Gamma^*$ terms become $^{(ii)}\Gamma^*$ terms, and therefore Γ terms. The treatment here given, or a simple extension of that of III., p. 987, shows that it also is legitimate to apply Gibbs's equation to Γ terms, *i. e.*, $^{(ii)}\Gamma^*$ terms, for boundaries that make linear combinations of Γ terms vanish. Thus the treatment of Guggenheim and Adam is sound except for the neglect of the gaseous phase.

It is only in the case of $^{(i)}\Gamma^*$ terms that single differentials of the surface tension can be expressed in terms of single adsorption terms. That is the reason that these terms have been used almost exclusively throughout the applications in IV. The physical meaning of these terms has been given in III., p. 982, and IV., p. 362 (in which latter place an error of units on p. 982 of III. is corrected). The values given by Guggenheim and Adam[10] for $\Gamma_2^{(i)}$ in their notation actually are values for Γ_{alcohol} for the boundary conditions $\Gamma_{H_2O}=0$, and $\Gamma_{\text{gas}}=0$. The question of values of individual Γ terms cannot be decided by thermodynamical reasoning from thermodynamical data, which cannot therefore supply an answer as to whether the layer of alcohol is unimolecular or not. A knowledge of Γ terms does not lead to information concerning the spatial distribution of particles in the interphase. The values for Γ_{alcohol} never exceed 0·04 molecules, and since closely packed hydrocarbon chains occupy an area of about 20·5 Å.^{2}, the data are not inconsistent with the hypothesis of a unimolecular or nearly unimolecular layer, because the surface excess could be packed into the area as such a layer. The way that Γ_{alcohol} varies with μ_{alcohol} is not readily interpreted. It is possible that the approximations of Guggenheim and Adam are valid, and that

their explanation that the curve is of this shape because of the position taken for the boundary in determining Γ will turn out to be correct. Further work is needed on this point.

Another type of problem arises in the work of Teorell (unpublished) on the adsorption of weak electrolytes, such as acid dyes, at benzene–water interphases. Benzene drops are passed up through an aqueous phase containing the dye, and the amount of dye transported is measured as the drops coalesce. The dye is practically insoluble in benzene, but is adsorbed at the interphase. Teorell kept the total concentration of $(HA+A^-)$ constant, and varied the pH. When the pH is greater than pK for the acid, this variation affects the concentration of HA more than that of A^- provided the pH is great enough to make $[A^-]_c \gg [HA]_c$. It was found that $\frac{1}{RT} \cdot \frac{\partial \gamma}{\partial lnc}$ gives a fair approximation to the quantity of dye recovered when the benzene drops coalesce, but only when c is the value calculated for the concentration of the neutral dye molecule HA, over a range of buffered pH values, and not if used for the concentration of A^-. This work differs from the more usual procedure where γ is determined as a function of $[A^-]_c$, $[HA]_c$, or $([A^-]_c + [HA]_c)$ at a given pH. In this case $RTln[H^+]_a + RTln[A^-]_a = -pK_{HA} + RTln[HA]_a$, so that for a constant pH if activity coefficients are neglected $[A^-]_c \propto [HA]_c$.

Teorell's experiments show that it is mainly neutral dye molecules, HA, which are adsorbed at the interphase, rather than A^- accompanied for the sake of electroneutrality by other cations such as Na^+. Thus if bulk phases of the original composition are liberated during the coalescence, the extra dye liberated is $\mathcal{T}_{dye}$. Agreement with Gibbs's equation is to be expected provided that for $\mathcal{T}_{H_2O}=0$, and $\mathcal{T}_{benzene}=0$, the $\mathcal{T}$ terms for salts such as NaA, and for $(2NaA - Na_2HPO_4)$, *i. e.*, $(2A^- - HPO_4^=)$, are negligible compared to $\mathcal{T}_{HA}$. It is important to stress, however, that the experiments do not give any evidence as to the degree of dissociation of HA in the interphase. Such A^- as is adsorbed is compensated electrically by hydrogen rather than sodium, but the methods do not tell anything about the ionization of HA in the interphase.

A similar problem is raised by the work of Donnan [12], Peters [13], [14], Jahrisch [15], and Danielli [16], who measured the interfacial tension lowering due to a fatty acid, HA, as a function of buffered pH. It is to be observed, however, that in these experiments the interfacial tension was lowered when the electrolytic dissociation increased, *i. e.*, at alkaline pH values. This, in fact, is the reverse of Teorell's results for the acid sulphophthaleïn dyes, where increased dissociation increased the interfacial tension. The reason for the contrary behaviour of the fatty acids and the aromatic indicator acids awaits explanation. The full details of ionic adsorption can only be worked out after a great deal of experimental work which is not as yet available for any of the systems just discussed Peters therefore was right in not applying Gibbs's equation to his data because they were not sufficiently comprehensive. Further data, combined if possible with measurements of interfacial potential differences should make the evaluation T of terms for the various ions a definite possibility. The use of an air–aqueous interphase would certainly make possible the collection of sufficient data for that system.

Two-Surface Phases.

Surface films are known to exhibit phenomena analogous to a change of phase, and under appropriate conditions it is possible to have two or more coexistent surface phases corresponding to the gaseous, liquid expanded, liquid condensed, or solid states. Coexistent surface phases must be at the same surface tension, and be in equilibrium with the same pressures, temperature, and chemical potentials of the different chemical components, since these quantities are constant throughout the bulk phases. Finally, for complete thermodynamic equilibrium local action currents must have ceased, or, alternatively, one or other of the two interphases is completely polarizable ; in both cases the two interphases should be polarized to the same surface potential. It follows that equation (8) of III. is valid, and that all electrocapillary equations are valid as before, except that equation (1) above becomes

$$\left[\left(\frac{\partial \gamma}{\partial \mathrm{E}}\right)_s = -\sum_1^c \left(\frac{\partial q_r}{\partial s}\right)_{\mathrm{E}_r} \left(\frac{\partial \mathrm{E}_r}{\partial \mathrm{E}}\right)_s\right]_{\mathrm{X}', 3, c-4}, \quad . \quad . \quad (5)$$

where the need for a third extensive degree of freedom to fix the relative areas of the two surface phases means that at least three q terms are necessary to describe the system. Since the equilibrium condition of the latter has to be capable of being reduced to the form $dZ = Ads + BdE$, where dZ is a complete differential, at least three q terms have to be kept constant in order to reduce $\left(\frac{\partial\gamma}{\partial E}\right)$ to a single $\left(\frac{\partial q}{\partial s}\right)$ term ; hence the suffix 2 in equation (1) becomes 3 in equation (5), and suffix $c-3$ becomes $c-4$ to retain the correct number of degrees of freedom. In equation (5) the $\left(\frac{\partial q_r}{\partial s}\right)$ terms refer to surface expansions of the composite interphase in contact with only two bulk phases, and s refers to the total surface area of the two interphases. Further, in the simplest case, where (5) reduces to

$$\left[\left(\frac{\partial\gamma}{\partial E_r}\right)_s = -\left(\frac{\partial q_r}{\partial s}\right)_{E_r}\right]_{X', 3, c-4}, \quad . \quad . \quad . \quad (6)$$

the surface expansion $\left(\frac{\partial q_r}{\partial s}\right)$ refers to an expansion at all intensive variables constant—in fact, to a change in the relative areas of the two surface phases associated with a change in total surface area.

In this simplest case let q_1, q_2, q_3 for the system of the combined surface phases be kept constant. Further, let a series of T terms be calculated for one surface phase for the conditions $T_1=0$, and $T_2=0$, also a similar series of T' terms for the other surface phase, subject to the conditions $T_1'=0$ and $T_2'=0$. Let the fraction of the surface covered by the surface phase corresponding to T terms be denoted by σ, and let the n_r of equation (4) of IV. be replaced by N_r terms corresponding to the total number of moles of the chemical component in question in the whole interphase of area s, so that the equation becomes

$$N_r = (\sigma s\lambda_1 + (1-\sigma)s\lambda_1')^1 x_r + (\sigma s\lambda_2 + (1-\sigma)s\lambda_2')^2 x_r + \sigma sT_r + (1-\sigma)sT_r' \quad . \quad . \quad (7)$$

Then at constancy of all intensive variables,

$$\left(\frac{\partial N_r}{\partial s}\right)=(\sigma\lambda_1+(1-\sigma)\lambda_1')^1x_r+(\sigma\lambda_2+(1-\sigma)\lambda_2')^2x_r+\sigma T_r$$

$$+(1-\sigma)T'_r+\frac{\partial\sigma}{\partial s}\{s(\lambda_1-\lambda_1')^1x_r+s(\lambda_2-\lambda_2')^2x_r+s(T_r-T_r')\}$$

$$+\sigma s.\frac{\partial\lambda_1}{\partial s}.{}^1x_r+(1-\sigma).s.\frac{\partial\lambda_1'}{\partial s}.{}^1x_r+\sigma s.\frac{\partial\lambda_2}{\partial s}.{}^2x_r$$

$$+(1-\sigma).s.\frac{\partial\lambda_2'}{\partial s}.{}^2x_r, \quad . \quad (8)$$

the conditions that $T_1=0$ and $T_2=0$ determine λ_1 and λ_2; that $T_1'=0$ and $T_2'=0$ determine λ_1' and λ_2'; and the position of the meniscus determines s. These conditions, except the last one, refer, however, to the behaviour of the individual surface phases. For the system of the two coexisting surface phases equation (8) becomes

$$\left(\frac{\partial N_r}{\partial s}\right)=A^1x_r+B^2x_r+T_r'+(T_r-T_r')\frac{d(\sigma s)}{ds}, \quad . \quad (9)$$

with zero values for T_1, T_2, T_1', and T_2'. These values, together with the conditions q_1 and q_2 constant imposed on equation (6) in the case now under discussion, allow A and B to be evaluated as zero, giving

$$\left(\frac{\partial N_r}{\partial s}\right)=T_r'+(T_r-T_r')\frac{d(\sigma s)}{ds}, \quad . \quad . \quad . \quad (9a)$$

and the value of $\frac{d(\sigma s)}{ds}$ is controlled by the values of T_3 and T_3' and the imposed condition of constancy of q_3, which means that $\left(\frac{\partial N^3}{\partial s}\right)=0$ at all intensive variables constant. Equation (6) can then be used to evaluate other $T_r'+(T_r-T_r')\frac{d(\sigma s)}{ds}$ terms which do not have a very direct relationship to properties of the actual interphase.

Corresponding to equation (6) a similar expression for temperature coefficients can be deduced, viz.

$$\left[\left(\frac{\partial\gamma}{\partial T}\right)_s=-\left(\frac{\partial S}{\partial s}\right)_T\right]_{X' \text{ except for T, 3, } c-3}, \quad . \quad . \quad (10)$$

and this is the surface analogy of the Clausius-Clapeyron equation. The term on the right-hand side is 1/T times the heat emitted during a surface expansion at all intensive variables constant and subject to three extensive restrictions such as constancy of q_1, q_2, q_3. Thus it corresponds to the heat of formation of the extra surface plus the heat emitted during a subsequent readjustment of σ. Equation (10) is therefore more complicated than the Clausius-Clapeyron equation.

The analogy with that equation is brought out by deducing the Clausius-Clapeyron equation for two bulk phases and one component as follows. Let the total volume of the system be denoted by V, its total entropy by S, the temperature by T, the pressure by p, the total number of moles of the substance by N, and its chemical potential by μ. Then for thermodynamically reversible processes

$$dE = TdS - pdV + \mu dN + \delta W'', \quad . \quad . \quad (11)$$

where E is the energy of the system and $\delta W''$ is other work done on it. For $\delta W'' = 0$ the two extensive degrees of freedom (for two coexisting phases) can be taken as V and N, and denoting a complete differential by dZ (11) can be converted to

$$[dZ = -SdT - pdV + \mu dN]_{\delta W''=0}. \quad . \quad . \quad (12)$$

It should be noted that

$$[dZ = -SdT + Vdp + \mu dN]_{\delta W''=0}$$

is not a valid expression, as it allows for only one extensive degree of freedom, N. It gives

$$\left(\frac{\partial V}{\partial T}\right)_{p,\,N,\,W''} = -\left(\frac{\partial S}{\partial p}\right)_{T,\,N,\,W''},$$

and this, though correct, merely states that $\infty = \infty$. Cross differentiation of (12) gives

$$\left[\left(\frac{\partial p}{\partial T}\right)_V = \left(\frac{\partial S}{\partial V}\right)_T\right]_{N,\,\delta W''=0}, \quad . \quad . \quad (13)$$

and $\left(\frac{\partial S}{\partial V}\right)_{T,\,N,\,W''}$ corresponds to an expansion at all intensive variables constant, *i. e.*, to a change of the relative amounts of the two phases. Thus $\left(\frac{\partial p}{\partial T}\right)_{V,\,N,\,W''} = \frac{\Delta S}{\Delta V}$,

where $\triangle S$ is the increase in partial molal entropy on conversion from the phase of lesser to the phase of greater volume, and $\triangle V$ is the corresponding increase in partial molal volume. Thus for two phases in equilibrium

$$\left[\frac{dp}{dT}\right]_{\text{two phases}} = \left(\frac{\partial p}{\partial T}\right)_{V,\,N,\,W''} = \frac{T\Delta S}{T\Delta V},$$

where $T\triangle S$ is the heat adsorbed per mole converted to the phase of greater volume. For the change $\left(\frac{\partial S}{\partial V}\right)_{T,\,N,\,W''}$ the pressure remains constant, and since $H \equiv E + pV$ for the whole system of two phases, (11) can be written

$$dH = TdS + Vdp + \mu dN + \delta W'',$$

so that for changes at p, N, and W'' constant $dH = TdS$. Since constancy of T means constancy of p, it follows that (13) becomes

$$\left[\frac{dp}{dT}\right]_{\text{two phases}} = \left(\frac{\partial p}{\partial T}\right)_{V,\,N,\,W''} = \frac{T\Delta S}{T\Delta V} = \frac{\Delta H}{T\Delta V}, \quad (14)$$

which is the more usual form of the expression.

Referring back to equation (10) and to the meaning of the constancy of q_1, q_2, and q_3, as explained by equation (9), it is evident that errors would be liable to arise in a simple straightforward application of the Clausius-Clapeyron equation to data concerning surface films (for such applications see references given by N. K. Adam [7]). The methods here developed could readily be extended to three or more coexistent surface phases, but the interpretation of the $\left(\frac{\partial q_r}{\partial s}\right)$ terms would become increasingly complicated.

Solution–Metal Interphases near the Potentials of the Reversible Metal—Metal Salt Potentials.

Changes in the electrical potential difference across a solution–metal interphase are the result of a modified distribution of charged particles in the interphase. As the metal is made electrically more positive the surface density of adsorbed anions increases. The adsorbed anions could also be regarded as adsorbed salt molecules, since a corresponding positive charge must occur in the interphase for every anion adsorbed. At potentials close

to that of the electrocapillary maximum for the given solution, the surface density of adsorbed salts of the ion M^{p+} of the electrode metal is low in the case of mercury and probably of all noble metals, and owing to electrostatic repulsion the salt probably forms an uncondensed film corresponding to a gaseous or vaporous film[7a]. If the metal is made more positive the surface density of the adsorbed salt increases, and the possibility arises that the adsorbed salt might form a condensed film or two co-existing surface phases. It seems probable that this would occur at potentials close to that of the reversible metal/precipitated metal salt electrode. If solid films of a given component exist they cannot be in thermodynamic equilibrium with a higher chemical potential of the substance than that corresponding to the pure three-dimensional solid under the given conditions of temperature, pressure, etc. Thus in the presence of solid precipitate, surface films should be at their maximum compression (for equilibrium conditions), and in some cases would be expected to be solid films. The existence of such films is not necessary, since it is found that many surface films can exist for prolonged periods in metastable states at compressions higher than those which they take up when in equilibrium with a crystal or lens of pure three-dimensional solid. Nevertheless it seems likely that condensed films would be formed before the formation of precipitated salts of the electrode metal. Some evidence in favour of this suggestion comes from the work of Müller and co-workers [17], who have polarized anodically horizontal electrodes of copper in saturated copper sulphate solutions and lead electrodes in sulphuric acid. Their results indicate in a quantitative manner that the area of exposed surface phase of bare metal is first reduced during anodic polarization owing to the growth of the precipitate or its adsorbed film in a direction parallel to the metal surface, and that subsequently the thickness of the salt precipitated on the horizontal electrode is increased. Müller, however, was using higher polarizing current densities than occur in electrocapillary work.

If condensed films are formed, they might be expected at a given surface potential to have a different surface charge from the gaseous film with which they are in equilibrium. It follows that $\left(\frac{\partial q_r}{\partial s}\right)$ terms for ionic adsorp-

tion and for the total charge over the whole interphase might become large in systems having two coexistent surface phases. The corresponding $\left(\frac{\partial N_r}{\partial s}\right)$ terms of (q_r) might tend to become of the order of T_r instead of T'_r if the value of $\frac{d(\sigma s)}{ds}$ is great enough. If T_r is much greater than T'_r considerable and rapid increases in $\left(\frac{\partial N_r}{\partial s}\right)$ terms might be expected in regions where there are two coexistent phases. In the case of electric charge, the difference between two surface phases at the same potential might well be considerable. The fact that high electrostatic capacities are calculated for solution–metal interphases from electrocapillary data at potentials close to those of reversible metal/metal salt electrodes is well known (see IV., p. 380). Under these conditions electrocapillary workers say that the anion has become "specifically adsorbed." For abrupt transitions from one surface phase to another with changing E_r values one would expect infinite capacities, as they are calculated from second differentials. The uniform capacities of cations and the abnormally high and variable capacities of anions are not easy to explain, but they could be accounted for by a change of surface phase that does not take place sharply at one surface tension, but gradually, over a small range of surface tensions. Such a gradual change, which is accompanied by some hysteresis, is known to occur in the transition from liquid expanded to liquid condensed films [7]; it is often supposed to occur with duplex films having also some water, and so applying to a triplex film. In the case of specific adsorption the film would perhaps be called quadruplex, with ions of the electrode metal, water, specifically adsorbed anions and attendant cations from the solution.

Measurements of surface tension by drop-weight methods, or by moving a meniscus up and down a fine capillary, always involve the use of freshly formed surfaces, and are not suitable therefore for detecting hysteresis. In addition, ageing effects are known to occur in the case of solution–metal interphases [18]. It is therefore suggested that the high capacities observed with specifically adsorbed anions might in part be due to the coexistence of

two surface phases of adsorbed anion at the interphase. In the absence of specific adsorption, the observed capacities for all ions would, on this view, be in the region of 18–30 μ-Farads cm.$^{-2}$, the existence of water-sheaths round the ions and at the interphases in fact tending to equalize the capacities of ions not interacting with the metal in this manner. It must be emphasized, however, that the varying and high capacities in the case of specific adsorption are more probably due to a fairly considerable potential across the diffuse portion of the double layer in the opposite sense to the total interfacial potential difference.

The authors would like to express their thanks to Prof. Rideal, F.R.S., and to Dr. J. H. Schulman for pointing out the need for an exposition of the thermodynamics of surface films and for stimulating discussion during the writing-up of this paper.

Summary.

(1) The electrocapillary equations developed in Papers III. and IV. of this series are extended to the case of surface films.

(2) The equations are applied to a typical and to a simplified case. Existing data are insufficiently detailed with respect to all the component ions to allow the practical use of the precise electrocapillary equations.

(3) The boundary conditions for evaluating $\mathcal{T}$ and Γ terms are discussed in relation to the types of experimental data available.

(4) The theory of two coexistent surface phases is discussed.

(5) A possible factor contributing to the high capacities of specifically adsorbed anions is the possible existence of a gradual change from gaseous to condensed films of adsorbed anion at potentials close to those corresponding to the formation of a solid precipitate of a salt of the metal in the capillary electrode.

(6) Measurements of surface tension and chemical potentials cannot alone supply information as to the degree of dissociation of a substance in an interphase or in a surface film.

References.

(1) Gibbs, Collected Works (i.) London (1928).
(2) Lippmann, *Ann. Chim. Phys.* (5) v. p. 494 (1875).
(3) I. Craxford, Gatty, and Philpot, Phil. Mag. (7) xvi. p. 849 (1933). II. *ibid.* (7) xvii. p. 54 (1934). III. *ibid.* (7) xix. p. 965 (1935). IV. Craxford, Gatty, and McKay, *ibid.* (7) xxii. p. 359 (1936). V. Gatty and McKay, *ibid.* (7) xxii. p. 402 (1936). VI. Craxford, Gatty, and McKay, *ibid.* (7) xxiii. p. 1079 (1937).
(4) Koenig, J. Phys. Chem. xxxviii. p. 11 (1934).
(5) Craxford, Dissertation, Oxford, D.Phil. (1936).
(6) McKay, Dissertation, Oxford, B.Sc. (1936).
(7) Adam, 'Physics and Chemistry of Surfaces,' p. 260; (7*a*) *ibid.* p. 330. Oxford (1938).
(8) Guggenheim, 'Modern Thermodynamics,' London (1933).
(9) Gatty and Spooner, 'The Electrode Potential Behaviour of Corroding Metals,' Oxford (1938).
(10) Guggenheim and Adam, Proc. Roy. Soc. A, cxxxix. p. 218 (1933).
(11) Butler and Wightman, J. A. C. S. p. 2089 (1932).
(12) Donnan, *Z. physikal. Chem.* xxxi. p. 42 (1899).
(13) Peters, Proc. Roy. Soc. A, cxxxiii. p. 140 (1931).
(14) Hartridge and Peters, *ibid.* B, ci. p. 348 (1922).
(15) Jahrisch, *Biochem. Z.* cxxxiv. p. 163 (1922).
(16) Danielli, Proc. Roy. Soc. B, cxxii. p. 155 (1937).
(17) Müller, "Die Bedeckungstheorie der Passivität der Metalle und ihre experimentelle Begründung." *Verlag Chemie* (1934); and references given in Evans, 'Metallic Corrosion and Passivity,' London, pp. 15, 43–46 (1937).
(18) Proskurnin and Frumkin, Trans. Farad Soc. xxxi. p. 110 (1935).

The Department of Colloid Science, Cambridge.
The Zoological Laboratory, Cambridge.
Médicinsk-Kemiska Institutionen, Upsala.

XCV. *A Note on Surface* pH.

By S. R. Craxford, O. Gatty, *and* T. Teorell *.

In a previous paper [1] it has been shown that electrocapillary measurements giving values for Γ_{H^+} and Γ_{A^-} assume H^+ and A^- to be component ions of the system; adsorbed HA counts therefore as adsorbed H^+ plus adsorbed A^-. The values of these Γ terms give no information about the degree of dissociation in an interphase, which in the general case is different from its value in either of the bulk phases. Moreover, an interphase is a non-homogeneous region, and if a degree of dissociation could be measured in it, it would be expected to vary from point to point at varying distances between the two phases. Considering the difficulty of

* Communicated by Sir Harold Hartley, F.R.S.

deciding upon a true degree of dissociation for concentrated solutions of strong electrolytes, which is a case that is far simpler than that of an interphase in that all elements of volume fixed with respect to the containing vessel have to be electrically neutral on a time average, it is reasonable to assume that existing methods will never reveal true degrees of dissociation in an interphase. If therefore pH is defined as $-\log_{10}$ (hydrogen ion concentration) it may be concluded that it cannot be estimated in any interphase, that it should vary with position in the interphase, and that in general it should differ from its value in either bulk phase. A definition of this type would be difficult to apply for another reason. The concentration in an interphase depends on the quantity of bulk phase associated with the non-homogeneous region; for volume concentrations in fact, the two coordinate axes lying in the plane tangential to the interphase are not equivalent to the axis perpendicular to this frame.

In practice pH is measured by the potential of a glass or hydrogen electrode against a saturated calomel electrode in the same solution, some workers correcting the observed potential for the liquid–liquid junction potential between the solution and the saturated KCl of the calomel electrode, using the formulæ either of Henderson or of Planck. Thus in practice pH would seem to be a measure of hydrogen ion activity rather than of hydrogen ion concentration. For a system containing two bulk phases, their interphase being permeable to H^+, let the calomel electrode remain in one of the bulk phases, and let the pH be defined always with reference to this electrode ; then the law of excluded perpetual motion shows that this pH would remain constant throughout both bulk phases and throughout the whole of the interphase. (The constancy of μ_{H^+}, the electrochemical potential of hydrogen ion throughout the bulk phases and the interphase has been shown for equilibrium conditions by Gibbs[2] and by Guggenheim[3]. (See also the constancy of $\underset{dN_r \to 0}{\mathrm{Lt}} \left(\frac{\delta W'}{dN_r}\right)_{p_1, p_2, T, N_k, \varepsilon_k}$ in Craxford, Gatty, and Philpot[4].) This conclusion follows because glass electrodes at different points of the system must all take up the same potential to prevent perpetual motion. The same argument applies to phases in true Donnan equilibrium if the membrane is permeable to H^+,

and to the similar ionic equilibria caused by the " diffusion effect " according to Teorell[5]. In the latter case the conclusions about glass electrodes have been confirmed experimentally by Teorell.

This second type of definition of pH is not satisfactory, however, because it would make the pH the same in both phases for the above case of Donnan equilibrium. Thus pH as normally understood is *not* a measure of the electrochemical potential of H^+ in the system, which is independent of the position throughout the system if the latter is permeable to hydrogen ions.

In the case of Donnan equilibrium a difference of pH is said to occur between the two phases because the potential of a glass electrode measured against a calomel electrode in the same place is found to depend on which phase contains the two electrodes. The two glass electrodes are at the same potential, and the discrepancy arises because there is a potential difference between the two calomel electrodes in the two different phases. It is evident that pH is a quantity that is related more closely to the chemical than to the electrochemical potential of hydrogen ions at that point of the system, but this statement cannot be made more precise without a fuller investigation of the theory of calomel electrodes.

If, however, pH be defined in terms of the potential difference between a glass electrode and an aqueous saturated calomel reference electrode (uncorrected for the liquid–liquid junction potential between the solution and the saturated KCl of the calomel electrode), both in the same bulk phase or both at points the same distance into the interphase, the definition is in accordance with what is ordinarily understood in discussions involving pH. A pH of this sort will in general be different in the two bulk phases for Donnan equilibria and also for systems of the type of $HClO_4$ partitioned between water saturated with nitromethane and nitromethane saturated with water. It will also be different in general in the interphase from its value in the bulk phases, and will vary according to the distance into the interphase at which it is measured by pairs of hypothetical (molecular sized) electrodes. A pH of this sort could never, however, be measured in practice. Exactly similar conclusions would hold if the pH were defined in terms of a movable aqueous saturated calomel electrode with the potentials corrected

for the liquid–liquid junction potential. This second type of pH would be still harder to arrive at owing to the difficulties of evaluating liquid–liquid junction potentials from aqueous saturated KCl into the interphase or into non-aqueous phases. In the last cases, for instance, the changes of the free energy of solvation would have to be considered for the ions in the diffusion region.

It follows that a surface pH defined in the third way, just discussed (whether the calomel electrodes are corrected or not for diffusion potentials by means of the formulæ of Henderson or of Planck), cannot be observed directly. But it will be different in the two bulk phases and at different depths into the interphase ; in this way it is somewhat analogous to the pH defined as $-\log_{10}$ (hydrogen ion concentration). In an interphase the relative amounts of ionized and unionized forms of an indicator would be expected to differ from the relative amounts of these two forms in either bulk phase in equilibrium with the interphase. For an interphase in equilibrium with a solution the thermodynamical dissociation constant in terms of activities is unaltered, but owing to the peculiar relationships possible between surface concentration and activity, a " concentration dissociation constant " $K_c = \frac{[H^+]_c\,[A^-]_c}{[HA]_c}$, which is, of course, not a true constant, may become modified in the interphase. Thus the observed colour of an indicator in an interphase may differ from its colour in a bulk phase for at least three reasons :—(i.) orientation factors, (ii.) in the surface $[H^+]_c$ differs from its value in the bulk phase, and so alters the observed ratio $\frac{[A^-]_c}{[HA]_c} = \frac{K_c}{[H^+]_c}$ by altering $[H^+]_c$, and (iii.) the observed ratio $\frac{[A^-]_c}{[HA]_c}$ is affected because K_c is different in the interphase to its value in bulk solutions. The colour change can be demonstrated as follows (unpublished experiments by Teorell). Pure nitrogen was bubbled as a " rain " of fine bubbles through a long cylinder containing a rather dilute solution of sodium bromthymol blue, to which some HCl had been added to change the colour to a greenish blue. After a while the top part of the solution turned yellowish and the bottom part became blue, which seems to indicate that it is mainly

the unionized (yellow) form of the indicator that is adsorbed at the nitrogen-dye solution interphase and carried upwards with the nitrogen bubbles. This is apparently a case of rather modified " adsorption hydrolysis " where the bulk solution of a salt of a weak acid becomes more alkaline, due to the surface adsorption of the acid molecules (*cf.* Teorell[6] for " partition hydrolysis," when an aqueous salt solution of a weak electrolyte is shaken with a non-aqueous solvent which can dissolve the free acid or base, as, for example, dimethylanilinehydrochloride shaken with carbon tetrachloride). Deutsch[7] had previously drawn attention to the colour change when several aqueous indicator solutions were emulsified with an organic liquid such as benzene, the colour developed corresponding in general to a more acid pH. Freundlich[8], however, is rather critical of the explanation depending on change of pH, and points to other possibilities of the type discussed above. Indicator colours may be affected perhaps by orientation, but if this factor is neglected it is safe to assert that one sees concentrations, whereas partitioning takes place according to electrochemical potentials (or to activities corrected for electrical potentials). Thus indicators will not give a direct solution of the problem of observing a surface pH.

It appears that the electrochemical potential definition of pH in terms of $\bar{\mu}_{R}^{+}$ is unsatisfactory, as it does not correspond to pH as ordinarily understood. Neither of the other two definitions is capable of direct observation; If they were, they would be expected to be different in an interphase from their values in either bulk phase. The repercussions of these conclusions on questions of reaction velocity, pH optima for enzymes, degree of coagulation, etc., are liable to be of great importance in biology, and possibly to have technical applications; they should form the subject of a separate investigation by other than thermodynamical methods. The whole question of surface pH has been brought up in a paper by Danielli[9], in which he omits to discuss which definition he proposes to adopt for pH.

The usually accepted idea of pH corresponds to a measurement of E.M.F. between a glass electrode and a calomel electrode in a similar region. Differences of pH in a system in equilibrium (the glass electrode is at the same potential throughout such a system) correspond to

differences of electrical potential between the two regions, and also to differences of diffusion potentials between the respective calomel electrodes in their respective regions. For difficulties of giving a precise thermodynamic treatment of liquid–liquid junction potentials, and for difficulties about the splitting of electrochemical potential into chemical and electrical components, see Gatty and Spooner[10]. A satisfactory theory must await a suitable theory of collisions and mean free paths in solutions.

The authors would like to thank Dr. J. H. Schulman for bringing this problem to their notice and for helpful discussions.

References.

(1) Craxford, Gatty, and Teorell, Phil. Mag. xxv. p. 1041 (1938).
(2) Gibbs, 'Collected Works,' London (1928).
(3) Guggenheim, 'Modern Thermodynamics,' London (1933).
(4) Craxford, Gatty, and Philpot, Phil. Mag. (7) xvii. p. 54 (1934).
(5) Teorell, J. Gen. Physiol. xxi. p. 107 (1937).
(6) Teorell, Skand. Arch. Physiol. lxvi. p. 304 (1933).
(7) Deutsch, *Z. physikal. Chem.* lx. p. 353 (1928).
(8) Freundlich, J.C.S. p. 164 (1930).
(9) Danielli, Proc. Roy. Soc. B, cxxii. p. 155 (1937).
(10) Gatty and Spooner, 'The Electrode Potential Behaviour of Corroding Metals,' Oxford (1938).

The Department of Colloid Science, Cambridge.
The Zoological Laboratory, Cambridge.
Médicinsk-Kemiska Institutionen, Upsala.

XCVI. *Thermal Diffusivity of the Soil at Colombo Observatory.* *By* J. P. Andrews, *D.Sc., F.Inst.P.**

Abstract.

The monthly means of underground temperatures at Colombo Observatory, derived from daily observations during the fifteen years 1919–33, are subjected to Fourier analysis. From the resulting series, it is found that the thermal diffusivity of the soil has a value of about 0·009 c.g.s. units.

UNDERGROUND temperatures have been recorded systematically at Colombo Observatory for many years; and averages from observations extending over

* Communicated by the Author.

the years 1919–1933 have been calculated and published recently by Mr. A. P. Kandasamy*. Such a long series of data ought clearly to yield information about the propagation of temperature waves into the earth, and this paper gives the results of the appropriate calculations.

The established method of calculating the thermal diffusivity K assumes that K is not a function of time. This may be nearly true in a land where "the rain it raineth every day"; but in Colombo there are two well-marked rainy seasons during which the water-content increases in the rather sandy soil. K is certain to have a different value at these times, and there is evidence that at these periods the temperature of the soil down to 10 ft. becomes almost constant, presumably owing to percolation of rain-water. The average value of K which is derivable from the imposing series of observations consequently has not the weight and precise significance that might otherwise have been expected. On the other hand, the annual variations of temperature in Colombo are so small, that a long series of measurements adds very materially to the reliability of the monthly averages upon which the calculation is based.

The Method of Measuring the Temperature.

The temperatures are read from mercury in glass thermometers which are normally suspended by chains inside narrow metal tubes, and at depths below the surface of 1, 2, 3, 4, 5, and 10 feet respectively. At selected times each day the thermometers are hauled to the surface and read. A mass of paraffin wax between the bulb and an outer glass vessel prevents any appreciable change of temperature in the bulb during this operation. The instruments are known as Symons Earth Thermometers. The various precautions taken are recounted in Kandasamy's paper.

Data.

The data for these calculations are taken from the same paper, where monthly averages are given, in addition to results on the diurnal variation. Table I. gives the

* Ceylon Jour. of Science (E) ii. 2, p. 93 (1937).

Table I.

Underground Temperatures. Monthly Averages.

Depth in ft.	Jan.	Feb.	Mar.	April.	May.	June.	July.	Aug.	Sept.	Oct.	Nov.	Dec.
1	83·4	85·6	87·9	87·6	86·0	85·0	85·3	86·2	86·5	85·2	83·9	83·1
2	84·0	85·9	87·6	87·7	86·2	85·4	85·4	86·1	86·5	85·5	84·4	83·9
3	83·9	85·4	87·1	87·4	86·3	85·4	85·3	85·9	86·3	85·5	84·4	83·9
4	84·0	85·2	86·7	87·3	86·4	85·5	85·3	85·8	86·2	85·6	84·7	84·1
5	84·3	85·3	86·6	87·3	86·6	85·8	85·5	85·9	86·4	85·9	85·0	84·5
10	84·4	84·5	85·2	85·8	85·9	85·6	85·3	85·3	85·5	85·5	85·1	84·7

Temperatures are in degrees Fahrenheit.

monthly averages, which have been taken as more suited to this calculation than the diurnal values *.

In fig. 1 these figures are plotted for depths of 1, 2, 5, and 10 feet, the others being omitted merely for the sake of clearness.

Analysis of the Data.

We express the temperature at a depth q feet, viz., v_q, thus :—

$$v_q = v_0 + A_{1q} \cos(\theta + \alpha_{1q}) + A_{2q} \cos(\theta + \alpha_{2q}) + \text{etc.} + A_{pq} \cos(\theta + \alpha_{pq}) + \text{etc.}, \quad (1)$$

Fig. 1.

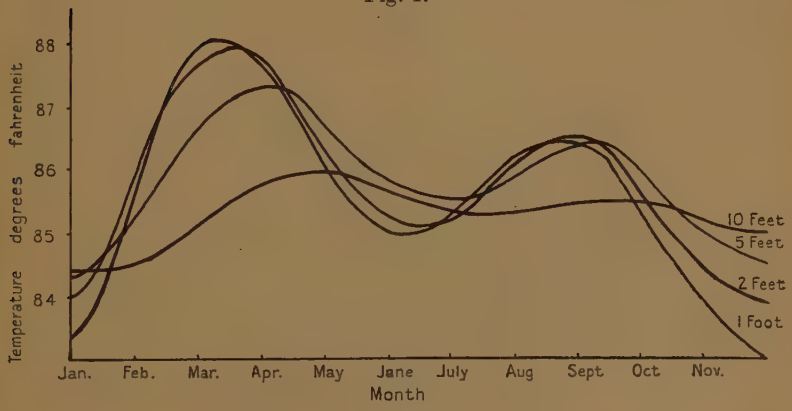

Annual variation of temperature.

where A_{pq} is the amplitude, and α_{pq} is the phase of the pth term of the series for a depth of q feet, and $\theta = 360\, t/s$, s being the number of seconds in a year. It is to be observed that θ must eventually be expressed in radians, but for present purposes it is conveniently expressed in degrees.

Table II. gives the values of A_{pq} and α_{pq} up to $p=4$. These values were obtained by subjecting the curves (fig. 1) to Fourier analysis by means of the scheme given in Whittaker and Robinson's 'Calculation of Observations,'

* The actual figures given here were taken from an unpublished MS. put at my disposal by the kindness of Dr. H. Jameson and Mr. Kandasamy. In the finally published account some of the figures differ by one-tenth deg. F. As will appear, this difference is of no importance to the calculation.

TABLE II.

Depths q feet.	Amplitudes A_{pq} (°F.)				Phases α_{pq}.			
	$p=1$.	$p=2$.	$p=3$.	$p=4$.	$p=1$.	$p=2$.	$p=3$.	$p=4$.
1	−1·212	−1·615	−0·240	−0·125	52° 37′	47° 4′	− 33° 38′	− 66° 30′
2	−1·042	−1·281	−0·190	−0·135	59° 1′	44° 1′	− 52° 4′	− 60° 15′
3	−1·026	−1·153	−0·158	−0·140	53° 17′	38° 6′	− 71° 31′	− 72° 36′
4	−0·905	−0·996	−0·151	−0·060	47° 47′	27° 36′	− 83° 32′	− 73° 29′
5	−0·808	−0·890	−0·126	−0·072	42° 59′	22° 3′	−105° 44′	− 83° 40′
10	−0·504	−0·416	−0·047	−0·034	14° 57′	−16° 1′	−135° 0′	−120° 19′

p. 270. The results have been checked by replotting the curves from the series.

The values of v_0 at different depths are given in Table III. Their approximate constancy shows that we are justified in considering the temperature fluctuations as due to the superposition of a series of simple periodic temperature variations in a mass of earth otherwise at a uniform temperature of about 85·6° F. We may then ignore v_0 in the ensuing calculations.

The method of analysis gives only terms up to $p=4$. An inspection of Table II., columns headed "$p=4$," where the values already vary erratically, indicates that the addition of further terms would not be justified.

TABLE III.

Depths (feet) .	1	2	3	4	5	10
v_0 (°F)	85·50	85·7	85·6	85·6	85·8	85·2

Calculation of Thermal Diffusivity.

If the surface of the earth be subjected to simultaneous simple periodic variations of temperature

$$C_1 \cos(\beta t+\gamma_1),\ C_2 \cos(2\beta t+\gamma_2),\ \ldots\ C_p \cos(p\beta t+\gamma_p) \text{ etc.},$$

where t is the time, it may be shown that the temperature at a depth x below the surface is given by

$$v_x=\sum_p C_p e^{-\sqrt{\frac{p\beta}{2K}}x} \cos\left(p\beta t-\sqrt{\frac{p\beta}{2K}}\,x+\gamma_p\right) \quad . \quad (2)$$

where K is the thermal diffusivity, and x will be measured generally in cm. Comparing with series (1), we have,

$$A_{pq}=C_p e^{-\sqrt{\frac{p\beta}{2K}}x}$$

or

$$\log_e A_{pq}=\log_e C_p-\sqrt{\frac{p\beta}{2K}}\,x \quad . \quad . \quad . \quad . \quad (3)$$

so that a graph of $\log_e A_{pq}$ and x for any one value of p, should be a straight line of slope $-\sqrt{\frac{p\beta}{2K}}$ from which K is determinable. In practice it was convenient to plot $\log A_{p1}/A_{pq}$ against x.

Similarly,

$$\alpha_{pq} = -\sqrt{\frac{p\beta}{2K}}\,x + \gamma_p \quad . \quad . \quad . \quad . \quad . \quad (4)$$

giving a second series of graphs from the slopes of which K may be found. For convenience in plotting, all phase angles (Table II.) may be written with the same sign by use of the relation $\cos(\theta+\delta) = \cos(\theta - 360 + \delta)$.

Fig. 2.

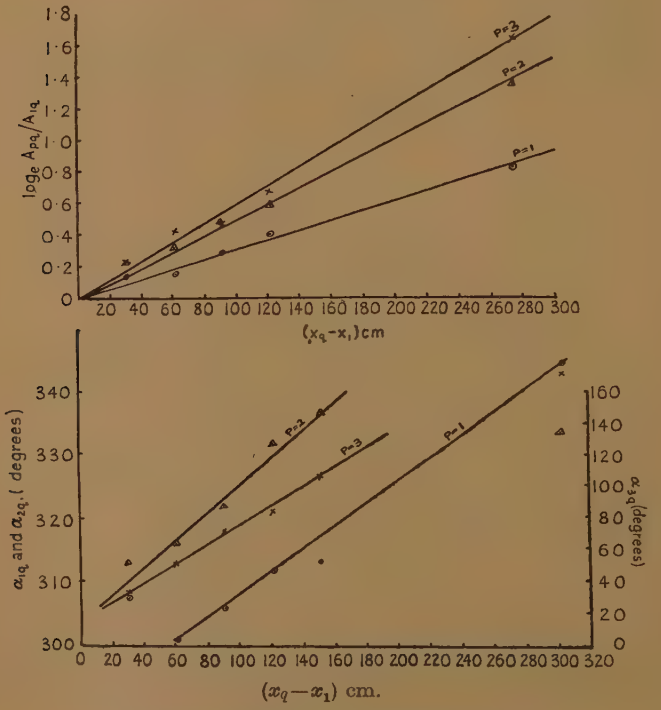

Rectilinear graphs for determination of K.

Graphs of these two kinds are shown in fig. 2 for values $p=1$, 2, and 3. The values for $p=4$ are too widely scattered to be of real use.

In Table IV. are given the values of the thermal diffusivity calculated from the slopes of the graphs, the angular measure and the units of length having been adjusted to radians and centimetres.

The results diverge rather widely, but if we may take the mean we obtain, to the order of accuracy which appears

to be justified, the value K=0·009 c.g.s. units. On comparing this value with other available results obtained in different parts of the world*, it appears that 0·009 is near the average value of all determinations.

Returning to the graphs of fig. 2, it is noticeable that although the points in the upper diagram (amplitudes) lie moderately well about straight lines, the points for 10 feet on the lower diagram (phases) are all much lower than would be expected. Now whatever variations from linearity occur in one set of graphs ought also to be found in the other if the assumptions made in the theory are applicable to the present problem. The most relevant of these assumptions is probably that of perfect homogeneity of the soil, and it therefore seems likely that a change in the nature of the soil occurs below 5 feet, or else that the section of earth in which the 10 ft. hole was sunk differs from the others. No data are available, however, to test this point. The smaller irregularities on the graphs may be due (*a*) to the disturbing effects of non-periodic variations not entirely eliminated in the monthly means, and (*b*) to the effects of percolation of rain-water, already referred to. It is worth observing that similar uncertainties must apply to other determinations made from the naturally occurring temperature cycle ; they are, however, of greater force in Colombo, owing to the small temperature variations.

TABLE IV.

Values of the Thermal Diffusivity.

Term.	From amplitudes.	From phases.
$p=1$.....	0·0102	0·0092
$p=2$.....	0·0077	0·0144
$p=3$.....	0·0083	0·0047

In conclusion, I desire to thank Dr. H. Jameson, Superintendent of Colombo Observatory, and Mr. A. P. Kandasamy for bringing the temperature records to my notice.

* See, for instance, ' Dictionary of Applied Physics,' article " Heat, Conduction of."

XCVII. *Electrolytic Water-Transport and Ionic Hydration Numbers.*

By H. C. Hepburn, *Ph.D.*, *Birkbeck College* (*University of London*) *.

Abstract.

A review of the various methods that have been employed to determine the hydration of electrolytic ions in aqueous solution indicates that the most consistent results have been obtained from those methods which are based upon the measurement of the amount of water transported with the ions during electrolysis. The author concludes that the most convenient of the latter methods is that involving the use of a parchment-paper diaphragm and consisting in the measurement of the volume changes produced during electrolysis. He has devised a sensitive form of apparatus for the purpose of such measurements and has developed an accurate expression for the electrolytic water-transport in terms of the observed volume change, the Hittorf transport number of the anion, and the partial molal volumes of the solute and of the solvent. A series of measurements has been carried out with solutions of sodium chloride in order to investigate a serious discrepancy shown by the earlier results relating to this salt. At the same time, the results of the author relating to solutions of copper sulphate and of cupric chloride, computed in former papers by means of an approximate expression, have been recalculated. The results so obtained for these solutions, together with those obtained for the sodium chloride solutions, have been employed to determine the true transport numbers and the hydration numbers of the respective ions; and the ionic complexity of cupric chloride solution is examined in the light of these results.

---

§1. *Introduction.*

It now appears to be generally accepted that most ions in aqueous solution are associated with water molecules to a greater or less extent. Attempts have been made to compute values for such hydration from the mobilities of the ions, by the application of Stokes's law regarding the

* Communicated by the Author.

motion of a sphere in a resistive medium[1]; other methods that have been employed to obtain hydration numbers include calculations from transport number data[2] from solution density and viscosity data[3], and from measurements of the distribution of a suitable substance between a non-aqueous solvent and the ionic solution under consideration[4]. Such methods, however, have yielded widely divergent results, and attention has therefore been drawn to the more direct methods which are based upon the determination of the amount of water transported with the ions during electrolysis.

Two distinct methods have been developed for the purpose of this latter determination. The first method, which is due to Nernst[5] and has been worked out by Buchbock[6] and by Washburn[7], involves the use of an indifferent (stationary) reference substance homogeneously distributed throughout the solution. The second method, which is referred to as the method of mechanical fixation, necessitates the use of a parchment-paper diaphragm which separates the two parts of the electrolyzing apparatus. The transport of water during electrolysis is determined by observing the volume changes produced[8], or, alternatively, by analysing the contents of each part of the apparatus before and after electrolysis[9].

The results obtained by means of the two methods referred to in the preceding paragraph, although much less divergent than those given by the indirect methods outlined in the first paragraph, are not altogether in satisfactory agreement. The most serious discrepancy arises in the important case of sodium chloride solution as between the results of the mechanical fixation (observation of volume changes) method and the other results (see Table I.). In view of such divergences, the author, during the past ten years, has endeavoured to develop an experimental technique which would lead to a greater degree of precision in the determination of electrolytic water-transport. The method finally decided upon was the physical variation of the mechanical fixation method, *i. e.*, the method involving the observation of the volume changes produced during electrolysis; and a special series of measurements has been made with sodium chloride solutions to confirm that the discrepancy pointed out in Table I. is not due to some flaw inherent in the method.

The mechanical fixation method appears to be of more

general application than that of Nernst in view of the difficulty, in the latter method, of finding in every case a suitable reference substance that will not interact with the ions of the solution, nor migrate in the electric field during electrolysis. The physical variation of the mechanical fixation method, moreover, involves no elaborate chemical analyses ; and the need for prolonged electrolysis is, in general, avoided. Velíšek and Vašíček[13] object to the physical variation on the ground that the transference of solute during electrolysis cannot be differentiated from the water transport. This difficulty, however, is readily resolved by a method developed by

TABLE I.

Sodium Chloride Solutions.

Concentration (gm.-equiv./litre).	Electrolytic water-transport (mols/faraday).	Observer.	Method.
1·182	0·81	Washburn[10].	Indifferent reference substance.
1·096	0·82	Washburn and Millard[11].	Ditto.
1·000	0·90	Baborovsky[9].	Mechanical fixation (chemical analysis).
1·000	1·4*	Remy and Reisener[12].	Mechanical fixation (observation of volume changes).

the author in the present paper which involves the utilization of the experimental data available for the Hittorf transport numbers of the ions and a knowledge of the partial molal volumes of the solute and of the solvent. The required values of the partial molal volumes have been specially determined by the author from solution-density data and are given in the appendix to the paper.

It has been pointed out that the employment of a diaphragm in the mechanical fixation method may introduce error in consequence of the electro-endosmotic effect of the diaphragm. The use of parchment paper as diaphragm material, however, appears to result in the

* Mean of six determinations. Two earlier determinations by Remy and Manegold[8] yield a mean value of 1·46, when necessary corrections are made.

elimination of this effect at normal concentration[14], and, in certain cases, at concentrations somewhat less than normal[15], [16].

The apparatus employed, which has already been described[15], was specially developed by the author. The high sensitivity of the apparatus enables results to be obtained at low current densities, thus minimizing the temperature rise due to the heating effect of the current. The author[15] has pointed out that in certain cases a considerable thermometric action arises from this heating effect, and he has devised a method which eliminates the error normally introduced by this cause.

The experimental work described in the present paper relates to solutions of sodium chloride; and values are computed for the electrolytic water-transport by means of an accurate expression obtained by the author in terms of the observed volume change, the partial molal volumes of the salt and of the solvent (water), and the experimental Hittorf transport number of the anion. At the same time, the former results of the author relating to solutions of copper sulphate[15] [17], and of cupric chloride[18], computed by means of an approximate expression, have been recalculated on a similar basis. The results so obtained have been employed to determine the true transport numbers and the hydration numbers of the respective ions by means of expressions due to Riesenfeld and Reinhold[2], and to Nernst[5]. The ionic complexity of cupric chloride solution is then examined in the light of these results.

The author considers that the experimental technique described in the present work and the use of the accurate expression derived for the electrolytic water-transport could be extended with advantage to solutions of other chlorides such as potassium chloride, lithium chloride, barium chloride, etc., and also to similar solutions containing (presumably unhydrated) heavy organic cations, with a view to obtaining further reliable data in regard to ionic hydration numbers.

§ 2. *Theoretical.*

The volume changes which occur during electrolysis, in consequence of (*a*) the transference of electrolyte from one electrode chamber to the other and (*b*) the chemical actions produced at the electrodes, have been referred

to by Remy and Reisener [12], who have applied certain corrections designed to eliminate these disturbing factors from the results obtained for the electrolytic water-transport by means of the physical variation of the mechanical fixation method. A systematic basis of correction, however, appears to be lacking, and the author has therefore developed a line of treatment similar to that employed by E. R. Smith [19] for the correction of transport numbers obtained by the moving-boundary method, to meet this need.

Consider the case of the electrolysis of a solution of sodium chloride, using a silver anode and a silver chloride cathode, the anode portion of the solution being separated from the cathode portion by means of a parchment-paper partition.

On the passage of 1 faraday of electricity, w_c equivalents of NaCl and x mols of water are added to the cathode solution. w_c is the true transport number of the cation, and x (mols/faraday) is the electrolytic water-transport from anode to cathode. The change ΔV in the volume V of the cathode solution, on the passage of Q faradays of electricity, is then given accurately by the following expression, provided $V/\Delta V$ is very large and assuming that the sodium chloride and the water added are evenly distributed throughout the solution :

$$\Delta V = \{w_c(\partial V/\partial n_1) + x(\partial V/\partial n_2) - \Delta V_e\}Q \quad . \quad (1)$$

$(\partial V/\partial n_1)$ and $(\partial V/\partial n_2)$ in equation (1) are the partial molal volumes of sodium chloride and of the solvent (water), respectively, *i. e.*, quantities representing the change in volume produced when 1 mol of solute or 1 mol of solvent is added to an infinite volume of solution. ΔV_e is the decrease in volume of the silver chloride cathode on the passage of 1 faraday of electricity, and is given by the expression $E_1/S_1 - E_2/S_2$, where E_1, E_2 are the equivalent weights and S_1, S_2 the densities of silver chloride and silver, respectively. Taking the values for these quantities given in the Landolt-Börnstein Tabellen [20] the magnitude of ΔV_e is found to be 15·49 cm.^{3}

Putting v_f in place of $\Delta V/Q$, and observing that $w_c = 1 - w_a$, we obtain from equation (1) the following expression for x, the electrolytic water-transport :

$$x = \frac{v_f}{(\partial V/\partial n_2)} + \frac{15{\cdot}49 - (1 - w_a)(\partial V/\partial n_1)}{(\partial V/\partial n_2)} \quad . \quad . \quad . \quad . \quad (2)$$

The electrolytic water-transport is represented approximately by the first term of the right-hand member of this equation, a similar expression having been employed in former papers in the case of solutions of copper sulphate and of cupric chloride. The second term represents the correction required for the volume change produced during electrolysis in consequence of (*a*) the transference of electrolyte from the anode chamber to the cathode chamber, and (*b*) the chemical change in the cathode.

The correction amounts to no less than 48·5 per cent. of the true value for x in the case of normal sodium chloride solution, but is much smaller (6·6 per cent.) in the case of normal potassium chloride solution. The corresponding corrections in the case of normal solutions of copper sulphate and of cupric chloride are respectively 6·8 and 0·6 per cent.; the effect of these latter corrections on the computation of the true transport numbers of the ions, for which purpose the former measurements were devised, being negligible.

The relation between the true transport number w_a and the experimental Hittorf transport number n_a, in the case of sodium chloride solution, is given by the following expression[1]:

$$w_a = n_a - cx \quad . \quad . \quad . \quad . \quad . \quad . \quad . \quad (3)$$

where c is the electrolyte concentration in equivalents per mol. Combining equations (2) and (3), we obtain an expression for x in terms of the experimental Hittorf transport number and other known quantities, viz.:

$$x = \frac{v_f + 15{\cdot}49 - (1 - n_a)(\partial V/\partial n_1)}{(\partial V/\partial n_2) + c(\partial V/\partial n_1)} \quad . \quad . \quad . \quad (4)$$

The corresponding expression which accurately represents the electrolytic water-transport in the case of solutions of copper sulphate and of cupric chloride (when copper electrodes are employed) is as follows:

$$x = \frac{v_f - 3{\cdot}56 + (n_a/2)(\partial V/\partial n_1)}{(\partial V/\partial n_2) + (c/2)(\partial V/\partial n_1)} \quad . \quad . \quad . \quad (5)$$

§ 3. *Experimental.*

The apparatus employed, which has already been described by the author[15] in a former paper, consisted

of two electrode chambers with side pieces (one chamber open to the air and the other closed, except for a capillary tube attached to it), the two chambers being separated by a diaphragm of parchment paper. The volume change produced by electrolytic transference, when an electric field was applied at the electrodes, was determined, as in the previous work, by observing the movement of the liquid thread in the capillary tube attached to the "closed" electrode chamber.

The apparatus was immersed in an electrically-heated water bath with a thermostatic device arranged to provide a temperature control within the limits $18° \pm 0{\cdot}1°$C.; and, to avoid thermometric effects, no heat was supplied to the bath immediately before or during the course of the measurements.

A silver anode and a silver chloride cathode, prepared after the manner recommended by Washburn[10], were employed. Each electrode was made up in the form of a large cylindrical spiral and was arranged to occupy the greater part of the vertical portion of the electrode chamber so that, as far as possible, the products of electrolysis were evenly distributed throughout the main part of the chamber. The more elaborate form of electrode (Type B), recommended by Washburn in the case of solutions of concentrations exceeding 0·2 normal, was found to be unnecessary in the present work as no prolonged electrolysis was required. A potential difference of 4 V. was applied between the electrodes.

Analytical reagent sodium chloride was used to prepare the solutions employed, the concentrations of which ranged from 0·1-normal to normal.

The experimental procedure followed that already described by the author[18], v_f, the ratio of the volume change ΔV to the quantity of electricity passing Q, being computed, as before, by means of the expression :

$$v_f = \frac{K_1}{2}\left(\frac{1}{T_1 I_1} + \frac{1}{T_2 I_2}\right) + \frac{K_1}{2T_s}\left(\frac{1}{I_2} - \frac{1}{I_1}\right) \quad . \quad . \quad . \quad (6)$$

T_1 (sec.) is the observed time for a volume displacement corresponding to 1 cm. length of the capillary, T_s (approximate value 5000 secs.) the time of a similar displacement due to gravitational movement outward, and I_1 (amp.) the mean current through the diaphragm. T_2, I_2 are the corresponding quantities obtained on reversal

of the current, and K_1 is the product $0{\cdot}00973 \times 96{,}540$. As explained in the former paper, equation (6) eliminates the correction for the heating effect of the current, and a precise measurement of the gravitational movement is found, in general, to be unnecessary.

The observed volume change ΔV was 0·00973 cm.^{3} in the case of concentrations 0·1 normal to 0·5 normal and 0·004865 cm.^{3} in the case of concentrations 0·6 normal to normal; and the values of $V/\Delta V$, V being the volume of solution surrounding each electrode, were approximately 8500 and 17,000 respectively. The limit of experimental error was about 1 per cent., so that the condition referred to in § 2 as necessary to secure accurate results

TABLE II.—Sodium Chloride Solutions.

Conc. (equivs./ litre).	Current I_1 (amp.).	Current I_2 (amp.).	Time T_1 (sec.).	Time T_2 (sec.).	Volume change v_f (cm.^{3}/faraday).
0·1	·02876	·03243	339·8	335·7	90·8 (3)
·2	·0600	·0590	305·4	402·2	45·4 (3)
·3	·0841	·0787	297·3	512·3	30·5 (0)
·4	·1119	·0991	219·6	1721·5	21·9 (8)
·5	·140	·130	311·6	518·6	17·7 (9)
·6	·165	·1505	322·8	611·2	13·9 (7)
·7	·1885	·1665	273·6	793·4	12·7 (3)
·8	·211	·1835	294·8	834·4	10·6 (8)
·9	·2295	·1975	314·0	861·6	9·35
1·0	·259	·2185	308·8	800·0	8·62

v_f is positive throughout, *i. e.*, the volume displacement at all concentrations is from anode to cathode.

by the application of equation (4) may be regarded as satisfied.

The experimental results are given in Table II.

§ 4. *Determination of Electrolytic Water-Transport and of True Transport Numbers.*

Sodium Chloride Solutions.—The interposition of a parchment-paper partition in the current path appears to be of negligible effect on the electrolytic water-transport in the general case of normal solutions[14], and, in the particular case of copper sulphate solutions, the evidence adduced by the author[15] suggests that the effect is also negligible in the case of concentrations less than normal,

but not less than 0·4 normal. In the circumstances, it will be assumed, in the first instance, that no material disturbance is introduced by the parchment-paper partition in the case of sodium chloride solutions of concentrations 0·8 normal and more. The observed volume change v_f at these concentrations (see Table II.) would then be attributed wholly to electrolytic transference ; and values for the electrolytic water-transport x (Table III.) are obtained on this assumption by means of equation (4), using the values for the partial molal volumes given in Table II. of the Appendix, and employing equation (7) (below) to obtain the values of the Hittorf transport number n_a.

TABLE III.—Sodium Chloride Solutions.

Conc. c (equiv./mol).	Electrolytic water-transport x (mol/faraday).	Hittorf transport number n_a.	True transport number w_a.	p.
0·	..	0·616	0·616	
·00181 (0·1 N.)	1·08	·618	·616	1·10
·00362 (·2 N.)	1·08	·620	·616	1·10
·00544 (·3 N.)	1·08	·622	·616	1·10
·00727 (·4 N.)	1·08	·625	·617	1·11
·00910 (·5 N.)	1·08	·627	·617	1·11
·01094 (·6 N.)	1·08	·629	·617	1·11
·01278 (·7 N.)	1·08	·631	·617	1·11
·01464 (·8 N.)	1·06	·633	·618	1·10
·01650 (·9 N.)	0·98	·635	·619	1·03
·01836 (1·0 N.)	0·93	·638	·621	1·00

The magnitude of the electrolytic water-transport x may also be deduced from a consideration of the values of the ionic transport numbers[2]. The most reliable experimental data for the Hittorf transport number n_a of the anion in the case of sodium chloride solutions appear to be those of Hopfgartner [21] (concentrations 0·1 normal and 0·9 normal), Taylor and Sawyer[22] (concentration 0·5154 normal), and Washburn and Millard[11] (concentration 1·096 normal). These data are accurately represented by the following linear relation :

$$n_a = 0{\cdot}616 + 1{\cdot}18\,c, \quad \ldots\ldots \quad (7)$$

where c is the electrolyte concentration in equivalents per mol.

The electrolytic water-transport x is given by the slope dn/dc of the straight line representing this equation, provided that the true transport number w_a of the anion is independent of concentration[17]; and this latter condition appears to be substantially satisfied in the case of sodium chloride solutions of concentrations not greater than 0·7 normal.

The value of dn/dc, given by equation (7) and representing a constant value of 1·18 for x in the case of concentrations not exceeding 0·7 normal, is in satisfactory agreement with the value of 1·08 obtained for x by Taylor and Sawyer[22] at concentration 0·5154 normal by means of the indifferent reference substance method. Taylor and Sawyer's value is also in close agreement with the author's value of 1·06 for x at concentration 0·8 normal; indeed, the slight difference between these two values of x may be regarded as accounted for by the change in the values of the true transport numbers from concentration 0·5154 normal to 0·8 normal (see § 5). It therefore appears that the specific effect of the parchment-paper diaphragm may be neglected at concentration 0·8 normal, *i. e.*, that the assumption made in the first paragraph of this section is justified. A constant value of 1·08 for x has been adopted in the case of concentrations 0·7 normal and less.

The decrease in the value of x to 0·93 at normal concentration (see Table III.) is discussed in § 5. The value of 0·93 is in satisfactory agreement with that of 0·90 obtained by Baborovsky[9] by means of the chemical analysis form of the mechanical fixation method, and is not greatly divergent from that of 0·82 obtained by Washburn and Millard[11] by means of the indifferent reference substance method. The somewhat lower value of Washburn and Millard is probably largely explained by the fact that their result relates to a concentration in excess of normal, *i. e.*, 1·096 normal.

The values obtained for x, the electrolytic water-transport, have been used to compute the values of the true transport number w_a of the anion by means of equation (3). It will be observed (Table III.) that the value of w_a at normal concentration is not materially different from that at infinite dilution, and w_a appears to be practically constant in the case of concentrations not greater than 0·7 normal.

The considerable values obtained for v_f in the case of the more dilute solutions examined (see Table II.) indicate a preponderating influence of the electro-endosmotic effect of the parchment-paper diaphragm, and it is proposed to discuss this effect in a subsequent paper.

Copper Sulphate solutions.—The values of x, the electrolytic water-transport, have been recalculated (see Table IV.) by means of equation (5) in the case of copper sulphate solutions of concentrations ranging from 0·4 normal to 1·8 normal, using the experimeutal data for v_f previously obtained by the author [15], [17]. The appropriate values

Table IV.—Copper Sulphate Solutions.

Conc. c (equiv./mol).	Electrolytic water-transport x (mol/faraday).	Hittorf transport number n_a.	True transport number w_a.	p.
0·	..	0·622	0·622	..
·00090 (0·05 N.)	1·45	·626	·625	0·68
·00180 (·1 N.)	1·45	·630	·627	·69
·00361 (·2 N.)	1·45	·637	·632	·71
·00722 (·4 N.)	1·45 (1·47)	·652	·642	·76
·00902 (·5 N.)	1·45 (1·44)	·659	·646	·78
·01082 (·6 N.)	1·45 (1·42)	·667	·651	·81
·01444 (·8 N.)	1·45 (1·48)	·681	·660	·87
·01805 (1·0 N.)	1·56	·695	·667	1·00
·02167 (1·2 N.)	1·61	·706	·671	1·07
·02530 (1·4 N.)	1·50	·714	·676	1·04
·02894 (1·6 N.)	1·41	·720	·679	1·01
·03295 (1·8 N.)	1·29	·723	·681	·94

of the partial molal volumes and of the Hittorf transport number n_a, required to effect the calculation, have been obtained from Table II. of the Appendix and from the author's former papers, respectively.

The resulting values for x over the concentration range 0·4 normal to 0·8 normal (indicated in brackets in column 2 of Table IV.) are practically constant, the maximum deviation from the mean value of 1·45 being about 2 per cent. The evidence adduced by the author in his former paper suggests that x is independent of concentration in the case of the more dilute solutions of copper sulphate, and a constant value of 1·45 for x has therefore been adopted for all concentrations less than normal. The

variation in x, with increasing concentration from 0·8 normal, is discussed in §5.

The values of w_a, the true transport number of the anion, have also been recalculated (Table IV.). The values so obtained, however, are not materially different from those previously given by the author, the maximum deviation from the former values being 0·3 per cent.

Cupric Chloride Solutions.—The values of the apparent Hittorf transport number n_a of the anion, in the case of solutions of cupric chloride of concentrations ranging from 0·1 normal to normal, have been obtained by graphical interpolation from the experimental data of Bein[23] and Denham[24]. The electrolytic water-transport x has then been determined (see Table V.) by means

TABLE V.—Cupric Chloride Solutions.

Conc. c (equiv./mol)	Electrolytic water-transport x (mol/faraday).	Apparent Hittorf transport number n_a.	Apparent true transport number w_a.
0·00180 (0·1 N.)	−1·43	0·597	0·600
·00361 (·2 N.)	−1·60	·606	·612
·00903 (·5 N.)	−1·76	·628	·644
·01808 (1·0 N.)	−1·83	·660	·693

of equation (5), using the experimental data obtained by the author[18] for v_f, and employing the appropriate values of the partial molal volumes given in Table II. of the Appendix. The values of the apparent true transport number w_a of the anion have been computed by means of equation (3), observing that x is negative in the case of cupric chloride solutions. The significance of these values, in relation to the apparently complex nature of cupric chloride in aqueous solution, is discussed in §5.

§5. *The Ionic Hydration Numbers.*

The hydration of an electrolytic ion in aqueous solution is regarded, for our present purposes, as including not only the water chemically bound to the ion, but also the addi-

tional water carried along by the ion in its movements through the liquid [15].

The electrolytic water-transport x is related to the hydration numbers h_a, h_c of anion and cation, respectively, according to the following equation [5]:

$$x = w_c h_c - w_a h_a \quad . \quad . \quad . \quad . \quad . \quad (8)$$

where w_a, w_c are the true transport numbers of the ions. h_a represents the number of mols of water associated with one equivalent of anions, h_c is the corresponding term relating to the cation.

Sodium Chloride Solutions.—A mean value of 3 is given by Remy [14] for the hydration number of the Cl^- ion in normal aqueous solution. This figure is based upon transference measurements with certain electrolytes containing a heavy organic cation and is arrived at on the assumption, which is supported by the conclusions of Hevesy [25] and Lorenz [26], that heavy organic cations are not hydrated. Remy's figure of 3 is in satisfactory agreement with that of 2·5 calculated by Schreiner [27] from activity data. Baborovsky [9] obtained the somewhat higher figure of 4 from a consideration of measurements of electrolytic water-transport with solutions of sodium chloride, potassium chloride, sodium bromide and potassium bromide. His result, however, appears to be based in part upon too low a value (0·605 in place of ·621, obtained by the author, and ·619 given by Remy [14] for the true transport number w_a of the Cl^- ion in the case of normal sodium chloride solution. Substitution of the author's value of ·621 for w_a gives a figure of 1·3 for the hydration number of the Cl^- ion, but this figure has not been adopted, as it seems probable that errors in the values taken for the transport numbers of the other ions considered may have affected the result to an appreciable extent.

Adopting 3·0 as the most probable value for the hydration number h_a of the Cl^- ion in normal solution, and utilizing the appropriate values of x and w_a given in Table III., we find from equation (8) that the hydration number h_a of the Na^+ ion in normal solution is 7·4. Remy [14], using a mean value of 0·98 (based upon all the available experimental results) for the electrolytic water-transport x in the case of normal sodium chloride solution, also obtained the value of 7·4 for h_c by taking a value of 0·619 for the true transport number w_a; but he appears

to favour the value of 8·1, obtained by considering only the values of x found by the mechanical fixation method. Remy and Reisener's[12] mean experimental value of 1·4 for x, however, yields the value of 8·6 for h_c; but it is evident, in the light of the present results, that 7·4 must be regarded as the most accurate value for this quantity.

In order to ascertain whether the quantities h_a, h_c vary with change in concentration, it is necessary, in the first place, to determine the effect on the value of the electrolytic water-transport x of the variations in the transport numbers w_a, w_c. This may be done by means of equation (8), taking constant values of 3·0 and 7·4 for h_a and h_c, and observing, in utilizing the values of w_a given in Table III., that $w_a+w_c=1$. The term p (Table III.) represents the ratio of the experimental value of x to the value of x obtained by means of the foregoing calculation. The values of p (see Table III.) do not depart greatly from unity; and p may be regarded as constant over the concentration range 0·1 normal to 0·8 normal. It therefore seems justifiable to conclude that h_a and h_c are also constant over this range of concentration. The decrease in the values of p, with increasing concentration from 0·8 normal, indicates that the hydration numbers undergo slight change, probably in consequence of variation in the mass of water carried along hydrodynamically by the ions.

The results of J. N. Sugden[4] for the hydration H (i. e., h_a+h_c) of sodium chloride, obtained by means of a method depending on the distribution of a suitable substance between a non-aqueous solvent and the aqueous solution of the salt, offer a basis of comparison with the present results. Precise agreement would not necessarily follow, since the method of distribution does not involve electrolytic migration, but J. N. Sugden's value of 7·0 for H in the case of normal sodium chloride solution is not greatly different from that of 10·4, *i. e.*, 3·0 plus 7·4, found in the present work. J. N. Sugden also finds that the values of H over the concentration range 0·1 normal to normal are "reasonably constant"—a result which may be regarded as parallel to that of the present work.

Copper Sulphate Solutions.—The hydration number h_a of the $[SO_4]^{-2}$ ion in normal solution, although not

directly available from the experimental results *, may be deduced from a consideration of the data obtained by J. N. Sugden [4] for the hydration H of certain sulphates and chlorides having a common cation. It should, perhaps, be pointed out that the terms H, h_a, h_c, for our present purposes, refer to equivalent (and not to molal) quantities of solute and ions. The comparative statement in Table VI. shows that J. N. Sugden's values for the hydration H of the three sulphates examined by him are in close agreement with the values for the corresponding chlorides. It thus appears, since the hydration H of the solute is given by the sum of the hydration numbers h_a, h_c of its constituent anion and cation, that the hydration number h_a of the $[SO_4]^{-2}$ ion is of practically the same magnitude as that of the Cl^- ion, *i. e.*, 3·0†. It may

TABLE VI.

Equivalent Hydration in Normal Solution.

Sulphate.	Equivalent Hydration H.	Chloride.	Equivalent Hydration H.
$\frac{1}{2}(Na_2SO_4)$	7·2	NaCl	7·0
$\frac{1}{2}(K_2SO_4)$	3·0	KCl	3·3
$\frac{1}{2}(MgSO_4)$	10·2	$\frac{1}{2}(MgCl_2)$	10·0

also be observed that Remy and Manegold's [8] measurements of electrolytic water-transport yield a value of 7·05 for the hydration number h_c of the Mg^{+2} ion in normal solution. This value, considered in conjunction with that of 3·0 obtained for the Cl^- ion, gives a figure of 10·05 for the hydration H of magnesium chloride, which is in close agreement with that of 10·0 obtained from J. N. Sugden's distribution measurements.

Adopting 3·0 as the hydration number h_a of the $[SO_4]^{-2}$ ion in normal solution, we find from equation (8), utilizing the appropriate values of x and w_a given in Table IV., that the hydration number h_c of the Cu^{+2} ion in normal solution is 10·7.

* An experimental method, designed to yield a value for the hydration number of the $[SO_4]^{-2}$ ion, has, however, been recently proposed by Baborovsky [28].

† Assigning a value of 3·0 to the hydration number of the Cl^- ion, we find that J. N. Sugden's results indicate that the K^+ ion, in normal aqueous solution, has little or no hydration.

The variation in the hydration numbers with change in concentration may be examined by means of the method used in connexion with the solutions of sodium chloride. The term p (Table IV.), which represents the ratio of the experimental value of x, the electrolytic water-transport, to the value of x obtained from equation (8) by taking constant values of 3·0 and 10·7 for h_a and h_c, may be regarded as "reasonably constant" over the concentration range normal to 1·6 normal; and it seems justifiable to conclude that there is no appreciable change in the values of H, h_a, and h_c over this concentration range. The decrease in the values of p with decreasing concentration from normal is considered in the following paragraph.

A review of the large body of data obtained from J. N. Sugden's distribution measurements[4] (N.B.—such measurements are not available in the case of copper sulphate solutions) indicates that hydration numbers, in the case of solutions of concentrations not greater than 2 normal, are, in general, independent of concentration, but that an abnormality arises in the case of the $[SO_4]^{-2}$ ion at concentrations less than normal. If, therefore, we assume that the decrease in the values of p, in the case of copper sulphate solutions of concentrations less than normal, is attributable to a change in the magnitude of the hydration number h_a of the $[SO_4]^{-2}$ ion, we may obtain values for this latter quantity by means of equation (8), taking a constant value of 10·7 for h_c and utilizing the values of x and w_a given in Table IV. The resulting values for h_a increase from 3·0 to 4·1 with decreasing concentration from normal to 0·1 normal. J. N. Sugden's distribution data, on the other hand, suggest that h_a decreases with decreasing concentration from normal; indeed, the diminution (3·0) in his value for the hydration H of magnesium sulphate, with decreasing concentration from normal to 0·1 normal, is equal to the value found for h_a in normal solution, thus indicating that the $[SO_4]^{-2}$ ion is completely dehydrated in 0·1 normal magnesium sulphate solution. It seems possible, however, that this apparent dehydration is attributable to a specific influence on the $[SO_4]^{-2}$ ion of the non-aqueous solvent employed in the method of distribution; and, bearing in mind the result obtained by the author, which indicates that the hydration H of copper sulphate increases somewhat with decreasing concentration from normal to 0·1 normal,

we are led to the conclusion that such apparent dehydration is not representative of the original solution.

Cupric Chloride Solutions.—The case of cupric chloride is of interest in view of the well-known colour change of aqueous solutions of this salt from green in concentrated solution to blue in dilute solution. Donnan and Bassett[29] have suggested that this colour change is due to the formation of complex anions of the form $[CuCl_4]^{-2}$, $[Cu_2Cl_6]^{-2}$, etc., the addition of water causing the complex radicals to break up into hydrated copper ions and chloride ions. Evidence in support of this suggestion is given by the transference measurements of Denham[24], which indicate that the apparent transport number n_c of the cation, as determined by the Hittorf method, decreases to an abnormally low value in the case of cupric chloride solutions and finally becomes negative as the saturation point (concentration >10 normal at room-temperature) is approached; an abnormally low value of n_c being consistent with the presence of anions of the form $[CuCl_4]^{-2}$ and a negative value with the presence of anions of the form $[Cu_2Cl_6]^{-2}$[30].

The change in colour of the solution and the abnormalities in the values of the Hittorf transport number apparently occur at concentrations considerably greater than normal; and the author[18], in a former paper, proceeded on the assumption that complex ion formation could be neglected in the case of the cupric chloride solutions (all of concentrations not exceeding normal) examined by him. The correctness of this assumption may now be tested, using the respective values of 3·0 and 10·7, obtained in the preceding sections of this paper, for the hydration numbers h_a, h_c of the Cl^- ion and the Cu^{-2} ion at normal concentration. Substituting these values in equation (8), and using the value of 0·693 (Table V.) obtained for the transport number w_a of the anion in the case of normal cupric chloride solution, we obtain the value of 1·2 for the electrolytic water-transport x. The experimental value of x, however, is $-1{\cdot}83$ (Table V.); there is thus an added effect, represented by a considerable water transport from the cathode to the anode. The most probable explanation of this added effect appears to be that hydrated complex anions are present in normal cupric chloride solution. A lower limit to the hydration

number of such complex anions (assumed to be of the form $[CuCl_4]^{-2}$) may be obtained from our present data by means of the following considerations.

Consider the electrolysis of a normal solution of cupric chloride in the ordinary type of migration apparatus, copper electrodes being employed.

If the true transport numbers of the Cu^{+2}, Cl^-, and $[CuCl_4]^{-2}$ ions are respectively w_c, w_a, and w_1, we have the relation:

$$w_c+w_a+w_1=1. \quad . \quad . \quad . \quad . \quad . \quad (9)$$

On the passage of 1 faraday of electricity, the net loss of cupric chloride from the solution surrounding the cathode is given by the expression: w_a+2w_1+cx (equivalents), where x is the electrolytic water-transport (considered as positive when from anode to cathode), and c is the concentration (equivs./mol). This expression represents the experimental Hittorf transport number n_a, and we therefore obtain the relation (*cf.* equation (3)):

$$n_a=w_a+2w_1+xc. \quad . \quad . \quad . \quad . \quad . \quad (10)$$

Finally, we have the following expression for the electrolytic water-transport x (*cf.* equation (8)), viz.:

$$x=w_ch_c-w_ah_a-w_1h_1 \quad . \quad . \quad . \quad . \quad (11)$$

where h_c, h_a, h_1 are the respective hydration numbers of the Cu^{-2}, Cl^-, and $[CuCl_4]^{-2}$ ions.

Substituting the values obtained in the foregoing sections for h_a and h_c, viz., 3·0 and 10·7, respectively, and utilizing the appropriate values for x and n_a given in Table V., viz., −1·83 and 0·660, respectively, we find from equations (9), (10), and (11) that the hydration number h_1 of the complex anion $[CuCl_4]^{-2}$ is given by the following expression:

$$h_1=16·7+3·0/w_1. \quad . \quad . \quad . \quad . \quad . \quad (12)$$

Observing that w_1 is $\geqslant 1$, we obtain the considerable value of 19·7 as the lower limit of h_1.

The present experimental results are thus consistent with the hypothesis that complex anions are formed in aqueous solutions of cupric chloride (and even in relatively dilute solution of normal concentration) and lead also to the conclusion that such complex anions are highly hydrated.

The Water Sheaths of the Ions.—The value of the water sheath of an electrolytic ion in aqueous solution is given by the product of the hydration number h and the ionic valency. The values so obtained, at normal concentration, for the various ions considered in the present work are collected in Table VII.

These values represent the total mass of water associated with the ions in the process of electrolytic transport; the evidence adduced by the author indicating generally that such values, in the case of solutions of concentration not greater than normal, suffer no appreciable change with variation in concentration.

The figures given in brackets in the case of the cations express the number of water molecules bound to the ions in aqueous solution by means of coordination linkages [31], [32], the differences between these figures and those

Table VII.

Ionic Water Sheaths at Normal Concentration.

Ion.	Na^+.	Cu^{+2}.	Cl^-.	$[SO_4]^{-2}$.	$[CuCl_4]^{-2}$.
Water sheath (mols) ..	7·4 (4)	21·4 (4)	3·0	6·0	>39

obtained by the author for the ionic water sheaths representing the additional water carried along by the ions in their movements through the liquid. Bernal and Fowler [31] conclude, from an examination of solution-density data, that most anions (notable exceptions being $[OH]^-$ and F^-) are not coordinated with water molecules in aqueous solution; but they assign, on theoretical grounds, a value of 4 for the coordination number of the Cl^- ion. This value, however, is in excess of that of 3·0 found for the water sheath.

§ 6. *Acknowledgment.*

The author desires to thank Prof. P. M. S. Blackett, F.R.S., for facilities provided and for the interest he has taken in this investigation.

References.

(1) See ' A Treatise on Physical Chemistry,' edited by H. S. Taylor, pp. 687, 688 (London, 1930).

(2) Riesenfeld, E. H., and Reinhold, B., *Z. phys. Chem.* lxvi. p. 672 (1909).

(3) Ingham, J. W., J. Chem. Soc. p. 1917 (1928).
(4) Sugden, J. N., *ibid.* p. 174 (1926).
(5) Nernst, W., *Götting. Nachr.* p. 1 (1900).
(6) Buchbock, G., *Z. phys. Chem.* lv. p. 563 (1906).
(7) Washburn, E. W., *ibid.* lxvi. p. 513 (1909).
(8) Remy, H., and Manegold, E., *Ibid.* cxviii. p. 161 (1925).
(9) Baborovsky, G., *ibid.* cxxix. p. 129 (1927).
(10) Washburn, E. W., J. Amer. Chem. Soc. xxxi. p. 322 (1909).
(11) Washburn, E. W., and Millard, E. B., *Ibid.* xxxvii. p. 694 (1915).
(12) Remy, H., and Reisener, H., *Z. phys. Chem.* cxxiv. p. 394 (1926).
(13) Velíšek, J., and Vašíček, A., ' Czechoslovak Chemical Communications,' Collection III, No. 1–2, p. 114 (1931).
(14) Remy, H., Trans. Faraday Soc. xxiii. p. 381 (1927).
(15) Hepburn, H. C., Proc. Phys. Soc. xliii. p. 524 (1931).
(16) Baborovský, J., *Chem. Listy*, xxix. p. 285 (1935).
(17) Hepburn, H. C., Proc. Phys. Soc. xliv. p. 267 (1932).
(18) Hepburn, H. C., *ibid.* xlv. p. 755 (1933).
(19) Smith, E. R., Bur. of Standards J. of Research, viii. p. 457 (1932).
(20) ' Landolt-Börnstein Tabellen,' pp. 290, 307 (1923).
(21) Hopfgartner, *Z. phys. Chem.* xxv. p. 115 (1898).
(22) Taylor, M., and Sawyer, E. W., J. Chem. Soc. p. 2095 (1929).
(23) Bein, H., *Z. phys. Chem.* xxvii. p. 1 (1898).
(24) Denham, H. G., *ibid.* lxv. p. 641 (1909).
(25) Hevesy, G., *Jahrb. Radioakt. Elektronik.* ii. p. 419 (1914); xiii. p. 273 (1916).
(26) Lorenz, R., *Z. anorg. Chem.* xciv. p. 265 (1916) *et seq.*
(27) Schreiner, E., *ibid.* cxxi. p. 321 (1922); cxxxv. p. 333 (1924).
(28) Baborovský, J., *Chem. Listy*, xxx. p. 5 (1936).
(29) Donnan, F. G., and Bassett, H., Trans. Chem. Soc. lxxxi. p. 939 (1902).
(30) Watkins, S. B., and Denham, H. G., J. Chem. Soc. cxv. p. 1269 (1919).
(31) Bernal, J. D., and Fowler, R. H., J. Chem. Phys. i. p. 515 (1933).
(32) Nernst, W., ' Theoretical Chemistry,' pp. 444, 445 (London, 1923).

APPENDIX.

The Determination of Partial Molal Volumes.

Introduction.—The use of partial molal volumes has been given prominence by Lewis and Randall[1] in connexion with the thermodynamic treatment of the activity of electrolytes in solution; and, in certain cases, such quantities have been evaluated by means of graphical methods[1] or by the application of empirical formulæ[2]. A complete body of data, such as the author requires for the accurate determination of electrolytic water-transport, is not, however, available, and he has therefore devised a convenient method for obtaining partial molal volumes in terms of the density and the concentration of the solutions under examination.

Partial Molal Volumes in Terms of Solution Density and Concentration.—Consider a solution containing n_1 mols of a substance X_1, n_2 mols of a substance X_2, etc., and designate the total volume of the mixture by V; $\bar{v}_1$, the

partial molal volume of X_1, is then defined as $\partial V/\partial n_1$; similarly, $\bar{v}_2$, the partial molal volume of X_2, is defined as $\partial V/\partial n_2$, and so on. If V is infinite, $\bar{v}$ is the increase in volume produced by the addition to the mixture of one mol of X.

Now consider a volume V (cm.^{3}) of a solution of a substance in water, containing n_1 mols of substance and n_2 mols of water. On the addition of ∂n_1 mols of the substance to the solution, let the solution density change from S to $S+\partial S$, and let the concentration of the solution (mols of substance per litre of solution) change from C to $C+\partial C$.

A simple analysis then gives the following expression for $\partial V/\partial n_1$, when small quantities of the second order are neglected, viz.:

$$\partial V/\partial n_1 = \frac{m_1 - 1000\ \partial S/\partial C}{S - C\partial S/\partial C} \quad . \quad . \quad . \quad . \quad (1)$$

Similarly, by considering the case in which ∂n_2 mols of water are added to the original solution, the following expression is obtained for $\partial V/\partial n_2$, viz.:

$$\partial V/\partial n_2 = \frac{m_2}{S - C\partial S/\partial C} \quad . \quad . \quad . \quad . \quad (2)$$

m_1 and m_2 are the molecular weights of the substance and of water, respectively.

Computation of Partial Molal Volumes.—The relationship between the density S_{18} and the concentration C(mols/litre), in the case of the solutions considered in the present work, is accurately represented by an equation of the form:

$$S_{18} = 0{\cdot}99860 + K_1C - K_2C^2. \quad . \quad . \quad . \quad (3)$$

The appropriate values of the constants K_1 and K_2 are given in Table I. and have been calculated by the author from the most reliable experimental data for the solution densities at 18° C.

The partial molal volumes have been calculated by means of equations (1) and (2) and are given in Table II.

Discussion of Results.—The negative values obtained for $\partial V/\partial n_1$ in the case of dilute solutions (concentrations 0·1 molal and less) of copper sulphate indicate that here

the addition of solute actually diminishes the total volume of the solution. A similar result was found by Lewis and Randall[1] (using a graphical method) in the case of magnesium sulphate solutions of concentrations less than

TABLE I.

Constants in Solution Density Equation.

Solution.	K_1.	K_2.	Observer and concentration range of data.
NaCl	0·04228	0·00158	Bousfield[3] (0·17 M. to 1·07 M.)
$CuSO_4$	·16154	·00676	Archibald[4] (0·05 M. to 0·25 M.; Kohlrausch[5] (0·5 M.); Hepburn[6] (0·7 M. to 0·9 M.).
$CuCl_2$	·1334	·0084	Heydweiller[7] (0·05 M. to 0·5 M.).

TABLE II.

Partial Molal Volumes (cm.^{3}) of the Solvent (Water) and of the Solute.

Conc. C (mols/ litre).	Solute.					
	NaCl.		$CuSO_4$.		$CuCl_2$.	
	$\partial V/\partial n_1$.	$\partial V/\partial n_2$.	$\partial V/\partial n_1$.	$\partial V/\partial n_2$.	$\partial V/\partial n_1$.	$\partial V/\partial n_2$.
0·05	—	—	−1·23	18·04	1·93	18·04
·1	16·51	18·04	−0·55	18·04	2·77	18·04
·2	16·83	18·04	0·80	18·04	—	—
·25	—	—	1·48	18·03	5·29	18·03
·3	17·14	18·04	2·16	18·03	—	—
·4	17·46	18·04	3·51	18·02	—	—
·5	17·77	18·03	4·86	18·01	9·48	18·00
·6	18·09	18·03	6·21	18·00	—	—
·7	18·40	18·03	7·55	17·98	—	—
·8	18·71	18·02	8·89	17·96	—	—
·9	19·02	18·02	10·23	17·94	—	—
1·0	19·33	18·01	—	—	—	—

0·07 molal. These results suggest that there is a strong ionic hydration effect in the case of such sulphate solutions[8].

The results, as a whole, show that $\partial V/\partial n_2$, the partial molal of the solvent (water), decreases slightly with increase in concentration; but all the values of this

quantity approximate to the value of the ordinary molal volume of water at 18° C. (18·04 cm.^{3}). On the other hand, $\partial V/\partial n_1$, the partial molal volume of the solute, increases, in each case, with increasing concentration.

References.

(1) Lewis, G. N., and Randall, M., ' Thermodynamics and the Free Energy of Chemical Substances,' p. 33 *et seq.* (New York. 1923).
(2) Lamer, V. K., and Gronwall, T. H., J. Phys. Chem. xxxi. p. 393 (1927).
(3) Bousfield, W. R., Phil. Trans. A, ccvi. p. 107 (1906).
(4) Archibald, J., Trans. Nov. Scot. Inst. ix. p. 335 (1897).
(5) Kohlrausch, *Wied. Ann.* xxvi. p. 161 (1885).
(6) Hepburn, H. C., Proc. Phys. Soc. xliv. p. 267 (1932).
(7) ' Landolt-Börnstein Tabellen,' p. 424 (1923).
(8) *Cf.* Bernal, J. D., and Fowler, R. H., J. Chem. Phys. i. p. 533 (1933).

XCVIII. *The Computation of Three-dimensional Fourier Syntheses in Crystal Structure Analysis.*

By T. H. Goodwin, *Ph.D., A.I.C., John Harling Fellow, University of Manchester, and* R. Hardy, *M.Sc.**

Abstract.

Two-dimensional Fourier projections of crystal structures may not lead to complete resolution of all the atoms. Three-dimensional syntheses do so. The method of computing such a synthesis is described for the most general case (no symmetry centre). Special reference is made to summation along lines such as (x_1y_1z) and over planes such as (xyz_1).

ONE of the most important stages in the analysis of crystal structures by X-rays is the computation of Fourier projections of the atoms, ions, or molecules on to convenient planes. With molecules which are themselves planar, such as all but a few of those to which the method has so far been applied, there is comparatively little ambiguity in the determination of atomic coordinates and hence of interatomic and intermolecular distances. The time has now arrived when it is desirable to extend these methods to compounds with non-planar

* Communicated by Prof. W. L. Bragg, F.R.S.

molecules. Clearly projections will be of less service here, for they will provide less perfect resolution of the atoms, and in certain cases, such as anhydro-sugars, where the molecules have three-dimensional polycyclic structures, complete resolution is theoretically impossible. To meet difficulties such as these the present work on the evaluation of three-dimensional Fourier syntheses has been developed, since these necessarily resolve all atoms perfectly if a sufficient number of terms is used.

At any point whose coordinates (xyz) are expressed as fractions of the cell edges a, b, c, the electron density $\rho(xyz)$ is given by

$$\rho(xyz)=\frac{1}{V}\sum_{-H}^{H}\sum_{-K}^{K}\sum_{-L}^{L}|F_{hkl}|\cos\{2\pi(hx+ky+lz)-\alpha_{hkl}\}, \quad . \quad (1)$$

where V is the volume of the cell, F_{hkl} is the absolute structure amplitude of the reflexion (hkl), and α_{hkl} is its phase angle. $\pm$H, $\pm$K, $\pm$L are the limiting values of (hkl), and represent, theoretically, a triply infinite series. (In practice several hundred planes will be used.) Since $|F_{hkl}|=|F_{\bar{h}\bar{k}\bar{l}}|$ and $\alpha_{hkl}=-\alpha_{\bar{h}\bar{k}\bar{l}}$, we may write (1) in the form

$$\begin{aligned}V.\rho(xyz)=&2\sum_{-H}^{H}\sum_{-K}^{K}\sum_{1}^{L}|F_{hkl}|\cos\{2\pi(hx+ky+lz)-\alpha_{hkl}\}\\&+2\sum_{-H}^{H}\sum_{1}^{K}F_{hk0}\cos\{2\pi(hx+ky)-\alpha_{hk0}\}\\&+2\sum_{1}^{H}|F_{h00}|\cos\{2\pi hx-\alpha_{h00}\}\\&+F_{000}, \quad . \quad . \quad . \quad . \quad . \quad . \quad . \quad . \quad . \quad . \quad . \quad . \quad (2)\end{aligned}$$

whereby the number of terms in the summation is almost halved. Further substantial reductions may frequently be made by virtue of the symmetry of the crystal. Thus, in the space-group $P4_2/n$, which is referred to later, the glide-plane makes it only necessary to sum over the range $h=-$H to H, $k=0$ to K, $l=0$ to L. (Due regard must be paid to the correct multiplicity of planes such as $\{hk0\}$ and $\{h00\}$.)

Considering now only the general expression (1), we may expand this to get (writing $|F|$ for $|F_{hkl}|$ and α for α_{hkl})

$$V.\rho(xyz)=\sum_{-H}^{H}\left[\sum_{-K}^{K}\sum_{-L}^{L}|F|\cos\{2\pi(ky+lz)-\alpha\}\right]\cos 2\pi hx$$

$$-\sum_{-H}^{H}\left[\sum_{-K}^{K}\sum_{-L}^{L}|\ F\ |\ \sin\{2\pi(ky+lz)-\alpha\}\right]\sin 2\pi hx. \quad . \ . \ . \quad (3)$$

If we call the square brackets [] $C_{yz\alpha}$ and $S_{yz\alpha}$ respectively, we have

$$C_{yz\alpha}=\sum_{-K}^{K}\left[\sum_{-L}^{L}|\ F\ |\ \cos\{2\pi lz-\alpha\}\right]\cos 2\pi ky$$
$$-\sum_{-K}^{K}\left[\sum_{-L}^{L}|\ F\ |\ \sin\{2\pi lz-\alpha\}\right]\sin 2\pi ky, \quad . \ . \quad (4)$$

$$S_{yz\alpha}=\sum_{-K}^{K}\left[\sum_{-L}^{L}|\ F\ |\ \sin\{2\pi lz-\alpha\}\right]\cos 2\pi ky$$
$$+\sum_{-K}^{K}\left[\sum_{-L}^{L}|\ F\ |\ \cos\{2\pi lz-\alpha\}\right]\sin 2\pi ky. \quad . \ . \quad (5)$$

Now calling the contents of the square brackets in (4) $C_{z\alpha}$ and $S_{z\alpha}$ respectively, we have

$$C_{z\alpha}=\sum_{-L}^{L}|\ F\ |\ \cos 2\pi lz.\cos\alpha+\sum_{-L}^{L}|\ F\ |\ \sin 2\pi lz.\sin\alpha, \quad . \quad (6)$$

$$S_{z\alpha}=\sum_{-L}^{L}|\ F\ |\ \sin 2\pi lz.\cos\alpha-\sum_{-L}^{L}|\ F\ |\ \cos 2\pi lz.\sin\alpha. \quad . \quad (7)$$

If we write C_α for $|\ F\ |\cos\alpha$ and S_α for $|\ F\ |\sin\alpha$, we may express equations (3) to (7) as follows :—

$$C_{z\alpha}=\sum_{-L}^{L}C_\alpha\cos 2\pi lz+\sum_{-L}^{L}S_\alpha\sin 2\pi lz, \quad . \ . \ . \quad (8)$$

$$S_{z\alpha}=\sum_{-L}^{L}C_\alpha\sin 2\pi lz-\sum_{-L}^{L}S_\alpha\cos 2\pi lz, \quad . \ . \ . \quad (9)$$

$$C_{yz\alpha}=\sum_{-K}^{K}C_{z\alpha}\cos 2\pi ky-\sum_{-K}^{K}S_{z\alpha}\sin 2\pi ky, \quad . \ . \quad (10)$$

$$S_{yz\alpha}=\sum_{-K}^{K}S_{z\alpha}\cos 2\pi ky+\sum_{-K}^{K}C_{z\alpha}\sin 2\pi ky, \quad . \ . \quad (11)$$

$$V.\rho(xyz)=\sum_{-H}^{H}C_{y:\alpha}\cos 2\pi hx-\sum_{-H}^{H}S_{yz\alpha}\sin 2\pi hx. \quad . \quad (12)$$

Thus the computation of a three-dimensional Fourier synthesis is carried out in four stages :

1. Calculation of C_α and S_α for all planes.
2. Arrangement of the planes into groups, the members of which have the same values of h and k with different

values of l (*e. g.*, the $\{3\bar{2}\,l\}$ planes) and calculation of $C_{z\alpha}$ and $S_{z\alpha}$ by means of (8) and (9).

3. Arrangement of these groups into "major groups," the members of which have the same values of h with different values of k (*e. g.*, the $\{3k\}$ groups) and calculation of $C_{yz\alpha}$ and $S_{yz\alpha}$ by means of (10) and (11).

4. Combination of these "major groups," which all have different values of h to calculate $V.\rho(xyz)$ by means of (12).

As in the method of evaluating two-dimensional projections described by Beevers and Lipson, use can be made of the facts that $\cos 2\pi hx = \cos 2\pi\bar{h}x$ and $\sin 2\pi hx = -\sin 2\pi\bar{h}x$. Thus at stage 3 (above) the combined contribution of any (hk) group and the corresponding $(h\bar{k})$ group to $C_{yz\alpha}$ is

$$= \{C_{z\alpha}(hk) + C_{z\alpha}(h\bar{k})\} \cos 2\pi ky - \{S_{z\alpha}(hk) - S_{z\alpha}(h\bar{k})\} \sin 2ky,$$

and to $S_{yz\alpha}$ is

$$\{S_{z\alpha}(hk) + S_{z\alpha}(hk)\} \cos 2\pi ky + \{C_{z\alpha}(hk) - C_{z\alpha}(h\bar{k})\} \sin 2\pi ky.$$

Thus by adding and subtracting the values of $C_{z\alpha}$ and $S_{z\alpha}$ for (hk) and $(h\bar{k})$ before multiplying by $\cos 2\pi ky$ and $\sin 2\pi ky$ considerable time may be saved.

In practice most workers will find it advantageous from the points of view of convenience and space to make the additions by summing separately terms such as $C_{z\alpha} \cos 2\pi ky$ and $S_{z\alpha} \sin 2\pi ky$ in (10), and taking the sum (or difference) of the appropriate totals instead of evaluating $C_{yz\alpha}$ for each (hk) group before adding.

However, since the number of $\{hkl\}$ structure factors must be as great as possible to effect the maximum resolution of the atoms, the process of evaluating a complete three-dimensional synthesis is very laborious. Even with the simplifications indicated above, and with the method of calculation described by Beevers and Lipson in which the cell edges are only divided into 60 parts, some 216,000 electrons densities might have to be calculated. It is therefore virtually impossible to proceed straight from the experimental structure factors and phase angles to a complete three-dimensional synthesis. One or more projections on convenient planes are essential

first, the more powerful method being used to resolve atoms not separated sufficiently by them.

Thus, if a projection on {001} shows a maximum at (x_1y_1) which is due to two atoms at $(x_Ay_Az_A)$ and $(x_By_Bz_B)$, three-dimensional syntheses will evaluate all six co-ordinates accurately. Clearly a synthesis along the line (x_1y_1z) will give the values of z_A and z_B, for, though this line will not in general pass through the centre of either atom, it will pass sufficiently close to both centres to produce definite maxima in the curve of variation of electron density with z. If independent evidence indicates that the two atoms must lie in (say) the lower half of the cell, it is unnecessary to evaluate $V.\rho(x_1y_1z)$ beyond $z=0{\cdot}5$. Having, in this way, determined the z-co-ordinates of both atoms, Fourier sections through $z=z_A$ and $z=z_B$ can now be made to find x_A, y_A, x_B, and y_B. Again, there is no need to carry out the calculation over the whole sections since only a small area of each round (x_1y_1), say $(x_1\pm{\cdot}05,\ y_1\pm{\cdot}05)$, is required. In this way more reliable determinations of all the coordinates may be made than are possible using projections only. If still greater accuracy is desirable new line syntheses through (x_Ay_Az) and (x_By_Bz) will give improved values for z_A and z_B, and these in turn can be used to construct new sections over the planes (xyz_A) and (xyz_B) to obtain slightly better results for (x_Ay_A) and (x_By_B).

A line synthesis is, of course, comparatively easy to carry out, and Tables I. to IV. have been included to illustrate the various stages of the work. To compute the electron density along the line (x_1y_1z) (in the tables along $(0{\cdot}181,\ 0{\cdot}070,\ z)$) the various terms C_α and S_α for all the planes (Table I.) are multiplied by the appropriate constants $\cos 2\pi hx_1$ and $\sin 2\pi hx_1$, and summed as in equations (8) and (9) to deduce $C_{x_1\alpha}$ and $S_{x_1\alpha}$ for each group of planes (*e. g.*, $\{h21\}$) in turn (Table II.). These are then multiplied by the corresponding constant values of $\cos 2\pi ky_1$ and $\sin 2\pi ky_1$, and totalled to give $C_{x_1y_1\alpha}$ and $S_{x_1y_1\alpha}$ for each "major group" (*e. g.*, $\{k1\}$) as in (10) and (11) (Table III.). Finally, $C_{x_1y_1\alpha}$ and $S_{x_1y_1\alpha}$ are multiplied by $\cos 2\pi lz$ and $\sin 2\pi lz$ over the required range (using the sine and cosine strips of Beevers and Lipson) to give $V.\rho(x_1y_1z)$ as indicated by equation (12) (Table IV.).

It should be noted that since $\phi=\cos\theta$ is symmetrical about $\theta=\pi$, while $\phi=\sin\theta$ is antisymmetrical, functions such as $V.\rho(xyz)$ in (12) may be evaluated when $z>0{\cdot}5$ by adding $\Sigma S_{x_1y_1\alpha}\sin 2\pi lz'$ (if $z'=1-z$), instead of calculating $S_{x_1y_1\alpha}\sin 2\pi lz$ and subtracting (see Table IV.).

Equation (2) shows that planes $\{hk0\}$ make contributions to the electron density along the line (x_1y_1z) which are constant and independent of z. Consequently it is not necessary to include them in the tables, as they do not help to determine the positions of the maxima but only their absolute magnitude. Their omission is responsible

TABLE I.

Section of Table required for Stage I. of a Line Synthesis.

hkl.	F_{hkl}.	α_{hkl}.	$C_\alpha(hkl)$.	$S_\alpha(hkl)$.	$F_{h\bar{k}l}$.	$\alpha_{h\bar{k}l}$.	$C_\alpha(\bar{h}kl)$.	$S_\alpha(\bar{h}kl)$.
021	19	90	0	19				
121	0	..	0	0	20·5	0	20·5	0
221	0	..	0	0	0	..	0	0
321	8·5	180	$\overline{8{\cdot}5}$	0	13·5	180	$\overline{13{\cdot}5}$	0
421	25	270	0	$\overline{25}$	7	270	0	7
521	26	0	26	0	14·5	180	$\overline{14{\cdot}5}$	0
621	0	..	0	0	11	270	0	$\overline{11}$

for the negative values of $V.\rho(x_1y_1z)$ in Table IV. Similarly $\{00l\}$ terms need not be included in calculating sections over planes (xyz_1).

In computing such a section $C_{z_1\alpha}$ and $S_{z_1\alpha}$ are deduced as for a line synthesis ((8) and (9)), but each must then be multiplied by several (or all) values of $\cos 2\pi ky$ and $\sin 2\pi ky$ and summed to give $C_{yz_1\alpha}$ and $S_{yz_1\alpha}$ as indicated by equations (10) and (11) before the multiplications and additions with respect to h and x are made over the required range of the latter (equation (12)).

These methods of evaluating three-dimensional syntheses were developed in connexion with the studies on pentaerythritol tetracetate $C(CH_2O.CO.CH_3)_4$ by the authors. This compound crystallizes in the space-group

TABLE II.

Section of Table required for Stage 2. ({*h*21} group.)

hkl.	$C_\alpha(hkl)$.	$C_\alpha(\bar{h}kl)$.	$C_\alpha(hkl)+C_\alpha(\bar{h}kl)$.	$\{C_\alpha(hkl)+C_\alpha(\bar{h}\bar{k}l)\}\cos 2\pi hx_1$.	$C_\alpha(hkl)-C_\alpha(\bar{h}\bar{k}l)$.	$\{C_\alpha(hkl)-C_\alpha(\bar{h}\bar{k}l)\}\sin 2\pi hx_1$.	$S_\alpha(hkl)$.	$S_\alpha(\bar{h}kl)$.	$S_\alpha(hkl)+S_\alpha(\bar{h}kl)$.	$\{S_\alpha(hkl)+S_\alpha(\bar{h}\bar{k}l)\}\cos 2\pi hx_1$.	$S_\alpha(hkl)-S_\alpha(\bar{h}\bar{k}l)$.	$\{S_\alpha(hkl)-S_\alpha(\bar{h}\bar{k}l)\}\sin 2\pi hx_1$.
021	0	..	0	0	0	0	19	.	19	19	19	0
121	0	20·5	20·5	8·6	$\overline{20{\cdot}5}$	$\overline{18{\cdot}7}$	0	0	0	0	0	0
221	0	0	0	0	0	0	0	0	0	0	0	0
321	$\overline{8{\cdot}5}$	$\overline{13{\cdot}5}$	$\overline{22}$	21·3	5·0	$\overline{1{\cdot}4}$	0	$\overline{7}$	32	5·2	$\overline{18}$	17·8
421	0	0	0	0	0	0	$\overline{25}$	0	0	0	0	0
521	26	$\overline{14{\cdot}5}$	11·5	9·5	40·5	$\overline{22{\cdot}7}$	0	0	0	0	0	0
621	0	0	0	0	0	0	$\overline{11}$	$\overline{11}$	$\overline{11}$	$\overline{9{\cdot}5}$	11	5·6
Totals				39·4		$\overline{42{\cdot}8}$				14·6		23·4

$C_{x_1\alpha}=39{\cdot}4+23{\cdot}4=62{\cdot}8.$

$S_{x_1\alpha}=\overline{42{\cdot}8}-14{\cdot}6=\overline{57{\cdot}4}.$

Table III.

Section of Table required for Stage 3.
($\{k\}1$ major group.)

kl.	$C_{x_1\alpha}$.	$C_{x_1\alpha}.\cos 2\pi ky_1$.	$C_{x_1\alpha}\sin 2\pi ky_1$.	$S_{x_1\alpha}$.	$S_{x_1\alpha}\cos 2\pi ky_1$.	$S_{x_1\alpha}\sin 2\pi ky_1$.
01	$\overline{35{\cdot}4}$	$\overline{35{\cdot}4}$	0	0	0	0
11	38·4	35·0	16·5	$\overline{31{\cdot}2}$	$\overline{23{\cdot}5}$	$\overline{13{\cdot}5}$
21	62·8	40·2	48·4	$\overline{57{\cdot}4}$	$\overline{36{\cdot}7}$	$\overline{44{\cdot}2}$
31	25·9	6·5	25·0	$\overline{41{\cdot}4}$	$\overline{10{\cdot}4}$	$\overline{40{\cdot}2}$
41	2·1	0·4	2·1	5·1	$\overline{1{\cdot}0}$	5·0
51	5·6	3·3	$\overline{4{\cdot}5}$	$\overline{37{\cdot}1}$	21·8	$\overline{30{\cdot}0}$
61	$\overline{24{\cdot}4}$	21·5	$\overline{11{\cdot}8}$	6·9	$\overline{6{\cdot}1}$	3·3
Totals*		70·7	75·7		$\overline{55{\cdot}9}$	119·6

$C_{x_1y_1\alpha} = 70{\cdot}7 - \overline{119{\cdot}6} = 190{\cdot}3.$

$S_{x_1y_1\alpha} = \overline{55{\cdot}9} + 75{\cdot}7 = 19{\cdot}8.$

* Summation is only necessary from $k=0$ to $k=$K (see p. 1097.)

Table IV.

Section of Table required for Stage 4.
(Final Result.)

z (in thirtieths)	0.	1.	2.	3.	4.	5.	6.
$\sum_1^L C_{x_1y_1\alpha}\cos 2\pi lz$	539	487	346	168	2	$\overline{115}$	$\overline{173}$
$\sum_1^L S_{x_1y_1\alpha}\sin 2\pi lz$	0	10	16	14	8	5	10
$\frac{1}{2}V.\rho(x_1y_1z)$* Diff.	539	477	330	154	6	$\overline{120}$	183
$\frac{1}{2}V.\rho(x_1y_1z)$* Sum	539	497	362	182	10	$\overline{110}$	$\overline{163}$
z (in thirtieths)	30	29	28	27	26	25	24

* $\frac{1}{2}$ because of limited range of summation (p. 1097).

$P4_2/n$. The $-CH_2O.CO.CH_3$ groups are equivalent, and the C=O bonds appeared to be parallel to this axis, since a large, sharp maximum at (0·275, 0·120) in the projection on (001) could only be accounted for in this way. By carrying out a line synthesis along (0·275, 0·120, z) the z-coordinates of these atoms were obtained and were then used to construct sections through the atoms to determine their x- and y-coordinates. In all three final sections and two final line syntheses were made and provided complete resolution of all the atoms in the cell. These led to unequivocal determination of all coordinates besides supplying what might be described as a stereoscopic picture of the distribution of scattering matter in the cell. Effectively some 1500 planes were used for this work, though in practice, owing to the multiplicity of planes in this space-group, only some 375 (approximately twice the number in the published list of F's) were included in the tables (see p. 1097).

The authors desire to express their warmest thanks to Prof. W. L. Bragg, F.R.S., for his constant interest, and to the University of Manchester for the John Harling Fellowship held by one of us (T. H. G.) while this work was carried out.

References.

Beevers, C. A., and Lipson, H., Phil. Mag. (7) xvii. p. 855 (1934); Proc. Phys. Soc. xlviii. p. 772 (1936).
Goodwin, T. H., and Hardy, R., Proc. Roy. Soc. A, clxiv. p. 369 (1938).

XCIX. *A Note on a suggested Intermetallic Reaction in a Liquid Antimony-Copper-Tin-Lead Alloy.* *By* G. C. Seager, *Ph.D.*, *and* F. C. Thompson, *D.Met.*, *M.Sc.**

DURING the course of experiments on the mechanical properties of some typical bearing metals †, it was observed that, although the results from both the high tin and the high lead alloys were repeatable, those for a material containing roughly 40 per cent. of tin and 50 per cent. of lead were distinctly erratic. One of the authors has been informed from another source that this

* Communicated by the Authors.
† H. Greenwood, J. Inst. Met. lv. no. 2, p. 77 (1934).

lack of reproducibility has been observed in other work on similar alloys.

It was suggested by Professor O. W. Ellis in 1925 * that, in a molten lead-base antifriction alloy containing—in addition to the lead—antimony, copper, and tin, there is the possibility of the occurrence of the reaction expressed by the equation

$$2Cu + SnSb \rightleftharpoons Cu_2Sb + Sn,$$

to which reaction were ascribed changes observed in the microstructure of the alloy. Since it appeared that such differences in the structures of the alloy due to changes which occurred to a varying extent prior to casting might lead to corresponding differences in their mechanical properties, it was decided to re-examine this point which, in addition to its technical interest, is of considerable

Fig. 1.

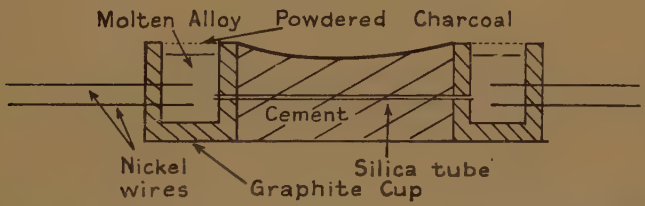

Apparatus used for the determination of the electrical resistance of a liquid alloy.

theoretical importance in view of our inadequate knowledge of the constitution of molten alloys and of the changes which they may undergo.

Since it was believed by Ellis that the reaction resulted in an abnormality in the temperature-resistivity curve of the liquid alloy, it was decided to re-determine this curve with a high degree of sensitivity. The composition of the alloy chosen was :—

Lead	48·6 per cent.
Antimony	10·5 ,, ,,
Copper	1·03 ,, ,,
Tin	39·8 ,, ,,

The apparatus used is shown in fig. 1, and since it is only the change of resistance with which we are here

* O. W. Ellis, J. Inst. Met. xxxiv. no. 2, p. 301 (1925).

concerned, no attempt has been made to obtain resistivity values in absolute units.

A silica tube of 1¼ mm. bore and 7 cm. long was filled with the alloy by suction. This was then cemented at each end into a circular graphite cup which was then also filled with the same alloy. Into each of these cups two nickel wires were fixed to act as electrical connexions for the resistance measurements, and the whole was embedded in fire-cement, leaving the tops of the cups open; the surface of the metal being protected from oxidation by a layer of powdered charcoal.

Fig. 2.

Resistance/temperature curve.

Near the centre of the narrow silica tube a gap was left in the cement to take a copper-constantan thermocouple, the E.M.F. of which was measured on a Cambridge potentiometer reading to 1 microvolt, *i. e.*, 0·025° C. The apparatus was heated in an electric muffle furnace.

The resistances were measured by means of a Kelvin double bridge on which the resistance could be measured to 5×10^{-6} ohms, *i. e.*, to about 0·01 per cent. The current and potential leads from the bridge being separate up to the point where they enter the molten metal, the effect of change of resistance of the nickel wires was reduced to negligible proportions. That this was so was verified by a "blank test" in which the silica tube was

replaced by a length of constantan wire. After a sufficiently high temperature had been reached the furnace was allowed to cool down, and the resistance and temperature read periodically.

The results, when plotted (fig. 2) gave a perfectly smooth curve until the temperature had fallen to 282° C., when a slight discontinuity occurred. As will be seen from the thermal cooling curve (fig. 3) this discontinuity corresponds to the commencement of solidification.

Fig. 3.

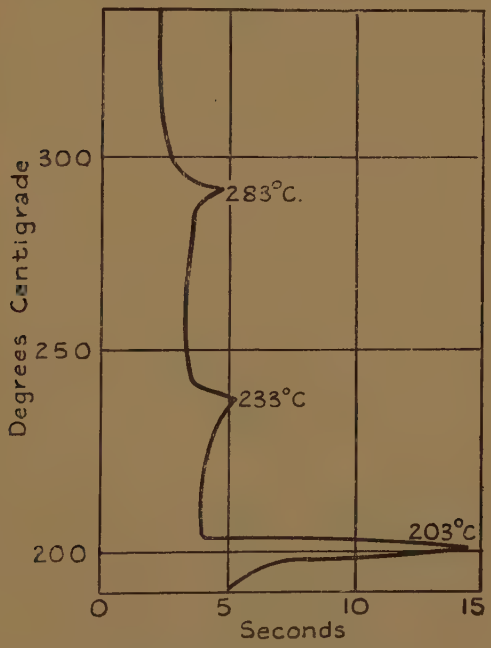

"Inverse rate" cooling curve.

So long then as the alloy is completely molten there is no evidence from these measurements of the slightest deviation from the smooth curve or, therefore, of the reaction suggested. The criticism has already been made by Desch * in the discussion on Ellis's paper that the abnormality in the latter's curve was due merely to the commencement of freezing, an explanation which would appear to receive strong support from the result here obtained.

* C. H. Desch, *loc. cit.* p. 322.

C. *The Specific Resistance and the Temperature Variation of Resistance of Tin Crystals.* *By* Bruce Chalmers, *B.Sc., Ph.D., F.Inst.P., and* R. H. Humphry, *M.Sc., F.Inst.P.**

Introduction

THE influence of impurities on the electrical resistance of metals has been the subject of numerous investigations, but in most cases the fundamental value of the results has been small owing to the possibility of variations of characteristics such as grain-size and orientation. In other investigations of specific resistance, notably those of Bridgman[1], these uncertainties have been overcome by using single crystals, but in many of these cases insufficient attention has been paid to the purity of the material used.

For these reasons the present investigation was undertaken with the object of measuring the specific resistance and the temperature coefficient of resistance of single crystals of tin of two different degrees of purity.

Preparation of the Specimens.

The specimens were prepared from tin of two grades, (*a*) Chempur tin (analysis, tin 99·987, copper 0·00132, antimony 0·00118, lead 0·00585, iron 0·00055, bismuth 0·00352, arsenic 0·00005, nickel 0·00003, silver 0·00018 per cent.; zinc, cobalt and sulphur, nil); and (*b*) Williams Harvey tin (analysis, tin 99·996, lead 0·0009, copper 0·0005, bismuth 0·0006, zinc 0·0005, iron 0·001, antimony 0·00014, arsenic 0·00005 per cent.; slight traces of silver, indium and calcium).

Since the structure of β tin is tetragonal it is only necessary to measure the specific resistance in two known directions in order to be able to calculate its value in any direction relative to the crystallographic axes. The same applies to the temperature coefficient of resistance. The two directions chosen were the extremes, *i. e.*, with the *c*-axis perpendicular and parallel respectively to the axis of the specimen.

The specimens were prepared by filling glass tubes of appropriate size, prepared with projections to accommodate the potential contacts as described later, with

* Communicated by the Authors.

tin ; all air-bubbles were removed by heating the tube in a furnace and evacuating with a Hyvac pump.

The specimens were recrystallized into single crystals of the chosen orientation by the moving furnace method, the furnace consisting of a small heating coil moved slowly along the specimen, sufficient heat being generated in the coil to melt the specimen locally. The orientation was predetermined by " seeding " with crystals known to have the required orientation [2]. These were prepared from a single seed by using appropriately curved glass tubes containing tin, the furnace travelling round the curve, the change of direction being a right angle to prepare a seed for the parallel orientation from one for the perpendicular position.

The orientations of all specimens were confirmed using the optical reflexion method previously described by one of the authors [3], and the specimens on which measurements had been made were all found, on removal of the glass, to be within 2° of the nominal values. An advantage of using the orientations described is that they are both easily identified by the optical method and that the change of resistivity with orientation is at a minimum at these values.

Resistance Measurements.

In the preparation of the single crystals it was necessary to use tubes not less than 1·8 mm. in diameter, in order to avoid air cavities, while other practical considerations set the limit of crystal length at about 20 cm. The resistance to be measured was thus of the order 0·005 Ω, and was determined by comparison with a standard resistance of 0·04 Ω having current and potential leads, by means of a double potentiometer arrangement. Current leads were connected to the crystals at the ends, which were exposed by heating the glass tube locally and plunging it into cold water, when the glass cracked off. Potential contacts were provided in the following manner :—the glass tube, prior to filling with tin, was heated in a fine blowpipe-jet at two points, and small pips were drawn out from it and sealed off. When the metal was melted in the tube it filled the two small cavities ; the crystal therefore had two very small excrescences, the tips of which were exposed by filing off the ends of the glass pips. The potential contacts

consisted of fine steel needle points soldered to strips of springy copper-foil, and inserted, after careful cleaning, into the tin crystal through the small apertures in the side of the glass tube. The copper strips were held securely in position by binding to the tube with wire in such a way as to impose a slight pressure on the contact, and they were then covered with a protective binding, the potential leads being soldered to the ends of the copper strips. These leads, together with the current lead to the lower end of the specimen, were passed through a cork which fitted the glass tube holder at the top and by which the specimen was held vertically.

A current of approximately 0·12 ampere was passed through the standard resistance and crystal in series, and the potential differences on each were balanced, in turn, on a potentiometer consisting of a fixed resistance R in series with a bridge wire 1 metre long and an adjustable resistance, using a galvanometer whose sensitiveness was 4 mm./μV. R was chosen of such value that the crystal p.d. could be balanced on the wire. In making a measurement, the p.d. at the terminals of the standard resistance was balanced against that at the ends R by adjustment of the potentiometer current, and then, switching over to the crystal, a balance was obtained for it on the potentiometer wire, which was provided with two contacts, one fixed near one end and the other movable. This wire was carefully calibrated over its whole length, and, it may be remarked, was found very uniform over the part used.

With the arrangement described the effect of any thermo-e.m.f.'s at the various contacts will be a residual one, due to slight differences in the contacts or in their temperatures. These residual effects were eliminated by the usual method of reversing the current. The heating effect of the current in the specimen was negligible, the rate of dissipation of energy being only 7×10^{-5} watt.

It may be shown simply that if L=distance between balance points for the crystal, corrected for calibration and thermo-effects, then the crystal resistance is proportional to L.

Measurements were made with the specimen at the ice-point, the steam-point, room-temperature as determined by standard thermometer, and the boiling-point of carbon

tetrachloride (76·7° C.). Observations at the two first-named points gave the mean temperature coefficient over the range 0°–100° C. and also the value of the resistance at 0° C., while those at the other points served to indicate whether, within the limits of measurement, the resistance was a linear function of temperature in the range considered. Measurements were made with several single crystals prepared from each sample of tin and for each orientation.

The specific resistance of the specimens was obtained from the resistance measured as described and observations of the distance between the potential contacts and the mean cross-sectional area, the last-named being determined from a large number of observations of the diameter in two directions at right angles after the glass tube had been removed from the specimen at a number of points along the crystal.

The accuracy of the final values of the temperature coefficient of resistance, α, and the specific resistance at 0° C., ρ_0, was estimated from the accuracy of the various measurements to be $\frac{1}{2}$ per cent. for α and $\frac{1}{2}$ per cent. for ρ_0.

Results.

The values of α obtained are shown in the following table, in which the results for two different specimens of each type are given.

Values of the Mean Temperature Coefficient of Resistance α over the range 0–100° C.

	∥.		⊥.	
	per °C.		per °C.	
Chempur	(1) 0·00460 (2) 0·00456	Mean 0·00458	(1) 0·00466 (2) 0·00466	Mean 0·00466
Williams Harvey.	(1) 0·00448 (2) 0·00455	Mean 0·00451	(1) 0·00466 (2) 0·00469	Mean 0·00467

The greater purity of the Williams Harvey tin thus appears to have no appreciable effect on the value of α for the ⊥ orientation, and the result is in good agreement with Bridgman's value [1], viz., 0·00469 per °C. On the other hand, the less pure material gives a perceptibly

greater value of α for the II orientation. Bridgman's value for this orientation is 0·00447 per °C.

The observations which were made at temperatures between 0° C. and 100° C. showed that a linear relation existed between resistance and temperature within the accuracy of the measurements. The values of ρ_0 obtained were as follows :—

Values of the Specific Resistance at 0° C.

	II.		⊥.	
	$\mu\Omega$-cm.		$\mu\Omega$-cm.	
Chempur	(1) 10·41 (2) 10·87	Mean 10·6	(1) 9·41 (2) 9·25	Mean 9·33
Williams Harvey.	(1) 11·2 (2) 10·8	Mean 11·0.	(1) 9·31 (2) 9·24	Mean 9·27

The purity of the metal appears to influence the value of ρ_0 to an extent which is only just perceptible. Bridgman's results for the specific resistance (when reduced to 0° C. using his values for α) are 9·05 $\mu\Omega$-cm. for the perpendicular and 13·14 $\mu\Omega$-cm. for the parallel orientation.

It therefore appears that the effect of small amounts of impurities is much more pronounced with the " parallel " orientation, and it may be suggested that this is due to some segregation of impurities along particular crystallographic planes during the process of recrystallization. This process would then be analogous to the internal surface effect which has been discussed by Goetz [4].

Summary.

Measurements are described and results given of the specific resistance and temperature coefficient of resistance for single crystals of tin in directions parallel and perpendicular to the *c*-axis. The tin used was of two degrees of purity, 99·987 and 99·996 per cent. The influence of this difference of purity is discussed.

Acknowledgment.

In conclusion, the authors wish to express their indebtedness to the International Tin Research and Development Council for providing the material for this work, and to

their Director of Research and Development, Mr. D. J. Macnaughtan, F.Inst.P., for his personal interest in it. One of the authors (B. C.) is further indebted to the International Tin Research and Development Council for a grant.

References.

(1) P. W. Bridgman, Proc. Amer. Acad. Arts & Sci. lx. p. 305 (1925).
(2) B. Chalmers, Proc. Royal Soc. clxii. p. 120 (1937).
(3) B. Chalmers, Proc. Phys. Soc. xlvii. p. 733 (1935).
(4) A. Goetz, International Conference on Physics, London, ii. p. 67 (1934).

The Sir John Cass Technical Institute,
London, E.C. 3.

CI. *A Definite Integral for Legendre Functions.*

By W. T. Howell *.

CONSIDER the value of the integral

$$\frac{1}{2\pi}\int_0^{2\pi} e^{-im\gamma}(\eta+\rho e^{-i\gamma})^{\lambda}(\xi-\sigma e^{i\gamma})^{-\mu}\,d\gamma$$

when m is integral and λ and μ are unrestricted.

Provided ξ and η are large enough we have, on expanding and integrating,

$$\frac{\Gamma(-\lambda-m)}{\Gamma(-\lambda)\Gamma(1-m)}\left(-\frac{\rho}{\eta}\right)^{-m}\eta^{\lambda}\xi^{-\mu} \times \mathrm{F}\left\{-\lambda-m,\,\mu;\;1-m;\;-\frac{\rho\sigma}{\xi\eta}\right\}. \quad (1)$$

Now

$$\mathrm{F}\left\{-\frac{s}{2}-\frac{n}{2},\,\tfrac{1}{2}-\frac{s}{2}+\frac{n}{2};\;1-s;\;-w^2\right\} = 2^{-s}\Gamma(1-s)\mathrm{P}_n^s(\sqrt{1+w^2}),$$

where $\quad |\arg w| < \frac{\pi}{2};\; s \neq 1\,2\,3\ldots$

So that, taking $\lambda = \frac{n}{2}-\frac{m}{2}$, $\mu = \frac{n}{2}+\frac{1}{2}-\frac{m}{2}$, we have

* Communicated by the Author.

$$\frac{1}{2\pi}\int_0^{2\pi} e^{-\iota m\gamma}(\eta+\rho e^{-\iota\gamma})^{\frac{n-m}{2}}(\xi-\sigma e^{\iota\gamma})^{-\frac{n-m+1}{2}}\,d\gamma$$

$$=(-2)^{-m}\,\frac{\eta^{\frac{n}{2}}}{\xi^{\frac{n+1}{2}}}\left(\frac{\sigma}{\rho}\right)^{\frac{m}{2}}\mathrm{P}_n^m\left(\sqrt{1+\frac{\rho\sigma}{\xi\eta}}\right)\times\frac{\Gamma\left(-\frac{n+m}{2}\right)}{\Gamma\left(-\frac{n-m}{2}\right)} \quad . \quad . \quad . \quad (2)$$

valid when m is integral or zero, but $\neq 1\,2\,3\ldots$, provided $n+m$ is not an even positive integer.

If ρ and σ are replaced respectively by $\iota\{(\xi\eta)^{\frac{1}{2}}+\mu\}$, $\iota\{(\xi\eta)^{\frac{1}{2}}-\mu\}$, we have the result

$$\frac{1}{2\pi}\int_0^{2\pi} e^{-\iota m\gamma}[\eta+\iota\{(\xi\eta)^{\frac{1}{2}}+\mu\}e^{-\iota\gamma}]^{\frac{n-m}{2}}$$

$$\times[\xi-\iota\{(\xi\eta)^{\frac{1}{2}}-\mu\}e^{\iota\gamma}]^{-\frac{(n-m+1)}{2}}\,d\gamma$$

$$=(-2)^{-m}\,\frac{\eta^{\frac{n}{2}}}{\xi^{\frac{n+1}{2}}}\left\{\frac{(\xi\eta)^{\frac{1}{2}}-\mu}{(\xi\eta)^{\frac{1}{2}}+\mu}\right\}^{\frac{m}{2}}\mathrm{P}_n^m\left(\frac{\mu}{\xi^{\frac{1}{2}}\eta^{\frac{1}{2}}}\right)\times\frac{\Gamma\left(-\frac{n+m}{2}\right)}{\Gamma\left(-\frac{n-m}{2}\right)}, \quad . \quad . \quad . \quad (3)$$

provided $|(\xi\eta)^{\frac{1}{2}}+\mu|<|\eta|$ and also $|(\xi\eta)^{\frac{1}{2}}-\mu|<|\xi|$, and n and m satisfy the conditions noted before.

Putting $m=0$ in (3), we get an apparently new definite integral for the Legendre function, viz.,

$$\mathrm{P}_n\left(\frac{\mu}{\xi^{\frac{1}{2}}\eta^{\frac{1}{2}}}\right)=\frac{1}{2\pi}\int_0^{2\pi}\left[1+\iota\left\{\frac{(\xi\eta)^{\frac{1}{2}}+\mu}{\eta}\right\}e^{-\iota\gamma}\right]^{\frac{n}{2}}$$

$$\times\left[1-\iota\left\{\frac{(\xi\eta)^{\frac{1}{2}}-\mu}{\xi}\right\}e^{\iota\gamma}\right]^{-\frac{n+1}{2}}d\gamma, \quad (4)$$

and writing $\xi=\mu x^2$, $\eta=\mu y^2$, we have

$$\mathrm{P}_n\left(\frac{1}{xy}\right)=\frac{1}{2\pi}\int_0^{2\pi}\left\{1+\frac{1+xy}{y^2}\,e^{-\iota\left(\gamma-\frac{\pi}{2}\right)}\right\}^{\frac{n}{2}}$$

$$\times\left\{1+\frac{1-xy}{x^2}\,e^{\iota\left(\gamma-\frac{\pi}{2}\right)}\right\}^{-\frac{n+1}{2}}d\gamma.$$

As an alternative to (1) we have

$$\frac{\Gamma(\mu+m)}{\Gamma(\mu)\Gamma(1+m)}\eta^{\lambda}\xi^{-\mu}\left(\frac{\sigma}{\xi}\right)^{+m}\mathrm{F}\left\{-\lambda,\ \mu+m;\ 1+m;\ -\frac{\rho\sigma}{\xi\eta}\right\}, \quad \ldots \quad (5)$$

provided $\mu+m \neq 0, -1, -2, \ldots$

Taking $\lambda=n$, $\mu=n+\alpha+1$, where n is a positive integer, and defining the Jacobi polynomials by

$$\mathrm{P}_n^{(\alpha,\beta)}(x)=(-)^n\frac{(\alpha+1)_n}{n!}\mathrm{F}\{-n,\ n+\alpha+\beta+1;\ \alpha+1;\ \tfrac{1}{2}(1-x)\},$$

equation (5) reduces to

$$(-)^n\frac{(n+\alpha+1)_m}{(n+1)_m}\frac{\eta^n}{\xi^{n+\alpha+1}}\left(\frac{\sigma}{\xi}\right)^{+m}\mathrm{P}_n^{(m,\alpha)}\left(1+\frac{2\rho\sigma}{\xi\eta}\right). \quad (6)$$

Replacing ρ, σ by

$$\iota\left\{\left(\frac{\xi\eta}{2}\right)^{\frac{1}{2}}+\left(\frac{\mu}{2}\right)^{\frac{1}{2}}\right\} \quad \text{and} \quad \iota\left\{\left(\frac{\xi\eta}{2}\right)^{\frac{1}{2}}-\left(\frac{\mu}{2}\right)^{\frac{1}{2}}\right\}$$

respectively, we get the result:

$$\frac{1}{2\pi}\int_0^{2\pi}e^{-\iota m\gamma}\left[1+\frac{\iota}{\eta}\left\{\left(\frac{\xi\eta}{2}\right)^{\frac{1}{2}}+\left(\frac{\mu}{2}\right)^{\frac{1}{2}}\right\}e^{-\iota\gamma}\right]^n \times\left[1-\frac{\iota}{\xi}\left\{\left(\frac{\xi\eta}{2}\right)^{\frac{1}{2}}-\left(\frac{\mu}{2}\right)^{\frac{1}{2}}\right\}e^{\iota\gamma}\right]^{-n-\alpha-1}d\gamma$$

$$=(-)^n\frac{(n+\alpha+1)_m}{(n+1)_m}(\iota)^{+m}\left\{\frac{\left(\frac{\xi\eta}{2}\right)^{\frac{1}{2}}-\left(\frac{\mu}{2}\right)^{\frac{1}{2}}}{\xi}\right\}^{+m}\mathrm{P}_n^{(m,\alpha)}\left(\frac{\mu}{\xi\eta}\right), \quad \ldots \quad (7)$$

where m is zero or a positive integer.

CII. *Notices respecting New Books.*

Introduction to Mathematical Probability. By J. V. Uspensky. [Pp. 411.] (McGraw-Hill Publishing Co., Ltd., 1937. Price 30*s*.)

LITTLE attempt has yet been made to present the modern developments of the mathematical theory of probability as a coherent whole, and this interesting and well-designed book deserves every encouragement. What with the attempts

at establishing an axiomatic basis for probability, the rapid rise of mathematical statistics both on the side of technique and in the field of logical inference, the extensions of the fundamental limit theorems of which Bernoulli's theorem was the origin, and the spread of applications in the sciences and in industry, there is room for various types of treatment and a need for selection of material. This is definitely a mathematical text-book, not concerned explicitly with applications, nor even with errors of observation, but equally not concerned with the axiomatic basis of the subject. Some essentially statistical developments are discussed, such as the theory of χ^2 and of Student's "t," but for the most part it is a thorough and, for an introduction, remarkably comprehensive exposition of the central problems as they have arisen out of the classical treatment.

Where there is so little to compare with and no established tradition of teaching, it is not easy to describe the ground covered or to assess the possible value of the book to students. No previous knowledge of probability is assumed and, although on the whole a considerable extent of mathematical analysis comes into use, this is introduced gradually as required and the notation is clear and as simple as possible. Of the classical problems, such as gambler's ruin, which have fallen into the background, as much is given as is warranted by their usefulness as examples of method. Attention is directed more to the law of large numbers, the central limit theorems, the concept of distribution for continuous and discontinuous variables, and methods of approximation. The problem of moments and the associated polynomials are discussed in a long appendix. There are numerous problems for solution, many of which are theorems which might equally well have been part of the text, the difference being that only an outline of the proof or a mere hint is given. This is good, provided these theorems are such as would otherwise be omitted as not essential to the argument; but this does not seem to be always the case, and the difference in emphasis may be misleading. For example, Cantelli's extension of Bernoulli's theorem, dealing with the series of relative frequencies in n, $n+1$, ... trials, is included in the text, while, in a later chapter, the strong law of large numbers, *i. e.*, the more general case of the means of samples of n, $n+1$, ... is set as a problem with indication of the line of proof.

References for further reading are supplied after each chapter, and at the end there are a one-page table of the error integral to four decimal places and a rather inadequate index, which might well be revised and extended. For instance, the important concept of chains of dependent trials, introduced

by Markoff, is made use of at each stage, but the term appears in the index under the letter " s " as " simple chains," while one reference alone appears also under Markoff. It is much to be hoped that there will be further editions of this valuable book in which this and other improvements can be made.

Synthetic Resins and Allied Plastics. Edited by R. S. Morrell, in collaboration with T. H. Barry, R. P. L. Britton, and H. M. Langton. [399 pages.] (Oxford University Press. London: Humphrey Milford, 1937. Price 21*s.* net.)

This book provides a comprehensive summary of the present position of an industry which, as regards most of its activities, is not more than twenty-five years old. Few sections of applied chemistry have grown more rapidly or thrown out more branches or achieved in so short a time a more bewildering degree of specialization. To this is doubtless to be attributed the fact that the book is the product of four collaborators. The rapid growth of the industry and the great variety of its manufactured products has caused its secrets to be closely guarded, and it is stated in the preface " Each class of industrial resins or plastics has its experts, who are seldom allowed to collaborate as authors."

The " General Introduction " contained in the first chapter indicates the methods of preparation and outstanding properties of the chief types of synthetic resins, which are then considered in detail in seven succeeding chapters. The types of machinery used for moulding and stamping are fully described, and numerous photographs are included. Two chapters deal with moulded and solid products suitable for use as insulators in the electrical industry.

A very pleasing feature of the book is the extended list of references appended to each chapter. These will be found extremely useful both by the academic and the industrial chemist, though their appeal to the one type of worker may be different from that exerted on the other. Thus, in Chapter 10, details of the preparation of the so-called Thiokol resins are given. These are prepared from ethylene dichloride and sodium polysulphides and appear to have " properties as regards extensibility and retractability comparable with natural rubber." The formation in certain reactions of resinous products of this type has, however, frustrated various syntheses which have recently been attempted from a purely academic standpoint in the reviewer's laboratory !

Although much attention is given to the physical properties of the various resins and to the preparation of substances bearing trade names, the fundamental chemical

aspects are never forgotten, and due regard is given to the historical development of the industry. This is instanced by the account in the first chapter of the early work, dating from an observation of von Baeyer's in 1872, which led up to the experiments of the American Baekeland and the production of Bakelite in 1909.

Among the specially interesting substances used as sources of plastics and resins are the mono- and divinylacetylenes, which in the hands of another American, Carothers, have yielded results which are equally of academic and industrial importance. By the action of hydrogen chloride, monovinylacetylene gives "chloroprene" or 2-chlorobutadiene, which polymerizes very rapidly to a substance called "Duprene." This is in some respects superior to the best natural rubber, being less affected by mineral oils, less permeable to hydrogen, and more stable to heat and oxidizing agents. The influence of the chlorine atom in promoting rapid polymerization (as compared with the much slower polymerization of butadiene) is of particular interest. Most of the work in this field has been carried out with the monovinyl compound as the starting-point, but some details are given regarding the polymerization of divinylacetylene, and the properties of the resulting products. There seems, however, to be no mention of the capriciously and dangerously explosive properties of the peroxide which it rapidly forms when exposed to air. These properties are italicized in Nieuwland's original paper, and should be borne in mind by all who may be concerned with the divinyl derivative.

One of the most important and longest chapters is that which deals with the causes of resinification, with the chemical and colloid-chemical properties of the products and with their molecular weight. Here the work of Staudinger, Haworth and Hirst, and of Rideal is summarized and discussed.

The book concludes with a discussion of the chemical and physical methods employed in the testing and identification of synthetic resins and plastics, a branch of the subject in which there is room for much further work. Some results of the X-ray examination are also described.

There is no doubt that this authoritative treatise—simultaneously a handbook and a work of reference—will be indispensable to the chemist engaged in this particular industry; the organic research worker will also find in it much to stimulate his curiosity. To lecturers in universities and technical colleges it will prove anunfailing source of information for those outlines of industrial processes which experience shows are so much appreciated by students, and which serve to demolish in their minds the unfortunate distinction between pure and applied chemistry.

Low Temperature Physics. By M. and B. RUHEMANN. [Pp. x+313.] (Cambridge University Press, 1937. Price 18*s*.)

THERE has recently been a remarkable convergence of interest, from many different directions, on phenomena at very low temperatures, and a general survey of the subject, such as is given in this book, is particularly opportune.

After a vivid account of the earliest successful experiments, the authors trace the developments in the methods of liquefying gases, and deal fully with methods now in use both for industrial and laboratory purposes. Attention was at first naturally focussed on problems inescapably involved in the methods for producing low temperatures, and it is appropriately with phase equilibrium that the first part of the book is concerned. Although this field is far from exhausted, interest now centres in the more general study of the properties of matter at the low temperatures which have been obtained. The work which has been done is surveyed in three parts under broad headings, "the solid state," "orbit and spin," and "the free electron." Under the first of these the stability of crystal structures, molecular rotations, specific heat, and the Nernst heat theorem are considered. The "orbit and spin" section deals with ortho- and parahydrogen, paramagnetism at low temperatures, and the method of magnetic cooling. Finally, thermal and electrical conductivity and supra-conductivity are considered.

The manuscript was completed at the end of 1935. This is no great drawback, as much of the work which has been done since is summarized in readily accessible reports. There is, moreover, a supplement of references up to May 1937.

The authors state that they "have taken pains to avoid the rigidity and professionalism of a text-book," and that they have deemed it preferable to be too elementary for the specialist than too advanced for the general physicist and the student. The aim is admirable, and on the whole the result is satisfying. Occasionally, however, a high degree of familiarity with specialized subject-matter on the part of the reader is implied in the disarming apparent simplicity of the presentation; and the casualness of exposition may sometimes irritate the specialist without bringing enlightenment to the beginner. In a subject so pervaded by thermodynamic arguments, moreover, a less piecemeal, and more organized and "professional" a presentation of the thermodynamic side would not have been a disadvantage.

The authors, working at the Physico-Technical Institute of Kharkov, are well qualified to write on this subject. They have the familiarity which comes from collaboration in the building up of a new centre of low temperature research.

They write with freshness and enthusiasm. Such criticisms as have been made in no way detract from the positive merits of the book, which can be strongly recommended as a stimulating and well-balanced survey of a fascinating field of physical investigation.

Mechanics. By W. F. Osgood. [Pp. 495+xv.] (Macmillan & Co.)

The author deplores the attitude of many teachers of elementary mechanics—that any way to get an answer is good enough—and insists upon the systematic inculcation of mathematical theory from the commencement of the study of mechanics. He sets out to combine a knowledge of the most elementary physical phenomena with the best mathematical methods and treats with completeness, clarity, and rigour the fundamentals of the subject.

This volume is suitable for first and second year university students, and its scope may be indicated by the following selection: statics of a particle, of a rigid body; motion of a particle, dynamics of a rigid body; relative motion and moving axes; Lagrange's equations, Hamilton's equations; contact transformations, solutions of Hamilton's equations. Numerous examples appear in the text, and a number of special topics are discussed in four appendices.

An Introduction to Nuclear Physics. By N. Feather. [Pp. 213+x.] (Cambridge University Press. Price 10*s.* 6*d.* net.)

Dr. Feather's book provides a valuable introduction for the specialist in nuclear physics and a useful summary for the general scientific reader whose desire is to have set before him the fundamental ideas necessary to an understanding of current research in this branch of physics. Of the four parts into which the subject-matter is divided, the first presents the evidence for the nuclear atom and for a nucleus with internal structure; and the later parts, which trace the developments following the adoption of this scheme of interpretation, include discussions of nuclear moments, artificial radioactivity, theories of β-emission, fast and slow neutrons, and Bohr's theory of the nucleus.

In view of the essentially non-mathematical treatment, this book will be especially welcomed by honours students of physics, and it should be given a place on the shelves of all who wish to keep in touch with the progress made in this fascinating subject.

Bessel Functions.—Part I. *Functions of Orders Zero and Unity.* [Pp. 288+xx.] (Published for the British Association at Cambridge University Press.)

Of the ten tables set out in this volume, Tables I. and III. give the functions $J_0(x)$ and $J_1(x)$ to ten decimal places for $x=0{\cdot}000\ (0{\cdot}001)\ 16{\cdot}000\ (0{\cdot}01)\ 25{\cdot}00$, and the functions $Y_0(x)$ and $Y_1(x)$ to eight decimal places for $x=0{\cdot}00\ (0{\cdot}01)\ 25{\cdot}00$. The first 150 zeros of J_0 and J_1 and the first 50 zeros of K_0 and K_1 appear in Tables II. and IV., together with the value of the one function at the zero of the other. Values of $I_0(x)$ and $I_1(x)$ to at least eight significant figures appear in Table VI. for $x=0{\cdot}000\ (0{\cdot}001)\ 5{\cdot}000$, while in Table VII. eight significant figure values of $K_0(x)$ and $K_1(x)$ for $x=0{\cdot}00\ (0{\cdot}01)\ 5{\cdot}00$ are listed. Each table is preceded by a catalogue of the chief properties of the functions concerned.

A number of auxiliary tables are also given. Table V. furnishes values of certain functions which permit the calculation of the J and K functions for any value of x in the range 25–6000. As it is not convenient to interpolate the Y and K functions for small values of x, certain easily interpolated functions are introduced, and their values are given in Tables III. A and VII. A. Eight figure values of the I and K functions for $x>5$ may readily be obtained from the easily interpolated functions $e^{-x}\mathrm{I}$ and $e^{x}\mathrm{K}$, which are listed in Table VIII., in conjunction with the exponential functions of Table IX.

In each table the second order differences of the function are listed, and Table X. provides the Everett and Besselian coefficient suitable for the interpolation of any of the tables given in the collection. The precautions taken to ensure the elimination of errors are described by Dr. Comrie in an introduction in which he pays a tribute to the painstaking skill of the compositors and readers of the Cambridge University Press. The compilation of these tables is a remarkable achievement, and we confidently accept Dr. Comrie's closing words, "There is every reason to believe that the tables are completely free from error."

[*The Editors do not hold themselves responsible for the views expressed by their correspondents.*]

INDEX TO VOL. XXV.

A.C. potentiometer — zero-shunt valve, 184.
Active nitrogen, some aspects of, 471.
Activity coefficients of potassium chloride and of calcium chloride, 45.
Airey (John R.), the radiation integrals $\int_x^\infty \frac{dx}{x^a(e^x-1)}$, 273.
Allen (J.), experiments on water waves of translation in small channels, 754.
Ampère's law, reciprocals to, 175.
Andrews (J. P.), thermal diffusivity of the soil of Colombo, 1066.
Annular quartz plates, radial and torsional vibrations of, 164.
Application of derivatives of line integrals, 549.
Approximations to functions and to solutions of differential equations, 740.
Astbury (N. F.), the primary standard of mutual inductance of the National Physical Laboratory, 290.
—— and Ford (L. H.), a screened sub-standard inductometer, 1009.
Ataka (Hikosaburo) on the extension of Thévénin's theorem, 663.
Atomic forces of solid state, on the, 111.
Bailey (C. R.) and Hale (J. B.), the infra-red absorption spectrum of phosgene, 98.
Banerjee (S. S.) and Joshi (R. D.), dielectric constant and conductivity of soil at high radio frequencies, 1025.
Bardhan (L. C.) on the nuclear structure of radioactive substances, 1033.
Beams, the bending of, on elastic foundations, 49.
Bell (R. P.), wave functions and permeabilities for a new type of potential barrier, 488.
Bending of beams on elastic foundations, 49.
Beta-particles, complete detection of, 393.
Beta-rays, the reflexion of, 322.
Beynon (W. J. G.), the ultra-violet absorption bands of ethyl-alcohol, *n*-propyl alcohol, and *n*-butyl alcohol in relation to magneto-optical dispersion, 443.
—— and Evans (E. J.), the ultra-violet absorption bands of methyl alcohol and allyl alcohol and their relation to magneto-optical dispersion, 476.
Bhatnagar (S. S.), Khanna (Mohan Lal), and Nevgi (M. B.), paramagnetism of the iron group, 234.
Bickley (W. G.), the secondary flow due to a sphere rotating in a viscous fluid, 746.
Bircumshaw (L. L.) and Preston (G. D.), studies on the oxidation of metals.—Part V. The oxidation of molten lead, 769.
Blocking layer photoelectric effect of cæsium oxide, on the, 269.
Books, new :—Francis Bitter, Introduction to Ferromagnetism, 189 ; R. W. Gurney, Ions in Solution, 190 ; Alfred Landé, Principles of Quantum Mechanics, 191 ; A. S. Ramsey, Electricity and Magnetism, 192 ; A. S. Ramsey, Dynamics.—Part II., 192 ; J. H. Michell and M. H. Belz, Mathematical Analysis, Volumes I. and II., 389 ; F. B. Pidduck, Lectures on the Mathematical Theory of Electricity, 389 ; Edward S. Allen, Plane Trigonometry, 390 ; A. S. Ramsey, Hydrostatics, 390 ; K. Henney, Electron Tubes in Industry, 391 ; A. V. Eastman,

The Fundamentals of Vacuum Tubes, 392; Harald Cramér, Random Variables and Probability Distributions, 583; J. W. Mellor, A Comprehensive Treatise on Inorganic and Theoretical Chemistry, Vol. XVI., Part and General Index, 584; Measurements of Radiant Energy, Editor, L. E. Forsythe, 703; Gerhard Herzberg, trans. J. W. T. Spinks, Atomic Spectra and Atomic Structure, 703; J. M. Thomas, Differential Systems, 704; H. Kestelman, Modern Theories of Integration, 811; Enrico Fermi, Thermodynamics, 812; S. Barnard and J. M. Child, Higher Algebra, 813; Herbert Dingle, Through Science to Philosophy, 814; Max Morris and O. E. Brown, Analytic Geometry and Calculus, 816; George Kaván, Factor Tables giving the Complete Decomposition into Prime Factors of all Numbers up to 256,000, 1004; C. V. Durell and A. Robson, Advanced Algebra, Vols. II. and III., 1005; A. Cornelius Benjamin, An Introduction to the Philosophy of Science, 1006; L. Susan Stebbing, Philosophy and the Physicists, 1007; J. V. Uspensky, Introduction to Mathematical Probability, 1115; Synthetic Resins and Allied Plastics. Editors:—R. S. Morrell, T. H. Barry, R. P. L. Britton, and H. M. Langton, 1117; M. and B. Ruhemann, Low Temperature Physics, 1119; W. F. Osgood, Mechanics, 1120; N. Feather, An Introduction to Nuclear Physics, 1120; Bessel Functions. —Part I. Functions of Orders Zero and Unity, 1121.

Bremmer (H.) and Pol (Balth. van der), the propagation of radio waves over a finitely conducting spherical earth, 817.

Cæsium oxide, on the blocking layer photoelectric effect of, 269.

Capacitance at ultra-high frequencies, 339.

Carwile (Preston B.), reciprocals to Ampère's law, 175.

——, suggested explanation of the contradiction between the Rayleigh-Jeans formula and experiment, 926.

Chakravarty (Kumar) and Khastgir (S. R.), direct determination of the electrical constants of soil at ultra-high radio-frequency, 793.

Chalmers (Bruce) and Humphry (R. H.), the specific resistance and the temperature variation of resistance of tin crystals, 1108.

Chalmers (J. Alan), the reflexion of β-rays, 322.

Charged colloid particles in an ultrasonic field, 426.

Coe (R. Thornton), the bending of beams on elastic foundations, 49.

Collective electron energy and specific heat, 899.

Colloid particles, charged, in an ultrasonic field, 426.

Complete detection of Beta-particles, 393.

Computation of three-dimensional Fourier synthesis in crystal structure analysis, 1096.

Craxford (S. R.), Gatty (O.), and Teorell (T.), the theory of electrocapillarity.—VII. The theory of surface films, 1041.

——, ——, ——, a note on surface pH, 1061.

Crystal structure analysis, the computation of three-dimensional Fourier syntheses in, 1096.

Curran (Samuel C.), the complete detection of Beta-particles, 393.

Cyclohexane, Raman effect in solid, 895.

Dasannacharya (B.), the development of the minor axis in a Foucault's pendulum, 601.

Davies (R. M.), the frequency of longitudinal and torsional vibration of unloaded and loaded bars, 364.

Definite integrals for Legendre functions, 1113.

Deflexion of beams and struts, remarks on the more accurate calculation of the, 678.

Development of the minor axis in a Foucault's pendulum, 601.

Dhar (S. C.) on the operational representation of M-functions of the confluent hypergeometric type, 416.

Dielectric constant of ionized gases.—II., 883.

—— and conductivity of soil at high radio frequencies, 1025.

Differential equations, approximation to functions and to solutions of, 740.
Differentiation of line integrals by parallel displacement, 1.
Diffusion of electrons in a magnetic field, 459.
Dock (E. H.), and Spencer-Gregory (H.), the effect of temperature on the thermal conductivity and the accommodation coefficient of hydrogen below 0° C., 129.
Dowling (John J.), the zero-shunt valve A.C. potentiometer, 184.
Duncan (W. J.), note on Galerkin's method for the treatment of problems concerning elastic bodies 628.
——, applications of the Galerkin method to the torsion and flexure of cylinders and prisms, 634.
Electrical constants of soil, direct determination of, at ultra-high radio-frequency 793.
Electro-capillarity, the theory of.—VII. The theory of surface films, 1041.
Electrolytic water-transport and ionic hydration numbers, 1074.
Electromagnetic waves, propagation of, in an ionized atmosphere, 148.
Electron energy, collective, and specific heat, 899.
Electrons, diffusion of, in a magnetic field, 459.
Equilibrium of a vortex maintained in a sudden expanding stream, 567.
—— of a thin plate, symmetrical loaded, resting on an elastic foundation of infinite depth, 576.
Evans (E. J.) and Beynon (W. J. G.), ultra-violet absorption bands of methyl alcohol and allyl alcohol and their relation to magneto-optical dispersion, 476.
Evaporation of atoms, ions, and electrons from tungsten, 834.
Experiments on water waves of translation in small channels, 754.
Fabian (W.), Lebesgue complex integration, 318.
——, Lebesgue complex integration and generalized differentiation, 807.
—— the zeta-function of Riemann, 321.
Ford (L. H.) and Astbury (N. F.), a screened sub-standard inductometer, 1009.
Form assumed by a steadily rotating thread, 193.
Foucault's pendulum, development of the minor axis in a, 601.
Fractional differentials, 540.
Fraser (Malcolm), thermo-electric effects in homogeneous conductors, 785.
Frazer (R. A.), Jones (W. P.), and Skan (Sylvia W.), note on approximations to functions and to solutions of differential equations, 740.
Frequency of longitudinal and torsional vibration of unloaded and loaded bars, 364.
Functions, class of, which are self-reciprocal in the Hankel transform, 622.
Galerkin method, applications of the, to the torsion and flexure of cylinders and prisms, 634.
—— ——, note on, for the treatment of problems concerning elastic bodies, 628.
Gangopadhyaya (Sukhamaya) and Khastgir (S. R.), dielectric constant of ionized gases.—II., 883.
Gardner (Harold Ward), the gradient diagram, 438.
Gatty (O.), Craxford (S. R.), and Teorell (T.), the theory of electro-capillarity.—VII. The theory of surface films, 1041.
——, ——, ——, a note on surface pH, 1061.
Gemant (Andrew) on fractional differentials, 540.
Gogate (D. V.), a relativistic study of Joule-Thomson effect and adiabatic processes in a gas.—Part I., 694.
Goodwin (T. H.) and Hardy (R.), the computation of three-dimensional Fourier syntheses in crystal structure analysis, 1096.
Görlich (P.), measurements on photocathodes in contact, 256.
Gradient diagram, the, 438.
Guggenheim (E. A.) and Wiseman (L. A.), the activity coefficients of potassium chloride and of calcium chloride, 45.
Hale (J. B.) and Bailey (C. R.), the infra-red absorption spectrum of phosgene, 98.
Hardy (R.) and Goodwin (T. H.), the computation of three-dimensional Fourier syntheses in crystal structure analysis, 1096.

Harmonic analysis, a method of.—A study of the rotational frequencies of screw propellers, 505.
Hepburn (H. C.), electrolytic water-transport and ionic hydration numbers, 1074.
Hermans (J. J.), charged colloid particles in an ultrasonic field, 426.
Hermite polynomials, a note on, 600.
Hogg, (A. H. A.), equilibrium of a thin plate, symmetrically loaded, resting on an elastic foundation of infinite depth, 576.
Howell (W. T.), integral representations for products of Weber's parabolic cylinder functions, 456.
——, a note on hermite polynomials, 600.
—— on a class of functions which are self-reciprocal in a Hankel transform, 622.
——, a definite integral for Legendre functions, 1113.
Hume-Rothery (William), and Raynor (Geoffrey Vincent), on the nature of intermetallic compounds of the type Mg_2Sn, 335.
Humphry (R. H.) and Chalmers (Bruce), the specific resistance and the temperature variation of resistance of tin crystals, 1108.
Hunter (W.) and Warburton Hall (H.) on the form assumed by a steadily rotating thread, 193.
Hurst (C.), the potential problem of a sphere lying between infinite conducting planes, 282.
Huxley (L. G. H.), the propagation of electromagnetic waves in an ionized atmosphere, 148.
——, supplementary note to the paper "The propagation of electromagnetic waves in an ionized atmosphere," 388.
Hydration and denaturation of proteins, 705.
Hypergeometric function, on Whittaker's confluent, 491.
Images, method of, by calculating electric and magnetic fields, 66.
Immelman (M. N. S.), point-discharge currents during thunderstorms, 159.
Impedance characteristics of short-wave dipoles, 981.
Inductometer, a screened substandard, 1009.
Infra-red absorption spectrum of phosgene, 98.
Integral representations for products of Weber's parabolic cylinder functions, 456.
Intermetallic compounds, nature of, the type Mg_2Sn, 335.
—— reaction, a note on a suggested, in a liquid antimony-copper-tin-lead alloy, 1104.
Ionic hydration numbers, electrolytic water-transport and, 1074.
Ionized gases, dielectric constant of.—II., 883.
Iron group, paramagnetism of, 234.
Jones (W. P.), Frazer (R. A.), and Skan (Sylvia W.), note on approximations to functions and to solutions of differential equations, 740.
Joshi (R. D.) and Banerjee (S. S.), dielectric constant and conductivity of soil at high radio frequencies, 1025.
Joule-Thomson effect and adiabatic processes in a gas, a relativistic study of.—Part I., 694.
Khanna (Mohan Lal), Nevgi (M. B.), and Bhatnagar (S. S.), paramagnetism of the iron group, 234.
Khastgir (S. R.), and Chakravarty (Kumar), direct determination of the electrical constants of soil at ultra-high radio-frequency, 793.
—— and Gangopadhyaya (Sukhamaya), dielectric constant of ionized gases.—II., 883.
Kimball (W. S.), application of derivatives of line integrals, 549.
——, differentiation of line integrals by parallel displacement, 1.
King (Ronold), capacitance at ultra-high frequencies, 339.
Koteswaram (P.) and Ramakrishna Rao (I.), additional Raman frequencies for water, 90.
Lebesgue complex integration, 318.
—— —— —— and generalized differentiation, 807.
Legendre functions, a definite integral for, 1113.
Lenses, thick, and combinations of thin lenses, 801.
Lessheim (H.) and Samuel (R.), note on numerical valency in polyatomic molecules, 667.
Line integrals, differentiation of, by parallel displacement, 1.

Line integrals, application of derivatives of, 549.
Linear variable networks, operational and matrix methods in, 585.
Lommel functions, 930.
McLachlan (N. W.), operational systems, 259.
McNeill (D. B.), some aspects of active nitrogen, 471.
MacRobert (T. M.), a proof by induction of the analytical continuations of certain generalized hypergeometric functions, 848.
Magnetic fields in transformers at low frequencies (25 to 75 cycles per second), 242.
Magnetism and the vibratory electron, 682.
Measurements on photocathodes in contact, 256.
Metcalfe (J.), Wheatcroft (E. L. E.), and Smith (R. B.), pre-striking currents in a thyratron, 649.
Meyerovitz (E. A.), the methods of images by calculating electric and magnetic fields, 66.
M-functions of the confluent hypergeometric type, operational representation of, 416.
Mitra (S. M.), Raman effect in solid cyclohexane, 895.
Miyadzu (Atsushi), note on the equilibrium of a vortex maintained in a sudden expanding stream, 567.
Molecular force and viscosity of gases, 865.
Mutual inductance, primary standard of, of the National Physical Laboratory, 290.
Nature of intermetallic compounds of the type Mg_2Sn, 335.
Nevgi (M. B.), Bhatnagar (S. S.), and Khanna (Mohan Lal), paramagnetism of the iron group, 234.
New forms of the theorem of three moments, 852.
Nuclear structure of radioactive substances, 1033.
Numerical valency in polyatomic molecules, 667.
Operational and matrix methods in linear variable networks, 585.
—— systems, 259.
—— theory of solid friction, 950.
—— representation of M-functions of the confluent hypergeometric type, 416.
Oxidation of metals, studies on.—Part V. Oxidation of molten lead, 769.
Parabolic cylinder functions, integral representations for products of Weber's, 456.
Paramagnetism of the iron group, 234.
Partridge (G. F.), a method of harmonic analysis.—A study of the rotational frequencies of screw propellers, 505.
Petrźilka (V.) and Žáček (A.), radial and torsional vibrations of annular quartz plates, 164.
Phosgene, infra-red absorption spectrum of, 98.
Photocathodes in contact, measurements on, 256.
Photoelectric effect, on the blocking layer, of cæsium oxide, 269.
Pipes (Louis A.), operational and matrix methods in linear variable networks, 585.
——, the operational theory of solid friction, 950.
Point discharge currents during thunderstorms, 159.
Pol (Balth. van der) and Bremmer (H.), the propagation of radio waves over a finitely conducting spherical earth, 817.
Porter (Alfred W.) on the calculation of surface tension from the measurement of sessile drops, 752.
Pöschl (Th.), remarks on the more accurate calculation of the deflexion of beams and struts, 678.
Potential barrier, wave functions and permeabilities for a new type of, 488.
—— problem of a sphere lying between infinite conducting planes, 282.
Potentials in curved surfaces, 783.
Preston (G. D.) and Bircumshaw (L. L.), studies on the oxidation of metals.—Part V. The oxidation of molten lead, 769.
Pre-striking currents in a thyratron, 649.
Primary standard of mutual inductance of the National Physical Laboratory, 290.
Proof by induction of the analytical continuations of certain generalized hypergeometric functions, 848.

Propagation of electromagnetic waves in an ionized atmosphere, 148.
—— of radio waves over a finitely conducting spherical earth, 817.
Prosad (K.) and Sen (D. N.) on the trajectory of ash particles in air and the determination of their size, 993.
Proteins, on the hydration and denaturation of, 705.
Radial and torsional vibrations of annular quartz plates, 164.
Radiation integrals $\int_x^\infty \frac{dx}{x^a(e^x-1)}$, 273.
Radio waves, the propagation of, over a finitely conducting spherical earth, 817.
Radioactive substances, on the nuclear structure of, 1033.
Ramakrishna Rao (I.) and Koteswaram (P.), additional Raman frequencies for water, 90.
Raman effect in solid cyclohexane, 895.
—— frequencies, additional, for water, 90.
Rayleigh-Jeans formula and experiment, suggested explanation of the contradiction between the, 926.
Raynor (Geoffrey Vincent) and Hume-Rothery (William) on the nature of intermetallic compounds of the type Mg_2Sn, 335.
Reciprocals to Ampère's law, 175.
Record (Frederick), thick lenses and combinations of thin lenses, 801.
Reflexion of β-rays, 322.
Reimann (A. L.), the evaporation of atoms, ions, and electrons from tungsten, 834.
——, zeta-function of, 321.
Relativistic study of Joule-Thomson effect and adiabatic processes in a gas.—Part I., 694.
Rigden (P. J.), the viscosity of air, oxygen, and nitrogen, 961.
Rotating thread, form assumed by a steadily, 193.
Samuel (R.) and Lessheim (H.), note on numerical valency in polyatomic molecules, 667.
Screened sub-standard inductometer, 1009.
Seager (G. C.), and Thompson (F. C.) a note on a suggested intermetallic reaction in a liquid antimony-copper-tin-lead alloy, 1104.
Secondary flow due to a sphere rotating in a viscuous fluid, 746.
Sen (D. N.) and Prosad (K.) on the trajectory of ash particles in air and the determination of their size, 993.
Sharma (J. L.) on Whittaker's confluent hypergeometric function, 491.
Shastri (N. A.) on Lommel functions, 930.
Short-wave dipoles, impedance characteristics of, 981.
Silberstein (Ludwik), summation of the series $1+x^3/3\,!+x^6/6\,!+\ldots$, 1003.
Skan (Sylvia W.), Frazer (R. A.), and Jones (W. P.), note on approximations to functions and to solutions of differential equations, 740.
Smith (R. B.), Metcalf (J.), and Wheatcroft (E. L. E.), prestriking currents in a thyratron, 649.
Soil, thermal diffusivity of the, at Colombo, 1066.
——, dielectric constant and conductivity of, at high radio-frequencies, 1025.
——, direct determination of the electrical constants of, at ultra-high radio-frequency, 793.
Solid friction, operational theory of, 950.
—— state, on the atomic forces of, 111.
Specific resistance and the temperature variation of resistance of tin crystals, 1108.
Spencer-Gregory (H.) and Dock (E. H.), the effect of temperature on the thermal conductivity and the accommodation coefficient of hydrogen below 0° C., 129.
Stibitz (G. R.), potentials in curved surfaces, 783.
Stoner (E. C.), collective electron energy and specific heat, 899.
Suggested explanation of the contradiction between the Rayleigh-Jeans formula and experiment, 926.
Summation of the series $1+x^3/3\,!+x^6/6\,!+\ldots$, 1003.
Surface films, the theory of, 1041.
—— pH, a note on, 1061.

Surface tension, on the calculation of, from the measurement of sessile drops, 752.
Taylor-Jones (E.), magnetism and the vibratory electron, 682.
Teichmann (Horst) on the blocking layer photoelectric effect of cæsium oxide, 269.
Temperature, effect of, on the thermal conductivity and the accommodation coefficient of hydrogen below 0° C., 129.
Teorell (T.), Craxford (S. R.), and Gatty (O.), the theory of electrocapillarity.—VII. The theory of surface films, 1041.
——, ——, ——, a note on surface pH, 1061.
Theorem of three moments, new forms of the, 852.
Thermal conductivity, the effect of temperature on, and the accommodation coefficient of hydrogen below 0° C., 129.
—— diffusivity of the soil at Colombo, 1066.
Thermo-electric effects in homogeneous conductors, 785.
Thévénin's theorem, on an extension of, 663.
Thick lenses and combinations of thin lenses, 801.
Thompson (F. C.) and Seager (G. C.), a note on a suggested intermetallic reaction in a liquid antimony-copper-tin-lead alloy, 1104.
Thomson (J. M.), magnetic fields in transformers at low frequencies (25 to 75 cycles per second), 242.
Thyratron, pre-striking currents in a, 649.
Tin crystals, the specific resistance and the temperature variation of resistance of, 1108.
Townsend (J. S.), diffusion of electrons in a magnetic field, 459.
Trajectory of ash particles in air and the determination of their size, 993.
Transformers, magnetic fields in, at low frequencies (25 to 75 cycles per second), 242.
Tungsten, the evaporation of atoms, ions, and electrons from, 834.
Turton (F. J.), new form of the theorem of three moments, 852,
Ultra-violet absorption bands of ethyl alcohol, *n*-propyl alcohol, and *n*-butyl alcohol in relation to magneto-optical dispersion, 443.
—— —— —— of methyl alcohol and allyl alcohol and their relation to magneto-optical dispersion, 476.
Valency in polyatomic molecules, note on numerical, 667.
Vibratory electron, magnetism and the, 682.
Viscosity of air, oxygen, and nitrogen, 961.
—— of gases, molecular force and, 865.
Viscous fluid, secondary flow due to a sphere rotating in a, 746.
Vortex maintained in a sudden expanding stream, note on the equilibrium of a, 567.
Walmsley (T.), impedence characteristics of short-wave dipoles, 981.
Warburton Hall (H) and Hunter (W.) on the form assumed by a steadily rotating thread, 193.
Wave functions and permeabilities for a new type of potential barrier, 488.
Waves of translation, experiment on water, in small channels, 754.
Wen-Po (Weng) on the atomic forces of solid state, 111.
——, molecular force and viscosity of gases, 865.
Wheatcroft (E. L. E.), Smith (R. B.), and Metcalfe (J.), pre-striking currents in a thyratron, 649.
Whittaker's confluent hypergeometric function, 491.
Wiseman (L. A.) and Guggenheim (E. A.), the activity coefficients of potassium chloride and of calcium chloride, 45.
Wright (C. E.), note on the paper "A note on the vibrations of a rotating rope," 387.
Wrinch (D. M.) on the hydration and denaturation of proteins, 705.
Žáček (A.) and Petržílka (V.), radial and torsional vibrations of annular quartz plates, 164.
Zero-shunt valve A.C. potentiometer, 184.
Zeta-function of Riemann, 321.

END OF THE TWENTY-FIFTH VOLUME.

Printed by Taylor & Francis, Ltd., Red Lion Court, Fleet Street, E.C.4.

Wool Research

Surface tension, on the calculation of, from the measurement of sessile drops, 752.
Taylor-Jones (E.), magnetism and the vibratory electron, 682.
Teichmann (Horst) on the blocking layer photoelectric effect of cæsium oxide, 269.
Temperature, effect of, on the thermal conductivity and the accommodation coefficient of hydrogen below 0° C., 129.
Teorell (T.), Craxford (S. R.), and Gatty (O.), the theory of electrocapillarity.—VII. The theory of surface films, 1041.
——, ——, ——, a note on surface pH, 1061.
Theorem of three moments, new forms of the, 852.
Thermal conductivity, the effect of temperature on, and the accommodation coefficient of hydrogen below 0° C., 129.
—— diffusivity of the soil at Colombo, 1066.
Thermo-electric effects in homogeneous conductors, 785.
Thévénin's theorem, on an extension of, 663.
Thick lenses and combinations of thin lenses, 801.
Thompson (F. C.) and Seager (G. C.), a note on a suggested intermetallic reaction in a liquid antimony-copper-tin-lead alloy, 1104.
Thomson (J. M.), magnetic fields in transformers at low frequencies (25 to 75 cycles per second), 242.
Thyratron, pre-striking currents in a, 649.
Tin crystals, the specific resistance and the temperature variation of resistance of, 1108.
Townsend (J. S.), diffusion of electrons in a magnetic field, 459.
Trajectory of ash particles in air and the determination of their size, 993.
Transformers, magnetic fields in, at low frequencies (25 to 75 cycles per second), 242.
Tungsten, the evaporation of atoms, ions, and electrons from, 834.
Turton (F. J.), new form of the theorem of three moments, 852,
Ultra-violet absorption bands of ethyl alcohol, *n*-propyl alcohol, and *n*-butyl alcohol in relation to magneto-optical dispersion, 443.
—— —— —— of methyl alcohol and allyl alcohol and their relation to magneto-optical dispersion, 476.
Valency in polyatomic molecules, note on numerical, 667.
Vibratory electron, magnetism and the, 682.
Viscosity of air, oxygen, and nitrogen, 961.
—— of gases, molecular force and, 865.
Viscous fluid, secondary flow due to a sphere rotating in a, 746.
Vortex maintained in a sudden expanding stream, note on the equilibrium of a, 567.
Walmsley (T.), impedence characteristics of short-wave dipoles, 981.
Warburton Hall (H) and Hunter (W.) on the form assumed by a steadily rotating thread, 193.
Wave functions and permeabilities for a new type of potential barrier, 488.
Waves of translation, experiment on water, in small channels, 754.
Wen-Po (Weng) on the atomic forces of solid state, 111.
——, molecular force and viscosity of gases, 865.
Wheatcroft (E. L. E.), Smith (R. B.), and Metcalfe (J.), pre-striking currents in a thyratron, 649.
Whittaker's confluent hypergeometric function, 491.
Wiseman (L. A.) and Guggenheim (E. A.), the activity coefficients of potassium chloride and of calcium chloride, 45.
Wright (C. E.), note on the paper "A note on the vibrations of a rotating rope," 387.
Wrinch (D. M.) on the hydration and denaturation of proteins, 705.
Žáček (A.) and Petržílka (V.), radial and torsional vibrations of annular quartz plates, 164.
Zero-shunt valve A.C. potentiometer, 184.
Zeta-function of Riemann, 321.

END OF THE TWENTY-FIFTH VOLUME.

Printed by TAYLOR & FRANCIS, Ltd., Red Lion Court, Fleet Street, E.C,4.

Wool Research